NBS SPECIAL PUBLICATION 300
VOLUME 5

Precision Measurement and Calibration

Frequency and Time

U.S.
DEPARTMENT
OF
COMMERCE
National
Bureau
of
Standards

Precision Measurement and Calibration

Volumes available or to be published in the NBS Special Publication 300 series

SP300, Vol. 1, Statistical Concepts and Procedures, H. H. Ku, Editor, Feb. 1969, 436 pages (SD Catalog No. C 13.10:300/v.1)* Price $5.50

SP300, Vol. 2, Temperature, J. F. Swindells, Editor, Aug. 1968, 520 pages (SD Catalog No. C 13.10:300/v. 2)* Price $4.75

SP300, Vol. 3, Electricity — Low Frequency, F. L. Hermach and R. F. Dziuba, Editors, Dec. 1968, 498 pages (SD Catalog No. C 13.10:300/v.3)* Price $4.50

SP300, Vol. 4, Electricity — Radio Frequency, A. J. Estin, Editor, June 1970, 450 pages (SD Catalog No. C 13.10:300/v.4)* Price $5.50

SP300, Vol. 5, Frequency and Time, B. E. Blair and A. H. Morgan, Editors, June 1972, 565 pages (C 13.10:300/v.5)* Price $6.00

SP300, Vol. 6, Heat, D. C. Ginnings, Editor, Feb. 1970, 400 pages (SD Catalog No. C 13.10:300/v.6)* Price $5.00

SP300, Vol. 7, Radiometry and Photometry, H. K. Hammond, III, and H. L. Mason, Editors, Nov. 1971, 690 pages (SD Catalog No. C 13.10:300/v.7)* Price $7.00

SP300, Vol. 8, Mechanics, R. L. Bloss and Mary J. Orloski, Editors, Jan. 1971, 590 pages (SD Catalog No. C 13.10:300/v.8) ½ Price $6.25

SP300, Vol. 9, Colorimetry, I. Nimeroff, Editor, June 1972, 460 pages (SD Catalog No. C 13.10:300/v.9)* Price $5.50

Volumes in Press**

SP300, Vol. 10, Ionizing Radiation, Elmer H. Eisenhower, Editor.

SP300, Vol. 11, Image Optics, Calvin S. McCamy, Editor.

---

* Available from the Superintendent of Documents, Government Printing Office, Washington, D.C. 20402. Order by the Supt. of Documents Catalog number as given for each volume.

** For announcements of new volumes as issued, complete the form (Notification key N-353) in the back of this volume and mail it to the Superintendent of Documents office.

UNITED STATES DEPARTMENT OF COMMERCE • PETER G. PETERSON, Secretary

Precision Measurement and Calibration

Selected NBS Papers on

Frequency and Time

B. E. Blair and A. H. Morgan, Editors

Institute for Basic Standards
National Bureau of Standards
Boulder, Colorado 80302

A compilation of previously published papers by the staff of the National Bureau of Standards, including selected abstracts by NBS and non-NBS authors. Issued in several volumes, see p. IV.

NBS Special Publication 300 — Volume 5

Coden Nat. Bur. Stand. (U.S.) Spec. Publ. 300, Vol. 5, 565 pages (June 1972)

Issued June 1972

For sale by the Superintendent of Documents, U.S. Government Printing Office, Washington, D.C. 20402 (Order by SD Catalog No. C.13.10: 300/v. 5), price $6.00.
Stock Number 0303-0916

Abstract

This is one of a series of volumes consisting of a group of selected papers and monographs by NBS authors, and abstracts of papers by non-NBS and NBS authors, dealing with the precision measurement of specific physical quantities and related topics. The contents should be useful to those in the scientific community who are engaged in frequency and time measurements or are otherwise interested in these physical quantities.

This volume contains selected reprints, and abstracts of very general papers, printed in chronological order in most cases from January 1960 through June 1969, covering the following general topics: Frequency and Time Standards, Time Scales, Distribution of Frequency and Time Signals, Statistics of Frequency and Time Standards, and Selected Frequency and Time References.

Key Words: Atomic beams, atomic clocks; atomic standards; atomic time; clock synchronization; coordinated U.T. dissemination of frequency and time; flicker noise; frequency and time standards; frequency measurement; frequency stability; international comparison of atomic standards; lasers; masers; radio frequency measurements; satellite timing; spectral density; standard frequency and time broadcasts; statistics of frequency and time measurements; time scales; time synchronizations; TV timing; VLF timing.

Library of Congress Catalog Card Number: 68–60042

Foreword

In the 1950's the tremendous increase in industrial activity, particularly in the missile and satellite fields, led to an unprecedented demand for precision measurement, which, in turn, brought about the establishment of hundreds of new standards laboratories. To aid these laboratories in transmitting the accuracies of the national standards to the shops of industry, NBS in 1959 gathered together and reprinted a number of technical papers by members of its staff describing methods of precision measurement and the design and calibration of standards and instruments. These reprints, representing papers written over a period of several decades, were published as NBS Handbook 77, Precision Measurement and Calibration, in three volumes: Electricity and Electronics; Heat and Mechanics; Optics, Metrology, and Radiation.

Some of the papers in Handbook 77 are still useful, but new theoretical knowledge, improved materials, and increasingly complex experimental techniques have so advanced the art and science of measurement that a new compilation has become necessary. The present volume is part of a new reprint collection, designated NBS Special Publication 300, which has been planned to fill this need. Besides previously published papers by the NBS staff, the collection includes selected abstracts and references by both NBS and non-NBS authors. It is hoped that SP 300 will serve both as a textbook and as a reference source for the many scientists and engineers who fill responsible positions in standards laboratories.

LEWIS M. BRANSCOMB, *Director.*

Preface

The general plan for this compilation has been reviewed by the Information Committee of the National Conference of Standards Laboratories. The plan calls for Special Publication 300 to be published in 12 volumes as presented on the inside of the front cover.

The division of subject matter has been chosen to assure knowledgeable selection of context rather than to attain uniform size. It is believed, however, that the larger volumes, of approximately 500 pages, will still be small enough for convenient handling in the laboratory.

The compilation consists primarily of original papers by NBS authors which have been reprinted by photoreproduction, with occasional updating of graphs or numerical data when this has appeared desirable. In addition, some important publications by non-NBS authors that are too long to be included, are represented by abstracts or references; the abstracts are signed by the individuals who wrote them, unless written by the author.

Each volume has a subject index and author index, and within each volume, contents are grouped by subtopics to facilitate browsing. Many entries follow the recent Bureau practice of assigning several key words or phrases to each document; these may be collated with titles in the index. Pagination is continuous within the volume, the page numbers in the original publications also being retained and combined with the volume page numbers, for example 100–10. The index notation 7–134 refers to volume 7, page 134 of this volume. A convenient list of SI (Système International) physical units and a conversion table are to be found inside the back cover.

The publications listed herein for which a price is indicated are available from the Superintendent of Documents, U.S. Government Printing Office, Washington, D.C. 20402 (foreign postage, one-fourth additional). Many documents in the various NBS nonperiodical series are also available from the NBS National Technical Information Service, Springfield, Va. 22151. Reprints from the NBS Journal of Research or from non-NBS journals may sometimes be obtained directly from an author.

Suggestions as to the selection of papers which should be included in future editions will be welcome. Current developments in measurement technology at NBS are covered in annual seminars held at either the Gaithersburg (Maryland) or the Boulder (Colorado) laboratories. These developments are summarized, along with a running list of publications by NBS authors, in the monthly NBS Technical News Bulletin.

HENRY L. MASON,
Office of Measurement Services,
NBS Institute for Basic Standards.

Editor's Note

Volume 5 gives broad coverage to work in the area of frequency and time for the decade 1960–1969. It contains 57 reprints of papers published by NBS authors and 23 abstracts, of which 12 constitute non-NBS authorship. These papers are given in the first four sections of Volume V. They show advances in atomic frequency and time scale standards, statistical means of time synchronization and methods of frequency and time dissemination, including satellites and TV timing. Section V.5, provides selected worldwide references of frequency and time, classified by area, written during the period 1960 to 1970 (February).

We wish to acknowledge the valuable assistance of the following persons in the preparation of this volume: J. A. Barnes, R. E. Beehler, and D. Halford for very helpful comments; J. Jespersen, D. H. Andrews, and other members of the Time and Frequency Division for aid in obtaining references and reprints; and Mrs. Louise Gaskill, Mrs. Carole Craig, and Miss Sandra Richmond for typing the manuscript copy.

B. E. BLAIR and
A. H. MORGAN, *Editors.*

Contents

1. Frequency and Time Standards—Continued

Abstracts

2. Time Scales

Papers

2. Time Scales—Continued

3. Distribution of Frequency and Time Signals

3. Distribution of Frequency and Time Signals—Continued

4. Statistics of Frequency and Time Measurements

4. Statistics of Frequency and Time Measurements—Continued

5. Selected References On Frequency and Time

January 1960—February 1970

Byron E. Blair

1. Frequency and Time Standards

Atomic Beam Frequency Standards

Richard C. Mockler

National Bureau of Standards, Radio Standards Division, Boulder, Colorado

Reprinted from

ADVANCES IN ELECTRONICS AND ELECTRON PHYSICS

Volume 15, 1961

Atomic Beam Frequency Standards

RICHARD C. MOCKLER

National Bureau of Standards, Boulder, Colorado

I. Introduction

It is natural to choose as a standard of frequency and time interval some periodic phenomenon appearing in nature that is especially uniform. The periodic rotation of the earth on its axis at one time provided a sufficiently uniform time base. As techniques of measurement improved it was demonstrated that the rotational period of the earth was slowly increasing,

an effect that has been attributed to tidal friction. In addition, there were observed irregular changes and almost periodic fluctuations in the length of the solar day. More recently (1956) astronomers have chosen the period of the orbital motion of the earth about the sun as the basis for the definition of time. This is the basis upon which time is defined (in the practical sense) today. There are secular variations in this period, but they are much more predictable than the changes in the length of the solar day. For this reason the second has been defined as 1/31,556,925.9747 of the tropical year at 12^h ET, 0 January, 1900.

Highly complex macroscopic systems such as our solar system probably are subject to some unpredictable changes and aging effects. For many purposes the periodic motions in microscopic systems of atoms would be more suitable for defining time intervals and frequency. To be sure, the separations of the quantum states of a completely isolated atom or molecule are expected to be fixed in time. The measurement of one of these separations by a suitable apparatus would provide a very excellent standard if the measurements can be made with the required precision.

Microwave and atomic beam magnetic resonance techniques provide a method of measuring state separations with probably the greatest accuracy and ease of interpretation of all the presently known spectroscopic techniques. Atomic beam techniques have the advantage that Doppler and collision broadening of the spectral line are practically eliminated. Certain atoms, especially the alkali metals, have intense spectral lines that are easily detected. Moreover, the transitions fall in a convenient range of the electromagnetic spectrum easily accessible to available coherent radiators.

A transition between the hyperfine structure (hfs) levels in the ground state of cesium provides the present working standard of frequency for the United States (*1*), the United Kingdom (*2*), Canada (*3*), and Switzerland (*4*). This transition can be measured with the remarkable precision of ± 2 parts in 10^{12}, and with an accuracy of ± 1.7 parts in 10^{11}.[1] It appears that even further improvements in precision and accuracy can be expected in the near future.

The frequency of the $(F = 4, m_F = 0) \leftrightarrow (F = 3, m_F = 0)$ transition in cesium has been measured in terms of the Ephemeris Second—the standard unit of time obtained through astronomical observations. This frequency is 9192631770 ± 20 cps (*5*). The probable error, ± 20 cps (or 2×10^{-9}), arises because of experimental limitations on the astronomical measurements and on long distance frequency comparisons. The astronomical data used in arriving at this figure were accumulated over a period of three years. A longer measurement time would reduce the probable error.

[1] Hereafter relative precisions and accuracies shall be written in the form 2×10^{-10}, for example. This has the meaning of 2 parts in 10^{10}.

With this relationship between astronomical time and the hfs separation of cesium, atomic frequency standards together with proper summing devices for counting equally spaced events can now make astronomical time immediately available, although even a temporary lapse in the summing device will irrecoverably lose the epoch at which the count was started. The long delays previously required to determine and publish the corrections to the propagated time signals are no longer necessary. Atomic time is also available with its greater uniformity. On the atomic time scale A.1 introduced by Markowitz (*5*) of the U.S. Naval Observatory, The frequency of cesium is assumed to be 9192631770.0 cps for atomic time. That is, there are that many cycles in one second of atomic time.

The present article deals primarily with cesium atomic beam frequency standards. It is not purported to be an exhaustive review. Its purpose is to provide: (a) some background in atomic beam spectroscopy in view of the fact that the area of atomic beam frequency standards is no longer solely of interest to the physicist,[2] (b) some design considerations of atomic beam standards, and (c) results of comparisons between various cesium standards.

The Introduction is followed by a description of the spectrum upon which the cesium standard is based (Sections II, III, and IV). Section V describes the beam apparatus and the salient features of its design. Section VI is a discussion of the excitation process. Inaccuracies in atomic beam measurements are considered in Section VII. In Section VIII, various cesium standards are compared using radio transmission data. A discussion of various other types of atomic standards and new developments and possibilities in the field is found in Section IX.

II. Atomic Hyperfine Structure

The quantum transitions employed in present day atomic beam standards occur between the hyperfine levels in the ground state of the alkali metal cesium. The hyperfine splitting arises because of the interaction between the magnetic moment of the nucleus and the magnetic field produced by the valence electron at the position of the nucleus. (See Fig. 1.)

The Hamiltonian for this interaction is given by

$$\mathcal{H} = -\boldsymbol{\mu}_I \cdot \mathbf{H}_{el}, \tag{1}$$

where $\boldsymbol{\mu}_I$ is the magnetic dipole moment of the nucleus, and $\mathbf{H}_{el}$ is the magnetic field at the nucleus produced by the electron. For hydrogenlike atoms, $\mathbf{H}_{el}$ can be estimated from some simple semiclassical considerations. The complete discussion is complicated (*9*).

The field at the nucleus has a contribution from both the orbital motion

[2] See also the general references on atomic and molecular beam spectroscopy (*6*, *7*, *8*).

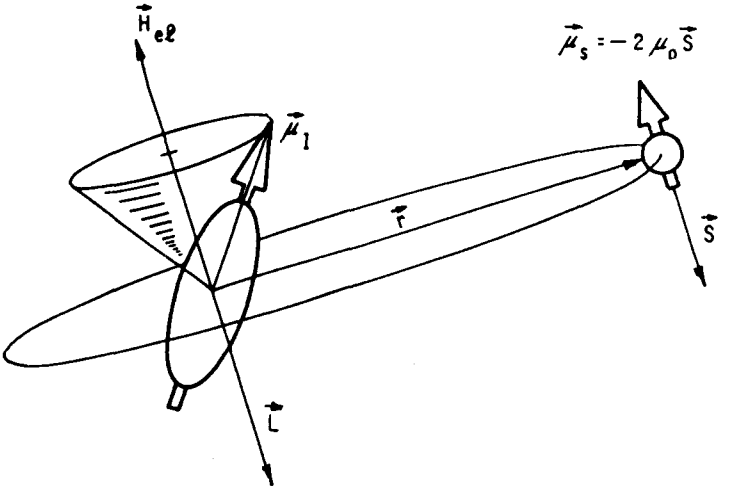

FIG. 1. Pictorial representation of the interaction of the nuclear magnetic moment with the fields produced by the orbital motion and spin of the electron.

of the electron and its intrinsic magnetic moment. Thus

$$\mathbf{H}_{el} = \mathbf{H}_{orbit} + \mathbf{H}_{spin}, \tag{2}$$

where $\mathbf{H}_{orbit}$ is the contribution from the orbital motion, and $\mathbf{H}_{spin}$ is the contribution from the spin moment. From the Biot-Savart Law,

$$\mathbf{H}_{orbit} = -\frac{e}{c}\frac{\mathbf{r}\times\mathbf{v}}{r^3} = -\frac{e}{mc}\frac{\mathbf{r}\times\mathbf{p}}{r^3}$$

or

$$\mathbf{H}_{orbit} = -\frac{e\hbar\mathbf{L}}{mcr^3} = -2\mu_0\frac{\mathbf{L}}{r^3}, \tag{3}$$

where $\mathbf{r}$ is the position vector of the electron relative to the nucleus, $\mathbf{v}$ is the velocity of the electron, $\hbar\mathbf{L}$ is the orbital angular momentum, and $\mu_0 = e\hbar/2mc$ is the Bohr magneton.

The field at the nucleus arising from the intrinsic magnetic moment of the electron can be obtained from the classical expression for the field of a dipole moment $\boldsymbol{\mu}_S = -2\mu_0\mathbf{S}$.

$$\mathbf{H}_{spin} = -\left[\frac{\boldsymbol{\mu}_S}{r^3} - \frac{3\mathbf{r}(\boldsymbol{\mu}_S\cdot\mathbf{r})}{r^5}\right] = \frac{2\mu_0}{r^3}\left[\mathbf{S} - \frac{3\mathbf{r}(\mathbf{r}\cdot\mathbf{S})}{r^2}\right], \tag{4}$$

where $\boldsymbol{\mu}_S$ is the magnetic moment of the electron.

We wish the average value of $\mathbf{H}_{el}$, and it will prove convenient to write this average as

$$\mathbf{H}_{el} = (\mathbf{H}_{el}\cdot\mathbf{J})\frac{\mathbf{J}}{J^2}, \tag{5}$$

463-560 O - 72 - 2

where $\mathbf{J} = \mathbf{L} + \mathbf{S}$. If the sum of (3) and (4) are inserted into (5),

$$\mathbf{H}_{el} = -\frac{2\mu_0}{r^3}[L^2 - S^2 + 3(\mathbf{e}_r \cdot \mathbf{S})\mathbf{e}_r(\mathbf{L} + \mathbf{S})]\frac{\mathbf{J}}{J^2}. \tag{6}$$

The unit vector $\mathbf{e}_r$ is in the direction of $\mathbf{r}$. The vectors $\mathbf{L}$ and $\mathbf{e}_r$ are perpendicular so that (6) becomes

$$\mathbf{H}_{el} = -\frac{2\mu_0}{r^3}[L^2 - S^2 + 3(\mathbf{e}_r \cdot \mathbf{S})^2]\frac{\mathbf{J}}{J^2}. \tag{7}$$

$(\mathbf{e}_r \cdot \mathbf{S})^2$ can be estimated from the vector model: $\mathbf{L}$ and $\mathbf{S}$ precess rapidly about $\mathbf{J}$ in the laboratory frame of reference. Consider the coordinate

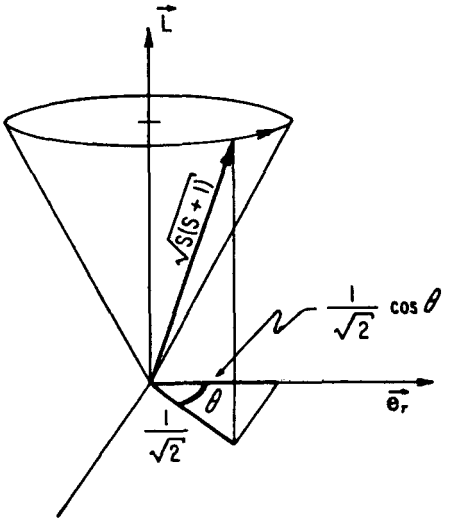

FIG. 2. Coordinate system in which $\mathbf{L}$ and $\mathbf{e}_r$ are fixed.

system in which $\mathbf{L}$ and $\mathbf{e}_r$ are fixed. In this system $\mathbf{S}$ precesses about $\mathbf{L}$ (Fig. 2). For one electron ($S = 1/2$), the average of the square of the projection of $\mathbf{S}$ on $\mathbf{e}_r$ is

$$\overline{(e_r \cdot \mathbf{S})^2} = \frac{1}{2\pi}\int_0^{2\pi}\left(\frac{1}{\sqrt{2}}\cos\theta\right)^2 d\theta = \frac{1}{4}.$$

Using this value for $\overline{(e_r \cdot \mathbf{S})^2}$ and the eigenvalues of L^2, S^2, and J^2 which are $L(L+1)$, $S(S+1)$, and $J(J+1)$ respectively, (1) becomes

$$\overline{\mathbf{H}_{el}} = -\frac{2\mu_0}{r^3}\left[L(L+1) - S(S+1) + \frac{3}{4}\right]\frac{\mathbf{J}}{J(J+1)}.$$

Since we have chosen the particular case for which $S = \frac{1}{2}$,

$$\overline{\mathbf{H}_{el}} = -\frac{2\mu_0}{r^3}\left[\frac{L(L+1)}{J(J+1)}\right]\mathbf{J}.$$

The hyperfine structure interaction is then given by

$$W = \langle J| -\boldsymbol{\mu}_I \cdot \mathbf{H}_{el}|J\rangle = -2g_I\mu_N\mu_0 \left\langle \frac{1}{r^3} \right\rangle \left[\frac{L(L+1)}{J(J+1)}\right] \mathbf{I}\cdot\mathbf{J}, \qquad (8)$$

where g_I is the nuclear g-factor, $\mathbf{I}$ is the nuclear angular momentum vector, and μ_N is the nuclear magneton. $\vec{\boldsymbol{\mu}}_I = g_I\mu_N\mathbf{I}$ and $\mu_N = e\hbar/2Mc = 5.05038 \times 10^{-24}$ erg/gauss where M is the mass of the proton.

The vector model for the hydrogenlike atom (assuming Russell-Saunders coupling) is shown in Fig. 3. It will be helpful in evaluating

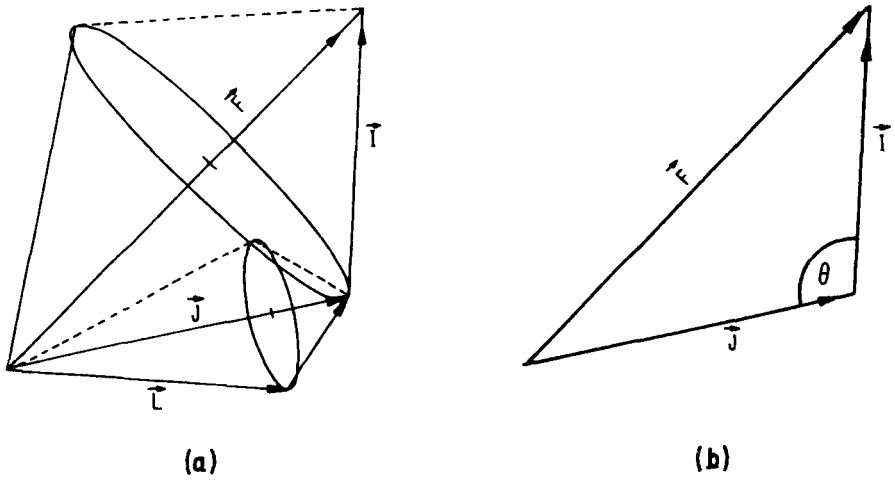

FIG. 3. Vector model for hydrogenlike atom.

$\mathbf{I}\cdot\mathbf{J}$, where $\mathbf{I}$ is the nuclear angular momentum vector, and $\mathbf{F}$ is the total angular momentum vector for the atom. $\mathbf{L}$ and $\mathbf{S}$ precess rapidly about $\mathbf{J}$ because of spin orbit interaction. $\mathbf{J}$ and $\mathbf{I}$ are magnetically coupled to a lesser degree and precess relatively slowly about $\mathbf{F}$. The angle θ of Fig. 3(b) is given by the law of cosines:

$$\cos\theta = \frac{I^2 + J^2 - F^2}{2IJ},$$

so that we may write

$$\mathbf{I}\cdot\mathbf{J} = \frac{1}{2}[I(I+1) + J(J+1) - F(F+1)].$$

Now

$$W = -g_I\mu_N\mu_0 \frac{L(L+1)}{J(J+1)}[I(I+1) + J(J+1) - F(F+1)]\left\langle \frac{1}{r^3} \right\rangle. \qquad (9)$$

The quantity $\langle(1/r^3)\rangle$ can be evaluated from the known wave functions of hydrogenlike atoms. The result is

$$\left\langle \frac{1}{r^3} \right\rangle = \frac{Z^3}{a_0^3 n^3 L(L+1)(L+\frac{1}{2})}, \tag{10}$$

where a_0 is the radius of the first Bohr orbit [$a_0 = (\hbar^2/me^2) = 5.2917 \times 10^{-9}$ cm], n is the principle quantum number, and Z is the charge on the nucleus. Finally,

$$W = \frac{g_I \mu_N \mu_0 Z^3}{a_0^3 n^3} \left[\frac{F(F+1) - I(I+1) - J(J+1)}{J(J+1)(L+\frac{1}{2})} \right]. \tag{11}$$

The various constants can be grouped and written in terms of the Rydberg and the fine structure constants, R_y and α:

$$R_y = \frac{me^4}{4\pi\hbar^3 c} \text{ (cm}^{-1}\text{)},$$

and

$$\alpha = \frac{e^2}{\hbar c}.$$

These have been determined more accurately than the result obtained for each by combining the separate constants. In terms of R_y and α

$$W = \pi\hbar c R_y \alpha^2 \left(\frac{m}{M}\right) \frac{g_I Z^3}{n^3} \left[\frac{F(F+1) - I(I+1) - J(J+1)}{J(J+1)(L+\frac{1}{2})} \right]. \tag{12}$$

Frequently, W is written as

$$W = a\mathbf{I} \cdot \mathbf{J},$$

where

$$a = \frac{2\pi\hbar c R_y \alpha^2 (m/M) g_I Z^3}{J(J+1)(L+\frac{1}{2}) n^3}.$$

It is evident from Eq. (12) that the interaction between the electron and nucleus splits a given electronic state into a number of hyperfine levels. They are designated by the various values of the total angular momentum quantum number F. The separations between the F levels fall in the radio and microwave frequency ranges of the electromagnetic spectrum. F can have the values

$$F = I + J, I + J - 1, I + J - 2, \ldots, I - J$$

if $I \geqq J$ or

$$F = J + I, J + I - 1, \ldots, J - I$$

if $J \geqq I$. The total number of possible F states is $2J + 1$ if $I \geqq J$ and $2I + 1$ if $I \leqq J$. Actually Eq. (12) is not valid for $L = 0$. In this case $\langle(1/r^3)\rangle$ vanishes (*9*). The more sophisticated relativistic caclulation yields the same result as (12) so that Eq. (12) is a valid approximation.

For hydrogen in its ground electronic state, $L = 0$, $J = \frac{1}{2}$, $g_I \approx 5.56$, and $I = \frac{1}{2}$ so that F can have only the two values, 1 and 0. Then, putting numerical values into Eq. (12), the separation between the $F = 1$ and $F = 0$ states is 1417 Mc. The experimental value obtained with atomic beam techniques is 1420.40573 $\pm$ 0.00005 Mc (*10*). More refined calculations yield almost exact agreement with experimental values for the hfs separation in hydrogen and deuterium.

The accurate calculation of the hfs separation for cesium has not been calculated nor is it likely to be in the near future. The large number of electrons, 55, for cesium makes the calculation extremely difficult. The frequency of this hfs separation in cesium is the present standard of frequency. The actual number is assigned with reference to astronomical time.

III. The Vector Model

The vector model is a simple and useful concept for the analysis of the fine and hyperfine structure of atoms in either very weak or very strong externally applied fields. For very precise measurements and for intermediate field conditions more detailed considerations are needed. These will be discussed in Section IV.

A. Weak Magnetic Fields

When the interaction between the spin and orbital motion of the electron is much greater than their interaction energy with the externally applied field, the field is considered weak. The resulting splitting that occurs is referred to as the Zeeman effect of the fine structure. Correspondingly, when the interaction energy between the nuclear moment with the electronic angular momentum is much greater than the interaction with an external field, the field is considered weak. It gives rise to the Zeeman effect of the hyperfine structure (hfs).

Consider an atom with zero nuclear spin. Under weak field conditions $\mathbf{L}$ and $\mathbf{S}$ add vectorially, and the total angular momentum is $\mathbf{J} = \mathbf{L} + \mathbf{S}$. $\mathbf{L}$ and $\mathbf{S}$ are strongly coupled and precess rapidly about $\mathbf{J}$. The vector $\mathbf{J}$, in turn, precesses slowly about the applied magnetic field $\mathbf{H}_0$. A given electronic state will be split into a number of substates. The energies of the various substates relative to the zero field energy are given by the Hamiltonian

$$\mathcal{H} = -\boldsymbol{\mu}_J \cdot \mathbf{H}_0 = g_J \mu_0 \mathbf{J} \cdot \mathbf{H}_0.$$

From the vector model (Fig. 4),

$$\mathbf{J} \cdot \mathbf{H}_0 = JH_0 \cos(\mathbf{J},\mathbf{H}_0) = m_J H_0$$

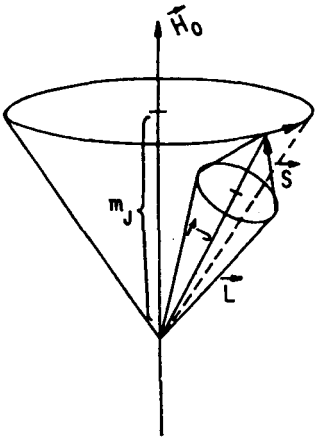

FIG. 4. Vector model of atom with zero nuclear spin.

so that

$$W = g_J \mu_0 m_J H_0, \tag{13}$$

where

$$m_J = J, J-1, \ldots, -J.$$

It is necessary to write g_J in terms of known quantities. It can be written in terms of the known g-factors of the electron, $g_S \approx 2$ and $g_L = 1$. This can be done in the following way. The projection of $\boldsymbol{\mu}_L$ and $\boldsymbol{\mu}_S$ on the direction of **J** is

$$|\boldsymbol{\mu}_J| = g_J \mu_0 J = g_L \mu_0 L \cos(\mathbf{L},\mathbf{J}) + g_S \mu_0 S \cos(\mathbf{S},\mathbf{J}).$$

Then

$$g_J = \frac{1}{J}[g_L L \cos(\mathbf{L},\mathbf{J}) + g_S S \cos(\mathbf{S},\mathbf{J})].$$

Using the law of cosines and the vector model in addition to the quantum mechanical equivalents of S^2, L^2, and J^2, we have

$$g_J = \left\{ g_L \left[\frac{J(J+1) + L(L+1) - S(S+1)}{2J(J+1)} \right] + g_S \left[\frac{J(J+1) + S(S+1) - L(L+1)}{2J(J+1)} \right] \right\}. \tag{14}$$

This expression for g_J, together with Eq. (13), gives the eigenvalues of the Hamiltonian when Russell-Saunders coupling applies. The important selection rules for transitions between sublevels of a given J and sublevels belonging to different J are $\Delta J = 0, \pm 1$ and $\Delta m_J = 0, \pm 1$.

Now suppose that the nucleus has a spin I different from zero. The vector model is shown in Fig. 3 and described in Section II page 6. **I** and **J** precess about **F**, and **F** precesses relatively slowly about the small field $\mathbf{H}_0$.

The portion of the total Hamiltonian of interest is

$$\mathcal{H} = a\mathbf{I} \cdot \mathbf{J} + g_F \mu_0 \mathbf{F} \cdot \mathbf{H}_0. \tag{15}$$

A quadrupole term is not included because we will confine ourselves to the case where $J = \frac{1}{2}$. For this case, the quadrupole term will not affect the state separations. The first term in Eq. (15) is the hfs interaction in zero field. It has been considered in Section II. The second term gives the splitting of the various possible F states in the weak field $\mathbf{H}_0$. Within the present approximation, the relative energies of the substates for a given F are

$$W_F = g_F \mu_0 m_F H_0. \tag{16}$$

The quantity g_F may be written in terms of g_J and g_I just as g_J had been previously written in terms of g_S and g_L.

From the vector model

$$g_F = \frac{1}{F} [g_J J \cos(\mathbf{J}, \mathbf{F}) - g_I I \cos(\mathbf{I}, \mathbf{F})]$$

and

$$g_F = g_J \left[\frac{F(F+1) + J(J+1) - I(I+1)}{2F(F+1)} \right] + g_I \left[\frac{F(F+1) + I(I+1) - J(J+1)}{2F(F+1)} \right]. \tag{17}$$

Equations (16) and (17) give a rather good quantitative estimate of the splitting in weak fields.

Let us consider the case when $J = \frac{1}{2}$—atoms in $^2S_{1/2}$ and $^2P_{1/2}$ states, for example. There are only two hyperfine levels—$F = I + \frac{1}{2}$ and $F = I - \frac{1}{2}$. Let these two values of F be designated by F_+ and F_-, respectively. The g-factors for these two levels are:

$$g_{F_+} = \left(\frac{1}{2I+1} \right) g_J + \left(\frac{2I}{2I+1} \right) g_I, \tag{18a}$$

and

$$g_{F_-} = -\left(\frac{1}{2I+1} \right) g_J + \left(\frac{2I+2}{2I+1} \right) g_I. \tag{18b}$$

Note that the g_F values are slightly different for the two values of F. The splitting in the two F levels in a weak field will then be slightly different. The energy level diagram may be drawn using Eqs. (16) and (18).

The diagram for cesium is shown in Fig. 5. The ground electronic state is $^2S_{1/2}$ so that $J = \frac{1}{2}$; the nuclear spin of cesium-133 is $\frac{7}{2}$. The best value

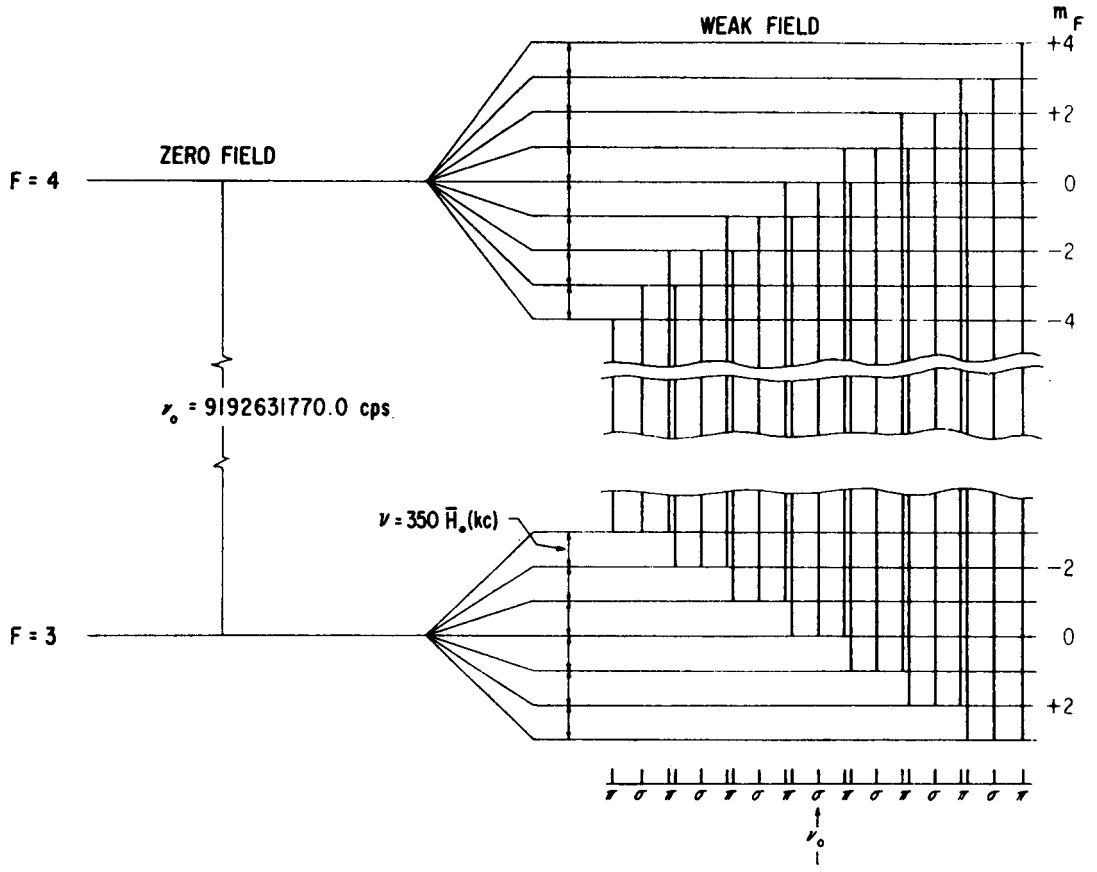

FIG. 5. Energy level diagram for Cs^{133}. The nuclear moment is positive, $I = 7/2$, and $J = 1/2$. The selection rules are $\Delta F = 0, \pm 1$; $\Delta m_F = 0, \pm 1$.

of g_I is obtained from the measured value of the magnetic moment of the cesium-133 nucleus:

$$\mu_{Cs} = +2.57887 \text{ in units of the nuclear magneton } \mu_N;$$

$$g_I = \frac{-(\text{magnetic moment in units of } \mu_N)}{(\text{angular momentum in units of } \hbar)},$$

$$g_I = -0.737.$$

In units of the Bohr magneton,

$$g_I = -0.737 \frac{m}{M} = -4.01 \times 10^{-4}.$$

Since Eq. (16) was written in terms of the Bohr magneton μ_0, these are the units of g_I that must be used.

The sequence of m_F states is inverted in the $F = 3$ level with respect to that in the $F = 4$ level as a result of the minus sign of the first term of Eq. (18b). The $F = 4$ level is higher than the $F = 3$ level. This can be seen

from the following considerations. The magnetic moment associated with the angular momentum **J** is antiparallel to **J**. The magnetic moment of the nucleus is parallel to **I** in the case of cesium (the usual circumstance). If **I** is parallel to **J**, the magnetic moments are antiparallel and the energy of interaction is evidently greater than if **I** is antiparallel to **J**. Thus when g_I is negative (and μ_I positive), the state $F = I + \frac{1}{2}$ lies above the state $F = \mathrm{I} - \frac{1}{2}$.

The closely spaced doublets appearing in Fig. 5—of which there are six—have a separation

$$\Delta\nu_{\text{doublet}} = \frac{\mu_0 H_0}{h}[2g_I] \sim 1.1 \times 10^3 \text{ sec}^{-1} \text{ gauss}^{-1},$$

which is a very small frequency separation at the field intensities normally used in atomic frequency standards (~0.010–0.100 oe). The transition $(F = 4, m_F = 0) \leftrightarrow (F = 3, m_F = 0)$ is chosen as the standard frequency transition because it is insensitive to the magnetic field. In fact, in the vector model approximation it is completely insensitive to the field. A more exact treatment shows a small quadratic field dependence of the transition frequency, as we shall see. The field sensitive lines provide a useful measure of the uniform field of the beam standard.

B. Strong Magnetic Fields

The vector model also provides a good approximation under conditions of very strong fields. The external field is said to be strong when the interaction energy between the nuclear moment and the electronic angular momentum is much less than the coupling with the field. Under these conditions **I** and **J** decouple and precess independently about the field direction (Fig. 6). The Hamiltonian is given by

$$\mathcal{H} = a\mathbf{I} \cdot \mathbf{J} + g_J\mu_0\mathbf{J} \cdot \mathbf{H}_0 + g_I\mu_N\mathbf{I} \cdot \mathbf{H}_0. \tag{19}$$

In this case the first term is not large compared with the other terms.

In the strong-field approximation $\mathbf{I} \cdot \mathbf{J}$ can be evaluated from the vector model (Fig. 6): **J** precesses much more rapidly about $\mathbf{H}_0$ than does **I**. We may then consider the average value of **J**—which is its component along $\mathbf{H}_0$—as interacting with **I**. Thus,

$$\mathbf{I} \cdot \mathbf{J} = IJ \cos(\mathbf{J}, \mathbf{H}_0) \cos(\mathbf{I}, \mathbf{H}_0),$$

and

$$\mathbf{I} \cdot \mathbf{J} = m_I m_J.$$

The energy eigenvalues are then given by

$$W = am_I m_J + g_J\mu_0 m_J H_0 + g_I\mu_N m_I H_0 \tag{20}$$

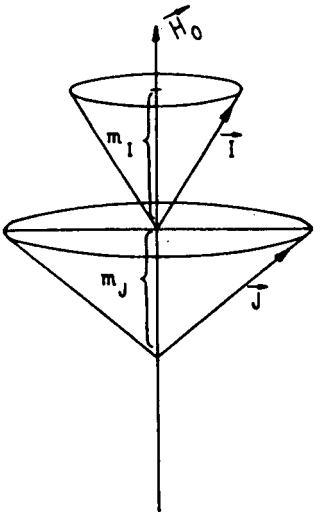

FIG. 6. Vector model of atom in strong magnetic field.

in very strong fields. This relation is a rather good approximation for cesium for fields greater than about 5000 oe.

IV. THE BREIT-RABI FORMULA (*7, 11*)

The vector model does not give an estimate of the energy separations in intermediate fields nor does it give a close enough approximation in weak and strong fields for precise beam experiments. The energy levels in any external magnetic field can be determined from the Hamiltonian:

$$\mathcal{H} = a\mathbf{I}\cdot\mathbf{J} + \mu_0 g_J \mathbf{J}\cdot\mathbf{H}_0 + \mu_0 g_I \mathbf{I}\cdot\mathbf{H}_0 + \frac{b[3(\mathbf{I}\cdot\mathbf{J})^2 + \tfrac{3}{2}\mathbf{I}\cdot\mathbf{J} - \mathbf{I}^2\mathbf{J}^2]}{2I(2I-1)J(2J-1)}. \quad (21)$$

The last term is due to the interaction between the electric quadrupole moment of the nucleus and the electronic charge distribution. There will be no quadrupole interaction in the case $J = \frac{1}{2}$ where the electronic charge distribution is spherically symmetric. This is the case that applies to existing atomic beam standards, and this is the only case that we will consider.

For $J = \frac{1}{2}$ it is necessary to diagonalize the secular determinant associated with the Hamiltonian

$$\mathcal{H} = a\mathbf{I}\cdot\mathbf{J} + \mu_0 g_J \mathbf{J}\cdot\mathbf{H}_0 + \mu_0 g_I \mathbf{I}\cdot\mathbf{H}_0.$$

The solutions are

$$W_{F=I\pm\frac{1}{2},\,m_F} = \frac{-\Delta W}{2(2I+1)} + \mu_0 g_I m_F H_0 \pm \frac{\Delta W}{2}\left[1 + \frac{4m_F x}{(2I+1)} + x^2\right]^{\frac{1}{2}}. \quad (22)$$

ΔW is the hfs separation in zero field ($\Delta W = h\nu_0$) between the states $F = I + \frac{1}{2}$ and $F = I - \frac{1}{2}$;

$$x = \frac{(g_J - g_I)\mu_0 H_0}{\Delta W}.$$

In accordance with the usual convention, the quantum numbers F and m_F are used with the understanding that at high fields these are the quantum numbers of the state from which the high field state is adiabatically derived. Equation (22) is called the Breit-Rabi formula, first given by Breit and Rabi in 1931 (*12*).

The energy level scheme is shown in Fig. 5 for weak applied magnetic fields. The transition most insensitive to the field is the $(F = 4, m_F = 0) \leftrightarrow (F = 3, m_F = 0)$ transition. The slight field dependence of the frequency of this transition is given by the Breit-Rabi formula, Eq. (22). Assuming small H_0:

$$\nu = \nu_0 + \frac{\nu_0}{2} x^2 - \frac{\nu_0}{8} x^4 + \cdots$$

Introducing the x-value for Cs^{133},

$$\nu = \nu_0 + 427.18 H_0^2 - 9.93 \times 10^{-6} H_0^4, \tag{23}$$

where ν is in cps and H_0 in oersted. The term involving H_0^4 is entirely negligible since H_0 falls in the range 0.1 to 0.01 oe for most cesium beam standards.

Equation (23) gives the zero field hfs separation ν_0 from the measured frequency ν after the value of H_0 is determined. The field H_0 can be easily evaluated by measuring any of the other observable transitions. For example, the microwave transitions ($\Delta F = \pm 1$, $\Delta m_F = 0$) for which

$$\begin{aligned} \nu_{(F=4,m_F)\leftrightarrow(F=3,m_F)} &= \nu_0 \left[1 + \frac{m}{4} x + \frac{1}{2}\left(1 - \frac{m_F^2}{16}\right) x^2 \right] \\ &= \nu_0 + 7.0062 \times 10^5 m_F H_0 + 26.699(16 - m_F^2) H_0^2. \end{aligned} \tag{24}$$

The very low frequency transitions between the sublevels of a given F state ($\Delta F = 0$, $\Delta m_F = \pm 1$) can also be used. In this case

$$\begin{aligned} \nu_{3,m_2\leftrightarrow 3,m_1} &= \frac{-\mu_0 g_I}{h} H_0 + \frac{\nu_0}{2}\left[\frac{1}{4} x - \frac{1}{32}(2m_1 - 1) x^2 \right] \\ &= 350.870 \times 10^3 H_0 - 13.349(2m_1 - 1) H_0^2, \end{aligned} \tag{25}$$

or

$$\begin{aligned} \nu_{4,m_2\leftrightarrow 4,m_1} &= \frac{\mu_0 g_I}{h} H_0 + \frac{\nu_0}{2}\left[\frac{1}{4} x - \frac{1}{32}(2m_1 + 1) x^2 \right] \\ &= 349.746 \times 10^3 H_0 - 13.349(2m_1 + 1) H_0^2. \end{aligned} \tag{26}$$

The magnetic quantum number m_1 is associated with the lower of the two substates involved in the transition. For the small values of H_0 ordinarily

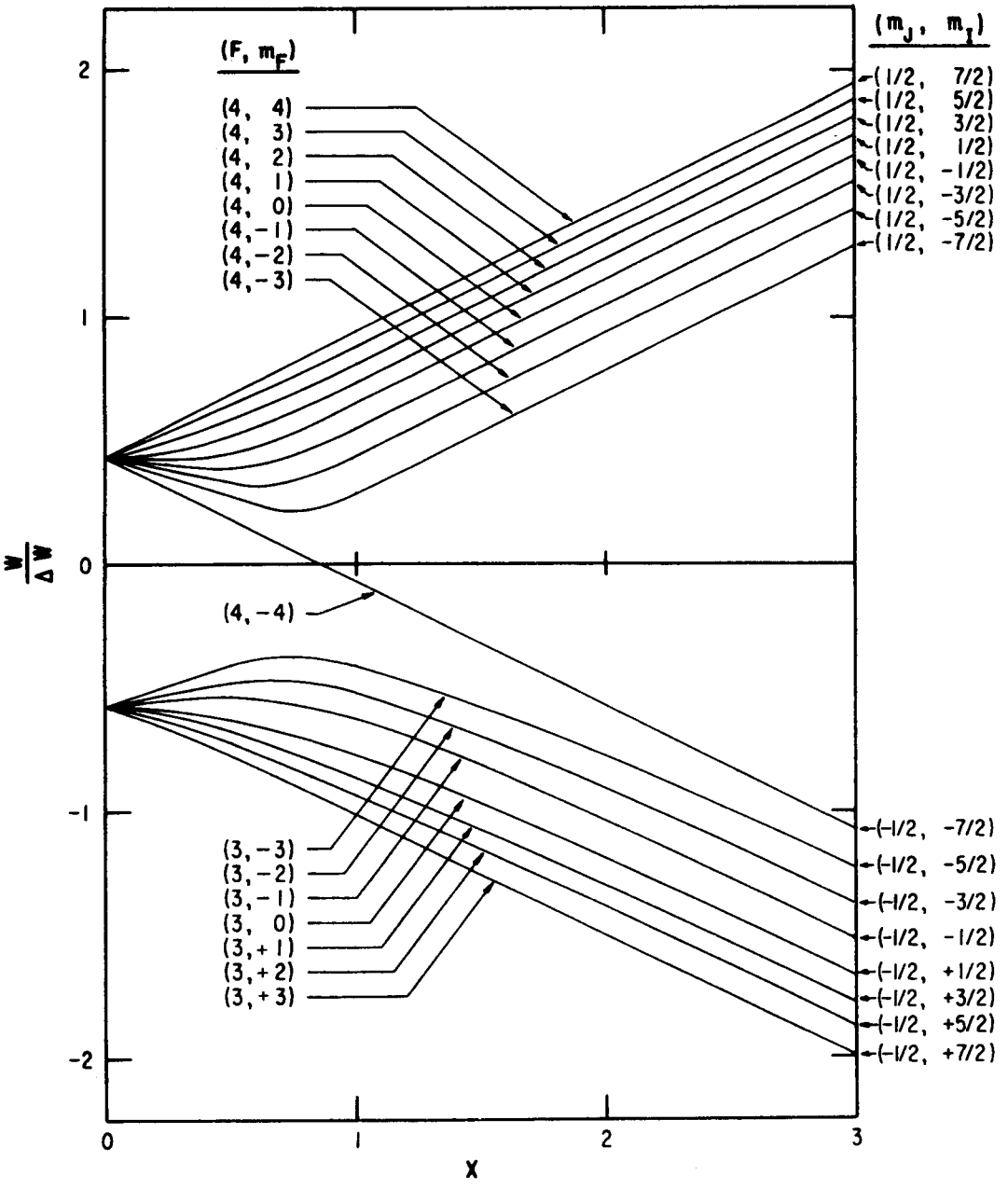

FIG. 7. Energy level diagram of Cs^{133} in the $^2S_{1/2}$ ground state as a function of the applied magnetic field. The hfs separation is $\Delta W = h\nu_0$.

used, all of the transitions of Eqs. (25) and (26) coincide at least for the practical purpose of measuring H_0.

Figure 7 shows a plot of the energy levels as H_0 varies from zero to very large values. The vector model applies in the extreme left hand and right hand sides of the graph. Equation (22) must be used for intermediate points.

V. The Atomic Beam Spectrometer

The frequencies of separation between the hfs levels in atomic spectra can be measured very precisely by means of atomic beam techniques. A schematic of a typical spectrometer used in atomic beam resonance experiments is shown in Fig. 8a, b. Many variations in design exist depending on the nature of the atom to be investigated. The design that will be discussed

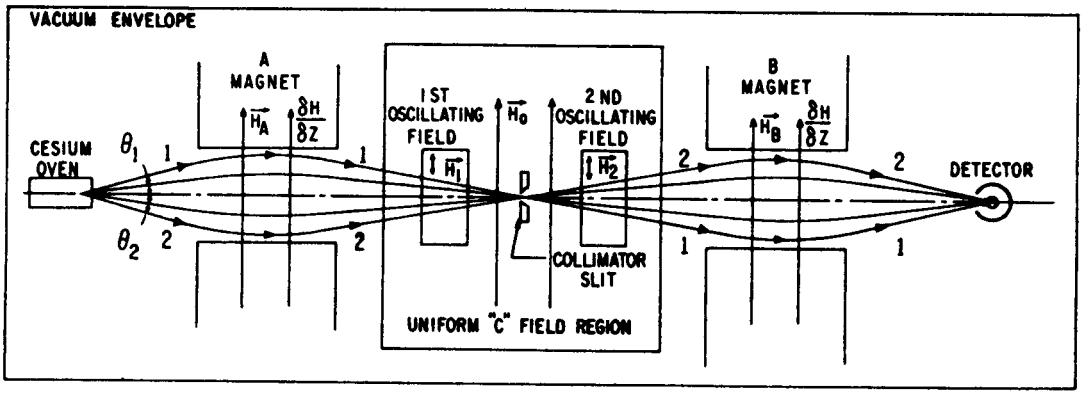

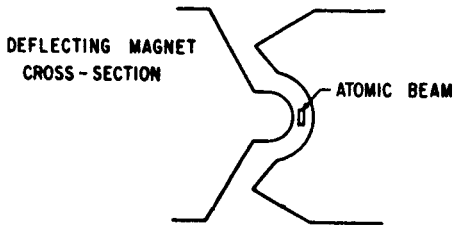

(a)

FIG. 8a. A schematic of a typical atomic beam spectrometer. The indicated trajectories are for atoms that make transitions.

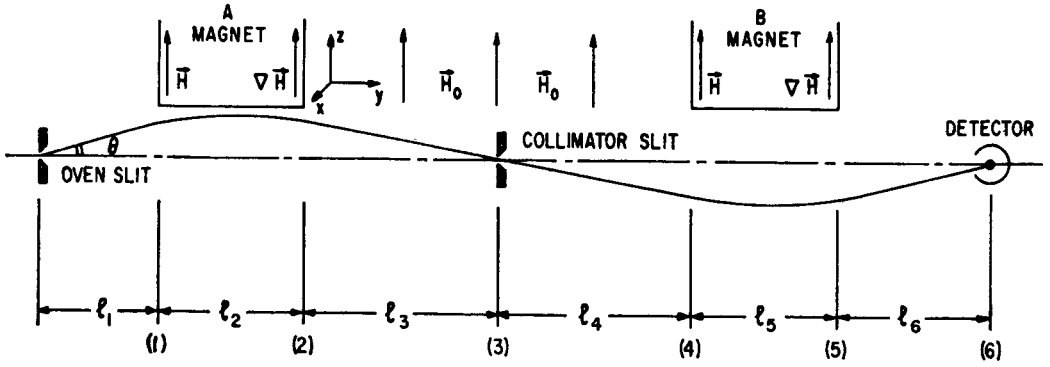

(b)

FIG. 8b. The trajectory of a single atom leaving the source at an angle θ and with a particular speed v.

here applies particularly to the longer of the two National Bureau of Standards cesium beam frequency standards (when specific numbers are given).

Neutral atoms effuse from the oven at the left in Fig. 8 and pass through the nonuniform magnetic field of the A deflecting magnet. The atoms have a magnetic dipole moment and consequently transverse forces act upon them in this nonuniform field. The magnitude and direction of this force depends upon which of the states a particular atom is in. Of all the atoms effusing from the oven at angle θ_1 and speed v suppose those in the upper group of levels of Fig. 8 (electron spin "up", or $m_J = +\frac{1}{2}$)[3] have their trajectories bent toward the axis and follow the path 1. All atoms in the lower group of levels (electron spin "down", or $m_J = -\frac{1}{2}$)[3] effusing at an angle $\theta_2 = -\theta_1$ with speed v will have their trajectories bent toward the axis also and follow a trajectory along path 2. Note that the atoms in the upper group of levels are subject to forces that are opposite in direction to the forces on atoms in the lower group—their moments have opposite sign.

The spin "up" atoms traversing the trajectory 1 and the spin "down" atoms traversing the trajectory 2 will cross the axis at the collimator slit, pass through the slit and enter the region of the B deflecting magnet. The B magnetic field is exactly like that of the A magnet. Consequently, the transverse forces of the atoms will be the same as in the A magnetic field. The spin "up" atoms will experience a downward force as before and the spin "down" atoms will experience an upward force, as before. However, now the atoms have crossed the center line at the collimator slit and the forces will tend to make the trajectories diverge from the center line. If, however, a radiation field is applied in the uniform C field region between the A and B magnets of frequency

$$\nu = \nu_0 + 427H_0^2,$$

transitions will take place between the states ($F = 4$, $m_F = 0$) and ($F = 3$, $m_F = 0$). The magnetic moments will be flipped. Atoms in the upper state will be induced to emit, and atoms in the lower state will absorb a quantum of energy—with a certain probability. Thus the sign of the magnetic moment will change for all atoms undergoing a transition. Consequently, the forces on these atoms will be opposite in the B magnet's field to what they were in the A magnet's field and they will be refocused unto the axis at the detector.

As the frequency of the exciting radiation is swept through ν, the detected signal will increase and reach a maximum at frequency ν and then decrease as the radiation frequency is varied beyond ν.

[3] It is assumed that the deflecting fields are strong fields for the purpose of qualitative discussion.

A. *Atomic Trajectories (6, 7)*

The atomic trajectories and deflections can be calculated rather simply for the elementary field configurations ordinarily used in the deflecting fields of atomic beam machines. The energy W of the atom is given by the Breit-Rabi formula, Eq. (22). This energy is a function of the magnitude of the field intensity H. The fields of the deflection magnets are conservative so that the force on the atom is given by[4]

$$\mathbf{F} = -\nabla W. \tag{27}$$

This can be rewritten as

$$\mathbf{F} = -\frac{\partial W}{\partial H}\nabla H, \tag{28}$$

provided that the only dependence of W on position is through the spatial variation of the magnetic field intensity H. $\mathbf{F}$ is different from zero only when the field has a gradient different from zero, i.e., when the field is nonuniform.

The partial derivative, $-\partial W/\partial H$, is called the effective magnetic dipole moment μ_{eff}. The effective dipole moment has, in general, a different value for each state:

$$\mu_{eff} = \mu_{F=I\pm\frac{1}{2},m_F}$$
$$= -g_I\mu_0 m_F \mp \left\{\frac{(x/2) + m_F/(2I+1)}{[1 + 4m_F/(2I+1) + x^2]^{\frac{1}{2}}}\right\}\mu_0(g_J - g_I) \tag{29}$$

for atoms with $J = \frac{1}{2}$. Note that μ_{eff} is a function of H. The magnetic moments given by Eq. (29) are plotted in Fig. 9 for cesium as a function of H (or x).

Equation (*28*) can be conveniently written as

$$\mathbf{F} = \mu_{eff}\nabla H. \tag{30}$$

The A and B deflecting magnets are designed such that the field configuration has a simple calculable form,[5] and so that the force has the components

$$F_x = 0,$$
$$F_y = 0,$$

and

$$F_z = \mu_{eff}\frac{\partial H}{\partial z} = \text{constant},$$

[4] Here $\mathbf{F}$ is the force vector and is not to be confused with the previous $\mathbf{F}$ which represented the total angular momentum vector.

[5] We consider here the field of two parallel wires with currents of equal magnitude flowing in the opposite direction. The fields themselves will be discussed more fully later.

within a reasonable approximation. Then

$$\ddot{z} = a = \frac{\mu_{eff}}{m}\frac{\partial H}{\partial z}, \tag{31}$$

where a is the acceleration imparted to the atom in the direction transverse to the axis of the spectrometer, and m is the mass of the atom. We choose the coordinate system where z is positive above the axis and negative below (Fig. 8b).

The acceleration a is different from zero only in the regions 2 and 5 where the field in nonuniform. Integration of Eq. (31) yields

$$\dot{z} = v_z = v_{zi} + a_i t \tag{32}$$

and

$$z = z_i + v_{zi}t + \tfrac{1}{2}a_i t^2, \tag{33}$$

where v_{zi} is the transverse velocity that the atom has as it enters the ith region, z_i is the z-coordinate of the particle as it enters this region, and t is the time spent in this region.

Atoms effuse from the source slit in all forward directions. Consider atoms emitted from the source with speed v and at an angle θ with respect to the center line of the machine. It is of interest to calculate the z-coordinate of these atoms at each of the y positions (1) through (6) (see Fig. 8b). The transverse velocity in region (1) is[6]

$$v_{z1} = v \sin\theta \approx v\theta$$

and the z-coordinate in plane (1) is

$$z_1 = v_{z1}t_1 = \theta l_1,$$

where $t_1 = (l_1/v)$.
The z-coordinate in plane (2) is given by

$$z_2 = z_1 + v_{z1}t_2 + \tfrac{1}{2}a_2 t_2^2,$$

where $t_2 = l_2/v$, so that

$$z_2 = (l_1 + l_2)\theta + \frac{1}{2}\frac{a_2 l_2^2}{v^2}.$$

Correspondingly,

$$z_3 = z_2 + v_{z2}t_3,$$

or

$$z_3 = (l_1 + l_2 + l_3)\theta + \frac{a_2 l_2(l_2 + 2l_3)}{2v^2};$$

$$z_4 = z_3 + v_{z2}t_4$$

[6] The angle θ will be very small for any atom that reaches the detector plane without collision. Hence $\sin\theta \approx \theta$ is a good approximation.

or

$$z_4 = (l_1 + l_2 + l + l_4)\theta + \frac{a_2 l_2}{2v^2}(l_2 + 2l_3 + 2l_4);$$

$$z_5 = z_4 + v_{z2}t_5 + \tfrac{1}{2}a_5 t_5^2$$

or

$$z_5 = (l_1 + l_2 + l_3 + l_4 + l_5)\theta + \frac{a_2 l_2}{2v^2}(l_2 + 2l_3 + 2l_4 + 2l_5) + \frac{a_5 l_5^2}{2v^2};$$

$$z_6 = z_5 + v_{z5}t_6$$

or

$$z_6 = (l_1 + l_2 + l_3 + l_4 + l_5 + l_6)\theta + \frac{a_2 l_2}{2v^2}(l_2 + 2l_3 + 2l_4 + 2l_5 + 2l_6) + \frac{a_5 l_5}{2v^2}(l_5 + 2l_6).$$

In order for an atom to pass through the collimating slit, z_3 must be zero. This imposes a condition on θ. In particular,

$$\theta = -\frac{a_2 l_2(l_2 + 2l_3)}{2v^2(l_1 + l_2 + l_3)}.$$

The displacement from the center line in the detector plane is then

$$z_6 = \frac{a_2 l_2(l_2 + 2l_1)(l_4 + l_5 + l_6)}{2v^2(l_1 + l_2 + l_3)} + \frac{a_5 l_5(l_5 + 2l_6)}{2v^2}.$$

From Fig. 9 it is evident that if a transition is induced for which $\Delta F = \pm 1$ and $\Delta m_F = 0$, the magnitude of the magnetic moment of the atom remains the same but the sign of the moment changes. Thus for this type of transition the forces would be equal but oppositely directed in regions (1) and (5) if

$$\left(\frac{\partial H}{\partial z}\right)_2 = \left(\frac{\partial H}{\partial z}\right)_5.$$

Hence a symmetrical apparatus would give a refocused beam at the detector wire. More specifically, if

$$l_1 = l_6,$$

$$l_2 = l_5,$$

$$l_3 = l_4,$$

and

$$\left(\frac{\partial H}{\partial z}\right)_2 = \left(\frac{\partial H}{\partial z}\right)_5,$$

463-560 O - 72 - 3

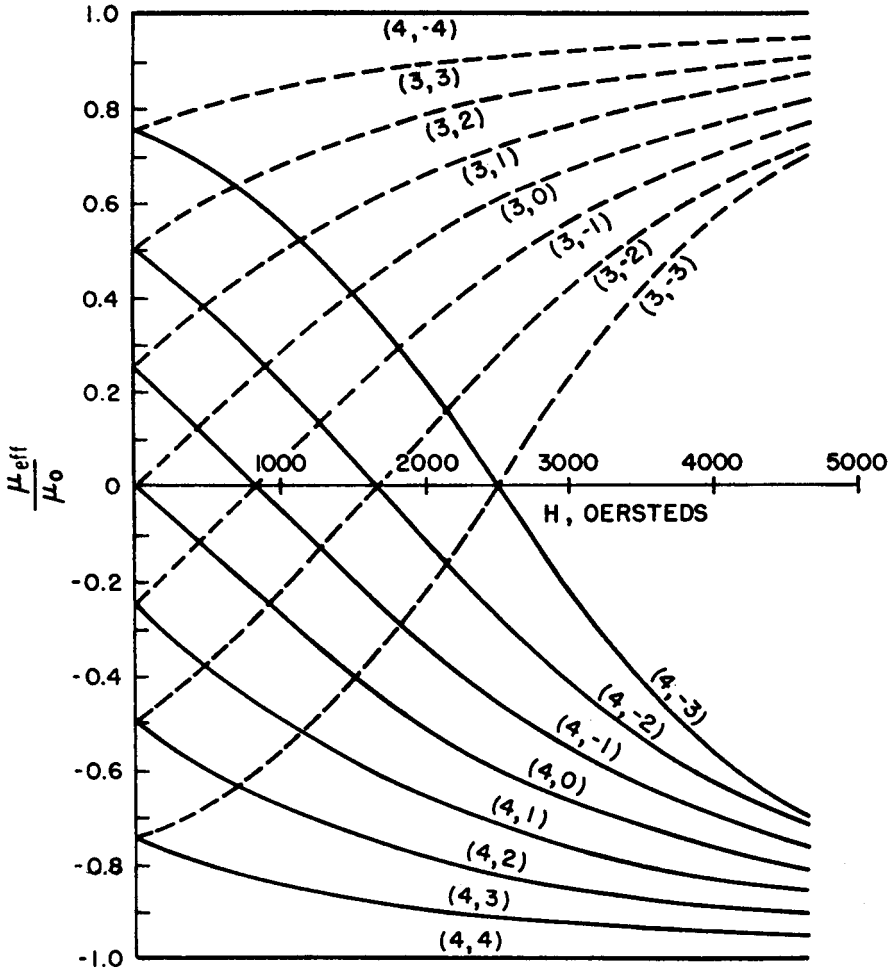

FIG. 9. The effective magnetic moment, μ_{eff}, relative to the Bohr magneton, μ_0, is plotted for the various magnetic substates in Cs^{133} as a function of the applied magnetic field.

then

$$z_6 = \frac{l_5(l_5 + 2l_6)}{2mv^2} [(\mu_{eff})_2 + (\mu_{eff})_5] \frac{\partial H}{\partial z}. \tag{34}$$

When a transition $\Delta F = \pm 1$, $\Delta m_F = 0$ is induced, $(\mu_{eff})_2 = -(\mu_{eff})_5$ and $z_6 = 0$ as described above.

Introducing some numbers, let

$$l_1 = l_6 = 24 \text{ cm},$$
$$l_2 = l_5 = 10 \text{ cm},$$
$$l_3 = l_4 = 100 \text{ cm},$$

and

$$\left(\frac{\partial H}{\partial z}\right)_2 = \left(\frac{\partial H}{\partial z}\right)_5 = 6800 \text{ oe/cm}$$

for a field at the position of the beam in the deflecting magnets of 2100 oe. For this particular value of the field intensity, $\mu_{eff} = 0.50 \times 10^{-20}$ erg/gauss. If the oven temperature is 150°C, the most probable velocity α of a cesium atom in the oven is 2.3×10^4 cm/sec and

$$z_6 = \frac{580}{4kT} [2\mu_{eff}] \frac{\partial H}{\partial z} = 0.17 \text{ cm}.$$

Although a symmetrical device is not the most suitable for observing the $\Delta F = 0$, $\Delta m_F = \pm 1$ transitions, these transitions are easily observed and they provide a useful measure of the magnitude of the uniform C field. The C field is essential in beam experiments in order to preserve the state identity of the atom as it progresses through the apparatus. All of the magnetic fields are arranged to have the same direction so that at no time will an atom in the beam pass through a region of zero field. This avoids the occurrence of nonadiabatic transitions or Majorani flop.

B. The Beam Intensity and Intensity Distribution (6, 7)

Evidently, from Eq. (34), the point at which an atom crosses the detector plane depends upon its velocity and its substate. Consider first the case when no forces are applied to the atoms of the beam, that is, when the deflecting magnets are switched off. The number of atoms striking the detector per unit time with velocities in the range v to $v + dv$ is given approximately by

$$dN = \frac{N_0 a A}{r^2} \left(\frac{m}{2\pi kT}\right)^{3/2} v^3 \exp\left(\frac{mv^2}{2kT}\right) dv. \tag{35}$$

This can be rewritten as

$$dN = I(v)dv = \frac{2I_0}{\alpha^4} v^3 \exp\left(-\frac{v^2}{\alpha^2}\right) dv, \tag{36}$$

where

$$I_0 = \frac{N_0 a A \bar{c}}{4\pi r^2} \tag{37}$$

is the total number of atoms striking the detector per unit time, N_0 is the number of atoms per unit volume in the oven, a is the oven slit area, A is the area of the detector, r is the total distance between the oven slit and the detector, $\bar{c}$ is the average speed of an atom inside the oven ($\bar{c} = \sqrt{8kT/\pi m}$), and α is the most probable speed inside the oven ($\alpha = \sqrt{2kT/m}$).

Equation (36) may be re-expressed in terms of the magnetic deflection: Let z_6 be designated as s_α when $v = \alpha$ and s otherwise so that

$$s_\alpha = \frac{2(\mu_{\text{eff}})_2}{2m\alpha^2}\left(\frac{\partial H}{\partial z}\right)_2 l_5(l_5 + 2l_6)$$

and

$$s = \frac{2(\mu_{\text{eff}})_2}{2mv^2}\left(\frac{\partial H}{\partial z}\right)_2 l_5(l_5 + 2l_6).$$

Evidently,

$$\frac{s}{s_\alpha} = \frac{\alpha^2}{v^2}$$

and

$$dN = I(s)ds = -I_0 \exp\left(-\frac{s_\alpha}{s}\right)\frac{s_\alpha^2}{s^3}\,ds \tag{38}$$

if the width of the parent beam is small compared to s.

Calculation of the actual intensity distribution must take into account the finite width of the beam. Figure 10 shows the trapezoidal beam shape

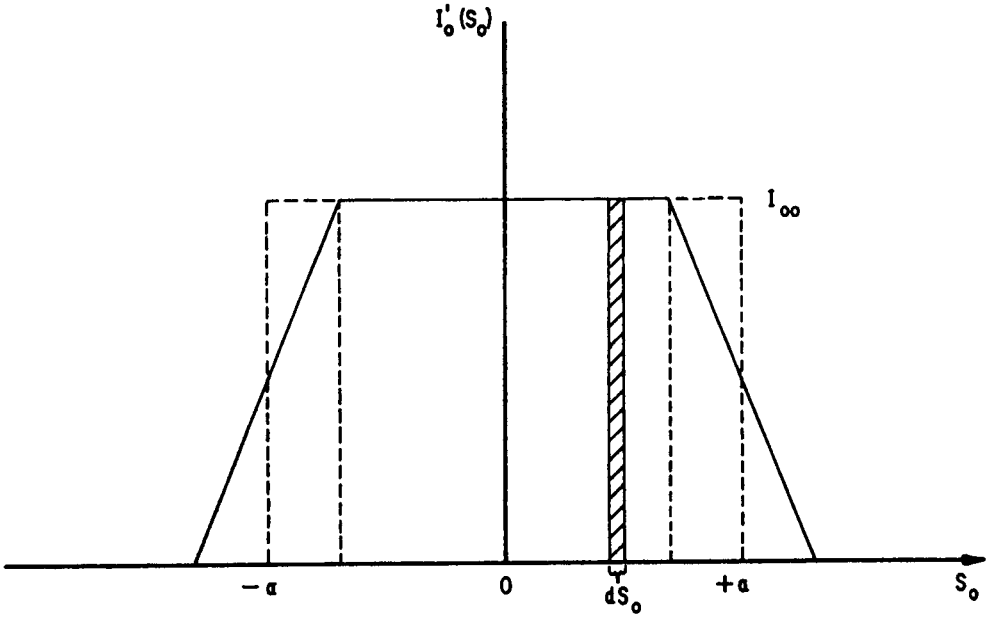

FIG. 10. Beam profile without deflection at the detector plane.

at the detector plane without deflection. The refocused beam would have the same shape if only atoms undergoing a moment change in the radiation field were considered.

Considering the finite width of the beam, the magnetic deflection is $s - s_0$ and

$$\frac{v^2}{\alpha^2} = \frac{s_\alpha}{s - s_0}.$$

Then the contribution to the intensity at s due to the infinitesimal width ds_0 at s_0 of the parent beam is given by

$$dI(s) = I_0'(s_0) \frac{s_\alpha^2}{(s - s_0)^3} \exp\left(-\frac{s_\alpha}{s - s_0}\right) ds_0, \tag{39}$$

where $I_0'(s_0)$ is the total number of atoms incident per second on the detector per unit width at the point s_0. If w is the width of the detector,

$$\int_{-w/2}^{+w/2} I_0'(s_0) ds_0 = I_0, \text{ approximately,}$$

where I_0 is given by Eq. (37).

In Eq. (39), $s - s_0$ must always have the same sign as s_α. When $s - s_0$ has the opposite sign from s_α there is no contribution at s and $dI(s) = 0$. Rather than introduce the trapezoidal shape of the undeflected beam into Eq. (39), it is usually sufficient to consider the equivalent rectangular beam shape of width $2a$ (Fig. 10). Integration of Eq. (39) yields

$$I(s) = I_{00}\left[\exp\left(-\frac{s_\alpha}{s+a}\right)\left(1 + \frac{s_\alpha}{s+a}\right) - \exp\left(-\frac{s_\alpha}{s-a}\right)\left(1 + \frac{s_\alpha}{s-a}\right)\right] \tag{40a}$$

for $s \geqq a$,

$$I(s) = I_{00}\left[\exp\left(-\frac{s_\alpha}{s+a}\right)\left(1 + \frac{s_\alpha}{s+a}\right)\right] \tag{40b}$$

for $-a \leqq s \leqq a$, and

$$I(s) = 0 \tag{40c}$$

for $s \leqq -a$. These equations apply when s_α is positive. The intensity distribution is (ideally) symmetrical about $s = 0$.

Figure 11 shows the intensity distribution for various values of s_α. It is evident from the curves that the maximum intensity occurs at a point considerably less than s_α. The probability of an atom emerging from the source slit is proportional to the velocity. Consequently, the most probable velocity in the beam is somewhat greater than the most probable velocity in the oven. In fact, the most probable velocity in the beam is $\sqrt{3/2}\alpha = 1.22\alpha$. The deflection of atoms in the beam will generally be less than s_α. The values of $|s|$ at the maxima of the curves occur at about $|s_\alpha|/3$ for large s_α ($s_\alpha \sim 10a$ or greater).

In the case of cesium, the beam is composed of atoms in 16 different states. A different μ_{eff} and s_α is associated with each state. The observed intensity distribution is then the composite of all of these separate intensity distributions. All of the separate distributions have approximately equal

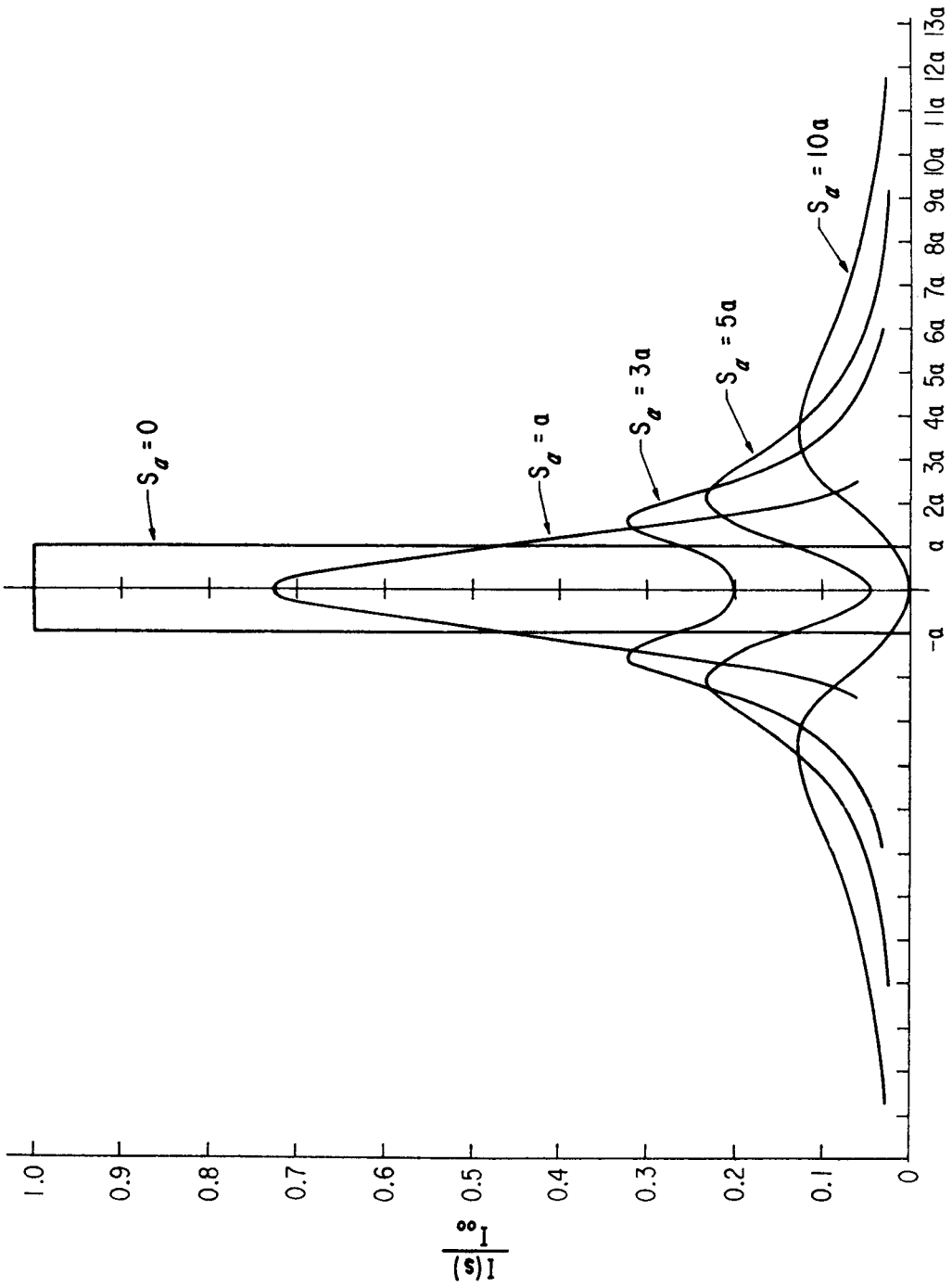

FIG. 11. The intensity distribution of the deflected beam for various values of s_a.

weight. The total intensity distribution is experimentally plotted by simply moving the detector transversely across the beam. This is a useful procedure in aligning the instrument. A suitable Stern-Gerlach peak separation is about 3 undeflected beam widths or $6a$ for a good signal-to-noise ratio of the refocused atoms. The deflecting magnets must be designed so that they are capable of providing an intensity distribution of this general character.

The observed signal in a beam experiment is the change in detector current due to the induced transitions. The total undeflected beam intensity seen by the detector centered at $s = 0$ is

$$I_0 = 16 I_{00} w, \qquad \text{if } w < 2a$$

and

$$I_0 = 16 I_{00} 2a \qquad \text{if } w > 2a,$$

where w is the width of the detector and I_{00} is the number of atoms of a single state colliding with the detector per second per unit width of detector.

Equation (37) gives a relation for I_0 if it is assumed that simple effusion occurs from the oven slit. At an oven temperature of 150°C the vapor pressure of cesium is about 5×10^{-3} mm Hg, and $N_0 \sim 1 \times 10^{14}$ atoms/cm^3. If the oven slit and detector widths are 0.015 in. and the equivalent beam height is 0.05 in., then

$$I_0 = \frac{N_0 a A \bar{c}}{4\pi r^2} \approx 8 \times 10^7 \text{ atoms/sec}$$

for $r = 268$ cm. For a surface ionization detector, the efficiency of ionization can be nearly 100%. In this case the detected current would be

$$(8 \times 10^7 \text{ electrons/sec})(1.6 \times 10^{-19} \text{ coul/electron}) = 1.3 \times 10^{-11} \text{ amp.}$$

Approximately one-eighth of this total detected intensity is contributed by the two states $(F = 4, m_F = 0)$ and $(F = 3, m_F = 0)$. When the deflection magnets are switched on, the intensity seen by the detector is

$$I' = \int_{-w/2}^{+w/2} I(s) ds.$$

If $w = a$, the integration yields

$$I' = \frac{a}{2} I_{00} [3 \exp(-2s_\alpha/3a - \exp(-2s_\alpha/a)]. \tag{41}$$

The total intensity is obtained by superposing the contributions made by all of the states, each state having in general a different s_α.

$$I'_{\text{total}} = \sum_{i=1}^{16} \eta_i I_{00} \frac{a}{2} [3 \exp(-2s_{\alpha i}/3a) - \exp(-2s_{\alpha i}/a)]. \tag{42}$$

η_i is the relative population of atoms in the ith state. If the transitions $(F = 4, m_F = 0) \leftrightarrow (F = 3, m_F = 0)$ are induced (with probability one), then the total detected intensity would be

$$I'_{\text{total}} = 2I_{00}a + \sum_{i=1}^{14} \frac{a}{2} I_{00} [3 \exp(-2s_{\alpha i}/3a) - \exp(-2s_{\alpha i}/a)], \quad (43)$$

where it is assumed that all states have equal populations. The first term is due to the refocused atoms. If the deflecting fields are very strong, then the $s_{\alpha i}$ are very nearly the same for all the states.

In order to observe the maximum change in detector signal when a transition occurs, the summation term of Eq. (43) should be made small relative to the term $2I_{00}a$ (see Fig. 11). A satisfactory practical choice of machine parameters to attain this condition are those for which $s_\alpha \approx 10a$.

Estimates of intensity by means of the foregoing relationships assume that simple effusion occurs at the oven slit and that the velocity distribution is not affected by the geometry of the apparatus. The oven slits are frequently made up of many long channels from which simple effusion does

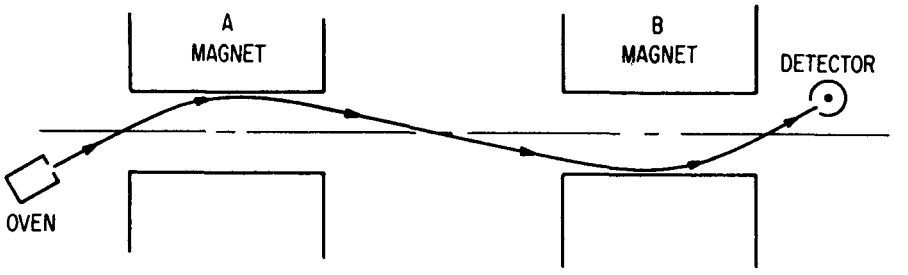

FIG. 12. Oven and detector offset arrangement for the selection of slower atoms. A narrower spectral line results.

not occur (*7*, *12*). This tends to concentrate the atoms effusing from the source within a smaller solid angle with a saving of oven material, in this case, cesium. The channeled source also tends to reduce the number of slow atoms detected because of this concentration of the beam—at least if the oven and detector are placed on the axis of the machine in the usual way.

The geometry of the apparatus will affect the velocity distribution. If the deflecting magnet pole shoes are too close together, the slow atoms that could be detected will be eliminated from the beam and the spectral line will be broad. It is useful to introduce a stop at the center of the undeflected beam for the purpose of eliminating very fast atoms. A reduction in intensity is incurred but the spectral line width will be narrower. It is thus useful to restrict the fast atoms but not the slow atoms.

Some economy in magnet construction can be gained by using deflecting magnets with rather narrow spacing between the pole shoes and off-

setting the oven and detector from the machine axis. Although the slowest atoms will be eliminated from the beam if the oven and detector are both on the machine axis, the slow atoms can be observed, together with the consequent narrower line, by offsetting the oven slit and detector (see Fig. 12). In this arrangement only emission or absorption is observed instead of both as in the usual circumstance.

C. The Deflecting Fields (6, 7)

Most atomic beam spectrometers employ iron magnets designed to produce the same field as two parallel wires carrying current in opposite directions. In a few cases, four- and six-wire field configurations have been used. The more common two-wire field will be considered first. Figure 13a

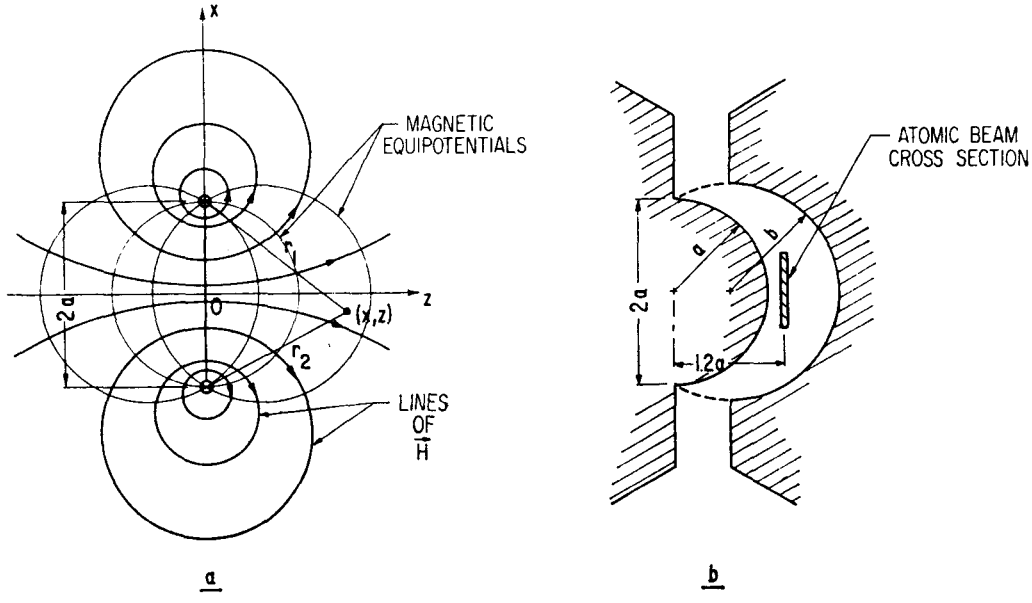

FIG. 13. (a) The field intensity lines and magnetic equipotentials of two parallel wires normal to the diagram at $x = a, z = 0$ and $x = -a, z = 0$. (b) An iron deflecting field contoured to produce a two-wire field.

displays the field intensity and the equipotentials of two parallel wires normal to the diagram at $(x = a, z = 0)$ and $(x = -a, z = 0)$. They carry a current I in opposite directions. The field intensity at the point (x, z) is given by[7]

$$H(x, z) = \frac{4Ia}{r_1 \cdot r_2} \tag{44}$$

and the gradient of the field is given by (see Appendix F in Ramsey, 7)

$$\frac{\partial H}{\partial z} = -4Ia\left(\frac{r_1^2 + r_2^2}{r_1^3 r_2^3}\right) z. \tag{45}$$

[7] In this relationship, I is measured in abamperes (1 abamp = 10 amp).

The value of this derivative $\partial H/\partial z$ is almost constant in the region $x = 0$, $z = 1.2a$. If the undeflected beam is centered at $z = 1.2a$ and the beam height does not exceed $1.4a$, the beam will be deflected without excessive distortion. It may be assumed in calculating atomic trajectories that $\partial H/\partial z$ and H both are constant in an adequately large region about this point.

At the point $y = 0$, $z = 1.2a$,

$$H = \frac{1.64I}{a},$$

$$\frac{\partial H}{\partial z} = \frac{1.61I}{a^2},$$

and

$$\frac{1}{H}\frac{\partial H}{\partial z} \approx \frac{1}{a}. \tag{46}$$

The current has been conveniently eliminated in this relationship.

The lines of **H** and the magnetic equipotentials form a system of orthogonal circles for two parallel wires. This same field configuration can be produced by an iron magnet by simply contouring the pole surfaces to coincide with two equipotential surfaces (see Fig. 13b). Suitably large deflections for cesium atoms can be obtained with rather simple low power magnets of this kind. In molecular beam experiments the effective magnetic moments of the molecules are ordinarily the order of a nuclear magneton; very large magnets are required and beam widths must be smaller. There appear to be some distinct advantages in using multipole deflecting fields. Multipole field configurations have been used successfully in atomic beam experiments (*13*, *14*, *15*) and in gaseous masers (*16*). A significant increase in intensity is gained—perhaps an order of magnitude—because these field configurations accept atoms from a relatively large solid angle. In atomic resonance beam experiments, however, a fraction of this gain is lost because of nonadiabatic transitions occurring as the beam enters and leaves the uniform C field region.

Figure 14 shows a cross section of a four-pole deflecting field. The surfaces of the iron pole pieces have been contoured to fall on the magnetic equipotentials whose intersection with the plane of the diagram form hyperbolas. The magnitude of the field intensity can be shown to be (ideally)

$$H = \frac{H_m}{R} r. \tag{47}$$

The transverse force on an atom within this magnet assembly is radial:

$$\mathbf{F} = -\nabla W = \left(-\frac{\partial W}{\partial H}\right)\frac{\partial H}{\partial r}\,\mathbf{e}_r, \tag{48}$$

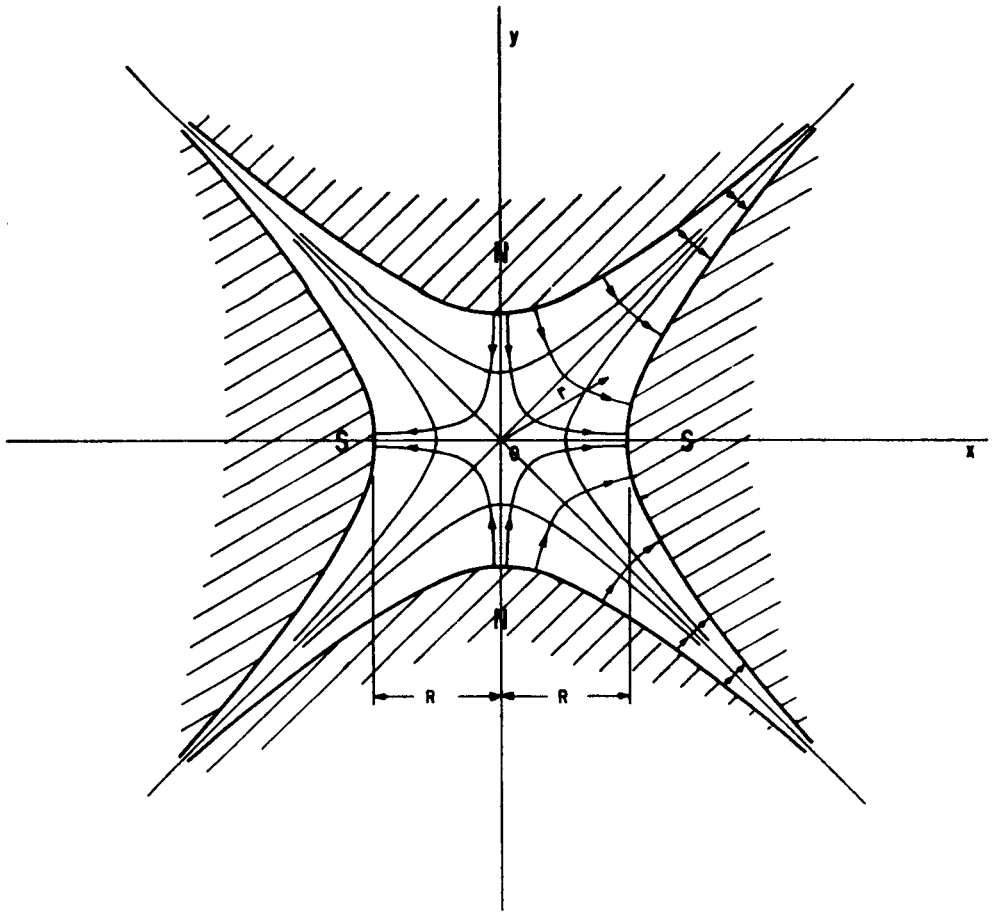

FIG. 14. Cross section of a four pole magnetic deflection field.

where $\mathbf{e}_r$ is a radial unit vector and

$$\frac{\partial H}{\partial r} = \frac{H_m}{R}. \tag{49}$$

R is the distance from the axis of the assembly to the nearest point on each of the four-pole surfaces, and H_m is the magnetic field at these points on the surfaces.

In general, W is a function of the magnitude of the field H and is given by the Breit-Rabi formula. If the field produced by the magnet assembly is sufficiently strong so that the magnetic interaction energy with the external field is large compared to the interaction energy between the nuclear and electronic angular momentum (Paschen-Back effect), then the atom will have a magnetic moment μ_{eff} of the order of a Bohr magneton independent of the magnetic field. As an example consider cesium: In strong fields

$$\mu_{eff} = -\mu_0 \text{ for } m_J = +\frac{1}{2} \text{ states}$$

and

$$\mu_{eff} = +\mu_0 \text{ for } m_J = -\frac{1}{2} \text{ states.}$$

Then

$$F_r = \mu_{eff} \frac{H_m}{R} = \mp \mu_0 \frac{H_m}{R} = \text{constant.} \tag{50}$$

Atoms for which μ_{eff} is positive are repelled from the axis, and atoms for which μ_{eff} is negative are attracted toward the axis. For atoms entering the deflecting field with a velocity vector in a plane containing the axis, the equations of motion have the same form as those previously calculated for a two-wire field. In general the atoms will execute a spiral motion through the deflecting field.

In order to consider μ_{eff} sufficiently independent of the field it would be necessary to adjust H_m to about 5 kgauss or higher for cesium and in addition a stop would be necessary on the axis so that atoms passing through the low field regions in the neighborhood of the axis would be eliminated from the beam. The stop would insure the validity of Eq. (50) which assumes μ_{eff} = constant. The field could also be operated at lower intensities in which case the force on an atom is approximately proportional to r, its distance from the axis. Cesium atoms in states ($F = 4$, $m_F = 0$) and ($F = 3$, $m_F = 0$), for example, in applied fields of 2 kgauss or less have an effective dipole moment approximately given by

$$\mu_{eff} = -\frac{\partial W}{\partial H_0} = \mp \frac{1}{2} \frac{[(g_J - g_I)\mu_0]^2}{\Delta W} H_0,$$

where the minus sign applies to the $F = 4$ state and the plus sign refers to the $F = 3$ state. The force on these atoms is

$$F_r = \mp \frac{1}{2} \frac{[(g_J - g_I)\mu_0]^2}{\Delta W} \left(\frac{H_m}{R}\right)^2 r = \mp kr, \tag{51}$$

where

$$k = \frac{1}{2} \frac{[(g_J - g_I)\mu_0]^2}{\Delta W} \left(\frac{H_m}{R}\right)^2. \tag{52}$$

Atoms in the ($F = 4$, $m_F = 0$) state are attracted toward the axis, and atoms in the ($F = 3$, $m_F = 0$) state are repelled from the axis. Atoms in the upper state would execute simple harmonic motion in passing through the deflecting field with angular frequency

$$\omega = \sqrt{\frac{k}{m}} = \mu_0 \frac{(g_J - g_I)}{(2m\Delta W)^{1/2}} \frac{H_m}{R} \tag{53}$$

A six-pole magnet with strong fields would also exert a force on the atoms proportional to r. Then

$$F_r = \mp \left(3\mu_0 \frac{H_m}{R^2}\right) r, \tag{54}$$

and

$$\omega = \sqrt{\frac{3\mu_0 H_m}{mR^2}}. \tag{55}$$

A beam device might be designed such that somewhat less than ¼ or ½ of a period of this harmonic motion occurred within each of the deflecting fields (see Fig. 15). Only flop-out experiments can be performed with these field configurations if the detector is placed on the axis as in Fig. 15a, b.

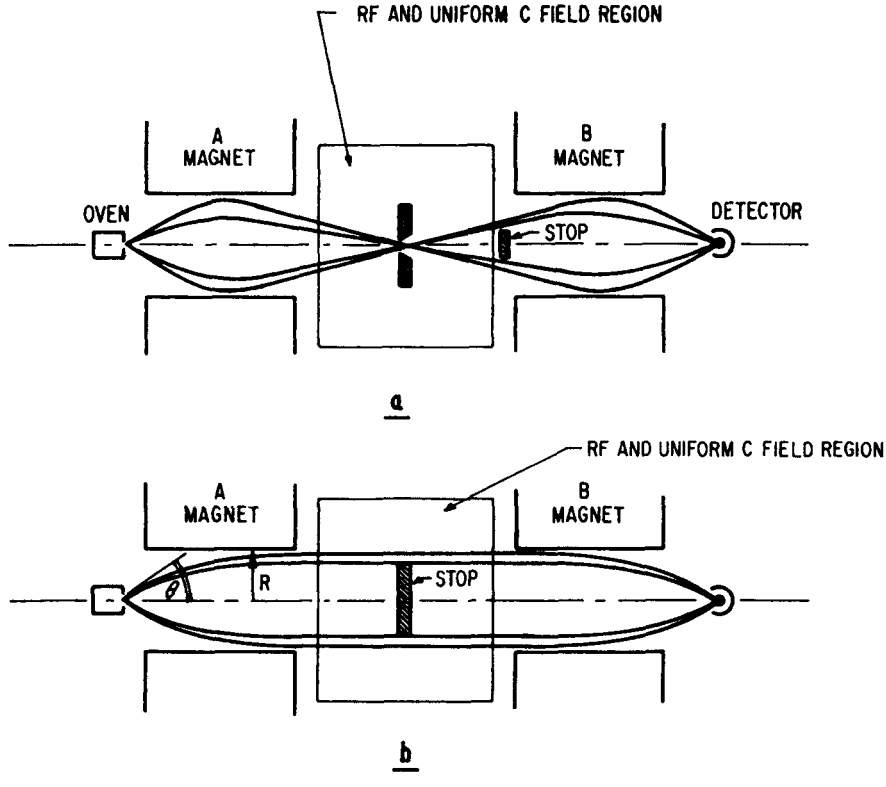

FIG. 15. (a) A beam device designed for ¼ the period of the harmonic motion occurring in the deflection magnet's field. (b) A beam device designed for ½ the period of the harmonic motion occurring in the deflection magnet's field.

The solid angle accepted from the source by the deflection magnet assembly can be determined in the following way. The increase in potential energy of an atom as it passes through the deflection field must be equal to the decrease in transverse kinetic energy that the atom experiences in passing through this field. Thus,

$$\frac{1}{2}m[v_{tr}(0)]^2 - \frac{1}{2}m[v_{tr}(R)]^2 = W(R) - W(0),$$

where $v_{tr}(0)$ is the transverse velocity of the atom as it enters the field (we assume that the oven orifice is on the axis at $r = 0$), $v_{tr}(R)$ is the transverse velocity at a distance R from the axis, and $W(R)$ and $W(0)$ are the potential energies of the atom at distances $r = R$ and $r = 0$ respectively. R is the radius of a circle inscribed within the pole pieces and touching the pole tips. For the fields considered $W(0) = 0$ and $W(R)$ are given by the Breit-Rabi formula. Presumably, only those atoms having $v_{tr}(R) \leqq 0$ will remain in the beam. An atom effusing from the source with velocity v can be emitted at a maximum angle θ_v and still remain in the beam. This angle will be sufficiently small so that we may write

$$v_{tr} = v \sin \theta_v \approx v\theta_v.$$

Now

$$\frac{1}{2}m[v_{tr}(0)]^2 = W(R) = \frac{1}{2}m[v\theta_v]^2,$$

or

$$\frac{1}{2}m[v\theta_v]^2 = \frac{kR^2}{2}.$$

The maximum solid angle accepted from the source is then

$$\Omega_v = \pi\theta_v^2 = \frac{\pi kR^2}{mv^2} \tag{56}$$

for atoms in the state considered and having velocity no less than v.

D. Beam Detection and Beam Sources (6, 7, 13, 17)

When an atom approaches a metal surface ionization processes are often possible. An atom will be ionized if an atomic electron tunnels to any unoccupied electronic state in the metal. This process occurs with particular ease for cesium. The atoms of the beam strike a hot wire, the ions are boiled off, collected, and measured with an electrometer or electron multiplier circuit. In Fig. 16 the metal is represented by a potential well of depth W_a filled with electrons to the Fermi level ζ. The work function ϕ is the minimum energy required to raise an electron to the energy continuum. The atom is represented by a second potential well which is occupied by an electron in one of the possible energy states. The ionization potential of the atom is denoted by V_I.

In order for ionization to take place, the energy level of the electron in the atom must coincide within narrow limits of a vacant energy level in the metal. The two states are then said to be in resonance and tunneling

may occur. The shapes of the potential wells of the metal and atom are deformed at close approach. This deformation is necessarily accompanied by a shift of the energy levels and consequently a shift in the ionization potential. Evidently, if an atom whose ionization potential is less than the work function of a metal strikes the metal surface, it can be re-evaporated as a positive ion (*18*). The metal must be sufficiently hot to prevent conden-

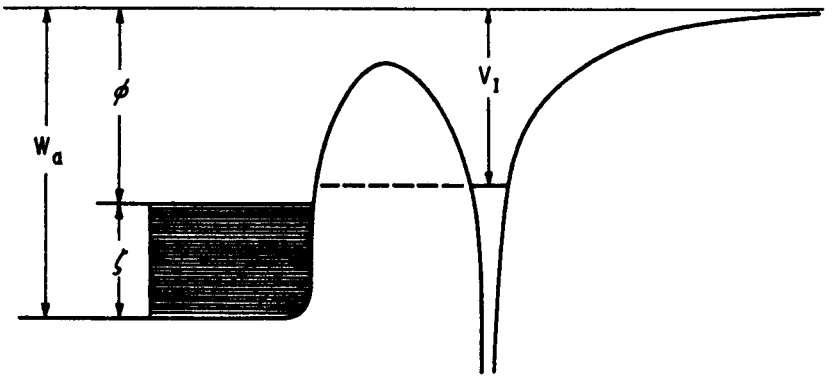

FIG. 16. A pictorial representation of the potential barrier between an atom and a metal surface.

sation. Cesium has a particularly low ionization potential (VI = 3.87 ev) and can be ionized with almost 100% efficiency on hot tungsten (ϕ = 4.5 ev) or hot platinum (ϕ = 5.1). The NBS standards employ a platinum-iridium alloy (80% Pt; 20% Ir) with somewhat improved behavior over either tungsten or platinum. There seem to be fewer impurity ions in the alloy than in tungsten. These ions create an undesirable and erratic background current.

The tungsten or Pt-Ir detector is usually in the form of a ribbon. Cesium is detected with good efficiency if the temperature of the ribbon is maintained at about 900°C. The ion current can be measured either with an electrometer or electron multiplier circuit. If an electrometer is used the ribbon is frequently surrounded by a collector ring, and if an electron multiplier is used, accelerating and focusing electrodes must be introduced. Frequently a mass spectrometer is used to analyze the ion beam, thus removing the impurity ions. The National Company Atomichron employs a tungsten ribbon together with an electron multiplier and mass spectrometer.

Electrometer circuits are capable of measuring currents as low as 1×10^{-17} amp. Those employed in the NBS standards have a background current of 4×10^{-15} amp when operating under ideal conditions. With the exciting radiation adjusted in frequency to the resonance peak of the atomic transition, the detected current is typically the order of 4×10^{-12} amp so that the signal-to-noise ratio is about 1000. Strictly speaking, this is the signal-to-noise ratio for Rabi excitation (see Section V,E). Most atomic

frequency standards employ Ramsey type excitation. The signal-to-noise ratio in this case is usually given by the ratio of the peak intensity less the intensity at the first minimum of the Ramsey interference pattern divided by the root-mean-square of the noise current. Because of the distribution of velocities in the beam, the first minimum does not go down to the noise level. In fact, typically, the current at this point is about $\frac{3}{4}$ or $\frac{2}{3}$ of the current at the peak of the spectral line. Thus the signal-to-noise ratio of the Ramsey line is about 330.

It is of interest to compare the electrometer and electron multiplier detectors. The electrometer circuit has the advantage of simplicity but the disadvantage of a longer time constant ($\sim$0.2 sec for typical current values).

A simplified model of an electrometer circuit is shown in Fig. 17. Let

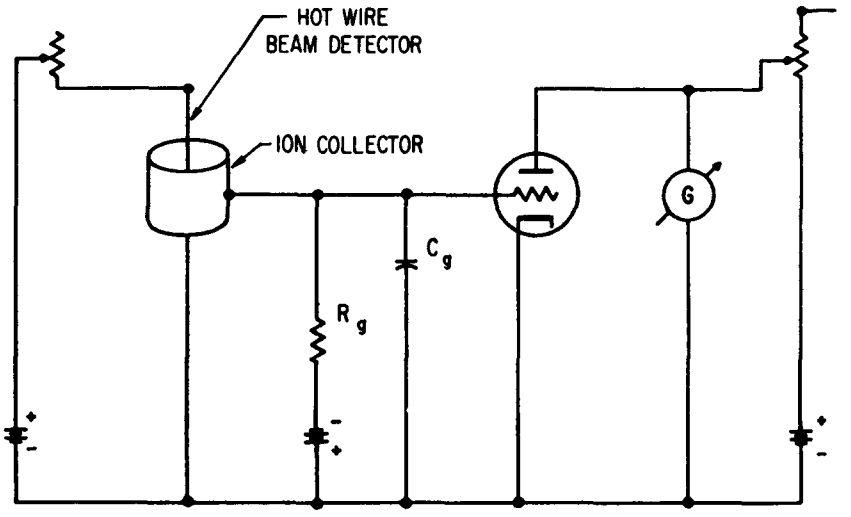

FIG. 17. Simplified electrometer circuit for the detection of atomic beam ion currents

us consider the noise in such a circuit. We will neglect the noise resulting from beam fluctuations and impurity ions boiled off the detector wire. The important sources of noise remaining are the Brownian motion of electricity in the grid circuit and the shot noise of the grid current. Using the Schottky and Nyquist relations, it can be shown (*19*, *20*) that the mean squared deviation of the grid current is given by

$$\overline{\Delta I^2} = \frac{(2kT/R_g) + eI}{2R_gC_g} \tag{57}$$

so long as the time constant τ of the galvanometer is much less than the time constant, R_gC_g, of the grid circuit. In Eq. (57), k is the Boltzman constant ($k = 1.38 \times 10^{-23}$ joules/°K), T is the absolute temperature of the grid resistor R_g, e is the electronic charge ($e = 1.60 \times 10^{-19}$ coul), and I is the grid current in amperes.

If the galvanometer responds much more slowly than the grid circuit, i.e., if $\tau \gg R_g C_g$, and if $(2kT/R_g) \gg eI$, then

$$\overline{\Delta I^2} = \frac{\pi kT}{\tau R_g}. \tag{58}$$

As an example suppose that $C_g = 20\mu\mu f$, $T = 300°K$, $R_g = 10^{10}$ ohms, and $I = 1 \times 10^{-12}$ amp. Using Eq. (57) and associated assumptions, the root-mean-square current deviation is

$$\Delta I_{rms} = 1.6 \times 10^{-15} \text{ amp.}$$

The signal-to-noise ratio is $I/\Delta I_{rms} = 630$. If the ionized beam current is measured with an electron multiplier, the primary contribution to the noise, ignoring the beam fluctuations and impurity ions, is shot-noise.

The mean squared deviation of the output noise current is given approximately by (*21*, *22*)

$$\overline{\Delta I_n^2} = 2eIM\left(\frac{mM-1}{m-1}\right)\Delta\nu, \tag{59}$$

where I is the average ion current incident on the first dynode, M is the total current multiplication factor, m is the average multiplication per stage, e is the charge on the electron, and $\Delta\nu$ is the bandwidth. It has been assumed in Eq. (59) that the probability of production of secondary electrons is given by a Poisson distribution which is only an approximately valid assumption (see *21*).

If $M = 10^6$, $m = 3$, $\Delta\nu = 5$ cps, and $I \times 10^{-12}$ amp, then the root-mean-square deviation of the output current is

$$\Delta I_{rms} = 1.5 \times 10^{-9} \text{ amp,}$$

and the signal-to-noise ratio is

$$\frac{MI}{\Delta I_{rms}} = 670,$$

which is not much different from the value obtained for the electrometer with the same time constant. This signal-to-noise ratio calculated for the electron multiplier would have to be reduced because the efficiency with which Cs^+ ions produce electrons at the first dynode is perhaps only 15% of the efficiency of an electron producing secondary electrons at this surface. Thus the estimated signal-to-noise ratio is about 100, and the electrometer appears to have some advantage over the electron multiplier. The real advantage of the electron multiplier seems to be for measuring very small currents as evidenced by Eqs. (58) and (59). Also, the time constant of the electrometer circuit becomes excessively long for very small currents.

463-560 O - 72 - 4

Various kinds of modulation schemes have come into use and are applicable to atomic beam frequency standards (*23, 24, 25*). Vibrating reed electrometers are used in both the United Kingdom and the United States frequency standards. They have some useful advantages over the dc electrometer (*26*).

The response time of electrometer circuits can be made sufficiently short for permissible modulation frequencies. (The modulation frequency must be less than the spectral line width.) By following the electron multiplier or electrometer with an amplifier and phase detector tuned to the modulation frequency, a correction signal may be obtained. This correction signal can then be used to lock the crystal oscillator from which the beam excitation is derived. Thus a signal source continuously locked to the atomic resonance is obtained. The National Company Atomichron employs this scheme of locking an oscillator to the cesium resonance (*27*).

The experience at NBS with servo devices is that manual measurements still provide the best, most consistent measurements. The feedback circuits sometimes introduce troublesome systematic errors. Even though precision and stability are good, there remains some uncertainty in accuracy. Considerable progress is being made in the improvement of the servo systems, however.

In the above considerations of noise in electrometer circuits and electron multipliers, the sources of noise originating from beam fluctuations and impurity ions boiled off of the hot wire were neglected. The noise from these sources may easily exceed those already discussed if proper care is not taken. The vacuum and beam excitation must be stable and the cesium in the source reasonably pure.

Distilled cesium of adequate purity may be obtained commercially in sealed glass ampoules. Cesium reacts with air and it is best but not necessary to break the ampoule in the oven under vacuum. The oven may also be filled with an inert gas after which the ampoule is broken and the oven immediately installed in the spectrometer. The vapor pressure of cesium as a function of temperature is shown in Fig. 18. Different groups operate the source at different temperatures ranging from about 70°C to 150°C. The source temperature depends upon the design of the oven slit and somewhat on the pumping speed. The NBS ovens are operated at 150°C at which temperature the vapor pressure of cesium is about 5×10^{-3} mm Hg. The mean free path for cesium at this pressure and temperature is approximately 5 cm. The oven slits may be channeled if it is desired to conserve cesium but they need not be unless the slit dimensions become comparable to the mean free path.

In the NBS devices, when operated with the oven slit and detector on the machine axis, it is found that the spectral line width is significantly

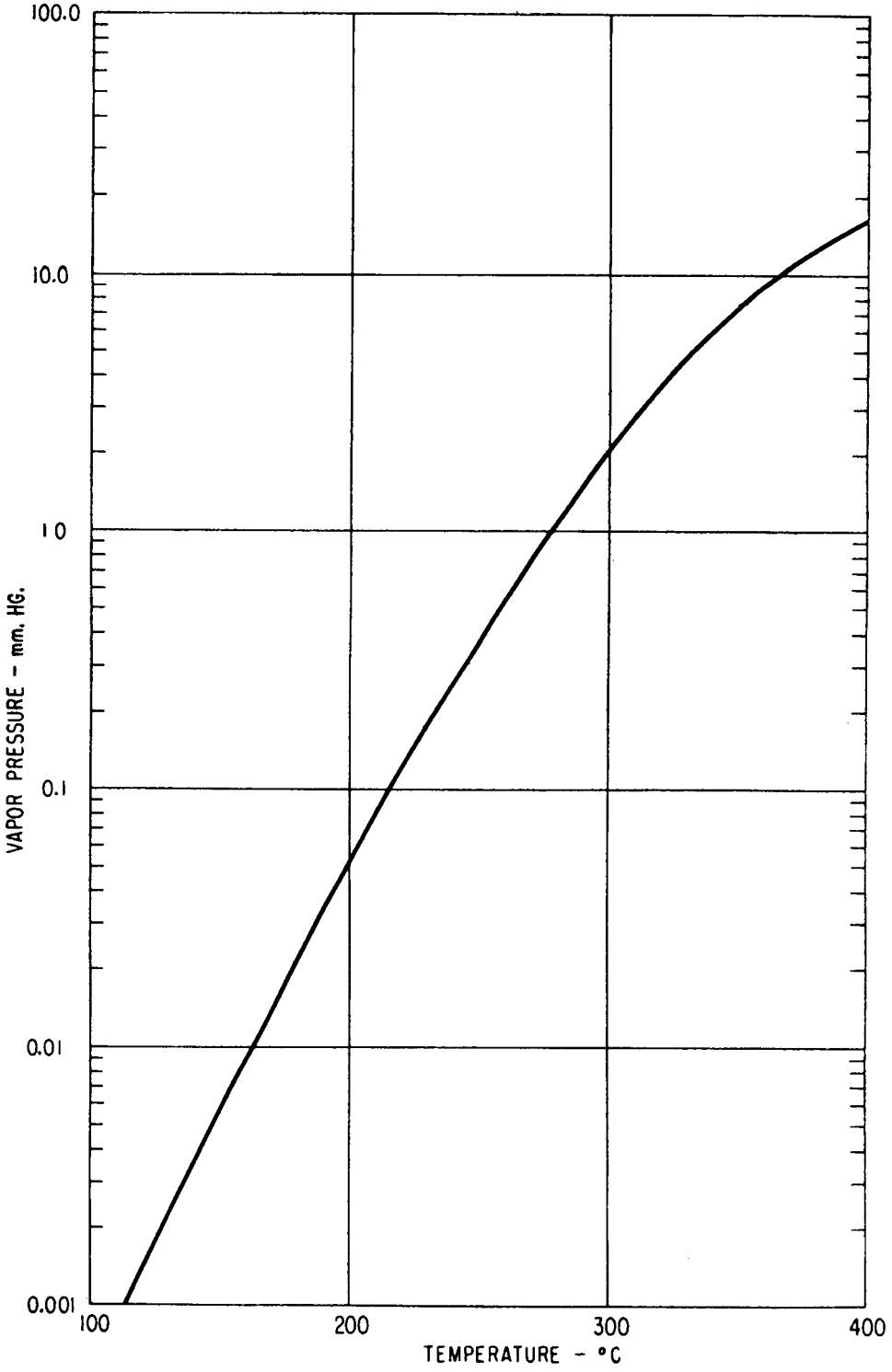

FIG. 18. The vapor pressure of cesium versus temperature.

broader when a thick channeled slit is used instead of a thin slit. It is presumed that the reason for this is that the thick slit concentrates more of the beam in a small solid angle about the normal. Slow atoms from the oven are selected by the deflecting fields only when they are emitted at relatively large angles from the normal. Ovens made of iron or stainless steel are popular, although copper and many other materials are quite likely to work satisfactorily.

VI. The Transition Process

In an atomic beam resonance experiment, the energy level scheme of the atom is determined by subjecting the beam to a radiation field. This field is applied in the C field region between the A and B deflecting magnets (see Fig. 8a). When the frequency of the radiation is swept through the frequency of an allowed transition, a change in moment of the atoms will occur. As a result of this moment change, the transverse force on the atoms in the second deflecting field also changes and a variation in detected beam current is observed.[8]

The width and intensity of the spectral lines—and consequently the transition probability as a function of frequency—are of considerable importance in the design, interpretation, and ultimate accuracy of an atomic beam experiment. The line width is given approximately by the Heisenberg relation:

$$\Delta\nu\tau \sim 1,$$

where $\Delta\nu$ is the line width and τ is the time the atom spends in the radiation field. In contrast with microwave absorption spectroscopy, collision and Doppler broadening can be made negligibly small in beam experiments. For purposes of atomic frequency standards, it is logical to choose states with long lifetimes so that the spectral line is not broadened by spontaneous emission processes.

The original Rabi method of exciting the atomic resonance employs a single oscillating field. In 1950, Ramsey introduced a method of excitation using two separated oscillating fields. There are a number of advantages to this method over the Rabi method. The Ramsey method improves the resolution of the spectrometer. It does not require as high a degree of uniformity of the static C field. It has a practical advantage when observing very high frequency transitions.[9] Two short oscillating fields separated by

[8] This is not strictly true. The moment of an atom as it passes through the A deflecting magnet will not differ from its moment in the B deflecting field for $\Delta F = 0$, $\Delta m_F = \pm 1$ ($m_F \neq I + \frac{1}{2}$) transitions if the deflecting fields are strong. Consequently, no change will be observed in the beam intensity when a transition of this type is induced (see Fig. 9).

[9] The oscillating field should be uniform in intensity and phase, and this is difficult to achieve when the oscillating field region is many free-space wavelengths long.

a distance L provide even higher resolution than a single ideal field covering the entire distance L. The advantage is gained at the expense of a reduction in signal-to-noise ratio that depends upon the velocity distribution in the beam.

A. The Transition Probability for a Single Oscillating Field

The Hamiltonian for an atom in the presence of a radiation field can be written as:

$$\mathcal{H}(t) = \mathcal{H}_0 + \mathcal{H}'(t), \tag{60}$$

where $\mathcal{H}_0$ is the Hamiltonian in the absence of the radiation field, and $\mathcal{H}'(t)$ is the interaction between the radiation field and the magnetic moment $\boldsymbol{\mu}$ of the atom. This second term may be written to sufficient approximation as

$$\mathcal{H}'(t) = -\boldsymbol{\mu} \cdot \mathbf{H} \cos \omega t, \tag{61}$$

where H is the magnitude of the oscillating magnetic field intensity and ω is the angular frequency of this oscillating field. In order to obtain the transition probability and the theoretical line shape, the time dependent Schrödinger equation must be solved. A complete solution may be obtained if certain assumptions are made. We will proceed to enumerate these assumptions.

(a) The two states involved in the transition are well isolated from other states.

(b) The diagonal elements of the interaction Hamiltonian are zero.

(c) The atom sees a finite portion of a cosine wave as it passes through the radiation field region. It enters the field at $t = 0$ and leaves at time τ. A substantial simplification can be made in the calculation without serious discrepancies in the results if it is assumed that the dipole moment interacts with a rotating field rather than an oscillating field. Instead of Eq. (61), write

$$\mathcal{H}'(t) = -\boldsymbol{\mu} \cdot (H \cos \omega t \mathbf{i} - H \sin \omega t \mathbf{j}), \tag{62}$$

where the z-axis is chosen along $\mathbf{H}_0$, the uniform C field, and H rotates with angular velocity ω in the x,y-plane. We have chosen the special case where the radiation field has a z-component equal to zero.

With these simplifying assumptions, the transition probability that an atom initially in state p, will be in state q after a time τ, is given by

$$P_{p,q}(\tau) = \frac{|2b|^2}{(\omega_0 - \omega)^2 + |2b|^2} \sin^2 \left\{ \frac{1}{2} [(\omega_0 - \omega)^2 + |2b|^2]^{1/2} \tau \right\}. \tag{63}$$

The quantity b is related to the matrix elements of the interaction Hamiltonian by

$$\mathcal{H}_{pq}' = \int \psi_p^* \mathcal{H}'(t) \psi_q d\tau = \hbar b e^{+i\omega t}, \tag{64}$$
$$\mathcal{H}_{qp}' = \int \psi_q^* \mathcal{H}'(t) \psi_p d\tau = \hbar b^* e^{-i\omega t},$$

and

$$\omega_0 = (W_q - W_p)/\hbar.$$

The maximum transition probability occurs at resonance ω_0 when b and τ are related by

$$|b|\tau = \frac{\pi}{2}$$

or

$$|b| = 1.57 \frac{v}{l} \tag{65}$$

where v is the velocity of the atoms, and l is the length of the oscillating field traversed by the atoms. The frequency width at half maximum for these optimum conditions is

$$\Delta\nu = 0.799 \frac{v}{l}. \tag{66}$$

If the velocity distribution of the atoms in the beam is taken into account (*6*, *7*)

$$|b| = 1.89 \frac{\alpha}{l} \tag{67}$$

where α is the most probable velocity in the source and the velocity distribution in the beam is assumed to be that for simple effusion through an ideal aperture. The line width in this case is

$$\Delta\nu = 1.07 \frac{\alpha}{l}. \tag{68}$$

The radiation field intensity required to produce the optimum transition probability is given by Eqs. (64) and (67). For the purpose of an estimate we make the following approximation. The radiation field interacts most strongly with the electronic magnetic moment, and we may write

$$\boldsymbol{\mu} = \boldsymbol{\mu}_J + \boldsymbol{\mu}_I \approx \boldsymbol{\mu}_J.$$

Then

$$\mathcal{H}'(t) = -\boldsymbol{\mu} \cdot (H \cos \omega t \mathbf{i} - H \sin \omega t \mathbf{j})$$
$$\approx g_J \mu_0 \mathbf{J} \cdot (H \cos \omega t \mathbf{i} - H \sin \omega t \mathbf{j}).$$

This can be rewritten as

$$\mathcal{H}'(t) = \frac{1}{2} g_J \mu_0 H [J_+ e^{i\omega t} + J_- e^{-i\omega t}],$$

where $J_\pm = J_x \pm iJ_y$. Now

$$2b = \frac{g_J \mu_0 H}{\hbar} \langle p|J_+|q\rangle = \frac{\mathcal{K}_{pq}' e^{-i\omega t}}{\hbar}, \tag{69}$$

and

$$2b^* = \frac{g_J \mu_0 H}{\hbar} \langle q|J_-|p\rangle = \frac{\mathcal{K}_{qp}'^* e^{i\omega t}}{\hbar}.$$

The nonvanishing matrix elements of J in the weak field representation (F, m_F) are (*28*)

$$\langle F, m_F|J_\pm|F, m_F \pm 1\rangle = A[(F \pm m_F)(F \mp m_F + 1)]^{1/2},$$
$$\langle F, m_F|J_z|F, m_F\rangle = Am_F,$$

where

$$A = \frac{J(J+1) - I(I+1) + F(F+1)}{2F(F+1)};$$

$$\langle F, m_F|J_\pm|F+1, m_F \pm 1\rangle = \pm B[(F \mp m_F + 1)(F \mp m_F + 2)]^{1/2},$$
$$\langle F, m_F|J_z|F+1, m_F\rangle = B[(F+1)^2 - m_F^2]^{1/2},$$

where

$$B = \left[\frac{(F+1-J+I)(F+1+J-I)(J+I+2+F)(J+I-F)}{4(F+1)^2(2F+1)(2F+3)}\right]^{1/2}; \tag{70}$$

$$\langle F, m_F|J_\pm|F-1, m_F \pm 1\rangle = \mp C[(F \pm m_F)(F \pm m_F - 1)]^{1/2},$$
$$\langle F, m_F|J_z|F-1, m_F\rangle = C[F^2 - m_F^2]^{1/2},$$

where

$$C = \left[\frac{(F-J+I)(F+J-I)(J+I+1+F)(J+I+1-F)}{4F^2(2F-1)(2F+1)}\right]^{1/2}.$$

The selection rules $\Delta F = 0, \pm 1$; $\Delta m_F = 0, \pm 1$ are derived from these matrix elements.

If the C field is very weak, as it is in atomic frequency standards, then the matrix elements (70) may be used directly in Eq. (69). In the event that there is a component of the radiation field in the z-direction—contrary to the assumption made in writing Eq. (62)—the matrix elements of J_z are necessary in calculating the transition probability. The $(F = 4, m_F = 0) \leftrightarrow (F = 3, m_F = 0)$ transition in cesium is a case in point.

Torrey has given a useful approximate evaluation of b for general values of the C field intensity (*29*). For π-transitions,

$$2b = \frac{2}{\hbar} H_x \left[\left(\frac{g_J \mu_0}{2} \pm \mu_{F,m_F}\right)\left(\frac{g_J \mu_0}{2} \mp \mu_{F',m_F \pm 1}\right)\right]^{1/2}, \tag{71}$$

where H_x is the component of the radiation field perpendicular to $\mathbf{H}_0$, and μ_{F,m_F} are the magnetic moments of the states F, m_F. These effective magnetic moments are given by

$$\mu_{I\pm\frac{1}{2},m_F} = \mp \left\{ \frac{x + (2m_F/2I+1)}{[1 + (4m_F x/2I+1) + x^2]^{\frac{1}{2}}} \right\} \frac{g_J \mu_0}{2},$$

if $m_F \neq \pm(I + \frac{1}{2})$, and

$$\mu_{I+\frac{1}{2},m_F} = \mp \frac{g_J \mu_0}{2},$$

if $m_F = \pm(I + \frac{1}{2})$.

For σ-transitions,

$$2b = -\frac{\mu_0}{\hbar}(g_J - g_I)\left[1 - \left(\frac{2m_F}{2I+1}\right)^2\right] \frac{H_z}{[1 + (4m_F x/2I+1) + x^2]^{\frac{1}{2}}}. \quad (72)$$

If g_I is neglected relative to g_J then,

$$2b = -\frac{2H_z}{\hbar}\left[\left(\frac{g_J \mu_0}{2}\right)^2 - (\mu_{F,m_F})^2\right]^{\frac{1}{2}}. \quad (73)$$

H_z is the component of the radiation field parallel to $\mathbf{H}_0$, and the quantity x has its previous value:

$$x = \frac{(g_J - g_I)\mu_0 H_0}{\Delta W}.$$

When there is a component of the radiation field in the direction of $\mathbf{H}_0$, the diagonal matrix elements of the interaction Hamiltonian do not vanish and one of the assumptions (b) used in the derivation of Eq. (63) is violated. If, however, $|\mathcal{H}_{pp'}|$ and $|\mathcal{H}_{qq'}| \ll h\omega_0$, which they are for the standard frequency transition, then Eq. (63) still provides a reasonably good approximation.

A more exact treatment of the transition probability for π-transitions using the rotating field approximation is given by H. Salwen (*11*, *30*). Salwen's theory includes the interaction between neighboring states. Small frequency shifts in the resonances result. Salwen makes the additional assumption that the widths of allowed lines are small compared to their separations. The analysis has not been made for σ-transitions which are of particular interest in atomic beam standards. The significance of these frequency shifts predicted by Salwen can be demonstrated by looking for a displacement of the resonance peak as a function of radiation field intensity. If a shift is not observable within the precision of measurement over a range of oscillator field intensity, then the frequency shifts are not significant in the measurements. Of course, radiation field dependent frequency

shifts can, and frequently do, result from instrumental difficulties quite apart from the effects produced by neighboring states in the spectrum.

Oscillating fields rather than rotating fields are employed in atomic beam experiments. Even when the effects of neighboring states are neglected, an oscillating field will produce a small shift in frequency which is not predicted by the rotating field approximation. An oscillating field solution to the time dependent wave equation was first obtained by Bloch and Siegert (*31*) for particles of spin ½. In their calculation it was assumed that the magnitude of the radiation field H is small compared to the uniform C field H_0 and that $\mathbf{H}$ and $\vec{\mathbf{H}}_0$ are perpendicular to each other. They calculated the frequency shift to be

$$(\nu_0' - \nu_0) = \frac{\nu_0}{16}\left(\frac{H}{H_0}\right)^2, \tag{74}$$

where ν_0' is the frequency at the peak of the resonance curve and ν_0 is the frequency separation of the two states. This relationship probably applies satisfactorily to the $\Delta F = 0$, $\Delta m_F = \pm 1$ transitions in the cesium standard provided that care is taken to keep H small relative to H_0. An estimate of this frequency shift for $\Delta F = \pm 1$, $\Delta m_F = \pm 1$ transitions can be made by inserting the value of the magnetic field at the position of the nucleus into (74) for H_0 rather than the magnitude of the C field intensity. This field is 3.3×10^6 oe for cesium. The theoretical analysis of the oscillating field induced $\Delta F = \pm 1$, $\Delta m_F = 0$ transitions has not been performed.

B. The Transition Probability for Two Separated Oscillating Fields (7)

In the Ramsey method of excitation, the beam passes through two separated oscillating fields contained within the uniform C field. The probability that an atom, initially in state p, will be in state q after passing through both oscillating fields is given by

$$P_{p,q} = 4\sin^2\theta\,\sin^2\frac{a\tau}{2}\left[\cos\frac{1}{2}(\lambda T - \delta)\cos\frac{a\tau}{2} - \cos\theta\sin\frac{1}{2}(\lambda T - \delta)\sin\frac{a\tau}{2}\right]^2, \tag{75}$$

where

$$\sin\theta = \frac{|2b|}{a}, \qquad \cos\theta = \frac{\omega_0 - \omega}{a},$$

$$a = [(\omega_0 - \omega)^2 + |2b|^2]^{1/2},$$

$$\omega_0 = \frac{W_q - W_p}{\hbar},$$

$$\lambda = \frac{\bar{W}_q - \bar{W}_p}{\hbar} - \omega,$$

τ is the time taken by an atom to pass through either of the two oscillating fields of length l, T is the time taken by an atom to traverse the distance L between the two fields,

$$\tau = \frac{l}{v}, \qquad T = \frac{L}{v},$$

and b is given by Eqs. (64) and (69). It is assumed, as for Eq. (63), that $\mathcal{H}_{pp'} = \mathcal{H}_{qq'} = 0$. The second oscillating field leads the first by the phase angle δ. $\bar{W}_p$ and $\bar{W}_q$ are the average energies of states p and q in the region between the two fields.

The transition probability, Eq. (75), provides the theoretical line shape for a single velocity beam. A probability of one is obtained at $\omega = \omega_0$ when $\delta = 0$ and $b\tau = \pi/4$. When $P_{p,q}$ is averaged over the velocity distribution of a beam effusing from an ideal aperture, the maximum transition probability is given at $\omega_0(\delta = 0)$ when

$$b = 0.942\,\frac{\alpha}{l}. \tag{76}$$

Notice that the field intensity required is about half that required for the optimum condition for a Rabi flop in an oscillating field of length l.

The halfwidth of the central peak of the Ramsey pattern is

$$\Delta\nu = 0.64\,\frac{\alpha}{L} \tag{77}$$

under the conditions of Eq. (*76*). The form of the Ramsey pattern is shown in Fig. 19. The pedestal upon which the interference pattern sits is usually much broader than the interference pattern. In some cases the pedestal width is over 700 times the width of the central peak. The minima of the Ramsey transition probability would decrease all the way to zero in the case of a single velocity beam. A distribution in velocity of the atoms tends to smooth out the interference pattern. Greater smoothing action occurs at larger frequency displacements from the central resonance peak.

When the phase of the second oscillating field leads that of the first by $\delta = \pi$ radians, a minimum occurs at ω_0 rather than a maximum (see Fig. 19b). When $\delta = (\pi/2)$, the transition probability takes the form of a dispersion curve about ω_0 (see Fig. 19c). It is evident that if a small phase difference exists ($\delta \neq 0$) between the two fields, the peak of the resonance will be shifted in frequency relative to ω_0. An apparent frequency shift arising from a phase difference between the oscillating fields can be, and frequently is, significant in atomic beam frequency standards.

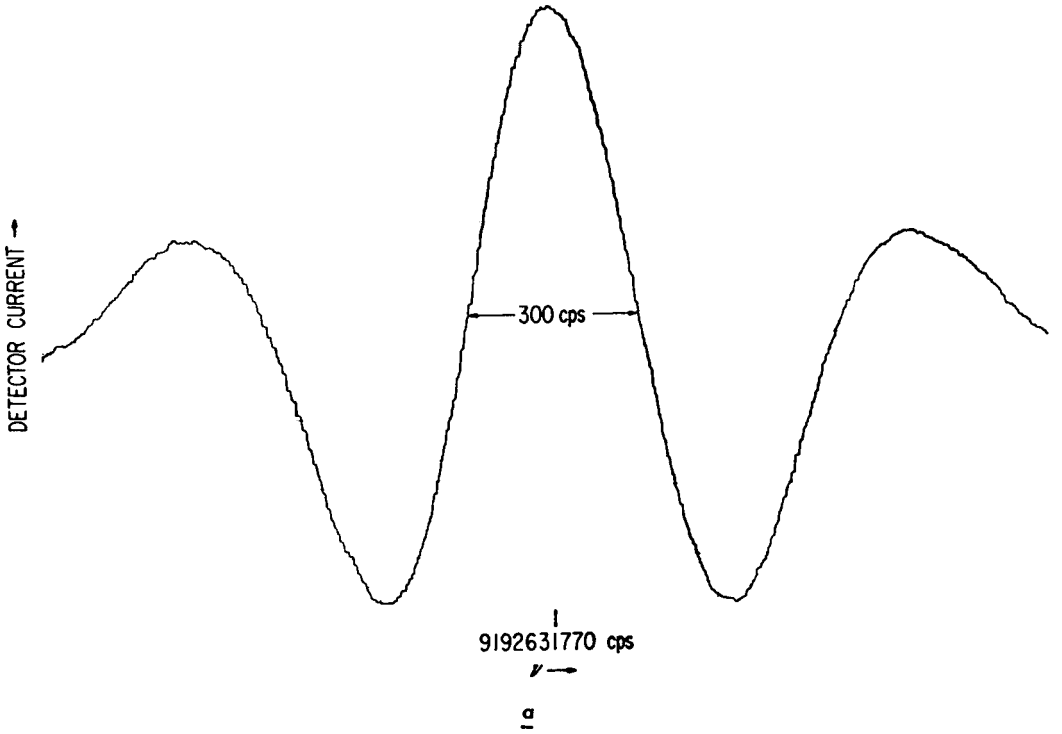

FIG. 19a. An actual trace of a Ramsey interference pattern when the two oscillating fields are in phase.

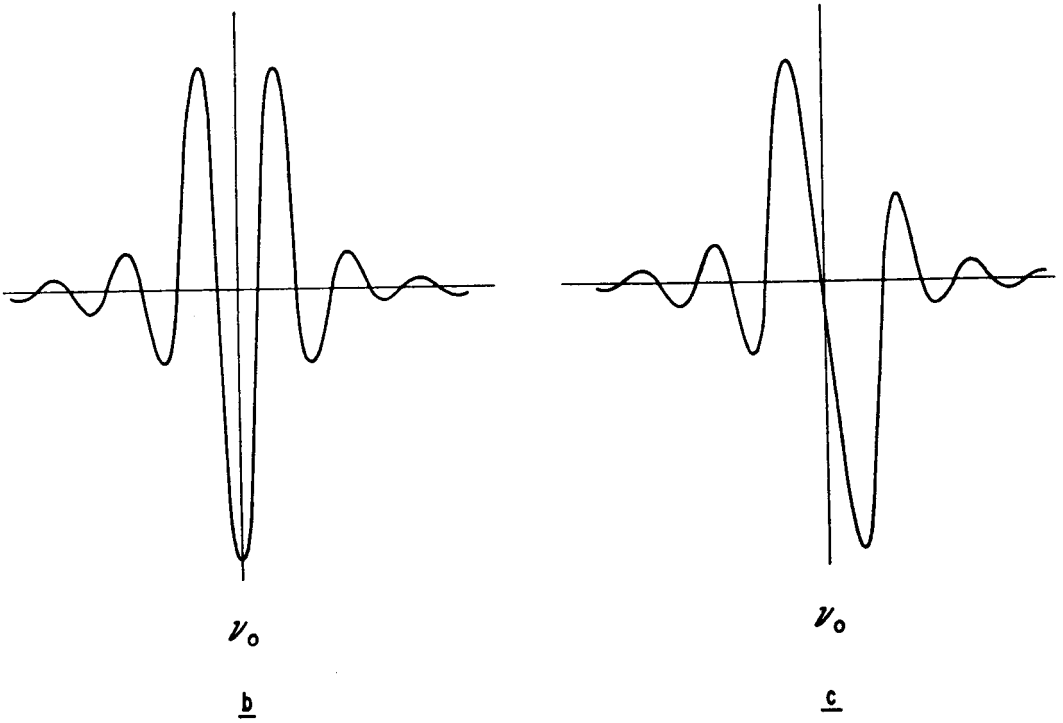

FIG. 19. (b) The form of the Ramsey pattern when the oscillating fields differ in phase by 180°. (c) The form of the Ramsey pattern when the oscillating fields differ in phase by 90°.

VII. Measurement Uncertainties

There are a number of uncertainties introduced into the absolute frequency measurements of a cesium standard. The ideal circumstance, of course, is to have the accuracy of these devices limited only by the random scatter in the data—all systematic frequency shifts having been measured or eliminated. Ideally then, the accuracy would be determined by the spectral line width and signal-to-noise ratio. At the present time systematic

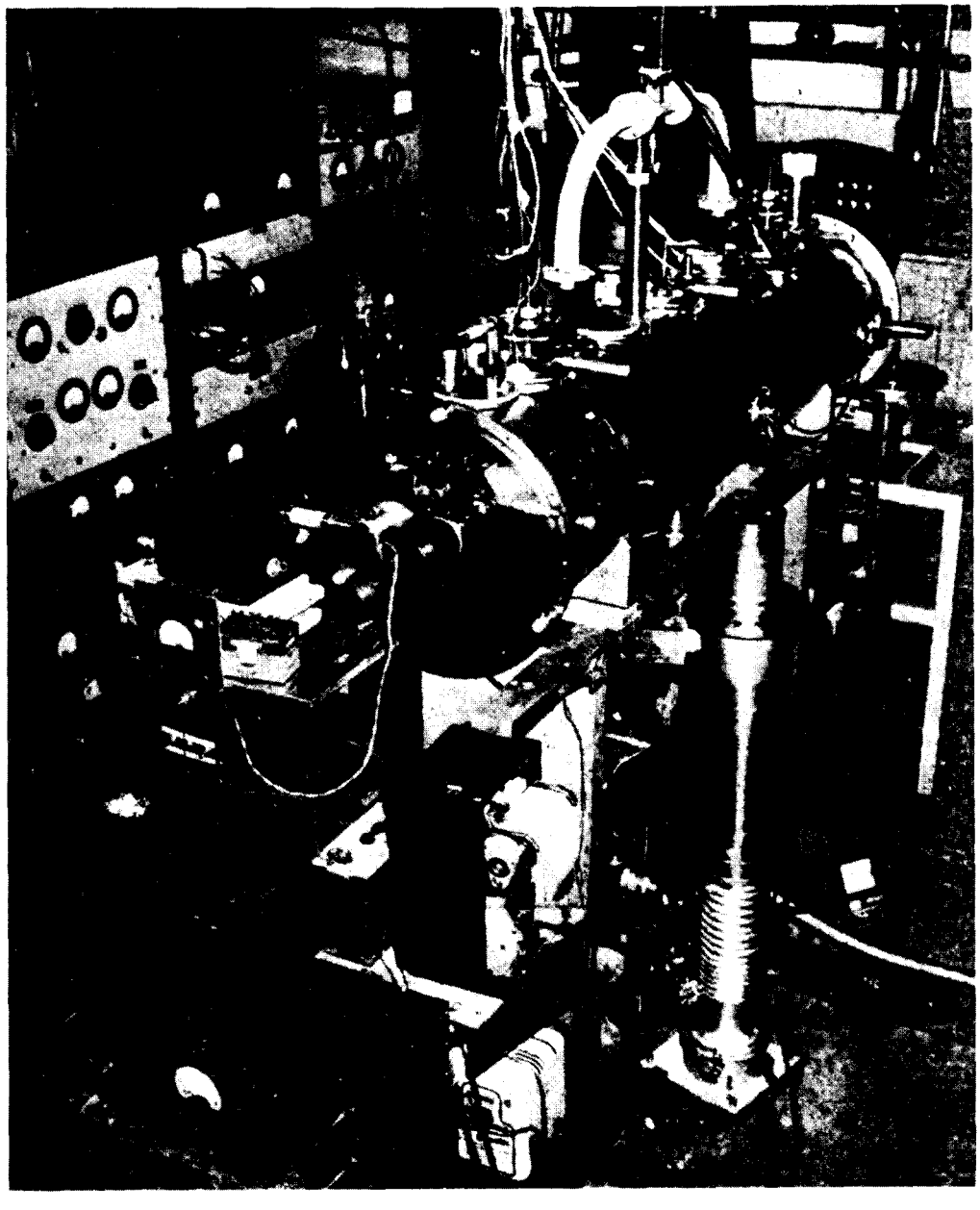

Fig. 20. NBS-I atomic beam frequency standard.

errors do limit the accuracy of cesium frequency standards. Beam devices with 300 cps line widths have demonstrated greater accuracy than those devices with much narrower resonances. As time progresses it is expected that longer machines will more closely approach their ideal capabilities.

Certain fixed parameters and effects that determine absolute frequency may be measured by auxilliary experiments. The effects that are now considered to contribute the greatest inaccuracies are:

(a) The magnitude and nonuniformity of the C field, including variations in the magnitude over long periods,

(b) A phase difference between the two oscillating field regions, and

(c) A lack of purity of the electromagnetic field exciting the atomic transition.

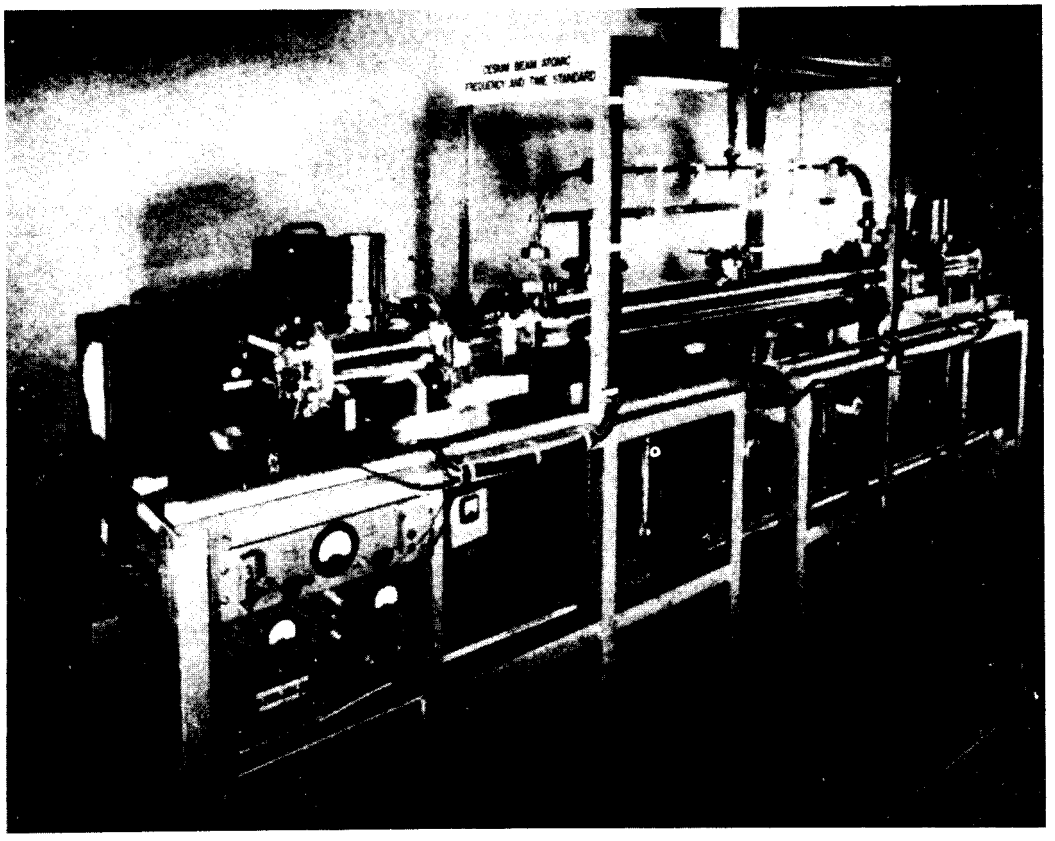

FIG. 21. NBS-II atomic beam frequency standard.

The method of measuring these effects and the results of the measurements together with the estimated uncertainty in absolute frequency will be presented for the United States Frequency Standard and alternate standard (see Mockler, *1*, *32*, *33*). The two devices are designated (NBS-II) and (NBS-I) respectively. They are shown in Figs. 20 and 21; their properties are given in the Appendix.

A. Magnetic Field Measurements

The magnitude of the C field is determined by observing a number of field sensitive microwave transitions, e.g., $(F = 4, m_F = \pm 1) \leftrightarrow (F = 3, m_F = \pm 1)$. The frequencies for these transitions are given by Eq. (24) which can be written to sufficiently good approximation as:

$$\nu = \nu_0 + 700.6 m_F \bar{H}_0, \tag{78}$$

where ν_0 is the hyperfine structure separation in zero field. The quantities ν and ν_0 are measured in kilocycles and $\bar{H}_0$ in oersteds.

The low frequency transitions for which $\Delta F = 0$, and $\Delta m_F = \pm 1$ are also used to measure the magnitude of the field and, in addition, the uniformity of the field. The frequency of these transitions is given by Eqs. (25) and (26). The abbreviated equation

$$\nu = 350 \bar{H}_0 \tag{79}$$

is a satisfactory approximation. The quantity ν is measured in kilocycles and $\bar{H}_0$ in oersteds. Small coils were placed at various positions (5 altogether) along the C field. The magnitude and uniformity of $\bar{H}_0$ is obtained by exciting each coil separately. A rotating coil fluxmeter, sensitive to 0.002 oe, provides still another method of measuring the field and its uniformity.

The uncertainty in the field measurements of amount δH_0 will produce an uncertainty in the standard frequency measurement given by

$$\delta \nu_0' = 854 H_0 \delta H_0; \tag{80}$$

$\delta \nu_0'$ is measured in cps and the field in oersteds. One would expect the average field $\bar{H}_0$ obtained from the microwave measurements to agree with the average of the local field measurements made at low frequencies and with the rotating coil fluxmeter, provided, of course, that a sufficient number of points are chosen along the field to give a good average. In NBS-I this is the case. The fields measured in the various ways agree within the precision of measurement. The maximum deviation in the C field in this instrument is ± 0.002 oe. In NBS-II there is a measured discrepancy of 0.004 oe in the average field measurements made by the different methods. This is still unexplained but seems to be associated with a deteriorating of the shielding properties of the μ-metal shields used to eliminate the earth's field, the fringing fields of the deflecting magnets, and other stray fields in the laboratory. When the shields were first installed there was no discrepancy between the various field measurements.

The average value of the square of the C field magnitude must be known in order to calculate the frequency ν of the peak of the resonance

curve and consequently the frequency of the exciting radiation at this point. It is obtained from Eq. (23) which can be written to sufficient approximation as:

$$\nu = \nu_0 + 427\overline{H_0^2}, \tag{81}$$

where ν and ν_0 are in cps and H_0 in oersteds. The zero field hyperfine separation, ν_0, is assumed to be 9192631770.0 cps for this calculation. The number 9192631770 $\pm$ 20 cps is the best value of ν_0 from astronomical time measurements as determined by Markowitz *et al.* (*5*). Additional significant figures are added simply to accommodate the additional stability of the atomic standards.

The average value of the field squared may be different from the square of the average field. Consequently, if the C field is not uniform, the low frequency measurements of H_0 at a sufficient number of points, n, would give the best value of $\overline{H_0^2}$. Using these data,

$$\overline{H_0^2} = \frac{1}{n}\sum_{i=1}^{n} H_{0i}^2,$$

where H_{0i} is the average field measured by the sensing coil at the ith position in the C field. The low frequency spectral line is subject to distortion and power shifts. Care must be taken to maintain the radiation field intensity H small compared to H_0 to avoid these "saturation" effects. Even at these low frequencies (7 to 21 kc) the Bloch-Siegert effect, Eq. (74), is unimportant (4–13 cps) insofar as the field measurements are concerned.

B. Phase Difference Errors

If the two oscillating fields of the Ramsey excitation structure are in phase, a maximum beam signal is observed at the resonance frequency. If the two fields are 180° out of phase, a minimum signal is observed at the resonance frequency. The central peak is shifted approximately a fringe width as the phase difference is shifted from 0° to 180°. Then if the width of the fringe is 120 cps, a phase difference of 1° will shift the frequency about 0.7 cps which is significant.

For the purpose of reducing the phase difference between the two fields, it was found quite effective to pass the beam through the two ends of a single rectangular resonant cavity electroformed in the shape of a *U*. The beam grazes the two end walls. The cavity is driven by the frequency multiplier chain through a coupling iris at the midpoint of the U. The cavity is made so that it may be rotated 180°, thus reversing the direction of traverse of the beam through the exciting structure. The frequency shift accompanying any phase difference will be in opposite directions for the

two orientations. The mean of the two frequencies is the line frequency and one-half the difference is the phase correction. Simple relationships for estimating this frequency shift from the plotted Ramsey pattern have been developed by Holloway *et al.* (*34*). Their method is less sensitive than the more common method of exchanging the oscillating fields.

C. Errors Resulting from Impure Radiation

The simple theory of spectral line shape assumes the atomic transition to be excited by pure sinusoidal or cosinusoidal radiation. If the electromagnetic field is not pure, rather large frequency uncertainties are possible in the measurements. Actually, of course, the transition is induced by a certain distribution of frequencies. This distribution is determined by the frequency multiplier and crystal oscillator from which the exciting radiation is derived. The radiation, in general, is composed of the carrier frequency, noise and discrete sidebands resulting from frequency modulation. The discrete sidebands are usually due to 60 cps—the power frequency—and multiples thereof. (In the cesium beam experiments it is possible to reduce the noise to a low enough level so that it is not the limiting factor in the precision of the frequency measurements). The sidebands are multiplied in

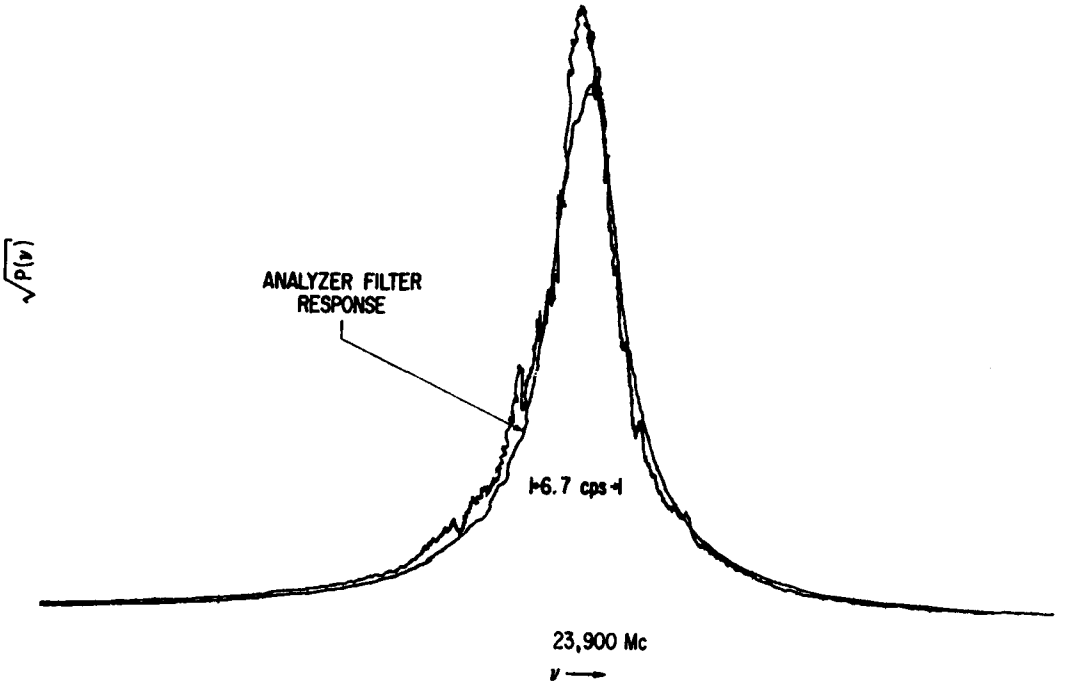

FIG. 22. The square root of the power spectrum of a 5 Mc quartz crystal oscillator multiplied in frequency to 23,900 Mc. This oscillator is used in the excitation chain of the United States Frequency Standard. The width and shape of the spectrum is essentially that of the response of the analyzing filter.

intensity by the factor of frequency multiplication. This factor is rather large (1836) and consequently these sidebands can introduce rather large frequency errors. Errors of this sort are particularly significant if the power spectrum is unsymmetrical.[10] Frequency shifts of a few parts in 10^9 have been observed by deliberately introducing sidebands unsymmetrically placed about the carrier.

Of course, if the power spectrum is known, the proper spectral line shape can be calculated in order to find the proper correction to the measured

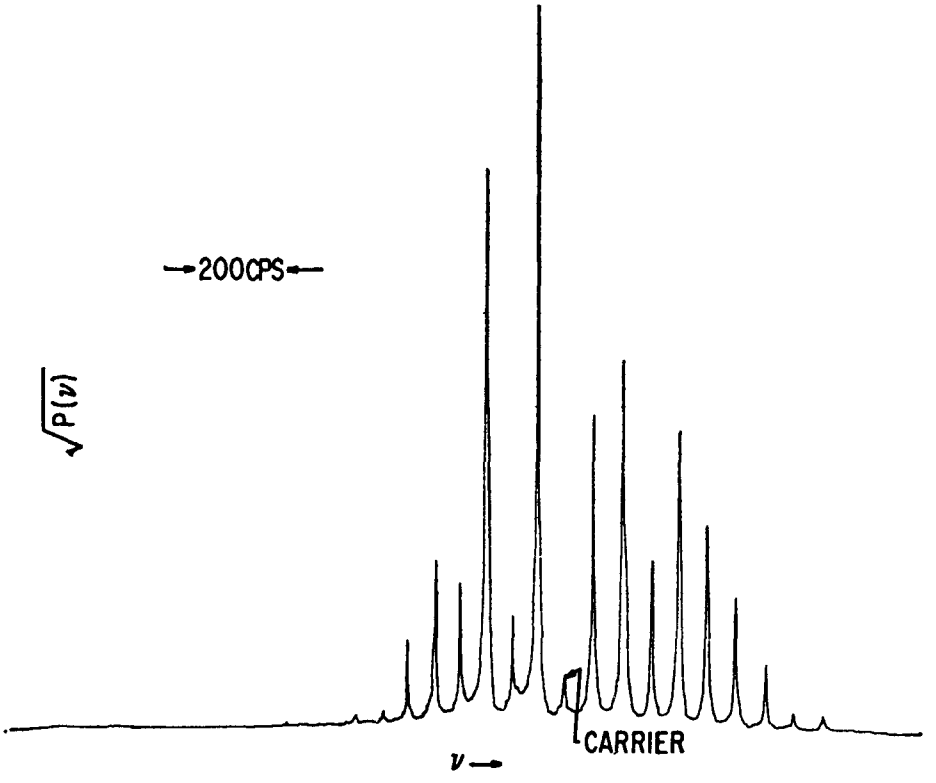

FIG. 23. The square root of the power spectrum of a 10 Mc quartz oscillator multiplied, in effect, to 15,000 Mc. Notice the 60 cps sidebands. The crystal in this oscillator is immersed in liquid helium.

frequency. It is both more desirable and much simpler to eliminate these sidebands so that the simple line shape theory applies. The square root of the power spectrum of a 5 Mc quartz crystal oscillator multiplied in frequency to 23,900 Mc is shown in Fig. 22. This is the oscillator used in the excitation chain of the United States Frequency Standard. Considerable care was taken with this oscillator to avoid 60 cps modulation. It was found necessary to use regulated dc power supplies in the filament circuits both

[10] An unsymmetrical power spectrum can arise when the carrier is frequency modulated with two or more different frequencies (*35*).

463-560 O - 72 - 5

in the oscillator and the frequency multiplier chain. Figure 23 plots the square root of the power spectrum of a similar oscillator circuit without regulation of the filament supply. The 60 cps sidebands are very prominent. Notice that the spectrum is quite unsymmetrical. In this spectrogram the 10 Mc oscillator was multiplied to 15,000 Mc.

The spectra of Figs. 22 and 23 were taken by means of an ammonia maser spectrum analyzer (*36*, *37*) developed by James Barnes and others in the Atomic Frequency and Time Standards Section of the National Bureau of Standards. The smooth trace in Fig. 22 is the response curve of the analyzer filter. It has been offset and reduced in intensity relative to the oscillator spectrum so that the two would not coincide. The resolution is insufficient to see the details of the spectrum. It can be said, however, that the spectrum has a width of 1 cps or less at 23,900 Mc. This is sufficiently narrow to assume that the cesium transition in the frequency standard is excited by a pure signal.

Low frequency crystal oscillators, for example, 100 kc oscillators, in most cases are unsuitable for exciting the cesium transition. The huge factors of frequency multiplication usually give power spectral widths greater than 1 kc at the cesium frequency. This is greater than the width of the cesium line. Ramsey (*7*, *38*) has considered the frequency shifts produced by exciting a transition with two or more signals close to each other.

D. Other Errors

The peak of the Ramsey pattern may be incorrectly determined if it is measured against a variable background of intensity. The cesium spectrum is essentially symmetrical about the $(F = 4, m_F = 0) \leftrightarrow (F = 3, m_F = 0)$ transition and overlap errors will tend to cancel. There may be, however, geometrical effects in the spectrometer that reduce the intensity of certain lines in the spectrum relative to their symmetrically placed counterpart. This would lead to an overlap error. The relative intensities of the lines on the high and low frequency side of ν_0 have been measured. The intensities of the $(F = 4, m_F = 1) \leftrightarrow (F = 3, m_F = 1)$ and $(F = 4, m_F = -1) \leftrightarrow (F = 3, m_F = -1)$ lines are found not to be the same but differ by about 25%. This leads to a calculated overlap error of about 1×10^{-12} at usual C field intensities. This estimate takes into account only superposition of the various lines of the spectrum. Lower fields will introduce still smaller errors. Transitions for which $\Delta m_F = \pm 1$, that is, π-lines, are not observable in the NBS standards and were not considered in the calculated estimate.

Saturation effects are thought not to contribute significantly to the frequency error because no frequency shifts were observable as the radiation field intensity was changed from very small values to rather large

values.[11] Beyond the values used, the line intensity was either too low or the line too broad for precise measurements. The problem of saturation as it applies to σ-transitions and the effect of the oscillating field in shifting the line frequency requires further theoretical study.

One would expect first order Doppler effects to broaden the spectral line by an unimportant amount. It is conceivable, however, that the small holes in the resonant cavity through which the beam passes radiate different amounts of energy. The entrance holes radiate differently than the exit holes. This radiation, though small, will be propagated against the beam from the entrance holes and in the direction of the beam from the exit holes. If both sets of holes radiate in the same way, the Doppler effect will broaden the line symmetrically. If they do not radiate in the same way the resonance peak will be shifted. A shift of this sort should be observable by rotating the waveguide exciting structure. It could be distinguished from a phase shift by changing the size of the holes. If the shift were very large, it would probably depend upon the radiation field intensity. No frequency shifts behaving in this way have been observed in the NBS standards.

Second order Doppler effect would introduce a fractional frequency shift of amount

$$\frac{\delta\nu}{\nu} = \frac{1}{2}\frac{\alpha^2}{c^2} \approx 5 \times 10^{-13},$$

where α is the most probable velocity of the atoms. This is a negligible shift for present experiments. Small but negligible frequency shifts arise from electric fields that might exist in the resonance excitation region. Haun and Zacharias (*39*) determined this shift experimentally and found it to be

$$\delta\nu_0 = 1.89 \times 10^{-6}\, E^2 \text{ cps},$$

where E is the electric field in volts/cm. For a field of 1 volt/cm,

$$\frac{\delta\nu_0}{\nu_0} = 2 \times 10^{-16}.$$

Frequency shifts incurred through frequency pulling of the resonant cavity are given approximately by

$$\Delta\nu_R = \left(\frac{Q_{\text{cavity}}}{Q_{\text{line}}}\right)^2 \Delta\nu_c$$

where $\Delta\nu_R$ is the shift in the peak of the atomic resonance line, and $\Delta\nu_c$ is the difference in frequency between the peak of the cavity response and the

[11] Relatively large saturation shifts are observed for π-transitions which are expected (*11*, *30*). These saturation shifts are also observed for σ-transitions if $m_F \neq 0$. The measured saturation shifts for the π transitions do not agree satisfactorily with Salwen's analysis.

peak of the spectral line. The estimated frequency shift from this source is about 4×10^{-14}.

E. Frequency Measurements

The fractional accuracy of the beam standard will be taken as the uncertainty in measurement of the Bohr frequency ν_0 relative to ν_0, i.e., $\delta\nu_0/\nu_0$. We suppose that ν_0 may have any number of significant figures required, so that the accuracy as defined here is limited only by the atomic standards themselves and not by inaccuracies in astronomical time measurements. Precision, on the other hand, will be understood to mean simply reproducibility. For example, if a fixed unknown phase difference exists between the two oscillating fields, the precision may be quite good but the accuracy is limited by the unknown phase shift.

An estimate of the fractional accuracy of a particular machine may be made by adding all of the experimentally determined fractional uncertainties contributed by the various effects considered in the preceding subsections of Section VII. Thus for NBS-II the uncertainty in the C field measurements introduces a frequency uncertainty of $\pm 8 \times 10^{-12}$, and the uncertainty in frequency due to a phase shift is $\pm 2 \times 10^{-12}$. Other effects discussed previously are expected to be negligible, or calculable. The estimate of the fractional accuracy is the sum or $\pm 1.0 \times 10^{-11}$ for NBS-II.

The uncertainty in the C field measurements of NBS-I give a frequency uncertainty of 4×10^{-12}. The uncertainty due to a phase shift is $\pm 2 \times 10^{-12}$, and the estimate of accuracy for NBS-I is 6×10^{-12}. There is a measurable phase error in NBS-I of 8×10^{-12}, however, this is a measurable shift and may be introduced as a correction. For one orientation of the NBS-I cavity the two devices disagree by 1.0×10^{-11}, and for the other orientation they disagree by 2.5×10^{-11}. The corrected measured zero field difference is 1.7×10^{-11}, which agrees with the sum of the individual estimates of accuracy for the two machines within the precision of measurement, which is 2×10^{-12}. These two standards are evidently limited in their accuracy by systematic errors and not by their line breadths, which are about 300 cps and 120 cps.

Comparisons between certain Atomichrons and the atomic frequency standard of the United Kingdom carried on at the National Physical Laboratory are discussed by Holloway *et al.* (*34*, *40*) and by McCoubry (*41*). Comparisons made through propagation data are given in Section VIII. Figure 24 shows a sample set of comparisons between NBS-I and NBS-II. The oscillator was noticeably more unstable the last half of the day for the measurements made in Fig. 24. This oscillator was less stable on this particular day than usual during the spring of 1960. The precision cited in the figure for the day's measurements is considered the standard

deviation of the mean which is

$$\sigma_M = \frac{1}{\nu_0}\left[\sum_{i=1}^{n} \frac{(\Delta\nu_i - \overline{\Delta\nu})^2}{n(n-1)}\right]^{1/2}.$$

The quantity $\Delta\nu_i$ is the ith measurement of the zero field frequency difference between the two standards, $\overline{\Delta\nu}$ is the average frequency difference and n is the total number of sets of measurements. For one method of comparison, see Mockler *et al.* (*1*). For the frequency multiplier chain circuits, see Schafer and Salazar (*42*). The circuits employed in the United Kingdom Standard are given by Essen and Parry (*43*).

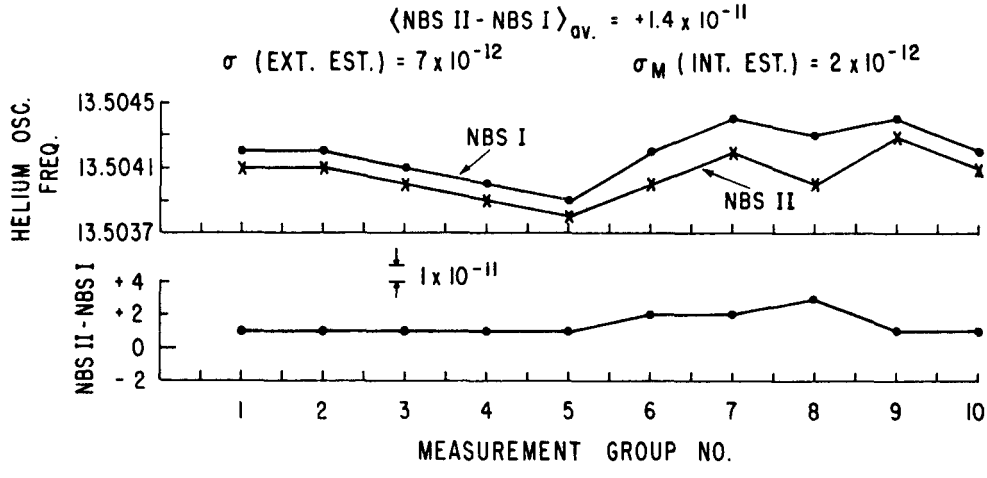

FIG. 24. A comparison of two cesium beam standards (NBS-I and NBS-II) by measuring the frequency of the same helium cooled crystal oscillator—one day's measurements. The crystal oscillator was unstable the last half of the day.

One method of measuring the frequency of a crystal oscillator in terms of the cesium resonance is shown in Fig. 25. This is the particular arrangement presently used with the United States standards. The ammonia maser stabilized crystal oscillator provides the most stable source for exciting the cesium transition that has been devised by the group. Other signal generators can be compared with this oscillator or with any signal output from either of the frequency multiplier chains for purposes of calibration. Also, any 5 Mc signal generator of sufficient stability may be used to drive the cesium beam chain directly for purposes of comparison with the cesium resonance.

It may prove practical to control the maser stabilized chain controlling the cesium excitation with a correction signal from the cesium beam. Thus the complete standard would be composed of an ammonia maser that would

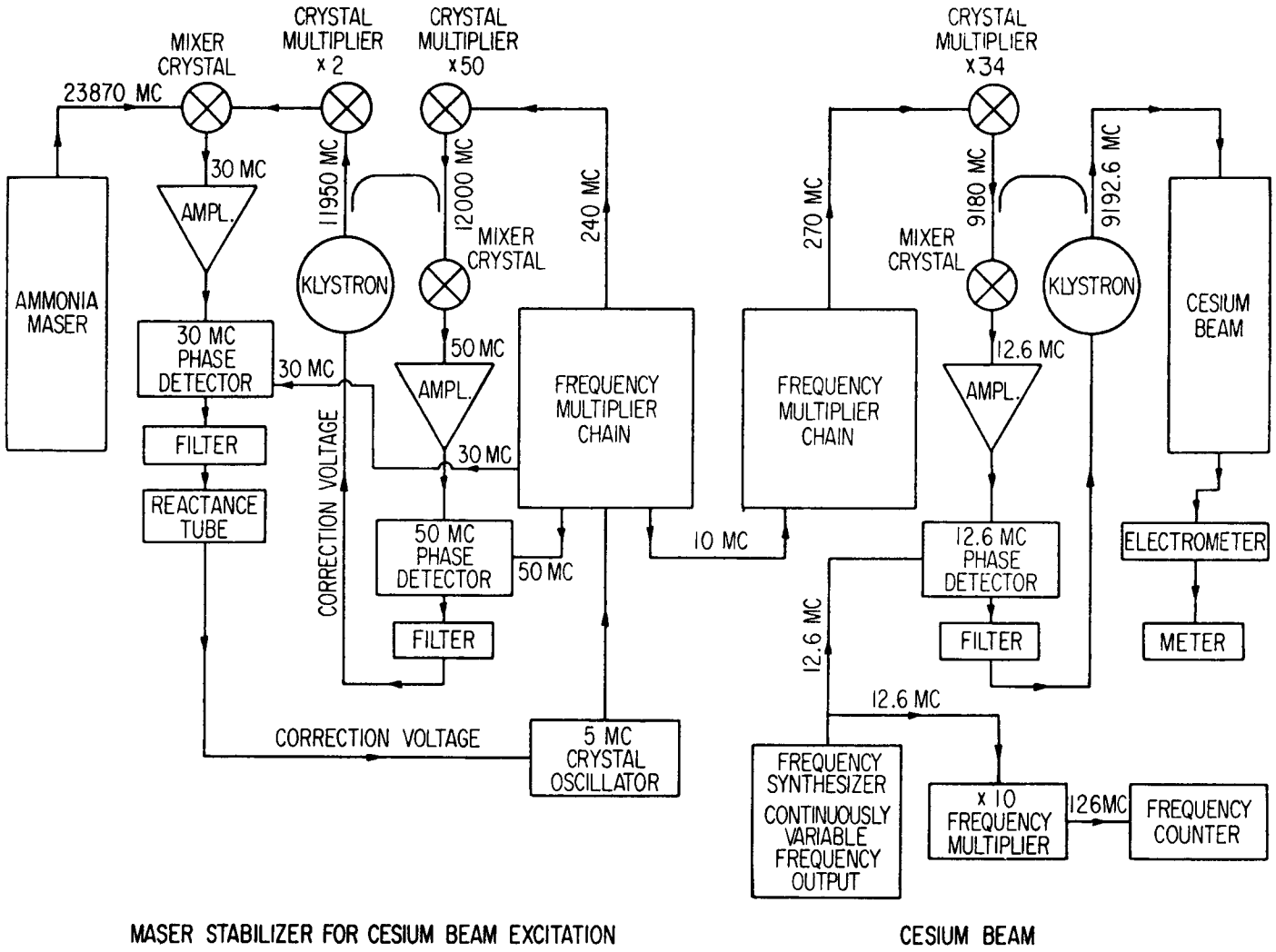

FIG. 25. A block diagram of the method of measuring the frequency of a crystal oscillator in terms of the cesium resonance used at the National Bureau of Standards. The crystal oscillator driving the cesium beam frequency multiplier is stabilized by an ammonia maser.

provide short term stability and the cesium beam which would determine the long term stability. If this device were operated continuously, and suitable scalars were added to accumulate cycles at, say, 5 or 10 Mc, then the device could properly be called an atomic clock.

VIII. Standard Frequency Comparisons between Cesium Standards via Propagation Data

Comparisons have been made through propagation data between the United States Frequency Standards, the United Kingdom standard at the National Physical Laboratory and four Atomichrons in the United States. The propagation data was obtained from the regular reports of: S. N. Kalra of the National Research Council of Canada; J. R. Pierce of the Cruft Laboratories; National Bureau of Standards Boulder Laboratories; Naval Research Laboratory, Washington, D. C.; and National Physical Laboratory, Teddington, England. The results are compiled in Table I. In this table the designation M_4 is the mean of the zero field frequencies of Atomichrons 106, 109, 110, and 112. The locations of these Atomichrons are indicated in the table.

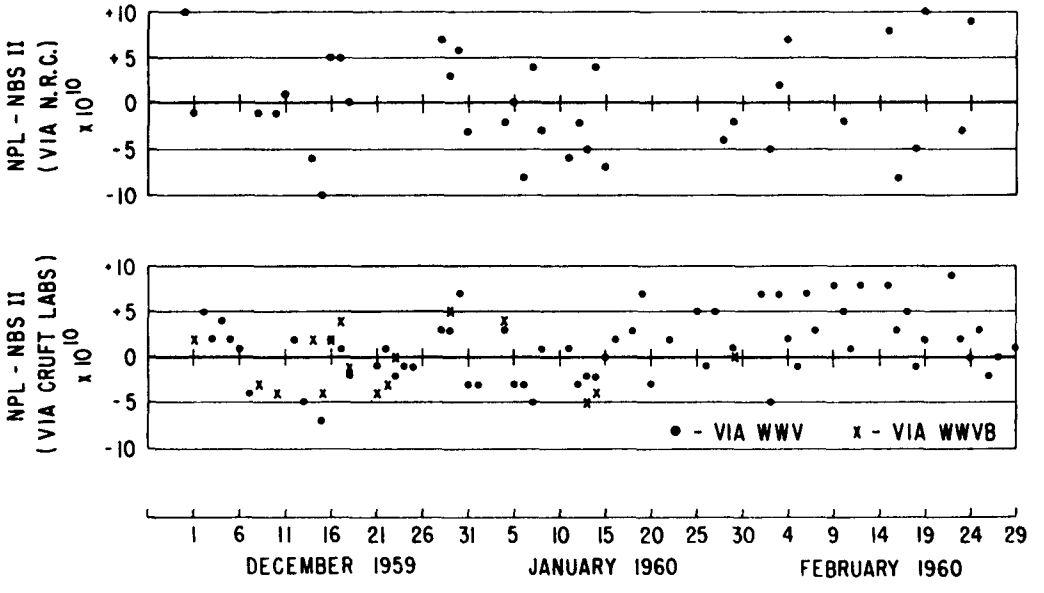

Fig. 26. Comparison of the United States Frequency Standard with that of the United Kingdom Standard using propagation data obtained from two different transmission links.

Figures 26 and 27 plot some of the data used in Table I and are given in order to display the scatter in the measurements. Figure 28 summarizes the propagation data available to date in terms of monthly averages.

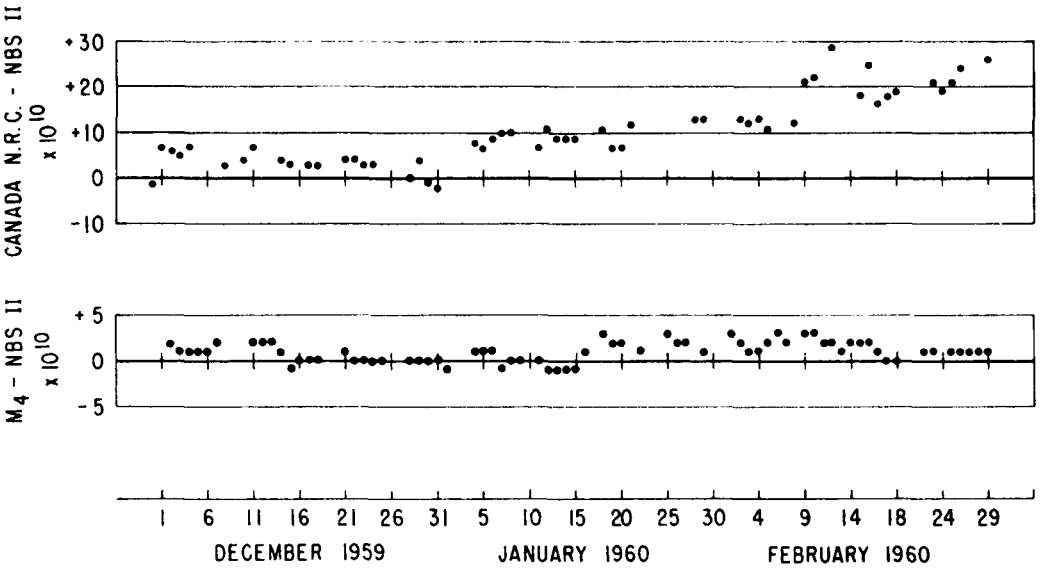

FIG. 27. Comparison of the United States Frequency Standard with that of Canada and with M_4.

TABLE I. SUMMARY OF 7-MONTH COMPARISONS BETWEEN NBS-II AND NPL, N.R.C. (CANADA), AND A GROUP OF 4 ATOMICHRONS[a]

Comparison	Number of daily comparisons used	Links used in the comparison
$(\text{NPL-NBS II})_{av} = +0.6 \times 10^{-10}$ via N.R.C. (Canada)	96	a. WWVB-NBS II b. WWVB-N.R.C. c. MSF-N.R.C. d. MSF-NPL
$(\text{NPL-NBS II})_{av} = +1.2 \times 10^{-10}$	128	a. 106-NBS II b. WWV-106—(30 day averages) c. WWV-112 d. MSF-112 e. MSF-NPL
$(\text{N.R.C.-NBS II})_{av} = +4.7 \times 10^{-10}$	128	a. WWVB-NBS II b. WWVB-N.R.C.
$(M_4\text{-NBS II})_{av} = +1.1 \times 10^{-10}$ 106—Boulder 112—Cruft 109—WWV 110—NRL	91	a. WWV-106 b. 106-NBS II c. WWV-110 d. WWV-112 e. WWV-109

[a] Data of Nov. 30, 1959 to June 30, 1960.

Discussions of the various frequency standards involved in these comparisons will be found in the published and unpublished literature (United Kingdom Frequency Standard, *2, 34, 40, 41, 43;* Canadian Frequency Standard, *3, 44;* The Atomichron, *27, 34, 40, 41;* The United States Frequency Standard, *1, 32, 33, 42*).

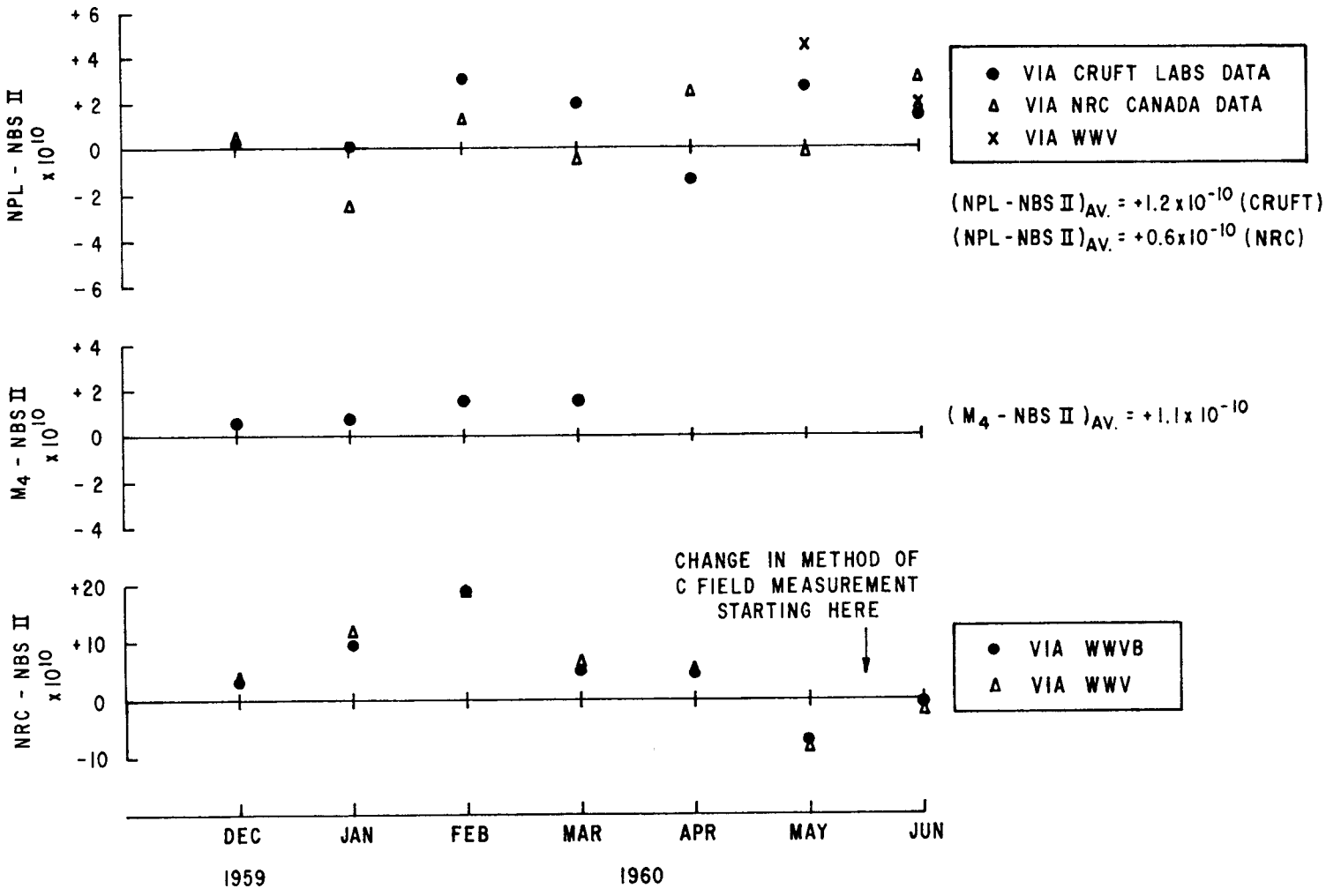

FIG. 28. Comparison of the United States Frequency Standard with the United Kingdom (NPL), Canadian (N. R. C.), and Atomichron standards using monthly averages.

IX. Thoughts on Future Developments

The atomic beam experiments that were carried on at the National Bureau of Standards demonstrate that beam devices of rather modest length (55 cm between the oscillating fields) can have a precision of 2×10^{-12} for measuring times the order of one hour. This is an order of magnitude better than the accuracy of these same machines. The limitation on the accuracy results from inadequate shielding and nonuniformity of the C field, and cannot be alleviated by narrowing the resonance line width. It appears that improvements in the C field would allow accuracies of 2×10^{-12} in these short beam devices. Until sufficiently uniform and permanent fields can be constructed, longer machines have limited usefulness insofar as accuracy is concerned. It does seem likely, however, that these developments will come about. Two long machines have been already put into operation. Essen and his group at NPL have an operating beam with the oscillating fields separated by 2.8 meters and a line width of about 50 cps. (*45*). The first estimate of accuracy was $1\text{–}2 \times 10^{-10}$ which was limited by the C field. Improvements in the magnetic shielding should yield higher accuracy.

Bonanomi and his group at Neuchâtel have a cesium beam with a 4-meter separation of the oscillating fields and a resonance line width of about 27 cps (*4*, *46*). Two long resonant cavities provide the two oscillating fields. In this way the Rabi pedestal is narrower and overlap errors should be smaller. Weaker C fields can be used, thus reducing the frequency uncertainty resulting from uncertainties in the C field. One disadvantage of this type of Ramsey structure is that it will likely be more difficult to measure phase shift errors. No estimate of the accuracy of this machine has been reported.

A. A Thallium Atomic Beam

Thallium-205 has been suggested by P. Kusch as a possible replacement for cesium in atomic beam standards (*47*). In view of the C field difficulties observed in the cesium standard, thallium is particularly attractive because it is much less field sensitive than is cesium.

The frequency of the field insensitive transition, $(F = 1, m_F = 0) \leftrightarrow (F = 0, m_F = 0)$, is given by

$$\nu(\mathrm{Tl}^{205}) = \nu_0(\mathrm{Tl}^{205}) + 20.4H_0^2, \tag{82}$$

where $\nu_0(\mathrm{Tl}^{205})$ is 21,310.835 ± .005 Mc (*48*). This is to be compared with

$$\nu(\mathrm{Cs}) = \nu_0(\mathrm{Cs}) + 427H_0^2$$

for the frequency of the field insensitive line of cesium. Thallium is 1/50th as sensitive to the magnetic field as cesium. Thallium has other advantages:

(a) The hfs separation ν_0 is more than twice that of cesium.

(b) There is a single σ-transition in thallium; there are seven in cesium. Frequency shifts due to overlap should be much less troublesome and a lower intensity C field can be used.

(c) There are only four states in the hfs of thallium (Fig. 29); there are 16 in cesium. Each thallium state, therefore, will have a higher population than the individual states of cesium. Higher signal intensities would then be observed for thallium if the detector efficiency were the same as for

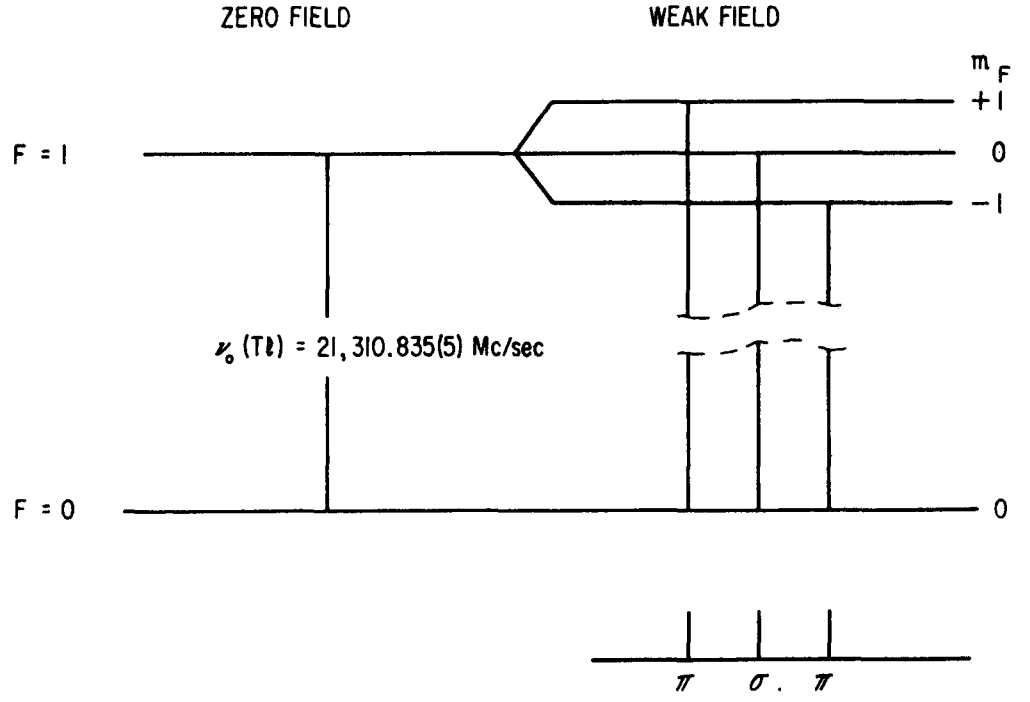

FIG. 29. The hyperfine structure of thallium (205) in the ground $^2P_{1/2}$ electronic state. $I = 1/2$.

cesium, which it is not. Thallium has the disadvantage that the method of detection is somewhat more difficult than the simpler method used for cesium. The relative efficiency must be determined experimentally before it can be said which atom will produce the better standard.

Both the National Bureau of Standards and the National Research Council of Canada are building thallium beams at the time of writing.

B. The Alkali Vapor Cell (49)

The alkali vapor frequency standard shows considerable promise although it has the disadvantage of inherent frequency shifts due to the buffer gases. These shifts are not sufficiently well understood to be treated

analytically; consequently certain recipes in construction would have to be prescribed if they were used as primary standards. Line breadths of 30 cps are attainable with much simpler apparatus than an atomic beam. Gas cell devices have been demonstrated by P. L. Bender and E. C. Beaty to have a frequency stability of 1×10^{-11} over a period of 1 month (*50*). A qualitative description of the operation of one of these devices follows.

Light from a rubidium-87 discharge is made incident upon a glass bulb containing Rb^{87} at a partial pressure of about 10^{-6} mm Hg. The bulb is contained within a resonant cavity tuned to the Rb^{87} hyperfine transition at 6835 Mc. The light radiation of interest from the lamp is the emission from the $5^2P_{3/2}$ and $5^2P_{1/2}$ states to the $5^2S_{1/2}$ ground state. By interposing a Rb^{85} absorption cell between the light source and the cavity, the light from one of the hfs lines emitted from the lamp (line *a* in Fig. 30b) can be subdued. Thus the Rb^{87} in the cavity cell will preferentially absorb b light. (The hfs of the optical radiation from both the $^2P_{1/2}$ and $^2P_{3/2}$ states will be about the same since the hfs intervals in the excited states are much less than in the ground state. The picture shown in Fig. 30b applies to both the $^2S_{1/2} \leftrightarrow {}^2P_{1/2}$ and $^2S_{1/2} \leftrightarrow {}^2P_{3/2}$ transitions.)

After excitation from the ground state to the excited states, rapid spontaneous decay back to the ground state occurs to both the $F = 2$ and $F = 1$ states with similar rates. An excess of population is accumulated in the $F = 2$ state since atoms are preferentially excited from the $F = 1$ state because of the Rb^{85} filter cell. Thus when the lamp is first switched on, the gas contained within the cavity is in thermal equilibrium and absorbs most strongly. After a time the population of the $F = 1$ state is depleted by the optical "pumping" of atoms out of this state and their subsequent accumulation in the $F = 2$ state. The gas cell becomes more transparent as indicated by an increased signal from the photo cell. If now microwave radiation of frequency 6835 Mc is applied to the cell, atoms will "flow" from the $F = 2$ state to the $F = 1$ state making more atoms available for excitation to the excited states. At this point the cell absorbs more of the incident light and a decrease in the photocell signal results. If the microwave radiation is swept through the 6835 Mc resonance the line shape may be recorded from the output of the photocell.

The inert buffer gas serves the purpose of prolonging the lifetime of the alkali metal atom in its $^2S_{1/2}$ ground state. In this state, the atoms can have many collisions with atoms of the inert buffer gas before having transitions induced between the $F = 2$ and $F = 1$ states by these collisions. Thus the lifetime of the atomic states will be prolonged by the collision processes. Collisions between the alkali atoms and the walls of the container will induce transitions, but the frequency of these collisions is drastically

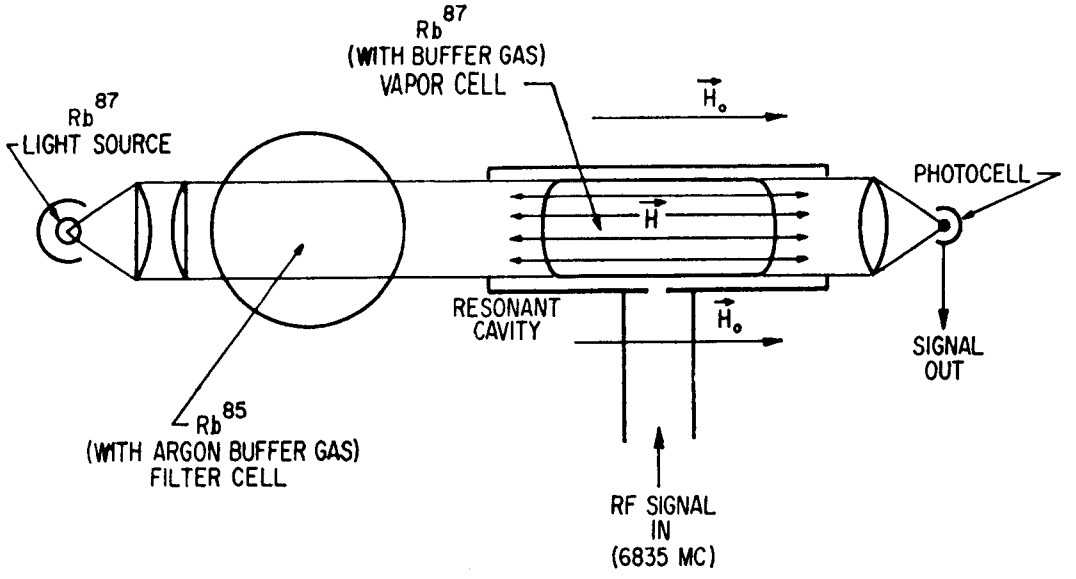

a

FIG. 30a. Rubidium-87 vapor cell. The hfs transition at 6835 Mc is observed by a change in intensity of the optical radiation transmitted through the vapor cell.

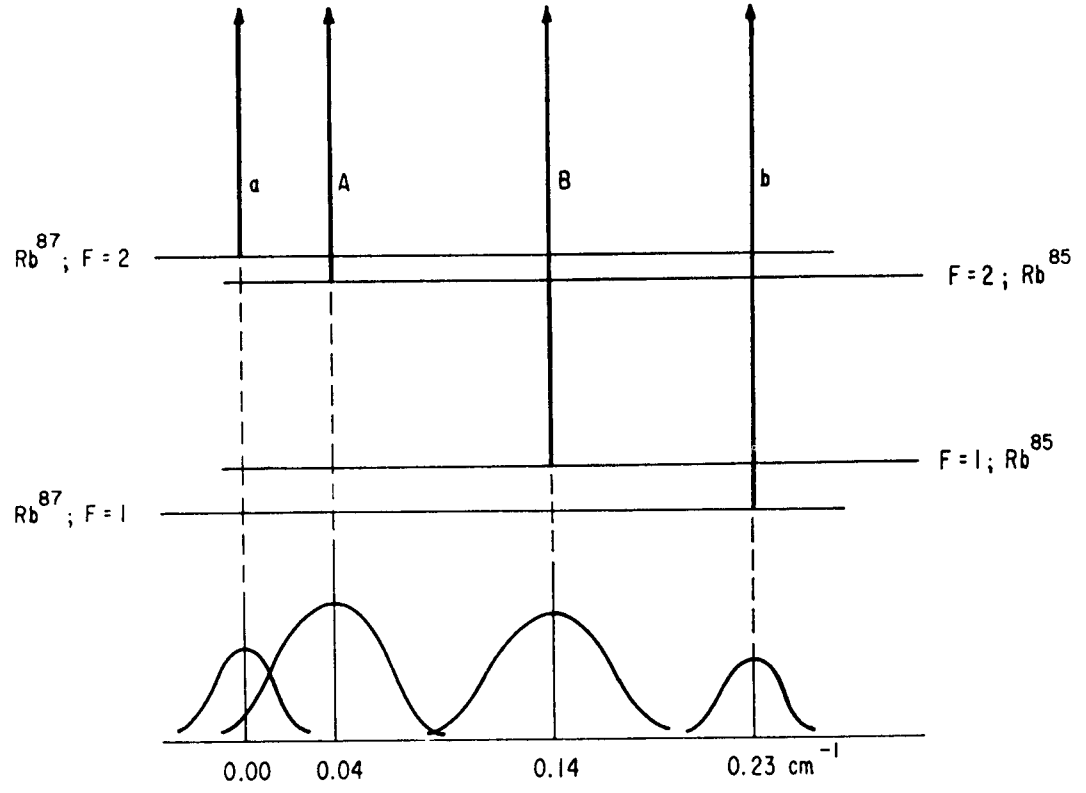

b

FIG. 30b. The filter action of the rubidium-85 bulb results from the overlap of lines a and A in the figure.

reduced by the presence of the relatively high pressure buffer gas. Doppler broadening is very small because the recoil momentum given to the radiating system by the emitted photons is distributed throughout the buffer gas via the many collisions that take place in the decay time (*51*, *52*). This "collision narrowing" is similar to the Mössbauer effect in which recoil-free gamma radiation is emitted by Fe^{57}, for example.

C. Molecular Beam Electric Resonance (53)

V. W. Hughes has suggested the $(J = 0) \leftrightarrow (J = 1)$ transition of Li^6F occurring at about 100 kMc as a frequency standard. It would employ the electric resonance beam technique which is similar to the atomic beam magnetic resonance technique. In electric resonance experiments deflections are produced through forces on the electric dipole moment in nonuniform electric fields. Electric dipole transitions are ordinarily observed. The molecular spectrum provides a much wider choice of frequencies and makes available much higher frequencies for use as a standard; higher frequencies will provide higher precision for a given signal-to-noise ratio. The molecules are distributed over a greater number of states than atoms in their ground state. Consequently, signal intensities will be substantially less. Signal intensities will generally be lower in electric resonance experiments than in a cesium beam experiment. This appears to be the primary drawback of the electric resonance method.

D. Masers

The ammonia maser has had considerable development as an extremely stable oscillator. An ammonia maser is used to stabilize the crystal oscillator driving the NBS cesium standards as mentioned previously (see Fig. 25). The measured stability for $N^{14}H_3$ masers is a few parts in 10^{12} for periods of a few minutes and about 2×10^{-11} for periods of several hours (*54*). The reproducibility of the $N^{14}H_3$ maser frequency is 2×10^{-10} (*55*). The best reproducibility, 3×10^{-11}, has been obtained using N^{15} ammonia by Bonanomi and his group (*4*). Ammonia containing N^{15} has the important advantage that the (3.3) line is single and not composed of a group of lines as is the (3.3) line of N^{14} ammonia. The relative intensities of the members of this group of lines will change with changes in the focusing voltage or beam intensity; this will cause a shift in frequency since this hfs is not resolved.[12]

Although the ammonia maser has good reproducibility for a given machine, it would probably be quite difficult to build other machines that

[12] Recently Barnes and Allan at NBS have obtained a reproducibility of 3×10^{-11} for N^{14} ammonia. They employ a servo system that continuously tunes the cavity to resonance. It uses Zeeman modulation to obtain the correction signal.

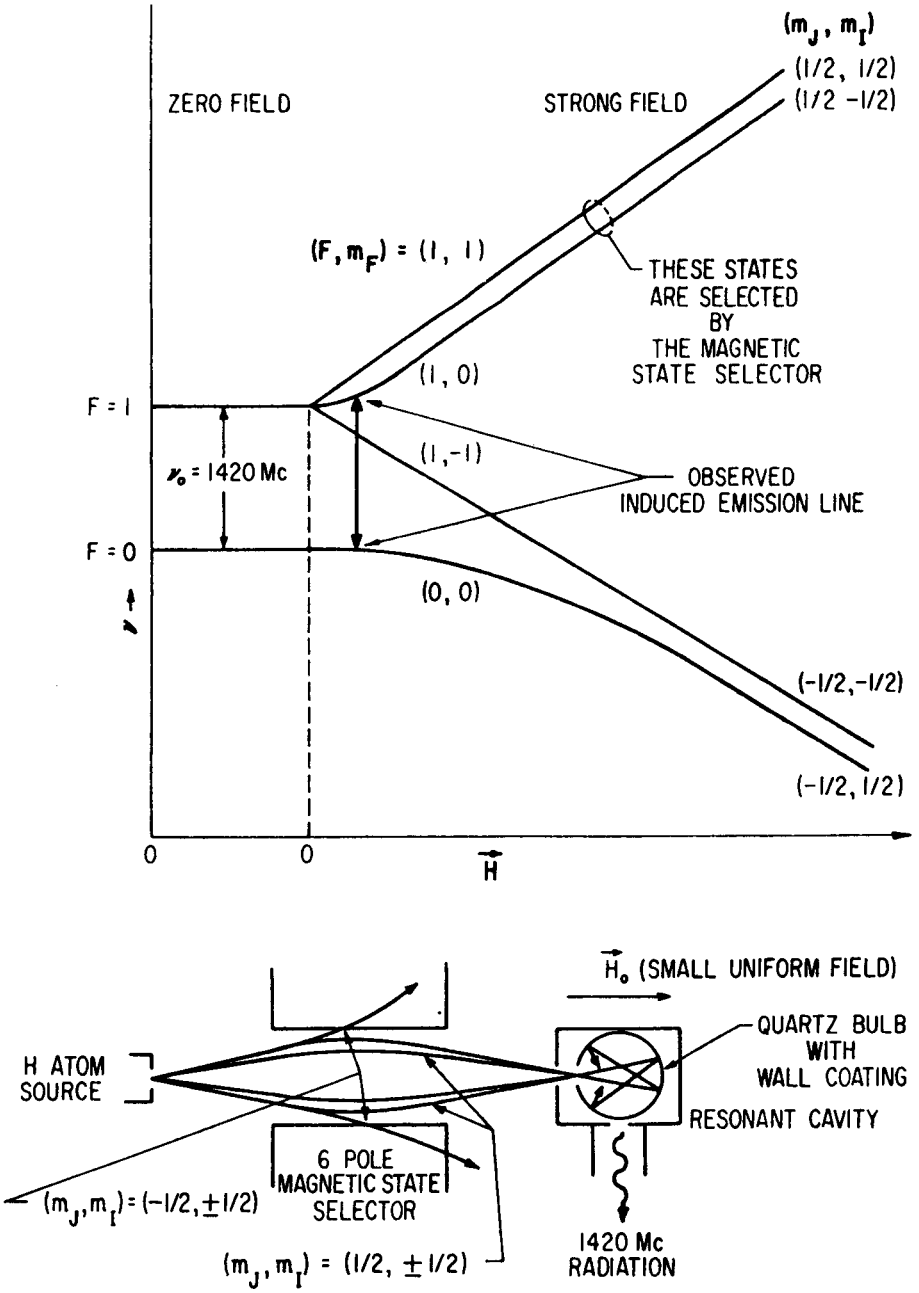

FIG. 31. The hydrogen atom beam maser.

would oscillate at frequencies closer than 1×10^{-9}. This places a rather severe limitation on its use as a primary standard. There are a number of parameters that must be carefully controlled. Furthermore, the Doppler shift cannot be precisely determined. The basic difficulty is that the frequency of the maser cannot be simply related to the Bohr frequency as it

can be for a cesium beam and the various parameters effecting the frequency require more delicate control. Other beam masers are being built to operate at higher frequencies (88 kMc, for example) by a number of laboratories, including NBS (*56*, *57*, *58*). These devices employ a Fabry-Perot interferometer as the resonator. Considerable progress has been made recently in the development of such resonators at millimeter wavelengths. Q's exceeding 100,000 are attainable (see the chapter entitled "Millimeter Wave Techniques," by W. Culshaw, in this volume).

Most recently Ramsey and his group at Harvard have succeeded in building a hydrogen atom maser (*59*) (Fig. 31). In this device hydrogen is dissociated in a discharge tube. A beam of hydrogen atoms effuses from the discharge tube and passes through a magnetic state selector. Atoms in the $F = 2, m_F = 1,0$ states are focused into a quartz bulb contained within a resonant cavity tuned to 1420 Mc, the hfs separation. The quartz bulb is coated with an inert, involatile film. Hydrogen atoms striking this film do not change their state—at least, not with a high probability. The atoms may have many wall collisions during the process of emission to the $F = 1$, $m_F = 0$ state. As a consequence of the long storage time in the cavity ($\sim$0.3 sec) by virtue of the wall collisions, the resonance line width (without regeneration) is about 1 cps.

The hydrogen beam maser differs significantly from the ammonia beam maser in two important ways: (a) The transitions are magnetic dipole transitions. (b) The radiating particles are retained in the resonating structure by wall collisions instead of passing directly through. It appears that this hydrogen maser is capable of higher stability than the ammonia maser because of its very narrow resonance width. However, there may be frequency shifts due to the wall collisions and perhaps some aging processes associated with the wall coatings.

Zero field solid state masers have been suggested by Bloembergen (*60*). Although such devices may provide highly stable oscillations, it is not certain how reproducible the frequency would be.

Acknowledgments

The author wishes to acknowledge the help of the various members of the Atomic Frequency and Time Standards Section of the National Bureau of Standards in the preparation of the manuscript.

The contributions of Messrs. Roger Beehler and James Barnes and Mrs. Mildred Beebe are of especial importance.

I wish to extend my gratitude to Drs. Peter Bender, William Culshaw, J. Holloway, L. Essen, J. Bonanomi, and Messrs. J. V. L. Parry, and P. Kartaschoff for many helpful discussions.

APPENDIX

The NBS Atomic Beam Frequency Standards Functional Data

	NBS-I	NBS-II
I. General dimensions (see Fig. 8b)		
l_1	11.5 cm	16.5 cm
l_2	5.1 cm	10.2 cm
l_3	46.0 cm	100.0 cm
l_4	46.0 cm	100.0 cm
l_5	5.1 cm	10.2 cm
l_6	11.5 cm	16.5 cm
II. Oven (adjustable)		
Temperature	150°C	150°C
Heater material	Nichrome	Nichrome
Heater current	0.8 amp	0.8 amp
Heater coil resistance (cold)	7 ohms	7 ohms
Slit dimensions	0.003 × 0.038 × 0.100 in.	0.015 × 0.100 × 0.187 in. (channeled)
III. Deflecting magnets (adjustable)		
Length	2.0 in.	4.0 in.
Gap width	0.040 in.	0.120 in.
Radius of convex pole piece, a (See Fig. 13.)	0.040 in.	0.120 in.
Radius of concave pole piece, b (See Fig. 13.)	0.050 in.	0.150 in.
Number of turns	200/magnet #22 wire	440/magnet #14 wire
Resistance of windings (cold)	2 ohms	1.6 ohms
Typical magnet current	1.4 amp	2–3 amp
Stern-Gerlach peak separation, each magnet	0.006 in.	0.040 in.
Power dissipation, each magnet	4 watts	5–14 watts
IV. Detector (adjustable)		
Material	80% Pt–20% Ir	80% Pt–20% Ir
Width	0.005 in.	0.015 in.
Current	0.6 amp	0.6 amp
Temperature	820°C	820°C
V. Center collimating slit (adjustable)		
Material	Plastic, brass, or aluminum	Plastic, brass, or aluminum
Width	0.003 in.	0.015 in.
VI. Resonant cavity		
Principle mode	$TE_{0,1,60}$	$TE_{0,1,100}$
Dimensions of beam holes	$\frac{1}{16} \times \frac{3}{16}$ in.	$\frac{1}{16} \times \frac{3}{16}$ in.
Coupling hole diameter	0.312 in.	0.328 in.
Loaded Q	~7000	~5500
Tuning range with adjustable probe opposite coupling hole	0.9 Mc	1.8 Mc
Separation of ends	56 cm	163 cm

463-550 O - 72 - 6

References

1. Mockler, R. C., Beehler, R. E., and Snider, C. S., *IRE Trans. on Instrumentation*, **I-9**, 120 (1960).
2. Essen, L., and Parry, J. V. L., *Phil. Trans. Roy. Soc.* **A250**, 45 (1957).
3. Kalra, S. N., Bailey, R., and Daams, H., *Nature* **183**, 575 (1959).
4. De Prins, J., and Kartaschoff, P., "Applications de la spectroscopie hertzienne à la mésure de frequences et du temps." Lab. suisse recherches horlogeres, Neuchâtel, Switzerland, 1960.
5. Markowitz, W., Hall, R. G., Essen, L., and Parry, J. V. L., *Phys. Rev. Letters* **1**, 105 (1958).
6. Kusch, P., and Hughes, V. W., *in* "Handbuch der Physik" (S. Flügge, ed.), Vol. 37, Part I, pp. 1–172. Springer, Berlin, 1959.
7. Ramsey, N. F., "Molecular Beams." Oxford Univ. Press, London and New York, 1956.
8. Kopfermann, H., "Nuclear Moments" (E. E. Schneider, ed. and transl.), Pure and Appl. Phys. Ser., Vol. 2. Academic Press, New York, 1948.
9. Bethe, H. A., and Salpeter, E. E., "Quantum Mechanics of One- and Two-Electron Atoms." Academic Press, New York, 1957.
10. Kusch, P., *Phys. Rev.* **100**, 1188 (1955); Wittke, J. P., and Dicke, R. H., *ibid.* **103**, 620 (1956); Anderson, L. W., Pipkin, F. M., and Baird, J. C., Jr., *Phys. Rev. Letters* **4**, 69 (1960).
11. Salwen, H., *Phys. Rev.* **101**, 623 (1956).
12. Breit, G., and Rabi, I. I., *Phys. Rev.* **38**, 2082 (1931).
13. King, J. G., and Zacharias, J. R., *Advances in Electronics and Electron Phys.* **8**, 1–83 (1956).
14. Friedburg, H., and Paul, W., *Naturwissenschaften* **38**, 159 (1951); Friedburg, H., *Z. Physik.* **130**, 493 (1951).
15. Lemonick, A., and Pipkin, F. M., *Phys. Rev.* **95**, 1356 (1954). Lemonick, A., Pipkin, F. M., and Hamilton, D. R., *Rev. Sci. Instr.* **26**, 1112 (1955).
16. Gordon, J. P., Zeiger, H. J., and Townes, C. H., *Phys. Rev.* **99**, 1264 (1955).
17. Zandburg, É. Ya., and Ionov, N. I., *Uspehki Fiz. Nauk* **57**, 581 (1959); English translation in *Soviet Phys.—Uspehki* **67**(2), 255 (1959).
18. Varnerin, L. J., Jr., *Phys. Rev.* **91**, 859 (1953).
19. Van der Ziel, A., *Physica* **9**, 177 (1942).
20. Strutt, M. J. O., and Van der Ziel, A., *Physica* **9**, 513 (1942).
21. Schockley, W., and Pierce, J. R., *Proc. IRE* **26**, 321 (1938).
22. Allen, J. S., *Proc. IRE* **38**, 346 (1950).
23. Daly, R. T., Ph. D. Thesis, Phys. Dept. Mass. Inst. Technol., Cambridge, Mass. (1954), unpublished.
24. Zacharias, J. R., Yates, J. G., and Haun, R. D., Mass. Inst. Technol., Research Lab. Electronics Quart. Progr. Rept. No.35 (1954), unpublished.
25. Milatz, J. M. W., and Bloembergen, N., *Physica* **11**, 449 (1946).
26. Polevsky, H., Swank, R. K., and Grenchik, R., *Rev. Sci. Instr.* **18**, 298 (1947).
27. "Instruction Manual for Atomichron Model NC-1001." National Company, Inc., Malden, Mass. 1957.
28. Condon, E. U., and Shortley, G. H., "Theory of Atomic Spectra," pp. 63–66. Cambridge Univ. Press, London and New York, 1951.
29. Torrey, H. C., *Phys. Rev.* **59**, 293 (1941).
30. Salwen, H., *Phys. Rev.* **99**, 1274 (1955).

31. Bloch, F., and Siegert, A., *Phys. Rev.* **57,** 522 (1940).
32. Mockler, R. C., Beehler, R. E., and Barnes, J. A., *in* "Quantum Electronics: A Symposium" (C. H. Townes, ed.) pp. 127–145. Columbia Univ. Press, New York, 1960.
33. Beehler, R. E., Mockler, R. C., and Snider, C. S., *Nature* **187,** 681 (1960).
34. Holloway, J., Mainberger, W., Reder, F. H., Winkler, G. M. R., Essen, L., and Parry, J. V. L., *Proc. IRE* **47,** 1730 (1959).
35. Black, H. S., "Modulation Theory," pp. 195–200. Van Nostrand, New York, 1953.
36. Barnes, J. A., and Heim, L. E., A high resolution ammonia maser spectrum analyser. *IRE Trans. on Instrumentation,* to be published.
37. Barnes, J. A., and Mockler, R. C., *IRE Trans. on Instrumentation* **I-9,** 149 (1960).
38. Ramsey, N. F., *in* "Recent Research in Molecular Beams" (I. Estermann, ed.), p. 107. Academic Press, New York, 1959. Ramsey, N. F., *Phys. Rev.* **100,** 1191 (1955).
39. Haun, R. D., Jr., and Zacharias, J. R., *Phys. Rev.* **107,** 107 (1957).
40. Essen, L., Parry, J. V. L., Holloway, J. H., Mainberger, W. A., Reder, F. H., and Winkler, G. M. R., *Nature* **182,** 41 (1958).
41. McCoubry, A. O., *IRE Trans. on Instrumentation* **I-7,** 203 (1958).
42. Schafer, G. E., and Salazar, H. F., A simple multiplier chain for excitation of cesium beam resonators. Natl. Bur. Standards (U.S.) report (1960), unpublished.
43. Essen, L., and Parry, J. V. L., *Proc. Inst. Elec. Engrs. (London), Pt. B* **106,** 240 (1959).
44. Kalra, S. N., and Bailey, R., *in* "Quantum Electronics: A Symposium" (C. H. Townes, ed.), pp. 121–126. Columbia Univ. Press, New York, 1960.
45. Essen, L., and Parry, J. V. L., *Nature* **184,** 1791 (1959).
46. Kartaschoff, P., Bonanomi, J., and De Prins, J., U. S. Army Signal Research and Development Lab., Ft. Monmouth, New Jersey, Proc. 14th Ann. Frequency Control Symposium (1960), pp. 354–360, unpublished.
47. Kusch, P., U. S. Army Signal Research and Development Lab., Ft. Monmouth, New Jersey, Proc. 11th Ann. Frequency Control Symposium, pp. 373–384 (1957), unpublished.
48. Lurio, A., and Prodell, A. G., *Phys. Rev.* **101,** 79 (1956).
49. Bender, P. L., *in* "Quantum Electronics: A Symposium" (C. H. Townes, ed.), pp. 110–121. Columbia Univ. Press, New York, 1960.
50. Carpenter, R. J., Beaty, E. C., Bender, P. L., Saito, S., and Stone, R. O., *IRE Trans. on Instrumentation* **I-9,** 132 (1960).
51. Dicke, R. H., *Phys. Rev.* **89,** 472 (1953).
52. Wittke, J. P., and Dicke, R. H., *Phys. Rev.* **103,** 620 (1956)
53. Hughes, V. W., *Rev. Sci. Instr.* **30,** 689 (1959).
54. Mockler, R. C., and Barnes, J. A., U. S. Army Signal Research and Development Lab., Ft. Monmouth, New Jersey, Proc. 13th Ann. Frequency Control Symposium, pp. 583–595 (1959), unpublished; Bonanomi, J., and Herrmann, J., *Helv. Phys. Acta* **29,** 224 and 451 (1956); Bonanomi, J., De Prins, J., Herrmann, J., and Karatschoff, P., *ibid.* p. 228; **30,** 492 (1957); Bonanomi, J., De Prins, J., and Herrmann, J., *ibid.* **31,** 282 (1958); Bonanomi, J., Herrmann, J., De Prins, J., and Kartaschoff, P., *Rev. Sci. Instr.* **28,** 879 (1957).
55. Mockler, R. C., Barnes, J. A., Beehler, R. E., and Fey, R. L., *IRE Trans. on Instrumentation* **I-7,** 201 (1958).
56. Gallagher, J. J., U. S. Army Signal Research and Development Laboratory, Ft.

Monmouth, New Jersey, Proc. 13th Ann. Frequency Control Symposium, pp. 604–617 (1959), unpublished.
57. Barnes, F. S., *in* "Quantum Electronics: A Symposium" (C. H. Townes, ed.), p. 57. Columbia Univ. Press, New York, 1960.
58. Culshaw, W., and Mockler, R. C., A Fabry-Perot maser. Natl. Bur. Standards (U.S.) report (1959), unpublished.
59. Goldenberg, H. M., Kleppner, D., and Ramsey, N. F., *Phys. Rev. Letters* **5**, 361 (1960).
60. Bloembergen, N., *in* "Quantum Electronics: A Symposium" (C. H. Townes, ed.), p. 160. Columbia Univ. Press, New York, 1960.

The Ammonia Beam Maser as a Standard of Frequency*

J. A. BARNES†, D. W. ALLAN†, AND A. E. WAINWRIGHT†

Introduction

The ammonia beam maser has presented certain problems when considered as a primary standard of frequency. These problems come about because the maser's frequency of oscillation is quite dependent upon a variety of parameters. Also, with several of these parameters there is no unambiguous way of selecting a particular value for the parameter. In the past these parameters have been difficult to control and caused undesirable drift rates.

Recently a servomechanism has been installed which has eliminated cavity-tuning effects;[1] *i.e.*, the cavity is continuously tuned to be at the resonant frequency of the molecule. The method will be shown later. The elimination of this parameter has also reduced the effects of the other parameters.

In the case of ammonia beam pressure and focusing voltage, there is no clear-cut way of selecting values in order to get the maser to oscillate at the "proper Bohr frequency."

In part, some of the trouble arises from the fact that the quadrupole moment of N^{14} in ordinary ammonia causes an asymmetric splitting of the $J=3$, $K=3$ inversion line. This trouble can be avoided by using $N^{15}H_3$ instead of the ordinary ammonia. The present experimental work has been confined to $N^{14}H_3$; however, as soon as a system capable of recirculating the ammonia is completed, data will be taken on $N^{15}H_3$. A considerable improvement in reproducibility when using $N^{15}H_3$ has been reported by others.[2]

With all of its problems, the ammonia beam maser using $N^{14}H_3$ has demonstrated a resettable frequency of better than $\pm 3\times 10^{-11}$.

Zeeman Modulation

It has been shown[3] that the cavity-pulling of the maser frequency is given approximately by

$$\nu_0 - \nu = \frac{\Delta\nu_l}{\Delta\nu_c}(\nu_0 - \nu_c) \tag{1}$$

where ν_0 is the natural resonance frequency of the ammonia molecule; ν is the frequency of oscillation of the maser; ν_c is the resonant frequency of the cavity; $\Delta\nu_l$ is the natural line width of the ammonia transition in the maser; and $\Delta\nu_c$ is the cavity bandwidth. It has been suggested by Shimoda, *et al.*[1,4] that a small magnetic field will cause a Zeeman splitting of the ammonia line and thus cause an effective broadening of the ammonia line width. If the cavity is tuned to a frequency other than ν_0, a frequency shift of the maser is observed with the application of the magnetic field.

Under the influence of a magnetic field, the line width is given approximately by (see Appendix)

$$\Delta\nu_l = \sqrt{(\Delta\nu_0)^2 + (\Delta\nu_H)^2} \tag{2}$$

where $\Delta\nu_0$ is the unperturbed line width for the ammonia transition and $\Delta\nu_H$ is the amount the lines are split by the magnetic field. (See Fig. 1.) It has been found[5] that $\Delta\nu_H$ is given by

$$\Delta\nu_H = \alpha H$$

where the constant α is approximately 718 cps/oersted.

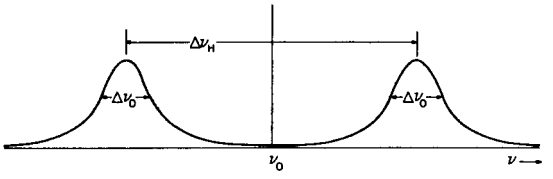

Fig. 1—Zeeman splitting of $J=3$, $K=3$ line of $N^{14}H_3$.

In order to obtain a continuous correction to the cavity tuning, the authors have found it desirable to apply a sinusoidally varying magnetic field to the maser; *i.e.*,

$$H = H_0 \sin \omega_m t.$$

Thus the line width will be given by

$$\Delta\nu_l = \sqrt{(\Delta\nu_0)^2 + (\alpha H_0)^2 \sin^2 \omega_m t}$$
$$= \sqrt{(\Delta\nu_0)^2 + \tfrac{1}{2}(\alpha H_0)^2 - \tfrac{1}{2}(\alpha H_0^2)\cos 2\omega_m t}.$$

* Received August 28, 1961. Presented at the WESCON Conf., San Francisco, Calif.; August 22–25, 1961.

† National Bureau of Standards, Boulder, Colo.

[1] J. C. Helmer, "Maser oscillators," *J. Appl. Phys.*, vol. 28, pp. 212–215; February, 1957.

[2] J. De Prins and P. Kartashoff, "Applications of Hertzian Spectroscopy to the Measurement of Frequency and Time," publication of Laboratoire suisse de recherches horlogeres, Neuchatel, Switzerland. (Topics on Radiofrequency Spectroscopy, August 1–17, 1960, International School of Physics, "Enrico Fermi," Varenna—Villa Monastero.)

[3] The reader is referred to J. P. Gordon, H. J. Zeiger, and C. H. Townes, "The maser," *Phys. Rev.*, vol. 99, pp. 1264–1274; August, 1955. While this is an approximate formula, it is sufficient to indicate the functional dependence of the maser frequency. Also a more elaborate theory[1] still suggests that $\partial\nu/\partial H = 0$ determines the natural resonant frequency which, incidentally, differs from other possible means of obtaining this frequency.

[4] K. Shimoda, T. C. Wang, and C. H. Townes, "Further aspects of the maser theory," *Phys. Rev.*, vol. 102, pp. 1308–1321; June, 1956.

[5] C. K. Jen, "Zeeman effect in microwave spectra," *Phys. Rev.*, vol. 74, pp. 1396–1406; November, 1948.

Applying the binomial theorem one obtains

$$\Delta\nu_l \approx \Delta\nu_0 \sqrt{1+\frac{x^2}{2}} - \tfrac{1}{2}\Delta\nu_0 \sqrt{1+\frac{x^2}{2}}\left(\frac{x^2}{2+x^2}\right)\cos 2\omega_m t + \cdots \quad (3)$$

where $x \equiv \alpha H_0/\Delta\nu_0$ and the approximation is valid to the degree that

$$\frac{x^2}{2+x^2} \ll 1.$$

Substitution of (3) into (1) gives

$$\nu = \nu_0 - \frac{\Delta\nu_0}{\Delta\nu_c}\sqrt{1+\frac{x^2}{2}}\,(\nu_0-\nu_c) + \frac{\Delta\nu_0}{\Delta\nu_c}\,\frac{1}{2\sqrt{2}}\,\frac{x^2}{\sqrt{2+x^2}}\,(\nu_0-\nu_c)\cos 2\omega_m t. \quad (4)$$

There are two things of interest in (4); first, the frequency of the modulation term is twice the frequency of the Zeeman field, as one would expect and, second, this modulation term is proportional to $\nu_0-\nu_c$. It is this latter property which enables one to simply construct a servosystem that will continually control the cavity tuning.

The authors have found that the most convenient and most noise-free method of demodulation is that of phase demodulation. The block diagram of the system used is shown in Fig. 2 and the equivalent servodiagram of the maser-crystal-oscillator phase-lock system is shown in Fig. 3. In Fig. 3 the transfer functions of the various components are indicated below the components.

From the theory of servosystems, the total transfer function for Fig. 3 is given by

$$\frac{\phi_0(\omega)}{\phi_m(\omega)} = \frac{K_1K_2K_3}{1+K_1K_2K_3}. \quad (5)$$

From this it follows that

$$\alpha(\phi_m(\omega)-\phi_0(\omega)) = V_1 = \alpha\phi_m(\omega)\left(1-\frac{K_1K_2K_3}{1+K_1K_2K_3}\right) = \alpha\phi_m(\omega)\left(\frac{1}{1+K_1K_2K_3}\right). \quad (6)$$

Substitution of the transfer functions into (6) yields

$$V_1(\omega) = \alpha\phi_m(\omega)\left[\frac{\omega^2\tau - j\omega}{\omega^2\tau+\alpha\beta-j\omega}\right]. \quad (7)$$

It is apparent that the bracketed expression in (7) has its maximum value when $\omega^2\tau \gg \alpha\beta$ which makes (7) have the value

$$V_1(\omega) \approx \alpha\phi_m(\omega). \quad (8)$$

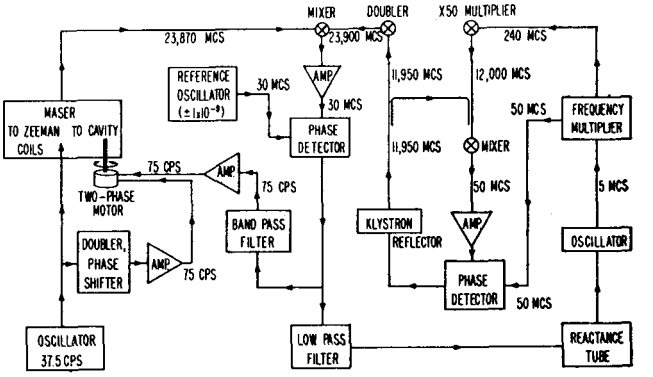

Fig. 2—Block diagram of complete system.

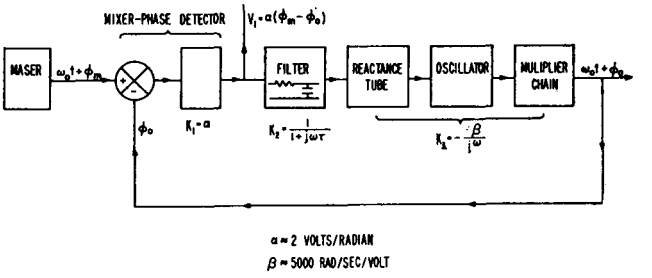

Fig. 3—Equivalent servodiagram for oscillator-maser phase-lock system.

As is customary in dealing with transfer functions, the quantities $\phi_m(\omega)$, $\phi_0(\omega)$ and $V_1(\omega)$ are the Fourier transforms of the time-dependent functions. Thus the voltage $V_1(t)$ can be obtained by taking the inverse Fourier transform of (8)

$$V_1(t) = \alpha\phi_m(t), \quad (9)$$

since α is a constant, and provided all important frequency components satisfy the relation $\omega^2\tau \gg \alpha\beta$.

Returning to (4), which can be written in terms of the total phase $\Phi(t)$,

$$\Phi(t) = \omega t + \phi_m(t) = 2\pi\left[\nu_0 - \frac{\Delta\nu_0}{\Delta\nu_c}\sqrt{1+\frac{x^2}{2}}\,(\nu_0-\nu_c)\right]t + \frac{\Delta\nu_0}{\Delta\nu_c}\,\frac{1}{2\sqrt{2}}\,\frac{x^2}{\sqrt{2+x^2}}\left(\frac{\nu_0-\nu_c}{2\nu_m}\right)\sin 2\omega_m t. \quad (10)$$

Comparison of (9) and (10) gives

$$V_1(t) = \gamma(\nu_0-\nu_c)\sin 2\omega_m t \quad (11)$$

where γ is the constant

$$\gamma = \left(\frac{\alpha}{4\sqrt{2}\nu_m}\right)\left(\frac{\Delta\nu_0}{\Delta\nu_c}\right)\left(\frac{x^2}{\sqrt{x^2+2}}\right) \quad (12)$$

and $(2\omega_m)^2\tau \gg \alpha\beta$.

Eq. (11), then, represents the demodulated signal from the maser. It should be noted here that the phase-

locked crystal oscillator's frequency is determined by the maser frequency and thus this servosystem serves a double purpose: 1) as a low-noise phase demodulator, and 2) as a precise frequency divider to facilitate comparison with other systems, *e.g.*, the cesium beam.

For the NBS maser system, γ has the value of approximately 3.5 mv per part in 10^{10} of $N^{14}H_3$ maser frequency. While this seems like a sufficiently sensitive detection system, it must be remarked that there still exist significant noise sources which will tend to limit the precision of balance. The most important of these sources is the crystal oscillator used in the maser phase-lock system. Any phase jitter of this oscillator signal after multiplication to K band will be detected as noise in the phase demodulator. It is interesting to note that if the maser is detuned one part in 10^{10}, the peak phase modulation on the maser is only about 0.14° at K band!

The oscillator which is used in the NBS maser system has demonstrated the most nearly pure spectrum of any oscillator analyzed to date.[6] In fact, except for a very small white-noise pedestal, it is difficult to be sure whether the maser or this oscillator has the more nearly monochromatic signal. Although some noise may be eliminated by narrow banding the demodulator, this process cannot be carried too far or the Nyquist conditions for stability of the servosystem will be violated.

The servoloop for the cavity tuning is completed by applying the amplified signal from the phase demodulator to one phase of a two-phase motor which in turn controls the depth of a small plunger in the maser's resonant cavity. The reference for the other phase of the motor is obtained by doubling the frequency of part of the signal from the Zeeman modulating field supply.

Due to inherent noise in the system, it has been found that a better time-averaged frequency is obtained from the maser if the gain is advanced to the point where small oscillations about the null modulation point just begin. Under these conditions, the servomotor is oscillating back and forth at a rate of about 2 cps, and at an amplitude of about ± 5 parts in 10^{10} in terms of maser frequency. An 8-sec average of oscillator frequency shows a standard deviation of about 3 parts in 10^{11}.

Returning to the condition on (11) that

$$(2\omega_m)^2\tau \gg \alpha\beta,$$

it is possible to determine the minimum time constant of the phase-lock filter. For the NBS system, the product $(\alpha\beta)$ is about 10^4 sec^{-1} and thus $\tau \gg 0.05$ sec. Typically, τ is chosen to be about 0.5 sec to 1.0 sec. Since this time constant must be taken this long, again the stability of the crystal oscillator must be very good or deterioration of the maser stability will result.

[6] J. A. Barnes and L. E. Heim, "A high-resolution ammonia-maser-spectrum analyzer," IRE TRANS. ON INSTRUMENTATION, vol. I-10, pp. 4–8; June, 1961.

BASIC MEASURING SCHEME

Quite an elaborate system is involved in detecting and dividing down the maser frequency. It is the purpose of this section to outline this system. See Fig. 2.

A 5-Mc crystal oscillator drives a multiplier chain. From this chain, 240 Mc is fed into a crystal multiplier; the 50th harmonic (12,000 Mc) of this and an 11,950-Mc signal from a klystron are fed into a crystal mixer. The 50-Mc beat note resulting is sent through an IF amplifier and then phase compared with 50 Mc from the multiplier chain. The phase difference is used as an error voltage to correct the klystron's frequency; hence, the klystron is phase locked to the 5-Mc crystal oscillator.

The klystron signal is sent to a crystal doubler giving 23,900 Mc. This signal goes in one side of a balanced crystal mixer. The maser's signal at approximately 23,870 Mc provides the reference into the other side of the above mixer. The 30-Mc beat note resulting goes to an IF amplifier and then to a phase detector. A frequency synthesizer, stable to better than a part in 10^8, is used as the reference into the other side of the phase detector. (One part in 10^8 at this reference gives a stability of about 1 part in 10^{11} at maser frequency.) The phase error resulting is then sent to a reactance tube which in turn corrects the frequency of the above-mentioned 5-Mc crystal oscillator. Therefore, the 5-Mc signal is phase locked to the maser's frequency, and hence the maser's stability can be analyzed by looking at the 5-Mc crystal oscillator or any multiple of it as derived from the multiplier chain.

EXPERIMENTAL RESULTS

Maser Frequency Dependence on Operating Conditions

It has been the intent of the authors to find most, if not all, parameters that give instability and that cause frequency shifts; also, the control of critical parameters has been of concern. Some of the frequency-dependent parameters are beam pressure, electrode focusing voltage, Zeeman modulation voltage, fluctuations in the magnetic field of the earth, background pressure in the maser's vacuum system, alignment of beam nozzles and electrodes with respect to the resonant cavity, temperature effects, and a few other influences, most of which are quite minor.

In connection with the beam pressure a variety of nozzles have been tried including klystron grid material, crimped foil, and special drilled single-hole nozzles. Most of the data have been taken with 0.02-inch single-hole nozzles; this is by no means the optimal nozzle to use, and this nozzle is used mainly for symmetry reasons in the NBS double-beam maser. Beam pressures typically used are in the vicinity of 6 mm of mercury; such a pressure gives a molecular mean free path (λ) of 8×10^{-4} cm. Since λ is smaller than the nozzle hole diameter, this disallows a Maxwellian velocity distribution, but rather gives cloud diffusion

which has a radial molecular intensity distribution. This system gives very uniform flow as can be illustrated from the frequency-time statistics, but quite a large consumption of ammonia (about 1 gr/hr).

Data were taken to determine the optimal beam pressure to use for frequency stability, and a typical family of curves is shown in Fig. 4. In another experiment the beam pressure was run up to about 14 mm of mercury to observe the continuation of the curves shown. It was found that the curves continued to approach each other and the second derivative became negative. This change in slope is attributed to a significant increase in the background pressure caused by the high flux of molecules.

By analyzing Fig. 4 one can quite easily observe the behavior of the focusing voltage V_F vs maser frequency since there is a 540-v difference between each of the curves in the family of curves plotted. The slope of maser frequency as a function of focusing voltage is positive with a positive second derivative also; the magnitude of the slope is in the vicinity of 1 part in 10^{10} of maser frequency per 200 v. This is rather severe for frequency stability, and the voltage has to be read to about 0.2 per cent in order to get resettability to 1 part in 10^{11}. This, of course, puts stringent requirements on the high-voltage power supply. One can further observe by analyzing Fig. 4 that the slope of frequency vs focusing voltage decreases for increasing beam pressures.

Another curve of interest is maser frequency vs the Zeeman frequency modulation voltage (see Fig. 5). If the Zeeman splitting coefficients are linear (the theory states they are to a first approximation—second-order effects are of the order[4] of 2×10^{-15} H^2—for all molecular frequency components within the range of the resonant cavity) then the slope of frequency vs modulation voltage should be zero. But the contrary result is that the curve has a negative slope of about 5 parts in 10^9 at maser frequency per oersted (rms); 2 volts rms applied to the magnetic-field coils of the NBS maser corresponds very closely to 1 oersted (rms) in the cavity. A similar effect has been observed on $N^{15}H_3$.[2]

With a slope as previously stated for maser frequency vs Zeeman modulation voltage, one might wonder if fluctuations in the earth's magnetic field would cause frequency shifts. From experiments performed it was found that the slope of this curve is essentially the same as for an ac field. Since the earth's magnetic field is about 0.56 oersted, a net shift of the maser's frequency of about 3 parts in 10^9 would be expected. Also, it was predicted that during fairly severe magnetic storms a frequency shift in the vicinity of 1 part in 10^{11} could be observed; an experiment was performed and an actual correlation was shown to exist. Since the shift due to magnetic storms is so small, it could be easily eliminated with a μ-metal shield around the maser's resonant cavity.

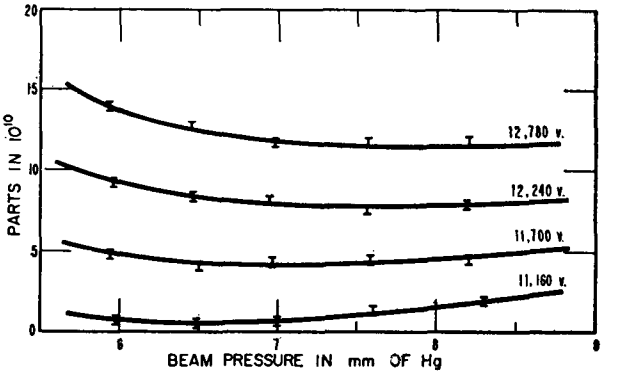

Fig. 4—Relative shift in maser frequency vs beam pressure.

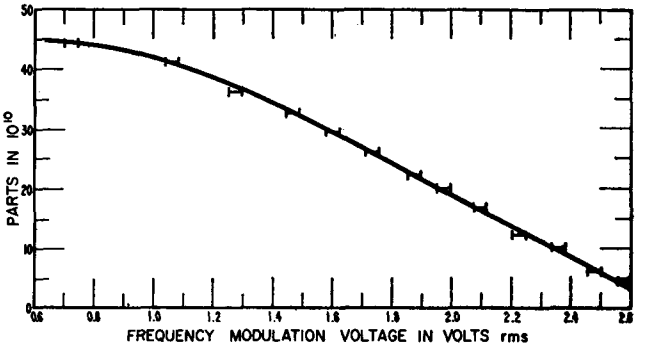

Fig. 5—Relative maser frequency vs modulation voltage applied to magnetic field coils.

Prior to the installation of the cavity-tuning servoloop, background pressure changes caused sizeable frequency shifts; for example, when the liquid-nitrogen cold traps on the maser's vacuum system were filled, of course the background pressure would change, and frequency shifts as high as 1 part in 10^9 were observed. Since the installation of the above-mentioned servoloop, cold trap filling and fairly large changes in the background pressure cause no measurable frequency shifts. Pressures typically used in the maser's vacuum system are 2×10^{-6} mm of mercury; no frequency shift has been observed up to pressures of 6×10^{-6} mm. Higher frequency shifts than this have been indicated though very marginal up to 1×10^{-5} mm.

The NBS maser has been taken apart and reassembled several times; each time a frequency shift has occurred along with changes in the parametric curves of Figs. 4 and 5, although the basic character of the curves has not changed. If pains are taken to duplicate alignment and configuration of nozzles, focusers, and cavity, the shift can be kept within 3 parts in 10^{10}—showing the critical nature alignment plays in the maser as a frequency standard. However, for any one alignment and configuration the stability for short term and long term is shown in Figs. 6 and 7. Such stability brings the maser to the status of a very good secondary standard.

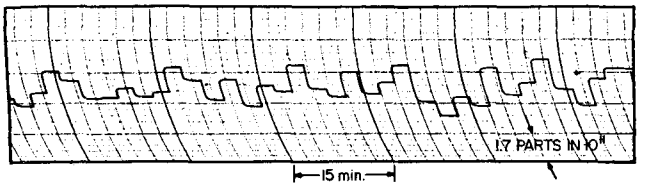

Fig. 6—Frequency of maser as a function of time. Each step represents an average frequency over an interval of approximately 78 sec. The record is 1½ hr long.

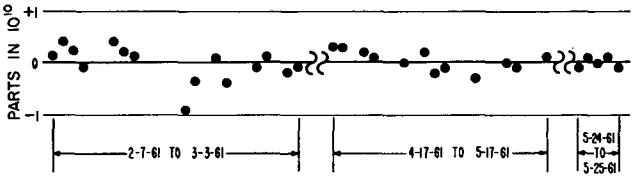

Fig. 7—NBS double-beam ammonia maser vs cesium beam (National Frequency Standard).

Maser Stability

In order to test the long- and short-term stability of the maser, comparisons have been made with a very stable (drift rate of about 6×10^{-12}/hr) quartz crystal oscillator and with the National Frequency Standard, cesium beam.

For short-term comparisons the oscillator that is phase locked to the maser is mixed with the oscillator mentioned above, and the period of the beat note is measured. Eight-second averages gave a standard deviation of 3 parts in 10^{11}; a large part of this is due to the oscillating cavity-tuning servoloop because the short-term stability of the free-running maser is only a few parts in 10^{12}.

The reader will remember that the period of oscillation of the cavity-tuning servoloop is about ½ sec; so if the time of averaging is long compared with the period of oscillation, the statistics should average out this oscillatory characteristic. Therefore, 78-sec period averages were taken, and a typical trace of the relative frequency fluctuations is shown in Fig. 6. This trace is 96 min long and gives a standard deviation of the mean of 1.3 parts in 10^{12}.

The long-term stability of the maser has been obtained by direct comparisons with the cesium beam. A plot of the day-by-day comparisons is shown in Fig. 7. Note that there are three sections; each one represents a new alignment and hence a different frequency (not indicated); the mean of each set is plotted on the same axis. Since the cesium beam usually has a standard deviation of the mean of less than 1 part in 10^{11} for any one measurement and the standard deviation for the plot in Fig. 7 is 3 parts in 10^{11}, one concludes that there is an unknown parameter in the maser system which is not in statistical control. It is felt at present that this is probably temperature-dependent elements in the maser system.

Conclusion

The experimental results show that an ammonia beam maser using the $J=3$, $K=3$ transition in ordinary $N^{14}H_3$ can be a very reliable secondary standard of frequency. As long as the alignment of the maser is not disturbed, its frequency is resettable to a precision which makes it quite competitive with the cesium beam and gas cell. The authors see no reason why such a maser system could not be run for years without deterioration of its resettability. With an improved servosystem, the short-term stability could probably approach that of the free-running maser itself and thus have this advantage over either the cesium beam or gas cell which depends on a quartz crystal oscillator for their short-term stability.

Perhaps one of the most encouraging aspects of the system is that everyone who has used $N^{15}H_3$ has reported a marked improvement over $N^{14}H_3$ in all operating parameters as theory predicts. It is hoped that the change to $N^{15}H_3$ may relegate this maser servosystem to a competitive primary standard of frequency.

Appendix

When a magnetic field is applied to the ammonia molecule, the spectral line for $J=3$, $K=3$ is split as shown in Fig. 1. Such a splitting, of course, changes the effective line width $\Delta\nu_l$ of the transition. Since this effective line width must be a function of the magnitude of the splitting only, it is reasonable, at least as far as functional dependence is concerned, to assume that the effective line width is related to the second moment of the perturbed line by the relation

$$\left(\frac{\Delta\nu_l}{2}\right)^2 = \frac{\int P(\nu)(\nu-\nu_0)^2 d\nu}{\int P(\nu)d\nu} \qquad (13)$$

where $P(\nu)$ is the probability of transition for the frequency ν, and ν_0 is the center of gravity of the line.

By a simple application of the parallel axis theorem one obtains

$$\left(\frac{\Delta\nu_l}{2}\right)^2 = \left(\frac{\Delta\nu_0}{2}\right)^2 + \left(\frac{\Delta\nu_H}{2}\right)^2 \qquad (14)$$

or equivalently

$$\Delta\nu_l = \sqrt{(\Delta\nu_0)^2 + (\Delta\nu_H)^2}. \qquad (15)$$

Acknowledgment

The authors wish to acknowledge the great amount of assistance given by R. E. Beehler and C. S. Snider in the comparisons with the cesium beam, and Dr. R. C. Mockler for some enlightening discussions and comments.

A Comparison of Direct and Servo Methods for Utilizing Cesium Beam Resonators as Frequency Standards*

R. E. BEEHLER†, W. R. ATKINSON†, L. E. HEIM†, AND C. S. SNIDER†

Summary—**Two systems, in which the frequency of a high quality quartz crystal oscillator can be controlled by a servo system employing as a reference frequency the ($F=4$, $m_F=0$)↔($F=3$, $m_F=0$) transition in the ground electronic state of cesium^{133}, have been in operation for about one year at the National Bureau of Standards. These systems are presently used in conjunction with the United States Frequency Standard, NBS II, and the alternate standard, NBS I, for measuring the frequencies of the United States Working Frequency Standards on a regular basis. The dependability, precision, and accuracy of the servo-derived measurements have been compared with the corresponding figures for the more direct manual method. Although both measurement systems have been found to be highly dependable, the servo method has significant advantages with respect to convenience of operation and measurement precision. These advantages can be utilized with no sacrifice of accuracy. Typical servo measurement precision is 2×10^{-12} for a 30-minute averaging time, while the measurement accuracy for both methods is 1.1×10^{-11}. For longer measurement periods of 12–14 hours, precisions and reproducibilities of 2×10^{-13} have been observed.**

Introduction

As a result of committee discussions held during the 1957 meeting of the Consultative Committee for the Definition of the Determining the Second, there arose a suggestion that, in studying and developing atomic frequency standards, preference should be given to systems in which the resonance absorption frequency is measured directly, as compared with devices which have an auxilliary oscillator whose frequency is controlled by a servomechanism. At the Boulder Laboratories of the National Bureau of Standards it was initially felt that the simplicity of measuring systems and techniques in which no feedback-type locking circuits are used would merit their exclusive use. In practice, however, the laboratory has come to utilize servo-type circuits to a larger and larger extent in the atomic frequency standards program. The use of these control systems has been expedient to the frequency measurements program primarily by reducing the labor involved in making a frequency measurement so that much more comparison data with an attendant gain in precision can be accumulated in a given amount of time than is possible by means of the more direct measuring technique involving manual determinations of frequency. In addition, the use of servo systems in some cases has resulted in a more useful measure of frequency.

Two systems, in which the frequency of a high quality quartz crystal oscillator can be controlled by a servo system employing as a reference frequency the ($F=4$, $m_F=0$)↔($F=3$, $m_F=0$) transition in the ground electronic state of cesium^{133}, have been in operation for over one year at NBS. These systems are presently used in conjunction with the United States Frequency Standard, NBS II, and the alternate standard, NBS I, for measuring the frequencies of the United States Working Frequency Standards on a regular basis. This paper is primarily concerned with the reliability of these servo-type measurements as compared with the more direct manual type of measurement.

Description of the Manual and Servo Measurement Systems

Block diagrams of the manual and servo measuring systems are shown in Figs. 1 and 2, respectively. In the manual system the unknown frequency f_x that is to be measured is multiplied by 1836 to approximately 9180 Mc. A klystron which excites the atomic resonance is then automatically electronically tuned by a servo, so that its beat note with the multiplied unknown is in phase synchronism with a variable frequency source whose frequency f at approximately 12.6 Mc is known to 1×10^{-8}. By changing the frequency f and observing the index of transition probability provided by the atomic beam detector current and displayed on a dc meter, it is possible to tune the klystron first to a frequency f_a about 50 cps above the cesium resonance and then to a frequency f_b equally offset below the cesium resonance. If f_u and f_l are, respectively, the frequencies of the tunable 12.6-Mc source corresponding to f_a and f_b, the unknown frequency f_x can easily be computed from the relation

$$1836 f_x + \frac{f_l + f_u}{2} = 9192631770.0 + \Delta f_0 \qquad (1)$$

where Δf_0 is the known frequency shift in the atomic resonance produced by the uniform magnetic C field, essential to the operation of the beam machine, and f_l and f_u are determined by electronic counter measurements. This method of measurement is referred to as the manual method because the frequencies f_l and f_u

* Received August 16, 1962. Presented at the 1962 International Conference on Precision Electromagnetic Measurements as Paper No. 8.3.

† National Bureau of Standards, Boulder, Colo.

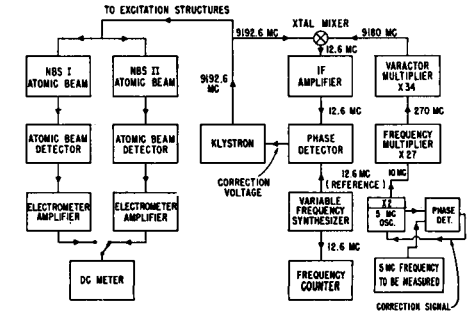

Fig. 1—Block diagram of the manual measurement system.

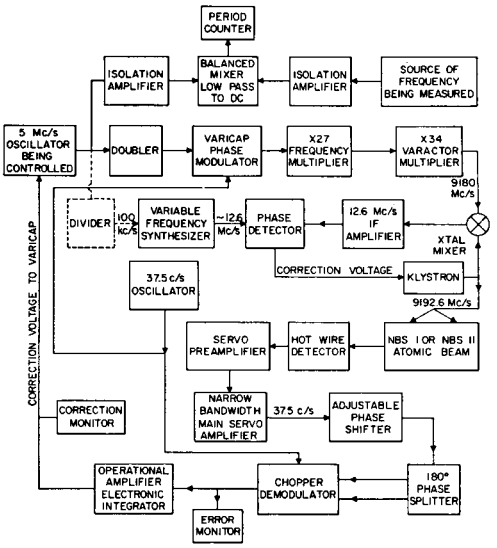

Fig. 2—Block diagram of the servo measurement system.

are alternately set by an operator so that the corresponding sequentially appearing beam currents are judged to be equal.

In the servo method of measurement shown in Fig. 2 the multiplier chain to 9180 Mc and the phase-lock klystron loop, including the source of the variable frequency f, are the same as used in the manual system. In this case, however, a high quality 5-Mc quartz-crystal oscillator, whose frequency f_s is to be controlled by the servo system, is used as the input to the multiplier chain. Phase modulation of a multiple of this frequency at a 37.5-cps rate is accomplished with the aid of a voltage-controlled diode capacitor in the output tank of the 5–10-Mc doubler. As a result of this modulation the beam current varies and the phase of the 37.5-cps component of the beam current depends on whether the average excitation frequency is above or below the cesium resonance frequency. In the postdetection servo electronics, a phase detector is used to develop a signed dc error signal which is integrated to produce a correction signal that is applied to a voltage-variable capacitor in the oscillator to control the frequency f_s at a particular value which depends on the value f of the variable source. With the servo loop closed, the frequency f_s at which the servo oscillator is locked can be computed from the relation

$$1836f_s + f = 9192631770.0 + \Delta f_0. \qquad (2)$$

Under normal operating conditions for the NBS II system, f is selected to be $\approx$12,632,000.0 cps and Δf_0 is 1.0 cps, which results in a value for f_s that is about 249×10^{-10} low relative to the nominal frequency of 5.0 $\cdots$ Mc. It should be noted that when f is derived from f_s through the use of a 5-Mc-to-100-kc divider and synthesizer, its appearance in (2) can be replaced by $(12.632/5)f_s$, where the numerical factor is exact. A measurement of the unknown frequency f_x is effected by measuring, with the servo loop closed, the period of the beat note between f_x and f_s—using an electronic counter. If the measured period is τ, then

$$|f_x - f_s| = \frac{1}{\tau} \qquad (3)$$

and f_x is determined since f_s is known from (2). The appropriate sign for the difference frequency, if not known, could be determined by shifting f_s in a known direction. The increased convenience of the servo measurement procedure over the manual is apparent, since the use of a digital recorder in conjunction with the period counter permits the accumulation of comparison data over long periods of time without the attention of operating personnel.

Both measurement systems have been used extensively at NBS and found to be highly dependable. The manual technique was used exclusively for a period of nearly two years and in conjunction with servo measurements for the past one year, while servo measurements have been emphasized more in the last year. Neither system has caused the loss of more than a few days of measurement time per year. Occasional problems with the manual system have been confined primarily to the electronic counter, klystron power supply, and components of the phase-lock klystron loop. These particular problems also affect the servo system operation which, in addition, has had minor troubles associated with faulty mechanical choppers and a malfunctioning power supply for the stabilized oscillator. Based on experience to date, then, no preference for one system or the other has been established with respect to dependability of operation.

Comparison With Respect to Measurement Precision

The term "precision," when used in connection with the NBS standards, refers to the extent to which a measurement of frequency is reproducible. Used in this sense the measure of precision would include contributions from both the standard itself and whatever source of frequency is being measured. The most commonly used

measure of precision for the NBS measurements is the standard deviation of the mean associated with the comparison data. For the manual method, the comparison data consists of a group of 20 to 50 determinations of the unknown frequency f_x, obtained by application of (1) to the raw data collected over a 30-minute period. Under normal measurement procedure, f_x is the 5-Mc output of one of the group of working standards maintained at NBS, consisting at present of 2 commercial cesium beam standards and 2 commercial rubidium vapor standards. A typical value of the measurement precision as defined above is about 8×10^{-12}. This precision figure can be reduced to 5×10^{-12} by collecting data over a $1\frac{1}{2}$-hour period. Representative groups of the manual data have been tested by using an appropriate computer program to determine the goodness of fit of a Gaussian distribution to the data. The primary significance of such a test stems from the central limit theorem of statistics. If the measurements did not exhibit a Gaussian distribution, it would be suspected that they were being influenced by at least one noncontrolled fluctuating variable that exerted a relatively large effect on the measurements. If the measurements did possess a Gaussian distribution, it would be suspected that, over the observation time, they vary because of the independent action of many variables which have about equal influence and that a significant improvement of precision could not be accomplished by controlling only a few of the variables that affect the outcome of a frequency measurement. A second reason for investigating the distribution bears on the usual interpretation of the standard deviation of the mean as providing limits within which lie 67 per cent of similarly determined means. This percentage is appropriate only for Gaussian distributions. The χ^2 test was used to give a single numerical measure of the over-all goodness of fit to a Gaussian distribution. In this test exact fit of the normal distribution curve to the experimental data would correspond to $\chi^2=0$, although such a value is extremely unlikely in practice because of statistical fluctuations. One group of 160 manual measurements was tested by dividing the data into 8 subgroups of 20 and computing χ^2 for each subgroup. The values of χ^2 ranged from 4 to 10 with an average of 6.6. One possible interpretation of this value is that because of statistical fluctuations there is a probability of about 60 per cent of finding a χ^2 value of 6.6 or higher even if the parent distribution of manual measurements is perfectly Gaussian. Therefore, one may conclude that a Gaussian distribution is a good fit to the observed distribution of the manual data.

The measure of precision for the servo-type measurements is taken to be the standard deviation of the mean of a set of frequency comparisons obtained from period measurements by using (2) and (3). When the frequency source to be measured is one of the NBS working standards, the precision is typically 2×10^{-12} for a 30-minute averaging period. This type of measurement is made on a daily basis at NBS and serves as the basis for published frequency measurements of the WWV, WWVL, WWVB, GBR, and NBA radio transmissions. Computer analysis of 519 measurements of 3 different working standards made over a period of several months gives an average χ^2 of 6.7—almost exactly the same as for the manual case and again indicative that a Gaussian distribution is a good fit to the data.

Comparisons have also been made between the two NBS frequency standards operating with independent servo systems. Data from two long comparison runs of 27 hours and 12 hours is shown in Figs. 3 and 4, respectively. Each point plotted on the uppermost curve in each figure is an average of 100 periods of the beat frequency between the two controlled oscillators. Since the period was 1.8 seconds, each point represents a 3-minute average followed by a counter display time of equal duration. The other plots in each figure indicate how the relative stability of the standards varies with the amount of time over which the data is averaged. The vertical bar at each point represents the precision of measurement. Analysis of the 27-hour run shows a precision of measurement for 30-minute averaging times of about 1.5×10^{-12}, compared to 2.5×10^{-12} for the servo comparisons with the working standards. If the 27-hour data is split into a 13-hour average and a 14-hour average, which are then compared with the 12-hour average obtained 5 days earlier, the three measurements of the frequency difference between the two standards differ by less than 2×10^{-13}. The value of χ^2 computed from the 267 values of the 27-hour comparison is 6.4, which once again is in close agreement with values obtained in other types of comparisons. From the uppermost plot in Fig. 3 it seems rather apparent that a significant amount of correlation is present among the 6-minute averages. In order to obtain some sort of quantitative measure of this effect the autocorrelation function was computed. The function drops to 49 per cent of the variance after 6 minutes but is still 20 per cent of the variance after 1 hour.

Comparison With Respect to Accuracy

The term "accuracy" refers to the degree to which the atomic frequency standard approaches the value f_0, the idealized resonance frequency for the cesium atom in its unperturbed state. This accuracy with respect to f_0 for the manual method of measurement is usually limited primarily by uncertainties associated with the uniform magnetic C field, phase differences between the two oscillating electromagnetic fields producing the atomic transition, the spectral purity of the excitation radiation, and effects of other neighboring atomic transitions.[1] An internal estimate of the accu-

[1] R. C. Mockler, R. E. Beehler, and C. S. Snider, "Atomic beam frequency standards," IRE Trans. on Instrumentation, vol. 9, pp. 120–132; September, 1960.

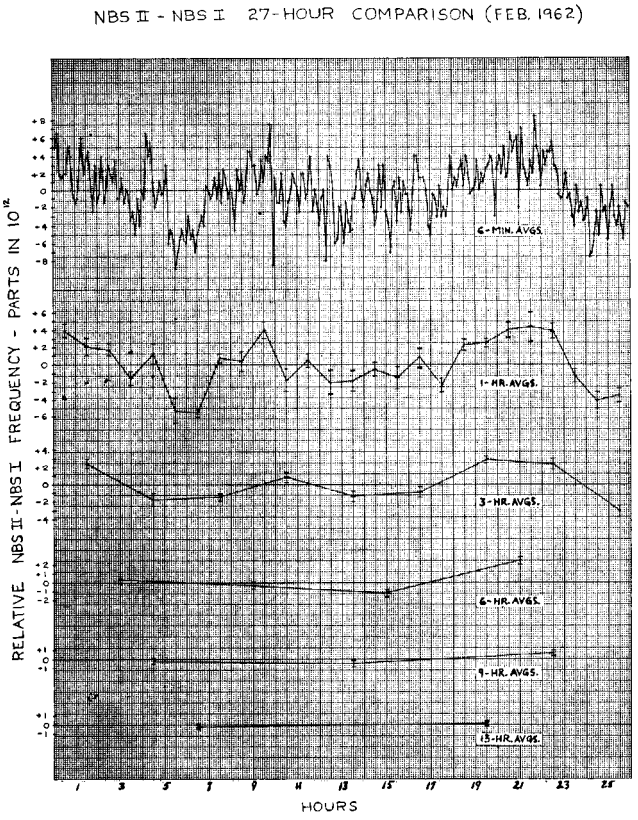

Fig. 3—27-hour frequency comparison of NBS I and II.

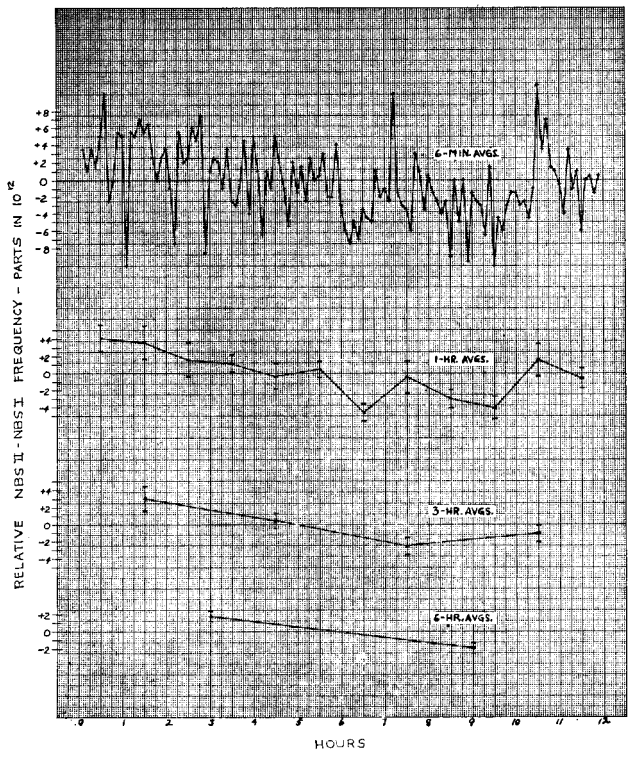

Fig. 4—12-hour frequency comparison of NBS I and II.

racy can be made by combining the estimates of possible frequency shifts due to the above causes.

For the case of NBS II the magnetic C field is produced by passing a current through a rectangular array of four parallel wires located within a triple-layer magnetic shield assembly. The field of about 0.047 oersted is calibrated by frequency measurements of the $(4, 1)\leftrightarrow(3, 1)$ and $(4, 1)\leftrightarrow(3, 0)$ microwave transitions of cesium which are strongly dependent upon the magnitude of the field. The field value for a given current is then determined from a least-squares fit of a straight line to the combined data. The uncertainty associated with this value is the computed standard deviation for a point interpolated from the least-squares line. The corresponding uncertainty in a frequency measurement is 5×10^{-12}, which serves as an estimate of possible inaccuracy due to incomplete knowledge of the C field. The measured nonuniformity of less than ±0.001 oersted does not contribute significantly to the accuracy figure.

If a phase difference exists between the two separated oscillating fields exciting the resonance in the Ramsey technique, a frequency shift will result. This effect may be observed by rotating the resonant cavity 180° and looking for a resultant frequency shift. For NBS II the measured shift is 4×10^{-12}, which means that one half of this amount or 2×10^{-12} is the actual frequency error produced by the phase difference. Since this amount can be applied with the appropriate sign as a correction to all frequency measurements, the only contribution to inaccuracy from this source is considered to be the uncertainty in the measurement which is about $\pm2\times10^{-12}$.

Another factor which has been observed to cause large frequency shifts under some conditions is the spectral purity of the radiation exciting the atomic transition. Shifts as large as 32×10^{-10} have been observed by exciting the resonance with a signal containing unsymmetrical sidebands in addition to a carrier frequency. This effect can be eliminated by proper design of the multipliers and, in the event the oscillator being measured is itself at fault, by utilizing an auxiliary oscillator phase-locked to the oscillator being measured with time constants chosen to make use of the long-term stability of the oscillator being measured and the short-term stability of the phase-locked oscillator. The auxiliary oscillator must not have troublesome sidebands and in addition, if the crystal current is high, noise effects will not be troublesome.

Another source of possible errors is the influence of neighboring transitions in the atomic spectrum. Significant frequency shifts may result in measurements made at low C fields, since the separation between transitions is proportional to the magnitude of the field. For measurements made with NBS II at a field of 0.020 oersted, for example, a systematic shift of 3.7×10^{-11} was detected. It has been found possible to eliminate this error by operating at sufficiently high fields (0.047 oersted for NBS II).

A final factor which has produced some error in the past in manual measurements of one particular commercial cesium beam standard involves the necessity for the operator to average by eye the observed beam variations. For this particular frequency source, oscillation in its servo loop produced a corresponding irregular oscillation in the beam current as observed on the dc meter. The manual measurement of this source showed a consistent error of 4×10^{-11} compared to a measurement not requiring the visual averaging of these oscillations. No measurable errors of this type have been found with more recent standards of this type or other frequency sources.

Other possible sources of error which have been investigated and found to make no measurable contribution to the inaccuracy of manual measurements include detuning of the resonant cavity, variations in the microwave power level, changes in the beam geometry and individual operator bias.

The figure of accuracy for a given manual measurement will depend upon the above estimates and the precision of the particular measurement. If we make the reasonable assumption that the above sources of error are independent and use 8×10^{-12} as the precision (typical of a 30-minute measurement), the over-all estimate of accuracy would be the square root of the sum of the squares of the separate estimates or about $\pm1\times10^{-11}$. If the measurement time extends over several days or if the measured source is unusually stable over the measurement period, it has been found possible to achieve a precision of 2×10^{-12} with a corresponding improvement in the accuracy estimate to 6×10^{-12}. An external estimate of the accuracy can be obtained by measuring the actual frequency difference between two similar atomic standards. If 6×10^{-12} is considered to be the accuracy for both NBS I and NBS II, the measured difference would not be expected to be much larger than the standard deviation associated with the difference frequency or 8.5×10^{-12}. The actual measured difference of $(1.6\pm0.4)\times10^{-11}$ or nearly two standard deviations could be expected with only about 5 per cent probability as a result of random sampling. In view of this apparent inconsistency between the internal and external estimates and because of the possible existence of sources of error not yet recognized the larger external estimate of $0.707\times1.6\times10^{-11}$ or 1.1×10^{-11} is considered a more appropriate accuracy figure with respect to f_0 for the manual measurement technique. Considerable confidence in this estimate has been gained during the past 3 years in view of the fact that the measured difference between NBS I and II of 1.6×10^{-11} has remained within a few parts in 10^{12} in spite of major changes in the magnetic shielding and method of producing the C field for both standards and replacement of the end sections of the resonant cavity in NBS I.

Possible sources of measurement error for the servo mode of operation include most of those already discussed for the manual case, plus effects associated with parameters of the servo system electronics. The only error sources characteristic of the manual system which are not applicable to the servo measurements are those of individual operator bias and effects of averaging beam variations by eye. The previously determined estimates of accuracy of 5×10^{-12} and 2×10^{-12} for C-field uncertainties and phase difference, respectively, should apply directly for the servo method also. The problem of the spectral purity of the radiation becomes much more complex for the servo case, since knowledge of the spectrum is generally not sufficient for predicting the existence or magnitude of any frequency shifts. Measurements to check for possible dependence of the frequency on cavity detuning and microwave power level were performed using the servo as well as the manual technique in order to take advantage of the higher precision capability of the servo system. Detuning of the resonant cavity by approximately 1 Mc produced a shift of 1×10^{-12}—well within the measurement precision. Variation of the microwave power level from 0.5 to 2.0 mw produced no significant frequency shift. This data is plotted in Fig. 5. The vertical bars at each point in this graph, as well as in the succeeding ones, represent the measurement precision in the sense defined previously.

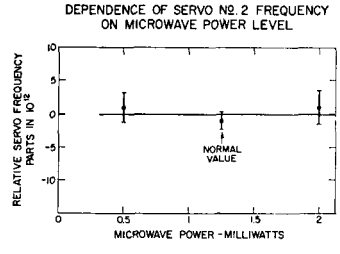

Fig. 5—Dependence of Servo No. 2 frequency on microwave power level.

Over a period of several months detailed investigations were made to determine to what extent 9 parameters of the servo system electronics might affect the frequency at which the controlled oscillator is locked. In each experiment the parameter under investigation was varied over as wide a range as possible while observing changes in the controlled oscillator frequency f_s relative to one of the secondary standard sources. Since the reliability of each experiment was rather strongly dependent upon the extent to which the secondary standard frequency, used as a reference, remained stable over the period of the measurements (usually several hours), great care was taken to select the particular secondary standard whose frequency was the most stable at the particular time as determined in most cases from auxiliary measurements. Both of the rubidium vapor standards and a commercial cesium beam standard were used at various times and, as a result of this careful selection procedure, the reference frequency could usually be depended on to remain within a few parts in 10^{12} over the

necessary time interval. In most cases at least one data point was rechecked to guard against erroneous conclusions being formed due to drift of the reference frequency. Results of these experiments are plotted in Figs. 6–17. In each curve the parameter being studied is plotted along the X axis and the relative frequency of the controlled oscillator in parts in 10^{12} is plotted along the Y axis. The straight lines drawn in are not least-squares fits to the data, but rather attempts to visually fit lines of zero slope to the data that are reasonably consistent with the measurement precisions.

Fig. 6 shows the dependence of the servo frequency on the amount of frequency correction applied to the servo oscillator when the loop is closed. The computed cor-

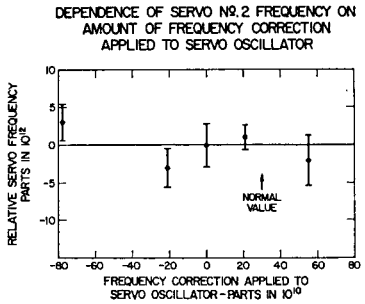

Fig. 6—Dependence of Servo No. 2 frequency on amount of frequency correction applied to servo oscillator.

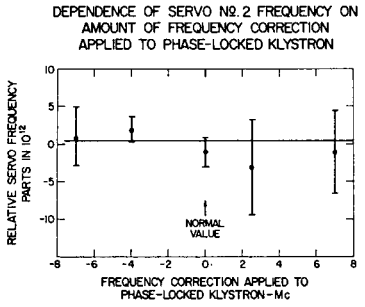

Fig. 7—Dependence of Servo No. 2 frequency on amount of frequency correction applied to phase-locked klystron.

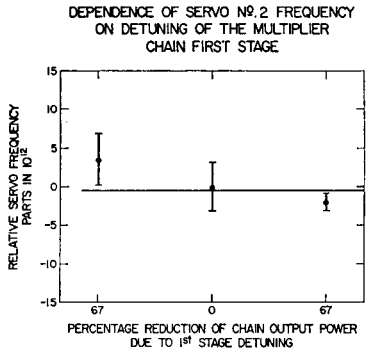

Fig. 8—Dependence of Servo No. 2 frequency on detuning of the multiplier chain first stage.

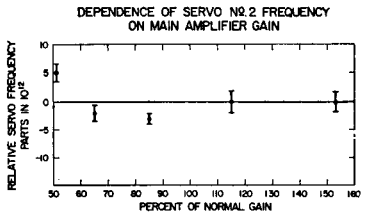

Fig. 9—Dependence of Servo No. 2 frequency on main amplifier chain.

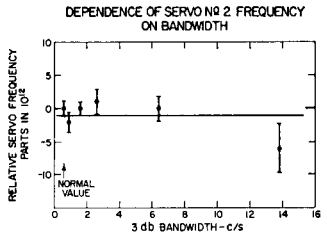

Fig. 10—Dependence of Servo No. 2 frequency on bandwidth.

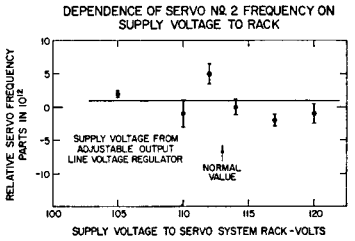

Fig. 11—Dependence of Servo No. 2 frequency on supply voltage to rack.

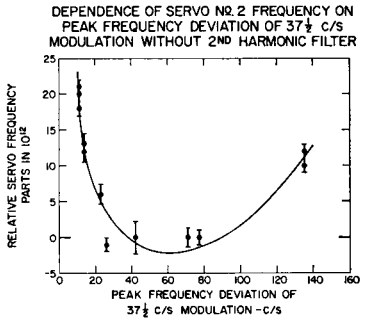

Fig. 12—Dependence of Servo No. 2 frequency on peak frequency deviation of 37½ cps modulation without 2nd-harmonic filter.

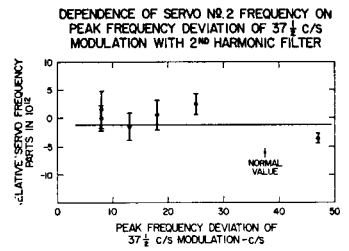

Fig. 13—Dependence of Servo No. 2 frequency on peak frequency deviation of 37½ cps modulation with 2nd-harmonic filter.

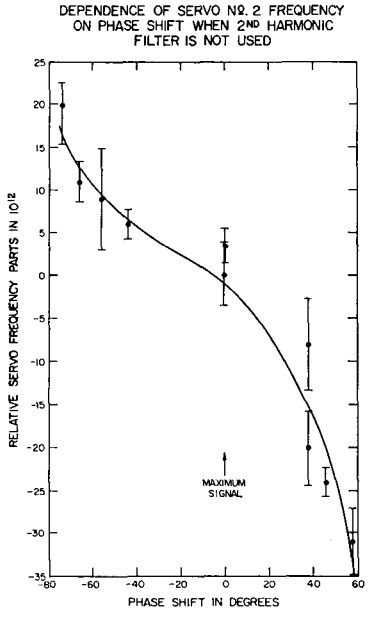

Fig. 14—Dependence of Servo No. 2 frequency on phase shift when 2nd-harmonic filter is not used.

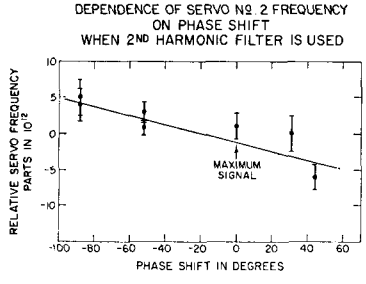

Fig. 15—Dependence of Servo No. 2 frequency on phase shift when 2nd-harmonic filter is used.

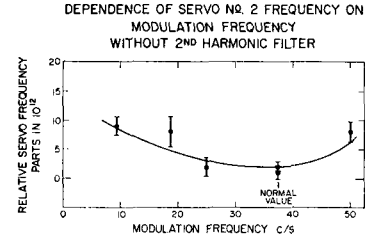

Fig. 16—Dependence of Servo No. 2 frequency on modulation frequency when 2nd-harmonic filter is not used.

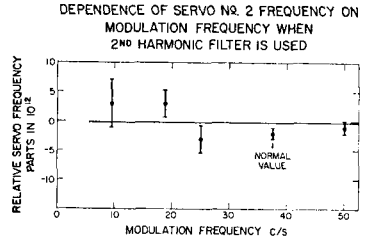

Fig. 17—Dependence of Servo No. 2 frequency on modulation frequency when 2nd-harmonic filter is used.

relation coefficient r for this data is 0.18. Since a value of r this large or larger would be expected in 20 per cent of similar measurements as a result of random sampling from an uncorrelated population, r is not significantly different from zero.

Fig. 7 shows the result of a similar-type experiment involving in this case the amount of frequency correction applied to the phase-locked klystron when its loop is closed. Although the measurement precisions were lower than normal for this experiment, a conclusion of no observable dependence on this parameter seems reasonable.

Fig. 8 presents the results of detuning the input stage of the (10–270)-Mc multiplier chain by equal amounts on each side of the maximum-signal position. Since the input stage is coupled rather directly to the (5–10)-Mc doubler output tank circuit where the phase modulation of f_s takes place, it was felt that, except for the 10-Mc doubler output tank circuit itself, frequency errors due to mistuning would be more severe in this stage than in any other part of the chain. The correlation coefficient is 0.32, a value that would be exceeded in only 15 per cent of such cases. However, when the data was divided rather randomly into 3 groups and r was computed separately for each group, all 3 values of r were not of the same sign. This result, together with the knowledge that the computed r values tend to be too large due both to sampling effects and instability of the reference frequency, lend support to a conclusion of no significant correlation in this case.

The parameter of interest in Fig. 9 is the gain of the main servo system amplifier, which is sharply tuned to the modulation frequency of 37.5 cps. The correlation coefficient of 0.29 for this data again is not unreasonable as a result of random sampling, especially in view of the result that division of the data into 3 subgroups produces 2 very small values of r and 1 larger value. The sign of all three values of r is the same, however, so that this may be considered a borderline case with respect to whether significant correlation exists.

Fig. 10 involves the dependence of the controlled oscillator frequency on the bandwidth of the main amplifier. Considering all the data plotted, the correlation coefficient is 0.40. A significant correlation would then seem to be indicated, since only 4 per cent of such experiments would produce r values this high as a result of the random sampling. However, there is some basis for disregarding the point for a bandwidth of 13.8 cps, because in this case a significant amount of 60-cps signal, which may be detrimental to the system in several respects, is allowed to be amplified. If r is redetermined neglecting this point, a much smaller value of 0.08 is obtained, which is much more consistent with a hypothesis of zero correlation.

The next parameter to be considered is the nominal 115-volt supply voltage to the rack containing the low-frequency portion of the servo system. Included in this rack are the 5-Mc oscillator, (5–10)-Mc doubler with

modulator, main servo amplifier, chopper-demodulator and operational amplifier. Results obtained by using an adjustable-output line voltage regulator to vary the supply voltage from 105 to 120 volts are shown in Fig. 11. This again seems to be somewhat of a borderline case, since the r value of 0.26 could be expected only 6 per cent of the time, due to random sampling from an uncorrelated population. Efforts to obtain more complete data of this type have been unsuccessful thus far because of higher-than-normal instabilities in the secondary standards.

Fig. 12 shows the significant dependence of the servo frequency on the peak frequency deviation of the 37.5-cps modulation for the case when components at the second harmonic frequency of 75 cps are present in the modulating signal at too high a level. The situation, with respect to second-harmonic shifts, is complicated by the fact that the amount of frequency error produced will in general depend on the phase as well as the amplitude of the 75-cps component. Although second-harmonic components may arise from several different sources in the system, the most likely origin is in distortion of the 37.5-cps modulating signal. The servo circuits do not permit the fundamental peak frequency deviation to be changed without simultaneously affecting the second harmonic frequency deviation; consequently, according to theory, the resultant frequency shift would be expected to depend on the setting of the peak frequency deviation control. Assuming this mechanism to be of major importance, an attenuating filter network tuned to the second harmonic frequency was inserted in the system between the oscillator that modulates the varicap and the phase modulator. The experiment was then rerun with the results shown in Fig. 13. The correlation coefficient for this data is only 0.15 so that the correlation with the second-harmonic filter is no longer significantly different from zero.

Figs. 14 and 15 show a similar effect with respect to dependence of the frequency on the relative phase of the 37.5-cps component from the beam detector. Again in this case the frequency dependence is significantly reduced by the second-harmonic filter, although certainly not eliminated completely. The r value of 0.50 for the measurements with the filter would result from chance in less than 0.2 per cent of similar cases. With reasonable assumption about the phase of the second harmonic, calculation shows that a second-harmonic distortion of 0.2 per cent would be sufficient to produce the dependence observed. The normal measurement procedure with the servo system in which the phase shifter is adjusted for maximum observed signal insures that any frequency error produced will not be very large, although it will also almost certainly not equal zero.

If second-harmonic distortion of the modulating audio signal is present due to distortion in the oscillator, then one might also expect resultant frequency shifts to depend on the modulation frequency. This effect with the filter out and in is shown in Figs. 16 and 17, respectively. The effect of the filter is not as pronounced in this case as for the other parameters. The r value of 0.19 for the data with filter has a reasonable expectation (26 per cent) of being exceeded as a result of random sampling from an uncorrelated population.

The determination of an over-all internal estimate of accuracy for the servo system based on the data discussed is made difficult by the uncertainties associated with the interpretation of the correlation results. From a general consideration of Figs. 6–17, however, it would seem unlikely that errors of more than a few parts in 10^{12} should arise due to the servo system parameters. Assuming a measurement precision of 1×10^{-12} (typical of 1-hour averages) and combining the various estimates of error as we did for the manual case, the internal estimate of accuracy for servo measurements is about 6×10^{-12}. It should be noted that for measurement times of 1 hour or longer the precision of measurement makes an insignificant contribution to the accuracy estimate.

Two methods are available with the NBS systems for obtaining an external estimate of any inaccuracies due to the servo system parameters alone. First, careful comparisons have been made of the measured frequencies of a stable source as determined by both the manual and servo methods. The measured discrepancy is $(0\pm3)\times10^{-12}$. Second, the difference between two independent servo systems of similar design has been measured (using second-harmonic filters in both systems) and found to be $(4\pm3)\times10^{-12}$. In both of these methods errors due to C-field uncertainties and phase difference in the resonant cavity do not enter in since they will be the same for all measurements. These latter comparisons then appear to substantiate the earlier conclusion that any additional contributions to inaccuracy above those present in the manual technique are less than a few parts in 10^{12}.

Since the accuracy figure for the manual case has been conservatively estimated to be about 1.1×10^{-11}, however, the small additional contribution from the servo parameters is relatively insignificant and for all practical purposes the two methods of measurement may be assumed to be equally accurate.

Conclusion

Based on several years experience, both the manual and servo measurement systems have proved highly dependable. Careful analysis of both systems has shown that the very significant advantages of the servo-type measurements in terms of convenience of operation and precision of measurement can be utilized with no significant sacrifice of accuracy. In view of the demonstrated frequency shifts that may occur under certain operating conditions of the servo system, however, it is recommended that any such system to be used with a primary frequency standard should be thoroughly evaluated before being put to routine use, and that periodic comparisons with manual measurements should continue after the system is in regular operation.

463-560 O - 72 - 7

Some Causes of Resonant Frequency Shifts in Atomic Beam Machines. I. Shifts Due to Other Frequencies of Excitation

JON H. SHIRLEY
National Bureau of Standards, Radio Standards Laboratory, Boulder Laboratories, Boulder, Colorado
(Received 27 August 1962)

The quantum theory of an atomic beam machine is set up in matrix form. A new method is then used to derive the Bloch–Siegert shift in the resonance. The results are extended to the case of Ramsey-type excitation. Finally the Bloch–Siegert shift is computed for the present atomic beam frequency standards and found to be well below the accuracy of measurement.

1. INTRODUCTION

IN the analysis of line shapes to be expected from atomic beam resonance experiments it has been customary to assume a special form for the matrix of the interaction which makes the resulting equations easy to solve [reference 1, Eq. V. 2]. These equations lead to expressions for the line shape agreeing with experiment. The effects of including other terms in the actual interaction have been discussed by Bloch and Siegert,[2] Stevenson,[3] and others,[4] and summarized in Ramsey's book.[1] In the case of magnetic resonance the usual approximation corresponds to a rotating (circularly polarized) excitation field, although oscillating (linearly polarized) fields are used in experiments. The effect of the antirotating component of an oscillating field has been found to be a normally negligible shift in the resonance frequency. A similar shift would be expected in observing the resonance in cesium used as a standard of frequency. Because of the high accuracy to which this frequency can be determined, the present calculations were undertaken to determine this shift quantitatively for the cesium beam machine now used as the U. S. standard of frequency.

Although the analytical results here reported have been obtained by others, the methods are somewhat different from those in the literature. In Sec. 2 the approximate equations for the state amplitudes are obtained from the exact ones by a simple, but general, method. A concise, but readily interpretable notation is used. The Rabi line shape is obtained quickly from these equations. Section 3 outlines a general method for treating rapidly oscillating perturbations and applies it to the equations of Sec. 2. This method is shorter than that of Bloch and Siegert,[2] but about comparable to the method of Stevenson[3] in labor required. Another method is indicated in the Appendix. The first-order solution for the amplitude is given in full. Section 4 derives the Ramsey line shape for separated oscillating fields, showing what happens to shifts present in the Rabi line shape. The physical situation treated corresponds more closely to the experimental case than that treated by Ramsey[5] but is no more difficult to work out. Finally, the resonant frequency shifts due to the antirotating field are evaluated numerically for the two cesium beam standards at the National Bureau of Standards.

2. THE RABI LINE SHAPE

Consider a quantum-mechanical system having two states of energies E_1 and E_2. Let a_1, a_2 be the respective probability amplitudes that the system is in one of these states. Let an oscillatory perturbation proportional to $\cos\omega t$ be applied to the system from time t_0 to time $t_0+\tau$. Call the matrix elements of the perturbation connecting the two states $2c$ and the diagonal elements $2d$ and $2f$. Assume that the matrix elements to any other states are zero. The Hamiltonian of the system is then:

$$H=\begin{pmatrix}E_1 & 0\\ 0 & E_2\end{pmatrix}+\begin{pmatrix}2d & 2c\\ 2c & 2f\end{pmatrix}\cos\omega t.$$

Since factors of the form $e^{i\nu t}$ in the amplitudes have no effect on the probabilities it is convenient to factor them out ahead of time so they do not clutter our equations later on. We define new probability amplitudes $\alpha=a_1e^{i\mu t}$, $\beta=a_2e^{i\nu t}$. Using these as a basis the Hamiltonian becomes[6]:

$$\begin{pmatrix}E_1-\mu & 0\\ 0 & E_2-\nu\end{pmatrix}+\begin{pmatrix}d & ce^{i(\mu-\nu)t}\\ ce^{-i(\mu-\nu)t} & f\end{pmatrix}(e^{i\omega t}+e^{-i\omega t}).$$

By choosing $\mu-\nu=\omega$ part of the perturbation matrix becomes time-independent. By choosing $\mu+\nu=E_1+E_2$ the time-independent part of the Hamiltonian H_0 becomes traceless, and hence has eigenvalues $\pm p$. The remaining time-dependent part of the Hamiltonian H_1 is treated as a perturbation. Substituting $\mu=\frac{1}{2}(E_1+E_2+\omega)$ and $\nu=\frac{1}{2}(E_1+E_2-\omega)$ and the ab-

[1] N. F. Ramsey, *Molecular Beams* (Oxford University Press, London, 1956).
[2] F. Bloch and A. Siegert, Phys. Rev. **57**, 522 (1940).
[3] A. F. Stevenson, Phys. Rev. **58**, 1061 (1940).
[4] S. Autler and C. H. Townes, Phys. Rev. **100**, 703 (1955).
[5] N. F. Ramsey, Phys. Rev. **100**, 1191 (1955). Compare also N. F. Ramsey, "Shapes of Molecular Beam Resonances," in *Recent Research in Molecular Beams*, edited by I. Estermann (Academic Press Inc., New York, 1959), pp. 115–117.
[6] To avoid unnecessary letters in the equations, $\hbar=1$ throughout this report. Thus energy and frequency have the same dimensions.

breviations $\omega_0=E_1-E_2$, $\Delta=(\omega-\omega_0)/2$:

$$H_0=\begin{pmatrix}-\Delta & c\\ c & \Delta\end{pmatrix},$$

$$H_1=\begin{pmatrix}2d\cos\omega t & ce^{i2\omega t}\\ ce^{-i2\omega t} & 2f\cos\omega t\end{pmatrix}.$$

Note that H_0 contains part of the effects of the perturbation, in fact the major part. For $\omega\gg c$ the effect of H_1 is very small. Neglecting H_1 is equivalent to the so-called rotating field approximation.[7] However, the present formulation is independent of whether or not the concept of a rotating excitation field has any physical meaning.

Neglecting H_1 the solution of the Schrödinger equation is

$$\Psi(t)=e^{-iH_0(t-t_0)}\Psi(t_0)$$

where

$$e^{-iH_0(t-t_0)}=\cos p(t-t_0)1-(i/p)\sin p(t-t_0)H_0.$$

If at $t=t_0$ the system is in the state 1, $\alpha(t_0)=1$ and $\beta(t_0)=0$. Then the solution is:

$$\Psi=\begin{pmatrix}\alpha\\ \beta\end{pmatrix}=e^{-iH_0(t-t_0)}\begin{pmatrix}1\\ 0\end{pmatrix}=\begin{pmatrix}\cos p(t-t_0)+i\dfrac{\Delta}{p}\sin p(t-t_0)\\ -i\dfrac{c}{p}\sin p(t-t_0)\end{pmatrix}.$$

Note that α and β oscillate with frequency p. The probability that a transition has occurred by the time $t_0+\tau$ is $|\beta|^2=(c^2/p^2)\sin^2 p\tau$. From det H_0 we find $p^2=c^2+\Delta^2$. Hence,

$$|\beta|^2=\frac{c^2}{c^2+\Delta^2}\sin^2(c^2+\Delta^2)^{\frac{1}{2}}\tau=\frac{\sin^2[(2c)^2+(\omega-\omega_0)^2]^{\frac{1}{2}}(\tau/2)}{1+(\omega-\omega_0)^2/(2c)^2},$$

the usual formula for the Rabi line shape [reference 1, Eq. V. 10]. For appreciable transition probability $\Delta=$ order of c, so $\omega\gg p$; i.e., H_1 oscillates rapidly compared to the solution neglecting it. Its effect on α,β should be slight when averaged over a few cycles of ωt.

3. EFFECT OF RAPIDLY VARYING PERTURBATION

The inclusion of H_1 in the Schrödinger equation has two effects. One is the production of a Fourier series in ωt. The rapidly oscillating terms are not observed experimentally and they average to zero. The second effect is a change in the frequency of the unperturbed solution from p to $q\equiv p(1+\lambda)$. This effect is important, as it may result in a shift of the maximum of the resonance line shape. This form of solution is suggested by Floquet's theorem[8] for second-order differential equations with periodic coefficients such as are satisfied by α,β, where iq corresponds to the characteristic exponent.

To determine an approximate solution when H_1 is included, we use an iteration method similar to ordinary perturbation theory, but modified to permit the shift from p to q in the slowly varying part of the solution. We write the Schrödinger equation as

$$i(d/dt)\Psi=H_0(1+\lambda)\Psi+(H_1-\lambda H_0)\Psi$$

and take the second half to be of smaller order. Write $\Psi=\Psi_0+\Psi_1+\Psi_2+\ \ldots$ and $\lambda=\lambda_2+\lambda_3+\ \ldots$. Substitute and equate parts of the equation of the same order (order equals the sum of subscripts in any one term)

$$i(d/dt)\Psi_0=H_0(1+\lambda)\Psi_0,$$
$$i(d/dt)\Psi_1=H_0(1+\lambda)\Psi_1+H_1\Psi_0,$$

$$i\frac{d}{dt}\Psi_n=H_0(1+\lambda)\Psi_n+H_1\Psi_{n-1}-\sum_{r=0}^{n-2}\lambda_{n-r}H_0\Psi_r.$$

Since H_0 is independent of t, the formal solution for a first-order linear equation can be used for these matrix equations. Let

$$U(\tau)=e^{-iH_0(1+\lambda)\tau}=\cos q\tau 1-(i/p)\sin q\tau H_0.$$

Then at $t_0+\tau$:

$$\Psi_0=U(\tau)\Psi(t_0),$$

$$\Psi_1=-iU(\tau)\int_0^\tau U^{-1}(t)H_1\Psi_0(t+t_0)dt,$$

$$\Psi_n=-iU(\tau)\int_0^\tau U^{-1}(t)\times[H_1\Psi_{n-1}(t+t_0)-\sum_{r=0}^{n-2}\lambda_{n-r}H_0\Psi_r(t+t_0)]dt.$$

The λ_i are chosen such that no secular terms (terms proportional to t) appear upon integration. Thus q is initially undetermined, but becomes determined to higher orders as the iteration progresses. The integration of $H_1\Psi_0$ where H_1 is purely oscillatory leads to no secular terms, so $\lambda_1=0$. The concept of changing a dominant frequency to eliminate secular terms is essentially the same as that used in Lindstedt's method for finding periodic solutions of nonlinear differential equations.

In our case where H_1 oscillates with frequency $\omega\gg p$ and magnitude c, the integration of $H_1\Psi_0$ will result in a factor c/ω in Ψ_1, thus making it small. However, $H_1\Psi_1$ contains terms in which the oscillatory factors have cancelled and upon integration yield a factor c/q which is not small. Thus to obtain all terms in the solution of

[7] For a spin $\frac{1}{2}$ particle in a rotating magnetic field, H_0 here is identical with $\mathcal{H}'$ in H. Salwen, Phys. Rev. **99**, 1274 (1955).

[8] E. T. Whittaker and G. N. Watson, *A Course of Modern Analysis* (Cambridge University Press, New York, 1927), 4th ed., p. 412.

order c/ω part of Ψ_2 must be computed. This peculiarity of the iteration procedure arises from the fact that we have equated orders in a differential equation and the orders of terms change upon integration. However, this does not invalidate the iteration procedure for no more c/ω terms occur beyond Ψ_2. In general, Ψ_{2n} is of order $(c/\omega)^n$ and higher. The same phenomenon occurs in the iteration procedure used by Bloch and Siegert, disguised by the algebra.

As an example we compute the lowest-order effects of two simple H_1's. To first order the effects of several such perturbations combine linearly, so it is only necessary to consider one at a time. Consider

$$H_0=\begin{pmatrix}-\Delta & c\\ c & \Delta\end{pmatrix}$$

and

$$H_1=\begin{pmatrix}0 & be^{i\Omega t}\\ be^{-i\Omega t} & 0\end{pmatrix}.$$

This is a generalization of the H_1 of Sec. 2, which allows us to consider perturbations at other frequencies.

Let

$$\alpha_0(\tau)=\cos q\tau+i\Delta/p\,\sin q\tau,\ \beta_0(\tau)=-ic/p\,\sin q\tau.$$

Then

$$U(\tau)=e^{-iH_0(1+\lambda)\tau}=\begin{pmatrix}\alpha_0 & -\beta_0\\ \beta_0 & \bar\alpha_0\end{pmatrix},$$

$$U(0)=1,$$

where the bar denotes complex conjugate.

$$\Psi_0(\tau+t_0)=\begin{pmatrix}\alpha_0(\tau)\\ \beta_0(\tau)\end{pmatrix}\quad\text{for}\quad\Psi(t_0)=\begin{pmatrix}1\\ 0\end{pmatrix}.$$

The exact integration of the equation for Ψ_1 is tedious and yields terms of all orders. However, we can easily integrate by parts such that the remaining integral is of higher order and is neglected.

$$\Psi_1(\tau+t_0)=-iU(\tau)\left[U^{-1}(t)\int^{t+t_0}H_1(t')dt'\Psi_0(t+t_0)\right]_0^\tau+O\left(\frac{b^2}{\Omega^2}\right),$$

$$=-iU(\tau)\left[U^{-1}(t)\begin{pmatrix}0 & \frac{b}{i\Omega}e^{i\Omega(t+t_0)}\\ \frac{b}{-i\Omega}e^{-i\Omega(t+t_0)} & 0\end{pmatrix}\begin{pmatrix}\alpha_0(t)\\ \beta_0(t)\end{pmatrix}\right]_0^\tau,$$

$$=U(\tau)U^{-1}(\tau)\begin{pmatrix}\frac{-b}{\Omega}e^{i\Omega(\tau+t_0)}\beta_0(\tau)\\ \frac{b}{\Omega}e^{-i\Omega(\tau+t_0)}\alpha_0(\tau)\end{pmatrix}-U(\tau)\begin{pmatrix}0\\ \frac{b}{\Omega}e^{-i\Omega t_0}\end{pmatrix},$$

$$=\begin{pmatrix}-\frac{b}{\Omega}(e^{i\Omega(\tau+t_0)}+e^{-i\Omega t_0})\beta_0(\tau)\\ \frac{b}{\Omega}[e^{-i\Omega(\tau+t_0)}\alpha_0(\tau)-e^{-i\Omega t_0}\bar\alpha_0(\tau)]\end{pmatrix}.$$

We now seek the lowest-order parts of Ψ_2.

$$H_1\Psi_1(t+t_0)=\begin{pmatrix}\frac{b^2}{\Omega}[\alpha_0(t)-e^{i\Omega t}\bar\alpha_0(t)]\\ -\frac{b^2}{\Omega}(1+e^{-i\Omega(t+2t_0)})\beta_0(t)\end{pmatrix}.$$

We forget the exponential terms as they contribute only to higher orders upon integration

$$U^{-1}H_1\Psi_1=\frac{b^2}{\Omega}\begin{pmatrix}|\alpha_0|^2-|\beta_0|^2\\ \alpha_0\beta_0-\alpha_0\beta_0\end{pmatrix}$$

$$=\frac{b^2}{\Omega}\begin{pmatrix}\frac{\Delta^2}{p^2}+\frac{c^2}{p^2}\cos 2qt\\ -\frac{\Delta c}{p^2}+\frac{\Delta c}{p^2}\cos 2qt+\frac{ic}{p}\sin 2qt\end{pmatrix}.$$

The constant terms yield unwanted secular terms upon integration. Therefore, we choose λ_2 such that

$$\frac{b^2}{\Omega}\begin{pmatrix}\frac{\Delta^2}{p^2}\\ -\frac{\Delta c}{p^2}\end{pmatrix}-U^{-1}\lambda_2 H_0\Psi_0=0.$$

U commutes with H_0, hence

$$U^{-1}(t)H_0\Psi_0(t)=H_0\Psi(t_0)=\begin{pmatrix}-\Delta\\ c\end{pmatrix}.$$

Then

$$\lambda_2=-b^2\Delta/\Omega p^2.$$

After some more work

$$\Psi_2(\tau+t_0)=(b^2/\Omega p^2)\begin{pmatrix}c\\ \Delta\end{pmatrix}\beta_0(\tau).$$

To first order the complete solution is

$$\Psi=\begin{pmatrix}\alpha_0-\frac{b}{\Omega}(e^{i\Omega\tau}e^{i\Omega t_0}\beta_0-e^{-i\Omega t_0}\beta_0)+\frac{b^2c}{\Omega p^2}\beta_0\\ \beta_0+\frac{b}{\Omega}(e^{-i\Omega\tau}\alpha_0-\bar{\alpha}_0)e^{-i\Omega t_0}+\frac{b^2\Delta}{\Omega p^2}\beta_0\end{pmatrix},$$

and

$$q=p-(b^2\Delta/\Omega p).$$

In the physical situation of an atomic beam machine the observed transition probability includes molecules entering the radiation field region at all initial times t_0, so that an average must be performed over t_0 (or equivalently over the phase of radiation seen by entering atoms). This averaging eliminates the contributions of Ψ_1 to Ψ. The resultant Ψ can be written

$$\langle\Psi\rangle_{t_0\text{average}}=\begin{pmatrix}\alpha_0-\frac{c}{\Delta}\lambda\beta_0\\ \beta_0-\lambda\beta_0\end{pmatrix}+O(\lambda^2).$$

Actually the probabilities rather than amplitudes should be averaged, but the error is of second order.

The transition probability is now

$$|\beta|^2=|-(ic/p)(1-\lambda)\sin q\tau|^2=(c^2/q^2)\sin^2 qt$$

to first order. To this order the effect of H_1 has been to replace p by q. The central maximum of $|\beta_0|^2$ as a function of Δ occurs where $dq/d\Delta=0$. Remembering that p depends on Δ

$$dq/d\Delta=(\Delta/p)-(b^2/\Omega p)+(b^2\Delta^2/\Omega p^3).$$

Neglecting the last term the maximum is at

$$\Delta_{\text{res}}=b^2/\Omega.$$

The Bloch-Siegert shift is obtained by setting $b=c$, $\Omega=2\omega$:

$$\omega_{\text{res}}-\omega_0=c^2/\omega.$$

For the case of an additional perturbation at frequency ω_1 with amplitude b:

$$\Omega=\omega-\omega_1,\quad \omega_{\text{res}}-\omega_0=2b^2/(\omega_0-\omega_1),$$

in agreement with Ramsey [reference 1, Eq. V. 17]. Note that if ω_1 is a sideband caused by frequency modulation of ω, its effect is exactly canceled by the corresponding sideband on the other side of the carrier, provided the power spectrum is symmetric.

Next we look for a shift due to

$$H_1=\begin{pmatrix}d & 0\\ 0 & f\end{pmatrix}2\cos\omega t.$$

Such diagonal elements of the perturbation matrix are usually assumed to be zero. However, this is not the case for $\sigma(\Delta m=0)$ transitions induced by an oscillating field parallel to the constant magnetic field. For then the Hamiltonian is

$$\begin{pmatrix}E_1 & \frac{1}{2}\mu g H_z\\ \frac{1}{2}\mu g H_z & E_2\end{pmatrix},$$

where

$$H_z=H_c+H_v\cos\omega t.$$

But the transitions observed are not between the zero field levels E_1, E_2, but between the levels with H_c diagonal. Diagonalizing the time independent part of the Hamiltonian and then performing the phase factoring as in Sec. 2 gives

$$H=\begin{pmatrix}-\Delta & c\\ c & \Delta\end{pmatrix}+\begin{pmatrix}2b\cos\omega t & ce^{2i\omega t}\\ ce^{-2i\omega t} & -2b\cos\omega t\end{pmatrix}$$

where

$$\Delta=(\omega-\omega_0)/2,$$
$$\omega_0=[(E_1-E_2)^2+\mu^2g^2H_c^2]^{\frac{1}{2}},$$
$$c=(E_2-E_1)\mu_0H_v/4\omega_0,$$
$$b=\mu gH_c\mu gH_v/4\omega_0.$$

In actual practice $b\ll c$.

Returning to the d and f case we again approximate the integration finding

$$\Psi_1(t_0+\tau)=-\frac{2i}{\omega}\begin{pmatrix}d[\sin\omega\tau\cos\omega t_0+(\cos\omega\tau-1)\sin\omega t_0]\alpha_0(\tau)\\ f\left[\sin\omega\tau\cos\omega t_0+\left(\cos\omega\tau-\frac{d}{f}\right)\sin\omega t_0\right]\beta_0(\tau)\end{pmatrix}.$$

Averaged over t_0, Ψ_1 vanishes.

$$H_1\Psi_1=-\frac{4i}{\omega}\begin{pmatrix}d^2(\sin\omega t-\sin\omega t_0)\cos\omega t\alpha_0\\ f^2\left(\sin\omega t-\frac{d}{f}\sin\omega t_0\right)\cos\omega t\beta_0\end{pmatrix}.$$

Integration of this gives no secular terms and

$$\Psi_2 = Od^2/\omega^2.$$

So $\lambda_2 = 0$ and thus H_1 is seen to have no effect other than small high frequency oscillations.

Variations of this method are possible, such as transforming to a representation in which H_0 is diagonal. The latter makes the integrations easier, but the transformation must be inverted at the end of the computation.

4. EFFECT ON RAMSEY LINE SHAPE

The preceding derivations apply to the single oscillating field method of atomic beam spectroscopy. The first-order effect is equivalent to replacing Δ by $\Delta' = \Delta - \delta\omega/2$, where $\delta\omega$ is the Rabi resonance frequency minus the Bohr frequency. We can easily use this solution to determine the shift observed with the separated oscillating field method of Ramsey. Let primes denote that Δ has been replaced by Δ' wherever it appears. Within each oscillating field region of length $l = v\tau$, Ψ is transformed by

$$U'(\tau) = \begin{pmatrix} \alpha_0' & -\beta_0' \\ \beta_0' & \bar{\alpha}_0' \end{pmatrix}.$$

In the distance $L = vT$ between the two oscillating field regions, $b = c = \delta\omega = 0$ and U becomes simply

$$V(T) = \begin{pmatrix} e^{i\Delta T} & 0 \\ 0 & e^{-i\Delta T} \end{pmatrix}.$$

Then for an atom traversing the entire apparatus, we have

$$\Psi(\tau + T + \tau + t_0) = U'(\tau)V(T)U'(\tau)\Psi(t_0),$$

$$= \begin{pmatrix} \alpha_0'^2 e^{i\Delta T} + \beta_0'^2 e^{-i\Delta T} \\ \alpha_0'\beta_0' e^{i\Delta T} + \bar{\alpha}_0'\beta_0' e^{-i\Delta T} \end{pmatrix}$$

for

$$\Psi(t_0) = \begin{pmatrix} 1 \\ 0 \end{pmatrix}.$$

The transition probability is:

$$|\beta|^2 = (4c^2/q^2)\sin^2 q\tau[\cos q\tau \cos\Delta T - (\Delta'/p')\sin q\tau \sin\Delta T]^2.$$

Near the center of the Ramsey pattern $\Delta \ll c$ so $q = p' \approx c$

$$|\beta|^2 \approx \sin^2 2c\tau[\cos\Delta T - (\Delta'/c)\tan c\tau \sin\Delta T]^2.$$

$$d|\beta|^2/d\Delta = (\sin^2 2c\tau)2[\cos\Delta T - (\Delta'/c)\tan c\tau \sin\Delta T] \times [-T\sin\Delta T - (1/c)\tan c\tau \sin\Delta T - (\Delta' T/c)\tan c\tau \cos\Delta T].$$

For the central maximum we set the last factor equal to zero:

$$\frac{\tan\Delta T}{T}\left(1 + \frac{\tan c\tau}{cT}\right) = -\frac{\Delta'}{cT}\tan c\tau = -\frac{\Delta}{cT}\tan c\tau + \frac{\delta\omega}{2cT}\tan c\tau.$$

For appreciable probability of transition $2c\tau \approx \pi/2$. Also $L \gg l$ or $T \gg \tau$, hence $cT \gg 1$. For small shifts ($\delta\omega \ll c$) $\Delta T \ll 1$ and the left side becomes just Δ. With these simplifying assumptions the shift in the peak of the Ramsey pattern is:

$$\omega_{res} - \omega_0 = \frac{\tan c\tau}{c\tau}\frac{l}{L} - \delta\omega.$$

Unlike the shift of the Rabi peak, the shift of the Ramsey peak depends on the velocity of the atom. However, for optimum value of c and the most probable velocities, the velocity dependent factor is about 1.2 and not strongly dependent on velocity, so about this value can be expected if a velocity average were performed. This derivation also holds for any other cause of a shift in the Rabi peak, such as that caused by matrix elements to other far away states, as long as the cause is effective only in the oscillating field regions and does not make the line asymmetric.

5. BLOCH-SIEGERT SHIFT FOR THE CESIUM BEAM FREQUENCY STANDARD

As a numerical example the Bloch-Siegert shift is estimated for the two cesium beam frequency standards currently operated at the National Bureau of Standards. There are actually sixteen hyperfine structure lines in cesium. However, in the frequency standards the oscillating field is parallel to the C field, which provides the Zeeman splitting. Under these conditions only the σ transitions are excited. All matrix elements between states with different m values vanish.[9] For each pair of states with the same m value the two-state analysis of this paper is valid. The observed spectrum is just the superposition of the seven lines for the seven possible σ transitions. In practice these lines are well separated by the order of one hundred times the Ramsey linewidth. As long as they are symmetrical about the center line, which is used as the standard, these other lines should not affect the position of the standard frequency resonance.

The Bloch-Siegert shift in the Rabi line is from Sec. 3, $\delta\omega = c^2/\omega_0$. The fractional shift in the Ramsey peak is then:

$$\text{F.S.} = (\omega_{res} - \omega_0)/\omega_0 = (\tan c\tau/c\tau)(l/L)(c^2/\omega_0^2).$$

Assuming the optimum value of c we have from [reference 1, Eqs. V. 42, 42a]:

$$2cl/\alpha = 0.600\pi$$

and the linewidth

$$\Delta\nu = 0.65\alpha/L.$$

Combining

$$c = 0.300\pi\alpha/l = 1.45(L/l)\Delta\nu$$

[9] H. C. Torrey, Phys. Rev. **59**, 293 (1940), Sec. II.

and

$$c\tau = 0.300\pi\alpha/v = 0.725$$

$$\text{F.S.} = 1.22\frac{l}{L}\left(\frac{1.45L\Delta\nu}{l2\pi\nu_0}\right)^2 = 0.065\frac{L}{l}\left(\frac{\Delta\nu}{\nu_0}\right)^2.$$

In this form we can use the experimental linewidths and need not compute c. For both machines $l=1$ cm, $\nu_0 = 9.2\times10^9$ cps. For NBS I:

$$L = 55 \text{ cm},$$
$$\Delta\nu = 300 \text{ cps},$$
$$\text{F.S.} = 3.8\times10^{-15}.$$

For NBS II:

$$L = 164 \text{ cm},$$
$$\Delta\nu = 120 \text{ cps},$$
$$\text{F.S.} = 1.8\times10^{-15}.$$

These figures are to be compared with the present accuracy of measuring the cesium resonance frequency of 1.7×10^{-11}.[10]

APPENDIX

Another, less general method for obtaining the solution to the Bloch–Siegert problem is one which requires deducing the form of the solution, and then solving for some undetermined coefficients. The equations are (cf. Sec. 3)

$$i\dot{\alpha} = -\Delta\alpha + c\beta + be^{i\Omega t}\beta,$$
$$i\dot{\beta} = \Delta\beta + c\alpha + be^{-i\Omega t}\alpha,$$

and the initial conditions $\alpha(t_0)=1$, $\beta(t_0)=0$. Letting the subscript "0" represent the functions in Sec. 3 with argument $t-t_0$, they satisfy:

$$i\dot{\alpha}_0 = (-\Delta\alpha_0 + c\beta_0)(1+\lambda),$$
$$i\dot{\beta}_0 = (c\alpha_0 + \Delta\beta_0)(1+\lambda).$$

We wish to add to α_0, β_0 terms with small coefficients which make the equations satisfied except for small terms. We note that when a function such as $Ae^{i\Omega t}\alpha(t)$ is differentiated, the result contains a term with a factor Ω, that is, a term with a larger order coefficient. Thus, to generate $be^{i\Omega t}\beta$ when α is differentiated, let us add to α_0 a term $Ae^{i\Omega t}\beta_0$. The derivative of this times i gives $A[-\Omega\beta_0 + (c\alpha_0+\Delta\beta_0)(1+\lambda)]e^{i\Omega t}$. Neglecting c and Δ compared to Ω we see that if $A=-b/\Omega$, we obtain $be^{i\Omega t}\beta_0$+smaller terms. Since $\beta=\beta_0$+smaller terms, we have thus satisfied the equation for α to lowest order.

However, we have several small terms left over. Those containing factors $e^{\pm i\Omega t}$ can be canceled by introducing terms of higher order. But the terms without this factor must be canceled by introducing similar terms with small coefficients into the approximate expressions for α and β. Thus we could add $B\beta_0$ to α and perhaps adjust B to cancel the other terms. We cannot add $C\alpha_0$, because this would violate the initial conditions.

After mulling over such considerations we are led to a trial solution in the form:

$$\alpha = \alpha_0 + A\beta_0 e^{i\Omega t} + B\beta_0,$$
$$\beta = \beta_0 + C(\alpha_0 e^{-i\Omega t} - \alpha_0 e^{-i\Omega t_0}) + D\beta_0,$$

where A, B, C, D are undetermined coefficients of order b/Ω and the initial conditions are satisfied. We substitute these expressions into the differential equations and equate the coefficients of terms of each order and functional type. In the α equation equating zero-order coefficients of $\beta_0 e^{i\Omega t}$ gives $-\Omega A = b$ or $A=-b/\Omega$ as noted previously. In the β equation from terms $\alpha_0 e^{-i\Omega t}$ we find similarly $\Omega C = b$ or $C=b/\Omega$. Now equating the first-order coefficients of α_0 and β_0 in the two equations we obtain

$$-\Delta\lambda + Bc = bC - cCe^{-i\Omega t_0},$$
$$c\lambda + B\Delta = -\Delta B + cD,$$
$$c\lambda + \Delta Ce^{-i\Omega t_0} + cD = -\Delta Ce^{-i\Omega t_0},$$
$$\Delta\lambda - cCe^{-i\Omega t_0} + \Delta D = Ab + Bc + \Delta D.$$

All told we have six equations in five unknown. However, these equations are consistent, with solutions:

$$\lambda = -b^2\Delta/\Omega p^2,$$
$$B = (c/\Omega)(b^2/p^2) - (b/\Omega)e^{-i\Omega t_0},$$

and

$$D = (\Delta b^2/\Omega p^2) - (2\Delta b/c\Omega)e^{-i\Omega t_0}.$$

These values give the same solution as in Sec. 3. Note that the first-order coefficients of $\alpha_0 e^{\pm i\Omega t}$, etc., do not cancel. This method, like the others, can be carried to higher order only with greatly increased labor as more undetermined coefficients must be inserted and more cross terms appear in the expansion.

[10] R. C. Mockler, R. E. Beehler, and C. S. Snider, IRE Trans. Instrumentation **I-9**, 120 (1960).

Some Causes of Resonant Frequency Shifts in Atomic Beam Machines. II. The Effect of Slow Frequency Modulation on the Ramsey Line Shape

JON H. SHIRLEY
Radio Standards Laboratory, Boulder Laboratories, National Bureau of Standards, Boulder, Colorado
(Received 27 August 1962)

The effect of slow frequency modulation of the exciting radiation on the Ramsey line shape observed in an atomic beam experiment is formulated theoretically. It is shown that the presence of second harmonic in the modulation can introduce measurable frequency shifts, whether observed directly or with a servo system.

1. INTRODUCTION

IN attempting to build a clock based on the cesium resonance frequency, a servo system is often used to lock a crystal oscillator to the peak of the Ramsey line shape. The exciting radiation is frequency modulated at a slow rate, such that the instantaneous frequency sweeps across the center of the Ramsey line. The detector output then contains a component at the modulation frequency which vanishes when the excitation frequency coincides with a maximum (or minimum) of the Ramsey pattern.

A closer analysis of this situation shows that the concept of sweeping the excitation frequency across the line shape is physically erroneous unless the rate of sweep is extremely slow. If the frequency changes slightly during the time an atom is between the two oscillating field regions, the atom sees a phase shift upon entering the second oscillating field region. Such phase shifts produce quite different line shapes.[1] As the apparent phase shift oscillates with the modulation, the line shape oscillates among its various forms for the corresponding phase shifts. For sinusoidal modulation the line shape has a time dependence which is readily Fourier analyzed into components at multiples of the modulation frequency. The servo system looks only at the fundamental component of this series, adjusting the excitation frequency to minimize the amplitude of this component. Calculations indicate that this component vanishes at the Bohr frequency in the case of pure sinusoidal modulation. However, if harmonics are present in the modulation, the fundamental component may vanish at a slightly different frequency.

An approximate analysis is carried out to determine the effect on the Ramsey line shape of a slow, but otherwise arbitrary phase modulation. The results are applied to pure sine-wave modulation and then to modulation including a small amount of second harmonic.

2. ANALYSIS FOR ARBITRARY PHASE DEPENDENCE

The derivation of the line shape for unmodulated excitation has been discussed in a previous paper.[2] Reference should be made to Sec. 2 of that paper for the formulation and notation used. In the derivation of the Rabi line shape let us replace $\cos\omega t$ by $\cos[\omega t+\phi(t)]$. Carrying out the same procedure as in reference 2 we find the same expression for H_0, except that Δ has been replaced by

$$\Delta'=[\omega+\dot{\phi}(t)-\omega_0]/2.$$

This depends on time, but we now make the assumption that the change in ϕ during the oscillating field region transit time τ is negligible compared with the Rabi linewidth. (In a typical case $\Delta\dot{\phi}/c$ is the order of 10^{-4} to 10^{-5}.) In the oscillating field regions we then treat ϕ as constant, that is, $\dot{\phi}(t_0+\tau)=\dot{\phi}(t_0)$.

For Ramsey excitation we take the time dependence of ϕ into full account in the interim between the two oscillating field regions. In the first oscillating field region we use in the U matrix

$$\Delta_1=\Delta+\tfrac{1}{2}\dot{\phi}(t_0),$$

in the second,

$$\Delta_2=\Delta+\tfrac{1}{2}\dot{\phi}(t_0+T).$$

In between, ΔT is replaced by $\Delta T+\frac{1}{2}\delta\phi$, where $\delta\phi=\phi(t_0+T)-\phi(t_0)$ is the apparent phase shift for an atom entering at time t_0 and traversing the apparatus in time T. Combining the transformation matrices as in Sec. 4 of reference 2 the transition amplitude of the Ramsey pattern becomes

$$\beta=e^{i(\Delta T+\frac{1}{2}\delta\phi)}\alpha_0(\Delta_1)\beta_0(\Delta_2)+e^{-i(\Delta T+\frac{1}{2}\delta\phi)}\beta_0(\Delta_1)\bar{\alpha}_0(\Delta_2).$$

Written out in full this expression becomes somewhat unwieldy. Over the central peak of the Ramsey pattern, however, $\Delta\ll c$ whenever $\tau\ll T$ or $l\ll L$. To first order in Δ and $\dot{\phi}$

$$\begin{aligned}|\beta|^2=\tfrac{1}{2}\sin^2 2c\tau\{&1+[\cos 2\Delta T-2(\Delta/c)\sin 2\Delta T\tan c\tau]\\&\times\cos\delta\phi-[\sin 2\Delta T+2(\Delta/c)\cos 2\Delta T\tan c\tau]\\&\times\sin\delta\phi-(c^{-1}\sin 2\Delta T\tan c\tau)\delta\omega\cos\delta\phi\\&-(c^{-1}\cos 2\Delta T\tan c\tau)\delta\omega\sin\delta\phi\},\end{aligned}$$

where $\delta\omega=\frac{1}{2}[\dot{\phi}(t_0)+\dot{\phi}(t_0+T)]$. Note that unless ϕ^2 terms are included the transition probability depends on ϕ only through the apparent phase shift $\delta\phi$ and the average frequency deviation $\delta\omega$. These depend on particle velocities through T, and on laboratory time through t_0.

If we observe the line shape over an extended period

[1] N. F. Ramsey, *Molecular Beams* (Oxford University Press, New York, 1956), p. 131.
[2] J. H. Shirley, J. Appl. Phys. 34, 783 (1963), preceding article.

of time, we see $|\beta|^2$ averaged over the entrance times of the atoms t_0. Let angular parentheses denote an average over t_0. The peak of the Ramsey pattern occurs at Δ_{res}, the root of $(d/d\Delta)|\beta|^2=0$. To the same approximation that $|\beta|^2$ was written

$$\tan 2\Delta_{res}T = -\frac{\langle\sin\delta\phi\rangle+[2(\Delta_{res}/c)\langle\cos\delta\phi\rangle+c^{-1}\langle\delta\omega\cos\delta\phi\rangle]\tan c\tau}{\langle\cos\delta\phi\rangle-[2(\Delta_{res}/c)\sin\delta\phi+c^{-1}\langle\delta\omega\sin\delta\phi\rangle]\tan c\tau}.$$

If $\langle\sin\delta\phi\rangle$ and $\langle\delta\omega\cos\delta\phi\rangle$ both vanish, $\Delta_{res}=0$ and there is no shift. If $\langle\sin\delta\phi\rangle\neq 0$, we have, neglecting terms of order $1/cT=O(l/L)$,

$$\tan 2\Delta_{res}T=-\langle\sin\delta\phi\rangle/\langle\cos\delta\phi\rangle,$$

or for a small shift:

$$\omega_{res}-\omega_0=-T^{-1}(\langle\sin\delta\phi\rangle/\langle\cos\delta\phi\rangle).$$

3. SIMPLE FREQUENCY MODULATION

Let us now consider the ideal case of pure sine-wave modulation

$$\phi=(b_1/\omega_m)\cos(\omega_m t+\delta_1).$$

Then

$$\delta\phi=-2(b_1/\omega_m)\sin(\tfrac{1}{2}\omega_m T)\times\sin(\omega_m t_0+\tfrac{1}{2}\omega_m T+\delta_1)=\delta\phi_1\sin W_1,$$

$$\delta\omega=-b_1\cos(\tfrac{1}{2}\omega_m T)\sin(\omega_m t_0+\tfrac{1}{2}\omega_m T+\delta_1)=\delta\omega_1\sin W_1.$$

We expand $\sin\delta\phi$ and $\cos\delta\phi$ in Fourier series in W_1, obtaining Bessel functions with argument $\delta\phi_1$ as coefficients[3]:

$$\sin\delta\phi=2J_1\sin W_1+2J_3\sin 3W_1+\cdots,$$

$$\cos\delta\phi=J_0+2J_2\sin 2W_1+2J_4\sin 4W_1+\cdots.$$

Now $\langle\sin nW_1\rangle=0$, so $\langle\sin\delta\phi\rangle=\langle\delta\omega\cos\delta\phi\rangle=0$ and no shift in the peak of the average line shape is expected.

We can go further and write out the Fourier expansion of $|\beta|^2$:

$$\begin{aligned}|\beta|^2=\tfrac{1}{2}\sin^2 2c\tau\Big\{&\Big[1+J_0\Big(\cos 2\Delta T-2\frac{\Delta}{c}\sin 2\Delta T\tan c\tau\Big)-J_1\frac{\delta\omega_1}{c}\Big]+\Big[-2J_1\Big(\sin 2\Delta T+2\frac{\Delta}{c}\cos 2\Delta T\tan c\tau\Big)\\&-J_0\frac{\delta\omega_1}{c}\sin 2\Delta T\tan c\tau\Big]\sin W_1\\&+\Big[-J_2\frac{\delta\omega_1}{c}\sin 2\Delta T\tan c\tau\Big]\cos W_1\\&+\Big[2J_2\Big(\cos 2\Delta T-2\frac{\Delta}{c}\sin 2\Delta T\tan c\tau\Big)\Big]\sin 2W_1\\&+\Big[(J_1-J_3)\frac{\delta\omega_1}{c}\cos 2\Delta T\tan c\tau\Big]\cos 2W_1+\cdots.\Big\}\end{aligned}$$

[3] See, for example, Harold S. Black, *Modulation Theory* (D. Van Nostrand Company, Inc., Princeton, New Jersey, 1953), p. 188, or any work on Bessel functions.

We see that the constant term and the coefficients of even harmonics are even functions of Δ. They have maxima (or minima) at $\Delta=0$. The coefficients of the odd harmonics are odd functions of Δ, vanishing at $\Delta=0$. Thus a servo system which looks at the first harmonic and adjusts Δ to minimize the amplitude, seeks the desired resonance frequency. This is also true for modulation at several incommensurable frequencies, since they do not interfere with each other. For commensurable frequencies the situation is different.

4. EFFECT OF SECOND HARMONIC IN THE MODULATION

We take

$$\phi=(b_1/\omega_m)\cos(\omega_m t+\delta_1)+(b_2/2\omega_m)\cos(2\omega_m t+\delta_2)$$

and use the abbreviated notation

$$\delta\phi=\delta\phi_1\sin W_1+\delta\phi_2\sin W_2,$$

$$\delta\omega=\delta\omega_1\sin W_1+\delta\omega_2\sin W_2,$$

where

$$\delta\phi_k=-2(b_k/k\omega_m)\sin(\tfrac{1}{2}k\omega_m T),$$

$$\delta\omega_k=-b_k\cos(\tfrac{1}{2}k\omega_m T),$$

and

$$W_k=(k\omega_m t_0+\tfrac{1}{2}k\omega_m T+\delta_k).$$

For simplicity we consider $\delta\phi_2\ll 1$, with $\delta\phi_1$ arbitrary and keep only first-order terms in $\delta\phi_2$.

$$\sin\delta\phi=2J_1\sin W_1+2J_3\sin 3W_1-\delta\phi_2 J_2\sin(2W_1-W_2)-\delta\phi_2 J_0\sin W_2\cdots,$$

$$\cos\delta\phi=J_0+2J_2\cos 2W_1-\delta\phi_2 J_1\cos(W_1-W_2)-\delta\phi_2 J_3\cos(3W_1-W_2)+\cdots.$$

The argument of all Bessel functions is $\delta\phi_1$.

$$\langle\sin\delta\phi\rangle=\delta\phi_2 J_2\sin(2\delta_1-\delta_2)\neq 0,$$

so a shift in the peak of the time-average line shape is expected, and will be approximately given by

$$\tan 2\Delta_{res}T=\delta\phi_2(J_2/J_1)\sin(2\delta_1-\delta_2).$$

Neglecting terms which will be of order l/L

$$|\beta|^2=\tfrac{1}{2}\sin^2 c\tau(1+\cos 2\Delta T\cos\delta\phi-\sin 2\Delta T\sin\delta\phi).$$

The first harmonic of the detector output is then proportional to

$$\delta\phi_2[J_1\cos(W_1-W_2)+J_3\cos(3W_1-W_2)]\times\cos 2\Delta T+2J_1\sin W_1\sin 2\Delta T.$$

The mechanics of the servo system involve filtering out this frequency and feeding it into a phase detector. The output of the phase detector is proportional to the time average of the product of the input signal and a reference signal of the same frequency. Let the reference signal be proportional to $\sin(W_1+\theta)$. Then the phase

463-560 O - 72 - 9

detector output is proportional to

$$\delta\phi_2[J_1\sin(2\delta_1-\delta_2+\theta)-J_3\sin(2\delta_1-\delta_2-\theta)]\times\cos 2\Delta T+2J_1\cos\theta\sin 2\Delta T.$$

This is the correction signal to control the excitation frequency. The servo adjusts the excitation frequency so that the correction signal vanishes. This occurs when

$$\tan 2\Delta_{res}T=-\tfrac{1}{2}\delta\phi_2[(1-J_3/J_1)\sin(2\delta_1-\delta_2)+\tan\theta(1+J_3/J_1)\cos(2\delta_1-\delta_2)].$$

Thus the servo locks onto a frequency shifted from the Bohr frequency. The magnitude of the shift is in general *different* from the shift observed in the time-average line shape. It depends on the magnitude and relative phas of the modulating frequencies, and on the phase of the reference signal for the phase detector.

An analysis of the power spectrum of the modulated signal considered in this section shows an asymmetry proportional to $\sin(2\delta_1-\delta_2)$. If the relative phases of the modulating frequencies are such as to give a symmetric power spectrum *and if* the relative phase of the reference signal vanishes, there will be no shift. On the other hand, for $\theta=\pi/2$, the shift can be sizeable (about 10^{-9} for cesium), so that it is desirable to observe the "in phase" component of the detector signal as well as to have symmetric power spectra in order to keep the shifts small. For $\delta\phi_1=O1$, $\delta\phi_2=O10^{-2}$, $\theta=0$, $T=O10^{-2}$,

$$(\omega_{res}-\omega_0)/\omega_0=2\Delta/\omega_0=O(\delta\phi_2/2\omega_0T)=O10^{-11}$$

for cesium. This estimate shows that the shift due to second harmonic in the modulation can be appreciable unless the amplitude of the second harmonic is kept very small. (Shifts due to the second harmonic have been observed and the dependence on the amplitudes and relative phases plotted by the National Company in their research on cesium beam frequency standards.[4] Unfortunately they did not present their theoretical work on the problem.)

The inclusion of higher harmonics only complicates the analysis. However, the odd harmonics alone do not produce any shifts. The general formula for the shift is always a sum of products of even and odd harmonics.

[4] Interim Development Report for Atomic Beam Frequency Standard, 4-28-57 to 7-27-57, National Company, Inc., Malden, Massachusetts (1957).

5. EFFECT OF VELOCITY DISTRIBUTION

In the preceding analysis no mention has been made of the velocity distribution and, in fact, no attempt has been made to average over velocities. We note that not only $\tan 2\Delta T$ and $\sin^2 c\tau$ depend on velocity, but also $\delta\phi_1$ and $\delta\phi_2$, hence all Bessel functions, also $\delta\omega_1$, $\delta\omega_2$, and θ (to compensate for T dependence in W_1). Ramsey's tables (reference 1, p. 423) do not include integrals of the form

$$\int_0^\infty e^{-\nu^2y^3}\sin\left(\frac{x}{y}\right)J_n\left(a\sin\frac{b}{y}\right)dy.$$

Qualitatively the results of this paper should not be changed appreciably by a velocity average from what they are using a single median velocity. If more than a rough value for the size of the shift were desired a numerical averaging would have to be performed to find a numerical magnitude for the shift. But because of the velocity distribution it is impossible to eliminate the shift simply by adjusting $\theta=0$ or $\delta\phi_1$ such that $J_1=J_3$, since these could hold only for a single velocity. However, since the sign of the shift can reverse, there must still exist conditions for which the shift seen by the servo, or the shift in the time-average line shape (but not both) vanishes. It would be difficult to compute these conditions theoretically, especially since they will depend sensitively on the power level of the excitation. But it should be possible by trying for a symmetric power spectrum and $\theta\approx 0$ to reduce the shift by one or two orders of magnitude below the estimate made in Sec. 4.

A change in excitation power level (c^2) changes the velocity for which the transition probability is a maximum, hence changes the relative effectiveness of the velocity components of the beam. Any velocity-dependent shift such as the one found in Sec. 4 then exhibits a marked and complex dependence on power level, and it is difficult to separate such shifts according to their causes.

National Bureau of Standards, Boulder, Colorado

Cesium Beam Atomic Time and Frequency Standards

By

R. E. Beehler, R. C. Mockler, and J. M. Richardson

(Received February 23, 1965)

With 10 Figures in the Text

Abstract

In recognition of the October 1964 declaration of the International Committee of Weights and Measures that the physical measurement of time be based on a particular transition between two hyperfine levels in the ground state of cesium 133, a review of the characteristics of cesium beam atomic frequency standards is presented. This article discusses the general requirements for frequency and time standards, advantages offered by the atomic standard as compared to astronomical standards, various other atomic standards in brief, the operating principles of cesium standards, measures of performance, error sources in cesium standards, characteristics of several standards in current operation, comparison of cesium standards, and atomic time standards derived from atomic frequency standards.

Introduction

The Twelfth General Conference of Weights and Measures, in October 1964, authorized the International Committee of Weights and Measures to designate an atomic or molecular frequency to be used temporarily for the physical measurement of time. The International Commitee declared that the transition to be used is that between the hyperfine levels $F = 4$, $m_F = 0$ and $F = 3$, $m_F = 0$ of the ground state $^2S_{1/2}$ of the atom of cesium 133, unperturbed by external fields, and that the value 9, 192, 631, 770 Hz is assigned to the frequency of this transition.

A review of the characteristics of cesium beam atomic frequency standards is therefore appropriate. This article discusses the general requirements for frequency and time standards, advantages offered by the atomic standard as compared to astronomical standards, various other atomic standards in brief, the operating principles of cesium standards, measures of performance, error sources in cesium standards, characteristics of several standards in current operation, the comparison of cesium standards, and atomic time standards derived from atomic frequency standards.

Requirements of Time Standards

The unit of the quantity time is the second. Before this unit can be useful in measurement, we must give a definition of it in order to specify its magnitude. The definition is an abstraction. It specifies the idealized concept which underlies the operational realization of the unit. It remains to construct and operate the actual physical apparatus which makes the idealized concept observable. At this point practical variations from ideality occur. We must then distinguish between the ideal definition and the practical apparatus which physically embodies the definition. The qualities of the apparatus are the subject of greatest study, and in our discussion we shall elect to call the apparatus the "standard". The term standard, then, will imply an apparatus based on a particular idealized concept, namely the definition.

It follows that the value provided by the standard may approach the value intended by definition to a greater or lesser degree. The degree to which any prescribed observation of the standard approaches the definition may be termed the accuracy of the standard with respect to the definition, or simply accuracy for short.

A standard of time is taken as a device which generates an ordered, nearly continuous sequence of states, or phases, which can be quantitatively identified and correlated by observation with events — in short, a clock. In practice, clocks are often based on phenomena which recur with almost uniform period. The unit of time will then be proportional to the period of the clock upon which its definition is based.

Since time is a basic quantity in the International System of Units, its standard should satisfy certain requirements deemed desirable for a standard of any quantity.

Firstly, it must have continuity of operation, because of the impossibility of "storing" the unit of time as one "stores", say, the unit of mass. Only if the unit is continuously generated and accumulated into its multiples is it possible to measure an arbitrary interval whenever desired. The only acceptable alternative to continuity is the ability to re-establish the unit and its multiples whenever and wherever needed.

Secondly, as time progresses, the standard must generate a unit which retains constant size with respect to other acceptable measures of time. Of course, a determinable and predictable variability in

the period of the standard is permissible if corrections may be applied which lead to a constant unit.

Thirdly, accuracy of the standard should equal or excel that of standards based on other possible definitions.

Fourthly, the standard should be accessible to all who need it. If it is not directly accessible, its properties must be made available by indirect means such as calibration or broadcast.

Fifthly, the characteristic period of the standard should be convenient with respect to the operations which are to be performed on it. Time standards give an observable phenomenon f (for example, angular position or voltage) nearly of the form $f(t) = f(t + 2\pi n/\omega)$ where t is the time, ω is the nominal angular frequency of the standard, and n is an integer. Necessary operations are averaging the period over large values of n for precision, taking Fourier transforms for large n for analysis of the standard, and generating multiples and submultiples of the period for measurement. It is convenient that ω be large so that these operations can be applied to conveniently small intervals as judged by a time characteristic of man's work, such as his lifetime or the time in which significant changes in techniques occur.

Finally, because of the need to locate events on a continuous scale of time running from some arbitrary origin and common to all observers, the standard should also be capable of continuously accumulating the units. This process will give what is often called epoch. Epoch means the state, or phase, of the standard expressed in the measure of time, as referred to some arbitrary initial state.

Astronomical and Atomic Time Standards

Up to now, time standards based upon the observed positions of celestial bodies undergoing known or assumed motions have best satisfied the requirements discussed above. Two of the many possible celestial "clocks" have major importance. These are the rotation of the earth as manifested by the apparent diurnal motion of the stars, and the orbital motion of the earth, as manifested by the apparent orbital motion of the sun. The apparent diurnal motion of the sun, which also serves as an important clock, is a combination of these phenomena.

The requirement of continuity of operation over the whole interest span of mankind, and beyond, can hardly be better satisfied than by these celestial standards.

Successive refinements in astronomical knowledge and techniques over the centuries have resulted in closer and closer realization of a unit nearly constant in time. One outstanding improvement was the replacement of the mean solar second by the ephemeris second as the accepted unit. The mean solar second, both in concept and in practice, is subject to fluctuations of the order of 1 part in 10^8 by comparison with other acceptable standards. The ephemeris second is constant in concept, and although there is no evidence that the practical realization of it is other than constant, unpredictable changes and aging effects could occur.

Astronomical standards have always satisfied the requirement of accuracy very well. The standard for the ephemeris second is the observed motion of the moon taken together with its theoretical relationship to the observed motion of the sun. The accuracy of this standard with respect to the definition is a few parts in 10^9.

The requirement of accessibility at any place on earth and at any time is well satisfied by celestial standards. As refinements have been made, however, it has been necessary to rely on a few well equipped observatories to make and reduce the observations and to disseminate the results by appropriate means.

The characteristic period of the celestial standard, presently the tropical year, is inconveniently long. Observations over a few years are necessary to attain precision comparable to the other factors which limit accuracy. Observations over centuries are necessary for an exhaustive understanding of the standard. Interpolation by auxilliary clocks is necessary between observations of the celestial standards.

Astronomical standards provide epoch extremely well. Their continuous operation precludes any lapse which would destroy the relationship of the present epoch to the initial epoch. Their long characteristic periods help avoid ambiguity of phase, even with infrequent observation.

Atomic frequency standards are based upon the frequency ν corresponding to a transition between two atomic states separated in energy by ΔE, according to the Bohr relation

$$h\nu = \Delta E\,, \tag{1}$$

where *his* Planck's constant. Atomic standards have been developed in the past decade to the point that they satisfy the requirements of good time standards to a degree competitive with astronomical standards.

Continuity of operation has been achieved for intervals of several years. In case of failure, it is possible to re-establish the unit of time with confidence.

Constancy in the size of the unit based on an atomic definition may be strongly presumed to hold by the nature of atomic energy levels. They are subject to the laws of quantum mechanics and electrodynamics, which enjoy a validity and permanence equal to that of the laws of dynamics underlying the astronomical standards. In particular the levels are determined by the interactions of relatively few elementary particles, and are often amenable to detailed theoretical analysis.

The greatest improvement of atomic standards over astronomical standards has been in the accuracy of the standard with respect to the definition. Accuracy of about 1 part in 10^{11} is now typical, and further improvement appears readily possible.

Atomic standards are widely accessible either by construction or purchase. They represent a modest investment in apparatus compared to that needed for astronomical time determinations. Wide radio dissemination of the output of a small number of good atomic standards still remains economically desirable, just as for astronomical standards.

The short characteristic period of the atomic standard is an advantage. Averages over the many cycles necessary to attain statistical precision of measurement are possible in minutes, hours, or days. For example, measurement precision of parts in 10^{13} are attainable for averaging times of 12 hours. For this reason, atomic standards make their results

available more promptly than astronomical standards. Small time intervals down to the nanosecond region are available directly from the standard because of its high frequency without recourse to a separately calibrated oscillator. Present engineering technology has enabled electronic integration of the period of the standard to provide large time intervals of typically several years with negligible error.

Epoch for an atomic time standard may be obtained by such electronic integration of periods. It is a matter of engineering to attain adequate reliability and redundancy. In case of failure of the period integrating apparatus, a lapse in the resulting time scale will occur. This lapse may be bridged by auxiliary standards, such as astronomical standards, but with some loss of accuracy in relating past epochs to present epochs. This loss of accuracy may be quite acceptable however, for many applications.

Atomic standards thus offer equivalent or improved characteristics over astronomical standards for time interval. Both the standards application and technological applications outside the scope of this paper call for the designation of an atomic unit of time interval and a time scale derivable from it. Other units of time interval and other time scales remain important for specialized applications. The ability to transform from one system to another is all that is needed to realize the advantages of all systems.

Various Atomic Frequency Standards

The cesium standard should be placed in perspective with respect to the various atomic frequency standards. Only in the years subsequent to 1945 did it appear technically feasible to try what had been recognized as possible in principle for some time — to control the rate of a clock by a frequency characteristic of an atom or molecule. I. I. RABI in his 1945 Richtmeyer Lecture before the American Physical Society made the specific suggestion, according to HERSHBERGER and NORTON (1948). The frequencies which appeared most suitable were either those characteristic of atomic hyperfine structure or molecular motions such as inversion or rotation. The techniques of observation which developed were absorption at resonance by the gas, the atomic beam method, the maser principle and the optical-microwave double resonance technique.

NH_3 Absorption. HERSHBERGER and NORTON (1948) gave early results using microwave absorption of the $(J = 3,\ K = 3)$ inversion line of NH_3 at 23,870 MHz. Basically the technique uses a microwave source, an absorption cell under low pressure to permit well resolved spectral lines, and a detector arranged to display absorption *vs* frequency. A practical NH_3 device (LYONS, 1952) gave precision of about 2 parts in 10^8 over a run of 8 days. The gas absorption technique is limited mainly by the wide spectral lines, typically 100 kHz, produced by Doppler and collision broadening. For this reason, the method is now obsolete for highly precise frequency standards.

Common Features. The remaining techniques of observation all have essential general features in common. Atoms are prepared in a pure state, the state is arranged to have a long lifetime against deexcitation, the atoms are stimulated by microwave radiation to emit (or absorb) in a way free of first-order Doppler effect, and the change of state is detected by convenient means.

Cesium Beam. Atomic beam techniques as described below have been successfully used for the magnetic hyperfine transitions of Cs^{133} at 9,192 MHz. ESSEN and PARRY (1957) at the National Physical Laboratory in England first reported complete success in using the *Cs* resonance to rate an oscillator on a routine basis. Since then, the development of cesium beam standards has been intensive. Several other national standards laboratories have reported results including Canada, United States, and Switzerland (see references).

National standards laboratories in four or five other countries are constructing instruments. Accuracy has been refined to about 1 part in 10^{11} as discussed below. The list of references is reasonably complete for cesium standards and reflects the extent of the development.

Thallium Beam. Successful thallium frequency standards have been reported (BONANOMI, 1962; BEEHLER and GLAZE, 1963). The transition used is between the two magnetic hyperfine levels in the ground state, $^2P_{1/2}$, arising from the coupling of the nuclear spin angular momentum and the electronic angular momentum. The transition is designated as

$$F = 0,\ m_F = 0 \rightleftarrows F = 1,\ m_F = 0\ .$$

The frequency is 21,310,833,945. 9 $\pm$ 0.2 Hz (BEEHLER and GLAZE, 1965). In principle thallium offers advantages over cesium in a lesser dependence of transition frequency on magnetic field, greater simplicity of the Zeeman spectrum, greater beam signal intensity (since a greater fraction of all atoms in the ground state is in the $m_F = 0$ states used for the standard frequency transition), and higher frequency than cesium by a factor of two so that a given absolute uncertainty in frequency measurement yields correspondingly greater relative precision. Increased experimental difficulties arise from greater difficulty of deflection and detection. The major limitation on accuracy appears to be phase shift of the *rf* radiation between the two separated field regions, as discussed below for cesium. Accuracy attained so far is comparable with the accuracy attained for cesium.

NH_3 Maser. The first maser used a beam of NH_3 molecules prepared in the upper inversion state of the $J = 3,\ K = 3$ rotational state by a quadrupolar electrostatic focuser, which focuses molecules in the upper state and defocuses those in the lower state. (GORDON, ZEIGER, and TOWNES, 1954; BASOV and PROKHOROV, 1955). The beam traverses a microwave resonator, in which the molecules are stimulated to emit by the existing microwave field. In the steady state the radiation emitted maintains a stored radiation field to stimulate further emission and supplies internal losses of the resonator and external loads. Many subsequent refinements have been developed. Nevertheless, the accuracy of the NH_3 beam maser has not proved as great as the accuracy of the cesium beam and the hydrogen maser, yet to be discussed. The reasons concern a complicated dependence of frequency on experimental conditions, partly associated with the unresolved structure of the inversion resonance line.

Hydrogen Maser. The hydrogen maser (GOLDENBERG, KLEPPNER, and RAMSEY, 1960) uses the transition

$$F = 1, m_F = 0 \rightarrow F = 0, m_F = 0 ,$$

between the magnetic hyperfine levels in the ground state, $^2S_{1/2}$, of atomic hydrogen. The frequency is 1,420,405,751.80 ± 0.03 Hz (CRAMPTON, KLEPPNER, and RAMSEY, 1963). The $F = 1$, $m_F = 0$ state is prepared by magnetic focusing of a beam of atoms, as in atomic beam techniques. A long lifetime in the excited state of 1 to 3 seconds is attained not by time of flight through free space as in the beam maser, but by storage in a bulb. The bulb has walls suitably coated so that wall collisions have a low probability of perturbing the prepared state. The bulb is contained in an electromagnetic resonator, which provides stimulation of radiation and power to external loads just as in the beam maser. First order Doppler shifts are effectively cancelled because of the random directions of the atoms. The technique has several advantages described in the literature (KLEPPNER, GOLDENBERG and RAMSEY, 1962). Stability of the radiation is reported to be about 3 parts in 10^{13} over a few days (VESSOT and PETERS, 1962). Accuracy is estimated at about 1 part in 10^{11}. Promise of further improvement is good (RAMSEY, 1965).

Optical-Microwave Double Resonance. The optical microwave double resonance technique, often designated as the optically pumped gas cell, emerged about 1957 (KASTLER, 1957). In Rb^{87}, for example, atoms are preferentially pumped out of the lower ($F = 1$) of two magnetic hyperfine levels by optical resonance radiation. Repopulation of this state by stimulated microwave emission from the $F = 2 \rightarrow F = 1$ transition is detected at microwave resonance by increased optical absorption of the pumping radiation. Lifetimes in the $F = 2$ state are prolonged by an inert buffer gas, collisions with which do not de-excite the $F = 2$ state. Inert wall coatings may be used in addition. The buffer gas also performs the essential function of reducing the Doppler width of the radiation. It confines the radiating atom to a region small compared with the wavelength. Thus the motion of the source does not cumulatively affect the phase of the emitted wave, as it does ordinarily in producing the Doppler effect. (DICKE, 1953; WITTKE and DICKE, 1956). Microwave-optical double resonance devices are convenient and provide short-term stability from day to day of about 1 part in 10^{11}. Accuracy with respect to the transition frequency of the unperturbed atom suffers from frequency shifts which are not adequately understood, and must be taken as perhaps 1 part in 10^{10}. These are associated with the buffer gas collisions and with the spectral distribution and intensity of the pumping radiation. Thus the technique is no longer considered suitable for the most accurate frequency standards.

Principles of Cesium Beam Operation

Hyperfine Structure. The hyperfine splitting in cesium arises because of the interaction between the magnetic moment of the nucleus and the magnetic field produced by the valence electron at the position of the nucleus.

In general, the valence electron produces a magnetic field at the nucleus by virtue of its orbital motion about the nucleus and also by virtue of its intrinsic magnetic moment. These two contributions to the field will be designated by $\vec{H}_{\text{orbit}}$ and $\vec{H}_{\text{spin}}$ and their sum by $\vec{H}_{\text{el}} = \vec{H}_{\text{orbit}} + \vec{H}_{\text{spin}}$. The Hamiltonian for the interaction can be concisely written as

$$\mathcal{H} = -\vec{\mu}_I \cdot \vec{H}_{el} , \qquad (2)$$

where $\vec{\mu}_I$ is the magnetic moment of the nucleus. For an alkali atom such as cesium, the ground electronic state is an S state and the orbital angular momentum is therefore zero. Since $\vec{H}_{\text{orbit}}$ is proportional to this angular momentum, the important contribution to $\vec{H}_{\text{el}}$ is $\vec{H}_{\text{spin}}$. The electron spin has two possible orientations, and we expect two different energy levels for the atom. The ground state for zero external field is thus split by the interaction into two levels and the separation of the two levels is referred to as the hyperfine structure (hfs) separation. If the appropriate quantum formalism is used, the separation W of the two levels is given approximately by (KOPFERMANN, 1948)

$$W = (I J F m_F \mid -\vec{\mu}_I \cdot \vec{H}_{el} \mid I J F m_F)$$
$$= \frac{g_I \mu_N \mu_0 Z^3}{a_0^3 n^3} \left[\frac{F(F+1) - I(I+1) - J(J+1)}{J(J+1)(L+\frac{1}{2})} \right], \qquad (3)$$

where g_I is the nuclear g-factor, μ_N is the nuclear magneton, μ_0 is the Bohr magneton, Z is the atomic number, a_0 is the radius of the first Bohr orbit ($a_0 = \hbar^2/me^2$), n is the principle quantum number, F is the total angular momentum quantum

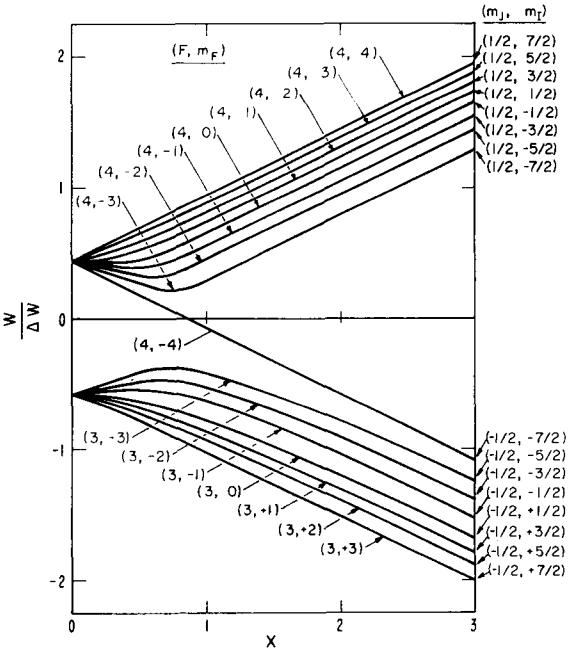

Fig. 1. Energy level diagram of Cs^{133} in the $^2S_{1/2}$ ground state as a function of the applied magnetic field

number, I is the nuclear angular momentum quantum number, J is the total electronic angular momentum quantum number ($\vec{J} = \vec{L} + \vec{S}$), L is the orbital angular momentum quantum number for the valence electron, and m_F is the magnetic quantum number associated with F. The level separation was first worked out by FERMI (1930) and FERMI and SEGRE (1933). Equation (3) reduces to their result for $J = 1/2$ and $L = 0$.

Effect of External Field. If an external field is applied, certain degeneracies are removed as shown in Fig. 1. This energy level diagram is for the ground state of cesium for which $I = 7/2$, and $J = 1/2$. In this case, since $F = I + J$, $I + J - 1, \ldots, I - J$, there are only two F levels: $F = I \pm 1/2$ or $F = 4$ and $F = 3$. Their energy as a function of the applied field H is given by the Breit-Rabi formula (RAMSEY, 1956):

$$W_{F=I\pm\frac{1}{2},\, m_F} = \frac{-\Delta W}{2(2I+1)} + \mu_0 g_I m_F H \pm$$
$$\frac{\Delta W}{2}\left[1 + \frac{4 m_F x}{(2I+1)} + x^2\right]^{\frac{1}{2}}, \qquad (4)$$

where ΔW is the hfs separation, given approximately by the Fermi-Segré formula, between the $F = I + 1/2$ and $F = I - 1/2$ states in zero field; and

$$x = \frac{(g_J - g_I)\,\mu_0 H}{\Delta W}.$$

For a small applied field $\vec{H}$ the energy levels may be drawn as in Fig. 2. From Fig. 1 and 2 it is evident that the states $(F = 4, m_F = 0)$ and $(F = 3, m_F = 0)$ are the least sensitive to

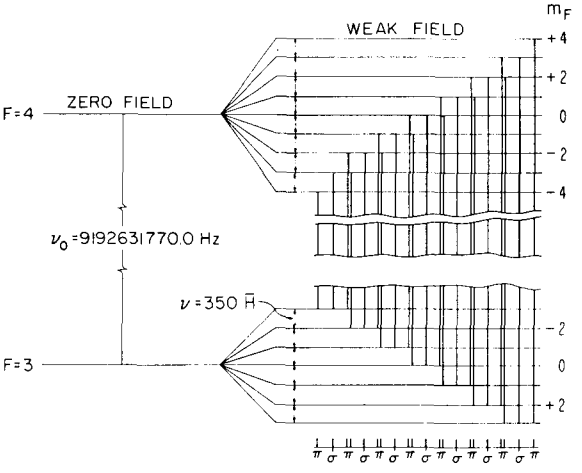

Fig. 2. Energy level diagram for Cs^{133} in a weak applied magnetic field

the applied field. Since the accuracy with which we can measure the transition frequency is partly determined by how accurately we can measure H, we choose this field insensitive transition for our frequency standard. The frequency is slightly field sensitive, and one can show from the Breit-Rabi formula that the frequency is given by

$$\nu = \nu_0 + 427\,H^2 \tag{5}$$

for small values of H, where ν is the frequency in Hz of the $(F = 4, m_F = 0) \longleftrightarrow (F = 3, m_F = 0)$ transition when the applied

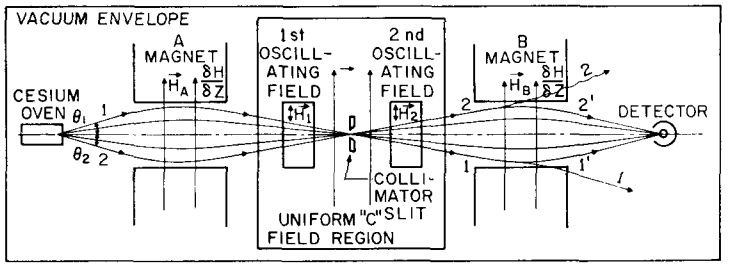

Fig. 3. A schematic of a typical atomic beam spectrometer

field has a magnitude of H (in oersteds). ν_0 is the transition frequency for $H = 0$; it has the value 9192631770.00...Hz.

Method of Observation. Now let us see how we observe these transitions with the atomic beam technique. The atomic beam spectrometer has the basic structure shown in Fig. 3. Neutral atoms effuse from the oven and pass through the non-uniform magnetic field of the A deflecting magnet. The atoms have a magnetic dipole moment μ and consequently experience a transverse force in this A-field region. This force is given by

$$F = -\nabla W = -\frac{\partial W}{\partial H}\nabla H,$$

where W is the potential energy of a dipole in the field and depends on H only according to the Breit-Rabi formula (4). The effective magnetic moment is

$$\mu_{eff} = -\frac{\partial W}{\partial H}, \tag{6}$$

by analogy with the case where the dipole moment is independent of H. Hence

$$\vec{F} = \mu_{eff}\,\nabla H. \tag{7}$$

The effective magnetic moment has, in general, a different value for each state:

$$\mu_{eff} = \mu_{F=I\pm\frac{1}{2},\,m_F} = -g_I\,\mu_0\,m_F \mp \left\{\frac{\frac{x}{2} + \frac{m_F}{(2I+1)}}{\left[1 + \frac{4\,m_F\,x}{(2I+1)} + x^2\right]^{\frac{1}{2}}}\right\} \mu_0\,(g_J - g_I). \tag{8}$$

Evidently, then, the force on the atom depends not only on the gradient of the field but also upon the particular state that the individual atom is in. The effective magnetic moment is positive for some states and negative for others. The magnet is designed so that the gradient of the field has a direction transverse to the beam and in the plane of the drawing of Fig. 3.

The quantity μ_{eff}/μ_0 is plotted as a function of the applied field H in Fig. 4. It is simply given by the negative derivatives of the curves plotted in Fig. 1. Suppose the positive z direction is in the upward direction perpendicular to the spectrometer axis in Fig. 4. Let $\vec{e_z}$ be a unit vector in the z direction. The magnets are designed so that

$$\vec{F} = \mu_{eff}\,\nabla H = \vec{e_z}\,\mu_{eff}\frac{\partial H}{\partial z},$$

and if μ_{eff} is negative, as it is for the (4, 0) state (i. e., the $F = 4$, $m_F = 0$ state, see Fig. 4), then the force is downward. If μ_{eff} is positive, as it is for the (3, 0) state, the force is upward in the figure. Atoms effusing from the oven in the θ_1 direction along trajectory 1 (see Fig. 3) that are in the (4, 0) state will experience a downward force. Some of them, those with the proper velocity, pass through the collimator slit and pass on to the second deflecting field region. Those atoms in state (3, 0) effusing in the θ_1 direction experience an upward force and do not pass through the collimating slit. They are eliminated from the beam. The opposite is true for atoms effusing in the θ_2 direction. Those in state (3, 0), experiencing an upward force pass through the collimator, and those in the (4, 0) state are eliminated from the beam and pass into the second deflecting field region. Normally the deflecting fields are high fields so that atoms in states 4, 4; 4, 3; 4, 2; 4, 1; 4, 0; 4, −1; 4, −2; and 4, −3 effusing at a positive angle θ_1 pass through the collimator. Correspondingly, atoms in states 4, −4; 3, 3; 3, 2; 3, 1; 3, 0; 3, −1; 3, −2; and 3, −3 effusing at a negative angle θ_2 pass through the collimator.

If the second deflecting field (that produced by the B magnet) is identical to the A-field, the atoms in, for example, the (4, 0) state following trajectory 1 (see Fig. 3) experience a downward force as in the A-field. They will not strike the detector. Similarly, atoms in the (3, 0) state, say, following trajectory 2 experience an upward force. They too will miss the detector. Suppose now that a radiation field is applied in the uniform field region (the C-field region, applied in order to preserve the state identy of an atom passing from the A-field to the B-field) of frequency appropriate to the $(4, 0) \longleftrightarrow (3, 0)$ transition. Atoms in the (4, 0) state are induced to emit a quantum of energy, and atoms in the (3, 0) state are induced to absorb a quantum of energy. Atoms that were in the (4, 0) state following a trajectory 1 now find themselves in the (3, 0) state. Atoms that were in the (3, 0) states following a trajectory 2 now find themselves in the (4, 0) state. Each sef atom that has made the transition has had its magnetic moments "flipped". As a result of this change in sign of the magnetic moment, the forces on these atoms in the B deflecting region will also change sign. These atoms will now follow the trajectories 1′ and 2′ in Fig. 3 and strike the detector.

By means of the well-known surface-ionization process (Zandberg and Ionov, 1959; Datz and Taylor, 1956) the atoms are converted into positively-charged ions with nearly 100% efficiency and can then be collected and measured. The resulting detected beam current goes through a maximum when the frequency of the radiation field is swept through the resonant frequency of the cesium transition. An actual recording of the spectral line shape, obtained in the process, is shown in Fig. 5 for the usual case of two separated excitation regions (Ramsey technique). The appearance of the auxilliary peaks on either side of the central resonance peak is a consequence of the separated oscillating-field technique. (Ramsey, 1950; Ramsey, 1956). The advantages offered by the Ramsey method

include a narrower width of the spectral line and less severe requirements on the uniformity of the C-field as compared to the single excitation region case (Rabi technique).

Unlike many other resonance experiments, the transition probability is examined by observing the effect of the radiation on the beam rather than the effect of the beam on the radiation field. The intensity of the signal does not depend upon the population difference of the two states but on the sum of their populations. The spectral linewidth is given by the uncertainty relation $\Delta E\, \Delta t \approx h$ or $\Delta\nu\, \Delta t \approx l$, where $\Delta\nu$ is the

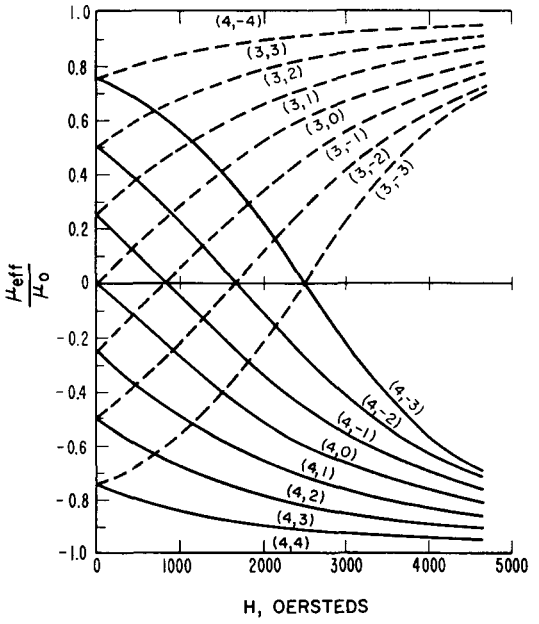

Fig. 4. The effective magnetic moment relative to the Bohr magneton for the various magnetic substates in Cs^{133} as a function of the applied magnetic field

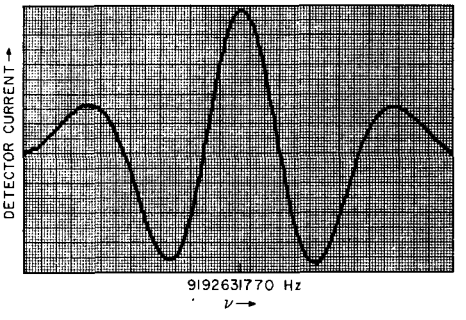

Fig. 5. Recording of the central portion of the Ramsey resonance line shape for one of the National Bureau of Standard's cesium standards

linewidth and Δt is the average transit time of an atom through the radiation field, if a single radiation field is used. If two radiation fields are used to induce the transition, then Δt is the average transit time for an atom to go from the first field to the second. The linewidth thus depends on the average velocity v in the beam and the length of the transition region, since $\Delta t = L/v$.

The process of measuring the frequency of an unknown source in terms of the cesium standard usually involves the direct comparison of the unknown frequency with the known frequency of an oscillator which is controlled in some manner by the atomic resonance. In the most common technique employed the control is done automatically and continuously by using an electronic servo system. The controlled oscillator frequency – normally near 5 MHz – is modulated at a low audio rate and then multiplied to the cesium frequency at 9192 MHz. If the multiplied frequency differs even slightly from that of the resonance maximum, the modulation results in the generation of a component of the detector current at the modulation frequency. If this component is amplified and phase-compared with the original modulation signal, it can be shown that the DC output signal of the phase detector has a magnitude proportional to the amount of deviation of the applied frequency from the atomic resonance frequency and a sign which depends on whether the applied frequency is higher or lower than the resonance. Thus, this signal may be used with appropriate circuitry to correct automatically and continuously the frequency of the 5 MHz oscillator to a value which bears a fixed and known relationship to the defined cesium frequency.

In a somewhat different technique used with some laboratory-type standards the control of the 5 MHz oscillator is accomplished manually. In this case an operator manually adjusts this frequency to a value which results in a maximum current from the detector corresponding to a maximum probability for the atomic transition.

Measures of Performance

There are no universally accepted measures for describing the performance of atomic frequency standards. Until common agreement on these measures is reached, each author is obliged to state exactly how his estimates of performance are to be interpreted.

Fluctuations may occur (a) among various observations for a given adjustment of a given instrument, (b) among various independent adjustments of a given instrument, and (c) among various independent instruments. Usually these fluctuations increase in magnitude in the order mentioned. Each of these types of fluctuations gives useful information about the performance of the standards. The fluctuations of type (a) arise from fluctuations of instrumental and environmental parameters during operation. The fluctuations of type (b) contain fluctuations of type (a) and also fluctuations in setting the adjustable parameters from time to time. The fluctuations of type (c) contain types (a) and (b) and also fluctuations from instrument to instrument in fixing the non-adjustable parameters.

Stability. A sequence of n readings of a particular standard in a particular adjustment, against a comparison oscillator assumed temporarily constant, will show fluctuations. The standard deviation of these observations is often called the stability of the standard. Its value will depend on the duration of the individual observations, and many be qualified as short term or long term stability. For example, if the average frequency over 1 second is measured for $n = 100$ successive times, the standard deviation of such a 1-second observation as estimated from the sample of 100 observations may be called the "short term stability" applicable to 1 second duration. In this sense, stability indicates the degree to which the standard in steady operation gives results constant in time.

Of interest is not only the magnitude of the frequency fluctuations but also their rate. Thus a more complete characterization of the stability of a given standard in a given state of adjustment would be all the statistical properties of the frequency fluctuations $F(t)$ about a mean frequency $\bar{\nu}$ considered as a function of time, that is $F(t) = \nu(t) - \bar{\nu}$ where $\nu(t)$ is the instantaneous frequency. These would be the moments of the amplitude distribution of $F(t)$, its spectrum, its autocorrelation function, and so forth. Studies of such properties are in progress but are beyond the scope of this paper.

Precision. Precision is considered a property of a measurement process, not of an instrument alone. It measures the random error in carrying out a prescribed observation. For example, if the prescribed observation is the mean of n successive readings taken as described in the preceding section, the sample standard deviation of the mean would appropriately measure the precision of such an observation.

Reproducibility. A sequence of comparisons for independent adjustments of a particular standard, against a reference standard assumed available and temporarily constant, will yield a mean and a standard deviation. The standard deviation of such observations may be called the reproducibility of the instrument. In this sense reproducibility indicates the degree of resettability of the instrument.

Accuracy. We use accuracy in this paper as the degree to which any prescribed observation of a particular standard approaches the definition. It requires (a) an estimate of the random error in carrying out the prescribed observation for a given adjustment (that is, precision), (b) an estimate of systematic errors incurred in adjusting the standard (that is, reproducibility), and (c) an estimate of systematic errors

incurred in constructing the standard. The measure of all these errors should be stated; that is, whether they represent limits of error, or one-, two-, or three-sigma estimates of a distribution of values. The method of combination should be stated. If the errors may be considered independent, for example, the square root of the sum of their squares may be taken as a proper estimate of the total error.

The estimate of precision of an observation has been discussed above.

We must now distinguish between possible ways of making the last two estimates, (b) and (c) depending on whether the standard to be evaluated stands in the highest echelon so that no higher reference standards is available, or whether the standard is in a lower echelon and may be compared with a reference standard. If the standard stands alone, the last two estimates must be made by a study of the effect of all known parameters on the frequency and an estimate of the uncertainty in these parameters in a given instrument or for a given adjustment.

A somewhat different viewpoint is possible if there are several standards of comparable quality in the highest echelon. We may then agree to consider all these as a sample from an ensemble of standards. They may be compared among one another with respect to the sample mean. Then the sample standard deviation may be taken as a single overall estimate of the accuracy of any one of the standards. This view assumes that all members of the ensemble randomly partake of variations in the parameters and are stationary over the time required in practice, often lengthy, to effect the comparisons.

If a reference standard is available, then accuracy *with respect to the reference standard* is often taken simply as the mean difference of successive comparisons for independent adjustments of the test standard. This view assumes that the precision of the comparison may be made arbitrarily small by increasing the number of observations.

Confusion of Terminology. Various authors have used the concepts explained here but under various names. We thus find "precision" used for our concept of "stability", as well as for our concept of "reproducibility". The reader is cautioned against this confusion.

Error Sources in Cesium Beam Standards

Systematic errors in cesium beam standards may arise from a great variety of sources. Fortunately, however, the atomic beam magnetic resonance technique used in cesium standard has the virtue that most of these errors can be kept quite small, providing that reasonable care is exercised in the design and construction of the standard. It has been found possible in at least two national standards laboratories to reduce the combined systematic error from all known sources to a level of $\pm 1 \times 10^{-11}$. In the following discussion an attempt will be made to mention at least briefly all the known error sources that may contribute significantly to the inaccuracy of a cesium standard. In some case quantitative results will be given based on the authors' experience with three independent laboratory-type standards at NBS. The error sources will be grouped depending on whether they produce a displacement of the resonance line, an asymmetrical distortion of the resonance line shape, or an erroneous measurement of the resonance peak even though the line is neither displaced nor distorted.

Errors Which Result from a Displacement of the Resonance

Uncertainty in Magnetic Field. The dependence of the cesium $(4, 0) \longleftrightarrow (3, 0)$ transition frequency on the magnitude of the uniform magnetic C field is given by

$$\nu = \nu_0 + 427\,\overline{H^2(x)}\,, \tag{9}$$

where ν and ν_0 are in Hz, H is in oersteds, and $\overline{\mathrm{H}^2\,(x)}$ is a spatial average over the length between the two oscillating field regions. Any uncertainties in determing $\overline{\mathrm{H}^2\,(x)}$ will lead to corresponding errors in frequency measurements referred to ν_0, the zero-field standard frequency. In practice, the field is determined from frequency measurements of various field-sensitive transitions in cesium by using theoretical relations between frequency and field magnitude. The most commonly used transitions for this puspose are the low frequency transitions between the various m_F levels within a single F state, such as the $(4, -4) \longleftrightarrow (4, -3)$ transition, and certain microwave transitions, such as the $(4, 1) \longleftrightarrow (3, 1)$ transition (see Fig. 2). The appropriate frequency-field relationships are:

$$\nu = 3.5 \times 10^5\,\overline{H(x)} \text{ for } (4, -4) \longleftrightarrow (4, -3) \tag{10}$$

and

$$\nu = \nu_0 + 7 \times 10^5\,\overline{H(x)} \text{ for } (4, 1) \longleftrightarrow (3, 1)\,. \tag{11}$$

The value of $\overline{\mathrm{H}\,(x)}$ obtained in this manner is then normally squared and used in equation (9) in place of $\overline{\mathrm{H}^2\,(x)}$, which is much more difficult to determine. Thus, frequency uncertainties resulting from this procedure arise from two sources:

(a) uncertainties in the value of $\overline{\mathrm{H}\,(x)}$, and

(b) uncertainties due to the use of $\overline{\mathrm{H}\,(x)}^2$ for $\overline{\mathrm{H}^2\,(x)}$.

In order to establish the uncertainty in frequency which results from an uncertainty in $\overline{\mathrm{H}\,(x)}$, we can give $\mathrm{H}\,(x)$ a constant increment $\Delta\mathrm{H}$ and compute the resulting $\Delta\nu$ from equation (9). Thus,

$$\nu + \Delta\nu = \nu_0 + 427\,[\overline{H(x)} + \Delta H]^2 \tag{12}$$

$$= \nu_0 + 427\,[\overline{H^2(x)} + 2\,\overline{H(x)}\,\Delta H + (\Delta H)^2]\,. \tag{13}$$

Neglecting the square of the differential and subtracting ν from both sides, again using (9), gives

$$\Delta\nu = 2\,(427)\,\overline{H(x)}\,\Delta H\,. \tag{14}$$

The procedure followed at NBS for determining the uncertainty in $\overline{\mathrm{H}\,(x)}$ consists of measuring four different independent microwave transitions for each setting of the current which produces the C field. A least-square fit of a straight line is made to these data, and the uncertainty to be associated with any field value obtained from this calibration is taken to be the computed standard deviation of a point from this line. This error contribution amounts to $\pm 1.9 \times 10^{-5}$ oersted or $\pm 1 \times 10^{-13}$ in frequency for the normal field value used of .050 oersted.

Longitudinal Non-uniformity of Magnetic Field. The uncertainty from the second source mentioned arises becauses $\overline{\mathrm{H}^2\,(x)}$, which is the quantity that determines the true value of ν, is not necessarily equal to $\overline{\mathrm{H}\,(x)}^2$, which is the value determined and used in practice. The error in Hz in using the latter quantity is given by

$$\Delta\nu = 427\,[\overline{H^2(x)} - \overline{H(x)}^2]\,. \tag{15}$$

It can readily be shown by direct substitution that if the C field is expressed as

$$\mathrm{H}\,(x) = \mathrm{H}_0\,(x) + cI\,, \tag{16}$$

where $\mathrm{H}_0\,(x)$ is the non-uniform residual field in the drift-space region with the current I turned off and c is a constant, then

$$\Delta\nu = 427\,[\overline{H_0^2(x)} - \overline{H_0(x)}^2]\,. \tag{17}$$

463-560 O - 72 - 8

If sufficiently detailed knowledge of the field uniformity can be obtained in some manner, this error can be evaluated and applied as a correction to all frequency measurements. Fig. 6 shows a plot of the residual field uniformity in one of the NBS standards obtained by drawing a very small sensitive magnetometer probe along the drift-space region in the position normally occupied by the atomic beam. From these data $[\overline{H_0^2(x)} - \overline{H_0(x)}^2]$ is found to be 0.14×10^{-6} oersteds^2 resulting in a frequency error given by equation (17) of less than 1×10^{-14}. Since this non-uniformity is measured only infrequently, however, and is known to be somewhat dependent on external conditions which may vary with time, it is considered preferable to treat the computed value $\Delta\nu$ as an uncertainty rather than a known correction.

Transverse Non-uniformity of Magnetic Field. Non-uniformity of field across the beam cross section may also produce frequency errors. This effect produces a broadening of the field-sensitive microwave resonance line with respect to the field-insensitive (4, 0)←→(3, 0)

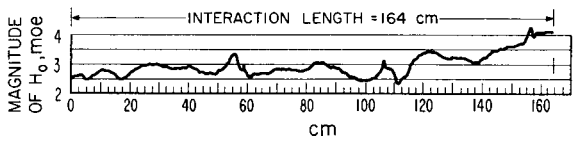

Fig. 6. Plot of the variation of the magnitude of the residual magnetic field $H_0(x)$ along the length of the C-field region in NBS II

line, thus offering a means of detecting the existence of this condition.

Doppler Effects. The presence of first and second order Doppler effects will also produce a displacement of the resonance. In general, one does not expect any first order Doppler shifts in this type of standard, since ideally the radiation field in the cavity consists of two equal traveling waves going perpendicular to the velocity of the atoms. If, however, due to imperfect alignment the atoms have a component of their velocity parallel to the radiation field and a net traveling wave exists in the cavity, a frequency shift $\Delta\nu$ may occur given by

$$\Delta\nu = \frac{1-R}{R}\nu\frac{\bar{v}}{c}\sin\alpha\,, \tag{18}$$

where R is the power reflection coefficient, v is the mean speed of the atoms in the beam, and α is the angle between the waveguide and a line normal to the beam. The experimental verification of such a shift has not as yet been made conclusively.

The unavoidable second order Doppler shift given by

$$\frac{\Delta\nu}{\nu} = v^2/2c^2 \tag{19}$$

amounts to about 3×10^{-13} and is negligible for most present applications.

Electric Fields. Possible frequency shifts due to electric fields are well beyond present measurement precision — at least for fields on the order of a few volts/cm. (HAUN and ZACHARIAS, 1957).

Errors Which Result from a Distortion of the Resonance Shape

Longitudinal Non-uniformity of Magnetic Field. If the C-field is non-uniform along its length in such a way that its magnitude at the two localized regions of oscillating field is not equal to its average value over the entire drift space, the Ramsey resonance pattern will not be centered on the broad Rabi resonance pedestal. The resultant asymmetrical distortion of the Ramsey line will lead to a frequency error, since the peak of the line is then shifted from its undisturbed value. Observation of the symmetry of the field-sensitive microwave transitions such as the (4, 1)←→(3, 1) provides a very sensitive indication of the longitudinal non-uniformity. The amount of observed asymmetry can be related to the degree of non-uniformity, thus permitting an estimate of the resultant error to be made.

RAMSEY has shown that if the magnitude of the C field varies within the small oscillating field regions large frequency shifts may result. (RAMSEY, 1959). The presence of such a shift may be detected rather easily, since the amount of error depends strongly upon the intensity of the radiation field in the cavity.

Polarity Dependent Shifts. In a number of standards now in operation frequency shifts of up to 1×10^{-10} have been observed upon reversing the polarity of the C field. (BONANOMI, 1962; BEEHLER and GLAZE, 1963; ESSEN, STEELE, and SUTCLIFFE, 1964). The sources of these shifts have been attributed to either a Millman effect or the influence of a rather large residual field in the transition region. The Millman effect is due to the beam experiencing an oscillating field which changes direction along the beam path. Such a condition may occur if there is leakage of the radiation field in the cavity out the beam entrance and exit holes. Since the direction of the resulting frequency shift changes upon reversal of the C-field direction, the error may be eliminated by making frequency measurements for both field polarities and using the mean value.

If a residual static field exists in such a direction as to cause the magnitude of the resultant field to vary when the component due to the C-field current is reversed, the measured transition frequency uncorrected to zero field will depend on the polarity. However, in this case the value of $\overline{H}$ given by the field calibration will also depend on the C-field polarity in such a way that no error should result in the measured frequency referred to zero field after the 427 H^2 correction is applied to the data.

Phase Difference. If a difference in phase exists between the radiation fields at the two ends of the microwave resonant cavity, the Ramsey resonance curve will be distorted asymmetrically with a resulting frequency error. Although in an ideal lossless single microwave resonant cavity there would be no phase difference, it is usually found in practice that unavoidable losses and electrical asymmetry do exist which causc phase shifts. KARTASCHOFF (KARTASCHOFF, 1962) has shown that the phase shift $\Delta\varphi$ due to an electrical asymmetry ξ in length units in a cavity of length L and attenuation constant per unit length α can be expressed as

$$\Delta\varphi = \alpha L\beta\xi\,, \tag{20}$$

where β is the propagation constant of the waveguide. Since the phase difference $\Delta\varphi$ will result in a frequency error $\frac{\Delta\nu}{\nu} = \frac{\Delta\varphi}{\pi Q}$, where Q = the quality factor of the

resonance line, the frequency shift can be computed for a given electrical asymmetry. Note that this particular error is independent of beam length. These relations place rather severe mechanical tolerances on the cavity, since an asymmetry of only 0.12 mm will produce an error of about 1×10^{-12}. Experience at NBS has shown that phase shifts sufficient to cause frequency errors of 1×10^{-11} may also develop gradually with time as a result of the accumulation of cesium and pump oil deposits within the cavity ends. Periodic cleaning of the cavity structure is necessary in this case.

A means of detecting the presence of cavity phase shifts and correcting for their effect is provided by the fact that the direction of the resulting frequency shift from the true value changes with the direction in which the beam traverses the cavity. Therefore, if the standard is designed to allow for the physical rotation of the cavity structure by 180° without disassembly of the cavity, or if the direction of beam traversal can be changed by interchanging the oven and detector, one-half of the frequency shift observed as a result of either of these operations can be used as a correction to all data, so that only the uncertainty in determining the phase shift contributes to the inaccuracy of the standard. Both methods have been utilized at NBS with the tentative conclusion that the more reproducible data is obtained with the second technique, possibly due to the unavoidable changing stresses caused by actual rotation of the cavity. The uncertainty in the correction as determined from the reproducibility is $\pm 3 \times 10^{-12}$ for NBS III. Attempts have also been made in some laboratories to detect phase shift errors by a careful examination of the Ramsey line symmetry. Signal-to-noise ratios achieved in present standards, however, limit the minimum detectable asymmetry to amounts corresponding to frequency shifts of 1×10^{-10} or greater.

Cavity Mistuning. A second possible error source associated with the microwave cavity is the cavity pulling effect which occurs if the resonance frequency of the cavity is not tuned exactly to the cesium frequency. The magnitude of this shift is given by

$$\Delta\nu_L = (Q_c/Q_L)^2 \Delta\nu_c \,, \tag{21}$$

where

$\Delta\nu_L$ = the frequency error of the Ramsey line
$\Delta\nu_c$ = the amount by which the cavity is mistuned
Q_c = the Q of the cavity
Q_L = the Q of the Ramsey line.

For a cavity Q of 5000 and a line width of 100 Hz the calculated shift is about 3×10^{-13} for a 1 MHz detuning. In practice, the cavity can usually be kept tuned to within much narrower limits than $\pm$ 1 MHz.

Neighboring Transitions. Another possible error contribution which may be quite significant under some conditions arises from distortion of the line by overlap of other microwave transitions in the cesium spectrum. Assuming that the parallelism of the C field and the oscillating fields is maintained properly so that π transitions ($\Delta m_F = \pm 1$) are not excited, the nearest transitions to the $(4, 0) \longleftrightarrow (3, 0)$ are the $(4, 1) \longleftrightarrow (3, 1)$ and $(4, -1) \longleftrightarrow (3, -1)$ σ resonances ($\Delta m_F = 0$) which are located symmetrically above and below the $(4, 0) \longleftrightarrow (3, 0)$ in frequency. Ideally these neighboring lines are symmetric about the $(4, 0) \longleftrightarrow (3, 0)$ both in frequency and intensity so that no net overlap shift should occur. However, it is usually found in practice that due to imperfect beam alignment the amplitudes of these two neighboring transitions are not equal. The resulting shift in the $(4, 0) \longleftrightarrow (3, 0)$ frequency in this case depends on the linewidths of the overlapping lines, the amount of asymmetry existing in the intensities, and especially on the separation in frequency of the overlapping lines from the $(4, 0) \longleftrightarrow (3, 0)$ (Mockler, Beehler, and Snider, 1960). This amount of separation depends on the magnitude of the C field according to (11), so that the surest way of avoiding this effect is to operate at a sufficiently high C field — normally, above 0.040 oersteds — so that significant overlap does not occur. In some of the early NBS work on cesium standards at fields of only 0.020 oersteds it was discovered that a systematic error of greater than 4×10^{-11} was being introduced into the data from an overlap effect.

Spectral Purity. The spectral purity of the microwave signal used to excite the cesium resonance has been found to be extremely important (Barnes and Mockler, 1960). When the transition is excited with a signal which contains sidebands at a significant level, particularly if the sidebands are asymmetrically distributed about the carrier, large frequency shifts in the $(4, 0) \longleftrightarrow (3, 0)$ standard frequency may result. For example, excitation of the cesium resonance in the original NBS cesium standard at one time yielded a frequency shifted by 32×10^{-10}. Examination of the spectrum using a high-resolution ammonia-maser spectrum analyzer system (Barnes and Heim, 1961) showed the presence of large, asymmetrical sidebands at the power line frequency and its harmonics. If the excitation contains a single unbalanced sideband at a frequency ν_s, the frequency shift produced is (Ramsey, 1956)

$$\frac{\Delta\nu}{\nu_0} = \frac{A_s}{A_0} \frac{W^2}{\nu_0 (\nu_0 - \nu_s)} \,, \tag{22}$$

A_s = amplitude of sideband
A_0 = amplitude of carrier at ν_0
W = resonance width
ν_0 = cesium resonance frequency.

The advantage of a narrow resonance line is readily apparent. This relation also applies if A is the difference in amplitude of two unbalanced sidebands. Since the sideband intensity is multiplied by the factor of frequency multiplication, those which originate in the driving oscillator (usually near 5 MHz) or early stages of the multiplier chain are particularly serious. For example, a sideband 100 db below the carrier at the oscillator frequency of 5 MHz will be only 35 db below the carrier at cesium frequency, even if the multiplier chain adds no noise of its own. If the most significant sidebands are due to power line frequencies and its harmonics, as is often the case, the spectrum may change as ground loops and electrical connections are changed in the laboratory resulting in time-varying frequency errors. Ideally, the spectrum of the excitation should be monitored frequently with a high-resolution spectrum analyzer. As a practical compromise at NBS, the beat frequency at approximately 100 Hz between the normal cesium excitation signal and a similar signal from another oscillator-multiplier

chain system which is known to have a clean spectrum is monitored regularly on an oscilloscope. The presence of noise, modulations, or other deviations from a sinusoid are watched for. This simple system is sufficiently sensitive that on several occasions undesirable modulations have been detected which were causing frequency errors of less than 2×10^{-11}.

Errors Which are Present Even When the Resonance is Perfect

Some contribution to inaccuracy arise because of errors involved in the measurement of the resonance peak, even though the line itself is undistorted and not displaced.

Random Fluctuations. Fig. 7 shows data from a 48-hour continuous comparison of two independent cesium standards, designated NBS II and NBS III, maintained at the National Bureau of Standards (NBS) in Boulder, Colorado. Each plotted point, representing the difference frequency averaged over 1 hour, is the mean of twenty 3-minute measurements of the period of the beat frequency. The length of the vertical bar drawn at each point represents the computed standard error of the 1-hour observation (standard deviation of the mean of the twenty 3-minute averages) and is thus an estimate of the relative precision of this process. This precision figure is typically $\pm 7 \times 10^{-13}$ for this data.

A second estimate of the frequency fluctuations appropriate for 1 hour averaging times can be obtained from these data by computing the standard deviation of the 48 1-hour averages. This value is $\pm 1 \times 10^{-12}$. It can easily be shown that if the measurement process is in statistical control — i. e., the individual 3-minute

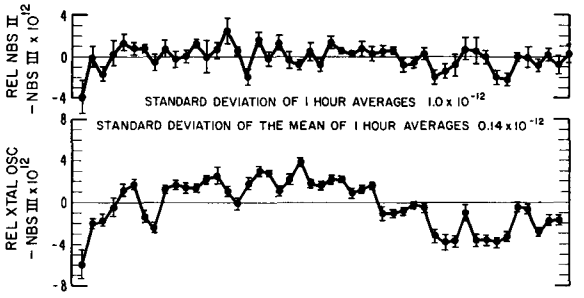

Fig. 7. 48-hour stability comparison between two cesium standards at the National Bureau of Standards (NBS II vs NBS III December 18— 20, 1963)

averages behave as random samples from a stable probability distribution — these two estimates should be equal. In view of the reasonably good agreement observed we can predict, in a probability, sense, that for any similar 1-hour frequency measurement the uncertainty in the result produced by the random variations would be about $\pm 1 \times 10^{-12}$. Although, in principle, it is possible to reduce this uncertainty to an insignificant level by making the measurement time sufficiently long, it is normally impractical to do so.

The primary source of these random fluctuations is the shot noise from the beam itself. The process by which a fluctuation in beam current may result in a frequency fluctuation of the oscillator controlled by the atomic resonance may be thought of in the following way. The servo system, as we have noted previously, responds to components of the detected beam current which are at or very near the modulation frequency. Such a component will normally occur only when the microwave frequency is not exactly equal to the cesium frequency. However, even if the microwave frequency is exactly tuned to the resonance peak, a beam fluctuation will have a frequency spectrum containing components at or near the modulation frequency. The servo system will interpret this component as a legitimate error signal and correct the oscillator accordingly, producing a momentary error in the controlled oscillator's frequency. The manner in which this resulting instability depends upon the more significant beam tube parameters may be seen from the much-simplified resonance line shape shown in

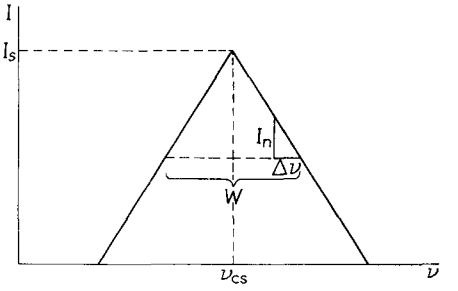

Fig. 8. Simplified resonance line shape for illustrating the relation between frequency fluctuations due to beam fluctuations and the signal-to-noise ratio and linewidth

Fig. 8. In this plot I_s is the peak detected current at the resonance maximum, W is the full resonance width where $I = I_s/2$, I_n represents a fluctuation of the beam current, and $\Delta\nu$ is the corresponding frequency fluctuation. Using the relation between the two similar triangles with sides $\Delta\nu$ and I_n in one case and $W/2$ and $I_s/2$ in the other, we can write immediately:

$$\frac{\Delta\nu}{I_n} = \frac{W/2}{I_s/2} = \frac{W}{I_s}, \tag{23}$$

or

$$\frac{\Delta\nu}{\nu_0} = \frac{W}{\nu_0}\frac{I_n}{I_s}. \tag{24}$$

Now, if we make the reasonable assumption that the main source of beam fluctuations is shot noise, we can use the fact that $\overline{I_n^2} \propto B$, where B is the bandwidth of the detection system by writing:

$$\overline{I_n^2} = \varrho_{no}^2 B, \tag{25}$$

where ϱ_{no}^2 is the mean square noise current per unit bandwidth. From (24) and (25) we have,

$$\left(\frac{\Delta\nu}{\nu_0}\right)_{RMS} = \frac{W}{\nu_0}\frac{\varrho_{no}}{I_s}\sqrt{B}. \tag{26}$$

Finally, since $B = 1/T$, where T = the time over which the measurement is made, we get

$$\left(\frac{\Delta\nu}{\nu_0}\right)_{RMS} = \frac{W}{\nu_0}\frac{\varrho_{no}}{I_s}T^{-\frac{1}{2}}. \tag{27}$$

This expression shows the advantages of a narrow resonance line, high signal-to-noise ratio, and long measuring time in minimizing frequency instability due to beam fluctuations. A more detailed consideration of the observed frequency instability would, of course, have to take into account the influence of the servo system corrections (CUTLER, 1964; KARTASCHOFF, 1964; LACEY, HELGESSON, and HOLLOWAY,

1964), but relation (27) is nevertheless very useful for comparing various beam-system designs.

Servo Errors. Systematic errors resulting from imperfections or misadjustments in the servo system used to develop a correction signal for electronically locking a quartz oscillator to the cesium resonance frequency also fit into this category. The main problem here is second harmonic distortion of the modulation signal which is usually chosen to be in the range 20— 100 Hz. The source of the distortion may be in the modulation oscillator itself or in the modulation circuitry due to non-linear response. The resulting frequency shift is

$$\Delta\nu = 1/2\ D\ \nu_d \sin\alpha, \text{ where} \quad (28)$$

$100\ D$ = percent second harmonic distortion,

ν_d = peak frequency deviation of the modulation, and

α = phase of the second harmonic relative to the fundamental.

Since the peak frequency deviation of the modulation is usually set to about one half of the resonance line width for optimum signal-to-noise ratio, the frequency error is less for a narrow resonance. Equation (28) shows that if this error is to be kept less than 5×10^{-12} in a standard with a 100 Hz line width, the distortion level must be held below 0.2% (assuming the worst case for the phase). One of the simplest checks for the presence of this error is to measure the frequency of the controlled oscillator as a function of ν_d. If a dependence is found, the second-harmonic distortion can sometimes be greatly reduced by inserting narrow-band rejection filters tuned to the second harmonic at appropriate points in the servo system. Square-wave modulating signals have also been employed in some systems instead of the usual sinusoidal form in order to reduce distortion at the source.

Other. Careful circuit construction techniques have been found necessary to prevent pickup at the modulation frequency and, in particular, to keep signals from the modulator portion from leaking into the sensitive error-signal processing circuitry. Other errors are possible which are related to imperfections in certain other servo components, but, in general, these must be evaluated for each particular servo system.

Multiplier chains may also contribute errors if transient phase shifts, such as due to temperature variations, are present. This effect may cause the output frequency to depart from an exact integral multiple of the input for significant periods of time. Since it is actually the output microwave frequency that is maintained by the servo system in synchronism with the cesium resonance, the chain input frequency from the controlled oscillator will be in error in this case.

Most investigators have found no definite dependence of the frequency on the microwave power level over reasonable ranges of power both up and down from the level corresponding to optimum transition probability. However, the frequency shifts resulting from some of the other error sources may be power dependent.

Table 1. *Contributions to Inaccuracy for* NBS III *Cesium Standard*

Source of Uncertainty	1 σ estimate in parts in 10^{12}	3 σ estimate in parts in 10^{12}
1. Uncertainty in $\overline{H(x)}$	$\pm$ 0.1	$\pm$ 0.3
2. Use of $\overline{H(x)}^2$ for $\overline{H^2(x)}$	–	$\pm$ 0.1
3. Doppler shifts	–	$\pm$ 1.0
4. Distortion effects arising from C-field non-uniformity	–	$\pm$ 0.5
5. Millman effect	–	$\pm$ 0.5
6. Uncertainty in cavity phase shift	–	$\pm$ 3.0
7. Cavity mistuning	–	$\pm$ 0.1
8. Overlap of neighboring transitions	–	$\pm$ 1.0
9. Spectral purity of excitation	–	$\pm$ 2.0
10. Random measurement errors (1 hr.)	$\pm$ 1.0	$\pm$ 3.0
11. 2nd harmonic distortion of servo modulation	–	$\pm$ 0.5
12. Miscellaneous servo-system effects	–	$\pm$ 2.0
13. Multiplier chain transient phase shifts	–	$\pm$ 1.0
14. Microwave power	–	$\pm$ 1.0
Total 3 σ Estimated Uncertainty (Square root of sum of squares)		$\pm$ 5.6

Combination of Errors

The process of determining an accuracy figure for a particular standard then consists of evaluating by one means or another the extent to which contributions from the various sources mentioned above may affect the accuracy of frequency measurements. These individual contributions must then be combined in some sense to arrive at an overall accuracy figure. Since the above contributions may reasonably be considered to be independent in the statistical sense, the combined uncertainty may be taken as the square root of the sum of the squares of the individual uncertainties.

An example of this procedure is summarized in Tab. 1, which gives the estimated individual contributions to inaccuracy for the newest NBS cesium standard, NBS III. The individual estimates given are subject to the following conditions:

(a) In most cases the estimates are considered to be reasonable limits of error, approximately corresponding to 3 σ estimates. Exceptions are the estimated uncertainties due to $\overline{H(x)}$ (Item 1) and random errors (Item 10), which were determined by statistical analysis as 1 σ limits.

(b) The estimates involving C-field effects, cavity phase shift, spectrum of the excitation, and servo effects are rechecked periodically.

(c) The estimates involving first order Doppler shift and multiplier chain transients are considered somewhat tentative, at present, due to a lack of conclusive experimental evidence in these areas.

Present accuracy figures quoted for NBS, NPL, and Neuchatel are $\pm\ 5.6 \times 10^{-12}$, $\pm\ 3 \times 10^{-11}$, and $\pm\ 1 \times 10^{-11}$, respectively. There is some variation in the methods used to make these estimates.

Cesium Standards in Operation

Cesium standards presently in operation may be usefully classified as laboratory standards or commer-

cial standards. The laboratory standards are those instruments which are capable of independent evaluation by the controlled variation of the many operating parameters discussed above. They are intended for stationary rather than transportable use. Thus they may have more elaborate power supplies, vacuum systems, signal sources, environmental control, etc. The commercial standards have the objective of transportable use in varied environments, often under limitations of size, weight, and power consumption. They are characterized by fixed design as a result of prior laboratory research and development.

The design and performance characteristics of most of the laboratory and commercial standards are available from the references. Thus we have elected merely to tabulate a few of the characteristics in Tab. 2 and 3 for the sake of illustration.

Accuracy of a cesium beam frequency standard is enhanced by providing a small line width and a large signal to noise ratio, as previously discussed. The requirement of small line width calls for a long interaction length, but the requirement of good signal-to-noise ratio calls for a short beam length in order to enjoy large aperture beam optics.

The laboratory instruments have in general elected to favor small line width by using a long interaction length. They overcome the shot noise error by accepting sufficiently long averaging times according to (27).

The commercial instruments have been forced to short tubes by size limitations. They have tended to compensate in two ways. The first is greater use of velocity selection of slow atoms, and the second is use of larger aperture and more sophisticated beam optics to improve the signal-to-noise ratio. This has a further benefit of improved stability over short averaging times.

Intensive further development of the commercial standards is continuing with the objective of further

Table 2. *Characteristics of Certain Laboratory Cesium Beam Standards*

Instrument	Approximate Date Of First Operation	Interaction Length (cm)	α^* $\times 10^{-4}$ cm-s^{-1}	$\bar{v}/\alpha$	Observed Line Width (Hz)	Servo?	Ascribed Accuracy $\times 10^{11}$	Reference
NPL-I (Cs 1)	1955	47	2.44	1	330	No	± 100	Essen and Parry, 1955; Essen and Parry, 1957.
NPL-II, Mod. 1	1959	265	2.30	0.9	52	No	± 3	Essen, Steele, and Sutcliffe, 1964.
NBS-I	1959	55	2.3	1.1	300	No	± 1	Beehler, Atkinson, Heim, and Snider, 1962.
NBS-II	1960	164	2.3	1.3	120	Yes	± 1	Beehler, Atkinson, Heim, and Snider, 1962.
NBS-III	1963	366	2.3	1.5	48	Yes	± 0.6	Beehler and Glaze, 1965.
LSRH-I	1959	100	2.16	–	–	No	–	—
LSRH-II	1960	409	2.25	0.7 1.1	20 35 42	Yes	± 1	Kartaschoff, 1962 Kartaschoff, 1964.
NRC-1	1958	80	–	–	230	No	100	Kalra, Bailey, and Daams, 1959.

* α is the most probable velocity of the Maxwell-Boltzmann distribution in the oven.

Table 3. *Characteristics of Certain Commercial Cesium Beam Standards*

Instrument Model No.	Interaction Length (cm)	$\alpha^* \times 10^{-4}$ cm-s^{-1}	$\bar{v}/\alpha$	Observed Linewidth (Hz)	Ascribed Accuracy $\times 10^{11}$	Reference
NC-1001 (National Company)	94	2.1	0.86	125	120 (100)	Reder, 1963 (data sheet)
NC-1501 (National Company)	24	2.2	0.64	375	± 20	,,
NC-1601 (National Company)	11	2.2	0.4	500	± 50 (data sheet)	,,
NC-2001 (National Company)	90	2.2	0.63	100	5	,,
HP-5060 A (Hewlett-Packard Company)	12.4	–	–	530	± 2	Bagley and Cutler, 1964, Hewlett-Packard Data Sheet (8/6/64)
P & B-3120 (Pickard and Burns Electronics)	–	–	–	260	± 5	Pickard and Burns Data Sheet 124

* α is the most probable velocity of the Maxwell-Boltzmann distribution in the oven.

improving accuracy, stability, packaging, and resistance to environmental changes. Improvements of one or two orders of magnitude are sought. The reader is advised to search the current periodical and report literature for details.

Comparison of Standards

The intercomparison of independent cesium beam standards provides an important check upon the estimates of accuracy assigned to the standards and should certainly be taken into account in any final accuracy assignments.

Direct Comparison. If the standards are located within the same laboratory the comparison is usually straightforward and can be made with high precision. An example of this sort of comparison is the direct measurement of the difference frequency between NBS II and NBS III over a 48-hour period, the results of which are shown in Fig. 7. Repeated measurements of this type over an extended time have shown the average frequency difference between these two independent standards to be 3×10^{-12}, which is consistent with the quoted accuracies of $\pm 1 \times 10^{-11}$ and $\pm 5.6 \times 10^{-12}$ for NBS II and NBS III, respectively.

Frequency Comparison by Radio. In order to compare standards in different locations, such as the various primary standards of frequency maintained by the national standards laboratories, several different techniques have been employed. The most widely used technique is the simultaneous (or approximately so) measurement of one or more standard frequency transmissions by a number of different laboratories in terms of their own atomic standard. Analysis of these data yields values for the differences among the monitoring cesium standards, although uncertainties due to propagation effects usually limit the precision of this type of comparison to one or two parts in 10^{11}, even when averages over many months are used. Best results are generally obtained for international comparisons when VLF transmissions, such as NBA (24 kHz) and GBR (16 kHz), are utilized.

Morgan, Blair, and Crow (1965) have used a statistical analysis-of-variance technique on 18 months of VLF monitoring data from seven different laboratories in the United States, Europe, and Canada in order to separate the variance of the observations at each laboratory into three components: (a) long-term mean differences among the atomic standards; (b) effects of the fluctuations of the receiving system, propagation effects peculiar to the particular radio path, and measurement errors; and (c) fluctuations of the transmitter signals and propagation effects common to all the radio paths. They concluded that during the July 1961-December 1962 period considered the means of all seven atomic frequency standards (commercial and laboratory types) agreed with the grand mean to within $\pm 2 \times 10^{-10}$, while the means of the four laboratory-type standards agreed with their grand mean to within $\pm 1 \times 10^{-10}$. An indication of the components of measurement fluctuations as observed at each of seven different laboratories is given in Tab. 4 and 5 for GBR and NBA, respectively. The values of $x_i - \bar{x}$ are the deviations of the 18 month mean for each atomic standard from the 18 month grand mean. These figures give an idea of the degree to which agreement among independent standards was attained and maintained over 18 months. The "$\hat{\tau}$ average" values are essentially an average standard deviation associated with the day-to-day fluctuations of the transmitted signal plus propagation effects common to all radio paths. Similarly, the "Av. $\hat{a}_i$" values represent average standard deviations associated with day-to-day fluctuations in the receiving system, including effects peculiar to the particular propagation path, measurement errors, as well as fluctuations in the local standard itself. Although the $\hat{\tau}$ and $\hat{a}_i$ are of comparable magnitude to the variations in the standards among each other ($x_i - \bar{x}$), the statistical treatment enables all these effects to be separated and estimated.

Time Scale Comparison. Another technique which has been used very successfully for the comparison of atomic standards at remote installations involves the comparison of independent time scales based on each of the cesium standards. For example, the NBS-A atomic time scale and the TA_1 atomic time scale based on the laboratory cesium standards at the National Bureau of Standards, Boulder, Colorado, USA and at the Laboratoire Suisse de Recherches Horlogeres,

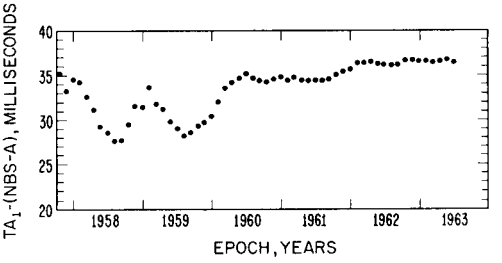

Fig. 9. Comparison of the atomic time scales TA_1 and NBS-A

Neuchatel, Switzerland, respectively, have been compared since 1958 (Bonanomi, Kartaschoff, Newman, Barnes, and Atkinson, 1964). Fig. 9 is a plot of the difference between the time scales as a function of epoch, where the ordinate is the reception time of the WWV time signals at Neuchatel on the TA_1 scale minus the emission time of the time signals on the NBS-A scale. Exact agreement of the two frequency standards would be indicated on this plot by a horizontal line. The obvious improvement occurring in 1960 was due to a change in standards at LSRH from an ammonia maser to a cesium standard and to the adoption of NBS II as the standard at NBS. The divergence of the scales equivalent to about 8×10^{-11} occuring from 1961.6 to 1962.1 was due to a temporary magnetic shielding problem with the LSRH standard as reported by Kartaschoff (Kartaschoff, 1962). If the observed rate of divergence of the two time scales from 1960.5 — 1961.6 and since 1962.2 is attributed entirely to a systematic difference between the two cesium standards, a frequency difference of 1×10^{-11} is indicated. This result is consistent with the quoted accuracy figures for both standards.

Portable Standards. Still another method of comparing two frequency standards at remote installations involves carrying a portable standard between the two laboratories, making frequency comparisons at both locations with the assumption that the portable

Table 4. *Errors in Terms of* GBR *Data and Indicated Standards*

$\hat{\tau}$ Average* $= 1.26 \times 10^{-10}$

$\hat{a}_i$ Average* per Station as follows:

Station	$(x_i - \bar{x}) \times 10^{10}$	Av. $\hat{a}_i \times 10^{10}$	No. Days Observed
CNET	1.68	1.05	278
CRUFT	−0.78	0.41	136
LSRH	−1.04	0.39	244
NBS	−0.68	0.66	244
NOB	−0.34	0.62	278
NPL	+0.05	1.00	278
NRC	+0.65	1.97	222

* RMS weighted Average

Station Indentifications

CNET Centre National d'Etudes des Telecommunications, Bagneux, Seine, France (Commercial standard).
CRUFT Cruft Laboratories, Harvard University, Cambridge, Massachusetts, USA (Commercial standard).
LSRH Laboratoire Suisse de Recherches Horlogeres, Neuchatel, Switzerland (Laboratory standard).
NBS National Bureau of Standards, Boulder, Colorado, USA (Laboratory standard).
NOB U. S. Naval Observatory, Washington, D. C., USA (Radio average of 9 standards).
NPL National Physical Laboratory, Teddington, Middlesex, England (Laboratory standard).
NRC National Research Council, Ottawa, Ontario, Canada (Laboratory standard).

Table 5. *Errors in Terms of* NBA *Data and Indicated Standards*

$\hat{\tau}$ Average* $= 0.68 \times 10^{-10}$

$\hat{a}_i$ Average* per Station as follows:

Station	$(x_i - \bar{x}) \times 10^{10}$	Av. $\hat{a}_i \times 10^{10}$	No. Days Observed
CNET	1.89	0.95	197
CRUFT	−1.05	1.13	131
LSRH	−0.99	0.63	197
NBS	−0.66	0.63	161
NOB	−0.27	0.51	197
NPL	−0.28	1.24	102
NRC	+1.30	1.82	113

* RMS weighted Average

Station Indentifications

CNET Centre National d'Etudes des Telecommunications, Bagneux, Seine, France (commercial standard).
CRUFT Cruft Laboratories, Harvard University, Cambridge, Massachusetts, USA (commercial standard).
LSRH Laboratoire Suisse de Recherches Horlogeres, Neuchatel, Switzerland (laboratory standard).
NBS National Bureau of Standards, Boulder, Colorado, USA (laboratory standard).
NOB U. S. Naval Observatory, Washington, D. C., USA (commercial standard).
NPL National Physical Laboratory, Teddington, Middlesex, England (laboratory standard).
NRC National Research Council, Ottawa, Ontario, Canada (laboratory standard).

standard's frequency remains stable between laboratories. This type of measurement has been made feasible by the recent development of highly-stable portable commercial cesium and rubidium standards. In June 1964, two commercial cesium standards which had been taken to Switzerland for an instrument exhibition were compared with the long cesium standard at LSRH in Neuchatel (BAGLEY and CUTLER, 1964). Four days later the commercial instruments were measured in terms of the NBS standard in Boulder, Colorado, after being kept in continuous operation during the intervening time. The results of these measurements again showed the Swiss and U. S. standards to be in agreement to better than 1×10^{-11}. The assumption of perfect stability of the commercial standards between comparisons did not appear to limit the measurements in view of the excellent long-term stability demonstrated by these instruments during one week's continuous operation in Switzerland.

Atomic Time Standards

Construction of Atomic Time Scales. An atomic time scale based upon the cesium transition can be constructed in several different ways. Basically, one needs to have some means of accumulating cycles of the periodic phenomenon (in this case, the cesium transition frequency) providing the unit from an arbitrarily chosen origin. Since most cesium standards employ a quartz-crystal oscillator which is electronically locked to the cesium resonance, the most direct method would be to divide the quartz oscillator frequency down to a suitable value for driving a clock directly. Because of the practical difficulty in keeping a complex system such as a cesium standard in continuous operation, however, an indirect technique has usually been used in which the clock is driven by a free-running quartz oscillator of nominal frequency ν_n which is periodically calibrated in terms of the cesium standard to give its actual frequency ν_a. These calibrations are then used to convert the sufficiently short indicated quartz time $\Delta\tau$ to atomic time Δt according to the relation $\Delta t = (\nu_n/\nu_a)\ \Delta\tau$ with the assumption that the oscillator frequency has drifted linearly between calibration points. The interval between calibrations ranges from 1 day for the A.1 (see below) and NBS-A scales to 10 days for the TA_1 scale. Errors introduced by departure of the actual oscillator drift from linearity as assumed, due to inherent oscillator noise and other causes, have been studied by a number of people (for example, DE PRINS, 1961).

Particular Time Scales. The various atomic time scales presently in use differ essentially only in the particular cesium standard or standards chosen for the basis of the scale. Thus, the A.1 atomic time scale developed at the United States Naval Observatory in 1958 is based upon a weighted average of 9 different laboratory and commercial cesium standards located in various laboratories throughout the world (MARKOWITZ, 1962 IRE). The published daily measurements of certain standard frequency transmissions, such as NBA and GBR, in terms of the various cesium standards are utilized to determine the frequency of the A.1 master oscillator in terms of the weighted average. The origin of the A.1 scale is chosen to be at $0^h\ 0^m\ 0^s$ on the UT 2 time scale on 1 January 1958*.

The TA_1 scale established in Switzerland by the Neuchatel Observatory is based upon the cesium resonance frequency as indicated by the cesium standard at the Laboratoire Suisse de Recherches Horlogeres (since 1960) (BONANOMI, KARTASCHOFF, NEWMAN,

* UT 2 is one of the Universal Time scales based on the rotation of the earth. Its rate is a measure of the mean speed of rotation of the earth with known periodic variations removed. UT 2 is still not uniform time, however, because of progressive changes in the speed of rotation of the earth.

BARNES, and ATKINSON, 1964). The origin of this scale was set to coincide with Ephemeris Time at $0^h\ 0^m\ 0^s$ UT 2 on 1 January 1958*.

Similarly, the NBS-A atomic time scale is based upon the United States Frequency Standard (USFS) maintained at the National Bureau of Standards, Boulder, Colorado, USA.

The epoch of this scale was set to be approximately equal to that of UT 2 at $0^h\ 0^m\ 0^s$ on 1 January 1958. The NBS-UA scale is also based on the USFS but the frequency offsets and step adjustments in epoch as announced by the Bureau International de l'Heure in Paris are incorporated, resulting in an interpolated "universal" time scale based on an atomic time scale.

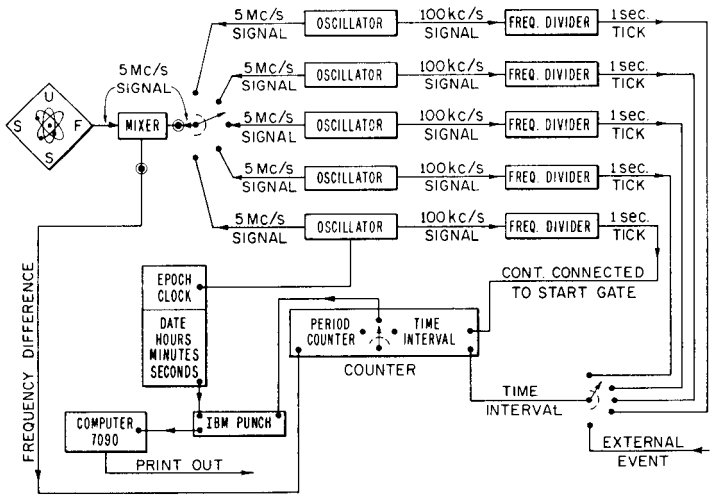

Fig. 10. Block diagram of the NBS-A atomic time scale

A block diagram of the components of the NBS-A scale is shown in Fig. 10. Each of the 5 oscillator-clock combinations operates independently of all others and a weighted average constitutes the time scale. A detailed description of the construction, operation, and results of the NBS-A and NBS-UA scales will be published (BARNES, 1965).

Synchronization of Clocks. A problem of interest involves the synchronization of clocks at remote locations. Interesting and novel techniques have been utilized during recent years for this purpose, including clock carrying experiments, the use of Loran-*C* transmissions and artificial earth satellites. In 1959 — 1960 the U. S. Army Signal Corp first demonstrated the feasibility of using airborne atomic clocks to obtain synchronization of widely separated clocks to within 5μsec (REDER, BROWN, WINKLER, and BICKART, 1961). Extensive use of portable, high-precision quartz clocks has been made by NBS personnel for synchronizing clocks at the Boulder, Colorado laboratories and at the WWV transmitter site in Maryland (BARNES and FEY, 1963). Uncertainties in the initial synchronization due to the portable clock were within 5 μsec. Later checks on this synchronization by means of further clock-carrying trips between Boulder and the WWV site were made with measurement accuracies approaching 1μsec. In June 1964, in connection with the previously mentioned flight of two commercial cesium standards between the United States and Switzerland, measurements made at the Naval Observatory and at Neuchatel, Switzerland, enabled the time at the two locations to be correlated to an accuracy of about 1μsec (BAGLEY and CUTLER, 1964). Further experiments of this type are planned.

Another method of synchronizing remote clocks uses the Loran-*C* navigation system transmissions at 100 kHz (DOHERTY, HEFLEY, and LINFIELD, 1960). These transmissions consist of pulses with typical rise times of 60 μsec, permitting time resoluting between the arrival of the ground wave and the more unstable sky wave. The resulting increase in timing accuracy over the 1 — 2 msec available by using HF or VLF transmissions allows remote synchronization of clocks within the Loran-*C* service area to 1 μsec. It is believed that extension of the Loran-*C* system would permit this capability to be available anywhere in the world.

Artificial earth satellites have also been used for highly-accurate synchronization of remote clocks. The Telstar satellite has been used to transmit microwave pulses between the United States and Europe with an uncertainty due to the satellite link of less than 1 μsec (MARKOWITZ, 1964). The advantages gained here include the reduced sensitivity of the microwave frequency to ionospheric disturbances and the use of a propagation path which lies mostly outside the ionosphere.

The (U. S.) Navy Navigational Satellite System may also be used for this purpose since the satellites carry clocks and radio transmitters (MARKOWITZ, 1962). It is expected that clocks in the United States and England can by synchronized to within 100 μsec initially and 10 μsec later using this means.

Summary

Any acceptable standard of time must satisfy the following requirements: continuity of operation, generation of a unit which remains constant with respect to other acceptable measures of time, accuracy greater than or equal to standards based on other definitions, accessibility to all who need it, a characteristic period of convenient size, and a capability for accumulating the units to give epoch. Although astronomical standards based on the observed positions of celestial bodies meet these requirements very well, atomic standards have been developed since 1945 which possess a much higher accuracy with respect to the definition and greatly improved precision, making it possible to provide better results in a much shorter averaging time. Various types of atomic standards have been developed and evaluated, including ammonia absorption cells, ammonia and atomic hydrogen masers, rubidium gas cell devices, and atomic beam devices using cesium and thallium. Cesium standards are the most highly developed at present with accuracies of $\pm 1 \times 10^{-11}$ having been achieved in several different laboratories.

Although there is no universal agreement on how to specify the performance of cesium standards, various estimates of accuracy, precision, stability, and reproducibility are often used. The specification of accuracy requires an appropriate combination of random and systematic components of error. These various components have been thoroughly analyzed both theoretically and experimentally for cesium by many different laboratories and commercial firms.

Different cesium standards have been compared both directly within a given laboratory and indirectly between remote locations by means of standard frequency and time

* Ephemeris Time is defined by the orbital motion of the earth about the sun and is determined, in practice, from observations of the orbital motion of the moon about the earth.

radio transmissions, comparisons of independent time scales constructed from the standards, and the carrying of portable clocks between the remote locations. Results show that frequency differences are within $\pm 2 \times 10^{-10}$ for all standards and $\pm 1 \times 10^{-10}$ for the laboratory-type standards.

A number of independent atomic time scales have been constructed based on either a group of cesium standards (A. 1) or on a particular standard (TA_1, NBS-A, NBS-UA). Clocks based on these time scales have been synchronized over intercontinental distances by clock-carrying experiments, use of radio transmissions, and use of artificial earth satellites. Accuracies of the order of 1 microsecond have been achieved.

References

1930 – 1954

[1] COHEN, V. W.: The nuclear spin of cesium. Phys. Rev. **46**, 713 (1934).

[2] DICKE, R. J.: The effect of collisions upon the Doppler width of spectral lines. Phys. Rev. **89**, 472 (1953).

[3] FERMI, E.: Über die magnetischen Momente der Atomkerne, Z. Physik **60**, 320 (1930).

[4] —, and E. SEGRÉ: Zur Theorie der Hyperfeinstruktur. Z. Physik **82**, 729 (1933).

[5] FRASER, R. G. J.: Molecular rays. Cambridge, England: Cambridge University Press 1931.

[6] FRASER, R.: Molecular beams. London: Metheun and Company 1937.

[7] GORDON, J. P., J. H. ZEIGER, and C. H. TOWNES, Molecular microwave oscillator and new hyperfine structure in the microwave spectrum of NH_3. Phys. Rev. **95**, 282 (1954).

[8] HERSHBERGER, W. D., and L. E. NORTON, Frequency stabilization with microwave spectral lines. R C A Rev. **9**, 38 (1948).

[9] KELLOGG, J. B. M., and S. MILLMAN: The molecular beam magnetic resonance method. The radio frequency spectra of atoms and molecules. Rev. Mod. Phys. **18**, 323 (1946).

[10] KOPFERMANN, H.: Nuclear moments, E. E. SCHNEIDER, translator, and H. S. W. MASSEY, editor, Pure and Appl. Phys. Ser., Vol. **2**, p. 114ff. New York: Academic Press 1958.

[11] LYONS, H.: Spectral lines as frequency standards. Ann. N. Y. Acad. Sci. **55**, 831 (1952).

[12] RAMSEY, N.: A molecular beam resonance method with separated oscillating fields. Phys. Rev. **78**, 695 (1950).

1955

[13] BASOV, N. G., and A. M. PROKHOROV: The molecular oscillator and amplifier. Uspekhi Fiz. Nauk. **57**, 485 (1955).

[14] ESSEN, L., and J. V. L. PARRY: An atomic standard of frequency and time interval. Nature **176**, 280 (1955).

[15] SMITH, K. F.: Molecular beams, London: Metheun and Company, and New York: John Wiley and Sons, Inc. 1955.

[16] ZACHARIAS, J. R., J. G. YATES, and R. D. HAUN: An atomic frequency standard. Proc. I. R. E. **43**, 364 (1955).

1956

[17] DATZ, S., and E. TAYLOR: Ionization on platinum and tungsten surfaces. I. The alkali metals. J. Chem. Phys. **25**, 389 (1956). II. The potassium halides. J. Chem. Phys. **25**, 395 (1956).

[18] ESSEN, L., and J. V. L. PARRY: Atomic and astronomical time. Nature **177**, 744 (1956).

[19] RAMSEY, N. F.: Molecular beams. Oxford, England: Oxford University Press 1956.

[20] WITTKE, J. P., and R. H. DICKE: Redetermination of the hyperfine splitting in the ground state of atomic hydrogen. Phys. Rev. **103**, 620 (1956).

1957

[21] ESSEN, L., and J. PARRY: The caesium resonator as a standard of frequency and time. Phil. Trans. Roy. Soc. London **250**, 45 (1957).

[22] HAUN, R. D., Jr., and J. R. ZACHARIAS: Stark effect on Cs-133 hyperfine structure. Phys. Rev. **107**, 107 (1957).

[23] KASTLER, A.: Optical methods of atomic orientation and of magnetic resonance. J. Opt. Soc. Am. **47**, 460 (1957).

[24] LYONS, H.: Atomic clocks. Sci. American. **196**, 71 (1957).

[25] PIERCE, J. A.: Intercontinental frequency comparison by very low frequency radio transmission. Proc. I. R. E. **45**, 794 (1957).

1958

[26] ESSEN, L., J. V. L. PARRY, W. MARKOWITZ, and R. G. HALL: Variation in the speed of rotation of the earth since June 1955. Nature **181**, 1054 (1958).

[27] — —, J. H. HOLLOWAY, W. A. MAINBERGER, F. H. REDER, and G. M. R. WINKLER: Comparison of caesium frequency standards of different construction. Nature **182**, 41 (1958).

[28] KALRA, S. N., R. BAILEY, and H. DAAMS: Cesium beam standard of frequency. Can. J. Phys. **36**, 1442 (1958).

[29] MARKOWITZ, W., R. G. HALL, L. ESSEN, and J. V. L. PARRY: Frequency of cesium in terms of ephemeris time. Phys. Rev. Letters **I**, 105 (1958).

[30] MCCOUBREY, A. O.: Results of the comparison: Atomichron-British cesium beam standard. IRE Trans. on Instr. **I-7**, 203, (1958).

[31] MOCKLER, R. C.: Etalons de temp atomiques et moleculaires au National Bureau of Standards, in proces verbaux des seamces, rapport et annexes, 1re session (1957), Comité Consultatif pour la Définition de la Seconde, pp. 38 – 42. (Comité International des Poids et Mesures.) Proces-Verbaux des Seances, 2. serie, tome 26-B. Paris: Gauthier-Villars 1958.

1959

[32] ANDRES, J. M., D. J. FARMER, and F. T. IONOUYE: Design studies for a rubidium gas cell frequency standard. IRE Trans. on Military Electronics **MIL-3**, 178 (1959).

[33] ESSEN, L., E. G. HOPE, and J. V. L. PARRY: Circuits employed in the NPL caesium standard. Proc. Inst. Elec. Engrs. (London), Pt. B **106**, 240 (1959).

[34] —, and J. V. L. PARRY: An improved caesium frequency and time standard. Nature **184**, 1791 (1959).

[35] Recent research in molecular beams, I. ESTERMANN, editor, New York: Academic Press, Inc. 1959.

[36] HOLLOWAY, J., W. MAINBERGER, F. H. REDER, G. M. R. WINKLER, L. ESSEN, and J. V. L. PARRY: Comparison and evaluation of cesium atomic beam frequency standards. Proc. I. R. E. **47**, 1730 (1959).

[37] KALRA, S. N., R. BAILEY, and H. DAAMS: Canadian cesium beam standard of frequency. Nature **183**, 575 (1959).

[38] —, C. F. PATTENSON, and M. M. THOMPSON: Canadian standard of frequency. Can. J. Phys. **37**, 10 (1959).

[39] KUSCH, P., and V. W. HUGHES: Atomic and molecular beam spectroscopy. Encyclopedia of Physics, p. 1, S. FLÜGGE, editor. Berlin-Göttingen-Heidelberg: Springer 1959.

[40] MCCOUBREY, A. O.: National's militarized cesium beam frequency standards. Proceedings of the 13th Annual Symposium on Frequency Control (U. S. Army Signal Research and Development Laboratory, Ft. Monmouth, N. J.) 276 (1959).

[41] RAMSEY, N. F.: Shapes of molecular beam resonances Recent Research on Molecular Beams, I. ESTERMANN, editor. New York: Academic Press, Inc. 1959.

[42] ZANDBERG, E., and N. IONOV: Surface ionization. Uspekhi Fiz. Nauk. **57**, 581 (1959); English Translation: Soviet Phys.-Usp. **2**, 255 (1959).

1960

[43] BARNES, J. A., and R. C. MOCKLER: The power spectrum and its importance in precise frequency measurements. IRE Trans. on Instr. **I-9**, 149 (1960).

[44] BEEHLER, R. E., R. C. MOCKLER, and C. S. SNIDER: A comparison of atomic beam frequency standards. Nature **187**, 681 (1960).

[45] CARPENTER, R. J., E. C. BEATY, P. L. BENDER, S. SAITO, and R. O. STONE: A prototype rubidium vapor frequency standard. IRE Trans. on Instr. **I-9** 132, (1960).

[46] DEPRINS, J., and P. KARTASCHOFF: Applications de la spectroscopie hertzienne a la mesure de frequences et du temps. Neuchatel, Switzerland: Laboratory Suisse Recherches Horlogeres 1960.

[47] DOHERTY, R., G. HEFLEY, and R. LINFIELD: Timing potential of Loran-C, Proceedings of the 14th Annual Symposium on Frequency Control (U. S. Army Signal Research and Development Laboratory, Ft. Monmouth, N. J.) 276 (1960).

[48] GOLDENBERG, H. M., D. KLEPPNER, and N. F. RAMSEY: Atomic hydrogen maser. Phys. Rev. Letters **5**, 361 (1960).

[49] KALRA, S. N., and R. BAILY: Experimental investigation of atomic beam resonance technique as applied to cesium clock, Quantum Electronics: A Symposium, p. 121. C. H. TOWNES, editor. New York: Columbia University Press 1960.

[50] KARTASCHOFF, P., J. BONANOMI, and J. DEPRINS: Description of a long cesium beam frequency standard, Proceedings of the 14th Annual Symposium on Frequency Control (U. S. Army Signal Research and Development Laboratory, Ft. Monmouth, N. J.) 354 (1960).

[51] MCCOUBREY, A.: Missileborn Atomichron frequency standard, Proceedings of the 14th Annual Symposium on Frequency Control (U. S. Army Signal Research and Development Laboratory, Ft. Monmouth, N. J.) 315 (1960).

[52] MERRILL, F. G.: Frequency and time standards. A status report. IRE Trans. on Instr. **I-9**, 117 (1960).

[53] MOCKLER, R. C., R. E. BEEHLER, and J. A. BARNES: An evaluation of a cesium beam frequency standard. Quantum Electronics, A Symposium, C. H. TOWNES, editor, p. 127. (Columbia University Press, New York, N. Y.: 1960).

[54] — —, and C. S. SNIDER: Atomic beam frequency standards. IRE Trans. on Instr. **I-9**, 120 (1960).

[55] — — NBS atomic frequency standards, Proceedings of the 14th Annual Symposium on Frequency Control (U. S. Army Signal Research and Development Laboratory, Ft. Monmouth, N. J.) 298 (1960).

[56] — Atomic beam frequency standards, Proceedings of the 1960 Brookhaven Conference on Molecular Beams. New York: Brookhaven National Laboratory, Upton, L. I., 1960.

[57] PIERCE, J. A.: The GBR experiment: a transatlantic frequency comparison between caesium-controlled oscillators. Proceedings of the 14th Annual Symposium on Frequency Control (U. S. Army Signal Research and Development Laboratory, Ft. Monmouth N. J.) 267 (1960).

[58] WINKLER, G.: A superior atomic clock for continuous long time operation. Proceedings of the 14 th Annual Symposium on Frequency Control (U. S. Army Signal Research and Development Laboratory, Ft. Monmouth, N. J.) 261 (1960).

1961

[59] ARDITI, M., and T. CARVER: Pressure, light and temperature shifts in optical detection 0-0 hyperfine resonance of alkali metals. Phys. Rev. **124**, 800 (1961).

[60] BARNES, J. A., and L. E. HEIM: A high-resolution ammonia maser spectrum analyser. IRE Trans. on Instr. **I-10**, 4 (1961).

[61] DEPRINS, J.: Applications des masers A $N^{15}H_3$ à la mesure et à la definition du temps. Unpublished, Université Libre de Bruxelles: Doctor of Sciences thesis 1961.

[62] MCCOUBREY, A. O.: Frequency control by microwave atomic resonance. Microwave Jl. **4**, 65 (1961).

[63] MOCKLER, R. C.: Atomic beam frequency standards, Advances in Electronics and Electron Physics, Vol. 15, p. 1. L. MARTON, editor. New York, N. Y.: Academic Press, Inc. 1961.

[64] RARITY, J., L. SAPORTA, and G. WEISS: The effects of frequency multipliers on the uncertainty of a frequency measurement. Proceedings of the 15th Annual Symposium on Frequency Control (U. S. Army Signal Research and Development Laboratory, Ft. Monmouth, N. J.) 261 (1961).

[65] REDER, F., P. BROWN, G. WINKLER, and C. BICKART: Final results of a world-wide clock synchronization experiment (Project WOSAC). Proceedings of the 15th Annual Frequency Control Symposium (U. S. Army Signal Research and Development Laboratory, Ft. Monmouth, N. J.) pp. 226 (1961).

1962

[66] BARNES, J. A., D. W. ALLAN, and A. E. WAINWRIGHT: The ammonia beam maser as a standard of frequency. IRE Trans. on Instr. **I-11**, 26 (1962).

[67] BEEHLER, R. E., W. R. ATKINSON, L. E. HEIM, and C. S. SNIDER: A comparison of direct and servo methods for utilizing cesium beam resonators as frequency standards. IRE Trans. on Instr. **I-11**, 231 (1962).

[68] BONANOMI, J.: A thallium beam frequency standard. IRE Trans. on Instr. **I-11**, 212 (1962).

[69] DEPRINS, J.: $N^{15}H_3$ double beam maser as a primary frequency standard. IRE Trans. on Instr. **I-11**, 200 (1962).

[70] ESSEN, L., and J. MCA. STEELE: The international comparison of atomic standards of time and frequency. Proc. Inst. Elec. Engrs. (London) Pt. B **41**, 109 (1962).

[71] GEORGE, J.: Recent advances in cesium beam technology and characteristics of Rabi and Ramsey cesium beam tubes 17 inches long. IRE Trans. on Instr. **I-11**, 250 (1962).

[72] KARTASCHOFF, P.: Operation and improvement of a cesium beam standard having 4-meter interaction length. IRE Trans. on Instr. **I-11**, 224 (1962).

[73] KLEPPNER, D., H. M. GOLDENBERG, and N. F. RAMSEY: Theory of the hydrogen maser. Phys. Rev. **126**, 603 (1962).

[74] — — — Properties of the hydrogen maser. Appl. Optics **1**, 55 (1962).

[75] MARKOWITZ, W.: The atomic time scale. IRE Trans. on Instr. **I-11**, 239 (1962).

[76] — Time measurement technique in the microsecond region. Engineers Digest **135**, 9 (1962).

[77] MIZUSHIMA, M.: Theory of resonance frequency shifts due to the radiation field. Proceedings of the 16th Annual Symposium on Frequency Control (U. S. Army Signal Research and Development Laboratory, Ft. Monmouth, N. J.) 267 (1962).

[78] PACKARD, M. E., and B. E. SWARTZ: The optically pumped rubidium vapor frequency standard. IRE Trans. on Instr. **I-11**, 215 (1962).

[79] RICHARDSON, J. M., R. E. BEEHLER, R. C. MOCKLER, and R. L. FEY: Les étalons atomiques de frequence au NBS. Comité Consultatif pour la definition de la Seconde aupres du Comité International des Poides et Mesures, 2- session – 1961, p. 57. Paris: Gauthier-Villars and C-- 1962.

[80] SHIMODA, K.: Ammonia masers. IRE Trans. on Instr. **I-11**, 195 (1962).

[81] STONE, R. R., Jr.: Synchronization of local frequency standards with VLF transmissions. Proceedings of the 16th Annual Symposium on Frequency Control (U. S. Army Signal Research and Development Laboratory, Ft. Monmouth, N. J.) 227, (1962).

[82] VESSOT, R. F. C., and H. E. PETERS: Design and performance of an atomic hydrogen maser. IRE Trans. on Instr. **I-11**, 183 (1962).

1963

[83] BARNES, J. A., and R. L. FEY: Synchronization of two remote atomic time scales. Proc. IEEE **51**, 1665 (1963).

[84] BEEHLER, R. E., and D. J. GLAZE: Experimental evaluation of a thallium beam frequency standard. Proceedings of the 17th Annual Symposium on Frequency Control (U. S. Army Research and Development Laboratory, Ft. Monmouth, N. J.) 392 (1963).

[85] CRAMPTON, S., D. KLEPPNER, and N. F. RAMSEY: Hyperfine separation of ground state atomic hydrogen. Phys. Rev. Letters **11**, 338 (1963).

[86] FARMER, D. J.: Performance and application of gas cell frequency standards. Proceedings of the 17th Annual Symposium on Frequency Control (U. S. Army Signal Research and Development Laboratory, Ft. Monmouth, N. J.) 449 (1963).

[87] GEORGE, J.: Development and performance of a miniaturized cesium beam tube. Proceedings of the 17th Annual Symposium on Frequency Control (U. S. Army Signal Research and Development Laboratory, Ft. Monmouth, N. J.) 438 (1963).

[88] GUY, H. D.: Problems of frequency multiplication in atomic standards. Proceedings of the 17th Annual Symposium on Frequency Control (U. S. Army Signal Research and Development Laboratory, Ft. Monmouth, N. J.) 482 (1963).

[89] MOCKLER, R. C.: Atomic frequency and time interval standards in the United States (1960 – 1963). Report to URSI U. S. National Committee-Commission I, February 8, 1963.

[90] NEWMAN, J., L. FEY, and W. R. ATKINSON: A comparison of two independent atomic tome scales. Proc. IEEE **51**, 498 (1963).
[91] REDER, F. H.: Achievements and problem areas of atomic frequency control. Proceedings of the 17th Annual Symposium on Frequency Control (U. S. Army Signal Research and Development Laboratory, Ft. Monmouth, N. J.) 329 (1963).
[92] SHIRLEY, J. H.: Some causes of resonant frequency shifts in atomic beam machines. I. Shifts due to other frequencies of excitation. J. Appl. Phys. **34**, 783 (1963).
[93] — Some causes of resonant frequency shifts in atomic beam machines. II. The effect of slow frequency modulation on the Ramsey line shape. J. Appl. Phys. **34**, 789 (1963).

1964

[94] BAGLEY, A. S., and L. S. CUTLER: A modern solid-state, portable cesium beam frequency standard. Proceedings of the 18th Annual Symposium on Frequency Control (U. S. Army Signal Research and Development Laboratory, Ft. Monmouth, N. J.) 344 (1964).
[95] — — A new performance of the flying clock experiment. Hewlett-Packard Company Journal **15**, No. 1, (July 1964).
[96] BONANOMI, J.: Les horlogues atomiques. Proceedings of the International Conference on Chronometry, Lausanne, 227 (1964).
[97] —, P. KARTASCHOFF, J. NEWMAN, J. A. BARNES, and W. R. ATKINSON: A comparison of the TA_1 and the NBS-A atomic time scales. Proc. IEEE **52**, 439 (1964).
[98] BRANDENBERGER, J. H., J. MICHAEL, P. KARTASCHOFF, and J. RACINE: Horlogue atomique avec tube à césium. Proceedings of the International Conference on Chronometry, Lausanne, 353 (1964).
[99] CUTLER, L. S.: Some aspects of the theory and measurement of frequency fluctuations in frequency standards. Interim Proceedings of the Symposium on the Definition and Measurement of Short Term Frequency Stability (Goddard Space Flight Center, Greenbelt, Maryland) II-73 (1964).
[100] ESSEN, L. J., J. McA. STEELE, and D. SUTCLIFFE: The NPL frequency standard. Proceedings of the 18th Annual Symposium on Frequency Control (U. S. Army Signal Research and Development Laboratory, Ft. Monmouth, N. J.) 308 (1964).
[101] GEORGE, J., E. WUNDERER, and T. ATHANIS: Recent progress in cesium beams at National. Proceedings of the 18th Annual Symposium on Frequency Control (U. S. Army Signal Research and Development Laboratory, Ft. Monmouth, N. J.) 322 (1964).
[102] HOLLOWAY, J. H., and R. F. LACEY: Factors which limit the accuracy of cesium atomic beam frequency standards. Proceedings of the International Conference on Chronometry, Lausanne, 317 (1964).
[103] —, and R. H. WOODWARD: Progress in the development of a cesium beam oscillator for aerospace guidance. Proceedings of the 18th Annual Symposium on Frequency Control (U. S. Army Signal Research and Development Laboratory, Ft. Monmouth, N. J.) 366 (1964).
[104] KARTASCHOFF, P.: Étude d'un étalon de fréquence a jet atomique de césium. Unpublished. Docteur Es Sciences Techniques thesis. Zürich: L'ecole Polytechnique Fédérale 1964.
[105] — Shot efiect influence on the frequency of an oscillator locked to an atomic beam resonator. Interim Proceedings of the Symposium on the Definition and Measurement of Short Term Frequency Stability (Goddard Space Flight Center, Greenbelt, Maryland) A-19 (1964).
[106] LACEY, R. F., J. H. HOLLOWAY, and A. L. HELGESSON: Short term stability of passive atomic frequency standards. Interim Proceedings of the Symposium on the Definition and Measurement of Short Term Frequency Stability (Goddard Space Flight Center, Greenbelt, Maryland) III-3 (1964).
[107] MARKOWITZ, W.: High precision frequency and clock synchronization techniques on an international basis. Proceedings of the 18th Annual Symposium on Frequency Control (U. S. Army Signal Research and Development Laboratory, Ft. Monmouth, N. J.) 251 (1964).
[108] MENOUD, C., J. RACINE, and P. KARTASCHOFF. Maser a hydrogène atomique. Quantum Electronics, p. 433. GRIVET, P., and N. BLOEMBERGEN, editors, New York: Columbia University Press 1964.
[109] MOCKLER, R. C.: Atomic frequency and time interval standards. URSI National Committee Report, XIV General Assembly Tokyo, September 1963, Commission I. Radio Science Journal of Research, Vol. **68 D**, No. 5, May 1964.
[110] PICKARD and BURNS Electronics, Data Sheet Number 24.

1965

[111] BARNES, J. A., and D. W. ALLAN: Private communication 1965.
[112] BEEHLER, R. E., and D. J. GLAZE: Private communication 1965.
[113] MORGAN, A. H., B. E. BLAIR, and E. L. CROW: Private communication 1965.
[114] RAMSEY, N. F.: The atomic hydrogen maser. Metrologia **1**, 7 (1965).

R. E. BEEHLER
National Bureau of Standards
Atomic Frequency and Time
Interval Standards
Radio Standards Laboratory
Boulder, Colorado

Offprint from „Metrologia"
Journal International de Métrologie scientifique — International Journal of scientific Metrology
Internationale Zeitschrift für wissenschaftliche Metrologie. Vol. 1, No. 3, July 1965, Pages 114—131

Springer-Verlag, Berlin · Heidelberg · New York

112-131

A Precision Pulse-Operated Electronic Phase Shifter and Frequency Translator

Since 1956, the definition of the unit of time (the second) has been in terms of the Ephemeris second, which must be determined by astronomical means. In October, 1964, the cesium beam was adopted internationally as an alternate standard to realize the unit of time. The frequency assigned to the appropriate atomic transition of cesium 133 was set at 9 192 631 770 Hz. However, all standard frequency and time transmissions, which are coordinated through the International Time Bureau (BIH) in Paris in accordance with CCIR regulations, do not presently broadcast the physical unit of time (the second).

Historically, this situation came about because one of the primary uses of precise time was in terrestrial (as opposed to space) navigation. In effect, what was needed could be more closely correlated with the Earth's angular position relative to the sun, rather than with an absolutely uniform time scale. Navigators (more specifically terrestrial navigators) had been accustomed to using a time scale called UT-2, which is essentially "mean solar time" corrected for a few known perturbations. To satisfy this need, the frequency of the "pendula" controlling the "time" markers of coordinated broadcasts has been slowed down to make the broadcast signals keep in approximate step with UT-2. Occasionally, steps of 0.1 second are also added when the UT-2 scale drifts outside of the predicted value. During 1965, the frequency offset of -150 parts in 10^{10} was incorporated in all coordinated broadcasts.[1] The value for 1966 is -300 parts in 10^{10}. According to CCIR regulations, these offsets are now restricted to an integral multiple of 50 parts in 10^{10}.

Thus, for a synchronous clock operating from an exact 100-kHz reference, the phase must be retarded at the rate of about one cycle per 5.5-minute interval for the -300×10^{-10} offset. Such slow phase shifts have normally been accomplished by electromechanical devices incorporating a resolver-type phase shifter. These devices being motor driven are notoriously wasteful of power and not nearly as reliable as solid-state electronics. Practically, one may realize a linearity with a resolver of about ±0.5 percent of one cycle or about ±50 ns for a 100-kHz signal. Because of these considerations, an all solid-state phase shifter was considered very desirable by the authors.

The heart of the phase shifters currently being used in the Atomic Frequency and Time Standards Section of the Radio Standards Laboratory of the National Bureau of Standards consists of a voltage variable delay line, a narrow-band filter, and a pulse shaper. The voltage variable delay line is a series of inductors, shunted to ground by a set of voltage variable capacitors (back-biased diodes work well) in a typical lumped-constant delay line fashion. A total of ten sections for the delay line has been used in the prototype models, which were designed to operate at 1 MHz.

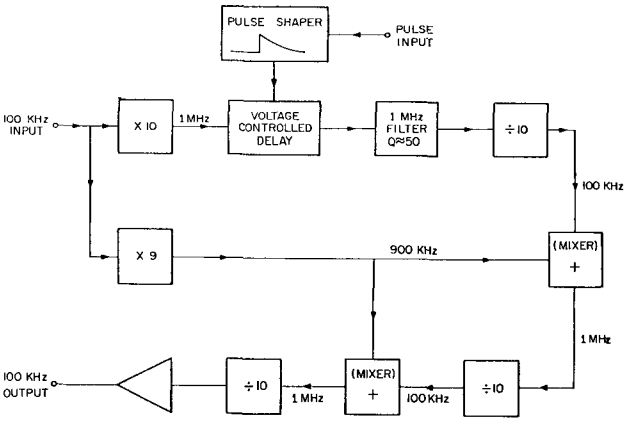

$\Delta\phi = 10$ ns/pulse

Fig. 1. Precision pulse operated phase shifter.

With a 1-MHz signal supplied to the delay line and the output signal fed to a narrow-band filter ($Q\approx50$), a voltage pulse is suddenly applied (risetime$\sim$0.1 μs) to the delay line. The amplitude of the pulse is so chosen that the delay is reduced by very nearly one microsecond. Due to propagation delays along the delay line for this pulse, the distortion in the output of the delay line persists for only about 1.5 μs for the prototype units. Since the duration of this perturbation is quite small relative to the reciprocal bandwidth of the filter, the output of the filter is essentially not disturbed by this process. Indeed, minimum variation in the amplitude of the 1-MHz signal from the filter is a reasonably sensitive criterion for pulse amplitude.

By now allowing the voltage on the delay line to slowly decay to its steady-state value, the frequency out of the delay line may be maintained within the bandpass of the filter, and thus exactly one cycle has been subtracted from the output signal in a smooth and continuous fashion relative to the input. In the prototype units constructed, the decay time of the pulse was set at 3 milliseconds, and thus the signal averages about 300 Hz off from the 1-MHz input during the decay time.

The generation of submultiples of this one cycle of phase is accomplished by using what amounts to a frequency error-multiplier run in reverse. First the 1-MHz signal out of the filter is divided to 100 kHz, which also divides the one cycle of phase shift by ten. That is, the steady-state phase shift of this 100 kHz is exactly $2\pi/10$ for each pulse supplied to the delay line. By mixing this 100-kHz signal with a 900-kHz signal derived from the input signal to the device, a new 1-MHz signal is obtained with phase shifts of exactly $2\pi/10$ or 0.1 μs for each pulse supplied to the delay line. Thus, by an iteration of frequency dividers and mixing with a signal that is phase coherent with the input, very precise submultiples of the one cycle of phase shift may be generated. A block diagram of an electronic phase shifter is shown in Fig. 1.

The limitations in accuracy of the phase shifts arise from the fact that there are several high "Q" circuits operating at essentially the same frequency, and hence "pick up" of a signal in a later stage can cause minor phase perturbations. By careful construction and shielding, it has been demonstrated at the National Bureau of Standards that a system similar to the one described here may be built such that accumulated phase perturbations are less than 0.01 percent of one cycle.

It remains now only to construct a pulsing circuit from a clock to pulse the phase shifter at the proper rate to generate the desired frequency offset.[2] Obviously, depending on the need, the granulations in this phase shifting process may be chosen for the particular application. The prototype units constructed at the Bureau generate ten nanosecond steps in the phase, and thus a series of pulses adjustable from 0 to 10 pulses in a two-second interval in steps of one pulse per two-second interval allows a wide choice of useful frequency offsets (0 to -500 parts in 10^{10} in steps of 50 parts in 10^{10}). While the output signal cannot be considered monochromatic, there are many applications where the granular nature of the phase is not significantly important (e.g., running a clock where precision of better than ten nanoseconds is not needed.

J. Barnes
A. Wainwright
National Bureau of Standards
Boulder Lab.
Boulder, Colo.

Manuscript received November 16, 1965.

[1] During the previous calendar years, the following offset frequencies have been used: 1959, -170×10^{-10}; 1960, -150×10^{-10}; 1961, -150×10^{-10}; 1962, -130×10^{-10}; 1963, -130×10^{-10}; 1964, -150×10^{-10}.

[2] R. C. Cumming, "Serrodyne frequency translator," *Proc. IRE*, vol. 45, pp. 175–186, February 1957.

Reprinted from the PROCEEDINGS OF THE IEEE
VOL. 53, NO. 12, DECEMBER, 1965

An Intercomparison of Atomic Standards

In early September, 1965, a group of atomically controlled oscillators was assembled at the National Bureau of Standards in Boulder, Colo. The main purpose of the two months of experiments was to obtain intercomparisons of the frequencies of the cesium beam, thallium beam, and hydrogen maser with accuracies substantially better than any previously obtained [1]–[4].

The participants in the experiments were personnel from the Quantum Electronic Devices (Q.E.D.) Division of Varian Associates, the Hewlett-Packard Company, and the Atomic Frequency and Time Standards Section of the National Bureau of Standards, Boulder, Colo. The equipment assembled for the experiments included the United States Frequency Standard NBS-III, a cesium beam; another cesium beam device constructed at Hewlett-Packard Company (incorporating a Varian Associates beam tube); two hydrogen masers constructed at the Q.E.D. Division of Varian Associates; and the NBS-II beam machine recently converted to thallium use. Unfortunately the conversion of NBS-II to thallium was not complete, and no significant numbers are at present available for this system.

The majority of comparisons among the two masers and the two cesium beam devices was obtained by period measurements of the beat frequencies between pairs of 5 MHz signals synthesized from the various controlling atomic transitions. It was recognized that for the precisions and accuracies which are realizable with these devices, 5 MHz is an unfortunately low frequency for comparison (it is worth noting that a slow phase drift of one-half cycle per day at 5 MHz constitutes a frequency offset of about one part in 10^{12}!). Nonetheless sufficient hardware and software existed at the 5 MHz range to make this the most desirable frequency for the present intercomparisons.

There were available three separate data acquisition systems capable of automatically punching data on cards for computer analysis, and thus data reduction was greatly facilitated. Indeed, such volumes of data were obtained during the comparisons that, to date, only a small fraction of the data has received attention. Thus the results reported here are preliminary and subject to a great deal of additional analysis. It is intended that a more comprehensive report of the intercomparisons will be published soon.

In order to have good reliability for the final results, it is desirable to substantiate that the various devices were operating properly and within specifications. Thus it is of value now to discuss briefly some of the experiments performed to establish a realistic and unbiased error budget for each instrument.

In regard to the two Varian hydrogen masers, each is equipped with magnetic shielding and with temperature control of source, cavity, and cavity loading. The magnetic shields of each maser were degaussed at the start of the experiments, and the magnetic fields were calibrated by exciting the Zeeman transitions. Almost daily checks of the cavity tuning of each maser were made with each maser being tuned independently of the other (each maser was used in turn as a stable reference to tune the other but its particular frequency was not considered).

Unfortunately it was not possible in the time available to perform a wall-shift experiment for the hydrogen masers. It was decided to use the values of the wall shift as determined by the Varian group sometime earlier [1].

Preliminary results indicated the frequency fluctuations of one maser relative to the other was within a few parts in 10^{13} from one second to several hundred seconds, and the frequencies of the two masers agreed to within one part in 10^{12} for the entire two-month period. The detailed analysis of the relative fluctuations of the two masers has not been completed, however.

While a realistic error budget for NBS-III has recently been published [5], it was decided that the very stable signals available from the two Varian masers would afford a unique opportunity for redetermining the magnitudes of some of the uncertainties associated with NBS-III. In particular, the oven and detector of NBS-III were interchanged four different times to determine phase-shift effects of the cavity. Also a completely different set of electronics was used to detect possible spectral difficulties or systematic errors in the servo systems.

The fluctuations in the frequency of the 5 MHz signal locked to NBS-III as compared to a hydrogen maser decreased with increasing sample time as $\tau^{-1/2}$ for τ ranging from 100 seconds to five hours. This is in complete agreement with theory [6]. A standard deviation of one part in 10^{13} was obtained for adjacent sample times of two hours. For adequate averaging times ($\tau \geq 200$ seconds), the new total estimated inaccuracy for NBS-III is 1.1×10^{-12} for a *one*-sigma value Beehler, Mockler, and Richardson [5] give a one-sigma value of about 1.9×10^{-12} ($3 \cdot \sigma = 5.6 \times 10^{-12}$).

The comparison of NBS-III with the Hewlett-Packard (H-P) cesium beam indicated a standard deviation for the frequency fluctuations of seven parts in 10^{13} for two-hour samples. If one assumes that the figure of one part in 10^{13} quoted above for the comparison of NBS-III and a hydrogen maser is caused primarily by shot noise modulating the frequency of NBS-III, it is possible to estimate the fluctuations on a shorter machine with a different flux of atoms [6]. Indeed, when this calculation is carried out for the H-P cesium beam, complete agreement with the experimental results of 7×10^{-13} for two-hour samples is obtained. Apparently, the electronic systems of these two independently constructed cesium beam devices function quite comparably.

The H-P cesium beam, being independently aligned, was available for about two weeks of comparisons. Assuming NBS-III as the primary standard, the average frequency of the 5 MHz output of the H-P unit was offset by -149.991 parts in 10^{10}. Since the unit was designed to generate a signal offset by -150 parts in 10^{10}, this indicates a discrepancy in frequency of only 9 parts in 10^{13} which is well within the estimated accuracies for the two beams.

It is thus felt by the authors that the behavior of the cesium beams and the hydrogen masers during this period have proved adequtely reliable to quote a significant frequency value for the hydrogen maser. It should again be emphasized that all data have not been analyzed, and refinements on the results may be expected. A preliminary value for the frequency of the appropriate transition of the hydrogen atom in free space, at zero magnetic field, and zero absolute temperature, is

$$1420{,}405{,}751.7860 \pm 0.0046 \text{ Hz}.$$

The uncertainty of 0.0046 Hz corresponds to 1) an assumed inaccuracy of 3 parts in 10^{12} due to uncertainties in the wall-shift effect in the hydrogen maser, compounded with 2) the inaccuracy of 1.1 parts in 10^{12} for the cesium reference to give a total uncertainty of 3.2 parts in 10^{12}.

Unfortunately, all aspects of wall shifts in the hydrogen maser are not sufficiently well understood to allow one to construct a realistic and objective error budget for the hydrogen maser. While the reproducibility of the wall shift is known to be better than one part in 10^{12}, the magnitude of the effect is not known to this accuracy, and the estimated inaccuracy of three parts in 10^{12} for the wall shift is considered an "outer limit" by the authors. It is, therefore, not on the same objective footing as the one-sigma value of 1.1 parts in 10^{12} for NBS-III.

The following is a list of values for the hydrogen frequency in terms of cesium as published elsewhere and the value given above.

1420,405,751.827 ± 0.02 (Varian-Naval Observatory, 1963) [1]

1420,405,751.800 ± 0.028 (Harvard-Naval Observatory, 1963) [2]

1420,405,751.778 ± 0.016 (Varian-H-P, 1964) [3]

1420,405,751.785 ± 0.016 (Varian-LSRH, 1964) [4]

1420,405,751.781 ± 0.016 (NASA-GSFC, 1965) [7]

1420,405,751.7860 ± 0.0046 (NBS-Varian-HP, 1-65, this letter).

The state-of-the-art for both cesium beams and hydrogen masers has undergone significant improvement. Absolute accuracy in the vicinity of a few parts in 10^{12} for frequency measurements is thus confirmed.

R. Beehler
D. Halford
R. Harrach
D. Allan
D. Glaze
C. Snider
J. Barnes
Radio Standards Lab.
National Bureau of Standards
Boulder, Colo.
R. Vessot
H. Peters
J. Vanier
Quantum Electronic Devices
Varian Associates
Beverly, Mass.

L. Cutler
L. Bodily
Hewlett-Packard Co.
Palo Alto, Calif.

References

[1] W. Markowitz, R. G. Hall, H. F. Hastings, R. R. Stone, R. F. C. Vessot, and H. E. Peters, "Report on the frequency of hydrogen," *Frequency*, vol. 1, no. 5, p. 46, July-August 1963. The frequency of 1420405751.734 ± 0.02 quoted in this reference was not corrected for second-order Doppler shift nor for wall shift. These corrections are given by J. Vanier, H. E. Peters, and R. F. C. Vessot, "Exchange collisions, wall interactions, and resettability of the hydrogen maser," *IEEE Trans. on Instrumentation and Measurement*, vol. IM-13, pp. 185–188, December 1964.
[2] S. B. Crampton, D. K. Kleppner, and N. F. Ramsey, "Hyperfine separation of ground-state atomic hydrogen," *Phys. Rev. Letters*, vol. 11, no. 7, pp. 338–340, October 1, 1963.
[3] H. E. Peters, J. Holloway, A. S. Bagley, and L. S. Cutler, "Hydrogen maser and cesium beam tube frequency standards comparison," *Appl. Phys. Letters*, vol. 6, no. 2, pp. 34–35, January 1965.
[4] H. E. Peters and P. Kartaschoff, "Hydrogen maser frequency comparison with Swiss cesium atomic beam standard," *Appl. Phys. Letters*, vol. 6, no. 2, pp. 35–36, January 1965.
[5] R. E. Beehler, R. C. Mockler, and J. M. Richardson, "Cesium beam atomic time and frequency standards," *Metrologia*, vol. 1, no. 3, pp. 114–131, July 1965.
[6] L. S. Cutler and C. S. Searle, "Some aspects of the theory and measurement of frequency fluctuations in frequency standards," *this issue*, page 136.
[7] E. H. Johnson and T. E. McGunigal, "Hydrogen maser frequency comparison with Hewlett-Packard 5060A cesium beam standard," NASA Technical Note TN D-3292 (August, 1965).

Reprinted from the PROCEEDINGS OF THE IEEE
VOL. 54, NO. 2, FEBRUARY, 1966
Pp. 301-302

The Performance and Capability of Cesium Beam Frequency Standards at the National Bureau of Standards

R. E. BEEHLER AND D. J. GLAZE

Abstract—NBS II, the older of the two cesium atomic beam frequency standards which are used alternatively as the United States Frequency Standard, has been operating for more than five years. The contribution to inaccuracy produced by uncertainties in the *C* field has been reduced by a factor of 30 to $\pm 2\times10^{-13}$. The average precision of measurement (standard deviation of the mean) has been demonstrated to be 1×10^{-12} for averaging times of 1 hour and 2×10^{-13} for 12 hours. The overall accuracy is considered to be $\pm 8\times10^{-12}3\sigma$. A new cesium standard, NBS III with an interaction length of 3.66 meters is in operation and has demonstrated an improved precision of 1×10^{-13} over 2 hours and an accuracy of $\pm 5\times10^{-12}3\sigma$. The C field contributions to inaccuracy in this machine have been reduced to $\pm 1\times10^{-13}$. Considerable effort has been devoted to the detection and elimination of small frequency shifts produced by various electronic components of the excitation systems. In spite of the various improvements effected, a small unexplained difference in frequency of about 1×10^{-12} continues to exist between the standards. The extremely high stability of the difference frequency, however, suggests that resolution of the difficulties should result in an accuracy capability of perhaps $\pm 1\times10^{-12}3\sigma$.

I. Introduction

THE PROGRAM at the National Bureau of Standards for the development, evaluation, and provision of atomic frequency and time standards has led to the development of two operating cesium standards and one thallium standard at the present time. In addition to these, the laboratory has two ammonia (N^{15}) masers which are used primarily as test instruments in the evaluation of atomic time and frequency standards. Also, a hydrogen maser has been operating since August, 1964.

It is the purpose of this report to discuss the progress made in this NBS program over the past three years, particularly that part of the program concerned with the evaluation and performance characteristics of the cesium atomic beam standards. The two cesium beams are used alternatively as the United States Frequency Standard. They also comprise the frequency element of the NBS Time Standard.

The three existing beam standards are designated NBS I, NBS II, and NBS III. The first of these, NBS I, is the oldest machine. It was originally operated using cesium but was converted in 1962 from cesium to thallium. NBS I is the shortest of the three standards, providing a spectral line width of about 300 Hz for cesium. NBS III is the newest and longest machine and provides a spectral line width of 48 Hz, while the line width for NBS II is 110 Hz.

The accuracy[1] of the cesium beams is considered to be $\pm 1\times10^{-11}$ for NBS I, $\pm 8\times10^{-12}$ for NBS II, and $\pm 5\times10^{-12}$ for NBS III. These figures are determined from an analysis of various auxiliary experiments and tests on a given machine and are confirmed by comparisons of the three independent machines. NBS II and NBS III have also been compared with the cesium standard at Neuchatel, Switzerland, by making use of radio signals [1] and portable atomic standards [2], [3]. The radio comparison data averaged over 1.3 years (1962.2–1963.5) indicated agreement to within 1×10^{-11} for that period. The more recent clock-carrying experiments gave the same result. The precision[1] associated with the NBS standards is at best 1×10^{-13} for two-hour averaging periods. More typically, values range from 0.5×10^{-12} to 1×10^{-12} for the one-half hour averaging periods normally employed in most measurements.

It appears that electronic problems and phase shifts in the resonant cavity are presently the most severe sources of uncertainty and that close attention must be given to them if accuracy is to be increased. Although time consuming, the solutions of these problems do not appear prohibitively difficult, at least for an improvement in accuracy of up to one order of magnitude. It is perhaps not too optimistic to expect an accuracy of $\pm 1\times10^{-12}3\sigma$ with the present standards within the next two years.

Some of the details of the analyses and characteristics of the NBS cesium beam standards are discussed in Section II.

II. The NBS Cesium Beam Standards

A. Comparison of NBS I and NBS II

NBS I was first placed into regular operation in the spring of 1959 as a cesium beam. It became the United

Manuscript received October 27, 1965.

The authors are with the National Bureau of Standards, Boulder, Colo.

[1] Accuracy and precision have the following meaning in this manuscript: 1. accuracy refers to the fractional uncertainty in determining an atomic state separation of the free atom and is expressed by 3σ limits for statistically determined quantities and by estimated extreme limits for other quantities; 2. precision refers to the fractional uncertainty within which a given machine provides a reproducible measurement and is expressed by 1σ limits unless otherwise noted.

States Frequency Standard (USFS) in the fall of that year. NBS II has been in use since 1960, and until the newest cesium beam, NBS III, was developed, NBS I and NBS II provided the USFS—each was a check on the other. Currently, NBS II and NBS III provide the USFS.[2]

NBS I and NBS II were intercompared for a period of three years [4]–[6]. During this period, practically all of the electronics and a number of the internal components of the beam apparatus were replaced, including deflecting magnets, *C*-field structures, and the waveguide excitation structure of NBS I. Also, both machines were partially disassembled and moved to a neighboring laboratory. With all these changes, the relative frequency difference between them remained fixed at 1.6×10^{-11} within a measurement uncertainty of $\pm2\times10^{-12}$. The average precision of frequency comparison (standard deviation of the mean) was 2×10^{-12} for an averaging time of one-half hour. The best precision that was attained was 2×10^{-13} (requiring an averaging time of 10 hours). The statistical behavior was good; χ^2 tests demonstrated a Gaussian distribution of the data [7]. The accuracy for each machine was considered to be $\pm1\times10^{-11}$. This figure was based on the measured frequency difference between the two standards and on the results of a group of auxiliary experiments designed to measure the *C*-field intensity and uniformity, the phase shift between oscillating field regions, the power spectrum of the exciting radiation, effects of neighboring resonances, cavity pulling, and the variation of frequency with power level. These tests were performed for each machine separately. The fixed frequency difference of 1.6×10^{-11} was never adequately explained and implies the existence of a systematic error which still has not been definitely identified.

The comparison of the NBS I and NBS II cesium beams was terminated in 1962 when NBS I was converted to a thallium beam.

B. Comparison of NBS II and NBS III

The newest cesium standard, NBS III, has been in operation since the summer of 1963. It represents an attempt to improve on previous standards with respect to both precision and accuracy by reducing random errors due to beam fluctuations and certain systematic errors that are line-width dependent. The separations between the oscillating field regions are 164 cm for NBS II and 366 cm for NBS III, with the corresponding spectral line widths being 110 Hz and 48 Hz. Figures 1 and 2 are photographs of these two instruments.

The procedure used in the evaluation of NBS III followed closely that previously used and reported in connection with NBS I and II [4]–[7]. Evaluation with respect to accuracy involved the study of each possible source of error in order to determine its maximum contribution to the overall measurement uncertainty. In many of the experiments, NBS II was used to provide the stable reference frequency for direct comparison with NBS III while the particular param-

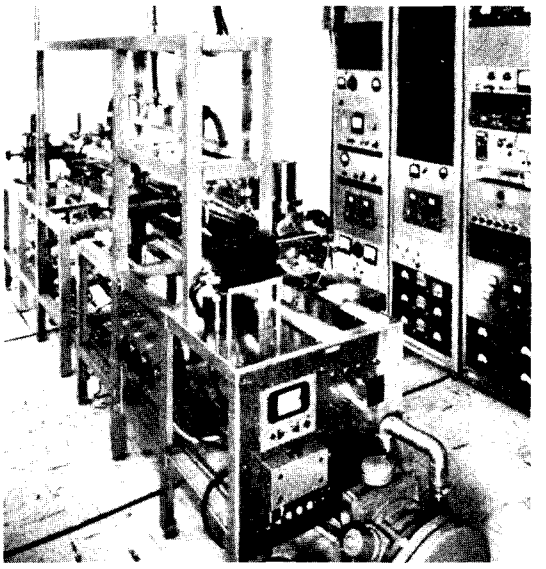

Fig. 1. Cesium atomic beam frequency standard, NBS II.

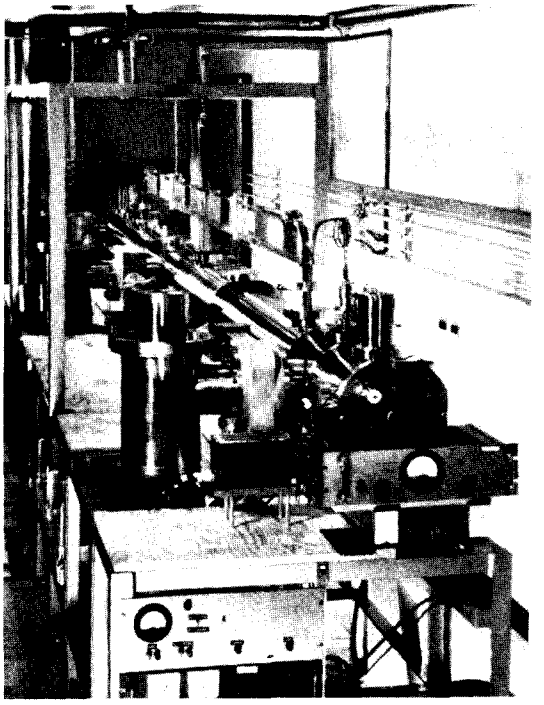

Fig. 2. Cesium atomic beam frequency standard, NBS III.

[2] The unit of frequency is defined by the frequency separation of the $F=4$ and $F=3$ hyperfine structure levels in the free cesium atom. This separation is defined to be exactly 9192631770 Hz. The machines themselves provide the means of measuring frequency in terms of this separation and are designated as standards. The unit of frequency provided by the standard can approach the idealized unit with a certain uncertainty determined by the particular standard and its analysis. Consequently, accuracy limits must be specified.

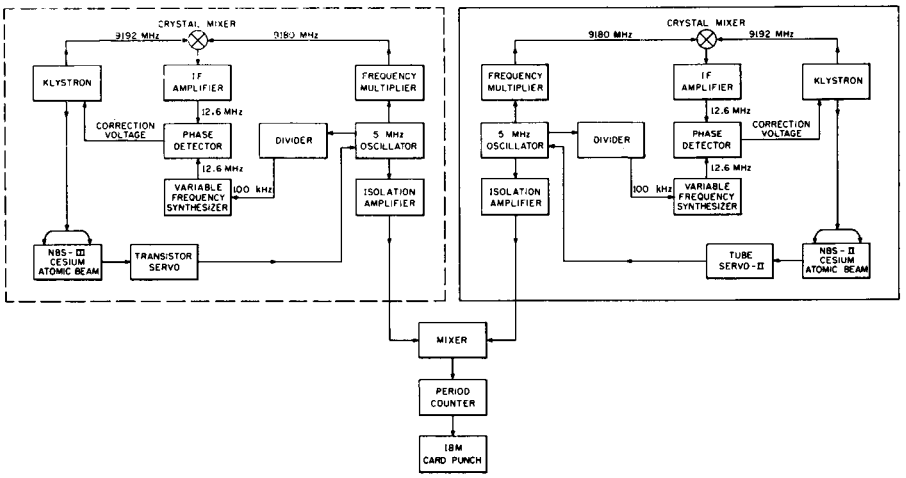

Fig. 3. Block diagram of measurement system for direct comparison of NBS II and NBS III.

eter being studied in the NBS III system was systematically varied. Figure 3 is a block diagram showing the actual method of comparison. Each standard controls a crystal oscillator by means of appropriate servo electronics, and the period of the beat frequency between these two oscillators is measured.

Data from two comparisons of this type are shown in Figs. 4 and 5. Each plotted point, representing the difference frequency averaged over one hour, is the mean of 20 three-minute measurements. The half-length of the vertical bar drawn at each point in Fig. 4 represents the computed standard error of the one-hour observation (standard deviation of the mean of the 20 three-minute averages) and is thus an estimate of the relative precision of this measurement process. This precision figure is typically 7×10^{-13} for these data. When the measurement averaging time of interest is one hour or less, somewhat better precision is usually obtained for comparisons between very high quality quartz crystal oscillators and NBS III than for the direct NBS II–NBS III measurements.

A second estimate of the frequency fluctuations appropriate for one-hour averaging times can be obtained from the data in Fig. 4 by computing the standard deviation of the 48 one-hour averages. This value for the NBS II–NBS III data is 1.0×10^{-12}. It can easily be shown that if the measurement process is in statistical control, i.e., the individual three-minute averages behave as independent samples from a stable probability distribution, these two estimates should be equal. In view of the resonably good agreement observed, we can predict, in a probability sense, that for any similar one-hour frequency measurement the uncertainty in the result produced by the random variations would be about $\pm1\times10^{-12}$. Analysis of a vast amount of comparison data accumulated over several years involving NBS II, NBS III, and many other frequency sources shows that the measurement precision for NBS III is usually two or three times better than for NBS II. Al-

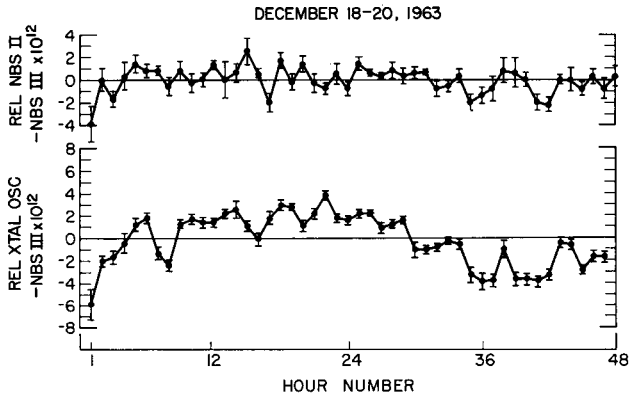

Fig. 4. 48-hour stability comparisons of NBS II, NBS III, and a crystal oscillator.

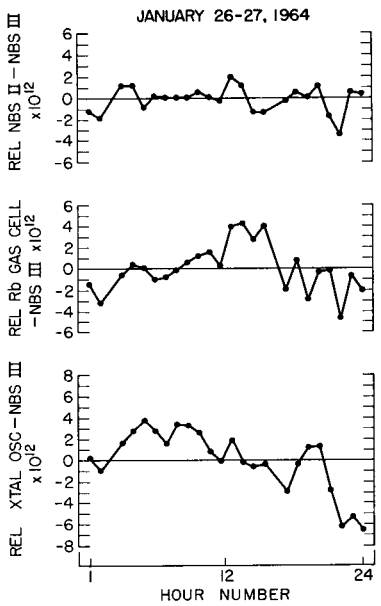

Fig. 5. 24-hour stability comparison of NBS II, NBS III, a crystal oscillator, and a Rb gas cell.

though precisions of 5×10^{-13} and 1×10^{-12} for NBS III and NBS II, respectively, are typical for one-hour averaging times, values of 2×10^{-13} have been obtained consistently during recent comparisons between NBS-III and the NBS hydrogen maser. No attempt has yet been made to determine the individual contributions of NBS III and the maser to this value.

In addition to these random measurement errors, a great variety of systematic error sources may exist which must be considered in determining an overall accuracy figure to be associated with a particular standard. Those sources of error which have been found to be most significant in the case of NBS II and NBS III include errors due to uncertainties associated with the uniform magnetic C field, phase shifts in the resonant cavity, the presence of unwanted sidebands in the spectrum of the microwave frequency exciting the cesium resonance, and certain other imperfections in the electronics system.

The cesium frequency for the $(F=4, m_F=0)\leftrightarrow(F=3, m_F=0)$ transition depends on the magnitude of the C field according to

$$\nu = \nu_0 + 427\overline{H^2(x)}, \tag{1}$$

where ν is the transition frequency (in Hz) in the magnetic field used, ν_0 is the cesium frequency (in Hz) in zero field, $H(x)$ is the magnitude of the C field (in oersteds), and $\overline{H^2(x)}$ is a spatial average over the length between the two oscillating field regions. Any uncertainties in our knowledge of $\overline{H^2(x)}$ will thus lead to corresponding errors in frequency measurements referred to ν_0.

In actual practice, since $\overline{H^2(x)}$ is difficult to determine directly, the procedure normally followed is to determine first the quantity $\overline{H(x)}$ from relatively simple measurements of various microwave transitions which depend linearly on the field, square the result to obtain $[\overline{H(x)}]^2$, and then compute the correction $427\ [\overline{H(x)}]^2$ for application to all measurements. Frequency uncertainties resulting from the use of this procedure arise, therefore, from two sources:

1) uncertainties in the value of $\overline{H(x)}$, and
2) uncertainties due to the use of $[\overline{H(x)}]^2$ for $\overline{H^2(x)}$.

The frequency uncertainty $\Delta\nu$ resulting from an uncertainty ΔH, independent of x, in $\overline{H(x)}$ or $H(x)$ can easily be computed from (1). Thus,

$$\nu + \Delta\nu = \nu_0 + 427[\overline{H(x)+\Delta H}]^2 \tag{2}$$

$$= \nu_0 + 427[\overline{H^2(x)} + 2\overline{H(x)}\Delta H + (\Delta H)^2]. \tag{3}$$

Neglecting the small term $(\Delta H)^2$ and subtracting ν from both sides, again making use of (1), gives

$$\Delta\nu = 854\overline{H(x)}\Delta H. \tag{4}$$

This uncertainty was evaluated in the following way for both NBS standards. The frequencies of each of the $(4, -1)\leftrightarrow(3, -1)$, $(4, 1)\leftrightarrow(3, 1)$, $(4, 2)\leftrightarrow(3, 2)$, and $(4, 3)\leftrightarrow(3, 3)$ transitions were measured. Theory relates these frequencies to the magnitude of the C field, and from these relationships $\overline{H(x)}$ can be obtained [5]. This gives four different measurements of the average field for each setting of the C-field current. The data so obtained were plotted, and a least-squares line was fitted to the points. The range over which the field was measured was between 0.045 Oe and 0.148 Oe. The field used for normal operation is about 0.048 Oe. This range of field values eliminates overlap effects caused by neighboring transitions and insures good linearity. The standard deviation of a point from this line is 0.000019 Oe. If this is taken to be the uncertainty in the magnitude of the C field ΔH, the corresponding uncertainty in the frequency of the $(4, 0)\leftrightarrow(3, 0)$ transition is $\pm1\times10^{-13}$. These figures apply to NBS III. Similar measurements for NBS II give an uncertainty of ±0.00004 Oe, corresponding to an uncertainty of $\pm2\times10^{-13}$ in the $(4, 0)\leftrightarrow(3, 0)$ frequency measurement. Previously, this uncertainty had been $\pm6\times10^{-12}$ and was the largest single contribution to the inaccuracy. More stable power supplies for the C-field current are now employed and account for the improvement. No changes have been made in the C-field structure of NBS II.

The uncertainty from the second source mentioned is a consequence of the nonuniformity of the C field, for in that case, $\overline{H^2(x)}$ is not equal to $[\overline{H(x)}]^2$. The error in Hz which results from using the latter quantity is given by

$$\Delta\nu = 427[\overline{H^2(x)} - [\overline{H(x)}]^2 \tag{5}$$

If the magnitude of the C field is expressed as

$$H(x) = H_0(x) + cI, \tag{6}$$

where $H_0(x)$ is the nonuniform residual field in the drift-space region observed with the current I producing the C field turned off, and c is a constant, it can readily be shown by direct substitution of (6) into (5) that

$$\Delta\nu = 427[\overline{H_0^2(x)} - [\overline{H(x)}]^2. \tag{7}$$

It is assumed here that the residual field $H_0(x)$ does not depend on I.

In the case of NBS II and NBS III, $H_0(x)$ has been measured by drawing a small sensitive magnetometer probe through the C-field region along the beam axis. A continuous plot of this field measurement for NBS II is shown in Fig. 6. The end points of the recording

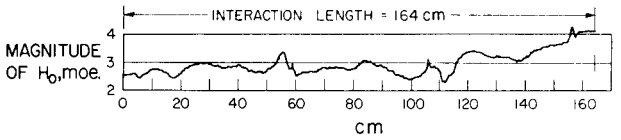

Fig. 6. Variation of magnitude of residual field H_0, along the length of C-field region of NBS II.

coincide with the positions of the openings in the magnetic shields where the two ends of the resonant cavity pass through the shields. Similar data for NBS III show slightly better uniformity even though the drift-space region is much longer. The average residual field in NBS II was 0.001 Oe about four years ago and has deteriorated to about 0.003 Oe at the present time. $\overline{H_0(x)}$ for NBS III is 0.0004 Oe. No degaussing of the magnetic shields has been employed to date. If the error $\Delta\nu$ is computed from (7) using the residual field data in Fig. 6, a value of less than 1×10^{-14} is obtained. Since it is impractical to measure this uniformity very often, however, it is considered that this effect may contribute a maximum uncertainty of perhaps $\pm1\times10^{-13}$ to the estimate of inaccuracy.

Certain other types of C-field nonuniformity can distort the observed cesium resonance asymmetrically, producing a frequency error as a result. Such an effect occurs, for example, if the average field in the region between the oscillating fields differs from the average field within the oscillating field regions. From an examination of the symmetry of the field dependent (4, 1) $\leftrightarrow$(3, 1) transition, which provides a sensitive indication of this condition, we conclude that any resultant errors should be less than $\pm5\times10^{-13}$ for both NBS II and NBS III. Local nonuniformity of the C field within the oscillating field regions can produce large frequency shifts, which are expected to be strongly dependent on the microwave power level. The absence of a large dependence of frequency on power level for either standard, together with the magnetometer data, suggests the lack of a significant contribution to inaccuracy from this source.

Reversing the polarity of the NBS III C field produced no frequency shift greater than the measurement precision of 5×10^{-13}.

The microwave cavity has been investigated in order to determine the existing phase difference between the oscillating field regions, dependence of the measured cesium frequency on cavity tuning, and the existence of possible fringing of the electromagnetic field at the beam coupling holes. Of these effects, the last was investigated by placing a horizontal wire grid across each opening in the resonant cavity end sections in an effort to reduce any existing leakage field. Measurements were then performed to determine the presence of a frequency shift, but none was observed. The measurements were obtained with NBS II as a reference.

A detuning of the resonant cavity by 1.3 MHz resulted in a frequency shift of 3×10^{-12}. It is believed, however, that this tuning change does not result in a pulling of the cesium resonance frequency, but rather results in a change in the phase shift between the two oscillating field regions of the resonant cavity. This is thought to be a result of asymmetry of the tuning mechanism. As long as the cavity is tuned to the cesium resonance, the phase difference should remain constant. The only contribution to uncertainty in the frequency measurements would then be the uncertainty in the phase difference determination.

The accurate determination of the frequency shift caused by phase differences existing in the cavity has proved to be one of the more difficult problems encountered with NBS III. The first method used to measure this effect consisted of measuring the NBS III resonance frequency relative to that of NBS II both before and after the entire NBS III cavity structure was physically rotated by 180°. One half of any frequency shift observed as a result of this operation may be attributed to a phase-difference effect and applied as a correction to all measurements. The physical rotation of this extremely long cavity, however, appears to deform the structure in an unreproducible manner to such an extent that the observed frequency shift is reproducible to only 5×10^{-12}. In an effort to minimize any such effects, a second method has recently been employed in which the direction of traversal of the beam through the cavity is reversed by interchanging the atomic beam oven and detector, while leaving the cavity undisturbed. Although this technique has been found to yield better reproducibility, the contribution from this source to the overall inaccuracy of NBS III is nevertheless considered to be $\pm3\times10^{-12}$.

Experiments to determine the existence of frequency shifts due to oven and detector offset in the horizontal plane have shown no net frequency shift greater than 1×10^{-12} for a position change of 1.7 mm. The normal operating point was included in this range. A horizontal misalignment of 0.5 mm would be considered excessive.

Another possible source of systematic frequency shifts may be a first-order Doppler effect. If, due to imperfect alignment, atoms have a component of their velocity parallel to the radiation field and a net traveling wave exists in the cavity, a frequency shift may occur, given approximately by

$$\Delta\nu = \left(\frac{1-R}{1+R}\right)\nu_0\frac{\bar{v}}{c}\sin\alpha,$$

where R is the power reflection coefficient, $\bar{v}$ is the mean speed of the atoms in the beam, and α is the angle between the waveguide and a line normal to the beam. Some measurements made with the NBS.I thallium standard suggested the existence of such a shift in that machine. Similar experiments performed recently, using NBS II, however, failed to disclose any such shifts.

The unavoidable second-order Doppler shift of $v^2/2c^2$ amounts to 4×10^{-13} for both standards.

The electronics systems for the atomic beam frequency standards have been extensively investigated as possible sources of systematic frequency errors. As the power level of the excitation signal was varied from 3 mW to 12 mW (normal value = 4 mW), the frequency of NBS III shifted -5×10^{-12}. A resonant cavity with a phase difference between the oscillating field regions usually produces such behavior, i.e., the frequency shift

is generally power dependent. Under these conditions, as long as the power is constant, the phase difference should be fixed, and no additional inaccuracy should exist.

The power spectrum of the frequency multiplier chain used with the cesium standards has been investigated at intervals with the ammonia maser spectrum analyzer [8]. Most recent results show the brightest sidebands to be down about 43 dB at 9180 MHz, which is the 34th harmonic of the 270 MHz output signal of the multiplier chain. Although sidebands down by this amount cannot cause sufficient distortion of the resonance to result in significant frequency shifts, an allowance must be made for the fact that the spectrum may change significantly from time to time. This has been found to be particularly true when the sidebands are due to the power line frequency and its harmonics, making the spectrum sensitive to changes in ground loops and various electrical connections in the laboratory. In arriving at estimates of inaccuracy for the standards, therefore, contributions of $\pm 2\times10^{-12}$ for NBS III and $\pm 6\times10^{-12}$ for NBS II are included for this possible error source. The larger contribution from NBS II reflects the fact that a wide spectral line is more sensitive to such errors than a narrow one. Although it is impractical to examine the spectrum very often using the maser analyzer, it has been found useful to monitor regularly with an oscilloscope the beat frequency at about 100 Hz between the normal cesium excitation signal and a similar signal from another oscillator-multiplier chain system that is known to have a clean spectrum. On several occasions, small spurious modulations have been detected on the beat signal which were causing frequency shifts of only 1×10^{-11}.

Servo system contributions to inaccuracy have been discussed in an earlier report [7]. Some effects have been studied in more detail since that time. Special effort has been made to measure the effects of second harmonic distortion of the 37.5-Hz modulating signal used in the servo systems of both machines. This was accomplished by using, for example, NBS III as a reference while a carefully controlled percentage of second harmonic distortion was added to the NBS II servo system. The frequency of NBS II was observed while the phase of the second harmonic distortion was varied relative to the phase of the 37.5 Hz fundamental. This experiment was performed at 0.4 percent, 1 percent, and 3 percent added second harmonic distortion. The dependence of the frequency of the standard on the second harmonic distortion is basically in accord with the relation $\Delta\nu = (1/2)Df_d \sin\alpha$ where $\Delta\nu$ is the shift in the transition frequency, D is a measure of the second harmonic distortion, f_d is the peak frequency deviation of the excitation signal due to the modulation, and α is the phase angle of the second harmonic signal relative to the fundamental. One percent distortion at a relative phase of 90° produced a frequency shift of 3×10^{-11}.

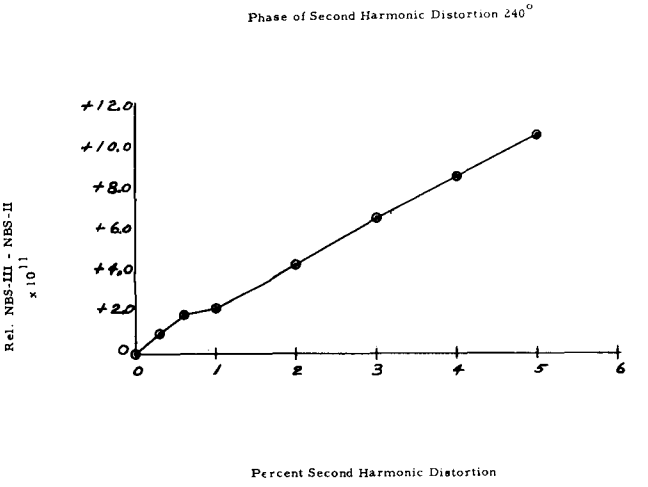

Fig. 7. Relative frequency of NBS II vs. percentage added second harmonic distortion.

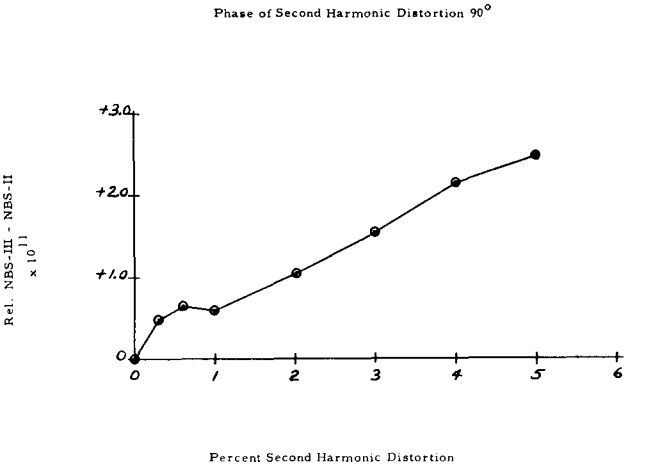

Fig. 8. Relative frequency of NBS III vs. percentage added second harmonic distortion.

The second set of experiments performed on both standards was the determination of the frequency dependence on the percentage of the second harmonic distortion added to the servo system. One standard was the reference in one experiment, while the situation was reversed for the other experiment. The phase of the second harmonic signal relative to the fundamental in each case was adjusted to the value which produced maximum shift of the transition frequency for any particular amount of second harmonic distortion. The results are shown in Figs. 7 and 8. It is apparent that the transition frequency as measured by NBS III is affected by second harmonic distortion less than one half as much as that for NBS II. NBS III therefore has an advantage over NBS II in this respect, due to its narrower line width.

The independent servo systems have been compared

recently via NBS III. Forty-minute measurements of the frequency of a high quality quartz oscillator taken alternately with the two servo systems show agreement to within 1×10^{-12}. The precision of each measurement was 0.9×10^{-12}. Similar results were obtained using NBS II.

Further sources of small errors which have been eliminated are large 60-Hz fields arising from physical layout of power outlets on NBS II and stray field leakage into the chopper demodulator in one of the servo systems. In addition, the frequency multiplier chain used with NBS II has been provided with better shielding, and the input impedance of this chain has been adjusted to 50 Ω. Possible frequency errors resulting from time dependent phase shifts in the multiplier chain have been considered, and some experimental work in this area is presently underway.

An overall estimate of inaccuracy for each of the standards may be made by combining in some appropriate manner the individual contributions to uncertainty discussed above. If we make the reasonable assumption that the individual effects are independent of one another, the proper method of combination is to use the square root of the sum of the squares as the overall estimate. Table I is a summary of the estimates of uncertainty due to the individual sources considered for both NBS II and NBS III. The combined total 3σ estimates of uncertainty are found to be $\pm8.0\times10^{-12}$ for NBS II and $\pm4.9\times10^{-12}$ for NBS III. The individual estimates given in the table are considered to be reasonable limits of error, approximately corresponding to statistically-determined 3σ estimates, for those effects not directly amenable to statistical analysis. The values given for Doppler shifts and multiplier-chain transient phase shifts are necessarily tentative at this time, due to a lack of conclusive experimental evidence.

TABLE I

CONTRIBUTIONS TO INACCURACY FOR NBS II AND NBS III

Estimated Uncertainty$\times10^{12}$

Source of Uncertainty	NBS II	NBS III
1) Random measurement errors (1 hr.) 3σ limits	±3.0	±1.5
2) Magnitude of $\overline{H(x)}-3\sigma$ limits	±0.6	±0.3
3) Overlap of neighboring transitions	±2.0	±1.0
4) Use of $\overline{H(x)}^2$ for $\overline{H^2(x)}$	±0.1	±0.1
5) Distortion effects arising from C field nonuniformity	±0.5	±0.5
6) C-field polarity effects	±0.5	±0.5
7) Cavity mistuning	±0.1	±0.1
8) Uncertainty in magnitude of cavity phase shift	±2.0	±3.0
9) Doppler shifts	±1.0	±1.0
10) Microwave power level	±1.0	±1.0
11) Spectral purity of excitation	±6.0	±2.0
12) Second harmonic distortion of servo modulation	±1.5	±0.5
13) Miscellaneous servo system effects	±2.0	±2.0
14) Multiplier chain transient phase shifts	±1.0	±1.0
Total 3σ Estimated Uncertainty (square root of sum of squares)	±8.0	±4.9

Checks upon the estimates of accuracy are obtained from comparisons of the cesium $(4, 0)\leftrightarrow(3, 0)$ transition frequency as measured by the two independent standards. The measured frequency difference between NBS II and NBS III contains data accumulated over a long period of time. Many of the data were obtained in the first stages of operation of NBS III when fluctuations were larger than they have been more recently.

Between September 1963 and March 1, 1964, measurements of the frequency difference between NBS III and NBS II were hampered by various electronic problems and a three-year accumulation of dirt and pump oil in the resonant cavity end sections of NBS II. This residue resulted in a large phase difference between the two oscillating field regions. A 180° rotation of the resonant cavity produced a frequency shift of 2.4×10^{-11}. After the cavity was cleaned on March 1, 1964, rotation produced a frequency shift of $(2.0\pm0.4)\times10^{-12}$, where the quoted uncertainty is the 1σ limit computed from the data. The average frequency difference during this period was 2×10^{-11}.

Between March 1 and May 22, the average frequency difference between the two standards was $(7\pm2)\times10^{-12}$. Two changes were made in this period: the input impedance of the frequency multiplier chain used with NBS II was brought down from 150 Ω to 50 Ω, and the shielding for this multiplier chain was made more adequate. From May 22, 1964 to June 1, 1965, the average measured difference between the two standards was

$$\text{NBS III} - \text{NBS II} = +\,(1.4 \pm 1.0) \times 10^{-12},$$

where the quoted uncertainty is once again the computed 1σ limit.

CONCLUSION

Experience gained at the National Bureau of Standards over a period of six years with three independent cesium standards has shown that realistic accuracy figures of $\pm5\times10^{-12}$ and measurement precisions of 1×10^{-13} in two hours are obtainable with existing standards. By reducing the uncertainties due to cavity phase shifts, random measurement errors, and spectral purity, and by careful attention to the remaining electronic problems, it is believed that an accuracy figure of $\pm1\times10^{-12}3\sigma$ may be realized for the NBS standards within the next one or two years.

ACKNOWLEDGMENTS

The authors would like to acknowledge the assistance of many members of the Atomic Frequency and Time Standards Section and, in particular, that of Dr. R. C. Mockler for his many helpful suggestions and continual encouragement, C. S. Snider for the general operation of the cesium standards, L. E. Heim for the servo system work, and J. A. Barnes and D. W. Allan for the spectrum analysis results.

References

[1] J. Bonanomi, P. Kartaschoff, J. Newman, J. A. Barnes, and W. R. Atkinson, "A comparison of the TA_1 and the NBS-A atomic time scales," *Proc. IEEE (Correspondence)*, vol. 52, p. 439, April 1964.

[2] A. S. Bagley and L. S. Cutler, "A new performance of the flying clock experiment," *Hewlett-Packard J.*, vol. 15, no. 11, July 1964.

[3] L. N. Bodily, "Correlating time from Europe to Asia with flying clocks," *Hewlett-Packard J.*, vol. 16, no. 8; April 1965.

[4] R. C. Mockler, R. E. Beehler, and C. S. Snider, "Atomic beam frequency standards," *IRE Trans. on Instrumentation*, vol. I-9, pp. 120–132, September 1960.

[5] R. C. Mockler "Atomic beam frequency standards," *Advan. Electron. Electron Physics*, vol. 15, L. Marton, Ed., New York: Academic, 1961, pp. 1–71.

[6] J. M. Richardson, R. E. Beehler, R. C. Mockler, and R. L. Fey, "Les etalons atomiques de frequence au NBS, 1961 Comité Consultatif pour la définition de la Seconde auprès du Comité International des Poides et Mesures, 2e session, Paris: Gauthier-Villars, 1962, pp. 57–67.

[7] R. E. Beehler, W. R. Atkinson, L. E. Heim, and C. S. Snider, "A comparison of direct and servo methods for utilizing cesium beam resonators as frequency standards," *IRE Trans. on Instrumentation*, vol. I-11, pp. 231–238, December 1962.

[8] J. A. Barnes and L. E. Heim, "A high-resolution ammonia-maser-spectrum analyser," *IRE Trans. on Instrumentation*, vol. I-10, pp. 4–8, June 1961.

Reprinted from IEEE TRANSACTIONS
ON *INSTRUMENTATION AND MEASUREMENT*
Volume IM-15, Numbers 1 and 2, March and June, 1966
pp. 48-55
THE INSTITUTE OF ELECTRICAL AND ELECTRONICS ENGINEERS, INC.
PRINTED IN THE U.S.A.

Evaluation of a Thallium Atomic Beam Frequency Standard at the National Bureau of Standards

R. E. BEEHLER AND D. J. GLAZE

Abstract—**The original NBS cesium standard (NBS I) has been converted to a thallium standard and was operated for one and one-half years with a typical precision of 2×10^{-12} and an accuracy of 1×10^{-11}. Experiments are described which were performed to establish these precision and accuracy estimates. These results, which are comparable to those obtained with longer cesium standards, are considered sufficiently encouraging to justify the conversion of a longer cesium standard to thallium for a more thorough evaluation.**

I. Introduction

In 1957, P. Kusch pointed out the possible advantages that thallium should have over cesium in atomic beam frequency standards [1]. The small quadratic dependence of the frequency on the uniform magnetic field in which the transition occurs is given by

$$\nu(\mathrm{Cs}^{133}) = \nu_0(\mathrm{Cs}) + 427H^2(\text{in Hz}), \quad (1)$$

$$\nu(\mathrm{Tl}^{205}) = \nu_0(\mathrm{Tl}) + 20.4H^2\ (\text{in Hz}). \quad (2)$$

The fractional uncertainties in frequencies resulting from uncertainties in H are given by

$$\left(\frac{\Delta\nu}{\nu_0}\right) = 9.1\times10^{-8}H\Delta H, \quad \text{for cesium, and} \quad (3)$$

$$\left(\frac{\Delta\nu}{\nu_0}\right) = 1.9\times10^{-9}H\Delta H, \quad \text{for thallium.} \quad (4)$$

Thus, the $(1, 0)\leftrightarrow(0, 0)$ transition in thallium is 1/50th as sensitive to the field as is cesium. This is no longer as great an advantage as it was originally, since the C fields have been so drastically improved in the cesium beams [2].

A further advantage for thallium arises from its simpler atomic spectrum, since there are only two microwave transitions neighboring the $(1, 0)\leftrightarrow(0, 0)$ σ transition already mentioned. These two π transitions are the $(F=1,\ m_F=1)\leftrightarrow(F=0,\ m_F=0)$ transition and the $(F=1,\ m_F=-1)\leftrightarrow(F=0,\ m_F=0)$ transition. Thus, with different C-field orientations necessary to excite these two sets of transitions, proper parallelism of the σ-oriented C field with the two oscillating field regions in the resonant cavity end sections should insure freedom from overlap of π transitions. Also, the simpler thallium spectrum should allow a greater signal intensity for the $(1, 0)\leftrightarrow(0, 0)$ thallium transition than for the corresponding $(4, 0)\leftrightarrow(3, 0)$ transition in cesium, since a greater percentage of the thallium atoms have energies in the desired states. Finally, the thallium transition frequency is more than double that of cesium, so that, for the same absolute uncertainty in the frequency, a higher relative precision of measurement is obtained for the thallium standard than for the cesium standard.

II. The NBS Thallium Beam Standard

These possible advantages led to the conversion of NBS I, the original NBS cesium standard with an interaction length of 55 cm, to a thallium standard in September, 1962. The thallium standard is shown in Fig. 1.

A considerable amount of time was spent in developing and improving a suitable detection system. Wire

Manuscript received October 27, 1965.

The authors are with the National Bureau of Standards, Boulder, Colo.

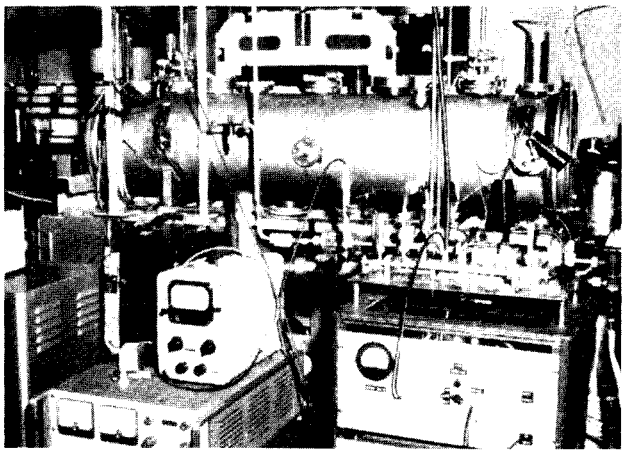

Fig. 1. Thallium atomic beam frequency standard.

0.013 cm in diameter drawn from a pure, single crystal of tungsten has given the most noise-free performance as a surface ionization detector for the thallium beam. Since thallium has an ionization potential of about 6.1 volts, the tungsten wire must be oxidized to provide a work function high enough to allow efficient ionization of the thallium atoms. The oxidation and operating procedures that have been developed are as follows:

1) Before the oven temperature is raised to its operating value of 610°C, pure oxygen is admitted to the vacuum system by opening a variable leak rate valve mounted on the detector cover plate of NBS I. The detector wire temperature is near 900°C as measured by an optical pyrometer.

2) Enough oxygen is admitted to raise the system pressure to one torr or higher.

3) The detector temperature drops below 700°C under these conditions. The temperature is, however, next increased to about 900°C. After approximately one minute, the variable leak rate valve is closed.

4) As the oxygen is being evacuated from the system, the detector current is decreased as necessary in order to maintain the temperature near 900°C.

5) Frequency measurements can be made when the system pressure falls below 3×10^{-6} torr, usually within 10 minutes, if the oven is up to temperature.

Although repeated oxidation of the detector with the oven hot no longer causes clogging of the oven slit, this procedure is detrimental to the molybdenum heater coils and is therefore used no more than is absolutely necessary.

The detector is normally operated at a relatively high temperature in order to decrease the "sitting" time of the atoms on the wire so that a servo technique of measurement involving 37.5 Hz modulation of the microwave excitation can be utilized. At 900°C–1000°C the oxide is stable for as long as 13 hours—this is the longest continuous operating time to date on the thallium system. During this and similar long-term runs, the oxide showed no tendency to deteriorate. Ionization efficiency for this system has been estimated to be at least 50 percent. Signal-to-noise ratios for the central peak of the Ramsey resonance curve are generally in the vicinity of 300–400.

The interaction length of 55 cm for the NBS I thallium standard results in a spectral line width of about 280 Hz as compared to 330 Hz for the same machine operated with cesium. The loaded Q of the resonant cavity is 2800. The frequency shift observed upon rotation of the cavity by 180° about a vertical axis, presumably resulting from a phase difference between the two oscillating field regions, is less than 2×10^{-12}. Two such rotations were performed.

During the course of the thallium investigations, this cavity was found to have become detuned by about 6 MHz. This detuning of the cavity from the thallium transition frequency was accompanied by a shift in this frequency of 4×10^{-11}. This detuning was attributed to a temperature-stress-tuning correlation even though this cavity had been provided with considerable mechanical bracing. Further, the measured thallium transition frequency depends significantly on the cavity tuning plunger position, with a frequency minimum occurring when the cavity is tuned to the thallium line frequency. This effect is not believed to be a result of frequency pulling by the resonant cavity, which is calculated to be only 0.0093 Hz or about 4.4×10^{-13} for a detuning of 6 MHz, but rather a result of a changing phase difference between the two oscillating field regions of the cavity due to possible asymmetry of the tuning mechanism.

This cavity, which is the second one constructed for the thallium system, has been provided with electroformed copper end sections, smaller beam coupling holes, and electroformed extensions out from the beam holes to minimize field fringing effects at these holes. As a result, the dependence of the measured thallium transition frequency on microwave power level that had been observed with the first cavity is eliminated, at least for power levels below 50 mW.

Considerations of accuracy are, for the present, necessarily confined to internal estimates. A second thallium standard is nearly ready for operation and should provide a better indication of accuracy.

In order to obtain an estimate for ΔH, the uncertainty in the magnitude of the uniform magnetic field, two independent calibrations of the field using the (4, 1) $\leftrightarrow$(3, 1) transition in cesium and the (1, 1)$\leftrightarrow$(0, 0) π transition in thallium were compared. At the relatively high field of 0.140 Oe used in most of the early measurements, the calibrations agreed to within 0.002 Oe. Considering ΔH to be ±0.001 Oe, we find $\Delta\nu/\nu$ to be $\pm3\times10^{-13}$. These data were taken with a power supply not as stable or well regulated as the one used for NBS II and NBS III, the NBS cesium standards.

To operate at 0.070 Oe reasonable evidence must exist that no overlap effects occur due to the π transitions. This evidence is obtained from two sources. First, care-

ful searches were made for π transitions with the C-field direction oriented for σ transitions. The signal-to-noise ratio of the σ transition was always as good as 200. No evidence of π transitions has ever been detected. Second, further evidence of the absence of overlap shifts is provided by the plot of the frequency of the normal $(1, 0)\leftrightarrow(0, 0)$ transition vs. the square of the C-field current shown in Fig. 2. The half length of the vertical bar at each plotted point represents the precision of measurement (standard error of the mean). Any overlap shifts should be most pronounced at low values of the C field. No significant deviation from linearity appears even at the lowest field used of 0.015 Oe, which corresponds to a C-field correction of only 2×10^{-13}. The rms deviation of the points from the least squares line is only 4×10^{-12}.

Reversal of the C-field polarity produced no frequency shift within the measurement precision of 2.5×10^{-12}. Such a shift had been observed with the earlier thallium cavity where significant leakage of the microwave radiation field from the beam holes was present.

Magnetic shielding of the C-field region is accomplished by an outer soft iron cylinder and an inner mumetal cyclinder. The measured nonuniformity of field along the length of the C-field region is within ±0.001 Oe at a field of 0.050 Oe. This and the residual field of ±0.001 Oe produce negligible uncertainties in the frequency measurements and are not considered limitations at present.

A block diagram of the servo measurement system appears in Fig. 3. The same two independent servo systems, employing 37.5 Hz modulation, that are used regularly with the NBS cesium standards are also usable in the thallium case. The only modification required is to increase the peak frequency deviation due to the modulation because of the greater relative line width for NBS I. Comparisons of recent manual measurements with servo measurements show agreement to within 2×10^{-12} The precision of measurement for the manual data was 2.4×10^{-12}, and that for the servo data was 1.5×10^{-12}. Interchange of the vacuum tube servo system with the transistorized servo system resulted in a frequency shift of less than 2.5×10^{-12}, which was the precision of measurement. A detailed evaluation of the vacuum tube servo system has been reported previously [3].

The power spectrum of the frequency multiplier chain used in the measurement system has been improved by the addition of more adequately filtered power supplies. The brightest sidebands of 60 Hz and 120 Hz are now down about 35 dB at the thallium transition frequency. Previous power supplies contributed time dependent, asymmetric sidebands which caused many nonreproducible frequency shifts in the thallium transition frequency.

The average precision of measurement for the thallium standard over one hour averaging times, as determined from more than one year's data, is 2×10^{-12} when

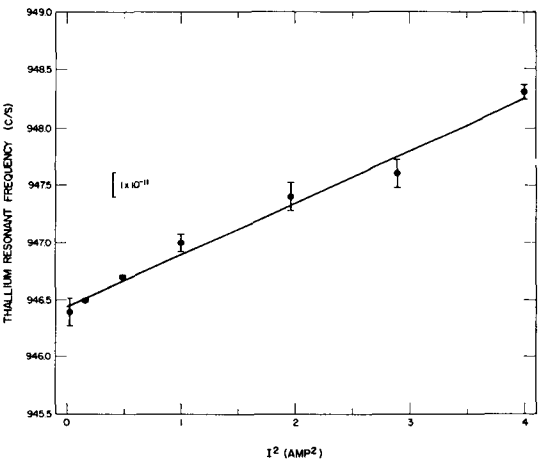

Fig. 2. Thallium resonant frequency vs. square of C-field current.

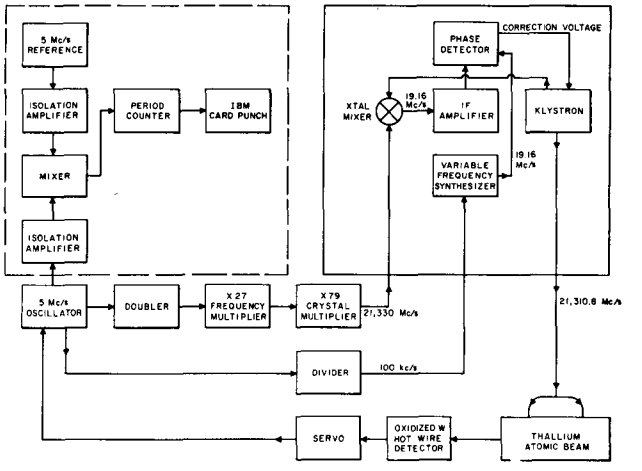

Fig. 3. Block diagram of the thallium servo measurement system.

compared with a high quality quartz oscillator or either of the NBS cesium standards. Occasionally, measurement precisions of 4×10^{-13} have been observed with one of the cesium standards as reference. When the average standard error of the mean of 2×10^{-12} for a one-hour measurement is compared to the standard deviation of 1×10^{-11} for daily measurements made over a period of months, a discrepancy is apparent, suggesting a lack of statistical control in the measurement process. For intermediate-length measurement periods of several hours within a given day, however, such as the thirteen-hour-frequency comparison of the thallium standard with NBS III, shown in Fig. 4, much better control is indicated. Here, the average precision of the one-hour measurements is 1×10^{-12}, while the standard error of the mean for the group of 13 one-hour points is about 6×10^{-13}, this being an indication of the precision expected for a measurement averaged over a thirteen-hour period. The one-hour precision for NBS III is typically 5×10^{-13} which is only about 4 times better than the corresponding figure for the much shorter thallium

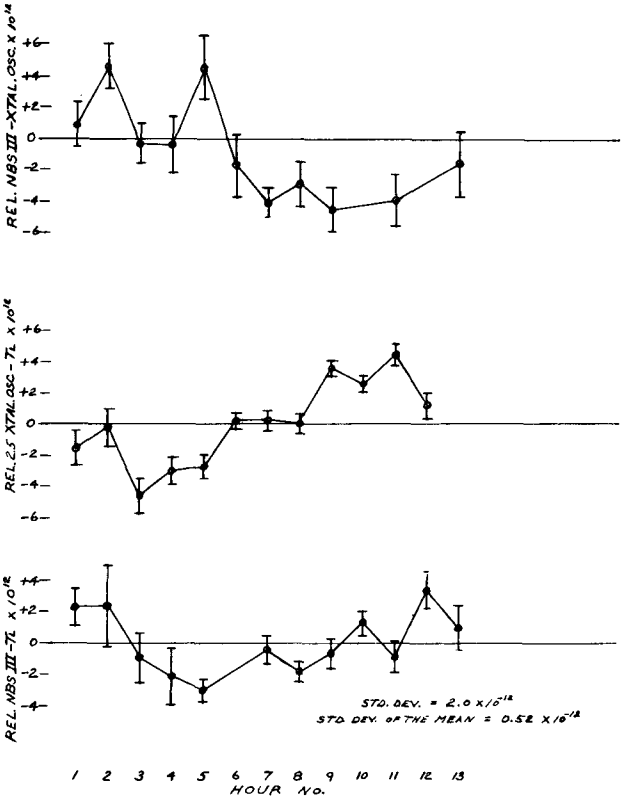

Fig. 4. 13-hour stability comparison of thallium standard, NBS III, and a crystal oscillator (April 16–17, 1964).

standard. In view of the ratio of the interaction lengths of about 7, this precision comparison is encouraging.

The precision associated with the thallium standard does depend on the oxide coating on the detector wire. As the detector wire ages and is oxidized away, the detection efficiency for the 0.013-cm wide beam drops, along with the intensity of the Ramsey pattern. As long as this intensity is a reasonable value ($2\text{–}5\times10^{-12}$ amperes of detected beam current), the precision is quite satisfactory.

The best value for the measured frequency of the $(F=1, m_F=0)\leftrightarrow(F=0, m_F=0)$ transition in thallium in zero magnetic field [with respect to an assigned frequency of 9192631770 Hz to the $(F=4, m_F=0)\leftrightarrow(F=3, m_F=0)$ transition in cesium] is

$$\nu_0(\mathrm{Tl}) = 21,310,833,945.9 \pm 0.2 \text{ Hz}.$$

The quoted accuracy figure of ±0.2 Hz or $\pm1\times10^{-11}$ is a tentative but best estimate from the accumulated data. This frequency determination agrees with that obtained by the Swiss group at Neuchatel Observatory (ν_0 21,310,833,945.1 $\pm$ 1.0 Hz) to within the quoted limits [4].

Future intentions for thallium standards include installation of permanent magnets of higher field intensity than those presently used in NBS I, and evaluation of NBS II as a thallium standard. The use of NBS II will allow direct comparison of two thallium standards with the added benefit of the narrower spectral line width of NBS II.

Conclusion

The results obtained from the short thallium standard have been sufficiently encouraging to justify an evaluation of a longer and more refined thallium system. Comparison of two independent thallium standards should provide a more reliable accuracy figure for comparison with cesium and hydrogen.

Acknowledgment

The authors would like to acknowledge the assistance of many members of the Atomic Frequency and Time Standards Section and, in particular, that of Dr. R. C. Mockler for his many helpful suggestions and continual encouragement, L. E. Heim for the servo system work, and J. A. Barnes and D. W. Allan for the spectrum analysis results.

References

[1] P. Kusch, "Precision atomic beam techniques," *1957 Proc. 11th Annual Frequency Control Symposium*, U. S. Army Signal Research and Development Lab., Fort Monmouth, N. J., pp. 373–384.

[2] R. E. Beehler and D. J. Glaze, "The performance and capability of cesium beam frequency standards at the National Bureau of Standards," *this issue*, pp. 51–57.

[3] R. E. Beehler, W. R. Atkinson, L. E. Heim, and C. S. Snider, "A comparison of direct and servo methods for utilizing cesium beam resonators as frequency standards," *IRE Trans. on Instrumentation*, vol. I-11, pp. 231–238, December 1962.

[4] J. Bonanomi, "A thallium beam frequency standard," *IRE Trans. on Instrumentation*, vol. I-11, pp. 212–215; December 1962.

Reprinted from IEEE TRANSACTIONS
ON *INSTRUMENTATION AND MEASUREMENT*
Volume IM-15, Numbers 1 and 2, March and June, 1966
pp. 55-58
The Institute of Electrical and Electronics Engineers, Inc.

An Intercomparison of Hydrogen and Cesium Frequency Standards

R. VESSOT, H. PETERS, J. VANIER, R. BEEHLER, D. HALFORD, R. HARRACH, D. ALLAN, D. GLAZE, C. SNIDER, J. BARNES, L. CUTLER, MEMBER, IEEE, AND L. BODILY, MEMBER, IEEE

Abstract—Intercomparisons of average frequency and of frequency stability were made among one Hewlett-Packard 5060A cesium beam, two Varian Associates H-10 atomic hydrogen masers, and the National Bureau of Standards NBS III cesium beam designated as the United States Frequency Standard. Each of the standards displayed a white noise frequency fluctuation behavior with a transition into an approximate flicker of frequency fluctuation behavior for longer time intervals. The rms fractional frequency fluctuation between adjacent samples, $\sigma(\tau, N=2)$, was $6\times10^{-11}\tau^{-1/2}$ down to a flicker level of about 3×10^{-13} for the hp 5060A cesium beam ($10^2\leq\tau\leq10^4 s$), $1\times10^{-11}\tau^{-1/2}$ down to a flicker level of less than 1×10^{-13} for NBS III cesium beam ($10^2\leq\tau\leq10^4 s$), and $5\times10^{-13}\tau^{-1/2}$ down to a flicker level of about 1×10^{-14} for the H-10 hydrogen masers ($1\leq\tau\leq10^4 s$). The accuracy capabilities of NBS III and H-10 #4 are now 1.1×10^{-12} and 0.47×10^{-12}, respectively (1σ estimate).

A discrepancy of only 1.1 parts in 10^{12} was observed between the average frequencies of the hp 5060A cesium beam and the NBS III cesium beam, with the former being higher in frequency.

In terms of the frequency of the Cs^{133} hyperfine transition ($F=4$, $m_F=0$)$\leftrightarrow$($F=3$, $m_F=0$), defined as 9 192 631 770.0000 Hertz, the measured frequency of the H^1 hyperfine transition ($F=1$, $m_F=0$) $\leftrightarrow$-$F=0$, $m_F=0$) was $\nu_H=1\ 420\ 405\ 751.7864\pm0.0017$ Hertz. This is believed to be the most accurate and precise measurement of any physical quantity.

I. Introduction

A SERIES of measurements involving hydrogen and cesium frequency standards [1] was made at the National Bureau of Standards (NBS), Boulder, Colo., during September and October 1965. The object of the measurements was to make intercomparisons of frequency between standards that then represented the state-of-the-art; to measure the frequency of the hyperfine separation of hydrogen in terms of the provisional international standard of frequency, the hyperfine separation of cesium 133, with higher accuracy than ever before; and to obtain statistical information that would give an insight into the nature of the perturbations that cause changes in frequency. Participating in the experiments were personnel from the NBS Atomic Frequency and Time Standards Section, the Hewlett-Packard Co., and the Quantum Electronics Division of Varian Associates. The equipment involved in the measurements were the NBS III cesium beam frequency standard used as the United States Frequency Standard located at Boulder, a Hewlett-Packard model hp 5060A cesium beam standard, and two atomic hydrogen masers model H-10 built by Varian Associates. A preliminary report of some of this work has been published [2].

Measurements involving time intervals ranging from 1 second to a maximum of 4×10^6 seconds were made between these standards by various techniques that are described in Section II of this paper. An effort was made to obtain statistically significant quantities of data to allow analysis of the spectral density of the phase or frequency fluctuations for sampling time intervals ranging from seconds to hours. For time intervals of greater duration, the number of samples available obviously diminishes and the relative magnitude of the confidence limits that apply to any given statistically determined parameter increases. Hence, it is difficult to make precise conclusions concerning the spectral density of the very low frequency fluctuations. Therefore, the long term data are presented in the form of relative frequency vs. the time of measurement, as well as in the form of $\sigma(\tau)$ vs. τ plots. The plots of frequency vs. running time can also help one to detect systematic behavior of the frequency fluctuations. These two forms of data presentation supplement each other.

Emphasis was placed on making measurements at what would normally be considered as the useful output frequency, 5 MHz, in order to include the effects due to the electronic circuits and frequency synthesizers that normally form part of the frequency control system. A great deal of the data was taken with a 5 MHz system developed at NBS using period measurement (Section II.A). This system was especially useful for measurements over continuous time intervals of 10^2 seconds to 10^4 seconds. For measurements between masers involving shorter time intervals, a different period measuring system (Section II.D) was used that referred the comparison to a common 5 MHz frequency and, by frequency multiplication back up to 1420 MHz, allowed greater resolution over the shorter time intervals. Relative stability measurements between masers

Manuscript received August 15, 1966. This paper was presented at the 1966 Conference on Precision Electromagnetic Measurements, Boulder, Colo.

R. Vessot and J. Vanier are with the Quantum Electronics Division, Varian Associates, Beverly, Mass.

H. Peters is with the NASA Goddard Space Flight Center, Greenbelt, Md.

D. Halford, D. Allan, D. Glaze, C. Snider, and J. Barnes are with the Radio Standards Laboratory, National Bureau of Standards, Boulder, Colo.

R. Beehler, L. Cutler, and L. Bodily are with the Hewlett-Packard Company, Palo Alto, Calif.

R. Harrach is with the Lawrence Radiation Laboratory, University of California, Livermore, Calif.

over intervals of days were made with this high resolution system by means of automatically printed period measurements and strip chart recordings of relative phase at 1420 MHz.

An important result from these experiments is a more accurate value of the hydrogen hyperfine frequency (Section IV) in terms of the cesium 133 hyperfine frequency assumed to be given by 9 192 631 770.0000 Hz. Due to improved understanding of the perturbations affecting the frequencies of the hydrogen and cesium devices, new error budgets (Section III) have been made for each which are more complete than those previously made. The frequency of the hyperfine separation of hydrogen is found to be 1 420 405 751.7864 $\pm$ 0.0017 Hz. The uncertainty of ± 0.0017 Hz is a 1σ (68 percent confidence) measure and corresponds to 1.2 parts in 10^{12}.

Very closely related to the problem of intercomparisons is the question of intrinsic frequency reproducibility between instruments and particularly between instruments made by different people. In the case of the two cesium devices having enormously different size, beam flux, and resonance linewidth, the data giving the average frequency over a run of several days duration indicated that the average frequencies agreed well within the accuracy limits assigned to each standard (Section II.D). The frequency fluctuations measured over a large range of time intervals τ are random and vary as $\tau^{-1/2}$, the behavior of a source which is frequency modulated by white noise (Section II.B).

Frequency reproducibility measurements between hydrogen masers constructed in different laboratories have been made [3]. However, since there are relatively few well stabilized H masers and since they are located in fixed installations, it is not yet possible to make definitive conclusions. It is possible to determine the frequency of the hyperfine separation of hydrogen for the idealized conditions of zero wall collision effects, zero magnetic field, zero absolute temperature, and zero electromagnetic pulling by applying suitable corrections. Though the reproducibility of *operating* frequency from one maser to another for masers made in a single laboratory is considerably better than the absolute reproducibility specified in the idealized manner previously mentioned, the reproducibility of hydrogen frequency given here is in terms of those ideal conditions.

II. Measurements and Techniques

A. Measurements with 5 MHz Comparison Systems

Long-term frequency comparisons among the cesium beam devices and hydrogen masers were made by measuring the period of the beat frequency between pairs of synthesized 5 MHz signals controlled by the various atomic transitions. The system is shown in block form in Fig. 1 and consists of two input channels at 5 MHz, each consisting of an isolator amplifier leading to a mixer. The output signal from the mixer, with peak-to-peak amplitude of 8 volts and having a frequency typically ranging from 0.001 Hz to 10 Hz, is led through a low pass filter to a period measuring counter connected to a card punch. Period data were automatically punched on cards.

As many as three such systems were used simultaneously during a run lasting 49 hours, during which the Hewlett-Packard cesium beam, the NBS cesium beam, and a Varian H maser were compared. Plots of these data are shown in Fig. 2 and some explanation of the circumstances should be given. Frequency offsets of a few tenths of a Hertz (cycle per second) from 5 MHz were arbitrarily chosen in order to obtain frequency differences suitable for making period measurements at 5 MHz. The Hewlett-Packard instrument was supplied with a -150×10^{-10} offset and was operated according to factory procedure, the NBS III instrument was operated at a nominal -249×10^{-10} offset, and the H maser digital synthesizing phase lock system was adjusted to the nearest 0.01 Hz at 1420 MHz so as to have a nominal zero offset of its 5 MHz output frequency. The data shown give the hour-by-hour variation between pairs of instruments. Each point is flagged with error bars representing the estimated standard deviations of the mean for each one-hour segment of the run as determined by computer analysis of the punched cards. On the average, during each hour there were 17 measurements for the Hewlett-Packard 5060A vs. NBS III, 25 measurements for the Hewlett-Packard 5060A vs. Varian H-10 #4, and 44 measurements for the H-10 #4 vs. NBS III.

At the beginning of the run a slow drift was observed in the H-10 #4 vs. NBS III data, due to the stabilizing of the maser cavity temperature control system, since a few hours prior to the beginning of this record both masers had been moved from a room having temperature of about 90°F to a room with ambient temperature of about 70°F. At 1500 hours September 14 local time the maser cavities were tuned and data taking was begun. At 2200 hours the same day the masers were checked and the cavity of H-10 #4 was found to have drifted high in frequency; it was retuned, the correction being 21×10^{-13} in $\Delta f/f$.

The tuning was checked at intervals during the run by observing the change in the beat frequency of H-10 #4 vs. H-10 #3 induced by a change in beam flux in H-10 #4. No interruption of the data resulted from this procedure; the offset introduced temporarily as a result of this process is of the order of a few parts in 10^{+13} in $\Delta f/f$ and is negligible. This tuning procedure is described in Section II.E and Section III.A.

There is evidence that the temperature control had not completely stabilized before the retuning at 2200 hours September 14. At 1500 hours September 15 it was found that H-10 #4 was 4.0×10^{-13} high, at 0200 on September 16 H-10 #4 was 3.8×10^{-13} high, and at 1800 September 16 it was found to be 1.2×10^{-13} high. During this run the instruments were not adjusted in any way except for the change in tuning of H-10 #4 at 2200 Sep-

tember 14, noted above. In the H-10 #4 vs. NBS III plot given in Fig. 2, the open circles represent the frequency offset observed under the conditions of tuning given above. The solid black points represent the frequency offset which would have been observed if H-10 #4 had been properly tuned.

Further data were taken for 50 days between Varian H-10 #4 and NBS III. The fractional differences of the synthesized frequencies, nominally at 5 MHz, are shown plotted against measurement number and date of measurement in Fig. 3. Further data between the hp 5060A and NBS III were taken for twelve days and are shown in Fig. 4. The hourly averages made during these two runs are shown as points with vertical flags indicating the estimated 1σ error of the averages that typically ranges from 1 to 3×10^{-13} in the case of the NBS III vs. H-10 #4 and from 5 to 9×10^{-13} in the case of comparisons involving the Hewlett-Packard instrument.

In addition to the 49 hour and 50 day runs just described, two more runs were made between H-10 #4 and NBS III using the 5 MHz comparison system. An 11 hour run was made on September 17 and a 52 hour run was made on September 23 through 25. The fractional frequency offsets are plotted against running time in Fig. 5. The data have been corrected for H maser cavity pulling and for magnetic field, cavity phase, power, and second-order Doppler shifts of NBS III. These corrections are discussed in Section III.

The circumstances of the 11 hour run were such that the noise level on the signals was very much lower than for the three other runs. This could be due to the fact that the runs were made during a quiet period on a Friday evening. As seen in Fig. 5, the 11 hour run data, taken in hourly groups of approximately 44 measurements, have a standard deviation for each group of about 1×10^{-13} in $\Delta f/f$, as compared to about 3 to 5×10^{-13} for the data of the 52 hour run. The 11 hour run was used for statistical analysis of σ as a function of sampling time τ in order to determine the frequency dependence of the spectral density of the relative instabilities of the signals. The analysis was performed using the method of Allan [4], which is outlined in the Appendix. A plot of $\sigma(\tau)$, the root mean square fractional relative frequency deviation for sampling time τ, vs. the sampling time, is given in Fig. 6.

Similar runs were performed using the Hewlett-Packard 5060A and the Varian H-10 #4 instrument. The σ vs. τ plots, given in Figs. 7 and 8 for two separate runs, show that the data are reproducible and follow closely tne $\tau^{-1/2}$ law described in Section II.B.

B. White Frequency Noise of Cesium Beam Standards: Short Term Frequency Stability

A comparison of the σ vs. τ plot for the NBS III instrument in Fig. 6, and that for the Hewlett-Packard 5060A instrument given in Figs. 7 and 8, indicates that the ratio of σHP to σNBS is about 5 to 1. This can be compared with the ratio predicted [5] from measured values of 1) the resonance linewidth, and 2) the signal-to-noise ratio at the output of the beam detector preamplifier (Fig. 9).

In notation consistent with the present paper, $\sigma(\tau)$ is taken as the fractional rms frequency deviation for a sample time interval τ, and

$$\sigma(\tau) = 0.387 \frac{\Delta f_l}{f_0} \frac{I_n}{I_m} \tau^{-1/2}, \tag{1}$$

where

Δf_l is the width of the atomic resonance,
f_0 is the center frequency of the atomic resonance,
I_n is the rms noise current from the detector preamplifier in a 1 Hz bandwidth centered at the modulation frequency, and
I_m is the peak signal current from the preamplifier.

In the case of the Hewlett-Packard instrument

$\Delta f_l = 550$ Hz,
$I_n/I_m = 1.92\times10^{-3}$, and
$\sigma(\tau) = 4.45\times10^{-11}\tau^{-1/2}$.

For the NBS III instrument

$\Delta f_l = 45$ Hz,
$I_n/I_m = 1.95\times10^{-3}$, and
$\sigma(\tau) = 3.7\times10^{-12}\tau^{-1/2}$.

The calculated ratio σHP/σNBS is 12 to 1 and should be compared with the measured ratio of 5 to 1. This discrepancy is largely due to the fact that in NBS III the frequency of the modulation is a large fraction of the resonance linewidth and results in a loss of recovered signal at the detector as compared to that obtained with slower modulation. The discrepancy in the ratio also may be due to the fact that only the noise contributions from the beam and the preamplifier are included in the calculation. The frequency lock system noise is not included, nor is the noise in the frequency comparison equipment. Over the complete range of time intervals, two minutes to four hours, of Figs. 6, 7, and 8, the data for both instruments show no evidence of systematic variations.

C. NBS III vs. Hewlett-Packard 5060A: Long Term Frequency Stability and Average Frequencies

The 12 day run (Fig. 4) was used to compare the average frequencies of the hp 5060A and NBS III cesium beam standards. To compare the standards in a way so as to yield the best average frequency relation, it is necessary to include corrections discussed in Section III.B. In Fig. 4 the data are shown plotted in the corrected form and the date of the measurement is indicated below the axis designated as "measurement number." The Hewlett-Packard instrument was operated at a design frequency offset of -150.00 parts in 10^{10} from the 9 192 631 770.0000 Hz frequency defined as the

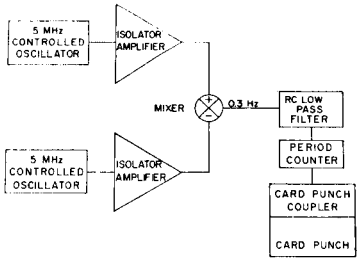

Fig. 1. NBS 5 MHz comparison system.

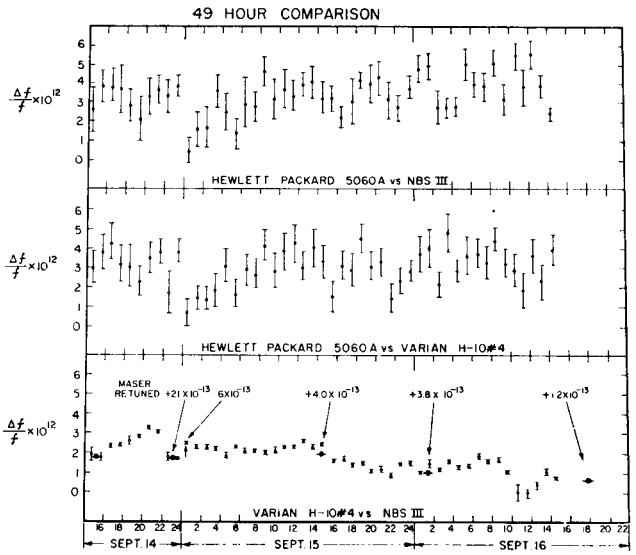

Fig. 2. Simultaneous measurements of frequency stability among NBS III, Varian H-10 #4, and Hewlett-Packard 5060A; 49 hour comparison.

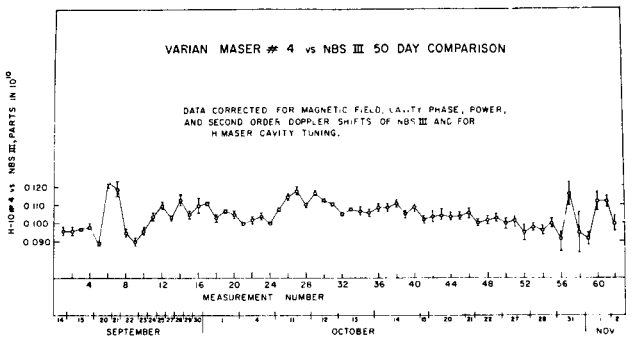

Fig. 3. 50 day plot of data between Varian H-10 #4 and NBS III.

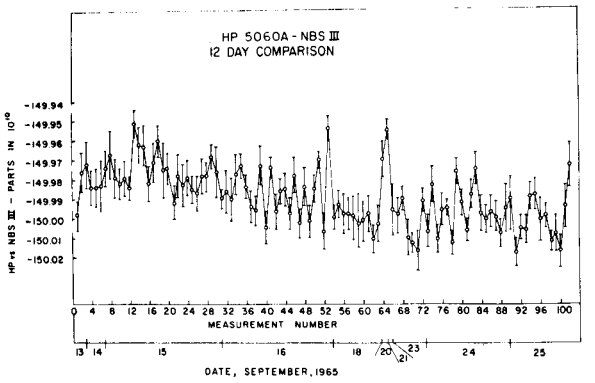

Fig. 4. 12 day plot of frequency offset between Hewlett-Packard 5060A and NBS III.

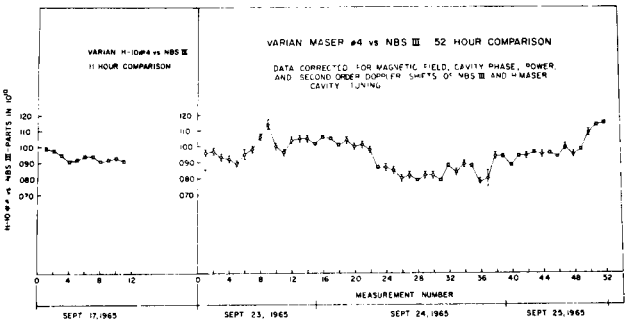

Fig. 5. 11 hour and 52 hour plots of data between Varian H-10 #4 and NBS III.

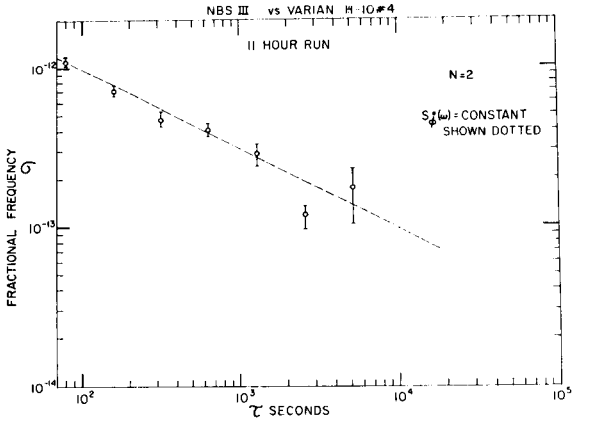

Fig. 6. Standard deviation of fractional frequency fluctuations as a function of sampling time, NBS III vs. Varian H-10 #4; 11 hour run.

frequency of the Cs^{133} hyperfine transition under ideal conditions of zero magnetic field, infinitesimal radiation field intensity, zero second order Doppler shift, and zero phase error between the cavities.

There were 102 measurements of length (τ) of one hour, and the dead time between measurements ($T-\tau$) ranged from a few seconds to greater than a day. A $\sigma(\tau)$ vs. τ plot of these measurements is in good agreement with the data of Figs. 7 and 8, with an indication of a flicker of frequency level [8], [4], [5] of 2 to 3 parts in 10^{13}. The flicker of frequency level for NBS III is known to be less than 1 part in 10^{13} for adjacent samples ($N=2$). The overall average of the 102 measurements was -149.989 parts in 10^{10} with a standard deviation σ of a measurement of 1.5 parts in 10^{12}. It is worth noting that the hp 5060A was calibrated in an internally consistent manner by adjusting the magnetic field to a predetermined level found by monitoring the field dependent hyperfine transitions at frequencies above and below the frequency of the ($F=4$, $m_F=0$)↔($F=3$,

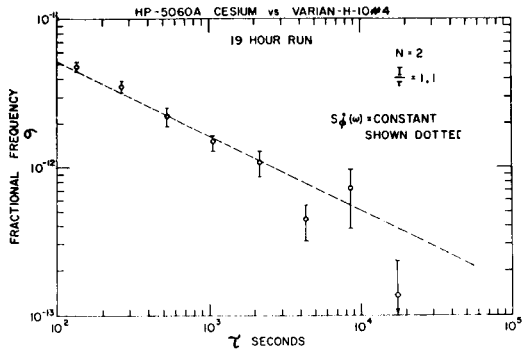

Fig. 7. Standard deviation of fractional frequency fluctuations as a function of sampling time, Hewlett-Packard 5060A vs. Varian H-10 #4; 19 hour run.

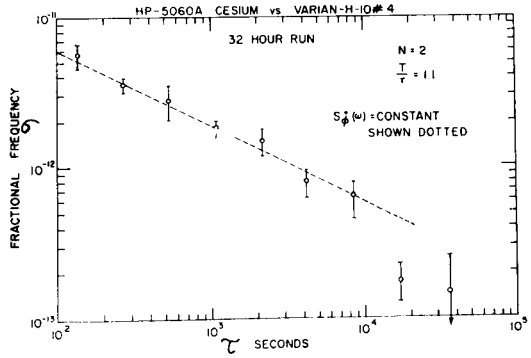

Fig. 8. Standard deviation of fractional frequency fluctuations as a function of sampling time, Hewlett-Packard 5060A vs. Varian H-10 #4; 32 hour run.

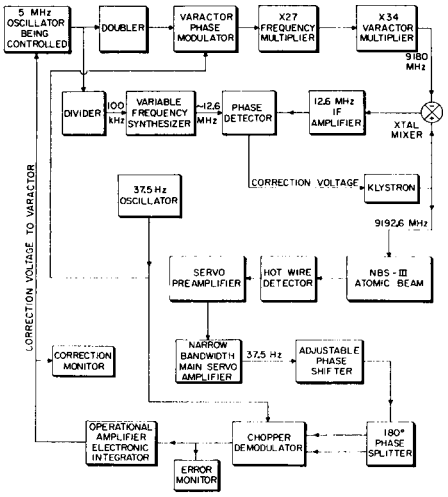

Fig. 9. Frequency lock system of NBS III cesium beam.

$m_F = 0$) transition. The NBS III instrument was operated in the manner described in reference [6]. A schematic of the NBS III frequency lock system is shown in Fig. 9. The discrepancy between the hp 5060A and NBS III is 1.1×10^{-12}, with the former being higher in frequency. The accuracy claimed for the hp 5060A by the manufacturer is $\pm 2 \times 10^{-11}$.

D. H Maser vs. H Maser: Short Term Frequency Stability

Measurements of short term relative frequency stability between masers were made using the system shown in Fig. 10. In this system a 5 MHz crystal oscillator is phase locked to Maser A and serves as a driver for a 1400 MHz multiplier serving as local oscillator for Maser B. The intermediate frequency signal f at 20.405 MHz is then compared with an offset signal from a digital synthesizer operating at f_2. The beat frequency $f_2 - f$ can be adjusted and allowed beat period measurements to be made over a range determined both by the beat rate $f_2 - f$ and by the number of periods chosen to represent the interval. As an example, if $f_2 - f = 1$ Hz, one can obtain 1 second averages by single-beat period measurements, 10 second averages by 10-beat period measurements, etc.

This method was used for runs of data typically involving several hundred measurements over a total time interval of one hour. An important parameter for each of these runs is the setting of the low pass filter which determines the amount of noise sideband power that accompanies the signal at the beat frequency. The behavior of the output fluctuations is a strong function of the filter setting for cases where additive white phase noise is present with the signal. The effect of this noise for fixed bandwidth B is given [5] by

$$\sigma = \frac{1}{2\pi f \tau} \sqrt{\frac{\overline{FkT}\,\overline{2B}}{P}}, \tag{2}$$

where FkT/P is the ratio of the additive noise power spectral density to the carrier power, and f is the frequency of the carrier. Low pass filtering of the beat signal has approximately the same effect on white phase noise as does band pass filtering of both carriers.

Under these conditions, one expects σ to vary as $1/\tau$ if the bandwidth is kept fixed. The presence of other spectral types of frequency fluctuation can be determined from the dependence of σ on observation time with different bandwidths or by relating the bandwidth to the reciprocal of the observation time and plotting the data in terms of $B\tau$ [7].

Data were taken by printing the period for a fixed number of beats and later transferring the data to card form for processing by a computer. In general, the number of samples was chosen to be some integral power of two for compatibility with the method used by Allan [4] and described in the Appendix. Plots of $\sigma(\tau)$ vs. sample time τ are given in Fig. 11 for two different bandwidths of the RC low pass filter. It is observed that the data are bandwidth dependent and are very much above the level predicted by the effect of known additive white noise of the microwave mixer. For the conditions $F = 10$, $kT \approx 4 \times 10^{-21}$ Joules, $P \approx 5 \times 10^{-13}$ watts, and a 2 Hz bandwidth low pass filter at the beat frequency, the value of σ given by the above equation for

white phase noise is

$$\sigma \approx 6 \times 10^{-14}\tau^{-1}.$$

It is clear from Fig. 11 that the measured instability is not due to the effect of added white noise of the microwave mixer. The tau dependence of $\sigma(\tau)$ in Fig. 11 is as $\tau^{-1/2}$ from 2 seconds to 120 seconds (i.e. white frequency noise) and is not the τ^{-1} dependence (i.e. white phase noise) described in (2). In addition, the σ values in Fig. 11 are greater than the values expected due to additive white noise. Other sources must be found to account for the instabilities observed. These may involve the frequency synthesis systems or interference pickup in the measurement system. Further study of the instabilities due to these components is in progress.

Figure 12 is a plot of relative fractional frequency vs. running time, as obtained from printed period data obtained from the system of Fig. 10. A constant frequency offset has been subtracted to emphasize the nature of the frequency fluctuations. It is seen that there is a reasonably regular frequency modulation with a peak-to-peak fractional frequency excursion of about 8×10^{-14} and having a modulation period of approximately one half-hour. The explanation of this modulation is still not available. However, there are several possible explanations including a cycling temperature-servo affecting the tuning of the maser cavity.

The presence of this periodic frequency modulation will have a distinct effect upon a $\sigma(\tau)$ vs. τ plot of the experimental data. If the chosen time interval τ is equal to one half of the period of the frequency modulation, then the value of $\sigma(\tau)$ will be a local maximum. If the chosen time interval is equal to one period, then the value of $\sigma(\tau)$ will be a local minimum. The same data as were presented in Fig. 12 are given in Fig. 13 in the form of a $\sigma(\tau)$ vs. τ plot. A local maximum value of $\sigma(\tau)$ is observed at $\tau \approx 800$ seconds, and a local minimum value is observed at $\tau \approx 1800$ seconds. This behavior of $\sigma(\tau)$ is due to the periodic frequency modulation evident in Fig. 12.

In general, the data beyond $\tau \approx 2000$ seconds exhibit a flicker of frequency level [8], [4], [5] of about one part in 10^{14}. This leveling-off of $\sigma(\tau)$ for $\tau > 2000$ seconds is not due to the periodic frequency modulation shown in Fig. 12. Data beyond 2.5×10^{4} seconds have a very large uncertainty indicated by the arrows.

An additional method of obtaining data was used in order to avoid the effects of having in the measuring loop the quartz crystal oscillator, the two multiplier chains, and the two digital synthesizers which were shown in Fig. 10. A technique is described in Fig. 14 where both maser signals are separately converted to 20.405 MHz using a common local oscillator signal which is fed through 60 dB isolators to two separate mixers. Each maser signal is fed through a total of 120 dB of isolation using four 30 dB ferrite circulators optimized to operate at 1420 MHz and connected in series. The data are taken by obtaining the beat fre-

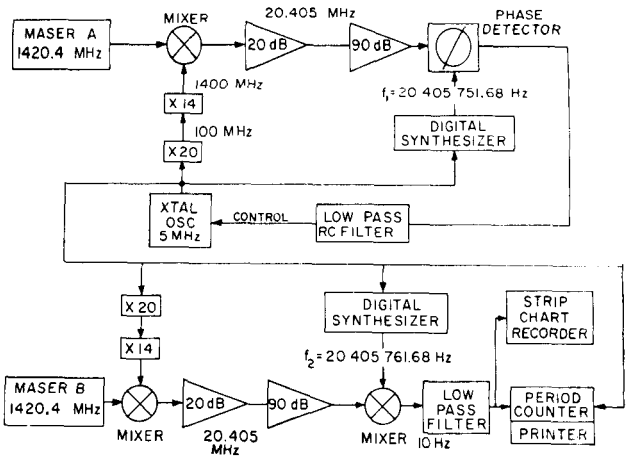

Fig. 10. Phase lock system for frequency comparison of H masers.

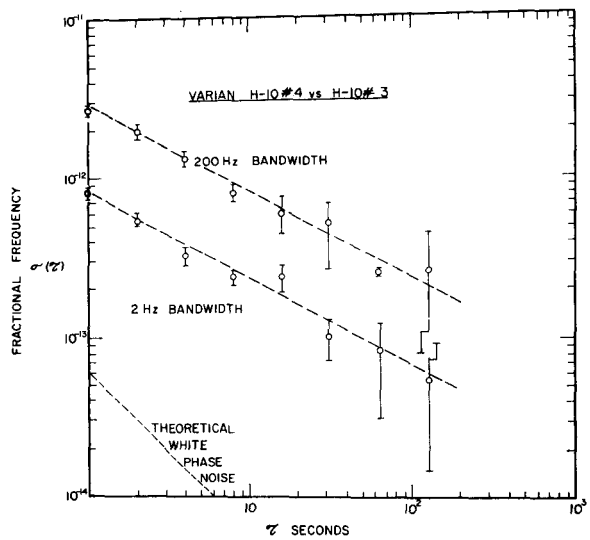

Fig. 11. Standard deviation of fractional frequency fluctuations between H masers as a function of sampling time and bandwidth, from automatically printed data.

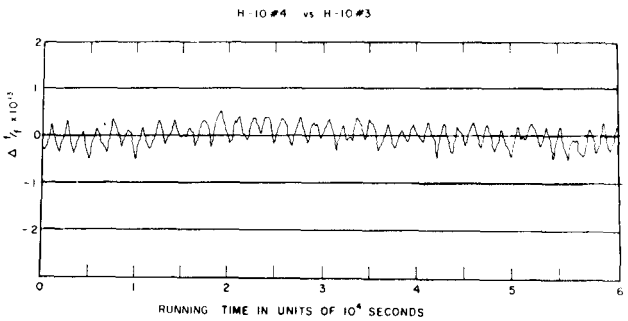

Fig. 12. Plot of relative fractional frequency fluctuations as a function of running time, Varian H-10 #4 vs. H-10 #3. A constant frequency offset has been subtracted to emphasize the nature of the frequency fluctuations.

463-560 O - 72 - 10

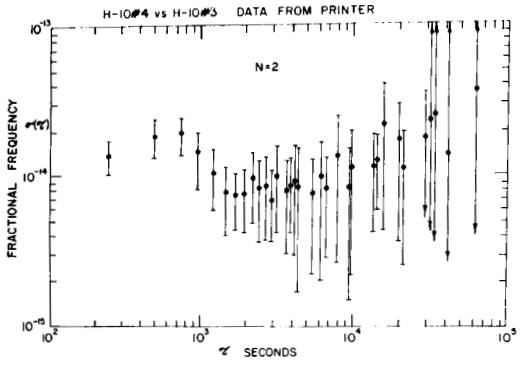

Fig. 13. Standard deviation of fractional frequency fluctuations between H masers as a function of sampling time, from automatically printed data.

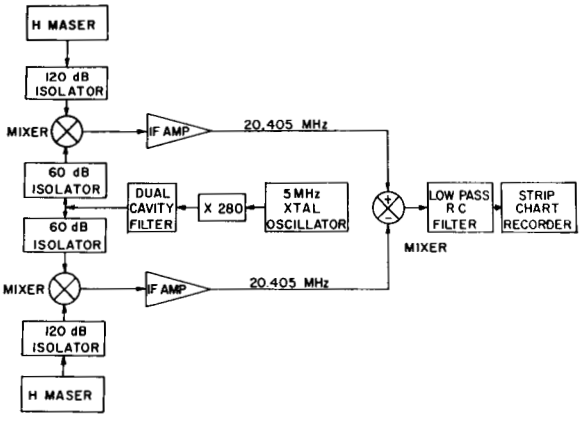

Fig. 14. An alternate system for comparison of H masers which avoids the use of phase lock electronics.

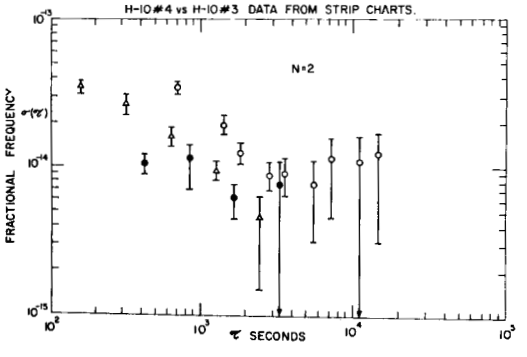

Fig. 15. Standard deviation of fractional frequency fluctuations between H masers as a function of sampling time, from strip chart data. The solid black points were obtained by the method of Fig. 14. All other points were obtained by the method of Fig. 10.

quency between the two 20.405 MHz intermediate frequency signals in a mixer and tracing the low-frequency beat directly on a strip chart recorder.

In Fig. 15 are σ vs. τ plots of chart data from one run (solid black points) using the method of Fig. 14 and of chart data from two runs (triangles and circles) using the method of Fig. 10. Analysis of the period data taken from charts was performed in the same manner as for the automatically printed data by using cards which

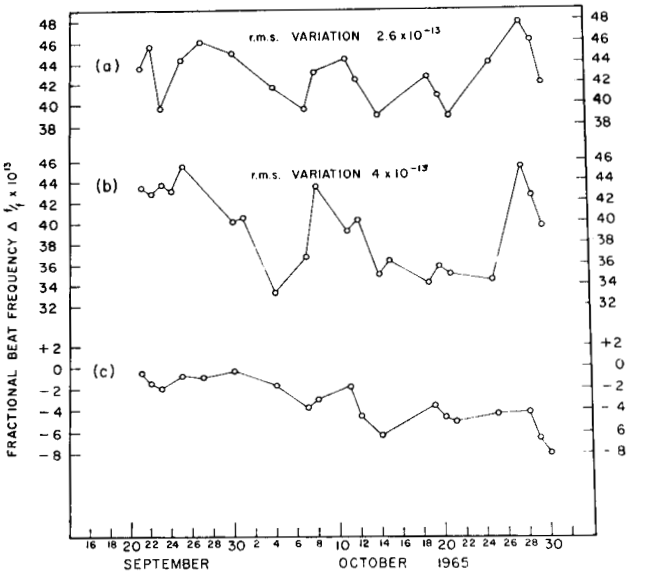

Fig. 16. (a) Fractional frequency difference of H masers as a function of time, corrected for cavity tuning effects in both masers. (b) Uncorrected fractional frequency difference of H masers as a function of time. (c) Cavity tuning effects in H-10 #4 as a function of time.

were manually punched using the same format as for the previously mentioned runs. By comparing Figs. 13 and 15, it is seen that the data taken with the method of Fig. 10 show the same general level of instability, whether from strip chart recordings or from automatically printed period measurements. In addition, it is seen that the data taken by the method of Fig. 14 show the same general level of instability as shown by the data taken by the method of Fig. 10. In Fig. 15 the white phase noise behavior evident between 10^2 and 10^3 seconds is due to random error in the estimation of phase from the strip chart recordings.

E. H Maser vs. H Maser: Long-Term Frequency Stability

Comparisons were made between the H masers for a period of five and one-half weeks. The masers were checked for cavity mistuning by varying the atomic hydrogen beam flux and monitoring the beat between the two masers. As the concentration of atomic hydrogen in the storage bulb is increased, the atomic resonance linewidth is broadened due to spin-spin exchange collisions between pairs of atoms in the maser storage bulb, and the magnitude of the cavity pulling, if any, is increased. When the cavity frequency is such that a variation in beam flux does not affect the output frequency, the maser is considered to be properly tuned. The tuning process is more fully described in Section III.A and in references [9]–[11].

Figure 16(b) shows, as a function of time, the hypothetical fractional beat frequency which would have been observed between the two masers if neither maser had been retuned during the run. The rms fractional frequency variation is 4.0×10^{-13}. Figure 16(a) shows the

corrected beat frequency which would have been measured had both masers been tuned. Here the rms variation is 2.6×10^{-13}, and the variations are due to unexplained processes which probably involve cavity pulling (see Section III.A).

Figure 16(c) shows a plot of the cavity pulling effect on H-10 #4. This was obtained by determining the frequency correction, using the tuning method described above, and plotting the correction in the output frequency as a function of time. There is evidence of a slow drift in the cavity tuning resulting in an output frequency drift of 7×10^{-13} in 50 days. This is probably due to a slow temperature variation, possibly due to a thermistor that had not been previously stabilized by aging in a temperature bath.

For these measurements there was an applied magnetic field offset in H-10 #3 of 37×10^{-13}. The average frequency of H-10 #3 was found to be 7 ± 2 parts in 10^{13} higher than the frequency of H-10 #4, after corrections for all known effects had been made. This discrepancy has since been reduced to less than ±2 parts in 10^{13} by renewal of the wall coating in the storage bulb of H-10 #3.

III. Accuracy of the Frequency Standards

A. Error Budget for Varian H-10 #4 Hydrogen Maser

Corrections are necessary to relate the output frequency of the hydrogen maser to the frequency of the hyperfine separation of the hydrogen atom under the least perturbed conditions. These conditions are [12]

1) zero collision rate,
2) zero absolute temperature,
3) zero magnetic field, and
4) zero cavity mistuning effect.

The effects from collisions are twofold, as there are collisions among the atoms as well as collisions with the walls of the storage bulb. In the latter case, while there is some question as to the actual mechanism of the frequency perturbation due to the wall collisions and also uncertainty as to the exact nature of the surface, it has been found that the Teflon[1] surfaces currently in use yield reproducible effects on the frequency of a maser. The wall shift is assumed to be proportional to the wall collision rate. By varying the wall collision rate through the use of different bulb dimensions, the value of the shift can be determined by extrapolation of the data to infinite bulb dimensions [12]. In the course of such measurements, a temperature dependence of the wall shift has been found. Recent measurements made by Varian Associates [3] indicate that for a $5\frac{1}{2}$ inch (14 cm) diameter spherical bulb, in the temperature range 27 to 45°C, the shift is $+2\times10^{-4}$ Hz per degree with an uncertainty of about 25 percent in the measurement. A semi-empirical relation to give the wall shift in the region of about 40°C can be written as

$$\delta f_w = K[1 + a(t - 40)]\frac{1}{D}, \qquad (3)$$

where D is the inside diameter of the bulb and t is the temperature of the bulb in degrees Celsius. The value of K determined by Varian Associates [13] from wall shift measurements at various temperatures is -0.208 ± 0.002 Hz inch (-0.528 ± 0.005 Hz cm), and the value of a is -5×10^{-3} per degree. The wall shift of the 6.87 inch (17.46 cm) diameter bulb of H-10 #4 is calculated using the above relation to be

$$\delta f_w(6.87 \text{ inch}, 45°\text{C}) = -0.0295 \pm 0.0006 \text{ Hz}.$$

The effect of collisions of pairs of hydrogen atoms has been studied by Bender [14], Crampton [15], Vanier [11], and others. A small frequency shift of about $\frac{1}{5}$ the spin exchange linewidth has been calculated for atomic hydrogen [14]. However, in the case of the atomic hydrogen maser, the collision-induced spin-spin exchange frequency shift depends upon the atomic resonance width in the same fashion as does the cavity pulling [16]; the tuning procedure involving the variation of the linewidth includes and cancels the effect of these collision shifts. The pertinent relation is [10][2]

$$f - f_H = \left[\left(\frac{f_c - f_H}{f_c}\right)Q - \left(\frac{13\sqrt{2}\,\bar{v}\hbar a_0^2}{32Q\mu_0^2\eta'}\right)\right]\Delta f_l, \qquad (4)$$

where

f is the output frequency of the maser,
f_H is the output frequency of the maser when tuned,
Δf_l is the linewidth of the atomic resonance,
f_c is the cavity resonance frequency,
Q is the loaded cavity resonance quality factor,
$\bar{v}$ is the mean speed of the H atoms in the storage bulb,
$\hbar$ is Planck's constant divided by 2π,
a_0 is the first Bohr orbit radius of hydrogen,
μ_0 is the Bohr magneton, and
η' is

$$\frac{\left(\int_b H_z dV_b\right)^2}{V_b\int_c H^2 dV_c},$$

where

V_c is the cavity volume,
V_b is the bulb volume,
H_z is the z component of the RF magnetic field in the cavity, and
H is the RF magnetic field in the cavity.

When the expression in the brackets is made zero (which is the "tuned" condition), the output frequency is independent of hydrogen pressure and is equal to f_H.

Second-order Doppler effect in the hydrogen maser due to thermal motion of the atoms is given by

[1] Du Pont's polytetrafluoroethylene.

[2] The second term of (4) as written in reference [10] contains an error of a factor of 2.

$$\Delta f_T = -f_H \frac{3kT}{2mc^2} = -1.9557 \times 10^{-4} T, \qquad (5)$$

where

k is Boltzmann's constant,
m is the mass of the hydrogen atom, and
c is the speed of light.

A change in the absolute temperature T of one degree K will give rise to a change in frequency of 1.38 parts in 10^{13}. Since the bulb temperature is known to better than ± 0.4°K, the probable error due to this cause is of the order of 5 parts in 10^{14}.

The value of the average of the square of the magnetic field H over the volume of the bulb affects the frequency of the oscillation in the amount $\Delta f_M \approx 2750\ \overline{H^2}$. It is possible to measure the average value of the magnetic field $\overline{H}$ in the bulb by inducing transitions among the $F=1$, $m_F=1$, 0, -1 states. The resonance is detected by observing a quenching or reduction in the maser output power. The transition resonant frequency (Zeeman frequency) is given by $f_z \approx 1.4 \times 10^{-6}\ \overline{H}$ and is normally measured with an uncertainty of a few Hertz. The uncertainty ΔH in $\overline{H}$ gives an uncertainty in Δf_M through the relation

$$\Delta(\Delta f_M) \approx 5500 H \Delta H.$$

Normally the maser is operated at a field of 0.5 milli-oersted making the total offset

$$\frac{\Delta f_M}{f} = +4.8 \times 10^{-13}.$$

Assuming a 10 Hz uncertainty in f_z, corresponding to 7 micro-oersteds, the uncertainty in $\Delta f/f$ due to magnetic effects is

$$\frac{\Delta(\Delta f_M)}{f} = \pm 1.3 \times 10^{-14}.$$

It will be noticed that there are two averaging methods involved in dealing with the magnetic field and that since $\overline{H^2}$ is always greater than or equal to $(\overline{H})^2$ there could be room for error in the determination of Δf_M. In this case, however, the possible error is not large since the effect of magnetic gradients would be detected by a large effect on the level of oscillation. An upper limit to the uncertainty due to these causes is estimated to be of the order of 5×10^{-14}.

The effect of cavity mistuning and the consequent "pulling" of the maser output frequency has already been discussed and the "tuned" condition has been described as the particular cavity resonance frequency chosen so that no output frequency shift results on changing the resonance linewidth. The sensitivity of this procedure depends in large part on the stability of the maser during the tuning process, the linewidth of the atomic resonance Δf_l, and the extent to which Δf_l can be broadened. There are several methods for broadening the line, such as by magnetic gradient quenching [17], by coherently or incoherently inducing transitions among the Zeeman levels [18], or by spin exchange line broadening. The last method, which has been used for some time, offers the greatest possible differential broadening of the line. If one assumes that the stability of the maser and its reference can be expressed by a maximum excursion $\pm \Delta f_b$ about the beat frequency, then the limits $\pm \Delta f/f$ within which the maser can be tuned will be given by

$$\frac{\Delta f}{f} = 2 \frac{\Delta f_b}{f} \frac{1}{\left[1 - \frac{\Delta f_{l_2}}{\Delta f_{l_1}}\right]}. \qquad (6)$$

Normally, the ratio $\Delta f_{l_2}/\Delta f_{l_1}$ lies between 1.5 and 2.0; taking this value as 1.5 and putting $\Delta f_b/f = 5 \times 10^{-14}$, then $\Delta f/f = 2 \times 10^{-13}$ is the maximum tuning error.

The error budget for the Varian hydrogen maser H-10 #4 is given in Table I.

TABLE I

CONTRIBUTIONS TO INACCURACY FOR VARIAN ATOMIC HYDROGEN MASER H-10 #4

Source	1σ estimate in parts in 10^{12}
Uncertainty in wall shift correction	± 0.42
Uncertainty in temperature for 2nd order Doppler shift	± 0.05
Uncertainty in C-field, $\overline{H_c}$	± 0.01
Use of $\overline{H_c}^2$ for $\overline{H_c^2}$	± 0.05
Cavity mistuning	± 0.2
Random measurement error (1 hour)	± 0.01
Total 1σ estimate of accuracy capability for Varian H maser H-10 #4 (square root of sum of squares)	$\pm 0.47 \times 10^{-12}$

B. Error Budget for NBS III Cesium Beam

A realistic error budget for the NBS III cesium beam standard was published [1] prior to the intercomparison described in this paper, giving ± 5.6 parts in 10^{12} as a 3σ estimate of accuracy uncertainty. However, the very stable signals available from the Varian hydrogen masers and recent theoretical work by Harrach [19] enabled a better determination to be made of some of the factors contributing to the uncertainty. Using one of the masers (H-10 #4) as an undisturbed reference frequency source, a set of evaluative experiments was performed on NBS III to study effects that result in systematic frequency offsets. These have been discussed in detail by Harrach and will only be summarized here.

The experiments consisted of measuring the radiation field dependence of the $(F=4, m_F=0) \leftrightarrow (F=3, m_F=0)$ cesium resonance frequency under varied conditions of beam direction through the apparatus, excitation spectrum, and magnetic C-field polarity and magnitude. From the analysis and interpretation of the experimental results, it was inferred that fractional corrections of -2.2×10^{-12} for dependence on radiation field intensity and of $+0.4 \times 10^{-12}$ for second order Doppler shift should be applied to the measured resonance frequencies. A more complicated correction was necessary

for beam direction dependence of the resonance frequency. The beam direction was reversed four different times by interchanging the oven and detector components, with the intention of evaluating and eliminating the effect of a cavity phase difference. It was found that the process of beam reversal slightly altered the phase difference magnitude, so that the necessary corrections varied from about 2 to 5 parts in 10^{12} for the different beam orientations, with an uncertainty of ± 0.8 part in 10^{12} for each determination.

The uncertainties in the fractional frequency corrections plus contributions from other sources, itemized in Table II, produce a 1σ estimate of accuracy capability of $\pm 1.1 \times 10^{-12}$ for NBS III. The term "accuracy capability" refers to the accuracy attained when a set of evaluative experiments is performed, as distinct from the accuracy of the standard when it is used for an extended period of time in an undisturbed, routine fashion. The term accuracy is used as defined in reference [1].

TABLE II

CONTRIBUTIONS TO INACCURACY FOR NBS III CESIUM BEAM FREQUENCY STANDARD

Source	1σ estimate in parts in 10^{12}
Uncertainty in average C-field magnitude, $\overline{H}_c$	± 0.1
Use of $\overline{H}_c^2$ for $\overline{H_c^2}$	± 0.03
Uncertainty in 1st and 2nd order Doppler shifts	± 0.1
Distortion from inequality of average C-field magnitudes in transition and drift regions, $\overline{H}_c(l) \neq \overline{H}_c(L)$	± 0.03
Uncertainty in C-field polarity-dependent shifts	± 0.1
Uncertainty in cavity phase difference (beam direction dependent shifts)	± 0.8
Cavity mistuning	± 0.03
Overlap of neighboring transitions	± 0.1
Uncertainty in power-dependent shifts	± 0.16
Random measurement error (1 hour)	± 0.16
2nd harmonic distortion of servo modulation	± 0.16
Miscellaneous servo system effects	± 0.5
Multiplier chain transient phase shifts	± 0.33
Total 1σ estimate of accuracy capability for NBS III (square root of sum of squares)	$\pm 1.1 \times 10^{-12}$

A comparison of the error budgets for the Varian maser (Table I) and the National Bureau of Standards cesium beam NBS III (Table II) shows that an apparatus-dependent effect is the major contributor to inaccuracy in each case. For the cesium beam, the frequency shift due to cavity phase difference is uncertain to $\pm 0.8 \times 10^{-12}$, or about 16 percent of its magnitude, while for the maser, the wall shift is considered known to $\pm 0.42 \times 10^{-12}$, or about two percent of its magnitude.

IV. HYDROGEN-CESIUM HYPERFINE FREQUENCIES RELATIONSHIP

An average value of the hyperfine separation of hydrogen in terms of that of cesium 133 can be obtained after suitable corrections are made for both the cesium device and the hydrogen maser.

A plot of $\Delta f/f$ vs. measurement number and date of measurement is shown in Fig. 3. These data include corrections made for magnetic field shift, power shift, phase shift, and second order Doppler shift of the cesium frequency. The data also include corrections for the effect of cavity mistuning in the hydrogen maser as determined by the procedure previously described. In order to relate the frequencies of the hyperfine separations of cesium and hydrogen to the synthesized frequencies, reference is made to the phase lock system in the upper half of Fig. 10. The varactor controlled 5 MHz quartz crystal oscillator is used to drive two frequency synthesizing systems. The first, which is simply a 280 times multiplier, provides about 2 milliwatts of power for the reference (local oscillator) input to the low noise (less than 10 dB noise figure) mixer where the maser signal is heterodyned to 20.405 MHz. This signal is amplified by about 110 dB and compared in phase with the output from the second synthesizing system driven by the 5 MHz oscillator. The latter system is a digital synthesizer which can be varied in increments of 0.01 Hz.

Analysis of the data of Fig. 3 gives a mean fractional frequency offset of 0.1044×10^{-10} with a root mean square deviation, σ, of 7.4×10^{-13} for 62 points. This represents a frequency offset of $0.1044 \times 10^{-10} \times 1420.405 \times 10^6 = 0.0148$ Hz. Further corrections are made to bring the hydrogen frequency to the ideal conditions discussed in Section III.A. The fully corrected hydrogen maser frequency is obtained in the following way:

Synthesized frequency	1 420 405 751.6800 Hz
Offset frequency from Cs comparisons	+0.0148
Correction for wall shift	+0.0295
Correction for magnetic field	−0.0001
Correction for second order Doppler effect	+0.0622
	1 420 405 751.7864 Hz

The 1σ accuracy estimate for the measurement is obtained by combining the error budgets of Tables I and II, giving an over-all accuracy of 1.2 parts in 10^{12}. In terms of the frequency of the Cs^{133} hyperfine transition $(F=4,\ m_F=0) \leftrightarrow (F=3,\ m_F=0)$, defined [20] as 9 192 631 770.0000 Hz, the frequency of the atomic hydrogen hyperfine transition $(F=1,\ m_F=0) \leftrightarrow (F=0,\ m_F=0)$ is

$$\nu_H = 1\ 420\ 405\ 751.7864 \pm 0.0017 \text{ Hz}.$$

Measurements previously made for the hydrogen frequency in terms of cesium with the wall-shift corrections then used are given in Table III. The last number in the table is the preliminary value reported earlier after a partial analysis of the data. The reduction of the standard error from 0.0046 Hz to 0.0017 Hz was made possible through improved measurements by Varian Associates [13], [3] of the wall shift and its temperature dependence.

From the frequency comparison data in Table III, it is seen that the frequency of the NBS III cesium standard differs from the frequency of the Laboratoire Suisse de Recherches Horologères, Neuchâtel, Switzerland (LSRH) cesium standard by $-7 \times 10^{-13} \pm 1.2 \times 10^{-11}$. This is the smallest discrepancy reported to date between these two national standards [25].

TABLE III

MEASUREMENTS PREVIOUSLY MADE FOR THE HYDROGEN FREQUENCY IN TERMS OF CESIUM

Experiment	Bulb diameter, inches	Wall shift correction, Hz	Second order Doppler correction, Hz and temperature	Corrected frequencies 1 420 405 751. Hz plus values given below
Varian-Naval Observatory 1963 [21]	6 ± 0.1	0.039 ± 0.008	0.06 40°C	0.827 ± 0.02
Harvard-Naval Observatory 1963 [15]	6.03	0.0298 ± 0.003	0.0602 35°C	0.800 ± 0.028
Varian-HP 1964 [22]	5.5 ± 0.1	0.040 ± 0.0023	0.0622 45°C	0.778 ± 0.016
Varian-LSRH 1964 [23]	5.5 ± 0.1	0.040 ± 0.0023	0.0622 45°C	0.785 ± 0.016
NASA-GSFC 1965 [24]	5.4	0.043 ± 0.0023	0.062 45°C	0.781 ± 0.016
NBS-Varian-HP 1966 [2]	6.87	0.0320 ± 0.0043	0.0622 45°C	0.7860 ± 0.0046

V. DISCUSSION

The main purposes of this paper have been to report the data obtained from a set of measurements, to offer some measure of the state-of-the-art of time and frequency control, and to report an improved measurement of the frequency of the hydrogen hyperfine separation. Since the arts of frequency standard design and instrumentation for making measurements are still progressing rapidly, one can conclude that these measurements will be followed by further and better measurements.

Long term measurements, yielding average frequencies between standards of different origin, have shown excellent agreement between the Hewlett-Packard 5060A instrument and the NBS III cesium beam designated as the United States Frequency Standard. The relationship between the statistics of the two devices is reasonably well understood, and the discrepancy of the frequency averages of the two instruments is within their accuracy specification.

At present, the resolution of the measurements is limited by random noise of the apparatus. Thus far, no *unexplained* systematic effects are observed. Future designs of beam standards with stronger beam flux and perhaps narrower linewidths will result in the obtaining of better data on systematic frequency shifts of both the beam tube and the frequency lock electronics.

In the case of measurements between two hydrogen masers with phase lock systems, the instabilities introduced by the phase lock-synthesizer system and the measuring system are not as well understood. The levels of instability in the 1 to 100 second sampling time range, though lower than those observed for the cesium devices, cannot be accounted for by the presence of white additive noise of the first mixer in each receiving system. The phase fluctuations due to the frequency multipliers, the digital synthesizers, and the period counting system as well as those of the masers themselves must still be subjected to further study in the 1 to 100 second range. While the present data will provide a measure of the possible performance of such a system, there is no doubt that this preliminary effort can be improved by more careful engineering.

A comparison of various measurements having sampling times ranging from 10^2 to 10^4 seconds is given in Fig. 17. Here the data from the hp 5060A, NBS III, and H-10 #4 are given together. The value of σ for H-10 #4 is obtained by dividing the value of σ from H-10 #4 vs. H-10 #3 by the square root of 2. Both cesium instruments exhibit the $\tau^{-1/2}$ behavior as discussed previously. The maser data show systematic variations at the 10^{-14} level, which are probably due to cavity detuning effects that are largely thermal in origin. By incorporating automatic self-tuning methods, using the spin exchange line broadening method described earlier, it is possible that the maser stability can be kept to better than 5×10^{-14} for sampling times greater than 10^4 seconds.

The accuracy of the hydrogen-cesium ratio is limited by the characteristics of the devices used to extract the information from the two respective atoms. The maser, in confining the atoms in a bulb, subjects them to wall interactions. These must be measured as a function of reciprocal bulb diameter $1/D$ and extrapolated to zero in $1/D$. In the case of the beam devices, the frequency resolution increases with increase of beam flux and inverse linewidth. Flux effects favor the construction of a short apparatus, and linewidth effects favor the construction of a long apparatus. It is important to control the intensity, spectral purity, and phase of the radio frequency excitation applied to the beam.

Further work in beam devices and masers will undoubtedly improve the accuracy of the hydrogen-cesium frequency ratio. The state-of-the-art has undergone considerable improvements, and the absolute accuracy of these devices is now at the 10^{-12} level, being 1.1 parts in 10^{12} for a cesium beam and 0.47 part in 10^{12} for a hydrogen maser. Frequency and time measurements using atomic standards are now, more than ever, the most accurate and precise physical measurements which can be made.

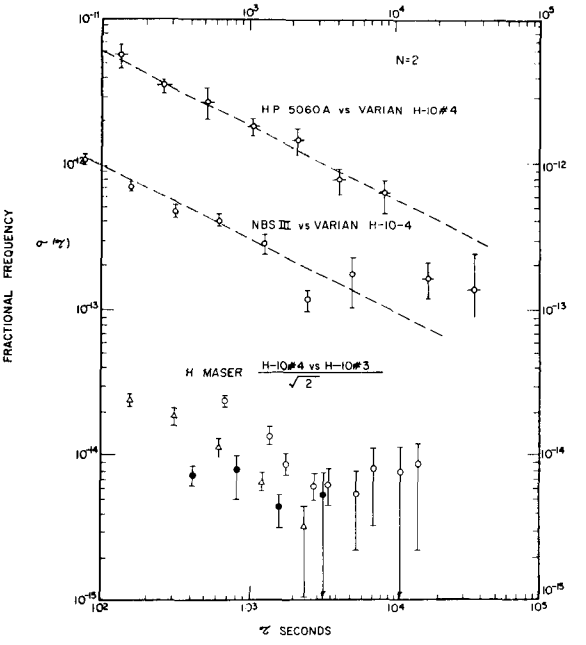

Fig. 17. Summary of frequency stability data as a function of sampling time τ.

Appendix

The variance σ^2 of the frequency fluctuations of a frequency standard is a useful parameter in determining quality factors for the unit. When finite data sampling is considered, this parameter is dependent on four independent variables of the analysis, i.e., the sample time τ, the period of sampling T, the number of samples taken N, and the system bandwidth ω_B.

For the experiments reported in this paper, T/τ and ω_B were constant for any given experiment, but they were not necessarily the same from one experiment to the next. For all σ versus τ plots where T/τ was a significant parameter, it was approximately equal to unity. N was always chosen equal to 2 and an ensemble average taken to determine a good statistical measure of the variance. The confidence limits are calculated on the assumption that each particular computed variance is uncorrelated with any other. A computer program based on the above method was used to analyze the data obtained in these measurements.

The variance is a function of the spectral density of the phase fluctuations of the system. By proper control of the above four analysis variables, it is possible to determine the frequency dependence of the spectral density of the phase fluctuations $S_\phi(\omega)$, as follows. If $\langle\sigma^2(\tau, T, N, \omega_B)\rangle = k\tau^\mu$, with k and μ constant over a sufficiently large range of τ, with $-2<\mu<+2$, then

$$S_\phi(\omega) = h\,|\,\omega\,|^\alpha, \tag{7}$$

where $\alpha=-\mu-3$, provided that N, T/τ, and ω_B are kept constant and that $\tau \gg 1/\omega_B$. If $\mu=-2$, a degeneracy of α occurs, and one may then use the dependence of the variance on the bandwidth,

$$\langle\sigma^2(\tau, T, N, \omega_B)\rangle = \frac{k}{\tau^2}\,|\,\omega_B\,|^{\alpha+1}, \qquad \alpha > -1,$$

for determining the frequency dependence of the spectral density. For a detailed treatment of the above see Allan [4].

References

[1] R. E. Beehler, R. C. Mockler, and J. M. Richardson, "Cesium beam atomic time and frequency standards," *Metrologia*, vol. 1, pp. 114–131, July 1965.

[2] R. Beehler et al., "An intercomparison of atomic standards," *Proc. IEEE (Letters)*, vol. 54, pp. 301–302, February 1966.

[3] R. Vessot et al., "A direct frequency comparison of hydrogen masers in separate laboratories by concurrent monitoring of Loran C signals," *Proc. IEEE (Letters)*, vol. 54, pp. 303–304, February 1966.

[4] D. W. Allan, "Statistics of atomic frequency standards," *Proc. IEEE*, vol. 54, pp. 221–230, February 1966.

[5] L. S. Cutler and C. L. Searle, "Some aspects of the theory and measurement of frequency fluctuations in frequency standards," *Proc. IEEE*, vol. 54, pp. 136–154, February 1966.

[6] R. E. Beehler et al., "A comparison of direct and servo methods for utilizing cesium beam resonators as frequency standards," *IRE Trans. on Instrumentation*, vol. I-11, pp. 231–238, December 1962.

[7] R. Vessot, L. Mueller, and J. Vanier, "The specification of oscillator characteristics from measurements made in the frequency domain," *Proc. IEEE*, vol. 54, pp. 199–207, February 1966.

[8] J. A. Barnes, "Atomic timekeeping and the statistics of precision signal generators," *Proc. IEEE*, vol. 54, pp. 207–220, February 1966.

[9] D. Kleppner et al., "Hydrogen-maser principles and techniques," *Phys. Rev.*, vol. 138, pp. A972–A983, May 17, 1965.

[10] J. Vanier, H. E. Peters, and R. F. C. Vessot, "Exchange collisions, wall interactions, and resettability of the hydrogen maser," *IEEE Trans. on Instrumentation and Measurement*, vol. IM-13, pp. 185–188, December 1964.

[11] J. Vanier and R. F. C. Vessot, "Cavity tuning and pressure dependence of frequency in the hydrogen maser," *Appl. Phys. Lett.*, vol. 4, pp. 122–123, April 1, 1964.

[12] D. Kleppner, H. M. Goldenberg, and N. F. Ramsey, "Theory of the hydrogen maser," *Phys. Rev.*, vol. 126, pp. 603–615, April 15, 1962.

[13] J. Vanier (to be published).

[14] P. L. Bender, "Effect of hydrogen-hydrogen exchange collisions," *Phys. Rev.*, vol. 132, pp. 2154–2158, December 1, 1963.

[15] S. B. Crampton, D. Kleppner, and N. F. Ramsey, "Hyperfine separation of ground-state atomic hydrogen," *Phys. Rev. Lett.*, vol. 11, pp. 338–340, October 1, 1963.

[16] S. B. Crampton, "Hyperfine and spin exchange experiments with the atomic hydrogen maser," Ph.D. dissertation, Harvard University, Cambridge, Mass., 1964, unpublished.

[17] J. Vanier and R. Vessot, "Relaxation in the level $F=1$ of the ground state of hydrogen: application to the hydrogen maser," *IEEE J. of Quantum Electronics*, vol. QE-2, pp. 391–398, September 1966.

[18] H. G. Andresen and E. Pannaci, "Servo-controlled hydrogen maser cavity tuning," *Proc. 20th Annual Symp. on Frequency Control*, 1966, to be published.

[19] R. J. Harrach, "Some accuracy limiting effects in an atomic beam frequency standard," *Proc. 20th Annual Symp. on Frequency Control*, 1966, to be published, and "Radiation field dependent frequency shifts of atomic beam resonances," to be published in *J. Appl. Phys.*

[20] *Comptes Rendus des Séances de la Douzième Conférence Générale des Poids*, Paris, France, October 6–13, 1964.

[21] W. Markowitz et al., "Report on the frequency of hydrogen," *Frequency*, vol. 1, p. 46, July–August 1963.

[22] H. E. Peter, et al., "Hydrogen maser and cesium beam tube frequency standards comparison," *Appl. Phys. Lett.*, vol. 6, pp. 34–35, January 15, 1965.

[23] H. E. Peter and P. Kartaschoff, "Hydrogen maser frequency comparison with Swiss cesium atomic beam standard," *Appl. Phys. Lett.*, vol. 6, pp. 35–36, January 15, 1965.

[24] E. H. Johnson and T. E. McGunigal, "Hydrogen maser frequency comparison with a cesium standard," NASA Technical Note TN D-3292, April 1966. The title and publication date of this technical note were not given correctly in reference [7] of Beehler et al. [2].

[25] J. Bonanomi et al., "A comparison of the TA_1 and the NBS-A atomic time scales," *Proc IEEE (Correspondence)*, vol. 52, p. 439, April 1964.

Some Accuracy Limiting Effects in an Atomic Beam Frequency Standard

Robert J. Harrach

National Bureau of Standards, Boulder, Colorado

Abstract

The accurate resonance frequency of the transition $(F, M_F) = (4, 0) \leftrightarrow (3, 0)$ in the ground state of cesium-133 is expressed in the form of an operational equation for an atomic beam spectrometer. Emphasized are the terms in this equation which correct for the beam direction dependence and radiation field dependence of measured resonance frequencies:

$$\tfrac{1}{2}\{\nu_{res_i}(P_1) + \nu_{res_j}(P_1)\} - \tfrac{1}{2}(S_i + S_j) P_1 ,$$

where i and j refer to opposite beam directions through the apparatus, P_1 is the microwave power exciting the transition, and S_i and S_j are the rates of linear frequency shift. The results of a detailed theoretical analysis are given which specify the contributions to these terms by various apparatus and fundamental shift-inducing effects.

This approach to accuracy specification is applied to the United States frequency standard, a National Bureau of Standards atomic beam machine designated NBS III, through a set of experiments using an atomic hydrogen maser as a highly stable reference frequency source. The corrections determined are -3.2×10^{-12} for beam direction dependence, -2.2×10^{-12} for power dependence, and $+0.4 \times 10^{-12}$ for second-order Doppler shift. The uncertainties in these corrections and contributions from other sources give a present 1σ estimate of accuracy capability of $\pm 1.1 \times 10^{-12}$ for NBS III. This figure should be reducible by one order of magnitude through efforts to eliminate systematic errors in the measurements of ν_{res_i} and ν_{res_j}

Up to the present time the lowest inaccuracy figure that has been quoted[1] for any frequency standard is $\pm 1.1 \times 10^{-12}$ as a single standard deviation (1σ) estimate for a National Bureau of Standards cesium beam machine designated NBS III. Attempts to improve on this value are resisted by the difficulty in identifying and making corrections for resonance frequency shifts induced by a variety of effects.

Intrinsic or fundamantal effects originate from the motion of atoms (Doppler effect), the structure of atoms (effect of neighboring energy levels), and properties of the transition-inducing radiation field (Bloch-Siegert and Stark effects). But the frequency shifts these generate are relatively feeble. Other effects are present because the atomic beam apparatus falls short of ideality. As examples, the phases of the pair of separated radiation fields are not exactly equal, the radiation fields are not strictly monochromatic, and the static magnetic c-field is not precisely uniform. The frequency shifts due to such "apparatus effects" establish the present limits of accuracy.

In this paper we consider a set of high precision experiments which enable identification of the particular effects which are most significant in limiting the accuracy of the NBS III beam machine. This work is one segment of a detailed study of atomic beam resonance frequency shifts.[2]

The standard of frequency is defined by the transition $(F, M_F) = (4, 0) \leftrightarrow (3, 0)$ in the ground state of cesium-133, for which the unshifted resonance frequency (Bohr frequency) is

$$\nu_B(H_c) \simeq \nu_B(0) + (426.4) H_c^2 , \qquad (1)$$

where H_c is the magnitude of a weak external magnetic field (in oersteds), and $\nu_B(0) \equiv 9,192,631,770$ cps. In Table 1 a summary is given of some of the resonance frequency shifts which are calculated for this transition. The notation $(\alpha, \ell, L, \nu_0, \bar{\nu}_0)$ used in the Table is the same as that used by Ramsey.[3] In particular, $\bar{\nu}_0$ and ν_0 are the Bohr frequencies corresponding to the average square c-field magnitudes in the drift region and transition regions, respectively.

The predicted frequency shifts depend on the level of microwave input power (P) exciting the transition, and on the beam direction through the apparatus (via the phase difference δ). This suggests the utility of relating the accurate frequency, $\nu_B(0)$, and measured resonance frequencies with an operational equation:

$$\nu_B(0) = \tfrac{1}{2}\{\nu_{res_i}(P_1, \bar{H}_{c_1}) + \nu_{res_j}(P_1, \bar{H}_{c_1})\} - (426.4)\bar{H}^2_{c_1} - (426.4)(\overline{H^2}_{c_1} - \bar{H}^2_{c_1})$$

$$- \tfrac{1}{2}(S_i + S_j)P_1 - \delta\nu_{Doppler} - \delta\nu_{c\text{-}field} - \cdots\cdots . \qquad (2)$$

The subscripts i and j refer to opposite beam directions through the apparatus, P_1 is the microwave input power which excites the transition, and $\bar{H}_{c_1}$ is the average c-field magnitude. The first term is just the mean frequency for opposite beam directions, and is aimed at eliminating the effect of phase difference. The second term corrects to zero magnetic field, and the third term adjusts for the use of $\bar{H}^2_c$ in the c-field calibration, rather than H^2_c. The fourth term corrects for effects which give a linear power-dependent shift that vanishes in the limit of zero excitation intensity and is independent of beam direction. (This includes four items in Table 1.) S_i and S_j are experimentally determined slopes (in cps per milliwatt, say) of a linear component of the observed frequency shifts. The fifth term subtracts out the second-order Doppler shift (given by Fig. 3), and the sixth term takes account of the distortion of the resonance due to inequality of the c-field magnitudes in the transition and drift regions (Fig. 2). The relation should be continued to include other contributions[6] which are not explicitly treated here, e. g., physical overlap, cavity pulling, multiplier chain transient phase shifts, and various servo system effects.

The set of experiments with the NBS III beam spectrometer were performed using an atomic hydrogen maser from Varian Associates as a highly stable reference frequency source.[1] The dependence of the $(4, 0) \longleftrightarrow (3, 0)$ resonance frequency on radiation field intensity was measured, under varied conditions of beam direction through the apparatus, c-field magnitude, and excitation spectrum.

The power-dependent frequency shifts observed for three successive reversals of the beam direction are shown in Fig. 4. Over the range of excitation intensities considered the shifts are linear, and data for opposite beam directions show a slightly different slope and a relative frequency offset. The important features of the data are the slopes, zero power (extrapolated) intercepts, and the average values of these quantities for

opposite beam directions. These are summarized in Table 2.

The interpretation of these results is found in terms of apparatus, rather than fundamental, effects. Evaluating the very small expected shifts due to the latter, using $\ell = 1.02$cm, $L = 366$ cm, and $\alpha = 2.3 \times 10^4$ cm/sec in Table 1, we have:

neighboring levels effect: $\delta\nu/\bar{\nu}_0 \simeq + (7.6) \times 10^{-16} \tan^2(\eta) P/P_0$

Bloch-Siegert effect: $\delta\nu/\bar{\nu}_0 \simeq + (3.8) \times 10^{-16} P/P_0$

Stark effect: $\delta\nu/\bar{\nu}_0 \simeq - (1.5) \times 10^{-18} P/P_0$

2nd-order Doppler effect: $(\delta\nu/\bar{\nu}_0)_{P_0} = - 4.4 \times 10^{-13}$.

The observed shifts are roughly $+ 3 \times 10^{-12} P/P_0$, with $P_0 \simeq 6.0$mW.

The relative displacement of the resonance frequency for opposite beam directions is attributed to a phase difference between the radiation fields. If the beam experiences a phase difference δ_i for one direction and δ_j for the other, the frequency difference is $\Delta\nu = \alpha(\delta_i - \delta_j) / 2\pi L$. For $\delta_j = - \delta_i$, the successive beam reversals would give a reproducible frequency difference. This was clearly not the case. For either beam direction the phase difference value was of order 10^{-3} radian, but in reversing the beam direction its precise magnitude was changed. It is felt that this irreproducibility is a consequence of the system being exposed to atmospheric pressure in order to interchange the oven and detector. Contaminants in the cavity ends which can contribute to a phase difference value then interact with air and moisture, resulting in a modified value. This circumstance can be avoided by designing the system so that it may be kept under vacuum while the oven-detector interchange is made. Both an oven and detector could be situated at each end of the apparatus, with adjustments for positioning the components so that either combination of oven and detector could be used.

The average rate of frequency shift for opposite beam directions was reproducible, with the magnitude

$$\frac{1}{2\bar{\nu}_o} (S_i + S_j) \simeq + 5.6 \times 10^{-13}/\text{mW}. \qquad (3)$$

Inbalance between pairs of sidebands in the excitation spectrum provides an interpretation of this result. A spectrum analysis revealed that the brightest sidebands were 44 db below the primary intensity at ± 60 cps and ± 120 cps

away from the primary frequency. Each pair was balanced to within an uncertainty of 2 db. If the sideband at - 60 cps was 1 to 2 db above that at + 60 cps, then the expression in Table 1 predicts a fractional shift of + 2.0 to + 4.5 parts in 10^{13} per milliwatt. Similarly, this inbalance in the ± 120 cps components would give an additional contribution half as large. When the excitation spectrum was changed, by using a different multiplier chain, the rate of shift was altered by more than a factor of two, confirming the interpretation as a spectrum effect.

The small beam direction-dependent contribution to the rate of shift,

$$\frac{1}{2\bar{\nu}_0}(S_i - S_j) \simeq 1.0 \times 10^{-13}/\text{mW}, \qquad (4)$$

is not satisfactorily understood. Phase difference is capable of making such a contribution, but the sign is wrong to account for the observations. A possible explanation is found in terms of a first-order Doppler shift due to leakage radiation from the cavity end slots into the drift region, but this has not been convincingly demonstrated.

Supplementary experiments indicated that the power-dependence of the resonance is unaffected by increasing the c-field magnitude above the 1/20 0e operating level, and by reversing c-field polarity. The displacements in the resonance frequency which accompanied performance of these operations were consistent with expectations based on the quadratic c-field dependence. For example, a residual average field component, $\bar{H}_0(x)$, along the direction of the applied c-field, $\bar{H}_a(x)$, causes the resultant c-field magnitude to change by approximately $2\bar{H}_o(x)$ when the polarity of the applied field is reversed. This shifts the (4, 0) $\leftrightarrow$ (3, 0) resonance frequency by about $(426.4)4\bar{H}_a(x)\bar{H}_o(x)$ cps, and the shift is removed when the applied field component is adjusted to restore the net c-field to its original value. From these supplementary experiments, we conclude that physical overlap of neighboring resonances, the Millman effect,[3] and the c-field difference quantity, $\bar{H}_c(\ell) - \bar{H}_c(L)$, make negligible frequency shift contributions.

The foregoing analysis determines the frequency corrections that should be applied to the NBS III standard, and helps to establish the limits of accuracy uncertainty. The device is normally operated with an input

power of 4.0 milliwatts, a c-field magnitude of 0.0484 0e, and with a beam direction corresponding to experiments (2) and (4) in Table 2. The correction for power-dependence, using equation (3) and $P_1 = 4.0$ mW, is then

$$-\frac{1}{2\bar{\nu}_o}(S_i + S_j)P_1 \simeq -2.2 \times 10^{-12}.$$

A second-order Doppler shift was too small to be resolved in the experiments, but a correction can be made on theoretical grounds. Using Fig. 3 for $P_1 = 2P_o/3$, and $\alpha = 2.3 \times 10^4$ cm/sec, we have

$$-\frac{1}{\bar{\nu}_o}(\delta\nu_{\text{Doppler}})\,P_1 \simeq +0.4 \times 10^{-12}.$$

Similarly, the shift due to c-field distortion was beyond experimental resolution. Calibrated line shape traces of the field-sensitive transitions, $(4,\pm 1) \leftrightarrow (3,\pm 1)$, showed that $|\bar{H}_c(\ell) - \bar{H}_c(L)| < 2 \times 10^{-3}$ 0e, so a theoretical upper limit for the correction magnitude is calculated, using the expression in Table 1 with $H_{c_1} = 0.0484$ 0e, to be less than 3×10^{-14}.

The most important, but most poorly defined correction is that for beam direction-dependence. A reasonable approach is to make this correction with respect to the average of the three determinations of $\frac{1}{2}(\nu_{\text{res}_i} + \nu_{\text{res}_j})$. Then, for example, if the beam has the orientation of experiment 2 in Table 2, the appropriate correction is -3.2×10^{-12}, with a maximum uncertainty estimated from the data to be no more than $\bullet\ 2.4 \times 10^{-12}$ (three times the rms deviation). However, if the beam machine is left undisturbed in a given orientation for long periods of time, this phase difference correction whould be considered to be much more uncertain.

The assessment of total accuracy uncertainty is made by considering the individual uncertainties in the terms that make up equation (2). An itemized account for the NBS III standard, including a discussion of the way that individual contributions should be combined to arrive at a total estimate, has been given by Beehler, et al.[6] A similar tabulation for NBS III, taking account of the results of this paper, is given in Table 3. The single standard deviation estimate of accuracy capability is approximately $\pm 1.1 \times 10^{-12}$.

The designation "accuracy capability" is meant to imply the limits of uncertainty when a set of evaluative experiments are performed, as distinct from undisturbed, routine operation of the standard.

The increasing availability of frequency devices (atomic beams and masers) capable of stabilities of a few parts in 10^{13} over a long duration (100 hours or more) gives promise of improved accuracies. A systematic experimental investigation using a reference frequency source of this high precision has not been carried out to evaluate most of the uncertainty factors in Table 3. Especially in the cases of miscellaneous servo system effects, multiplier chain phase shifts, and the first-order Doppler effect, it is lack of information which makes the estimated uncertainties as large as they are. These experiments, coupled with efforts to reduce systematic errors in the measurements of ν_{res_i} and ν_{res_j} (for which the installation of the alternate oven-detector system mentioned earlier would be a starting point) can reasonably be expected to improve the NBS III accuracy capability figure by an order of magnitude.

ACKNOWLEDGMENTS

I wish to express my gratitude to R. E. Beehler for many helpful discussions during the course of this work. The experiments which have been described were performed by him, D. J. Glaze, and C. S. Snider.

REFERENCES

(1) R. Beehler, D. Halford, R. Harrach, D. Allan, D. Glaze, C. Snider, J. Barnes, R. Vessot, H. Peters, J. Vanier, L. Cutler, L. Bodily, "An intercomparison of atomic standards, "Proc. IEEE (Letter), 54, 301-302, February 1966.

(2) R. Harrach, "Radiation field dependent frequency shifts of atomic beam resonances," to be published.

(3) N. Ramsey, MOLECULAR BEAMS. London, England: Oxford University Press, 1956.

(4) N. Ramsey, "Shapes of molecular beam resonances," in RECENT RESEARCH IN MOLECULAR BEAMS (I. Estermann, ed.). New York: Academic Press, 1959.

(5) R. Haun, Jr. and J. Zacharias, "Stark effect on Cs-133 hyperfine structure, "Phys. Rev., 107, 107-109, July 1957.

(6) R. Beehler, R. Mockler, and J. Richardson, "Cesium beam atomic time and frequency standards," Metrologia, 1, 114-131, July 1965.

TABLE I

approximate shift, ($\nu_{res} - \bar{\nu}_o$), at optimum excitation intensity, in cps.	Effect	Power-dependence	Reference
$-\alpha\delta/2\pi L$	Phase difference, $\delta_2 - \delta_1 = \delta$ (rad) where 1 and 2 refer to first and second radiation fields	Fig. 1	(2)
$+ \nu(\nu_o - \bar{\nu}_o)/L$ $+ \frac{2\ell}{L}(426.4)\bar{H}_c(i)\{\bar{H}_c(i) - \bar{H}_c(L)\}$	c-field non-uniformity, which makes the average field magnitude in the drift region, $\bar{H}_c(L)$, differ from the average magnitude in the transition regions, $\bar{H}_c(i)$	Fig. 2	(2)
$+ \frac{\int(0.045)\alpha^2\nu_i}{i\,\ell L(\nu_o-\nu_i)}$	Sidebands in an impure excitation spectrum. The ratio of the intensity of the sideband at frequency ν_i to the primary intensity at $\bar{\nu}_o$ is $\nu_i \pm P_{sb}/P$. The optimum primary intensity is P_o(in mW, say).	linear; take times P/P_o	(4),(2)
$- \bar{\nu}_o 3\alpha^2/4c^2$	Second-order Doppler effect; c = speed of light	Fig. 3	(2)
$+ \frac{(0.09)\alpha^2}{4\ell L\bar{\nu}_o}$	Bloch-Siegert effect	linear; take times P/P_o	(3)
$- \frac{\ell}{L}(2.29)10^{-10}\overline{E_o^2}$	Stark effect; $\overline{E_o^2}$ is the mean square electric field component when the radiation field is at optimum intensity	linear; take times P/P_o	(5)
$+ \frac{(0.045)\alpha^2\tan^2(\eta)}{\ell L\bar{\nu}_o}$	Neighboring levels; η is the angle between the oscillating radiation field and the static c-field	linear; take times P/P_o	(4),(2)

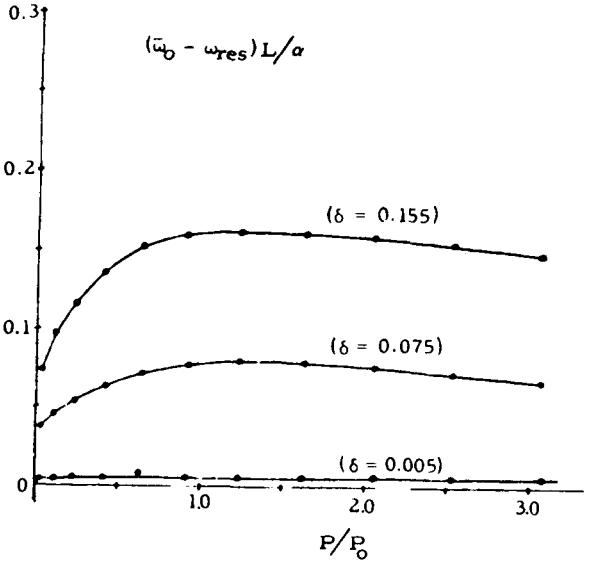

Fig. 1 Theoretical frequency shift induced by a small phase difference, δ(radians), as a function of excitation intensity.

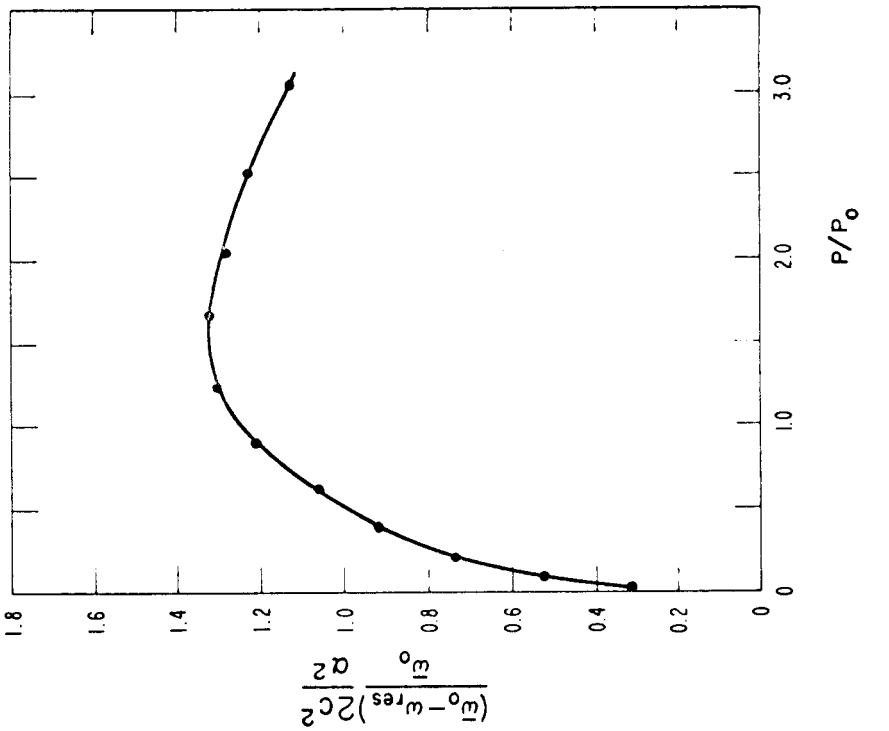

Fig. 3 Theoretical frequency shift due to a second-order Doppler effect, as a function of excitation intensity

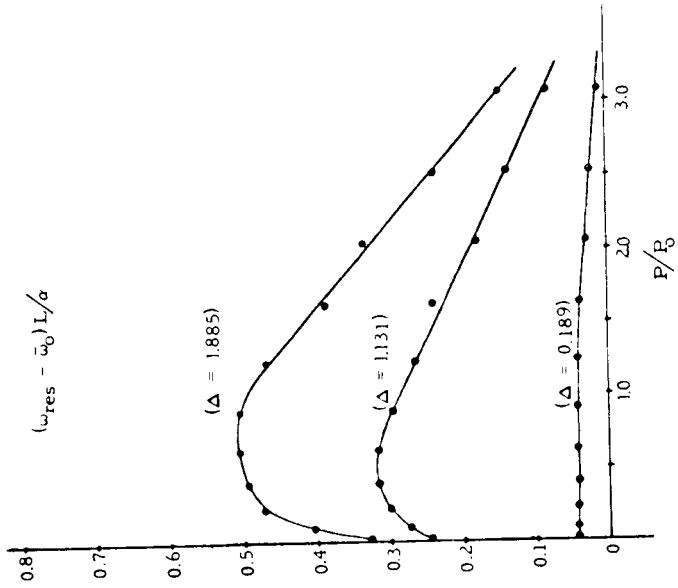

Fig. 2 Theoretical frequency shift induced by c-field non-uniformity which makes $\nu_o \neq \bar{\nu}_o$. The parameter labeling the curves is $\ell = 8\pi(\nu_o - \bar{\nu}_o)/\alpha$.

463-560 O - 72 - 11

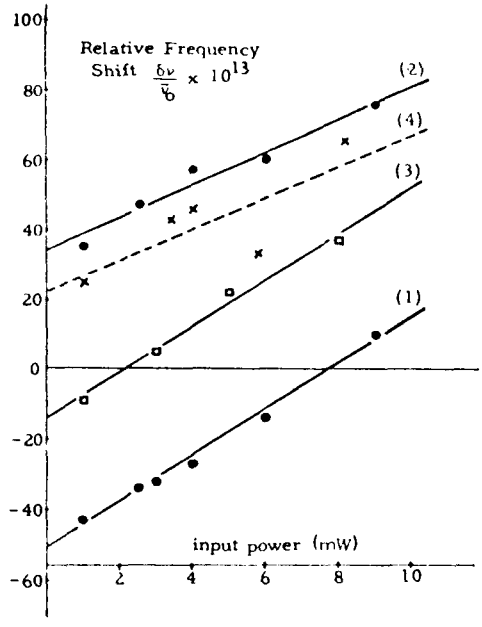

Fig. 4 Power-dependent frequency shifts of the (4,0)←→(3,0) transition in the NBS III atomic beam spectrometer. The least squares determined lines (1) and (3) represent one beam direction, and (2) and (4) the other, in chronological order. The zero point for the frequency shift relative to the H-maser reference is arbitrarily chosen. The data points for lines (1), (2), and (3) are means for 1/2 hour averaging times with standard deviations of 2 to 4 parts in 10^{13}. Line (4) was determined in a more brief experiment. The time duration between successive experiments was about 5 days.

TABLE 2

Summary of experimental results in Fig. 4. The slopes and intercepts, together with their standard deviations, are derived by least squares analysis

Experiment	Slope, S (parts in 10^{13}/mW)	Avg. slope, $\frac{1}{2}(S_1+S_2)$ (parts in 10^{13}/mW)	Difference slope $\frac{1}{2}(S_1-S_2)$ (parts in 10^{13}/mW)	Zero power intercept (parts in 10^{13})	Avg. zero power intercept (parts in 10^{13})
1	6.58 ± 0.32	5.63 ± 0.33	0.96 ± 0.33	- 51.3 ± 1.6	- 8.8 ± 1.7
2	4.67 ± 0.58	5.67 ± 0.40	1.00 ± 0.40	+ 33.8 ± 3.0	+ 9.6 ± 2.0
3	6.66 ± 0.53	5.58 ± 0.78	1.08 ± 0.78	- 14.6 ± 2.7	+ 3.9 ± 4.0
4	4.49 ± 1.49			+ 22.3 ± 7.5	

TABLE 3

Contributions to inaccuracy for NBS III cesium beam frequency standard

Source	3σ estimate in parts in 10^{12}
Uncertainty in $\bar{H}_c$	± 0.3
Use of $\bar{H}_c^2$ for $\overline{H_c^2}$	± 0.1
Uncertainty in 1st- and 2nd-order Doppler shifts	± 0.3
Distortion from $\bar{H}_c(t) \neq \bar{H}_c(L)$	± 0.1
Uncertainty in *c-field polarity dependent shifts*	± 0.3
Uncertainty in cavity phase difference	± 2.4
Cavity mistuning	± 0.1
Overlap of neighboring transitions	± 0.3
Uncertainty in power-dependent shifts	± 0.5
Random measurement error (1 hr)	± 0.6
2nd harmonic distortion of servo modulation	± 0.5
Miscellaneous servo system effects	± 1.5
Multiplier chain transient phase shifts	± 1.0
Total 3σ estimate of uncertainty (square root of sum of squares)	± 3.2

A Historical Review of Atomic Frequency Standards

R. E. BEEHLER

Abstract—**An attempt is made to trace the historical development of the leading contenders in the atomic frequency standards field—cesium and thallium atomic beam devices, rubidium gas cell standard, and the hydrogen maser. Many of the important experiments leading to the development of techniques basic to the various types of standards, such as the magnetic resonance method, optical pumping, buffer gases and wall coatings, and maser techniques are briefly described. Finally, the application of these basic techniques to the development of the specific types of atomic standards is discussed.**

Introduction

ALTHOUGH the exploitation of atomic frequency standards on a large scale dates back to less than 10 years ago when they came into general use as basic reference standards in many laboratories, some of the basic techniques involved had been developed almost fifty years ago. It is the purpose of this paper to review some of the early experiments and outline the subsequent development of basic techniques which have led to the present atomic frequency standards. The discussion will be confined to those standards which are presently available commercially to the general user or are at least under active development by several commercial or national standards laboratories—namely, cesium and thallium atomic beam devices, rubidium gas cell devices, and hydrogen masers. Because of the scope of the subject, it will often be impossible to include many details of the principles of operation of equipment, measurement procedures, and general performance results. However, an attempt will be made to give adequate references in all cases. The historical development of the most important *basic* techniques will first be described without regard to specific frequency standards, followed by a discussion of the later application of these basic techniques to the development of specific types of atomic standards. For an analysis of the relative merits of the different types of atomic standards discussed here and for an up-to-date status report of their performance achievements reference is made to the article by A. McCoubrey in this issue [1].

Development of Basic Techniques

Atomic Beam and Magnetic Resonance Techniques

The first experiments using atomic or molecular beams were those of the French physicist A. L. Dunoyer in 1911 [2]. Dunoyer's apparatus, shown schematically in Fig. 1, consisted simply of a 20-cm-long glass tube with three separately evacuated chambers which served as source, collimation, and observation chambers. He observed that when sodium was heated sufficiently in *A*, a deposit was formed in *C* whose distribution could be explained by the assumption that the sodium atoms traveled in straight lines.

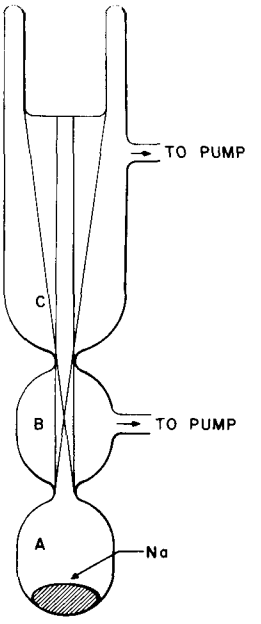

Fig. 1. Schematic diagram of Dunoyer's original atomic beam apparatus [2].

Nine years later at the University of Frankfurt in Germany, Otto Stern became the first to use a molecular beam technique for making physical measurements. In these experiments to measure directly the speed of gas molecules, a source of silver atoms at the center of an evacuated jar produced a beam of atoms which was collimated by a narrow slit and detected by deposition on a glass plate near the jar's surface. The principal parts were mounted such that they could be rotated about a vertical axis inside the bell jar at speeds of 1500 rpm. Stern observed, in agreement with the results of Dunoyer's experiments, a narrow sharp deposit explainable by straight line atomic trajectories as long as the apparatus was stationary. However, for rotational speeds of 1500 rpm the deposited pattern was shifted slightly and also appeared fuzzy. From the amount of the shift Stern could calculate the average velocity of the atoms, which turned out to agree with the predictions of kinetic theory to within a few percent. The fuzziness of the deposit showed that a distribution of speeds existed in the beam.

Manuscript received January 6, 1967; revised February 16, 1967.
The author is with the Frequency and Time Division, Hewlett-Packard Company, Palo Alto, Calif.

Less than two more years elapsed before Stern and a colleague, Walther Gerlach, performed their celebrated "Stern-Gerlach experiment" [3] which was to have a most profound effect on the development not only of molecular beam techniques but also of quantum mechanics in general. The results of this experiment supported the concept of spatial quantization—i.e., the seemingly unlikely idea that the magnetic moment of an atom in an external magnetic field can have only a few possible discrete orientation angles with respect to the external field lines. If the atom is considered to behave as a small bar magnet of magnetic moment μ in an external field, H, its change in energy, when placed in the field, would be given by $\Delta E = \mu H \cos\theta$, where θ is the angle between the magnet and the field lines. Until the performance of the Stern-Gerlach experiment, it was generally believed that a large number of such atoms in a field would show a random distribution of the angle θ, and hence would have energy values anywhere between $+\mu H$ and $-\mu H$. An opposing view, however, was suggested by observations made as early as 1896 by the Dutch physicist Pieter Zeeman that certain spectral lines split into two or more sharp lines when the radiating atom is placed in an external magnetic field. This effect could be explained by postulating that the energy of atoms in a magnetic field is quantized, resulting in the observed spectral emission lines produced by transitions between these discrete energy levels being limited to a few sharply defined frequencies through the relation $E_1 - E_2 = h\nu$, where E_1 and E_2 are the energies of the two levels involved in the transition, h is Planck's constant, and ν is the frequency of the emitted spectral line. If the atoms could have random orientations, and hence energies, in the field, one would expect to observe a blurred spectral line corresponding to a spread in energy of the levels of $2\mu H$, contrary to the experimental evidence.

In 1921 Stern conceived an experiment for testing for space quantization using a beam of silver atoms. He realized that the force exerted on a silver atom with magnetic moment μ by a magnet designed to produce a field with a large gradient $\partial H/\partial z$ across the gap would be given by $-\mu(\partial H/\partial z)\cos\theta$ and would thus vary continuously from $+\mu(\partial H/\partial z)$ to $-\mu(\partial H/\partial z)$ if atoms were oriented randomly. On the other hand, if space quantization existed, the force on silver atoms would be either $-\mu(\partial H/\partial z)$ or $+\mu(\partial H/\partial z)$. By shooting a beam of silver atoms between the poles of such a magnet and observing the deflection pattern produced, one should observe either a single broad fuzzy line (if random orientations are possible) or two discrete sharp lines (if space quantization exists). Performing the experiment with Gerlach, who had a magnet of the proper design, Stern did indeed observe two separated lines in the deflection pattern.[1] As we shall see shortly, magnets similar to that used in the Stern-Gerlach experiment are a basic component of today's atomic beam frequency standards, being useful for obtaining a beam of atoms in a specific energy state.

In 1923 Stern became head of the Department of Physical Chemistry at the University of Hamburg. During the next 10-year period he and his students published a series of some 30 papers which served to establish many of the basic principles and techniques used in today's atomic beam devices. Particular emphasis was placed upon the development of atomic beam methods for greatly improved measurements of magnetic moments.

In 1932 O. Frisch and E. Segrè used an atomic beam technique with potassium to detect transitions produced by subjecting the atoms to a sudden variation in the direction of a static magnetic field located between two Stern-Gerlach magnets [4]. The first magnet acted as a polarizer, separating the atomic beam into two beams differing in magnetic state. One of these beams was then blocked by the obstruction of part of the magnet gap, producing a beam with atoms only in the desired state. These remaining atoms were then passed through a second Stern-Gerlach magnet which acted as an analyzer to detect whether the magnetic state had been changed in the region between the magnets. When the static field with its rapid reversal in direction was applied in the center region, a change was noted in the number of atoms reaching the atomic beam detector located after the second magnet. This indicated that some of the atoms had made transitions to different energy states (and thus had their magnetic moment reversed in direction), producing a change in their deflection by the second magnet. This apparatus, used some 35 years ago, differed primarily from present atomic beam tubes only in the method of producing the transitions between the atomic energy levels.

Six years later in 1938 at Columbia University, I. I. Rabi, one of Otto Stern's former students, made the next major advance in atomic beam techniques by developing his magnetic resonance method, which permitted the detection of transitions between the closely spaced energy levels resulting from the interaction of an external magnetic field with an atom or molecule [5]. Rabi's apparatus, shown schematically in Fig. 2, was similar to that used by Frisch and Segrè, except that transitions between the magnetic states of an atom or molecule were produced by applying an oscillating RF field of proper magnitude and direction and whose frequency satisfied the resonance condition, $W_1 - W_2 = h\nu$, for the two energy levels of interest.

Although the field directions in the A and B Stern-Gerlach magnets were the same, the field gradients were arranged to be in opposite directions, so that, in the absence of transitions in the C region, molecules from the source O would undergo equal and opposite deflections by the two magnets and therefore strike the detector D. Application of the proper frequency RF field in the region R, however, produced a change from one energy state to another, such that the resultant change in magnetic moment produced a sufficiently different deflection in the B magnet to cause the molecule to miss the detector. The surface-ionization type detector used by Rabi ionized nearly all of the molecules striking the 0.001-inch wide surface and thus produced an

[1] Because the existence of electron spin with its effect on effective magnetic moments was not yet known in 1921, Stern actually expected to observe three discrete lines instead of two. Thus, while this experiment supported the concept of space quantization an additional mystery was introduced which was not resolved until 1925.

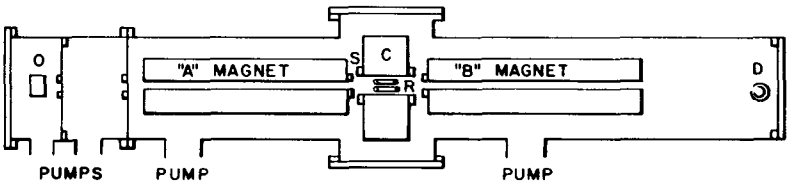

Fig. 2. Schematic diagram of Rabi's magnetic resonance apparatus [5].

electrical signal proportional to the number of molecules striking the wire per second. As the excitation frequency was varied through the resonance value for a particular transition between two energy states, Rabi observed a sharp decrease in the detector output signal.[2] The first resonance curve ever observed by this magnetic resonance technique is shown in Fig. 3. It was published by Rabi and his colleagues in February, 1938, and represents a resonance between two spatial quantization states of the lithium nucleus obtained with a beam of LiCl molecules in a strong enough C field to decouple completely the nuclear magnetic moments from one another and from the molecular rotation [5]. From the measured values of the frequency at resonance and the static C field in which the transition occurred, Rabi was able to calculate much improved values for several nuclear magnetic moments.

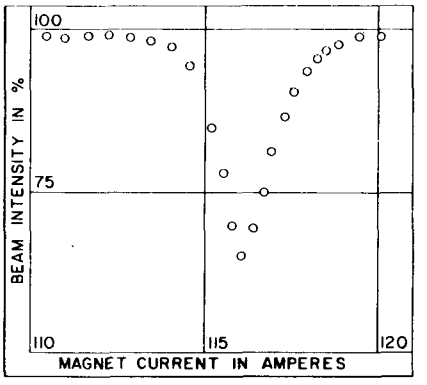

Fig. 3. First published resonance curve using Rabi's magnetic resonance technique [5].

Soon thereafter another member of the Columbia group, P. Kusch, extended the new atomic beam magnetic resonance technique to measurements of separations of the closely spaced hyperfine structure levels in the ground state of atoms [6]. Hyperfine-structure level separations in several isotopes of lithium and potassium were measured to a precision of 0.005 percent. Relative to earlier hyperfine-structure measurements by optical means, the atomic beam magnetic resonance results were simpler to interpret, much more accurate, and of much higher resolution.

A further refinement in the atomic beam magnetic resonance technique, which proved to be of extreme importance in the application of the technique to frequency standards, was introduced by N. F. Ramsey at Harvard University in 1950 [7]. In the conventional atomic beam apparatus at that time the oscillating RF field for producing transitions in the beam was applied over a relatively short region, being limited by the requirements of maintaining uniform phase and uniform static magnetic field (C field) over the entire region of interaction between the atoms and the RF field. A lengthened interaction region is desirable for many experiments, however, because the longer the interaction time, the more sharply defined are the atomic energy levels and thus also the resonance frequencies associated with transitions among them. Ramsey developed a method which increased the effective interaction time without adversely affecting the phase and field uniformity requirements. He replaced the usual single oscillating field region with two such regions separated by a relatively large distance and showed that the effective interaction time was now the entire length separating the two RF regions. Moreover, the observed resonance width under these conditions is 40 percent less than that for a single Rabi-type excitation of length equal to the separation of the two Ramsey fields and the C field uniformity requirements are actually less severe for the Ramsey case. Application of this technique to atomic beam frequency standards has resulted in resonance linewidths of less than 50 Hz at 9192 MHz.

Before discussing the specific development of cesium and thallium atomic beam frequency standards based upon the basic techniques described up to this point, let us first consider the historical evolution of some other methods and techniques which led to other types of atomic standards, such as the optically pumped gas cell devices and the hydrogen maser.

Optical Pumping Techniques

Optically pumped gas cell frequency standards, such as the Rb^{87} gas cell devices currently available commercially, represent a completely different approach to the problem of detecting a condition of resonance in the hyperfine structure levels of the ground state of an atom. In the atomic beam devices, as we have seen, the occurrence of transitions excited by RF resonance radiation is detected by observing resultant changes in the trajectories of the atoms comprising the beam. In gas cell devices, on the other hand, a double resonance technique is used in which the RF resonance condition is detected by the resultant changes in the intensity of transmitted optical radiation at the proper fre-

[2] In the early experiments described here the transition frequencies of interest depended linearly on the magnitude of the static magnetic field provided in the C region. For reasons of experimental convenience resonance curves were actually obtained by keeping the frequency fixed and sweeping the field through the corresponding resonance value.

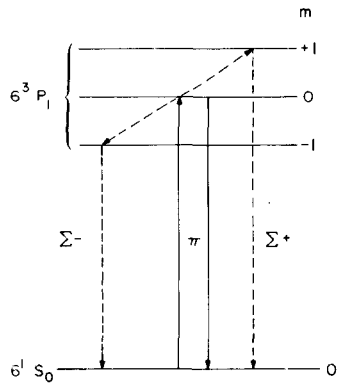

Fig. 4. Simplified energy level diagram for mercury showing states used in early double resonance experiments [12].

quency to produce transitions between the ground and first excited states of the atom.

The development of the optical pumping and double resonance techniques, which are basic to the operation of gas cell standards, can be traced back to 1949 when Prof. F. Bitter at the Massachusetts Institute of Technology showed that the frequency, intensity, and polarization of optical radiation emitted by an atom in a $^2P \rightarrow {}^2S$ (ground state) transition are all altered if the atom is simultaneously subjected to a weak oscillating RF field whose frequency is near resonance for the hyperfine levels of one of the energy states involved in the optical radiation process [8]. About this same time A. Kastler and J. Brossel of the Ecole Normale Superieure in Paris suggested a double resonance technique as a sensitive means of gaining information about the structure of energy levels [9]. The first application of this technique was to one of the excited states of the mercury atom by Brossel and Bitter in 1950 [10].

As an aid to understanding the way in which the double resonance technique was first used, consider the simplified energy level diagram for mercury shown in Fig. 4. The levels indicated are the 6^1S_0 ground state and the three Zeeman levels of the 6^3P_1 excited state. If mercury vapor is illuminated by optical resonance radiation at 2537 Å, transitions will occur from the ground state to one of the excited-state levels, the particular one depending on the polarization of the radiation. In the experiment of Brossel and Bitter a polarization (labeled π in Fig. 4) was used which selectively populated the $m=0$ level of the triplet. Under these circumstances the emitted light from spontaneous transitions back to the ground state also contains only π radiation. If now an RF field is applied perpendicular to the static magnetic field producing the Zeeman splitting and its frequency is adjusted to the proper value for resonance between the $m=0$ and the $m=\pm 1$ levels, transitions will be induced to the $m=\pm 1$ states. Decay from these levels back to the ground state will now cause Σ components to appear in the emitted light. Since the intensity and polarization of the emitted light are thus altered in the process, a means is available for optically detecting the occurrence of the RF resonance. A set of RF resonance curves for mercury obtained in this manner by Brossel and Bitter is shown in Fig. 5. Each curve corresponds to a different amplitude of the RF field.

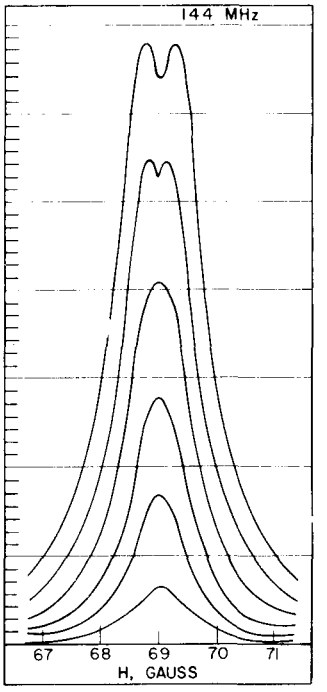

Fig. 5. Set of RF resonance curves obtained with double resonance technique for mercury [10].

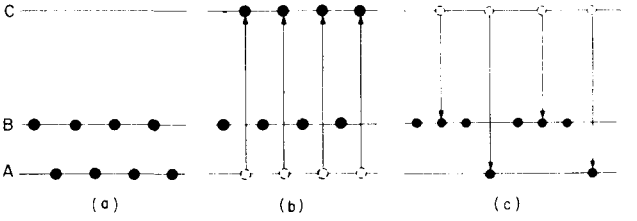

Fig. 6. Simplified optical pumping method.

The development of the method of optical pumping as applied to the building up of the population of one certain level at the expense of others in the *ground* state of atoms is due primarily to Kastler [11], [12]. Consider the much simplified energy level diagram shown in Fig. 6, where A and B represent two closely-spaced energy states in the hyperfine structure of the ground state of an atom and C represents one of the levels of the first excited state. Transitions $A \rightarrow C$ and $B \rightarrow C$ occur at optical excitation frequencies, while transitions $A \leftrightarrow B$ are in the RF range. Before application of any excitation radiation to the system, atoms are equally distributed between levels A and B of the ground state as in Fig. 6(a). If optical resonance radiation from which the $B \rightarrow C$ component has been removed by some means such as filtering is now used to illuminate the system, atoms in level A absorb an optical photon and make transitions to C, as indicated in Fig. 6(b). Since lifetimes in the excited state are very short, however, the atoms in C sponta-

neously re-emit a photon and fall either to level A or B with approximately equal probabilities. As shown in Fig. 6(c), the net effect at this point has been to increase the population of B at the expense of A. Now, since there are still atoms in A which can be excited to C by the optical resonance radiation, the cycle is repeated until (ideally) all the atoms end up in level B. This is then the process of optical pumping for changing the population distribution among the ground state levels.

If an RF excitation is now applied which is adjusted in frequency to the resonance value corresponding to the frequency separation of A and B, the pumped atoms in B will be stimulated to make transitions back to A, at which point the optical pumping process resumes. In 1956 H. G. Dehmelt at the University of Washington developed the technique of monitoring the intensity of the light transmitted through the sample as a means of detecting the occurrence of the RF transitions [13]. Using a photocell detector, one observes an output current which increases to a constant maximum value (maximum transparency of the sample) for the condition in Fig. 6(c), since at that point no atoms are available to be pumped $A \rightarrow C$ by absorbing part of the incident light. As the RF signal is swept through resonance, however, atoms transfer to A where optical absorption again takes place, producing a sharp drop in the transmitted light. The detection of RF resonances by this means is extremely sensitive. For example, a sample of vapor at a pressure of only 10^{-7} torr can reduce the intensity of the transmitted light by 20 percent when the correct RF is applied. A very large effective energy gain occurs with the optical detection technique, since the optical photon detected has an energy approximately 10^4 to 10^5 times greater than the energy of the RF photon involved in the microwave transition. As we shall see in more detail later, the use of optical pumping and optical detection with atomic systems of Na^{23}, Cs^{133}, and Rb^{87} has made possible the development of extremely compact atomic frequency standards relative to the atomic beam devices.

Buffer Gas Techniques

While the optical pumping technique as briefly described in the preceding section will, in principle, produce a large population buildup in level B of Fig. 6, collisions of atoms in the sample with each other and with the walls of the containing vessel actually provide a relaxation mechanism whereby atoms can "leak" back to level A without the application of RF. Even in very dilute samples atoms make about 10 000 collisions per second with the walls. Since this is usually greater than the number of optical photons which the atom can absorb per second for repumping to level B, the pump effectively becomes very leaky and at best only weak RF resonances can be observed.

In 1955 in the laboratory of A. Kastler a fortunate accident occurred during some experiments with sodium vapor in highly-evacuated glass bulbs which was to provide the key for significantly improving the efficiency of the optical pumping process. When a vacuum system failure allowed hydrogen gas to be introduced into one of his sodium bulbs, Kastler and his colleagues were amazed to find that the optical pumping was greatly increased! The foreign gas introduced was found to act as a buffer between the sodium atoms and the walls where disorienting collisions take place. It was found in later experiments that, because of collisions between atoms of the sample and those of the buffer gas, the average diffusion time to the walls could be increased from 10^{-4} second (without buffer gas) to nearly a second. It is, of course, necessary to use a buffer gas which does not itself disorient the sample atom's magnetic state during collisions. In general, use of sample atoms in a $^2S_{1/2}$ ground state with its spherical symmetry appears to be the best way to insure minimum interaction during buffer gas collisions.

In addition to producing an enhancement of the optical pumping process by increasing the effective time during which RF transitions can be excited, the use of buffer gases also causes a reduction in the observed resonance linewidth as compared to the normally observed Doppler broadened value. This "collision-narrowing" effect in a buffer gas was first predicted by R. H. Dicke in 1953 [14] and was observed experimentally by J. Wittke and Dicke at Princeton University in 1954 [15]. Measuring the hyperfine splitting in the ground state of atomic hydrogen by a microwave absorption technique, they found that atomic hydrogen at a pressure of 5×10^{-4} torr in a buffer gas of clean molecular hydrogen at 0.2 torr produced a resonance width of only 3 kHz or one-sixth of the normal Doppler width.

In 1956 H. G. Dehmelt performed optical pumping experiments with sodium in argon buffer gas and observed relaxation times of up to 0.21 second which corresponds to an amazing 10^8 sodium-argon collisions occurring before disorientation of the sodium atom [13]. Dehmelt pointed out at that time that such long relaxation times (0.21 second) used in future RF resonance experiments with optical pumping would provide extremely narrow linewidths. Even longer relaxation times (up to 2 seconds) were obtained by Dehmelt's group by replacing the buffer gas with a solid buffer wall coating chosen to have minimum magnetic interaction with colliding rubidium atoms [16]. Using eicosane ($C_{20}H_{42}$), they obtained strong resonances in rubidium and found that at least 600 collisions occurred before appreciable disorientation. W. Hawkins, working at Yale University, also obtained favorable results with wall surfaces of absorbed air molecules on Apiezon L grease and on copper [17]. Several years later, however, during the early development phase of commercial gas cell standards, R. M. Whitehorn at Varian Associates concluded that use of solid buffer coatings for commercial applications presented too many technical problems [18]. To date, all commercial gas cell standards have used buffer gases.

Storage Techniques for Increasing Interaction Times

The advantages to be gained in terms of narrower resonance lines by increasing the interaction time between an atomic beam and the applied RF resonance radiation have already been mentioned briefly in connection with the de-

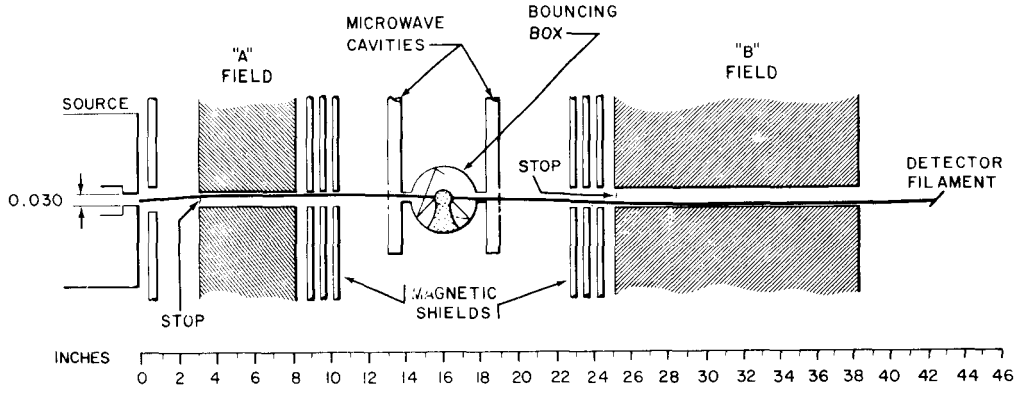

Fig. 7. Schematic diagram of "broken-beam" apparatus [21].

velopment of Ramsey's separated oscillating fields technique. In 1957 Ramsey pointed out that it should be possible to further increase the interaction time in such an experiment by "storing" the atoms in a bounce box having a suitable non-disorienting wall coating and located between the two RF field regions of an atomic beam apparatus [19]. If the collisions with the walls of the bounce box do not appreciably affect the magnetic state of the atom, an effective increase in the separation of the two fields is realized without physically lengthening the apparatus.

Kleppner, Ramsey, and Fjelstadt reported in 1958 the first successful results using this "broken-beam" technique [20]. The bounce box was designed so that an atom had to make at least two collisions in order to pass through and contribute to an observed resonance. Employing a beam of atomic cesium, they were able to observe resonances between the hyperfine states for wall coatings of teflon heated to 100°C, eicosane, and polyethylene. The authors at this time stated their intention to test other substances for wall coatings for application in a "high-precision atomic clock incorporating both the storage box and maser principles."

Further experiments with a cesium beam and a variety of wall coatings, using the apparatus shown schematically in Fig. 7, were reported in 1961 by Goldenberg, Kleppner, and Ramsey [21]. For storage bulbs coated with "Paraflint" (a mixture of long chain paraffins), resonance widths of only 150 Hz were obtained as compared with 2 kHz without the storage bulb. This result implied that at least 200 collisions could occur before relaxation of the hyperfine states became a problem. One unfavorable feature of the experimental observations was a rather large shift of several hundred Hz in the resonance frequency resulting from slight displacements of the energy levels during each collision process. This type of shift was minimized later in the hydrogen maser applications because of the much lower polarizability of the hydrogen atom compared to cesium.

Maser Techniques

The development of maser techniques in 1953, initially using ammonia, represented still another approach to the problem of using microwave resonances in atoms or molecules as frequency standards. The maser was invented by C. H. Townes of Columbia University [22] but was also proposed independently by N. G. Basov and A. M. Prokhorov of the U.S.S.R. [23]. In this device, a collimated beam of ammonia molecules effuses from a source and then passes through an inhomogeneous electrostatic field designed to spatially separate the two energy states of the inversion spectrum, just as a Stern-Gerlach magnet separates magnetic states of atoms in the magnetic resonance method. The electrostatic state separator applies a radially outward force to molecules in the lower inversion state, but a radially inward force on the upper energy state molecules. The upper-state molecules are thus focused into a high-Q cylindrical microwave cavity tuned to the resonance frequency for the ammonia inversion transition ($J=3$, $K=3$) at 23 870 MHz. The resulting large excess population of upper energy state molecules in the cavity is then favorable for stimulated transitions from upper to lower inversion states with an accompanying emission of an RF photon.

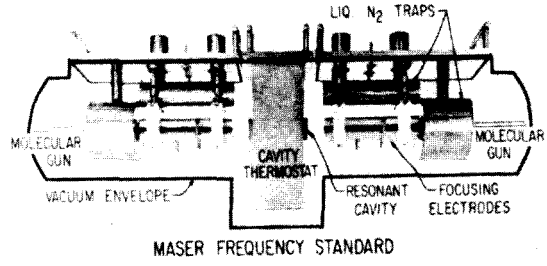

Fig. 8. Diagram of an early ammonia beam maser showing arrangement of components (courtesy of National Bureau of Standards, Boulder, Colo.).

Townes was able to get a sufficient flux of molecules into the cavity so that the emitted microwave energy exceeded the losses involved, and a small amount of excess energy could be coupled out of the cavity for external use. Operation of the maser in this manner as an oscillator was found to require a flux of at least 5×10^{12} molecules per second per square centimeter. Figure 8 shows the physical arrangement of the components in an ammonia maser, modified for operation with two beams to reduce Doppler effects.

Following the first successful operation of a maser in

1953, J. P. Gordon, H. J. Zeiger, and Townes studied in detail the characteristics of the maser oscillation frequency and found rather strong dependencies of the output frequency upon the ammonia source pressure and the voltage applied to the electrostatic focuser [24]. The strong coupling between the ammonia beam and the resonant cavity also causes the output frequency to depend significantly on the tuning of the cavity.

In spite of intensive research efforts in the United States, the U.S.S.R., Japan, Switzerland, and several other countries during the next few years to develop adequate techniques for controlling the critical maser parameters and for achieving a reproducible frequency from one maser to another, it has now become apparent that, except possibly for its high short-term frequency stability, the ammonia maser cannot compete with other types of atomic devices for use as a primary or secondary frequency standard. Its importance is mainly that it led to the development of one of the present-day leading contenders for the best atomic frequency standard—the hydrogen maser.

Application of Basic Techniques to the Development of Specific Types of Atomic Frequency Standards

Development of the World's First "Atomic Clock"

The first operational complete "atomic clock" system was developed at the National Bureau of Standards (NBS), Washington, D. C., in 1948–1949 by H. Lyons and his associates [25]. This system consisted basically of a quartz crystal oscillator, electronically stabilized by the $J=3$, $K=3$ absorption line in ammonia at 23 870 MHz, together with suitable frequency dividers for driving a 50-Hz clock from the stabilized oscillator. This historic accomplishment was the culmination of many years of experimental interest in the absorption spectrum of ammonia, extending back to 1933 and the remarkable experiments of C. E. Cleeton and N. H. Williams in which they were able to observe absorption lines in ammonia more than 10 years before the development of most microwave equipment and techniques [26]. Aided by the rapid development of microwave techniques for radar applications during World War II, B. Bleaney and R. P. Penrose succeeded in observing the rotational fine structure of ammonia in 1946 [27]. About this time R. V. Pound proposed stabilizing a klystron with one of the ammonia spectral lines [28]. This was accomplished by W. V. Smith et al. in 1947 [29] and shortly thereafter by W. D. Hershberger and L. E. Norton at RCA [30].

The NBS system, developed specifically for use as a frequency standard, was first operated on August 12, 1948. A photograph of this first "atomic clock" is shown in Fig. 9. The heart of the system, a 25-foot long waveguide absorption cell filled with ammonia at a pressure of 10–15 microns, is shown wrapped around the clock mounted on top of the equipment cabinets. The $J=3$, $K=3$ absorption line obtained by sweeping the excitation frequency through the molecular resonance can be seen displayed on the oscilloscope in the photograph. A block diagram of the complete atomic clock system (in a somewhat modified form from that shown in Fig. 9) is presented in Fig. 10. Two versions of the NBS ammonia clock were built with demonstrated long-term stabilities of 1×10^{-7} and 2×10^{-8}. Work on a third version was eventually halted when it became apparent that atomic beam techniques offered more promise for frequency standard development.

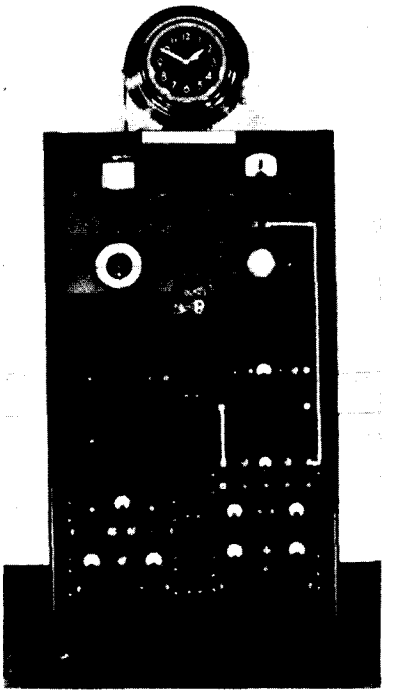

Fig. 9. Original NBS ammonia clock (courtesy of National Bureau of Standards, Boulder, Colo.).

Development of Atomic Beam Standards Utilizing Cesium or Thallium

According to Hershberger and Norton [30], I. I. Rabi made the specific suggestion of using atomic or molecular transitions in an atomic clock in his January, 1945 Richtmyer lecture before the American Physical Society. Four and one-half years later a program was initiated at the National Bureau of Standards to develop an atomic beam frequency standard utilizing cesium, which would hopefully avoid the problems of collision and Doppler broadening encountered in the ammonia absorption cell work.

The NBS group, led by H. Lyons and J. Sherwood, was able to obtain the services of Prof. P. Kusch of Columbia University as a consultant and set out to construct a machine using Rabi's magnetic resonance technique, with the excitation radiation at 9192 MHz being applied to the cesium beam over a 1-cm path by means of a single short-circuited section of X-band waveguide. At the 1952 New York meeting of the American Physical Society, J. Sherwood reported the first successful observation of the $(F=4,\ m_F=0) \leftrightarrow (F=3,\ m_F=0)$ microwave transition [31]. A photograph of the original apparatus involved is shown in Fig. 11. Shortly thereafter, this apparatus was modified for opera-

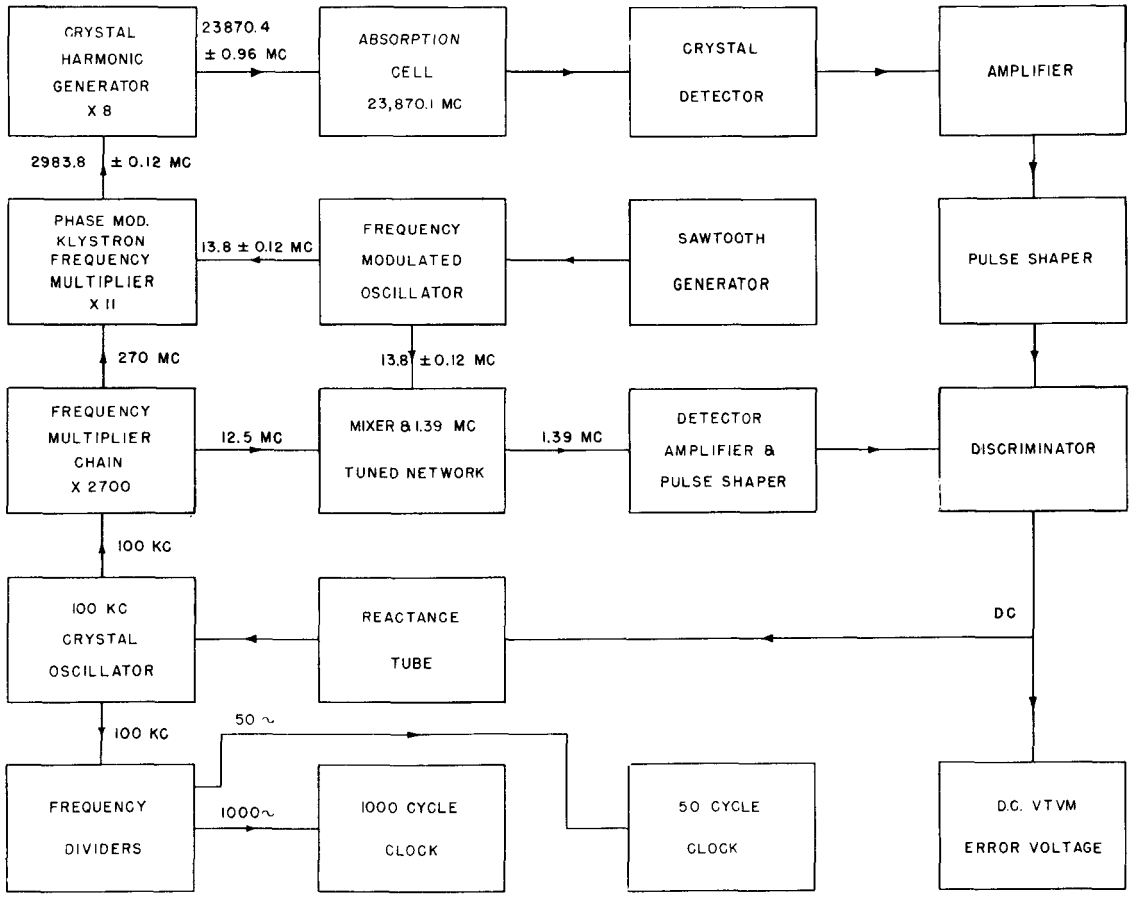

Fig. 10. Block diagram of NBS ammonia clock (courtesy of National Bureau of Standards, Boulder, Colo.).

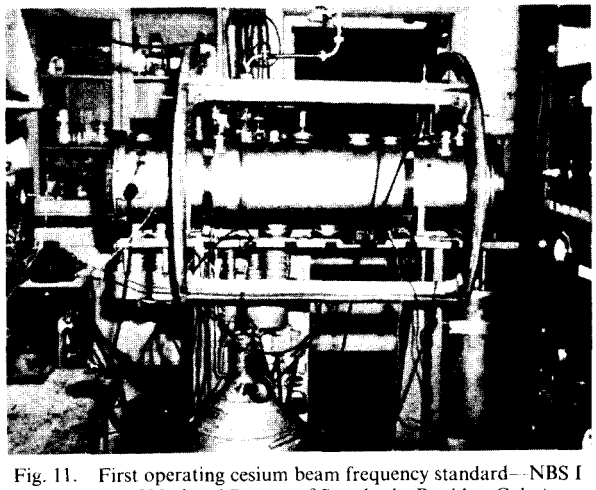

Fig. 11. First operating cesium beam frequency standard—NBS I (courtesy of National Bureau of Standards, Boulder, Colo.).

tion with the Ramsey technique of separated oscillating fields. Using a separation of 50 cm, a Ramsey resonance was observed with a line Q of 30 million, which corresponds to a linewidth of the central peak of the Ramsey resonance pattern of only 300 Hz at 9192 MHz [32]. Based on these results, Lyons predicted an eventual accuracy capability of 1×10^{-10}. The apparatus was soon thereafter disassembled completely and moved to the new NBS site at Boulder, Colo., where, under the direction of R. Mockler, it was eventually reassembled with many new components and improved electronics and used to thoroughly evaluate the precision and accuracy capabilities of cesium beam frequency standards [33]. It was not until the 1958–1959 period that this first cesium beam standard was used to more or less routinely calibrate the frequencies of the NBS working standards.

Meanwhile, L. Essen and his associates at the National Physical Laboratory (NPL) in Teddington, England, had placed a similar cesium beam apparatus with a Ramsey linewidth of 340 Hz and an accuracy of 1×10^{-9} into operation in June, 1955 [34]. This standard, a photograph of which is shown in Fig. 12, was the first to be used on a regular basis for the calibration of secondary working frequency standards. Frequency measurements made with this standard, averaged over the 1955–1958 period, were combined with data from the U. S. Naval Observatory to obtain a determination of the cesium transition frequency (reduced to zero magnetic field conditions) in terms of the astronomical units of time interval [35]. From these measurements resulted the now familiar cesium frequency of 9192.631770 MHz in terms of the Ephemeris second. More recently, in 1964, this value was used to *define* an atomic unit of time interval.

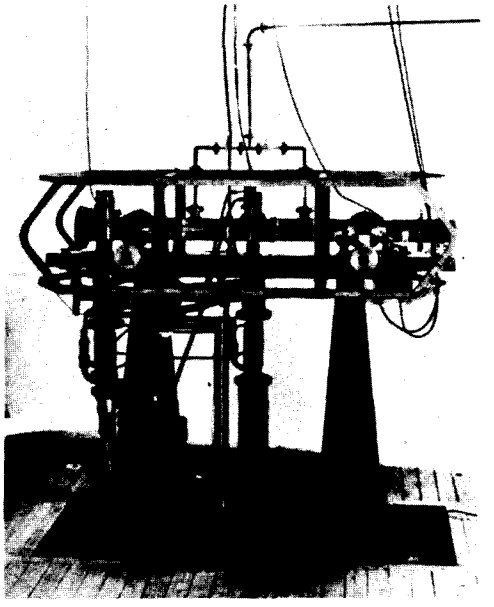

Fig. 12. Original NPL cesium beam frequency standard—NPL I (courtesy of National Physical Laboratory, Teddington, England—crown copyright reserved).

Successful operation of another laboratory-type cesium standard was reported in 1958 by S. Kalra, R. Bailey, and H. Daams at the National Research Council (NRC) in Ottawa, Canada [36]. They achieved a Ramsey linewidth of 290 Hz, a measurement accuracy of better than 1×10^{-9}, and a measurement precision of 1×10^{-10}. During the next year the first cesium standard at the Laboratoire Suisse de Recherches Horlogeres (LSRH) in Neuchatel, Switzerland was operated by J. Bonanomi, J. de Prins, and P. Kartaschoff [37].

In the case of all these early cesium beam standards developed by the various national standards laboratories, the frequency of the oscillator providing the cesium transition excitation was first adjusted manually to the peak of the resonance curve and then compared with the unknown frequency to be measured. Several years earlier, however, in 1954, J. Zacharias, J. Yates, and R. Haun at the Massachusetts Institute of Technology had been able to electronically stabilize the frequency of a quartz oscillator with the $(4, 0) \leftrightarrow (3, 0)$ transition in cesium [38]. By choosing the time constants of the servo-loop properly, it was possible to combine the superior short-term stability of the oscillator with the excellent long-term stability of the atomic resonance itself in order to achieve optimum overall performance. The authors suggested that this technique together with a sealed-off cesium beam tube should make a commercial cesium standard feasible.

Building upon these results, R. Daly and others at the National Company, Malden, Mass., developed the first commercial cesium beam frequency standard, termed the "Atomichron," in 1956 [39]. Utilizing a cesium beam tube about 6 feet in overall length, this instrument had a specified stability after one-hour warmup of 5×10^{-10} for measuring periods of greater than 5 seconds for the life of the instrument and an accuracy of 1×10^{-9}. These specifications were later significantly improved as more experience was accumulated. A photograph of one of the early Atomichrons is shown in Fig. 13.

The relative portability of the Atomichron made it possible in March, 1958 to transport two of these instruments to England for direct comparisons with the National Physical Laboratory cesium standard of L. Essen [40]. The results showed that the two Atomichrons agreed to within 1×10^{-10} but differed from the NPL standard by 2.2×10^{-10}. The measurement uncertainties were considered to be $\pm 5 \times 10^{-11}$. The relatively close agreement observed, considering the state-of-the-art at that time, was even more remarkable in view of the wide differences existing in terms of the electronics used, the beam optics employed, and the general construction techniques followed for the commercial and NPL instruments.

As new, improved versions of cesium standards evolved in the various laboratories based on the experiences with the early instruments, a trend developed in the various national standards laboratories toward very long machines with the resulting narrow linewidths, while commercial emphasis was directed more toward very short tubes with higher-efficiency beam optics, high reliability, and reduced size, weight, and electrical power consumption.

Long-beam instruments, employing separations between the two oscillating field regions ranging from 2.1 to 4.1 meters, were constructed at NPL in 1959 [41], at LSRH in 1960 [37], at NBS in 1963 [42], and at NRC in 1965 [43]. As a result of the long interaction times between the beam and the RF field, extremely narrow resonance linewidths have been achieved—as low as 20 Hz in the LSRH instrument. In all cases, except for NPL, servo systems have been incorporated in order to stabilize the frequency of a quartz oscillator with the cesium resonance. Comparisons among these four long-beam standards by means of the most recent Hewlett-Packard Company "flying clock" experiment [44] (using cesium standards) indicate agreement to within 4×10^{-12}. The best precision and accuracy figures achieved to date with cesium standards are believed to be $\pm 2 \times 10^{-13}$ (one sigma estimate for one-hour averaging time) and $\pm 1.1 \times 10^{-12}$ (one sigma estimate), respectively, reported by Beehler et al., for the NBS standard [45]. Detailed characteristics and performance results for the various individual standards discussed are given elsewhere, in the literature.

Commercial development of cesium beam standards has proceeded rapidly since 1956 with primary contributions from National Company, Varian Associates, Pickard and Burns Electronics, and Hewlett-Packard Company. Recently, the first non-U. S. commercial cesium standard has been introduced by Ebauches, S.A., in Switzerland. These instruments typically weigh about 60 pounds, require ≈ 50 watts of electrical power, use solid-state electronics extensively, and fit into about 9 inches of standard rack space [46], [47]. Quoted performance characteristics include

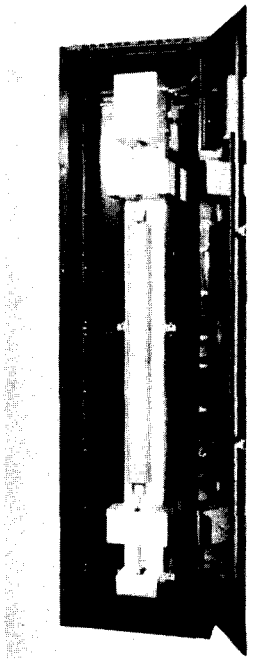

Fig. 13. Early model of National Company Atomichron (courtesy of National Company, Malden, Mass.).

$\pm 1 \times 10^{-11}$ accuracy [46], $\pm 1 \times 10^{-11}$ long-term stability[3] [46], and 11 000-hour mean time between failures [48]. Considerable progress [49] has been made in the development of a highly refined 27-inch cesium beam tube and associated electronics for the U. S. Air Force with a long-term stability specification of $\pm 5 \times 10^{-14}$.

In parallel with the development of cesium beam devices, several laboratories have also constructed atomic beam standards utilizing thallium. Prof. P. Kusch first pointed out in 1957 that thallium should have significant advantages over cesium in an atomic beam frequency standard in terms of its higher transition frequency, its much-reduced sensitivity to external magnetic fields, its much simpler atomic spectrum resulting in the ability to utilize a higher fraction of the atoms comprising the beam with reduced overlap effects from neighboring transitions, and its lower vapor pressure [50]. Disadvantages pointed out were the greater difficulty in detecting the atomic beam and the requirement for larger deflecting magnets.

In 1962 J. Bonanomi was successful in building a thallium atomic beam standard at Neuchatel Observatory in Switzerland [51]. A resonance linewidth of 135 Hz, corresponding to a line Q of 1.6×10^8, was obtained. The difficult problem of detecting thallium atoms was resolved by using the surface ionization technique, as with cesium, but with an oxygenated tungsten detector wire to increase its work function. In assessing the accuracy of the instrument, Bonanomi concluded that all contributions to inaccuracy from the beam tube itself were too small to be detected.

A few months later another thallium standard was placed into operation by R. Beehler and D. Glaze at the National Bureau of Standards [52]. Experiments there also confirmed the high accuracy potential of thallium standards, indicating that for similar-length devices, thallium provides at least as good an accuracy figure as cesium.

Much more recently, R. Lacey at Varian Associates has developed a small (28-inch length), portable thallium beam tube similar to the sealed-off commercial cesium beam tubes [53]. This tube makes use of a heated silver tube as a controllable oxygen leak for continuous oxidation of the tungsten detector ribbon. A novel double-resonance technique, first developed for thallium by J. Bonanomi, was also used by Lacey in order to reduce the size of deflecting magnets needed by making use of atoms which are in states having larger magnetic moments while in the A and B deflection magnet regions of the apparatus. A resonance linewidth of only 178 Hz was achieved and the observed signal-to-noise ratio implies a frequency stability of less than 1×10^{-11} for one-second averaging times, provided that shot noise of the beam is the limiting factor.

Development of Practical Gas Cell Frequency Standards

The successful incorporation of the double-resonance, optical pumping, and optical detection techniques into operating frequency standards using alkali metals, such as sodium, cesium, and rubidium, was achieved by a number of independent laboratories starting in 1958. In that year M. Arditi and T. Carver at the International Telephone and Telegraph Laboratories [54] and W. Bell and A. Bloom at Varian Associates [55] first used the optical detection technique mentioned earlier to observe the field-independent hyperfine resonance in Na^{23}. The former, using argon and neon buffer gases, obtained a linewidth of 400 Hz and were able to measure shifts of the resonance frequency as a function of the buffer gas pressure.

About the same time, P. Bender (NBS), E. Beaty (NBS), and A. Chi (Naval Research Laboratory) developed a practical cesium gas cell standard operating on the same $(4, 0) \rightarrow (3, 0)$ hyperfine transition used in the cesium atomic beam standards [56]. The optical pumping radiation—the $A \rightarrow C$ component in the simplified scheme of Fig. 6—was obtained from an argon discharge light source operated in a magnetic field of 5000 gauss so that one of the argon emission lines was Zeeman-shifted to a frequency near that of the desired $A \rightarrow C$ component. Resonance linewidths of as low as 40 Hz, corresponding to a Q value of 2×10^8, were achieved with neon and helium buffer gases. Extensive data on pressure shifts of various buffer gases with cesium were obtained both in these NBS experiments and in similar ones conducted by Arditi at ITT Labs [57]. In 1959 Arditi reported some performance results of his cesium gas cell standard [58], including a short-term stability (several seconds) of $\pm 2 \times 10^{-10}$, a long-term stability (minutes or hours) of $\pm 1 \times 10^{-10}$, and an accuracy of ± 3–4×10^{-10}.

The Rb^{87} hyperfine resonance had been used in gas cell work as early as 1957 by T. Carver of Princeton University [59]. Utilizing optical pumping to increase the population difference within the hyperfine structure of the rubidium

[3] Total drift for the life of the beam tube.

ground state but detecting the microwave transition by observing the microwave absorption, rather than the optical transmission, Carver obtained linewidths of approximately 200 Hz with an argon buffer gas. Shortly thereafter, P. Bender et al. at the National Bureau of Standards developed a new technique [60] for the optical pumping of Rb^{87}. A diagram of their experimental apparatus is shown in Fig. 14. The innovation here was the method used to obtain selective pumping from only one of the hyperfine levels of the ground state up to the excited state. Light from a rubidium spectral lamp was filtered by a mixture of Rb^{85} and 5 cm Hg of argon. The broadening of the Rb^{85} absorption lines produced by the argon in the filter cell caused one of the absorption lines to overlap the lower frequency component ($B \rightarrow C$ in Fig. 6) of the Rb^{87} lamp emitted light. Therefore, the light reaching the sample cell contained mainly the higher-frequency component ($A \rightarrow C$) and the optical pumping process proceeded efficiently. This filtering scheme proved so effective that all present commercial Rb gas cell standards use it. With the apparatus shown, Bender et al. were able to achieve linewidths of only 20 Hz for Rb^{87} ($Q = 3 \times 10^8$). They also reported a precision of 5×10^{-11} in setting the microwave signal frequency on the center of the resonance line.

With the accumulation of extensive data on cesium and rubidium gas cell standards from ITT Laboratories, NBS, Varian Associates, Space Technology Laboratories, and NPL (England), among others, three main factors which limited gas cell performance emerged. The first is the nature and density of the particular buffer gas used in the cell. Frequency shifts were found to be directly proportional to buffer gas pressure and were positive for light gases and negative for heavy gases. By using mixtures of positive and negative coefficient buffer gases it was found possible to nearly cancel out the effect. The second factor is the linear dependence of the frequency on the temperature of the gas cell. This effect can also be minimized by proper mixtures and pressures of buffer gases in the cell, but a single choice of such conditions does not minimize both the pressure and temperature shifts. R. Carpenter et al. at NBS obtained temperature coefficients of less than $1 \times 10^{-11}/°C$ with rubidium as early as 1960 [61]. Both the NBS and ITT Laboratories groups have published measured temperature and pressure shift coefficients for a variety of buffer gases with cesium and rubidium systems [61], [62].

The third limitation on performance is an observed dependence of the frequency on the intensity of the optical pumping light. This is also a linear shift (at least for low buffer gas densities) and is reduced by operating at relatively high buffer gas pressures and gas cell temperatures. A number of other methods have been proposed to reduce this "light shift" and at present manufacturers of commercial gas cell frequency standards are still devoting much effort to this problem. Data from several laboratories show that if frequency is plotted versus cell temperature for different light intensities, a series of lines result which converge to a single frequency that agrees within experimental uncertainties with the values determined by atomic beam methods

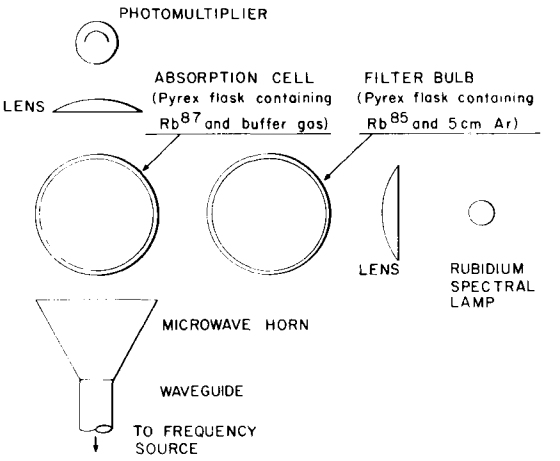

Fig. 14. Schematic diagram of NBS Rb^{87} gas cell frequency standard [60].

(after extrapolation of the gas cell data to zero magnetic field and zero buffer gas pressure).

Manufacturers of rubidium gas cell standards, such as Varian Associates and General Technology Corporation, have been able to select and control the important parameters well enough to achieve long- and short-term stabilities of 1×10^{-11} per month and 1×10^{-11} for one second, respectively, in extremely compact packages employing solid-state electronics [63]. Because of the frequency dependence on buffer gas the device must be calibrated initially with respect to a primary standard. From then on, however, the gas cell performs admirably as a secondary standard with typical stabilities as quoted above.

Development of the Atomic Hydrogen Maser

The atomic hydrogen maser, first developed at Harvard University in 1960 by N. Ramsey, M. Goldenberg, and D. Kleppner [64], was an outgrowth of several of the basic techniques discussed earlier, including those involving buffer gases, atomic beam experiments with stored atoms, and ammonia maser principles. Maser action had not been achieved previously with gaseous atoms in the ground state, primarily because of the much smaller values of the relevant magnetic dipole matrix elements as compared to the electric dipole matrix elements characterizing molecular transitions such as the $J = 3$, $K = 3$ resonance used in ammonia masers. This difficulty was overcome in the atomic hydrogen maser by using a "storage bulb" with a non-disorienting wall coating in order to achieve very long effective interaction times of the order of one second.

The hydrogen maser developed at Harvard combined in a single device several outstanding advantages previously offered in part by a number of different types of atomic frequency standards. For example, an extremely narrow linewidth of about 1 Hz results from the long interaction time. The spectral line is of very high purity in contrast to the complex structure of the ammonia line. Shifts due to first-order Doppler effect are essentially eliminated by virtue of the averaging process as the typical atom makes about 10^4

random bounces off the storage bulb walls before undergoing magnetic relaxation from the desired energy state or escapes from the bulb. Finally, the high signal-to-noise ratio characteristic of the maser technique helps to produce the best short-term frequency stability yet observed with any atomic frequency standard.

A schematic diagram of Ramsey's original apparatus is shown in Fig. 15. Atomic hydrogen from a Wood's discharge source first passes through a state separator, just as in the ammonia maser. However, because the transition of interest in hydrogen is a *magnetic* dipole transition, the state separator consists of a hexapole deflecting magnet rather than an electrostatic version. Atoms in the higher energy state of interest ($F=1$, $m_F=0$) are focused into the quartz storage bulb as indicated by the dashed lines, while the lower-state atoms ($F=0$, $m_F=0$) are defocused. The storage bulb is centered within a cylindrical resonant cavity tuned to the frequency of the $(1, 0)\leftrightarrow(0, 0)$ hyperfine transition at 1420 MHz. While bouncing around within the bulb the atoms radiate to the lower energy state and eventually leave the bulb through the entrance aperture after about a second. With the paraffin wall coating first used, at least 10^4 collisions with the walls could occur without seriously perturbing the energy states. Teflon coatings have been found to perform even better. With sufficient beam flux ($\approx 4\times 10^{12}$ atoms per second) and high enough cavity Q, maser oscillation was achieved. Not shown in Fig. 15 is a system of Helmholz coils for applying a small dc magnetic field to the cavity region, corresponding to the C field in atomic beam magnetic resonance devices. A photograph of this first Harvard hydrogen maser is shown in Fig. 16.

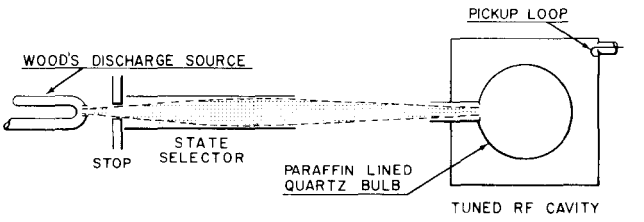

Fig. 15. Schematic diagram of Ramsey's original hydrogen maser [64].

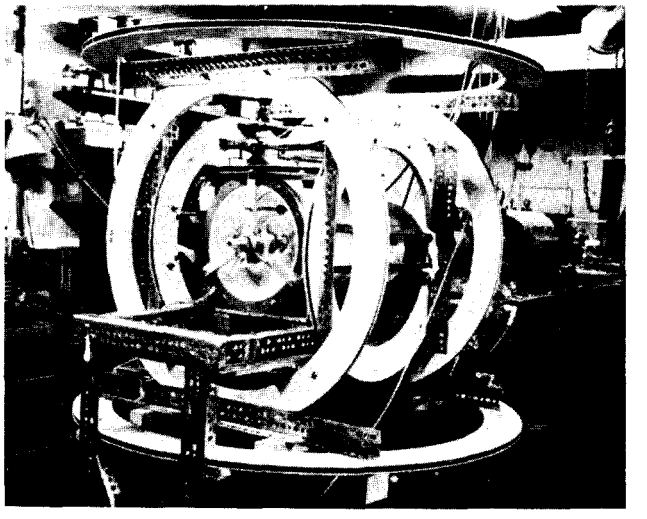
Fig. 16. Ramsey's first hydrogen maser (courtesy of N. Ramsey, Harvard University, Cambridge, Mass.).

As in the case of the earlier experiments with buffer gases and wall coatings mentioned previously, the maser oscillation frequency was shown both experimentally and theoretically [65] to depend on the wall coating used. Since the collision rate is an important factor, the "wall shift" depends on the bulb size. For bulb diameters normally used the shift amounts to a few parts in 10^{11} but appears to be stable with time. Wall shifts have been measured both at Harvard [66] and by R. Vessot et al. of Varian Associates [67] by measuring maser frequency for different sizes of storage bulbs.

Work on hydrogen masers was undertaken at Varian Associates and at LSRH in Switzerland in 1961. C. Menoud and J. Racine at LSRH [68] and Vessot and Peters at Varian [69] reported successfully operating masers in 1962. The Varian maser has been commercially available for several years and employs many refinements developed for commercial applications, such as elaborate temperature control of the resonant cavity to reduce cavity-pulling frequency shifts due to mistuning, provision for effective degaussing of the three-layer magnetic shielding, use of oil-free ion pumps to reduce the possibility of contaminating the wall coating and changing the wall shift, and control of the hydrogen flux by a temperature-controlled palladium leak. More recently, H. Andresen at the U. S. Army Electronics Command (Ft. Monmouth, N. J.) has developed a servo system for automatically keeping the resonant cavity tuned to the frequency of the atomic resonance [70]. Further work on hydrogen masers is currently in progress at many laboratories throughout the world.

For a summary of the present status of hydrogen maser performance results the reader is referred to the article by A. McCoubrey in this issue. It is worth noting, however, that maser stabilities of 1×10^{-14} for averaging periods in the vicinity of 30 minutes and absolute inaccuracies of less than 1×10^{-12} have already been achieved [71]. Since 1963, a number of intercomparisons have been made between hydrogen masers and cesium beam standards involving equipment and personnel from five different laboratories in the U. S. and one in Switzerland. The results [45], [71], with one exception in 1963, show that all measured values of the hydrogen frequency in terms of cesium (after application of appropriate corrections to both the hydrogen and cesium raw data) agree to within the quoted measurement uncertainties, which ranged from 2×10^{-11} to 1.2×10^{-12}.

Conclusion

An attempt has been made to at least touch upon the highlights of the historical development of the better known types of present atomic frequency standards. A number of other types, or modifications of existing types, of atomic standards are being investigated in various laboratories and may eventually prove superior to all those discussed here. In this class would be included the large-bulb (60-inch diameter) hydrogen maser now under construction at

Harvard University for reduction of wall shifts and cavity-pulling shifts, the rubidium maser with its extremely high short-term stability, masers using other atoms with optical pumping, electric resonance molecular beam devices operating at several hundred GHz, and possibly even lasers if the large frequency gap between RF and the optical region can be successfully bridged. In view of the large amount of effort and resources being put into the development of improved atomic frequency standards at present in many countries of the world it seems likely that the performance of atomic frequency standards will continue to improve rapidly in the foreseeable future.

References

[1] A. O. McCoubrey, "Relative merits of atomic frequency standards," this issue.

[2] L. Dunoyer, *Comptes Rend.*, vol. 152, p. 594, 1911.

[3] W. Gerlach and O. Stern, "On the quantization of direction in a magnetic field," *Ann. Physik*, vol. 74, pp. 673–699, 1924.

[4] R. Frisch and E. Segrè, "On the adjustment of the direction of quantization," *Z. Physik*, vol. 80, p. 610–616, 1933.

[5] I. I Rabi, J. R. Zacharias, S. Millman, and P. Kusch, "A new method of measuring nuclear magnetic moment," *Phys. Rev.*, vol. 53, p. 318, February 1938.

[6] P. Kusch, S. Millman, and I. I. Rabi, "The radiofrequency spectra of atoms," *Phys. Rev.*, vol. 57, pp. 765–780, May 1940.

[7] N. F. Ramsey, "A molecular beam resonance method with separated oscillating fields," *Phys. Rev.*, vol. 78, pp. 695–699, June 1950.

[8] F. Bitter, "The optical detection of radiofrequency resonance," *Phys. Rev.*, vol. 76, pp. 833–835, September 1949.

[9] J. Brossel and A. Kastler, *Compt. Rend.*, vol. 229, pp. 1213–1215, 1949.

[10] J. Brossel and F. Bitter, "A new double resonance method for investigating atomic energy levels. Application to $Hg^3P_1^*$," *Phys. Rev.*, vol. 86, pp. 308–316, May 1952.

[11] A. Kastler, *J. Phys. et Rad.*, vol. 11, p. 255, 1950.

[12] ——, "Optical methods of atomic orientation and of magnetic resonance," *J. Opt. Soc. Am.*, vol. 47, pp. 460–465, June 1957.

[13] H. G. Dehmelt, "Slow spin relaxation of optically polarized sodium atoms," *Phys. Rev.*, vol. 105, pp. 1487–1489, March 1957.

[14] R. H. Dicke, "The effect of collisions upon the Doppler width of spectral lines," *Phys. Rev.*, vol. 89, pp. 472–473, January 1953.

[15] J. P. Wittke and R. H. Dicke, "Redetermination of the hyperfine splitting in the ground state of atomic hydrogen," *Phys. Rev.*, vol. 96, pp. 530–531, October 1954.

[16] H. G. Robinson, E. S. Ensberg, and H. G. Dehmelt, "Preservation of spin state in free atom-inert surface collisions," *Bull. Am. Phys. Soc.*, vol. 3, p. 9, January 1958.

[17] W. B. Hawkins, "Optical pumping, buffer gases, and walls," *Proc. 11th Annual Frequency Control Symp.*, pp. 318–323, May 1957.

[18] R. M. Whitehorn, "Gas cell frequency standards using buffer gases and buffer walls," *Proc. 13th Annual Frequency Control Symp.*, pp. 648–654, May 1959.

[19] N. F. Ramsey, "Resonance experiments in successive oscillatory fields," *Rev. Sci. Instr.*, vol. 28, pp. 57–58, January 1957.

[20] D. Kleppner, N. F. Ramsey, and P. Fjelstadt, "Broken atomic beam resonance experiment," *Phys. Rev. Lett.*, vol. 1, pp. 232–233, October 1958.

[21] H. Goldenberg, D. Kleppner, and N. F. Ramsey, "Atomic beam resonance experiments with stored beams," *Phys. Rev.*, vol. 123, pp. 530–537, July 1961.

[22] J. Gordon, H. Zeiger, and C. Townes, "Molecular microwave oscillator and new hyperfine structure in the microwave spectrum of NH_3," *Phys. Rev.*, vol. 95, pp. 282–284, July 1954.

[23] N. Basov and A. Prokhorov, "The use of molecular beams in the study of the spectra of molecules by radio spectroscopy," *J. Exp. Theoret. Phys. (U.S.S.R.)*, vol. 27, pp. 431–438, 1954.

[24] J. Gordon, H. Zeiger, and C. Townes, "The maser—new type of microwave amplifier, frequency standard, and spectrometer," *Phys. Rev.*, vol. 99, pp. 1264–1274, August 1955.

[25] H. Lyons, "Microwave spectroscopic frequency and time standards," *Electronic Engrg.*, vol. 68, p. 251, March 1949.

[26] C. Cleeton and N. Williams, "Electromagnetic waves of 1.1 cm wavelength and the absorption spectrum of ammonia," *Phys. Rev.*, vol. 45, pp. 234–237, February 1934.

[27] B. Bleaney and R. Penrose, "Ammonia spectrum in the 1 cm wavelength region," *Nature*, vol. 157, pp. 339–340, March 1946.

[28] R. Pound, "Electronic frequency stabilization of microwave oscillators," *Rev. Sci. Instr.*, vol. 17, pp. 490–505, November 1946.

[29] W. Smith, J. de Quevedo, R. Carter, and W. Bennett, "Frequency stabilization of microwave oscillators with spectral lines," *J. Appl. Phys.*, vol. 18, pp. 1112–1115, December 1947.

[30] W. Hershberger and L. Norton, "Frequency stabilization with microwave spectral lines," *RCA Review*, vol. 9, pp. 38–49, March 1948.

[31] J. Sherwood, H. Lyons, R. McCracken, and P. Kusch, "High frequency lines in the hfs spectrum of cesium," *Bull. Am. Phys. Soc.*, vol. 27, p. 43, 1952.

[32] H. Lyons, "Spectral lines as frequency standards," *Ann. N. Y. Acad. Sci.*, vol. 55, pp. 831–871, November 1952.

[33] R. Mockler, R. Beehler, and J. Barnes, "An evaluation of a cesium beam frequency standard," in *Quantum Electronics, A Symposium*, C. H. Townes, Ed. New York: Columbia University Press, 1960, pp. 127–145.

[34] L. Essen and J. Parry, "Atomic standard of frequency and time interval," *Nature*, vol. 176, pp. 280–282, August 1955.

[35] W. Markowitz, R. Hall, L. Essen, and J. Parry, "Frequency of cesium in terms of ephemeris time," *Phys. Rev. Lett.*, vol. 1, pp. 105–107, August 1958.

[36] S. Kalra, R. Bailey, and H. Daams, "Cesium beam standard of frequency," *Can. J. Phys.*, vol. 36, pp. 1442–1443, 1958.

[37] P. Kartaschoff, J. Bonanomi, and J. de Prins, "Cesium frequency standards: Description and results," *Helv. Phys. Acta*, vol. 33, pp. 969–973, 1960.

[38] J. R. Zacharias, J. G. Yates, and R. D. Haun, Jr., "An atomic frequency standard," *Proc. IRE (Abstract)*, vol.43, p. 364, March 1955.

[39] W. Mainberger, "Primary frequency standard using resonant cesium," *Electronics*, vol. 31, pp. 80–85, November 1958.

[40] A. McCoubrey, "Results of comparison: Atomichron–British cesium beam standard," *Proc. 12th Annual Frequency Control Symp.*, pp. pp. 648–664, 1958.

[41] L. Essen and J. Parry, "An improved cesium frequency and time standard," *Nature*, vol. 184, p. 1791, December 1959.

[42] R. E. Beehler and D. J. Glaze, "The performance and capability of cesium beam frequency standards at the National Bureau of Standards," *IEEE Trans. on Instrumentation and Measurement*, vol. IM-15, pp. 48–55, March–June, 1966.

[43] A. Mungall, H. Daams, and R. Bailey, "The Canadian cesium beam frequency standard," *Proc. 20th Annual Frequency Control Symp.*, pp. 436–447, 1966.

[44] L. Bodily, D. Hartke, and R. Hyatt, "World-wide time synchronization, 1966," *Hewlett-Packard J.*, vol. 17, no. 12, pp. 13–20, August 1966.

[45] R. Beehler, D. Halford, R. Harrach, D. Allan, D. Glaze, C. Snider, J. Barnes, R. Vessot, H. Peters, J. Vanier, L. Cutler, and L. Bodily, "An intercomparison of atomic standards," *Proc. IEEE (Letters)*, vol. 54, pp. 301–302, February 1966.

[46] Model 5060 Data Sheet, Hewlett-Packard Company, Palo Alto, Calif., October 1, 1966.

[47] NC 3501 Data Sheet. National Company, Melrose, Mass.

[48] L. Bodily, "Performance characteristics of a portable cesium beam standard," *Proc. 20th Annual Frequency Control Symp.*, pp. 448–463, 1966.

[49] J. Holloway and R. Sanborn, "Characteristics of a high performance cesium beam frequency standard," *Proc. 19th Annual Frequency Control Symp.*, pp. 344–368, 1965.

[50] P. Kusch, "Precision atomic beam techniques," *Proc. 11th Annual Frequency Control Symp.*, pp. 373–384, 1957.

[51] J. Bonanomi, "A thallium beam frequency standard," *IRE Trans. on Instrumentation*, vol. I-11, pp. 212–215, December 1962.

[52] R. Beehler and D. Glaze, "Experimental evaluation of a thallium beam frequency standard," *Proc 17th Annual Frequency Control Symp.*, pp. 392–407, 1963.

[53] R. Lacey, "A thallium atomic beam tube for frequency control," *Proc. 20th Annual Frequency Control Symp.*, pp. 416–423, 1966.

[54] M. Arditi and T. Carver, "Optical detection of zero-field hyperfine splitting of Na^{23}," *Phys. Rev.*, vol. 109, pp. 1012–1013, February 1958.

[55] W. Bell and A. Bloom, "Optically detected field-independent transition in sodium vapor," *Phys. Rev.*, vol. 109, pp. 219–220, January 1958.

[56] E. Beaty, P. Bender, and A. Chi, "Narrow hyperfine absorption lines

of Cs^{133} in various buffer gases," *Phys. Rev.*, vol. 112, pp. 450–451, October 1958.
[57] M. Arditi and T. Carver, "Frequency shift of the zero-field hyperfine splitting of Cs^{133} produced by various buffer gases," *Phys. Rev.*, vol. 112, p. 449, October 1958.
[58] M. Arditi, "Evaluation of a breadboard gas cell frequency standard," *Proc. 13th Annual Frequency Control Symp.*, pp. 655–667, 1959.
[59] T. Carver, "Rubidium oscillator experiments," *Proc 11th Annual Frequency Control Symp.*, pp. 307–317, 1957.
[60] P. Bender, E. Beaty, and A. Chi, "Optical detection of narrow Rb^{87} hyperfine absorption lines," *Phys. Rev. Lett.*, vol. 1, p. 311–313, November 1958.
[61] R. J. Carpenter, E. C. Beaty, P. L. Bender, S. Saito, and R. O. Stone, "A prototype rubidium vapor frequency standard," *IRE Trans. on Instrumentation*, vol. I-9, pp. 132–135, September 1960.
[62] M. Arditi and T. Carver, "Pressure, light, and temperature shifts in optical detection of 0-0 hyperfine resonance of alkali metals," *Phys. Rev.*, vol. 124, pp. 800–809, November 1961.
[63] Manufacturer's specification sheets.
[64] H. Goldenberg, D. Kleppner, and N. Ramsey, "Atomic hydrogen maser," *Phys. Rev. Lett.*, vol. 5, pp. 361–362, October 1960.
[65] D. Kleppner, H. Goldenberg, and N. Ramsey, "Theory of the hydrogen maser," *Phys. Rev.*, vol. 126, pp. 603–615, April 1962.
[66] S. Crampton, D. Kleppner, and N. Ramsey, "Hyperfine separation of ground-state atomic hydrogen," *Phys. Rev. Lett.*, vol. 11, pp. 338–340, October 1963.
[67] J. Vanier, H. E. Peters, and R. F. C. Vessot, "Exchange collisions, wall interactions, and resettability of the hydrogen maser," *IEEE Trans. on Instrumentation and Measurement*, vol. IM-13, pp. 185–188, December 1964.
[68] C. Menoud and J. Racine, "Atomic hydrogen maser, description and preliminary results," *Helv. Phys. Acta*, vol. 35, pp. 562–567, September–October 1962.
[69] R. F. C. Vessot and H. E. Peters, "Design and performance of an atomic hydrogen maser," *IRE Trans. on Instrumentation*, vol. I-11, pp. 183–187, December 1962.
[70] H. Andresen and E. Pannaci, "Servo-controlled hydrogen maser cavity tuning," *Proc. 20th Annual Frequency Control Symp.*, pp. 402–415, April 1966.
[71] R. Vessot, H. Peters, J. Vanier, R. Beehler, D. Halford, R. Harrach, D. Allan, D. Glaze, C. Snider, J. Barnes, L. Cutler, and L. Bodily, "An intercomparison of hydrogen and cesium frequency standards," *IEEE Trans. on Instrumentation and Measurements*, vol. IM-15, pp. 165–176, December 1966.

Reprinted from the PROCEEDINGS OF THE IEEE
VOL. 55, NO. 6, JUNE, 1967
pp. 792-805

463-560 O - 72 - 12

PRESSURE SHIFT AND BROADENING OF METHANE LINE AT 3.39 μ STUDIED BY LASER-SATURATED MOLECULAR ABSORPTION*

R. L. Barger and J. L. Hall
Joint Institute for Laboratory Astrophysics,† Boulder, Colorado 80302
(Received 21 October 1968)

We study broadening and the anomalously small shift of a 3.39-μ rotation-vibration line of methane at millitorr pressures. Saturation by the laser intracavity field allows investigation of the very sharp natural linewidth, without Doppler broadening. Two lasers were independently locked to this transition with an offset of less than ±1 kHz, a reproducibility of $\pm 1 \times 10^{11}$.

By the use of laser saturation of molecular absorption, we have obtained at 3.39 μ an emission feature in laser power centered on a methane vibration-rotation line. In this paper we report measurements of the broadening and exceptionally low shift of the line due to pressure, temperature, and other experimental conditions, and measurements of the reproducibility of line center. The emission feature is a very sharp Lorentzian line, its width being determined by collisional and interaction time effects. In this preliminary work we have obtained widths as narrow as 150 kHz half-width at half-maximum intensity, i.e., $\Delta\nu_{1/2}/\nu \approx 1 \times 10^{-9}$ (the ultimate attainable half-width, as would be determined by the radiative lifetime, is $\Delta\nu_{1/2}/\nu \approx 1 \times 10^{-12}$). We have stabilized to the line center with a reproducibility of better than $\pm 1 \times 10^{-11}$. This reproducibility is 2.5 orders of magnitude better than that of the primary standard of length, which is defined by the 6057-Å line of Kr^{86}.

Several reviews of laser-stabilizing methods are available.[1,2] For a discussion of laser-wavelength standard accuracy problems the reader is referred to a recent paper by one of us (J.L.H.).[3] Essentially all previous absolute methods rely on an atomic transition as the fundamental wavelength reference. Molecules are attractive as the reference on several counts. First, molecular vibration-rotation transitions have characteristically longer radiative lifetimes. Second, we deal with absorption from a thermally accessible state, a fact which will be an important aid to understanding the residual effects of collisions. Third, we may select a system with a favorable branching ratio to maximize the absorption per unit linewidth, and fourth, as mentioned by many workers,[4] the richness of molecular spectra makes more likely an "accidental" coincidence within the 2- or 3-ppm tuning range of the typical laser. By now, many such overlaps are known.[4,5]

The CH_4 absorption of the 3.39-μ radiation of the helium-neon laser is a remarkably happy case.[6] It is a transition [$P(7)$ line of the ν_3 band] which starts from a level that is well populated thermally even at liquid-nitrogen temperatures and below. The natural lifetime is estimated to be about 10 msec.[7] The absorption coefficient is very large, about 0.18 cm^{-1} $Torr^{-1}$,[7] so that relatively modest laser power densities are required to obtain usable saturation. The transition lies about 100 MHz blue of the helium-neon line center,[7] but one can pressure-shift the laser into very good coincidence with the methane absorption. See Fig. 1(a). In addition, the high helium pressure (≃12 Torr) greatly increases the laser homogeneous width and thus allows single frequency oscillation. Even at these pressures the 3.39-μ laser line has high gain, which allows the use of an intracavity gas cell to obtain high power density and high sensitivity to small absorption. Uehara, Sakurai, and Shimoda[8] have shown that this methane line is also free from Stark shift. Magnetic interaction with the earth's field is expected to produce about $\frac{1}{2}$ kHz of splitting. Spin-rotation interaction may be of the order of 3 kHz.

Our work is based on the synthesis of this background with an idea of Lee and Skolnick,[9] who reported saturation of the absorption of pure neon placed within the cavity of a He-Ne oscillator. Their point is that the absorption profile is so sharp that a Doppler shift is generally required to bring the laser frequency into resonance with the absorber. As the laser frequency approaches the natural (molecular) absorption frequency, absorbers with smaller longitudinal velocities are involved. Ultimately, at line center, both counter-running cavity waves interact with the same zero-longitudinal-velocity subgroup. For suitably large cavity power density, this doubled interaction rate will reduce the actual number of resonant absorbers and thus give rise to an

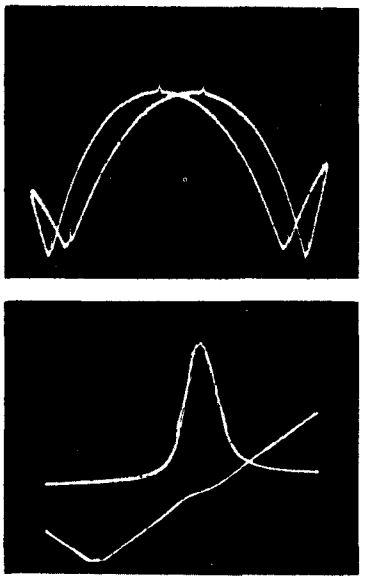

FIG. 1. (a) Output power versus laser-cavity tuning. Only the upper 20% of the 1-mW output is displayed in the full ten divisions. The horizontal axis is calibrated as 28 MHz/div by the cusps where the order of the interferometer changes by 1 and the frequency jumps by 200 MHz. The saturated absorption peak is about 2% amplitude and 400 kHz wide, and is nicely centered on the Ne^{20} Doppler gain curve. (b) Upper trace is output power versus cavity tuning, similar to (a) except here the scale is 2 MHz/div. Lower trace (ordinate is the "optical" oscillation frequency (beat frequency against a local oscillator laser) versus the same cavity sweep as the upper trace. The frequency "hangup" occurs as the oscillation frequency is strongly pulled by the methane's rapidly varying phase shift.

"emission" feature precisely at line center. It is important to note that even if the two running waves are of unequal intensity, there is no systematic shift of line center, assuming the cell to be isothermal. The linewidth of the interaction is seen to be the homogeneous width due to collisions, natural decay rate, intensity broadening, Stark and Zeeman broadening, etc. For very favorable absorber systems, nearly free from the above-mentioned sources of broadening, one may observe the linewidth anticipated on the basis of the finite interaction time. This time should scale proportional to the laser spot size and inversely with the thermal velocity of the absorber molecules. In the experiments to be described, the corresponding partial linewidth is in the neighborhood of 100 kHz half-width at half-maximum (1×10^9).

Experiment. —Since much of our success in these measurements is directly due to the novel experimental techniques employed, it may be of interest briefly to summarize the salient features of the apparatus. To minimize environmental disturbances, all experiments have been carried out in an isolated underground laboratory (vault). The three lasers, Nos. 1 and 3 with and No. 2 without methane cells, and the methane-gas handling system are mounted on a 3-ton, 4-ft×12-ft, cast-iron–surface table. The cavities of lasers Nos. 1 and 3 are about 60 cm long. They are spaced with three fused-silica rods, 19 mm in diameter, which are cemented into lightweight aluminum plates with an acoustically lossy epoxy. The cavity is divided roughly equally between the rf excited helium-neon gain cell and the methane absorption cell. Power densities up to $2\frac{1}{2}$ W/cm^2 are obtained in the methane cell. Mirrors are scanned with electrostrictive crystals to give frequency modulation at frequencies up to 10 kHz. With methane inside the cavity, the phase shift accompanying the extremely sharp absorption slows the cavity tuning rate at line center by a factor of about 3. See Fig. 1(b). Thus to obtain a proper line shape we must program the scan over the line as a frequency input rather than a cavity-tuning input.

Excellent automatic frequency locks are obtained with specially designed high-stability servo systems. We lock laser No. 1 to line center (zero-slope point) by using the central zero of the first derivative with respect to frequency of the laser power. Using laser No. 2 as a local oscillator, we obtain beat frequencies between lasers Nos. 1 and 2 and between lasers Nos. 2 and 3. Signals proportional to beat frequency are obtained with linear frequency-to-voltage converters and fed into the servos to perform the locks. We call this technique "frequency-offset locking." With the No. 1-No. 2 frequency-offset lock held constant at, say, 5000.0 kHz, the frequency of the No. 2-No. 3 can be varied from $\frac{1}{4}$ to about 15 MHz to scan over the methane line of the No. 3 laser. Frequency-offset locking yields beat frequencies with about ±50-Hz fluctuations for a $\frac{1}{10}$-sec averaging time. The line-center lock has total frequency excursions of about 1 kHz. Thus, with the "frequency-offset locking" technique, stability can be transferred from one laser to another with almost no loss of precision.[10] (The average offset frequencies drift by less than 1 kHz/h.)

Data have been taken in the form of X-Y plots of the derivative with respect to frequency of laser No. 3's output power. Some representative

first-derivative line shapes are shown in Fig. 2. The modulation used, 50-kHz peak-to-peak, is small enough that no important correction for finite modulation width is required. The linewidth was measured at 15 methane pressures between 0.02 and 48 mTorr. In another set of experiments at a constant 13-mTorr methane pressure, xenon was used as the pressure-broadening agent. Xenon pressure ranged from 0 to 88 mTorr. The resulting line shapes, similar to those of Fig. 2, are all accurately described by the Lorentz derivative function. The broadening results may be well expressed by the following (least-squares fitted) linear relation

$$\Delta\nu_{\frac{1}{2}} = 150\ \text{kHz} + (13.9 \pm 0.4\ \text{kHz/mTorr}) \times P_{\text{Xe}} + (16.3 \pm 0.6\ \text{kHz/mTorr}) \times P_{\text{CH}_4}.$$

Here $\Delta\nu_{1/2}$ is the half-width at half-maximum intensity of the Lorentz power signal. This half-width, according to the arguments given by Bennett,[11] corresponds approximately to twice the half-width of each Lorentz hole. Thus for pure CH_4 self-broadening we report 8.1 ± 0.3 kHz/mTorr as the "phase-memory" linewidth Γ_2 ($\Gamma_2 = 1/\pi T_2$ in the usual resonance jargon, T_2 being the polarization coherent relaxation time).

Gerritsen and Ahmed[12] report the slope of the absorption linewidth versus pressure to be 7.4 $\pm$ 0.5 kHz/mTorr for pure methane. The small difference between these two results, 0.7 ± 0.8 kHz/mTorr, may well arise from a small error in absolute calibration of the pressure measurement. (Our measurements were made with a high-pressure ion gauge calibrated for methane against a McCloud gauge using a capacitance manometer as the null detector.) However, the sign of the difference is not inconsistent with the possibility that phase and frequency shifts of interest to us can arise from weaker collisions than those which affect the high-pressure experiments of Ref. 12. It will be very interesting for us to study the signal size (as well as linewidth) as a function of saturation parameter and pressure, since we should be able to determine separately the rate of energy loss, Γ_1, and the rate of loss of phase coherence, Γ_2.

We now turn to the interesting question of the line shift with pressure, power, and other experimental conditions, that is, to the question of accuracy and freedom from spurious systematic frequency offsets. We are easily able to measure pressure-induced broadening as reported above. However even with excellent digital data (similar to those illustrated in Fig. 2) and computer line-shape analysis, we are not yet able reliably to measure the pressure-induced shift

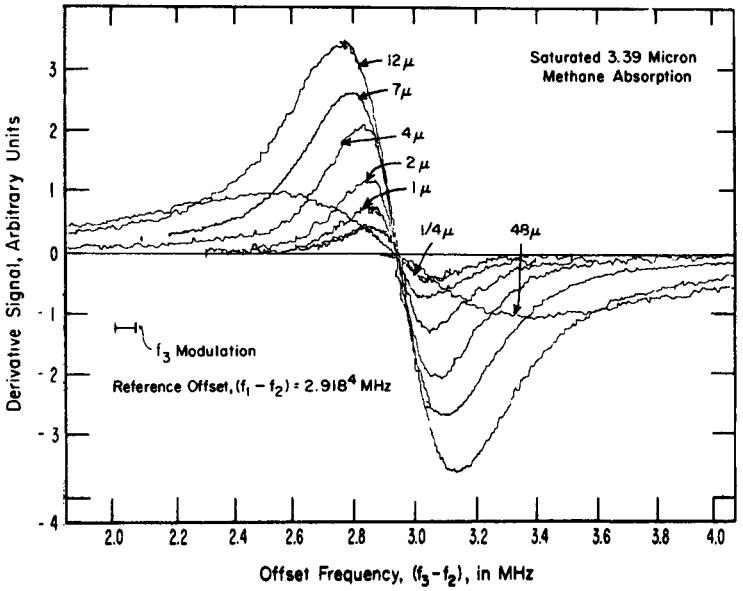

FIG. 2. First derivative of the output power of laser No. 3 versus offset-lock frequency $f_3 - f_2$. The several curves are labeled by the CH_4 (in mTorr) in laser No. 3. Laser No. 1 was stabilized to the center of its methane line. Laser No. 2, local oscillator for both optical-heterodyne detectors, was stabilized against laser No. 1 with a 2.918⁴-MHz offset. The curves are very accurately described by the Lorentz-derivative function.

in pure CH_4. The present best value is 75 ± 150 Hz/mTorr. Thus the shift-to-width ratio for CH_4-CH_4 interaction is 1:200 rather than the roughly 1:4 ratio usually obtained for Van der Waals interactions. Our result, an upper limit, is obviously already pleasant in connection with wavelength-standards applications of this work. We believe this remarkably small shift can be directly understood in terms of the high symmetry of the methane molecule, the beautifully regular spacing of the relevant rotational energy levels, and the low kinetic energy of the collision partners. Interestingly enough, xenon also gives an unmeasurable shift, 29 ± 150 Hz/mTorr.

To develop some appreciation of the accuracy of the lock-to-line center, we have looked for a frequency difference between lasers Nos. 1 and 3 with the lasers independently line-center locked. The finite slope of the laser power curves beneath the methane peaks contributed less than $\frac{1}{2}$-kHz offset. For methane pressures below about 10 mTorr, we observe an asymmetric power broadening.[13] This disappears for low power density (below $\sim\frac{1}{2}$ W/cm^2), where adequate signal-to-noise ratio is still obtained. Shift of the zero-slope point is about 1 kHz at a power density of 1 W/cm^2. Thus, we have extrapolated to the limit of low power for various methane pressures. We find no frequency difference to within our experimental uncertainties of ± 1 kHz between the two independently locked methane saturated-absorber systems. This demonstrated reproducibility of ± 1 part in 10^{11} is better by 2.5 orders of magnitude than the present primary standard of length, and to our knowledge is 2 orders of magnitude better than any figure previously reported for wavelength reproducibility.[14]

Some early experiments with two separated interaction regions ("Ramsey two-cavity method") were partially successful in demonstrating the expected interference effects at very low pressures, but the relative phase of the excitation in the two interaction zones could not be adequately controlled in those first experiments. Probably the two most interesting directions for further immediate progress are the following: (a) to enlarge the beam diameter in the interaction region and to refrigerate the methane, both of which sharpen the resonance, and (b) to build a ratio-type experiment outside the laser cavity. Our interesting, but still preliminary, results on the second approach will be reported at a later time. In addition to the interest as a potential wavelength standard, these techniques should allow study of gas-phase collision effects with a sensitivity never before available.

The authors are happy to express their appreciation to their colleagues R. N. Zare and P. L. Bender for their interest and their useful comments. One of us (J.L.H.) has profited greatly from several conversations with D. W. Halford on frequency standards and related topics.

---

*Work supported in part by National Aeronautics and Space Administration, Advanced Development Division, Goddard Space Flight Center, Greenbelt, Md., and in part by the National Bureau of Standards, of which the authors are staff members.

†Of the University of Colorado and the National Bureau of Standards.

[1]A. D. White, IEEE J. Quantum Electron. QE-1, 349 (1965).

[2]G. Birnbaum, Proc. IEEE 55, 1015 (1967).

[3]J. L. Hall, IEEE J. Quantum Electron. QE-4 (to be published).

[4]R. N. Zare (Joint Institute of Laboratory Astrophysics), private communication; K. M. Baird (National Research Council of Canada, Ottawa, Canada), private communication; G. Gould (Polytechnic Institute of Brooklyn), private communication; V. P. Chebotayev, in the Proceedings of the Fifth International Conference on Quantum Electronics, Miami, Florida, May, 1968 (to be published).

[5]C. B. Moore, to be published.

[6]Methane has also been suggested for an absolute standard by K. Shimoda, in Conference on Precision Electro-Magnetic Measurements, Boulder, 1968, U. S. Atomic Energy Commission Report No. CONF 66 0644 (U. S. Government Printing Office, Washington, D. C., 1968).

[7]H. J. Gerritsen, in the Proceedings of the Third International Congress on Quantum Electronics, Paris, 1963, edited by P. Grivet and N. Bloembergen (Columbia University Press, N.Y., 1964), p. 581.

[8]K. Uehara, K. Sakurai, and K. Shimoda, to be published. Result quoted in Ref. 6.

[9]P. H. Lee and M. L. Skolnick, Appl. Phys. Letters 10, 303 (1967).

[10]These techniques will be reported in more detail at a later time.

[11]W. R. Bennett, Jr., in the Proceedings of the Third International Congress of Quantum Electronics, Paris, 1963, edited by P. Grivet and N. Bloembergen (Columbia University Press, N.Y., 1964), p. 450.

[12]H. J. Gerritsen and S. A. Ahmed, Phys. Letters 13, 41 (1964).

[13]These very interesting changes in line shape at high power are presently being investigated.

[14]Our "material" fractional linewidth is (within a factor of 2 or so) equal to that of the hydrogen maser, the present standard of excellence for reproducibility. Our cavity Q of 20×10^6 is about 50 times higher than that of a "typical" H maser. Our measured signal-to-noise ratio is about 50 dB in a 1-Hz bandwidth, about

the same as the H maser. However, a refrigerated photocell and a He-Ne optical preamplifier should each add about 10 dB. The higher cavity Q will require greater bandwidth in the cavity stabilizing feedback loop, but the signal-to-noise ratio should be ample. With a methane cell of four-times larger aperture, cooled to 76°K, we should closely approximate the H-maser stability.

Reprinted from
Physical Review Letters
Volume 22, No. 1
January 6, 1969

USE OF LASER-SATURATED ABSORPTION OF METHANE FOR LASER FREQUENCY STABILIZATION*

R. L. Barger and J. L. Hall
Joint Institute for Laboratory Astrophysics†
Boulder, Colorado

Using laser saturation of molecular absorption, we have obtained at 3.39 μ an emission feature in laser power centered on a methane vibration-rotation line [P(7) line of the ν_3 band].[1,2] We report here the results of using this feature to stabilize laser frequency. The width of this very sharp Lorentzian line is determined by collisional and interaction time effects. Methane collisional self-broadening is measured to be 8.1 ± 0.3 kHz/m Torr, and an upper limit for the exceptionally low self-induced pressure shift is 75 ± 150 Hz/m Torr. We have obtained widths as narrow as 150 kHz halfwidth at half-maximum intensity, i.e. $\Delta\nu_{1/2}/\nu \approx 1\times10^{-9}$. Of this, about 100 kHz is due to time of flight across the laser beam; the remainder is due to power broadening. The asymmetry previously observed[2] in power broadening has been reduced to a negligible level. Beat frequency measurements between two independent, dissimilar methane stabilized lasers show that we have stabilized laser frequency to line center with a reproducibility of better than ± 1×10^{-11}. An analysis of the frequency noise spectrum is given in the figure.

* Supported in part by NASA, Advanced Development Division, Goddard Space Flight Center, Greenbelt, Md. and in part by the National Bureau of Standards, of which the authors are staff members.

† of the University of Colorado and the National Bureau of Standards.

1. J. L. Hall, IEEE J. Quantum Electron. QE-4, 638 (1968).

2. R. L. Barger and J. L. Hall, Phys. Rev. Letters 22, 4 (1969).

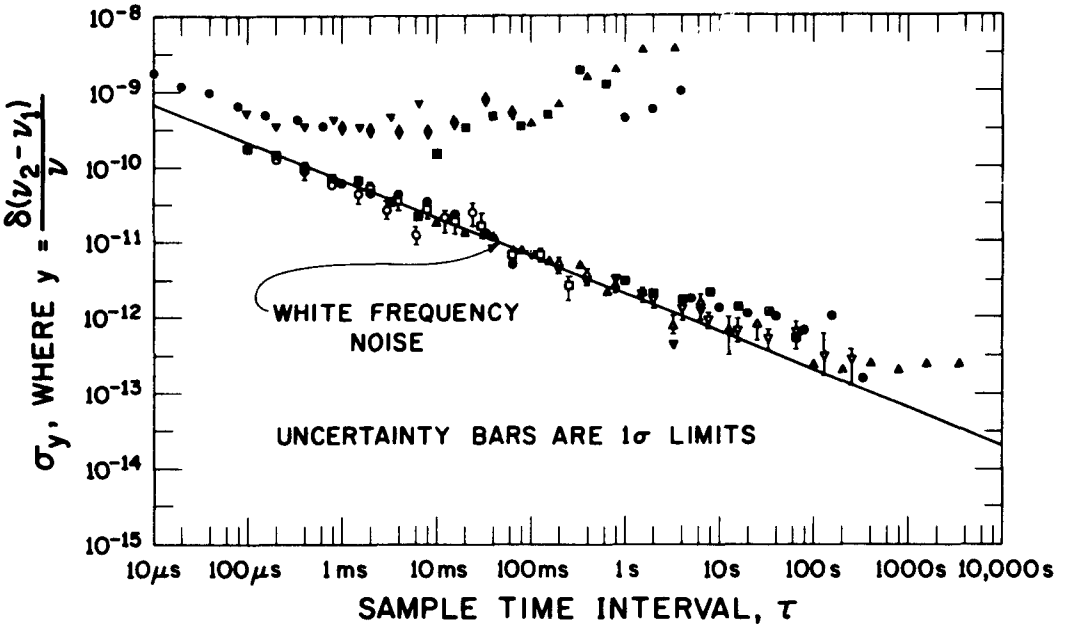

Frequency fluctuations versus sample time interval of (a) Beat between two free running He-Ne lasers (upper set of measurement points). (b) Beat between two He-Ne lasers, each independently controlled by a methane absorption cell. (Lower set of measurement points).

Plotted is the Allan variance.* Number of samples N = 2; ratio of dead time plus sample time to sample time r = 1; bandwidth B > 1 MHz.

*D. Allan, Proc. IEEE 54, p. 221 (1966).

Reprinted from: Proc. of the 23rd Ann. Symp. on Freq. Cont. (U. S. Army Electronics Command, Ft. Monmouth, N. J., May 6-8, 1969) p. 306 (May 1969)

The Atomic Hydrogen Maser

Norman F. Ramsey [1]

The atomic hydrogen maser is described. In this device hydrogen atoms in the upper hyperfine state are focused onto the entrance aperture of a teflon coated quartz bulb in which the atoms are stored for about a second. This bulb is surrounded by a cylindrical radio-frequency cavity. When the cavity is tuned to the hyperfine frequency of atomic hydrogen, maser radiation is produced. Due to the large line Q resulting from the long storage time, the radiation is highly stable in frequency. Results are given of theoretical calculations on the threshold flux of atoms required for maser oscillations, on the various relaxation processes that limit the effective storage time, and on the possible sources of frequency shifts of the maser. Results are given on the relative stability of two hydrogen masers. Measurements of the atomic hyperfine frequency of atomic hydrogen and deuterium give $\Delta_H = 1{,}420{,}405{,}751.800 \pm 0.028$ cps and $\Delta_D = 327{,}384{,}352.5 \pm 1.0$ cps on the A.1 time scale with $\Delta^{Cs} = 9{,}192{,}631{,}770.0$ cps. The method by which the deuterium has been measured depends upon the effect of a deuterium magnetic resonance transition upon the intensity of the hydrogen maser oscillation amplitude when a mixture of hydrogen and deuterium is used. This method should be capable of extension to a number of different atoms. The hydrogen maser apparatus has been used to measure the spin exchange collision cross section between atomic hydrogen and a number of different gases. Results of some of these measurements are reported. Measurements of the dependence of the hydrogen hyperfine frequency upon a strong externally applied electrostatic field are given.

Metrologia, Vol. 1, No. 1, 7–15 (January 1965).

Manuscript received October 24, 1964

[1] Lyman Physics Laboratory, Harvard University, Cambridge, Mass. 02138, U.S.A.

Automatic Tuning of Hydrogen Masers

H. Hellwig and E. Pannaci

Beam-intensity modulation based on varying the power of the hydrogen RF-discharge was used in an automatic tuning system. Two hydrogen masers were tuned automatically and simultaneously. Their beat frequency was measured to have a long-term stability of 3×10^{-13}.

Proc. IEEE, Vol. 55, No. 4, 551-552 (April 1967).

ON THE NATURAL SHIFT OF A RESONANCE FREQUENCY
NBS TECHNICAL NOTE 346

Robert J. Harrach
National Bureau of Standards, Boulder, Colorado

September 29, 1966

ABSTRACT

The natural resonance frequency shift, caused by the transition-inducing radiation field, is examined for a magnetic dipole transition between hyperfine structure levels in the ground state of a thallium atom. A calculation predicts, for an atomic beam experiment, a natural shift magnitude of 1.4 parts in 10^{10} of the thallium resonance frequency, per mW/Oe. In the experiment, frequency shifts caused by overlap of neighboring resonances were observed, but the natural shift was unresolved, indicating that its size is more than an order of magnitude below the calculated value. Subsequently it has been shown that the natural shift was inhibited by the particular radiation field mode used in the experiment. When the theory correctly takes this mode into account, the calculated natural frequency shift is consistent with the experimental results.

Key Words: Atomic Beam, Frequency Shift, Radiation Field, Resonance, Thallium

The Relative Merits of Atomic Frequency Standards

A. O. McCoubrey [1]

The relative merits of atomic frequency standards based upon resonances in hydrogen, rubidium, or cesium depend upon the particular application and the specific requirement for each of several performance factors combined with physical characteristics. While the properties of an ideal atomic frequency standard may be established, practical instruments depart from the ideal as the result of compromises in the apparatus design and construction. The resonance line sharpness is an important factor which is dependent upon the apparatus; however, others may have a greater influence upon the essential characteristics. These include instrumental offsets due to atomic collisions with neighboring atoms or walls and magnetic fields. The intensity of the resonance signal is also essential in the determination of merit. These factors are discussed in relationship to hydrogen maser rubidium gas cell and cesium beam atomic frequency standards and the merits of each are compared. The possible merits of frequency standards based upon thallium beams are also discussed; however, a lack of extensive operating experience limits the knowledge in this case.

Proc. IEEE, 55, No. 6, 805–814 (June 1967).

Manuscript received March 31, 1967.

[1] Central Research Laboratory, Varian Associates, Palo Alto, Calif. 94304, U.S.A.

BARIUM OXIDE BEAM TUBE FREQUENCY STANDARD

Barium oxide beam tube frequency standard, H. Hellwig, R. McKnight, E. Pannaci and G. Wilson, Proc. 22nd Ann. Symp. on Freq. Contr. (U.S. Army Electronics Command, Ft. Monmouth, New Jersey, April 22-24, 1968), 529-538 (1968).

In a paper at the 21st Frequency Control Symposium last year a barium oxide molecular beam tube for frequency control application was proposed.[2]

Since that time further detailed theoretical investigations have been made and the experimental work has been initiated. An experimental model of the beam tube has been built with a physical size of 21-inch length and 3-inch diameter. Both dimensions could be reduced significantly if necessary. Special attention was paid to the oven, which is the main technical problem for a practical beam tube. The oven is a small iridium tube surrounded by a triple heat shield, and heated by electron bombardment. In its present design a power of 50 W is required to bring the oven to its operating temperature of 1500° C. A new design is expected to cut the necessary power in half.

The design of the beam tube and its characteristic performance data will be presented. This includes a discussion of the properties of the beam tube elements, the electronic system and the beam intensity, and lifetime expectations of the tube. The theoretical results will be summarized by stating the requirements for a frequency accuracy of better than 10^{-12} with respect to the unperturbed molecular transition frequency.

The barium oxide molecular beam tube, currently being developed in the Electronic Components Laboratory, is expected to have a frequency accuracy approaching 10^{-13} and, in addition, to be small in size and light in weight, which is a major consideration for a practical device.

---

2. H. Hellwig, Proc. 21st Annual Symposium on Frequency Control, 1967, p. 484.

UNITED STATES DEPARTMENT OF COMMERCE
Maurice H. Stans, Secretary
NATIONAL BUREAU OF STANDARDS • A. V. Astin, Director

TECHNICAL NOTE 373

ISSUED JUNE 1969

Nat. Bur. Stand. (U.S.), Tech. Note 373, 116 pages (June 1969)
CODEN: NBTNA

RADIO-FREQUENCY MEASUREMENTS IN THE NBS INSTITUTE FOR BASIC STANDARDS

[Abstracted to include only sections related to time and frequency.]

EDITED BY ROBERT S. POWERS
AND WILBERT F. SNYDER

Institute for Basic Standards
National Bureau of Standards
Boulder, Colorado 80302

CONTENTS

*Special Publication 300-Vol. 5, includes only sections relating to time and frequency (pp. 1-12-1 of Tech. Note 373).

ABSTRACT

This volume is a collection of diagrams, tables, and text material, which has been assembled to show the interrelationships between various radio frequency measurements made by the Institute for Basic Standards (IBS). In particular, the measurements are those which lead to services provided to the public or to other government agencies. These services include not only calibrations made for fees, but the broadcast services of the four NBS radio stations. Measurements made as part of the IBS research and development program are not included.

The information included is designed to give the users and potential users of the radio frequency services a clearer understanding of the origins of the measurement output of IBS in this field.

Key words: accuracy; calibration services; measurements; measurement techniques; radio frequency; uncertainties of measurement.

RADIO-FREQUENCY MEASUREMENTS IN THE NBS INSTITUTE FOR BASIC STANDARDS

Edited by Robert S. Powers
and Wilbert F. Snyder

INTRODUCTION

This volume is being published to give users of the National Bureau of Standards calibration services at radio frequencies a collection of information about the uncertainties given in Report of Calibration. It is a collection of diagrams, tables, and text material which shows the interrelationships among various radio frequency measurements made by the Institute for Basic Standards (IBS). In particular, the measurements are those which lead to services provided to the public or to other government agencies. These services include not only calibrations made for fees, but also the broadcast services of the four NBS radio stations. Measurements made as part of the IBS research and development program are not included.

It is hoped that this information will give the users and potential users of the radio-frequency services a clearer understanding of the origins of the measurement output of IBS in this field.

Generally, the sequence of measurements which leads to an output calibration or other service is shown by measurement flow charts. The notations of these charts are explained on page 5.

Each measurement may have errors arising from many sources. Typical values of these errors are given in one of two ways. In most cases, known or suspected sources of bias error are listed along with typical values of the random errors (or imprecision). In addition, in many instances, Error Flow Diagrams have been included to show more explicitly the way the various sources of uncertainty enter the measurement chain.

The study that led to these charts and tables was initiated to provide the management of the Institute and its divisions with a fairly detailed analysis of how the elements of the NBS part of the national system of radio measurements relate to each other. This was to help identify those parts of the "NBS subsystem of radio measurement" which could make the greatest contributions to improving the output of

the subsystem as a whole, if given the limited funds that are available. The principal suggestion arising from the study was that significant gains in the overall performance of the IBS system could result from improvement in the treatment and reporting of the known error sources. At this time, a program to improve the reporting of uncertainties is under way.

This information is current as of approximately January, 1969. It serves to update, and present in a different form, some of the information in NBS Technical Note 262.*

The term "error" means the difference between the value actually measured and some "true value" which would have been obtained from a hypothetical "perfect" experiment.** The term "uncertainty" refers to the range within which the metrologist believes the actual error, as defined above, does fall. Thus, an error does have a particular value, although the metrologist does not know that value; the uncertainty is a range of values specified by the metrologist to indicate his best knowledge about the likely value of the error.

The phrase "bias uncertainties" has been used rather than the more commonly used "systematic errors" to express the uncertainty about the sources of error listed. If the error itself could be evaluated, a correction would be made. The phrase "random error" is used to represent observed deviations of measurements from the mean of a set of measurements.

In perusing these pages, the reader will observe that the values for errors are sometimes shown with plus and minus signs (±) and sometimes without the signs. There is no significant difference between the two designations, it being mostly a matter of personal choice. Prepared material for this volume came from a number of sources, and no particular effort was made to bring the use of plus and minus signs into uniformity. To do so would have required extensive redrafting and retyping.

---

* NBS Technical Note 262, Accuracy in measurements and calibrations, 1965, edited by W. A. Wildhack, R. C. Powell, and H. L. Mason, issued June 15, 1965.

** The concept of "true value" is discussed in some detail by Churchill Eisenhart in his paper, Realistic evaluation of the precision and accuracy of instrument calibrating systems, J. Res. NBS 67C, 161 (1963).

Bias Uncertainties:

The uncertainties shown in these tables are typical values and in general may vary somewhat, depending on the range of frequency, the magnitude of the measurand (the quantity being measured), or the nature of the particular device being calibrated. Sometimes the magnitude is given as a single typical value and sometimes as a range of values. More details can be obtained from the person(s) listed under Personnel.

Where error flow diagrams were available, they were used in place of tables.

Random Errors:

In general, the number given for the random error represents approximately three times the estimated standard deviation (3σ) for a representative set of measurements.

Total Uncertainty:

The total uncertainty figure represents the sum of the estimated bias uncertainties and the 3σ random errors. Note that in a rather large number of the radio frequency measurements the random errors are quite negligible with respect to the bias uncertainties. The terms "limits of uncertainty" and "limits of error" are often used interchangeably with "total uncertainty."

Uncertainty quoted customer:

The uncertainty quoted to the customer is not always equal to the total uncertainty as described above. It is sometimes larger due to round-off, and sometimes larger to include an additional margin of safety in the estimate of possible error. Reporting practice is tending more and more toward quoting the actual number obtained as above, rather than the larger figures.

Notes:

The notes include information and comments which are intended to clarify the diagrams and charts or otherwise help the reader to understand some aspect of the measurement.

463-560 O - 72 - 13

References:

The lists of references are not intended to be complete, but rather to supply the reader with at least one source of published information concerning the measurement, as made by NBS. Sometimes no such sources are available. Where references are given, they often include extensive bibliographies on the subject measurement. Unpublished information can often be obtained from the personnel whose names are listed.

Personnel:

The name of the person(s) responsible for each measurement is given. Anyone requiring more detailed information about any of the measurements is invited to write to the appropriate person at

National Bureau of Standards
Institute for Basic Standards
Boulder, Colorado 80302

or telephone (303) 447-1000 and ask for the person named.

These names are also listed to give credit to those who helped to prepare the charts and other information on the various measurements.

MEASUREMENT REPRESENTATION

The Symbol :	Represents :
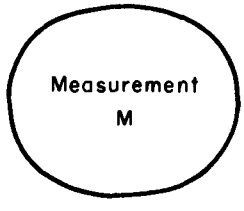	A measurement technique or device
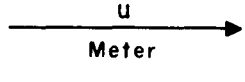	The output of one measurement and input to other measurements; e.g., a calibrated meter having uncertainty u. The uncertainty is expressed either as a percentage, as a fraction, or as a quantity with dimensions; e.g. "5%", "3×10^{-7}", or "10μsec". These outputs are usually available to NBS customers.
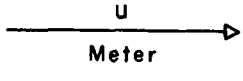	A measurement output available to NBS customers.

TIME AND FREQUENCY STANDARDS

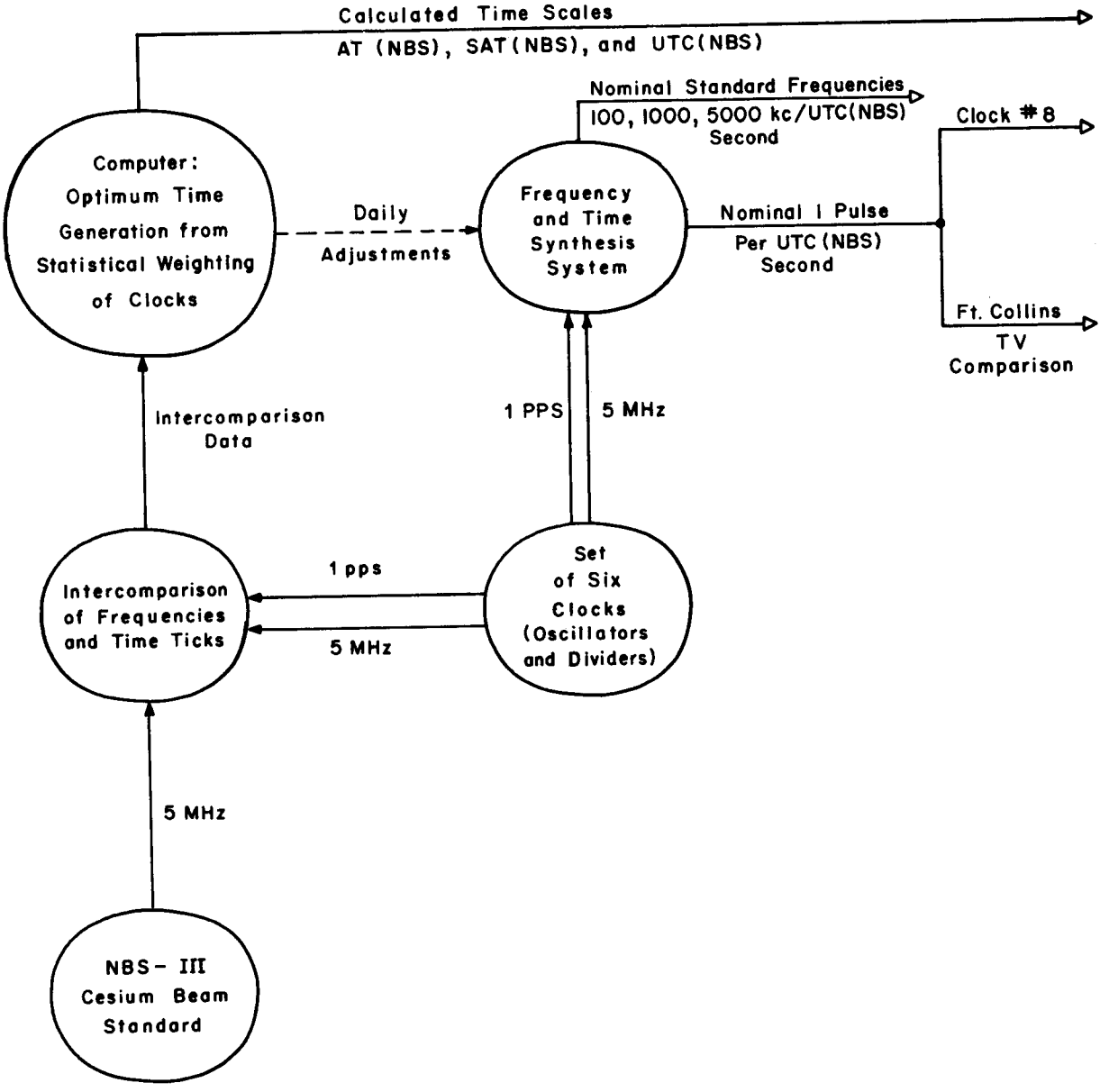

Bias Uncertainties:

Source of Uncertainty	Fractional Uncertainty	
Magnitude of $\overline{H(x)}$ (3σ limits)	0.3	(parts in 10^{12})
Overlap of neighboring transitions	1.0	
Use of $H(x)^2$ for $H^2(x)$	0.1	
Distortion arising from C-field nonuniformity	0.5	
Cavity mistuning	0.1	
Uncertainty in magnitude of cavity phase shift	3.0	
Doppler shifts	1.0	
Microwave power level	1.0	
Spectral purity of excitation	2.0	
Second harmonic distortion of servo modulation	0.5	
Miscellaneous servo system effects	2.0	
Multiplier chain transient phase shifts	1.0	
Random Errors (one hour averaging, 3σ):	0.5	
Total Uncertainty (square root of sum of squares):	4.7	(parts in 10^{12})

Notes: Error sources listed here contribute to the uncertainty in determining the frequency of a particular atomic state separation of the free cesium atom. The fractional uncertainty is given as 3σ limits for statistically determined quantities and by estimated extreme limits for other quantities.

The random error given above refers to the random variations between successive frequency comparisons (with one hour averaging time) between the NBS-III cesium beam machine and another highly stable oscillator. The contribution of NBS-III to the relative fluctuation between the pair of signals generated can be identified (approximately) because the stability of the second signal generator is known from comparisons with still other oscillators.

NBS-III cannot be operated continuously -- the NBS time scale is actually computed from the data obtained by daily intercomparisons between NBS-III and the signals from five sources (two crystal and three cesium) which do operate continuously. Data obtained from these intercomparisons may be

used to adjust the frequencies of the five working sources, when necessary, as shown on page 6.

The standard signals used to control the NBS broadcast stations are generated from one of the working oscillators. The AT (NBS) time scale is derived directly from the frequency of the cesium atom, as realized by NBS-III. The UTC (NBS) scale is generated from a signal having a frequency offset which has been promulgated by the Bureau International de l'Heure to make the time scale correspond approximately to the UT2 time scale.

USNO and NBS Time Coordination

On 1 October 1968 the epochs of the UTC (NBS) and the UTC (USNO) time scales were within one microsecond of each other. Since there was a slight rate difference between the master clocks at these two institutions, this time coincidence would not have continued. Hence, the USNO and the NBS agreed to each change their rates by nominally half the difference on 1 October 1968, and from thenceforth coordinate the rates so that the master clock at the USNO and the master clock at the NBS would remain near synchronous. It was initially felt and agreed upon that the time difference could be kept less than 5 μs.

In the figure (page 6), the abbreviation "pps" means "pulses per second."

Reference: R. E. Beehler and D. J. Glaze, The performance and capability of cesium beam frequency standards at the National Bureau of Standards, IEEE Trans. Instr. Meas., IM-15, 48 (1966).

Personnel: D. Halford
D. W. Allan

TIME AND FREQUENCY DISSEMINATION – WWVL

19.9 or 20.5 and 20.0 kc/(sec-UTC)
UTC (NBS) Time Scale

AT BOULDER :

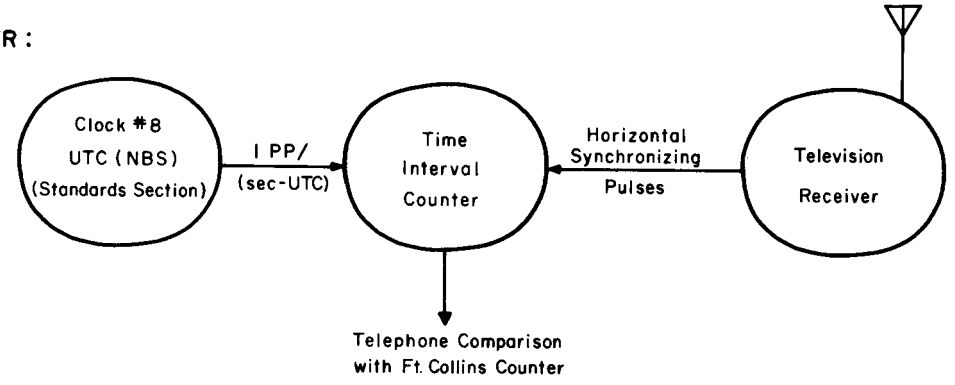

AT FT. COLLINS :

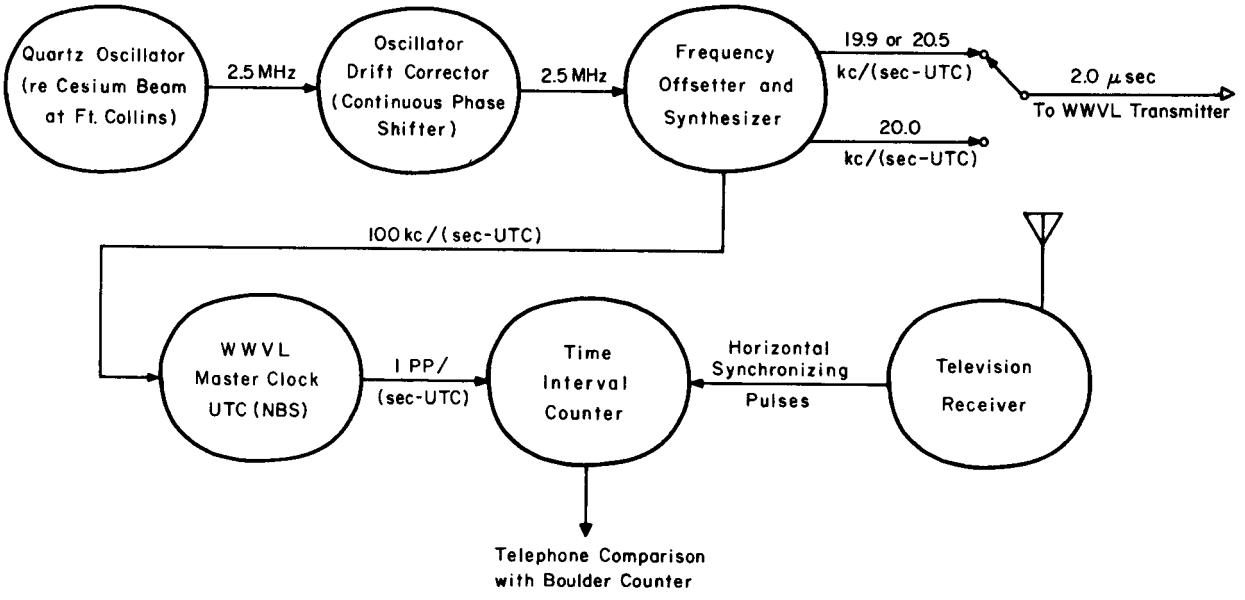

TIME AND FREQUENCY DISSEMINATION – WWVB

60 kHz SAT (NBS) Time Scale

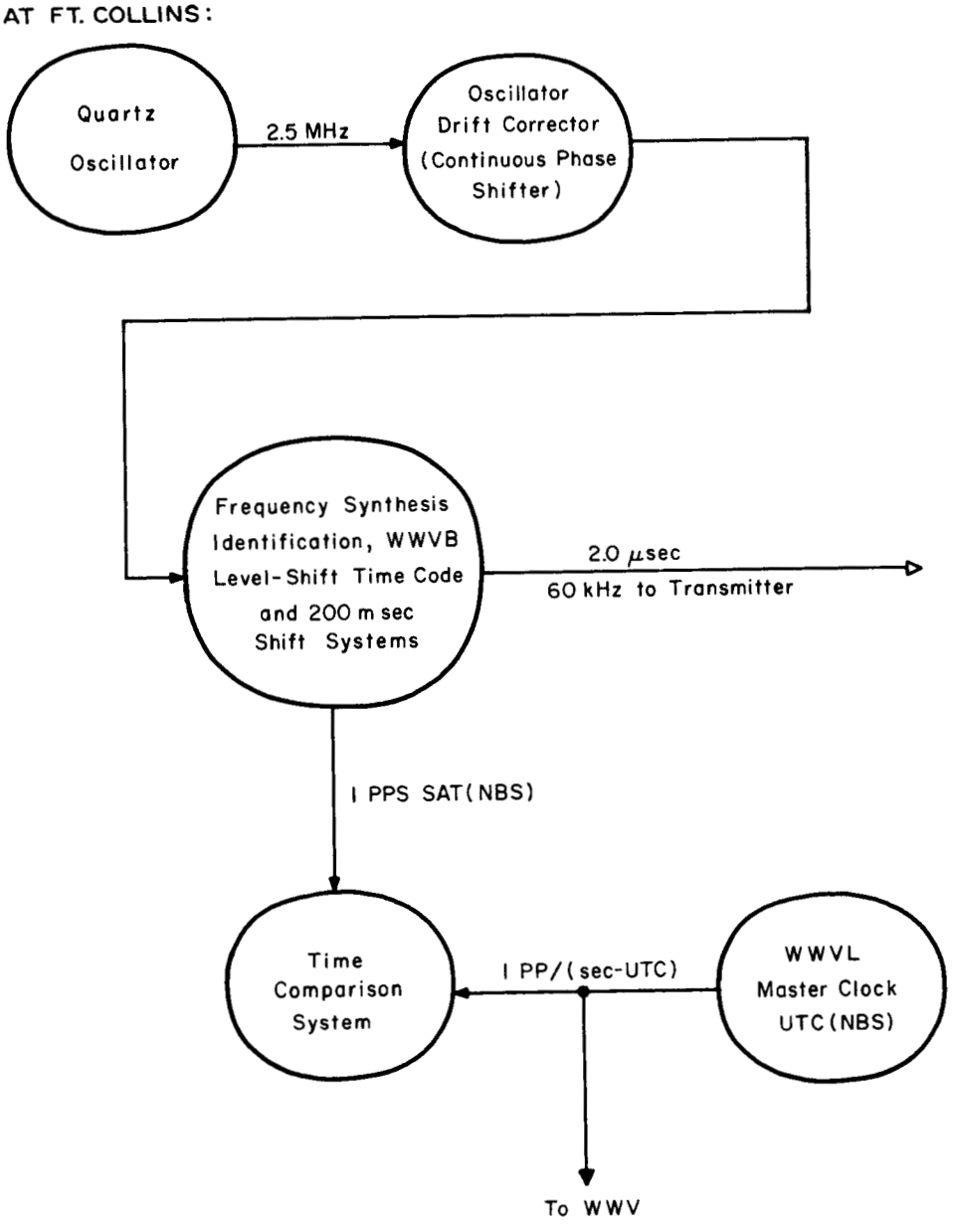

TIME AND FREQUENCY DISSEMINATION – WWV

2.5, 5, 10, 15, 20 & 25 Mc/(sec-UTC)
UTC (NBS) Time Scale

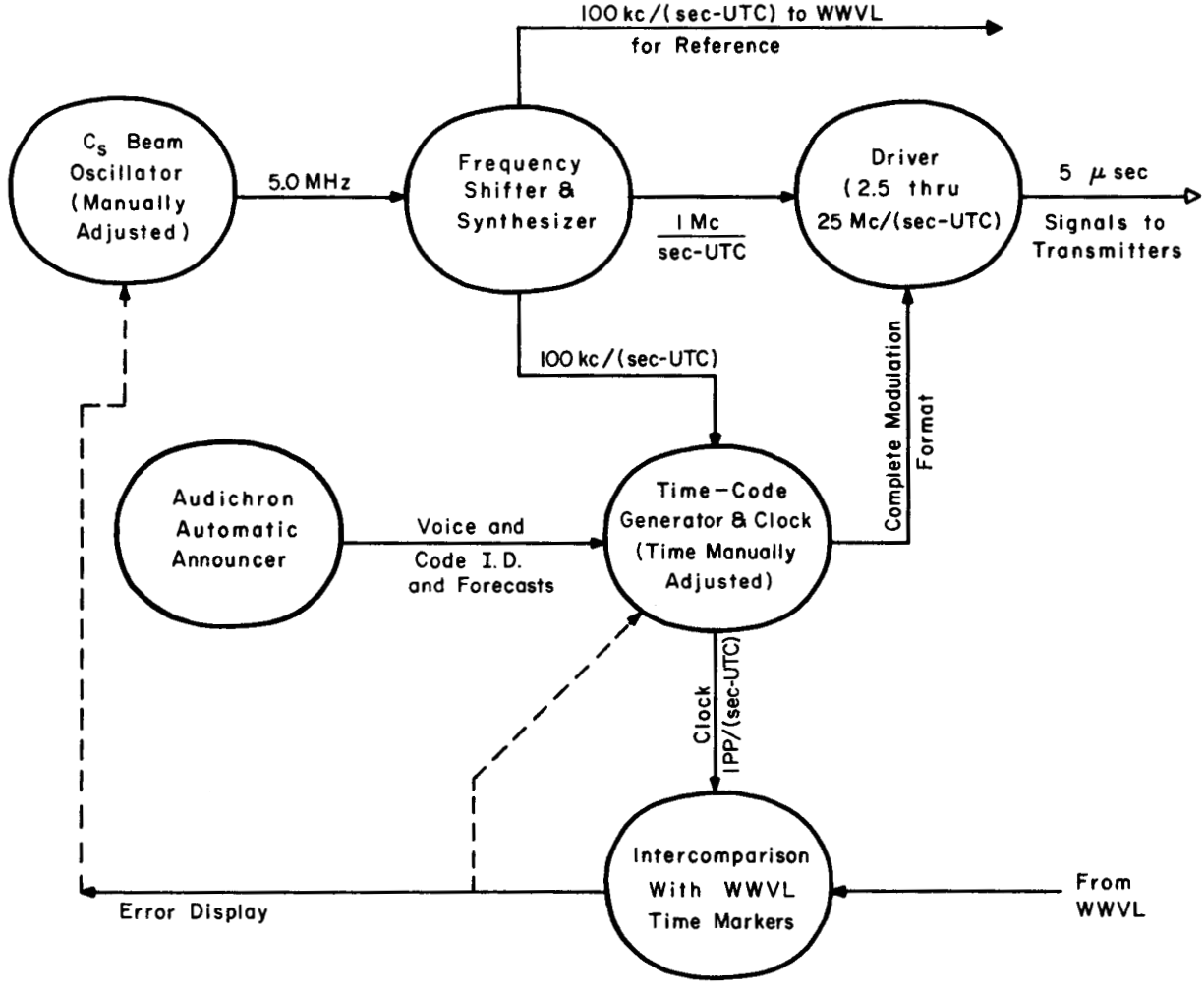

TIME AND FREQUENCY DISSEMINATION - WWVH

2.5, 5, 10 & 15 Mc/(sec - UTC)
UTC (NBS) Time Scale

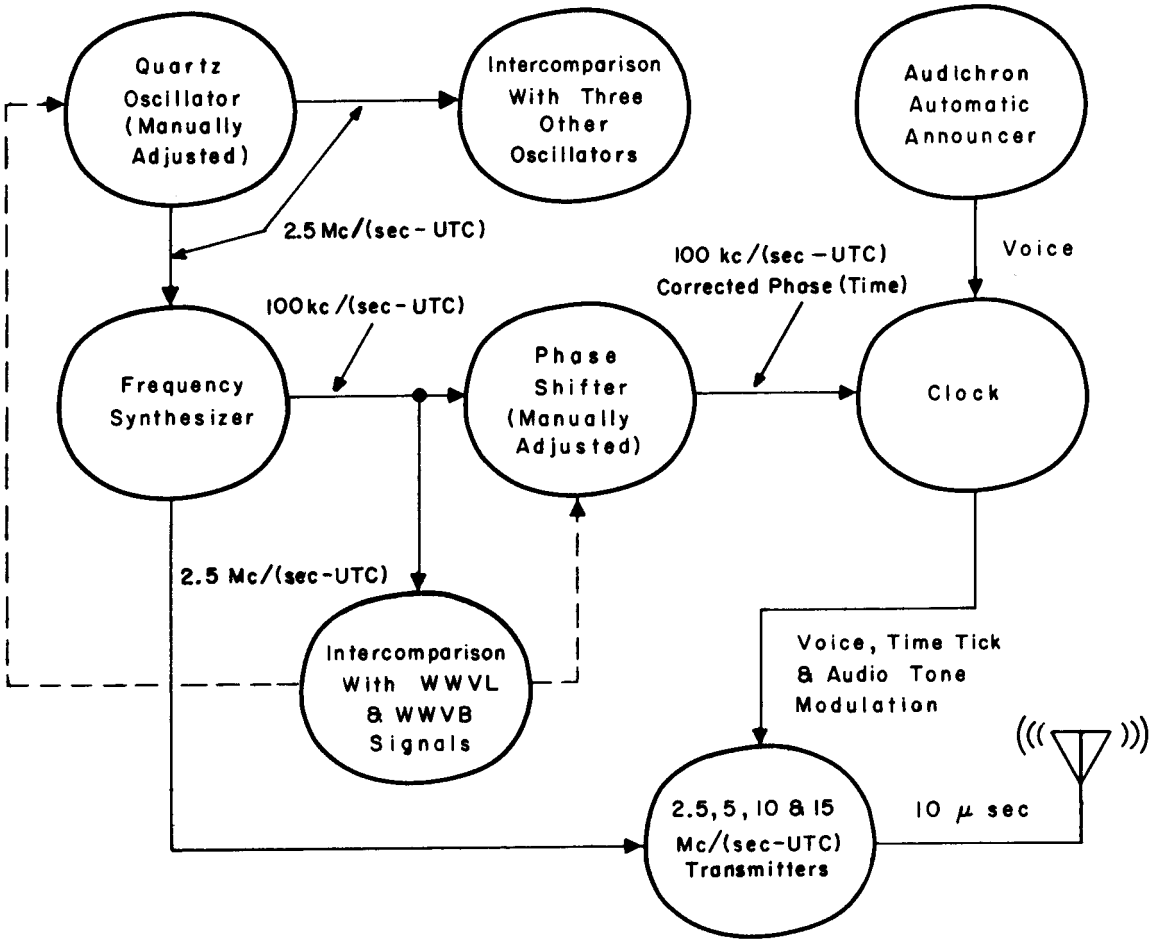

WWVL, WWVB, WWV, and WWVH:

Bias Uncertainties: Since the signals from all the stations are controlled by the standards in Boulder, as shown on pages 7-10 , there is no significant long-term bias in the phase of the broadcast signals relative to the NBS time scales.

Random Errors: The phase (time) uncertainties given below are random fluctuations due to weather-caused changes in antenna impedance and to operator and equipment limitations.

Station	Maximum Phase Error [re SAT(NBS) or UTC(NBS)] (microseconds)
WWVL	2.0
WWVB	2.0
WWV	5.0
WWVH	10.0

Total Uncertainty: Same as Random Errors

Notes: Standard time and frequency signals are broadcast from four radio stations operated by the National Bureau of Standards. WWVL, WWVB, and WWV are located near Ft. Collins, Colorado; WWVH is on the island of Maui, Hawaii. For detailed description of the information available on each signal, see the reference below.

The unit of frequency, Hz, is used to denote one cycle per second, where the second is that defined internationally in terms of a transition in cesium. The unit, c/(sec -UTC), denotes one cycle per second where the second is derived from the UTC(NBS) time scale.

The frequency offset from the internationally defined atomic frequency required to generate the UTC(NBS) time scale is determined annually by the Bureau International de l' Heure (BIH) in Paris. At present the offset is -300 parts in 10^{10}.

SAT(NBS) is a Stepped Atomic Time scale based on the atomic frequency with periodic retardations to approximate UT-2.

Time synchronization between the NBS coordinated time scale UTC(NBS) and the clocks at the Ft. Collins transmitter sites is checked daily.

Reference: NBS Standard Frequency and Time Services, Special Pub. 236 (1968). (Revised annually).

Personnel: P. Viezbicke

DIRECT COMPARISON:

In addition to obtaining time information from the broadcast signals, one can also make direct comparisons between the NBS clocks at Boulder and a portable clock.

Bias Uncertainties: See Notes

Random Errors: See Notes

Total Uncertainty: See Notes

Uncertainty quoted customer: See Notes

Notes: Comparison between AT(NBS) and the customer clock can be made with a precision of about 1 n sec. and an accuracy of about 100 n sec.

Reference: D. W. Allan, R. L. Fey, H. E. Machlan, J. A. Barnes, An ultraprecise time synchronization system designed by computer simulation, Frequency 6, #1, 11 (1968).

Personnel: D. W. Allan

CAVITY WAVEMETERS

100 MHz – 90 GHz

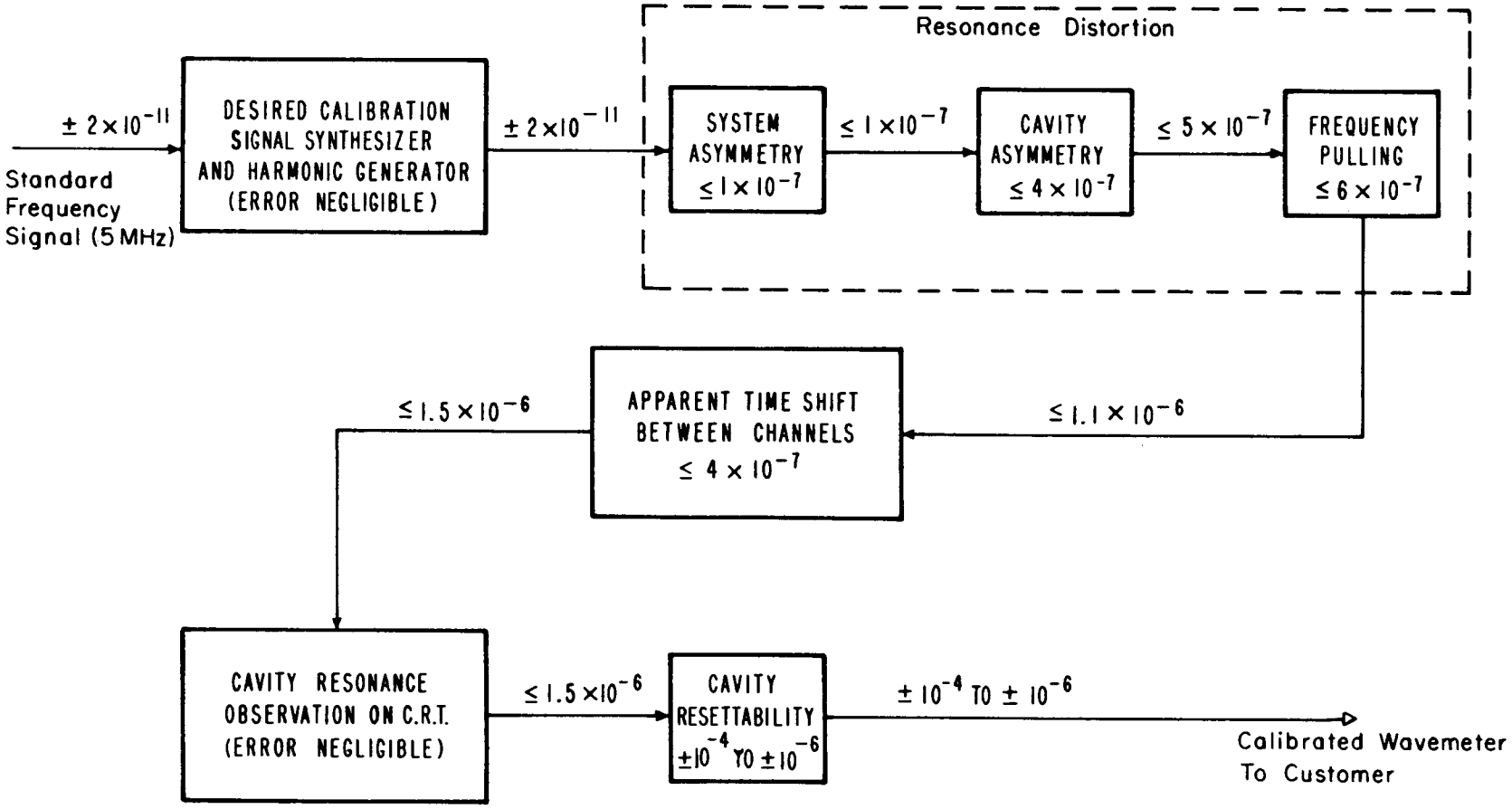

Cavity Wavemeters

100 MHz - 90 GHz

Bias Uncertainties:

Random Errors:

Total Uncertainty:

Uncertainty quoted customer:

See Error Flow Diagram, page 11

Notes: None

Reference: C. G. Montgomery, Techniques of microwave measurements, Radiation Laboratory Series, No. 11, pp. 291-293 (1947).

Personnel: R. E. Larson
C. K. S. Miller

STABILITY OF STABLE OSCILLATORS AND OTHER SIGNAL SOURCES: FREQUENCY, PHASE, TIME, AND AMPLITUDE STABILITY

Carrier Frequency : 0 Hz - 12.4 GHz
Frequency Domain: 10^{-6} Hz - 10^{6} Hz Fourier Frequency
Time Domain : 10^{-6} s - 10^{6} s Time Interval

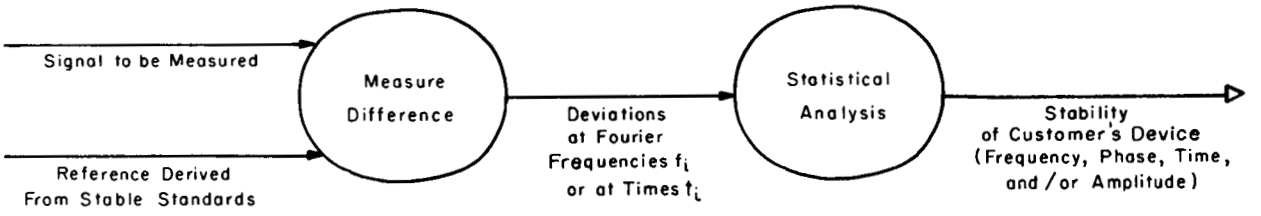

Stability of Stable Oscillators and Other Signal Sources: Frequency, Phase, Time, and Amplitude Stability

Carrier Frequency:	0 Hz - 12.4 GHz
Frequency Domain:	10^{-6} Hz - 10^{6} Hz Fourier Frequency
Time Domain:	10^{-6} s - 10^{6} s Time Interval

Bias Uncertainties: Less than 3dB typical, to as low as 0.1dB

Random Errors: Less than 3 dB typical, to as low as 0.1 dB

Total Uncertainty: Less than 5 dB typical, to as low as 0.2 dB

Uncertainty quoted customer: Same as Total Uncertainty.

Notes: These calibrations can be performed on quartz crystal oscillators, atomic frequency standards, signal generators, frequency synthesizers, frequency multiplier chains, frequency dividers, amplifiers, buffers, phase shifters, and in general any device which generates or processes a frequency, phase, or time signal. Spectrum analysis can be done directly at Fourier frequencies f greater than 1 hertz, with an analyzer bandwidth as narrow as 1 hertz. The entire range of frequency domain stability can be obtained by Fourier transformation of time domain data.

References: D. W. Allan, Statistics of atomic frequency standards, Proc. IEEE, 54, 221 (1966), and L. S. Cutler and C. L. Searle, Some aspects of the theory and measurement of frequency fluctuations in frequency standards, Proc. IEEE, 54, 136 (1966).

Personnel: J. H. Shoaf
D. Halford

IMPROVEMENTS IN CESIUM BEAM FREQUENCY STANDARDS AT THE NATIONAL BUREAU OF STANDARDS

by D. J. Glaze and J. A. Barnes, Time and Frequency Division, National Bureau of Standards, Boulder, Colorado, U. S. A.

The National Bureau of Standards Frequency Standard, NBS-III, a cesium beam with a 3.66 meter interaction region, has been in operation since 1963. The last published (1966) accuracy capability for NBS-III was 1.1×10^{-12} (1σ). With this performance NBS-III was used in the measurement of the frequency of the hyperfine separation of hydrogen. This was, and is, the most accurate published measurement of any physical quantity. A number of improvements are being made in NBS-III to improve its accuracy capability.

In early 1966 the vacuum system was modified to use three commercial 200 liter per second ion pumps. The resulting ultimate pressure was improved by a factor of 10 to 2×10^{-8} torr.

Several new solid state, broadband frequency multiplier chains have been constructed with particular attention given to reduction of both power-line related sideband levels and random phase noise sideband levels. Reduction of the random phase noise by more than 20 dB compared to the previous state of the art has been obtained consistently. One of these frequency multiplier chains is presently in use in the 9.192 ... GHz excitation system.

In addition a solid state servo system has been employed to control the frequency of the 5 MHz slave oscillator. This servo system and the new frequency multiplier chain have improved both the reliability and long term stability of NBS-III.

Comparisons were made between NBS-III and one of the commercial cesium standards in the NBS Clock Ensemble. The relative fractional frequency stability of σ ($N = 2$, $\tau = 1$ day, $T = 7$ days) $= 1 \times 10^{-13}$ was observed for nine weekly comparisons. Presently at NBS there are no hydrogen masers or thallium beams capable of being used in meaningful measurements against NBS-III.

The long term frequency accuracy for this recently improved NBS-III system has not been evaluated fully. Due to the improvements in both electronics systems and evaluative techniques, however, an accuracy of 5×10^{-13} (1σ) for a single evaluative experiment has been observed.

Substantial NBS effort is being expended toward improvement of the accuracy and figure of merit (presently 10) for NBS-III. Improved designs and associated components for new beam optics have been completed, and the modified NBS-III system will be designated NBS-5. It is expected to be in operation in early 1970 and to exhibit a figure of merit in excess of 500.

Reprinted from:
International Union of Radio Science (U. R. S. I.)
XVIth General Assembly Abstracts
(Ottawa, Canada--August 18-28, 1969, Commission I/VII), p. 8 (1969)

Paper to be published in:
Progress in Radio Science 1966-1969
Part I, Proc. XVIth General Assembly of URSI, Ottawa
C. E. White, Editor (in press)

2. Time Scales

463-560 O - 72 - 14

A COMPARISON OF TWO INDEPENDENT ATOMIC TIME SCALES

Reprinted from the PROCEEDINGS OF THE IEEE
VOL. 51, NO. 3, MARCH, 1963

A Comparison of Two Independent Atomic Time Scales*

Although the use of atomic beam devices clearly permits the measurement of time intervals of up to several years with a precision which is 100 times better than that available from astronomical measurements, the problem of preserving epoch exists if it is wished to replace the traditional astronomical timekeeping methods by quantum electronic techniques.

Two main approaches to this problem exist. The first involves securing reliable nonintermittent operation of an atomic frequency standard with clock-driving quartz oscillators locked to the instrument for realizing the atomic transition. With this approach, more than one atomic standard is necessary in each laboratory, since the expected lifetime for reliable operation of a single instrument is far from infinite.

The second, less expensive method requires intermittent use of the atomic standards to calibrate free-running quartz oscillators which drive clocks. These calibrations are then used to convert indicated quartz time to atomic time. The accuracy of this method depends on, among other things, how often the calibrations are made. One must also consider possible systematic errors arising from the possibility that the oscillators exhibit cyclic frequency variations having a frequency conciding with the frequency with which the calibrations were made. This type of error could arise, for instance, if during the measuring process the loading on the oscillator changed and this in turn induced a change in the frequency at which the oscillator was operating. This type of error could happen also if frequency measurements were made at an interval which is some integral multiple of 24 hours. Ambient temperatures and supply voltages ordinarily have 24-hour periods. Therefore, if the voltage and temperature regulating circuits of the oscillator were not functioning adequately because of design or deterioration of the components, a systematic error might be expected. Such a mechanism is known to have affected the measurements reported below by about 1 part in 10^{11}. However, some quartz oscillators which were designed more recently than those used in obtaining data for this paper show smaller accumulated time errors due to diurnal frequency variations even though the frequency measurement schedule was maintained on a daily basis over a period of several months.

The National Bureau of Standards, Boulder, Colo., has assigned atomic times to WWV pulses on a daily basis for a period of over four years. These assignments are made using daily frequency measurements of WWV based on the United States Frequency Standard assuming an atomic second as equivalent to 9,192,631,770.000 . . . oscillations of a source resonant with the zero-field hyperfine level spacing of Cs^{133}. They have been compared to similar assignments made by the U. S. Naval Observatory, Washington, D. C., according to their A.1 scale.[1] The variations in the daily differences in times as assigned by the Naval Observatory and by NBS are plotted in Fig. 1.

One would expect that over a period of 4 years measuring techniques would improve, causing a plot such as Fig. 1 to have smaller variations; and systematic errors would be found and eliminated, causing an approach to a more nearly horizontal line as time progresses. The latter has not happened, as is shown in Fig. 1. Analysis of the data seems to indicate that, although the general agreement tends to be within one part in 10^{10}, a persistent slope of about

* Received December 7, 1962.
[1] "Time Service Notice," the U. S. Naval Observatory, Washington, D. C., No. 6; January 1, 1959.

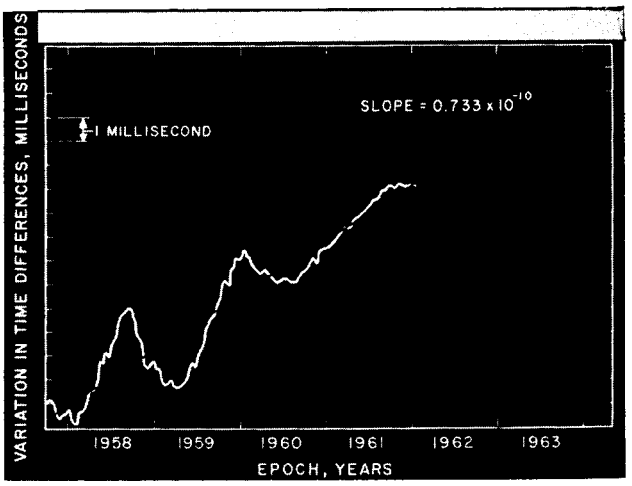

Fig. 1—Comparison via WWV of Naval Observatory A.1 atomic time scale and NBS atomic scale constructed from WWV frequency corrections. Positive slope implies Naval Observatory is slow or NBS is fast.

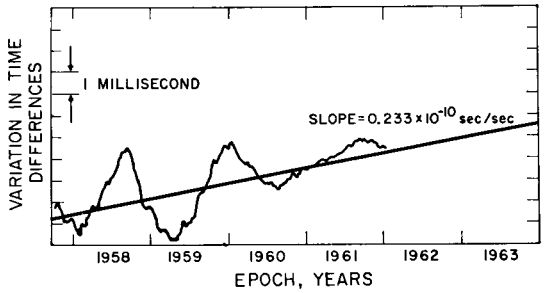

Fig. 2—Comparison of Naval Observatory and NBS atomic time scales after removal of 0.5×10^{-10} discrepancy

0.7×10^{-10} sec/sec exists, upon which is superimposed irregular fluctuations whose significance, if any, is not known. These fluctuations are much smaller for the last part of the curve than for the first.

A large part of the slope is probably caused by lack of agreement among laboratories concerning the correction which is applied to the nominal frequency output of Atomichrons. This output was given as 9,192,631,840 cps before the common usage of 9,192,631,770 cps as the zero-field Cs frequency. Therefore, in order to obtain the operating output frequency of Atomichrons in terms of the presently accepted value of the Cs frequency a correction must be applied. The basic correction used in the construction of the A.1 scale[2,3] is 74.0×10^{-10}, while some laboratories, *e.g.*, Cruft,[2,4] use the value 74.5×10^{-10}. (NBS also used 74.5×10^{-10} prior to June 13, 1960, when the use of an Atomichron was discontinued and NBS II was adopted as the United States Frequency Standard.) This discrepancy accounts for most of the slope shown in Fig. 1. Fig. 2 shows a comparison of the two atomic time scales after the removal of the 0.5×10^{-10} sec/sec discrepancy, which leaves a slope of only about 2×10^{-11} sec/sec to be attributed to systematic errors.

Two clocks diverging at the rate of 2×10^{-11} sec/sec would require of the order of 100 years before their relative error would be as large as the error now present in the best measurements of astronomical time.[5]

The time pulses of WWV have been related to an atomic time base determined by the United States Frequency Standards in Boulder for the period of October 9, 1957, to the present, in addition to being related to the Atomic Time Scale A.1 of the Naval Observatory. The variations of these pulses from A.1 are regularly published by the Naval Observatory.[6] NBS intends to publish the variations of WWV pulses relative to the NBS Atomic Time Scale in the near future.

The authors would like to thank E. T. Woodbury, who assisted in checking the machine computations, and V. Heaton, who compiled the data utilized in this study.

J. Newman
L. Fey
W. R. Atkinson
Radio Standards Lab.
National Bureau of Standards
Boulder, Colo.

[2] W. Markowitz and R. G. Hall, "Frequency Control of NBS on an International System (I)," U. S. Naval Observatory, Washington, D. C.; January 12, 1961.

[3] R. G. Hall, private communication.

[4] "Cruft Laboratory Frequency Comparison Reports," Cruft Lab., Harvard University, Cambridge, Mass., unpublished reports.

[5] W. Markowitz, R. Glenn Hall, L. Essen, and J. V. L. Parry, "Frequency of cesium in terms of ephemeris time," *Phys. Rev. Lett.*, vol. 1, pp. 105–108; August, 1958.

[6] "Bulletin B, U. S. Naval Observatory Time Signals," U. S. Naval Observatory, Washington, D. C. (published periodically by the Naval Observatory).

On the Redefinition of the Second and the Velocity of Light*

G. E. HUDSON†, AND W. ATKINSON‡

Summary—**This summary article resulted from an informal discussion period held during the International Conference on Precision Electromagnetic Measurements, August 14–17, 1962. This session was presided over by Prof. Norman Ramsey of Harvard University. The Radio Standards Laboratory of the National Bureau of Standards in Boulder, Colorado, sponsored the meeting along with the IRE Professional Group on Instrumentation and the AIEE Instrumentation Division. Partial support for the conference came from a grant from the National Science Foundation.**

On the Redefinition of the Second and the Velocity of Light

A VERY POPULAR session at the International Precision Electromagnetic Measurements Conference was the Thursday night meeting called to discuss the proposed atomic definition of the second, and methods for measuring the speed of light. This discussion was moderated and stimulated by Prof. Ramsey, who entertained the participants throughout the two hour meeting with remarks such as his invitation to the proponents of the pendulum clock to speak up, with his diplomatic attempts at quelling various semantic debates, and with his impartiality in requesting the advocates of the various atomic devices to speak out for their systems.

* Received November 5, 1962.
† Physics Department, New York University, New York, N. Y.
‡ Radio Standards Laboratory, National Bureau of Standards, Boulder, Colo.

After Prof. Ramsey's opening remarks, the first part of the meeting was devoted to the redefinition of the second. Dr. J. M. Richardson gave a résumé of the historical developments that had set the stage for the discussion. The International Committee of Weights and Measures will make, in 1966, a recommendation to adopt a definition of the second based on an atomic system. It has created a subcommittee, the Consultative Committee for the Definition of the Second (CCDS) to study this question. During the evening, numerous proponents of cesium, thallium, hydrogen, ammonia, rotational molecular transitions, and optical pumped devices were found who made statements about the suitability of the substances or techniques for redefining the unit of time. Among them were several members of the CCDS subcommittee, namely, Drs. Essen, Markowitz, De Prins, Bonanomi, Henderson, Mockler, and Richardson. The consensus was that it seems to be too early to consider the inadequacy of any of the techniques presently under development. Prof. Ramsey summarized the information expressed in a few remarks to which there was no voiced objection. In effect, he said: We ought to stick to the 1966 date for defining the new unit of time. The definition ought to be the best that can be determined somewhat before that date by keeping our eyes open during the next two years for what will prove itself to be the best. Cesium is a good

horse with a good head start and any other horse must show itself to be a really first rate one. There are some possibilities but no certainties that it will be overtaken.

Should some standards prove to be better than cesium it would be difficult with present techniques to effect the comparison between laboratories that would prove this. Dr. De Prins noted that estimated precisions obtained in a single laboratory are sometimes in parts of 10^{12}–10^{13} range, but comparisons between separate laboratories are reported in the 10^{10}–10^{11} range. There was a brief description of statistical difficulties in making intercomparisons. Among these are not only the discontinuities in data due to gaps in reporting by the several laboratories studied, but also the observed non-Gaussian nature of the fluctuations in frequency reported by the monitors. As a result, it was noted that atomic time comparisons have some advantage over frequency comparisons. However, a slide presented at the meeting to give a comparison of atomic times assigned to WWV pulses by the Naval Observatory and by the NBS showed over a four-year period a discrepancy that averaged to six parts in 10^{11} but at times was in parts in 10^{10} range. Dr. Bender expressed the opinion that the need for a system capable of comparing time scales to the 1-μsec level is a problem that needs a solution before 1966. Dr. Markowitz indicated that there was hope in using the Loran C modification by March 1963 between the European and North American continent for this purpose. During the week of the meeting, it was noted that a radio news broadcast told of the satellite Telestar making such intercomparisons.

Concerning the multiplicity of time scales, it may be noted that there are seven types of time for scientific purposes. One can, of course, have several scales of time such as a civil scale and a scientific scale that would have the same unit of interval, but the civil scale could differ by incorporating discontinuities in it similar to leap year.

The second part of the evening discussion was concerned with experiments in progress, or proposed, for determining the speed of light. Among these was described a microwave interferometer of the Michelson type to measure 50-kMc waves at the Boulder laboratories. Dr. Boyne of the NBS in Washington analyzed a novel method utilizing an optical maser as a source. Dr. Essen of the National Physical Laboratory is of the opinion that their determination of c will be to a few parts in 10^8.

During this part of the discussion, Mr. McNish made the point that present light speed measurements are all less accurate than length and time interval measurements. Dr. Ramsey also stated that since we have an MLT system, the speed of light must still be determined experimentally even though it is a theoretically invariant constant. In response to an expressed interest of Dr. Richardson as to just what are the present theoretical limitations in concept on the constancy of the speed of light, Dr. Shimoda noted that the possibility of a non-zero photon rest mass resulting in dispersion of light seems to yield a figure of one part in 10^{16} as an interesting region for investigation.

It is apparent that the main functions and results of these discussions were to raise and pose more questions than could be considered in detail in such a meeting. Some remarks of especial interest to the writers indicated a grave concern for the limitations which our present relativistic notions of space and time place on the definition of a standard clock, dissemination of time information over the earth, and the concept of the universal constancy of the phase speed of light. In fact, in his opening remarks, Dr. Richardson had expressed the thought that it would be wise to state in the report of the CCDS experimental limits to support the idea that what we call time, or more appropriately proper time, is in reality a single simple concept. We wish to add here a few comments on these questions and shall develop them at length in a later analysis.

We maintain the point of view of the theory of relativity and hold that time and space are relative concepts and the presence of gravitational fields is a manifestation of the curvature of space time. It is ordinarily asserted that a standard clock in an inertial frame of reference will record the *proper* time. The proper time intervals generated by two clocks in relative motion in different inertial frames are related by a Lorentz transformation. However, one should note that it is not possible to realize ideally the requirement that all parts of an atomic time standard should operate in a single inertial frame of reference. Consequently, studies should be made of the effect of departures of a clock from an ideal device. One should then be able to correct the standard unit generated by an operating device to ideal field-free conditions. Present estimates, for example, indicate that the elastic distortions produced by operation in a reference frame on the earth's surface yield negligibly small effects. We feel at present that the main contribution of such studies will lead to conceptual clarification rather than to significant numerical corrections for some time to come.

Concerning the speed of light, one should carefully distinguish between the coordinate speed which can depart quite widely from the value c and the speed as measured locally in proper units in an inertial frame of reference. The latter speed is always c. Any deviation from this using proper time and length units would be remarkable. Because the curvature of space time near gravitating masses produces an unavoidable distortion of our coordinate systems over an extended region, one can observe coordinate deviations of the speed of light. This should be interpreted as reflecting a change in local coordinate scale units and not in the proper light speed. The magnitude of such an effect on our coordinate scale units due to a difference in gravitational potential can be as much as one or two parts in 10^9 near the earth.

To describe, convert, and compare happenings at large distances and different times, people use coordi-

nate systems. These coordinate systems must be specified by physical means. The question arises as to the effect of the rotation of the earth on the assignment of time and space scales at each point of the earth's surface. Since the earth is nearly spherical, gravitational field effects over the surface are small. Nevertheless, if one imagines clocks attached to the surface and generating at each point the proper time unit characteristic of that place, he will find that the spatial coordinate lines of latitude and longitude cannot be stationary; but if the time coordinate for the earth is generated by a single clock in the inertial system of the fixed stars and a stationary spatial network is introduced, the proper time at any point on the surface of the earth will depend on the latitude. Also, the coordinate speed of light will be different when measured from east to west or from west to east. These coordinate effects are reflections of the effect that no rigidly rotating frame of reference exists whose space time coordinate axes are all orthogonal in the relativistic sense. One method for generating a coordinate time scale for the earth is to use a clock in a satellite. In this case, in order to determine the proper time at a point, one would need, of course, to correct for the Doppler shift including the gravitational effect. To sum up, we emphasize that an inertial reference frame which covers the earth continuously cannot be found for which the spatial axes are always and everywhere perpendicular, for which the time coordinate measures the proper time, and for which the speed of light has the one coordinate value c. Space does not permit us a more detailed examination of these questions. We merely hope that our remarks have made clearer the limitations which must be considered in adopting a conceptually correct redefinition of the unit of time. It is our opinion that the conceptual requirements of relativity, indeed, furnish us with additional reasons why an atomic standard for proper time as well as one for length should be adopted.

Reprinted from IEEE TRANSACTIONS
ON *INSTRUMENTATION AND MEASUREMENT*
Volume IM-12, Number 1, June, 1963
PRINTED IN THE U.S.A.

Synchronization of Two Remote Atomic Time Scales*

Any time scale in use at present is generated from the combination of two basic functions. First is provision of some periodic phenomenon (frequency standard) to serve as the prototype for the unit length of time. Second is the addition of a means for counting the number of cycles (cycle accumulation) executed by this periodic phenomenon. Before the appearance of crystal oscillators and atomic clocks, these elements commonly took the form of 1) the pendulum, and 2) the escapement driving the hands. An atomic clock requires the same elements but they appear in different form: 1) a quartz crystal oscillator whose frequency of oscillation is controlled by an atomic transition, and 2) various electronic dividers and comparison circuitry.

Since October 9, 1957, the National Bureau of Standards has maintained an atomic time scale (NBS-A) in which the atomic transition is that of the United States Frequency Standard (USFS) at the Boulder Laboratories of the NBS. From October 9, 1957, until April 24, 1963, time accumulation for NBS-A was performed near Washington, D. C., by the same quartz crystal oscillator and electronic dividers which produce time pulses for the broadcasts of radio station WWV. As described previously,[1] atomic times were assigned to WWV pulses on a daily basis. The atomically-controlled WWV broadcast is set to agree closely with Universal Time, which is presently falling behind atomic time at the rate of 130×10^{-10} sec/sec. Therefore, during this time, NBS-A consists of a record of the lateness of WWV time pulses relative to an ideal clock referenced to the cesium frequency taken as 9,192,631,770.00 · · · cps. NBS-A was set to be coincident with the A.1 time scale[2] of the United States Naval Observatory, Washington, D. C., on January 1, 1958.

In July, 1962, a time-accumulation system composed of quartz crystal oscillators, dividers and synchronous clocks was put into operation in a laboratory adjacent to the USFS in the Boulder Laboratories of the NBS. Since the oscillators are controlled by the USFS, this system provides an improved method of maintaining atomic time, as well as bringing both elements of the clock to the same location. The entire system has proved capable of operation without interruption since its beginning and should be capable of continuous operation indefinitely. Since high-frequency radio propagation introduces uncertainties of an appreciable fraction of a millisecond in comparison between the time pulses from WWV and those from the Boulder atomic time scale, a more precise method was used to synchronize the two scales. This was done on April 24, 1963, by transporting a high-precision quartz clock from Boulder, Colo., to the WWV transmitter at Greenbelt, Md. (near Washington, D. C.), and returning it to Boulder in order to observe directly the time difference between the two time scales.

TABLE I

Transmitter and Location	Receiver Location	Propagation plus receiver delay measured by portable clock	Theoretical delay*
Loran C Cape Fear, N. C.	U. S. Naval Observatory	1839± 5 μsec	1840 μsec†
Loran C Cape Fear, N. C.	NBS, Boulder, Colorado‡	8489± 10μ sec	8492 μsec‖
Loran C Cape Fear, N. C.	WWV Greenbelt, Md.	——	1855 μsec ‖
WWV Greenbelt, Md.	U. S. Naval Observatory	316± 50 μsec	——
WWV Greenbelt, Md.	NBS, Boulder, Colorado	9008± 50 μsec	9.23 msec§

* These delays include the measured receiver delays involved in the total delay.
† Adopted by the U. S. Naval Observatory.
‡ This includes a microwave link from the receiver at Table Mesa to the NBS Boulder Laboratories.
‖ Secondary phase factors based on National Bureau of Standards Circular No. 573.
§ NBS Tech. Note No. 22.

Measurement of the time of occurrence of the Boulder time scale pulses before and after the trip agreed to within 5 μsec. It may then be concluded that on April 24, 1963, the Boulder time scale was brought into synchronism with the Washington time scale within these limits. Since this date the Boulder clock is taken as the clock of the National Bureau of Standards which maintains the atomic time scale NBS-A. The Washington time scale will assume a subordinate position, relatable to the one at Boulder by future clock carrying or observation of various pulse reception times.

Another type of time signal broadcast, with microsecond timing capabilities in the ground wave propagation region, is the East Coast Loran C system with a master station near Cape Fear, N. C., whose time signals are controlled by the U. S. Naval Observatory. In order to make additional checks of the WWV time pulses relative to the NBS-A time scale, and to make propagation and receiver delay measurements using Loran C signals, the portable clock was also taken to the U. S. Naval Observatory and to the master Loran C transmitter. Since there is no Loran C receiver as yet at the WWV transmitter, the propagation delay of the Loran C signals at the WWV transmitter could not be measured. The results of the clock-carrying experiment are summarized in Table I. The uncertainties shown for the measured values are due to the uncertainties in the portable clock (±5 μsec) and fluctuations (primarily due to propagation) in the time pulses as received. In addition to measuring some propagation and receiver delays of the Loran C signals, it was determined that the emission of the Loran C signal was 1247 ±5 μsec after the emission of the WWV seconds pulse on April 24, 1963.

Since the Loran C signals are received both at Boulder and the U. S. Naval Observatory, it is now possible to tabulate rather precisely an absolute time difference between the two atomic time scales, A.1 and NBS-A, by noting the arrival times on the respective time scales available at each place, and correcting for the receiver and propagation delays.

We are sincerely indebted to Miss Jean Newman, Robert Doherty, Earl Berger, and Fred Sera of the National Bureau of Standards; Dr. W. Markowitz of the U. S. Naval Observatory, and Cmdr. Edwards of the U. S. Coast Guard, without whose cooperation these measurements would not have been possible.

J. A. Barnes
R. L. Fey
Radio Standards Laboratory
National Bureau of Standards
Boulder, Colo.

Reprinted from

PROCEEDINGS OF THE IEEE

November 1963

* Received August 7, 1963.

[1] J. Newman, L. Fey, and W. R. Atkinson, "A comparison of two independent atomic time scales," Proc. IEEE (*Correspondence*), vol. 51, pp. 498–499; March, 1963.

[2] W. Markowitz, "Time measurement techniques in the microsecond region," *Engineers Digest*, pp. 9–18; July–August, 1962.

A Comparison of the TA_1 and the NBS-A Atomic Time Scales

The Observatory of Neuchatel, Switzerland, publishes information[1] from which it is possible to determine the reception time in Neuchatel of the time signals emitted by the standard frequency and time-interval broadcast station WWV, located in Greenbelt, Md., and operated by the United States National Bureau of Standards. In this communication the reception times of the WWV time signals on the TA_1 atomic time scale are compared with the emission times assigned to the WWV signals according to the NBS-A atomic time scale. The TA_1 scale was established in 1957 and is maintained by the Laboratoire Suisse de Recherches Horlogeres in Neuchatel, while the NBS-A scale was also established in 1957 and is maintained by the National Bureau of Standards. Each of the scales has been established with the intention that the frequency of the cesium transition widely used as a frequency standard shall be 9192631770.00 . . . cycles per unit time interval. In the following discussion and figure this unit of time interval is called a second since it is believed[2] to differ from the second as presently defined by no more than a few parts in 10^9.

The origin of the NBS-A time scale has been set with the intention that this scale shall assign $0^h0^m0^s$ as the occurrence time to an event occurring at $0^h0^m0^s$ UT2 time on January 1, 1958. The National Bureau of Standards does not have facilities for determining the occurrence times of events on the UT2 scale so that reception times of WWV pulses on the A.1 scale, as listed in the U. S. Naval Observatory Time Service Notice 6, January 1, 1959, were used to set the origin. Recent measurements made by the National Bureau of Standards in cooperation with the U. S. Naval Observatory have indicated that 0.316 msec is the effective propagation time between the WWV transmitter and the U. S. Naval Observatory.[3] In setting the origin of NBS-A, the 0.316-msec figure has been used.

The TA_1 scale was intended originally to coincide as closely as possible with Ephemeris Time on January 1, 1958, 0^h UT. Since the accuracy with which ET is known is rather poor, the origin of TA_1 with respect to ET is to be considered uncertain.

The TA_1 scale and the NBS-A scale are constructed from independently obtained frequency measurements made with the aid of atomic frequency standards located in the laboratory constructing the time scale. Fig. 1 shows the comparison.

Over the course of years, various refinements in techniques and instrumentation for atomic timekeeping have evolved and have been incorporated into either the procedure or the equipment used to establish the time scales TA_1 and NBS-A. Two changes which occurred near June, 1960, and which resulted in a significant improvement of the time scale comparison are the switch by LSRH from the $N^{14}H_3$ maser to a Cs resonator for a frequency standard, and the adoption of NBS II as the United States Frequency Standard.[4]

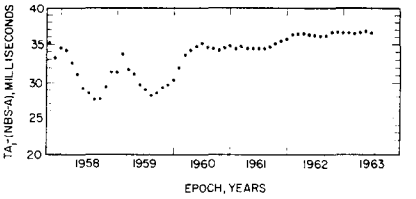

Fig. 1—Comparison of the time scales TA_1 and NBS-A.

The curve of Fig. 1, as expected, becomes smoother as time progresses and as more and more refinements are incorporated into the timekeeping procedure and apparatus. Since, as mentioned above, the origin of the TA_1-scale is not the same as that of NBS-A, the magnitude of the difference in Fig. 1 has little significance, although about 22.8 msec[5] is due to propagation delay. The quantity plotted in Fig. 1 is the reception at Neuchatel of the 0700 UT WWV pulse on the TA_1 scale minus the emission time of the 0700 UT WWV pulse on the NBS-A scale.

During the last several years, Fig. 1 shows that the NBS-A and TA_1 scales were diverging at a rate of $\sim 3\times10^{-11}$ sec/sec. If this divergence is entirely attributed to a difference in the NBS and LSRH atomic frequency standards, then it would appear that if the two groups were presented with the problem of determining the frequency of identical sources, the LSRH group would report a value $\sim$3 parts in 10^{11} less than the NBS group would report. Both laboratories monitor the frequencies of the very low frequency stations, NBA and GBR. During the years 1961–62 the measurements on GBR indicate that the average frequency reported by LSRH is 1.7 parts in 10^{11} less than the frequency reported by NBS. During this same period the measurements on NBA indicate that the average frequency reported by LSRH is 3.4 parts in 10^{11} less than the frequency reported by NBS. This rather good agreement between Fig. 1 and records made by monitoring GBR and NBA is found not only in the averages for the two-year period 1961–62, but also during shorter periods such as the period from 1961.6 to 1962.1. There the average VLF reported by LSRH is about 8 parts in 10^{11} less than that reported by NBS. This is explained by temporary poor shielding of the C-Field region of the LSRH Cs Beam Tube and bas been reported by Karatschoff [4]. A new improved shield was installed in March 1962. From 1960.5 to 1961.6, and since 1962.2, the rate of divergence of NBS-A and TA_1 has been about 1 part in 10^{-11}, with the points plotted in Fig. 1 having a standard deviation of 0.2 msec. This rate of divergence is consistent with the estimated accuracies of both standards,[6,7] and illustrates the practicality of keeping time by using the techniques of quantum electronics.

J. Bonanomi
Observatoire Cantonal
Neuchatel, Switzerland
P. Kartaschoff
Lab. Suisse de Recherches Horlogeres
Neuchatel, Switzerland
J. Newman
J. A. Barnes
W. R. Atkinson
Radio Standards Lab.
National Bureau of Standards
Boulder, Colo.

Manuscript received November 18, 1963.

[1] "Bulletin horaire de l'Observatoire de Neuchatel," Series A–D, published monthly by the Observatory of Neuchatel, Switzerland.

[2] W. Markowitz, R. G. Hall, L. Essen, and J. V. L. Parry, "Frequency of cesium in terms of ephemeris time," *Phys. Rev. Letters*, vol. 1, pp. 105–107; August, 1958.

[3] J. A. Barnes and R. L. Fey, "Synchronization of two remote atomic time scales," to be published.

[4] J. Newman, L. Fey, and W. R. Atkinson, "A comparison of two independent atomic time scales," Proc. IEEE, vol. 51, pp. 498–499; March, 1963.

[5] George W. Haydon, Radio Systems Division, National Bureau of Standards, Boulder, Col., private communication.

[6] P. Kartaschoff, "Operation and improvement of a cesium beam standard having 4-meter interaction length," IRE Trans. on Instrumentation, vol. I-11, pp. 224–230; December, 1962.

[7] R. E. Beehler, W. R. Atkinson, L. E. Heim, and C. S. Snider, "A comparison of direct and servo methods for utilizing cesium beam resonators as frequency standards," IRE Trans. on Instrumentation, vol. I-11, pp. 231–258; December, 1962.

Reprinted from the

PROCEEDINGS OF THE IEEE

VOL. 52, NO. 4, APRIL, 1964

of time and the atom . . .

The current international standard for the physical measurement of time is based on the use of atomic-frequency control devices that are now being studied intensively in the search for an ultimate basis for the precise definition of time. The author is assistant chief of the Physics Division of the NBS Radio Standards Laboratory, Boulder, Colo., where the atomic-frequency standard is being actively investigated.

By George E. Hudson

In 1952, Harold Lyons[1] of the National Bureau of Standards put into brief operation an atomic clock of the ammonia-absorption type, and thus reflected the intense interest in devising atomic standards for measuring time intervals. This interest has grown rather than diminished. As progress continued with the advent of cesium-beam frequency controls—first with L. Essen and J. V. L. Parry[2] at the National Physical Laboratory in England, and later with the models investigated[3, 4] at the Boulder Laboratories of the NBS, and by Bonanomi in Neuchatel, Switzerland, by Kalra in Canada, and by McCoubrey and Holloway of the National Company in the United States—the standard for time measurement of highest possible accuracy was removed in effect from the astronomic realm to the atomic. In collaborating with Essen, W. Markowitz of the US Naval Obsevatory[5] determined in 1958 the frequency characteristic of the cesium standard in terms of the accepted international unit of time, the ephemeris[6] second. Since the international adoption of a temporary atomic standard to realize the unit of time, the figure they gave with a considerable uncertainty,

9 192 631 770 Hz,

must be regarded not as a measured value, but rather as an exactly defined one, accurate to any number of significant figures. The uncertainty of 2 or 3 parts in 10^9 that originally attached to the measurement was evidently due to the uncertainties and inconvenience in the methods used to realize the ephemeris second; that is, the limitation lay in the astronomical observations, not in the atomic device.

As a result of this situation, the transition has finally become formalized by the pronouncement of the International Committee of Weights and Measures at its meeting in Paris in October 1964 that, for the physical measurement of time, the international standard of time interval to be used is to be temporarily based on the frequency of emission or absorption associated with the change in state,

$$|F = 4, m_F = 0> \leftrightarrow |F = 3, m_F = 0>,$$

of the cesium-133 atom.[7, 8] The size of the unit is still defined to be the invariable ephemeris second—the fraction 1/31 556 925.9747 of the tropical year at 12 hours Ephemeris Time on 0 January 1900 (i.e., December 31, 1899).

The Institute of Basic Standards of the National Bureau of Standards is charged by Congress with the improvement, maintenance, and development of the standards whereby the basic physical units are realized and disseminated in the United States. The list includes the standard of length (already an atomic one utilizing the wavelength of a krypton line) and those of mass, temperature, and electric charge. It also includes frequency.

The United States Frequency Standard (USFS) is maintained in the Radio Standards Laboratory in Boulder, Colo. The standards of time and frequency have the unique property that they can be disseminated to the general public via radio broadcasts. In fact, the time signals sent out by NBS Station WWV in Greenbelt, Md., have long been used for navigation, surveying, and other technical purposes, and recently these emissions have been strictly regulated by comparison with the USFS in Boulder via very-low-frequency transmissions from NBS Station WWVL in Fort Collins, near Boulder.[9]

Traditionally it was the province of the astronomical observatories to tell time by means of the courses of the stars and other heavenly bodies, this being the most accurate way to measure time. It has also been a necessary activity of the US Naval Observatory since there is a direct relationship between time told this way and the navigation of ships. Anyone interested in a detailed account can consult, for example, the *Explanatory Supplement*

to the Astronomical Ephemeris and the American Ephemeris and Nautical Almanac.[10] What is of importance here is the basic fact that modern, accurate measurement of time is accomplished with a standard-frequency generator. A brief description of the standard atomic clock situated at NBS Boulder Laboratories and the standard time scale generated by it may help in understanding how this is done. (See Fig. 1.)

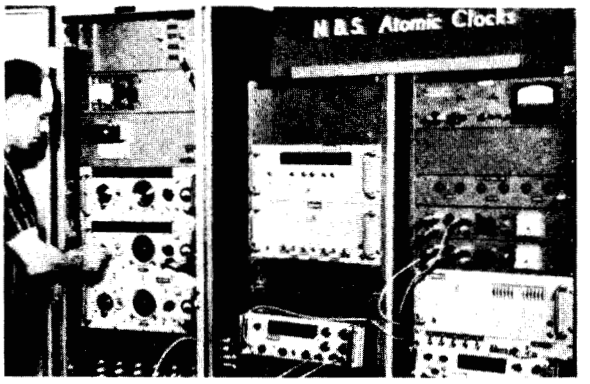

Fig. 1. D. Allan of the Boulder Laboratories adjusts the setting of the universal scale for the NBS atomic-clock system.

First, how does the frequency standard work? A beam of cesium atoms in a variety of states (among which are the $|F=3, m_F=0>$ and $|F=4, m_F=0>$ states) is directed down the axis of a long tube, with the aid of a magnetic lens. It converges to a focus through a collimating slit midway, and then diverges. At the far end of the tube is a similar second magnetic lens, followed by a detector of cesium atoms working in accordance with the principle of surface ionization. If the atoms do *not* change state, the second lens serves to disperse the beam still more and very few of the atoms can be detected. However, if the atoms in one of the states,

$$|F=3, m_F=0> \text{ or } |F=4, m_F=0> ,$$

undergo a transition into the other state (by absorption in the first case, or by emission in the second, of a quantum of radiation of frequency $\nu_s = 9\,192\,631\,770$ Hz), then the second magnetic lens brings them again to a focus and they are detected. Such transitions are induced by electromagnetic radiation of nearly this frequency introduced into the tube from an external oscillator through a waveguide. In this way, when one registers a maximum detection signal, he knows the external oscillator has the standard frequency—by definition—except for errors.

Now, if one should maintain such an external oscillator continuously "on frequency," and count the cycles of oscillation, n, in a given time interval to be measured, then clearly the time elapsed is

$$t = \frac{n}{\nu_s} .$$

Unfortunately, it is neither convenient to operate the primary frequency standard continuously, nor is it desirable from the point of view of reliability to generate a continuous time scale from a single oscillator.

A solution to this problem can be obtained if one recognizes and applies the natural extension of the relation: time equals cycles divided by frequency. Formally, the general relation is

$$t = \int_0^n \frac{dn'}{\nu(n')} ,$$

where $\nu(n)$ is the frequency of some periodic device measured frequently enough in terms of the frequency standard that its variation with the number of cycles n can be accurately followed. Then t is the time elapsed while the device oscillates n times (of course, n need not be an integer). All that is needed is to measure the frequency $\nu(n)$ against the standard and to count the number of cycles. J. Barnes, in collaboration with L. Fey[11] of NBS-BL, has accomplished exactly this. To insure reliability there are five oscillators (one is a rubidium gas cell; the other four are high-quality quartz-crystal oscillators) whose frequencies are measured daily in terms of the USFS. This is often enough. The cycles are counted—actually an accumulated total is kept—and by a suitable weighted average of the five, the time of any event may be determined to an accuracy equal to that of the USFS—that is, to one part in 10^{11}. (This accuracy is attained only after the fact, since a computer program must be used to evaluate the equivalent of the integral and the required average).

This is the A scale of time, and it has been extended continuously and uninterruptedly back to the fall of 1957 by the assignment of atomic times to the occurrence of the time signals of WWV. Beginning January 1, 1958, a composite time scale, known as the A1, was computed from weighted averages of frequencies from several standards laboratories. This was done at the US Naval Observatory. However, it is not yet clear whether such an average yields a time scale which is more meaningful than that derived from a single standard. As has been remarked, a time scale generated by one device will "walk away" in a statistical sense from any time scale generated by another device, even though both may be based on the same type of frequency standard. This is related to the well-known random-walk phenomenon. At any rate, the early establishment of an atomic time scale had the important consequence of confirming the presence of

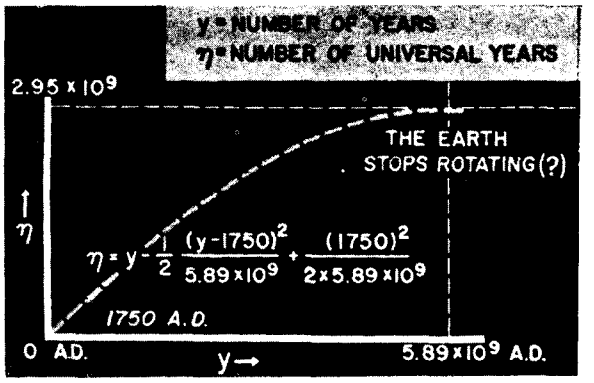

Fig. 2a. Relation between the universal scale and the uniform ephemeris time scale.

previously discovered erratic changes in the earth's motion, and of demonstrating the feasibility of atomic timekeeping. A comparison between the A scale and the A1 scale has shown[12] a very minor fractional difference in scale of perhaps 0.2 parts in 10^{10}. A similar comparison has been made with the TA_1 scale, itself established in 1957, and maintained by the Laboratoires Suisse de Recherches Horlogères, with the Cs transition defining its fundamental unit since July 1960. The observed deviation between TA_1 and NBS-A is about 3 parts in 10^{11}. It is fair to say that the present A scale is one of the most accurate single atomic time scales in existence.

What was the immediate consequence of the establishment of methods of atomic timekeeping? Did it mean that people everywhere forgot about the stars or the earth as a basis for telling time? Did it mean that the internationally accepted unit of time, the ephemeris second, was immediately disseminated for use by the scientific public? Not at all; first, the use of the earth to tell time for rough purposes is far too convenient and easy; second, navigation is based on the scale derived from the earth's motion. The US Naval Observatory continues to circulate its "Time Service" announcements[13] which are widely used to obtain approximations to the UT2 scale of time, useful to navigators. NBS's radio station WWV continues to broadcast time signals based on this scale, or rather an approximation to it called the universal atomic scale, with code broadcast of differences which may be applied to come as close as possible to the UT2 scale insofar as it is known at the moment of broadcast.

There is a disadvantage in the indefinite, unmodified, continuation of this system. The time ticks from WWV are not one second apart, nor does the time scale called UT2 have the international ephemeris second as its basic unit. It has what is called the mean solar second as its basis. This interval is obtained by a process of calculating from theory and reducing observational data and applying the resulting corrections for the motions of the earth's poles and then applying a smoothing procedure to observations of the earth's rotation.

Thus the UT2 interval is in essence the "second" that your clock ticks off if it is adjusted to tick 86 400 ($= 24 \times 60 \times 60$) times per mean solar day, while the earth rotates once on its axis. Such a time interval is not equal in length to the international unit of time interval, the second. That is, it is neither an atomic nor an ephemeris second.

The time between WWV ticks is longer than a second, because the earth is rotating too slowly on its axis to make the universal scale agree with the international (ephemeris or atomic) scale. Back about 1750 it was presumably rotating just about at the speed it should in order that one 86 400th part of a day would equal one international second as now defined. Before that time it was rotating too rapidly, and since then, too slowly. It has slowed down so much that the (universal) year of 365¼ days is between one-half and one second longer than it was in 1750. The approximate empirical relationship[14] (see Fig. 2a) is, on the average and in round numbers,

$$\tau = t - \frac{(y - 1750)^2}{380} + \frac{(1750)^2}{380},$$

τ = number of (universal) mean solar seconds which have elapsed since the year 0 AD,

t = number of seconds since 0 AD $= 31 \times 10^6 \times y$,

y = number of (ephemeris) years since 0 AD.

The parabolic form indicates that the earth is slowing down in its axial rotation and would stop in about 6 billion years if this law were to persist (time to get off?). The fact that the days are longer than they were in 1750, reflects that the earth is rotating more slowly—not that it is *slowing* down an additional one-half second or more each year. The deceleration figure is actually about 1/190 sec/yr each year. Differentiation of this relation also gives

$$\frac{d\tau}{dt} = 1 - \frac{y - 1750}{190}\,\frac{dy}{dt},$$

where $$\frac{dy}{dt} = \frac{1}{31 \times 10^6} \text{ years/sec},$$

so that the rate at which the universal scale increases is less than the ephemeris rate—or universal scale units are longer than one second, and are getting longer as y increases. The quantity

$$\frac{y - 1750}{190 \times 31 \times 10^6}$$

is called the *average* fractional offset. About the

year 1750, the two scales progressed at the same rate, since

$$d\tau = dt \text{ when } y = 1750.$$

It must be re-emphasized that these are only rough average figures and do not reflect short term variations in the earth's rotation. (See Fig. 2b.)

Apart from the empirical relationship mentioned above, there are theoretical arguments, based on considerations of tidal friction and the concomitant recession of the moon, which indicate that in something less than 50 billion years the earth will present a fixed face to the moon, while the moon rotates about the earth every 47 days.[17,18] Following this, the earth's rotation would continue to slow down gradually due to solar tidal effects until it rotates once on its axis each year. However, a relation between τ and t has been published by Brouwer,[14] which he deduced from observational data; his relation yields numbers slightly different from mine which were obtained from information communicated to me privately by W. Markowitz of the US Naval Observatory. The year 1750 would be replaced by 1779, and the denominator 380 would be replaced by 334. However, for the short span of observation time available, the difference has no practical consequence, especially since the relation describes only the average rotation. It is interesting that, despite the extreme extrapolation involved, theory and observation yield very roughly comparable results.

In any event, since the atomic (or ephemeris) second is shorter than the unit of universal time, the mean solar second, a decision had to be made. There were several choices open, and one was selected. An international agreement relating to the broadcast of time signals and standard frequencies was arrived at and concurred in by many governments via the organization known as the International Radio Consultative Committee (CCIR). It had the support of the various astronomical laboratories and of standards laboratories in many countries, including the US, the UK, and the USSR. In the light of subsequent natural occurrences, hindsight indicates that what was agreed upon may not have been the wisest thing.

It seemed so easy at first. The earth was rotating too slowly. So let there be broadcast from stations like WWV, GBR, and NBA a carrier frequency which is too low in the same proportion.[15] At the time when this decision was taken, the fractional offset in frequency amounted to —130 parts in 10^{10}. The time ticks which occurred every so many cycles were more widely spaced, and for a time the system worked well—until about a year later. Mother Earth began to swing her weight around, still more slowly, and the time signals not only did not indicate seconds, but they did not even indicate mean solar (universal) seconds! Adjustments in phase of these ticks were called for about two or three times a year, to keep them within about 0.1 seconds of the universal scale, UT2. Also, an additional adjustment in the fractional frequency offset seemed in order, and was carried out. It was changed to —150 parts in 10^{10} in 1964. But now people became worried, particularly at the National Bureau of Standards, which has the mission of accurately disseminating the basic standards of frequency and time interval; what was being broadcast or what was contemplated was a kind of variable or rubber standard, from which the international second can be obtained, somewhat inconveniently, by applying the known correction. Superimposed on the average rate of increase of the fractional frequency offset (1.7 parts in 10^{10} per year) are large random fluctuations of several parts in 10^9. Attempts to follow these fluctuations by adopting different offset values from time to time necessitate major revisions in existing equipment, which is not good.

Faced with such a situation, the best thing is to admit the difficulty and to take steps toward resolving it. It was not possible to get the international CCIR agreement modified so quickly and to include recognition and coordination of direct broadcasts of an un-offset second and carrier frequency as a desirable aim, though it soon may be. The United States CCIR Study Group VII, of which the author is chairman, is charged with the study of standard-frequency and time-signal broadcasts and regulations. It met during the summer and fall of 1964 to mull over the implications of the forthcoming international atomic-time-standard pronouncements, as requested by the corresponding international CCIR Study Group, headed by B. Decaux of the National Telecommunication Study

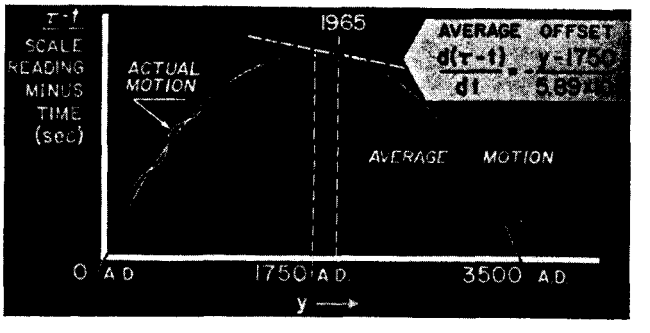

Fig. 2b. Earth motion and the universal scale offset. The average earth motion produces a parabolic relation between the universal scale and the ephemeris scale. The slope of this parabola at any point is a measure of the average offset in frequency. The actual motion of the earth produces fluctuations around this parabolic trend.

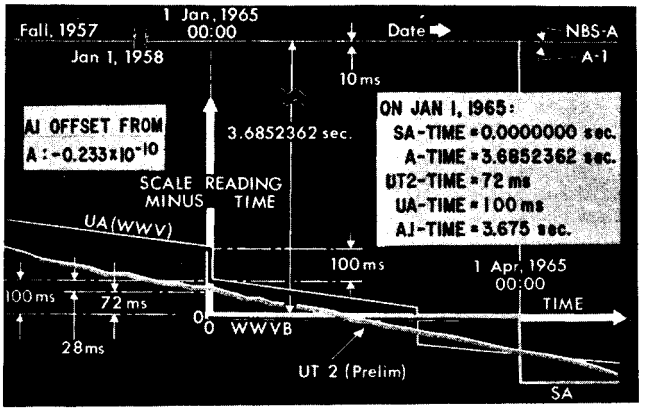

Fig. 3. Relations between time scales. On January 1, 1965, radio station WWVB began broadcasting intervals of one second shown by horizontally stepped line marked SA (stepped atomic). Due to the frequency offset the time intervals broadcast by WWV and other coordinated stations are longer than one second, as shown by sloped and stepped line.

Center in Paris and to see what could be done about the offset question. A positive approach was taken, later augmented by suggestions adopted by the international Study Group meeting at an interim session in Monte Carlo during March 1965. It was decided that experimental broadcasts and studies should be made to study how best to broadcast the interval of time and the epoch of UT2 in the same radio emissions. This is exactly what is being done. Radio Station WWVB, under the management of D. Andrews (who also directs the broadcasts from NBS stations WWV, WWVH, and WWVL) of the NBS Boulder Laboratories, began on January 1, 1965,[16] to broadcast time ticks derived from the A-scale of the National Bureau of Standards with an accuracy of $\pm 2 \times 10^{-11}$. (See Fig. 3.) The controlling element is, of course, the atomic clock incorporating the United States Frequency Standard. The carrier frequency of WWVB is 60 kHz, and is without intentional offset. This is allowable since the frequency offset of WWVB is not specifically regulated internationally. The only frequency corrections which might need to be made are those introduced by slight disturbances in radio transmission and control. These amount, typically, to less than 0.02 parts in 10^{10}, averaged over a month, with a daily rms deviation of $\pm$ 0.06 parts in 10^{10}, and are published by the NBS in the "Standard Frequency and Time Notices" of the *Proceedings* of the IEEE (correspondence). Every few months, the times of occurrence of the ticks from WWVB will be shifted uniformly by a two-tenths-of-a-second step adjustment without changing the length of the subsequent intervals between successive pulses. This keeps them within about 0.1 second of the UT2 scale. Thus, navigators need have no fear of using such stepped atomic signals. Adjustments may need to be made no more often than with the frequency-offset-plus-one-tenth-second-step-adjustment system. Moreover, physicists have directly available the international standard of time interval.

One cannot say as yet that this system is the ultimate one to be used, nor has it been decided that the Cs beam is to serve as the ultimate basis for atomic timekeeping. The hydrogen maser is already a top competitor, both commercially and in scientific research; one is completed and being thoroughly investigated at NBS-BL and another is under construction. One can only say, along with Xenophenes, that "in the course of time, through seeking, men find that which is the better—for all is but a woven web of guesses."

(See addendum on facing page).

References

1. H. Lyons, Ann. N.Y. Acad. Sci. **55**, 831-871 (1952).
2. L. Essen and J. V. L. Parry, Phil. Trans. Roy. Soc. (London) **A250**, 45 (1957).
3. R. E. Beehler, R. C. Mockler, and J. M. Richardson, private communication on cesium beam atomic time and frequency standards.
4. R. C. Mockler, R. E. Beehler, and C. S. Snider, IRE Trans. Instr. **9**, 2, 120 (1960).
5. W. Markowitz, R. G. Hall, L. Essen, and J. V. L. Parry, Phys. Rev. Letters **1**, 105 (1958).
6. D. H. Sadler, Occ. Notes Royal Astron. Soc. **3**, 103 (1954).
7. G. E. Hudson and W. Atkinson, *Physics Today*, May 1963, p. 30.
8. Nat. Bur. Std. Tech. News Bull. **48**, 209 (1964).
9. D. H. Andrews, "LF-VLF Frequency and Time Services of the National Bureau of Standards" (to be published).
10. W. Markowitz, *Explanatory Supplement to the Ephemeris* (distributed by the British Information Services, New York, 1961) Chap. 3, p. 66.
11. J. A. Barnes, D. H. Andrews, and D. W. Allan, private communication on the NBS—a time scale—its generation and dissemination.
12. J. Bonanomi, P. Kartaschoff, J. Newman, J. A. Barnes, and W. R. Atkinson, Proc. IEEE **52**, 439 (1964); see also: J. Newman, L. Fey, and W. R. Atkinson, Proc. IEEE **51**, 498 (1963).
13. US Naval Observatory Weekly Bulletin, "Preliminary Emission Times for Signals from NBA, GBI, WWV, CHU, and other Co-ordinated Stations."
14. D. Brouwer, Astron. J. **57**, 125 (1952).
15. International Radio Consultation Committee, *Documents of the Xth Plenary Assembly* (International Telecommunications Union, Geneva, 1963) Vol. III, p. 193.
16. The US Federal Register, December 19, 1964, p. 18095.
17. H. Jeffreys, *The Earth*, (Cambridge University Press, New York, 1959) 4th ed., pp. 246-250.
18. G. Gamow, *Biography of the Earth*, (Mentor Press, New York, 1959) p. 187.

Reprinted from
AUGUST 1965 • PHYSICS TODAY

(Addendum to "Of Time and the Atom", G. E. Hudson, Physics Today, 34, August 1965)

Time marches on: The atomic frequency and time standards maintained at the NBS are no longer called the USFS and the USTS, but are called NBSFS and NBSTS. This change results from the scientifically valid reason that all such correctly constituted and calibrated atomic standards, wherever they may be, are equivalent; that is, each is an equally valid (metric) instrument for measuring time intervals or frequency. Moreover, it is important that these be maintained independently (except for calibration of rate, in terms of nearby suitable reference standards) in any locale, since they may then be used to measure the local properties of the large coordinated networks now being established (e.g., Loran C, Omega, Satellite Timing, Aircraft Collision Avoidance Timing (ACAS) Systems). These systems themselves, when properly defined and accurately realized, constitute large, extended, nonlocal standards, and each furnishes a means for synchronizing those clocks coordinated in its framework, i.e., "attached" to it. Sometimes two such systems will not yield the same synchronization. This operational point of view, while not assuming the validity of Relativity theory, is not inconsistent with it. But it does drop the unwarranted assumption of Newtonian Absolute Time.

The International System (SI) of Units has now adopted the atomic cesium transition as the standard for the second. This action was taken on Friday, 13 October 1967 at the CGPM meeting in Paris.

But this leaves the problem of precise definition (and subsequent realization) of the large nonlocalized standard systems of timing, which can be referred to as "coordinate time systems." The A.1 scale of the USNO is now independently based on a variety of locally maintained cesium clocks and oscillators. The relations between the broadcast times by NBS stations and others, such as the many Navy ones, are now measured very effectively, by a large atomic clock-carrying service directed by the USNO. In this way, in the US, the USNO maintains large standard (nonlocal) coordinate time networks, and measures their properties by independent local metric standards.

The question concerning the time scale or scales to be used at the "origin" of the various nonlocal coordinate time systems is still being discussed internationally. The US CCIR Executive Committee has forwarded, for international consideration, a proposal to form an International Working Party to study these matters. The CIPM, through an ad hoc subcommittee of the CCDS, is also considering the problem of forming an International Atomic Scale of Time which would be at the "origin" of the coordinate time system coordinated by the BIH. (1968).

The NBS-A Time Scale—Its Generation and Dissemination

J. A. BARNES, D. H. ANDREWS, SENIOR MEMBER, IEEE, AND D. W. ALLAN

Abstract—**In conjunction with the United States Frequency Standard (USFS) located at the National Bureau of Standards, Boulder Laboratories, two time scales have been established. The NBS-A time scale is referenced to the USFS in accordance with the definition of the atomic second as adopted by the 12th General Conference of Weights and Measures in October, 1964. The epoch of this scale was set to be nearly coincident with the epoch of UT-2 at 00:00 hour January 1, 1958. The NBS-UA time scale is also referenced to the USFS but the frequency offsets and shifts in epoch as announced by the Bureau International de l'Heure (BIH) in Paris are incorporated in this time scale. Thus, NBS-UA is an atomically interpolated approximation to UT-2.**

The accuracies of time interval measurements referenced to these time scales are believed to have essentially the accuracy of the USFS [1]—the accuracy of the USFS is about one part in 10^{11}. The NBS-UA time scale is presently being disseminated by the NBS radio stations WWVL, WWVH, and WWV. The phases of WWVL transmissions have been maintained coherent with the NBS-UA time scale with a precision of about ± 3 μs and the epoch of the WWV transmissions with a precision of about ± 10 μs since January, 1964. Since January 1, 1965, the WWVB phase has been maintained coherent with NBS-A.

INTRODUCTION

A CLOCK SYSTEM or time scale is obtained by summing up small "time intervals" or "units of time." The time scale usually has as its origin some rather arbitrary event in the remote past. The time indicated by the clock, usually called "epoch" (for example, the epoch of some event might be 10:46 AM, December 7, 1964), is obtained by summing up the "units of time" ever since the origin of the time scale.

The basic unit of time, the second, as adopted by international agreement, has undergone an extensive evolutionary process. Prior to 1956 the second was defined as one/86 400th part of the time required for an average rotation of the earth on its axis with respect to the sun. This "second" of time was discovered to have certain irregularities and thus in 1956 the ephemeris second was adopted. The ephemeris second is defined as the fraction 1/31 556 925.9747 of the tropical year for 1900, January 0 at 12:00 ephemeris time.

The uncertainties arising in astronomical observations have limited the precision of measurement of this unit of time to about two parts in 10^9 and thus in October, 1964, the 12th General Conference of Weights and Measures at its meeting in Paris temporarily adopted an alternate definition of the second based on a transition of the cesium atom. The exact wording of the action of the 12th General Conference was: "The standard to be employed is the transition between the two hyperfine levels $F=4$, $m_F=0$ and $f=3$, $M_F=0$ of the fundamental state $^2S_{1/2}$ of the atom of cesium 133 undisturbed by external fields, and the value 9 192 631 770 Hertz (Hz) is assigned." This atomic second is reproducible

Manuscript received March 10, 1965.

The authors are with the National Bureau of Standards, Boulder, Colo.

with a much greater precision than the ephemeris second.

In spite of this definition, nations have also been committed by international agreement to the broadcast of approximate UT-2 time. The time scale, UT-2 is essentially mean solar time corrected for such things as the migration of the poles, etc. The length of a UT-2 "second" is not constant in terms of the present internationally defined atomic second. The Bureau International de l'Heure (BIH) in Paris determines a reasonable approximation of the UT-2 "second" in terms of the atomically defined second and all coordinated broadcasts emit this approximate "second" of UT-2 time. This difference between the approximate UT-2 "second" and the atomic second (presently the approximate UT-2 "second" is 150×10^{-10} seconds longer than the atomic second) is determined and set for each year and announced by BIH. By "summing up" these UT-2 "seconds" an approximation to UT-2 (epoch) time is obtained. Occasionally step adjustments are needed in this approximate UT-2 scale to maintain it within 0.1 seconds of the astronomically determined, true UT-2 epoch.

Thus it is that the National Bureau of Standards has maintained two time scales for the past several years: 1) the NBS-A time scale is based on the present international definition of the atomic second with the resonance of the appropriate cesium transition being used by the United States Frequency Standard (USFS); the epoch of NBS-A was set in coincidence with UT-2 on January 1, 1958, in cooperation with the United States Naval Observatory, and 2) the NBS-UA time scale is also based on the USFS but the frequency offsets and step adjustments in epoch as released by the BIH are incorporated to make an interpolated "universal" time scale from an atomic time scale. The NBS time scales have thus accumulated about 3.6 seconds difference (NBS-UA being late relative to NBS-A) since January 1, 1958.

The clock system maintaining NBS-A and NBS-UA has evolved with the state-of-the-art in frequency and time measurements. The present system is believed to have a precision and accuracy of time interval measurements which is limited only by the USFS itself for time intervals longer than a few days. The accuracy of the USFS [1] is about one part in 10^{11}. For time intervals of the order of one day or less the clock system contributes an additional uncertainty to the relative error of the time interval measurements of about 3×10^{-12}.

The NBS-UA time scale, prior to January 1, 1965, was disseminated by the radio stations WWV, WWVL, WWVB, and WWVH. The signals emitted by these transmitters were phase coherent with the NBS-UA time scale such that the standard deviation of the time error between a clock run from these signals and the NBS-UA time scale is 3 μs for the WWVL/B signals and 10 μs for the WWV signals.

On January 1, 1965, radio station WWVB (60 kHz from Fort Collins, Colo.) began operation without offset from the atomic definition of the second. The phase of the transmitter for WWVB is phase-locked to the NBS-A time scale while WWVL, WWVH, and WWV maintain coherence with the NBS-UA time scale. The epoch of the one second "ticks" on the carrier of WWVB is shifted in increments of 200 ms in order to maintain synchronism with UT-2 to within about 100 ms.

The NBS-A and NBS-UA Time Scales

The Clock System

The NBS-A and NBS-UA clock system has undergone considerable evolution since its beginning in 1957. Starting on October 9, 1957, the National Bureau of Standards assigned atomic times to the pulses of radio station WWV on a daily basis in terms of the United States Frequency Standard; this was the beginning of the NBS-A time scale [2]. The epoch of NBS-A time was set to agree within about 0.1 ms with that of the A.1 atomic time scale maintained by the U. S. Naval Observatory on January 1, 1958. In this way the NBS-A standard time scale became a continuation of the time sequence of events used to synchronize observers everywhere. Its continuously generated epoch forms an easily accessible reference scale for all events. This is a prerequisite for all standard time scales. Time continued to be generated for NBS-A at WWV until a more precise clock system was constructed at the National Bureau of Standards, Boulder, Colo., in July, 1962. On April 24, 1963, synchronization occurred to within ±5 μs between WWV and the Boulder clock system via a portable clock [3]. Since that time, the NBS-A time scale has been maintained at the National Bureau of Standards in Boulder, having the very desirable feature of being located in close proximity to the USFS so that radio propagation is no longer a part of the measuring scheme.

The NBS-UA time scale is also generated by the same clock system generating NBS-A. Its direct synchronization with WWV was accomplished in the same clock transport of April 24, 1963 [3].

The present clock system consists of four quartz crystal oscillators and one rubidium gas cell. Each oscillator has coupled to it a clock to count cycles; the 100 kHz nominal frequency from the oscillator is divided down and generates indicated time intervals of about one second. Each of the five clock combinations is left to run freely except when its frequency exceeds its nominal frequency by more than one part in 10^8; it runs independently of all of the other four, and hence from each a time scale can be constructed.

Time is determined in the following fashion. It has been found that as a good quartz crystal oscillator ages, its frequency drift rate approaches a constant, and that after a relatively short time (of the order of a few weeks) the oscillator can be assumed to a very good approximation to have a frequency drift which is linear with the indicated time. Most approximately-periodic devices

463-560 O - 72 - 15

whose true frequency f can be measured sufficiently often in terms of a standard may be used to generate time. If the nominal frequency of such a device is f_n, and the number of oscillations (periods) in the true time t is N, then the indicated time τ for this interval is

$$\tau = N/f$$

or for infinitesimal fractions of a cycle dN

$$d\tau = dN/f_n.$$

On the other hand, the actual time elapsed for this same small fraction of a period is

$$dt = dN/f. \tag{1}$$

Substitution and integration leads immediately to the expression for the total elapsed time

$$t = \int_0^\tau \left(\frac{f_n}{f}\right) d\tau \tag{2}$$

in terms of the indicated time. Now the defined frequency of the standard f_s which is identical with its true frequency by definition, is a certain multiple r of the true frequency of the clock, i.e., $f_s/f = r$. In general, r depends on the indicated time. Hence, one can write

$$t = \frac{f_n}{f_s} \int_0^\tau r d\tau. \tag{3}$$

If the clock were the standard itself, then one would have $r = 1$, and $t = \tau$. The frequency standard would also be the time standard. In actual practice, this is not convenient, and the time may be calculated from accumulated data on the value of the function r. Since f differs only slightly from f_n, r may be written in the form

$$r = f_s/f_n + \delta r$$

where δr is a small quantity relative to f_s/f_n. Thus the true atomic time is given by the expression

$$t = \tau + \frac{f_n}{f_s} \int_0^\tau \delta r d\tau. \tag{4}$$

The second term is generally a very small correction, and is approximated by a summation of discrete measurements. In fact, this integral is approximated by a sum of terms based on the assumption of a linear drift in frequency between measurements of δr.

The assumption of a linear frequency drift for a quartz crystal oscillator between daily calibrations is at variance with certain perturbations often observed in the frequency of quartz oscillators. These variations are due to fluctuations in the ambient temperature and in the 60 Hz line voltage; there have been frequency shifts due to a change in load on an oscillator, and inherent circuit noise has been observed to induce statistical fluctuations which cause an oscillator to depart from the predominant linear frequency drift behavior. All but the last of these effects can and have been controlled by proper electronic design and laboratory techniques. The interesting problem of statistical fluctuations caused by inherent oscillator noise has stimulated a great deal of study by several people in order to determine the statistical characteristics of the noise and its effect on the time error and precision of various types of oscillators [4]. Recently some additional results, not yet published, have been established by the authors. One result is that the deviation in the incremental time accumulated by a quartz crystal oscillator during one calibration interval is almost completely independent of the deviations obtained in previous intervals so that the errors compound by nearly a random walk process. As an example this "rms time error" for our best oscillator is 0.3 μs for one day (or 3 parts in 10^{12}). If one were to make daily measurements on the oscillator for 100 days, the rms time error would be $\sqrt{100} \times 0.3$ or 3 μs for approximately three months (or 3 parts in 10^{13}). The conclusion is that as time progresses the relative precision of the NBS-A time scale approaches that of the standard rather than that of the clock system, in the sense that the ratio of the accumulated error in time to total elapsed time approaches zero as $t^{-1/2}$, so that the accuracy of the time scale approaches that of the USFS for long elapsed time.

Various experiments have been conducted by the authors to determine if systematic errors are present in the oscillators. One quite conclusive experiment was to compare two of the oscillator clocks as independent time generators. One of these was a quartz crystal oscillator and the other was the rubidium gas cell, each in different rooms, at different temperatures, and under basically different operating conditions. The divergence between the two could be explained entirely in terms of the random walk phenomenon. Moreover, if systematic errors were present, they were less than 5×10^{-13}.

Typically, each oscillator is compared to the USFS for approximately fifteen minutes each working day. The integration of (4) is approximated on the basis of a linear frequency drift between calibrations.

Comparison With Other Time Scales

Regardless of the confidence limits one assigns to the NBS-A time scale due to internal consistencies, it is desirable to make external measurements to help insure that no significant, undiscernible, systematic errors exist in the system. Comparisons have been made with Laboratoire Suisse de Recherches Horlogères (LSRH), Neuchatel, Switzerland, and with the United States Naval Observatory.

The modus operandi of the LSRH atomic time scale (denoted TA_1) is very similar to that of NBS-A in that it employs cesium^{133} as the standard, and high quality quartz crystal oscillators coupled with clocks to interpolate time and frequency between calibrations in terms of the standard. In spite of these basic similarities, the fact that TA_1 is completely independent of NBS-A indicates that a comparison between the two should be very significant.

The comparison [5] was made using the NBS con-

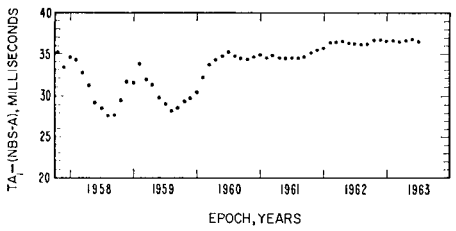

Fig. 1. Comparison on the time scales TA_1 and NBS-A.

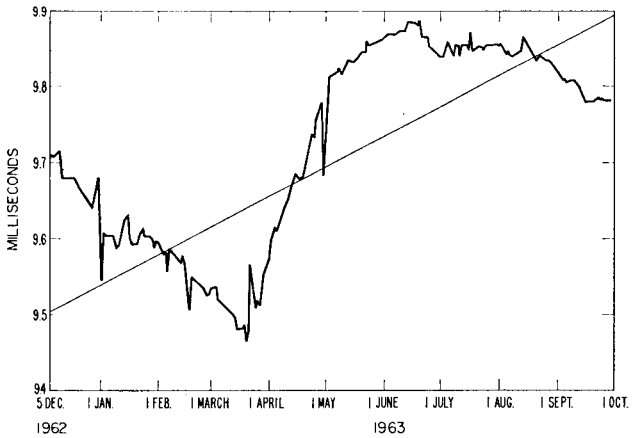

Fig. 2. Arrival time of Loran C pulses on the NBS-UA time scale.

trolled radio station, WWV, Greenbelt, Md. Figure 1 shows a plot of the reception times of pulses on the TA_1 time scale since 1957 minus the emission times of the corresponding WWV pulses on the NBS-A time scale. The standard deviation for each data point plotted is about 0.2 ms, and the propagation delay is of the order of 25 ms, determined roughly from the distance.

It is interesting to note the effect exhibited by the curve in 1960 when the United States adopted the laboratory cesium beam standard, NBS-II, as the USFS, and LSRH changed from the $N^{14}H_3$ maser to Cs^{133} as their standard. The divergence over-all is $\sim 3\times10^{-11}$ s/s; from epoch 1962.2 on, the divergence is $\sim 1\times10^{-11}$ s/s, with TA_1 high in frequency relative to NBS-A. This latter divergence is just the stated accuracy for each of the standards involved. In June 1964, L. Cutler and A. S. Bagley [6] carried two portable cesium beam standards to Neuchatel, Switzerland, and measured the frequency of the LSRH cesium standard and then traveled to Boulder and measured the frequency of the USFS. Assuming no change in the portable standards during travel, the frequency of the USFS agreed with that of the LSRH standard to within 1×10^{-11}.

The Loran C master is basically the Naval Observatory's approximation to UT-2 controlled in terms of the scale A.1, and hence the comparison of A.1 with NBS-A was accomplished by monitoring the arrival time of the Loran C pulses on the NBS-UA time scale. A plot of hese reception times on the NBS-UA time scale is shown in Fig. 2. The straight line least squares fit to the data shows a divergence rate (slope) of 1.5×10^{-11} s/s with the Loran C master being low in frequency relative to the NBS-UA time scale.

The Automatic Generation of a Time Scale

The computer typically takes two weeks of data before the individual times of each of the five clocks are calculated and averaged to yield NBS-A and NBS-UA. In this situation one cannot determine the time an event occurred, as measured by any one of the clocks in the system, until after the computer has processed the data. Therefore, it was very desirable to construct a clock that is on time and on frequency. Such a device would have great utility in the immediate dissemination of time and frequency. A uniform frequency and time generator was therefore constructed at the NBS Boulder Laboratories. The idea for the device was conceived by L. Fey; concurrently and independently a commercial concern constructed a similar one. The device called a Drift Corrected Oscillator (DCO) utilizes the characteristic of a good quartz crystal oscillator mentioned earlier: Its frequency drift rate after aging is nearly constant. The utilization is accomplished by cascading two mechanical ball disk integrators and coupling the output to a continuous phase shifter; the phase shifter in turn is inserted on the output of a good quartz oscillator. The combination generates a stable frequency and a nearly uniform time scale which approximates NBS-UA.

A DCO has been maintained to approximate the NBS-UA time scale since November, 1963, and has been controlling the time and frequency transmissions of the NBS since January 17, 1964. The standard deviation from the NBS-UA scale of the time pulses from this device since it began operation is 3 μs, and the standard deviation of its fractional frequency offset determined in terms of the USFS, has been 5×10^{-12} on a daily basis, 4×10^{-12} on a weekly basis, and 2×10^{-12} on a monthly basis.

The Dissemination of NBS-UA

The NBS-UA time scale is available to the public through the NBS broadcasting services. NBS directly controls the broadcasts from four different stations: WWV (2.5 MHz, 5 MHz, 10 MHz, 15 MHz, 20 MHz, 25 MHz) and WWVH (5 MHz, 10 MHz, 15 MHz), high-frequency stations known and used for many years; WWVB (60 KHz), a low-frequency station initiated at Boulder in the mid-fifties and rebuilt at Fort Collins in 1963; and WWVL (20 KHz), a very low-frequency station started in 1960 at Sunset, Colo., and rebuilt at Fort Collins in 1963.

The Atomic Frequency and Time Interval Standards Section provides signals suitable for controlling precision broadcasts which are maintained within close tolerances to the USFS and NBS-UA. This constitutes the first step in disseminating these standards.

The second step occurs in relating this information to the LF and VLF broadcasts at Fort Collins. This is accomplished as follows: The LF and VLF signals broadcast from Fort Collins are phase monitored at NBS, Boulder; the phases of these signals are compared with the standard reference signal; error signals with appropriate sense and magnitude are transmitted by FM to Fort Collins; these error signals drive servosystems to accomplish the required transmitted phase corrections for both frequencies so that each is directly related to the standards provided.

This system reduces the transmitted phase variations received at Boulder to the point where the actual transmitted phase is coherent with the reference phase to a tolerance of ± 0.1 μs. The complete system, to be described in detail elsewhere, has proven to be very reliable, well-engineered, and adequate for present needs.

The third step in disseminating the frequency and time standards is to relate the HF broadcasts from WWV and WWVH to WWVB and WWVL and thence directly back to NBS-UA.

This is accomplished at present by phase monitoring WWVB and WWVL at the HF stations and using this information to control the operating oscillators. Thus, WWV is phase-locked to WWVL which in turn is phase-locked to NBS-UA, just as synchronous electric clocks are phase-locked to the 60 Hz power line. Until now no attempt has been made to control WWVH to tolerances better than 1 ms but WWV has been the subject of experimental efforts to determine the best tolerance limits which could be applied realistically to frequency and time control of a remote station.

Using the signals from WWVL as a reference, the operator at WWV was instructed on January 18, 1964, to maintain his oscillator by incremental adjustments as needed to maintain phase with Fort Collins. These adjustments were to be limited to a part in 10^{11} or less.

The results of this experiment are as follows:

Date	Clock at WWV relative to NBS-UA
April 24, 1963	On time (by definition) [2]
March 3-5, 1964	508 μs fast
May 4, 1964	524 μs fast
May 18, 1964	517 μs fast
May 23, 1964	512 μs fast
July 22, 1964	518 μs fast
September 14, 1964	518 μs fast

The data tabulated here were accumulated by portable clock carrying techniques using both commercially available clocks and NBS built clocks of the crystal oscillator type. The agreement of the measurements on a round-trip basis indicate a measurement accuracy approaching a microsecond.

An examination of the complete data over this period reveals the fact that WWV, since the middle of January, 1964, has been time controlled to NBS-UA within a tolerance of ± 10 μs. This is a positive improvement in time dissemination.

It is desirable to indicate several steps that must be taken in the future to improve the control of a remote oscillator.

1) Continuous drift compensation in place of present incremental adjustments in the remote oscillator system.
2) Improved VLF receivers to provide greater accuracy and redundancy.
3) Development of techniques to correct for propagation time variations.

Conclusion

The National Bureau of Standards has established and maintained an atomic time scale (NBS-A) and an atomically controlled approximation to UT-2 (NBS-UA), with their beginnings in late 1957. Since that time many improvements both in the United States Frequency Standard and the clock systems accumulating the time scales have taken place. The present system, located entirely at the Boulder Radio Standards Laboratory, Institute of Basic Standards, of the National Bureau of Standards, is believed to have a timing precision of 0.3 μs for a one day interval and is limited primarily by the accuracy and precision of the USFS (accuracy of one part in 10^{11} and precision of two parts in 10^{12} for fifteen minute averages) for longer intervals.

The standard frequency broadcast stations WWVB and WWVL are directly phase controlled by the auxiliary continuously generated approximation to the NBS-UA scale. It is, therefore, possible to make use of the properties of LF and VLF propagation to hold any number of clocks at quite remote locations in very precise (± 10 μs) synchronism indefinitely with the NBS-UA scale and hence with each other. Experiments at radio station WWV have proven the feasibility of this mode of time control.

Acknowledgment

The authors wish to acknowledge the aid of many colleagues; most significant among these are R. E. Beehler, R. L. Fey, J. Milton, P. Kartaschoff, and Dr. R. C. Mockler.

References

[1] R. C. Mockler, R. E. Beehler, and C. S. Snider, "Atomic beam frequency standards," *IRE Trans. on Instrumentation*, vol. I-9, pp. 120–132, September 1960.

[2] J. Newman, L. Fey, and W. R. Atkinson, "A comparison of two independent atomic time scales," *Proc. IEEE (Correspondence)*, vol. 51, pp. 498–499, March 1963.

[3] J. A. Barnes and R. L. Fey, "Synchronization of two remote atomic time scales," *Proc. IEEE (Correspondence)*, vol. 51, p. 1665, November 1963.

[4] W. R. Atkinson, L. Fey, and J. Newman, "Spectrum analysis of extremely low frequency variations of quartz oscillators," *Proc. IEEE (Correspondence)*, vol. 51, p. 379, February 1963.

[5] J. Bonanomi, P. Kartaschoff, J. Newman, J. A. Barnes, and W. R. Atkinson, "A comparison of the TA_1 and the NBS-A atomic time scales," *Proc. IEEE (Correspondence)*, vol. 52, p. 439, April 1964.

[6] L. S. Cutler and A. S. Bagley, "A new performance of the 'flying clock' experiment," *Hewlett-Packard J.*, vol. 15, pp. 1–5, July 1964.

AN ANALYSIS OF A LOW INFORMATION RATE TIME CONTROL UNIT

Lowell Fey, James A. Barnes, and David W. Allan

National Bureau of Standards, Boulder, Colorado

Timing systems which are driven by unadjusted quartz crystal oscillators accumulate errors due to oscillator frequency instability. To realize maximum timekeeping precision, assuming a frequency calibration is available intermittently, the oscillator frequency must be correspondingly readjusted or the clock must be reset, or a bookkeeping method employed to systematically account for errors. At best, none of these procedures is as satisfactory as having a stable frequency available continuously; besides being time consuming, the above expedients always introduce a possibility for error. In an operational system, the problem is compounded because coordination is required among a number of people in a number of stations. To minimize these disadvantages and in some cases improve accuracy, a method of operation which retains oscillator synchronization as automatically as possible is desired.

In first approximation, to keep separately located clocks in synchronism, it is only necessary that their driving oscillators operate at the same nominal frequency. As shown by Barnes,[1] this specification is not sufficient because of the occurrence of a particularly troublesome low frequency (flicker) noise in oscillators. This noise causes a statistical divergence in the times kept by clocks driven by separate oscillators even though their frequencies are nominally the same. For clock synchronism over an indefinitely long period, their driving frequencies must be locked together continuously. Within the same laboratory, this is not difficult to accomplish; the problem of interest is to maintain remotely located clocks in synchronism. Practical methods for arbitrary locations involve some type of radio propagation. The limitations of high frequency broadcasts such as those from WWV, are well-known to prevent synchronism to better than about 1 millisecond. With VLF propagation, however, ionospheric conditions are sufficiently stable to permit phase comparison, and thus synchronization, between oscillators at receiver and transmitter. Unattended operation of such a system is made impractical by diurnal shifts in received phase, making visual interpretation necessary to extract frequency comparison information from a record of received carrier phase compared to local oscillator phase. In doing this, the most reliable data results if phase difference is determined for the most stable period each day. Generally, this period is that of a few hours near midday on the propagation path; during the night, oscillator phase is degraded by increased propagation fluctuation and a phase offset error occurs as a result of sunrise and sunset diurnal phase changes. In order to overcome these difficulties as well as to permit compensation for local oscillator frequency drift without step frequency adjustments, the concept of a multiple loop servo system has been developed.

Such a system evolves from a single loop system such as used in VLF phase tracking receivers as follows. The conventional idealized single loop servo diagram is illustrated in Figure 1. Here the reference phase $\omega_o t$ is assumed to result from a constant angular frequency, ω_o, while the local oscillator phase is equal to $\omega_o t$ plus a small difference $\xi(t)$. The function of the servo loop is to maintain the corrected phase output from the local oscillator, ξ_{out}, in agreement with the reference phase, $\xi_{ref.}$. This is done by integrating the error between these two phases with respect to time to produce a rate of change of phase in a direction that will reduce the phase error. A step function error will thus produce a correction which decreases as e^{-At}. The time constant associated with this loop is seen to be $\tau = \frac{1}{A}$. If instead of a step function phase error, a frequency difference, $\Delta\omega$, exists between reference and local oscillator, the uncorrected phase errors will increase linearly with time. The action of the feedback loop will then be to supply a continuous phase correction while operating, of necessity, with a steady state phase error of magnitude $\frac{\Delta\omega}{A}$. The addition of a second loop will improve this situation as shown in Figure 2.

If a frequency difference, $\Delta\omega$, exists between reference and local oscillators, the phase error will be corrected as before with time constant τ_1. At the same time the second loop integrator also contributes an error correction, reducing the correction necessary by the first loop until, at steady state, all the correction is supplied by the second loop and no residual error is required as input to the first integrator. In effect, an error different from zero for finite length of time has been integrated to a constant by the first integrator. This constant input to the second integrator produces an output correction which has the desired property of increasing linearly with time. Since such a system, now has the possibility of being unstable, the time constants $\tau_1 = \frac{1}{A_1}$ and $\tau_2 = \frac{1}{A_2}$ must be adjusted, as treated in the usual servo theory,[2] to provide stability and optimum transient response. After equilibrium has been reached, since no steady state phase error is required to actuate the servo loops, the reference may be removed and the output phase will continue to follow the reference phase even though a frequency difference exists between reference and local oscillator. Carrying this procedure one step further, a third loop may be added, extending the performance capability to that of compensating for a linear change in oscillator frequency, that is for oscillator drift. Then, as before, after equilibrium has been reached, the system will adjust itself so that the necessary oscillator drift correction is shared by the 2nd and 3rd loops with none required of the first loop. Consequently the output frequency will again continue to remain constant after the reference frequency has been removed. No further comparison to the constant reference frequency would be necessary if it were not for previously mentioned flicker fluctuations which perturb the oscillator frequency.

A realistic model of the behaviour of a good quartz crystal oscillator is to consider it as a source of frequency which increases at a constant rate, (drift), upon which is superimposed low frequency fluctuations known as

flicker frequency modulation. This is a type of fluctuation having a power spectrum proportional to $\frac{1}{f}$ where f now refers to frequency components of the fluctuation. Thus $\bar{\phi}(t)$ is composed of a deterministic portion due to oscillator frequency offset from the reference and oscillator frequency drift plus a random portion due to flicker noise. The effect of flicker noise is to prevent a precise determination of oscillator frequency and drift rate since difficulty arises in separating flicker noise from drift.

This difficulty is illustrated in Figure 3. The ordinate, variance $\frac{(\bar{\phi}\ (t + \tau) - \bar{\phi}(t)}{\tau}$ presents a measure of spread, or fluctuation, in the phases (times) accumulated by an ensemble of oscillators as a function of sample time, τ, given on the abscissa. The negative slope region for short sample time corresponds to thermal or white noise and indicates that improvement in precision can be made by increasing measuring time. At times of the order of one second, flicker noise begins to predominate and has the effect of preventing further increase of precision with increasing sample time as well as producing the annoyance of a divergence of frequency fluctuation with increasing N, the number of samples. For illustration of differences, representative time series samples of various types of noise are shown in Figure 4. The most widely known is white noise, upper left, having the property of no correlation in time from point to point, and thus no frequency dependence in its power spectrum. At the lower left is flicker noise which has been shown[3] to apply to the frequency fluctuations of quartz crystal oscillators. It exhibits correlation in time and a $\frac{1}{f}$ frequency dependence. For further comparison successively higher correlation and frequency dependence are shown in random walk, $\frac{1}{f^2}$ and flicker walk $\frac{1}{f^3}$, (corresponding to the phase noise for $\frac{1}{f}$ FM), upper and lower right.

The servo design problem now becomes one of optimizing the loop time constants to provide the most stable operation in the presence of flicker noise, assuming periodic synchronization to a standard reference frequency. Since detailed analysis of a third-order feedback system requires numerical techniques even without treatment of noise, and servo running times of months or years are contemplated making real time experiments impractical, and since an efficient technique has recently been developed for computer generation of flicker noise,[4] it was decided to carry out the initial investigation entirely with the use of a digital computer.

Figure 5, obtained from a digital computer plot, illustrates the behaviour of the system with no noise input assuming a linear drift in local oscillator frequency and therefore a quadratic change in phase with time. Initial conditions were set so that the system correction rate was not adjusted to the quadratic input. Thus as time progressed, an error resulted which was reset to zero periodically, corresponding to synchronization of a real device to a constant reference frequency. The resulting transient response appears on the left. In this case time constants were

such that the transient response became negligibly small after a few settings. Thereafter, prediction of the quadratic input was perfect, as theory requires, and the error remained at zero in the open loop condition.

Figure 6 shows the same system in steady state with only flicker noise and no oscillator drift input. The noise magnitude was taken to be that of a characteristic high quality quartz crystal oscillator, 2×10^{-12}, which means that the variance of frequency fluctuations with sample size $N = 2$ is expected to be 2×10^{-12}. The resulting errors are reset to zero daily, permitting only the small variation seen about the zero line.

Figure 7, again shows transient response assuming the same flicker noise plus a realistic frequency drift of 5×10^{-11} per day. If only a second order system were used, the daily errors shown would have remained constant at the initial value instead of dying out.

In all of these cases, the time constant of the first loop was taken to be negligibly small compared to the time constants of the other two loops, enabling phase error to be corrected to zero immediately upon application of a reference frequency. Comparison of behaviour using various 2nd and 3rd loop time constants under the above-mentioned realistic assumption for oscillator frequency drift and flicker noise, led to the choice of 1.1 days for the 2nd loop time constant and 20 days for the 3rd loop time constants as reasonably optimum. Figure 8 shows a steady state plot of error from such a system, with daily synchronizations for the first half of the running period. During the second half of the plot, synchronization to the reference was suspended. After 40 days, due to the effects of uncorrected flicker noise, the error had reached 12 microseconds, a value quite small compared to that resulting from an isolated free running oscillator.

Realization of a practical device could be accomplished either with an electromechanical system consisting of motors, gear reductions and ball and disk integrators or with an all electronic system using an electronic phase shifter such as developed by Barnes and Wainwright.[5]

In addition to using such a system with a VLF receiver and programming the reference to be applied during the best propagation time each day, the system could also be used in a continuously referenced mode in a laboratory with an atomic frequency standard. Should the standard fail the system could serve as a standby frequency source. Similarly in a laboratory which makes periodic calibration of oscillators that drive clocks, use of the device would reduce time fluctuations of the clocks over those occurring when oscillator frequency adjustments are made.

A different mode of operation might make use of synchronization by means of meteor burst propagation. In this case propagation between two points depends on reflections from dense ionization accompanying the frequent but random occurrence of meteors in the D region of the ionosphere. Using this method, Sanders,[6] et al., have observed microsecond stability over an 880-km path.

REFERENCES

1. J. A. Barnes, "Atomic timekeeping and the statistics of precision signal generators," Proc. IEEE, Vol. 54, p. 207, February 1966.

2. H. Chestnut and R. W. Mayer, Servomechanism and Regulatory System Design, New York, Wiley, 1951.

3. W. R. Atkinson, L. Fey, and J. Newman, "Spectrum analysis of extremely low frequency variations of quartz oscillators," Proc. IEEE (correspondence), Vol. 51, p. 379, February 1963.

4. D. Halford, to be published.

5. J. Barnes and A. Wainwright, "A precision pulse-operated electronic phase shifter and frequency translator," Proc. IEEE (correspondence) Vol. 53, p. 2143, December 1965.

6. W. R. Sanders, D. L. Albright, S. Tashiro, and D. N. March, "A meteor burst time synchronization experiment," to be published.

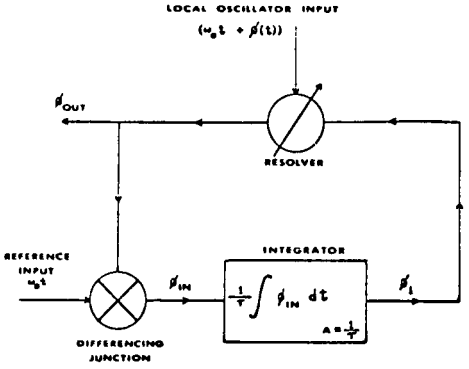

figure 1

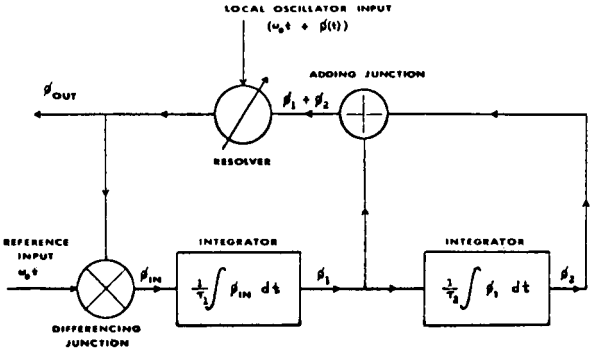

figure 2

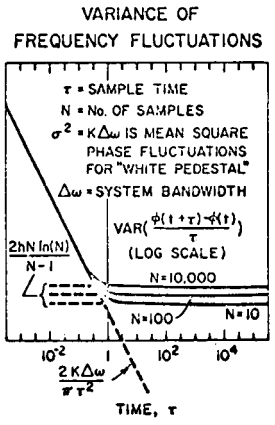

figure 3

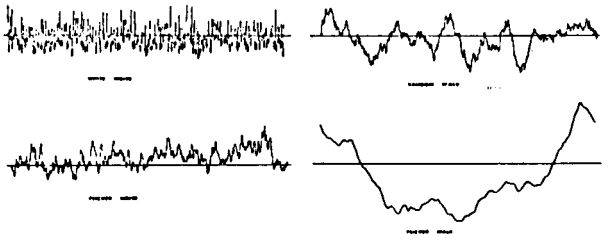

figure 4

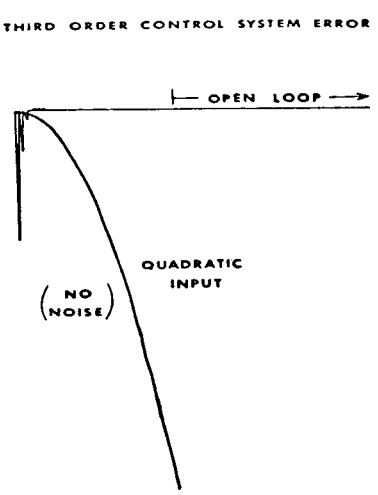

figure 5

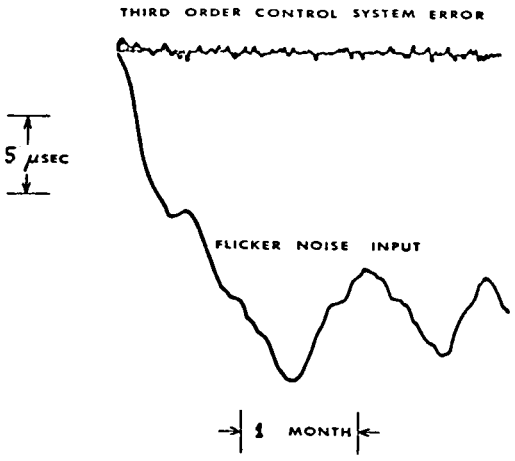

figure 6

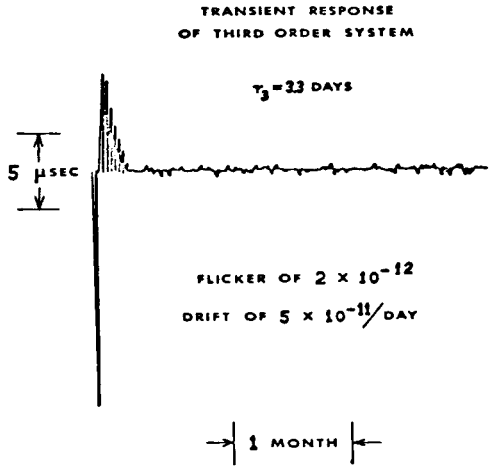

figure 7

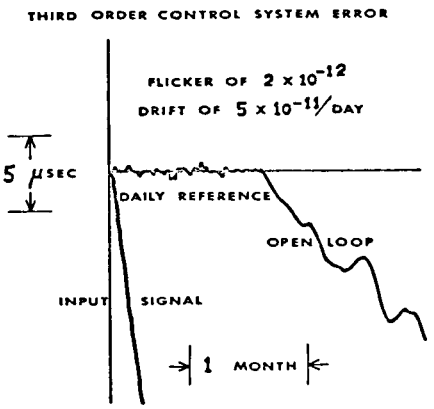

figure 8

Some Characteristics of Commonly Used Time Scales

GEORGE E. HUDSON

Abstract—**Various examples of ideally defined time scales are given. Realizations of these scales occur with the construction and maintenance of various clocks, and in the broadcast dissemination of the scale information. Atomic and universal time scales disseminated via standard frequency and time-signal broadcasts are compared. There is a discussion of some studies of the associated problems suggested by the International Radio Consultative Committee (CCIR).**

I. Introduction

SPECIFIC PROBLEMS noted in this paper range from mathematical investigations of the properties of individual time scales and the formation of a composite scale from many independent ones, through statistical analyses of the properties of realized scales in actual use in broadcasts or proposed for use. How to determine the most efficient and most useful system for broadcasting time and frequency signals is a difficult question. Its answer requires a type of information and operation analysis used in current investigations of electromagnetic frequency spectrum conservation problems. The diverse needs and ideas of many different types of scientists (e.g., geodesists, electronics engineers, physicists, astronomers, geologists) and of many different large groups of users (e.g., military and space agencies, industrial standards laboratories, watch and clock industry) must be taken into account.

We describe (Section III) some broadcast time-dissemination methods and some relevant properties of their associated time scales. The role of the universal scales in furnishing information for the earth sciences and astronomy as well as for navigation is noted (Section II), and the need for supplying this information adequately and simultaneously by standard frequency and time-signal broadcast systems is emphasized (Section III). Finally, we show that nature has posed such a difficult problem in confronting us with diverse important time scales that it is not yet possible to settle on time information-dissemination techniques which are finally acceptable to all users. Moreover, it should be noted that studies of timekeeping and time scales are also important partly because of the close relationship of time-scale properties to the foundations of gravitation and atomic theories [1].

II. Some Time Scales

A. Examples

1) Atomic Scales: In the United States, a precision atomic clock, NBS(A), is maintained at the National Bureau of Standards to realize one international unit of time [2]. As noted in the next section, it realizes the atomic time scale, AT (or A), with a definite initial epoch. This clock is based on the NBS frequency standard, a cesium beam device [3]. This is the atomic standard to which the non-offset carrier frequency signals and time intervals emitted from NBS radio station WWVB are referenced; nevertheless, the time scale SA (stepped atomic), used in these emissions, is only piecewise uniform with respect to AT, and piecewise continuous in order that it may approximate to the slightly variable scale known as UT2. SA is described in Section II-A-2).

The properties of hydrogen maser standards and cesium beam standards have been and are continuing to be studied in great detail, but detailed discussion of experiments with these devices is not properly in the context of the present paper [4], [5].

A contribution to a composite single atomic scale is now made by hydrogen maser frequency standards maintained at the U. S. Naval Research Laboratory. The composite scale is the A.1 scale, maintained by the U. S. Naval Observatory. It is widely used as a reference scale; NBS(A) and A.1 have differed very slightly since their common initial epoch on January 1, 1958 [3], [6]. The present difference in epoch amounts to about 10 ms, and is presently being determined to a much greater precision by a cooperative program undertaken between NBS and USNO. The accuracy of the NBS(A) scale is believed to approach that of the NBS cesium frequency standard—about 5 parts in 10^{12}. There are, of course, several other atomic time scales and frequency standards maintained throughout the world—among these are TA1 at the LSRH (Laboratoire Suisse de Recherches Horlogères), Neuchâtel, Switzerland, and that maintained at NPL (National Physical Laboratory), Teddington, England [7]–[9]. On the basis of some of these scales, the composite one, A.1, was determined for a time by W. Markowitz at the U. S. Naval Observatory. It is now based on several high-quality commercial cesium frequency standards at the Observatory. The hydrogen maser serves as the "flywheel" of this atomic clock. The existence of several independent atomic *clocks* is certainly not to be deplored on scientific grounds since many useful statistical and operating data are obtained via their intercomparison. It does pose the problem, however, of how best to determine a composite "most uniform" and reliable realization of the atomic scale. This certainly is a subject worthy of cooperative consideration by the best scientific and engineering

Manuscript received March 27, 1967.
The author is with the National Bureau of Standards, Boulder, Colo.

minds that can be devoted to it. A promising start on this problem was made by E. L. Crow [10], at the instigation of J. M. Richardson of the Radio Standards Laboratory, NBS-BL. An extension of such theoretical studies combined with the experience of the Naval Observatory in forming the composite A.1 scale is very desirable.

2) Universal Scales: An astronomical time scale known as the universal scale, UT, is a slightly nonuniform one, relative to the atomic time scale, AT. UT is commonly known as Greenwich Mean Time (GMT), when epochs (the times of occurrence of the "ticks") need be specified to no better accuracy than 0.1 second. UT is obtained via interpolation between successive observations of the sidereal time of nearly periodic events (such as the zenith transits of a star) which is then transformed to mean solar time by means of a ratio. The interpolation is accomplished by means of a free-running oscillator driving a clock at nearly the correct rate. The zenith observations and the ratio are used to correct this clock rate so that it ticks off 86 400 intervals, each one nearly one second long, between successive transits of the "mean sun" each day [11]. The scale thus defined locally at an observatory is called UT0. Five slightly different universal time scales now being used are designated respectively as UT0, UT1, UT2, universal atomic (UA), and stepped atomic (SA). UT1 is obtained from UT0 by applying a correction for polar motion specified by data furnished by different observatories. UT2 is derived from UT1 by applying a periodic correction having a maximum amplitude of 0.03 second [12], for annual and semiannual seasonal variations [13]-[15]. Despite these corrections, UT2 is still known to be somewhat nonuniform. The knowledge of UT2 (or even better, UT1) yields information directly concerning the rotational position of the earth about its axis. UA is a piecewise uniform scale which approximates the universal time scale, UT2, within about 0.1 second. It is a "stepped offset" scale (offset pulse rate, stepped pulse epoch) and is derived by making adjustments in offset and epoch from the uniform atomic time scale. The SA scale is a piecewise uniform one derived from the atomic scale by step adjustments in pulse epoch only in order to approximate UT2 within about 0.1 second. All universal scales need be defined and realized only to an accuracy of a few ms [16], [17] due to refraction limitations on astronomical observations, but in view of their definitions the UA and SA scales have the ultimate accuracy of the atomic scale.

Because the rate of occurrence of UT2 markers has been variable and less than the rate of occurrence of seconds markers, UT2 readings were about 5.31 seconds behind A.1 readings on January 1, 1967; on January 1, 1958, at 00:00 GMT, A.1 and NBS(A) epochs were set equal to that of UT2. At present (1966 and 1967) there are 0.94 fewer scale intervals over a year in the UT2 scale than in the more uniform atomic scale, AT.

The importance of UT for celestial navigation, in determining longitude, must be pointed out [18], [19]. The essential principle is simple. By some means, one obtains information that the earth, in rotating on its axis, is in a certain orientation relative to the "fixed" stars at a given instant. In that orientation, tables show that various known stars will have certain elevations above the horizon, in the east-west direction, depending on the longitude of the observer, which can thus be determined. The orientation information is furnished from the epoch of UT1, since successive scale intervals of UT1 (mean solar "seconds") correspond to equal increments (15 arcseconds) of rotation of the earth with respect to the universal mean sun. (Fifteen arcseconds equal about 1/4 nautical mile at the equator.) Conversion to rotation relative to the stars (Sidereal Time) is accomplished by use of the ratio of the length of the mean solar day to the mean sidereal day, about 1.00275.

Universal scales are clearly nonuniform relative to atomic time due to variations in the earth's rotation rate. Nevertheless, the importance of their use in furnishing information about the earth's position on its axis cannot be denied and insures the necessity for their continued dissemination in some suitable form, via radio broadcast [17], [18].

B. Specific Trends in UT

The variations in UT scales or earth rotation rates have been studied extensively by Brouwer [20] and many others [14], [21], [22]. In this article, we need only point out the general nature and size of the variations which have been observed. The reason this is important here is to give the reader some background indication of the kind of data which are encountered in attempts to make both UT information (usually UT2) and more uniform time and frequency information available on the same broadcasts from radio stations. Brouwer's study covered a long period of time; the curves shown in Fig. 1 summarize much of his data

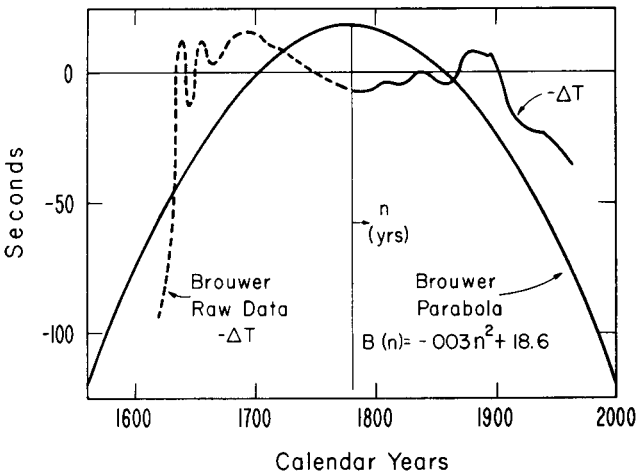

Fig. 1. Trend of $-\Delta T = UT - ET$. The difference $-\Delta T$ in readings of the two scales, UT and ET, is plotted versus the date, which is proportional to ET. The slope of this graph is proportional to the offset in marker rate of UT with respect to that of ET. The parabola represents Brouwer's suggested average trend. Random effects in $-\Delta T$ are evidently present. ET (ephemeris time) is an astronomical time scale which may be considered for present purposes to be uniform with respect to AT [24].

and analysis. They reflect the random behavior [22] of UT, marked on occasion by sudden erratic changes [23].

As specified in the figure, the abscissas are proportional to the astronomical time scale known as ephemeris time, ET. At present ET can be considered uniform with respect to AT [24]. It is a good comparison scale to be used in detecting long-term properties of a time scale.

A study [25] of the trend of UT2 relative to the uniform atomic scale has shown that over a recent 7 1/2-year interval the difference between UT2 scale readings and atomic scale readings was representable by the sum of the Brouwer average parabola (Fig. 1) and a sinusoidal term having a period of 24.1 years and an amplitude of 2.56 seconds. This study was found useful in making short-term predictions of UT2 and as a summary of fluctuation sizes over the interval. The residual difference from the smooth trend has an rms deviation of 16 ms and a maximum of 40 ms. A maximum of the sinusoid occurred at the beginning of 1967.

III. Some Characteristics of Broadcast Scales and Systems

A. Some Specific Systems

1) CCIR Considerations: In the XIth Plenary Session of the CCIR in Oslo, Norway, during the summer of 1966, there was specifically recognized by Study Group VII the possibility of a great many *systems* for broadcasting universal and atomic time information, on the same emission. Moreover, nonuniform time scales, in particular some broadcast ones, as has been noted [17], [26]–[35], have many different properties. The number of possible signal systems increases if one offsets carrier-signal frequencies in various ways from their nominal values to achieve occasional desired adjustments in the pulse rates of time signals. This problem has been noted in various CCIR documents approved by the Assembly, details of which can be found in the published Volume III of the Assembly proceedings. Some documents are indicated by numbers in parentheses in the next paragraph.

For this discussion, we refer especially to the suggestion that experiments and studies be made of how to provide both epoch of UT and the international unit of time interval in the same emission, and how various user requirements can be met by the emission of a single time scale (Opinion 26). We also point to the recommendation (Rec. 374.1) of the use of several international time systems coordinated by the BIH (Bureau International de l'Heure) which were designed for the broadcast of both UT and AT information. Two are called the UTC and SAT systems. We call attention to a report (Rept. 365) comparing these systems statistically for 1965, and finally to a report (Rept. 366) suggesting one method of classification of emission systems which yield standard frequency and time information.

It should be expressly understood that the existence of the two systems SAT and UTC is to be regarded as a step in the evolution and adoption of a single practicable world-wide system which will be internationally acceptable. Thus, it seems important to exhibit here briefly a method of characterization of systems which can be used to fulfill various needs, but which require further study.

2) A Classified Listing of Systems: Systems for broadcasting time and frequency information can be classified according to the method adopted in Tables I and II. A system may utilize more than one time scale. If so, two or more columns would be used under the heading *entry*, in constructing such a table. An *entry* Yes, or No, indicates whether or not a specified property is indicated directly on a broadcast by the time markers (pulses) and the use of piecewise constant carrier frequencies (but not codes). Under additional remarks, specify when an adjustment in a property may be made, how large it is to be, what the known relation between pulse (marker) and carrier phase is, which universal or uniform scale is being approximated, and what the relations are to these scales (e.g., how closely approximated).

As examples, the UTC system is so classified in Table I, and the SAT system is classified in Table II. Both systems are coordinated by the BIH and are currently in use. The UTC system is used by a large number of stations, and the SAT system, an experimental but coordinated one, is used at present only by stations WWVB in Fort Collins, Colo., and DCF77, in Mainflingen, West Germany.

Other possible systems also can be so classified. For example, the system used by station HBG in Switzerland differs from the UTC system (Table I) only in that (as in Table II) the carrier is not offset (Item A) and the time markers and carrier signals are not phase-locked (Item D). Hence, by an appropriate pulse generator locked to the received carrier signal, a clock yielding a time scale which is very close to AT and whose pulse rate need never be adjusted, can be constructed, just as with the SAT coordinated system carrier signals (Table II, Item F). Time signals emitted following any one coordinated system must be synchronized to 1 ms.

It is to be hoped that the experimentation with and study of various systems for yielding both UT information and AT information, on the same broadcast emission, will lead to a suitable format acceptable to most if not all users in the next few years. Toward this end, several coordinating groups of the U. S. Preparatory Committee, Study Group VII, CCIR, have been appointed. One object is to study the deplorable problem raised by the existence of a great variety of auxiliary time scales, some denoted by a random nomenclature. Since the initiation of the SAT system on January 1, 1967, the ad hoc name SAB for the signals disseminated by WWVB has been dropped. WWVB's control clock is now called NBS(SA), just as WWV's and WWVH's is called NBS(UA). Another more important requirement, which has been noted by many international organizations, is to eliminate carrier-frequency offsets. It seems appropriate at this point to give a more technical discussion of offsets in frequency and in pulse rates.

TABLE I

SYSTEM—UTC

Name(s) of Scale(s)	UA	Universal Atomic
Property	Entry	Additional Remarks
A) Carrier offset	Yes	Adjusted, when necessary, on the first of a year by a positive, negative, or zero integral multiple of 50 parts in 10^{10} to follow UT2.
B) Marker rate offset	Yes	Same adjustment as A).
C) Epoch steps	Yes	Phase of markers adjusted on first of a month, when necessary, by 100-ms steps to follow UT2.
D) Marker-carrier phaselocked	Yes	None.
Contains time markers which:		
E) Yield universal scale	Yes	UA approximates UT2 within about 0.1 second.
F) Yield uniform scale with respect to AT	Yes	By correcting for the offset and the step adjustments, AT can be found, but correction information must be obtained from additional signals or a supplementary historical log.
G) Made up of more than one broadcast time scale	No	Voice or code can, of course, be used to supply information in F), or a better knowledge of (preliminary) UT2.

TABLE II

SYSTEM—SAT

Name(s) of Scale(s)	SA	Stepped Atomic
Property	Entry	Additional Remarks
A) Carrier offset	No	None.
B) Marker rate offset	No	Except at moment of epoch adjustment.
C) Epoch steps	Yes	200-ms steps to follow UT2 made on the first of a month, when necessary.
D) Marker-carrier phaselocked	Yes	None.
Contains time markers which:		
E) Yield universal scale	Yes	Approximate UT2 within about 0.1 second.
F) Yield uniform scale with respect to AT	Yes	Differs from AT by $0.2n$ seconds, where n is a positive, negative, or zero-integer which must be obtained from supplemental information. During March, 1967, $n=28$. An AT scale can be generated by phase-locking to carrier.
G) Made up of more than one broadcast time scale	No	Voice or code can, of course, be used to supply the information in F), or a better knowledge of (preliminary) UT2.

B. Offsets, Steps, and Trends in Some Broadcast Time and Frequency Signals

1) Offsets: For a long time, oscillators whose frequencies are deliberately offset from their nominal values measured relative to atomic standards have been used to control time and frequency signals emitted from various United States radio stations, e.g., from WWV and WWVH, as well as NSS and NBA [18]. At present, adjustments in this offset are introduced on the first of a year into the emitted carrier frequency in accordance with some of the adjustments required by the definition of the commonly used broadcast (piecewise uniform) time scale UA belonging to the UTC system.

Figure 2 shows the history of WWV carrier-frequency offsets since 1957. The improvement in frequency control is evident and may be directly ascribed to improvements in standards and phase-lock control techniques. The trend should be compared with the fitted-offset trend of the UT2 scale marker rate to judge how well the broadcast offset approximated it. Beginning January 1, 1960, the time pulses emitted from WWV were locked to the carrier frequency, as was true for many other time broadcasts. Thus, the rate of emission of the time pulses was controlled by varying the carrier-frequency offsets. This is still the method in use for stations following the UTC system.

2) Steps and Trends: Figure 3 is a summary comparison of realizations of all the various scales considered for the nine years since 1957. Ordinates plotted are the differences between the reading on a given scale or clock at a given epoch and the simultaneous corresponding reading on the atomic scale. The slope of a trend on such a plot, when divided by 31.5×10^6 (the number of seconds per year), is the offset rate from that of the reference clock. In addition to NBS(UA), SAB, and UT2, the average long-term Brouwer trend is shown [20]. One sees that the average marker-rate offset of UT2 from the more uniform atomic scale would ultimately become indefinitely large, if the long-term Brouwer trend were to persist. It is also clear that the UT2 scale and offset undergo large fluctuations about their long-term average trends. A smooth fit to the UT2 data, shown by the dotted curve, has been represented over this period by a sinusoidal plus a parabolic function. The amplitude of the sinusoidal component is about 2.56 seconds, although the rms deviation of the data from the curve-fit is only about 16 ms.

3) Comparisons in 1956 and 1966: In the following, certain statistics relating to the "stepped offset" (epoch steps, pulse rate and carrier frequency offset), or UTC, system for broadcasting UT and AT information are compared with similar statistics relating to the "stepped" system utilizing

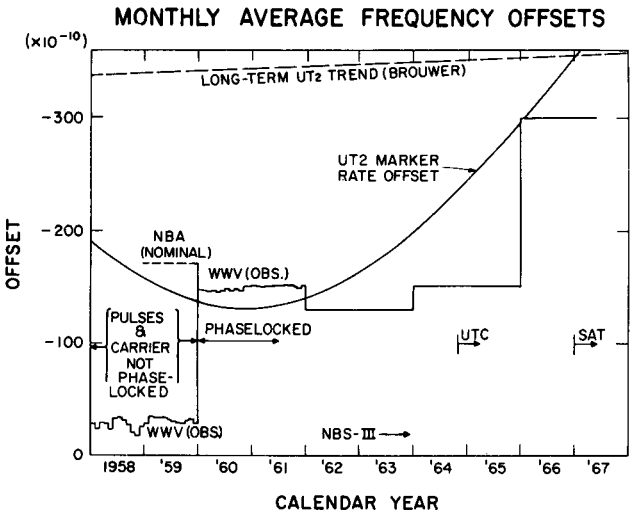

Fig. 2. The recent history of frequency offsets. Since the long-term trend of the UT2 scale seems to be parabolic, its long-term trend in offset marker rate is linear, shown dashed. Fluctuations in UT2 produce the (smoothed) offset trend about the long-term one shown by the solid curve. The NBS frequency standard of course is not offset, as indicated by the bottom horizontal line. Improvement in frequency control is evident in the step "approximation" to UT2; the UTC system, inaugurated as a continuation of the former coordinated "signal" system in 1964, led to the offset of -300×10^{-10} in transmissions in 1966 and 1967 in an attempt to follow more closely the UT2 fluctuating trend.

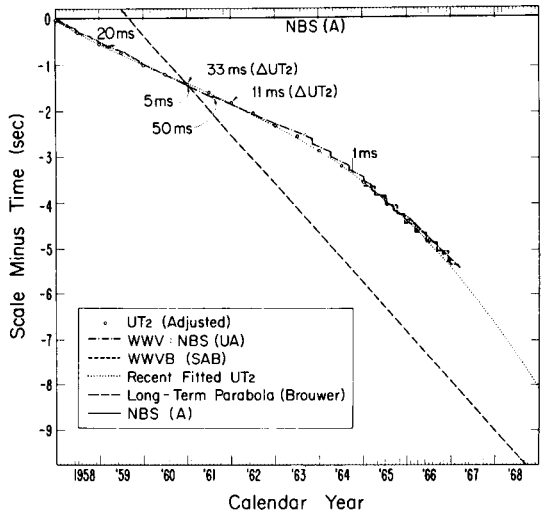

Fig. 3. Summary of broadcast time-scale trends. All scale trends are indicated by plotting as ordinates the number of nominal seconds decreased by the number of seconds (atomic scale) which have elapsed since January 1, 1958. The long-term parabolic Brouwer trend in UT2 is shown dashed; the broadcast scale for WWV is indicated by the tilted stepped curve, with step retardations of 100 ms since 1964, and that for WWVB is shown at the right by the step approximation to the UT2 trend with step retardations of 200 ms. The UT2 (adjusted) points are plotted after removing the discontinuities due to redetermination of various observatories' coordinates; the dates and sizes of these discontinuities are indicated. The nonoffset trend of the atomic scale, as generated by the NBS clock, is shown by the top horizontal line.

SAB (stepped atomic, WWVB). Such data may contribute toward an answer to the CCIR-suggested studies.

The data for 1956 and 1966 may be represented conveniently by plotting aginst the calendar date, for each realized scale, NBS(UA) and SAB, respectively, the difference between the number of scale markers (nominally seconds pulses) since the beginning of January, 1958 (i.e., the scale reading) and the number of seconds pulses, AT, since that epoch. The trends for 1965 and 1966 are shown in Fig. 4. The solid curve represents the smooth curve-fit to UT2 (shown by circles) using a sinusoid plus parabola. The portion of this curve from August 1, 1965, to December 31, 1965, was drawn before the data points shown were known. It therefore constitutes a prediction of the trend of UT2 for the latter portion of 1965 and was good to better than 40 ms. Also shown in Fig. 4 (dashed) is the long-term parabolic trend analyzed by Brouwer [20].

Various statistical data are evident from Fig. 4. Although both the UA and SAB scales satisfied stated conditions for ship navigation, and were within about 0.1 second of UT2 (corresponding to a "fix" of about 150 feet at the equator) there is some distinction to be made in the closeness of approximation measured by the absolute deviation and percent departure time in favor of UA. The improvement since 1963 in the approximation of UT2 by such stepped, offset methods is evident. In terms of mean deviations there is a small distinction between SAB and UA in favor of SAB.

Because of the offset (or slope), the UA scale markers of course are separated by intervals which are longer than one second. The corresponding SAB intervals are one second long. Both scales are piecewise uniform and piecewise continuous with respect to AT. If it seems desirable to retain the goal of broadcasting directly signals which approximate UT2 to the highest accuracy, and which on the same emission directly yield atomic time and frequency information and the international second, then the best method has not yet been found.

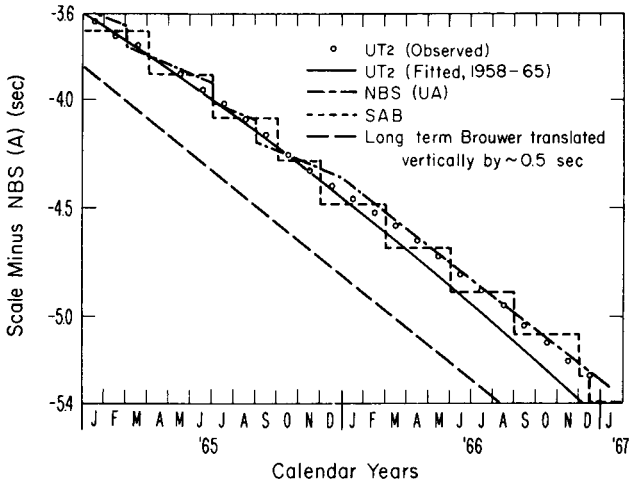

Fig. 4. Trends in SAB and NBS(UA) during 1965 and 1966. The trend in the NBS(UA) clock reading, following the UTC system, is indicated by the slanted (i.e., offset), stepped (100 ms) approximation to the UT2 data, represented by dots. The fitted trend UT2 is shown by the solid curve, and the SAB stepped (200 ms) scale trend is also indicated. The ordinate magnitudes represent lag times with reference to the scale readings of the NBS time standard or clock, NBS(A).

C. Possible Future Trends in the Broadcast of UT and AT Signals

The investigations reported here summarize preliminary attempts at resolving the CCIR question of how to broadcast UT and AT signals, satisfactorily, on the same emission. A few comments regarding the possible future status of these two kinds of signals would seem to be appropriate. There should soon be advances in the scientific analyses of information concerning the properties and trends of the slightly variable universal scales of time. These should take the form of statistical and trend analyses of the ever-increasing store of data concerning the earth rotation rates and the development of appropriate physical theories. There probably will be improvements in the overall coordination of national and international standard transmissions of time signals as more atomic frequency standards are adopted [8], [9]. There may be wider adoption of atomic scales not only for synchronization purposes, but also for epoch determination, in conjunction with the astronomical ephemeris time scale, ET [24], [34], [35]. In this fashion, it may become more commonly recognized that the primary and important role of universal scale transmissions is not that of a source of uniform time, but of essential geological information useful in tracking, navigation, and scientific studies of the environment.

It should be emphasized that both present coordination methods, UTC and SAT, described herein, furnish UT and AT information on the same broadcast. Yet each requires either the broadcast, or other communication, of additional information before AT or UT2 itself (or, perhaps more directly useful, the earth's rotational position obtained by correcting UT2 to UT1) can be determined from the broadcast pulses, as accurately as they can be known at a given moment. The same can be said for some other simpler methods which have been suggested, such as the straightforward broadcast of an atomic time scale. For example, with no adjustments save an occasional renaming of a particular second from time to time, i.e., by occasionally inserting or deleting a few seconds, or a minute, the atomic scale, so modified, could keep approximately in phase with UT, but would not lead directly to UT information of sufficient accuracy for some purposes.

Celestial navigators who use UT information now require the use of tables noting star positions versus UT. It may soon prove desirable and possible, however, for astronomers to prepare supplementary tables of UT versus AT (or ET) well within the requisite accuracy limits and sufficiently far in advance for the ready use of celestial navigators.

Alternatively, quite accurate broadcasts of preliminary UT epoch information (within 10 ms) might prove feasible, by a modification of the present UTC method. Adjustments made every month, in offset, or in epoch, or both, which are a known multiple of a small increment in relative offset (say, 50×10^{-10}) or a small time interval (say, 10 ms) have been suggested. It may appear that UT1, in fact, would be the appropriate universal scale to follow for this purpose. It would be very important, even essential, for reference and synchronization purposes, to have available, on the same broadcast, standard, "uniformly" spaced, *clearly marked* atomic time pulses interspersed with the UT pulses, say at 5- or 10-second intervals. Or the desirable choice might be to have more widely spaced universal time pulses to indicate closely the earth's position, with a background of seconds pulses for reference. The solution of the problem will depend on time-sharing studies and determination of user needs.

Everyday users would not need to be concerned about the introduction of an occasionally modified, atomic scale of time. Various local universal times, standardized by convention, such as Mountain Standard Time (MST), differ from GMT [36] by an integral number of hours, depending on locations. Such local time scales are often adjusted periodically by one-hour steps to yield "daylight savings time," or to return to "standard" time. Similar local times could be derived just as well from an atomic scale, by similar adjustments and zoning, and by the deletion, every few years, of a small number of "one-second leaps" or, alternatively, in about 50 years, a "one-minute leap." In this way, approximate epochal coherence with the rising and setting of the sun would be retained, and there need be no fear of a radical departure from solar time for "everyday" purposes.

It should be emphasized that the coordinated methods which have been used to broadcast UT and AT information, or which have been discussed or mentioned herein, are only a few of the possible ones.

IV. Concluding Remarks

We list here a few concluding statements about problems and information which have been discussed in the foregoing.

1) The practical use of universal scales (UT) as a navigational aid and for yielding other information concerning the rotational position of the earth cannot be denied. Suitable methods for disseminating a suitably accurate universal scale separately, and in combination with, a more uniform scale must be studied, experimented with, and discussed.

2) It should not be held that UT is the only kind of time for "everyday" use. Unadjusted atomic scales will not diverge from UT by more than a few seconds every few years and differences could easily be removed, on occasion, by proper adjustment. These adjustments would be far smaller in magnitude than similar adjustments already in common use under the headings of daylight savings time, leap year day, and reference to the mean sun instead of the visible apparent sun.

3) The invention of physically different time scales, such as a nuclear-based one [37], should be regarded as a desirable scientific activity; but the proliferation of artificial derived scales is to be deplored.

4) There is a need for intensive study of the formation and properties of composite time and frequency standards and time scales. Many competent laboratories maintain

463-560 O - 72 - 16

their own precise instrument standards founded on fundamental readily accessible phenomena of nature. This is indeed an evident trend which occurs in other standards areas. Thus, here is clearly a need for coordination in the use, dissemination, and intercomparison of such standards.

5) The CCIR is attempting to stimulate further investigations of the need and use of more uniform scales of time on broadcasts, better ways to present universal scale information of use in the study and use of earth rotation rates and positions, the more efficient use of the electromagnetic spectrum for these broadcasts, and the international definition of a composite, more uniform, reference scale of time.

6) The action of national and international committees in defining and calling attention to problems and needs, and in stimulating research and development is an extremely important one, as well as their function in keeping the overall scope in proper perspective. They also perform a needed general recommendatory function, as exemplified by the CCIR documents; they certainly assist in maintaining a uniform level for specifying operating procedures and standards.

7) The technological study of improvements in the methods of giving time and geological information simultaneously on standard broadcasts is an important example of a general problem now being recognized more formally on a broad scale. This is the scientific and efficient technological use of the electromagnetic frequency spectrum.

Acknowledgment

The basic researches by Dr. R. C. Mockler, Dr. J. A. Barnes, R. E. Beehler, R. L. Fey, and Dr. J. M. Richardson on atomic time and frequency standards made it imperative for me to learn from them, by conversations and reading, the essential background in this field. I am indebted to my predecessor, the late W. D. George, and to Dr. Y. Beers, A. H. Morgan, and D. H. Andrews, for my education in the fascinating art and science of time and frequency standard dissemination by radio broadcasts.

Collaboration with Mrs. M. Cord in making the current studies of the properties of time scales, some results of which are reported herein, is gratefully acknowledged. The contributions of all other co-workers and colleagues, including secretaries Mrs. L. Canaday and Miss C. Nielsen, are sincerely appreciated.

References

[1] R. Dicke, "Gravitational theory and observation," *Phys. Today*, vol. 20, pp. 55–70, January 1967.

[2] CIPM, *Comptes Rendus des Séances de la Douzième Conférence Générale des Poids et Mesures*. Paris: Gauthier-Villars, 1964, p. 93.

[3] J. A. Barnes, D. H. Andrews, and D. W. Allan, "The NBS-A time scale its generation and dissemination," *IEEE Trans. on Instrumentation and Measurement*, vol. IM-14, pp. 228–232, December 1965.

[4] R. E. Beehler, R. C. Mockler, and J. M. Richardson, *Metrologia*, vol. 1, pp. 114–131, July 1965.

[5] R. Vessot, H. Peters, J. Vanier, R. Beehler, D. Halford, R. Harrach, D. Allan, D. Glaze, C. Snider, J. Barnes, L. Cutler, and L. Bodily, "An intercomparison of hydrogen and cesium frequency standards," *IEEE Trans. on Instrumentation and Measurement*, vol. IM-15, pp. 165–176, December 1966.

[6] J. Newman, L. Fey, and W. R. Atkinson, "A comparison of two independent atomic time scales," *Proc. IEEE (Correspondence)*, vol. 51, pp. 498–499, March 1963.

[7] J. Bonanomi, P. Kartaschoff, J. Newman, J. A. Barnes, and W. R. Atkinson, "A comparison of the TA1 and the NBS-A atomic time scales," *Proc. IEEE (Correspondence)*, vol. 52, p. 439, April 1964.

[8] L. U. Hibbard, "Atomic frequency standards," *At. Energy (Australia)*, vol. 7, pp. 21–26, October 1964.

[9] A. G. Mungall, R. Bailey, and H. Daams, "Atomic transition sets Canada's time," *Canad. Electronics Engrg.*, vol. 37, pp. 23–27, August 1965.

[10] E. L. Crow, "The statistical construction of a single standard from several available standards," *IEEE Trans. on Instrumentation and Measurement*, vol. IM-13, pp. 180–185, December 1964.

[11] E. W. Woolard and G. M. Clemence, *Spherical Astronomy*. New York: Academic, 1966, pp. 326–375.

[12] *B.I.H. Bulletin Horaire (Paris)*, p. 2, January–February 1964.

[13] W. Markowitz, "Variations in the rotation of the earth, results obtained with the dual rate moon camera and photographic zenith tubes," *Astron. J.*, vol. 64, pp. 106–113, April 1959.

[14] W. H. Munk and G. D. F. MacDonald, *The Rotation of the Earth*. London: Cambridge University Press, 1960, ch. 8.

[15] Kuiper and Middlehurst, *Telescopes: Stars and Stellar Systems*, vol. I. Chicago: University of Chicago Press, 1960, ch. 7.

[16] Société Suisse de Chronométrie, *Proc. Congrès Internat'l de Chronométrie Lausanne*, Neuchâtel, Switzerland, pp. 157–174, June 1964.

[17] J. Kovalevsky, "Astronomical time," *Metrologia*, vol. 1, pp. 169–180, October 1965.

[18] U. S. Naval Observatory and Royal Greenwich Observatory, *Explanatory Supplement to the Astronomical Ephemeris and the American Ephemeris and Nautical Almanac*. London: Her Majesty's Stationery Office, 1961, pp. 443–453.

[19] U. S. Naval Observatory, *The American Ephemeris and Nautical Almanac for the Year 1968*, Washington, D. C.: U. S. Gov't Printing Office, 1966, pp. 468–485.

[20] D. Brouwer, "A study of the changes in the rate of rotational of the earth," *Astron. J.*, vol. 57, pp. 125–146, September 1952.

[21] W. Markowitz, "Latitude and longitude, and the secular motion of the pole," in *Methods and Techniques in Geophysics*, S. K. Runcorn, Ed. London: Interscience, 1960, pp. 325–361.

[22] R. B. Blackman and J. W. Tukey, *The Measurement of Power Spectra*. New York: Dover, 1958, pp. 151–159.

[23] S. Iijima, N. Matsunami, and S. Okazaki, "On the abrupt change in the earth's rotation at the beginning of 1963," *Ann. Tokyo Astron. Observatory*, 2nd ser., vol. VIII, pp. 207–217, August 1964.

[24] W. Nicholson and D. Sadler, "Atomic standards of frequency and the second of ephemeris time," *Nature*, vol. 210L, p. 187, April 1966.

[25] M. Cord and G. E. Hudson, "Some trends in UT," to be published.

[26] I. Newton, *Principia*, rev. transl. by F. Cajori. Berkeley, Calif.: University of California Press, 1947, p. 6.

[27] R. B. Lindsay and H. Margenau, *Foundations of Physics*. New York: Wiley, 1936, pp. 72–78.

[28] H. Margenau, *The Nature of Physical Reality*. New York: McGraw-Hill, 1950, ch. 7.

[29] *Van Nostrand's Scientific Encyclopedia*, 3rd ed. Princeton, N. J.: Van Nostrand, 1958, pp. 1691–1692.

[30] J. M. Richardson, "Time standards," in *Encyclopedic Dictionary of Physics*, suppl. vol. 1. Oxford: Pergamon, 1966.

[31] , "Time and its inverse," *Internat'l Science and Technology*, pp. 54–76, June 1962.

[32] G. E. Hudson, "Of time and the atom," *Phys. Today*, vol. 18, pp. 34–38, August 1965.

[33] J. M. Richardson and J. Brockman, "Atomic standards of frequency and time," *Phys. Teacher*, vol. 4, p. 247, September 1966.

[34] G. Becker, "Von der astronomischen zur atomphysikalischen Definition der Sekunde," pts. I and II, *PTB Mitteilungen*, no. 4, pp. 315–323 and no. 5, pp. 415–419, 1966.

[35] G. C. McVittie, *General Relativity and Cosmology*. Urbana, Ill.: University of Illinois Press, 1965, pp. 89–90.

[36] "Frequency and time standards," Frequency and Time Division, Hewlett-Packard Co., Appl. Note 52, pp. 1–2, 1965.

[37] L. A. Khalfin, "A fundamental method for measuring time," *Soviet Physics JETP*, vol. 12, pp. 353–345, February 1961.

The Development of an International Atomic Time Scale

JAMES A. BARNES

Abstract—**The paper reviews briefly the methods of generating atomic time and the errors inherent in the resulting scales. An atomic clock consists of an atomic frequency standard and an "integrator" to accumulate the phase of the signal. Because of noise perturbing the instantaneous frequency, an ensemble of identical atomic clocks will show a distribution of (epoch) times which is unbounded as the system evolves in time. The recognition of this problem has important consequences in national and international coordination of time scales and the construction of average atomic time scales.**

Also of significance is the not completely resolved question of weighting of individual standards in the construction of average time scales. In spite of these difficulties, it is pointed out that through coordination and proper data handling, most of the advantages of astronomical time scales can be realized by atomic time scales. A statement of some of the problems facing any attempts at coordination is presented without any suggested solutions.

I. The Construction of an Atomic Time Scale

A. Introduction

WHEN one thinks of a clock, it is customary to think of some kind of pendulum or balance wheel and a group of gears and a clock face. Each time the pendulum completes a swing, the hands of the clock are moved a precise amount. In effect, the gears and hands of the clock "count" the number of swings of the pendulum. The face of the clock, of course, is not marked off in the number of swings of the pendulum but rather in hours, minutes, and seconds.

One annoying characteristic of pendulum type clocks is that no two clocks ever keep exactly the same time. This is one reason for looking for a more stable "pendulum" for clocks. In the past, the most stable "pendulums" were found in astronomy. Here one obtains a significant advantage because only one universe exists—at least for observational purposes, and time defined by this means is available to anyone—at least in principle. Thus, one can obtain a very reliable time scale which has the property of universal accessibility. In this paper, time scale is used to refer to a conceptually distinct method of ordering events in time.

In a very real sense, the pendulum of ordinary, present-day, electric clocks is the electric current supplied by the power company. The power companies normally are careful that just the right number of swings of the pendulum occur each day, the length of the day being determined by observatories. Since all electric clocks which are powered by the same source have, in effect, the same pendulum, these clocks will neither gain nor lose time relative to each other. Indeed, they will remain close to astronomical time.

Manuscript received December 19, 1966; revised March 7, 1967.
The author is with the National Bureau of Standards, Boulder, Colo.

It has been known for some time that atoms have characteristic resonances or, in a loose sense, "characteristic vibrations." The possibility, therefore, exists of using the "vibrations of atoms" as pendulums for clocks. The study of these "vibrations" has normally been confined to the fields of microwave and optical spectroscopy. Presently, microwave resonances (vibrations) of atoms are the most precisely determined and reproducible physical phenomena that man has encountered. There is ample evidence to show that a clock which uses "vibrating atoms" as a pendulum will generate a time scale more uniform than even its astronomical counterpart.

But due to intrinsic errors in any actual clock system, one may find himself back in the position of having clocks which drift relative to other similar clocks. Of course, the rate of drift is much smaller for atomic clocks than the old pendulum clocks, but nonetheless real and important. If at all possible, one would like to gain the attribute of universal accessibility for atomic time also. This can be accomplished only by coordination between laboratories generating atomic time. Both national and international coordination are in order.

It is the purpose of this paper to review briefly the methods of constructing atomic time scales and, in doing so, to point out the limitations and difficulties facing an internationally, or, for that matter, a nationally accepted standard of atomic time (epoch). Within the literature one can find numerous papers treating time, both astronomical and atomic. It is not the purpose of this paper to review the entire field of timekeeping and show the relation of atomic time to other forms of time. For such a review, the reader is referred to the literature [1], [2]. Similarly, one may find extensive literature which covers the detailed limitations of atomic frequency standards.[1] The rather modest aim of this paper is to recognize the common difficulties of atomic frequency standards in general and develop the consequences for an international standard of atomic time. The author hopes to accomplish two things in the present treatment: first, to formulate a clear and concise statement of some of the technical (as opposed to political, personality, or traditional) problem areas to be overcome and second, to convey to individuals who are not intimately involved in the field the present, rather volatile state of affairs in atomic timekeeping.

[1] See, for example, R. E. Beehler, "A historical review of atomic frequency standards," this issue; A. O. McCoubrey, "The relative merits of atomic frequency standards," this issue; and the Special Issue on Frequency Stability, *Proc. IEEE*, vol. 54, February 1966.

It is of value in comparing time scales to consider four significant attributes of some time scales:

1) accuracy and precision,
2) reliability,
3) universal accessibility,
4) extension.

In the areas of accuracy and precision, atomic time scales have a clear advantage over their astronomical counterpart. Atomic clocks may be able to make a reasonable approach to the reliability and accessibility of astronomical clocks. The extension of time to past events (indeed, remote, past events) is a feature which atomic clocks will never possess. Their utility for future needs, however, is quite another matter. The needs of the general scientific community and, in particular, the space industries are making ever greater demands on accurate and precise timing covering longer time intervals. Often these needs cannot be met by astronomical time.

B. The Basic System

An ordinary clock consists of two basic subsystems: a periodic phenomenon (pendulum), and a counter (gears, clock face, etc.) to count the periodic events. An atomic clock differs from conventional clocks only in that the frequency of the periodic phenomenon is, in some sense, controlled by an atomic transition (atomic frequency standard) [3], [4]. Since microwave spectroscopic techniques allow frequencies to be measured with a relative precision far better than any other physical quantity, the desirability of extending this precision to the domain of time measurement has long been recognized.

It is customary to define the instantaneous (angular) frequency, $\Omega = 2\pi f$, of a signal generator by the equation

$$\Omega \equiv \frac{d\phi}{dt}, \tag{1}$$

where ϕ is the phase of the signal output and t is the time. This definition is consistent with the theory of operation of atomic frequency standards [5]–[7]. Thus, if Ω_s is the angular frequency of an atomic frequency standard and ϕ_s is the instantaneous phase, then one interprets t as atomic time. It is convenient to assume that $\Omega_s = \Omega_s(\phi_s)$, and then, the solution of (1) becomes

$$t_1 - t_0 = \int_{\phi_0}^{\phi_1} \frac{d\phi_s}{\Omega_s(\phi_s)}. \tag{2}$$

For the case where $\Omega_s = 2\pi f_s$ is constant, one may obtain from (2)

$$t_1 - t_0 = \frac{N_1 - N_0}{f_s}, \tag{3}$$

where $N_1 - N_0$ is the number of cycles (not necessarily an integer) elapsed during the interval $t_1 - t_0$ of atomic time.

It is customary to set

$$t_0 = N_0 = 0$$

at some arbitrary point in time. Several atomic scales [8]–[10] have chosen the "zero point" at zero hours, January 1, 1958 (UT2), but this is not universal among all atomic scales in existence today.

Thus, an atomic clock may consist of an atomic frequency standard and synthesizer-counter system which contains the current value of N/f_s. In practice, one normally maintains a running count of the atomic time (N/f_s) on some visual display capable of being read to the nearest second. Also a device is operated which generates a very precise electrical pulse each time the counter (N) increases its count by the numerical value of f_s (i.e., each atomic second). Fractions of one second then are determined by interpolation between the one-second ticks of the clock. For precision measurements, the usual method of interpolation is to use an electronic frequency counter operated in the time interval mode, and determine the time interval between a tick of the atomic clock and the observed event. Measurements to one nanosecond are possible by this technique and the use of "vernier methods" [11].

C. Reliability and Redundancy

In the past, reliable operation of atomic frequency standards has been a significant problem. Presently, however, commercial units with a mean time between failure (MTBF) exceeding one year are not uncommon. As with most solid-state devices, the first six to twelve months is the biggest problem, although finite atom source lifetime prevents unlimited operation without interruption.

It is true that an MTBF exceeding one year reflects significant engineering accomplishments, but this is far from comparable to the high reliability of astronomical time. The obvious solution is to introduce redundancy in the clock system. One can use several atomic clocks in the system and this should certainly be the best approach in the sense of accuracy and reliability—it is expensive, however. An alternative is to use secondary standards or crystal oscillators as "fly wheels" during down times of the primary frequency standard. A reasonable, economical compromise is probably a mixture of these two possibilities.

Suppose the synthesizer-counter subsystem of a clock system should jump a small amount and cause a discontinuity in its indicated time. It is possible that such a transient malfunction could occur with no outwardly apparent signs of malfunction of the apparatus. It is also apparent that if only two clocks are available for intercomparison, it is impossible to decide which clock suffered the transient malfunction. Thus, three clocks (not necessarily all atomic) constitute an absolute minimum for reliable operation. If one or more of these has an extended probable down time (e.g., while the atom source is replenished in an atomic device), then four or five clocks become a more workable minimum.

It should be noted here that one could assemble a large group of clocks into one system and the system MTBF calculated from the individual MTBF's might extend into geologic time intervals. This system MTBF is undoubtedly over-optimistic due to neglect of the possibilities of catastrophes or operator errors. Nonetheless, with various

atomic clocks spread over the earth, it should be possible to maintain an epoch of atomic time with a reliability that could satisfy almost any future demand.

D. Propagation of Errors in an Atomic Clock

In any actual atomic frequency standard, there are always noise processes which prevent its frequency from being absolutely constant. Here it is necessary to reconcile the idea of nonconstancy with the idea of a standard. Conceptually, a standard is often defined in certain highly idealized ways. The actual physical embodiment of a standard is always less than ideal [12]. In a cesium or thallium beam device, for example, the effects of shot noise of the beam itself can be reduced by going to a high flux of atoms but the effects cannot be eliminated entirely.

Define Ω_0 now to be the "ideal" (instantaneous) frequency of an atomic frequency standard (the numerical value of Ω_0 is set by definition) and let ε represent the departure of the actual frequency Ω_s from the ideal, i.e.,

$$\Omega_s = \Omega_0 + \varepsilon.$$

Under these conditions, (2) becomes approximately

$$T \approx \frac{N}{f_0} - \frac{1}{(2\pi f_0)^2}\int_0^{\phi_1} \varepsilon(\phi)d\phi \tag{4}$$

for $|\varepsilon/f_0| \ll 1$. T is the ideal (though unobservable) time.

The most favorable class of noise which one might reasonably expect for an actual frequency standard is that ε is a band-limited white noise with zero mean. Another, entirely possible spectral type of noise, is flicker $(1/f)$ noise. The sources of systematic errors and the noise sources are adequately covered in other papers (for example, Beehler et al. [12]). Defining $t_1 \equiv N/f_0$, the indicated time, (4) may be written in the form

$$t_1 \approx T + \frac{1}{2\pi f_s}\int_0^{t_1} \varepsilon_1(t)dt \tag{5}$$

where $\phi = 2\pi f_0 t$, $\varepsilon_1(t) = \varepsilon(2\pi f_0 t) = \varepsilon(\phi)$, and $|\varepsilon/f_0| \ll 1$. For $\varepsilon_1(t)$, a white noise process, the integral on the right of (5) is a "Brownian motion" or Wiener-Lévy process. A characteristic of such a process is that while its average value is zero, its excursions away from zero can be arbitrarily large as t_1 becomes large. It is easiest to imagine a large ensemble of identical clocks which were set together at $t_1 = 0$, i.e., a Dirac δ function for the initial distribution density of the clocks. As this system evolves in time, each clock will wander away from the others, and at some later time ($t_1 > 0$) there will be a spread to the distribution density of the clocks. It is a characteristic of Brownian motion that the width of this distribution increases proportionally to $\sqrt{t_1}$. If $\varepsilon_1(t)$ is other than a white noise with zero mean, the above statements do not hold. For example, if $\varepsilon_1(t)$ is a flicker $(1/f)$ noise process, the uncertainty of the value of the integral grows linearly with t even though it is a nondeterministic process. It is thus important to know what types of noise predominate in actual standards and how closely they approach theoretical limitations.

The omnipresent flicker $(1/f)$ noise in electronic equipment encourages one to conclude that this type of noise will be the ultimate limitation of stability of all atomic frequency standards. Within the author's experience, all atomic frequency standards *do* "flicker out" eventually when left undisturbed. The effects of occasional realignments of system parameters on the continuation of flicker noise are difficult to evaluate. It is reasonable to expect that complete alignments of the standard do destroy correlations which give rise to the flicker noise. Based on this reasoning, it is reasonable then to weight laboratory-type standards more heavily than the hermetically sealed commercial units which have been in operation for some time.

Typical values for the coefficient of the linear increase in the time uncertainty (assuming a flicker noise frequency modulation) range from 10^{-14} for hydrogen masers to a few times 10^{-13} for good cesium beams [4]. For the present state-of-the-art, the uncertainties due to systematic offsets are significantly greater than these values (10^{-11} to 10^{-12}), and thus the noise processes do not directly limit the accuracy of the instrument. The noise processes do, however, determine its precision (uniformity). One significant conclusion from these considerations may be stated: No matter how carefully systematic differences between elements of an ensemble of frequency generators are removed, the spread of times indicated by the various clocks will grow at least as $t^{\frac{1}{2}}$ and very possibly as t itself.

While these statements seem pessimistic, it is of value to recognize that Brouwer [13] determined that the random processes which affect the rotation of the earth on its axis caused the rms fluctuations in Universal Time to increase as $t^{\frac{3}{2}}$, for t greater than one year. For periods of the order of a year or less it appears that the variations in the UT2 time scale cause the rms fluctuations to increase as the first power of t (flicker noise frequency modulation). The coefficient of this linear term is about 2×10^{-9} or almost a factor of 10^4 worse than some cesium clocks.

The present means of determination of Ephemeris Time (ET) are not adequately precise to allow definitive statements about possible variations of ET [1].

It is, of course, difficult to conceive of an ensemble of solar systems to give operational meaning to some of these comments. The fact that only one solar system is used solves the problems of drifting astronomical time scales by default. The fluctuations in Universal Time are, nonetheless, observable and subject to classification by statistical techniques. A unique time scale which would be universally accessible is certainly desirable.

II. Construction of an Average Atomic Time Scale

A. Introductory Comments

As mentioned in Section I-C, there is often reason to construct average scales even within a given laboratory. In actual practice, average scales have been constructed in laboratories which, themselves, do not possess a primary

atomic frequency standard. This is accomplished by using standard radio transmissions of other laboratories. This method, on the face of things, has certain advantages. By referring to a select set of primary frequency standards one hopes to accomplish two things: obtain a time scale with less bias and greater uniformity than any of the individual standards, and construct a scale which may be reproduced in any other laboratory that wishes to duplicate results. To accomplish either of the above results is difficult in practice. These difficulties arise from two sources: There are difficulties of quantitatively assessing the value of an individual standard relative to the others used in the construction of the average scale, and there exists the possibility of an inadvertent introduction of additional "Brownian motion" terms in the constructed scales.

B. Weighting Factors

There exist two possible criteria which might be considered for determining a set of weighting factors for the individual standards in establishing an average standard. A perfectly reasonable and realizable approach is to weight an individual standard inversely proportional to its mean square variation in frequency over some time interval which may be determined (at least in principle) by comparing the standard with an ensemble of other precision signal sources. With the weighting factors determined in this way, the resulting average standard should, in fact, be more uniform than any of its individual constituents (i.e., *uniformity* of rate, not necessarily *accuracy* of rate). One must consider here some of the problems of long-term stability.

An alternative is to weight the individual standards proportionally to the individual probabilities of being correct. The problem here, of course, is how to determine the accuracy of the individual standards. Does one believe the individual claims? Are the claims based on the same objective criteria? One can show that, if there is a variation in the accuracy capabilities of the individual standards and one *assumes* that they are equally reliable (equal weighting), the resulting scale is often closer to the worst in its performance than to the best. While this seems to be a significant dilemma, some very useful suggestions have come from some statistical studies [14]–[16].

Statisticians seem reasonably agreed that the simple mean (equal weighting) may, in specific situations, not be the best estimate. What is needed here is a compromise between minimum bias and safety from far-out values. The author is not aware of any laboratory that is attempting to implement the rather recent suggestions by statisticians.

In the author's opinion, the most reasonable approach is the former alternative—to base the weighting factors on the stability of the individual standards. To this end, the methods employed by Blair, Crow, and Morgan [17], [18] may prove quite useful.

C. Averages of Frequency and Time

Historically, the average time scales which have been constructed have been based on *frequency* measurements of the various standard broadcasts. Because of frequency measurement errors, it is seen that if two laboratories attempt to duplicate results in constructing average scales, relative *time* errors between the two laboratories tend to accumulate in (at best) a random walk fashion. In this situation, one has not acquired the redundancy and reliability of time measurements that is desirable.

In constructing an average time scale, two alternative data handling techniques are possible. One alternative is to treat the select set of atomic standards as simply defining frequency, as has been done in the past. In so doing, frequency measurement errors $\varepsilon_m(t)$ are introduced which are probably not correlated with errors of other laboratories observing the same set of frequency standards. Thus, each average time scale constructed on this basis has its own (independent of others) "Brownian motion." That is, even though all laboratories attempt to handle data in exactly the same way, the average scales gradually walk away from each other regardless of the fact that they are using the same set of standards and the same weightings.

The more reasonable alternative is to derive the average time scale from an average of the times (as opposed to frequencies) of the set of select time scales. This average should probably be other than the simple mean as noted above. By this technique, the measurement errors do not accumulate in an unbounded fashion as in a "Brownian motion." The problem here is obtaining comparisons of epoch for the necessary scales. While it is true that some standard broadcasts are phase-locked to their primary time scales [8], this is a fairly recent innovation and not all such broadcasts incorporate this technique. Portable clocks are an obvious, though expensive, solution [19], [20].

It should be noted that the average scale still has "Brownian motion" terms inherent in its construction. The significant point here is that the "Brownian motions" are common to all laboratories that construct the average scale and, thus, the times kept by these laboratories do *not* "walk away" from each other in an unbounded fashion. In effect, the (weighted) average epoch of the select set of atomic clocks can be considered to exist independently of its observation by some laboratory. Although there will always be some error of observation of the average, these errors of observation do not compound with the errors of subsequent observations and, hence, are not a "Brownian motion" or "random walk" type of error. By this method one has effectively recaptured the property of universal accessibility for the atomic scale.

III. Coordination of Atomic Time Scales

A. Introductory Comments

There are compelling reasons to consider an international coordination of atomic time scales to be desirable. The present paper does not pretend to solve the problems of coordination but merely to delineate and recognize some of the technical problem areas which will have to be faced by any coordination proposal. What follows is a statement of some of the technical problems which the author considers most significant.

B. Extent of Coordination

It must be decided if only one average international standard of atomic time should exist with all stations maintaining close correlation to this standard or if a more relaxed coordination should prevail. As an example, individual nations maintain their own standard of the volt and these are intercompared to define an international volt. Each country knows the relation of its volt to the international volt, but within the country the individual standards are used. An analogous system is possible with the epoch of atomic time.

In the author's opinion, a fairly close coordination is desirable. Since uniformity and precision are the most salient features of atomic time, it is inconsistent to gain coordination of atomic time scales by discrete steps in the indicated epoch of coordinating broadcast stations. It seems reasonable to maintain the broadcast time signals near the coordinated time by very small (approaching the accuracy limitations) variations in the reference frequency. The fundamental constituent time scales used in determining the one coordinated time scale would be intercompared either by portable clocks or via published values for the broadcast, coordinated time scales.

C. The Sanctity of the Individual Atomic Time Standard

Because of the problems discussed in Section II-B, most laboratories which maintain their own atomic time scales are quite reluctant to "contaminate" their scales with questionable data and techniques. Of all the problems facing coordination, this problem may well prove the most difficult. As is shown in Section II, the methods of constructing an average time scale are not closed issues. One may reason that the extreme reliability and great convenience of a closely coordinated time system should be adequate inducement to laboratories to cooperate in such an arrangement.

D. Nomenclature

As time scales have appeared throughout the world, an amazing array of different naming schemes have evolved. There exist A. 1, A. 3, TA1, NBS-A, UTC, and NBS-UA, to name a few. There is no reason why a coherent naming procedure cannot be adopted—this will probably be resolved in the near future. One could logically adopt a nomenclature which first gives the generic type of time scale (e.g., AT—atomic time) and then in parentheses the laboratory actually making the measurement [e.g., AT(NBS) would mean the atomic time scale maintained at the National Bureau of Standards]. This is quite similar to the notation used by the BIH [9].

References

[1] J. Kovalevsky, "Astronomical time," *Metrologia*, vol. 1, October 1965.

[2] G. Becker, "Von der astronomischen zur atomphysikalischen Definition der Sekunde" (in German), *PTB Mittlg.*, no. 4, pp. 315–323, and no. 5, pp. 415–419, 1966.

[3] A. O. McCoubrey, "The relative merits of atomic frequency standards," this issue.

[4] R. F. C. Vessot, H. Peters, J. Vanier, R. Beehler, D. Halford, R. Harrach, D. Allan, D. Glaze, C. Snider, J. Barnes, L. Cutler, and L. Bodily, "An intercomparison of hydrogen and cesium frequency standards," *IEEE Trans. on Instrumentation and Measurement*, vol. IM-15, pp. 165–176, December 1966.

[5] J. A. Barnes and R. C. Mockler, "The power spectrum and its importance in precise frequency measurements," *IRE Trans. on Instrumentation*, vol. I-9, pp. 149–155, September 1960.

[6] J. H. Shirley, "Some causes of resonant frequency shifts in atomic beam machines. I—Shifts due to other frequencies of excitation," *J. Appl. Phys.*, vol. 34, pp. 783–788, April 1963.

[7] J. H. Shirley, "Some causes of resonant frequency shifts in atomic beam machines. II—The effects of slow frequency modulation on the ramsey line shape," *ibid.*, pp. 789–791.

[8] J. A. Barnes, D. H. Andrews, and D. W. Allan, "The NBS-A time scale—its generation and dissemination," *IEEE Trans. on Instrumentation and Measurement*, vol. IM-14, pp. 228–232, December 1965.

[9] B. Guinot, "Temps atomique," *Bull. Horaire du Bureau Internat'l de l'Heure*, ser. J, no. 7, January–February 1965.

[10] W. Markowitz, "The system of atomic time, A. 1" *Proc. 13th Ann. Symp. on Frequency Control* (U. S. Army Signal R & D Lab., Ft. Monmouth, N. J.), p. 316, May 1959.

[11] "Practical nanosecond timer developed," *Missiles and Rockets*, pp. 34–35, May 24, 1965.

[12] R. E. Beehler, R. C. Mockler, and J. M. Richardson, "Cesium beam atomic time and frequency standards," *Metrologia*, vol. 1, pp. 114–131, July 1965.

[13] D. Brouwer, "A study of the changes in the rate of rotation of the earth," *Astron. J.*, vol. 57, pp. 125–146, September 1952.

[14] E. L. Crow, "The statistical construction of a single standard from several available standards," *IEEE Trans. on Instrumentation and Measurement*, vol. IM-13, pp. 180–185, December 1964.

[15] F. J. Anscombe and B. A. Barron, "Treatment of outliers in samples of size three," *J. Research NBS*, vol. 70B, pp. 141–147, April–June 1966.

[16] T. A. Willke, "A note on contaminated samples of size three," *J. Research NBS*, vol. 70B, pp. 149–151, April–June 1966.

[17] A. H. Morgan, E. L. Crow, and B. E. Blair, "International comparison of atomic frequency standards via VLF radio signals," *J. Research NBS*, vol. 69D, July 1965.

[18] B. E. Blair, E. L. Crow, and A. H. Morgan, "Five years of VLF worldwide comparison of atomic frequency standards," *J. Research NBS*, to be published.

[19] L. N. Bodily, "Correlating time from Europe to Asia with flying clocks," *Hewlett-Packard J.*, vol. 16, pp. 1–8, April 1965.

[20] L. N. Bodily, D. Hartke, and R. C. Hyatt, "Worldwide time synchronization, 1966," *Hewlett-Packard J.*, vol. 17, pp. 13–20, August 1966.

Reprinted from the PROCEEDINGS OF THE IEEE
VOL. 55, NO. 6, JUNE, 1967
pp. 822-826
THE INSTITUTE OF ELECTRICAL AND ELECTRONICS ENGINEERS, INC.
PRINTED IN THE U.S.A.

By computing the root mean square of the third difference of the fluctuations of Universal Time for various sample times, a spectral classification of the fluctuations can be made. For periods from 0.02 years to 20 years, the data indicate a power spectral density for the fluctuations which varies as $|\omega|^{-\alpha}$, where α lies in the range $3 \leq \alpha \leq 5$.

Based on the spectral classification, some simple and practical methods of predicting frequency offsets for coordinated Universal Time are compared to theoretically optimum (linear) prediction. Three methods are considered and are applied to past UT 2 data for comparison. A conclusion from the paper is that the frequency offset for the coordinated time scales (following present regulations) may be predicted such that no resets of epoch are required for roughly 60 per cent of the years for which the prediction is made.

KEY WORDS: ***Universal Time, Prediction, Coordinated Universal Time.***

Reprinted from FREQUENCY, Vol. 5, No. 6, pp. 15-20 (November/December 1967)

AN APPROACH TO THE PREDICTION OF COORDINATED UNIVERSAL TIME

JAMES A. BARNES and DAVID W. ALLAN

INTRODUCTION

Prior to the year 1956, the definition of the second was the fraction 1/86,400 of the mean solar day. Since the late 1930's, however, astronomers have been aware of fluctuations in the Earth's rate of rotation.[1,2] In 1952 a statistical classification of these fluctuations was presented by Brouwer.[3] His conclusion was that the *rate* of rotation behaved as an "accumulation of random digits," i.e., a random walk.

Because of the fluctuations in the Earth's rate of rotation, a new definition of the unit of time (the second) was adopted in 1956. This definition is based upon the Earth's orbital motion around the sun and is called Ephemeris time (ET). In 1964 an alternate standard for measuring the second received international acceptance. This standard is the cesium beam atomic clock and generates a second of time which does not differ from the Ephemeris second within the present limits of measurement (limitations in the measurement stem from difficulties in the precise determination of ET).

Late in the 1950's, several laboratories began to maintain an epoch of atomic time based upon the cesium atom's frequency. Of significance for this paper are two atomic time scales, the A.1 scale of the U. S. Naval Observatory[4] and the A.3 scale of the International Time Bureau (BIH)[5] in Paris. Regular comparisons between these time scales and Universal time (UT, based upon the rotation of the Earth on its axis) are available covering the interval from 1956 to the present. As is considered below, this allows one to significantly augment the ET-UT data by virtue of the high precision of the atomic measurements, which allow more frequent determination of the UT epoch.

Universal time (UT) is significant because many forms of navigation depend upon fairly accurate knowledge of the Earth's angular position relative to the sun and stars. For this reason all time signals broadcast by stations coordinating with the International Time Bureau (BIH) in Paris, in accordance with international regulations, maintain close agreement with UT 2 (mean solar time with corrections for some known perturbations).

Present CCIR regulations require some[6] coordinated "time" signals (UTC) to be offset in rate relative to the atomic second by integral multiples of 50 parts in

10^{10}. The offset in frequency is announced by the BIH in the fall of the year preceding the year in which it is to be used. When UT 2 and coordinated "time" signals differ in excess of 0.1 second, the coordinated "time" signals are reset exactly one tenth of a second as announced by BIH. Thus, each year various observatories and laboratories are interested in predicting the Earth's rotational rate for the next year.

CLASSIFICATION OF UT 2 BEHAVIOR

The methods of analysis used here may be found in the Special Issue of the Proceedings of the IEEE, Vol. 54, No. 2, February, 1966. In particular, Cutler and Searle,[7] Vessot, et al.,[8] Allan,[9] and Barnes[10] use time domain analysis to infer power spectral density. The present authors considered it worthwhile to apply some of these techniques to Universal time.

By correcting Universal time (UT) for the migration of the Earth's poles one obtains UT 1. Then by removing the remaining yearly periodic fluctuations one obtains UT 2. Numerous observatories determine UT 2. Some of the most extensive data may be found in the publications of the BIH. In particular, data of UT 2 relative to an atomic time scale may be found in reference 5 covering the years 1956.0 to 1965.0 at 10-day intervals. The rms third difference[10] of these data is plotted in Figure 1 as a function of the delay time, τ. The third difference is given by

$$\Delta^3\varphi = \varphi(t+3\tau) - 3\varphi(t+2\tau) + 3\varphi(t+\tau) - \varphi(t) . \quad (1)$$

Also plotted in Figure 1 is the rms third difference of UT-ET as obtained from Brouwer[3] for the years 1820.5 to 1900.5 and from reference 11 for the years 1901.5 to 1962.5. While UT differs from UT 2, the corrections from UT to UT 1 are too small to be resolved in the data for periods longer than one year and the UT 1 to UT 2 corrections are periodic at one year, which is exactly the sampling rate. While one may question the reliability of the ET measurements, there is as yet no significant indication that ET differs from Atomic time (AT). The precision of determination of ET is not nearly as high as for AT[12], but for periods of two years or longer the measurement errors of ET are not significant for Figure 1. Thus Figure 1 may be considered to reflect the fluctuations in UT 2 relative to a uniform clock.

The confidence limits indicated by Figure 1 were computed according to the number of independent, non-overlapping third differences used to calculate the rms third difference according to reference 13. The limits indicated on Figure 1 are calculated for a 90 per cent confidence. The single "best" straight line is not, in fact, contained within 90 per cent of the confidence intervals shown. This single "best" line has a slope of about 1.36.

The same data of Figure 1 are plotted on Figure 2 with two straight lines intersecting at about one year.

It is interesting to note that Brouwer,[3] using a bit more extensive data than the ET-UT data used here, concludes that: "The resulting value for the secular increase in the length of the day is $+0.^s00135 \pm 0.^s00038$ (s = seconds) per century. The principal uncertainty in these evaluations is due to the random process which causes the amplitude of the fluctuations to increase proportionally to the power 3/2 of the time . . ." (We note that if the rms amplitude of fluctuations increase in proportion to the 3/2 power of time, then the rms third difference does also.) Although Brouwer's remarks were based on data with a spacing of one year and although a line of slope 3/2 cannot be contained within very many confidence intervals of Figure 1, one cannot completely rule out the possibility of a 3/2 power law for the amplitude of the fluctuations for

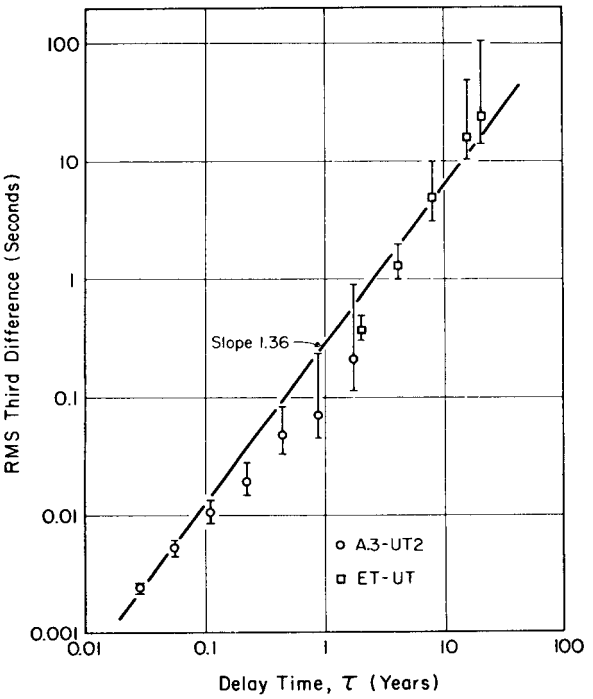

Figure 1 — RMS third difference of UT data.

times smaller than one year. One is tempted however, to draw the lines as indicated in Figure 2. A line of slope 1 fits the data very well for times less than one year. There are additional reasons, which will be covered later, to suspect that for times longer than one year a slope of 2 as shown in Figure 2 is not real.

One may construct a table relating the τ dependence of the rms third difference of a time series to the frequency dependence of the power spectral density of that series. The first four values of Table I were obtained from Vessot, et al.,[8] Allan,[9] and Barnes.[10] The remaining values were obtained by extending their mode of analysis.

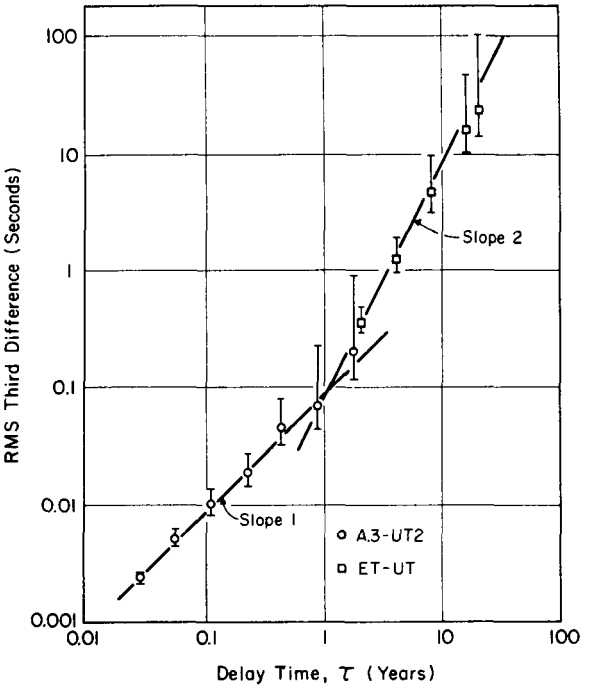

Figure 2 — RMS third difference of UT data.

Also, it should be noted that Brouwer[3] states that "the observed fluctuations in the moon's mean longitude are compatible with the hypothesis that the rate of rotation of the earth is affected by cumulative random changes." Thus, Brouwer's model is completely consistent with the fifth line of Table 1.

Table I

τ-dependence of the third difference for power law spectra

Noise Spectral Type	α	τ-Dependence of rms Third Difference	Name of Noise
$S(\omega) = k$	0	$\sim \tau^0$	White
$= \frac{k}{\lvert\omega\rvert}$	1	$\sim \ln(\tau\omega_h)$	Flicker
$= \frac{k}{\lvert\omega\rvert^2}$	2	$\sim \tau^{1/2}$	Random Walk
$= \frac{k}{\lvert\omega\rvert^3}$	3	$\sim \tau$	Flicker Rate
$= \frac{k}{\lvert\omega\rvert^4}$	4	$\sim \tau^{3/2}$	Random Walk Rate
$= \frac{k}{\lvert\omega\rvert^5}$	5	$\sim \tau^2$	Flicker Acceleration

where ω_h is a high frequency cutoff.

A Noise Model

It is possible to construct a filter[14-16] whose transfer function, $K(\omega)$, is approximated by $\left(\frac{1}{j\omega}\right)^{\frac{\alpha}{2}}$. Assume that $\varphi(t)$ is the output of such a filter when white noise is the input to the filter. Davenport and Root[17] show [their Eq. (11-57)] that the minimum mean square error of prediction for $\varphi(t+\tau)$ is given by

$$\varepsilon_{min} = \int_0^\tau |g(\eta)|^2 \, d\eta$$

where $g(\eta)$ is the impulse response function of the filter which is processing the white noise (of unit power). The impulse response function, $g(\eta)$, is defined as the Fourier transform of the transfer function, $K(\omega)$; i.e.,

$$g(\eta) = \frac{1}{2\pi}\int_{-\infty}^{\infty} K(\omega) e^{i\omega\eta} \, d\omega.$$

For the case of a filter with transfer function $K(\omega) = \left(\frac{1}{j\omega}\right)^{\frac{\alpha}{2}}$, the impulse response function is[18]

$$g(\eta) = \frac{1}{\Gamma\left(\frac{\alpha}{2}\right)} \eta^{\frac{\alpha}{2}-1} . \qquad (2)$$

The minimum mean square error of prediction then becomes

$$\varepsilon_{min} = \left(\frac{1}{\Gamma\left(\frac{\alpha}{2}\right)}\right)^2 \int_0^\tau \eta^{\alpha-2} \, d\eta,$$

Thus, for a signal, $\varphi(t)$, whose power spectral density (relative to an angular frequency to be consistent with references 9 and 10) is given by

$$S_\varphi(\omega) = h|k(\omega)|^2 = h|\omega|^{-\alpha} , \alpha > 1, \qquad (3)$$

where h is the input power spectral density (relative to ω), the minimum mean square error of prediction is expected to be

$$\varepsilon_{min}^2 = \frac{2\pi h}{\Gamma^2\left(\frac{\alpha}{2}\right)} \left(\frac{\tau^{\alpha-1}}{\alpha-1}\right), \alpha > 1. \qquad (4)$$

The factor of 2π occurs because (3) is a density relative to an angular frequency rather than a cycle frequency.

The Prediction Problem

By virtue of the fact that α is not precisely determined by the data, it was not possible to determine *the* best method of prediction. Instead, it was considered simplest by the authors to predict on the basis of an equation of the form

$$\hat{\varphi}(t+\tau) = \sum_{n=1}^{M} a_n \varphi(t-b_n\tau) \qquad (5)$$

where the coefficients $\{a_n, b_n\}$ are to be determined (1) on the basis of available data and (2) "near" optimum prediction for that range of α which is consistent with the previous analysis. (By "Optimum Prediction" one means to predict with a minimum resulting mean square error.)

The first sets of $\{a_n\ b_n\}$ investigated by the authors were constructed with the assumption that the actual predicted value, $\hat{\varphi}(t+\tau)$, would satisfy an equation in which the m-th finite difference is zero. As an example, the third difference of the variable χ_n is given by

$$\Delta^3\chi_n = \chi_{n+3} - 3\chi_{n+2} + 3\chi_{n+1} - \chi_n,$$

and thus the predicted value would be given by

$$\hat{\varphi}(t+\tau) = 3\varphi(t) - 3\varphi(t-\tau) + \varphi(t-2\tau). \qquad (6)$$

In general the errors based on the finite difference method of prediction are significantly worse than optimum prediction. Figure 3 shows a plot of the ratio of finite difference prediction to optimum prediction for various orders of differencing and as a function of α. Figure 3 was obtained from (4) and (6) and references 9 and 10 for $1 < \alpha \leq 3$. The method of analysis cited in the previous references was extended for the range $3 < \alpha < 7$.

If one accepts the possibility that, out to periods of one year, the Earth's behavior is dominated by an $|\omega|^{-3}$ behavior of $S_\varphi(\omega)$ (slope 1 in Figure 2), then a second difference method is only 20 per cent worse than optimum (see Figure 3).

If, however, one accepts Brouwer's $\tau 3/2$ dependence, one can show that optimum prediction is accomplished by a simple continuation of the instantaneous rate. (This is exactly analogous to noting that, for a gambler playing at even odds, the gambler's total funds are as likely to increase as decrease during the next few plays.) The instantaneous rate, however, is not exactly measurable, and one logically retreats to a prediction based upon an equation of the form

$$\hat{\varphi}(t+\tau) = \varphi(t) + \frac{\tau}{T}(\varphi(t) - \varphi(t-T)). \qquad (7)$$

Assuming that the errors of measurement of $\varphi(t)$ and $\varphi(t-T)$ are each five milliseconds[12], the error in $\hat{\varphi}(t+\tau)$ arising from the measurement of $\varphi(t)$ and $\varphi(t-T)$ can be shown to become near to the error of optimum prediction at a T value of about 2 weeks (15×10^5 sec.) for $\tau = 1$ year.

If one accepts an $|\omega|^{-5}$ dependence for the spectral density of the fluctuations in the Earth's angular position, then one finds the variance of the second difference of the position does not exist (Figure 3). This is equivalent to saying that the secular (mean) increase in the length of the day is not a measurable quantity. Based on the more extensive data in Brouwer's[3] paper and some recent results of coral growth,[19-23] however, the secular increase in the length of the day seems well understood. If an $|\omega|^{-5}$ dependence is real, it probably does not extend to frequencies much below one cycle per century. Munk and MacDonald[24] (their Figure 8.1) indicate this behavior stops at about one cycle per 30 years. Dicke[25] has also discussed the long term fluctuations in the rotation of the Earth.

Because of the rather steep slope to the date of Figure 2 for periods longer than one year, a prediction method which is a compromise between a pure third difference and a pure second difference was also investigated. The form of the prediction studied is given by

$$\hat{\varphi}(t+\tau) = 2\varphi(t) - \varphi(t-\tau) + \frac{\tau^2}{T^2}[\varphi(t) - 2\varphi(t-T) + \varphi(t-2T)]. \qquad (8)$$

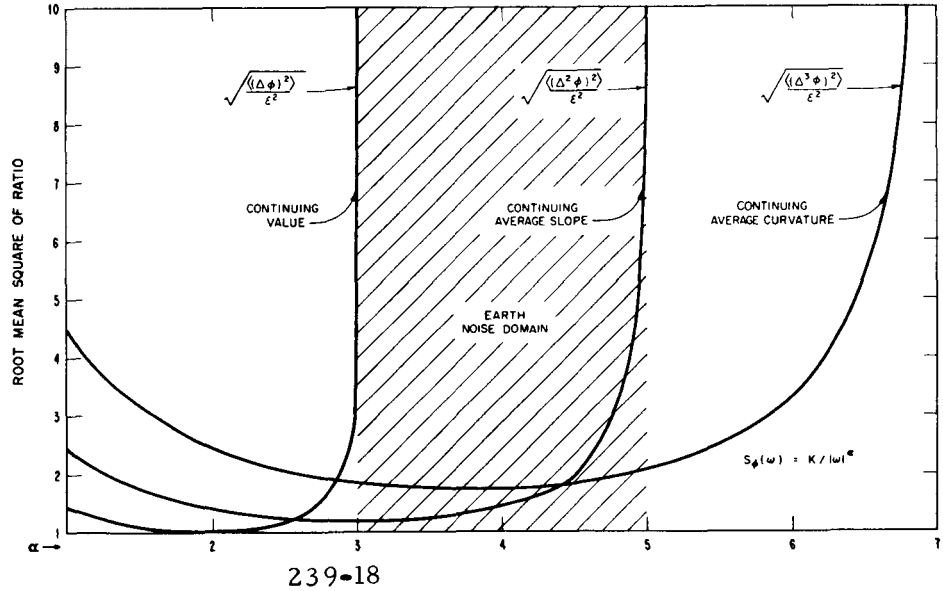

Figure 3 — Ratio of prediction based on finite differences to optimum.

Prediction Results

Because the U. S. Naval Observatory regularly supplies the National Bureau of Standards with current values of the time difference between A.1 (the U. S. Naval Observatory atomic time) and UT 2, "predictions" for the past years were computed on the basis of a second difference and also on the bases of (7) and (8) ($T = 3\tau$) using the A.1 - UT 2 data. In actual practice the frequency offset (relative to atomic time scales) is announced in the fall of the year preceding the year it is used.

The authors chose to predict the year-end value of UT 2 - UTC for the Nth year from early September (Nth year) values using one of the prediction schemes. Based on this year-end value and the desire to reduce this error to zero during the (N + 1)th year, frequency offsets, $\frac{\Delta f}{f}$, computed from each of the simple methods were predicted. The results of such calculations for each of the three prediction methods are presented in Table II for the past years and for 1967. The frequency offsets were held to integral multiples of 50 parts in 10^{10}, and if the UT 2-UTC value exceeded 0.1 second a "reset" is assumed to have occurred. While these are the current conditions which UTC satisfies, it should be remarked that these conditions were *not* actually used during the earlier part of the period covered. Thus this table should not be compared naively to actual past performance although it may be considered as an indication of what these prediction methods might yield in the future.

On the basis of the data presented in Table II, it appears that no one technique is obviously more reliable than the others. Certainly the second-difference method and the method based on (7) are simpler than (8), and may be preferred for this reason.

The predictions for 1968 are -250×10^{-10} for both the second difference method and on the basis of (7). Based on (8) one would predict -300×10^{-10} for 1968.

Table II

Prediction Results

Year	Second Difference		Equation 7		Equation 8 ($T=3\tau$)	
	$(\Delta f/f) \times 10^{10}$	number of resets	$(\Delta f/f) \times 10^{10}$	number of resets	$(\Delta f/f) \times 10^{10}$	number of resets
1958	−150		−150			
1959	−150		−150			
1960	−150		−200	1		
1961	−150		−150			
1962	−100	1	−100			
1963	−150		−200		−150	1
1964	−250	1	−200		−200	1
1965	−250		−350	2	−250	
1966	−250	1	−300		−300	
resets/years		3/8		3/8		2/4
1967	−250		−300		−300	

CONCLUSIONS

An analysis of recent UT 2 data has shown that Brouwer's 3/2 power law is reasonable for periods shorter than one year. That is, even for short periods of time, "the observed fluctuations . . . are compatible with the hypothesis that the rate of rotation of the earth is affected by cumulative random changes" — as Brouwer[3] commented in regard to times longer than a year. Based only on these recent UT 2 data, however, a better fit to the data is a flicker noise (1/f) law affecting the rate of rotation of the earth for periods shorter than one year.

Three methods of predicting the offset frequencies for Coordinated Universal time (UTC) have been considered which are not "far" from an optimum prediction scheme. These schemes of prediction have been applied to past UT 2 data to test their reliability (Table II). Because all three schemes seem roughly equivalent, one is tempted to choose the simplest, i.e., a second-difference method of prediction.

REFERENCES

1. Jones, Sir Harold Spencer, Ann. Cape Obs., 13, Part 3, 1932.
2. Jones, Sir Harold Spencer, *M. N.*, 99, 541, 1939.
3. Brouwer, D., "A Study of the Changes in the Rate of Rotation of the Earth," *Astronomical Journal*, Vol. 57, No. 5, pp. 125-146, September 1952.
4. Markowitz, W., "The System of Atomic Time, A. 1," *Proc. of the 13th Annual Symposium on Frequency Control*, New Jersey: U. S. Army Signal Research and Development Laboratory, p. 316, May 1959.
5. Guinot, B., "Temps Atomique," *Bulletin Horaire du Bureau International de l'Heure*, Series J., No. 7, January-February 1965.
6. Hudson, G. E., "Some Characteristics of Commonly Used Time Scales," *Proc. IEEE*, Vol. 55, No. 6, June 1967.
7. Cutler, L. S., and C. L. Searle, "Some Aspects of the Theory and Measurement of Frequency Fluctuations in Frequency Standards," *Proc. IEEE*, Vol. 54, No. 2, pp. 136-154, February 1966.
8. Vessot, R. F. C., L. Mueller, and J. Vanier, "The Specification of Oscillator Characteristics From Measurements Made in the Frequency Domain," *Proc. IEEE*, Vol. 54, No. 2, pp. 199-207, February 1966.
9. Allan, D. W., "Statistics of Atomic Frequency Standards," *Proc. IEEE*, Vol. 54, No. 2, pp. 221-230, February 1966.
10. Barnes, J. A., "Atomic Timekeeping and the Statistics of Precision Signal Generators," *Proc. IEEE*, Vol. 54, No. 2, pp. 207-220, February 1966.
11. U. S. Naval Observatory and Royal Greenwich Observatory, 1967, *American Ephemeris and Nautical Almanac*, Her Majesty's Stationery Office, London, p. vii. U. S. Naval Observatory and Royal Greenwich Observatory (1961), Explanatory Supplement to the Astronomical Ephemeris and Nautical Almanac (Her Majesty's Stationery Office, London), pp. 443-453.
12. Kovalevsky, J., "Astronomical Time," *Metrologia*, Vol. 1, No. 4, October 1965.
13. Crow, E. L., F. A. Davis, and M. W. Maxfield, *Statistics Manual, with Examples Taken From Ordnance Development*, China Lake, Calif., (or Dover, 1960), U. S. Naval Ordnance Test Station, p. 242, 1955.
14. Heaviside, O., *Electromagnetic Theory*, Dover Publication, New York, pp. 128-129, 1950.
15. Carlson, G. E. and C. A. Halijak, "Approximations of Fractional Capacitors $(1/s)^{1/n}$ by a Regular Newton Process," *IEEE Trans. on Circuit Theory*, pp. 210-213, June 1964.
16. Roy, S. C. D. and B. A. Shenoi, "Distributed and Lumped RC Realization of a Constant Argument Impedance," *Journal of the Franklin Institute*, Vol. 282, No. 5, pp. 318-329, November 1966.
17. Davenport, W. B., Jr., and W. L. Root, *Random Signals and Noise*, McGraw-Hill, New York, Chap. 11, 1958.
18. Campbell, G. A., and R. M. Foster, *Fourier Integrals*, Van Nostrand, New York: p. 50, pair 521, 1948.
19. Wells, J. W., "Coral Growth and Geochronology," *Nature, 197*, p. 948, (1963).
20. Scrutton, C. T., "Periodicity in Devonian Coral Growth," *Palaeontology, 7*, p. 552 (1964).
21. Runcorn, S. K., "Changes in the Earth's Moment of Inertia," *Nature, 204*, p. 823 (1964).
22. Lamar, D. L. and P. M. Marfield, "Length of Devonian Day From Scrutton's Coral Data," *J. Geophys. Res. 71*, 4429 (1966).
23. Runcorn, S. K., "Corals As Paleontological Clocks," *Sci. Am.*, Vol. 215, No. 4, pp. 26-33, October 1966.
24. Munk, W. H., and G. J. F. MacDonald, *The Rotation of the Earth*, Cambridge, 1960, Chapters 8 and 11.
25. Dicke, R. H., *The Earth-Moon System*, Plenum Press, New York: 1966, pp. 98-164.

Any two independent time scales will exhibit time departure due to two main causes, i.e., systematic differences in the frequency standards and inherent random noise processes. For time synchronization, theoretical considerations indicate that a third-order feedback system will automatically remove the systematic difficulties of typical frequency standards used in time scale work. The whole system is simulated with a computer to determine the systems feasibility and operating parameters. In this treatment we assume that time comparisons for synchronization would be intermittent and that the frequency standard may be represented by a systematic linear frequency drift with a random flicker noise spectrum (1/|f|) of the frequency fluctuations.

On the basis of the computer results an electromechanical system was designed and built. When the input to the system is the frequency from a high quality quartz crystal oscillator, the output frequency has no measurable frequency drift. If synchronization is performed every 12 hours, the rms time error predicted by the system for the time of the next synchronization is 70 nanoseconds, which is near theoretical optimum.

KEY WORDS: Time scales; Time synchronization; Computer simulation; Flicker noise; Optimum prediction; Frequency drift; Third order feedback system.

Reprinted from FREQUENCY, Vol. 6, No. 1, pp 11-14 (January 1968).

AN ULTRA-PRECISE TIME SYNCHRONIZATION SYSTEM DESIGNED BY COMPUTER SIMULATION

D. W. ALLAN, L. FEY, H. E. MACHLAN, and J. A. BARNES

Radio Standards Laboratory, National Bureau of Standards, Boulder, Colorado

DESCRIPTION OF THE TIME CONTROL SYSTEM

Consider a *master clock* to which synchronization of an independently operating secondary clock is desired. By *independently operating* is meant a clock which is physically remote from the master and for which time comparisons with the master are only intermittently available. These conditions apply to an important class of timing problems, the case for instance, where a master clock exists at the U. S. Naval Observatory or the National Bureau of Standards and where numerous secondary clocks throughout the country or world require synchronization with the master. Usually comparisons may be made only intermittently either daily by radio or less often by the use of portable clocks. The master clock consists of an ultrastable frequency source, such as a cesium beam standard, driving a set of frequency dividers to produce a time scale. The secondary clock is similar but may contain a less stable oscillator, typically a high quality quartz crystal oscillator. Generally, crystal oscillators exhibit two types of frequency instabilities: (1) a systematic linear change in frequency with time, known as drift, and (2) a random fluctuation exhibiting a power spectrum proportional to $1/|f|$ (flicker noise), where f is the fluctuation frequency. These instabilities occur simultaneously.

Both types of instability will cause the time scale kept by the secondary clock to depart from that of the master clock.[1] The systematic instability may in principle be predicted and is thus removable while the random fluctuations are not. It is these random fluctuations which prevent independently running clocks from remaining synchronized without intercomparison and indeed also prevent the precise determination, and thus removal, of the systematic instability. The present discussion describes the use of computer simulation techniques to determine the design parameters and the behavior of a multiloop servo system which is to correct for the systematic instability of a secondary clock also having random frequency fluctuations. Some of the work presented here has already been reported at the 1966 Frequency Control Symposium.[2]

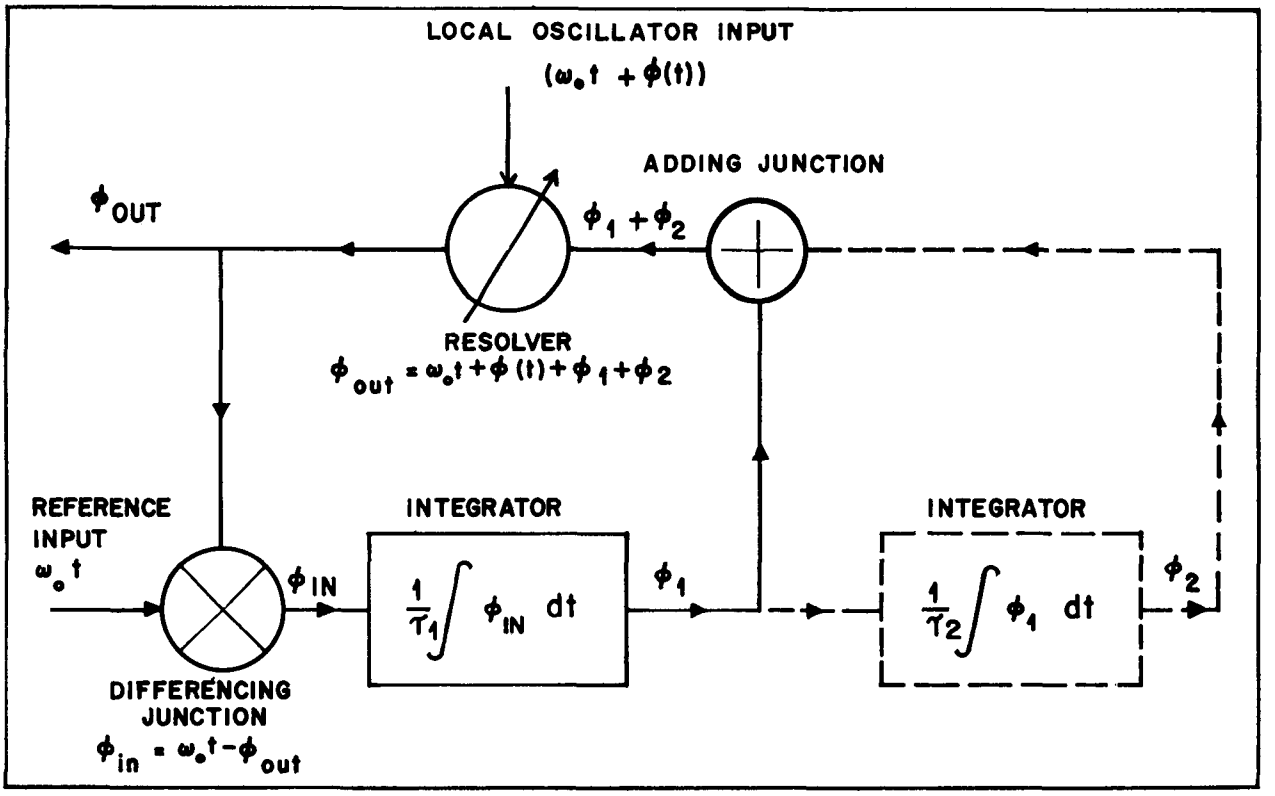

Fig. 1 — Block diagram of second order time control system.

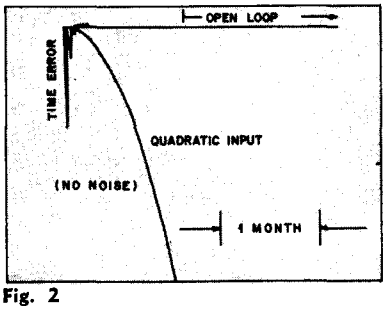

Fig. 2

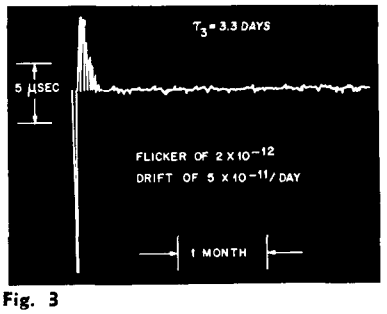

Fig. 3

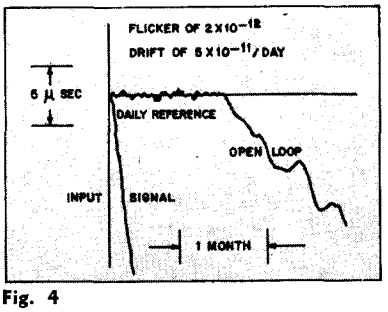

Fig. 4

The conventional idealized single loop servo diagram is illustrated in Fig. 1 (solid lines). The reference phase $\omega_0 t$ is assumed to result from a constant angular frequency, ω_0, from the master oscillator. The local oscillator phase from the secondary oscillator is equal to $\omega_0 t$ plus a small difference $\phi(t)$ which includes both systematic and random fluctuations about $\omega_0 t$. The function of the servo loop is to maintain the modified phase output from the local oscillator, ϕ_{out}, in agreement with the reference phase. This is done by integrating the difference between these two phases with respect to time to produce a change of phase in a direction that will reduce the phase error. By virtue of the fact that this is a negative feedback system, a step function in $\phi(t)$ will produce a servo correction which decreases as $\exp(-t/\tau_1)$, where τ_1 is the loop time constant. If instead of a step function phase error, a frequency difference, $\triangle\omega$, exists between reference and local oscillator, the uncorrected phase errors will increase linearly with time. The action of the single feedback loop will then be to supply a continuous phase correction while operating, of necessity, with a steady state phase error of magnitude $\triangle\omega\tau_1$. If now a second feedback loop is added as shown by the dotted line in Fig. 1, the phase error will be corrected as before with time constant τ_1. At the same time the sec-

Fig. 2 — Third order time control system error with linear frequency drift and no flicker noise.

Fig. 3 — Transient response of third order time control system with both linear frequency drift and flicker noise.

Fig. 4 — Open loop behavior of a third order time control system with flicker noise and after linear frequency drift removal.

ond loop integrator also contributes an error correction, reducing, with time constant τ_2, the correction necessary by the first loop until, at steady state, all the correction is supplied by the second loop, and no residual error is required as input to the first integrator. Since such a system now has the possibility of being unstable, the time constants τ_1 and τ_2 must be adjusted[3] to provide stability and desired transient response. After equilibrium has been reached, since no steady state phase error is required to actuate the servo loops, the reference may be removed and the output phase will continue to follow the reference phase even though a frequency difference exists between reference and local oscillator.

Carrying this procedure one step further, a third loop may be added, extending the performance capability to that of compensating for a linear frequency drift, that is, for oscillator aging. Then, as before, after equilibrium has been reached, the system will adjust itself so that the necessary oscillator drift correction is shared by the second and third loops with none required of the first loop. Consequently the output frequency will again remain constant after the reference frequency has been removed. After equilibrium has been reached no further comparison to the constant reference frequency would be necessary if it were not for previously mentioned random fluctuations which perturb the oscillator frequency.

If a third order feedback system is analyzed using Nyquist's stability criteria, the following time constant relationship is obtained:

$$\tau_3 > \tau_1.$$

This relationship is derived for a system where the reference is continuously available. Because the reference is typically available only intermittently, and because of the random fluctuations of the frequency of the clock to be synchronized, it is convenient to analyze the system via computer simulation techniques.

COMPUTER SIMULATION OF THE TIME CONTROL SYSTEM

A computer program was written to simulate the error response of a third order feedback time control system. The pertinent time constants and system parameters were left as variables so that optimization as well as stability might be achieved. The third time constant τ_3 is expected to be longer than the reset interval (about one day) for many of the system's applications. The time required to reduce the system's transient response to a negligible value must be longer than τ_3, therefore, testing the system in real time for optimum operating conditions would be very impractical. If flicker noise is now introduced into the system, a determination of the characteristic response will be an overwhelming problem if the analysis need be done in real time. In real time several days would be required to evaluate one set of time constants even without random fluctuations. Several sets of time constants must be evaluated. With the addition of the random fluctuations several sets of such evaluations would be necessary for each set of time constants. Because of these problems, computer simulation becomes extremely expeditious, since it allows a time compression of at least 10^6. The systems feasibility, limiting characteristics, and optimum operating parameters may also be determined prior to construction, which in this case saved considerable time and money.

Fig. 2 is a computer plot of the output time error signal with the input being a simulated frequency drift (quadratic time departure as shown). The time is reset once each day and allowed to free-run between synchronizations. One can observe the transient response as the drift rate is automatically subtracted out; and then after several time constants the reference signal is no longer provided for synchronization (open loop), but the time error remains essentially zero.

Computer simulation of flicker noise is a recent and significant development.[4] This development along with the insertion of a linear frequency drift provides an excellent computer simulated model of a large and important class of frequency standards.

Simulated flicker noise was next generated in the computer and added to the frequency drift. Various levels of flicker noise and of frequency drift were tried and the system's simulated response was analyzed. Variation of the system's time constants showed pronounced effects on the transient response, and time constants could be chosen that would make the system either stable or unstable.

Realistic levels of flicker noise had little effect on the simulated system's response except to increase the instability if the system were unstable and to slightly increase the length of the transient response. Fig. 3 shows the transient response and the error signal for a fractional frequency drift of 5 parts in 10^{11} per day and a flicker noise level of 2×10^{-12}. The level of flicker noise is measured by computing the square root of the variance of the frequency fluctuations for an ensemble of paired, adjacent samples.[5]

Fig. 4 shows the effect of providing no correction signal (open loop) after the system has adjusted for the frequency drift of a signal having both linear frequency drift and flicker noise. The accumulated error is about 9 microseconds after 1 month in the open loop condition.

The following time constant information resulted from the computer simulation. If τ_1 is very short (about 1 second), then τ_2 need be longer than the time between synchronizations for the system to be stable. For critical damping during the transient response, τ_3 need be at least 3 times longer than τ_2. Longer times for τ_3 gave no noticeable degradation in the level of the residual error signal, but gave a proportional increase in the length of the transient response.

REALIZATION OF THE TIME CONTROL SYSTEM

On the basis of the computer results an electromechanical third order drift control system was constructed on a fairly compact layout occupying 7 vertical inches in a

19 inch relay rack. The main components include: two ball and disc integrators, three gear differentials, two 60-Hz synchronous motors, one dc servo motor and amplifier, one resolver, and one phase detector. Other components include: isolation filters and amplifiers, gear trains, mechanical counters, and a dc power supply.

The parameters such as loop time constants, frequency and drift ranges, allowable gear backlash, etc., were determined from the characteristics of the crystal oscillator to be controlled, the desired precision of the output phase, the specifications of available electromechanical devices, and the constraints determined by the computer analysis.

A 100 kHz signal derived from a high quality 2.5 MHz crystal oscillator was the signal to be controlled. This particular oscillator had a drift rate of -1×10^{-11} per day and exhibited a flicker noise level of 0.86×10^{-12}. The nonlinearities of the system contributed no more than ± 25 nanoseconds time error. The system's time can be synchronized to the reference to within 10 nanoseconds.

Since it is necessary to operate the control system continuously for a period of at least a few months, optimum loop time constants as determined by computer were modified somewhat by the limited range of the mechanical integrators and discrete values of stock items such as motor speeds and gear combinations.

The loop time constants used in this device are:

Loop 1 (phase loop), $\tau_1 \approx 2$ sec;
Loop 2 (frequency loop), $\tau_2 = 1.56$ days;
Loop 3 (drift loop), $\tau_3 = 8.68$ days.

The frequency range of the system is limited by the integrators to 18.75×10^{-10}. This allows for about six months of operation with this oscillator before both the integrator in the drift loop and the oscillator must be reset.

Synchronization between the input signal and the 100 kHz reference, which is derived from the master clock cesium beam standard oscillator, occurs automatically every twelve hours. A record of the time difference between the output of the automatic time control system and the cesium beam standard is taken on a strip-chart recorder.

The accumulated time error of the system was analyzed 12 hours after each synchronization (just prior to the next synchronization). The rms time error was 70 nanoseconds. If the systematic frequency drift is assumed to be effectively removed by the automatic time control system, the accumulated time errors will be due to the flicker noise fluctuations. An equation may be written which gives the optimum predicted rms error obtainable when flicker noise fluctuations predominate:[5,6]

$$\delta t_{rms} = \tau (\ln 2)^{-\frac{1}{2}} [\sigma(2,\tau)],$$

where $[\sigma(2,\tau)]$ is the previously defined flicker noise level. The calculated optimum predicted rms error for a flicker noise level of 0.86×10^{-12} and a prediction time, τ, of 12 hours is 45 nanoseconds. This is to be compared with the experimental result of 70 nanoseconds. The computer simulation of the system on the same basis gave an rms error of 65 nanoseconds in good agreement with the physically realized system.

REFERENCES

1. Barnes, J. A., "Atomic Timekeeping and the Statistics of Precision Signal Generators," *Proc. IEEE,* Vol. 54, February 1966, p. 207.

2. Fey, L., J. A. Barnes, and D. W. Allan, "An Analysis of a Low Information Rate Time Control Unit," *Proc. 1966 20th Annual Symp. on Frequency Control,* pp. 629-635.

3. Chestnut, H., and R. W. Mayer, *Servomechanism and Regulating System Design,* New York, Wiley, 1951.

4. Halford, D., to be published.

5. Allan, D. W., "Statistics of Atomic Frequency Standards," *Proc. IEEE,* Vol. 54, February 1966, p. 221.

6. Barnes, J. A., and D. W. Allan, "An Approach to the Prediction of Coordinated Universal Time," *Frequency,* November/December, 1967, pp. 15-20.

463-560 O - 72 - 17

ATOMIC SECOND ADOPTED AS INTERNATIONAL UNIT OF TIME

13th General Conference on Weights and Measures Also Agrees on Changes in Terminology

■ A new definition of the international unit of time, the *second*, was adopted Friday, October 13, 1967, in Paris by the 13th General Conference on Weights and Measures.[1] The second has now been defined in terms of a characteristic rate of electromagnetic oscillation of the cesium-133 atom. The Conference also made terminological decisions in regard to the "micron," the "degree Kelvin," and the "candela"; and it added several to its list of derived units in the International System.

The General Conference on Weights and Measures, convened every few years, is a meeting of delegates from the countries (now numbering 40) adhering to the Treaty of the Meter. It is the principal body concerned with working out international agreements on physical standards and measurements. The U.S. delegation to the 13th General Conference was led by A. V. Astin, Director of the National Bureau of Standards.

Speaking for the governments represented, which include those of all the leading scientific and industrial countries, the Conference agreed overwhelmingly that the moment had come to replace the existing definition, based on the earth's orbital motion around the sun, by an "atomic definition."

The Conference decided that:

> The unit of time of the International System of Units is the second, defined in the following terms:
>
> "The second is the duration of 9,192,631,770 periods of the radiation corresponding to the transition between the two hyperfine levels of the fundamental state of the atom of cesium–133."

and abrogated the resolutions giving the earlier definition.

The frequency (9,192,631,770 Hz) which the definition assigns to the cesium radiation was carefully chosen to make it impossible, by any existing experimental evidence, to distinguish the new second from the "ephemeris second" based on the earth's motion. Therefore no changes need to be made in data stated in terms of the old standard in order to convert them to the new one.

On the other hand, the atomic definition has two important advantages over the preceding definition: (1) it can be realized (i.e., generated by a suitable clock) with sufficient precision, ± 1 part in a hundred billion (10^{11}) or better, to meet the most exacting demands of current metrology; and (2) it is available to anyone who has access to or who can build an atomic clock controlled by the specified cesium radiation,[2] and one can compare other high-precision clocks directly with such a standard in a relatively short time—an hour or so as against years with the astronomical standard.

The development in the last few decades of atomic clocks, without which the new definition could not have been considered seriously, has laid the preliminary groundwork for an eventual experimental assault on a fundamental question: Are the time scales based respectively on gravitational, electrical, and nuclear forces compatible and consonant with each other? And if (as some think) they are not, then why not?

Laboratory-type atomic clocks are complex and expensive, so that most clocks and frequency generators will continue to be calibrated against a standard such as the NBS Frequency Standard, controlled by a cesium atomic beam, at the Radio Standards Laboratory in Boulder, Colo. In most cases the comparison will be by way of the standard-frequency and time-interval signals broadcast by NBS radio stations WWV, WWVH, WWVB, and WWVL.[3] Similar services are supplied by several radio stations of the U.S. Navy. NBS broadcasts have been monitored by an atomic frequency standard since 1957. The Radio Standards Laboratory has also developed a rubidium-vapor (instead of cesium), portable (39 lb), battery-operated frequency standard with a short-term stability of ± 1 part in 10^{10}, which has proved useful for time comparisons at isolated facilities.[4] Similar atomic standards, weighing only about 20 lb, but at some cost in accuracy, have been developed for use in aircraft where they serve as components in precision navigation systems.

Cesium atomic clocks had already become so good by 1964 that the International Committee on Weights and Measures, acting under authority of the 12th General Conference held in that year, designated the present atomic definition for temporary use for measurements requiring maximum precision.[5] Continued improvements of the cesium clock are anticipated; and, in the not too distant future, clocks based on other than cesium radiations are expected to open the way to substantial further increases in precision. The present

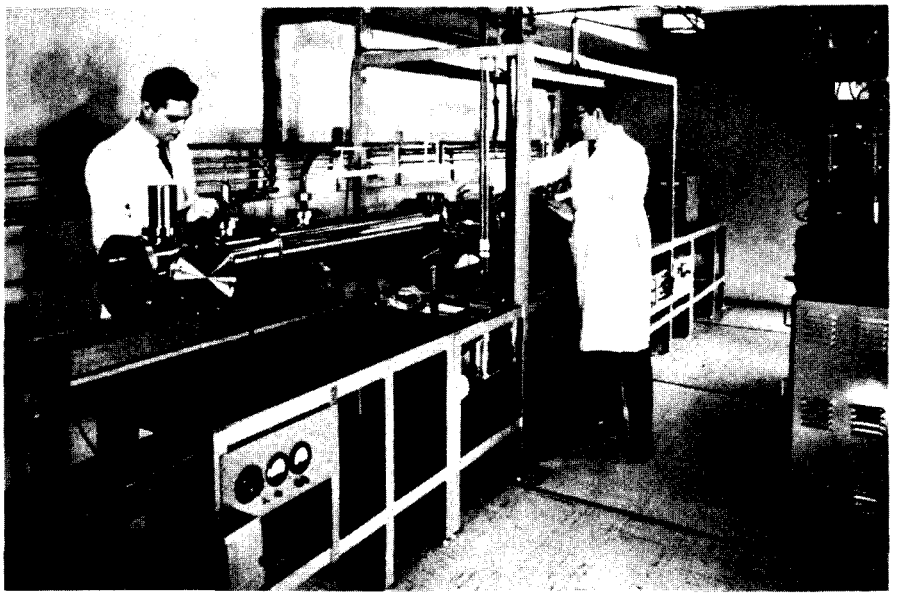

The cesium atomic clock at the NBS Radio Standards Laboratory generates the second—the SI unit of time. A quartz-oscillator-controlled microwave signal is held at 9,192,631,770 Hz by continuous comparison with the cesium-133 resonance at that frequency. A beam of cesium-133 atoms passes left to right through the long metal cylinder (center) and interacts with microwaves brought in by waveguide components (above cylinder).

(13th) Conference adopted a resolution urging that research and development programs along these lines be pursued with all possible vigor.

The Path to the New Second [6]

The founders of the metric system (in its present-day version known as the International System) did not define a unit of time. But, by convention among scientists, time had long been measured in terms of the rotation of the earth, the scientific unit of time—the second—having once been defined as 1/86,400 of a mean solar day. But the rotation of the earth has proved too erratic to meet modern scientific needs for keeping time—it is subject to periodic fluctuations within a year and to unpredictable fluctuations from year to year—and, therefore, the mean solar second is continually changing. The inconsistencies created by this are small—of the order of a part in 10^8—yet enough so that the time scale kept by the rotation of the earth on its axis now lags behind that kept by the revolution of the earth about the sun by about 30 seconds, reckoning from the year 1900.

A partial remedy was achieved in 1956 when the International Committee on Weights and Measures redefined the second for scientific use as 1/31.556,925.9747 of the tropical year at 1200 hours, ephemeris time, 0 January 1900. This imposing number was obtained from Simon Newcomb's equation for the apparent motion of the sun across the celestial sphere. This so-called ephemeris second is made available in practice with the aid of atomic clocks, but only retrospectively, as an average value over several years, by means of continual observations of the position of the moon. It can be determined experimentally with an uncertainty of a few parts in 10^9, a large uncertainty compared with the exactness implied by the multidigitality of the definition.

This 1956 definition of the second—though a great improvement for astronomers—still had one serious fault. No one else could measure an unknown interval of time with it by direct comparison. But even as this redefinition of the second was being formulated, a spectacular revolution in the measurement of time was taking place in the laboratory, where experimental techniques in molecular and atomic physics had been advancing rapidly.

Physicists had been able to excite some of the lower energy states of atoms and molecules, the associated frequencies of which, in accordance with Planck's equation $E=h\nu$, fall within the microwave part of the spectrum. These frequencies could be measured by comparison with laboratory oscillators and expressed in terms of the germane time-inverse unit of frequency, the cycle-per-second (now called the hertz, abbreviated Hz). Even in the early experiments, frequencies could be compared

Continued

The SI unit of luminous intensity is the candela. The light-colored porcelain cylinder with black cable coiled around it has a relatively narrow and deep vertical cavity containing platinum. Rf current in the coil keeps the cavity at the freezing temperature of platinum (2042 K). The opening at top of the cavity then radiates 60 candelas per square centimeter in the direction perpendicular to the plane of the opening.

ATOMIC SECOND *continued*

repeatedly with an agreement to within parts in 10^8 or 10^9. Subsequently, atomic beams, masers, and absorption cells were developed which also proved to be very stable standards for frequency and time; not only could they be compared with each other with a precision of 1 part in 10^{10}, or better, during an observing time of an hour or so, but cesium-beam resonators, independently constructed in different laboratories, agreed in frequency to a few parts in 10^{11} (equivalent to a second of cumulative error in 3000 years). It was apparent that if the second were defined as the interval of time corresponding to x cycles of a suitably selected atomic resonance frequency, the second could be realized more easily and more exactly than by the ephemeris second.

Other Actions Taken by Conference

The 13th General Conference also made the several other decisions summarized below.

Length. The name "micron," for a unit of length equal to 10^{-6} meter, and the symbol "μ" which has been used for it, are dropped. The symbol "μ" is to be used solely as an abbreviation for the prefix "micro-," standing for multiplication by 10^{-6}. Thus the length previously designated as 1 micron should be designated 1 μm.

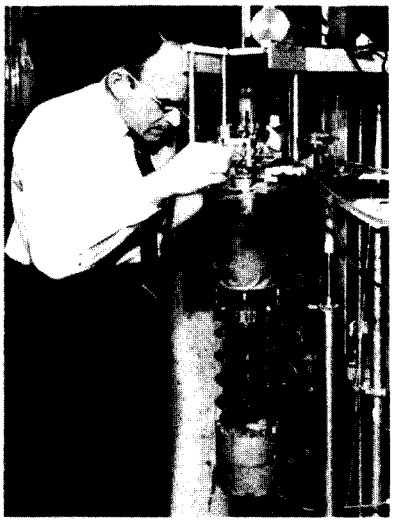

L. A. Guildner adjusts valves on the NBS gas thermometer which measures temperature in kelvins as a function of pressure changes of a constant volume of a nearly perfect gas.

Temperature. The Conference recognized the urgency of revising the International Practical Scale of Temperature of 1948. Noting that the laboratories competent in the area are agreed on the main lines of the changes required, it authorized the International Committee on Weights and Measures to take the steps necessary to put a new International Practical Scale of Temperature into effect as soon as possible.

The name of the unit of thermodynamic temperature was changed from *degree Kelvin* (symbol: °*K*) to *kelvin* (symbol: *K*). The definition of the unit of thermodynamic temperature now reads:

> The kelvin, the unit of thermodynamic temperature, is the fraction 1/273.16 of the thermodynamic temperature of the triple point of water.

It was also decided that the same name (*kelvin*) and symbol (*K*) be used for expressing temperature intervals, dropping the former convention which expressed a temperature interval in *degrees Kelvin* or, abbreviated, *deg K*. However, the old designations are acceptable temporarily as alternatives to the new ones. One may also express temperature intervals in *degrees Celsius*.

Photometry. Recognizing that photometry must take into account the principles and techniques of colorimetry and radiometry, the Conference approved plans drawn up by the International Committee on Weights and Measures to expand the scope of its activities to include the fundamental metrological aspects of colorimetry and radiometry.

The definition of the unit of luminous intensity, the *candela*, was rephrased to meet the objections of critics who found a certain awkwardness in its wording. The meaning of the definition, which was never in doubt, remains the same. The reformulated definition follows:

> The candela is the luminous intensity, in the direction of the normal, of a blackbody surface 1/600,000 square meter in area, at the temperature of solidification of platinum under a pressure of 101,325 newtons per square meter.

Derived units. To the derived units and associated symbols that the 11th General Conference (1960) had included in its Resolution 12, which introduced the International System of Units (official abbreviation: SI, from the French designation, Système International d'Unités), the 13th General Conference added the following:

Wave number	1 per meter	m^{-1}
Entropy	joule per kelvin	J/K
Specific heat	joule per kilogram kelvin	J/kg K
Thermal conductivity	watt per meter kelvin	W/m K
Radiant intensity	watt per steradian	W/sr
Activity (of a radioactive source)	1 per second	s^{-1}

A proposal to have the *mole* defined by the 13th General Conference was deferred.

[1] The Proceedings of the Conference will be published by Gauthier-Villars & Cie., Paris. A summary will appear in the journal, Metrologia.

[2] A description of such clocks is given in Atomic frequency standards, NBS Tech. News Bull. **45**, 8–11 (Jan. 1961). For more recent developments and technical details, see Cesium beam atomic time and frequency standards, by R. E. Beehler, R. C. Mockler, and J. M. Richardson, Metrologia **1**, 114–131 (July 1965).

[3] The services provided by these stations are described in NBS Misc. Publ. 236, 1967 edition, NBS Standard Frequency and Time Services, for sale at 15 cents per copy by the Superintendent of Documents, U.S. Government Printing Office, Washington, D.C. 20402.

[4] Portable atomic frequency standard, NBS Tech. News Bull. **49**, 4–5 (Jan. 1965).

[5] The Twelfth General Conference on Weights and Measures, by H. Moreau, Metrologia **1**, 27–29 (Jan. 1965).

[6] This section is an excerpt, with minor changes, from Measurement standards, by A. G. McNish, International Science and Technology, No. 47, 58–66 (Nov. 1965).

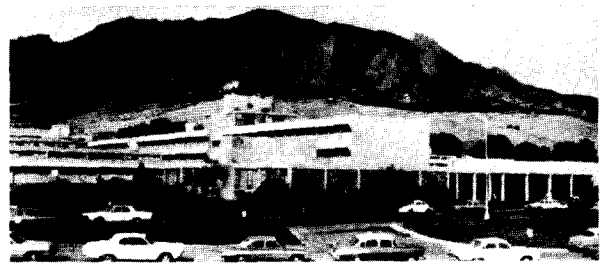

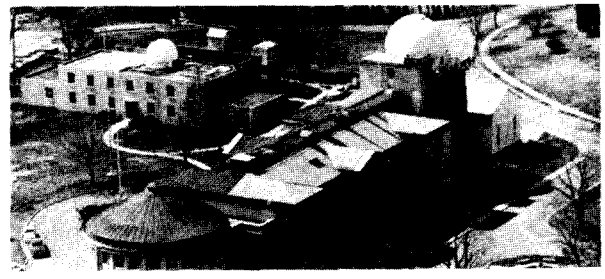

The Nation's two "time keepers"—the National Bureau of Standards, Boulder, Colo. (top) and the U.S. Naval Observatory, Washington, D.C.—recently synchronized their clocks to provide the country with a unified time system of unsurpassed accuracy.

NATION GETS Unified Time System

NBS and Naval Observatory Synchronize Time to About 1 Microsecond

A UNIFIED TIME SYSTEM of unsurpassed accuracy for the entire country was achieved recently when the Nation's two "time keepers"—the National Bureau of Standards and the U.S. Naval Observatory (USNO)—synchronized their clocks. On October 1, 1968, these agencies cooperated to effect a much more precisely coordinated time system than has ever before existed. The action taken by these agencies was the synchronization of their Coordinated Universal Time (UTC) clocks to within about 1 microsecond of each other. Synchronization was achieved when the NBS Time and Frequency Division (Boulder, Colo.) increased the rate of its UTC(NBS) clock by 4 parts in 10^{13}, while the Naval Observatory (Washington, D.C.) decreased the rate of its UTC(USNO) clock by 4 parts in 10^{13}.

The Bureau and the USNO have been cooperating under regulations of the International Radio Consultative Committee (CCIR), which for the past several years has required synchronization of standard time broadcasts to one thousandth of a second. This has been adequate for most users, but as technology has advanced, many precise timing needs have developed that cannot be met by this tolerance. More than a year ago, the desirability of synchronizing the USNO and NBS frequency and time standards to much finer tolerances than 1 millisecond was recognized.

In anticipation of a coordinated coordinate rate for USNO and NBS, on August 24, 1967, the Coordinated Universal Time clock of the Bureau, UTC(NBS), and all UTC transmissions of NBS were advanced by 200 microseconds. This left NBS about 35 microseconds early relative to USNO.

As the rate of the USNO clock has been high relative to the NBS clock by about 1 part in 10^{12}, the two clocks drifted toward each other. Their time lines converged on about October 1, 1968, and the time difference between the USNO clock, UTC(USNO), and the NBS clock, UTC (NBS), became zero. At that time USNO reduced the rate of its clock by 4 parts in 10^{13}, and NBS increased the rate of its clocks controlling NBS standard transmissions by 4 parts in 10^{13}. (A clock running fast by 4 parts in 10^{13} accumulates about 35 billionths of a second error per day. This rate of error would require about 80 000 years to accumulate one second in error.) The present specified absolute accuracy of the rate of the NBS clock is ± 5 parts in 10^{12}.

Measurements made after October 1 with portable clocks indicate that the time difference between the USNO and the NBS coordinated clocks is within one microsecond. By mutual agreements between USNO and NBS, small frequency adjustments ($<10^{-12}$) will be made infrequently to assure that this time difference remains less than about three microseconds.

Among scientists requiring more precise time measurements are geodesists, who, in attempting to measure the Earth very accurately, must sight on an artificial satellite from distant locations at very nearly the same instant of time. The sightings must be made within about 100 microseconds of each other, but the geodesists would prefer that the time error be within 10 microseconds. There are also military and NASA requirements that require synchronization accuracies in the microsecond range. It should be emphasized that this is synchronization accuracy and not absolute time-of-day accuracy.

Meanwhile, there is a general trend in technology toward tighter tolerances on synchronization. For example, the planned Aircraft Collision Avoidance System (ACAS) specifies worldwide synchronization accuracy of 0.5 microsecond, which is possibly beyond the current state-of-the-art.

To meet such needs, the National Bureau of Standards and U.S. Naval Observatory are engaged in a joint effort to provide a unified time service to all the United States. The new system is near the limit of the present state-of-the-art in its ability to provide accurate time and time synchronization to remote locations. This synchronization system is expected to provide a working model of a coordinate time system suitable for extension to worldwide coverage at some later date.

A COORDINATE FREQUENCY AND TIME SYSTEM

G. E. Hudson, D. W. Allan, J. A. Barnes
National Bureau of Standards, Boulder, Colo.

and

R. Glenn Hall, J. D. Lavanceau, G. M. R. Winkler
U. S. Naval Observatory, Washington, D. C.

SUMMARY

A coordinate frequency and time system, suitable for extension to worldwide coverage, is described in relation to the form evolving in the United States. It consists of a network of component primary and associated stations, at fixed locations and altitudes, and a reference coordinating component at a reference location and altitude.

Each primary station is a source of coordinate frequency and time signal emissions steered directly in rate and epoch by a steering element; for coordination purposes this element is offset slightly in rate from an associated independently running "proper" local atomic standard. The local independent atomic standards are each evaluated for internal accuracy of realization of the standard Cesium frequency value assigned in the International System (SI) of Units, and for reliability and stability of operation.

A unified local atomic standard for the system serves as the coordinating component. It is defined in terms of a weighted average of the independent local atomic standard frequencies whose weights are chosen on the basis of reliability, stability, internal accuracy, and independence. It is a "proper paper standard" regarded as normally located at the system origin, at a standard reference altitude. In its definition, the frequency of the unified atomic standard is taken equal to the value f(Cs).

When completely coordinated, the carrier frequencies and signal epochs received at the origin from a participating station have average values equal to the assigned coordinate values when measured by the unified atomic standard. But if the measurement were made by the unified standard at the emission site, this would not be the case, in general, because of the small Pound-Rebka carrier frequency shift. Moreover, referred to emissions from a coordinated station A, there is no fractional difference in average rate and frequency of signals received at A, if they are emitted from another coordinated station, B.

An analysis of this network leads to the necessary conditions on the average frequencies emitted from the participating stations when coordinated, and to the frequency values of the independent local atomic standards referred to the unified one.

The system could be extended internationally, by regarding the national unified standards as components of an international one whose assigned frequency would equal f(Cs). Again, a physical link must be established between the components in real time. This leads to the recognition of small individual frequency offsets of emissions and of national unified standards needed to achieve a well-defined international coordinate frequency and time system.

Reprinted from:
Proc. of the 23rd Ann. Symp. on Freq. Contr.
(U. S. Army Electronics Command, Ft. Monmouth, New Jersey, May 6-8, 1969)
pp. 250-262 (May 1969).

I. INTRODUCTION

A. General Consideration

There are three aspects of a time and frequency information dissemination system which require three quite distinct types of activity by associated personnel.

1) The system must be administered. This means that its effects on the users served by it must be continually evaluated to see if their needs are met. Policy decisions must be taken with an eye toward future developments, as well as toward safeguarding of commonly accepted practice, and technical feasibility.

2) It must be operated and maintained consistently and efficiently. By its nature all component portions of the system must be coordinated continually to insure internal consistency. Internal records of the regular operations, adjustments, changes in system, and data collected by monitoring activity must be kept in a uniform way and be available to system administrative, operating, and engineering staff.

3) The technical characteristics of the system, including its limitations, must be investigated and continually reexamined in the light of technological advances and the requirements of the system users and potential users. There must be a clear understanding of the existing system physically and from an information theory point of view. This understanding must be both on a conceptual and operational level and be both deep enough and broad enough to yield a proper technical perspective concerning the relation of the system to others, existing or proposed.

These three requirements account for the sextuple authorship of this short paper. The authors can be identified roughly, but not exclusively, in pairs with these aspects. They are paired because the system proposed herein stems from experience with and observation of the joint effort made between two major institutions of the many government agencies interested in establishing a single coordinate frequency and time system for the United States. In making this coordination effort we have observed that it may be feasible to extend its use with small modifications to wider coverage, an aim explicitly stated in the "terms of reference" of Study Group VII of the CCIR. In passing, it should be noted that the terms "coordinated" and "coordinate" -- since they refer to an agreed upon method for referring time to a common reference, are almost synonymous and may be used in the present text interchangeably (except for syntax).

There are, of course, many other individual contributions, including industrial concerns and government agencies, to this systematic effort in addition to the six authors and their respective two agencies. It perhaps suffices to cite in this respect the members of U. S. Study Group VII.

B. The USNO-NBS Coordination

As a guide in discussing the present coordination effort we list seven prerequisites descriptive of the kind of coordinate time system being set up and maintained (although not yet completely formalized!) in the United States for general use.[1]

1) The system contains component member stations and laboratories.

2) Each member has similar identifiable items of equipment or portions of equipment systems, which we shall call elements of the local system component.

3) The component members of the system are evaluated and given statistical weights on the basis of certain criteria agreed upon by the members.

4) Adjustment procedures are formulated in the sense of designating at what portions of the system coordinating adjustments are to be made, and when they are to be made, and tolerance limits of various kinds are specified.

5) Maintenance procedures are formulated and followed in the sense of collection, recording, and reporting of data to be used in order to maintain the smooth operation of the system.

6) Provisions are made for the participation of associated member stations, whose atomic clocks are used at the station for control and stability, but are not maintained sufficiently independently to be included in the component weighting procedure of the system. Such stations are monitored and emit signals within the prescribed tolerance limits -- i. e. ,

they disseminate the coordinate time and frequency information in the way agreed upon, but do not have a commercial or government standards laboratory directly working with them as part of the system.

7) A reference location and initial epoch must be designated; a reference time scale (a "paper" clock) must be defined as an average (using the weights chosen in item 3) of the component independent atomic frequency and time standards. It should be noted that the system origin so specified should be in terms of a physical object--e. g. , a laboratory building, and a well-defined physical event. Moreover, the record of differences between the reference scale and other well-defined scales such as UT2 and ET must be kept continuously as a necessary part of the coordinate time system.[2]

Since the independent local atomic standards and clocks are usually averages of several physically distinct but similar atomically controlled or calibrated clocks, the name independent local mean standard will be used for them. (Sometimes we shall use the term: "local atomic standards" as an alternative one.) Similarly, the average time scale at the system spatial origin will be designated the national mean scale --or sometimes the "unified atomic standard. "

We can retrace these points in terms of the present USNO-NBS coordinated effort for the United States.

1) Obviously, the two present components of the system are:

(1) the U. S Naval Observatory in Washington, D. C. , in close association with the laboratories of NRL and commercial standards laboratories which furnish the USNO with information and assistance in evaluating their atomic Cesium standard oscillators and clocks.

(2) the National Bureau of Standards Laboratory at Boulder, Colorado.

2) The essential basic elements for each component have been identified and are illustrated schematically in Figure 1. They are:

(a) local atomic Cesium frequency standards and independent mean time scales. At the USNO Time Service Division, in Washington there is maintained a set of from ten to sixteen independent atomic clocks whose readings are recorded and averaged almost every day by a statistical weighting procedure. The average reading is the independent mean paper time scale IM (USNO). This scale is also known as A. 1. The rate of running of each clock in the set is controlled by the radiation frequency characteristic of the well-known energy transition of atomic Cesium. The statistical procedure chosen insures a high degree of internal stability, reliability, and independence of IM (USNO) from other physical systems. Although not a direct realization in the sense of standards laboratories of the base units of time interval and frequency adopted in the SI, this "proper" time scale yields a close approximation. It is an example of a local atomic standard for the coordinate time system described herein.

At the NBS Time and Frequency Division, in Boulder there is maintained a local Cesium atomic frequency standard known as NBS-III, used to calibrate the rates of running of a set of crystal-oscillator and atomic-oscillator controlled clocks. A statistically weighted average of those readings is used to compute the "paper" atomic time scale known as AT (NBS). The internal accuracy of the reference frequency standard, NBS-III, is continually evaluated to determine the confidence with which the standard realizes the SI base unit of time interval, the second (or its inverse, the hertz). The statistical procedure is chosen to ensure that the AT (NBS) scale realizes the internal accuracy of the local atomic frequency standard, at this moment, 5×10^{-12} (3σ).

Redundancy and reliability are furnished by the crystal and atomic clock system, while long-term stability, as well as accuracy, is computed from the calibrations relative to the NBS-frequency standard. This portion of the NBS system is an example of an independent local proper atomic standard for the coordinate time system, and may be designated IM (NBS). Its scale is identical with what has been known as NBS-A, but is now known as AT (NBS).

(b) coordinating elements whereby necessary corrections and adjustments for coordination are introduced into the local control equipment or perhaps are kept only as a record and guide for coordination. Some detailed methods for the calculation of these corrections are discussed in a later section. No standard name has yet been given to these internal system records; but each component certainly keeps such records. It is probable that they should be continuously available to both components.

(c) Steering elements can be identified at both component stations. They are the respective clocks and oscillators used to control or steer the carrier frequencies, signal pulse rates, and time epochs. One may designate them as coordinate clocks and frequency standards. They should be set physically to maintain the agreed coordination. At the USNO, the steering element is called the master clock, but might be designated for system purposes TC(USNO). Similarly, the NBS time scale or clock keeping coordinate time may be called TC(NBS). When these clocks and scales become coordinated internationally, they could be designated UTC(USNO) and UTC(NBS) respectively; the U denotes "universal", and the TC denotes "coordinated time".

(d) There are, of course, radio emissions of time signals and carrier frequencies closely associated in spatial location with each component. For NBS, this is WWV and WWVL, and for the USNO, this is NSS. There are other emissions closely associated with them, but, because they are not from nearby radio stations, we prefer to distinguish them as "associated stations".

(e) Finally, at each locale there are monitoring and maintenance facilities whereby data required for maintaining continuous coordination are collected and recorded.

3) The initial coordination between the USNO and NBS took place on 1 October 1968. It was necessary at that time to correct relatively large divergences in rate of the respective emissions amounting to about 8 parts in 10^{13}. Hence, it was decided, as an interim measure, without following the format discussed here, to shift the steering rates sufficiently over a period of time, to eliminate the major portion of this discrepancy.[1]

This has now been accomplished. Accordingly, more refined adjustments for coordination, which will take into account small effects such as the Pound-Rebka gravitational red-shift,[3] and relative random walks of the two local atomic standards, will be made in the future. In order to do this, it has been decided to attach equal weight to the two standards. In our notation, this means $\alpha_1 = \alpha_2 = 0.5$. Briefly, this decision resulted from a consideration of several incommensurate requirements at the two components. It is very important that the coordinate scale have nearly one "second" as the base unit of time at the coordinate time origin. This is the "second", as defined in the International System (SI) of units. It is part of the mission of NBS to attempt to realize, via the frequency standard NBS-III, this unit. At the same time, it is also important to keep the coordinate time scale as stable as possible, and insure its reliability, of prime consideration for the USNO.

4) Every few months, as a result of continuous monitoring via radio observations and portable clock intercomparisons, a new adjustment of the steering elements and the radio emissions must be made, to insure that the frequencies and rates of all system emissions, as observed at the USNO (i. e., near sea level), have the nominal values assigned them, measured relative to the unified mean standard of the system. Because of differences produced by propagation, and differences in rate between the local mean standards and the system's unified one, the rates as emitted from the stations and measured by the respective local standards will not have the nominal values but will be slightly offset. This is discussed more fully in the next section.

5) The USNO maintains a large portable clock service, and is charged by the DOD with assuring uniform standards of practice in frequency and time throughout the DOD. Coupled with the radio monitoring facilities both at NBS and the USNO, data are collected which result in a value for the fractional rate difference, S_{12}, between the USNO and NBS independent mean standards.

Based in part on this measurement, and on the weight value chosen, other quantities of importance for maintaining coordination are inferred as described in the third section.

6) We mention briefly the stations and emissions which can be considered as associated ones. This means that NBS-station WWVH, in Hawaii, being at a different altitude, should emit signals at a rate very slightly different than the rate of WWV -- even when both rates were measured by ideally identical local standards at the two sites. The Loran-C chain and the forthcoming Omega system, as well as other U. S. Navy standard frequency and time signal stations may be considered as associated stations;[4] monitoring data yields differences between their emitted signal rates and those necessary to be correctly coordinated with this system. Broadcast stations, too, if considered as associated coordinate time and frequency stations need similar information.

7) The USNO continually make observations of star transits, and this information is used by the International Bureau of Time (BIH) in constructing the astronomical time scale known as UT2 (roughly the same as Greenwich Mean Time). The knowledge of UT2 and the coordinate time system emissions is a necessary prerequisite for maintaining the coordinate time scale and UT2 as different aspects of the same coordinate time system. Necessary redundancy and convenience in using it for navigational purposes is thereby built into the system.

We have designated the USNO as the spatial origin location of this national coordinate time system. The initial epoch chosen is, provisionally, set at 1 January 1958 at 0000 UT.

II. THE MEANING OF COORDINATE TIME AND METRIC TIME

Coordinate time systems as spatially extended physical objects have long been envisioned in physics, and employed in astronomy. The importance of giving an explicit operational definition of such a system has recently been stressed by several authors -- notably in a presidential address to the Royal Astronomical Society by D. H. Sadler.[5,6,7]

It is our purpose here to explain the distinction between coordinate time and metric time. Very briefly, and roughly, it is analogous to the distinction between master-slave radio stations, and independently running oscillators.

More exactly, let us imagine many clocks, chosen for their stability and reliability, and because each, when calibrated by an atomic frequency standard at the same location, is determined to run freely at a rate very closely approximating that specified in the International System. The clocks can then be distributed over a large area and at different fixed altitudes, at fixed locations on the earth. Each then continues to run with its proper (Fr: propre ≡ self) rate. It is a local atomic standard, and can be used to measure rates and time intervals in terms of the SI base units for frequency and time. It is therefore called a "metric" instrument. This agrees with the strict mathematical sense of metric since we do not envision the possibility of changes in location or "small" accelerations as affecting its rate. It is a good piece of laboratory equipment for measuring time intervals.

Now, two such real clocks when in juxtaposition will normally diverge very slowly, but randomly, in reading and rate, because of tiny random effects which are not eliminated. A suitable average can produce an average reading and rate, which is presumably more stable --

and the stability properties of such a mean clock may be very desirable. However, one cannot necessarily say that the average clock is a better realization of the SI unit of time than either one of the two. This is certainly a matter for further investi gation in each case. More important, however, is the fact that two such clocks at a distance would run quite independently, and at their own (proper) rates.

However, to obtain a time epoch and a frequency which is uniform over a large spatial volume, a uniform physical link with some standard clock must be established. It is a remarkable fact that radio signal pulses or carriers, used to establish such a link, and when measured by two standard metric clocks A and B, at a distance from eath other, show very little difference in frequency or rate relative to these. This is illustrated in Figure 2. However, a small systematic effect[3] has been observed in the frequency of electromagnetic radiation when it is propagated through a difference, gH, in gravitational potential, over an altitude difference H- even though the gravitational acceleration field, $\vec{g}$, is a constant. This difference is sometimes ascribed to a difference in rate of the metric clocks. But the argument from physical grounds shown in Figure 3, indicates that the radio waves, or photons, themselves change energy, and therefore frequency, by having work done on them as they move in a direction with a component parallel to the field vector $\vec{g}$. The computed value of this effect on radio carrier frequencies between Boulder, Colorado, and Washington, D. C. is 1. 8 parts in 10^{13} or an accumulative effect over a year of 6 μs. (phase difference in time units).

This can be described geometrically by attributing different radii of curvature to different portions of the spacetime map on which are plotted events happening to two clocks, A and C, at a distance and at different altitudes. In this way the relative difference between the received pulse rate at C and the metric clock rate at C can be portrayed. This is shown in Figure 4.

So it is easy to see, as also shown on Figure 5, that one coordinates time at different locales and altitudes, by sending radio pulses from an origin(say at sea level) so that the coordinate clocks at various locales are "slaved" to the agreed time scale at the system origin. Naturally other propagation effects and random effects must be taken into account, by a suitable collection of data. But the main point made here is that coordinate times (and frequencies) must be carefully determined by establishing physical links with a suitable origin time scale. Moreover, it is by no means obvious that all such physical links will lead to the same coordination. Hence, it is essential to define the method used to establish this link very carefully, and to follow well-prescribed procedures in measuring (by metric clocks) and recording the "behavior " of the extended system.[8]

In this system, coordinate clocks slaved together by radio means are needed for synchronization and epoch interpolation. Independent, proper, metric clocks are needed for time interval and rate measurement and calibration. Radio dissemination is needed in order to define the time coordinate spacing operationally. A unified system mean clock at the origin forms, together with adequate records, a useful reference and transfer standard, if its rate is nearly that prescribed in the International System.

III. PRINCIPLES AND ANALYSIS OF THE SYSTEM

We have enunciated, at least by implication, four main principles necessary for the quantitative definition of the kind of coordinate time system emerging from the USNO-NBS coordination.

1) A national mean standard or unified atomic clock and frequency standard is defined by the weighting process at the system origin. Its fractional rate difference from the average of the set of local mean atomic standard rates is zero.

2) Natural astronomical events are related to the national mean clock readings via UT2.

3) No radio waves or pulses used to synchronize the system should "disappear" -- ideally there is conservation of phase so that in every closed circuit (including equipment) the net phase change is zero.

4) Disseminated coordinated frequencies and rates measured as received at the origin in terms of the national mean standard must have their assigned (i. e., nominal) coordinate values.

In view of these requirements we may write down certain relationships between measured, inferred, or assigned quantities and quantities needed for making adjustments in emissions in order to attain coordination. First, let us define a few symbols. Let

N = number of component stations and laboratories in the system.

$\alpha_1, \alpha_2, \ldots \alpha_N$: weights assigned to the respective components.

$S_{12}, S_{13}, \ldots S_{1N}$: measured or inferred fractional frequency deviations of the rate of the first local mean atomic standard (its metric element) from the other component local mean time and frequency standards, as if in juxtaposition.

$F_1, F_2 \ldots F_N$: fractional frequency deviations of the rate of the respective local mean standards from the national one.

$E_1, E_2, \ldots E_N$: fractional frequency deviations of steering elements from local mean standards--recorded in the coordinating elements and introduced into the steering elements to compensate for random and systematic differences of the component local standards and emissions from the national mean at the system origin.

$G_1, G_2, \ldots G_N$: fractional frequency deviations introduced by the gravitational Pound-Rebka shift into the radio time and frequency signals used for synchronization and dissemination as they travel to the system origin.

$D_1, D_2, \ldots D_N$: ideal fractional frequency deviations of the respective emitted signals from their respective local mean atomic standards in order to follow the presently defined UTC system.

It should be understood that the frequencies as actually emitted and received may not at any one time agree with the ideal values. The system records should show the ideal values, and the departures from them which would be regarded as errors in the coordinate time system.

Figure 6 is a schematic diagram of a national system with N components. On it, one may trace for each component, the part of the component circuit in which each of the quantities defined above appear.

The national mean standard is denoted by the letters UAS (unified atomic standard).

On the figure, certain quantitative relations are shown which we now derive.

$$\sum_{i=1}^{N} \alpha_i = 1 \ . \tag{1}$$

By the first principle, we may also write

$$\sum_{i=1}^{N} \alpha_i F_i = 0 \ . \tag{2}$$

The definition of the pairwise measured (or inferred) fractional frequency deviation of the first local standard from the others yields

$$\left.\begin{aligned} S_{12} &= F_1 - F_2 \\ S_{13} &= F_1 - F_3 \\ &\vdots \\ S_{1N} &= F_1 - F_N \end{aligned}\right\} \ . \tag{3}$$

It is useful to note that $S_{ij} = F_i - F_j$ and therefore that $S_{1j} = S_{1i} + S_{ij}$, for i and j having values 1, 2, ... N.

One immediately infers that

$$F_1 = \sum_{j=2}^{N} S_{1j}\,\alpha_j \qquad (4)$$

a relation which may be used in place of Equation (2).

The gravitational radiation shifts are easily evaluated from the differences in altitude of the component emission stations from the system reference altitude. Let these altitude differences be $H_1, H_2, \ldots H_N$, in kilometers.

Then

$$G_j = \frac{gH_j}{c^2} \quad (j=1, \ldots N) \qquad (5)$$

where $g = 9.8\ m/s^2$

$c = 3 \times 10^8\ m/s.$

This effect must be included to help satisfy principle 4).

The present UTC-system necessitates the insertion of a constant frequency offset for all UTC-coordinated emissions from the nominal assigned values in order to partially synchronize the time signals with UT2. Thus we have, at present

$$D_j = E_j - 300 \times 10^{-10} \qquad (6)$$

There are discussions at present aimed at eliminating this large frequency offset, and attaining the very rational requirements of the navigators by a different, simpler, and improved means. When, and if, this is done, the distinction between D and E will vanish. Until then, all UTC-carrier signals used for calibration purposes ought to be corrected on reception by this amount.

In any event, this frequency offset only furnishes part of the information required for a more accurate immediate knowledge of UT2, important to many users. Such information is, or can be, supplied by voice or simple code on the same emissions.

Principles 3) and 4) lead to the equations

$$E_j + F_j + G_j = 0, \quad (j = 1, 2, \ldots N) \qquad (7)$$

That is, for j=1, for example, the ideal fractional frequency deviation, E_1, between the first local mean atomic standard and the emitted signal rates, added to the gravitational shift, G_1, in the emitted radiation, ought to exactly compensate for the inferred random difference, F_1, in rates of the first local mean standard and the national unified mean standard. The difference between E_1 and D_1 can be ignored, since it is both added and subtracted in making the first, or any, circuit in the system.

Now, if one is given all the α_j -values, and measures, or infers from observations, all the S_{1j}-values, then all the F_j-values can be determined from Equations 1, 3, and 4. The E_j-values are determined from (7), and the D_j-values from (6). One represents most of these relations easily on a frequency level diagram as in Figure 7.

Associated with each component station there are two levels: the level determined by the fractional frequency difference, S_{1j}, of the first station's local mean standard from the j^{th} local mean standard, and the level determined by the gravitational shift, G_j, determined from the altitude difference of the station from the system origin reference level.

Positive quantities are represented by vectors pointing up, negative ones by vectors pointing down. Hence, a station at a high altitude will have a gravitational level below the reference level, indicated by UAS in Figure 7, and conversely. Figure 8 also depicts the situation for the case N= 2 as it existed for the USNO-NBS coordination. As explained, however, the adjustments made did not quite follow this procedure because of the large value of S_{12}. (The values of G_1 and G_2 were taken to be zero for this initial adjustment.)

IV. CONCLUSIONS

Let us summarize the foregoing discussions, briefly. In order to set up this coordinate time system, there seem to be nine essential procedural steps.

(1) The components must be identified-both the associated and the member stations and laboratories.

(2) The essential system elements belonging to each component member must be identified: the local mean atomic standard, the coordinating element, the steering element, and the local coordinated radio station emitting specified time and frequency signals.

(3) The reference origin in space and time must be specified.

(4) Intercomparison measurements of the component local mean atomic time and frequency standard rates and epochs must be made, leading to the values of S_{1j}, (j= 2, . . . N).

(5) Statistical weights (α) must be chosen for each component.

(6) The national mean standard is then defined by determining the deviations (F) of all the local independent mean atomic standards from it.

(7) Astronomical events must be measured in terms of the unified national mean standard, utilizing UT2.

(8) The desired ideal emission rate offsets (E) from their respective local mean standards must be determined and the present UTC value D ($D = E - 300 \times 10^{-10}$) determined for UTC coordinated emissions.

(9) Continuous monitoring procedures must be set up to continually redetermine and publish -- for the system at least -- the weights and

(a) F - values
(b) E, D - values
(c) Differences between actual and ideal emission rates and epochs.
(d) Differences between actual and ideal reception rates and epochs.

If these procedures are permanently implemented, and the present USNO-NBS coordination appears to assure that this will be the case, the system can become a model for more extensive worldwide application, and for other national coordinate time systems. It already is a specific well-defined portion of what is often called the "National Measurement System".[9]

Some modifications may be needed for worldwide use. For example, the weighting process becomes a truly knotty problem, with political overtones. To insure proper statistical procedures, it is essential that all component members keep truly independent standards, and evaluate them exhaustively for reliability, stability, and accuracy. A certain amount of knowledge of how each of these national standards and their components (observatories, laboratories, and radio stations) are linked by physical means and coordination procedures must be available to the designated international coordinating agency. We are fortunate that there is already in existence a traditional agency, the International Bureau of Time (BIH), which receives all the essential astronomical information to construct the UT2 scale, and acts as coordinator for the present UTC system. In fact,

the BIH maintains an average atomic scale of time which satisfies some of the prerequisites to serve as an international mean time scale and standard (the scale known as A. 3). Questions concerning the weighting procedure, i. e., how to use the data furnished the BIH --(both national mean scale data and individual component data) should be answered.[10, 11, 12]

Again, the CCIR has established an International Working Party charged for the moment with considering the improvement of the UTC system to meet modern requirements. So it would be natural for this group, IWP VII/1, to continue to act as an advisory body to the FAGS (steering committee for the BIH) and to the BIPM (the international bureau engaged in metric standardization activities). These are clearly interdisciplinary matters which are the concern of the sciences of astronomy, geophysics, radio engineering, physics, and politics. This is a matter for future consideration in the CCIR.[13]

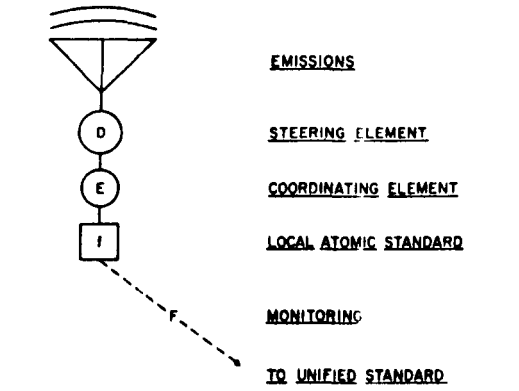

Figure 1: The symbols D, E, F refer to fractional frequency offsets explained in the text. The symbol "f" stands for the rate or frequency of the local mean clock or frequency standard--close to the prescribed SI-value.

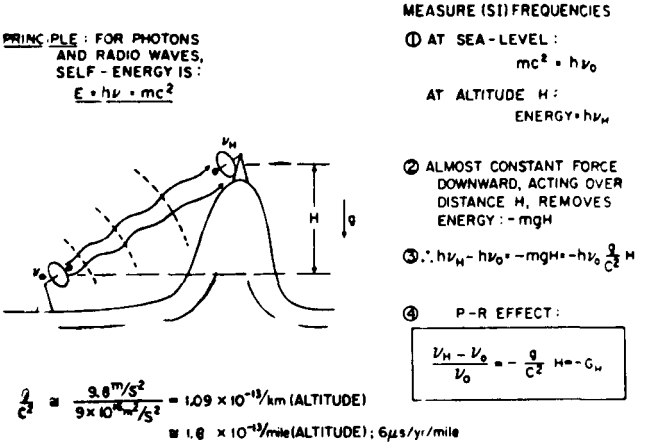

Figure 3: The Pound-Rebka, or gravitational frequency shift has been experimentally verified to one percent for gamma rays using the Mössbauer effect. It is a consequence of the general relativistic theory of gravitation.

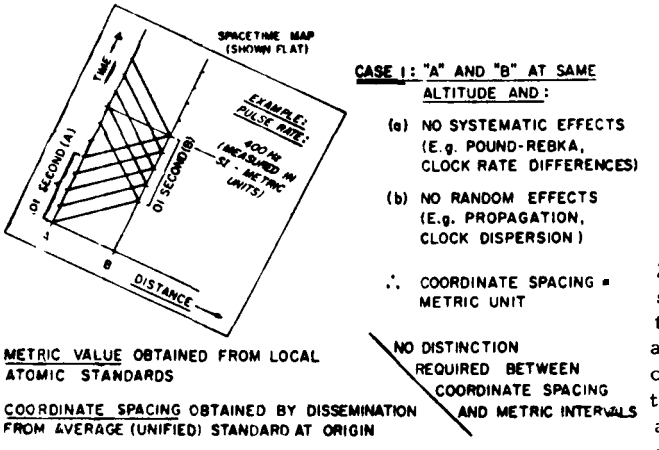

Figure 2: The schematic spacetime map shows radio pulses transmitted to B and returned to A to synchronize their clocks. A and B are separated by about 2.25×10^3 km (~1400 miles).

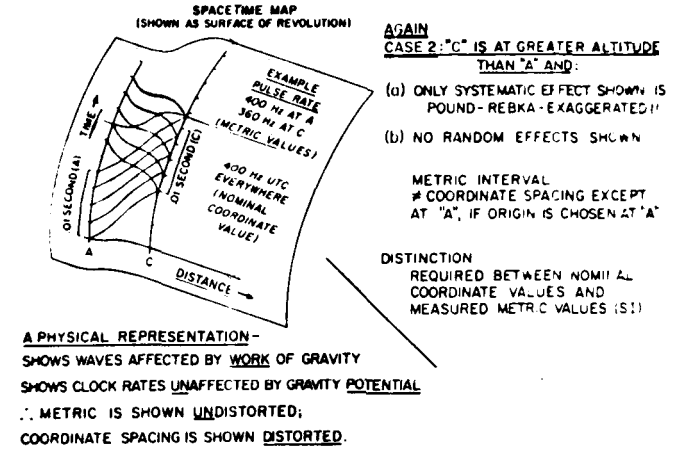

Figure 4: A and C are again separated by about 2.25×10^3 km. Their coordinate clocks are synchronized by radio pulses, and the rates of these are measured by the metric clocks running at their own (proper) SI rates. The curvature of the schematic map is introduced to show that the intervals of the two metric clocks are equal at the two respective locations differing in altitude. Only altitude changes produce the P-P effect, although for pictorial purposes, horizontal distances as well are combined with differences in altitude.

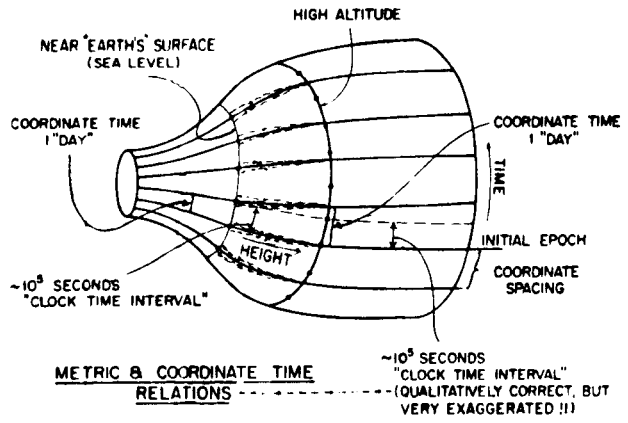

Figure 5: This is an even more exaggerated portrayal of the spacetime curvature needed to show the difference between coordinate intervals and metric intervals. The center of the "earth" is at the smallest cross section of the "bottleneck". The generators of the surface follow roughly the variation in gravitational potential with altitude. Unlike Figure 4, no horizontal distances are involved.

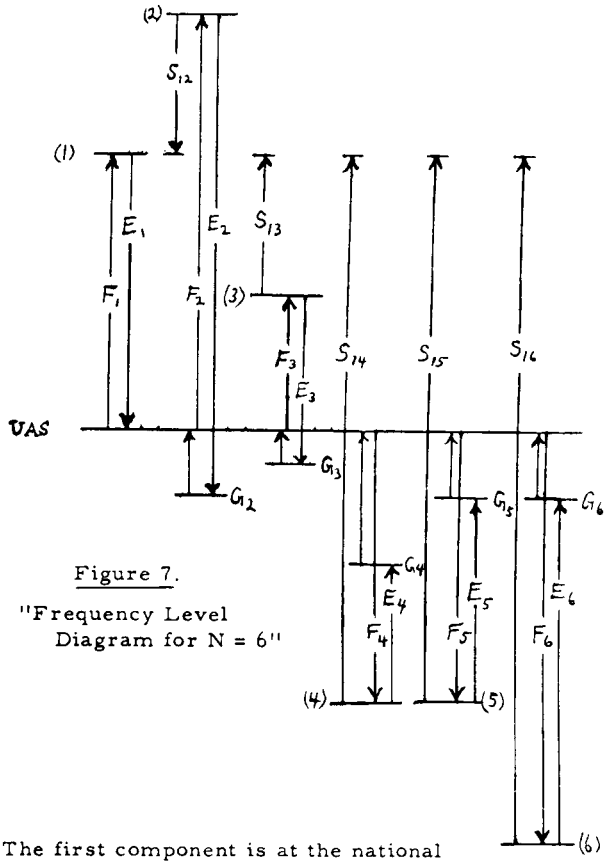

Figure 7.

"Frequency Level Diagram for N = 6"

The first component is at the national mean reference level, (UAS), so $G_1 = 0$.

Positive quantities are associated with upward arrows. Weights are not shown.

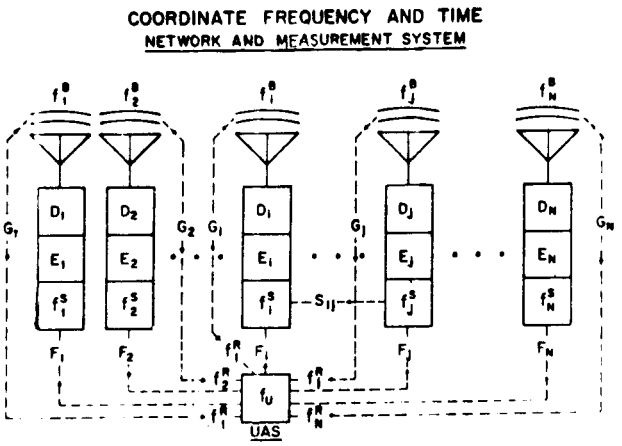

$$F_j = F_i - S_{ij}\,, \quad \Sigma \alpha_j = 1\,, \quad \Sigma \alpha_j F_j = 0\,, \quad E_j + F_j + G_j = 0\,, \quad G_j = \frac{g}{c^2} H_j$$

Figure 6: The coordinate time system resembles an electrical network. Ideal values of emitted frequencies f_j^B, are indicated, as are ideal values f_j^R, of received frequencies, and the rates f_j^S of the standards, and f_u of the system unified mean standard. Not shown are the observed emitted frequencies f_j^E, and actually received frequencies f_j^A. The measured or inferred rate intercomparison of the i^{th} and j^{th} local standards is indicated by the fractional frequency difference S_{ij}.

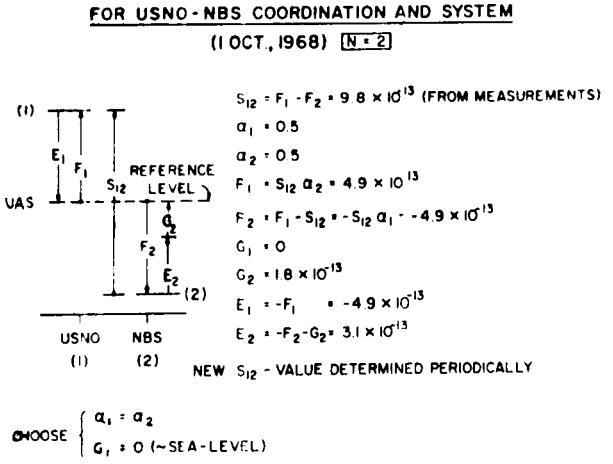

Figure 8: The values shown are of the correct orders of magnitude, but are for illustrative purposes only. Presently, the difference in rates of the local mean standards is considerably less, so that the importance of the gravitational shift is relatively greater.

463-560 O - 72 - 18

V. REFERENCES

1) A. Guetrot, D. W. Allan, and L. S. Higbie, National Bureau of Standards and J. Lavanceau, USNO, "An Application of Statistical Smoothing Techniques of VLF Signals for Comparisons of Time between USNO and NBS", Proc 23rd Annual Frequency Control Symposium, USAECOM, (6-8 May 1969).

2) Nautical Almanac Office, USNO and Her Majesty's Nautical Almanac Office, Royal Greenwich Observatory "The American Ephemeris and Nautical Almanac for the Year 1969" --U. S. Government Printing Office, Washington, D. C. (1967). (Also see: "Explanatory Supplement to the Astronomical Ephemeris and the American Ephemeris and Nautical Almanac", Her Majesty's Stationery Office, London (1961)).

3) R. V. Pound and G. A. Rebka, Physics Review Letters 4, p. 337 (1960).

4) G. M. R. Winkler "Recent Improvements in the U. S. Naval Observatory Timekeeping and Time Distribution Operations", Proc. 22nd Annual Symposium on Frequency Control, USAECOM, p. 383, (April, 1968).

5) D. H. Sadler, "The Presidential Address -- Astronomical Measures of Time", Q. Jour. Royal Astronomical Society, 9, pp. 281-293 (1968).

6) G. C. McVittie, "General Relativity and Cosmology", p. 89 & ff, University of Illinois Press, Urbana (1965).

7) G. E. Hudson, "Spacetime Coordinate Systems" Proc. of the International Conference on Chronometry, 1, pp. 197-221, Lausanne (June 1964)

8) J. L. Synge, "Relativity, the Special Theory" (p. 7), J. Wiley and Sons, 2nd ed. (1965).

9) R. D. Huntoon, "Concepts of the National Measurement System", Science, 158, No. 3797, pp. 67-71 (1967).

10) B. Guinot, "Formation of a Mean Atomic Time Scale" (to appear in Astro. Bulletin)(1967).

11) J. A. Barnes, "The Development of an International Atomic Time Scale", Proc. IEEE, 55, No. 6, pp. 822-826, (June 1967).

12) L. Essen, "Time Scales" Metrologia 4, No. 4, pp. 165-168, (Oct. 1968).

13) G. E. Hudson, "Some Characteristics of Commonly Used Time Scales", Proc, IEEE, 55, No. 6, pp. 815-821, (June 1967).

Astronomical Time

Jean Kovalevsky [1]

A definition of time-scales and criteria of uniformity of a time-scale are introduced in the first part of the paper. These considerations are applied to time-scales currently used in Astronomy: Sidereal and Universal Times. Each of them is defined, their equivalence is proved, and the precision with which each can be determined is discussed. The irregularities of the rotation of the Earth are the causes of the non-uniformity of these time-scales. A uniform gravitational time, Ephemeris Time, is then defined and the precision of its determination is discussed. All the three astronomical time-scales have a necessity of their own and cannot be interchanged. In order to reach a better understanding of the concept of time, it is necessary that all time-scales—including atomic time—should coexist and be compared with the highest possible precision.

Metrologia, Vol. 1, No. 4, 169–180 (October 1965).

Manuscript received August 6, 1965.

[1] Bureau des Longitudes, Paris 6e/France

Von der Astronomischen zur Atomphysikalischen Definition der Sekunde

G. Becker [1]

According to resolutions of the 12th General Conference on Weights and Measures and of the International Committee on Weights and Measures of Oct. 1964, precise measurements of time may be performed by means of a resonance frequency of the cesium atom as an atomic time and frequency standard. The problems of the definition of the second and the reasons which led to this development are discussed.

PTB-Mttlg, No. 4, 315–323, and No. 5, 415–419, (1966). (In German)

[1] Physikalisch-Technische Bundesanstalt (PTB), West Germany

TIME SCALES

By L. Essen

Time scales have traditionally provided the time of day and the season of the year, as well as time interval, and if it is to be of universal use the atomic scale must be coordinated with astronomical scales. Two major steps in the coordination have already been taken: the atomic unit has been defined in terms of the second of Ephemeris Time, and the scales were made to agree on 1st January 1958. If the rotation of the Earth were constant the scales would continue to agree, but because of the variations in the rate of rotation the atomic scale will diverge from the astronomical scale unless some adjustments are made to bring them together. The present method of adjustment is to apply a frequency offset from the nominal value to the oscillator from which the 1s timing pulses are derived and when necessary a step adjustment to the epoch of the signals. This method possesses serious disadvantages and it is suggested that all standard transmissions should operate at their nominal values provision being made to supply those users needing astronomical time with the difference between atomic and astronomical time.

Metrologia, Vol. 4, No. 4, 161-165 (October 1968)

Note on Atomic Timekeeping at the National Research Council

A. G. Mungall, H. Daams, and R. Bailey

Three different experimental atomic time scales have been maintained at the National Research Council of Canada. One has been based on an HP 5061A cesium standard, another on a free-running crystal oscillator, calibrated daily with respect to the NRC 2.1 m primary cesium standard, and a third on the HP 5061A calibrated weekly by the primary standard. VLF and Loran C intercomparisons with the United States Naval Observatory and the National Bureau of Standards indicate that the third is probably the most accurate of the three time scales. Agreement between this scale and those of the USNO and NBS is of the order of 1 μsec or 1×10^{-13} in frequency over a four-month period.

Metrologia, Vol. 5, No. 3, 73-76, (July 1969)

3. Distribution of Frequency and Time Signals

3. Distribution of Frequency and Time Signals—Continued

WIDELY SEPARATED CLOCKS WITH MICROSECOND SYNCHRONIZATION AND INDEPENDENT DISTRIBUTION SYSTEMS

Thomas L. Davis and Robert H. Doherty
National Bureau of Standards
Boulder Laboratories
Boulder, Colorado

Summary

In a majority of timing applications, a problem exists in setting two or more clocks to agree with one another. Present techniques using WWV or other high frequency broadcasts allow clocks to be synchronized within one millisecond. This paper describes a method which offers an improvement in synchronization of three orders of magnitude.

Microsecond synchronization is obtained by use of the Loran-C navigation system as the link between a master clock at Boulder, Colorado and any slaved clock anywhere in the Loran-C service area.

The timing system also includes a unique method for distribution of several time code formats on a single UHF channel.

Introduction

Three solutions to the problem of time synchronization of widely separated clocks have been proposed by Morgan [1]. These methods are:

(a) Transportation of a master clock to each location where synchronization is desired,

(b) two-way transmission of radio signals between a master clock and the slave clock, and

(c) one-way transmission of radio signals from a master clock to a slave clock.

The timing system which is described here uses one-way transmission of LF radio signals (method c) to synchronize a slave clock to a master clock and one-way transmission of UHF radio signals to distribute time to the user from the slave clock.

The WWV transmissions are perhaps the most widely known and for many applications the most useful broadcasts. The equipment required is both inexpensive and readily available. Their major disadvantage is in the accuracy of time synchronization available. While millisecond time is accurate enough for many applications, modern scientific measurements require at least one or two and often three orders of magnitude better than this. For this reason, several studies have been made on the stability of signals at LF and VLF [2, 3, 4, 5]. As a result of these and other studies, several systems have been proposed which would supply standard frequency and time on a world wide basis. One of these, Loran-C, is already in operation as a precise 100 kc navigation system [6]. The operation of Loran-C is such that when synchronized to a time and frequency standard, microsecond synchronization is available anywhere within the service area of the system [7].

Once a clock has been synchronized with the master clock, the time information must be distributed to the user. In order to cover the wider range of recorder applications, serial time codes are generated at rates from one ppm to 1000 pps. All these codes are time-division multiplexed on a single UHF channel for distribution to the user. This equipment will be described after the clock and its synchronization have been discussed.

I. MICROSECOND SYNCHRONIZATION

The Loran-C Navigation System

The Loran-C navigation system is a precise 100 kc pulse system which obtains its accuracy by means of pulse sampling. Figure 1 shows the manner in which this sampling is accomplished. A signal reflected from the ionosphere will arrive at the receiver with a random phase relationship some time after the direct or ground wave signal. A gate samples the signal ahead of the arrival of the sky wave so that only the ground wave is used to synchronize the system. The propagation time of the ground wave can be calculated to one microsecond over a land path and to one-tenth of a microsecond over a sea-water path.

† The work described in this paper is sponsored by the United States Air Force, Ground Electronics Installation Engineering Agency (GEEIA), Eastern GEEIA Region, Brookley Air Force Base, Mobile, Alabama.

The system consists of at least three stations, a master and two or more slaves. On the East Coast Chain, the slave stations are located at Jupiter Inlet, Florida and Martha's Vineyard, Massachusetts. The master station is located at Cape Fear, North Carolina. When used as a navigation system, a hyperbolic line-of-position is determined by the master station and each of the slaves. The intersection of these lines-of-position (LOP's) gives the location of the receiver to better than 1000 feet at ranges of 1000 miles over sea water and land.

The National Bureau of Standards is proposing to synchronize the Loran-C system, which is operated by the U. S. Coast Guard, with the United States Frequency Standard (USFS) at Boulder, Colorado [8]. Signals from the Loran-C station at Cape Fear will be monitored and compared against the USFS. Corrections will be made to the master oscillator at Cape Fear to keep the synchronization well within a microsecond of the USFS. Another more refined and more expensive plan proposes the establishment of a Loran-C station between Cape Fear and Boulder. This plan has two very definite advantages. First, the East Coast Chain would be expanded to a star, providing navigation coverage of the Great Lakes and the Gulf of Mexico. Second, very good ground wave signals would be available at Boulder. This star chain plus a station located in the southwestern United States would provide Loran-C coverage for the entire continental United States. The entire system could be easily monitored at Boulder.

A Loran-C Clock

In order to fully utilize the capabilities of the Loran-C system for timing, a clock of some type is required. This clock must be capable of resolving time to one microsecond, it must be capable of being easily synchronized by the Loran-C signals, and the time in the clock must be in a format that can be used external to the clock. Such a clock has been constructed at the Boulder Laboratories of the National Bureau of Standards. Figure 2 shows the manner in which this clock is constructed. The Loran-C receiver fits in the space on the right. The space on the left is occupied by the clock. A visual readout is visible directly above the monitor oscilloscope in the center section.

Clock Divider

The clock divider consists of 15 trochoidal beam-switching tubes operating as decimal counters. These tubes are arranged so that the first operates at one megacycle, the second at 100 kc, and so on to the 15th which operates every 100 days.

Figure 3 shows a typical divider stage. The carry output for the previous stage is produced by gating the input pulse rate with the number nine output from the previous beam-switching tube. This method reduces the carry propagation time through the divider to less than one microsecond. The carry output is used to trigger a bistable multivibrator which drives the beam-switching tube. An additional input to the bistable multivibrator allows counts to be added to each decade as an aid to synchronizing the clock.

The first counter is driven directly by the megacycle pulses from the pulse generator and no gating is involved. The seconds and minutes counters are arranged to reset to zero by themselves on their 60th count. The hours counters are reset automatically to zero on their 24th count. The days counters are allowed to count to 399 before they reset. This requires a manual clock reset once a year.

Readout Register and Display

The readout register must, upon command, store and display the time of the command. The manner in which this is accomplished is demonstrated in Figure 4. Since the read command can occur randomly, it is used to select one of the microsecond pulses. This pulse is then delayed less than a microsecond to insure that all the beam switching tubes are in a stable state. Each output from the beam-switching tubes is connected to one input of an "and" gate. The delayed read command is connected to the other gate input and to the reset input of a bistable multivibrator. The gate output triggers a monostable multivibrator. The pulse from the monostable multivibrator trailing edge is fed to the set input of the bistable. Thus, ten bistable multivibrators will store the number in the decade until the next read command. The time between successive read commands must be sufficient to allow the monostable multivibrators to recover. The prototype requires 200 microseconds to recover. This means the read commands cannot occur closer together than 400 microseconds.

Two types of display are available. The output from the bistable is permanently connected to an incandescent display. This readout is always visible to the operator and is required to synchronize the clock. Also available is a high speed photographic readout. The output from the monostable multivibrator flashes a "nixie" indicator tube for 200 microseconds. This readout is useful for rapidly recording the time of a discrete event to the nearest microsecond.

Synchronization of the Clock

The Loran-C receiver provides two types of information to the clock, both of which must be used to obtain the desired microsecond synchronization. This information is derived from the 100 kc carrier and from the pulse rate which is transmitted.

Frequency Synchronization. Before any thought can be given to synchronizing a clock in time, a stable and accurate frequency source must be available. Figure 5 shows the manner in which this frequency is derived from the Loran-C receiver. The local oscillator supplies 500 kc to two phase shifters. The number one shifter is driven directly from a servo motor and number two is driven by the same motor through a clutch. The output from the first phase shifter is divided by five to supply the local 100 kc signal for the Loran-C receiver. The output from the second phase shifter is used to generate pulses at a megacycle rate for the clock. The clutch output also drives an integral control unit which adjusts the frequency of the oscillator. If the Loran-C receiver loses synchronization with the transmitter, the clutch is disengaged and the oscillator is allowed to free run. The clock accuracy, until synchronization is re-established, then depends upon the stability of the local oscillator.

Time Synchronization. Loran-C is not presently instrumented to resolve time increments larger than 50 milliseconds. However, identification of one second increment could be instrumented without affecting the navigation accuracy. Increments of time not resolved by Loran-C can easily be resolved by WWV.

Loran-C pulses are broadcast in groups of eight with a group repetition rate (GRR) of twenty per second[1]. The first pulse in one of these group of eight occurs exactly on the second at the master transmitter. Figure 6 shows some of these pulse groups and their relation to the pulse transmitted by WWV for a hypothetical site.

WWV must be used to set the correct time into the clock down to 50 milliseconds. It may be used below this, but is not necessary. Loran-C is now used to set the clock correct to the nearest microsecond. In order to demonstrate the technique used, the following example is given:

> Assume, first, a location 1000 miles from a slave transmitter with an all sea water propagation path; and second, a Loran-C receiver with an instrumentation delay of 25 microseconds.

This information is now used to calculate the total delay from the master transmitter to the GRR output of the receiver.

Propagation time-master to slave:

	2711.8 μsec
Slave coding delay:	12000.0 μsec

Propagation time-1000 mi of sea water:

	5373.1 μsec
Receiver delay:	25.0 μsec
Total delay:	20109.9 μsec

Figure 6 shows the manner in which these delays are related.

At any time after the second, the first six counters will have advanced some number of microseconds. This number may be read out and displayed by commanding the readout storage register. When this read command is derived from the Loran-C receiver as shown in Figure 6, the number of microseconds will be 20110. This is the sum of all propagation and instrumentation delays from the master transmitter to the receiver output.

If the readout register does not display this number of microseconds, that is, if the second pulse in the clock does not coincide with the second pulse at the master transmitter, then the counters are adjusted until this number is displayed. Once the microsecond counters have been set and the counters from seconds to days have been set using WWV, no further adjustments need be made. Since the oscillator is phase-locked to the one at the master transmitter, any tendency to drift is immediately corrected.

This completes the discussion of the clock and the methods for microsecond synchronization. Since microsecond time alone is not sufficient for this application, serial time codes are generated for recorders. The generation and distribution of these codes will now be discussed.

II. DISTRIBUTION OF MICROSECOND TIME

Generation and Distribution of Time Codes

Most timing distribution systems in current usage generate all required codes at a central location then distribute each code separately to the user. Therefore, a terminal site may have several channels carrying time information to it. In the system to be described, the single channel is an integral portion of the time code generator. That is, the code is not generated on time until the required information reaches the terminal site. The system can be described in three sections:

> (1) The encoder, which receives time information from the clock and supplies code information to the link,
>
> (2) The link, a UHF transmitter and receiver, and

[1] Based on the East Coast Chain. Fractional repetition rates can be handled by modified instrumentation techniques.

(3) the decoder, which takes the coded information from the link and generates the necessary time codes.

The Encoder

The encoder takes time information from the clock in decimal form and encodes it in such a manner that all the information can be transmitted on a single channel. The information which is included in the prototype system includes four proposed time codes for the Inter-Range Instrumentation Group (IRIG) combination code, five time codes for the Atlantic Missile Range (AMR), and one countdown, or "T"-time, code. The IRIG codes include both binary-coded-decimal (BCD) and straight, or pure, binary (SB). The AMR codes are coded binary (CB).

The encoder may be further divided into several subsections. These are the time generator, the rate generator, the code generators, and the code multiplexer.

The Time Generator. The time generator receives 10-line decimal time from the clock and produces three binary time format outputs. Ten decimal-to-BCD conversion matrices produce the BCD output in a 4-line format from tenth of seconds to hundreds of days. The coded binary time is produced by three registers of bistable multivibrators. The first register counts seconds up to 59 when it is reset by a pulse from the clock. This register produces a 6-line output for seconds. A second register counts minutes up to 59 when it is reset by a pulse from the clock. Again a 6-line output is generated for minutes. Finally, a register counts hours up to 23 when a clock pulse resets it. A 5-line output is generated. In order to generate the time of day in straight binary seconds, a register of 17 bistable multivibrators are used[2]. This register counts seconds from the clock and is reset once a day by a pulse from the clock.

Rate Derivation and Format. In order to send 10 time codes over a single-channel information link, some method of multiplexing the code information is required. Such a scheme, employing time-division multiplexing, is shown in Figure 7.

Because the fastest code rate to be transmitted is 1000 pps, this rate was selected as a basic rate for the system. The information to be transmitted is always contained within a 1000 microsecond sync interval. In order to position the information properly in the interval, the encoder must sample the time one millisecond early, then delay the information to the proper position in the sync interval. The receiver then selects the information from the sync interval and uses the following 1000 pps sync pulse to generate the time codes. An additional 30 microseconds of time advance are introduced so that the propagation time may automatically be corrected within six miles of the transmitter.

The codes and rates which are derived are:

IRIG Codes	AMR Codes	Rates
1 ppm	1 ppm	1 ppm
	1 pps	1 pps
2 pps		2 pps
	20 pps	20 pps
100 pps	100 pps	100 pps
	500 pps	500 pps
1000 pps		1000 pps

A total of nine code formats at seven rates result. An additional rate of 20 kpps is derived and is used to correctly position the pulses in the sync interval. The technique used to derive these rates is shown in Figure 8. A 100 kpps rate is gated to derive a 20 kpps rate which is 30 microseconds early. This rate is then gated down to 1000 pps, also 30 microseconds early. All rates following are derived from the 1000 pps gate 1030 microseconds early.

Code Generators. The code generators must use the desired rates to generate a signal which is multiplexed into the sync interval. Two methods are available to perform this generation, one conventional and one not so conventional.

The conventional method uses two parallel registers and produces a serial output. One register counts time and is transferred into the second, which is a shift register. The information is shifted out of the register and generates a time code at the output. In the second, and unconventional method which is used in this encoder, prior knowledge is used to sample time information stored in a register. Figures 9 and 10 demonstrate the required information and how it is used.

In order to determine the proper place in the sync format at which a particular point in the time register must be sampled, the time code must be inspected. Figure 9 shows the first portion of a proposed IRIG 100 pps code. Because the time code is desired at the correct time at the terminal equipment, advance sampling of 1030 microseconds is used at the transmitter.

For example, in order for the 10 second bit to occur at the terminal equipment exactly on index count number six, the 10 second BCD output must be sampled during the index interval beginning on count five. Since, for this code, index count five always corresponds to a time 50 milliseconds after the second, outputs from the beam-

[2] This SB register is not included in the prototype equipment but the CB registers may be rewired to provide SB time.

switching tubes in the divider are used to select this interval for sampling. Figure 10 shows the logical "and" gate used to sample this time while Figure 11 shows a timing diagram of the sampling operation. In order to avoid ambiguity between 50 milliseconds and 150 or 250 milliseconds, the zero output from the tenth second counter (marked as 000 milliseconds) is used along with the number five output of the ten millisecond counter (marked as 50 milliseconds). This sampling technique is used for each information bit in this code.

This method will obviously only generate a "one" for the time bits. Some simple method must be devised to generate "zeros" for the time bits and for all other index counts except the reference marks as well as to generate the reference marks. Figure 10 also shows the method used to generate a "zero" unless a "one" or a "mark" is to be generated. The rate, in this case 100 pps, is used to set a bistable multivibrator whose output feeds a 3-input and gate. This bistable multivibrator is reset after two milliseconds. The other two gate inputs are inhibited by other bistable multivibrators, one for the "one" code and one for the "mark". If neither bistable multivibrator is set by a "one" or a "mark" pulse, then the output of the "zero" bistable multivibrator appears at the code output. If either the "one" or "mark" bistable multivibrator is set, the "zero" output is inhibited. The "one" and "mark" are mutually exclusive as is seen from the code format.

The reset pulses for the bistable multivibrators are derived from the clock divider. The "mark" set pulses are derived in the same manner as the "one" pulses, except a 3-input and gate is used[3].

Code Multiplexer. The code multiplexer takes the information from the nine code generators (four IRIG, five AMR) and multiplexes it onto a single channel for broadcast over the UHF link. Figure 12 shows a portion of the multiplexer which demonstrates how this is accomplished.

The 1000 pps rate, which synchronizes the receiver, is fed directly to the code multiplexer output. The inputs from the code generators must each be delayed to its unique position in the sync interval. The information which is actually broadcast consists of set and reset pulses. This information is derived from the rate and length of the code generator output pulse. Since all codes of the same rate, regardless of format, turn on at the same time, each rate is delayed to its correct position in the sync interval and transmitted. The 20 kpps rate is used as a reference to correctly position the pulse exactly on a 50 microsecond mark in the interval. This is demonstrated for the 100 pps rate in Figure 12. In order to generate the reset pulse for the code, the output of the code generator is differentiated to initiate its delay. Again, the 20 kpps rate is used to re-establish the system accuracy. This procedure is repeated for each rate and code.

It should be noted that the relative position of the pulses within the sync interval is inmaterial. Because of the system logic the set pulse will always occur in an interval which precedes the reset pulse. However, because of some symplifications made in the demodulator, the 100 pps reset pulses should appear as shown in Figure 7. This will be discussed shortly.

The Information Link

The link must transmit the information from the output of the encoder to the input of the decoder. A UHF distribution system is employed in the prototype system. This includes a single transmitter at a central location and a receiver at each recording site.

The Transmitter. The transmitter which is used in this system is a simple pulsed cavity oscillator. A blocking oscillator is used to pulse the cavity which operates at a frequency of 1.75 Gc[4]. A coaxial transmitting antenna is mounted at a height above nearby obstacles.

The Receiver. The receiving antenna is a dipole mounted in a corner reflector or horn. The antenna feeds a crystal mixer. The local oscillator is another cavity oscillator which operates continously. A 60 Mc IF strip provides the required gain. The detected output from the IF strip is fed directly to the input of the decoder.

Using this relatively simple system, signals were received at a range of 40 miles with a signal-to-noise ratio of 20 db.

The Decoder

The decoder must take the output from the receiver, separate the sync pulses, examine the sync interval for information, and generate the time codes. Two units are used to perform these functions, a sync interval demodulator, which separates the sync pulses from the rest of the information and generates a ramp output, and a time code demodulator, which uses the ramp and sync pulses to examine the sync interval for information to generate a time code and rate output.

The Sync Interval Demodulator. The sync interval demodulator is required at every site in order to separate the 1000 pps sync pulses and to generate the ramp which is required

[3] Special techniques are used on the 500 and 1000 pps codes.

[4] Gc = Gigacycles = 10^9 cps.

for the code demodulator.

The broadcast code format is such that the last 100 microseconds of the sync interval are always vacant and alternate sync intervals are usually vacant (Figures 7 and 14). These empty spaces are used to simplify the synchronization of the demodulator. The manner in which the sync demodulator operates is shown in Figures 13 and 14. The first pulse, no matter when it occurs, passes through an "and" gate and triggers a bootstrap ramp generator. The bootstrap inhibits the gate for the length of the ramp, 900 microseconds. After the bootstrap has removed the gate inhibition, the next pulse is allowed through to repeat the cycle. If the first pulse occured in the middle of some particular sync interval, then the ramp will turn off in the middle of the following interval, which will probably be empty. Figure 14 shows how the unsynchronized ramp would be synchronized by the IF output using the sync pulses and empty intervals.

The outputs which are produced by the sync interval demodulator are: First, the ramp, which is used to generate the delays required for the code demodulator; second, the sync pulses, which are used to synchronize the various time codes within a microsecond; third, a clamp output, which is used to discharge capacitors for high speed operation; and fourth, a test pulse, which would be used as an aid for tests and alignment. This test pulse is derived in exactly the same manner as the rate, or synchronized set, pulses in the code demodulator and is usually adjusted for a one pps output.

Time Code and Rate Demodulator. The code demodulator must take the outputs from the sync demodulator and use them, along with the IF output, to generate the desired time code. One such demodulator is required for each code output desired. Figures 15 and 16 describe the operation of a typical demodulator[5].

The ramp output from the sync demodulator is used with a delay pickoff to select a portion of the sync interval to be examined. The portion of the interval which is examined is different for each code. Because of the manner in which the codes are generated in the encoder, the set pulse will occur in an interval which is several milliseconds ahead of the interval containing the reset pulse. Therefore, the relative position of the set and reset pulses in the sync interval is arbitrary. When a set pulse occurs in the interval at the point where the delay pickoff is sampling, a gate is opened which allows the next sync pulse to set a bistable multivibrator. This is the bistable multivibrator which produces the code output. This synchronized pulse occurs at the code rate, correct in time, and is brought out separately as a repetition rate. When the reset pulse occurs in the interval and is recognized by the delay pickoff, it is used directly to reset the output bistable multivibrator. This means that the reset pulse is not synchronized with the 1000 pps sync rate. The effect of this operation on the code output is negligible. The difference between a pulse 2000 microseconds wide and one 2050 microseconds wide is barely discernable at a 100 pps rate and is even less so at the slower code rates. Since the percentage error is potentially greatest on the 100 pps code, these reset pulses are spaced closest to the front of the interval.

The instrumentation used for the 500 and 1000 pps codes is different partially because of format and partially because of speed. The 500 pps (AMR) code is a presence-absence code which is sent for only 38 milliseconds each second. The 1000 pps (IRIG) code occurs at the same speed as the sync pulses. Instead of using separate set and reset pulses for these codes, a single pulse technique is used along with monostable multivibrators. Approximately the same technique is used in the 1000 pps demodulator as is used in the code generators to produce a "zero" output unless instructed otherwise. This eliminates the need of sending 1000 pps code information in every interval.

Closing Comments

While this system is designed primarily for missile range timing, there are many other applications where timing to the indicated accuracy is desired. Some examples of these applications are:

(1) The positioning of high altitude aircraft by means of a UHF pulse broadcast from the aircraft and received at several locations against a common time base,

(2) the location of thunderstorms by precisely fixing lightning discharges,

(3) the accurate position fixing of nuclear detonations by similar techniques, and

(4) the precise measurement of time variations on high frequency transmissions such as WWV as an aid to better understanding of propagation phenomena.

The distribution of accurate time in large metropolitan areas can be accomplished by use of the system described, but using a television station for the link. In this manner, one centrally located clock could supply microsecond time to an entire metropolitan area such as Los Angeles.

During the summer of 1960, the system was completed by the National Bureau of Standards,

---

[5] All the demodulators are identical except for the 500 and 1000 pps codes.

Boulder Laboratories, Central Radio Propagation Laboratory, Navigation Systems Section. Except for the beam-switching tubes in the divider, the UHF transmitter and receiver, and portions of the Loran-C receivers, solid state circuitry is used throughout.

Acknowledgements

The authors wish to acknowledge the contributions of Mr. Gifford Hefley, Mr. Robert F. Linfield, and Mr. Earl L. Berger, all of NBS-BL, and Mr. Phillip J. Kiser of Eastern GEEIA Region for their aid in the design and construction of the equipment described. We also wish to thank Mr. Ernest Komarek and Mr. William Mansfield for their comments and suggestions on the manuscript. The figures were prepared under the direction of Victor Brackett and the typing was done by Jane L. Rhomberg.

BIBLIOGRAPHY

[1] A. H. Morgan, "Precise Time Synchroniaztion of Widely Separated Clocks," NBS Technical Note No. 22, July 1959.

[2] A. D. Watt and R. W. Plush, "Power Requirements and Choice of an Optimum Frequency for a Worldwide Standard Frequency Broadcasting Station," NBS Jour. of Research, Vol. 63D, No. 1, July-August 1959, pp. 35-44.

[3] J. R. Johler, W. J. Kellar, and L. C. Walters, "Phase of the Low Frequency Ground Wave," NBS Circular No. 573, June 1956.

[4] J. R. Johler and L. C. Walters, "On the Theory of Reflection of Low and Very Low-Radiofrequency Waves from the Ionosphere," NBS Jour. of Research, Vol. 64D, No. 3, May-June 1960, p. 269.

[5] J. R. Wait, "Diurnal Change of Ionospheric Heights Deduced from Phase Velocity Measurements at VLF," Proc. I.R.E., Vol. 47, No. 5, May 1959, p. 998.

[6] W. P. Frantz, W. Dean, and R. L. French, "A Precision Multipurpose Radio Navigation System," 1957 I.R.E. Convention Record, Part 8, p. 79.

[7] R. H. Doherty, G. Hefley, and R. F. Linfield, "Timing Potentials of Loran-C," presented at the 14th Annual Frequency Control Symposium, Fort Monmouth, New Jersey, sponsored by U. S. Army Signal Research and Development Laboratory, Proceedings to be published.

[8] Staff, NBS-BL, "National Standards of Time and Frequency in the United States," (letter) Proc. I.R.E., Vol. 48, No. 1, January 1960, p. 105.

GLOSSARY

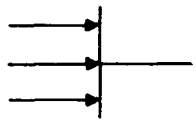

Logical "or" Circuit

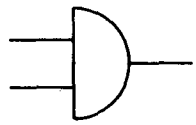

Logical "and" Circuit

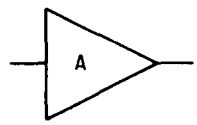

Amplifier (no inversion)

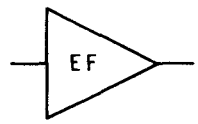

Emitter Follower

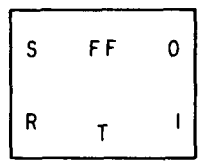

Bistable Multivibrator (flip-flop)

S = set input } cannot be used together
R = reset input }
T = toggle input
(for symmetrical triggering)
0 = output after reset
1 = output after set

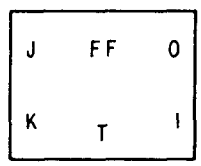

Bistable Multivibrator (flip-flop)

J = set input } can be used together
K = reset input }

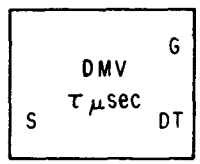

Monostable Multivibrator
(one-shot or delay multivibrator)

S = set input
G = gate output
DT = delayed trigger output
τ = duration of delay

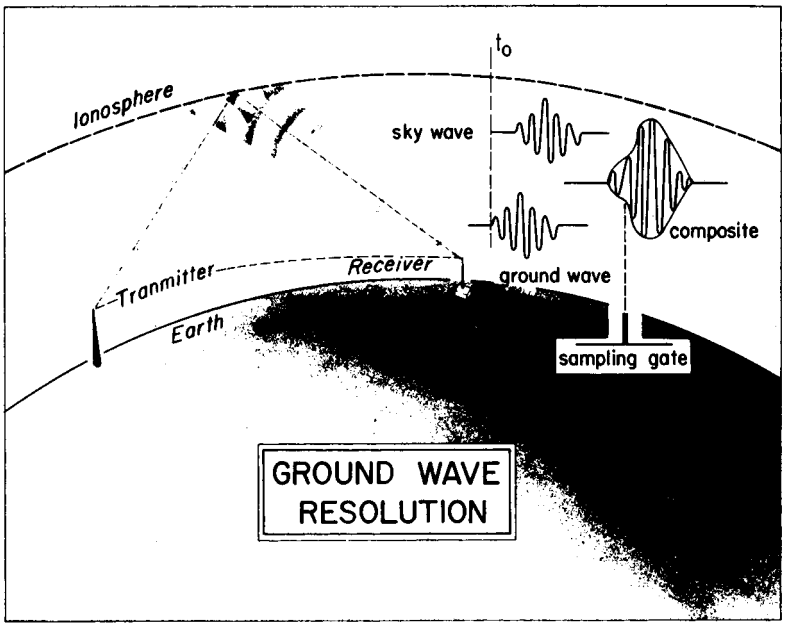

Fig. 1. Ground wave resolution.

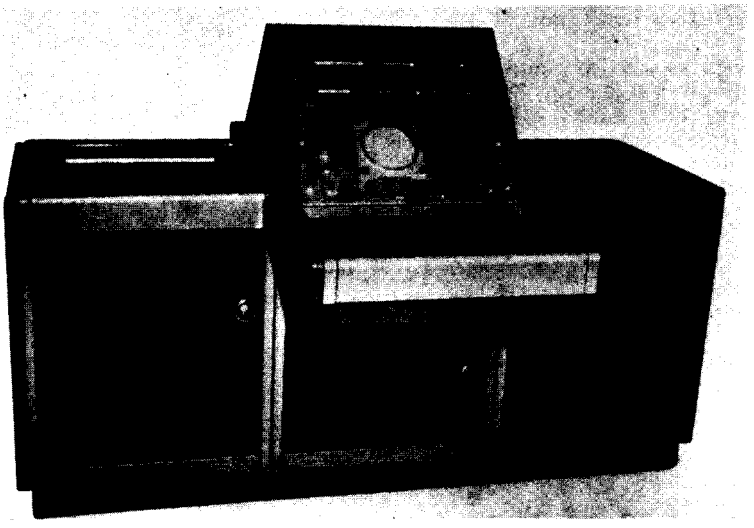

Fig. 2. A Loran-C clock.

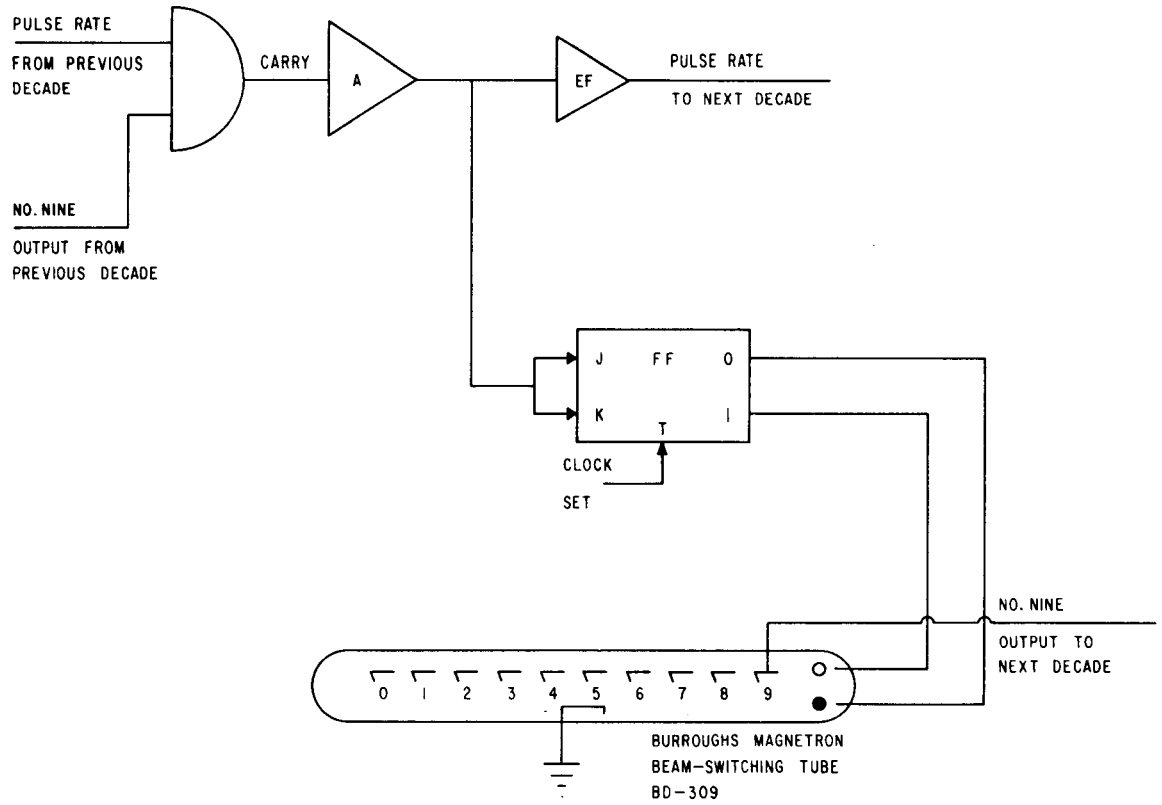

Fig. 3. Typical divider decade.

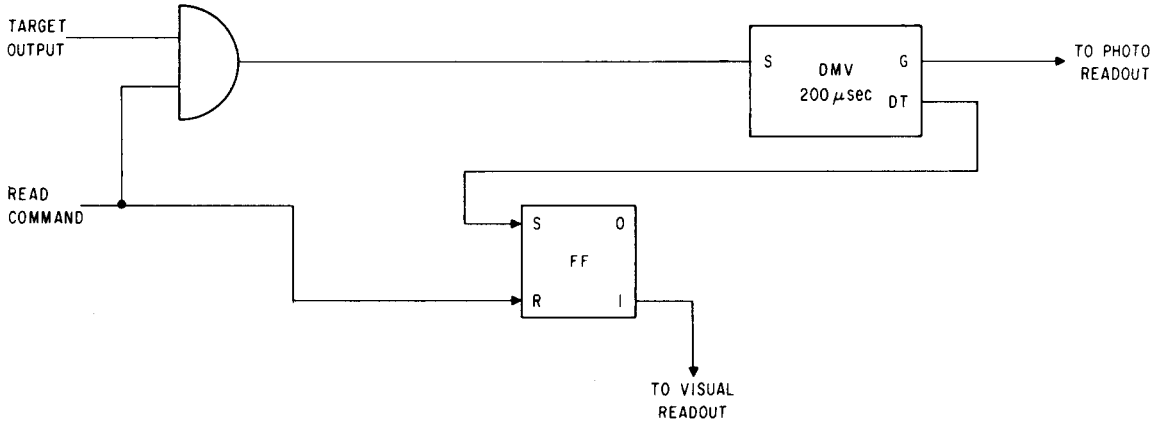

Fig. 4. Readout logic diagram.

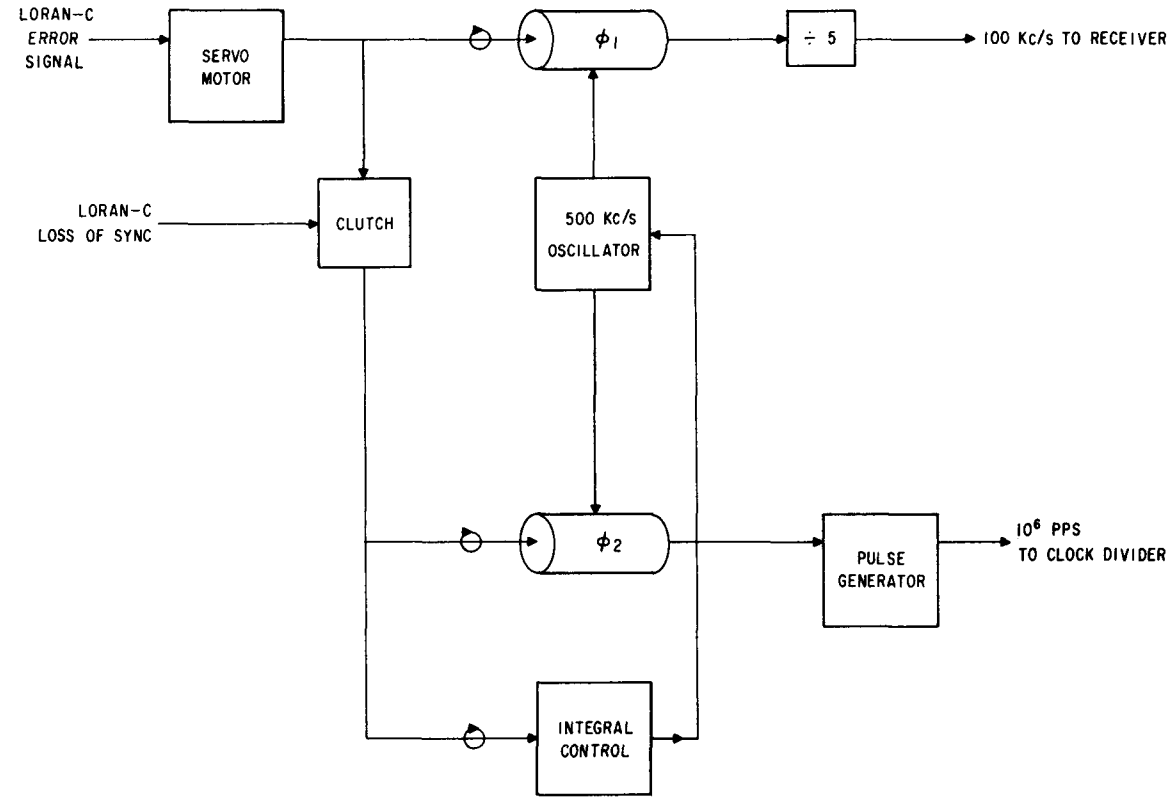

Fig. 5. Frequency control.

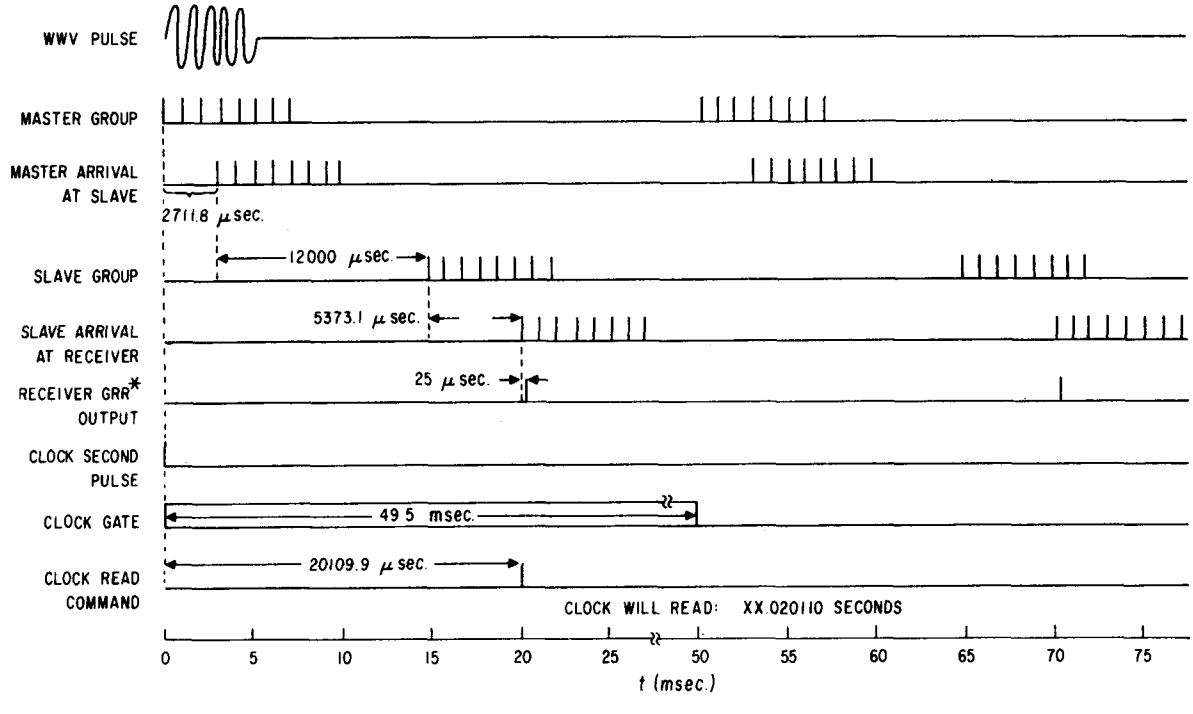

Fig. 6. Example of the time relationship for WWV and Loran-C pulses.

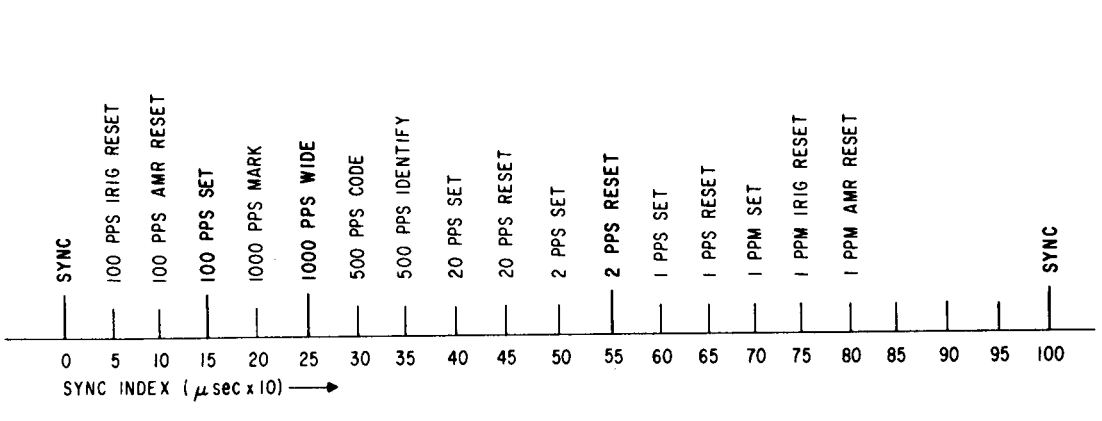

Fig. 7. Synchronizing interval format.

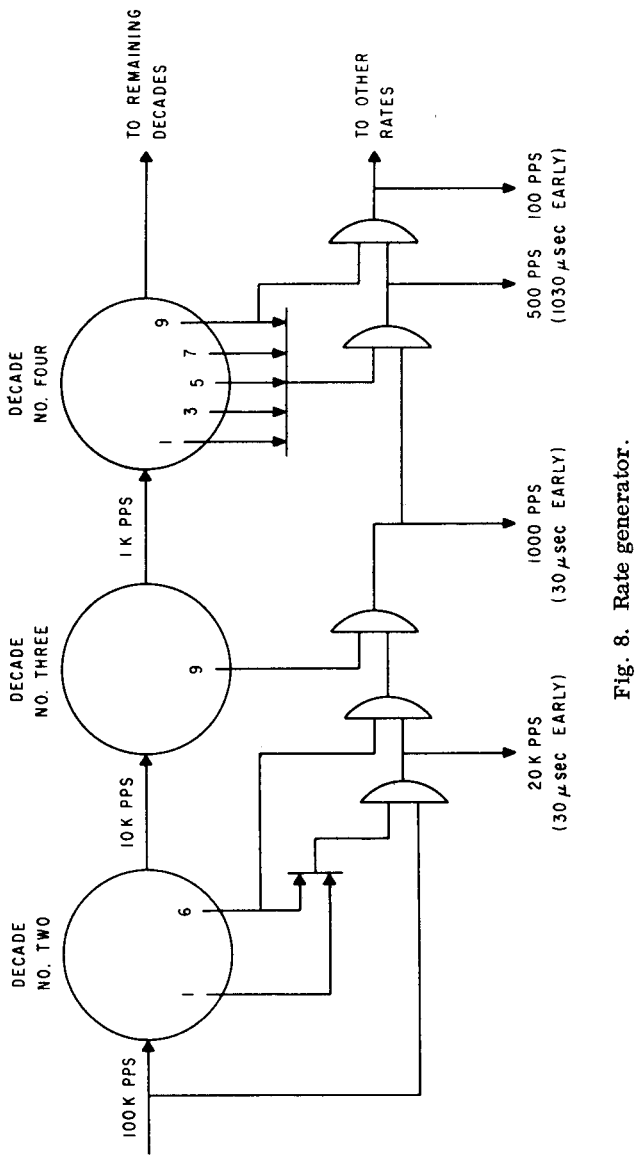

Fig. 8. Rate generator.

463-560 O - 72 - 19

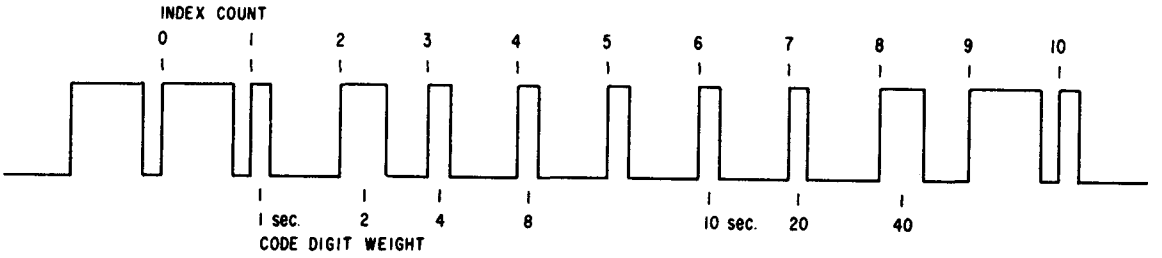

Fig. 9. Example of a 100-pps time code.

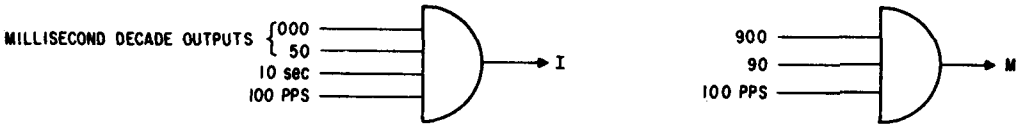

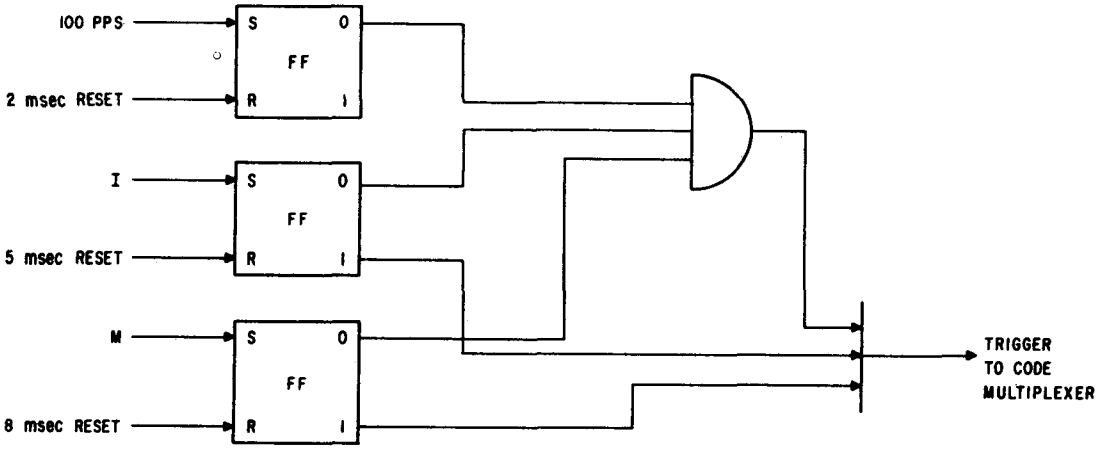

Fig. 10. Example of a 100-pps time code generator.

Errata to Widely Separated Clocks With Microsecond Synchronization and Independent Distribution Systems.

p. 14, Figure 10 -
Output from FF No. 1 should come from "1" instead of "0".

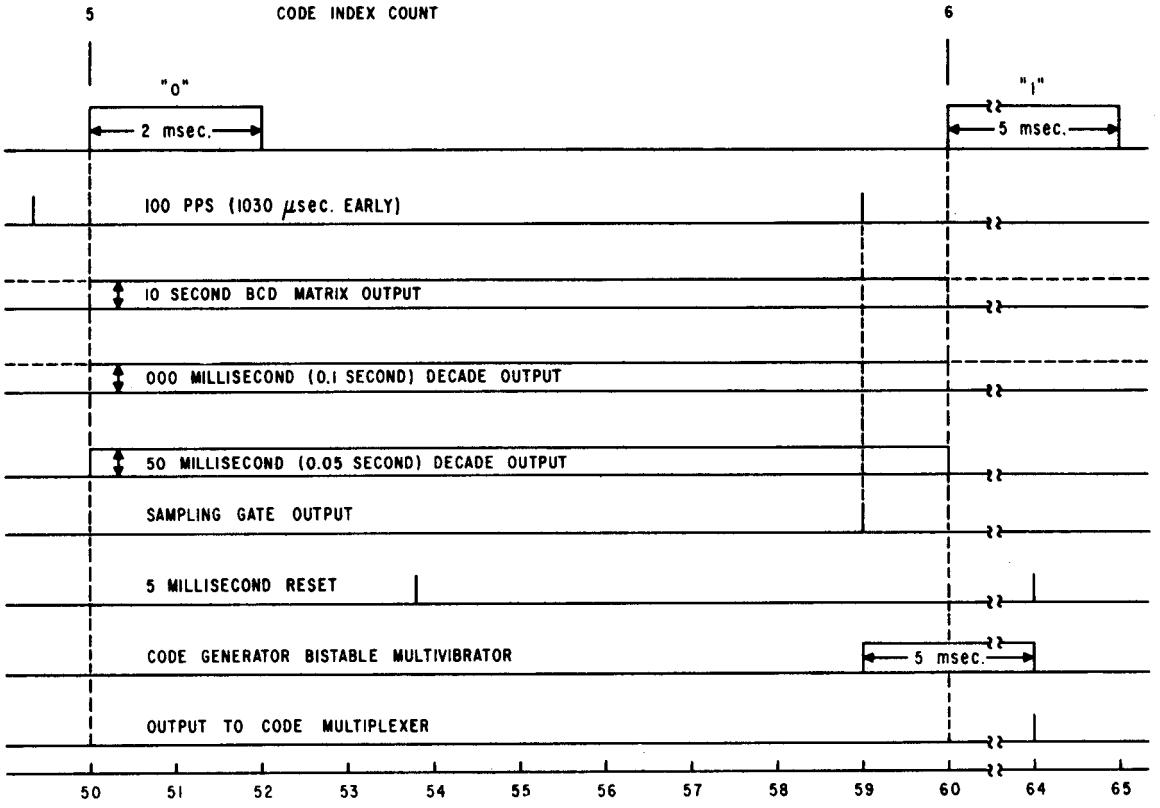

Fig. 11. Code generator timing diagram.

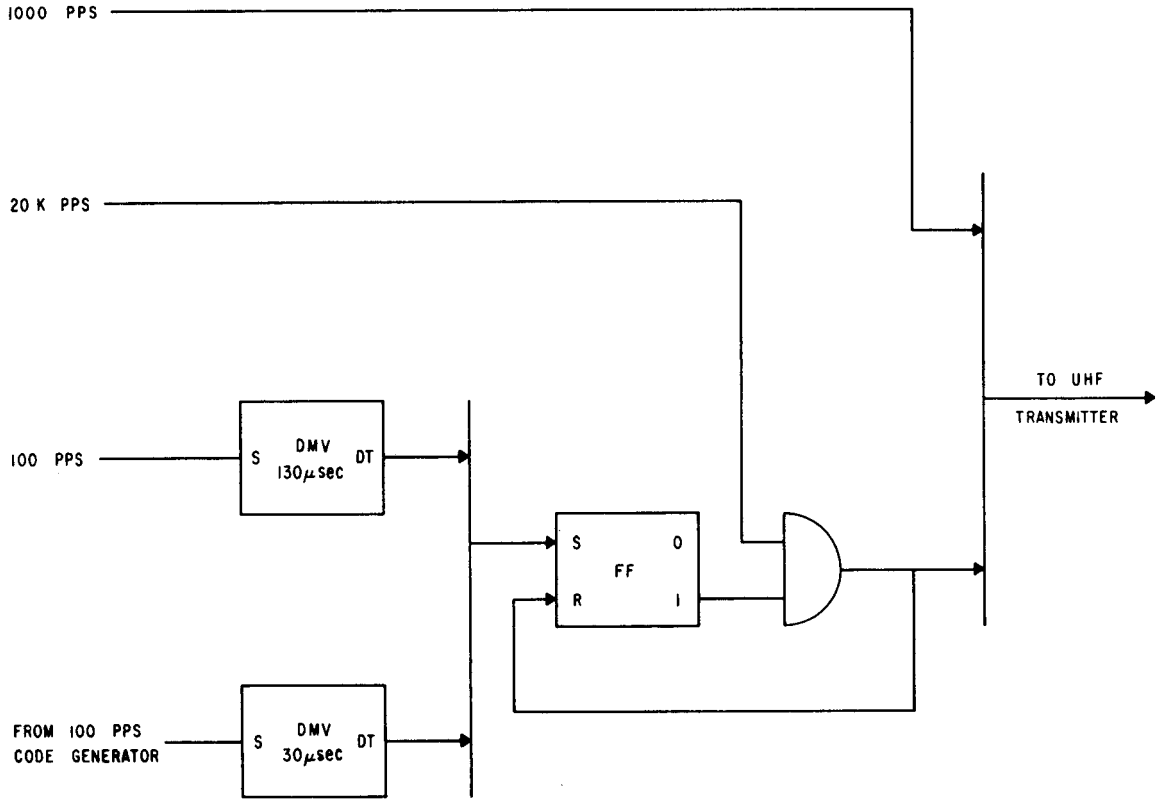

Fig. 12. Code multiplexer.

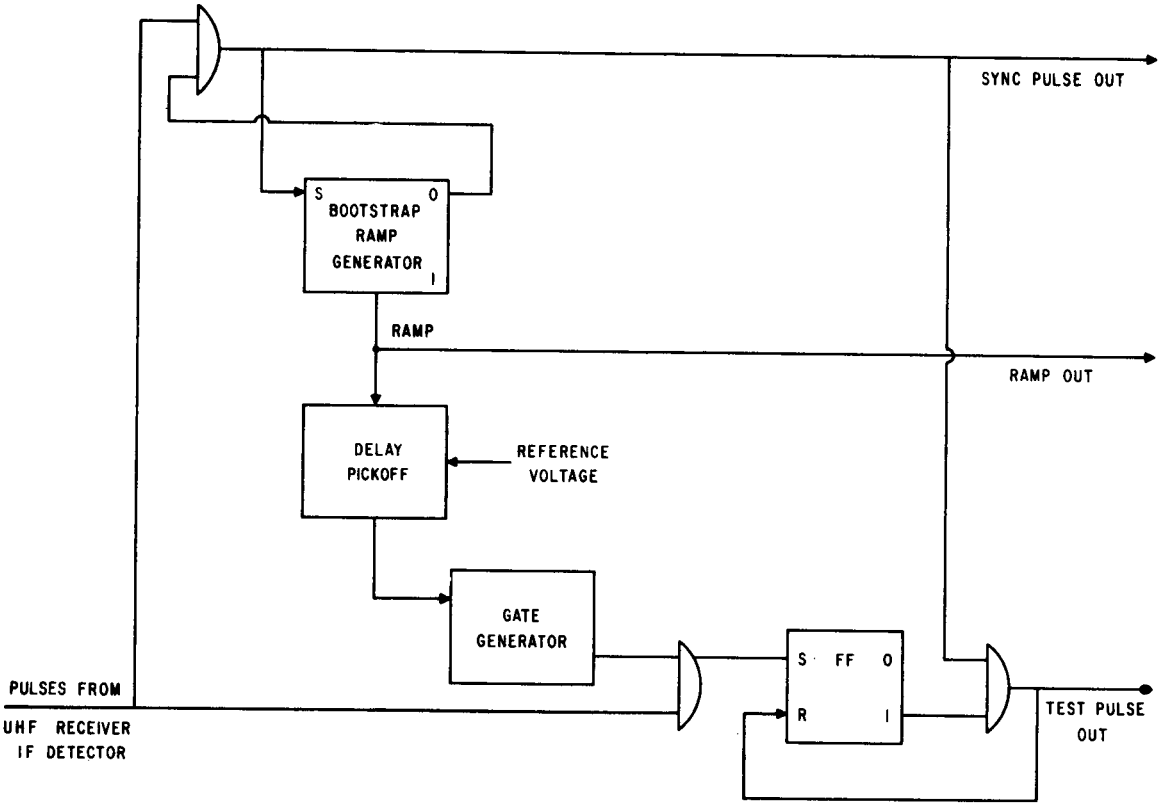

Fig. 13. Synchronization interval demodulator.

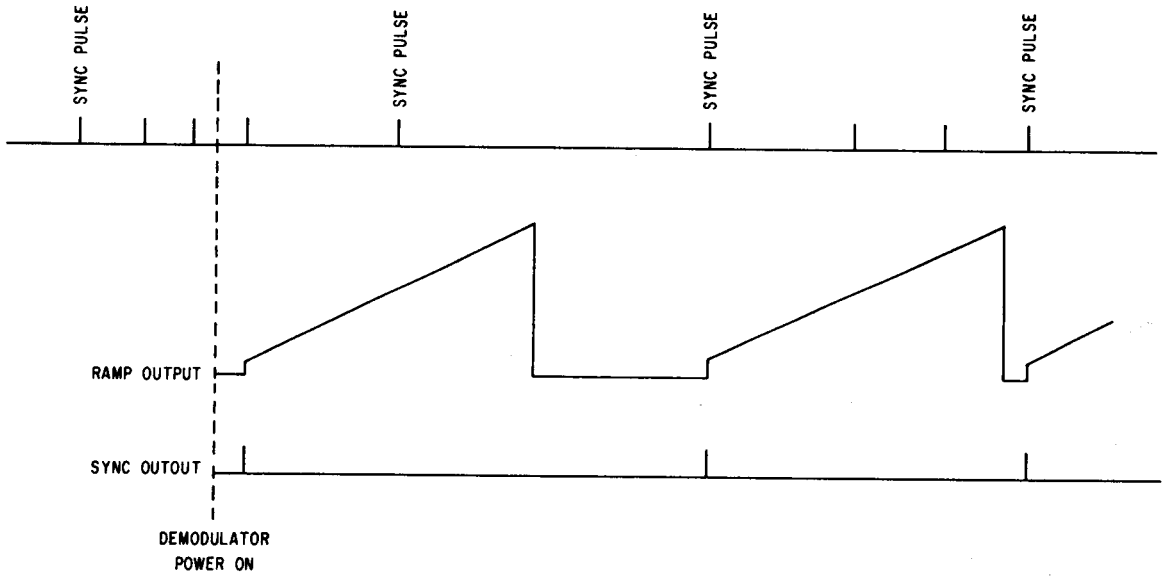

Fig. 14. Demodulator synchronization.

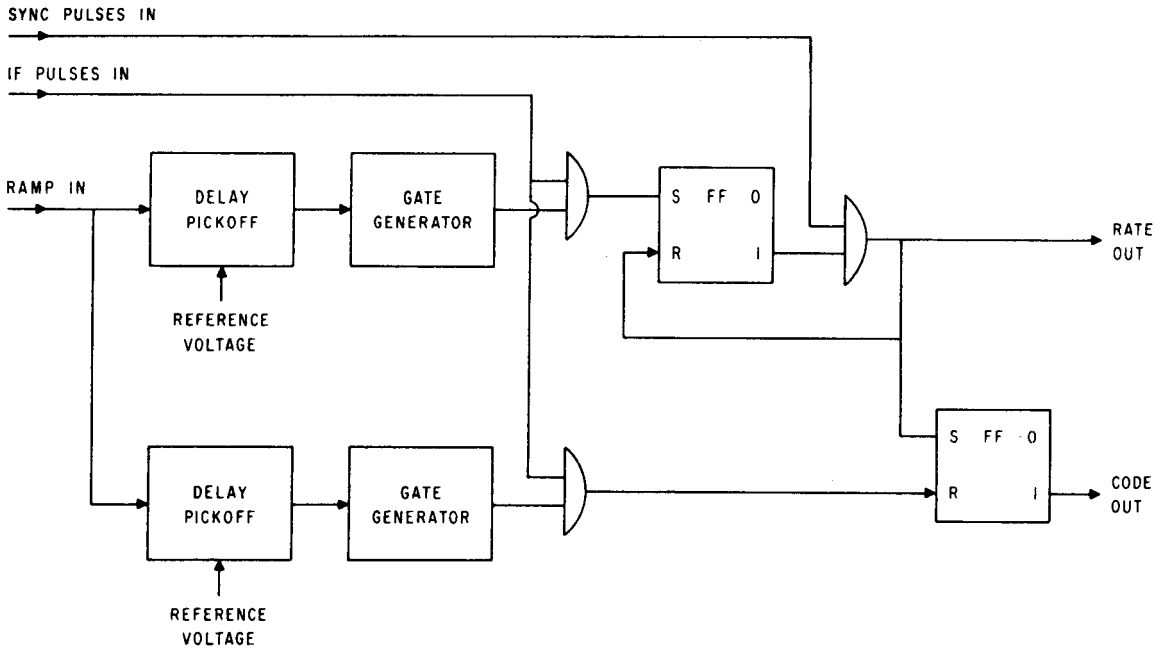

Fig. 15. Time code demodulator.

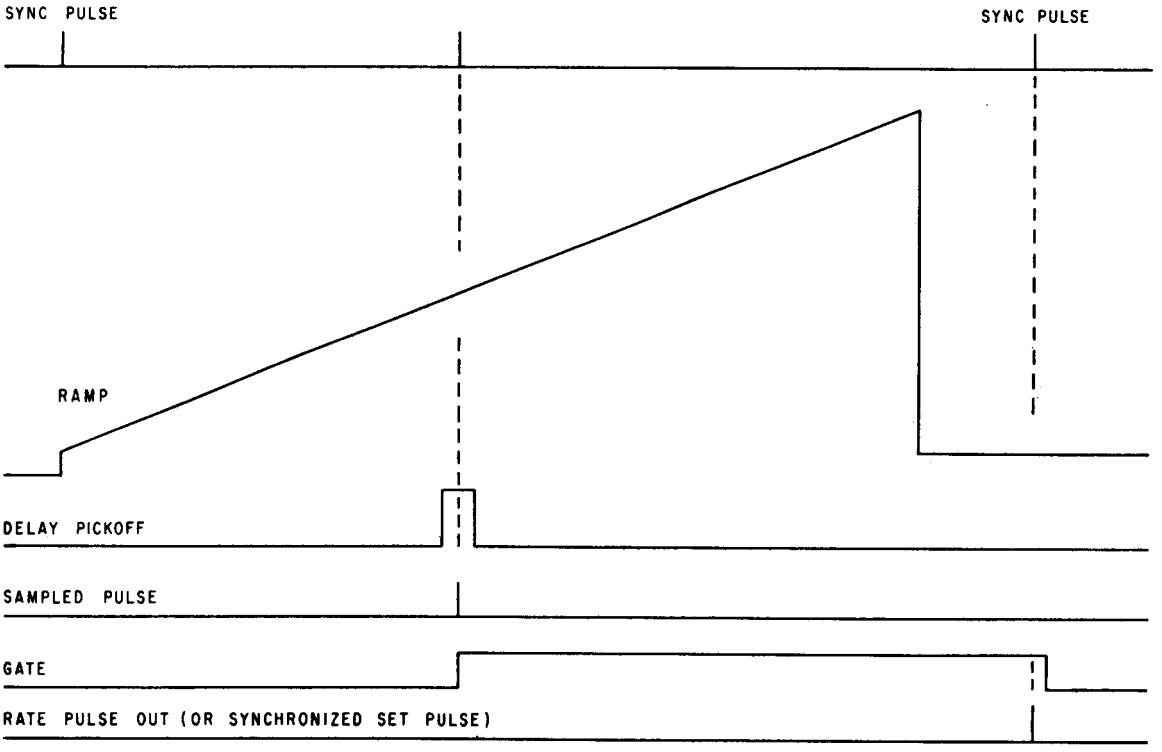

Fig. 16. Demodulator timing diagram

Timing Potentials of Loran-C*

R. H. DOHERTY†, SENIOR MEMBER, IRE, G. HEFLEY†, AND R. F. LINFIELD†, SENIOR MEMBER, IRE

Summary—**The Loran-C navigation system is capable of synchronizing and setting clocks to a relative accuracy of better than 1 μsec throughout the system's service area. A Loran-C receiver functions as a slaved oscillator and a trigger generator. The generated triggers bear a time relationship to the triggers at the master transmitter, which is known to within a microsecond. Clocks operating from these sources are compared with clocks operating from independent free-running oscillators.**

A fundamental relationship between time and position is considered. Loran-C as a navigation and timing system can provide both position and time simultaneously. The East Coast Loran-C chain will be time synchronized. The national frequency standards and uniform time source located at Boulder will be used to monitor these signals. Time synchronization and time distribution have been demonstrated on the Atlantic Missile Range. Inter-range time synchronization and precise time for large areas of the world could be provided in the future.

Appendix I describes briefly the results of ground wave measurements made on the Loran-C (Cytac) system. Appendix II describes the results of sky wave measurements made with the system.

* Received by the IRE, June 30, 1960; revised manuscript received, August 28, 1961.

† Radio Systems Division, National Bureau of Standards, Boulder, Colo.

I. INTRODUCTION

IN the majority of timing applications a problem exists in setting two or more clocks to agree with one another. The greater the requirement for precise agreement between these clocks, the more difficult the problem becomes and, if the clocks are in widely separated locations, the difficulty is further increased. The reading of a single clock is meaningful only as it relates to its own frame of reference. For example, a clock may gain or lose with respect to the periodicity of the earth as it revolves about its own axis or about the sun.

Accurate astronomical time depends on long-term observations, but is ultimately limited by unpredictable variations in the earth's rotation. Furthermore, any astronomical time can be determined only to an accuracy of several milliseconds for a single set of observations. The initial settings of individual clocks may, therefore, differ by amounts of the order of milliseconds. These differences combined with the gains or losses of individual clocks are of such magnitude that

Reprinted from the PROCEEDINGS OF THE IRE
VOL. 49, NO. 11, NOVEMBER, 1961

independently operating clocks or clocks synchronized by existing radio timing signals are unable to make measurements more precise than a millisecond at different locations.

When it is necessary to measure time at two or more locations to an accuracy of 1 μsec or better, such measurements must all be made within the same frame of reference, that is within a single clock system. The term "clock system" as used in this paper means a master clock at a convenient central location and other clocks at widely separated locations which are slaved to the master in such a way that each will track the master. Such a clock system must also provide for a means to synchronize or set each slave clock to agree accurately with the master clock. A number of Loran-C clocks will function as such a clock system with initial setting or synchronizing accuracies of 1 μsec or better using ground wave reception. Accuracies of 10 μsec or better should be obtainable using sky wave reception. Other methods may be used to set remote clocks, such as flying atomic standards from place to place, but they do not offer the convenience or reliability of Loran-C.[1]

The National Bureau of Standards at Boulder, Colo., maintains the nation's primary frequency standard. A fail safe clock operating from this standard would provide an extremely uniform time source that could be related in retrospect to any astronomical time measurements. This uniform time source is the proposed means for monitoring the aforementioned master clock.

II. Loran-C Operation and Its Timing Application

Loran-C[2] is a pulse navigation system operating on a basic frequency of 100 kc and normally consisting of a master station and two or more slave stations. Several Loran-C chains are operational or under construction. The presently operating U. S. East Coast Loran-C chain, and the previously operated Cytac (later named Loran-C) chain are shown in Fig. 1. The master station is located at Cape Fear, N. C., and the two slave stations at Martha's Vineyard, Mass., and Jupiter Inlet, Fla. The area over which a ground wave could be received for timing purposes would extend approximately 3000 km seaward or 2000 km landward from any one transmitter.

The Loran-C system utilizes synchronous detection techniques for measuring phase, and methods for determining a fixed sampling point early on the pulse, independent of pulse amplitude. By this means the ground wave is completely resolved from the sky waves. See Fig. 2. To a first approximation the ground wave transmission time is proportional to distance. Secondary corrections, however, usually have a magnitude in the range of 1 to 10 μsec. These corrections are determined

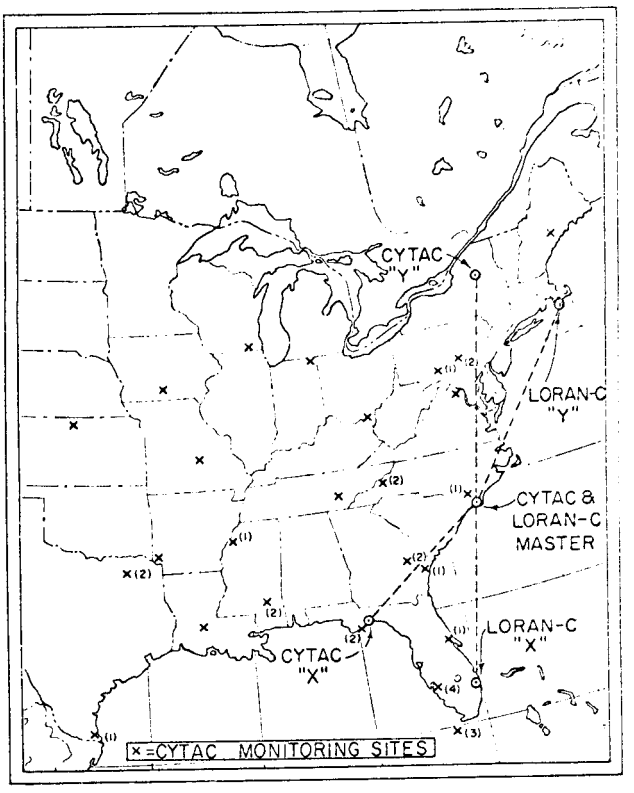

Fig. 1—Loran-C and Cytac locations.

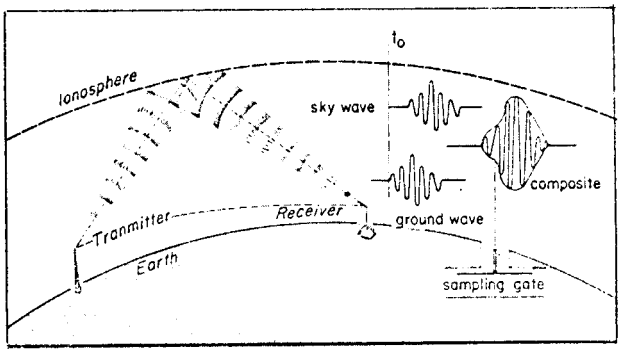

Fig. 2—Ground wave resolution with Loran-C.

largely by the conductivity of the path and to a much smaller extent by the dielectric constant and the index of atmospheric refraction.[3,4] Both the conductivity and the dielectric constant of sea water are accurately known. Consequently, the transmission time over sea water can be computed accurately. Transmission times over paths involving land cannot be as accurately calculated since the conductivity of land is not well known. However, by correlating time difference measurements[5]

[1] F. H. Reder, M. R. Winkler and C. Vickart, "Results of a long range clock synchronization experiment," Proc. IRE, vol. 49, pp. 1028–1042; June, 1961.

[2] W. P. Frantz, W. Dean and R. L. Frank, "A precision multipurpose radio navigation system," 1957 IRE National Convention Record, pt. 8, pp. 79–97.

[3] J. R. Johler, W. J. Kellar and L. C. Walters, "Phase of the Low Radiofrequency Ground Wave," Natl. Bureau of Standards, Boulder, Colo., NBS Circular No. 573; June, 1956.

[4] K. A. Norton, "The propagation of radio waves over the surface of the earth and in the upper atmosphere," Proc. IRE, vol. 25, pp. 1203–1236; September, 1937.

[5] All time difference measurements are determined by phase differences at 100 kc.

with generalized assumptions of ground conductivity, individual path conductivities may be deduced. For example, it has been demonstrated that the best single value of conductivity which can be assigned to the eastern half of the U. S. is 0.005 mho/meter. The average error between time differences computed using this conductivity and those measured in a test program (see Appendix I) was approximately 0.8 μsec. The algebraic average was nearly zero and the maximum error among all sites was 2.5 μsec. The largest errors were associated with sites located in mountainous terrain. Until better prediction methods are developed it must be assumed that systematic errors of the order of 1 μsec may exist for land and mixed paths unless the transmission time has been measured by the use of two transmitters, such as is done over the Loran-C baselines.

The East Coast Loran-C chain operates on a basic repetition rate of twenty pulse groups per second.[6] A pulse group consists of eight phase coded pulses with a uniform spacing of 1 msec. The Loran-C system, as presently operated, does not resolve time increments larger than the repetition period or 50 msec. Larger increments could be resolved without interference to the system, but at this time there appears to be no pressing requirement for such a change. The 50-msec interval between pulse groups can be resolved conveniently by the WWV seconds' pulses. In order to use WWV and Loran-C in such a manner the two transmitting systems must be synchronized, as they would be since WWV is transmitting uniform time.[7] See Fig. 3.

The Loran-C navigation system operating on a basic frequency of 100 kc performs the vitally important function of slaving all oscillators in the system to the oscillator at the master transmitter. By virtue of the technique of slaving a number of relatively cheap oscillators to a master oscillator, all clocks operated from such oscillators will, by definition, have an average drift rate of zero. The instantaneous deviation of any one clock from the average is primarily determined by the factors listed below:

1) Signal-to-noise ratio.
2) Relative and absolute quality of slave and master oscillators.
3) Integration time.
4) Tightness of coupling of the slave oscillator.

The positioning system requires a means for selecting a given cycle and a point on that cycle. It is obvious that this criteria for the positioning system satisfies the requirements for synchronizing a timing system. The instrumentation being utilized in the navigation system has a resolution of a few hundredths of

[6] Fractional Loran rates can also be used for the operation of a clock by gating the received pulses and using only those transmitted on the second to set the clock.

[7] A. H. Morgan, "Precise Time Synchronization of Widely Separated Clocks," Natl. Bureau of Standards, Boulder, Colo., NBS Tech. Note No. 22; July, 1959.

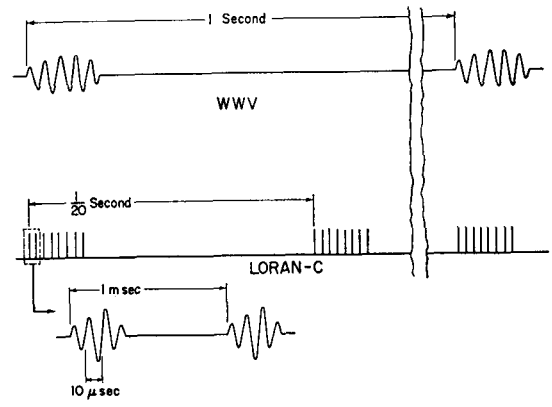

Fig. 3—Synchronization of Loran-C with WWV time signals.

1 μsec. The time variations in propagation due to changes in refractive index, conductivity, etc. are substantially less for all times than the previously mentioned prediction capability. Standard deviations of 0.2 to 0.3 μsec may be expected. (See Appendix I.)

In order to relate the Loran-C system to the primary frequency standard it has been proposed that an extremely high quality secondary frequency standard be installed at the Loran-C master station, and that the master transmissions be monitored at Boulder and that corrections be published periodically.

Measurements of Loran-C sky wave signals from the East Coast made in Boulder in 1955 and 1961 (Appendix II) showed that the propagation time can be determined to an absolute accuracy of about 1 μsec with an integration time of less than one minute. The standard deviation of such measurements (daytime) is less than 0.5 μsec. A better receiving antenna has made it possible to use the ground wave signal and achieve a substantially better measurement of the Loran-C master oscillator frequency.

III. Setting a Loran-C Clock

In order to set a slave clock to agree with the master clock it is first necessary to determine the amount by which the apparent time at the slave is slow with respect to the master.

After the signal has reached the antenna, additional time is required for it to pass through the receiver and produce a trigger suitable for starting or synchronizing the clock. This time depends solely on the receiver design. For timing purposes the Loran-C receiver should be designed in such a way that the transmission time through it remains constant over a wide range of environmental conditions.

The apparent time at the receiver is slow by the amount of time required for the signal to propagate from the master transmitter and through the Loran system to the receiver, plus the transmission time through the receiver plus any additional systematic delays such as the coding delay normally used in a Loran system. This is illustrated by the following example:

Given: 1) Receiver 2000 km from slave transmitter.
2) Sea water path.
3) Receiver delay 25.0 μsec.

Propagation time 2000 km sea water	6,675.3
Propagation time Master to Slave	2,711.8
Slave coding delay	12,000.0
Receiver delay	25.0
Total Delay	21,412.1

It is assumed that a pulse is transmitted from the master station precisely at each second. The corresponding pulse from the slave station would produce a time trigger at the receiver output 21,412.1 μsec later. Therefore, the clock at the receiver should read 0.021412 second when this time trigger is used as a read command. The calibration of this clock to read the correct fraction of a second is accomplished by adding counts to the divider chain, and the clock will maintain the same uniform time as the master clock. A one second or one minute output from the clock will occur within 1 μsec of the respective output from any other Loran-C clock in the system.

Fig. 4 is a front view of the developmental model of a Loran-C clock.[8] The panel immediately above the oscilloscope contains a 15-digit visual display covering from 1 μsec to 1000 days. When the clock is given a read command this display reads out the time and holds the reading until the next read command is received.

IV. Slaved Clocks vs Independent Clocks

The comparison of Loran-C clocks (slaved clocks) with independent clocks running from oscillators of different qualities is shown in Fig. 5. This comparison assumes that two independent clocks are drifting apart at a drift rate equal to the maximum rate indicated. The independent clocks must be initially synchronized and must run continuously without interruption. The Loran-C clocks may be interrupted and resynchronized at random without affecting the accuracy.

If a clock operating from the slaved oscillator of a Loran-C receiver is correctly set and if that clock and receiver are moved a distance of 300 meters toward the Loran-C transmitter, the clock will then be 1 μsec fast. Similarly, if the clock is moved 300 meters in the opposite direction it will be 1 μsec slow. In contrast, if the same clock were operating from an independent oscillator it would neither gain nor lose as a result of motion.

If a Loran-C clock is used in a moving vehicle its position must always be taken into account. In either ships or aircraft the fixes available from the Loran-C navigation system can provide the necessary information. However, the computations required to convert the time difference readings to distance from the transmitters are rather involved and may necessitate the use of a separate computer. An independent clock may be more satisfactory than a slaved clock in a moving vehicle if the clock does not have to maintain the correct time for a long period. Even the best clocks (or oscillators) will drift with respect to other clocks. In cases where drifts of the order of a microsecond are important, the slaved clock is a virtual necessity.

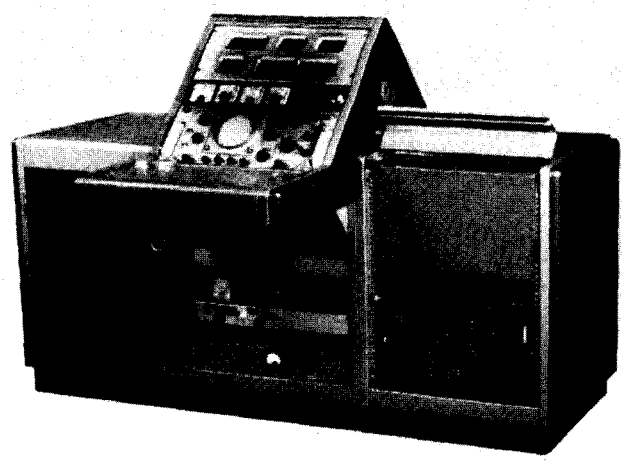

Fig. 4—Loran-C clock.

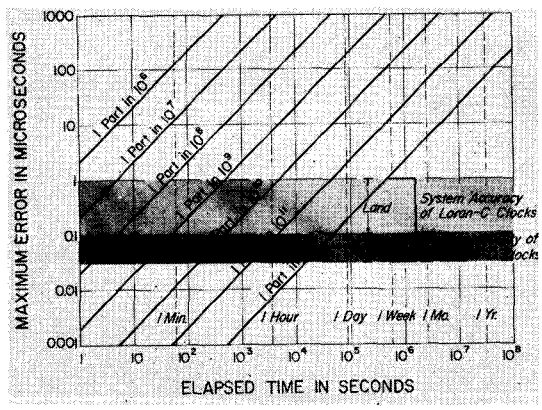

Fig. 5—Comparison of slaved and independent clocks.

As the accuracy of clocks within a timing system is increased, the location of each clock becomes correspondingly more important. Fig. 6 illustrates this simple relationship. The timing precision of Loran-C and WWV are also shown for an integration time of approximately one minute. Much longer integration times would improve the accuracies obtainable with WWV.[7]

V. Missile Range Timing

The National Bureau of Standards demonstrated Loran-C timing potentials on the Atlantic Missile Range in October, 1960. These tests were conducted using two experimental Loran-C clocks and a UHF timing distribution system.[8] The clocks were rather complex devices consisting of modified Loran-C receivers and counting and read-out circuits. The two clocks were synchronized on two separate transmitters and an external read command was used to check any variation

[8] T. L. Davis and R. H. Doherty, "Widely separated clocks with microsecond synchronization and independent distribution systems," IRE Trans. on Space Electronics and Telemetry, vol. SET-6, pp. 138–146; December, 1960.

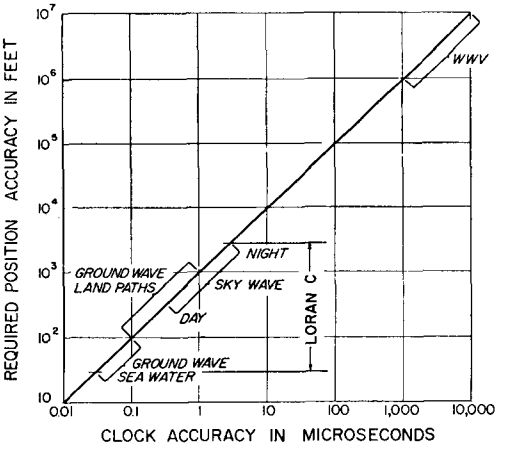

Fig. 6—Time-position accuracy relationship.

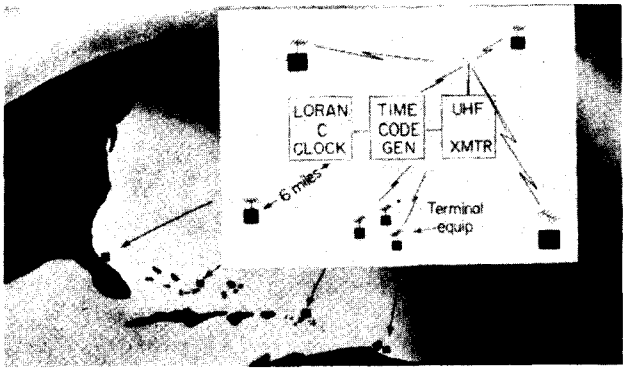

Fig. 7—UHF time distribution system.

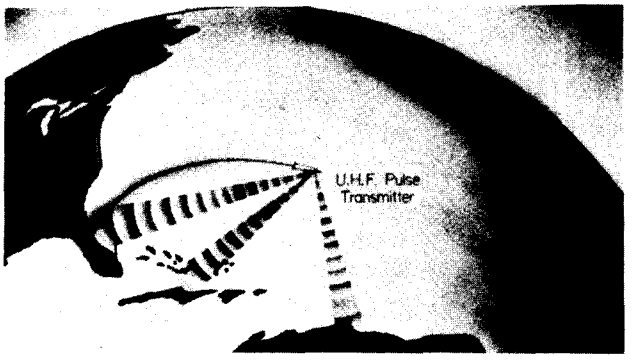

Fig. 8—Trajectory determination by precise timing.

between the clocks. When a large number of equipments requiring time are operated in close proximity, a single clock can serve them all by means of an appropriate UHF timing distribution system.[8] This basic system of time measurement and distribution could be duplicated at any number of locations within the coverage area of a Loran-C chain. See Fig. 7.

Loran-C ground wave coverage extends down range as far as Trinidad. The various down-range sites to that distance can be provided with absolute timing accuracy of approximately 1 μsec. Beyond Trinidad and down to Ascension Island the Loran-C clocks must be synchronized on sky waves. It is important to note that the absolute accuracy involves an allowance for *systematic* propagation errors which cannot be measured independently by any existing system or method. The repeatability of time measurements at any one station, however, will in general be better than 0.1 μsec. In some cases, repeatability may be at least as important as absolute accuracy. For example, the trajectory of a missile or the position of a satellite[9] could be determined by transmitting very short pulses at UHF or microwave frequencies from the missile and recording their time of arrival at a number of time synchronized stations. See Fig. 8. Systematic time errors among the observing stations would result in a corresponding error in the absolute position of the trajectory, but the changes from reading to reading would be influenced only by the stability of the individual clocks and the stability of the propagation medium between the missile and the ground stations.

On the basis of theory[10] and measurements (Appendix II) there is little doubt that Loran-C clocks can be quite accurately synchronized even on second and/or third hop sky waves. Second hop sky wave time differences from the Cytac (Loran-C) transmitters (Forestport, N. Y., Cape Fear, N. C., and Carrabelle, Fla.) were measured at distances up to 5000 km. Standard deviations of these differences were less than 2 μsec day or night. Sunrise and sunset effects corresponding to 18 to 20 km change in ionospheric height were observed. When only the first reflected signal was utilized these sunrise and sunset effects rarely lasted more than 30 minutes. The height variations agree well with other observations for oblique incidence.[11,12] At distances beyond ground wave range there is no satisfactory way to accurately measure sky wave delays. But there is no reason to distrust computed values based on theoretical calculations, former observations and recent electron density rocket information.[10–13] Based on this information, it should be possible to establish time at ranges from 2000 to 8000 km at least within 10 μsec.

The Atlantic and Pacific missile ranges can be linked with a common timing system which will provide 1 μsec accuracy. The link between the two ranges requires the

[9] G. Hefley, R. F. Linfield and R. H. Doherty, "Timing and Space Navigation with an Existing Ground Based System," presented at AGARD 10th General Assembly, Istanbul, Turkey, October, 1960, Pergamon Press Inc., New York, N. Y.; 1961.

[10] J. R. Johler and L. C. Walters, "On the theory of reflection of low and very-low radiofrequency waves from the ionosophere," *J. Res. NBS*, vol. 64D, pp. 269–285; May–June, 1960.

[11] J. R. Wait, "Diurnal change of ionospheric heights deduced from phase velocity measurements at VLF," PROC. IRE (Correspondence), vol. 47, p. 998; May, 1959.

[12] J. M. Watts, "Oblique incidence propagation at 300 kc using pulse techniques," *J. Geophys. Res.*, vol. 57, pp. 487–498; December, 1952.

[13] A. H. Waynick, "The present state of knowledge concerning the lower ionosphere," PROC. IRE, vol. 45, pp. 741–749; June, 1957.

installation of additional Loran-C stations in a generally east-west direction across the Continental U. S. Possible locations for these stations are shown in Fig. 9. Such a configuration would provide inter-range synchronization as well as excellent navigational coverage over the Continental U. S.

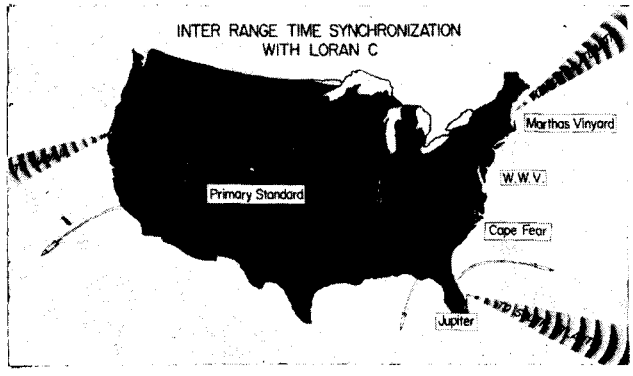

Fig. 9—Possible transmitter locations.

The inter-range synchronization only could be obtained on a very reliable basis by providing a transmitter in Illinois and another transmitter and secondary frequency standard near the West Coast. The western transmitter would be located within ground wave range of Boulder and could be steered by the primary frequency standard. If a number of Loran-C chains were synchronized, one to another, in order to provide coverage over very long ranges, the synchronization accuracy would be degraded to some extent. As far as is known, synchronization errors are of a random nature and therefore can be expected to add as the root-sum-square. For example, if the synchronization error in each transmitter is 0.03 μsec, the accumulated error in synchronizing six stations would be $\sqrt{6(0.03)^2}$ or 0.073 μsec.

The synchronization accuracy of the present Loran-C system could be improved by the use of better oscillators and longer integration times. It is not obvious, however, how much improvement could be achieved before reaching the point of diminishing returns.

The total noise or synchronization errors which can be expected in synchronizing a chain in the Hawaiian Islands from the U. S. should be substantially less than the prediction error in a land or mixed path.

VI. Additional Uses of Precise Time

Some scientific and commercial uses of a precise timing system that may have direct or indirect military applications are:

1) The positioning of high-altitude aircraft from the ground by using the UHF pulse technique.

2) The location of thunderstorms by precisely measuring the location of the lightning discharge.

3) The accurate position-fixing of nuclear detonations by a similar means.

4) A precise evaluation of the fluctuations of the periodicity of the earth's rotation and other astronomical phenomena by relating observations made at widely separated points.

5) The precise measurement of time variations on high-frequency transmissions such as WWV as an aid to better understanding of propagation phenomena.

6) Similar measurements on forward scatter communication links and other types of communication could also be made.

7) The surveying of offshore islands and remote areas.

8) The investigation of Loran-C sky waves to give a better understanding of ionospheric conditions.

9) The precise time from a single Loran-C clock could be made economically feasible for a variety of users in industry and research by the application of a VHF or UHF distribution system. Relatively inexpensive distribution would result if sufficient users were located within range of the distribution system. Existing facilities such as television transmitters could be utilized for this purpose.

Appendix I

Loran-C Ground Wave Measurements

The data presented in this appendix have been abstracted from a report concerned with the position fixing aspects of the Loran-C (formerly Cytac) system.[14]

The data were obtained primarily in the service area (see Fig. 1) during 1954 and 1955. The data are presented in the form of time difference measurements, since the position-fixing information was of prime concern. Although individual propagation paths were not resolved, these measurements were entirely consistent with the individual round-trip paths observed at the transmitters. Since no appreciable differences were detected, the time difference data in the service area were considered to be representative of single path propagation times. Data presented in Appendix II, comparing various sky wave time modes with the ground wave signal, are also consistent with this assumption.

These time-difference (TD) measurements were made in two stages. An envelope measurement was made automatically by subtracting the derivative of the envelope from the envelope and detecting an axis crossing with a servo loop. A cycle measurement was made automatically using synchronous detection techniques and a null seeking servo system. In all cases, the master signal was used to control the reference frequency, and the time differences (X − M and Y − M) were measured with respect to the master. The difference between the envelope TD readings and the cycle TD readings was denoted as the discrepancy. If this discrepancy did not exceed plus or minus 5 μsec, cycle identification was assured by the envelope reading. A typical plot of the cumulative distribution of this reading is illustrated in Fig. 10. Within ground wave recep-

[14] R. F. Linfield, R. H. Doherty, and G. Hefley, "Evaluation of the Propagation Aspects of the Cytac System," private communication; March 18, 1957. (Originally classified confidential.)

tion, the discrepancy was always well within reasonable limits.

The differences between observed and predicted readings were either position dependent or time dependent. The variations related to the position are thought to be caused by an incorrect assumption of the value of the conductivity. Fig. 11 shows a plot of data from locations where the signals arrived over land path. It appears that 0.005 mho/meter is a good average for the M-X pair, but that a higher value of conductivity from the Y transmitter would better approximate the M-Y paths.

The mean of the observed phase readings was compared to predicted phase readings calculated using an assumed conductivity of 0.005 mho/meter for land and 5 mhos/meter for sea water. Differences between the mean and the calculated readings are listed in Table I. Also shown are the distances from the transmitters, the hours of observation, and the standard deviations of the two time differences. The hours of observation were distributed randomly, day or night, throughout the period of operation at each location.

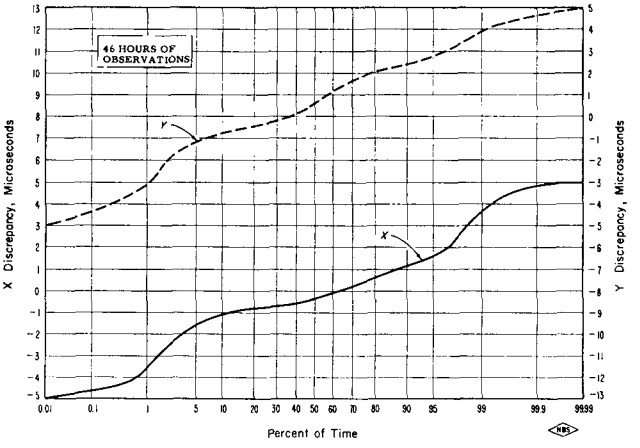

Fig. 10—Cumulative distribution of discrepancy readings—Wisconsin.

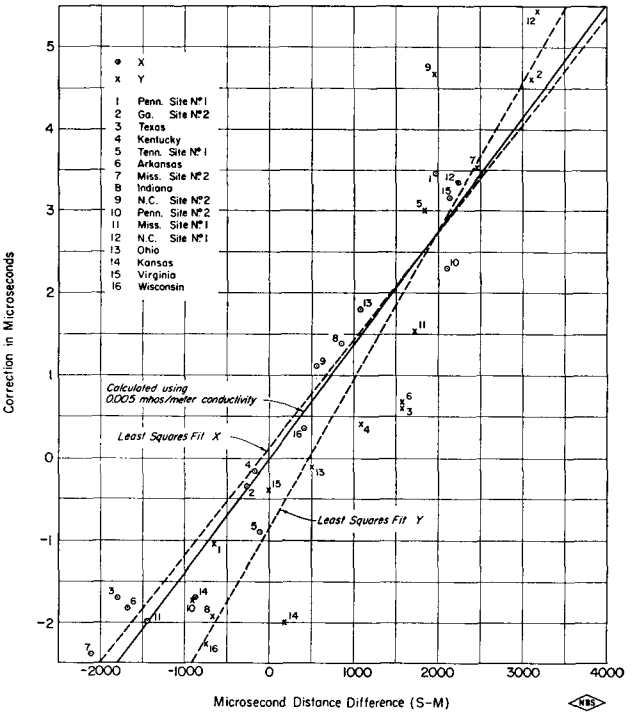

Fig. 11—Comparison of theoretical phase of secondary field difference corrections and measured data.

TABLE I

RESULTS OF CYTAC MONITORING PROGRAM

Receiver Location	Distance to Transmitters km			Total Observations	Days At Site	Mean (all Observations) Minus Predicted (μsec)		Std. Deviation of the Observations	
	M	X	Y	(hours)		M-X	M-Y	M-X	M-Y
Miss.—1	1187	753	1704	800	341	+0.10	−0.47	0.11	0.47
N. C.—1	84	756	1028	750	316	+0.35	+1.01	0.16	0.53
Ohio	670	993	825	200	102	+0.48	−1.20	0.10	0.21
Texas—1	2055	1312	2781	98	64	−1.25		0.15	
Maine	1322	2051	437	92	11		−0.07		0.23
Tenn	663	630	1214	58	5	−0.76	+0.78	0.10	0.24
Missouri	1339	1120	1556	52	5	−0.04	−2.88	0.14	0.25
Penn.—1	666	1252	472	52	3	+1.30	−0.09	0.12	0.05
Indiana	1039	1294	839	51	5	+0.29	−1.04	0.07	0.09
Wisconsin	1324	1430	1101	46	5	−0.13	−1.33	0.11	0.13
Florida	656	401	1717	34	7	−0.51	+0.89	0.16	0.27
Kansas	1939	1696	2010	30	5	−0.60	−2.22	0.17	0.19
N. C.—2	499	670	1084	27	2	+0.54	+2.24	0.05	0.09
Iowa	1573	1469	1542	22	2	+0.28	−1.58	0.11	0.10
Penn.—2	681	1314	409	17	3	−0.15	−0.43	0.09	0.07
Virginia	545	1184	544	16	2	+0.63	−0.33	0.26	0.06
Georgia—1	412	368	1408	16	3	+0.32	+0.14	0.12	0.15
Georgia—2	440	359	1371	14	2	−0.05	+0.38	0.11	0.07
Florida—2	816	37	1754	9	1	−0.01	+0.65	0.06	0.17
Louisiana	1414	780	2063	9	2	−0.81	−1.59	0.05	0.23
Arkansas	1519	1015	1990	8	2	+0.48	−1.37	0.04	0.22
Florida—3	1118	655	2182	8	2	−0.03	−0.03	0.08	0.12
Miss.—2	1079	449	1818	8	2	+0.43	+0.07	0.10	0.18
Florida—4	927	454	1983	7	2	+0.02	+0.02	0.06	0.10
Texas—2	1669	1133	2141	7	1	+0.80	−1.19	0.03	0.16

The standard deviation of the mean minus the predicted values listed in Table I for the M-X pair is 0.5 μsec, the mean deviation is 0.43 μsec and the algebraic average is +0.06 μsec. For the M-Y pair the standard deviation is 1.17 μsec, the mean deviation is 0.92 μsec, and the algebraic average is −0.41 μsec. The Millington[15] method for combining conductivities was used for evaluating predictions for 13 sites, but this did not appreciably improve the standard deviations. However, the only conductivity values[16] that were available were measured at broadcast frequencies and over limited areas and are, therefore, not considered applicable at 100 kc. By assuming conductivities for the Y path ranging from 0.004 to 0.008 mho/meter, the standard deviation of the mean-predicted values for the M-Y pair was reduced to 0.69 μsec, and the average error was reduced to 0.51 μsec. Even though the two paths (receiver to M and receiver to X or Y) cannot be separated this method could provide a means for empirically evaluating conductivity at 100 kc in areas where Loran-C measurements are available.

Figs. 12–16 present cumulative distributions of the time difference readings taken at 2.5 minute intervals for sites where the total observation time was limited. Figs. 17–20 present cumulative distributions of the daily average readings for sites where observations were made for several months.

From these figures it can be seen that variations were within 1 μsec during a very high percentage of the time. It may be noted that the M-Y (northern) pair generally had greater deviations than the M-X (southern) pair. This is also quite obvious from Figs. 21–24 where the daily averages are plotted for the fixed sites. Figs. 25 and 26 indicate some typical diurnal variations on the M-X and M-Y pairs. Again it can be seen that the M-Y variations were greater than the M-X variations.

The reason for the larger time variation associated with the northern path was never completely resolved although many contributing factors can be listed. Errors of this magnitude do not exist on the northern pair of the present east-coast Loran-C system.

Most of the data presented here were obtained from signals that were not phase coded. Multihop sky wave contamination was not eliminated and could contribute toward time variations (see Fig. 27). During the first few months of operation some variations were probably due to inexperience of operating personnel.

The operation was not continuous and evidently instabilities accompanied shut down periods. Fig. 28 shows such changes recorded at four stations when the operating periods were compressed into a single plot. Correlation coefficients were calculated using simultaneous data from these four sites. The correlation coefficients are shown in Table II.

In a further investigation, the variations were divided into two categories or components: 1) purely random variations and 2) variations which would produce correlation at the observation points. Since servos in the different pieces of equipment were not adjusted to have identical damping characteristics, the data were normalized to the average characteristics of the four equipments. The results indicated in Table III demonstrate that the maximum variations that could positively be attributed to propagation did not exceed 0.03 to 0.04 μsec.

Although the time fluctuations have sometimes been shown to correlate with weather phenomena, particularly temperature, it has not been conclusively established that the variations were not partially within the antenna system. The typical Loran-C installation includes a 600-foot top loaded transmitting antenna, and a 30- to 90-foot receiving whip within a few hundred meters of the transmitting antenna. Impedance changes of the transmitting antenna would affect the phase characteristics of the receiving antenna. An attempt to check this effect was made by using a receiver on the base-line extension. Any effect due to the antenna impedance change was evidently masked by larger variations.

The large time variations on the northern pair (M and Y) were probably the result of a combination of multihop sky wave contamination, and the first-hop sky wave contamination. The first-hop contamination could occur if the signal were sampled too late, that is, after the first-hop sky wave had started to arrive. The base-line path of the northern pair during the Cytac tests was quite long (over 1000 km); it was all over land (causing maximum delay of the ground wave), and it was at a high geomagnetic latitude.

A subsequent Loran-C chain located in the arctic (high geomagnetic latitude) has encountered trouble with very short first-hop sky wave delays because of the lower ionospheric heights at these latitudes. This situation was encountered even though the base lines were over sea water.

The Loran-C chain located on the East Coast of the United States has been relocated since 1955. The northern base line is now partially over sea water and the northern station is at a slightly lower geomagnetic latitude. With continuous operation and the new locations, the variations have been reduced by an order of magnitude.

Amplitudes of the ground wave signal out to ranges as great as 3700 km are shown in Fig. 29. The paths that the signals traversed were partially land, but primarily sea water. The agreement between predicted and measured values is fairly good in the range of 2400 to 3700 km. The deviation from the predictions at ranges less than 2400 km is greater than can be explained by experimental error.

[15] G. Millington, "Ground wave propagation over an inhomogeneous smooth earth," *Proc. IEE*, vol. 96, pt. III, pp. 53–64; January, 1949.

[16] R. S. Kirby, *et al.*, "Effective Radio Ground Conductivity Measurements in the United States," Natl. Bureau of Standards, Boulder, Colo., NBS Circular No. 546; February, 1954.

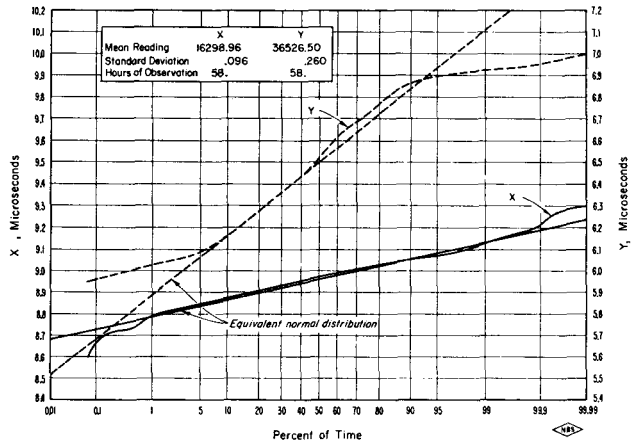

Fig. 12—Cumulative distribution of time difference readings—Tennessee Site 1 (2.5 minute intervals).

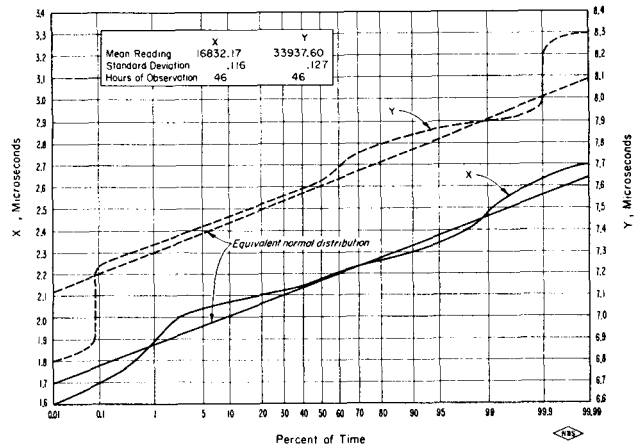

Fig. 13—Cumulative distribution of time difference readings—Wisconsin (2.5 minute intervals).

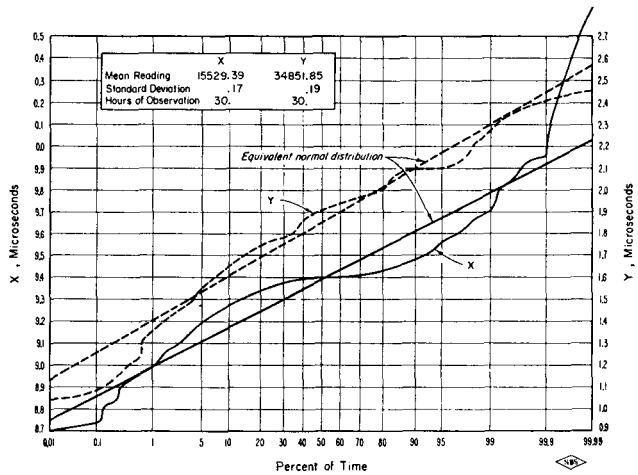

Fig. 14—Cumulative distribution of time difference readings—Kansas (2.5 minute intervals).

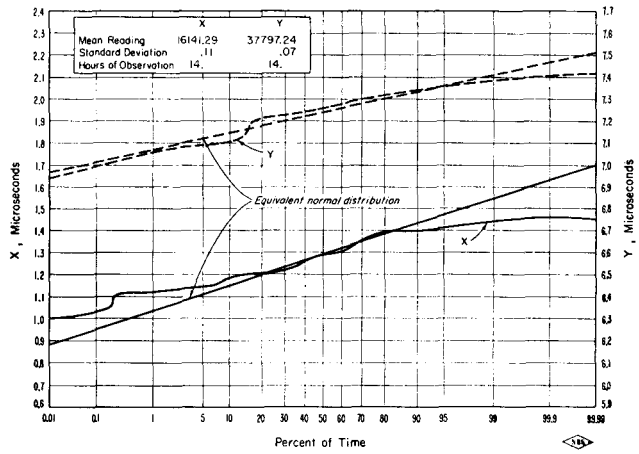

Fig. 15—Cumulative distribution of time difference readings—Georgia Site (2.5 minute intervals).

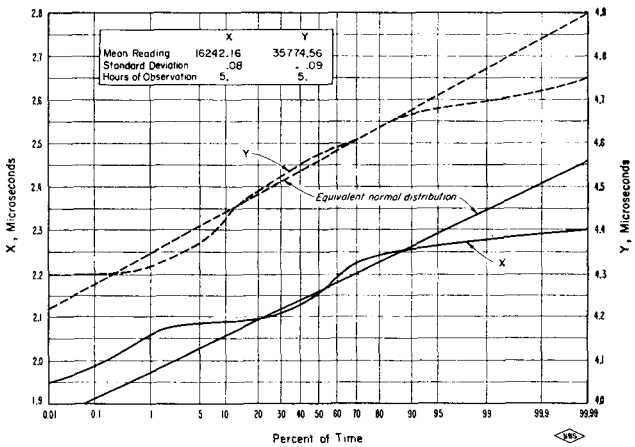

Fig. 16—Cumulative distribution of time difference readings—Kentucky (2.5 minute intervals).

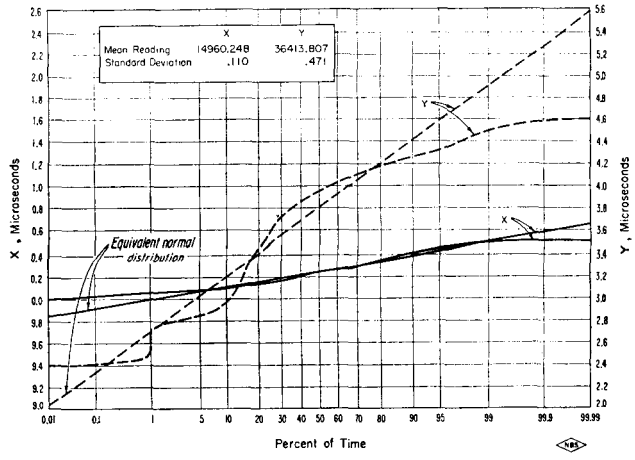

Fig. 17—Cumulative distribution of daily averages —Mississippi Site 1 (November 1954–1955).

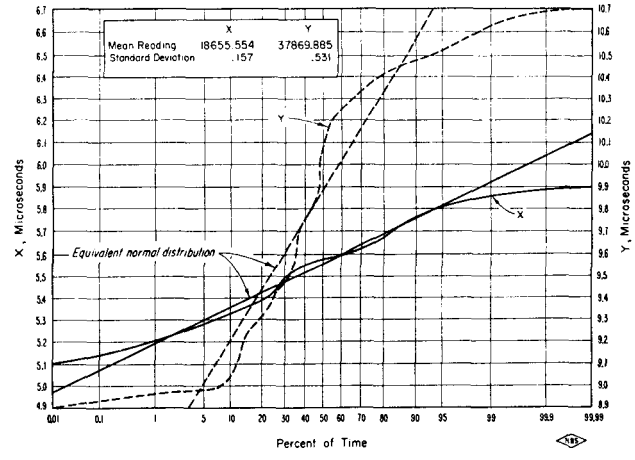

Fig. 18—Cumulative distribution of daily averages —North Carolina Site (January–October 1955).

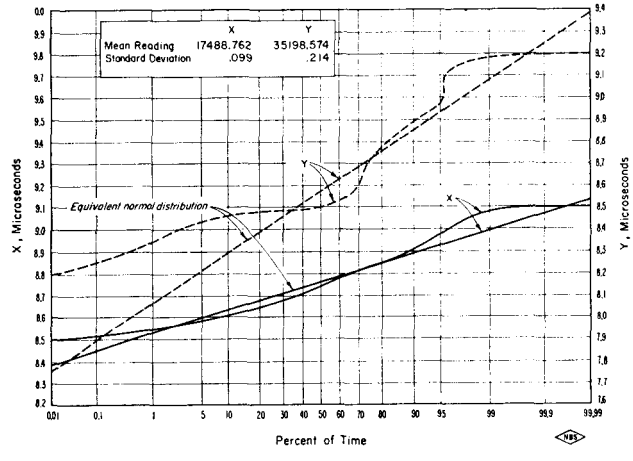

Fig. 19—Cumulative distribution of daily averages —Ohio (January–February 1955).

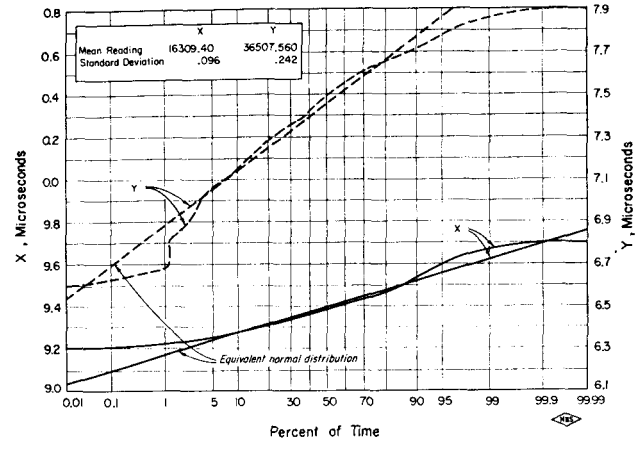

Fig. 20—Cumulative distribution of daily average —Tennessee Site 1 (March–November 1955).

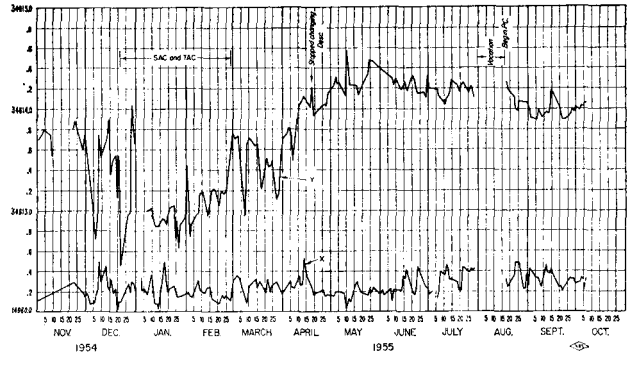

Fig. 21—Daily average X and Y cycle readings—Mississippi Site 1.

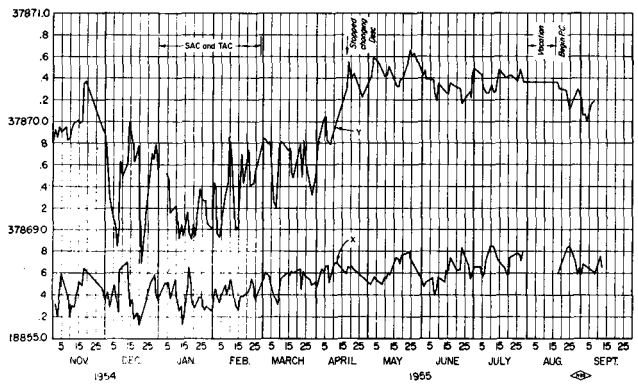

Fig. 22—Daily average X and Y cycle readings —North Carolina Site 1.

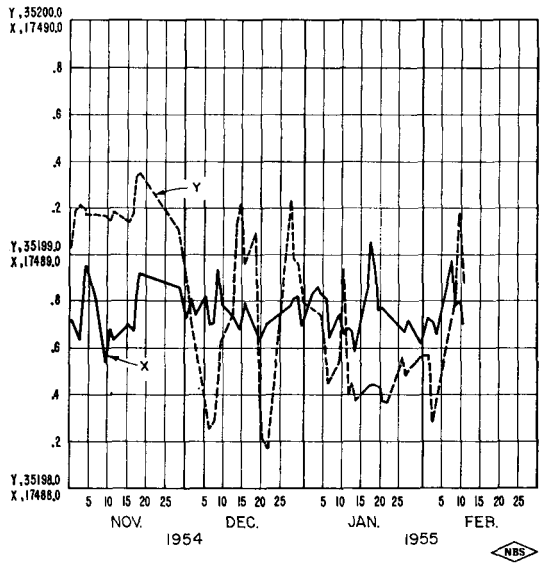

Fig. 23—Daily average X and Y cycle readings—Ohio.

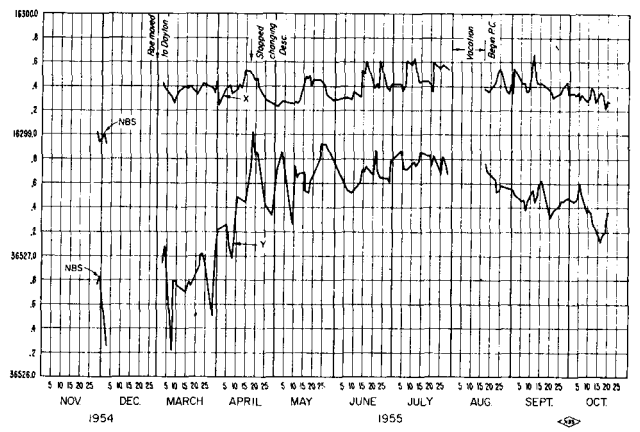

Fig. 24—Daily average X and Y cycle readings—Tennessee Site 1.

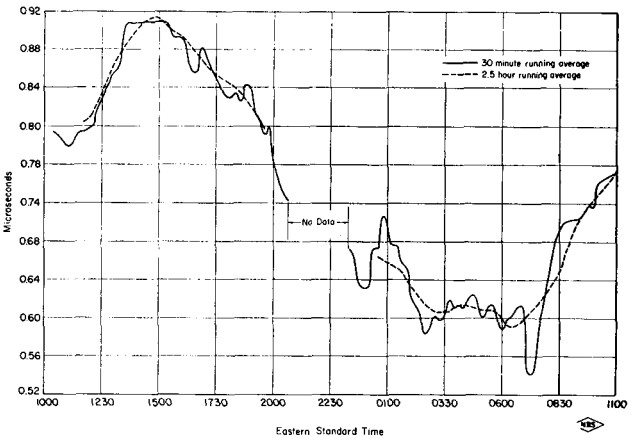

Fig. 25—Running average of Y time difference—North Carolina Site 1 (November 30–December 1, 1954).

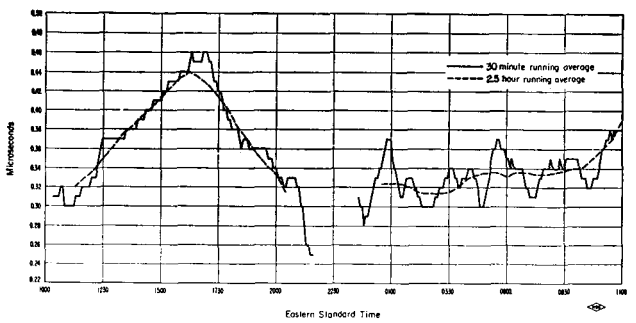

Fig. 26—Running average of X time difference—North Carolina Site 1 (November 30–December 1, 1954).

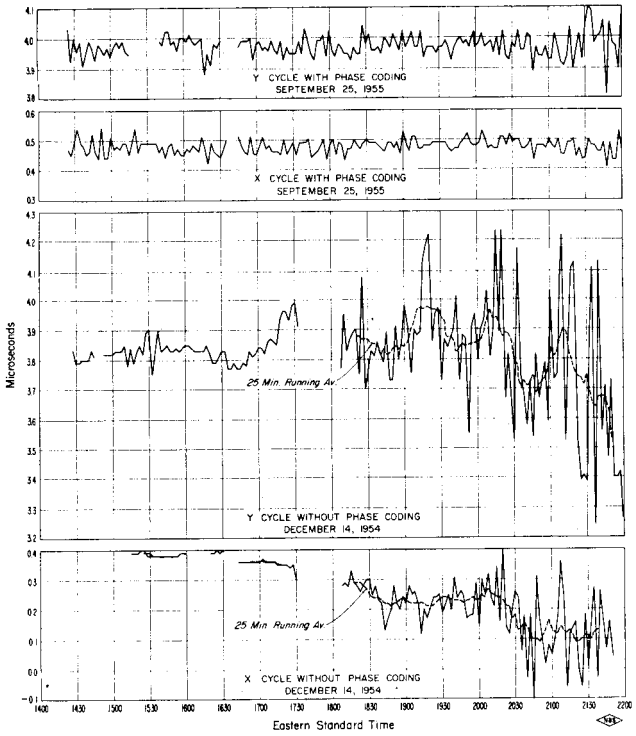

Fig. 27—Cycle readings with and without phase coding—Mississippi Site 1.

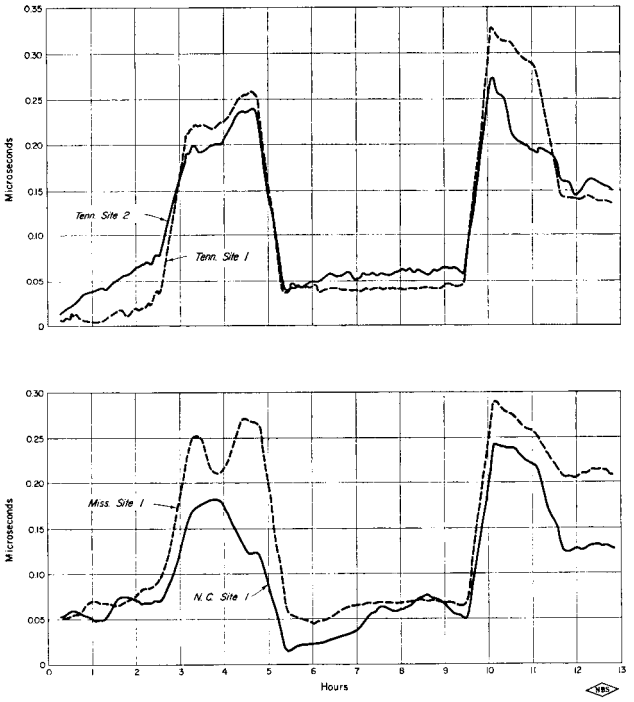

Fig. 28—37.5 minute running averages of X readings (13.1 hours of data, September 1–13, 1955).

TABLE II

CORRELATION OF S_1 PAIR

	Tenn. Site 1	Tenn. Site 2	Miss. Site 1	N. C. Site 1
Tenn. Site 1		0.930	0.934	0.901
Tenn. Site 2	0.930		0.934	0.855
Miss. Site 1	0.934	0.934		0.870
N. C. Site 1	0.901	0.855	0.870	

CORRELATION OF S_2 PAIR

Tenn. Site 1		0.526	0.658	0.620
Tenn. Site 2	0.526		0.543	0.442
Miss. Site 1	0.648	0.543		0.669
N. C. Site 1	0.620	0.442	0.669	

TABLE III

	Measured	Normalized	Noise Component	Synchronous Component
		S_1 PAIR		
Tenn. Site 1	0.107	0.077	0.011	0.076
Tenn. Site 2	0.081	0.081	0.009	0.076
Miss. Site 1	0.092	0.081	0.003	0.076
N. C. Site 1	0.068	0.082	0.032	0.076
		S_2 PAIR		
Tenn. Site 1	0.057	0.038	0.024	0.029
Tenn. Site 2	0.043	0.043	0.032	0.029
Miss. Site 1	0.043	0.035	0.019	0.029
N. C. Site 1	0.105	0.037	0.022	0.029

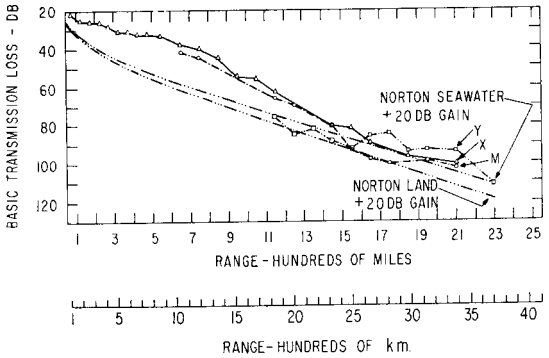

Fig. 29—Predicted and measured ground wave signal amplitude.

463-560 O - 72 - 20

APPENDIX II

LORAN-C SKY WAVE MEASUREMENTS

Loran-C is a pulse navigation system utilizing sampling techniques to select the ground wave and discriminate against the sky wave signal. These same sampling techniques can be utilized to select one sky wave signal and discriminate against all other sky wave signals at ranges beyond ground wave reception. This provides a means for measuring the phase and amplitude of a particular sky wave time mode rather than a composite signal as is done in CW measurements. Many measurements that have been made with Loran-C indicate that the phase of a particular time mode is very stable, but the amplitude of that time mode is quite unstable. Furthermore, the variations occurring on one time mode do not necessarily correlate with variations occurring on another time mode.

If a number of vectors of different fixed phases but of variable amplitudes are added together, the phase of the resultant will change as a result of the amplitude variations. Similarly, the phase of a CW signal varies in accordance with the amplitudes of the different time modes. Consequently, the phase variations do not necessarily indicate phase changes in the individual time modes nor changes in ionospheric height.

At ranges beyond ground wave reception the first signal arriving via the ionosphere was normally observed. At shorter ranges uncontaminated higher order multihop sky wave signals were observed. Sky wave signals have been observed at distances as great as 12,000 km (Johannesburg, S. A. from Jupiter, Fla.). A large number of measurements listed in Table IV have been made between 3000 and 5000 km. Multihop measurements listed in Table V have been made at ranges as short as 500 km.

Figs. 30–31 illustrate typical daytime first-hop sky waves observed at Boulder, Colo. (about 3000 km from the transmitters). All of the data available suggest an excellent sky wave phase stability when a single propagation mode is studied. The Boulder data recorded over a period of more than one month had short term variations of only 0.25 μsec and day to day variations of only 0.5 μsec. This data was obtained by comparing a first-hop sky wave from one transmitter with the ground wave from another (southern pair). Nighttime measurements were not made in 1955 because the transmitters did not operate on a 24-hour basis during September and October. Similar measurements made at Boulder in 1961 indicate nighttime stabilities to be at least within 5 μsec (see Fig. 32).

TABLE IV

Mode	Distance (Kilometers)	Time (Day or Night)	Delay (μsec)	σ Standard Deviation (μsec)
BELIZE, BRITISH HONDURAS				
X Gnd. Y Gnd.	1425 3133	D	− 0.4	0.944
X Gnd. Y 1st	1425 3133	D	+ 29.9	1.012
X Gnd. Y 1st	1425 3133	N	+ 43.1	1.219
X Gnd. Y 3rd	1425 3133	D	+102.8	0.541
X Gnd. Y 2nd	1425 3133	N	+103.9	1.460
X Gnd. Y 4th	1425 3133	N	+267.7	0.904
KINGSTON, JAMAICA				
M Gnd. X Gnd.	1786 1539	D	− 0.7	0.551
X Gnd. Y Gnd.	1539 3829	N	+ 0.3	0.366
M Gnd. Y Gnd.	1786 3829	D	+ 1.0	0.356
PUERTO CABEZAS, NICARAGUA				
X Gnd. Y Gnd.	1763 3356	D	− 2.21	1.235
X Gnd. Y 1st	1763 3356	D	+ 30.0	1.436
X Gnd. Y 1st	1763 3356	N	+ 49.7	1.234
X Gnd. Y 3rd	1763 3356	D	+211.4	1.018
M Gnd. X Gnd.	2286 1763	N	− 1.9	0.255
BUENAVENTURA, COLOMBIA				
M Gnd. X Gnd.	3339 2983	D	− 2.64	0.590
M 1st X 1st	3339 2983	N	− 2.06	0.415
M 1st Y 1st	3339 4385	N	+ 0.0	0.936
M Gnd. Y 2nd	3339 4385	D	+ 37.5	1.864
M Gnd. Y 3rd	3339 4385	D	+105.3	0.909
X 1st Y 4th	2983 4385	D	+222.7	1.309
X Gnd. Y 4th	2983 4385	D	+235.9	1.015
GUAYAQUIL, EDUADOR				
M 1st X 1st	4024 3574	N	− 1.98	0.299
M 1st Y 2nd	4024 5086	N	+ 56.6	0.527
M 1st X 1st	4024 3574	D	− 0.50	1.812

TABLE V

Distance Kilometers	Transmitter	Total Delay (μsec)	Amplitude (in μv/m)	Most Probable Hop	Corresponding Layer Height km
WOODSTOCK, KENTUCKY					
817	X	304	9.6	3rd	65.0
817		Nothing could be observed for 4th			
817	X	784	10.3	5th	65.5
817	X	1024	10.8	6th	63.6
1051	Y	285	19.2	3rd	69.5
1051	Y	505	14.4	4th	71.8
1051	Y	753	11.2	5th	71.7
1051	Y	993	9.6	6th	69.6
SPRING CREEK, NORTH CAROLINA					
496	M	815	24.4	4th	68.0
496	M	1050	20.0	5th	64.0
676	X	454	—	3rd	74.2
676	X	752	13.2	4th	74.0
1078	Y	1083	—	6th	74.0
BOULDER, COLORADO					
2526	Y	32	—	1st	*
2526	Y	448	—	5th	78.8
2526	Y	618	—	6th	78.3
2518	Y	34	—	1st	*
2518	Y	298	2.0	4th	77.4
2518	Y	440	—	5th	77.5
2510	M	34	—	1st	*

* Since the apparent heights are obtained from a graph based on geometrical-optical considerations, and the distance for first-hop sky wave is far beyond that obtainable by geometrical-optical theory, any apparent heights assigned to these first-hop reflections would be completely meaningless.

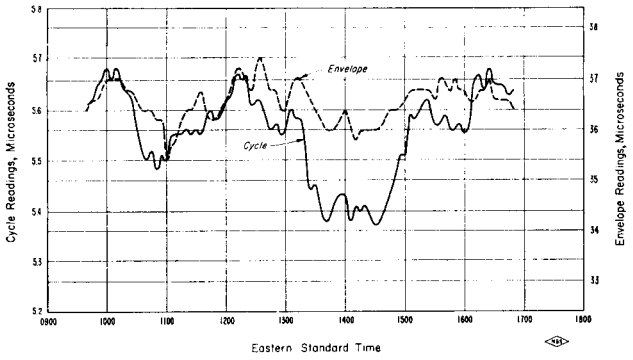

Fig. 30—Envelope and cycle readings, first-hop sky wave—Boulder, Colo. (September 13, 1955).

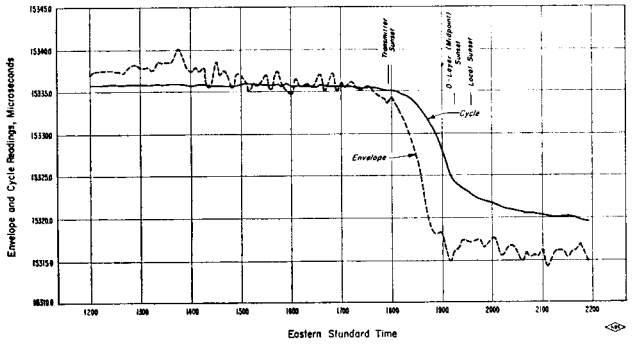

Fig. 31—First-hop sky wave measurements—Boulder, Colo. (October 6, 1955).

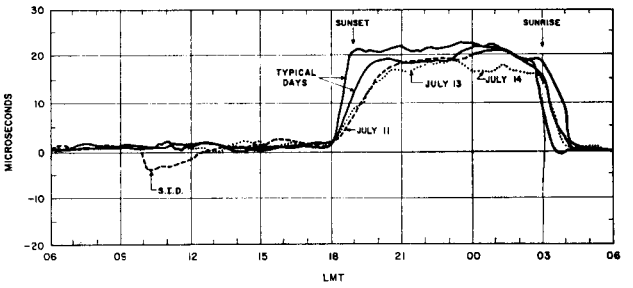

Fig. 32—First-hop sky wave from Cape Fear, N. C.—Boulder, Colo. (1961). Approximately 3000 km.

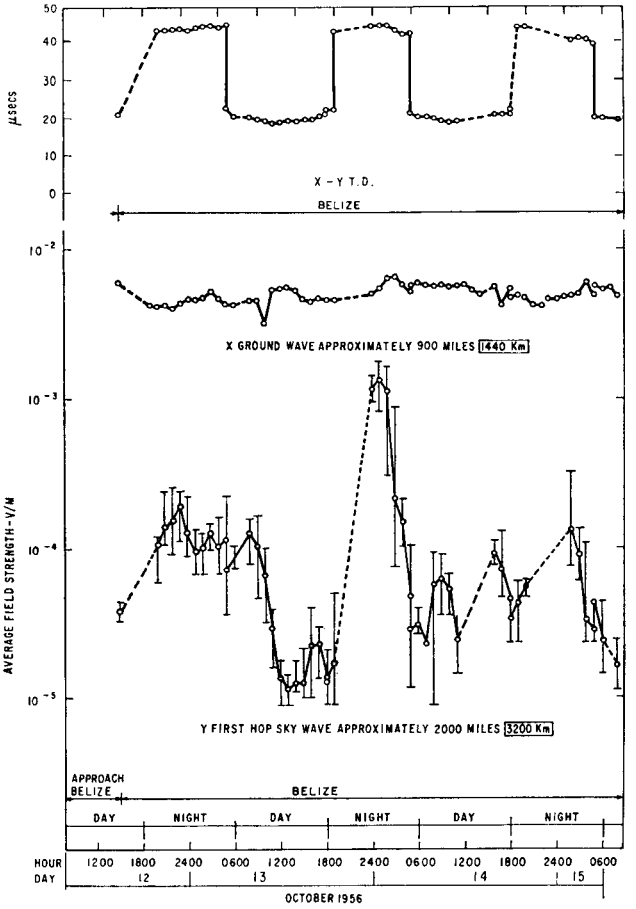

Fig. 33—Phase and amplitude of Loran-C sky wave referred to ground wave.

The standard deviations listed in Table IV were typical of observations for an entire day or night made in Central and South America in 1956. These standard deviations again suggest excellent stability of the sky wave phase. The delays listed are delays as compared to the predicted arrival time of the ground wave signal. These delays seem to be quite reasonable for the propagation mode being measured. Fig. 32 illustrates the phase change resulting from an S.I.D. occurring on July 11, 1961. The event was rated at about $3\frac{1}{2}$ on a scale of 4. VLF records indicated a change of up to 30 μsec. This first-hop sky wave signal showed a total phase change of 4.5 μsec. This phase decrease was accompanied by an amplitude increase of more than 12 db. The slower sunset effect seems to be related to the flare and the magnetic storm that followed the event. On July 13th and 14th (dotted curves) a magnetic storm occurred that disturbed the phase of VLF CW measurements.

Fig. 33 presents a three-day plot of both the phase and amplitude of a first-hop sky wave signal, the upper plot representing the T.D. between a first-hop sky wave signal from 3200 km and the ground wave signal from 1440 km. Again rather good phase stability is suggested. The lower plots are the measured amplitudes of the two signals. The amplitude of the sky wave signal is quite variable and not obviously correlated with any phase changes.

The amplitudes of the various time modes present vary relative to one another, often quite rapidly. Fig. 34 illustrates several time modes of the Loran-C master pulses observed at Boulder. The relative amplitudes of the several time modes obviously do not correlate. A CW measurement made at this frequency would show phase changes due to these relative amplitude changes alone.

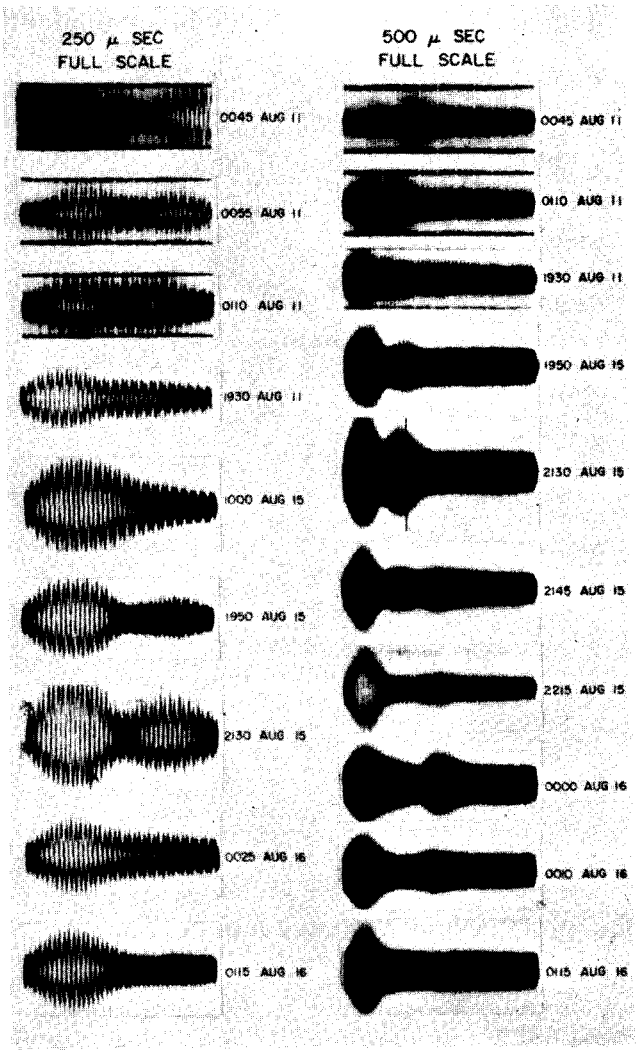

Fig. 34—Multihop sky waves master signal observed at Boulder, Colo.

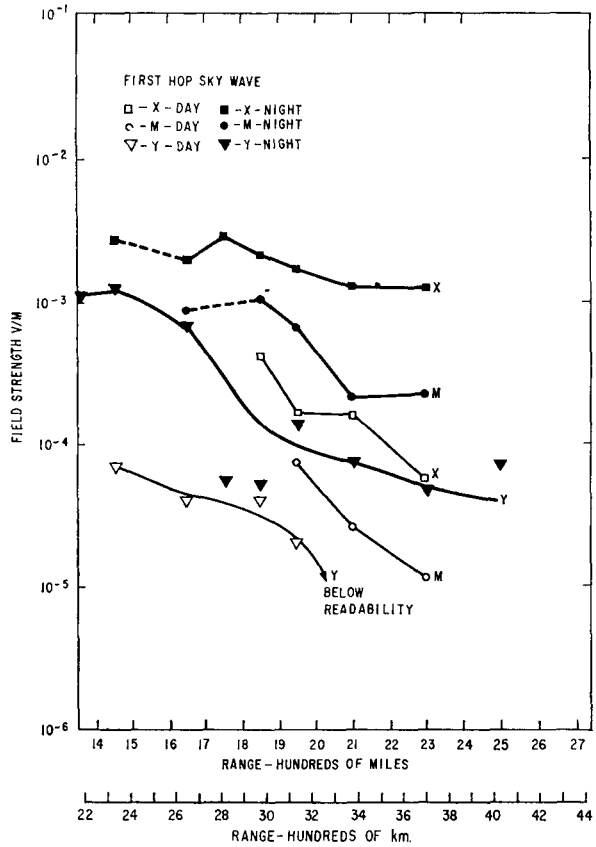

Fig. 35—Field strength of Loran-C sky wave on north-south paths.

Fig. 35 represents average amplitudes observed on a predominantly north-south path. Since these plots are strictly amplitude versus distance and the Y transmitter was about 15° farther north than the X transmitter, a strong latitude effect on signals propagated by the ionosphere is suggested. The average nighttime sky wave field intensity was about 20 db larger than the average daytime field intensity.

Table V presents other interesting observations made at relatively short ranges. It was noted that high-order multihop sky waves were present at most locations. It was further noted as can be seen from the tabulations that often the amplitude of the nth hop would be as great as or greater than the amplitude of the nth-1 hop. Assumptions made as to predominant time modes or negligible time modes for CW measurements may be somewhat questionable in view of these observations.

VII. Acknowledgment

Special acknowledgment is given to P. J. Kiser, of the Air Force Eastern GEEIA Region, for his engineering contributions to the Loran-C clock and his assistance in the preparation of this paper.

The entire Loran-C clock and UHF distribution system has been developed by the National Bureau of Standards, Boulder Laboratories under the sponsorship of Headquarters, Eastern GEEIA Region.

JOURNAL OF RESEARCH of the National Bureau of Standards—D. Radio Propagation
Vol. 65D, No. 6, November–December 1961

Worldwide VLF Standard Frequency and Time Signal Broadcasting

A. D. Watt,[1] R. W. Plush,[1] W. W. Brown, and A. H. Morgan

Contribution From the Boulder Laboratories, National Bureau of Standards, Boulder, Colo.

(Received June 15, 1961)

Recent studies and measurements have shown that the phase stability of the signals in the VLF region is very much higher than in the HF spectrum. This fact, along with its excellent coverage characteristics, has caused considerable interest in employing this medium for the wide distribution of standard frequencies and time reference. Basic limitations in stability of the received signals are discussed, including path phase distortion, carrier-to-noise and envelope delay variations as related to precise synchronization of clocks, and highly accurate frequency calibrations.

Also included is a discussion of the present services of standard frequency and time signal stations throughout the world at HF, LF, and VLF.

1. Introduction

The requirement for better standards for precise measurements of frequency and time which are readily available has constantly increased with advances in various fields of science. The scientific unit of time is determined astronomically, and is determined to an uncertainty of a few parts in 10^9 in the course of a year. Since frequency is related inversely to time interval, this uncertainty, strictly speaking, must be transferred to the specification of absolute frequency. Frequency generators, however, stable to parts in 10^{10} or 10^{11} now exist, and form the basis for relative measurements of frequency which for many purposes satisfy the increased requirements mentioned above.

The history of the development of our present system of time is an extremely fascinating subject and it is interesting to note Newton's definition of time, "Absolute, true and mathematical time, of itself, and by its own nature, flows uniformly on, without regard to anything external," [Mach, 1942]. Most of man's time systems have been based on an attempt to find a reference which "flows uniformly on." The very great influence upon our lives and surroundings caused by the revolution of the earth around the sun and the rotation of the earth on its axis has resulted in various definitions [2] of time in terms of years (orbital rotation), days (axial rotation), and subdivision of these units in hours, minutes, and seconds. Time based on apparent solar days (from noon to noon) although apparently satisfactory as a time reference for many applications was shown by astronomical observations to have appreciable nonuniformity.

Since apparent solar days are variable in length with season, mean solar time was devised and the tabulation of this difference between the apparent value and the mean value is called the equation of time. This difference has a maximum value a little in excess of 16 min. Apparent solar days are variable in length with season for two reasons: partly because of the variation in the angular velocity of the sun along the ecliptic in accordance with Kepler's second law of planetary motion, and partly because the inclination of the ecliptic to the celestial equator introduces a variation in the rate at which the projected coordinate of the apparent sun moves along the celestial equator. The mean sun is a fictitious body which moves along the celestial equator at a uniform rate equal to the mean rate of the apparent sun. Because of the fact that a solar time reference (date and time of day, etc.) will depend upon the observer's position, Universal Time (also known as Greenwich mean time) was established with the mean solar time reference based on the prime meridian at Greenwich, England. The problem of relative position for civil purposes has been solved by dividing the earth into various time zones usually differing by one hour with lines of demarcation chosen to minimize the inconvenience caused by crossing time zones in heavily populated areas.

Three kinds of Universal Times are: UT0, which is uncorrected mean solar time; UT1, is Universal Time corrected for observed polar motion and represents the true angular rotation of the earth about its axis;[3] UT2, is Universal Time corrected for both observed polar motion and seasonal variation in speed of rotation of the earth on an extrapolated basis.

The fundamental unit of time was until very recently the mean solar second which was defined as $\frac{1}{86{,}400}$ of a mean solar day. This fundamental unit

[1] Present address of A. D. Watt and R. W. Plush: DECO Electronics, Inc., Boulder Division, 8401 Baseline Road, Boulder, Colo.

[2] An interesting and useful description of time and time signals is contained in "United States Naval Observatory Circular No. 49," published by the U.S. Naval Observatory, Washington 25, D.C. (March 8, 1954). See also "Astronomical Time," G. M. Clemence, Rev. Mod. Phys. 29, 1 (January 1957) and "The Way Things Are," P. W. Bridgman, pp. 135–141 (Harvard University Press, Cambridge, Mass., 1959).

[3] Because of the increased precision with which the earth's rotation can be measured with respect to a reference star rather than the sun, the period of the earth's rotation with respect to the vernal equinox, called a sidereal day, is used for precise determination of the earth's rotation.

of time based upon the mean solar day appeared to be entirely satisfactory until astronomical observations and advances in the fields of communication, electronic frequency standards, and precision instrumentation showed that in fact the earth was not rotating in a strictly constant manner. Even after the corrections of UT1 and UT2, time based on this reference did not flow on uniformly as our definition of it would require. A more uniform astronomical time based on the yearly motion of the earth about the sun, called Ephemeris Time, has long been known. The present definition of the second is $\frac{1}{31,556,925.9747}$ of the tropical year for January 0, 1900 at 12 hr Ephemeris Time [Markowitz, 1959]. This was adopted by the International Committee of Weights and Measures in 1956 and ratified by the 11th General Conference on Weights and Measures in 1960. Discussion of various astronomical and atomic times has been given by Markowitz [1959].

Although quartz crystal clocks were instrumental in revealing many of the variations in rotation of the earth, it was not until atomic standards were placed in use that a new reference of time became conceivable. The use of molecular and atomic spectral lines as frequency standards [Lyons, 1952] has led to the speculation that perhaps here we have a reference which can be made highly independent of external variable influences and as a result may produce a time base of greatly improved uniformity and convenience. The difficulty of keeping molecular and atomic clocks in operation for long periods of time has up until recently prevented their use as a basic time reference. A determination of the atomic transition frequency of cesium in terms of Ephemeris Time by Markowitz, Hall, Essen, and Parry [1958] indicated a value of 9,192,631,770 ± 20 c/s which is the best value available at present. The deceleration in the rotation of the earth about its axis as determined by the cesium standard is in the order of 1.16×10^{-5} radians/year^2, i.e., 0.16 seconds/year^2 [4], which is in good agreement with values obtained by the moon camera of 0.17 seconds/year^2 for that period (June 1955 to June 1958). It is possible [Bullard, 1955] that Ephemeris Time and Atomic Time may not have the same rates; however, further careful experiments will be required to determine this. The stability of the best long time interval bases, which at present are quartz clocks steered by atomic standards is limited to values in the order of one part in 10^{10}. Frequency comparisons quoted to higher precisions are relative, and may be made in two ways. One is to intercompare two oscillators directly for the short term, and the other is to compare one with the mean of a group of three or more of the same quality and assume that their variations are independent, so obtaining a statistical increase in precision for the group. The resonance of cesium is known in terms of the Ephemeris Second to an accuracy of only about 2 parts in 10^9, the limitation being set by the uncertainty in the determination of the Ephemeris Second. Thus, high quality clocks closely steered by atomic standards will not realize the presently defined unit of time with any greater accuracy than this because of the nature of the definition itself. Presently, maximum available relative frequency stabilities for periods of several hours are in the order of: 1 part in 10^{11} for Crystal standards and 1 part in 10^{12} for the Ammonia Maser.

[4] This means that if an atomic clock and "earth" clock were started together, at the end of a year the "earth" clock would be 0.08 sec behind the atomic clock.

2. Basic Limitations of Precision in the Frequency and Time Standards Via Radio Signals

With the availability of very stable time references and frequency standards, it is obvious that considerable care must be exercised if these standards are to be distributed over large areas of the world without appreciable deterioration. If the terrestrial propagation of radio wave energy was at a constant velocity equal to the velocity of light in a vacuum and with a noise free background, it would be a relatively simple matter to distribute frequency and time signals with essentially no loss in stability and accuracy. Under these conditions, the received frequency would be unaffected and the time signals would have a given correctable constant delay of $T'_d=d/v_0$ where: d is the distance and v_0 is the velocity of light $\simeq3\times10^5$ km/s. In practice the radio energy is transmitted along a path with an effective velocity (v) which varies with the characteristics of and conditions along the transmission path so that the actual delay, T_d, may vary also. It is obvious that the time indicated at a given receiving site is $T_r=T_t+T_d$, where the receiving clock can be made to indicate transmitted time T_t by subtracting T_d from the received time T_r during clock setting. At the high frequencies, 2.5 to 30 Mc/s, presently employed for the distribution of frequency and time signals, multiple propagation paths frequently exist with appreciably different delays which can introduce large apparent errors in the received frequency and time. For any given path it may be possible by the proper choice of frequencies to have essentially one dominant mode of propagation; however, even a single mode may have appreciable variations in transmission time.

2.1. Phase Distortion Limitations

In figure 1 the straight dashed line represents the distortionless transmission in free space where the phase delay in radians could be given as

$$\phi'=\frac{2\pi fd}{v_0} \tag{1}$$

where: f is the frequency in cycles per second, and d is the path length expressed in kilometers.

The actual propagation medium, assuming one mode of multiple path to be dominant, may be considered as an electrical network with phase and amplitude versus frequency characteristics which vary as a function of time. The actual time

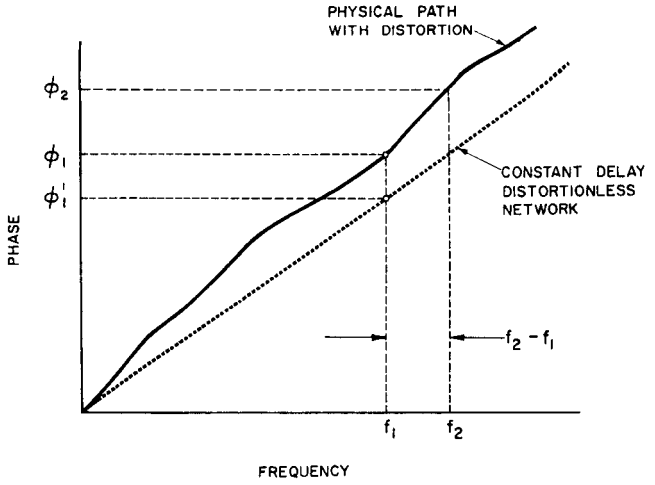

FIGURE 1. *Transmission path phase characteristics.*

delay is

$$T_d = d/v_p \tag{2}$$

where v_p is the average path phase velocity in kilometers per second. It is well known in electrical circuit theory that various types of network delays exist, and if we are to consider the phase delay defined in eq (1), v must be expressed in terms of path phase velocity rather than envelope velocity.

The actual path phase velocity relative to the velocity of light, v_p/v_0, is known to be a function of frequency and the path involved. Important factors may include ionospheric conditions, ground conductivity, and surface roughness. In the VLF region, Jean, Taylor, and Wait [1960] have shown good agreement between experimentally and theoretically determined values of v_p over the 4 to 20 kc/s frequency range. (See also Wait [1961a] and Wait and Spies [1961].) At night they have found values of v_p/v_0 to be $\simeq$1.03 at 4 kc/s, 1.01 at 10 kc/s, and 1.003 at 20 kc/s. Many references pertinent to the velocity of propagation are contained in the paper by Jean, Taylor, and Wait [1960]. In general, v_p increases with surface conductivity, and decreases with increase in ionospheric height and earth's surface roughness.

An actual physical path phase characteristic may look somewhat like the solid wavy curve of figure 1 where a frequency f_1 would be delayed by the phase ϕ_1. This phase delay in seconds can be written as

$$T_d = \frac{\equiv\phi_1}{2\pi f_1} \tag{3}$$

where T_d is the equivalent time delay in seconds. It should be pointed out that the particular phase versus frequency curve illustrated will only apply for a given distance and at a given time and that it may vary in its exact position as a function of time. The effect of these short term variations of phase as a function of time is to limit the precision with which a given standard frequency can be received.

To obtain the value of the received frequency

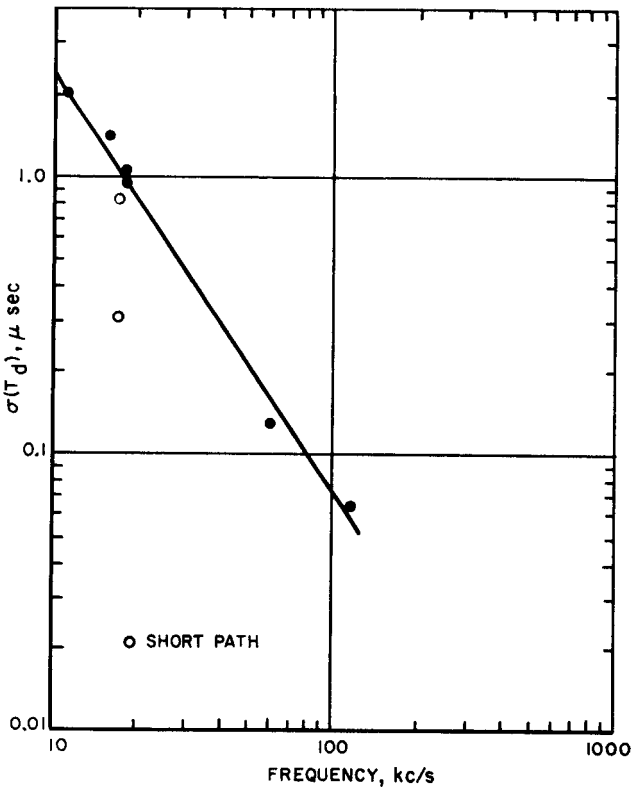

FIGURE 2. *Short term propagation time (phase) stability daytime paths, normalized to single reflection sky wave.*

from the phase measurements it is clear from the definition of frequency that the average departure from the transmitted frequency, $\overline{\Delta f}$, observed in terms of the final and initial phase delays is given by:

$$\overline{\Delta f} = \frac{\phi(T) - \phi(0)}{2\pi T} \tag{4}$$

where T is the time interval, in seconds, over which the phase comparison is made.

The relations governing the transmission path phase stability and signal-integration times required for specific frequency-comparison precisions have been described previously in considerable detail [Watt and Plush, 1959]. In general, where possible, observations should be made near noon at the center of the path. At such time, the phase variations, due to diurnal and random short term effects, are expected to be minimal. Pierce [1957] has experimental evidence over a 5200 km path that the total diurnal phase variation of the 16 kc/s Rugby signal is surprisingly constant throughout the year being in the order of 34 $\pm$1 μsec. Jean[5] over a 7500 km path has observed that the diurnal variation of the phase of the 16 kc/s Rugby signal has substantial variations in pattern. The observed average phase change of $\sim$42 μsec yields about the same effective change in ionospheric height; i.e., $\Delta h \simeq 16$ km using a method described by Wait [1959]. The diurnal patterns observed by Jean

[5] A. G. Jean, private communication. See also C. J. Chilton [1961].

appear to change systematically with seasons and appreciably particularly during ionospherically disturbed conditions. The daytime transmission delay appears to be much less affected by these disturbances than the nighttime phase.

The short time variations in propagation time resulting from path phase instabilities can, in general, be assumed to be randomly distributed about an average time delay $\overline{T_d}$ with a rate of change similar to the fade rate. This means that a single measured value of the delay ranges roughly between $\overline{T_d} \pm \sigma\ (T_d)$, where $\sigma\ (T_d)$ is the standard deviation of the random time delay variable. In general, there will be different values for both $\overline{T_d}$ and $\sigma\ (T_d)$ for day or night paths. Expected standard deviations of short time propagation time delays are shown in figure 2 as a function of frequency for a single reflection daytime skywave in the VLF and LF regions. It should be emphasized that this trend does not continue up into the HF region. The data are obtained from table B–1 [Watt and Plush, 1959] with the additional point at 10.2 kc/s from Tibbals.[6]

2.2. Time Reference and Clock Setting

It is obvious that if a single precisely known uniform frequency were available at a receiving location, that it could be employed in the control of a time standard clock, provided: (a) that the clock could be properly set initially, and (b) that there were no interruptions in the frequency standard or clock. Since neither of these can be guaranteed, it becomes apparent that some method of establishing a time or phase reference at the receiving location is necessary, and that the problem of transmitting a precise time reference is much more difficult than a standard frequency transmission. At the higher frequencies where bandwidth limitations are not severe, this is accomplished by transmitting rather short pulses whose leading edges at the transmitter are quite steep. The delay of these time pulses is also variable but it is not the same as the phase delay described in eqs (2) and (3). Since the pulses are applied in the form of modulation on the rf carrier, the "envelope delay" as defined by Nyquist and Brand [1930] in terms of the slope of the phase characteristic, $d\phi/df$, is the important factor. As we will see in the next section, the HF paths are very instable in both phase and envelope time delay and the timing accuracy obtainable with these pulses is considerably less than that available at the transmitter.

In view of the much more stable phase delay conditions in the VLF region as described by Pierce [1957] and Allan, Crombie, and Penton [1956] along with its excellent coverage characteristics, considerable interest has been exhibited in employing this medium for the distribution of standard frequencies and time reference. The channel bandwidths available in this frequency region, along with the very narrow bandwidths of the transmitting antenna, prevent the use of short-time pulses for the establishment of coarse time markers which could be used in identifying a particular rf cycle. An alternate method employing two closely spaced and alternately transmitted related frequencies is being considered. A description of this method is given by Morgan [1961]. The transmitted and received waveforms for such a narrow band time signal system are shown in figure 3 where it is apparent that the envelope of the voltage difference produces time reference markers with ambiguities spaced by the reciprocal of the frequency difference. Coarse time markers may, if desired, be provided by the times of frequency switching. On-off keying can also be considered for date time code. In a dual frequency system, transmitted waveforms are given as:

$$e_1 = \cos \omega_1 t \tag{5}$$

$$e_2 = \cos \omega_2 t \tag{6}$$

while the envelope of the phasor sum is given as

$$E(t)_{\text{envelope}} = \sqrt{2+2\cos(\omega_2-\omega_1)t} \tag{7}$$

It can be observed that at the transmitter, zero time is our phase reference. At the receiver, the phases of e_1 and e_2 are delayed and these two signals are

$$e_{1r} = \cos[\omega_1 t + \phi_1] \tag{8}$$

$$e_{2r} = \cos[\omega_2 t + \phi_2] \tag{9}$$

Since these two signals can be employed to phase lock high quality local oscillators, it is possible to have two highly constant amplitude sinusoids as indicated. The envelope voltage waveform at the receiver is then

$$E(t)_{\text{envelope received}} = \sqrt{2+2\cos[(\omega_2-\omega_1)t+(\phi_2-\phi_1)]} \tag{10}$$

where it is evident that the important phase is now

[6] M. L. Tibbals, private communication.

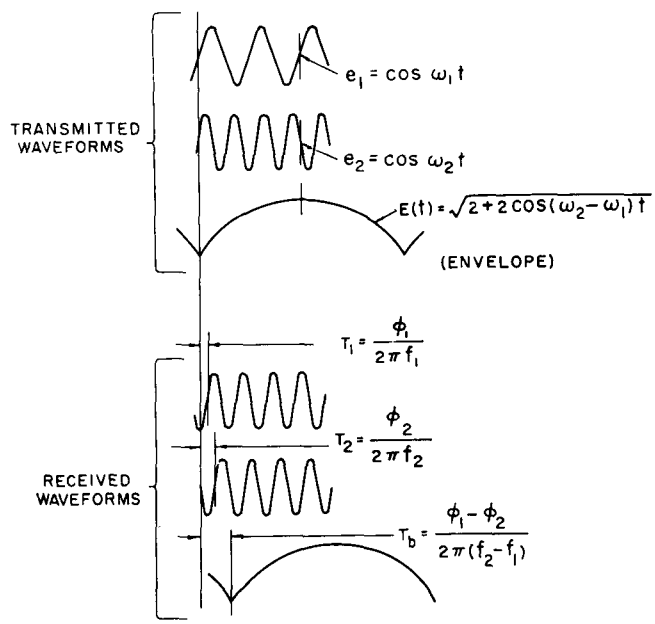

FIGURE 3. *Standard frequency and time signal waveforms.*

$\phi_2-\phi_1$ and the resulting time delay is

$$T_b=\frac{\phi_2-\phi_1}{2\pi(f_2-f_1)} \tag{11}$$

where T_b is the envelope delay in seconds.

If the individual frequencies concerned are separated far enough, the path phase fluctuations become independent and the standard deviation of T_b would be

$$\sigma(T_b)=\frac{\sqrt{2}\sigma(\phi)}{2\pi(f_2-f_1)} \tag{12}$$

assuming that $\sigma(\phi_1)=\sigma(\phi_2)=\sigma(\phi)$.

It can be seen that the time variations will decrease with an increase in frequency separation. It should be emphasized that as the frequency separation is reduced the relative phases tend to become correlated and as a result the envelope reference time variation does not increase without limit since the phase difference tends to approach zero. Measured standard deviations of envelope delay variations for a 1 kc/s frequency spacing in the VLF band are shown by Casselman, Heritage, and Tibbals [1959] to be in the order of ± 20 μsec. (See also Stone, Markowitz, and Hall, 1960.)[7]

Employing the ionospheric roughness parameter described by Watt and Plush [1959] the standard deviation of short term phase variation; i.e., $\sigma(\phi)$, of a VLF carrier received over a 4200 km path is found to be in the order of 0.09 radians. When this value is used in (12) the expected $\sigma(T_b)$ expressed in microseconds is shown in figure 4. Experimental values for $\sigma(T_b)$ obtained from Heritage and Tibbals[8] for spacing of 200, 1,000, and 3,000 c/s appear to substantiate the general level and trend of this curve.

In order to permit identification of a specific cycle of the carrier frequency f_1, it is obvious that $\sigma(T_b)$ must be less than $0.5/f_1-\sigma(T_d)$ which at 20 kc/s will be in the order of ± 22 μsec. Until such time as the expected reduction in $\sigma(T_b)$ due to integration for time intervals long compared to the fade periods is obtained, it appears that frequency separations in the order of 1 kc/s will be required for carrier cycle identification in the 20 kc/s region. If the frequency separation chosen is rather large, the (f_2-f_1) markers may be difficult to resolve from the on-off keying envelope. This is due in part to the normal build up time required by the narrow antenna bandwidths, see typical shapes in figure 5, and the variation in position of this envelope as received due to path envelope delay. Should the on-off keying phase markers received with time delay variations $\sigma(T_e)$ not be stable enough to resolve (f_2-f_1) markers, it may be necessary to employ an additional frequency providing an intermediate reference, viz $(f_3-f_1)<(f_2-f_1)$.

Since the precision of frequency comparison is defined as the phase jitter divided by the observing period T (7.3 of Watt and Plush, 1959) we can write

$$\epsilon=\sqrt{2}\sigma(\phi)/2\pi fT. \tag{13}$$

The time delay for a given phase delay is $T_d=\phi/2\pi f$, and since $\sigma(T_d)=\sigma(\phi)/2\pi f$, we can write (13) as

$$\sigma(T_d)=\epsilon T/\sqrt{2}. \tag{14}$$

Figure 6 shows the manner in which this relationship can be employed to determine the variations expected in a given clock relative to a standard clock T seconds after it has been set to coincidence with the standard clock. It is interesting to note that if an all daylight radio path such as the 16 kc/s transatlantic path observed by Pierce [1957] is employed, the maximum standard deviation of time difference is less than 2 μsec.

It should be pointed out that the problem of subtracting out the mean true transmission time, $\overline{T_d}$,

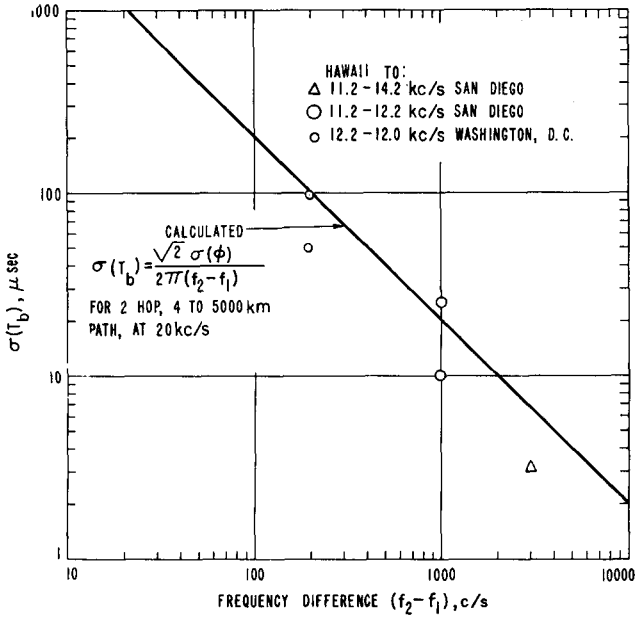

FIGURE 4. *VLF transmission path envelope phase stability.*

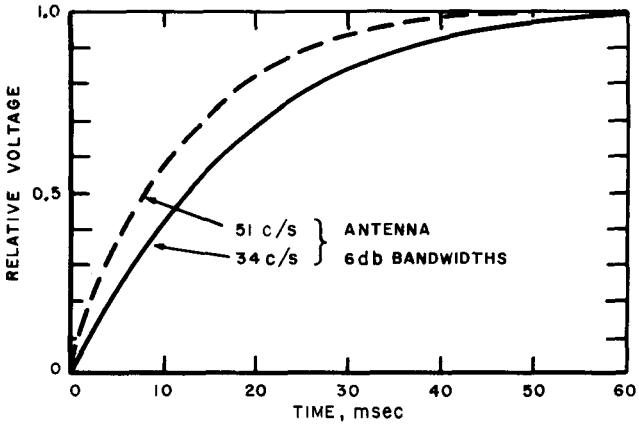

FIGURE 5. *Keying response envelope of typical VLF transmitting antenna.*

[7] Stone, Markowitz, and Hall in a recent paper [1960] have indicated VLF time comparisons of 500 μsec at Washington, D.C., from NBA in Panama. Employing a 6 db transmitting bandwidth of 44c/s on fig. 4 and assuming that the envelope matching would approach that of two frequencies spaced by the 6 db bandwidth we obtain $\sigma(T_b)\cong 450$ μsec for a path of comparable length. Actually the spacing chosen should likely be less which would yield better agreement.

[8] Private communication.

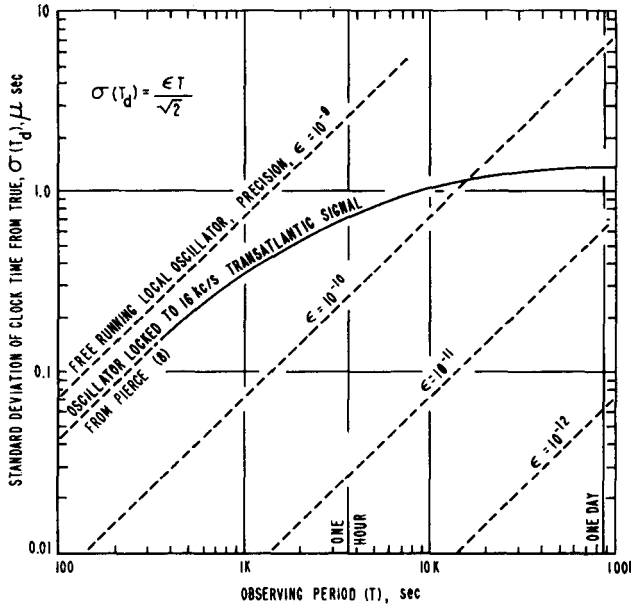

FIGURE 6. *Clock-time deviations from original setting as a function of observing period.* ([8] Pierce 1957).

whether it be a phase delay or envelope delay, still exists. Ionospheric disturbances caused by solar related proton storms or meteoric showers have the largest apparent effect on the nighttime phase delay [Chilton, 1961]. As a result, the midday values of $\overline{T_d}$ are expected to be relatively constant from day to day with the exception that solar flares effect the day values. Over some paths, it is possible that there may be appreciable seasonal variations in even the midday value of $\overline{T_d}$. Additional studies are required before the errors likely in predicting $\overline{T_d}$ can be specified as closely as desired. If two or possibly three VLF standard frequency and time signal stations are operating simultaneously at different rf frequencies but with a common frequency base as well as a common time reference, it is expected that the average delays due to transmission time can be obtained with greater accuracy. Once the average path delays have been subtracted out, a clock at a given receiving site can be set with a high degree of precision (probably limited mainly by the ability to determine absolute average path delay), to the time generated by the network of VLF standard frequency and time signal broadcasting stations.

2.3. Carrier to Noise Limitations

The limitations of noise to precision of frequency comparison have been previously described [Watt and Plush, 1959] and we shall only calculate the effects of rms carrier to rms thermal noise ratio on time signal accuracy.

From equation (C1) of Watt and Plush [1959] and (3)

$$\underset{\text{(noise)}}{\sigma(T_d)} = \frac{N/C}{2\sqrt{2}\pi f_1} \tag{15}$$

where $\sigma(T_d)$(noise) is now the standard deviation of the time reference in seconds derived from the carrier frequency (f_1) phase, and N/C is the rms noise to carrier ratio in the receiver. With post detection filtering or integration following a linear detector, N should be calculated in the effective bandwidth of the integrator. If we consider noise density or in particular, the noise voltage per 1 kc/s bandwidth concept where $N_{1\text{ kc}}$ has the dimensions volts/$\sqrt{\text{kc/s}}$, we obtain

$$\underset{\text{(noise)}}{\sigma(T_d)} = \frac{\sqrt{B_r/1{,}000}}{2\sqrt{2}\pi f_1 C/N_{1\text{ kc}}} \tag{16}$$

where B_r is the effective receiver bandwidth in cycles per second.

When timing is derived by an envelope beat pattern between two carriers, the effects of noise are given by

$$\underset{\text{(noise)}}{\sigma(T_b)} = \frac{N/C}{2\pi(f_2 - f_1)} \tag{17}$$

or

$$\underset{\text{(noise)}}{\sigma(T_b)} = \frac{\sqrt{B_r/1{,}000}}{2\pi(f_2 - f_1)C/N_{1\text{ kc}}} \tag{18}$$

where it is obvious that the time stability for these conditions is poorer for a given $C/N_{1\text{ kc/s}}$ ratio than obtains for $\sigma(T_d)$ (noise).

We can also determine the stability of a time reference obtained from a keyed envelope obtained at the one half amplitude point of the leading edge with coherent detection. For a single sample this is shown in the appendix to be

$$\underset{\text{(noise, sampled)}}{\sigma(T_e)} = \frac{1}{(C/N)2B_t} \tag{19}$$

where: $\sigma(T_e)$ is in seconds and B_t is the transmitter 6 db bandwidth in c/s. If the carrier is keyed on periodically (for example, once each second) the resulting envelope reference can be integrated to reduce the effects of noise. The improvement is equal to the square root of the number of individual pulses, and if the repetition rate is F

$$\underset{\text{(noise, integrated)}}{\sigma(T_e)} = \frac{1}{(C/N)B_t\sqrt{TF}} \tag{20}$$

or

$$\sigma(T_e) = \frac{\sqrt{B_r/1{,}000TF}}{(C/N_{1\,kc})B_t} \tag{21}$$

where: T is the integration period, TF is the number of samples averaged, B_r is the effective receiver bandwidth in c/s. It is apparent from (21) that the time reference derived from the envelope leading edge improves directly as the carrier to noise ratio and as the first power of the transmitting antenna bandwidth and as the square root of the

integration time. In all the derivations involving the rms carrier to noise ratios, the significant noise background considered is of thermal type. The actual background will normally be atmospheric noise which in a wide bandwidth has a very different statistical nature [Watt and Maxwell, 1957]. The effects of atmospheric noise upon radio systems are in general quite different from those of thermal noise [Watt, Coon, Maxwell, and Plush, 1958]. For a pulse sampling system with integration, the required rms C/N may be appreciably less than indicated in eqs. (20) and (21). Hefley[9] [1960] for example has found with Loran-C systems that for equivalent performance the carrier to atmospheric noise ratio can be much less than the carrier to thermal noise ratio; however, it must be remembered that this system employs a very wide RF bandwidth.

When carrier phase or frequency stability is considered, the narrow bandwidths (0.1 c/s or less) employed will make the atmospheric noise statistics the same as thermal noise [Watt and Maxwell, 1957] and in these cases the formulas given (15) through (18) should apply if linear receivers are employed.

3. Present Services

There are at present quite a large number of standard-frequency and time-signal stations in use throughout the world. VLF, LF, and HF are employed for large area coverage with some higher frequencies being used for local distribution. A description of the stations operating along with their location and characteristics is given in Annex I of CCIR Report 66 [1956].

Annex II of the same document describes the characteristics of projected standard frequency and time signal stations at four additional locations. In general, the high frequency stations all employ pulse modulation of the carrier frequency for time signal transmissions and many of them in addition have standard audiofrequencies employed as modulation at various times. The stability as broadcast is usually very good, for example with the National Bureau of Standards station WWV [1960a] the carrier and audiotones have stability of one part in 10^9 at all times with normal daily deviations of less than two parts in 10^{10}. The time signals have essentially the same stability and the maximum deviation from UT–2 is about ± 50 msec. Final corrections to the frequency as broadcast versus the U.S. Frequency Standard are published monthly by the National Bureau of Standards [1960b] in the Proceedings of the IRE while final corrections to the time signals versus UT–2 time are published by the U.S. Naval Observatory.

3.1. HF Standard Frequency and Time Services

Because of the variation in the propagation medium at HF, the frequency as received is generally much less stable than that transmitted. Actually, for high precision measurements it is frequently necessary to use long averaging periods of 10 to 30 days. Ideally, the following conditions should prevail at the time measurements are being made; (a) all daylight (or darkness) over radio path, (b) no ionospheric disturbance in progress, (c) no part of the radio path should pass near either auroral zone, (d) single mode propagation should be existing. In general, frequency determinations can be made either by a direct comparison or by means of the time pulses. Some idea of the precision of frequency comparison obtainable can be seen from figure 7 which shows the precisions available from WWV and WWVH over paths ranging from approximately 2,000 to 8,000 km. Line A shows that for short period samples, such as 100 sec, the precision available is in the order of 2 parts in 10^7. If similar 100-sec samples are made each day, after 30 days the precision has improved to one part in 10^8. It should be emphasized that this type of frequency comparison does not make full use of the transmissions and that the improvement with observing period is not as great as would be predicted if all the actual information received was fully utilized for the total periods shown. Line B shows the results obtained at Boulder employing time pulses compared for approximately 10 sec near noon each day and averaged by means of a clock. Here the daily averaging time is 24 hr. The point shown for 30 days is arrived at as follows. Daily comparisons of the local clock versus the received time of WWV are used to obtain running 10-day averages of time difference. Each day one new daily value is added and the 11-days old value is dropped and the re-

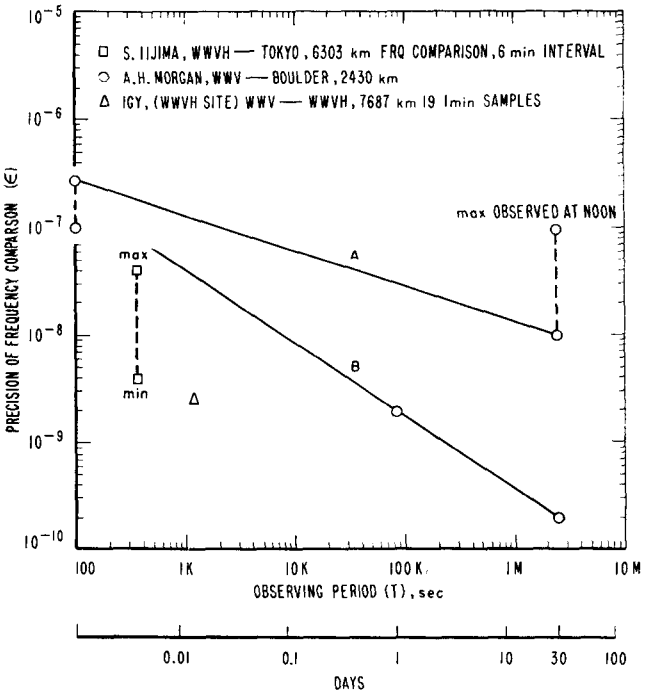

FIGURE 7. *Frequency comparison precision at 10 Mc/s.*
Line A=100 sec samples, frequency comparisons 1 sample/day at noon.
Line B=24-hr average each day, time pulses, compared at 10 a.m. local time.
All values are standard deviation and at best time of day (disturbed day data not included).

[9] Private communication.

sultant 10 time differences averaged. The 30-day running averages of the above 10-day averaged values are obtained in a similar manner. The precisions obtained are appreciably better, being in the order of ± 2 parts in 10^9 for 1 day and approximately ± 2 parts in 10^{10} for 30 days.

3.2. LF Standard Frequency Transmissions

At present there are at least six low frequency standard transmissions being operated including MSF at 60 kc/s in Rugby, England; WWVB at 60 kc/s in Boulder, Colo.; DCF77 at 77.5 kc/s in Mainflingen, Germany; OLP at 50 kc/s in Czechoslovakia; HBJ at 96.04 kc/s in Switzerland; and A5XA at 133⅓ kc/s at Fort Monmouth, N.J., U.S.A. Other characteristics of these transmissions are described in Annex III of CCIR Report 66 [1956]. Pierce [1957] has shown the standard deviation of frequency comparison for MSF transmissions on a transatlantic path to be in the order of 1 times 10^{-10} for a 30-minute observing period. Further calculations for LF transmissions are compared with experimental results by Watt and Plush [1959] and shown here in figure 8. Pierce [1958] has shown average frequency comparison precisions from WWVB (60 kc/s) as received at Cruft Laboratory, of 1.4 parts in 10^{11} in an observing period of about one hr. From equation (14) this would correspond to a short term time variation $\sigma(T_d) \simeq 0.36$ μsec.

Recent plans to distribute time signals via Loran-C navigation system, pulse transmissions at 100 kc/s, have been described by Doherty [1961]. Very precise time signal distribution in the order of 0.2 μsec is possible within the ground wave coverage range of about 1,500 km. By employing sky wave modes, timing precision in the order of 1 μsec appears likely out to about 3,500 km.

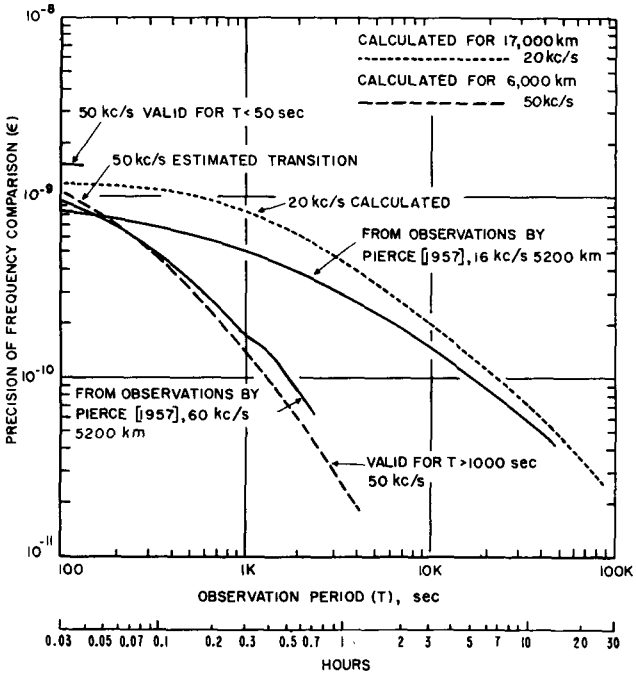

FIGURE 8. *Experimental and theoretical precisions.*

NOTE: Due to diurnal phase change observing periods of longer than 10 K nclude several days.

It is obvious from this and the preceding sections that in a limited area the LF systems (50 to 100 kc/s) will provide for more precise comparison of frequency and time than the VLF systems (15 to 20 kc/s). The propagation loss, however, is much higher in the 50 to 100 kc/s band which restricts the useful range to distances of about 3,000 to 4,000 km. LF transmissions at 60 kc/s in England [Steele, 1955] have shown that timing can be obtained to ± 15 μsec by pulse envelope methods.

3.3. VLF Standard Frequency Transmissions

Annex III of CCIR Report 66 [1956] describes the transmissions from GBR at 16 kc/s which has been used as a basis for much of the pioneer work on standard frequency broadcasting in the very low frequency region. The precisions available from this transmission, and GBZ on 19.6 kc/s, based primarily on observations by Pierce [1957, 1958] and Allan, Crombie and Penton [1956], are included in sections 2.2 and 4. Stabilized transmissions with phase locked master-slave relationship from Hawaii and San Diego have also served as a valuable source of information for VLF path phase stability as described by Casselman, Heritage, and Tibbals [1959]. Recently interim station broadcasts of the U.S. frequency standard have been initiated from WWVL on 20 kc/s from near Boulder, Colo. Time and stabilized frequency broadcasts from NBA at 18 kc/s also recently have been initiated.[10] Additional VLF transmissions are in the process of being stabilized in frequency which should make them available for path phase stability measurements. In the VLF region both theory and experiment show that greater observing times are required for a given degree of frequency comparison precision than is true in the LF region; however, when long range paths are considered the low attenuation rates obtaining in the VLF band make emissions in this frequency region useful for worldwide coverage.

4. Characteristics and Expected Coverage for a VLF Standard Frequency and Time Signal Broadcasting Station

Based on the previous analysis [Watt and Plush, 1959] the precision of frequency comparison expected as a function of observing period T was prepared and is shown as figure 8 [Pierce, Winkler, and Corke, 1960].[11] It is obvious when comparing figures 7 and 8 that a VLF broadcast will provide one or two orders of magnitude improvement over present HF broadcasts in precision of frequency comparison for a given observing period. This great increase in performance has clearly indicated the desirability of designing and constructing a high quality VLF standard frequency broadcasting station or network of 2 or 3 stations whose primary

[10] Precise time and stabilized frequency broadcasts at 18 kc/s over NBA, Summit, Canal Zone, were announced in U.S. Naval Observatory Time Service, Notice No. 8, 18 November 1959. See also a recent paper by Stone, Markowitz, and Hall [1960].

[11] A recent paper by Pierce, Winkler, and Corke [1960] describes results at 16 kc/s over a 5,200 km path that indicate possible precisions of 2×10^{-11}.

function is to provide extremely precise standard frequency and time signals.

Because of the desirability of having such a station near the U.S. standard of frequency located at Boulder, Colo., a study has been made to determine design parameters and service obtainable at various locations. Seventeen different receiving sites were chosen and the total number of measurements obtainable each day for 99 percent of all hours were calculated based on a radiated power of 100 kw. Calculations were made for a range of radiated powers from 25 to 100 kw and the resulting number of measurements obtainable as a function of the cost per measurement was determined. The results of this study [Watt and Plush, 1959] indicated a preference for a radiated power in the order of 100 kw.

The results of this study are summarized in table 1, where the various assumptions made are indicated along with a tabulation of the total number of measurements obtainable for 99 percent of all hours with 100 kw radiated at 20 kc/s [12] for the months of June and December assuming a precision of frequency comparison of 1 part in 10^9. The method of analysis and some of the assumptions made in this analysis are contained in the following sections.

4.1. Propagation Path Attenuation Rates

It is relatively well known that the attenuation rate (a) to be employed in field strength equations such as (2) in the paper by Watt and Plush [1959], expressed in decibels per 1,000 km (db/K), is dependent upon a number of factors including: frequency, ionospheric conditions, earth's surface conditions, and the earth's magnetic field.

Experimental and theoretical studies indicate that there is a broad minimum in the attenuation-versus-frequency curve which is centered somewhere in the vicinity of 16 to 18 kc/s. The shape of this attenuation curve is likely to vary between day and night conditions, and is also likely to be different for east-to-west and west-to-east propagation. It would appear from an analysis of results obtained from many different sources that the east-to-west (magnetic) attenuation rate in some cases may be as much as 1 or 2 db/K greater than the west-to-east attenuation rates. This effect is expected to be more pronounced at night; in addition this difference in attenuation rate with direction is expected to be greater at the lower frequencies; viz, 10 to 14 kc/s, and relatively small in the vicinity of 20 kc/s. These effects have been discussed by various authors [H. J. Round, T. E. Eckersley, K. Tremellen, and F. C. Lunnon, 1925; K. G. Budden, 1951 and 1952; J. R. Wait, 1958 and 1961b; and D. D. Crombie, 1958].

Approximate values for the average daytime attenuation rate (a) in the vicinity of 20 kc/s are: sea $\simeq$2, average land $\simeq$4, estimated values for permafrost and icecap are 7 and 18. When mixed surface conditions are encountered along the path, as is usually the case in practice, the total average path attenuation will not always be exactly equal to the sum of the attenuations expected from each individual portion of the path. This may be due in some cases to a transfer of energy from the dominant to higher order modes caused by the discontinuities in conductivity at the surface. It is also likely that low conductivity at the earth's surface will produce appreciably greater attenuation during the day when the ionosphere is low than at night when it is higher.

After determining the various amounts of surface types along the individual paths, expected average attenuation rates have been assigned for each of the receiving locations in table 1. In some cases reciprocal path values have been employed and, in general, values quoted are as high as anticipated from a consideration of all possible attenuation mechanisms.

Field strengths anticipated for these particular paths have been calculated employing the relationships given by Watt and Plush [1959]; the results are shown in column 5 of table 1 for an assumed radiated power of 100 kw at a frequency of 20 kc/s.

4.2. Expected Availability and Precision of Frequency Comparison

The carrier to noise available at the receiving location may in some cases be the limiting factor as regards the time required to obtain a frequency comparison of, say, 1 part in 10^9. Median atmospheric noise fields expected for the various receiving locations have been obtained from Crichlow, Smith, Morton, and Corliss [1955] and the results presented in columns 6 and 7 of table 1. Combining the previous information regarding carrier field intensities with the noise field intensity data, we have obtained the minimum expected observation times required to compare frequency to 1 part in 10^9 for 100 kilowatts radiated as shown in columns 14 and 15.

Pierce [1957] has shown that the transmission path phase is very stable and that the diurnal variations caused by sunrise or sunset along the Rugby to Cambridge path are surprisingly constant throughout the year. During the all sunlight period the path phase appears more stable than at night for frequencies of 16 to 60 kc/s. We have determined, on the basis described by Watt and Plush [1959], the minimum observing times required to obtain a precision of 1 part in 10^9 based on path phase variations expected for both day and night conditions. It should be noted that $\sigma(\phi)$ has been assumed to increase as the square root of distance which is what one would expect of sections of variable delay wave guides connected in series. These results are presented in columns 12 and 13.

Although it is obvious that in a case where minimum observing times based on path phase variability and carrier-to-noise ratio are nearly the same, the combined effect will require a longer observation time than indicated for either limitation. We have neglected this effect and have considered only the one condition which requires the longer period.

In order to get some idea of the relative service obtainable from the proposed standard frequency and time signal broadcast, the total number of

[12] It should be noted that 20 kc/s has been employed in these calculations because: (1) 20 kc/s is an internationally assigned standard frequency, (2) the power requirements for worldwide coverage are expected to be near a minimum at this frequency, (3) considerable propagation data is available in this region. Further research on attenuation and phase stability should be conducted over the whole VLF spectrum to determine the suitability of other frequencies for standard frequency and time distribution.

TABLE 1 – STANDARD VLF BROADCAST STATION ANTICIPATED RECEPTION CAPABILITIES – 100 kw AT 20 kc/s RADIATED NEAR BOULDER, COLO.

1	2	3	4	5	6		7	8	9	10	11	12	13	14	15	16				17			
No.	LOCATION	DIST., km	(ESTIMATED) PATH ATTEN. DAYLIGHT α, db/1000 km	CARRIER FIELD FOR 100 kw RAD. db RELATIVE TO 1 μv/m	MEDIAN NOISE FIELD db RELATIVE TO 1 μv/m, 1 kc/s BAND		hr ALL DAYLIGHT ON PATH		No. hr ALL NIGHT ON PATH		MIN. OBSERVATION TIME – hr FOR ε=10⁻⁹ BASED ON PATH PHASE VARIATION		MIN. OBSERVATION TIME – hr FOR ε=10⁻⁹ BASED ON C/N WITH 100 kw RADIATION		TOTAL No. OF MEASUREMENTS OBTAINABLE FOR 99% OF ALL HOURS, 100 kw						
																JUNE			DECEMBER				
					JUNE	DECEMBER	JUNE	DECEMBER	JUNE	DECEMBER	DAY	NIGHT	JUNE	DECEMBER	DAY	NIGHT	TOTAL	DAY	NIGHT	TOTAL
1.	WASHINGTON, D.C.	2 370	5.0	59.1	45.0	35.0	12.8	7.2	12.8	7.2	0.001	0.07	0.0145	0.0069	882	102	984	1 042	182	1 224
2.	MONTREAL, Canada	2 370	5.0	59.1	40.0	32.0	12.9	6.7	12.9	6.7	0.001	0.07	0.01	0.0054	1 289	95	1 384	1 239	184	1 423
3.	THULE, Greenland	4 470	5.5	43.7	30.0	26.0	14.8	4.2	14.8	4.2	0.002	0.14	0.015	0.011	985	29	1 014	380	104	484
4.	KEFLAVIK, Iceland	5 770	5.0	38.7	32.0	30.0	11.48	0/(1)	11.48	0/(1)	0.006	0.18	0.026	0.022	440	4	444	44	60	104
5.	RUGBY, England	7 400	4.5	33.8	44.0	34.0	8.3	1.5	8.3	1.5	0.01	0.24	0.096	0.044	85	5	90	33	32	65
6.	PARIS, France	7 770	4.5	31.7	40.0	35.0	8.0	1.4	8.0	1.4	0.01	0.28	0.084	0.057	94	4	98	23	27	50
7.	TORINO, Italy	9 000	4.5	26.0	42.0	35.0	7.1	1.1	7.1	1.1	0.02	0.3	0.15	0.088	46	2	48	11	22	33
8.	MOSCOW, U.S.S.R.	8 880	5.5	30.5	40.0	35.0	6.3	-1.7	6.3	-1.7	0.02	0.3	0.09	0.062	69	–	69	–	20	20
9.	NEW DELHI, India	12 850	5.0	-0.1	45.0	40.0	2.6	-2.0	2.6	-2.0	0.5	1.0	1.4	0.96	1	–	1	–	2	2
10.	FAIRBANKS, Alaska	3 880	5.0	39.5	30.0	28.0	14.3	4.1	14.3	4.1	0.002	0.12	0.0098	0.0082	1 458	32	1 490	499	116	615
11.	SAN DIEGO, California	1 450	5.0	65.6	40.0	35.0	13.8	8.8	13.8	8.8	0.001	0.04	0.006	0.0043	2 799	220	3 019	2 045	344	2 389
12.	HONOLULU, Hawaii	5 470	3.0	51.2	35.0	35.0	10.6	6.6	10.6	6.6	0.004	0.18	0.0125	0.013	847	35	882	506	58	564
13.	TOKYO, Japan	9 560	2.5	42.5	40.0	35.0	7.0	2.0	7.0	2.0	0.03	0.31	0.036	0.024	193	5	198	63	21	84
14.	LOWER HUTT, New Zealand	12 650	2.0	41.6	35.0	40.0	6.8	6.8	6.8	6.8	0.05	0.44	0.026	0.039	135	14	149	135	14	149
15.	BYRD LAND, Antarctica	14 430	3.0	24.2	30.0	32.0	0/(1)	9.2	0/(1)	9.2	0.08	0.52	0.069	0.06	11	16	27	114	1	115
16.	JOHANNESBURG, So. Afr.	16 150	4.5	17.6	35.0	48.0	3.7	2.7	3.7	2.7	0.1	0.6	0.17	0.45	20	3	23	5	5	10
17.	BUENOS AIRES, Argentina	9 840	4.5	22.5	35.0	45.0	9.0	8.6	9.0	8.6	0.03	0.34	0.17	0.34	51	24	75	24	25	49

1. "NUMBER OF MEASUREMENTS" REPRESENT THE NUMBER OF FREQUENCY COMPARISON MEASUREMENTS POSSIBLE DURING THE TOTAL TIME OF COMPLETE DAYLIGHT AND COMPLETE DARKNESS BETWEEN BOULDER AND THE "LOCATION OF MEASUREMENTS"
2. PRECISION OF EACH FREQUENCY COMPARISON MEASUREMENT – 1 PART IN 10^9
3. HIGHER PRECISION THAN 1 PART IN 10^9 WILL BE OBTAINABLE BY MAKING MEASUREMENTS FOR PERIODS LONGER THAN THE MINIMUM TIMES LISTED. OVER PATHS WHERE DAYLIGHT IS PRESENT FOR 2 HOURS OR MORE, PRECISIONS RANGING FROM 3 PARTS IN 10^{10} TO POSSIBLY 3 PARTS IN 10^{11} ARE EXPECTED.

measurements with a precision of 1 part in 10^9 obtainable per 24 hr for 99 percent of all hours have been obtained by dividing the number of hours of all-day or all-night over the particular path by the appropriate minimum observing times and adding, as shown in columns 16 and 17 for the months of June and December. It can be seen from this tabulation that the service provided at various locations is appreciably different; however, it is interesting to observe that in all but one case an appreciable number of measurements can be made throughout each day, and that in the worst case, for transmissions to New Delhi, at least one comparison with a precision of 1 part in 10^9 is expected in each day. In many of the closer more favorable locations, it would appear that precision of 3 parts in 10^{10} or better can be expected where observing times of at least 2 hr or more over daylight paths are possible. The maximum precision obtainable that can be expected and any locations can readily be calculated using the procedures outlined earlier [Watt and Plush, 1959].

5. Appendix

5.1. Timing Accuracy Obtainable With an On-Off Keyed Carrier in the Presence of Thermal Noise

It is well known that the slope of the envelope at the one-half amplitude point of a keyed carrier passed through a filter with a 6 db bandwidth B_t is

$$\frac{dv}{dt}\simeq EB_t \tag{A1}$$

where E is the maximum or locked keyed carrier voltage, and dv/dt is the slope observed at the one-half carrier envelope amplitude point.

When thermal type noise is present, the envelope of the keyed carrier can be expected to have a standard deviation in amplitude of $\sigma(a)$ for $C/N\gg 1$ with an envelope detector or for all C/N ratios if a synchronous detector is employed. If the point at which the noise free keyed carrier crosses the $E/2$ point is chosen as a reference T_0, it can be seen that the actual crossing point in the presence of noise will vary about this point. The standard deviation of this crossing time is defined as $\sigma(T_e)$, and it is easily seen that

$$\sigma(a)/\sigma(T_e)=dv/dt=EB_t \tag{A2}$$

$$\sigma(T_e)=\sigma(a)/EB_t \tag{A3}$$

Since $E=\sqrt{2}\ C$ where C is the rms carrier and $\sigma(a)=\sqrt{2}\ N$ where N is the rms noise in the receiver IF band pass filter, we can write

$$\sigma(T_e)=\frac{1}{(C/N)B_t} \tag{A4}$$

When the receiver effective bandwidth is B_r(c/s) and we use the convention of $C/N_{1\ kc}$, i.e., the rms carrier to rms noise in a one kc/s effective band, we

obtain for a single sample

$$\sigma(T_e)=\frac{\sqrt{B_r/1{,}000}}{(C/N_{1kc})B_t} \qquad \text{(A5)}$$

The authors have benefited from many helpful discussions with numerous individuals. In particular, we would like to acknowledge information and suggestions obtained from J. R. Wait, J. A. Pierce, A. G. Jean, R. C. Kirby, W. Markowitz, K. A. Norton, J. M. Richardson, W. D. George, D. H. Andrews, and D. D. Crombie. The assistance of Mrs. Winifred Mau in the preparation of this manuscript is also gratefully acknowledged.

6. References

Allan, A. H., D. D. Crombie, and W. A. Penton, Frequency variations in New Zealand of 16 kc/s transmissions from GBR Rugby, Nature **177,** 178 (1956).

Budden, K. G., The reflection of very low frequency radio waves at the surface of a sharply bounded ionosphere with superimposed magnetic field, Phil. Mag. **42,** 833–851 (1951).

Budden, K. G., The propagation of a radio atmospheric—II, Phil. Mag. **43,** 1179–1201 (1952).

Bullard, E. C., Definition of the second of time, Nature **176,** 282 (Aug. 1955).

Casselman, C. J., D.P. Heritage, and M. L. Tibbals, VLF propagation measurements for the Radux-Omega navigation system, Proc. IRE **47,** No. 5, 829–839 (May 1959).

CCIR VIII Plenary Assembly, Vol. I, Report 66, p. 362 (Warsaw, 1956).

Chilton, Charles J., VLF phase perturbation associated with meteor shower ionization, J. Geophys. Research **66,** No. 2, 379–383 (Feb. 1961).

Crichlow, W. Q., D. F. Smith, R. N. Morton, and W. R. Corliss, World-wide radio noise levels expected in the frequency band from 10 kc to 100 Mc, U.S. Dept. of Commerce, NBS Circ. 557 (Aug. 1955). (U.S. Govt. Printing Office, Washington 25, D.C.) See ITU, Geneva (1957).

Crombie, D. D., Differences between east-west and west-east propagation of VLF signals over long distances, J. Atmospheric and Terrest. Phys. **12,** 110–117 (1958).

Doherty, R. H., G. Hefley, R. F. Linfield, Timing potentials of Loran-C, to be published in Proc. IRE (1961).

Jean, A. G., W. L. Taylor, and J. R. Wait, VLF phase characteristics deduced from atmospheric waveforms, J. Geophys. Research **65,** 907–912 (March 1960).

Lyons, H., Spectral lines as frequency standards, Annals, N.Y. Academy of Sciences, p. 831 (May 1952).

Mach, Ernst, Science of mechanics, 5th English ed., p. 272 (Open Court Publishing Co., LaSalle, Ill., 1942).

Markowitz, William, Astronomical and atomic times, U.S. Naval Observatory, Washington 25, D.C. (9 March 1959). See also: Time measurement, Encyclopedia Britannica **22,** 224–228 (1959).

Markowitz, W., R. G. Hall , L. Essen, and J. V. L. Parry, Frequency of cesium in terms of ephemeris time, Phys. Rev. Letters **1,** No. 3, 105–107 (Aug. 1, 1958).

Morgan, A. H., Proposal for a new method of time signal modulation of VLF carriers (to be published as an NBS Tech. Note, 1961).

National Bureau of Standards, Boulder Laboratories, Standard frequency and time signals, WWV and WWVH, NBS Misc. Publ. 236 (1960).

National Bureau of Standards, Boulder Laboratories, National standards of time and frequency in the United States, Proc. IRE **48,** No. 1, p. 105 (Jan. 1960).

Nyquist, H., and S. Brand, Measurement of phase distortion, Bell System Tech. J. **IX,** 522–543 (July 1930).

Pierce, J. A., Intercontinental frequency comparison by VLF radio transmission, Proc. IRE **45,** 794 (1957).

Pierce, J. A., Recent long distance frequency comparisons, IRE Trans. on Instrumentation **I–7,** pp. 207–210 (Dec. 1958).

Pierce, J. A., G. M. R. Winkler, and R. L. Corke, The 'GBR experiment': A trans-Atlantic frequency comparison between caesium-controlled oscillators, Nature **187,** 914–916 (July–September 1960).

Round, H. J., T. E. Eckersley, K. Tremellen, and F. C. Lunnon, Report of measurements made on signal strength at great distances during 1922 and 1923 by an expedition sent to Australia, J. Inst. Elec. Engrs. (London) **63,** No. 346, 933–1011 (Oct. 1925).

Steele, J. McA., The standard frequency monitor at the National Physical Laboratory, Proc. Inst. Elec. Engrs. (London), Part B, **102,** 155–165 (1955).

Stone, R. R., Jr., W. Markowitz, and R. G. Hall, Time and frequency synchronization of Navy VLF transmissions, IRE, Trans. on Instrumentation **I–9,** No. 2, 155–161 (Sept. 1960).

Wait, J. R., A study of VLF field strength data, both old and new, Geofisica pura e applicata **41,** 73–85 (1958/III).

Wait, J. R., Diurnal change of ionospheric heights deduced from phase velocity measurements at VLF, Proc. IRE **47,** 998 (1959).

Wait, J. R., A comparison between theoretical and experimental data on phase velocity of VLF radio waves, Proc. IRE **49,** 1089–1090 (June 1961).

Wait, J. R., A new approach to the mode theory of VLF propagation, J. Research NBS (Radio Prop. **65D,** No. 1, 37–46 (Jan.–Feb. 1961).

Wait, J. R., and K. P. Spies, A note on phase velocity of VLF radio waves, J. Geophys. Research **66,** 992–993 (March 1961).

Watt, A. D., and E. L. Maxwell, Measured statistical characteristics of VLF atmospheric radio noise, Proc. IRE **45,** 55–62 (Jan. 1957).

Watt, A. D., R. M. Coon, E. L. Maxwell, and R. W. Plush, Performance of some radio systems in the presence of thermal and atmospheric noise, Proc. IRE **46,** No. 12, 1914–1923 (Dec. 1958).

Watt, A. D., and R. W. Plush, Power requirements and choice of an optimum frequency for a world-wide standard-frequency broadcasting station, J. Research NBS (Radio Prop.) **63D,** No. 1, 35–44 (July–Aug. 1959).

(Paper 65D6—164)

Remote Phase Control of Radio Station *WWVL*

THE standard very-low-frequency 20-kc. emission from the National Bureau of Standards radio station *WWVL* at Sunset, Colorado, has been synchronized with the frequency of a working atomic standard located at the National Bureau of Standards Laboratories in Boulder, Colorado, eleven miles from the transmitter site. The phase-lock loop for this purpose uses a servosystem similar to that described by Looney[1], with the system elements necessarily divided between the two locations. At Boulder Laboratories is located a 20-kc./s. receiver, phase detector, atomic standard and a 50 Mc./s. F.M. auxiliary transmitter for returning error and reference phase signals, by means of duplexing, to a 400 c.p.s. two-phase servomotor with gear reduction which drives a resolver at the transmitter site. The resolver, which is located electrically between the local crystal oscillator and transmitter input, thus corrects the transmitter input phase so as to maintain the transmitted output phase, as received at Boulder Laboratories, in synchronism with the phase of the controlling atomic oscillator. This system therefore corrects for frequency drift of the transmitter control oscillator as well as for changes in phase which in general are known to occur in the transmitter and antenna system (ref. 2 and Watt, A. D., private communication). Comparisons made on a very-low-frequency monitor between the phase of the received 20-kc./s. signal at Boulder Laboratories and that derived from the working atomic standard oscillator show that any uncorrected random phase variations may amount to no more than 0·05 μsec. phase shift so that transmitted phase stability is essentially that of the working atomic oscillator.

From the results of daily comparisons of the controlling atomic oscillator with that of the United States frequency standard[3], daily variations of the frequency of the working atomic standard are of the order of 1 or 2 in 10^{-11}.

R. L. FEY
J. B. MILTON
A. H. MORGAN

National Bureau of Standards,
Boulder Laboratories,
Radio Broadcast Services,
Boulder, Colorado.

[1] Looney, Chesley H., *Proc. Inst. Rad. Eng.*, **49**, 448 (1961).
[2] Watt-Carter, D. E., and Cork, R., L., *Nature*, **191**, 1286 (1961).
[3] Mockler, R. C., Beehler, R. E., and Snider, C. S., *Trans. Inst. Rad. Eng.*, 1-9, 120 (1960).

Printed in Great Britain by Fisher, Knight & Co., Ltd., St. Albans.

(Reprinted from Nature, Vol. 193, No. 4820, pp. 1063 1064, March 17, 1962)

RADIO SCIENCE Journal of Research NBS/USNC-URSI
Vol. 68D, No. 11, November 1964

A VLF Timing Experiment [1]

A. H. Morgan [2] and O. J. Baltzer [3]

(Received April 22, 1964; revised May 22, 1964)

The purpose of the experiment given in this paper was to measure the differential phase stability of two VLF carriers (19.9 kc/s and 20.0 kc/s) as received at Austin, Tex., as a function of the observing time, using the former low power standard frequency broadcasts of WWVL, Sunset, Colo.

These measurements indicate that, at the distance involved (1400 km) and with an averaging time of a few hours, the envelope or group delay variations will cause a "jitter" in the received envelope zeros at the receiver of less than one cycle at 20.0 kc/s. Therefore, a particular cycle of the 20.0 kc/s carrier as transmitted may be identified at the receiver, thus providing "microsecond" timing.

1. Introduction

It is well known that the precision of high-frequency (HF) signals is several orders less than that of very low-frequency (VLF) signals due to the severe and unpredictable variations in the propagation medium. This sets an upper limit to the precision with which widely separated clocks may be synchronized using HF timing signals and with which frequency comparisons may be made (fig. 1).

Because of their high phase stability and low attenuation rates, VLF signals are well suited for the dissemination of standard frequencies. This was the basis for changing to their use in 1961 in calibrating and controlling the frequencies as broadcast at WWV. The marked improvement that resulted is clearly evident in figure 1, where S^2 is the sample variance and S the sample standard deviation of the mean, in parts in 10^{10}. Further evidence in the high stability of LF and VLF signals is given in figure 2, which shows the excellent agreement of the signals of the NBS standard LF (WWVB) and VLF (WWVL) stations as received at WWV.

If the precisions of frequency comparison of a few parts in 10^{11} [Pierce, 1958] were obtainable in the dissemination of time signals, it would permit synchronization of clocks to 1 μsec over wide areas of the world. Because of the narrow bandwidths available at VLF and the high Q factors of the antennas, it has not been possible to use sharply rising pulses as precise time markers.

This appears to be a basic limitation, and if so, it could not be circumvented by trick circuitry. In any case, the bandwidths needed for such pulses are simply not available. Moreover, even if they were, it appears that the high ambient noise levels at VLF would be a severe problem in the effective use of wideband systems.

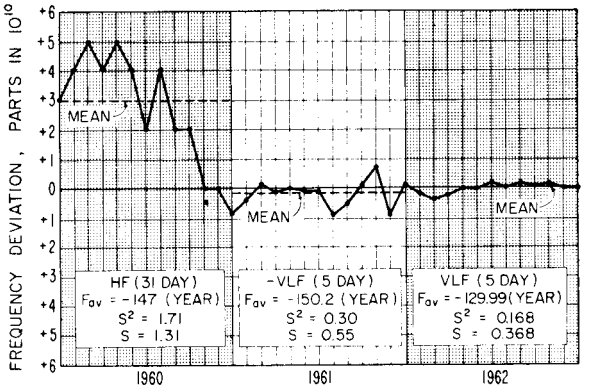

FIGURE 1. *Improvements in the frequency control of WWV.* The units of S are in parts in 10^{10}.

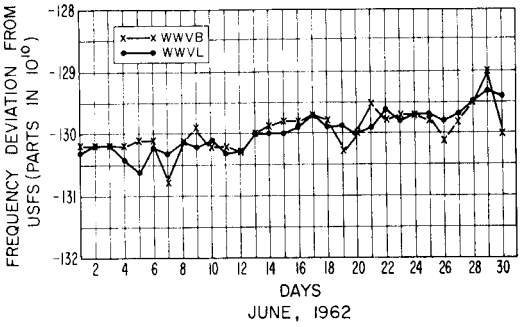

FIGURE 2. *Agreement of values of frequency of WWVL and WWVB as received at WWV.*

The positive zero crossovers of the carrier wave, however, do provide the desired precision for timing marks, but at 20 kc/s, for instance, there are ambiguities in the time every 50 μsec. To resolve these ambiguities another carrier frequency, 19.9 kc/s, for example, may be transmitted every second. The much more widely spaced zero crossovers of the received envelope serve as coarse time markers to identify certain cycles of the carrier. They, in turn,

[1] This paper was given at the VLF Symposium in Boulder, Colo., August 13, 1963.
[2] Radio Standards Laboratory, National Bureau of Standards, Boulder Laboratories, Boulder, Colo.
[3] Senior Vice President, Tracor, Inc., Austin, Tex.

463-560 O - 72 - 21

may be identified by reference to other time scales such as the signals of WWV.

However, high differential phase stability is necessary in order to be able to identify the correct carrier cycle with this method.

The group delay of these signals, as given in a previous paper [Watt et al., 1961] is

$$t_d=\frac{\phi_2-\phi_1}{\omega_2-\omega_1}, \tag{1}$$

where $\phi=\omega t$. As pointed out in the previous paper the received phase, ϕ, at each carrier frequency may consist of a constant term, ϕ', and a fluctuating term, $\pm\delta\phi'$, due to effects of the propagation medium; i.e., $\phi=\phi'\pm\delta\phi'$. This would also indicate that the group delay time could be similarily expressed; i.e., $t_d=t_d'\pm\delta t_d'$. If these expressions are put into (1), the result is

$$t_d'\pm\delta t_d'=\frac{(\phi_2'-\phi_1')\pm(\delta\phi_2'-\delta\phi_1')}{\omega_2-\omega_1}. \tag{2}$$

The differential phase is the quantity of interest, and is given as

$$\delta t_d'=\frac{(\delta\phi_2'-\delta\phi_1')}{(\omega_2-\omega_1)} \tag{3}$$

or, briefly, as

$$\Delta(\delta\phi')=\Delta\omega\delta t_d', \tag{4}$$

where

$$\Delta(\delta\phi')\equiv(\delta\phi_2'-\delta\phi_1') \text{ and } \Delta\omega\equiv(\omega_2-\omega_1).$$

In the previous paper a discussion was given of the basic limitations in the stability of the VLF signals, including path phase distortion, carrier-to-noise, and group delay variations as related to the time dissemination problem.

2. Purpose of the Experiment

The purpose of this experiment was to measure the differential phase stability of two VLF carriers (19.9 kc/s and 20.0 kc/s) as received at Austin, Tex., as a function of the length of the observing time. These results were obtained by using the former low power standard frequency broadcasts of WWVL, Sunset, Colo.

It may be shown from (1) that a change in the phase of zeros of either carrier wave as received will cause a change in the antiphase points that is larger by a factor equal to the ratio of the carrier frequency (which everyone is chosen for the timing) to the envelope frequency. In this case (at 20 kc/s) the factor is 20,000 c/s|100 c/s=200.

3. Description of the Experiment

Such signals, phase locked [Fey et al. 1962] to the working frequency standard (fig. 3) by means of a VHF radio link to eliminate the effects of phase shifts in the VLF antenna system and transmitter, were transmitted from Sunset, Colo., and received at Austin, Tex., a distance of about 1400 km. The receiving equipment used consisted of two phase-locked receivers, one at each carrier frequency, with provision to record a voltage analog of the received phase of each.

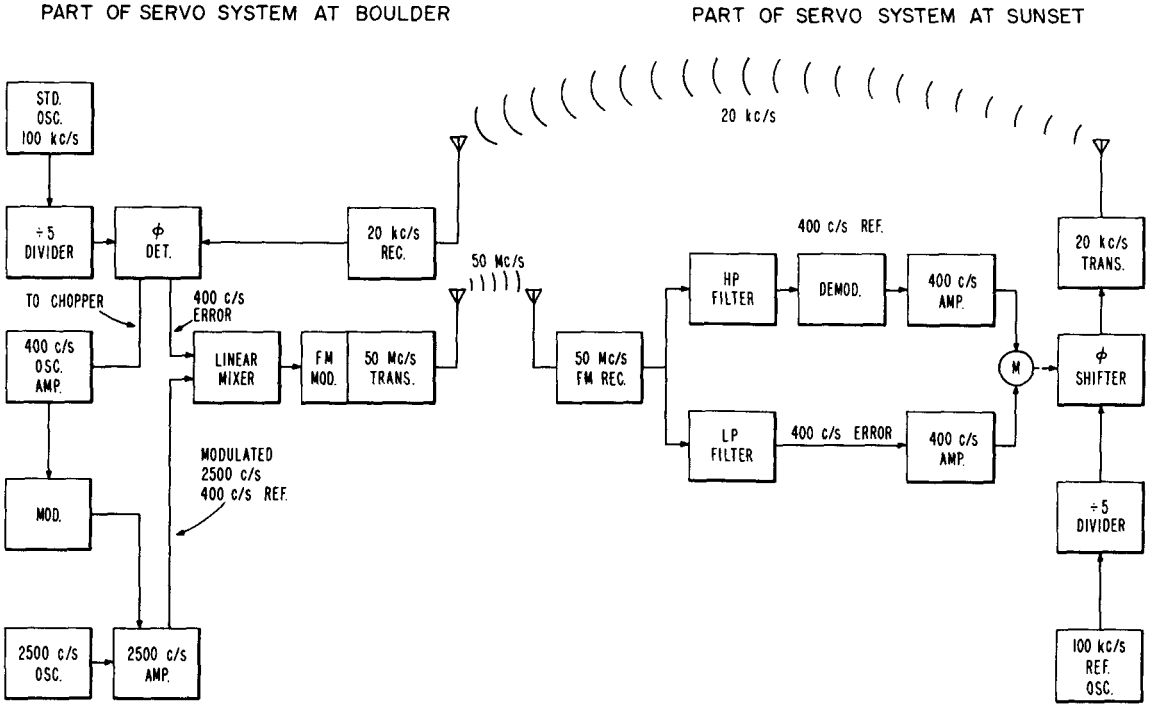

FIGURE 3. *Sunset phase-lock system for WWVL (20 kc/s).*

A simplified block diagram of a typical phase-lock receiver is shown in figure 4. As may be seen, the signal available to the user is not the received signal but one locally generated and kept in phase lock with it. Therefore, the receiver output signal is: (1) very constant in amplitude and (2) relatively free of noise perturbations, both very important considerations. The receiving system acts as a very narrow band filter (bandwidths of 0.01 to 0.001 cycle) which permits use of signals several tens of decibels below the noise in a 1 kc/s bandwidth.

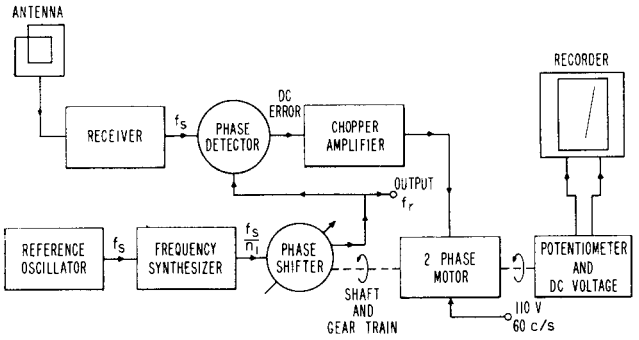

FIGURE 4. *Phase-lock receiving system.*

A block diagram of the receiving system used is shown in figure 5. It may be seen that a differential phase meter was also included to record continuously the differences in phase of the two signals. A typical set of records is shown in figure 6, where the lower parallel traces represent the received phase of the 20.0 and 19.9 kc/s carriers. That the traces of the two signals follows each other very closely is quite apparent. The upper trace is the magnified phase difference between the two carriers.

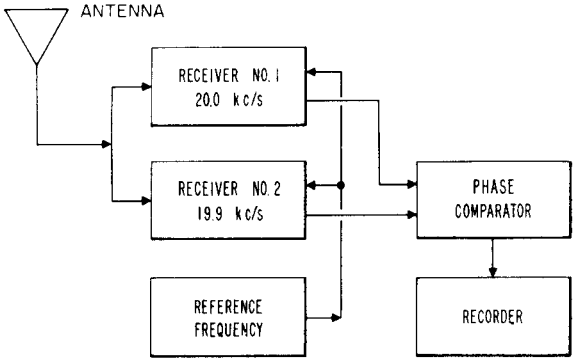

FIGURE 5. *Diagram of receiving system at Austin, Tex.*

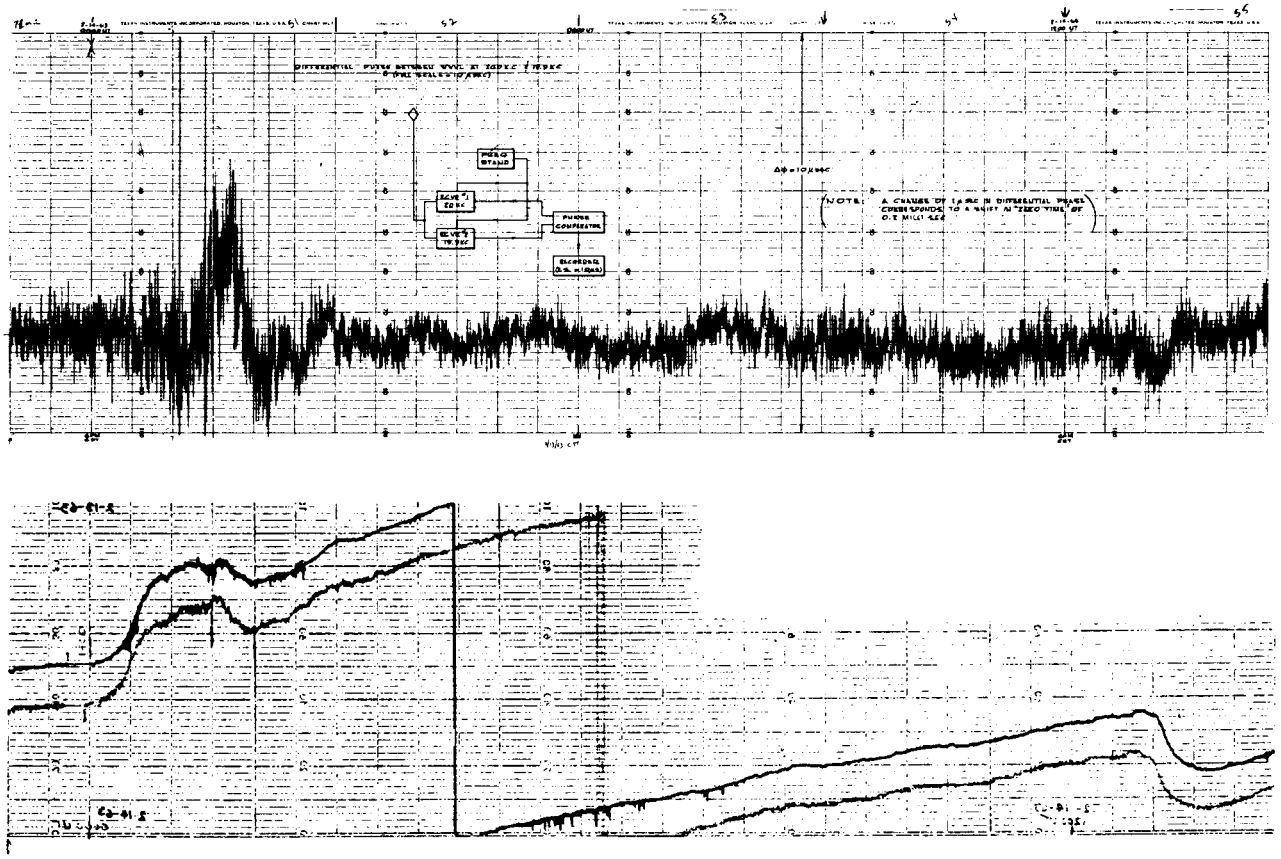

FIGURE 6. *Typical set of recordings, February 1963.*

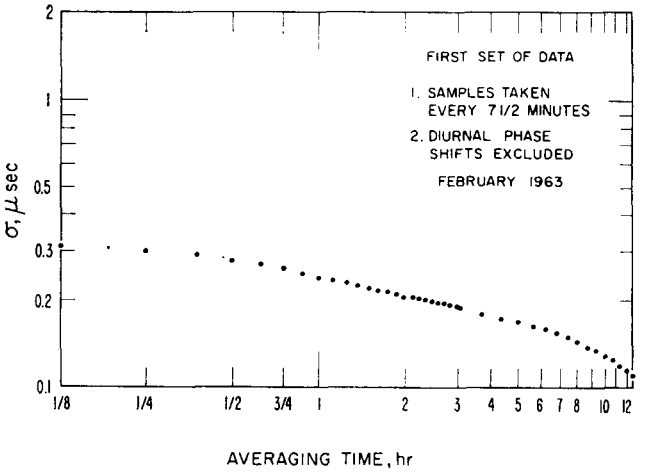

FIGURE 7. *Differential phase stability.*
(Sampling time=7.5 min.)

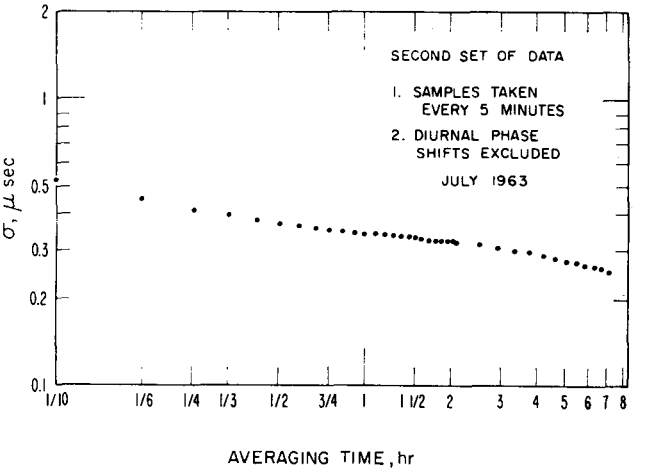

FIGURE 8. *Differential phase stability.*
(Sampling time=5.0 min.)

4. Preliminary Results Obtained

Two sets of several days recordings, as described above, were made at Austin, Tex., and the data analyzed.

For analysis by a digital computer, the data on the differential phase records were scaled at intervals of 7½ min for the first set of records and at 5-min intervals for the second set, but excluding periods of diurnal phase shifts. The calculated results are shown in figures 7 and 8. They are a plot of the sample standard deviation, in microseconds, as a function of the averaging time in seconds, of the differential phase converted to differential time, as given in (3), between the 19.9 and 20.0 kc/s signals as received in Austin, Tex.

The results given in figures 7 and 8 indicate that, with an averaging time of a few hours, the envelope or group delay variations will cause a "jitter" in the envelope zeros at the receiver of about ± 50 μsec, or about 1 cycle at 20 kc/s, during periods of no diurnal phase change. This means that a particular cycle of the carrier as transmitted may be identified at Austin, Tex., provided the group delay time over the path is known. In that case, a precise clock in Austin could be synchronized to one in Boulder to "microsecond" accuracy using the zero crossovers of the 20.0 kc/s signals.

The contributions of L. Fey, E. Marovich, and E. L. Crow are hereby acknowledged. Also, the manuscript was typed by Miss C. A. Merkling.

5. References

Fey, R. L., J. B. Milton, and A. H. Morgan (March 17, 1962), Remote phase control of radio station WWVL, Nature, **193,** No. 4820, 1063–1064.

Pierce, J. A. (December 1958), Recent long-distance frequency comparisons, IRE Trans. Instr. **I–7,** No. 3–4, 207–210.

Watt, A. D., R. W. Plush, W. W. Brown, and A. H. Morgan (1961), J. Res. NBS **65D** (Radio Prop.) No. 6, 617–627.

(Paper 68D11–423)

RADIO SCIENCE Journal of Research NBS/USNC-URSI
Vol. 69D, No. 7, July 1965

International Comparison of Atomic Frequency Standards Via VLF Radio Signals[1]

A. H. Morgan, E. L. Crow, and B. E. Blair

National Bureau of Standards, Boulder, Colo.

(Received December 31, 1964; revised February 23, 1965)

A study was made of data obtained over an 18-month period (July 1961 to December 1962, inclusive) on the comparison of atomic frequency standards located in seven laboratories in the United States, Europe, and Canada, using the VLF signals of GBR (16 kc/s), Rugby, England, and NBA (18kc/s), Balboa, Canal Zone. Each laboratory observes the accumulated difference in phase over a 24-hr period (the same for all laboratories, or nearly so) between its own standard (either laboratory or commercially constructed) and the received VLF signal. A statistical analysis was designed to separate the observations at each laboratory into three components: (a) long-term mean differences among the atomic standards; (b) estimates of the standard deviations, $\hat{\alpha}_i$, at each receiving station; and (c) estimates of the transmitter standard deviations, $\hat{\tau}$. Each $\hat{\alpha}_i$ includes receiver fluctuations, propagation effects perculiar to the path, and measurement uncertainties; $\hat{\tau}$ includes the transmitter fluctuations and propagation effects common to all paths.

The study shows that $\hat{\alpha}_i$ at each receiver varied from a low of 0.39×10^{-10} units of fractional frequency (that is, 0.39 parts in 10^{10}) (GBR data) at LSRH to a high of 1.97×10^{-10} (GBR data) at NRC with an average for all stations of 1.01×10^{-10} measured against GBR and 0.99×10^{-10} when measured against NBA. Also, the average $\hat{\tau}$ for GBR is 1.26×10^{-10} and for NBA is 0.68×10^{-10}. Finally, it is shown that: (1) the means of the frequencies of the seven individual laboratories agreed with the grand mean of these seven laboratories to within ± 2 parts in 10^{10} for the 18-month period, and (2) the laboratory-type standards agreed with their grand mean to within ± 1 part in 10^{10}.

1. Introduction

The agreement between atomic frequency standards of varied construction in many laboratories distributed widely over the world is noteworthy. This agreement establishes confidence in such atomic devices as standards of time and provides a basis for defining an atomic second [NBS, 1964]. This present paper tests the agreement between atomic frequency standards through the medium of VLF radio signals and derives measures of their individual precisions.

The atomic frequency standards of seven laboratories located in the United States, Europe, and Canada were compared by means of a fairly complete statistical analysis of data gathered and exchanged over an 18-month period, July 1961 through December 1962. Each laboratory operates one or more atomic standards, which may be either laboratory designed and constructed or commercially constructed, and makes daily measurements of the received phase of stabilized VLF signals from stations GBR and NBA. Each then reports the deviations of the frequencies of the received signals from nominal (i.e., the rated frequency as defined by its own atomic standard). The reported values are 24-hr averages centered at about the same value of UT.

Six of the laboratories involved are: Centre National d'Études des Télécommunications (CNET), Bagneux, Seine, France; Cruft Laboratories (CRUFT), Harvard University, Cambridge, Mass.; Laboratoire Suisse de Recherches Horlogères (LSRH), Neuchatel, Switzerland; National Bureau of Standards (NBS), Boulder, Colo.; National Physical Laboratory (NPL), Teddington, Middlesex, England; National Research Council (NRC), Ottawa, Ontario, Canada. Also included are the data obtained by the U.S. Naval Observatory (NOB), Washington, D.C., which obtains a "mean atomic standard" by using weighted results from nine laboratories including the above six [Markowitz, 1962].

A number of comparisons of atomic frequency standards by radio transmissions, VLF transmissions in particular, have already been published [e.g., Pierce, 1957; Essen, Parry, and Pierce, 1957; Holloway, Mainberger, Reder, Winkler, Essen, and Parry, 1959; Pierce, Winkler, and Corke, 1960; Markowitz, 1961; Richardson, Beehler, Mockler, and Fey, 1961; Essen and Steele, 1962; Mitchell, 1963; Markowitz, 1964]. The summary statistics of these papers have been primarily mean differences and standard deviations of differences. In addition, Mitchell analyzed data from pairs of laboratories to separate out standard deviations associated with each laboratory and with the transmitter. The present paper provides an analysis similar to Mitchell's applicable to any number of laboratories simultaneously.

[1] A condensed version of this paper was presented at the URSI XIV General Assembly in Tokyo, Japan, September 1963. [Morgan, Blair, and Crow, 1965.]

2. Stabilized Very-Low-Frequency Transmissions Used

The stabilized VLF transmissions of GBR (16 kc/s), Rugby, England, and NBA (18 kc/s), Balboa, Panama Canal Zone, were used by all the laboratories concerned to obtain the comparison data. The VLF transmitters are directly controlled by oscillators, which require regular periodic calibration and adjustment, and give transmitted stabilities (standard deviations of fractional frequency) of the order of 1 or 2 parts in 10^{10}. The transmitted carrier frequencies are held as constant as possible with reference to an atomic standard but are offset in frequency so that the transmitted time pulses may be kept in closer agreement with the UT−2 scale. The amount of fractional frequency offset is determined in advance for each year by the Bureau International d l'Heure, Paris, France, through cooperative efforts of several astronomical observatories throughout the world, and is based on the assumed value of the cesium resonance of 9,192,631,770 c/s.

3. Brief Description of Measurement Techniques

Figure 1 shows the locations of the laboratories participating in these studies and the radio transmission paths to each from GBR and NBA. Each laboratory maintains one or more atomic frequency standards, makes daily measurements of GBR and NBA, and reports the deviation of the received VLF signals from nominal (as indicated by the local atomic frequency standards). Table 1 lists the location, type, and stated accuracy of such standards at the receiving laboratories. Usually the received phase of each transmission is recorded in terms of a local, reference quartz oscillator which, in turn, is calibrated periodically by an atomic frequency standard.

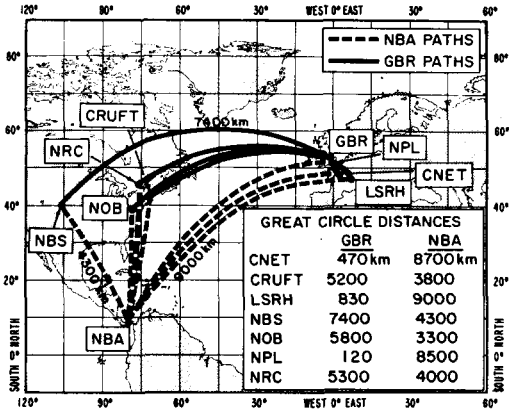

FIGURE 1. *Location of transmitters and receiving laboratories.*

Table 1. Characteristics of Laboratory Atomic Standards

(These are not complete. In particular, the averaging time with which the accuracy or precision should be associated is not listed.)

Laboratory	Abbreviation	Approximate Geographic Location	Type of Atomic Standard	Reported Accuracy x 10^{-10}	Reported* Precision x 10^{-11}	Reference for Accuracy and Precision	Method of Distributing Results by Laboratory Concerned
Centre National d'Études des Télécommunications Bagneux, Seine, France	CNET	48° 48' N 2° 19' E	Cs Beam (Atomichron #107)	+2.2 (Sys. Dev. from Avg. of 6 labs)	2-3	Decaux [1963]	L'ONDE Electrique and monthly circulation
Cruft Laboratories Harvard University Cambridge, Mass., USA	CRUFT	42° 22' N 71° 6' W	Cs Beam (Atomichrons #202; #112)	5 (Mfg.'s guarantee)	2	Pierce [1963]	Monthly circulation
Laboratoire Suisse de Recherche Horlogère Neuchatel, Switzerland	LSRH	47° 00' N 6° 57' E	Cs Beam	0.3	2.7	Kartaschoff [1962]	Observatoire de Neuchatel Bulletin Série c - monthly
National Bureau of Standards Boulder, Colorado, USA	NBS (USFS) (U. S. Frequency Standard)	40° 00' N 105° 16' W	Cs Beam	0.1	0.2	Beehler et al. [1962]	NBS - FM monthly report*** from Frequency-Time Dissemination Research Section
National Physical Laboratory Teddington, Middlesex England	NPL	51° 25' N 0° 20' W	Cs Beam	0.3	?	Essen & Steele [1962], NPL [1963; 1964]	Electronic Technology and monthly circulation
National Research Council Ottawa, Ontario, Canada	NRC	45° 25' N 75° 43' W	Cs Beam	3**	-	Kalra [1961]	Monthly circulation
U. S. Naval Observatory Washington, D. C., USA	NOB	38° 55' N 77° 39' W	Cs Beam (weighted average of 9 Cs resonators including Atomichrons)	0.2	-	Markowitz [1962]	Time Service Bulletins and weekly circulation

*Standard deviation is often but not always specified.

**The term "stability" was used, so that this result perhaps should be in the "precision" column.

***About 10 per cent more days of data were used in the present analysis than was reported in the FM monthly reports.

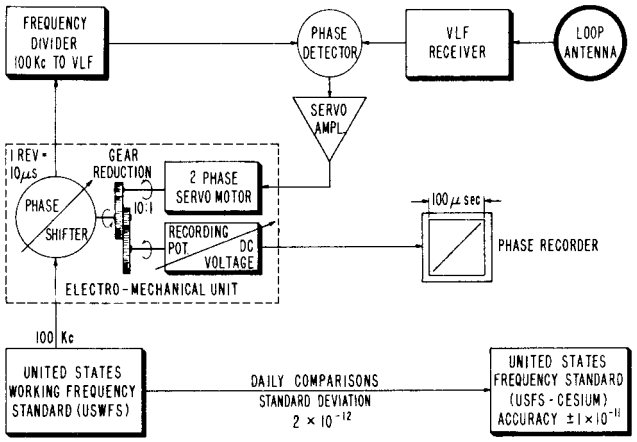

FIGURE 2. *Block diagram of typical VLF phase comparison at NBS, Boulder, Colo.*

One prevalent VLF measuring system employs a phase-lock receiver such as shown in the simplified diagram of figure 2 [Morgan and Andrews, 1961]. In such a system the servodriven phase-shifter continuously phase locks a synthesized signal from the local standard to the received VLF signal. A linear potentiometer, connected to a constant direct voltage, generates the voltage analog of the phase-shifter position. The sensitivity of the voltage analog recorder is determined by the gear ratio between the potentiometer shaft and the phase-shifter shaft. The overall frequency bandwidth of a typical phase-lock servosystem is in the range of 0.01 to 0.001 c/s. The maximum fractional frequency difference between an incoming signal and the local standard that may be tracked is usually near 5 parts in 10^8 (or a change of about 3 μsec per minute).

The measuring system of figure 2 (located at NBS) produces phase records of width 4.5 in. for the full scale sensitivity of 100 μsec, with coordinate lines at intervals of 2 μsec. The time scale, controlled by the recorder speed, normally provides 1/4 in. per 20 min, which is the interval between coordinate lines. Measurements on the phase records are made during the time the propagation path is sunlit and phase fluctuations are minimal. The duration of such a quiet period varies with the seasons; it ranges, however, from about 2 hr to 8 or 10 hr. (The standard deviation of phase fluctuations in NBA recordings at NBS during the daytime was found to be several tenths of a μsecond for a series of 20-min measurements taken over a 7-hr period.)

The error of observing the accumulated phase at each laboratory has not been completely evaluated; any measurement system, however, introduces measurement error. The measuring system may also introduce a smoothing or averaging effect, especially if it produces a continuous record. Such smoothing may reduce fluctuations of interest, from frequency standards and propagation in the present case, as well as measurement error. Fluctuations of periods as short as 5 min are visible on the NBS records; this implies that the averaging time of the system is of the order of 2 min or less. Consequently, only a negligible proportion of the accumulated phase difference over 24 hr could be averaged out.

The phase records from the system of figure 2 are read to the nearest μsec. (They could be read more closely, but the improvement might be marginal relative to the other errors.) The resulting maximum reading error of 0.5 μsec corresponds to 6 parts in 10^{12} over a 24-hr period. Taking account of the two independent readings, initial and final, needed to produce the 24-hr increment in phase and assuming a uniform distribution of errors up to the maximum, leads to the figure of 0.05 parts in 10^{10} for the standard deviation of the fractional frequency due to reading error. This is a contribution to the estimated standard deviation $\hat{\alpha}_i$ of the local atomic standard defined in section 4 and evaluated in figures 5 and 6, but it is an order of magnitude less than the total. There may be appreciable measurement error beyond the reading error. No attempt has been made to survey the measurement errors of the laboratories other than NBS.

The reported frequency values, obtained from phase measurements at each laboratory, represent 24-hr averages centered at the same value of UT, 0300 UT, except for one set of values—those reported by NBS for NBA transmissions. These were centered at 0600 UT to avoid diurnal side effects during the winter sunrise periods.

4. Methods of Statistical Analysis

The purpose of the statistical analysis is to attempt to separate the relative observations at each laboratory into components associated with: (a) the long-term mean differences between the atomic standards; (b) effects of the fluctuations of the receiving system, propagation effects peculiar to the particular radio path, and measurement errors; and (c) fluctuations of the transmitter signals and propagation effects common to all the radio paths.

The daily values of fractional frequency differences were placed into a matrix with the columns representing laboratories and the rows representing days. Each matrix contained one quarter of a year of data, so that there were six matrices included in the 18-month period of study. Each matrix is regarded in the analysis as a sample of observations from an infinite ensemble or population of daily values from the given laboratories. The method required that no data be missing in any cell of the matrix; therefore, when any laboratory omitted a daily value, the complete row of data for all laboratories was discarded. This admittedly reduced the amount of usable data, but the average number of days remaining per quarter, about 40, is believed to be sufficient.

The analysis of the relative frequency observations at several receiving laboratories into components associated with each laboratory standard and the transmitter can be accomplished in several ways, of which a relatively simple one will be described. The expectation of a random variable, or average over a

population, will be denoted by $E[\ ]$. This and other statistical concepts may be found in books such as that by Cramér [1946].

Let k be the number of receiving laboratories and n the number of days that observations are made by each laboratory. Let x_{ij} be the observed fractional difference in frequency of received and local standard signals, in parts in 10^{10}, at the ith receiving laboratory on the jth day ($i=1, 2, \ldots, k$; $j=1, 2, \ldots, n$). The observations x_{ij} include (1) any systematic differences between the ith local standard and the oscillator used by the transmitter; (2) fluctuations associated only with the ith standard; (3) fluctuations associated only with the transmitter oscillator, and (4) radio propagation fluctuations. Thus we can represent x_{ij} by the equation

$$x_{ij}=\mu_i+a_{ij}+t_j (i=1, 2, \ldots, k; \quad j=1, 2, \ldots, n), \tag{1}$$

where

μ_i = systematic (long-term) mean fractional frequency difference at the ith receiver (i.e., $\mu_i=E[x_{ij}]$;

a_{ij} = daily fluctuations of fractional frequency difference associated with the ith receiver on the jth day, in particular fluctuation of its standard but including also propagation effects peculiar to the ith path and measurement errors;

t_j = daily fluctuation of the transmitted signal, including any effects, propagation in particular, common to all received signals.

Thus $E[a_{ij}]=E[t_j]=0$, and we assume that a_{ij} and t_l are uncorrelated, so that $E[a_{ij}t_l]=0$. Likewise we assume that $E[a_{ij}a_{hl}]=0$, $i\neq h$ or $j\neq l$, and $E[t_jt_l]=0$, $j\neq l$.

The systematic mean frequency difference μ_i is easily estimated by the sample mean at the ith receiver,

$$\hat{\mu}_i=x_{i.}=\frac{1}{n}\sum_{j=1}^{n}x_{ij} (i=1, 2, \ldots, k), \tag{2}$$

where the circumflex accent denotes "estimate of." It is known that $\hat{\mu}_i$ is a best estimate in the sense that it is an unbiased estimate of μ_i and has variance less than that of any other unbiased estimate that is a linear combination of the observations.

Following in part the notation of Mitchell [1963], we let α_i be the "true" (long-term) standard (root-mean-square) deviation of the a_{ij}, associated with the ith receiver, and τ the true standard deviation of the t_j, associated with the transmitter. Variance being defined as the square of a standard deviation, we may for brevity refer to α_i^2 as the ith receiver variance and τ^2 as the transmitter variance. Let σ_i be the true standard deviation of the observations x_{ij} at the ith receiver. Then it follows from (1) and the above assumptions that

$$\sigma_1^2=\alpha_1^2+\tau^2,\ \sigma_2^2=\alpha_2^2+\tau^2,\ \ldots,\ \sigma_k^2=\alpha_k^2+\tau^2. \tag{3}$$

The purpose of further analysis is to estimate α_1, α_2, . . . α_k, and τ from the kn observations x_{ij}. Let the sample variance of the n observations from the ith receiver be denoted by

$$s_i^2=\frac{1}{n-1}\sum_{j=1}^{n}(x_{ij}-\bar{x}_{i.})^2. \tag{4}$$

Since s_i^2 is an unbiased estimate of σ_i^2, substitution in (3) gives k equations for the $k+1$ unknowns $\hat{\alpha}_1$, $\hat{\alpha}_2$, . . ., $\hat{\alpha}_k$, $\hat{\tau}$, where $\hat{\alpha}_i^2$ and $\hat{\tau}^2$ are unbiased estimates of α_i^2 and τ^2. The one required additional equation is furnished by calculating the means

$$\bar{x}_{.j}=\frac{1}{k}\sum_{i=1}^{k}x_{ij} (j=1, 2, \ldots, n) \tag{5}$$

over all k receivers for each day and then calculating the sample variance of these averages,

$$s_0^2=\frac{1}{n-1}\sum_{j=1}^{n}(\bar{x}_{.j}-\bar{\bar{x}})^2, \tag{6}$$

where $\bar{\bar{x}}$ is the mean of all kn observations. It can be shown that s_0^2 is an unbiased estimate of

$$\sigma_0^2=\tau^2+\frac{1}{k^2}(\alpha_1^2+\alpha_2^2+\ldots+\alpha_k^2). \tag{7}$$

Solving (3) and (7) and substituting estimates for true values, we obtain the unbiased estimates

$$\hat{\tau}^2=\frac{k}{k-1}\left(s_0^2-\frac{1}{k^2}\sum_{i=1}^{k}s_i^2\right), \tag{8}$$

$$\hat{\alpha}_i^2=s_i^2-\hat{\tau}^2 (i=1, 2, \ldots, k). \tag{9}$$

For $k=2$, that is, two receivers, the estimates (8) and (9) reduce essentially to Mitchell's estimates [1963].

The theoretical precisions of the estimates (8) and (9) have been derived under the assumption of independence of the measurements from day to day; it is hoped to include formulas for these precisions in a further paper, along with approximations for the degree of dependence. The precision of $\hat{\alpha}_i$ (and of $\bar{x}_{i.}$) would appear in theory to be improved by using all observations available at the ith receiver (including those on days when other receivers provide no data) to calculate s_i^2, but s_0^2 can be obtained only by using days common to all receivers.

The above model for separating $\hat{\alpha}_i$ and $\hat{\tau}$ is in effect included in that of Grubbs [1948] for separating measurement errors of several instruments from the product variability which the instruments are measuring.

5. Discussion of Results

Mean values. The mean fractional differences in frequency recorded at each receiver from both GBR and NBA were calculated for each month and for the entire 18-month period, using all the daily observations.

Likewise a grand mean over all months and receivers was found for GBR to be -130.06 parts in 10^{10} relative to the assumed cesium resonance frequency of 9,192,631,770 c/s. The corresponding grand mean for NBA was -129.78. The 18-month means, $\bar{x}_{i.}$, deviations from grand mean, $\bar{x}_{i.} - \bar{x}$, and standard deviations, s_i, of daily recorded values over the 18-month period are listed in table 2 for GBR and in table 3 for NBA.

The mean deviations of individual laboratories from the grand mean range from about $+2$ to -1 parts in 10^{10} measured against either transmission and in general appear to be statistically significantly different from 0 due to the large number of observations. The statistical significance cannot be greater than that based on regarding each daily observation as statistically independent of those for other days (whereas in fact there is some autocorrelation). Based on this assumption and the standard deviations and numbers of daily observations in tables 2 and 3, the standard deviations of the means range from 0.04 to 0.19 (parts in 10^{10}), and it would follow that all values of $\bar{x}_{i.} - \bar{x}$ except those for NPL in tables 2 and 3 would be significantly different from zero at the 5 percent probability level.

However, a more refined test of significance of differences of means of the "common" data is possible by means of a two-factor analysis of variance with standards and days as factors, which eliminates the transmitter and common propagation variation (and hence also any autocorrelation due to these) [Cramér, 1946, pp. 543–546]. This more refined test still neglects the effect of any autocorrelation in individual standards. If this neglect is kept in mind, it is still impressive that all such tests result in significance beyond the 0.1 percent (0.001) probability level. Hence it is believed that even if any autocorrelation in individual standards is accounted for, the values of $\bar{x}_{i.} - \bar{x}$ will prove to be significantly different from zero. In other words, the observed average differences of standards from their grand mean are concluded to be real systematic differences, though a few standards differ little in pairs, like NOB and NPL.

The reality of the differences between laboratories is further shown by the mean deviations from the grand mean over the years 1959–60 calculated from the data of Essen and Steele [1962] and given in the "ES" column of tables 2 and 3. These indicate that systematic differences between many of the laboratories continued over the years 1959 or 1960 through 1962.

The difference in grand mean frequencies received from GBR and NBA from all data reported in the 18-month period, -0.28 parts in 10^{10}, is replaced by -0.15 parts in 10^{10} when only the "common" (C) data are considered. If a formal Student t test of the difference of two means is made using standard errors derived from (6), the difference -0.28 is found to be significant at the 5 percent probability level, whereas the difference -0.15 is not. Since significance of the differences would be lessened by taking account of the effect of autocorrelation, no significant average difference between the transmitters GBR and NBA is claimed.

The monthly means of "common" data for each laboratory are shown in figures 3 and 4; these figures

Table 2. Means and Standard Deviations of Frequencies Compared with GBR

July 1961 - December 1962

(unit, 1 part in 10^{10})

Atomic Standard	No. of Days		$\bar{x}_{i.}$ Mean		$\bar{x}_{i.} - \bar{x}$ Deviation from Grand Mean			s_i Standard Deviation of Daily Values	
	T	C	T	C	T	C	ES	T	C
CNET	478	278	-128.27	-128.14	+1.79	+1.68	+1.52	1.73	1.77
CRUFT	388	136	-131.14	-130.60	-1.06	-0.78	-1.91	1.87	1.39
LSRH	422	244	-130.99	-130.86	-0.93	-1.04	-1.22	1.48	1.49
NBS	469	244	-130.70	-130.50	-0.64	-0.68	-	1.56	1.55
NOB	486	278	-130.28	-130.16	-0.22	-0.34	-	1.49	1.51
NPL	476	278	-129.93	-129.77	+0.13	+0.05	+0.41	1.59	1.66
NRC	458	222	-129.37	-129.17	+0.69	+0.65	+1.39	2.19	2.35
GRAND MEAN, $\bar{x}$			-130.06	-129.82					

Note: 1. In applying the notation $\bar{x}_{i.}$, s_i, and $\bar{x}$ to all data, the definitions in equations (2), (4), and that for $\bar{x}$ under equation (6) are understood to be extended to unequal numbers of days, n_i, for each receiver.

2. T indicates total data reported; C indicates data common to stations within quarters. ES denotes mean deviations from grand mean (with signs appropriately reversed) calculated from Table 2 of Essen and Steele (1962) for the years 1959-60, except that only last half of 1960 is given for LSRH and NRC.

Table 3. Means and Standard Deviations of Frequencies Compared with NBA

July 1961 - December 1962

(unit, 1 part in 10^{10})

Atomic Standard	No. of Days		$\bar{x}_{i.}$ Mean		$\bar{x}_{i.} - \bar{x}$ Deviation from Grand Mean			s_i Standard Deviation of Daily Values	
	T	C	T	C	T	C	ES	T	C
CNET	427	197	-127.90	-127.78	+1.88	+1.89	+1.72	1.43	1.38
CRUFT	385	131	-131.00	-130.72	-1.22	-1.05	-1.45	1.66	1.66
LSRH	437	197	-130.74	-130.66	-0.96	-0.99	-1.05	1.14	1.17
NBS	369	161	-130.26	-130.33	-0.48	-0.66	-	0.99	0.96
NOB	474	197	-129.89	-129.94	-0.11	-0.27	+0.53	0.89	0.88
NPL	375	102	-129.98	-129.95	-0.20	-0.28	-0.17	1.43	1.45
NRC	363	113	-128.75	-128.37	+1.03	+1.30	-	1.96	1.97
GRAND MEAN, $\bar{x}$			-129.78	-129.67					

Note: 1. In applying the notation $\bar{x}_{i.}$, s_i, and $\bar{x}$ to all data, the definitions in equations (2), (4), and that for $\bar{x}$ under equation (6) are understood to be extended to unequal numbers of days, n_i, for each receiver.

2. T indicates total data reported; C indicates data common to stations within quarters. ES denotes mean deviations from grand mean (with signs appropriately reversed) calculated from Table 2 of Essen and Steele (1962) for July-December 1960.

show that not only are observations for individual days missing for particular laboratories but even series for entire months or more. The variability of monthly means is visibly greater than that of the 18-month means reported above, but variations in laboratory data common to all laboratories for a given transmitter are apparent. Similar results were given by Mitchell [1963, fig. 4] for the same period for LSRH, NBS, and NPL.

Standard deviations. The standard deviations s_i of tables 2 and 3 are estimates of the σ_i of (3). They tend not to vary greatly for a given transmitter because each contains the common variation of the transmitter and common propagation effects. The standard deviation of the common effects, $\hat{\tau}$, is plotted for each quarter and each transmitter in figures 5 and 6. The component standard deviation associated with each receiver, $\hat{\alpha}_i$, is also similarly plotted. A comparison of $\hat{\alpha}_i$ for each receiver as determined from both the GBR and NBA transmissions is plotted in figure 7.

The quarterly receiver (local standard) and transmitter (NBA and GBR) standard deviations are all roughly of the same order of magnitude, 1 part in 10^{10}, but there is substantial variation, between transmitters, from receiver to receiver, and from quarter to quarter. Thus the quarterly $\hat{\alpha}_i$ vary from a low of zero to a high of 2.24 (parts in 10^{10}), and the quarterly $\hat{\tau}$ vary from 0.28 to 1.01 for NBA and from 0.73 to 1.48 for GBR.

Whether these variations are significant, that is, reflect differences among the true values α_i and τ, or are only to be expected statistically in estimates from small samples, can be judged from the standard deviations of the estimates, which have as yet been evaluated only under the assumption of independence from day to day. Even under this assumption each α_i and τ is estimated from all 18 months of data with 95 percent confidence limits roughly 15 percent below and 20 percent above the estimates $\hat{\alpha}_i$ and $\hat{\tau}$, except that the four smaller $\hat{\alpha}_i$ obtained from GBR data (Cruft, NBS, LSRH, NOB) have larger percentage errors, with 95 percent confidence limits up to 100 percent above or below the estimate $\hat{\alpha}_i$. The effect of day-to-day dependence is to extend these limits even farther. However, it is evident that some receivers have consistently, and hence probably significantly, lower values of α_i than others.

Since the above confidence limits show that much of the fluctuating behavior of $\hat{\alpha}_i$ and $\hat{\tau}$ is not significant, it is reasonable to compute weighted root-mean-square average values of $\hat{\alpha}_i$ and $\hat{\tau}$ over all quarters; these averages are tabulated in figures 5 and 6. The smallest average $\hat{\alpha}_i$ are 0.51 when measured against NBA transmissions, obtained for the Naval Observatory, and 0.39 when measured against GBR, obtained for LSRH. The corresponding largest average $\hat{\alpha}_i$ are 1.82 and 1.97, both obtained for the National Research Council of Canada.

It is of interest to compare these results with those obtained by Mitchell [1963] over the same six quarters of 1961 and 1962. He compared three receivers, NBS (USFS), NPL, and LSRH, in pairs using both NBA and GBR transmissions. The comparative re-

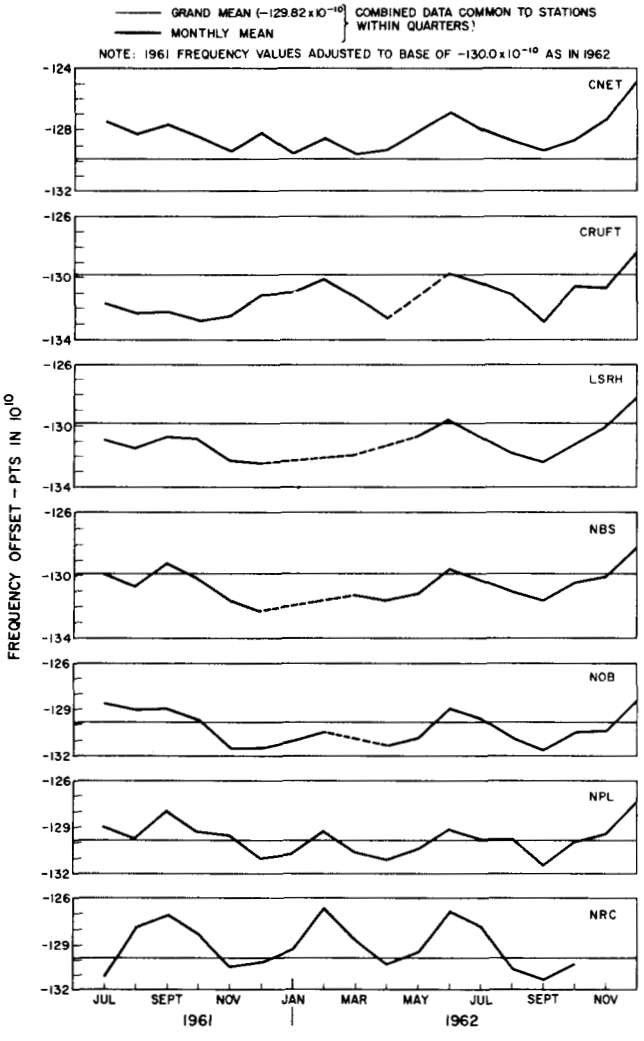

FIGURE 3. *GBR monthly means versus grand mean of all laboratory standards.*

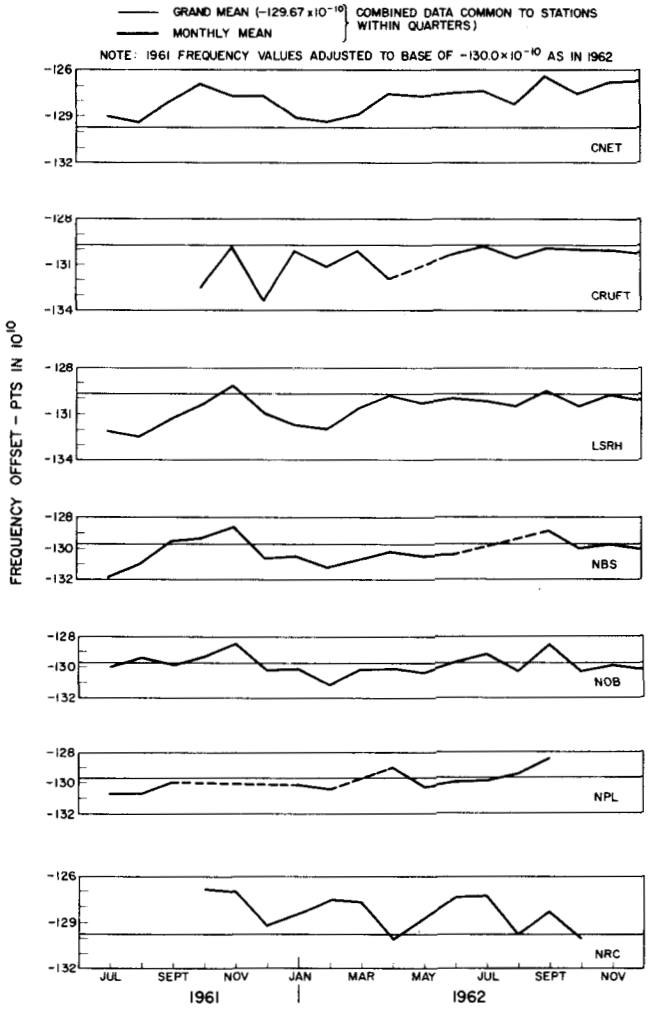

FIGURE 4. *NBA monthly means versus grand mean of all laboratory standards.*

sults are as follows (standard deviations in parts in 10^{10}):

		Present analysis		Mitchell (average)
		GBR	NBA	
NBS (USFS)	$\hat{\alpha}_1$	0.66	0.63	0.7
LSRH	$\hat{\alpha}_2$	.39	.63	.6
NPL	$\hat{\alpha}_3$	1.00	1.24	1.1
Transmitter	$\hat{\tau}$	1.26	0.68	1.1 (GBR), 0.7 (NBA)

The check between the two sets of results is almost complete, to the expected precision. This is not surprising, since essentially the same data for these receivers are used. However, the present analysis should tend to yield a more precise estimate of τ by virtue of using 5 to 7 receivers for its estimation, whereas Mitchell's method should tend to yield more precise values of s_i by virtue of having fewer missing data in the pair-by-pair treatment (although a general treatment is possible using all data). The average number of daily pairs of observations per quarter used by Mitchell was about 60, whereas the number of daily sets of observations per quarter used herein is about 40. The principal justification of the present method is the simultaneous analysis of data from any number of receiving laboratories.

Since the $\hat{\alpha}_i$ include propagation as well as local standard fluctuations and $\hat{\tau}$ includes possibly fluctuations from sources other than the transmitter oscillator, it is desirable to attempt further separation. This should be possible from internal estimates of precision of local standards but has not yet been carried through. Mitchell [1963] estimated the standard deviation of transmission time fluctuations in transatlantic comparisons of cesium-controlled oscillators at 0.2×10^{-10}, which would leave the standard devia-

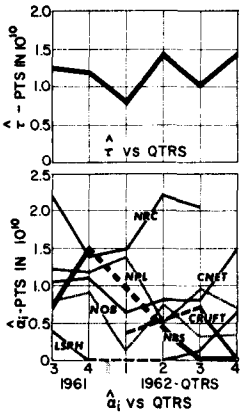

$\hat{\tau}$ AVERAGE* = 1.26 x 10^{-10}
FROM ALL STATIONS/6 QTRS

$\hat{\alpha}_i$ AVERAGE* PER STATION AS FOLLOWS:

STA.	AV. $\hat{\alpha}_i$	Nº QTRS	Nº DAYS
CNET	1.05×10^{-10}	6	278
CRUFT	0.41×10^{-10}	3	136
LSRH	0.39×10^{-10}	5	244
NBS	0.66×10^{-10}	5	244
NOB	0.62×10^{-10}	6	278
NPL	1.00×10^{-10}	6	278
NRC	1.97×10^{-10}	5	222

* rms WEIGHTED AVERAGE WITH WEIGHTS EQUAL TO NUMBER OF DAYS PER QUARTER MINUS 1.

FIGURE 5. *Estimated standard deviations, $\hat{\alpha}_i$, of receiver variations (including noncommon propagation variations) and estimated standard deviation, $\hat{\tau}$, of variations of transmitter GBR (including common propagation variations).*

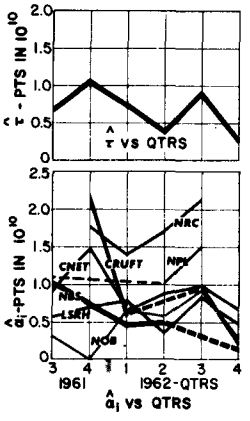

$\hat{\tau}$ AVERAGE* = 0.68 x 10^{-10}
FROM ALL STATIONS/6 QTRS

$\hat{\alpha}_i$ AVERAGE* PER STATION AS FOLLOWS:

STA.	AV. $\hat{\alpha}_i$	Nº QTRS	Nº DAYS
CNET	0.95×10^{-10}	6	197
CRUFT	1.13×10^{-10}	4	131
LSRH	0.63×10^{-10}	6	197
NBS	0.63×10^{-10}	5	161
NOB	0.51×10^{-10}	6	197
NPL	1.24×10^{-10}	3	102
NRC	1.82×10^{-10}	4	113

* rms WEIGHTED AVERAGE WITH WEIGHTS EQUAL TO NUMBER OF DAYS PER QUARTER MINUS 1.

FIGURE 6. *Estimated standard deviations, $\hat{\alpha}_i$, of receiver variations (including noncommon propagation variations) and estimated standard deviation, $\hat{\tau}$, of variations of transmitter NBA (including common propagation variations).*

tions estimated above essentially unaltered (due to the combination by squares).

The mathematical model (1) implies the condition that all daily measurement intervals are simultaneous, whereas the NBS measurements of NBA transmissions were offset 3 hr from all the others, which were simultaneous. An upper bound to the effect of this offset can be derived by assuming that the transmitted fluctuations during the 3-hr offset are uncorrelated with the transmitted fluctuations for which they substitute at the other end of the 24-hr period. The maximum expected effect on $\hat{\tau}$ is to multiply it by the factor $[1 - 1/(8k^2)]^{1/2}$, where k is the number of receiver stations, so that to correct for the effect one would divide by this factor. Since k is 5 or 6, the maximum effect on $\hat{\tau}$ is 0.25 percent, or 0.002×10^{-10} for the $\hat{\tau}$ average, a negligible amount. The effect on $\hat{\alpha}_i$ varies somewhat with $\hat{\alpha}_i$ but is at most 0.43 percent for any $\hat{\alpha}_i$ average.

As noted earlier, the method used for estimating α_i and τ requires restriction of the data to those measurements common to all stations compared within a given quarter. To estimate the effect of such restriction, a comparison was made of the column (station) variances for both restricted (C) and total reported data (T) of each station for the entire 18-month period for both the GBR and NBA transmissions. These data are plotted in figure 8, and the square roots or standard deviations are given in tables 2 and 3 for the GBR and NBA data, respectively. As can be seen there is close agreement in all instances except Cruft-GBR; this exception can be attributed to having only three quarters represented in the restricted data. A new estimate of α_i, say $\hat{\alpha}_i'$, was calculated on the basis of the relative increase or decrease of the restricted data in terms of the total reported data for the overall 18-month period. The previously derived transmitter variance estimate, $\hat{\tau}^2$, was employed in these calculations. For the NBA data the new $\hat{\alpha}_i'$ differed from -5 to $+6$ percent from the previous estimate, $\hat{\alpha}_i$. With the exception of the Cruft data, the new $\hat{\alpha}_i'$ for the GBR data differed from -11 to $+3$ percent from $\hat{\alpha}_i$. The $\hat{\alpha}_i$ calculated from the total reported data for the Cruft GBR data was about three times the $\hat{\alpha}_i$ computed from the quarterly restricted data. This new value, however, is much more in line with that computed from the Cruft NBA data. Thus, with the exception of the Cruft GBR data, the restriction to data days common within quarters has no disturbing effect on the estimation of the atomic standard deviations α_i.

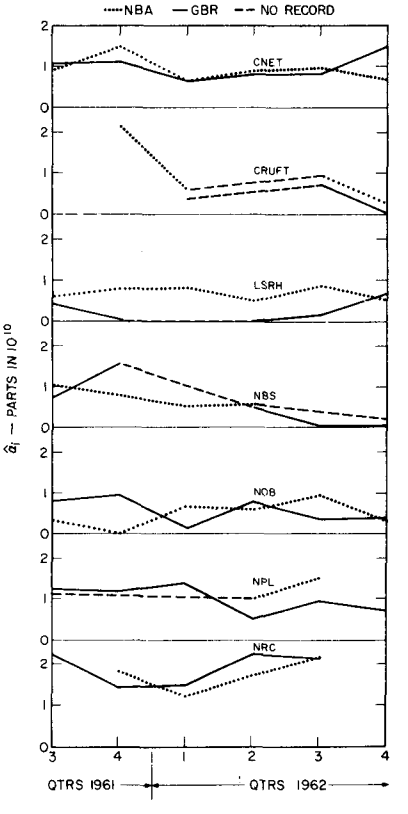

FIGURE 7. *Comparison of each laboratory standard $\hat{\alpha}_i$ using either GBR or NBA signals.*

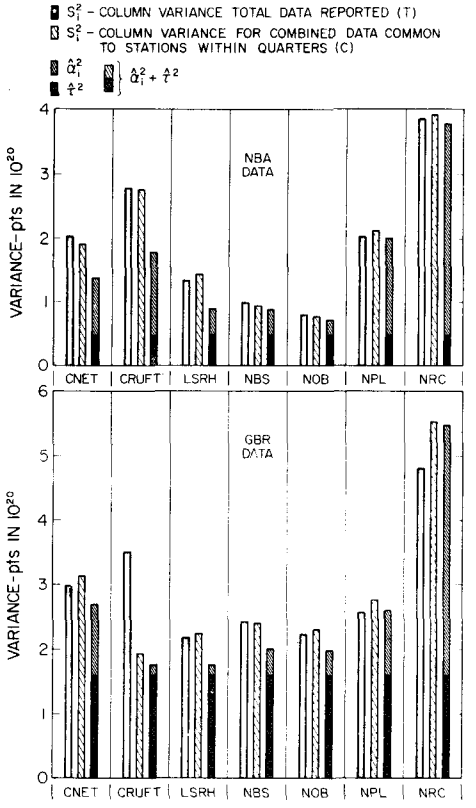

FIGURE 8. *Comparison of variances for GBR and NBA data groups.*

Another factor affecting the estimates of α_i and τ is the elimination of possible variation of mean values from quarter to quarter. Hence, figure 8 includes the $\hat{\alpha}_i^2+\hat{\tau}^2$ values which were determined from the averaged quarterly values of $\hat{\alpha}_i^2$ and $\hat{\tau}^2$ in figures 5 and 6. This sum would equal s_i^2, the column variance for each station based on data days common to all stations within quarters, in accordance with (9), except for the fact that the column variances plotted in figure 8 were obtained for the overall 18-month period and include variability due to differences among the quarterly means. It is therefore seen that the quarterly means contribute appreciable variation in 7 out of the 14 comparisons; the greatest percentage excess of s_i^2 over $\hat{\alpha}_i^2+\hat{\tau}^2$, occurring for LSRH-NBA, is 60 percent, which would correspond to 26 percent increase in both $\hat{\alpha}_i$ and $\hat{\tau}$ if their ratio is unchanged, that is, to 0.81 and 0.86 part in 10^{10}. The second greatest percentage increase in $\hat{\alpha}_i$ and τ would be 24 percent, for Cruft-NBA. The other estimated changes in $\hat{\alpha}_i$ and $\hat{\tau}$ due to variability of quarterly means are all increases but range down to a negligible 0.5 percent.

6. Possible Future Improvements in VLF Measurements

One improvement envisioned for VLF phase comparison measurements is the use of the higher-power WWVL (20 kc/s) transmissions (1 to 2 kW radiated power) which commenced from the new NBS Fort Collins Standard Radio Transmitting Site in August 1963 [Richardson, 1964; Blair and Morgan, 1965].

A large increase in coverage is anticipated over the lower-power broadcasts so that many more laboratories may be able to measure their standards directly in terms of the USFS.

The periodic adjustment of quartz crystal oscillators at VLF transmitters may cause undesired phase changes in the transmitted signals. Phase changes in the transmitting antenna may also occur due to the effects of the weather and cause changes [Watt-Carter and Corke, 1961] of at least 1 part in 10^{10}. By means of a VHF radio link from the USWFS (United States Working Frequency Standard) to the VLF transmitter and a continuously phase-locked servosystem [Milton et al., 1962] these sources of error have been eliminated from the WWVL broadcasts.

Another improvement in comparing atomic standards, and especially for separating out propagation errors, now appears possible through the use of portable quartz crystal clocks. Their advantages are their low power consumption, small weight and size, reliability, and excellent stability. A 2.5–Mc/s oscillator, with a stability (standard deviation) of a few parts in 10^{11}, is employed in an experimental portable clock at NBS. The effects of temperature, vibration, and environmental and voltage changes are being carefully evaluated, so that optimum results may be obtained. Preliminary results obtained with portable clocks are very promising, and further developmental work on them is under way at NBS.

We wish to acknowledge the contributions of Catherine Barclay, Joan Berube, and Kenneth Yocum in the data processing; and, to thank the contributing laboratories listed in table 1 who so kindly permitted the use of their data in this paper. We also express thanks to Carole Craig for the careful typing of this paper.

7. References

Beehler, R. E., W. R. Atkinson, L. E. Heim, and C. S. Snider (Dec. 1962), A comparison of direct and servo methods for utilizing cesium beam resonators as frequency standards, IRE Trans. Instr. **I-11**, 231–238.

Blair, B. E., and A. H. Morgan (1965), Control of WWV and WWVH Standard Frequency Broadcasts by VLF and LF Signals, Radio Sci. J. Res NBS **69D**, No. 7, 915–928.

Cramér, H. (1946), Mathematical Methods of Statistics (Princeton University Press, Princeton, N.J.).

Decaux, B. (June 1963), private communication.

Essen, L., J. V. L. Parry, and J. A. Pierce (Sept. 14, 1957), Comparison of caesium resonators by transatlantic radio transmission, Nature **180**, 526.

Essen, L., and J. McA. Steele (Jan. 1962), The international comparison of atomic standards of time and frequency, Proc. IEE **43B**, No. 3752M, 41–47.

Grubbs, F. E. (1948), On estimating precision of measuring instruments and product variability, J. Am. Statist. Assn. **43**, 243–264.

Holloway, J., W. Mainberger, F. H. Reder, G. M. R. Winkler, L. Essen, and J. V. L. Parry (Oct. 1959), Comparison and evaluation of cesium atomic beam frequency standards, Proc. IRE **47,** 1730–1736.

Kalra, S. N. (Mar. 1961), Frequency measurement of standard frequency transmissions, Can. J. Phys. **39,** 477.

Kartaschoff, P. (Dec. 1962), Operation and improvements of a cesium beam standard having 4-meter interaction length, IRE Trans. on Instr. **I-11,** 224–230.

Markowitz, W. (April 1961), Définition, détermination et conservation de la seconde, Comité Consultatif pour la Définition de la Seconde auprès du Comité International des Poids et Mesures, 2e session, Annexe 2 (Gauthier-Villars & Cie, Paris), 45–51.

Markowitz, W. (December 1962), The atomic time scale, IRE Trans. on Instr. **I-11,** 239–242.

Markowitz, W. (July–August 1964), International Frequency and Clock Synchronization, Frequency, **2,** No. 4, 30–31.

Milton, J. B., R. L. Fey, and A. H. Morgan (March 17, 1962), Remote phase control of radio station WWVL, Nature **193,** No. 4820, 1063–1064.

Mitchell, A. M. J. (June 22, 1963), Frequency comparison of atomic standards by radio links, Nature **198,** No. 4886, 1155–1158.

Morgan, A. H., and D. H. Andrews (April 1961), Méthodes et Techniques de contrôle des ondes kilométriques et myriamétriques aux Boulder Laboratories, Comité Consultatif pour la Définition de la Seconde auprès du Comité International des Poids et Mesures, 2e session, Annexe 6 (Gauthier-Villars & Cie, Paris), 68–72.

Morgan, A. H., B. E. Blair, and E. L. Crow (1965), International comparison of atomic frequency standards via VLF radio signals, Progress in Radio Science 1960–1963, **1,** Radio Standards and Measurements, (Elsevier Publishing Company, Amsterdam/London/New York, 1965), 40.

NBS (Dec. 1964), World sets atomic definition of time, NBS Tech. News Bull. **48,** 209–210.

NPL (1963), Report for year 1962, standards division, electrical and frequency measurements, NPL (Teddington, England), 217.

NPL (1964), Report for year 1963, standards division, electrical and frequency measurements, NPL (Teddington, England), 216, 217.

Pierce, J. A. (June 1957), Intercontinental frequency comparisons by very low frequency radio transmission, Proc. IRE **45,** 794–803.

Pierce, J. A., G. M. R. Winkler, and R. L. Corke (September 10, 1960), The 'GBR Experiment': A trans-Atlantic frequency comparison between caesium-controlled oscillators, Nature **187,** No. 4741, 914–916.

Pierce, J. A. (July 1963), private communication.

Richardson, J. M., R. E. Beehler, R. C. Mockler, and R. L. Fey (April 1961), Les étalons atomiques de fréquence au N.B.S., Comité Consultatif pour la Définition de la Seconde auprès du Comité International des Poids et Mesures, 2e session, Annexe 5 (Gauthier-Villars & Cie, Paris), 57–67.

Richardson, J. M. (January 1964), Establishment of new facilities for WWVL and WWVB, Radio Sci. J. Res. NBS **68D,** No. 1, 135.

Watt-Carter, D. E., and R. L. Corke (September 23, 1961), VLF transmitting system phase transfer variations, Nature **191,** No. 4795, 1286.

Note added in proof. A mistake in the calculation of the rms weighted average $\hat{\alpha}_i^2$ for LSRH using GBR transmissions has been discovered; it should be 0.0156 rather than 0.156, resulting in an rms average $\hat{\alpha}_i$ of 0.12 rather than 0.39 (parts in 10^{10}). The change should be made in the abstract, the table on page 911, and the table within figure 5. The apparently considerable change is of doubtful significance because, as stated on page 910, the confidence limits on this α_i are about 100 percent above and below the estimate $\hat{\alpha}_i$. In fact the further data for 1963 and 1964 (502 days) yield 0.43, and when these are combined with the 244 days of data in 1961 and 1962, the overall rms average $\hat{\alpha}_i$ is 0.36.

(Paper 69D7–524)

RADIO SCIENCE Journal of Research NBS/USNC-URSI
Vol. 69D, No. 7, July 1965

Control of WWV and WWVH Standard Frequency Broadcasts by VLF and LF Signals

B. E. Blair and A. H. Morgan

National Bureau of Standards, Boulder, Colo.

(Received October 21, 1964; revised January 22, 1965)

Since 1961 the NBS VLF and LF signals have improved the calibration and frequency control of the WWV (Maryland) HF broadcasts. Similarly, better control of the WWVH (Hawaii) HF broadcasts was achieved in early 1963 by monitoring the NBS VLF broadcasts in terms of the WWVH control oscillator. In mid 1963 WWVL (20 kc/s) and WWVB (60 kc/s) were relocated from two sites near Boulder, Colo., to a single site near Ft. Collins, Colo., and the transmitter power for both broadcasts was increased several fold. These higher powered broadcasts resulted in more precise control of both HF broadcasts. Through the VLF and LF signals the 24-hr average frequency values of WWV are related to the United States Frequency Standard (USFS) within a few parts in 10^{11}.

This paper describes the NBS low-frequency broadcasts, the method of using them to control and calibrate the HF broadcasts, and gives an analysis of the precision of frequency control obtained at WWV over a 21-month period. An appendix discusses the short-term phase stabilities and diurnal phase shifts observed in the low-frequency signals at WWV and WWVH, and examines the accuracy-limiting effects of propagation path characteristics and background noise levels in such received signals.

1. Introduction

The accuracy of the United States Frequency Standard (USFS) has improved greatly over the last four decades from approximately one part in 10^4 in 1920 to a present value of 5 parts in 10^{12}. One way such technological advances have met the needs of science and industry is through the NBS standard frequency broadcasts, as graphically shown in figure 1. The abrupt change in the slope of the curve in 1957 was due to a technological "breakthrough" culminating in commercial, atomic frequency standards. Laboratory models of atomic (cesium-beam) frequency standards were developed and built at NBS and in 1960 two such units became the basis of the USFS [Mockler et al., 1960]; continued improvements followed [Beehler et al., 1962] and are reflected in figure 1. By late 1961 the NBS low power WWVL (20 kc/s) and

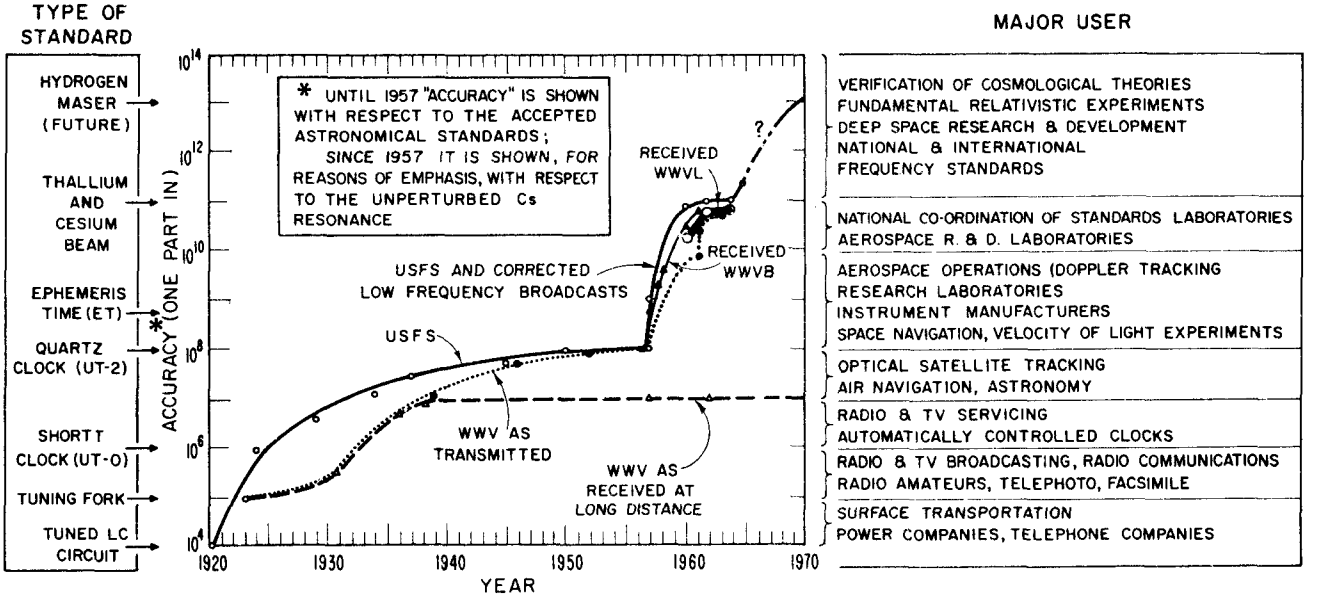

FIGURE 1. *Improvements in the accuracy of the USFS and its dissemination.*

WWVB (60 kc/s) broadcasts disseminated the USFS with a transmitted accuracy of several parts in 10^{11} (fractional frequency units) through control by transfer (working) atomic frequency standards. Regularly published corrections relate such values to the USFS as shown in figure 1.

Prior to 1961, WWV was calibrated at NBS, Boulder, by comparing received WWV time signals with the USFS, and was frequency controlled on the basis of these calibrations. This technique, briefly described in a previous publication [Watt et al., 1961], will not be discussed here except to note that the precisions achieved, using the HF time signals alone, were several parts in 10^{10} for 30-day running averages. Similarly, until early 1963, calibration and control of the WWVH broadcasts relied on the WWV time signals as received in Hawaii. Because of the inadequacy of this method, a new technique was introduced at WWV in January 1961, using the NBS low-frequency signals received from WWVL and WWVB. It is well known that the received phase stability of VLF and LF radio signals at large distances is several orders of magnitude better than that of HF [Pierce, 1958; Crombie et al., 1958; Watt et al., 1961] and that the VLF signals propagate over large distances with small attenuation. Thus, such characteristics of the NBS low-frequency signals enabled the calibration and control of the HF broadcasts with a precision nearly equivalent to the stability of atomic frequency standards.

The improvement in the WWV frequency control is evident in figure 2 where the monthly means are plotted for 4 years. The variances, S^2, are pooled estimates obtained from monthly daily values which are based on running averages for the indicated periods. For the period 1960 to 1963 the standard deviations, S, decrease from 1.2 to 0.31 parts in 10^{10}. For WWVH the improvement is a little less as evidenced by figure 3. Clearly shown, however, is the smaller variation in the WWVH monthly means that occurred with the initiation of VLF control in March 1963.

This paper will describe the NBS standard frequency broadcasts; the method of using the NBS low-frequency signals for calibration and control of the HF broadcasts; the relative agreement between the received 20 and 60 kc/s signals at WWV; and the effects of increased WWVL and WWVB transmission power. Variations in short-term phase stabilities and diurnal phase shifts, observed in low-frequency recordings at WWV and WWVH, are given in the appendix.

2. NBS Standard Frequency Broadcasts

WWVL and WWVB, presently located at Ft. Collins, Colo., lie nearly on a great circle path between WWV at Greenbelt, Md., and WWVH at Maui, Hawaii. WWVH is over twice as far (5300 Km) from Ft. Collins as is WWV (2400 Km). The HF broadcasts of WWV are at 2.5, 5, 10, 15, 20, and 25 Mc/s while those at WWVH are at 5, 10, and 15 Mc/s; characteristics of the NBS radio stations have been given previously [Morgan, 1962 and 1963; Richardson, 1964].

2.1. Role of Frequency Standards in NBS Broadcasts

The frequency reference of the NBS standard frequency broadcasts is the USFS which consists of two cesium beam units [Mockler et al., 1960] designated as NBS–I and NBS–II. Because these do not operate continuously, the U.S. Working Frequency Standard

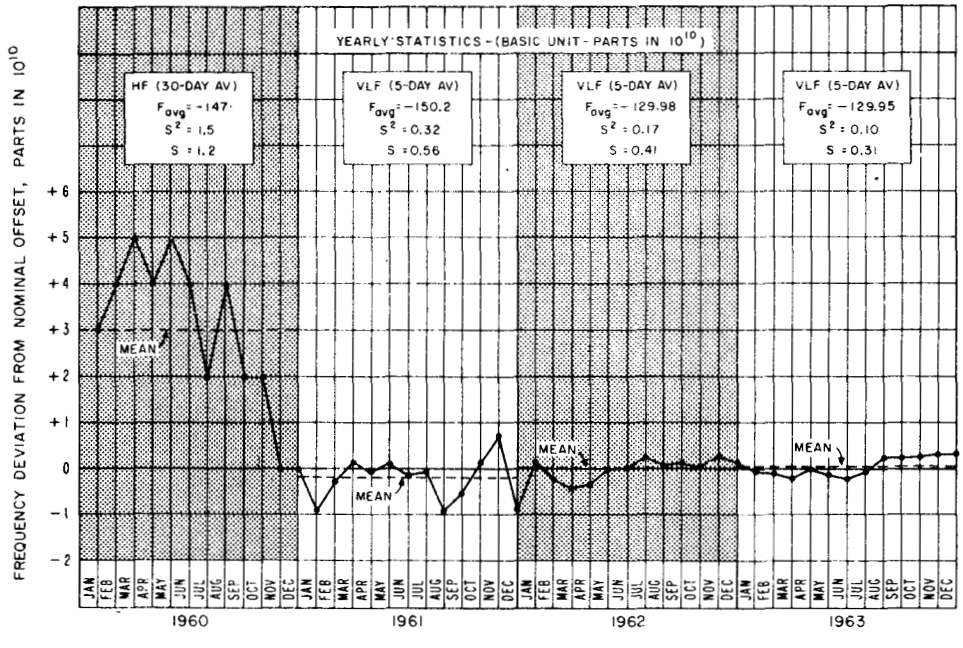

FIGURE 2. *Improvements in the frequency control of WWV.*
(Ordinate in fractional frequency).

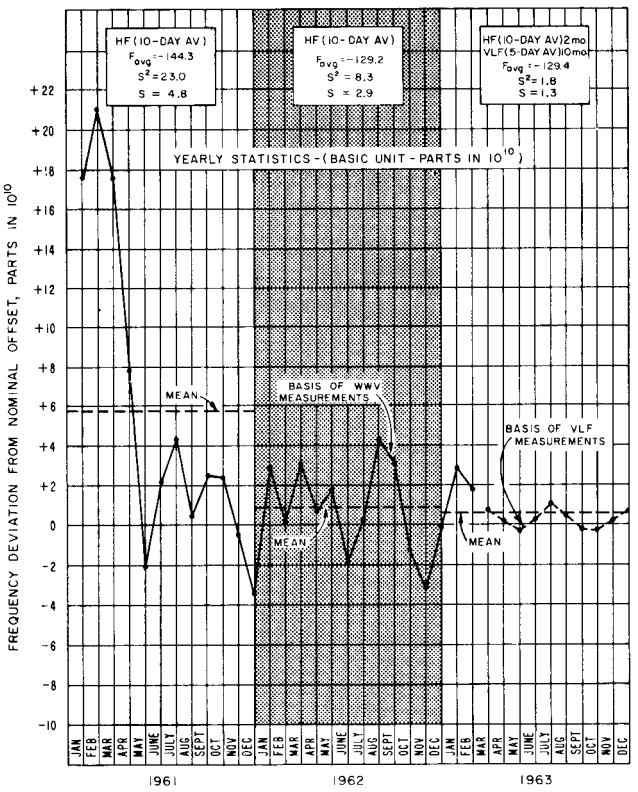

FIGURE 3. *Improvements in the frequency control of WWVH.* (Ordinate in fractional frequency).

(USWFS), consisting of a group of oscillators, provides continuity in the calibration and frequency control of the NBS standard frequency broadcasts. Figure 4 shows the relationship of the USWFS to the USFS and the function of the former in controlling NBS stations WWV, WWVH, WWVL, and WWVB.

To improve the transmitted stability of the 20 kc/s signals, in October 1961 a remote phase-locking system, operating at VHF, was placed into operation between Boulder and WWVL when this station was located at Sunset, Colo. [Fey et al., 1962]. A similar system now controls the low-frequency broadcasts from the new Ft. Collins site [NBS, 1963]. The phase-lock system continuously keeps the transmitted phase of both the WWVL and WWVB signals in agreement with that of the USWFS at the Boulder Laboratories. Such a system corrects for frequency drift of the oscillator which controls the transmitter as well as for phase fluctuations introduced by the transmitter or antenna system in the broadcast signals. Measurements indicate that the transmitted low-frequency stability (standard deviation) is essentially that of the USWFS, which in the case of rubidium standards is equal to or less than 2 parts in 10^{11} [Blair et al., 1965].

2.2. Description of NBS VLF Broadcasts

NBS began broadcasting a low power, standard 20 kc/s on April 5, 1960 [NBS, 1960], from Sunset, Colo. (18 km from NBS, Boulder). This was the first known standard frequency broadcast at 20 kc/s [the specific frequency adopted for such use by the International Telecommunications Union (ITU) in December 1959].

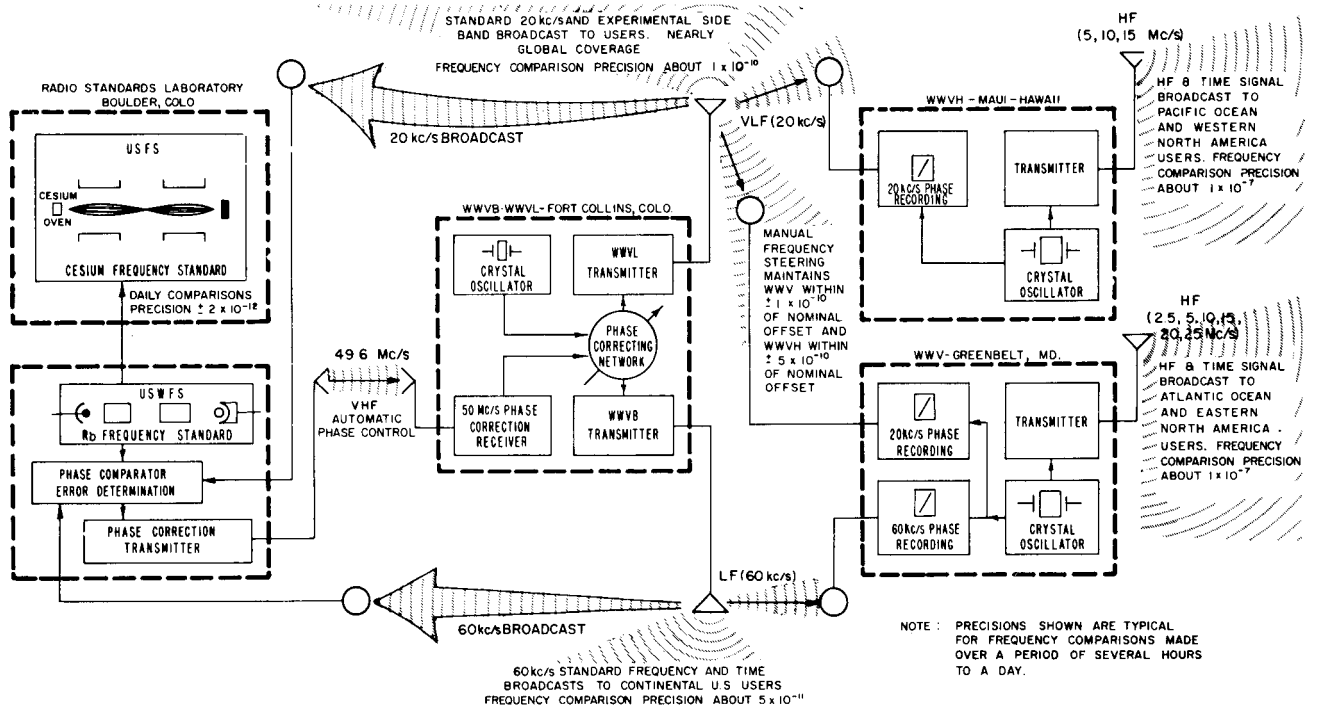

FIGURE 4. *USFS reference and frequency control of NBS standard frequency broadcasts.*

463-560 O - 72 - 22

Great Britain, however, has pioneered in broadcasting standard frequency signals in both VLF and LF bands. The Sunset station operated for nearly 3½ years, and was relocated with modified equipment at Fort Collins, Colo., August 1963 [NBS, 1963; Richardson, 1964]. This new station (WWVL—latitude 40°40′51″ N—longitude 105°03′00″ W) provided a much larger antenna and more powerful transmitter; thus, the radiated power was increased from 15 W to about 1 kW.

2.3. Description of NBS LF Broadcasts

In 1956 a standard 60 kc/s broadcast was begun from the grounds of NBS at Boulder, Colo. [NBS, 1957]. The call letters KK2XEI were used initially but were changed to WWVB in March 1960. Because of the low power (about 2 W radiated) these signals were of limited use. Nevertheless, station WWV received such signals and confirmed the stability of LF signals as propagated over long distances. A rubidium atomic frequency standard directly controlled the 60 kc/s broadcast from August 1961 to June 1963. Casual checks revealed no appreciable errors introduced into the broadcasts through antenna and/or transmitter variations, although the WWVB signals were not continuously phase-locked to the USWFS during this period. On July 5, 1963, WWVB (latitude 40°40′28″ N—longitude 105°02′39″ W) began radiating about 5 kW of power from the new station at Ft. Collins, Colo.

3. Calibration and Frequency Control of the HF Broadcasts

Calibration of the WWV broadcasts since 1961 consists of relating the WWV daily frequency values to the USFS through the NBS low-frequency received signals. For frequency control of the WWV broadcasts, such signals also indicate when adjustments of the controlling oscillator are necessary to maintain the HF broadcast frequency within set limits. (± 1 part in 10^{10} of nominal for WWV). The frequency measurements at the HF stations are obtained with conventional, phase-lock receiving systems [Looney, 1961; Morgan et al., 1961]. The overall effective bandwidth of the tracking-receiver systems employed at WWV in Maryland is about 0.001 c/s, and the sensitivity is between 0.1 and 1 μV. The system can follow a maximum frequency difference of about 2 parts in 10^8 between an incoming signal and the local standard, (i.e., about 1 μsec of equivalent phase difference per minute). At WWVH, in Hawaii, the VLF tracking receiver has an effective bandwidth of 0.006 c/s and a sensitivity near 0.01 μV.

The concept of the frequency control for WWV and WWVH is portrayed also in figure 4. This method of control relies on a manual link between the phase-lock receiving systems and the controlling oscillator at the HF stations. At WWV, the phase of both the WWVL and WWVB signals is recorded continuously in terms of the controlling oscillator; the accumulated phase differences are read daily at 24-hr intervals when the sun is at high noon over the center of the path (1800 UT). At the Boulder Laboratories these observations are used to compute the WWV frequency in terms of the USFS. Such assigned daily values provide the calibration of the WWV broadcasts. To smooth out day-to-day variability, a 5-day running average of the WWV daily frequency is calculated for each day, and such values are published monthly in the PROCEEDINGS—IEEE. The WWVH values are related to the USFS similarly through the WWVL signals.

4. Typical VLF Signal Phase Recordings

Figures 5, 6, and 7 show typical recordings of low-frequency signals as received at stations WWV and WWVH. (NBA signals have been used for spot checks, and a typical recording made at WWV is shown in fig. 5.) It is from such records that the accumulated phase is measured at 24-hr intervals. The diurnal variations shown in these records are of considerable interest. Rapid phase shifts occurring at both sunrise and sunset are caused by changes in the ionospheric-reflection height. (Such height changes have been interpreted through mode theory [Wait, 1962].) The shape of the transitions at 20 kc/s is worth noting. At sunrise, the reflection height begins to drop and the phase of the received signals first decreases by 5 to 10 μsec and then increases to the average daytime value. At sunset an initial decrease is followed by a short increase in phase with a gradual decrease to the nighttime level. Such changes are very regular and repeat with consistency from day to day. This behavior presumably results from mode interference effects at this frequency over this path [Wait, 1963; Crombie, 1964]. Although this is not seen on the 60 kc/s records at WWV, another characteristic frequently appears: one cycle, or an integral multiple of one cycle, of the received signal is lost during the sunrise period. This is shown in the WWVB recordings of June 5 and October 10 in figures 5 and 6. In figure 5 a dashed curve has been drawn, indicating where the analog recording of the phase should have been. Such behavior can result from destructive interference between several rays with changing amplitude and phase [Burtt, 1963]. A similar effect at sunset has been reported for the 60 kc/s signals as received at Austin, Tex. [Tracor, 1964]. Short-term phase stabilities and diurnal phase changes, obtained from low-frequency phase recordings made at WWV and WWVH, are tabulated in the appendix.

5. Relative Agreement Between Received 20 and 60 kc/s Signals—Effects at WWV of VLF and LF Transmission Power

The VLF–LF method of calibration and control is predicated upon the relative phase stability and frequency agreement between the received 20 and 60 kc/s signals. Since frequency is the time rate of change of phase, frequency values may be derived from phase measurements. A discussion of the agreement between the received frequencies, coupled with an

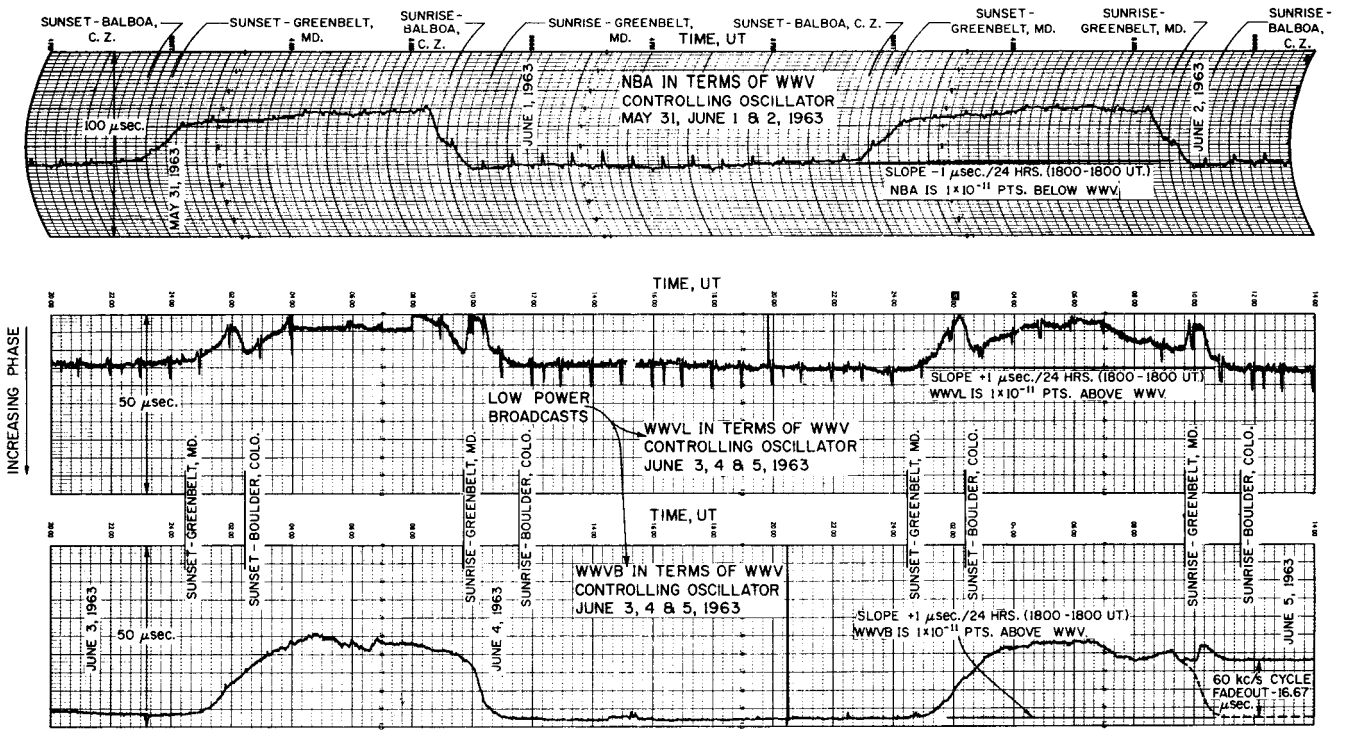

FIGURE 5. *Typical records of NBA, WWVL and WWVB (low power) as received at station WWV–June 1963.*

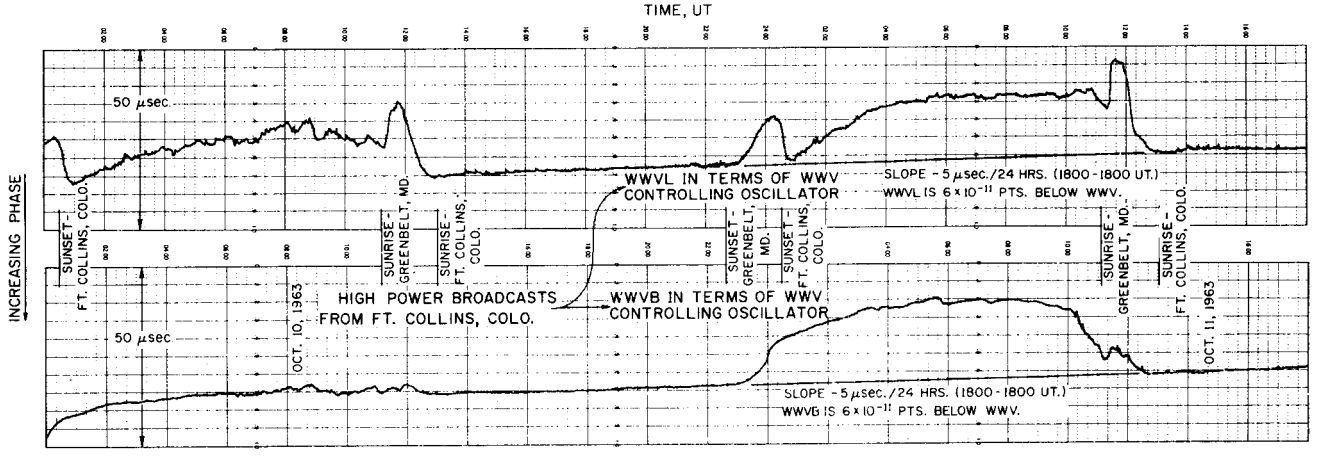

FIGURE 6. *Typical records of WWVB and WWVL (high power) as received at station WWV–October 1963.*

evaluation of the effects of increased transmission power of the Ft. Collins broadcasts, follows.

5.1. Comparison of WWV Frequency in Terms of 20 and 60 kc/s as Received at WWV

The average daily frequency of WWV as determined by received VLF and LF NBS signals is shown in figures 8 and 9 for both low- and high-power transmission periods in October 1962 and 1963, respectively. As can be seen, good agreement exists. For comparison, NBA data are shown in figure 8. In both figures, the variation in the WWVB values is smaller than that for WWVL, and the 1963 combined groupings show a lesser variation than the corresponding 1962 data. Because the same oscillator was used at WWV in both instances, the improvement in the data is believed to result, at least in part, from the higher power signals. The scatter about the least square lines, shown by the standard error of estimate, $S_{y/x}$ [Crow et al., 1960], results presumably from oscillator variations at WWV, with small contribution from propagation effects and

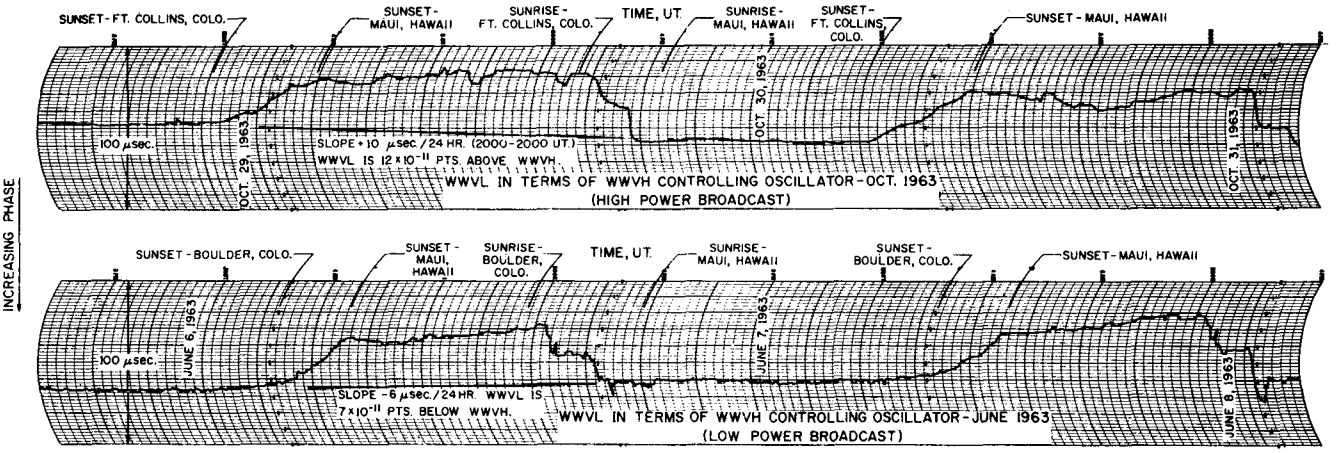

FIGURE 7. *Typical records of WWVL as received at station WWVH (Maui)–June and October 1963.*

measurement errors. Note that in 1963, figure 9, there appears to be a very high correlation between the 20 and 60 kc/s points in the combined plot. Since the WWVL and WWVB broadcasts at Ft. Collins are controlled by a common oscillator, the correlated variation noted in these points, as referred to the same WWV oscillator, is felt to result either from fluctuations in the WWV controlling oscillator, common propagation effects, or both. Such good agreement does not always occur as is shown later in the November–December data.

5.2. Daily Agreement Between Received 20 and 60 kc/s Signals at WWV

The average daily frequency differences between the WWVL and WWVB signals as received at station WWV have been divided into two groups for a 21-month period of study: period 1 covers the low-power broadcasts from April 1, 1962 to June 30, 1963; period 2 includes the high-power broadcasts from July 1 to December 30, 1963. (The low-power 20 kc/s signals and high-power 60 kc/s signals were used to obtain the July 1963 data.) The agreement between WWVL and WWVB as received at WWV is shown by the difference in nominal offset between the two broadcasts.

Figure 10 shows the daily variations in offset frequency differences for the two periods. Figures 11 and 12 give plots of monthly average differences $\bar{X}$, and standard deviations, S_d, for the 21-month period. The variation of these statistics in figures 10 through 12 shows a definite decrease for the period 2 data. Also apparent is the increased variability in November 1962 and November–December 1963. The cause of such variation is unknown at this time, although seasonal propagational effects likely are major contributing factors.

Figure 13 gives histograms of the two data groups. The grand mean offset differences, $\bar{\bar{X}}_1$ and $\bar{\bar{X}}_2$, between WWVL and WWVB as received at WWV are negligible for both levels of power transmission. Still, the period 2 average standard deviation, S_{d2}, reduces to about half that for period 1. (The November 1962 and November–December 1963 data were omitted in computing these statistics on the basis of nonhomogeneity of their variances [Box, 1953].) The lesser variation for period 2 may result from at least three factors: (1) The better signal to noise ratio of the high power Ft. Collins broadcasts permitted more reliable phase tracking at WWV; (2) during period 1 the WWVB signals, although directly controlled by an atomic standard, were not continuously phase-locked to this USWFS. Thus, small offset differences may have existed between these low-power WWVL and WWVB signals as broadcast; and (3) during period 2, as noted before, there was essentially a constant frequency difference between the WWVL and WWVB signals as broadcast.

Superimposed on the histograms in figure 13 are fitted normal curves based on statistics of the observed samples. As can be seen, the general form of the histograms is somewhat similar to that of the normal curve but with a greater central tendency or high frequency of values near the mean. Significant departure from normality was found, as expected, for both periods by a chi² statistical test. In addition, a curve type criterion, β_2, was calculated for each data group. (β_2 is the ratio of the sample 4th moment about the mean to the sample variance squared. This ratio equals 3.0 for the normal distribution.) Values of β_2 equal to 3.5 and 7.5 were obtained for periods 1 and 2 respectively. Such values, greater than 3.0, are in agreement with the concentration of the data about the mean.

The statistical limits shown in figure 10 through 12 are based on a normal distribution and independence of the individual observations. The importance of this latter factor will be considered in subsequent studies, while a discussion of the effects of a nonnormal distribution follows. Figure 10 shows tolerance limits [Crow et al., 1960] for the daily offset differences. Nonparametric tolerance limits [Somerville, 1958], were computed also and gave results not significantly different from those based on a normal distribution. Thus, although the tolerance limits as shown are not strictly justified, they are at least approximately correct.

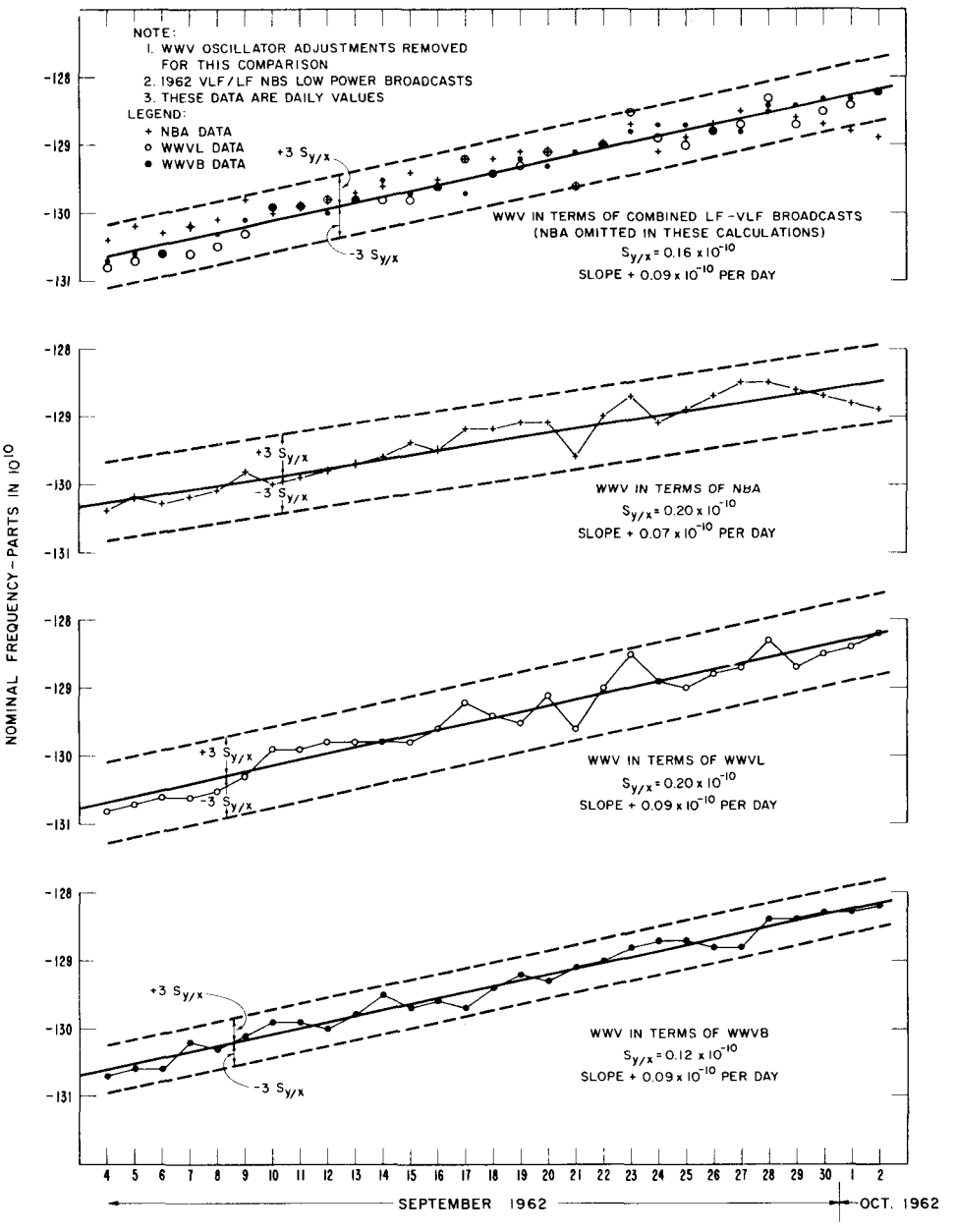

FIGURE 8. *Comparison of VLF/LF determinations of WWV frequency (low power–1962).*

Confidence limits shown in figure 11, about the monthly offset differences, $\bar{X}$, also are believed to be reasonable, since the means of even small samples essentially are normally distributed even if the basic data are not [Davies, 1957]. On the other hand, confidence limits for standard deviations are quite dependent upon a normal distribution of the parent data. Thus, such confidence limits, shown in figure 12, should be used with caution.

6. VLF Measurements at WWVH

The calibration and frequency control of the WWVH broadcasts by the 20 kc/s signals is largely experimental at this time, although significant improvements have been obtained since their introduction in April 1963. In figure 14 the WWVH frequencies, in terms of the WWVL broadcasts, are seen to agree generally with 30-day running averages based on WWV HF meas-

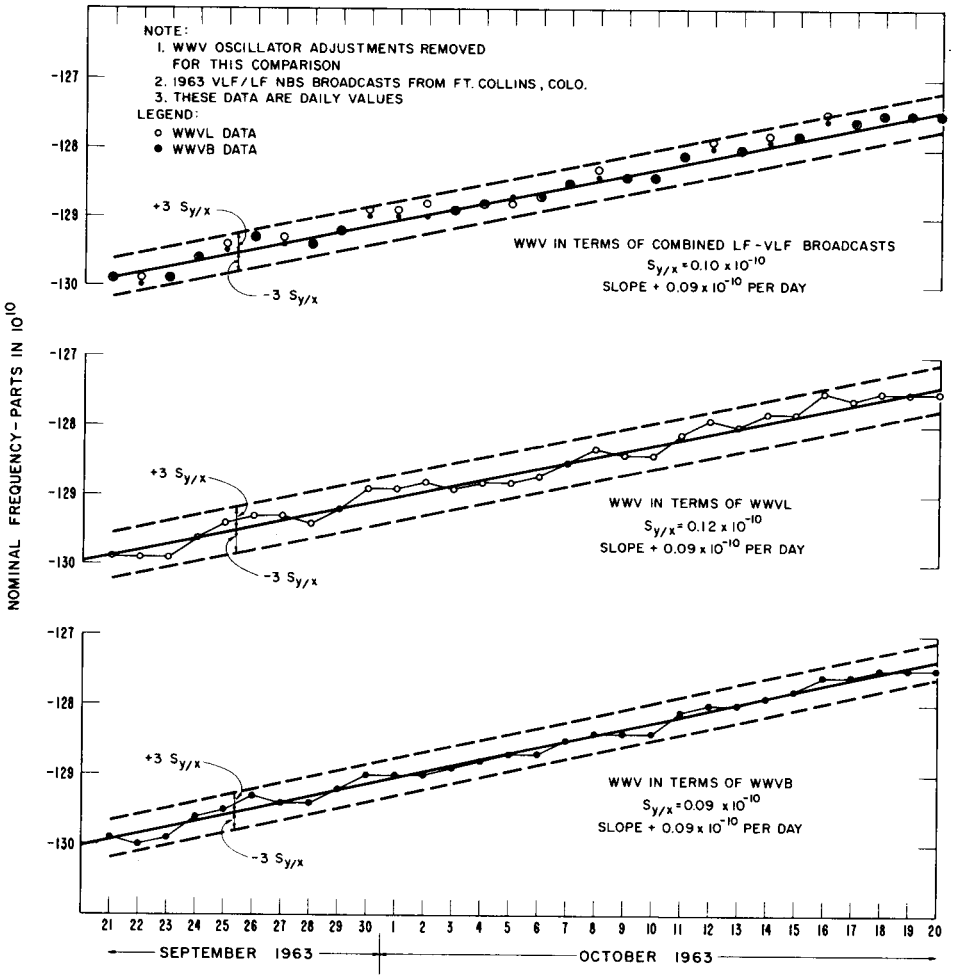

FIGURE 9. *Comparison of VLF/LF determinations of WWV frequency (high power–1963).*

urements for a period in May–June 1963. (The WWV HF values for this same period are included for comparison.) The running average procedure clarifies the general trend of a variable set of measurements sensitive to time by smoothing the short-term, or day-to-day fluctuations. The large daily variations in the WWVH data presumably result from fluctuations in the WWVH controlling oscillator. It is expected that the WWVH broadcasts will eventually have a stability equivalent to that of WWV through the use of the low-frequency signals from Ft. Collins.

7. Calibration and Frequency Control Results

Measurements made at station WWV for a 21-month period of time indicated only negligible bias in the average offset difference between the WWVL and WWVB received signals; also, the standard deviation of the average daily differences was about 1 or 2 parts in 10^{11}. In other words, this was the net effect of all variation producing influences such as propagation effects and instrument errors. Tolerance limits for including 90 percent of the daily variations at WWV with a probability of 95 percent are near ± 4 parts in 10^{11} and such values indicate the calibration uncertainty during this period. The day-to-day frequency variations of the controlling oscillator at WWV are near several parts in 10^{11}. Such fluctuations would be present of course in the WWV transmitted signals.

This method of calibration and frequency control by NBS low-frequency signals would be equally applicable to other HF or similar broadcasts requiring such accuracy. (The HF station ZUO, in South Africa, presently frequency controls its broadcasts by the WWV HF signals [CCIR, 1963].) The dissemination of the USFS through these low-frequency broadcasts provides a readily available reference directly traceable to NBS.

8. Conclusions

Improvement in the NBS HF broadcasts since 1961 has resulted from frequency-steering by the NBS low-

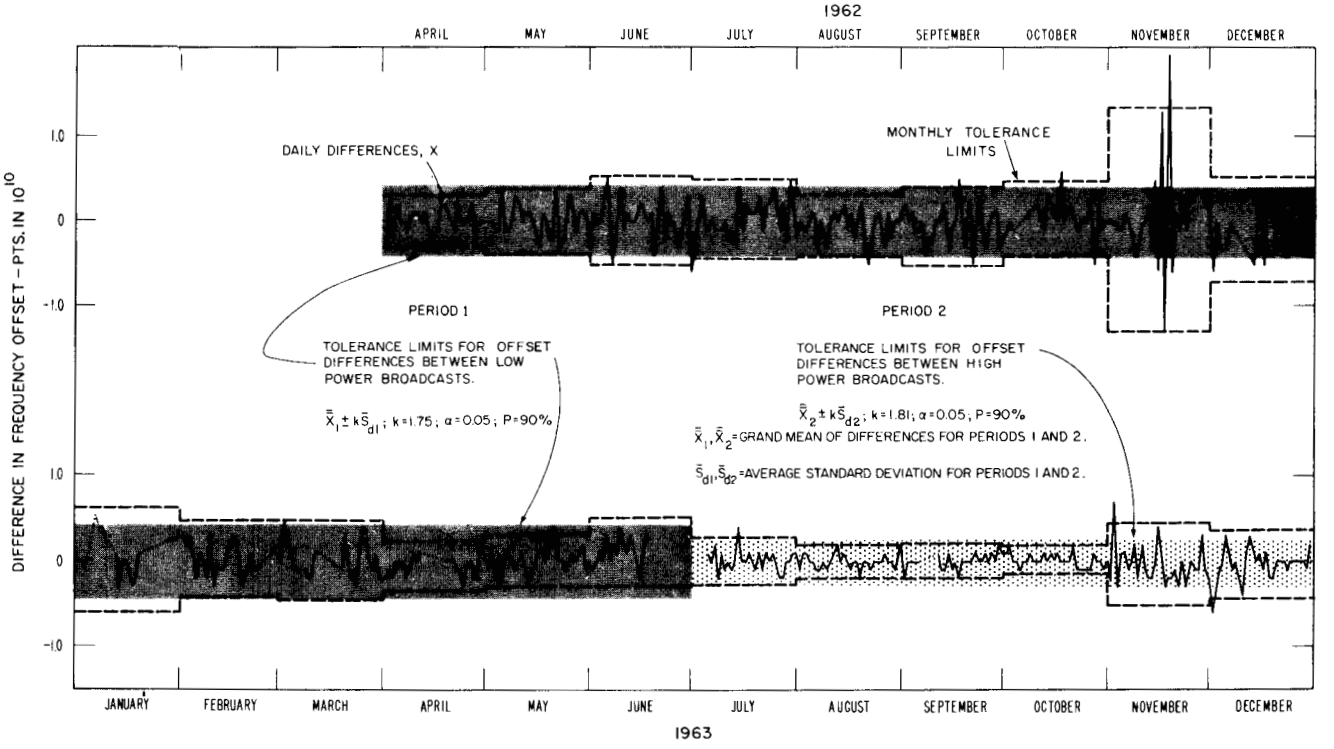

FIGURE 10. *Daily variations in offset differences between WWVL and WWVB as received at station WWV.*

frequency signals. The stability of the HF broadcasts is nearly equivalent to that of the received VLF and LF signals. The higher power broadcasts from Ft. Collins give results at WWV which are less variable and closer to the offset frequency of the USWFS than the former low-power broadcasts. The nonnormality of the WWVL and WWVB difference data was manifested by a strong central tendency about the mean; this, however, with the exception of confidence limits for standard deviations, has small effect on the computed statistical limits. VLF and LF standard frequency broadcasts can be used to control HF broadcasts with a precision of several parts in 10^{11}.

9. Appendix. VLF and LF Propagation Data

In the course of calibrating and controlling the HF broadcasts, VLF and LF propagation data was obtained. This appendix presents a study of the short-term phase stability and diurnal phase shifts observed in low-frequency signals received at WWV and WWVH. Knowledge of propagation variations over diverse paths is a matter of increased concern in fields such as frequency and time dissemination [Looney, 1964] and long-range navigational aids [Pressey et al., 1961; Blackband, 1964].

9.1. VLF and LF Short-Term Phase Stability

The phase stability of some VLF and LF signals was analyzed for several 10-day periods in October 1962 and June/October 1963. The data involved the WWVL, WWVB, and NBA signals, as received at stations WWV and WWVH. Measurements on the phase recordings consisted of fitting a least square line to phase points taken at 1/2-hr intervals for either all daylight or all darkness on the path for a given day; calculating the daily standard error of estimate about this fitted line; and, averaging these daily standard error of estimates to obtain the mean variation, $S_{\text{avg (ph)}}$, for each 10-day period. A summary of these statistics is given in table 1. Several interesting observations can be made from these data: (1) The LF stability appears to be considerably better than that for the VLF measurements during the daytime; (2) the nighttime variations for both frequency bands are comparable; (3) in each frequency band, fluctuations during the daytime are much less than those at night; and, (4) generally, some improvement in phase stability is associated with the NBS high power low-frequency broadcasts.

Phase fluctuations observed at a receiver output result from a combination of effects, due to: (1) The

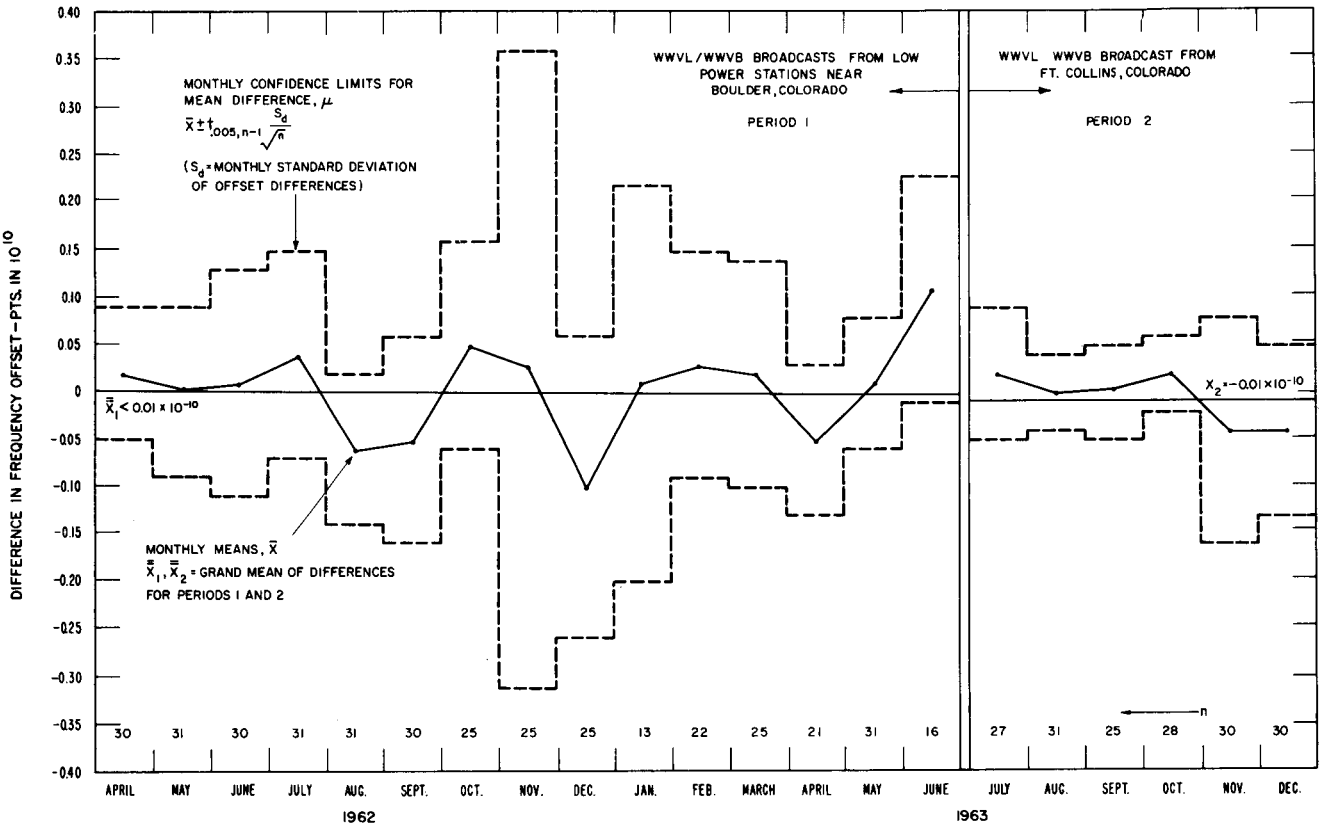

FIGURE 11. *Monthly average offset differences between WWVL and WWVB as received at station WWV.*

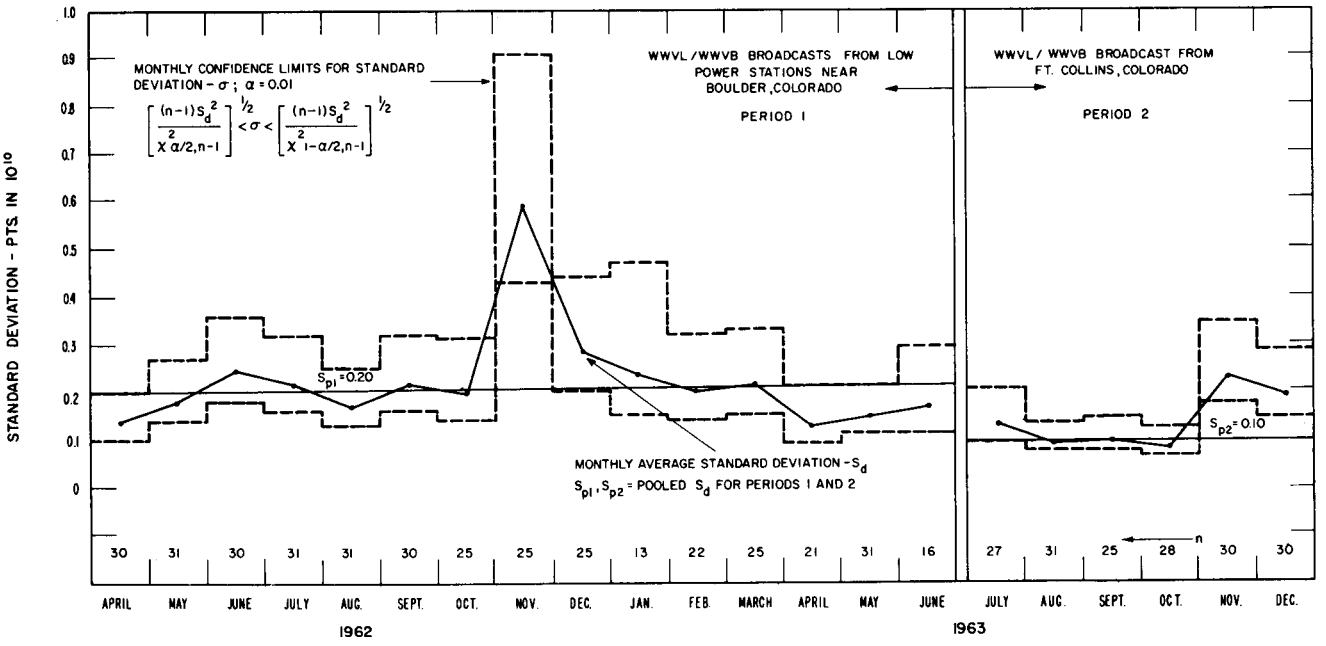

FIGURE 12. *Monthly average standard deviations of offsets between WWVL and WWVB as received at station WWV.*

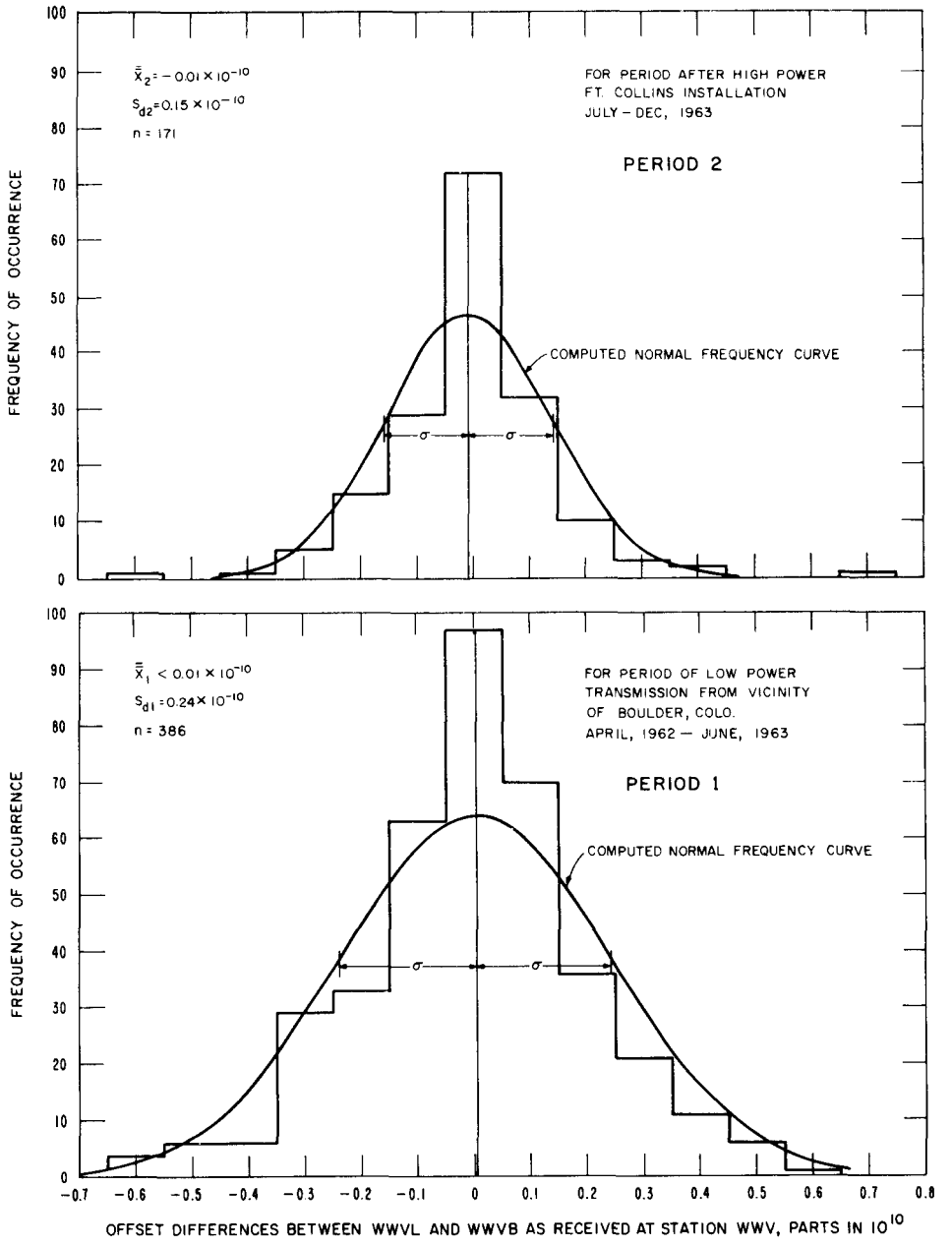

FIGURE 13. *Histograms of WWVL/WWVB offset differences for low power and high power broadcasts.*

transmitting system; (2) the propagation medium; (3) atmospheric and other types of noise; and (4) the receiving system. The standard deviations of short time fluctuations in the transmitted phase of the WWVL and WWVB signals is believed to be about 0.1 μsec. Since the receiving systems employed also introduce phase errors which are believed to be about 0.1 μsec, the total rms instrumentation threshold is near several tenths of a μsec. In view of this, phase fluctuations near this threshold are not believed significant in showing the influence of the other two factors—the propagation path and the received noise. It has been shown [Watt et al., 1959] that this latter factor produces a noise-induced standard deviation of phase, $S_{\text{avg (noise)}}$, where

$$S_{\text{avg (noise)}} \approx \frac{1}{\sqrt{2}\,(C/N)^2}$$

and C and N are the effective carrier and noise power at the phase measuring point in the receiving system. In this paper the phase variations induced by noise refer to this last described factor as distinguished from phase variations caused by propagation factors.

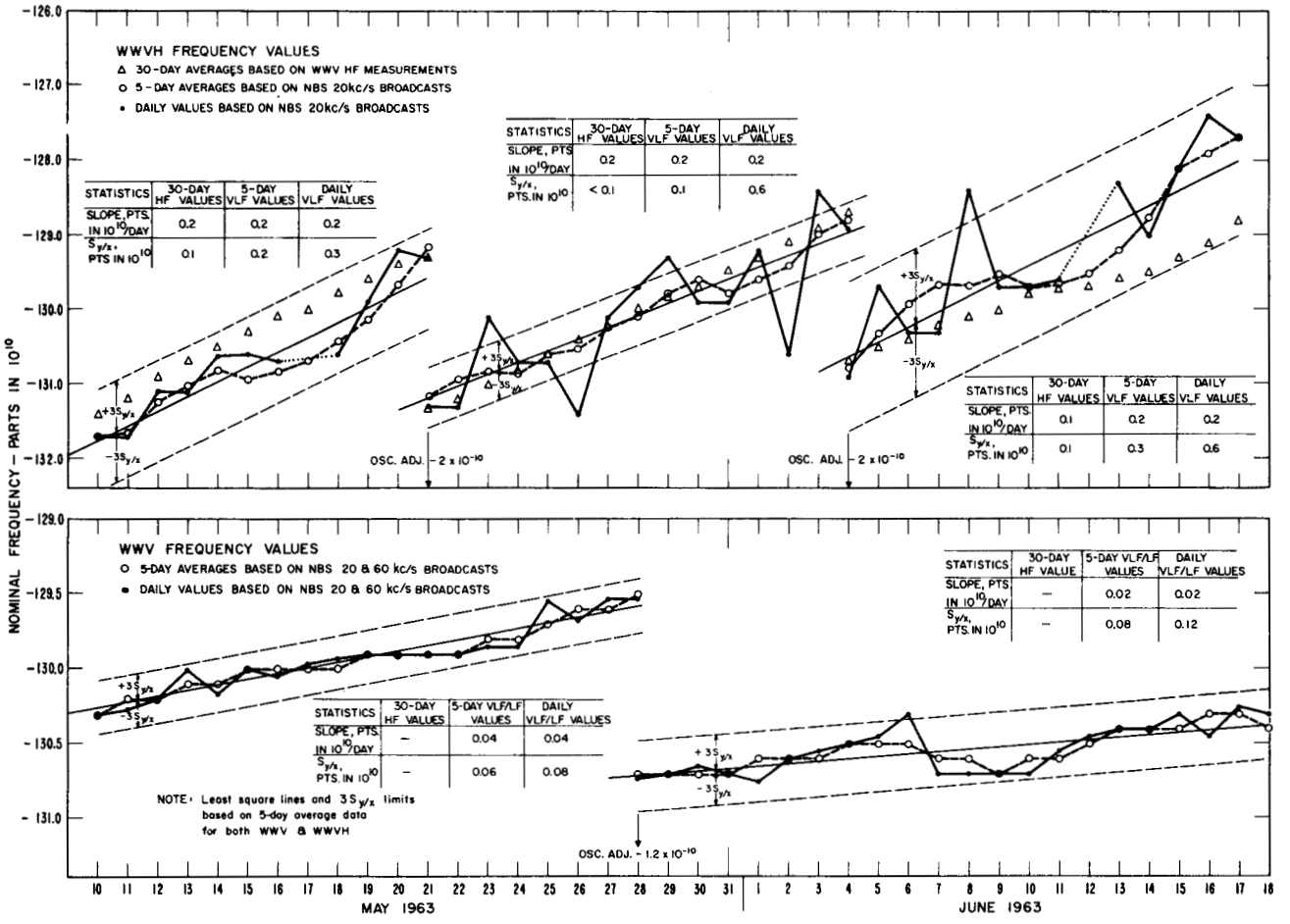

FIGURE 14. *Comparison of running averages and daily values of WWVH and WWV frequencies.*

On the basis of a calculated signal-to-noise ratio for the low-power 20 kc/s broadcast, the standard deviation of the phase attributable to noise is of the order of 0.5 μsec [Watt et al., 1959]. A similar figure was obtained for the low power, 60 kc/s broadcast [Watt, 1964]. Such values seem to be comparable with the records as shown in figures 5 and 6. Because the signal-to-noise ratio is improved by higher radiated power (an increase in power of about 50 and 3000 in the case of the 20 and the 60 kc/s signals respectively), the phase variation contributed by noise should be considerably reduced with the higher power broadcasts from Ft. Collins.

The precision, ϵ, of frequency comparisons with fixed bandwidth at VLF, using techniques employed in these studies has been shown [Watt et al., 1959] to be

$$\epsilon \cong \frac{(N/C)^{1/2}}{\omega T}$$

where N and C are the narrow band noise and carrier powers, respectively, $C/N \gg 1$, $\omega = 2\pi f$, and T is the averaging time, $\epsilon = \frac{\sigma f_d}{f}$ where σf_d is the standard deviation of the frequency difference between the received frequency and the local standard frequency, f. If the precision of the measurement is limited by the carrier-to-noise ratio, then an increase in the carrier level would improve the results, that is, ϵ is reduced. For the WWVL broadcasts C/N was increased by 50, and we would expect a reduction in ϵ of about 7 to 1, if the precision was limited only by a fixed noise level. With a time varying noise level, the expected improvement would of course be less. In addition, a fixed threshold, consisting both of propagation phase variation and instrument limitations, could limit the improvement obtained by increasing power. It is likely that all of the above effects contribute in causing the observed improvement to be only 2 to 1.

The short-term stabilities shown in this report approach the limit of precision obtainable with present oscillators, receivers, and recorders in use at WWV and WWVH. Much additional work is required to reduce instrument system errors and to ascertain seasonal and reciprocal path effects. From such work, and by use of comparison oscillators with stabilities better than 1 part in 10^{11}, it may be possible to deduce the ultimate phase stability of VLF and LF signals [Brady, 1964].

Table 1. Summary Statistics of Phase Stability Measurements

Transmitter	Receiving Station	October 1962						October 1963						June 1963					
		Day			Night			Day			Night			Day			Night		
		$S_{avg\,(ph)}$	n	k	$S_{avg\,(ph)}$	n	k	$S_{avg\,(ph)}$	n	k	$S_{avg\,(ph)}$	n	k	$S_{avg\,(ph)}$	n	k	$S_{avg\,(ph)}$	n	k
WWVB	WWV	0.2 μs	18	10	0.7 μs	13	10	0.1 μs	19	10	0.7 μs	13	10	0.2 μs	15	10	0.6 μs	11	10
WWVL	WWV	0.6 μs	19	8	0.9 μs	13	10	0.3 μs	18	10	0.9 μs	13	10	0.6 μs	17	10	0.7 μs	10	10
	WWVH	-	-	-	-	-	-	0.7 μs	14	10	1.8 μs	15	10	0.8 μs	15	8	2.7 μs	13	10
NBA	WWV	0.8 μs	17	10	1.3 μs	17	10	-	-	-	-	-	-	0.6 μs	16	10	0.7 μs	12	10
	WWVH	-	-	-	-	-	-	-	-	-	-	-	-	0.7 μs	15	10	1.0 μs	10	10

Statistics Denoted as Follows:

$S_{avg\,(ph)}$ = average phase stability given by standard error of estimate.

n = number of 0.5 hours measurements.

k = number of days for which measurements made.

Table 2. Diurnal Characteristics of VLF and LF Signals

Transmitter	Receiving Station	Distance Between Transmitter and Receiver Km	Measurement Time UT	DIURNAL DATA 1/ June 1963				October 1963			
				$\bar{\bar{X}}_{di}$ μsec.	$S_{avg\,(di)}$ μsec.	n	k	$\bar{\bar{X}}_{di}$ μsec.	$S_{avg\,(di)}$ μsec.	n	k
WWVB	WWV	2400	0400-0900	18.7	1.1	11	10	19.8	0.8	11	10
	WWVH	5300	-	-	-	-	-	-	-	-	-
WWVL	WWV	2400	0400-0900	10.2	1.4	11	9	15.2	1.3	11	10
	WWVH	5300	0500-1200	29.1	2.9	14	10	32.0	1.8	15	10
NBA	WWV	3300	0200-0900	28.9	1.5	14	10	-	-	-	-
	WWVH	8300	0530-1100	44.9	1.3	10	6	-	-	-	-

1/ Statistics Denoted as Follows:

$\bar{\bar{X}}_{di}$ = grand average of diurnal phase change.

$S_{avg\,(di)}$ = average standard deviation of diurnal phase measurements.

n = number of 0.5 hour measurement periods per night.

k = number of days for which measurements made.

9.2. VLF and LF Diurnal Phase Shifts

Sample diurnal variation measurements were made on the records of WWVL, WWVB, and NBA, and the results are shown in table 2. (The average diurnal phase change $S_{avg\,(di)}$, is determined by comparing a series of phase readings taken during the nighttime portion of the recordings with the average daytime phase level of the preceding and following days.) The data admittedly are sparse as they are essentially single distance measurements for each station during a 2-month period. They do, however, indicate the magnitude of the diurnal changes observed for several different carrier frequencies and propagation distances together with the standard deviations of the measurements. Blackband [1964] has found that, for distances greater than about 4800 km in the frequency range of 18 to 20 kc/s, the magnitude of the diurnal phase changes tends to increase linearly with distance.

Wait [1963] has shown that mode theory substantiates Blackband's experimental data. Since some of the measurements given here were taken outside this frequency range, and within the critical second, or higher order, mode distances, and were quite sparse, direct correspondence with Blackband's results may not be expected. (See also [Volland, 1964].)

An additional effect should be considered [Watt, 1964]: considerable variation may occur when diurnal shifts are measured at points which are equidistant but in different directions from the same transmitter, because of differences in day and night phase velocities corresponding to each direction. Also, this directional effect may vary for land or sea paths and with geographical latitude. Such characteristics have been predicted previously by Wait [1962].

The constancy of the diurnal phase shift is an important factor in the day-to-day intercomparisons of frequency standards via low-frequency signals. The imminent improvement in atomic frequency standards [Stoyko, 1964] will necessitate thorough intercomparison of such standards, and, if evaluated by low-frequency radio signals, the limits introduced by propagation factors must be considered.

The results of this study were made possible through the combined efforts and cooperation of many people. At stations WWV and WWVH the measurements were made by the staffs of Fred Sera and Sadami Katahara, respectively. Catherine Barclay and Vincent Heaton of the NBS, Boulder Laboratories contributed much in the day-to-day calibration and frequency steering work. We have also benefited from many helpful discussions with A. D. Watt, D. D. Crombie, E. L. Crow, and J. F. Brockman. The computer program analysis resulted from the work of Kenneth Yocum, John Devenney, Jean Petersen, and Joan Berube. The NBA recordings made at WWVH were made available by D. D. Crombie. The assistance of Carole Craig in the preparation of this manuscript is gratefully acknowledged.

10. References

Beehler, R. E., W. R. Atkinson, L. E. Heim, and C. S. Snider (Dec. 1962), A comparison of direct and servo methods for utilizing cesium beam resonators as frequency standards, IRE Trans. Instr. **I-11,** No. 3–4, 231–238.

Blackband, W. T. (1964), Diurnal changes in the time of propagation of V.L.F. waves over single mode paths, Propagation of radio waves at frequencies below 300 kc/s, (Pergamon Press), chap 16, 219–229; forward, VI.

Blair, B. E., A. H. Morgan, and L. J. Edlin (1965), Performance characteristics of commercial Rb atomic frequency standards (private communication).

Box, G. E. P. (1953), Non-normality and tests on variances, Biometrika **40,** 318–335.

Brady, A. H. (Mar. 1964), On the long term phase stability of the 19.8 kc/s signal transmitted from Hawaii, and received at Boulder, Colorado, Radio Sci. J. Res. NBS **68D** No. 3, 283–289.

Burtt, G. J. (Nov. 1963), Observations on phase stability of signals from NBA (18 kc/s) Panama as received in New Zealand, Proc. IEE **110,** No. 11, 1928–1932.

CCIR (Nov.–Dec. 1962), Standard frequencies and time signals, Frequency **1,** No. 1, 28–31.

Crombie, D. D., A. H. Allen, and M. Newman (May 1958), Phase variations of 16 kc/s transmissions from Rugby as received in New Zealand, Proc. IEE **105B,** 301–304.

Crombie, D. D. (Jan. 1964), Periodic fading of VLF signals received over long paths during sunrise and sunset, Radio Sci. J. Res. NBS **68D,** No. 1, 27–34.

Crow, E. L., F. A. Davis, and M. W. Maxfield (1960), Statistics manual, 18, 104, 147–165 (Dover Publications, Inc.).

Davies, O. L. (Ed) (1957), Statistical methods in research and production, 16–17, 61–62 (Hafner Publishing Company).

Fey, R. L., J. B. Milton, and A. H. Morgan (March 17, 1962), Remote phase control of radio station WWVL, Nature **193,** No. 4820, 1063–1064.

Looney, C. H., Jr. (Feb. 1961), A very low frequency synchronizing system, Proc. IRE **49,** No. 2, 448–452.

Looney, C. H., Jr. (January 1964) VLF utilization at NASA satellite tracking stations, Radio Sci. J. Res. NBS **68D,** No. 1, 43–45.

Mockler, R. C., R. E. Beehler, and C. S. Snider (Sept. 1960), Atomic beam frequency standards, IRE Trans. Instr. **I-9,** No. 2, 120–132.

Morgan, A. H., and D. H. Andrews (Apr. 1961), Méthodes et techniques de contrôle des ondes kilométriques et myriamétriques aux Boulder Laboratories, Comité Consultatif pour la Définition de la Seconde auprès du Comité International des Poids et Mesures, 2^{e} session, Annexe 6, (Gauthier-Villars & C^{ie}, Paris), 68–72.

Morgan, A. H. (Aug. 1962), Frequency and time calibration services at the Boulder Laboratories of the National Bureau of Standards, NBS Miscellaneous Publication 248, Proc. 1962 Standards Laboratory Conference, 37–43.

Morgan, A. H. (June 1963), Time and frequency broadcasting, ISA Journal **10,** No. 6, 49–54.

NBS (July 1957), Experimental standard frequency broadcasts on 60 kc/s, NBS Tech. News Bull. **41,** 99–100.

NBS (May 1960), Standard frequency broadcasts on 20 kc/s, Journal des Telecommunications **27,** 118f–119f.

NBS (October 1963), New facilities dedicated for WWVB and WWVL, NBS Tech. News Bull. **47,** No. 10, 178–180.

Pierce, J. A. (Dec. 1958), Recent long distance frequency comparisons, IRE Trans. Instr. **I-7,** No. 3–4, 207–210.

Pressey, B. G., G. E. Ashwell, J. Hargreaves (Mar. 1961), The phase variation of very-low frequency waves propagated over long distances, Proc. IEE **108-B,** No. 38, 214–226.

Richardson, J. M. (Jan. 1964), Establishment of new facilities for WWVL and WWVB, Radio Sci. J. Res. NBS **68D,** No. 1, 135.

Somerville, P. N. (1958), Tables for obtaining non-parametric tolerance limits, Ann. Math. Stat. **29,** 599–601.

Stoyko, A., M. N. Stoyko (Jan.–Feb. 1964) La rotation de la terre et le problème de l'heure au Symposium International des Marées Terrestres et au Congrès International de Chrometrie, Bull Horaire n°7 (série 6) 186–187.

Tracor (Mar.–Apr. 1964), Goings-on in LF and VLF, IEEE Digest, Frequency **2,** No. 2, 12–13.

Volland, Hans (1964), Diurnal phase variation of VLF waves at medium distances, Radio Sci. J. Res. NBS **68D,** No. 2, 225–238.

Wait, J. R. (1962), Electromagnetic waves in stratified media, (Pergamon Press, Ltd., Oxford).

Wait, J. R. (1963), A note on diurnal phase changes of very low frequency waves for long paths, J. Geophys. Res **68,** 338–340.

Watt, A. D., and R. W. Plush (July–Aug. 1959), Power requirements and choice of an optimum frequency for a world-wide standard frequency broadcasting station, J. Res. NBS **63D** (Radio Prop.), No. 1, 35–44.

Watt, A. D., R. W. Plush, W. W. Brown, and A. H. Morgan (Nov.–Dec. 1961), Worldwide VLF standard frequency and time signal broadcasting, J. Res. NBS **65D** (Radio Prop.), No. 6, 617–627.

Watt, A. D. (May 1964), private communication.

(Paper 69D7–525)

LF-VLF Frequency and Time Services of the National Bureau of Standards

DAVID H. ANDREWS, SENIOR MEMBER, IEEE

Abstract—**The United States Frequency Standard and National Bureau of Standards Time Scale are described, and the techniques by which they are used to control the broadcasts from WWVB and WWVL, Fort Collins, Colo., are presented. A practical method for control of frequency and time broadcasts from WWV, Greenbelt, Md., is described and actual results shown.**

Introduction

RECENT ADVANCES in space technology have imposed upon timing systems a greater need for precise time synchronization between ground stations separated by thousands of miles. The National Bureau of Standards is meeting this challenging requirement with improved standards and improved techniques for disseminating them by means of radio broadcasts at LF and VLF.

Frequency Standard

The National Bureau of Standards maintains the United States Frequency Standard at its laboratories in Boulder, Colo. The USFS has a defined frequency of 9 192 631 770.00 Hz for the $(F=4,\ m_F=0)\leftrightarrow(F=3,\ m_F=0)$ transition in the ground electronic state of cesium^{133}.

This frequency standard is physically realized in atomic beam devices designated NBS-II and NBS-III. NBS-II and its forerunner, NBS-I, are fully described elsewhere[1] by Mockler and others of his staff. NBS-III has a separation of 366 cm for its perturbing oscillating field as against 164 cm for NBS-II, which results in the narrower line width of 50 Hz compared with the 120 Hz line width of NBS-II.

These devices realize the USFS with an uncertainty of $\sim 1\times10^{-11}$ and have precisions approaching 2×10^{-12}.

Upon this standard all of the frequency and Time Services of the National Bureau of Standards are based.

NBS-A Time Scale

The frequency of a continuously running device is measured daily in terms of the United States Frequency Standard (the devices designated NBS-I, NBS-II, and NBS-III are high-quality laboratory machines, unsuited by nature and complexity to continuous operation), and it is possible to generate a time scale with the same uncertainty and stability as that of the USFS. This derives partly from the fact that frequency and time interval are inversely related.

The National Bureau of Standards Atomic (NBS-A) time scale, described by Barnes, Andrews, and Allan,[2] approaches the USFS uncertainty very closely. Actually five continuously running frequency generators are compared with the USFS each working day. These generators are well aged and are assumed to have a linear frequency drift between measurements. At intervals of about two weeks the daily frequency measurements are examined with the aid of a computer to obtain the deviation of each one from a straight line. Time is computed then on the basis of the group of generators weighted inversely as the square of the deviation of the frequency of each generator from the straight line.

This system produces an extremely good time scale which, however, has the same disadvantage, from an operating point of view, as the devices used to realize the USFS. It presently is incapable of producing a continuously available time reference incorporating the full accuracy of the USFS.

NBS-UA Time Scale

Time signals presently broadcast from the NBS radio stations are an approximation to UT (Universal Time) based on a fixed annual offset from the atomically determined frequency and with step time adjustments of 100 ms as needed to keep the time as broadcast within about 150 ms of actual UT2. During the calendar year 1964 the frequency used to approximate UT2 is 150 parts in 10^{10} lower than the atomically determined frequency.

The National Bureau of Standards derives the NBS-UA time scale by applying the appropriate offset frequencies and time jumps as required to the NBS-A time scale.

This still lacks the continuity necessary to operate radio stations.

A further approximation, having the desired continuity, is made by applying drift-rate correction to the output of one of the frequency generators. Since the generator used for this purpose has very good stability and very nearly linear drift rate, it is quite practical to "program out" the drift. At Boulder a system for ac-

Manuscript received March 15, 1965.

The author is Chief of the Frequency-Time Broadcast Services, National Bureau of Standards, Boulder, Colo.

[1] R. C. Mockler, R. E. Beehler, and C. S. Snider, "Atomic beam-frequency standards," *IRE Trans. on Instrumentation*, vol. I-9, pp. 120–132, September 1960.

[2] J. A. Barnes, D. H. Andrews, and D. W. Allan, "The NBS-A time scale—its generation and dissemination," this issue, page 228.

complishing this mechanically is used. The system was developed concurrently, but independently, with a commercial system, and was in use at Boulder prior to the availability of a commercial unit. This drift-rate corrector consists [2] of a phase shifter driven by two ball-disk integrators in cascade with appropriate gear reduction units and synchronous motors.

The time derived from the drift-corrected oscillator is compared frequently with time computed on the NBS-UA time scale. Corrections are made to the drift-rate settings as necessary to keep the drift-corrected time in close agreement with the NBS-UA time scale. In practice it has been possible to do this within a few microseconds tolerance, at the same time holding the frequency within 1 or 2×10^{11} of the USFS.

The previously described system provides the broadcasting services with a continuous source of standard frequency which is time-locked to the NBS-UA time scale for all practical purposes.

Phase-Lock Link

Since the high field strengths associated with transmitters make it highly undesirable to have them in close proximity to precision laboratories, the LF and VLF transmitters are located about fifty miles away from the Boulder laboratories at Fort Collins, Colo. This adds to the problem of precise control of the transmitted frequencies. Also phase fluctuations normally occur due to temperature variations at the transmitters and shifting of the antenna system due to winds, ice, and thermal expansion.

All these fluctuations and the relating of the frequency to the drift-corrected oscillator are taken care of in the phase-lock system in use between Boulder and Fort Collins.

The phases of the signals transmitted at 20 kHz and 60 kHz are monitored at the Boulder laboratories and compared with the phases of signals generated by the drift-corrected oscillator.

When the phase of the received signal varies from the phase of the reference signal, an error voltage is produced. Then this error signal is made to produce appropriate FM signals feeding a transmitter operating at 50 MHz. This transmission is beamed by a directional antenna array to Fort Collins.

Signals as received at Fort Collins operate servo systems to control the transmitted phases at each frequency. The transmission system actually broadcasts both the reference signal and the error signal for each correction servo system. By this technique it has been possible to eliminate most of the propagation fluctuations due to the control link in the phase of the transmitted signals at 20 kHz and 60 kHz.

Figure 1 shows in block diagram form the steps involved in making possible the accurate transmissions from WWVB and WWVL at Fort Collins. Later the significant part these transmissions play in the control of WWV will be described.

Figure 2 illustrates in block diagram form the Boulder end of the phase-lock system. From left to right this diagram shows the LF and VLF receivers, phase detectors, oscillators, modulator amplifiers, and the mixer necessary to provide the reference and error signals to the 50 MHz FM transmitter.

Figure 3 continues the phase-lock system at the Fort Collins end of the link. The 50 MHz receiver at the upper right of the diagram picks up the signals beamed from Boulder. The received signal is split then into its three component signals whose frequencies are 400 Hz, 5.4 kHz, and 10.5 kHz. The three frequencies carry, respectively, the reference phase information, the 20 kHz error phase information, and the 60 kHz

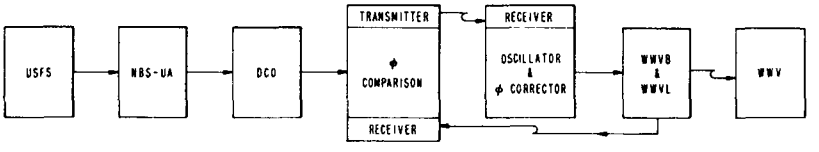

Fig. 1. Frequency-time control of WWV.

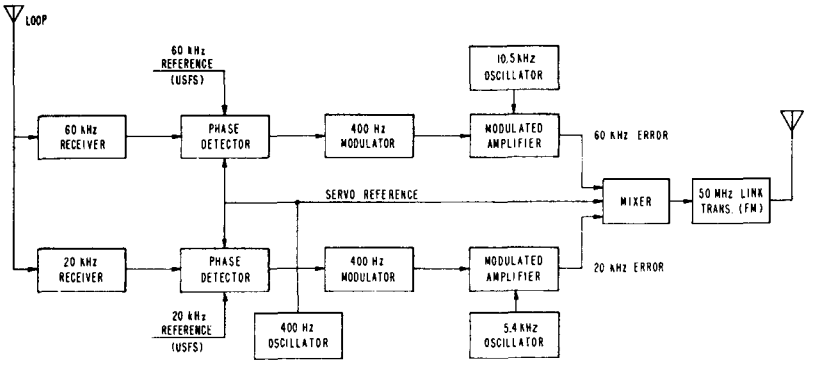

Fig. 2. Phase-lock system, Boulder section.

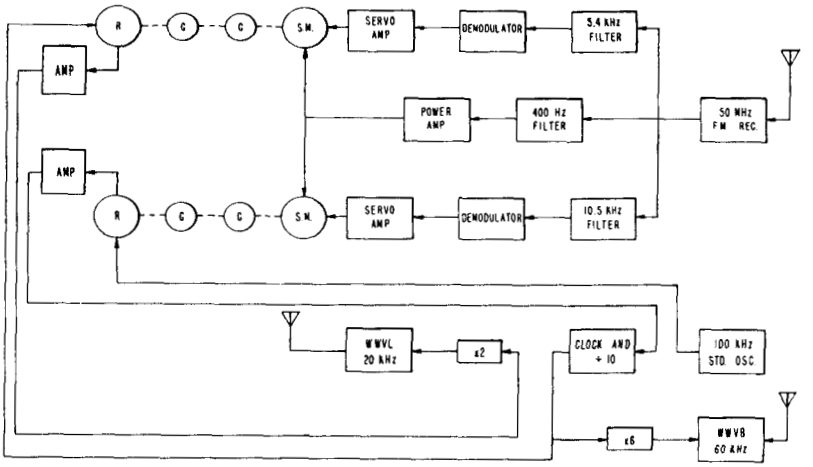

Fig. 3. Phase-lock system, Fort Collins section.

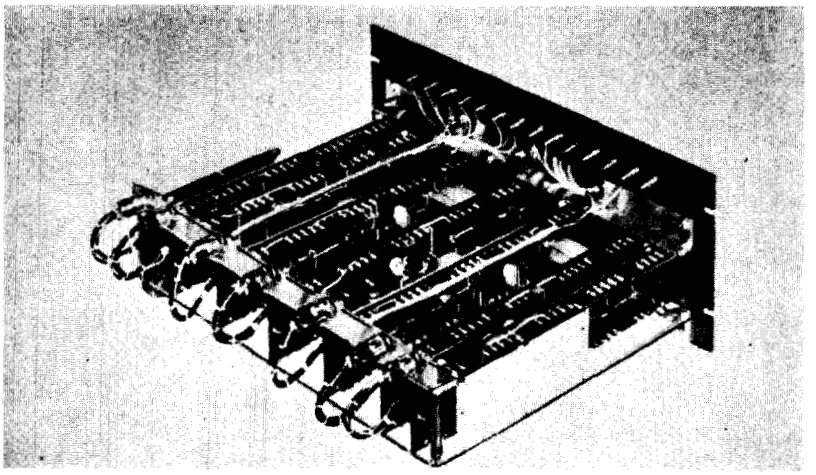

Fig. 4. Boulder phase correction equipment.

error phase information. As will be noted the 60 kHz system bears the brunt of the oscillator drift correction, and the 20 kHz system compensates mainly for variations in the phase of the VLF antenna system. This serves to share the load on the servo systems when both transmitters are working. It can also be seen that the system will function quite well with either frequency alone.

The system is basically a simple servo system with an FM link coupling the phase detectors to the servo motors and phase correcting devices.

The performance of this system has been remarkably excellent. Very few malfunctions have been observed in more than a year's operation. The circuitry is almost entirely transistorized.

Figure 4 shows the Boulder part of the phase correction equipment. The unit at Fort Collins is constructed along similar lines. The 50 MHz transmitter and receiver are not included in this photograph. They are commercial items which have been modified for this purpose by the National Bureau of Standards.

The system maintains the transmitted phase of each signal within about 0.1 μs of the reference phase at Boulder. Short term variations of a few microseconds occurring with a period of several seconds, may occur when heavy winds are blowing at Fort Collins causing the antenna to sway and detune.

LF-VLF Antenna Properties

At this point it may be well to describe briefly the LF and VLF antenna properties at Fort Collins.

Two large diamond shaped antennas each supported by four 400-foot masts are used for radiating the power from two 50 kW transmitters operating at 20 kHz and 60 kHz. The radiated power from these antenna systems is presently about 500 watts at 20 kHz and 4 kW at 60 KHz. It is expected that improvements that will be made in 1965 will raise the transmitted power to 1 kW at 20 kHz and 10 kW at 60 kHz.

The radiation pattern is believed to be substantially omnidirectional. Field studies are planned which will determine what effect the mast configuration and nearby mountains have on the concentricity of the radiation pattern.

Monitoring at WWV

Having described briefly the frequency standards maintained by the Boulder laboratories and shown how the signals from WWVB and WWVL are related to these signals, it is now possible to proceed with the methods and techniques presently in use by NBS to control WWV at Greenbelt, Md.

The transmissions at both 20 kHz and 60 kHz are received at WWV using techniques referred to by Morgan and Andrews[3] in an earlier publication. The reference signal at WWV is taken from the oscillator controlling the broadcasts.

Each week the phase records taken at both frequencies are mailed to Boulder, and have been analyzed for time drift of WWV's signals relative to the stabilized phase transmissions from Fort Collins.

It has been possible to maintain good records, even during the time when WWVB and WWVL were on the air for only six hours a day. This is quite practical when the oscillator at the receiving site is of such stability that the daily drift never exceeds a half cycle of the frequency being monitored.

The monitoring records are most favorable when readings are taken at the time when noon occurs at the midpoint of the path between the transmitter and the receiver. For this path the best observation time is 1 P.M. EST or 11 A.M. MST. Converted to Universal Time, this is 1800.

For the purpose of this study readings were taken each day at 1800, 1900, 2000, and 2100 UT and averaged. The phase records were taken with a 50 μs full scale at 20 kHz and with a $16\frac{2}{3}$ μs full scale at 60 kHz. These scale widths equal a full cycle at each frequency and conveniently avoid phase ambiguities occurring due to diurnal effects.

Experimental Results

The experimental results obtained in time control of WWV during five months in the first half of 1964 are presented in four charts that will be described in detail.

On January 18, 1964, the drift corrected oscillator, referred to previously, was put in control of WWVB and WWVL by means of the phase-lock link between Boulder and Fort Collins. At that time, the operator at WWV was instructed to maintain phase between the WWV master oscillator and the transmissions of WWVB and WWVL as closely as possible by simple step adjustments of the controlling oscillator in increments not exceeding 1×10^{-11}. Pending the availability of more sophisticated equipment to do this task this technique has been in effect for all of 1964 except the first half of January.

Results of this experiment are shown in Figs. 5–8. The abscissa of each of these figures is time of the year blocked off by months. The ordinate scale of Fig. 5 is blocked off in 10 μs increments. The values plotted are

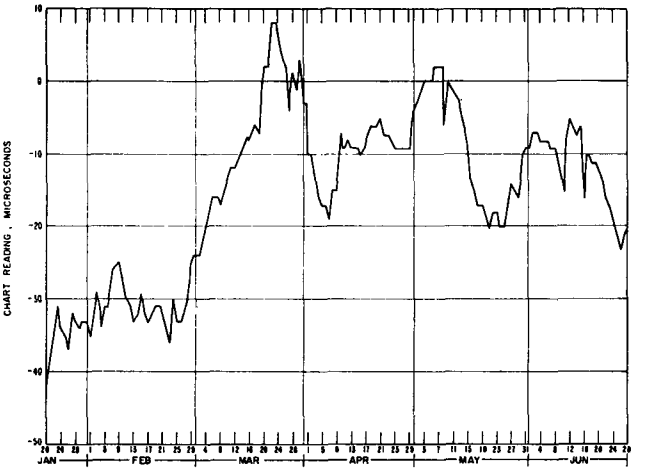

Fig. 5. Monitor chart readings of WWVL at WWV.

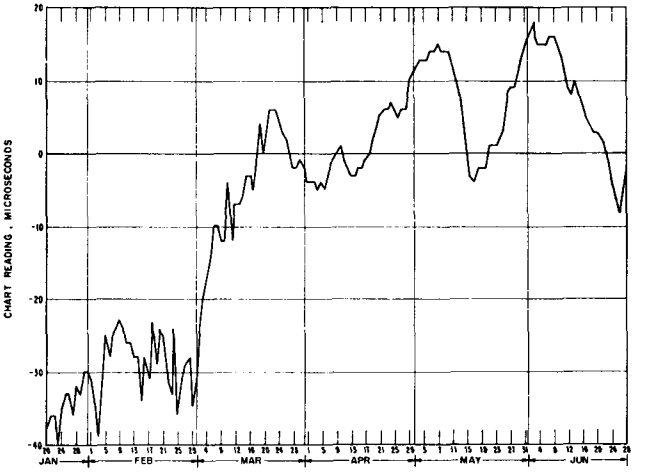

Fig. 6. Monitor chart readings of WWVB at WWV.

actual chart readings in microseconds with an arbitrary zero point. The curve consists of daily values plotted point by point. This shows the raw data as observed on the monitor at WWV recording WWVL. Even though this curve is quite jagged, it is immediately evident that WWV time has been maintained within ±25 μs of WWVL phase throughout this period.

The jaggedness of the raw data plot is thought to be attributable, at least partly, to propagation variations. Experience with the controlling oscillator at WWV indicates that the variations from day to day are in excess of any that can be attributed to the oscillator.

Figure 6 shows a very similar curve, this time being a plot of WWVB as monitored at WWV. Again the ordinate is the monitoring chart reading plotted in microseconds with an arbitrary zero.

Perhaps the most significant point to note in this plot is the jaggedness of the curve during January and February. During these months the curve fluctuated much more severely when monitoring WWVB than when monitoring WWVL. While not so pronounced, there seems to be the reverse effect during May and

[3] A. H. Morgan and D. H. Andrews, "Frequency calibration receiving systems and techniques using standard LF and VLF signals," April 2, 1962, private communication.

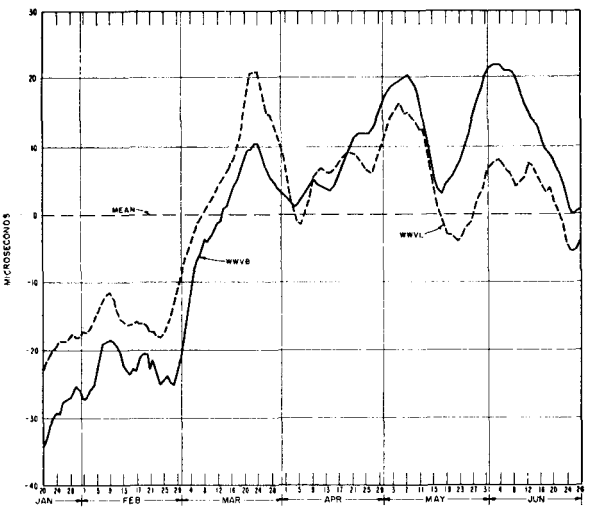

Fig. 7. Five-day-average deviations of WWVB and WWVL as monitored at WWV.

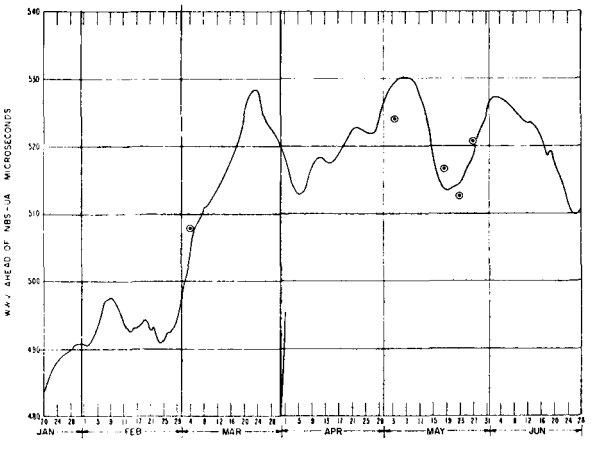

Fig. 8. Daily values of WWV clock time vs. standard clock at Boulder.

June, in that the monitoring records of WWVL show greater fluctuations than those of WWVB.

To obtain the curves presented in Fig. 7 several operations were performed on the raw data previously shown. Firstly, somewhat smoother curves were obtained by using five day averages of the raw data instead of daily values. This is justifiable upon the premise that propagation variations, such as might be caused by the effective height of the ionosphere changing from day to day, would be random in nature and thus average out in several days.

In addition to smoothing of the data by using five-day running averages, the mean value for the period of time shown was obtained for the data taken for WWVB and WWVL. Secondly, the curves were related to each other by making the mean value of each curve equal to zero microseconds on an arbitrary ordinate scale.

Thirdly, an average was taken of the curves shown in Fig. 7 and is plotted in Fig. 8. Notice now, however, that the ordinates are on a new scale which is the time relationship of the clock pulse at WWV with respect to the NBS-UA time scale. To establish this scale a number of trips were made with a portable clock between the NBS-UA clock at Boulder and the station clock at WWV. The relative time differences between the clocks obtained by these measurements are plotted as encircled points in Fig. 8. To fit the curve to the points the average values were obtained for the curve on the clock-point days and matched to the average value of the time differences obtained from the portable clock measurements. The scatter of the points relative to the monitoring time curve shows a standard deviation of less than 1.5 μs.

It should be noted that the portable clock measurements are made customarily on a round-trip basis so that the time loop can be closed and thus avoid gross errors in the measurements. In general, it has been possible to make a clock trip to WWV with a closure time of from 1 to 3 μs, which is consistent with the scatter of the points on the monitoring time curve.

Conclusions

Using a combination of LF and VLF monitoring of WWVB and WWVL at WWV, Greenbelt, Md., it has been possible to establish a gain-or-loss time curve for the WWV clock relative to NBS-UA which controls WWVB and WWVL by phase-lock techniques described earlier.

Further, it has been possible to establish within a very few microseconds the actual time relationship between the gain-or-loss time curve at WWV and the NBS-UA time scale by means of portable clocks.

The techniques described here can be refined. Improvements can be made in LF-VLF station control, in monitoring techniques, in techniques for minimizing the effects of scatter in monitoring data due to propagation effects, in smoother control of the remote clock oscillator, and in the portable clocks.

It is concluded that the combination of 1) LF and VLF monitoring, 2) portable clock synchronization, 3) a high quality local clock, and 4) simple manual adjustments of the oscillator in the local clock can maintain the time synchronization between widely separated clocks within ± 10 μs.

Acknowledgment

The author wishes to acknowledge monitoring data provided by F. Sera and H. Luzier, WWV, Greenbelt, Md., and portable clock measurements by J. Barnes, D. Allan, and L. Fey. The help of others who have contributed suggestions incorporated in this paper also is appreciated.

The aid of V. Heaton in reducing the mass of monitoring data to the curves presented herein is also appreciated sincerely.

References

[1] J. A. Barnes and R. L. Fey, "Synchronization of two remote atomic time scales," *Proc. IEEE (Correspondence)*, vol. 51, p. 1665, November 1963.

[2] R. L. Fey, J. B. Milton, and A. H. Morgan, "Remote phase control of radio station WWVL," *Nature*, vol. 193, pp. 1063–1064, March 17, 1962.

Reprinted from IEEE TRANSACTIONS ON *INSTRUMENTATION AND MEASUREMENT*
Volume IM-14, Number 4, December, 1965

463-560 O - 72 - 23

RADIO SCIENCE, Vol. 1 (New Series), No. 12, December 1966

New Measurements of Phase Velocity at VLF

G. Kamas, A. H. Morgan, and J. L. Jespersen

Radio Standards Laboratory, National Bureau of Standards, Boulder Laboratories, Boulder, Colo. 80302, U.S.A.

(Received June 6, 1966; revised July 13, 1966)

The purpose of this note is to describe some new phase velocity measurements using signals from the VLF stations NPG (18.6 kc/s) near Seattle, Wash., and WWVL (20.0 kc/s) near Fort Collins, Colo. Previous experimental results have been described by Wait [1961].

The new measurements consisted of determining the accumulated phase over a known distance along the surface of the earth. These measurements are related to the phase velocity by the following expressions. By definition, the phase velocity at a point R is given by

$$V_p(R)=\frac{2\pi f}{d\phi/dR} \tag{1}$$

where f is the radio frequency and ϕ is the phase. Therefore, the total phase accumulated over a distance D is

$$\phi_T=2\pi f\int_0^D \frac{dR}{V_p(R)}.$$

If V_p is a constant, then

$$V_p=\frac{2\pi fD}{\phi_T}; \tag{2}$$

otherwise, (2) gives some average effective velocity.

The measurements were accomplished using phase-locked VLF receivers and very stable atomic reference frequency standards mounted in a mobile laboratory which traversed a roughly north-south path from Boulder, Colorado, to Austin, Texas. This method is the opposite of that used in VLF navigation, where the velocity of the wave is assumed known and position is then determined [Stanbrough and Keily, 1964; Stanbrough, 1965] from the measurements of the phase.

The results in terms of the quantity, $\Delta\phi$, are shown in figure 1. The term $\Delta\phi$ is the measured accumulated phase in microseconds minus the phase that would have accumulated if the phase velocity of the wave equaled that of light, c, in a vacuum. It is plotted as a function of radial distance R from the transmitter. The phase in microseconds is related to the phase in radians by the expression, ϕ microseconds $=\phi$ radians$/2\pi f$, where f is the radio frequency. Each value of $\Delta\phi$ at the two frequencies, 18.6 and 20.0 kc/s is an average of six measurements obtained on different days within 4 hours of local noon at the midpoint of the path. There was no unusual solar activity during any of the measurements. Because the measurements did not start at the transmitter, the accumulated phase between the transmitter and the starting point is unknown. Therefore, we have arbitrarily set $\Delta\phi$ equal to zero for the point closest to the transmitter at each of the two frequencies. The error due to uncertainties in the great-circle-path length, the reference-oscillator frequency, and the phase-measurement equipment is less than 0.5 μs.

Although it is not our intention in this paper to discuss these results in any detail, there are two features of the data which deserve comment. First, the standard deviation of the measurements is considerably more than one would expect from the measurement errors alone. This spread in the data is probably due, primarily, to varying local anomalies and to differences in the ionosphere between measurements. Second, the phase in general does not accumulate uniformly with distance at either frequency, but rather appears to have an oscillatory pattern whose amplitude decreases with distance from the transmitter. This is to be expected, since ionospheric waveguide mode theory shows [Wait, 1962] that the phase pattern across the ground depends upon the interaction of several ionospheric waveguide modes. Near the transmitter several modes are important; however, the higher-order modes are attenuated rapidly with distance, so that at great distances the phase pattern is primarily due to mode 1. All of the measurements shown in figure 1 appear to be in an oscillatory pattern except, perhaps, for the four most distant measurements at 18.6 kc/s whose average values lie on a straight line. Assuming that these four values are produced primarily by mode 1, we have calculated the phase velocity by fitting a line, using the least-squares method, to the phase versus distance measurements. The slope of this line, by (1), is inversely proportional to the phase velocity. Although there is no guarantee that more distant measurements would not have shown further oscillations, it is interesting to note that the result obtained was

$$V_p/c-1=-0.0026\pm0.0007. \tag{3}$$

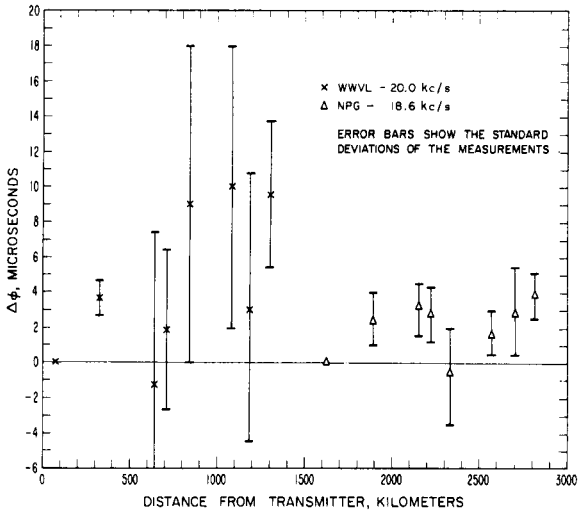

FIGURE 1. *Measured phase minus calculated accumulated phase, in microseconds, at discrete distances from the transmitter.*

This value, within the precision of the measurement, agrees with a previous experimental result, using a different method, obtained by Steele and Chilton [1964] where they interpret their measurement as applying to mode 1. The value is also in agreement with a theoretical mode 1 value obtained by Wait and Spies [1964] for an

exponential model of the ionosphere with a reference height of about 80 km (case with no earth magnetic field). In this model the conducting parameter ω_r varies with height, z, as $e^{+\beta z}$, where $\beta = 0.3$ km^{-1} and where $\omega_r = 2.5 \times 10^5$ sec^{-1} at the reference height. The ground conductivity is assumed infinite.

As a statistical check, the phase velocity, using the same method, was obtained from the rest of the 18.6-kc/s measurements with the result that $V_p/c - 1 = -0.0003 \pm 0.0007$. It may be shown that this value differs from the previous value at the 5-percent significance level, thus indicating that no meaningful phase velocity may be obtained by fitting a straight line to all of the 18.6-kc/s data.

Since figure 1 shows rapid fluctuations in $\Delta\phi$ with distance at 20.0 kc/s, no attempt was made to apply (1) to this data. To determine the phase velocity as a function of distance, where more than one mode is significant, measurements must be made sufficiently close together along the path to accurately sample the variation. A later paper will report on the results of such closely spaced measurements and on the extension of the measurements reported above.

References

Stanbrough, J. H., Jr. (1965), A VLF radio relative navigation system, Navigation **11,** 4, 417–428.

Stanbrough, J. H., Jr., and D. P. Keily (1964), Long range navigation by means of VLF transmissions, Deep-Sea Res. **11,** No. 2, 249–255.

Steele, F. K., and C. J. Chilton (1964), Measurement of the phase velocity of VLF propagation in the earth-ionosphere waveguide, Radio Sci. J. Res. NBS **68D,** No. 12, 1269–1273.

Wait, J. R. (1961), A comparison between theoretical and experimental data on phase velocity of VLF radio waves, Proc. IRE **49,** No. 6 1089–1090.

Wait, J. R. (1962), Electromagnetic Waves in Stratified Media (Pergamon Press, New York, N.Y.).

Wait, J. R., and K. Spies (Dec. 30, 1964), Characteristics of the earth-ionosphere waveguide for VLF radio waves, NBS Tech. Note No. 300.

(Paper 1–12–168)

A Dual Frequency VLF Timing System

L. FEY AND C. H. LOONEY, JR., SENIOR MEMBER, IEEE

Abstract—**The use of high precision portable clocks and radio signals is discussed in relation to synchronization of remotely located clocks. The demonstrated inherent phase stability, approximately ten μs rms, of very-low-frequency (VLF) propagation and its low attenuation rate with distance, have led to various approaches to exploit these virtues in timing applications. The system considered here employs two carrier frequencies with timing information contained in their difference frequency to permit identification of a specific cycle of one of the carrier frequencies. Such a system makes stringent demands on phase stabilities of the transmitted signals and of the receiving system as well as that of the propagation medium itself.**

The present system, whose development has been supported jointly by NBS and NASA, makes use of NBS radio station WWVL at Fort Collins, Colo. Receivers are of the standard VLF phase tracking servo type. A special signal generator is used in conjunction with the local clock to simulate the transmitted signal in order to relate the local time scale to that at the transmitter.

One of the carrier frequencies is maintained at 20 kHz. With a second frequency (500 Hz removed from this frequency), carrier cycle identification was achieved on about 90 percent of the days for over a month on the path from Fort Collins, Colo., to Greenbelt, Md. Since January 4, 1966, the difference frequency has been 100 Hz, with somewhat more fluctuation in results. However, lower precision is required for the initial synchronization. The results of averaging to improve this performance will be discussed.

TWO BASIC methods are used for synchronizing remotely located high precision clocks. One is transportation of operating clocks between locations where clocks are to be synchronized; the other is propagation of radio signals which contain timing information.

Until recently, high-frequency (HF) propagation such as from radio station WWV, rather than the portable clock method, offered the higher practical precision of synchronization, with modest investment in receiving equipment. This system employs amplitude modulation of an HF carrier with time ticks once per second. The bandwidth used is limited by considerations of spectrum availability rather than any inherent equipment limitations. Propagation is by means of the E and F ionospheric layers, whose inherent instabilities limit precisions of synchronization to around one millisecond from day to day so that no additional advantage accrues from increasing the present bandwidth. On the other hand, improvements in the uniformity with which time scales can be kept, and the development of portable quartz crystal clocks and atomic oscillator clocks, now permit synchronization with precisions of the order of one microsecond using portable clocks [1], [2]. Since many of the demands in such areas as satellite and missile tracking, geodesy, seismology, and sophisticated communications systems are in the range which can only be satisfied by portable clocks, increasing use is now being made of these devices. The difficulty with this approach is that extreme reliability is required of clocks to maintain synchronization for long periods after they have been synchronized. Furthermore, even without clock failures it has been shown [3] that time kept by clocks driven by crystal oscillators may be expected to depart from that of a uniform standard in a random walk fashion, necessitating periodic resynchronization.

One obvious approach in solving this problem is to make use of the extreme stability of very-low-frequency (VLF) propagation compared to that of HF propagation. This stability is that of the ionospheric D layer by which VLF signals propagate and is such that day-to-day repeatabilities of better than 10 microseconds are possible. A further advantage is the reliability of this mode of propagation and its extremely low attenuation rate, permitting worldwide reception from a single station [4], [5]. The simplest way to make use of these advantages is to synchronize a remote clock by use of a portable clock, then maintain the remote clock's synchronization by manual adjustment of its oscillator frequency, obtaining the necessary corrections from VLF reception. For direct time synchronization, however, the VLF approach has serious limitations when carried out in the same way as the high-frequency case—that is, using pulse modulated timing information. This limitation is due to the combination of low carrier frequency and high transmitting antenna Q which severely restricts the useful bandwidth and prevents the broadcast of fast rise time pulses by VLF.

Essentially, then, the difference between HF methods and VLF methods arises from the comparatively narrow bandwidth capability but high propagation stability available at VLF which make new techniques necessary if the potential synchronization stability is to be reached. An early description of a VLF system having such a potential was given by Casselman and Tibbals at the 1958 IRE Conference on Military Electronics [6]. The original suggestion for this system, which is known as Omega, was attributed to J. A. Pierce of Harvard, who also first established that VLF transmissions possessed extremely good phase stability [7].

Manuscript received June 23, 1966. This work was partially supported by NASA under Contract S-49285 (G), and was presented at the 1966 Conference on Precision Electromagnetic Measurements, Boulder, Colo.

L. Fey is with the National Bureau of Standards, Boulder, Colo.
C. H. Looney, Jr., is with the Goddard Space Flight Center, Greenbelt, Md.

The Omega system was proposed for and is currently under active study as a worldwide navigation system [8]. Here it is the position on the earth's surface which is to be determined, but the necessary measurement is a time comparison between CW signals received from pairs of transmitting stations. However, a single CW signal is insufficient, since time measurements on a CW signal would have ambiguities equal to the period of the signal (between about 30 μs to 100 μs for the VLF band) resulting in position ambiguities spaced by a few miles. In order to resolve these ambiguities, the navigator would require independent knowledge of his position to better than one-half the spacing of the ambiguities, which corresponds to previous synchronization uncertainty of less than one-half of a carrier period. Omega employs coherent, closely spaced, multiple frequency CW broadcasts to overcome this difficulty. In essence, the difference frequency between a pair of closely spaced carrier frequencies, having a longer period than either carrier frequency, is used to resolve ambiguities of the carrier phase. The difference frequency period fluctuations need only be less than one-half the carrier period to permit a particular carrier cycle to be unambiguously associated with a zero crossover of the difference frequency for this resolution. The Omega system carries out these resolutions in several steps, starting with a relatively small difference frequency period to resolve carrier ambiguities, and then resolving difference frequency ambiguities in turn with longer difference frequency periods. This process continues until position ambiguities are too widely spaced for the navigator to be uncertain as to which location he is nearest. This multi-step procedure is necessary in a navigation system where only a short averaging time is allowed for each determination of position, and where the measurement must be made at any time of day or night rather than at the time propagation conditions are best. The NBS-NASA timing system requirements are less stringent in that receiving locations are fixed and synchronization information is not needed so often as navigation position information. For example, at NASA tracking stations [9], employing atomic oscillators or ultra-stable crystal oscillators and the resultant highly uniform time scales, it is now thought sufficient to make a time synchronization determination once a day during the time of most stable propagation conditions.

NBS-NASA System Description

The NBS-NASA system, while using the same techniques as Omega, is simpler in that only one transmitter location is used, making transmission time sharing among stations unnecessary. Ultimately the system may employ more than one difference frequency, but tests have been made using only one at a time for a period of several months each. The frequencies used in the NBS-NASA tests are the 20.0 kHz standard frequency carrier, offset from the United States Frequency Standard (USFS) to conform to the coordinated Universal Time scale, with either 20.5 kHz or 19.9 kHz as the single auxiliary frequency for a given test period. These frequencies are all synthesized from a common source which is phase locked to the offset USFS. Carrier period ambiguities are thus 50 μs; difference frequency period ambiguities are either 2 ms or 10 ms. Frequency shift keying is employed to utilize the single transmitter and antenna at Fort Collins, Colo., allowing 10 seconds transmission time alternately for each frequency. In order to relate these transmissions to Universal Time (UTC) the phases of the two frequencies being broadcast are adjusted at the transmitter to go through zero simultaneously in a positive direction coincident with a seconds tick of UTC. These phase relations are maintained, upon reception, with the time of simultaneous phase agreement delayed by an amount depending on the phase velocity of the signals and on the distance of receiver from transmitter. Since there is a slight dependence of phase velocity on frequency, an additional small phase shift of the difference frequency will occur. In order to extract timing information from the signals, one or, with a little more convenience, two conventional phase tracking VLF receivers may be used.

It is necessary to relate the phases of the received signals to the time scale operating at the receiving site in order to perform a time synchronization. This is done by making use of an auxiliary device, referred to as a calibrator, to generate from the local time scale the same two frequencies as transmitted, with the same simultaneous phase relationship conditions. The calibrator actually consists of a sawtooth waveform generator, which is synchronized by a 100 pulse-per-second rate taken from the local time scale divider chain. This waveform has the desired properties that all harmonics of the fundamental frequency exist, (in particular, 19.9 kHz, 20.0 kHz, and 20.5 kHz) and all go through zero in a positive direction coincident with each pulse of the 100 pps clock output which is in turn synchronized with the 1 pps clock output. An interchange of signals from the receiving antenna with the calibrator output permits a measurement to be made of the pair of phase differences. From these two measured quantities, the relation between transmitter time scale and receiver time scale may be calculated, provided only that the carrier propagation phase delays are known. In order to study propagation fluctuations on the path from Fort Collins, Colo., to the Goddard Space Flight Center at Greenbelt, Md., however, the clocks at the two locations have been kept synchronized by the use of portable clocks and propagation delay[1] treated as the unknown quantity. If Δt_1 denotes the measured time difference between the phase

[1] For purposes of simplicity, the treatment of this paper assumes that propagation is dispersionless so that no distinction between phase velocity and group velocity is made. The term propagation delay will thus be used throughout in referring to either phase or group delay; effects of dispersion will be treated later as a correction.

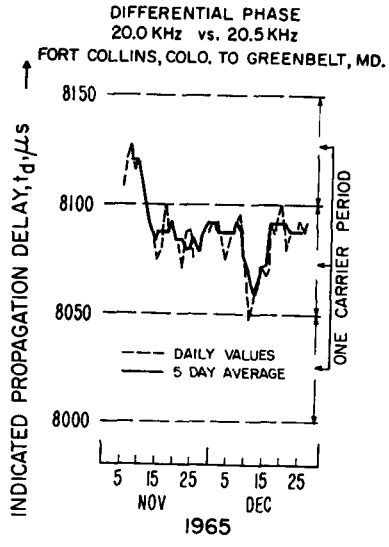

Fig. 1.

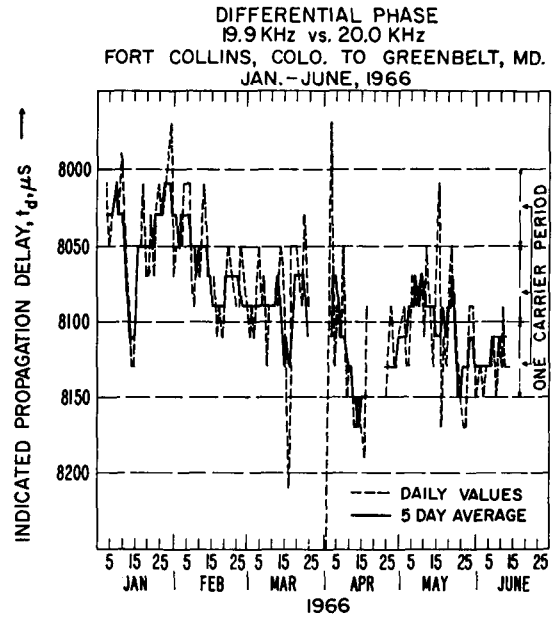

Fig. 2.

of the received signal and locally generated signal of the lower frequency f_1, and Δt_2 denotes measured time difference similarly for the higher frequency f_2, then it is shown in the Appendix that when the transmitter and receiver clocks are synchronized, the propagation delay t_d, as determined from the difference frequency, is

$$t_d = (\Delta t_2 - \Delta t_1)\left[\frac{f_1}{f_2 - f_1}\right] + \Delta t_2.$$

Using this formula with measurements made around noon each day at Greenbelt, Md., propagation delay has been calculated for data taken from late October 1965 to June 1, 1966. From October to January 4, the two frequencies broadcast were 20.0 kHz and 20.5 kHz. From January 4 to June the frequencies were 20.0 kHz and 19.9 kHz. Results are shown in Figs. 1 and 2, which display a plot of indicated propagation delay as derived from the difference frequency measurements. The data were obtained from the μs-counter dial of a pair of commercial VLF receivers which have a resolution of 0.1 μs. This accounts for the steps in indicated propagation delay, and also points out the severe requirement on relative phase stability of the two carrier frequencies. Even though each transmitted frequency is nominally phase-locked to a common reference, there has been some long term differential phase fluctuation. This made daily local measurement of differential phase, as transmitted, necessary. The data in Figs. 1 and 2 have been corrected for this fluctuation. On May 24 an improved AGC circuit was installed in the transmitter phase control servos, resulting in considerable improvement in the transmitted phase stability as shown in Fig. 2. In order to gain a knowledge of longer term propagation fluctuation, the data has been smoothed by making five-day averages. These results are also shown in Figs. 1 and 2. The value for $(\Delta t_2 - \Delta t_1)$ for the months of February through early June 1966 approximates -9.5 μs, which corresponds to a propagation delay of approximately 8100 μs. Portable clock measurements indicate a value for propagation delay of approximately 8050 μs. This difference of 50 μs between VLF and portable clock measurements is equivalent to a 0.25 μs bias in $(\Delta t_2 - \Delta t_1)$ which may be due to the variation of phase velocity with frequency.

According to mode theory calculations of Wait and Spies [10], propagation phase velocity decreases with increasing frequency in the neighborhood of 20.0 kHz, resulting in about 0.2 μs delay of the 20.0 kHz signal over that of 19.9 kHz and about 0.7 μs delay of the 20.5 kHz signal over that of 20.0 kHz signal. These values of 0.2 μs and 0.7 μs, when applied to the measured data shown in Figs. 1 and 2, do indicate a value of approximately 8050 μs for propagation time, thus bringing the VLF and portable clock data into close agreement. This correction is of theoretical interest, and arises from the dispersive properties of the earth ionosphere waveguide which cause the phase and group velocities to be different. It is necessary in making predictions of propagation delay to receiving points for which portable clock measurement is not readily accessible. At present, the measured values of propagation delays must also be extrapolated with care for another reason. Measurements made using portable receiving equipment indicate that as much as one microsecond bias error in the phase of the difference frequency may occur as a result of close proximity of the receiving antenna to long metallic structures, such as power lines, pipes, or buildings. This error in phase could cause an indicated propagation delay error of as much as 200 μs and makes evident that, where precise synchronization is required, propa-

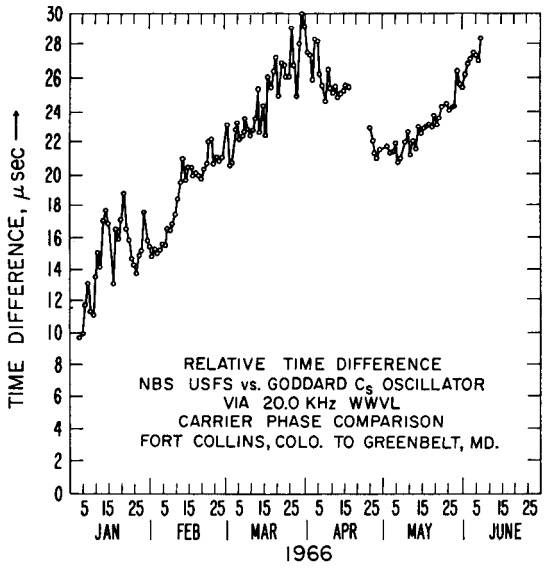

Fig. 3. Residual daily VLF time fluctuations assuming correct carrier cycle identification each day.

gation delay should be determined with a portable clock.

As can be seen in Fig. 2, phase stability of the received 100 Hz difference frequency was not sufficient to permit identification of the same carrier cycle every day measurements were made. For this to have occurred, the measurements would have to all be between two of the indicated dashed horizontal lines. If the system were being used for timing, an error of 50 μs would have occurred in indicated time each day the measurements shifted from one band into an adjacent band. Taking five-day averages improves the synchronization at the expense of a delay in making a determination. The degree of objection to such delay depends on the uniformity which can be ascribed to the local time scale. Catastrophic failures would, of course, make a complete resynchronization necessary.

In order to evaluate the maximum stability of synchronization of the system over the path under discussion, the day-to-day time variation of the received carrier is plotted in Fig. 3. This would be the system synchronization capability if the same carrier cycle had been identified each day. The capability of VLF in comparing frequencies to better than 1 part in 10^{12} is readily apparent from this figure. Between January and March the mean slope is about 2 parts in 10^{12}.

In order to permit positive carrier cycle identification continuously during day and night, it is apparent that several difference frequencies must be transmitted simultaneously. More effort is needed to determine the optimum frequencies; but it appears that if both 500 and 100 cycle frequencies had been used simultaneously, cycle identification could have been accomplished nearly every day in two steps, with an initial synchronization certainty of ± 5 milliseconds from WWV transmissions. A completely self-sufficient VLF system is clearly preferable; possibly this system would provide the convenient frequencies of 1 Hz, 100 Hz, and 1000 Hz in a multiple transmission from an NBS VLF station, and we believe would permit time synchronization of better than 10 μs throughout most of the world.

Appendix

In deriving an expression for the propagation phase delay of the difference frequency, it is convenient to refer to Fig. 4, which displays phase relationships of the two carrier frequencies at significant times at transmitter and receiver. The dotted line represents the traveling wave of the signal from the transmitter as it progresses in distance, on the vertical axis, and in time, on the horizontal axis. The slope of the dotted line then indicates phase velocity. The time origin is $t=t_0$, the time of occurrence of a seconds tick. This time is synchronized at transmitter and receiver locations using a portable clock.

The phases of f_1 and f_2, the lower and upper frequency carriers, are identically zero at $t=t_0$ from both the transmitter, represented by Φ_{1tx} and Φ_{2tx}, and from the calibrator at the receiver, represented by $\Phi_{1\text{cal}}$ and $\Phi_{2\text{cal}}$. Assume that the phase relationships of two signals emitted from the transmitter at time $t=0$ may be observed during propagation to the receiver. If propagation phase velocity is the same for each frequency, their phases will remain at zero and they will arrive at the receiver with that relationship as represented by Φ_{1rx} and Φ_{2rx}. Meanwhile, the phase of each signal emitted from the calibrator will have advanced. The observed phase difference between received signal and calibrator signal of f_1 will be

$$\Phi_{1rx} - \Phi_{1\text{cal}} = \phi_1 \tag{1}$$

and of f_2 will be

$$\Phi_{2rx} - \Phi_{2\text{cal}} = \phi_2. \tag{2}$$

We denote the total phase advance of calibrator phase of f_1 during propagation of the signal from transmitter to receiver by θ_1 and, similarly, the total phase advance of f_2 by θ_2. Now θ_2 will advance more rapidly as a function of distance than θ_1, since $f_2 > f_1$. Let the distance d of the receiver from the transmitter be sufficiently small so that during propagation time t_d from transmitter to receiver θ_2 has advanced over θ_1 by less than one complete cycle. The consequences of removing this restriction will be considered later. Therefore, let the number of complete cycles advance by either θ_1 or θ_2 from the calibrator during t_d be denoted by N. Then

$$\theta_1 = 2\pi N + \phi_1 \tag{3}$$

and

$$\theta_2 = 2\pi N + \phi_2, \tag{4}$$

where $\phi_2 > \phi_1$. From (3) and (4),

$$\theta_2 - \theta_1 = \phi_2 - \phi_1. \tag{5}$$

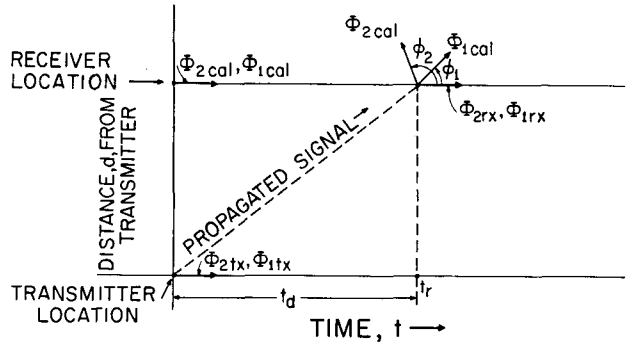

Fig. 4. Phase relationships of calibrator signal and propagated signal.

The propagation time t_d is equal to calibrator phase advance in cycles at either frequency multiplied by the period τ_1 or τ_2 of that frequency; hence,

$$t_d = \theta_1 \frac{\tau_1}{2\pi} \tag{6}$$

$$= N\tau_1 + \frac{\phi_1 \tau_1}{2\pi} \tag{6a}$$

from (3), or

$$t_d = \theta_2 \frac{\tau_2}{2\pi} \tag{7}$$

$$= N\tau_2 + \frac{\phi_2 \tau_2}{2\pi} \tag{7a}$$

from (4). Then

$$\theta_2 = \theta_1 \frac{\tau_1}{\tau_2} \tag{8}$$

from (6) and (7). Substituting for θ_2 in (5) and solving for θ_1,

$$\theta_1 = \frac{\phi_2 - \phi_1}{\frac{\tau_1}{\tau_2} - 1}. \tag{9}$$

Substituting θ_1 into (6),

$$t_d = \frac{(\phi_2 - \phi_2)}{\frac{\tau_1}{\tau_2} - 1} \frac{\tau_1}{2\pi} \tag{10}$$

$$= \frac{\phi_2 - \phi_1}{f_2 - f_1} \cdot \frac{1}{2\pi}$$

which is seen to be group delay [11]. The quantities ϕ_2 and ϕ_1 are generally not measured directly by VLF receivers. Instead, the corresponding time changes Δt_1 and Δt_2, where

$$\phi_1 = 2\pi \frac{\Delta t_1}{\tau_1} \tag{11}$$

and

$$\phi_2 = 2\pi \frac{\Delta t_2}{\tau_2}, \tag{11a}$$

are often obtained in the following way.

VLF receivers are commonly equipped with counters which totalize in steps of 0.1 μs changes in time between the phase of the received carrier and the local oscillator reference. This is a useful form of presentation when the receivers are used to measure time accumulation between local clock and transmitter clock, since this quantity does not depend on carrier frequency while phase accumulation does.

Using a receiver so equipped in order to make a time measurement, the time readings corresponding to received phases Φ_{1rx} and Φ_{2rx} are noted. Interchanging receiver VLF input from antenna to calibrator, the time readings corresponding to calibrator phases Φ_{1Cal} and Φ_{2Cal} are noted. Only the differences Δt_1 and Δt_2 between these sets of readings are meaningful, since the measurements themselves depend on unknown receiver phase shifts which are assumed constant throughout the measurement and therefore cancel out.

Substituting (11) and (11a) into (10) and rearranging,

$$t_d = (\Delta t_2 - \Delta t_1)\left[\frac{\tau_1}{\tau_1 - \tau_2}\right] + \Delta t_1. \tag{12}$$

Using the definitions

$$\tau_1 = \frac{1}{f_1} \tag{13}$$

and

$$\tau_2 = \frac{1}{f_2}, \tag{13a}$$

(12) becomes

$$t_d = (\Delta t_2 - \Delta t_1)\left[\frac{f_2}{f_2 - f_1}\right] + \Delta t_1, \tag{14}$$

or

$$t_d = (\Delta t_2 - \Delta t_1)\left[\frac{f_1}{f_2 - f_1}\right] + \Delta t_2. \tag{14a}$$

This is the time corresponding to propagation delay as determined from the difference frequency. Once determined, it is used to resolve carrier cycle ambiguities in the following way.

First, round the first term in (14a) to the nearest integral multiple of the carrier period τ_2, 50 μs. That is the coarse time determination and follows recognition that, from (6a), (11a), and (14a),

$$N\tau_2 = (\Delta t_2 - \Delta t_1)\left[\frac{f_1}{f_2 - f_1}\right]. \tag{15}$$

If the errors in determination of Δt_2 and Δt_1 produce an error of less than $\frac{1}{2}\tau_2$, this roundoff procedure will pro-

duce the correct value for N_{T_2} and avoid error due to the magnification term $[f_1/(f_2-f_1)]$. Then the time Δt_2, the second term of (14a), is added to this integral number of periods to give the final answer or the fine time determination.

The case where the phase of f_2 advances by more than one cycle over that of f_1 will be considered. This evidently occurs when distance d is so large that propagation delay t_d is greater than the period T_{diff} of the difference frequency. This period corresponds to a distance of one wavelength λ_{diff} of the difference frequency, where approximately

$$\lambda_{\text{diff}} = cT_{\text{diff}}$$

with c = velocity of light. In this case, when calculated by (14a), t_d is too small by one or more periods of the difference frequency. This situation causes no problem for difference periods under discussion here. For instance, the two ms periods correspond to one complete wavelength of difference frequency, being somewhat less than 400 miles. If d is uncertain by less than half this amount, then the correct value of t_d can be readily determined by observing which value of n, for $n=0$, 1, 2, 3, . . . results in (t_d+nT_{diff}) being nearest the value of propagation delay calculated from d and the velocity of light. This situation is illustrated in Fig. 5. where the distance and time scales have been lengthened to include two periods of the difference frequency. Ambiguities of distance occur at $n=1$ and $n=2$ where all phases return to their values at $t=t_0$. When t_d is $>\frac{1}{2}T_{\text{diff}}$, values of t_d calculated from (14a) may be negative. This merely means that they are to be subtracted from $(n+1)T_{\text{diff}}$, rather than added to nT_{diff}, and illustrates again that distance must be known to better than half a wavelength of the difference frequency.

A sample set of data taken at Goddard Space Flight Center is given in Table I to illustrate the above procedure.

From these data $\Delta t_1=22.3$ μs; $\Delta t_2=12.8$ μs; $\Delta t_2-\Delta t_1=-9.5$ μs; and $f_1/(f_2-f_1)=199$; so that, from (14a) first term, $t_d\cong-1890.5$ μs. With a difference frequency of 100 Hz, $T_{\text{diff}}=10\,000$ μs. The distance from Fort Collins, Colo., to Greenbelt, Md., is about 2400 km so that nT_{diff} is closest to a calculated propagation delay of about 8000 μs when $n=1$. Subtracting the measured value of 1890.5 μs from 10 000 μs results in a measured value for propagation delay of 8109.5 μs which rounds to 8100 μs as the time corresponding to the nearest integral number of 20.0 kHz carrier periods. To this is added time Δt_2, 12.8 μs so that measured propagation delay, finally, is 8112.8 μs for this example.

It remains to point out how this system could be used for time synchronization if propagation delay t_d were known. In that case

$$\Delta T = (\Delta t_2 - \Delta t_1)\left[\frac{f_1}{f_2 - f_1}\right] + \Delta t_2 - t_d, \qquad (16)$$

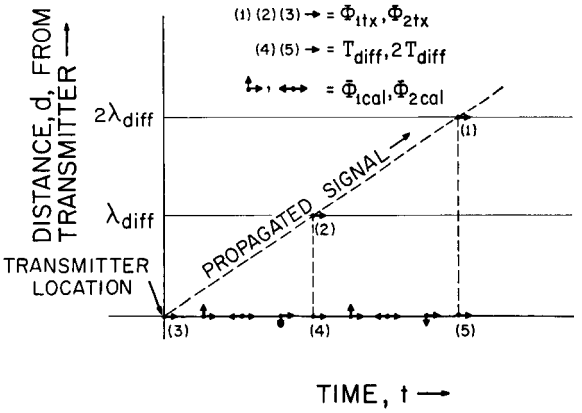

Fig. 5. Phase repetition relationships of calibrator signal and propagated signal showing ambiguities.

TABLE I

	Receiver Counter Reading	
Frequency	19.9 kHz	20 kHz
Propagated Signal	1306.7 μs	1302.4 μs
Calibrator Signal	1284.3 μs	1289.6 μs

where ΔT is time delay of the receiver clock compared to the transmitter clock. Ambiguities would now appear as before but would be in time, rather than distance, as illustrated by identical phases at times T_{diff} when $n=1$ and $2T_{\text{diff}}$ when $n=2$. In order to make a correct synchronization, the receiver clock would need to be synchronized independently to better than $\frac{1}{2}T_{\text{diff}}$. For the case of $T_{\text{diff}}=10$ ms this could be achieved with WWV when it can be received. For $T_{\text{diff}}=2$ ms use of WWV is questionable.

References

[1] J. A. Barnes and R. L. Fey, "Synchronization of two remote atomic time scales," *Proc. IEEE (Correspondence)*, vol. 51, p. 1665, November 1963.

[2] L. N. Bodily, "Correlating time from Europe to Asia with flying clocks," *Hewlett-Packard J.*, vol. 16, pp. 1–8, April 1965.

[3] J. A. Barnes, "Atomic timekeeping and the statistics of precision signal generators," *Proc. IEEE*, vol. 54, pp. 207–220, February 1966.

[4] A. D. Watt and R. W. Plush, "Power requirements and choice of an optimum frequency for a worldwide standard-frequency broadcasting station," *J. Res. NBS (Radio Science)*, vol. 63D, pp. 35–44, July–August 1959.

[5] A. D. Watt, R. W. Plush, W. W. Brown, and A. H. Morgan, "Worldwide standard frequency and time signal broadcasting," *J. Res. NBS*, vol. 65D, pp. 617–627, November–December 1961.

[6] C. J. Casselman and M. L. Tibbals, "The Radix-Omega long range navigation system," *1958 Proc. Second Nat'l Conv. on Military Electronics*, pp. 385–389.

[7] J. A. Pierce, "The diurnal carrier-phase variation of a 16-kilocycle transatlantic signal," *Proc. IRE*, vol. 43, pp. 584–588, May 1955.

[8] J. A. Pierce, "Omega," *IEEE Trans. on Aerospace and Electronic Systems*, vol. AES-1, pp. 206–215, December 1965.

[9] C. H. Looney, Jr., "VLF utilization at WASA satellite tracking stations," *J. Res. NBS (Radio Science)*, vol. 66D, pp. 43–45, January 1964.

[10] J. R. Wait and K. P. Spies, "Characteristics of the earth-ionospheric waveguide for VLF radio waves," NBS, Washington, D. C., Technical Note 300 (Supplement) February 1965.

[11] C. A. Coulson, *Waves*. New York: Interscience, 1947, pp. 128–133.

Distribution of Standard Frequency and Time Signals

A. H. MORGAN, MEMBER, IEEE

Abstract—**This paper reviews the present methods of distributing standard frequency and time signals (SFTS), which include the use of high-frequency, low-frequency, and very-low-frequency radio signals, portable clocks, satellites, and RF cables and lines. The range of accuracies attained with most of these systems is included along with an indication of the sources of error. Information is also included on the accuracy of signals generated by frequency dividers and multipliers.**

Details regarding the techniques, the propagation media, and the equipment used in the distribution systems described are not included. Also, the generation of the signals is not discussed.

I. Introduction

THE DISTRIBUTION of standard frequency and time signals (SFTS) with the highest accuracy over long distances has become increasingly important in many fields of science. It is essential for the tracking of space vehicles, worldwide clock synchronization and oscillator rating, international comparisons of atomic frequency standards, radio navigational aids, astronomy, national standardizing laboratories, and some communication systems. Methods used include use of high-frequency (HF), low-frequency (LF), and very-low-frequency (VLF) radio transmissions, portable clocks, satellites carrying a clock or a transponder, and RF cables and lines.

This paper will review these distribution systems and some of their limitations and also indicate some promising techniques for future study. Recent advances [1] in the distribution of SFTS will be included, but they will not always be specifically pointed out. Information will be included on the accuracy of SFTS signals generated by frequency dividers and multipliers. Details regarding the techniques, the propagation media, the equipment involved in the distribution systems described, and the generation of the SFTS are not included.

The definition of the terms *stability*, *precision*, and *accuracy* as used in this paper are essentially the same as those given in another paper [2].

II. Distribution by Radio Signals

A. Distribution by HF and VHF Signals (3 to 300 MHz)

At present there are about 15 standard HF and time-signal broadcasting stations [3], [4] operating in the allocated bands between 2.5 and 25 MHz. Table I lists them along with certain characteristics, such as location, carrier frequencies and power, period of operation, carrier offset, etc. The characteristics of the HF and VHF stations that broadcast standard frequency and time signals [3] in additional frequency bands are given in Table II. Many of these stations participate in the international coordination of time and frequency and are identified in the tables. The signal emission times of the coordinated stations are within 1 millisecond of each other and within about 100 ms of UT2; their carrier frequencies are maintained as constant as possible with respect to atomic standards and at the offset from nominal as announced each year by the Bureau International de l'Heure (BIH) [4]. The fractional frequency offset in 1966 was -300 parts in 10^{10}, and this value is to be used in 1967.

The long and widespread experience with standard HF and time signals, and their present world-wide use, underlines their importance to a large body of users. There are international organizations, such as the International Radio Consultative Committee (CCIR) [5], the BIH [4], and the International Scientific Radio Union (URSI) [6], [7], that are concerned with many aspects of their operation and utilization, such as reduction of mutual interference, broadcast accuracy, synchronized emission times, etc. For instance, the CCIR not only publishes information on signals but also is engaged in a study program designed to improve the services and uses of the present stations.

A technique employed by NBS to improve the transmitted accuracy of the frequencies of WWV[1] and WWVH was to use the received signals of WWVB (60 kHz) and WWVL (20 kHz) at these stations to remotely control them [8]. The NBS atomic standards are located at Boulder, Colo., and the transmissions of WWVL and WWVB, which stations are located about 50 miles away, are remotely phase-controlled by means of a VHF phase-lock system [9] connected between them and the atomic standard at Boulder so that their transmitted frequency accuracy is essentially that of the NBS standard. Because of the high received frequency accuracy of LF and VLF signals, it was thus possible to improve the frequency control of WWV and WWVH. Later, the carrier frequencies and time signals of WWV and WWVH were phase-locked to the received signals of WWVL and WWVB, so that they might be used to obtain time (epoch) [42].

The received accuracy of the HF time interval and epoch signals depends on many factors, such as the averaging time, the length of the radio path from transmitter to receiver, the condition of the ionosphere, whether the path is partially in light and darkness or not, the frequency used,

Manuscript received December 13, 1966; revised January 6, 1967.
The author is with the National Bureau of Standards, Boulder, Colo.

[1] WWV was located at Beltsville, Md., until December 1, 1966, and is now at Ft. Collins, Colo. All references in this paper are to the Beltsville location.

TABLE I

CHARACTERISTICS OF STANDARD-FREQUENCY AND TIME-SIGNAL EMISSIONS IN THE ALLOCATED BANDS

Station				Carrier				Time Signals			Operation	
Call sign	Approximate location	Latitude Longitude	Coordination	Frequencies MHz	Power kW	Offset $\times 10^{-10}$	Accuracy $\times 10^{-9}$	Modulation 1 Hz	Duration Minutes	100-ms Steps	Days Week	Hours Day
ATA	New Delhi India	28° 34′ N 77° 19′ E		10	2		20	yes	continuous		5	5
FFH	Paris France	48° 59′ N 2° 29′ E		2.5	0.3		2	yes	10/20	yes	2	8 1/2
HBN	Neuchatel Switzerland	46° 58′ N 6° 57′ E	yes	5	0.5	−300	0.1	yes	5/10	yes	7	24
IAM	Rome Italy	41° 52′ N 12° 27′ E		5	1		0.5	yes	10/15	yes	6	1
IBF	Turin Italy	45° 3′ N 7° 40′ E		5	0.3		0.1	yes	35/60	yes	6	1 1/3
JGZAR	Tokyo Japan	35° 42′ N 139° 31′ E		0.02	3		0.5	yes	continuous	yes	5	2
JJY	Tokyo Japan	35° 42′ N 139° 31′ E	yes	2.5; 5; 10; 15	2	−300	0.5	yes	continuous	yes	7	24
LOL	Buenos Aires Argentina	34° 37′ S 58° 21′ W	yes	5; 10; 15	2	−300	20	yes	4/60	yes	6	5
MSF	Rugby United Kingdom	52° 22′ N 1° 11′ W	yes	5, 5; 5; 10	0.5	−300	0.1	yes	5/10	yes	7	24
OMA	Prague Czechoslovakia	50° 7′ N 14° 35′ E		2.5	1		1	yes	15/30	50 ms	7	24
RWM-RES	Moscow U.S.S.R.	56° 37′ N 36° 36′ E		5; 10; 15	20		5	yes	10/120	$n \times 10$ ms	7	19
WWV	Fort Collins Colo.	40° 41′ N 105° 2.5′ W	yes	2.5; 20; 25 5; 10; 15	2.5 10	−300	0.02	yes	continuous	yes	7	22 1/2
WWVH	Hawaii U.S.A.	20° 46′ N 156° 28′ W	yes	2.5 5; 10; 15	1 2	−300	0.1	yes	continuous	yes	7	22 1/2
WWVL	Fort Collins Colo.	40° 41′ N 105° 3′ W		0.02	1.8	−300	0.02				7	24
ZLFS	Lower Hutt New Zealand	41° 14′ S 174° 55′ E		2.5	0.3		50				1	3
ZUO	Johannesburg South Africa	26° 11′ S 28° 4′ E	yes	10	0.25	−300	0.5	yes	continuous	yes	7	24
ZUO	Olifantsfontein South Africa	25° 58′ S 25° 14′ E	yes	5	4	−300	0.5	yes	continuous	yes	7	24

TABLE II

CHARACTERISTICS OF STANDARD-FREQUENCY AND TIME-SIGNAL EMISSIONS IN ADDITIONAL BANDS

	Station			Carrier				Time Signals			Operation	
Call sign	Approximate location	Latitude Longitude	Coordination	Frequencies kHz	Power kW	Offset $\times 10^{-10}$	Accuracy $\times 10^{-9}$	Modulation 1 Hz	Duration Minutes	100-ms Steps	Days Week	Hours Day
CHU	Ottawa Canada	45° 18′ N 75° 45′ W	yes	3330 7335 14670	0.5 3 5	−300	5	yes	continuous	yes	7	24
DCF77	Mainflingen Germany	50° 1′ N 9° 9′ W		77.5	12			yes		200	6	6
	Droitwich United Kingdom	52° 16′ N 2° 9′ W		200	400		10				7	18–20
GBR	Rugby United Kingdom	52° 22′ N 1° 11′ W	yes		300 40	−300	0.1	yes	4/5	yes	7	22
HBG	Prangins Switzerland	46° N 6° E		75	20		0.02	yes	continuous	yes	7	24
Loran-C	Carolina Beach N. C.	34° 4′ N 77° 55′ W		100	300		0.05		continuous	50	7	24
MSF	Rugby United Kingdom	52° 22′ N 1° 11′ W	yes	60	10	−300	0.1	yes	5/10	yes	7	1
NAA	Cutler Me.	44° 39′ W 67° 17′ W	yes	17.8	2000 1000	−300	0.05				7	24
NBA	Balboa Canal Zone	9° 4′ N 79° 39′ W	yes	24	300 30	−300	0.05	yes	continuous	yes	7	24
NPG-NLK	Jim Creek Wash.	48° 12′ N 121° 55′ W	yes	18.6	1200 250	−300	0.05				7	24
NPM	Lualualei Ha.	21° 25′ N 158° 9′ W	yes	26.1	1000 100	−300	0.05				7	24
NSS	Annapolis Md.	38° 59′ N 76° 27′ W	yes	21.4	1000 100	−300	0.05				7	24
OMA	Podebrady Czechoslovakia	58° 8′ N 15° 8′ E		50	5		1	yes	23 hours/day	50	7	24
RWM-RES	Moscow U.S.S.R.	55° 45′ N 37° 33′ E		100	20		5	yes	40/120	$n \times 10$	7	21
SAJ	Stockholm Sweden	59° 20′ N 18° 3′ E		15×10^4	0.06		0.1				1	2
SAZ	Enkoping Sweden	59° 35′ N 17° 8′ E		10^5	0.1		5				7	24
VNG	Lyndhurst Australia	38° 0′ S 145° 12′ E		5425 7515 12005	0.5 0.5–10 10		1			yes	7	24
WWVB	Fort Collins Colo.	40° 40.5′ N 105° 2.5′ W		60	13		0.02	yes	continuous	200	7	24
ZUO	Johannesburg South Africa	36° 11′ S 28° 4′ E		10^5	0.05		0.5		continuous	yes	7	24

Fig. 1.

etc. [10]. In general, higher accuracies of received frequency and time interval are associated with longer averaging times, with all daylight or all darkness on the radio paths, a quiet ionosphere, and the highest useful HF frequency. For example, the HF broadcasts of WWV, averaged over a 30-day period, were used to compare to about 1 ms three atomic time scales, two of them separated from each other by about 2400 km [11], and from the third by about 7400 km [12].

From studies made in Japan and Sweden, the one-sigma standard deviation of a single HF time measurement was found [13] to vary from about 0.01 ms at short distances to about 0.5 ms at distances around 18 000 km. This is in good agreement with results [10] obtained in the U. S.

Frequency comparisons to a few parts in 10^{10} were made between Boulder, Colo., and Washington, D. C., using the HF time signals of WWV averaged over a period of 30 days [14], [8]. When short-term (one second to one hour observing time) frequency measurements are made, the fluctuations may vary [15] from a few parts in 10^8 to a few parts in 10^7. The limit of received accuracy at HF is set by the propagation medium regardless of the length of the observation period.

Figure 1 shows the locations of the standard frequency and time transmitters of the world.

B. Distribution by LF Transmissions (30 to 300 kHz)

There are about seven stations broadcasting standard frequency and time signals in the LF band, with transmitted frequency and time interval accuracies ranging from 0.2 to 50 parts in 10^{10}. (See Tables I and II.) Experiments [13] have shown that the time signals of HBG (75 kHz) may be received with a precision of 0.1 ms at distances of 1000 km, and the phase of the ground wave is typically stable to about ± 2 μs at 500 km.

The received frequency and phase accuracy is much better at LF than at HF because of the higher stability of the propagation medium. For instance, the rms phase fluctuations of WWVB (60 kHz) as received at distances of 2400 km were 0.1 to 0.2 μs during the daytime and around 0.6 μs at night [8]. Each measurement was averaged over a 30-minute period. Within the ground-wave range, the Loran-C stations at 100 kHz provide signals with high stability at the receiver. At Washington, D. C., the signals from the Cape Fear Loran-C Station (Table II) were used to measure time interval to a precision of about 0.1 μs and to make frequency comparisons to about one part in 10^{12} in one day [16]. Others have reported similar results [17]. Sources of error in using Loran-C signals included identification of the wrong RF cycle in the pulse (3rd one usually used) and uncertainty in propagation delays.

C. Distribution by VLF Transmissions (10 to 30 kHz)

There are about eight VLF stations broadcasting standard frequency and time signals with transmitted accuracies of a few parts in 10^{11} or better. Tables I and II list them and their main characteristics.

Of all the radio transmissions available, those at VLF have proven to be the best for the accurate distribution of standard frequencies over large areas of the world [18]–[22]. They have been in use for over a decade [18] but have been widely used for this purpose only during the last five or six years.

Atomic frequency standards in different countries have been continuously intercompared by means of VLF transmissions ever since they first became available [20], [23]–[29]. As a result of greater understanding of VLF propagation and the improvements in the accuracy of the atomic standards and the VLF receiving equipment, frequency comparisons over long distances with precisions better than one part in 10^{11} are now possible. For example, an analysis of data on the comparison by VLF for an 18-month period of several widely separated atomic frequency standards [25], [26] indicated that long-term precisions of this order are realizable. Although the analyses did not separate the fluctuations due to the propagation medium from those due to the transmitter or receiving system, the internal consistency of results indicated that the propagation effects were not limiting the measurements. Short-term VLF frequency measurements of NPM (19.8 kHz), Hawaii, were made [30] at Boulder, Colo., with precisions ranging from 2.5×10^{-11} (24-hour observing time) to 3.1×10^{-12} (8-day observing time).

Time signals on VLF transmissions of NBA (18 kHz) using a pulse technique provided a received precision [31] of about one-half millisecond in Washington, D. C. The limiting factor is the low signal-to-noise ratio as set in the wideband receiver required for reproducing the pulse.

Another more promising technique, devised at NBS [32], [14], [34], uses two or more alternately transmitted closely spaced carriers; its feasibility has been shown for distances of about 1400 km [34] and 2400 km [38]. It is based on the same principle as the proposed Radux-Omega Navigation System [33]; however, the NBS VLF time distribution system was developed independently. The positive zero crossings of the received VLF carrier may serve as "time markers" if they are phase-locked to a local signal. Their accuracy is limited by the phase fluctuations. At, say,

20 kHz, these "markers" are separated by 50 μs and may be identified by use of the interference nulls produced by a second nearby carrier which is also phase-locked. The ambiguity of identification of these nulls will be the period of the beat between the two wider-spaced carriers (if more than two are used). Coarser time markers are obtained by either a third closer-spaced carrier or conventional time signals or both. As in all timing systems using radio transmissions, both the phase and group delays of the signals must be known in order to synchronize widely spaced slave clocks to the transmitter or to each other. This is necessary because the dispersion in the propagation medium will cause the phase and group velocities to be different.

The National Aeronautics and Space Administration has reported interest in this VLF time distribution system for use at its satellite tracking stations [35]. Further investigations of its utility as a worldwide accurate time distribution system are underway at NBS [36] and elsewhere [37], [38]. Another similar system for VLF distribution of time signals has been reported [39], [40]. It has been studied theoretically, but as yet no field tests have been made.

The Omega Navigation System [41] is based on the same principle as the above-mentioned multiple carrier VLF timing system, and if it is placed into operation with eight stations as planned, it will be possible to distribute time with it to any point on the globe. The received time (epoch) accuracy has not yet been established.

A recent method that may be used to maintain widely spaced clocks in synchronism, after they have been set together by other methods (such as portable clocks), is to use the received phase of WWVL (20 kHz). These signals have been phase-locked [9] to the controlling NBS standards at Boulder, which in turn are held at nearly constant phase with respect to the NBS-UA time scale [42]. By observing the daily change between a zero crossover of the 20-kHz signal and a suitable time signal from the local clock, it is possible to keep the local clock correct to within a few microseconds.

Recent results [27] on the comparisons of atomic frequency standards by VLF gave values approaching those obtained with portable clocks, as shown in Table III(a). From this study and others [30] it is concluded that the stability of the propagation medium at VLF for paths up to 7500 km may be around two or three parts in 10^{12}. Apparently the limit of the stability of the medium has not been reached yet during times of quiet ionosphere.

Sources of error in using VLF for frequency comparisons include: 1) undetected loss of one cycle of the received signal during diurnal phase-shifts, 2) phase-jumps in the receiver synthesizer, 3) variations in the phase of the transmitted signals [9] due to the antenna system, 4) phase variations introduced by the receiving antenna, 5) lack of knowledge of the stability of the propagation medium, 6) occurrence of sudden phase anomalies (SPA) on the path, and 7) mode interference in the region between the useful ground-wave range and out to about 2500 km from the transmitter.

Sources of error in time comparisons include all of the above-mentioned factors and the lack of knowledge of the phase and group velocities in the given radio path.

III. Distribution by Portable Clocks

The most accurate method of distributing standard frequency and time over great distances to individual users, in wide use today, is by use of portable clocks, a technique first proposed [10] by NBS in 1959. Following this proposal, the first set of experiments of transporting cesium clocks [43] by air, to test the possibility of synchronizing remote slave clocks, were begun in 1959. Some preliminary measurements were made in 1960 [44], [45], but the final results were reported [46] in 1961. These results were that the slave clocks were synchronized to about 5 μs.

Another experiment conducted in 1963, in which a quartz clock was transported by air, produced similar results. It was reported that a time closure of about 5 μs was obtained in the comparisons of the portable clock with the standard before and after being transported [47].

A recent series of "flying clock" experiments was undertaken in 1964 in which atomic clocks were flown by commercial airlines to several countries to intercompare the various standards [48]–[50]. The results are shown in Table III(a) which also includes some comparisons of the same standards using VLF radio transmissions [25]–[27]. The frequency and time of the portable clocks were compared directly with those of the standards in the laboratories visited. Frequency comparisons were made to uncertainties of a few parts in 10^{12} and time comparisons to about one microsecond.

Sources of error relating to portable clocks include: 1) undetected changes in the clock during transit, 2) undetected phase-jumps in the frequency dividers, and 3) environmental effects on the rate of the clock, such as shock, vibration, voltage, and temperature changes, etc.

IV. Distribution by Satellites

Two experiments in the use of satellites to distribute time have been reported. In the first one, the satellite Telstar was used to compare clocks at Andover, Me., and Goonhilly Downs, Cornwall, U. K. [51], [52]. The clocks were compared to a precision of about 1 μs.

The second experiment made use of Relay II to compare [53], [54] clocks in Kashima, Japan, with those at Mojave, U. S. The precision of determining the arrival time of pulses on a photograph was about 0.1 μs, but it was believed there were systematic errors of around 1 μs.

Sources of error in these measurements include the nonreciprocity of the propagation paths used, lack of simultaneity of the time of the observations at each end of the paths, and resolution of the pulse arrival time.

V. Distribution by Transmission Lines and Cables

Many distribution systems use telephone lines or coaxial cables to carry the SFTS between two points; for example, between a distribution amplifier and a transmitter, between the transmitter and the antenna, or between locations several miles apart from one another.

TABLE III

(a) FREQUENCY COMPARISONS IN TERMS OF AN ARBITRARILY SELECTED STANDARD (NBS)

(Unit is 1×10^{-12})

	VLF			Portable Clocks†		
References	Mitchell [25]	Morgan et al. [26]	Crow et al. [27]	Bagley and Cutler [48]	Bodily [49]	Bodily et al. [50]
Year	1961–1962	1961–1962	1965	1964	1965	1966
CNET		+245*	−8			−12
FOA			+4		+6	−2
LSRH	−51	−34	+2	+7	−5	+2
NPL	+68	+55	−9		+23	−2
NRC		+164*	+5		+5	−3
PO						+15
PTB					+34	−14
RRL			−2		0	+2
USNO		+36	+37	−5**		−2**

* Standard was changed some time after these measurements were made.

** Not the same standard that was used with the VLF comparisons.

† The last measurement made each year was used here. For convenience, the values given here are rounded off to the nearest unit of 1×10^{-12}.

(b) TIME COMPARISONS IN TERMS OF AN ARBITRARILY SELECTED STANDARD (NBS)

(Unit is 1 μs)*

References	Bodily [49]	Bodily et al. [50]**	Time Change ΔT	UT or A Time
Year	1965	1966		
CNET	−242	−142 +358	+100	UT-2
FOA	−883	−868 −368	+15	UT-2
HBN	+1353	+389 +889	+964	A
NPL	+705	+296444† +496944	+295739	A
NRC	+6‡	+352† +200852	+346*	A
PO	−752	−160 +340	+591	UT-2
RGO	+5019	−437 +63	−5456	A
RRL	+1001	+977 +1477	−24	UT-2
USNO	−342	+420 +80	−76	UT-2
WWV	−481	+492 +8	−11	UT-2
WWVH	−231	−494 +6	−363	UT-2

* For convenience, the values are arbitrarily rounded to the nearest microsecond.

** The lower figures for each station are, to the nearest μs, as reported by Bodily et al. [50]; the upper figures are adjusted to take account of retardation of 500 μs in time of NBS-UA standard on April 15, 1966.

† A −200-ms adjustment of other time scales which occurred during the period between measurements was subtracted.

‡ Clock was set by portable clock.

LABORATORIES INVOLVED IN COMPARISONS

CNET—National Center for Commun. Studies, Bagnieux, France
FOA —Swedish Nat'l Defense Institute, Stockholm, Sweden
LSRH—Laboratoire Suisse de Recherche Horlogere, Neuchatel, Switzerland
NBS —National Bureau of Standards, Boulder, Colo.
NPL —National Physical Laboratory, Teddington, England
NRC —National Research Council, Ottawa, Canada
PO —Paris Observatory, Paris, France
PTB —Phys.-Tech. Bund., Braunschweig, Germany
RGO —Royal Greenwich Observatory, Herstmonceux Castle, England
RRL —Radio Research Laboratory, Tokyo, Japan
USNO—U. S. Naval Observatory, Washington, D. C.

*Note added in proof (1970):

The value of 346 μsec for NRC in Table III(b) should be 17 μsec. [See Mungall, A. G., et al., "Atomic Hydrogen Maser Development," Metrologia, Vol. 5, No. 3, p. 93 (1968).]

A. Distribution by Telephone Lines[2]

Underground telephone lines are used to carry a 10-kHz signal, derived from a hydrogen maser, from the Naval Research Laboratory to the Naval Observatory (both in Washington, D. C.) and back, a distance of about 10 miles each way [55]. Using 10-kHz amplifiers with bandwidths of 1 kHz, the fractional frequency changes introduced by the amplifiers and the 20-mile telephone wire loop were about 1×10^{-12}, averaged over 24 hours. This was determined by comparing the signal sent around the loop with that as transmitted.

A similar system, using a 1-kHz signal with outside telephone lines part of the way, was found to have diurnal phase shifts due to the daily ambient temperature cycle [56]. The relationships were determined between 1) the phase shift and the temperature change, 2) a change in the dc line resistance and the temperature change, and from these was found 3) the resistance change versus phase shift, in ohms per microsecond equivalent phase change. The latter was used in the design of an automatic phase corrector introduced into the line so that a change in the dc resistance of the line would provide the error signal to the phase corrector. A reduction of a 30-μs phase shift to a 1-μs phase shift, averaged over 5 hours, was attained on the 46-mile (round-trip) line. Averaged over 48 hours, the phase shift was still 1 μs, which represents a long-term fractional frequency stability of about 6 parts in 10^{12}.

Sources of error in the received signals include pickup of stray signals on the line and environmental effects on the group and phase-delay of the line.

B. Distribution by Coaxial Cables

Measurements of phase variations [57] on 163 km of coaxial cable between Birmingham and London, England, revealed changes of from 4 degrees to 7 degrees on signals sent completely around the loop at 1 kHz. This would cause time errors of about 20 μs at the receiver on this particular coaxial cable. The authors did not state whether the cable was underground or not.

A few limited measurements at the NBS [58] on 1000 feet of RG-58/U coaxial cable indicated that during periods of rapid temperature changes, there are significant phase and frequency changes. This was observed several times with the cable outside in the open sunlight. An increase in temperature caused a decrease in phase delay in the cable. This work is being extended to include other cables and other environmental conditions and also their effects on timing pulses.

Sources of error are the same as for the telephone lines.

VI. Frequency Synthesizers

An important function in the distribution of SFTS is the synthesis of other frequency (and time) signals from the standard frequency, each of which still retains the accuracy of the standard. Two common devices that are important in this process are (a) frequency multipliers, and (b) frequency dividers.

A. Frequency Multipliers

The phase variations occurring in vacuum-tube-type frequency multipliers were investigated in Japan [59], and the investigation included theoretical as well as experimental work. It was reported that the prime causes of the phase fluctuations in the multipliers were the temperature variations of the tuned circuits. Other factors included the fluctuations in the filament and plate supply voltages and the number of multiplier stages. The exact effects of tube noise, especially at low frequencies, were not determined.

For averaging times of 10 seconds, the fractional frequency fluctuations, $\Delta f/f$, were about one part in 10^{11} when multiplying from either 100 kHz to 100 MHz or 100 kHz to 1900 MHz. In multiplying up to the same frequencies the fluctuations were one order of magnitude less when the input was at 10 MHz. By increasing the averaging time to 100 seconds, the fluctuations given above were reduced another order of magnitude. Fluctuations in the power supply contributed less than one part in 10^{-13} for a 10-second observing time.

A Russian investigator obtained similar results [60]. He reported that for vacuum tube multipliers the calculated fractional frequency fluctuations, $\Delta f/f$, were:

a) 0.3×10^{-10} for 1 second averaging time
b) 0.3×10^{-12} for 100 seconds averaging time
c) 0.3×10^{-14} for 10 000 seconds averaging time.

The experimental results reported were that, with a multiplication factor of 2.25×10^6, $\Delta f/f$ was less than 2×10^{-11}.

More recently, a frequency multiplier less susceptible to noise has been reported [61]. The noise level of the multiplier is less than -145 dBm/Hz bandwidth at the 100 MHz output. This would permit frequency comparisons with precision of about one part in 10^{14} in 1-second observing time, with a 10-kHz bandwidth if only the multiplier noise is considered. The spectra of the source would limit the precision to much worse than this.

B. Frequency Dividers

It appears that there is very little quantitative data on the performance of frequency dividers. Some data found in the Russian literature [62] showed that fractional frequency errors of from one part in 10^8 to one part in 10^{10} may be introduced by frequency dividers. However, no details were given concerning the type of dividers or the division ratios used.

VII. Promising Techniques for Future Study

There are several techniques for distributing SFTS which appear to be promising and should receive further study. They involve use of: 1) satellites, 2) meteor trial reflections of VHF radio signals (also called "meteor burst"), 3) NBS multiple-carrier technique and the Omega Navigation System at VLF for distributing time, 4) "round-trip" transmissions at HF, and 5) E-layer reflections at HF.

[2] The type of transmission lines used were not stated.

Satellites, multiple-carrier VLF timing, and round-trip HF transmissions are suitable for SFTS distribution over long distances (global), but the uses of meteor trial and E-layer reflections are limited to shorter ranges (up to about 1200 miles).

As mentioned before, the multiple carrier VLF technique devised by NBS [32], [14], [34], possibly a similar one under study in Italy, [39], [40], and the Omega System appear to be promising for the worldwide distribution of SFTS, as shown by theoretical [14], [39], [40] and experimental studies [34], [36]–[38]. The technical and economic advantages of such a system are: 1) it requires a relatively narrow bandwidth; 2) it will provide continuous and worldwide signals for clock synchronization and time interval requirements; 3) the transmissions are from a single site (a suitable backup in cases of emergency may be provided at another site) and therefore it does not have the transmitter synchronization problems inherent in other possible worldwide systems; 4) the reliability and continuity of its signals at a receiver will be many times greater than that of a network of transmitters that must be kept accurately synchronized at all times if the timing signals are to be useful; and 5) the cost of operating and maintaining a single transmitting station would obviously be much less than that of a network.

It is only fair to say that one of the stations in the network of transmitters could be used, during periods when the network was not synchronized, as a single source of the signals. However, there might be some uncertainty as to its correctness unless special provisions were made.

Some preliminary studies [63]–[65] made of the phase velocity stability of VHF signals reflected by meteor trials indicated "nanosecond" phase stability. However, it cannot be inferred directly from this that the (pulse) group velocity stability is the same, and therefore, that the system is capable of nanosecond time (epoch) distribution. Phase measurements may be made in a relatively narrow frequency band, but pulsed signals with nanosecond resolution require a very wide band; for the same transmitted power the received S/N ratio for the two cases will be very much different. Furthermore, the dispersion characteristics of the propagation medium and multipath distortion become very important for pulsed signals. It can be shown by information theory that time (epoch) information cannot be sent by utilizing only the phase of a sinusoidal carrier signal.

In another experiment, in which pulses were used and their received stability measured, it was reported [66] that the "meteor burst" system was capable of supporting microsecond and fractional microsecond timing accuracies. The results were not verified by independent methods.

A preliminary timing system using pulses has been developed at NBS to determine the best accuracy (and related parameters) of meteor trail reflections. One recent result is that two atomic clocks separated by about 1600 km were synchronized with this system to about 10 microseconds. This was indicated by bringing the two clocks together [67].

The two reported experiments [51]–[54] in distributing time by means of satellites indicate the high potential accuracy of this system. Two types of satellites with two types of distribution equipment that may be used for this are stationary and nonstationary satellites carrying either a clock or a transponder. From theoretical studies made at NBS [68], it was concluded that three synchronous equally spaced satellites carrying atomic clocks could distribute time over all the globe except a small area around each pole.

Some problems to be solved include: 1) devising one or more easy and accurate methods of determining the propagation delays of the time signals from the satellite to the receiver, 2) development of an atomic clock that will run for long periods of time in the satellite, and 3) a quick and easy method of providing information to users on corrections to be applied to time signals received from satellites.

A system proposed by NBS [10] in 1959 to distribute more accurate time and frequency at HF is to use "round-trip" measurements. This requires the use of a transponder at the slave clock in order to be able to measure the propagation delay of the time signals from the transmitter to the slave clock and back. If the time pulses are sent at a rapid rate, say 100 pulses per second, the propagation medium will then change but little from pulse to pulse. The one-way delay time, obtained from the round-trip measurements, will be more accurately known than at present; and it will be updated continuously.

Reflection of HF time signals from the E-layer appears to be a promising method of distributing time over distances of about 800 to 1200 miles. The proper choice of transmitted frequencies, the proper angle of take-off of the signal at the transmitting antenna and the correct pattern of the receiving antenna would be necessary to insure that the E-layer rather than the F_2-layer was being utilized. Higher accuracies achieved by this method depend on the greater stability of the E-layer. Of course, the system would be limited to daylight periods over the path.

Acknowledgment

Helpful comments on the manuscript were received from H. M. Altschuler, J. A. Barnes, D. D. Crombie, and D. H. Andrews. Also, assistance from B. E. Blair was received in preparing Table III. Mmes. Eddyce Helfrich and Carole Craig carefully typed several versions of the paper, including the last one.

Bibliography

References

[1] J. M. Richardson, "Progress in the distribution of standard time and frequency," presented at the URSI XVth General Assembly, Munich, September 1966.

[2] R. Beehler, R. C. Mockler, and J. M. Richardson, "Cesium beam atomic time and frequency standards," *Metrologia*, vol. 1, pp. 114–131, July 1965.

[3] Preliminary Doc. VII/90-E, Study Group VII, Internat'l Radio Consultative Committee (CCIR), Oslo, 1966.

463-560 O - 72 - 24

[4] *Bull. Horaire de Bureau International de l'Heure (BIH)*, ser. J, no. 7, January–February 1965.
[5] "Fixed and mobile services, standard frequencies and time signals, monitoring of emissions," *Documents of the Xth Plenary Assembly*, Internat'l Radio Consultative Committee (CCIR), vol. III, Geneva, 1963.
[6] *Progress in Radio Science 1960–1963 (Radio Standards and Measurements)*, vol. I, R. W. Beatty, Ed. Amsterdam/London/New York: Elsevier, 1965.
[7] *Radio Standards and Measurements*, Commission I, URSI XIVth General Assembly, vol. XIII-1, Tokyo, 1963.
[8] B. E. Blair and A. H. Morgan, "Control of WWV and WWH standard frequency broadcasts by VLF and LF signals," *J. Res. NBS (Radio Sci.)*, vol. 69D, pp. 915–928, 1965.
[9] R. L. Fey, J. B. Milton, and A. H. Morgan, "Remote phase control of radio station WWVL," *Nature*, vol. 193, pp. 1063–1964, March 17, 1962.
[10] A. H. Morgan, "Precise time synchronization of widely separated clocks," Nat'l Bureau of Standards, Boulder, Colo., Tech. Note 22, July 1959.
[11] J. Newman, L. Fey, and W. R. Atkinson, "A comparison of two independent atomic time scales," *Proc. IEEE (Correspondence)*, vol. 51, pp. 498–499, March 1963.
[12] J. Bonanomi, P. Kartaschoff, J. Newman, J. A. Barnes, and W. R. Atkinson, "A comparison of the TA_1 and the NBS-A time scales," *Proc. IEEE (Correspondence)*, vol. 52, p. 439, April 1964.
[13] "Stability and accuracy of standard-frequency and time signals as received," Preliminary Doc. VII/1006-E, XI Plenary Assembly, Internat'l Radio Consultative Committee (CCIR), Oslo, 1966.
[14] A. D. Watt, R. W. Plush, W. W. Brown, and A. H. Morgan, "Worldwide VLF standard frequency and time broadcasting," *J. Res. NBS (Radio Prop.)* vol. 65D, no. 6, pp. 617–627, 1961.
[15] S. Iijima, "An interpretation of frequency change in WWVH signals as received in Tokyo," *Tokyo Astron. Bull.*, 2nd ser., no. 138, 1961.
[16] W. Markowitz, "International frequency and clock synchronization," *Frequency*, vol. 2, no. 4, pp. 30–31, 1964.
[17] R. Doherty, G. Hefley, and R. Linfield, "Timing potentials of Loran-C," *Proc. 14th Annual Symp. on Frequency Control*, pp. 276–297, 1960.
[18] J. A. Pierce, H. T. Mitchell, and L. Essen, "World-wide frequency and time comparisons by means of radio transmissions," *Nature*, vol. 174, pp. 922–923, November 1954.
[19] J. A. Pierce, "Intercontinental frequency comparison by very low-frequency radio transmission," *Proc. IRE*, vol. 45, pp. 794–803, June 1957.
[20] J. A. Pierce, G. M. R. Winkler, and R. L. Corke, "The GBR experiment: A trans-Atlantic frequency comparison between cesium controlled oscillators," *Nature*, vol. 187, no. 4741, pp. 914–916, 1960.
[21] A. D. Watt and R. W. Plush, "Power requirements and choice of an optimum frequency for a world-wide standard frequency broadcasting station," *J. Res. NBS (Radio Prop.)*, vol. 63 D, no. 1, pp. 35–44, 1959.
[22] K. Nakajima, K. Suzuki, Y. Azuma, K. Akatsuka, and K. Nakamura, "Equipment for the international VLF comparison and results of measurements of phase variation between Hawaii and Tokyo," *J. Radio Res. Lab. (Japan)*, vol. 10, pp. 127–136, March 1963.
[23] L. Essen, J. V. L. Parry, and J. A. Pierce, "Comparison of cesium resonators by transatlantic radio transmissions," *Nature*, vol. 180, p. 526, 1957.
[24] L. Essen and J. McA. Steele, "The international comparison of atomic standards of time and frequency," *Proc. IEE (London)*, vol. 109B, pp. 41–47, January 1962.
[25] A. M. J. Mitchell, "Frequency comparison of atomic standard by radio signals," *Nature*, vol. 198, pp. 1155–1158, June 1963.
[26] A. H. Morgan, E. L. Crow, and B. E. Blair, "International comparison of atomic frequency standards via VLF radio signals," *J. Res. NBS (Radio Sci.)*, vol. 69D, pp. 905–914, July 1965.
[27] E. L. Crow, B. E. Blair, and A. H. Morgan, unpublished results, 1966.
[28] A. G. Mungall, R. Bailey, and H. Daams, "Atomic transition sets Canada's time," *Canadian Electronics Engrg.*, vol. 9, pp. 23–37, August 1965.
[29] ——, "The Canadian cesium beam frequency standard," *Metrologia*, vol. 2, pp. 97–104, July 1966.
[30] A. H. Brady, "On the long term phase stability of the 19.8 kc/s signal transmitted from Hawaii and received at Boulder, Colorado," *J. Res. NBS (Radio Sci.)*, vol. 68D, pp. 283–289, 1964.
[31] R. R. Stone, Jr., W. Markowitz, and R. G. Hall, "Time and frequency synchronization of Navy VLF transmissions," *IRE Trans. on Instrumentation*, vol. I-9, pp. 155–161, September 1960.
[32] A. H. Morgan, "Proposal for a new method of time signal modulation of VLF carriers," Nat'l Bureau of Standards, Boulder, Colo., unpublished rept., February 1959.
[33] C. J. Casselman and M. L. Tibbals, "The Radux-Omega long range navigation system," *Proc. 2nd Nat'l Conf. on Military Electronics*, pp. 385–389, June 1958.
[34] A. H. Morgan and O. J. Baltzer, "A VLF timing experiment," *J. Res. NBS (Radio Sci.)*, vol. 68D, pp. 1219–1222, November 1964.
[35] C. H. Looney, Jr., "VLF utilization at NASA satellite tracking stations," *J. Res. NBS (Radio Sci.)*, vol. 68D, pp. 43–45, 1964.
[36] G. Kamas, A. H. Morgan, and J. L. Jespersen, "A new measurement of phase velocity at VLF," *Radio Science*, vol. 1 (new series), December 1966.
[37] A. Chi and S. N. Witt, "Time synchronization of remote clocks using dual VLF transmissions," *Proc. 30th Annual Symp. on Frequency Control*, 1966.
[38] L. Fey and C. H. Looney, Jr., "A dual frequency VLF timing system," *IEEE Trans. on Instrumentation and Measurement*, vol. IM-15, pp. 190–195, December 1966.
[39] C. Egidi and P. Oberto, "Modulazione d' ampiezza con le tre righe spettrali aventi ampiezza e fosi qualunque," *Alta Frequenza*, vol. 33, pp. 144–156, 1964; see Fig. 11.
[40] ——, "Generally distorted three spectral lines amplitude modulation," *Archiv. Elekt. Ubertragung*, vol. 18, no. 9, pp. 525–536, 1964; see Fig. 10.
[41] J. A. Pierce, "Omega," *IEEE Trans. on Aerospace and Electronic Systems*, vol. AES-1, pp. 206–215, December 1965.
[42] J. A. Barnes, D. H. Andrews, and D. W. Allan, "The NBS-A time scale—its generation and dissemination," *IEEE Trans. on Instrumentation and Measurement*, vol. IM-14, pp. 228–232, December 1965.
[43] F. H. Reder and G. M. R. Winkler, "World-wide clock synchronization," *IRE Trans. on Military Electronics*, vol. MIL-4, pp. 366–376, April–July 1960.
[44] F. H. Reder and C. Bickart, "Preliminary flight tests of an atomic clock," *Nature*, vol. 186, pp. 592–593, May 1960.
[45] F. H. Reder, G. M. R. Winkler, and C. Bickart, "Results of a long-range clock synchronization experiment," *Proc. IRE*, vol. 49, pp. 1028–1032, June 1961.
[46] F. H. Reder, P. Brown, G. M. R. Winkler, and C. Bickart, "Final results of a world-wide clock synchronization experiment," *Proc. 15th Annual Symp. on Frequency Control*, 1961.
[47] J. A. Barnes and R. L. Fey, "Synchronization of two remote atomic time scales," *Proc. IEEE (Correspondence)*, vol. 51, p. 1665, November 1963.
[48] A. S. Bagley and L. S. Cutler, "A new performance of the 'flying clock' experiment," *Hewlett-Packard J.*, vol. 15, pp. 1–5, July 8, 1964.
[49] L. Bodily, "Correlating time from Europe to Asia with flying clocks," *Hewlett-Packard J.*, vol. 16, pp. 1–8, April 1965.
[50] L. Bodily, D. Hartke, and R. C. Hyatt, "World-wide time synchronization," *Hewlett-Packard J.*, vol. 17, pp. 13–20, August 1966.
[51] W. Markowitz, see [16].
[52] J. McA. Steele, W. Markowitz, and C. A. Lidback, "Telstar time synchronization," *IEEE Trans. on Instrumentation and Measurement*, vol. IM-13, pp. 164–170, December 1964.
[53] Radio Research Laboratory Frequency Standards Section and Kashima Branch, "Report on clock pulse synchronization experiment via Relay II satellite," *J. Radio Res. Lab. (Japan)*, vol. 12, pp. 311–316, 1964.
[54] W. Markowitz, C. A. Lidback, H. Uyeda, and K. Muramatsu, "Clock synchronization via Relay II satellite," *IEEE Trans. on Instrumentation and Measurement*, vol. IM-15, pp. 177–184, December 1966.
[55] H. F. Hastings, "Transmission to Naval Observatory of reference frequency derived from hydrogen masers at NRL," *NRL Progress Rept.*, pp. 46–47, March 1965.
[56] F. K. Koide, "Standard frequency transmission on phase-compensated telephone lines," 20th Instr. Soc. Am. Conf. and Exhibit, Preprint, 1965.

[57] P. G. Redgment and D. W. Watson, "Very-long-wave phase differences between spaced aerial systems," *J. IEE (London)*, vol. 94, pt. IIIA, no. 16, pp. 1016–1022, 1947.
[58] A. H. Morgan and G. Kamas, unpublished results, 1966.
[59] S. Saburi, Y. Yasuda, and K. Haroda, "Phase variations in the frequency multiplier," *J. Radio Res. Lab. (Japan)*, vol. 10, pp. 137–175, March 1963.
[60] M. Z. Klumel', "Phase stability of frequency multipliers," *Meas. Tech.* (English transl. of *Izmeritel'naya Tekhnika*), vol. 1, pp. 69–74, January–February 1958.
[61] H. P. Stratemeyer, "A low-noise phase-locked-oscillator multiplier," *Proc. IEEE-NASA Symp. on Short-Time Frequency Stability*, NASA, SP-80, pp. 211–215, November, 1964.
[62] E. V. Artem'eva and V. F. Lubentsov, "Additional frequency errors due to the transmission of electrical oscillations," *Meas. Tech.* (English transl. of *Izmeritel'naya Tekhnika*), vol. 1, pp. 226–229, March–April 1958.
[63] D. K. Weaver, P. C. Edwards, A. E. Bradley, and D. N. March, "Final Report—Meteor-burst time synchronization experiments," Electronics Research Lab., Montana State University, Bozeman, ERL Tech. Rept., August 1963.
[64] V. R. Latorre and G. L. Johnson, "Time synchronization techniques," *IEEE Internat'l Conv. Rec.*, pt. 6, pp. 422–427, 1964.
[65] V. R. Latorre, "The phase stability of VHF signals reflected from meteor trails," *IEEE Trans. on Antennas and Propagation*, vol. AP-13, pp. 546–550, July 1965.
[66] W. R. Sanders, "A meteor-burst clock synchronization experiment," private communication, June, 1966.
[67] L. Gatterer and D. Hilliard, unpublished results, October 1966.
[68] J. L. Jespersen, unpublished report, 1966.

Additional Pertinent Publications

[69] D. H. Andrews, "LF-VLF frequency and time services of the National Bureau of Standards," *IEEE Trans. on Instrumentation and Measurement*, vol. IM-14, pp. 233–237, December 1965.
[70] W. T. Blackband, "Diurnal changes of transmission time in the arctic propagation of VLF waves, *J. Res. NBS (Radio Sci.)*, vol. 68D, pp. 205–210, 1964.
[71] ——, "Diurnal changes in the time of propagation of VLF waves over single mode paths," in *Propagation of Radio Waves at Frequencies Below 300 kc/s.* New York: Pergamon, 1964, ch. 16, pp. 219–299.
[72] K. G. Budden, *The Waveguide Mode Theory of Wave Propagation.* New York: Prentice-Hall, 1961.
[73] B. Burgess, "Propagation of VLF waves over distances between 1000 and 3000 km," *J. Res. NBS (Radio Sci.)*, vol. 68D, pp. 15–16, 1964.
[74] G. J. Burtt, "Observations on phase stability of signals from NBA (18 kc/s) Panama as received in New Zealand," *Proc. IEE (London)*, vol. 110, pp. 1928–1932, November 1963.
[75] D. D. Crombie, "Periodic fading of VLF signals received over long paths during sunrise and sunset," *J. Res. NBS (Radio Sci.)*, vol. 68D, pp. 27–34, January 1964.
[76] D. D. Crombie and H. L. Rath, "Reversal of the diurnal phase variations of GBR (16 kilocycles per second) observed over a path of 720 kilometers," *J. Geophys. Res.*, vol. 69, pp. 5023–5027, December 1964.
[77] D. D. Crombie, "Further observations of sunrise and sunset fading of very-low-frequency signals," *Radio Sci.*, vol. 1 (new series), pp. 47–51, January 1966.
[78] K. Davies, *Ionospheric Radio Propagation.* New York: Dover, 1966.
[79] K. Davies and D. M. Baker, "On frequency variations of ionospherically propagated HF radio signals," *Radio Sci.*, vol. 1 (new series), pp. 545–556, May 1966.
[80] B. Decaux and A. Gabry, "Some particular observations on diurnal variations of VLF transmissions received in Paris," *J. Res. NBS (Radio Sci.)*, vol. 68D, 21–25, 1964.
[81] M. R. Epstein, V. R. Frank, G. H. Barry, and O. G. Villard, Jr., "A comparison of long-distance HF radio signal reception at high and low receiving sites," *Radio Sci.*, vol. 1 (new series), pp. 751–762, July 1966.
[82] Special Issue on Frequency Stability, *Proc. IEEE*, vol. 54, February 1966.
[83] D. E. Hampton, "An experimental study of the phase stability of VLF signals," *J. Res. NBS (Radio Sci.)*, vol. 68D, pp. 19–20, 1964.
[84] "Frequency and time standards," Hewlett-Packard Co., Application Note 52, 1966.
[85] J. R. Johler, "The propagation time of a radio pulse," *IEEE Trans. on Antennas and Propagation*, vol. AP-11, pp. 661–668, November 1963.
[86] A. H. Morgan and J. A. Barnes, "Short-time stability of a quartz-crystal oscillator as measured with an ammonia maser," *Proc. IRE*, vol. 47, p. 1782, October 1959.
[87] "Standard frequency and time services," Nat'l Bureau of Standards, Boulder, Colo., NBS Misc. Publ. 236, 1966.
[88] F. H. Reder, C. J. Abom, and G. M. R. Winkler, "Precise phase and amplitude measurements on VLF signals propagated through the arctic zone," *J. Res. NBS (Radio Sci.)*, vol. 68D, pp. 275–281, 1964.
[89] A. M. Thompson, R. W. Archer, and I. K. Harvey, "Some observations on VLF standard frequency transmissions as received at Sydney, N.S.W.," *Proc. IEEE*, vol. 51, pp. 1487–1493, November 1963.
[90] H. Volland, "Diurnal phase variations of VLF waves at medium distances," *J. Res. NBS (Radio Sci.)*, vol. 68D, pp. 225–238, 1964.
[91] J. R. Wait, *Electromagnetic Waves in Stratified Media.* New York: Macmillan, 1962.
[92] ——, "A note on diurnal phase changes of very low frequency waves for long paths," *J. Geophys. Res.*, vol. 68, pp. 338–340, 1963.
[93] J. R. Wait and K. P. Spies, "Characteristics of the earth-ionosphere waveguide for VLF radio waves," Nat'l Bureau of Standards, Boulder, Colo., Tech. Note 300, December 1964.
[94] J. R. Wait, "A possible mechanism for excessive mode conversion in the earth-ionosphere waveguide," *Radio Sci.*, vol. 1 (new series), pp. 1073–1076, September 1966.
[95] D. Walker, "Phase steps and amplitude fadings of VLF signals at dawn and dusk," *J. Res. NBS (Radio Sci.)*, vol. 69D, pp. 1435–1443, 1965.
[96] A. D. Watt and R. D. Croghan, "Comparison of observed VLF attenuation rates and excitation factors with theory," *J. Res. NBS (Radio Sci.)*, vol. 68D, pp. 1–9, 1964.

Reprinted from the PROCEEDINGS OF THE IEEE
VOL. 55, NO. 6, JUNE, 1967
pp. 827-836
THE INSTITUTE OF ELECTRICAL AND ELECTRONICS ENGINEERS, INC.
PRINTED IN THE U.S.A.

RADIO SCIENCE, Vol. 2 (New Series), No. 6, June 1967

Five Years of VLF Worldwide Comparison of Atomic Frequency Standards

B. E. Blair,[1] E. L. Crow,[2] and A. H. Morgan [1]

(Received January 19, 1967)

The VLF radio broadcasts of GBR(16.0 kHz), NBA(18.0 or 24.0 kHz), and NSS(21.4 kHz) have enabled worldwide comparisons of atomic frequency standards to parts in 10^{10} when received over varied paths and at distances up to 9000 or more kilometers. This paper summarizes a statistical analysis of such comparison data from laboratories in England, France, Switzerland, Sweden, Russia, Japan, Canada, and the United States during the 5-year period 1961–1965. The basic data are differences in 24-hr average frequencies between the local atomic standard and the received VLF radio signal expressed as parts in 10^{10}. The analysis of the more recent data finds the receiving laboratory standard deviations, $\hat{\alpha}_i$, and the transmission standard deviation, $\hat{\tau}$, to be a few parts in 10^{11}. Averaging frequencies over an increasing number of days has the effect of reducing $\hat{\alpha}_i$ and $\hat{\tau}$ to some extent. The variation of the $\hat{\alpha}_i$ with propagation distance is studied. The VLF-LF long-term mean differences between standards are compared with the recent portable clock tests, and they agree to parts in 10^{11}.

1. Introduction

Six years ago in London, the XIIIth General Assembly of URSI adopted a resolution (No. 2) which strongly recommended continuous very-low-frequency (VLF) and low-frequency (LF) transmission monitoring throughout the world by atomic frequency standards (Decaux, 1961). URSI proposed such tests to obtain the day-to-day phase stabilities of VLF and LF radio signals and to determine their usefulness for precise time and standard frequency comparisons at distant points. Since that time, some 10 laboratories have collected and exchanged atomic standard frequency data, obtained through such transmissions as GBR (England, 16 kHz), NBA (Canal Zone, 18 or 24 kHz), WWVL (U.S.A., 20 and 19.9 kHz), NSS (U.S.A., 21.4 kHz), and WWVB (U.S.A., 60 kHz). Since the Twelfth General Conference of Weights and Measures authorized a temporary atomic designation for the physical measurement of time in October 1964 (General Conference of Weights and Measures XII, 1964), these comparisons of atomic frequency standards have taken on added significance.

This paper supplements a previous 18-month comparison of atomic frequency standards (Morgan, Crow, and Blair, 1965) and covers the period 1961 up through part of 1966. Many previous comparison studies through VLF and LF radio transmissions have been reported. In addition to those references given in our previous paper, see Nakajima, Suzuki, Azuma, Akatsuka, and Nakamura (1963); Reder, Åbom, and Winkler (1964); and Mungall, Bailey, and Daams (1966). These past 6 years have seen tremendous improvement in atomic frequency standards (McCoubrey, 1966); microsecond time synchronization at remote points via satellites (Steele, Markowitz, and Lidback, 1964; Markowitz, Lidback, Uyeda, and Muramatsu, 1966); improvements in the transmission of VLF and LF radio signals (Milton, Fey, and Morgan, 1962; Barnes, Andrews, and Allan, 1965; Bonanomi, 1966; U.S. Naval Observatory, 1966); and side-by-side worldwide comparisons of atomic frequency standards via portable cesium (Cs) standards to parts in 10^{12} (Bagley and Cutler, 1964; Bodily, 1965; Bodily, Hartke, and Hyatt, 1966).

In the light of such advances, it is the purpose of this paper to analyze the 5-year accumulation of daily observations of atomic frequency standards systematically made at certain laboratories by means of received VLF radio signals, to note the present-day status of such comparisons, and to contemplate further work and events which could eventually lead to a universal standard which might control an international atomic time-scale system (CCIR, 1966).

2. Characteristics of Atomic Frequency Standards

Characteristics of the atomic frequency standards located at the various receiving laboratories are listed in table 1. Figure 1 shows the locations of both the laboratories and the VLF and LF transmitters engaged in these studies, together with great circle distances between applicable transmitters and receivers. These propagation distances range from 50 to 9470 km, and all such paths lie in the northern hemisphere.

3. Summary of Statistical Analysis

The methods of comparison and statistical analysis have been described by Morgan, Crow, and Blair (1965). Each laboratory records the received VLF signals in

[1] National Bureau of Standards, Boulder, Colorado 80302.
[2] Environmental Science Services Administration, Boulder, Colorado 80302.

Table 1. Characteristics of Atomic Frequency Standards

Laboratory	Laboratory Abbreviation	Approximate Laboratory Geographic Location	Atomic Standard: Type	Atomic Standard: Period of Observation	Atomic Standard: Designation	Interaction Length-cm	Reported* Accuracy pts in 10^{11}	Reference
All-Union Research Institute of Physical Technical and Radio Technical Measurements Moscow, Russia	ARIM	UNKNOWN	--	Jan 1, 1964 to Dec 31, 1965	--	--	--	--
Centre National D'Études des Télécommunications Bagneux, France	CNET	48° 48' N 2° 19' E	Cs-Commercial	Jan 1, 1961 to Apr 30, 1965	A107	94	±22	Decaux (1963)
			Cs-Combination Commercial-Laboratory	Apr 30, 1965 to Present	Cs 2	25	± 2	Decaux (1967)
Cruft Laboratories Harvard University Cambridge, Mass., USA	CRUFT	42° 22' N 71° 6' W	Cs-Commercial (inactive)	Jan 1, 1961 to Dec 31, 1963	S 203	94	±50 (Mfr's guarantee)	Pierce (1963)
Research Institute of National Defence-FOA Stockholm, Sweden	FOA	59° 20' N 18° 3' E	Cs-Commercial	Mar 1, 1965 to Present	--	12.4	± 2	Bodily (1966), Bodily, Hartke, and Hyatt (1966)
Laboratoire Suisse de Recherche Horlogère Neuchâtel, Switzerland	LSRH	47° 00' N 6° 57' E	Cs-Laboratory	Jan 1, 1961 to Dec 31, 1963	LSRH-II	409	± 3(1σ)	Kartaschoff (1962)
				Jan 1, 1964 to June 30, 1966			± 1(1σ)	Kartaschoff (1964, 1967)
National Bureau of Standards Boulder, Colorado, USA	NBS	40° 00' N 105° 16' W	Cs-Laboratory	Jan 1, 1961 to Jun 30, 1962	NBS-I	55	± 1(3σ)	Beehler, Glaze (1966), Glaze (1967)
				Jul 1, 1962 to Aug 31, 1963	NBS-II	164	± 0.8(3σ)	
				Sept 1, 1963 to May 31, 1965	NBS-III	366	± 0.5(3σ)	
				Jun 1, 1965 to present				
U. S. Naval Observatory Washington, D. C., USA	NOB	38° 55' N 77° 39' W	Cs-Beam (weighted average of 9 Cs stds)	Jan 1, 1961 to May 31, 1965	A.1	varied	± 2	Markowitz (1962, 1964)
			Cs-Commercial	Jun 1, 1965 to present	Cs-60	12.4	±0.9(ref H_1)	Buchanan, Pritt, and Hastings (1965)
National Physical Laboratory Teddington, Middlesex, England	NPL	51° 25' N 0° 20' W	Cs-Laboratory	Jan 1961 to Nov 1963	NPL-II, MOD 1	265	± 3	Essen, Steele, and Sutcliffe (1964), Essen (1967)
				Dec 1963 to Jan 1964	NPL-II, MOD 2			
				Jan 1964 to Jan 1965	NPL-II, MOD 3			
				Jan 1965 to present	NPL-II, MOD 4			
National Research Council Ottawa, Ontario, Canada	NRC	45° 25' N 75° 43' W	Cs-Laboratory	Jan 1, 1961 to Nov 6, 1962	NRC-1	80	±30	Kalra (1961)
				Feb 17, 1965 to Present	NRC-2	210	± 1.9	Mungall, Bailey, and Daams (1966)
Tokyo Astronomical Observatory Mitaka, Near Tokyo, Japan	TAO (RRL)	35° 40' N 139° 32' E	$N^{14}H_3$-Laboratory	Aug 14, 1964 to Present	--	--	± 3 (resetability)	CCIR (1964)

*Methods of determining vary. Consult applicable reference for complete details for a particular standard. In most cases the precision of short-term measurements is reported also, but the methods of determining vary widely.

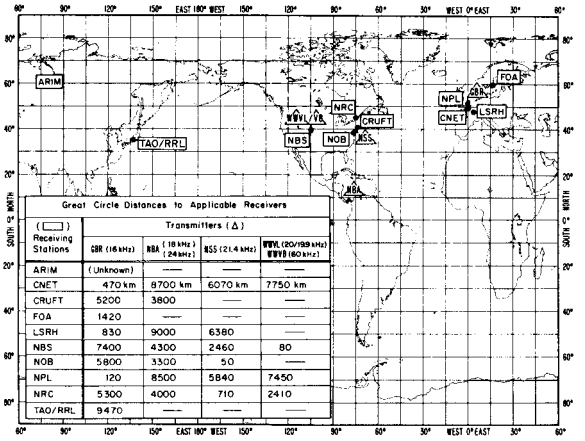

FIGURE 1. *Locations of receiving laboratories and VLF and LF transmitters.*

terms of a transfer oscillator, which is periodically calibrated in terms of the primary frequency standard. It should be emphasized that the data analyzed are thus only measurements at certain laboratories possessing atomic standards and systematically recording signals from VLF transmitters and do not include any measurements at the VLF transmitters. From the reduction of such phase recordings, daily (24-hr) averages of the received frequencies are determined and exchanged among the different laboratories.

Initial analysis of these data yields the long-term mean of the daily observations at each receiving laboratory and the variance s_i^2 (or standard deviation s_i) of these observations. The means give immediately the long-term mean differences between the atomic standard frequencies of the receiving laboratories. By averaging the daily observations from all receiving laboratories and a little further statistical analysis (see Morgan et al., 1965), the variance $\hat{\tau}^2$, common to all receiving laboratories, is obtained. Thus $\hat{\tau}$ includes variations of the transmitter oscillator, the transmitting system, and propagation variations common to all receiving stations. A decomposition of s_i^2 into two components can then be achieved, $\hat{\tau}^2$ being one component; the other component, $\hat{\alpha}_i^2$, may be defined simply as $\hat{\alpha}_i^2 = s_i^2 - \hat{\tau}^2$. It follows that $\hat{\alpha}_i$ consists of all variations of the measurements at the ith receiving laboratory *not* common to all laboratories, and thus includes variations of both primary and transfer oscillators, other parts of the receiving system, and of the propagating signal peculiar to the ith transmission path.

3.1. Long-Term Mean Differences Between Atomic Standards

It is of interest to test the mean frequencies measured simultaneously by receiving laboratories over periods as long as a year for the presence of systematic differences between atomic standards. Hence, the

differences, Δ_i, of yearly means from the yearly grand mean for all laboratories are shown in tables 2 and 3 for GBR and NBA or NSS for the years 1961–1965. (NBA suspended operations for about a year in 1965, and NSS was then monitored instead.)

The mean differences of tables 2 and 3 are also combined and displayed in figure 2. We formulate the following generalizations from tables 2 and 3 and figure 2:

(a) The maximum of the yearly mean difference in table 2 between atomic frequency standards decreased from 39 parts in 10^{11} in 1961 to 8 parts in 10^{11} in 1965 (aside from one standard introduced in 1964); table 3 shows a similar decrease, from 42 to 5. Thus, as shown in figure 2, the mean difference of each standard from the grand mean has tended to decrease.

(b) Before 1965, the grand mean for each year and each transmitter differed up to 8 parts in 10^{11} from the prescribed fractional frequency offset of -1500 or -1300 parts in 10^{11} and up to 14 parts in 10^{11} from that of the other transmitter. However, these differences reduced to just 0.1 part in 10^{11} in 1965. (The prescribed fractional frequency offset, which is presently -3000 parts in 10^{11}, is an approximation, agreed upon internationally, to the difference in the rate of occurrence of time ticks on the universal time scale (UT2) and second pulses on the atomic or ephemeris time scales (Hudson, 1965).) However, among the differences between the two transmitters as measured by any given receiving laboratory, i.e., between corresponding means (Δ_i) of tables 2 and 3, the maximum absolute difference ranges only between 2 and 5 parts in 10^{11}.

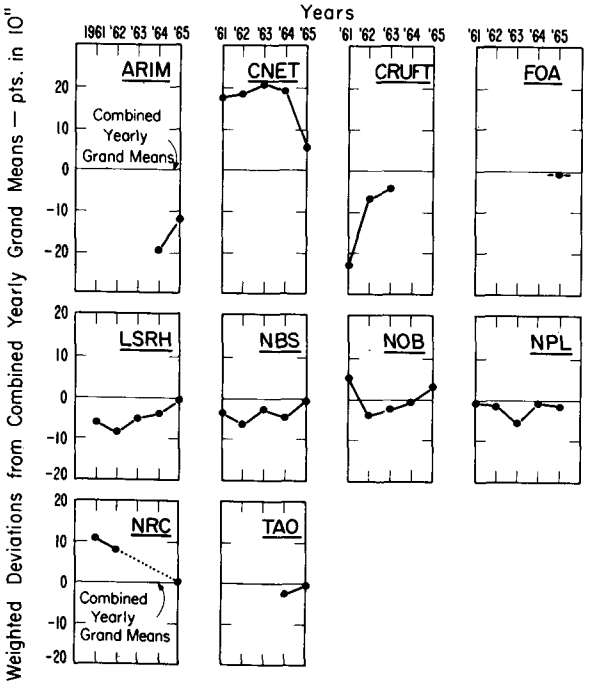

FIGURE 2. *Average agreement among atomic standards, 1961–1965 as indicated by transmissions of GBR and NBA (NSS, 1965) combined.*

(Some receiving stations have reported frequency values only in terms of GBR. Thus the deviations only from the GBR yearly grand means are shown for ARIM, FOA, TAO, and NRC (1965).)

3.2. Day-to-Day Fluctuations Associated with Receiving Laboratories

The part of the fluctuation from day to day of the daily frequency measurement (of a transmitted signal) by the ith receiving laboratory, which is associated uniquely with that laboratory, is characterized by a standard deviation α_i. This includes system errors and propagation effects peculiar to the ith path as well as receiver atomic standard variations. The estimate of α_i from any given quarter (of a year) is denoted by $\hat{\alpha}_i$. (Since the simultaneous statistical analysis for all $\hat{\alpha}_i$ requires complete sets of daily observations from all laboratories, using data in quarterly groups turned out to be desirable.) Yearly average estimates of α_i, denoted by $\bar{\hat{\alpha}}_i$, are presented in this paper, obtained as weighted root-mean-square combinations of the $\hat{\alpha}_i$ with weights equal to the number of days per quarter, minus 1.[3] Figures 3 and 4 give the $\bar{\hat{\alpha}}_i$ for the various laboratories reporting reception of GBR, NBA, and NSS during 1961–1965. We formulate the following generalizations from figures 3 and 4 and from approximate confidence intervals that are not shown:

(a) The standard deviation $\hat{\alpha}_i$ for most laboratories tended to decrease from 1961 to 1965, whether derived from GBR transmissions or NBA and NSS transmissions. If this decrease were attributed to improvement in atomic standards, it would have to be assumed that the standards contribute a major portion of the α_i; however, it seems likely that the measuring systems have been improved too, and it is possible that propagation fluctuations decreased.

(b) The $\bar{\hat{\alpha}}_i$ derived from GBR transmissions and the corresponding $\bar{\hat{\alpha}}_i$ derived from NBA or NSS transmissions tend to be near each other. All of the values for 1965, with one exception, fall between two and six parts in 10^{11}. The recently reported within-laboratory standard deviations of atomic standard average frequencies for 1-day periods are at least an order of magnitude less than these values; that is, a few parts in 10^{12} (McCoubrey, 1966).

(c) Three of the $\bar{\hat{\alpha}}_i$ from GBR and NBA transmissions are zero (LSRH and NBS from GBR in 1962 and NBS from NBA in 1964). These and other substantial variations are easily accounted for by the uncertainties in the estimates. Even 95 percent confidence intervals based on independence of daily observations place upper limits for these two values of α_i at five parts in 10^{11}, and intervals taking account of dependence would

[3] See Morgan et al. (1965) for a more complete explanation of the theory and notation. In brief, α_i and τ are standard deviations of theoretical distributions that could be known only if infinite observations were made; $\hat{\alpha}_i$ and $\hat{\tau}$ are estimates of α_i and τ made from a finite number of observations, here generally restricted to 1 per day for a quarter of a year; $\bar{\hat{\alpha}}_i$ and $\bar{\hat{\tau}}$ are rms averages of the four $\hat{\alpha}_i$ and four $\hat{\tau}$ for each year.

Table 2. Yearly Means Δ_i and Standard Deviations s_i of 24-hour Average Frequencies Transmitted by GBR and Measured by Various Standards.

The Δ_i are deviations from the yearly grand mean of all standards (positive if ith standard is low).
n_i = number of 24-hour average frequencies

Frequency unit - 1 part in 10^{11}

Atomic Frequency Standard	1961			1962			1963			1964			1965		
	n_i	Δ_i	s_i	n_i	Δ_i	s_i	n_i	Δ_i	s_i	n_i	Δ_i	s_i	n_i	Δ_i	s_i
ARIM	-	-	-	-	-	-	-	-	-	238	-19.5	17.4	144	-12.8	10.3
CNET	323	+16.4	31.9	323	+17.8	17.9	345	+21.2	13.2	350	+20.1	10.4	310 * (230)	+6.4 (+0.4)*	14.3 (8.0)*
CRUFT	246	-22.9	32.0	282	-7.3	14.9	304	-5.0	10.9	-	-	-	-	-	-
FOA	-	-	-	-	-	-	-	-	-	-	-	-	258	-1.0	7.8
LSRH	329	-6.1	33.4	268	-7.8	14.9	330	-5.0	8.2	355	-2.7	9.9	342	-0.1	8.5
NBS	326	-4.2	32.4	302	-6.9	14.1	347	-3.1	8.8	350	-3.9	9.5	328	-0.9	7.8
NOB	321	+ 2.9	29.3	317	-4.6	13.1	319	-3.0	9.1	352	+0.7	10.4	350	+2.9	9.3
NPL	317	-0.6	29.6	304	-0.1	15.2	331	-6.4	8.2	351	+ 0.2	7.2	341	-1.4	7.7
NRC	339	+9.3	39.8	286	+ 6.9	21.9	-	-	-	-	-	-	285	0.0	9.4
TAO	-	-	-	-	-	-	-	-	-	135	-2.7	13.2	339	-1.0	11.8
GRAND MEAN	-1492.3			-1299.3			-1295.8			-1504.5			-1499.9		

*New standard, Apr.-Dec. 1965. Mean of new standard not included in grand mean.

Table 3. Yearly Means Δ_i and Standard Deviations s_i of 24-hour Average Frequencies Transmitted by NBA (NSS in 1965) and Measured by Various Standards.

The Δ_i are deviations from the yearly grand mean of all standards (positive if ith standard is low).
n_i = number of 24-hour average frequencies

Frequency unit - 1 part in 10^{11}

Atomic Frequency Standard	1961			1962			1963			1964			1965		
	n_i	Δ_i	s_i	n_i	Δ_i	s_i	n_i	Δ_i	s_i	n_i	Δ_i	s_i	n_i	Δ_i	s_i
CNET	251	+ 18.4	14.6	299	+18.9	12.8	276	+19.2	9.0	240	+17.5	9.3	204 (174)*	+ 1.7 (-3.0)*	13.0 (6.2)*
CRUFT	238	-23.8	15.2	263	-7.1	9.1	249	-4.6	9.0	-	-	-	-	-	-
LSRH	322	-6.1	11.9	284	-9.1	10.2	296	-5.4	5.6	257	-5.7	6.4	224	-1.1	8.1
NBS	230	-3.3	12.7	257	-6.0	8.6	297	-3.1	4.2	236	-6.4	4.3	245	-0.9	5.5
NOB	294	+ 6.5	11.6	316	-3.8	9.2	273	-2.3	4.3	290	-2.6	5.0	270	+2.1	7.1
NPL	259	+ 0.1	14.6	241	-2.9	14.2	205	-5.0	6.3	154	-3.2	8.0	169	-2.7	7.2
NRC	133	+13.8	22.4	240	+ 9.2	18.0	-	-	-	-	-	-	-	-	-
GRAND MEAN	-1506.2			-1295.1			-1298.9			-1495.9			-1500.0		

*New standard, Apr.-Dec. 1965. Mean of new standard not included in grand mean.

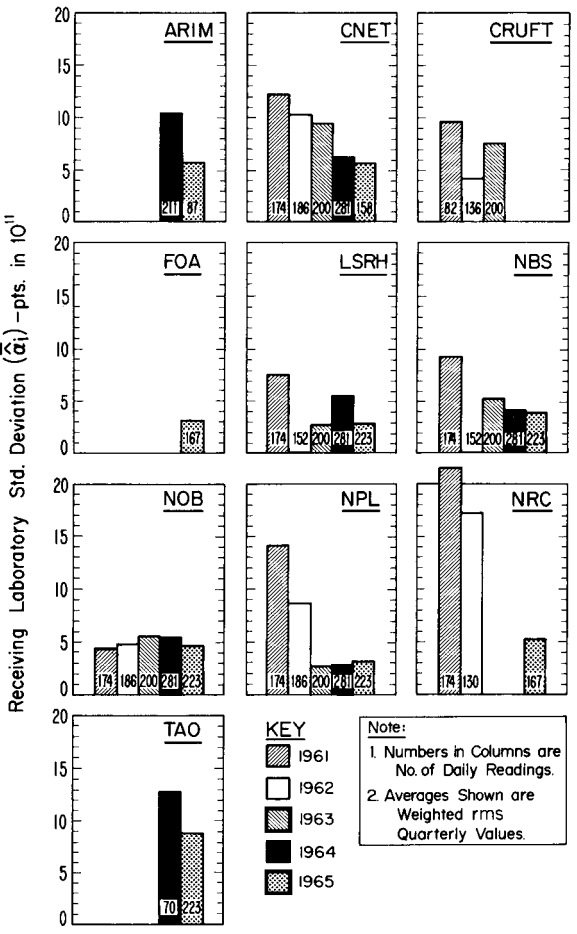

FIGURE 3. *Derived standard deviations, $\bar{\hat{\alpha}}_i$, (associated with receiving laboratories) of daily average frequency measurements of GBR transmissions.*

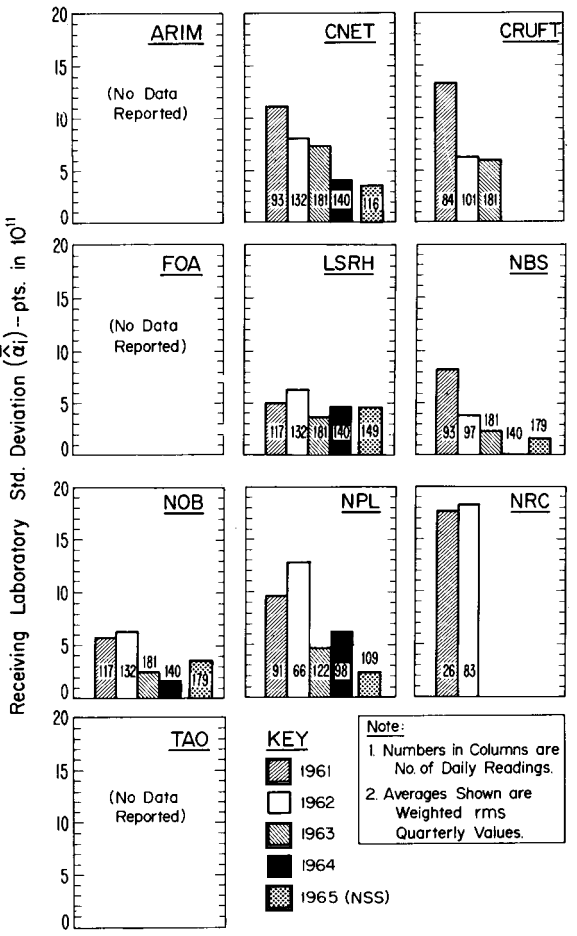

FIGURE 4. *Derived standard deviations, $\bar{\hat{\alpha}}_i$, (associated with receiving laboratories) of daily average frequency measurements of NBA (NSS in 1965) transmissions.*

place them even higher. (Uncertainties in estimates are discussed further in section 4.)

3.3. Day-to-Day Fluctuations of Transmissions

The day-to-day fluctuations in transmissions are characterized by a standard deviation τ, which includes transmitting system variability and propagation variability common to all receiving stations included in the analysis as well as transmitter oscillator variability. The data do not permit analysis into components arising from these three sources. Figure 5 shows the estimated standard deviations $\bar{\hat{\tau}}$ of transmission errors for GBR and NBA for each year 1961 through 1964, as well as 1965 values for GBR and NSS, and values for NSS and WWVL for parts of 1966. From 1961 through 1963 the $\bar{\hat{\tau}}$ decreased by 60 or 65 percent, after which they leveled off to values of less than 7 parts in 10^{11}. This improvement is believed to result from improved transmitter-oscillator control.

4. Effects of Averaging VLF Frequency Data

To show the effects of long-term averaging of standard frequency data, averages over consecutive nonoverlapping intervals of 7, 15, 30, 60, 120, and 240 days were computed for the 1963–64 GBR data and for similar intervals for the 1965 GBR data. Then the values of $s_i^2, \hat{\alpha}_i^2$, and $\hat{\tau}^2$ were calculated using these longer-term averages as the individual observations. An example of the effective reduction in the magnitude of s_i^2, $\hat{\alpha}_i^2$, and $\hat{\tau}^2$ is shown graphically in figure 6. The variances s_i^2 and variance components, $\hat{\alpha}_i^2$ and $\hat{\tau}^2$, are plotted with logarithmic scales because, in the case of independent observations from a stable distribution (as well as asymptotically in at least some cases of autocorrelated observations), they should vary inversely with the first power of the length of the averaging interval. (The variances s_i^2 of 1-day averages, as well as the $\hat{\alpha}_i^2$ and $\hat{\tau}^2$ derived from them, are determined from a large number of days, whereas the variances

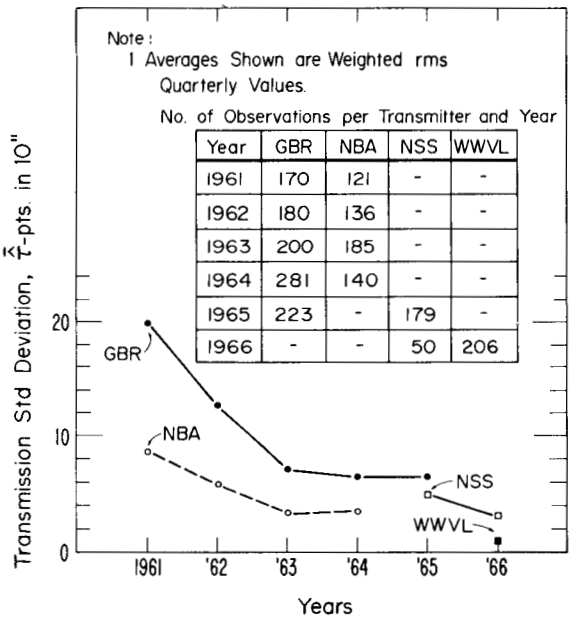

FIGURE 5. *Derived standard deviations, $\bar{\hat{\tau}}$, associated with transmitter (GBR, NBA, NSS, or WWVL), of daily average frequency measurements by receiving laboratories.*

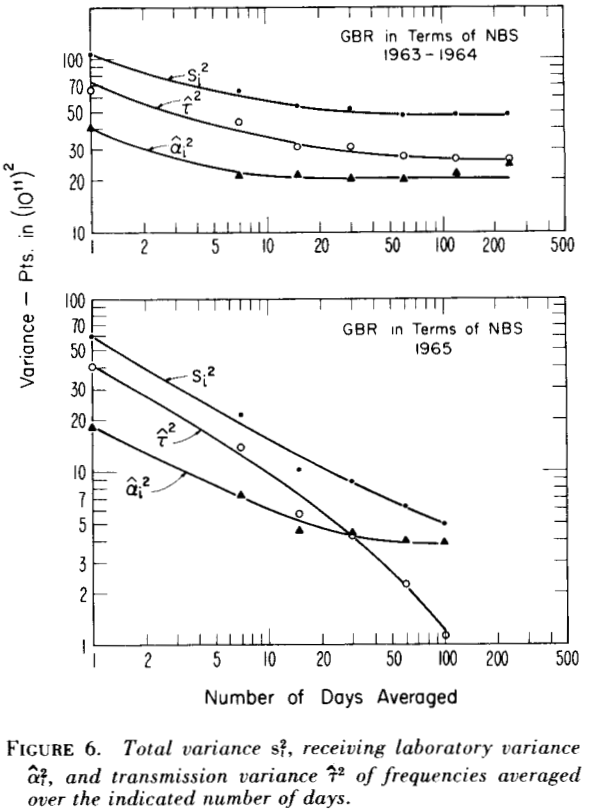

FIGURE 6. *Total variance s_f^2, receiving laboratory variance $\hat{\alpha}_f^2$, and transmission variance $\hat{\tau}^2$ of frequencies averaged over the indicated number of days.*

s_f^2 of 60-day averages are determined from 12 values for 1963–1964 and from 3 values for 1965. Other points are proportionally limited.)

We see from figure 6 that although there is at least an initial decrease as the averaging interval length increases, s_f^2 levels off at about ½ of its value for 1-day averages in the 1963–1964 data, but decreases steadily as about the −0.6 power of the averaging interval length in the 1965 data. The leveling off in 1963–1964 is associated with substantial spectral components of periods longer than the averaging interval that are not included in values of s_f^2, $\hat{\alpha}_f^2$, and $\hat{\tau}^2$ calculated from short-term (such as 1-day) averages. Figure 6 may be compared with Allan's figures 4–7 (1966), McCoubrey's figure 17 (1966), and Bodily's figure 5 (1966), which graph within-laboratory standard deviations of atomic standard frequencies against averaging intervals up to about 1 day. These graphs, showing the variation of measurement for averaging intervals of 1 day or less, indicate a slope near −0.5 for cesium standards, corresponding to a slope for variances near −1. Our figure 6 includes both propagation and measuring system variation, as well as atomic standard variation. Which components are substantial for periods beyond 1 day still appear to be incompletely known. The limited reduction in variances through averaging may result, at least in part, from long-term variations in the ionosphere such as solar-cycle, seasonal, and lunar-tide variations (Chilton, Crombie, and Jean, 1964). (An editorial reader, J. A. Barnes, notes that this limited reduction might be explained by the hypothesis that flicker noise frequency modulation is present, a fact recognized in several papers on crystal oscillators and in Vessot et al. (1966) for atomic devices.)

The relatively slow decrease of variability with increasing interval length (or number of observations) exemplified in figure 6 renders the classical confidence intervals based on independent observations too short and is the reason for not including them in this paper. The effect of averaging intervals, on s_f^2, $\hat{\alpha}_f^2$, and $\hat{\tau}^2$ and their uncertainties is under further study.

5. Relation of Precision of Frequency Comparison With Distance

Since Pierce's pioneering work nearly a decade ago on the precision of short-term phase measurements of 16-kHz signals received over a 5200-km path (Pierce, 1957), there has been considerable question whether such precision depends upon distance. Pierce, Winkler, and Corke (1960) later extended the short-term results to observations over 24-hr periods. They found standard deviations of about 2 parts in 10^{11} for GBR frequency measurements over the same 5200-km path. The frequency measurements given in the present paper were made at consecutive 24-hr times, generally near the center of the all-daylight period, to minimize effects from the diurnal height changes of

the ionosphere. The daily phase variations in such frequency data, attributable to ionospheric effects, are believed to result largely from day-to-day height changes of the reflecting layer of the ionosphere. Pierce et al. (1966) state that phase changes due to ionospheric height changes that are common to the whole path would be proportional to distance. Superimposed on these day-to-day variations are shorter-term phase fluctuations, whose contribution is difficult to assess at this point. Pierce et al. (1966) show some indication that these shorter-term variations in a received VLF signal increase with distance to the 1/4 power.

Our analysis of the observed variance s_i^2 of average frequency fluctuations into components $\hat{\tau}^2$ associated with the transmitter and $\hat{\alpha}_i^2$ associated with the receiver (including the path to the receiver) provides data for analyzing the variation with distance more specifically. Since the true variance $\hat{\alpha}_i^2$ for the ith receiver includes contributions from its atomic standard and measurement system that have nothing to do with distance from the transmitter, a simple reasonable model for it would be of the form

$$\alpha_i^2 = \alpha_{0,i}^2 + \gamma^2 (D_i - L)^{2\beta}, \qquad L \leq D_i \leq U,$$

where D_i is the great-circle distance from the transmitter to the receiver over which the signal is received and $\alpha_{0,i}$, β, γ, L, and U are constants to be determined. A more refined model would be expected to have all of the constants depending on i, since path position and orientation, proportion of water below the path, and interference between short and long great-circle paths are factors. In addition, the model can be tested only by sample values $\hat{\alpha}_i^2$ (or averages thereof, $\bar{\hat{\alpha}}_i^2$), which are subject to considerable sampling error not included in the above equation; there is more relative error in $\hat{\alpha}_i^2$ than in the s_i^2 from which it is derived by subtracting $\hat{\tau}^2$.

However, it is possible to give outside bounds for the limiting distances L and U. Certainly U is no larger than the circumference of the earth, 40,000 km. A lower limit to L is provided by the distance beyond which first-order mode theory is satisfactory; the value of L so indicated is somewhat arbitrary, but the work of Wait (1957, 1962) suggests 2000 to 3500 km for daytime propagation. For shorter distances, higher-order modes interfere with no simple dependence on distance. In figure 7 we have plotted the yearly average receiver standard deviations, $\bar{\hat{\alpha}}_i$, against distance for the nine receiving stations recording at least one of GBR, NBA, and NSS during 1963–65. (The earlier values were not included because they tend to be larger than the values for the period 1963–65 which seems characterized by approximate stability.) Although the carrier frequencies of the transmitters vary from 16 to 24 kHz, and Pierce et al. (1966) normalize phase variations by division by the carrier frequency, we have not done this because $\hat{\alpha}_i$ includes atomic standard and system measurement variations as well as propagation variations and the effect is relatively small here anyway.

We observe from figure 7 that distance D does not appear to explain a major portion of the variation of $\bar{\hat{\alpha}}_i$. However, if we exclude the data for $D < 2000$ km on the basis of interfering modes as indicated above, there is a substantial correlation with distance, consistent with the model $\alpha^2 = 2^2 + (D - 2.5)^2$ for $2.5 \leq D \leq 10$ with D in megameters.

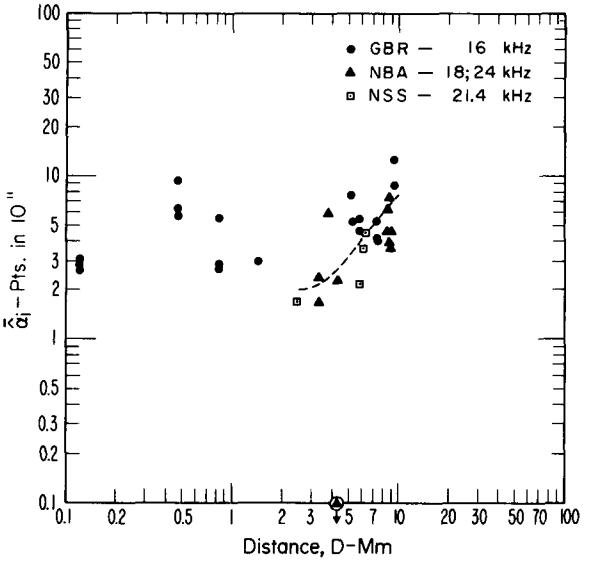

FIGURE 7. *Receiving laboratory standard deviation,* $\bar{\hat{\alpha}}_i$, *plotted against VLF propagation distance,* D.

6. Relation of Long Term VLF-LF Measurements to Direct Measurements With Portable Cesium Standards

Recently there have been several "flying clock" experiments in which portable atomic frequency standards have been intercompared side by side with atomic standards located in worldwide laboratories for short observation periods (Bagley and Cutler, 1964; Bodily, 1965; Bodily, Hartke, and Hyatt, 1966). Comparison between such measurements and the long-term VLF-LF data is shown in table 4 for the 1965 and 1966 data. (These data are in terms of deviations from NBS measurements to facilitate comparisons between the portable Cs standards and the VLF-LF measurements.) In most cases the direct measurements with portable Cs standards are within parts in 10^{12} of the VLF-LF mean values. Figure 8 gives the distribution of the differences of the daily observations of three receiving laboratories from those of NBS. (Superimposed on these distributions are fitted normal curves.) Also shown are several of the portable clock direct measurements.

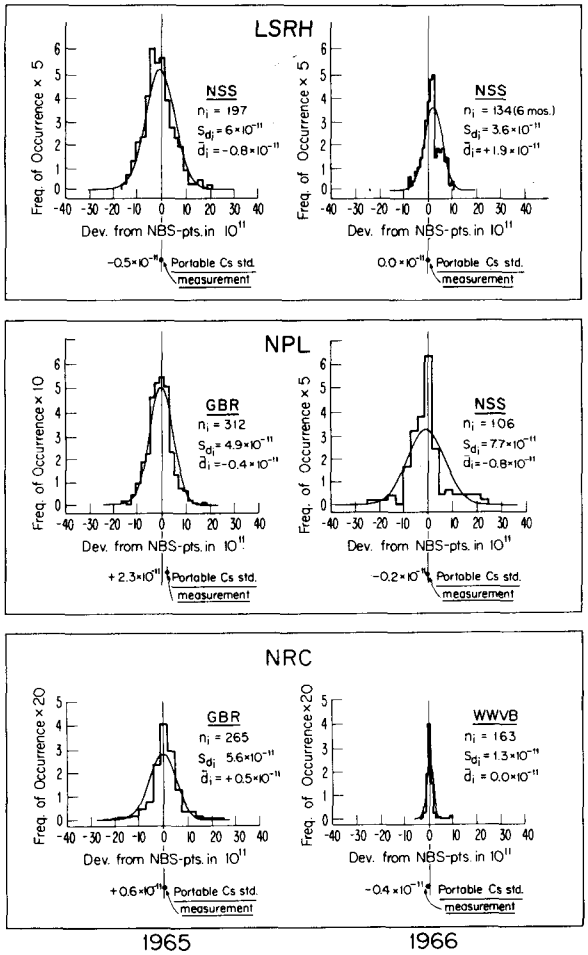

FIGURE 8. *Relation of portable Cs standard data to frequency distributions of differences of VLF–LF daily measurements by NBS and those by three other laboratories.*
(The portable Cs standard data are also shown as differences from NBS. Basic data are from Bodily (1965) and Bodily, Hartke, and Hyatt (1966).)

If one assumes that all the receiving laboratory standards are randomly selected members of a population of atomic standards and that the portable reference standards do not change systematically, a standard error of the mean difference between the receiving laboratories and the portable standards, $s/\sqrt{n}$ (where s is the standard deviation of the observed differences of the frequencies of n laboratories from those of the portable standards), can be computed for both 1965 and 1966, and confidence limits for the mean differences constructed. The 1965 and 1966 95 percent confidence limits are as follows:

$$\left.\begin{aligned}(1965)\ -5.1 < +8.2 < +21.5\ (n=7)\\ (1966)\ -3.2 < +1.1 < +5.4\ (n=13)\end{aligned}\right\}\ \text{pts. in } 10^{12}.$$

Thus, there is no statistically significant mean difference between the assumed population of receiving laboratory atomic standards and the population of portable Cs standards. This latter population has been studied by Bodily (1966), whose histogram shows that 95 out of a population of 100 portable cesium standards fall within about ±5 parts in 10^{12} of the reference cesium frequency.

7. Future Remote Comparisons of Atomic Frequency Standards

With the increased gains in the stability of atomic frequency standards, one can foresee the eventual need of comparing such standards at remote points with errors less than parts in 10^{12}. Longer period measurements may permit this to some extent, but improvements in transmitter control and long-term comparison studies using portable clocks as indicated below should obtain fuller realization of the maximum possible precision.

Transmitter improvements: Improved transmitter control has resulted in a reduction by a factor of three or more of the transmission standard deviation associated with VLF broadcasts (fig. 5). Thus, the WWVL transmission standard deviation, $\bar{\hat{\tau}}$, for 9 months in 1966, is less than 1 part in 10^{11}. The GBR transmitter has been modified recently (British Post Office, 1964) to radiate with increased power under control of an atomic frequency standard (Essen, 1965). The phase stability of the NSS, VLF transmitter has been improved within the past year by means of automatic antenna tuning (Williams, 1966), and the U.S. Navy Omega stations are using Cs standards for primary oscillator control (U.S. Navy, 1966). Since a goodly part of the standard deviation of reported daily frequency values at each receiving laboratory is attributable to transmitter fluctuation, one can expect less variation in the received daily frequencies in the future.

More detailed experiments: As Mitchell (1963) pointed out, the present precision of comparing atomic frequency standards via VLF signals is influenced also to a large extent by system measurement errors at the receiving station. It is apparent that further analysis of such receiving errors is essential to added gains in the precision of VLF measurements. Because of the success of the direct comparisons using portable Cs standards, we recommend long-term portable Cs standard experiments of a statistical design to (a) determine the propagation effects limiting the transfer and comparison of standard frequencies via VLF/LF at various distances and paths, (b) analyze and assess the receiving station error into components of primary and/or transfer oscillator instabilities, receiving equipment variations from the receiving antenna to the comparison instrumentation, and internal measurement errors in comparing, recording, and reducing the daily frequency observations, and (c) determine whether the ultimate precision of frequency standards measurements via long-distance radio paths can be improved through allowance for or prediction

Table 4. Comparison of Frequencies Derived from Radio Propagation and Portable Clock Data*

Frequency unit - 1 part in 10^{12}

Laboratory	VLF-LF DATA												Portable Clock Data[a]	
	1965						1966 (5-6 mos.)						1965	1966
	GBR			NSS			WWVL/VB			NSS				
	n_i	$\bar{d}_i$	s_{d_i}	n_i	$\bar{d}_i$	s_{d_i}	n_i	$\bar{d}_i$	s_{d_i}	n_i	$\bar{d}_i$	s_{d_i}	p_i	p_i
CNET	208	3	55	154	-16	34	129	-21 (WWVL)	31	114	-17	30	--	-12
FOA	233	+ 4	41	--	--	--	--	--	--	--	--	--	+6	+ 2
LSRH	308	+ 9	76	197	- 8	60	--	--	--	134	+19	36	-5	0
NOB	320	+40[b]	55	243	+33[b]	48	--	--	--	143	0	12	+6	- 2
NPL	312	- 4	49	154	-20	46	134	- 3 (WWVL)	40	106	- 8	77	+23	- 2
NRC	265	+ 5	56	--	--	--	163	0 (WWVB)	13	--	--	--	+ 6	- 4
Paris Observatory	--	--	--	--	--	--	--	--	--	65	+22	64	--	+16
RRL (TAO)	310	- 2	89	--	--	--	--	--	--	--	--	--	+ 1	+ 2

*Frequency data are deviations from NBS, i.e., NBS - Station standard (positive if NBS has the higher frequency)

a - (Bodily, 1965; Bodily et al., 1966)

b - weighted mean standard (Markowitz, 1962)

The column notation is as follows:

n_i = number of daily frequency deviations of ith receiving laboratory from NBS

$\bar{d}_i$ = mean daily frequency deviation of ith receiving laboratory from NBS

s_{d_i} = standard deviation of daily deviations

p_i = mean difference between NBS and ith receiving laboratory as measured by portable clocks

of propagation influences as alluded to by Chilton, Crombie, and Jean (1964).

With the improving state of the art in atomic frequency standards, the possibility of establishing an international atomic time scale as contemplated by the CCIR (1966) takes on new significance.

8. Conclusion

The worldwide comparison of atomic frequency standards over the past half decade has improved several fold in precision. The standard deviations characteristic of the receiving stations, $\bar{\alpha}_i$, are of the order of a few parts in 10^{11}. The average agreement between the VLF-LF long-term measurements and the portable Cs standards measurements is to parts in 10^{11}, or less, as good as the average agreement within the VLF-LF measurements. Averaging of daily frequency observations over long periods of time provides some improvement in the standard deviations associated with the transmitter and the receiving laboratories. There is some evidence that for those path distances which correspond to single mode dominance of VLF transmission, a linear dependence of precision on distance may apply; however, further work is necessary to substantiate this. Various VLF transmissions are being improved, and the standard deviations of some VLF transmissions, $\bar{\hat{f}}$, have quite steadily decreased to parts in 10^{11}, or less. We recommend long-term round-robin experiments with portable cesium standards that are designed specifically to delineate the propagation limitations and to analyze the receiving station errors.

We acknowledge the work of Judith Stephenson and Ursula Palmer in the data processing and programming, and thank the many contributing laboratories that so regularly exchange standard frequency data with us. We are also grateful to D. D. Crombie, J. A. Barnes, and A. D. Watt for helpful comments.

9. References

Allan, D. W. (1966), Statistics of atomic frequency standards, Proc. IEEE **54**, No. 2, 221–230.

Bagley, A. S. and L. S. Cutler (1964), A new performance of the "flying clock" experiment, Hewlett-Packard J. **15**, No. 11, 1–4, 8.

Barnes, J. A., D. H. Andrews, and D. W. Allan (1965), The NBS–A time scale—Its generation and dissemination, IEEE Trans. Instr. Meas. **IM-14**, No. 4, 228–232.

Beehler, R. E. and D. J. Glaze (1966), The performance and capability of cesium beam frequency standards at the National Bureau of Standards, IEEE Trans. Instr. Meas. **IM-15**, Nos. 1 and 2, 48–55.

Bodily, L. N. (1965), Correlating time from Europe to Asia with flying clocks, Hewlett-Packard J. **16,** No. 8, 1–8.
Bodily, L. N. (1966), A summary of some performance characteristics of a large sample of cesium-beam frequency standards, Hewlett-Packard J. **18,** No. 2, 16–19.
Bodily, L. N., D. Hartke, and R. C. Hyatt (1966), World-wide time synchronization, 1966, Hewlett-Packard J. **17,** No. 12, 13–20.
Bonanomi, J. (1966), HBG, European time service on 75 kHz, Circular No. 2, The Observatory, Neuchatel, Switzerland, 1–12.
British Post Office (1964), Short news items: The transmitter at the Post Office Radio Station, Electronic Engineering **36,** No. 442, 851.
Buchanan, O. R., D. L. Pritt, and H. F. Hastings (1965), Preliminary results of the investigation of the frequency characteristics of two H-P 5060A cesium beam frequency standards. Rept. of NRL Progress, PB 167330, 45–46, U.S. NRL, Washington, D.C.
CCIR (1964), Japan-JJY Standard Frequency and Time-Signal Emissions, Study Group VII, Preliminary Document VII/20 E.
CCIR (1966), Intercomparisons of time scales by various methods, Study Group VII, Preliminary Document VII/1008–E, Oslo XIth Plenary Assembly, Norway.
Chilton, C. J., D. D. Crombie, and A. G. Jean (1964), Phase variations in VLF propagation, Propagation of Radio Waves at Frequencies Below 300 Kilocycles, ch. 19, 257–290. (Pergamon Press, Oxford).
Decaux, B., Editor (1961), Monograph of Radio-electric Measurements and Standards, XIIIth General Assembly of URSI, London 1960, 113–114. (Elsevier Publishing Company, Amsterdam/London/New York).
Decaux, B. (1963, 1967), Private communications.
Essen, L. (1965, 1967), Private communications.
Essen, L., J. McA. Steele, and D. Sutcliffe (1964), The NPL frequency standard, Proc. 18th Annual Symp. on Freq. Con., (U.S. Army Sig. Res. and Dev. Lab., Ft. Monmouth, N.J.), 308–321.
General Conference of Weights and Measures, XII (1964), Document No. 17 and Document No. 21.
Glaze, D. (1967), Private communication.
Hudson, G. E. (1965), Of time and the atom, Physics Today **18,** No. 8, 34–38.
Kalra, S. N. (1961), Frequency measurement of standard frequency transmissions, Can. J. Phys. **39,** No. 3, 477.
Kartaschoff, P. (1962), Operation and improvements of a cesium beam standard having 4-meter interaction length, IRE Trans. on Instr. **I-11,** 224–230.
Kartaschoff, P. (1964), Étude d'un étalon de fréquence a jet atomique de césium. Unpublished Docteur Es Science Techniques thesis, Zürich, L'école Polytechnique Fédérale.
Kartaschoff, P. (1967), Private communication.
Markowitz, W. (1962), The atomic time scale, IRE Trans. Instr. **I-11,** Nos. 3 and 4, 239–242.
Markowitz, W. (1964), International frequency and clock synchronization, Frequency **2,** No. 4, 30–31.
Markowitz, W., C. A. Lidback, H. Uyeda, and K. Muramatsu (1966), Clock synchronization via relay II satellite, IEEE Trans. Instr. Meas. **IM-15,** No. 4, 177–184.
McCoubrey, A. O. (1966), A survey of atomic frequency standards, Proc. IEEE **54,** No. 2, 116–135.
Milton, J. B., R. L. Fey, and A. H. Morgan (1962), Remote phase control of radio station WWVL, Nature **193,** No. 4820, 1063–1064.
Mitchell, A. M. J. (1963), Frequency comparison of atomic standards by radio links, Nature **198,** No. 4886, 1155–1158.
Morgan, A. H., E. L. Crow, and B. E. Blair (1965), International comparison of atomic frequency standards via VLF radio signals, Radio Sci. J. Res. NBS **69D,** No. 7, 905–914.
Mungall, A. G., R. Bailey, and H. Daams (1966), The Canadian cesium beam frequency standard, Metrologia **2,** No. 3, 98–104.
Nakajima, K., K. Suzuki, Y. Azuma, K. Akatsuka, and K. Nakamura (1963), Equipment for the international VLF comparison and results of measurements of phase variation between Hawaii and Tokyo, J. of Radio Res. Lab. (Japan) **10,** No. 48, 127–136.
Pierce, J. A. (1957), Intercontinental frequency comparisons by very low frequency radio transmission, Proc. IRE **45,** No. 6, 794–803.
Pierce, J. A. (1963), Private communication.
Pierce, J. A., W. Palmer, A. D. Watt, and R. H. Woodward (1966), Omega, A World-wide Navigational System, Pickard and Burns Electronics Pub. No. 886B, Defense Documentation Center No. AD–630 900 (2nd ed.), Sect. 3, 26–29.
Pierce, J. A., G. M. R. Winkler, and R. L. Corke (1960), The 'GBR Experiment,' A trans-Atlantic frequency comparison between cesium-controlled oscillators, Nature **187,** No. 4741, 914–916.
Reder, F. H., C. J. Åbom, and G. M. R. Winkler (1964), Precise phase and amplitude measurements on VLF signals propagated through the Arctic zone, Radio Sci. J. Res. NBS **69D,** No. 3, 275–281.
Steele, J. McA., W. Markowitz, and C. Lidback (1964), Telstar time synchronization, IEEE Trans. Instr. Meas. **IM-13,** No. 4, 164–170.
U.S. Naval Observatory (1966), Developments in VLF transmissions; MSK and Omega, Time Service Announcement.
Vessot, R., H. Peters, J. Vanier, R. Beehler, D. Halford, R. Harrach, D. Allan, D. Glaze, C. Snider, J. Barnes, L. Cutler, and L. Bodily (1966), An intercomparison of hydrogen and cesium frequency standards, IEEE Trans. Instr. Meas. **IM-15,** No. 4, 165–176.
Wait, J. R. (1957), The attenuation vs. frequency characteristics of VLF radio waves, Proc. IRE **45,** 768–771.
Wait, J. R. (1962), Electromagnetic Waves in Stratified Media, 278, 284. (Pergamon Press, Oxford.)
Williams, J. C. (1966), Private communication.

(Paper 2–6–233)

Satellite VHF Transponder Time Synchronization

J. L. JESPERSEN, GEORGE KAMAS, LAWRENCE E. GATTERER, MEMBER, IEEE, AND PETER F. MACDORAN, MEMBER, IEEE

Abstract—**This paper describes an experiment designed to transfer accurate time between two widely separated clocks using a VHF satellite transponder. The satellite used was the NASA Applications Technology Satellite, ATS-1. The experiment used atomic oscillators to maintain accurate time at each station, and the synchronization was accomplished by measuring the round-trip delay times between the stations. The goal of the experiment was to evaluate a VHF system, because of the low-cost ground equipment involved, in contrast to microwave systems. The paper discusses the results and the various factors that contributed to the timing errors.**

INTRODUCTION

THE NASA Applications Technology Satellite (ATS-1) has been used in a series of experiments to explore one method of synchronizing widely separated precision clocks. The synchronization was achieved by making round-trip time delay measurements, via the satellite transponder, between master and slave clock locations. Similar experiments have been conducted [1], [2] previously using satellites with microwave transponders. The present experiment was conducted with the ATS-1 VHF transponder. Although the microwave frequency region is ideal from the point of view of avoiding atmospheric signal distortion, the VHF system has an advantage in that relatively simple and low-cost ground equipment may be used. Synchronization of the clocks was achieved to within a few microseconds.

Manuscript received December 22, 1967; revised May 2, 1968.

J. L. Jespersen, G. Kamas, and L. E. Gatterer are with the National Bureau of Standards, Boulder, Colo.

P. F. MacDoran is with the U. S. Coast and Geodetic Survey, Rockville, Md.

THE SATELLITE VHF TRANSPONDER

The NASA satellite ATS-1 was launched December, 1966, in near synchronous orbit. A part of the ATS satellite system is devoted to supporting experiments at VHF. The VHF repeater or transponder operates as a frequency translator. Signals received at 149.220 MHz with frequency modulation are heterodyned to an intermediate frequency, 29.95 MHz, and then heterodyned to 135.600 MHz for retransmission to earth. An eight-element phased-array antenna system operating in duplex is used for both receiving and transmitting, while signal limiting and bandwidth filtering are employed simultaneously in the satellite signal chain. Because of this, amplitude modulation is not possible at

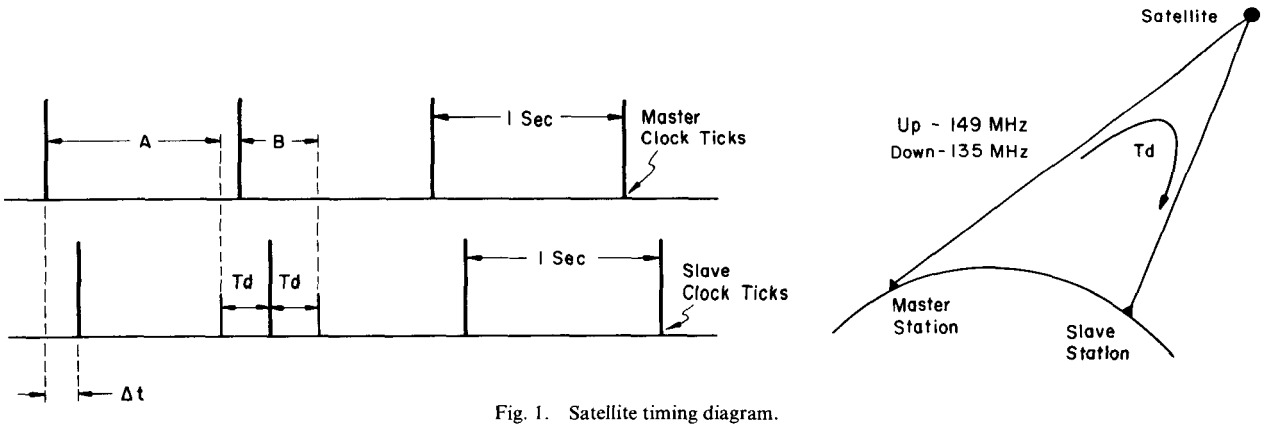

Fig. 1. Satellite timing diagram.

full satellite power levels and the overall system bandwidth is restricted to 100 kHz. For this experiment frequency modulation was employed.

System Description

Fig. 1 shows the geometry of the timing experiment and a timing diagram which is used to derive the equations necessary for the synchronization. The description here is simplified to make clear the general principles of operation. As will be described in more detail in later paragraphs in this section, the synchronization was initiated by transmitting 1-pps pulses from the master station. For this experiment, it was assumed that the master and slave clocks did not differ initially by more than one second. If this condition had not been met, then a slower pulse rate would have been used to unambiguously set the slave clock to the master clock. Since one of the main considerations in the experiment design was simplicity of operation, particularly at the slave site, the signal was adjusted in time and transmitted from the master station to arrive "on time" at the slave station with respect to the slave station clock. This adjustment was achieved by maintaining a communication link between the master and slave stations. The operator at the slave station simply told the master station operator to either advance or retard the transmitted tick until it appeared to arrive in coincidence with the slave clock tick. This was done by the use of a voice channel over the satellite or by telephone communication. The amount of time by which the transmitted pulse leaving the master transmitter must be delayed with respect to the master station clock to arrive "on time" with respect to the slave clock is designated A in Fig. 1.

By inspection, from the figure,

$$A = \Delta t + (1 - T_d). \tag{1}$$

Δt is the time difference between the master and slave clocks and T_d is the one-way path delay from one ground station, via the satellite, to the other ground station.

After A was determined and recorded at the master station, the slave station transmitted pulses directly from the slave station clock without adjustment. These pulses arrived via the satellite at the master station B seconds late with respect to the master clock. Again, by inspection from the figure,

$$B = \Delta t + T_d. \tag{2}$$

Since both A and B were measured at the master station, the master station operator could determine the difference between the master and slave clocks by solving (1) and (2) simultaneously to obtain

$$\Delta t = (A + B - 1)/2. \tag{3}$$

Strictly speaking, (3) holds only if $0 \leq \Delta t \leq T_d$. In most practical cases Δt will be less than T_d (0.25 second) so that (3) will be applicable. However, there are two other possible cases. If

$$T_d \leq \Delta t \leq 1 - T_d,$$

then

$$\Delta t = (A + B)/2,$$

and if

$$1 - T_d \leq \Delta t \leq 1,$$

then

$$\Delta t = (A + B + 1)/2.$$

Since T_d is approximately known in advance, it was possible to inspect the measured values of A and B and then to select the correct one of the three possible cases. The actual choice was easy because both A and B had to fit the inequality. A range of values for A and B was computed using the known range to the satellite.

Details of System Operation

Fig. 2 shows block diagrams of the master and slave stations. As stated in the previous section, synchronization is initiated by the master station. The master station transmits 10-kHz tone bursts that are adjusted in time to arrive at the slave station nearly coincident with the slave clock pulse. A 1-pps rate is used first to avoid ambiguity. When the 1-pps pulses have been adjusted to arrive very nearly on time, the pulse rate is increased to 100 pps. This higher rate aids the detection process and increases the precision of measurement.

After it had been established that the pulses transmitted by the master station were "on time" with respect to the slave clock at the slave station, the direction of transmission

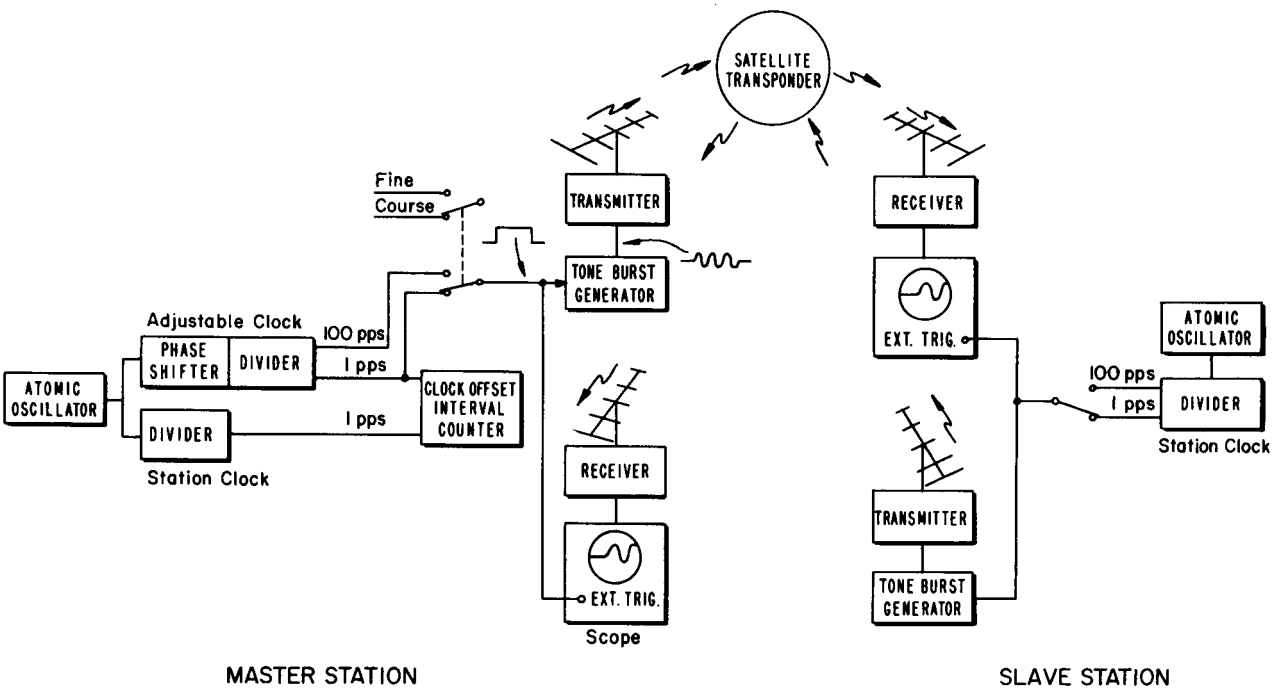

Fig. 2. System block diagram.

was reversed. The slave then transmitted its own clock pulse to the master without any adjustment. First a 1-pps rate was used and then a 100-pps rate. The master then measured the quantity B, which was the difference between the arrival of the slave time tick and the master clock.

At both master and slave stations, the "clocks" consisted of coherent 100-pps and 1-pps dividers driven by an atomic standard. The digital clock output was used to trigger a sine-wave tone burst generator which in turn frequency modulated the transmitter. The tone burst started at zero phase and lasted for one-half second or 5 milliseconds, depending on the pulse rate chosen.

Because the bandwidth of the system would not transmit the necessary spectrum to reproduce the start of the tone burst without distortion, the actual time "mark" used was the start of the third cycle of the burst. The first cycle was easy to see and the operator simply counted zero crossings to find the third cycle.

The equipment delays at each station were measured by converting a sample of the transmitter output to the receiver frequency using a broad-band mixer. In this way, using the modulation format of the timing system, the combined transmitter-receiver delay could be measured. Next the transmitter was driven by the tone burst generator and a sample was again converted with a broad-band mixer to a reasonably low frequency for direct display of the frequency modulation on an oscilloscope. The receiver and transmitter delays could then be separated. Based upon equipment delay measurements made over periods of several days, it was concluded that the variability is ± 2 μs. The actual delay was about 150 μs for each set of equipment used.

The time coincidence detector used in this experiment was a triggered oscilloscope. The station clock was used to trigger the sweep and the receiver video output was displayed. Prior to each run, the time bases of the oscilloscopes were calibrated using the atomic standard divided output.

Sources of Error

1. Equipment Delay Measurements

In the derivation of the timing equations in a previous section, no mention was made of equipment delays. If it can be assumed that the equipment delays from master to slave and slave to master are equal, then the equations as derived are valid, since the equipment delays can be assumed to be included in the term T_d. In fact, the delays are not identical, and the measurements must be corrected for these delays before the equations can be applied. As previously mentioned, the variability was found to be ± 2 μs, and the magnitude of the equipment delay for one transmitter-receiver set was about 150 μs.

2. Signal-to-Noise Considerations

There will be a certain amount of error due to the fact that the signal is received in a noisy environment. Table I gives a signal-to-noise calculation which typifies the down link operation.

The rms jitter in the arrival time of a zero crossing of the signal is

$$\text{rms jitter} = \frac{t_r}{(2S/N)^{1/2}}$$

where t_r is the period of the modulation and S/N is the signal-to-noise power ratio. Substituting the appropriate values into this equation, we obtain

TABLE I

SIGNAL-TO-NOISE CALCULATION

Down link	135.6 MHz
Satellite transmitter power, dBW	16.0
Satellite antenna gain, dB	9.0
Ground station antenna gain, dB	10.0
Space attenuation, dB	−167.0
Received power	−132.0 dBW
Noise temperature, dB	30.0
Boltzmann's constant, dBW	−228.6
Bandwidth (30 kHz), dB	44.8
Received noise power	−153.8 dBW
Carrier-to-noise ratio, dB	21.8
FM improvement,* dB	4.8
Signal-to-noise ratio, dB	26.6

* For 10-kHz deviation and 10-kHz modulation.

$$\text{rms jitter} \sim \frac{100\ \mu s}{(457)^{1/2}} \cong 5\ \mu s$$

on the zero crossings of the 10-kHz tone bursts. This calculation assumes that the S/N ratio received at the satellite is sufficient for the transponder to retransmit a clean signal at its maximum output of 40 watts. A calibration was run to determine how much effective radiated power from the ground station was required to obtain a clean satellite signal. On the basis of this test it was determined that an effective radiated power of 2500 watts was sufficient to obtain full signal power from the satellite.

3. Faraday Rotation

Because of the presence of the earth's magnetic field, the ionosphere is a birefringent medium which causes a linearly polarized wave to split into two elliptically polarized components with opposite senses of rotation. As a result of this splitting, a linearly polarized signal changes its orientation as it passes through the ionosphere so that there is no assurance that maximum signal will be received at either the satellite or ground receiving antennas simply by aligning the transmitting and receiving antennas. In principle, it is possible to calculate the amount of rotation if the electron content and the earth's magnetic field are known along the propagation path. In practice, it is easier to either rotate the ground transmitting and receiving antennas until maximum signal is received or to use circularly polarized ground transmitting and receiving antennas. Both techniques were used in this experiment. The error introduced by the Faraday rotation is indirect in the sense that the effect is as though the satellite transmitter power has been reduced.

4. Amplitude and Phase Scintillations

Amplitude and phase scintillations on the timing signals are due to the presence of irregularities in the refractive index of the ionosphere which move between the signal source and the observer. Generally, the period of the scintillations is of the order of minutes. By amplitude scintillations it is meant that the signal appears to fluctuate in brightness, whereas for phase scintillations it is meant that the location (or angle of arrival of the signal) appears to change with time [3]. In general, both of these effects are related to phase distortion of the signal. That is, the phase front of the signal is distorted in the region of the ionosphere containing the irregularities. As the signal propagates away from this region, the distorted wave interferes with itself to produce amplitude modulation of the signal which is a function of the distance from the irregularities and upon the amount of initial phase distortion at the irregularities. Typically, at 100 MHz at medium latitudes, the amplitude fading (when it is present) is about 10 percent of the mean signal strength, which will cause no particular problem for timing experiments [4]. However, on some occasions, particularly at either high or low latitudes, the signal fluctuations could be considerably greater and could possibly, on some rare occasions, render the system inoperable. The phase scintillations introduce path length fluctuations which at most would not amount to more than a few centimeters (1 km $\sim$3 μs), which is negligible from the point of view of this timing system.

5. Ionospheric Absorption

In the scintillations discussed above, there is no net loss of energy, just a redistribution. However, the ionosphere could also produce a true absorption, particularly at times of solar disturbances. But observations [5] indicate that, at 100 MHz, under even the most disturbed conditions, the absorption should not exceed 1 dB.

6. Path Nonreciprocity Effects

An explicit assumption for the proper operation of the system is that the electromagnetic path between the master and slave stations is reciprocal. Strictly speaking for ATS-1, this assumption is not correct, for the following three reasons.

1) The up and down links to the satellite differ by 13.62 MHz so that there will be some differential delay due to the slight difference in group velocities at these two frequencies. However, we estimate that with reasonably normal ionospheric conditions, this difference should not exceed 0.1 μs.
2) ATS-1 is not in an absolutely synchronous orbit. However, the amount of error introduced by the satellite motion during the few minutes required for clock synchronization does not exceed 1 μs in the worst case [6].
3) The amount of delay in the satellite itself is of no consequence as long as it does not change appreciably during the course of the clock synchronization. Experiments conducted prior to the launch indicate that the satellite delay should be stable in this respect to 0.1 μs or less [7].

OBSERVATIONS

Experiments were conducted for a 10-day period during June and July of 1967. Signal exchanges were made between the NASA STADAN field site near Barstow, Calif., and stations located at the WWVH site at Maui, Hawaii,

463-560 O - 72 - 25

the NBS Laboratories at Boulder, Colo., and a satellite-tracking station at Gunbarrel Hill, operated by the U. S. Environmental Science Services Administration, about 10 miles north of Boulder. Two independent sets of equipment were located in the same room at Boulder. To check the accuracy of the procedure, portable cesium clocks which were checked prior to and after the experiments were located at the NBS, ESSA, and Maui sites. In addition, a crystal clock was available at the STADAN site. Several different kinds of comparisons were made. For example, by exchanging signals between Maui and STADAN the difference between the STADAN crystal and Maui cesium clocks was determined. At the same time, however, the Boulder sites could monitor this exchange. A few minutes after the STADAN-Maui exchange, a STADAN-Boulder exchange was made to determine the difference between the STADAN and Boulder clocks. In the meantime, these exchanges were being monitored at Maui. By comparing the difference between the STADAN and Boulder clocks and between the STADAN and Maui clocks, it was possible to determine the difference between the Maui and Boulder clocks with the STADAN clock as an intermediary. It might be objected at this point that some error could arise because of the fact that the STADAN station did not have a cesium clock; but since the complete set of signal exchanges occurred in a few minutes of time, the amount of drift in the crystal clock was negligible. Table II gives the results of various intercomparisons. The accuracy shown is the average of the absolute value of the time difference for all observations. The standard deviation is given as the error.

The values given in Table II were obtained by comparing the measured difference determination via the satellite with the known clock differences. The difference between the cesium clocks was known to within one-half microsecond at all times during the experiment. Earlier, the rms phase jitter of the zero crossing was calculated to be about 5 μs. For almost all of the observations, visual inspection of the oscilloscope trace indicated a peak-to-peak jitter of about 15 μs. From the tabulation of the data we see that the accuracy of all intercomparisons was about 4 ± 2 μs. Thus, the measured and computed results are in good agreement. Even though the signals showed a large peak-to-peak jitter, it was possible, by observing the trace, to estimate the average arrival time to within a few microseconds. In fact, recalling that equipment delay measurements had a variation of ±2 μs, it is apparent that one can estimate the average arrival time with good precision.

Another interesting fact is that the accuracy of the clock setting, within the precision of the measurements, does not depend upon the geographical clock separation. This is not particularly surprising since the round-trip distance from slave to master station via the satellite does not depend very strongly upon the distance between the master and slave stations.

Finally, the comparisons between Boulder and Maui via STADAN are as accurate as any of the others, although an extra measurement step is involved. We attribute this to the fact that better receivers and higher gain antennas are available at the NASA STADAN site so that the signal jitter is less than that observed at the other stations.

TABLE II

Locations	Accuracy, μs	Number of Observations
Boulder-STADAN-Maui	4.2 ± 2.0	5
Boulder-Gunbarrel Hill	4.1 ± 1.8	8
Boulder-Maui	4.0 ± 2.6	4
Boulder-Boulder	3.0 ± 2.8	4

Conclusions

A synchronous satellite (ATS-1) containing a VHF transponder has been used to synchronize widely spaced clocks to a few microseconds. The techniques involved exchanging radio timing signals, via the satellite, between the locations of the clocks to be synchronized. An analysis is made of the various factors which might affect the accuracy of the system and it is concluded that the predominant errors were probably related to variations in equipment delays and to fundamental limitations based upon signal-to-noise calculations. Although the signals were in the VHF region, the ionospheric perturbations of the signals produced errors which were negligible compared with other error sources in the system; and it appears that these ionospheric errors did not exceed one microsecond. However, with more sophisticated equipment and stronger signals from the satellite, it is probable that ionospheric limited synchronization could be achieved.

Acknowledgment

The authors would like to thank the following for their help during the experiment: J. P. Corrigan and the STADAN personnel of NASA; A. H. Morgan, D. Hilliard, and S. Canova of NBS; S. Katahara and the station personnel of WWVH, Maui, Hawaii; S. Gerrish of the HANDS group of ITSA; J. Puerner and J. Hutt of NESC; and, in particular, R. N. Grubb of the HANDS group of ITSA whose participation in the design and organization of this experiment were crucial to its successful conclusion.

References

[1] J. McA. Steele, W. Markowitz, and C. A. Lidback, "Telstar time synchronization," *IEEE Trans. Instrumentation and Measurement*, vol. IM-13, pp. 164–170, December 1964.

[2] W. Markowitz, C. A. Lidback, H. Uyeda, and K. Muramatsu, "Clock synchronization via Relay II satellite," *IEEE Trans. Instrumentation and Measurement*, vol. IM-15, pp. 177–184, December 1966.

[3] J. L. Jespersen and G. Kamas, "Satellite scintillation observations at Boulder, Colorado," *J. Atmos. Terr. Phys.*, vol. 26, pp. 457–473, 1964.

[4] R. S. Lawrence, J. L. Jespersen, and R. C. Lamb, "Amplitude and angular scintillations of the radio source Cygnus-A observed at Boulder, Colorado," *J. Research NBS*, vol. 65D, pp. 333–350, July–August 1961.

[5] C. G. Little and R. S. Lawrence, "The use of polarization fading of satellite signals to study the electron content and irregularities in the ionosphere," *J. Research NBS*, vol. 64D, pp. 335–346, July–August 1960.

[6] E. Metzger, NASA Goddard Space Flight Center (private communication).

[7] R. Boucher, Hughes Aircraft Company (private communication).

This report shows the possibilities of clock synchronization using time signals transmitted at low frequencies. The study was made by observing pulses emitted by HBG (75 kHz) in Switzerland and by WWVB (60 kHz) in the United States.

The results show that the low frequencies are preferable to the very low frequencies. Measurements show that by carefully selecting a point on the decay curve of the pulse it is possible at distances from 100 to 1000 kilometers to obtain time measurements with an accuracy of ±40 microseconds.

A comparison of the theoretical and experimental results permits the study of propagation conditions and, further, shows the desirability of transmitting seconds pulses with fixed envelope shape.

Reprinted from FREQUENCY, Vol. 6, No. 9, pp 13-21 (September 1968),

RECEPTION OF LOW FREQUENCY TIME SIGNALS

DAVID H. ANDREWS
P. E., Electronics Consultant*

C. CHASLAIN, J. DePRINS
University of Brussels, Brussels, Belgium

I. INTRODUCTION

For several years the phases of VLF and LF carriers of standard frequency transmitters have been monitored to compare atomic clocks.[1,2,3]

The 24-hour phase stability is excellent and allows frequency calibrations to be made with an accuracy approaching 1 x 10^{-11}. It is well known that over a 24-hour period diurnal effects occur due to propagation variations. Fig. 1 shows this effect over a 24-hour period relatively small for LF at medium distances.

While this method is adequate for frequency comparisons of atomic clocks, it does not suffice for clock synchronization (epoch setting). Presently, the most accurate technique requires carrying portable atomic clocks between the laboratories to be synchronized. No matter what the accuracies of the various clocks may be, periodic synchronization must be provided. Actually the observed frequency deviation of 3 x 10^{-12} between cesium controlled oscillators amounts to a timing error of about 100T microseconds, where T, given in years, is the interval between synchronizations.

Another approach is to effect synchronization by means of HF time signals (3-30 MHz). Such signals are usually provided by carrier modulation for a short interval at a frequency near 1 kHz (Fig. 2). Epoch is obtained by observing the time of a significant point, say the first maximum of the modulation pulse.

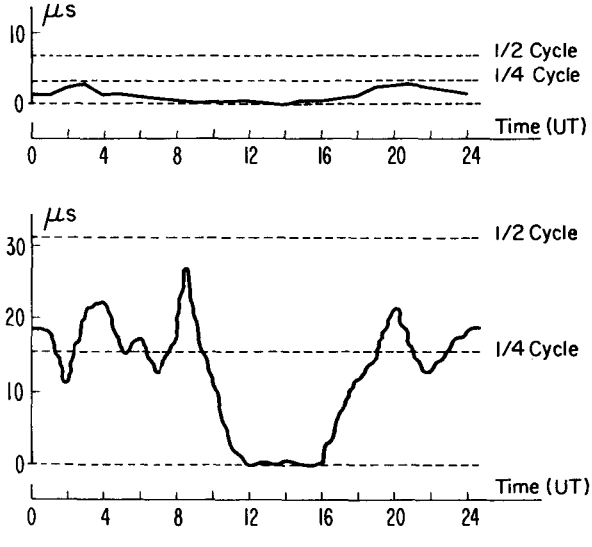

Figure 1 — (Top) Diurnal phase variation of HBG; (Bottom) Diurnal phase variation of GBR.

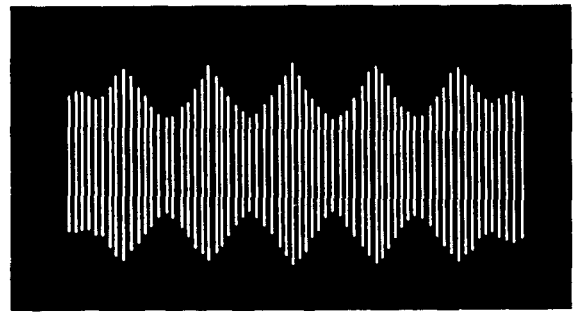

Figure 2 — High frequency time signals.

* *This work was performed before Mr. Andrews' retirement from the National Bureau of Standards, Boulder, Colo.*

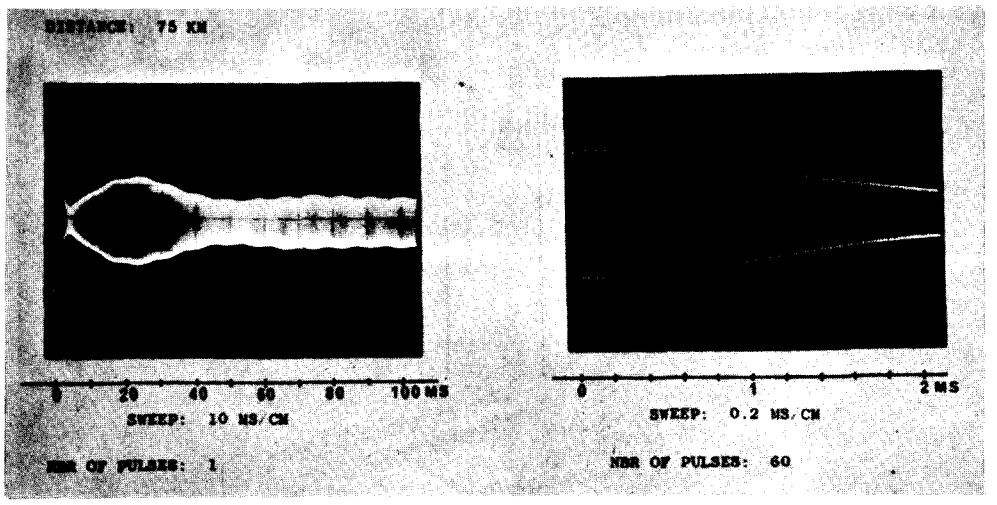

Photo 1 — Boulder, 8 April, 1967, 8H (U.T.)

Clearly, for high frequencies, the shape of the received modulation signal depends neither upon the antenna characteristics, nor, in general, upon the receiver characteristics. But, propagation conditions change the effective path length, and variations in arrival time of the pulse may reach hundreds of microseconds.

The daily phase stability at LF (Fig. 1), indicates that a single mode of propagation is dominant at 500 km. It would appear, then, that low frequencies are suitable for transmitting time signals. The low frequencies, however, cannot utilize modulation like that used at HF because the high antenna "Q" strongly affects the desired modulation shape. The receiver system will also degrade the modulation envelope.

The system studied utilizes carrier modulation by a square pulse, which undergoes some degradation by the transmitter tuning system. The antenna tuning and its "Q" depend upon weather conditions so that the radiated pulse varies in the course of time.

The pulse is further distorted by the receiver. Photo 1, made of WWVB in Boulder, shows a typical envelope. The length of the decay time (about 2 ms) with respect to the desired accuracy makes it difficult to define a suit ble "timing" point.

Ideally one could find the exact analytical expression for the complete envelope and by comparison with experimental results define the arrival time. Such an approach is not feasible with present transmitting conditions.

The purpose of this work has been to select and measure a suitable "timing" point. A precision of ±40 microseconds is assured by the system here proposed. In Brussels, for example, this method has provided time synchronization with this accuracy, and frequency measurements on a yearly basis were in error by less than 7 parts in 10^{12}. These results were obtained using a quartz clock. The economic appeal of this method is strong since the synchronizing equipment can be set up for a few hundred dollars and gives results comparable to those obtained using atomic clocks costing from $10,000.00 to $20,000.00.

Improvements in emission, particularly in the transmitted envelope shape, coupled with synchronization between transmissions at LF and VLF would permit synchronization to the order of a microsecond, if the path delay is known.

In conclusion, we note that this accuracy is actually attained, in a restricted area (East Coast U.S.A.) with the Loran-C navigation system using a low frequency.[4,5,6] It would be very interesting, in view of the Loran-C results and some of the aforesaid considerations, to build a transmitter solely devoted to synchronization and which does not have the drawbacks of Loran-C, namely, difficulty in pulse identification and pulse repetition rate, and inadequate coverage except in Eastern United States.

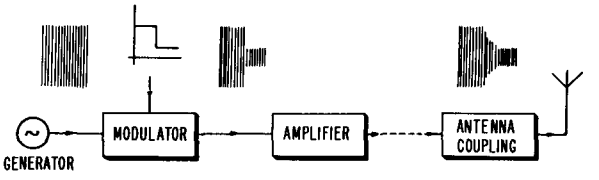

Figure 3. — Simplified block diagram of a transmitter.

II. EMISSION OF TIME SIGNALS

A transmitter is shown schematically in Fig. 3, including the waveshapes resulting in the final radiated signal.

At low power, the carrier is amplitude modulated by a rectangular pulse. The resulting signal is then amplified to the required power, about 30 kilowatts, and coupled through a transmission line to a resonant antenna.

Characteristics of the transmitters studied are given in Table I.

TABLE I

Transmitter

	HBG	WWVB
Location *[7]	Prangins (Switzerland) 46°N 6°N	Fort Collins (USA) 40°40.5′N 105° 2.5′E
Frequency	75 kHz	60 kHz
Power	20 kW	13 kW
Carrier frequency	AT (1)	AT (1)
Phase control	No	Yes
Time Signal System	UTC (2)	SAT (3)
Modulation Characteristics	Carrier cut-off each second (4)	WWVB Time Code [11]

(1) AT = atomic time [7]

(2) UTC = coordinated universal time [7]

(3) UTC is approximated by AT with 200-ms steps

(4) The minute is identified by two successive 100-ms carrier cut-offs separated by 100 ms.

* Numbers in brackets refer to references.

III. THEORETICAL ENVELOPE SHAPE

While the low power driving signal is basically a square wave, this is not true for the emitted signal, nor for the received signal. The modulated signal is distorted both by the electronic circuits in the transmitter and receiver and also by propagation of the electromagnetic waves through the ionosphere.

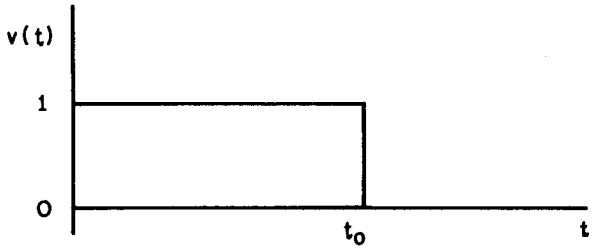

Figure 4.

To calculate the envelope shape it is hardly possible to consider in detail all the electronic circuits of the transmitter and receiver. The following simplifying hypotheses are made:

a. The transmitter and receiver are linear amplifiers with tuned RLC circuits.

b. The envelope shape remains unchanged for the propagation mode considered.

The most important results are contained in the remainder of the report. Details of the calculations involving Laplace transforms may be found in Chaslain's paper.[8]

III-1. *Response of circuits tuned to different frequencies to a single pulse*

The driving modulation signal v(t) is shown in Fig. 4, where

$$v(t) = u(t) = 1 \qquad 0 < t < t_o$$
$$= 0 \qquad t < 0,\ t > t_o$$

The theoretical response for three circuits in series is given by:

$$i_3(t) = \frac{\beta}{L_1L_2L_3}\left\{\sum_{i=1}^{3}\frac{\rho_I}{\eta_i c_i}\, e^{-\mu_i t}\sin(\eta_i t+\varphi_i) - \sum_{i=1}^{3}\frac{\rho_i}{\eta_i c_i}\, e^{-\mu_i(t-t_o)}\sin[\eta_i(t-t_o)+\varphi_i]u(t-t_o)\right\} \qquad \{1\}$$

where ω_i, L_i, R_i refer to the frequency, inductance, and resistance of the ith circuit, and where

$$\rho_i = \sqrt{[(\omega_i^2+2\mu_i^2)\delta_i + 2\mu_i\eta_i\gamma_i]^2 + [\delta_i(\omega_i^2+2\mu_i^2) - 2\mu_i\eta_i\delta_i]^2}$$

$$c_i = (A_{ij}^2+B_{ij}^2)(A_{ik}^2+B_{ik}^2)(1-\varepsilon_{jk})$$

$$\varepsilon_{jk} = \begin{cases} 1, & j = k \\ 0, & j \neq k \end{cases}$$

$$\mu_i = \frac{\omega_i}{2Q_i};\quad Q_i = \frac{\omega_i L_i}{R_i};\quad \eta_i^2 = \omega_i^2 - \mu_i^2$$

$$A_{ij} = (\omega_j^2-\omega_i^2) + 2\mu_i(\mu_i-\mu_j)$$

$$B_{ij} = 2\eta_i(\mu_i-\mu_j)$$

$$\delta_i = (A_{ij}A_{ik}-B_{ij}B_{ik})(1-\varepsilon_{jk})$$

$$\gamma_i = (A_{ij}B_{ik}+A_{ik}B_{ij})(1-\varepsilon_{jk})$$

$$\operatorname{tg}\varphi_i = \frac{\gamma_i(\omega_i^2+2\mu_i^2) - 2\mu_i\eta_i\delta_i}{\delta_i(\omega_i^2+2\mu_i^2) + 2\mu_i\eta_i\gamma_i}$$

III-2. *Study of the effects on a carrier amplitude modulated with a square wave.*

The signal to be transmitted is shown in Figure 5 and is given by:

$$v(t) = A\sin\omega t - c\sin\omega t\,u(t-t_o),$$

where u is the previously defined modulation signal.

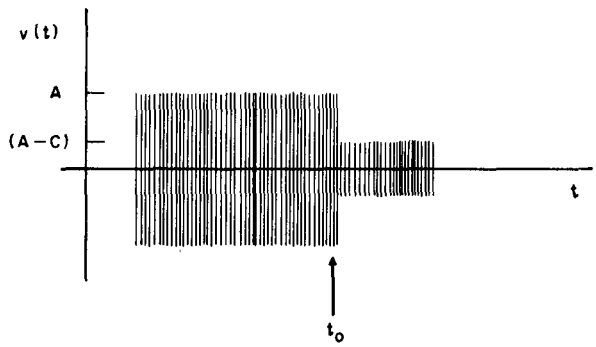

Figure 5.

For n circuits in series tuned to the same frequency, their behavior, during carrier suppression, is given by:

$$i_n(t) = \frac{kA}{2^n \prod_{i=1}^{n}(\mu_i L_i)}\left\{\sin\omega t - \frac{c}{A}\left[\sin\omega t - \sum_{i=1}^{n}\frac{\omega}{\eta_i}\,\frac{e^{-\mu_i t}}{\prod_{\substack{j=1\\ j\neq i}}^{n}\left(1-\frac{\mu_i}{\mu_j}\right)}\right.\right.$$

$$\left.\left. L_i(t-t_o)\right]u(t-t_o)\right\} \qquad \{2\}$$

with the symbols:

$$L_i(t-t_o) = \frac{1}{\omega}\left\{\{\rho_i\sin[\eta_i(t-t_o)+\varphi_i] - \mu_i\sin\omega t_o\sin\eta_i(t-t_o)\right\}$$

$$\operatorname{tg}\varphi_i = \frac{\eta_i}{\omega}\operatorname{tg}\omega t_o$$

$$\rho_i = \omega\sqrt{1-\frac{1}{4Q_i^2}\sin^2\omega t_o}$$

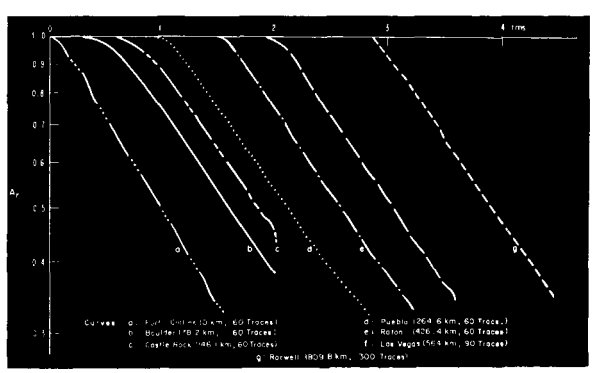

Figure 6. — Envelope shape versus distance between transmitter and receiver.

If the beginning of the pulse is synchronized with the carrier and if $4Q_i^2 >> 1$, we get

$$i_n(t) = \frac{kA}{\omega^n}\prod_{i=1}^{n}\left(\frac{Q_i}{L_i}\right)\left\{1-\frac{C}{A}\left[1-\sum_{i=1}^{n}\frac{e^{-\frac{\omega}{2Q_i}t}}{\prod_{\substack{j=1\\ j\neq i}}^{n}\left(1-\frac{Q_j}{Q_i}\right)}\right]u(t-t_o)\right\}\sin\omega t. \qquad \{3\}$$

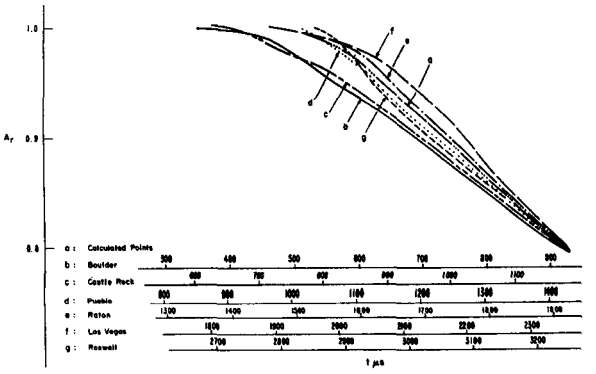

Figure 7. — Envelope shape versus distance between transmitter and receiver.

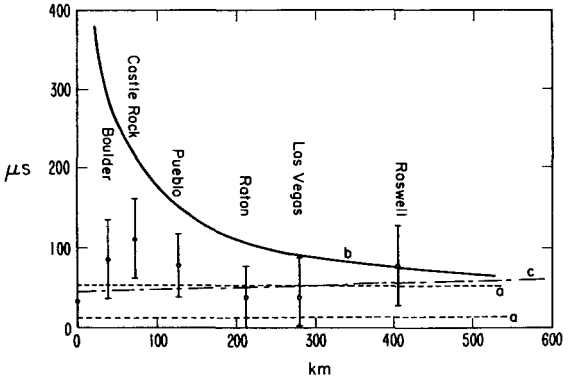

Figure 8. — Curve a: Ground wave. Curve b: Wave reflected once at an altitude of 70 km. Curve c: Linear regression curve.

III-3. *Remarks.*

1. In assuming a simplified model composed of two tuned circuits, one for the transmitter and the other for the receiver, we obtain a response curve which immediately shows several discrepancies. For instance, it is very reasonable for the "Q" of the transmitting antenna to vary by 10% due to atmospheric changes. In this case, for realistic conditions, time variations for fractional amplitudes between 0.5 and 1.0 are given in Figure 13.

This graph seems to show that it should be possible to synchronize at the beginning of the time pulse. But experimentally this cannot be done precisely due to the slow rate of change of amplitude at the beginning of the pulse. The amplitude decreases by 0.5% during the first 100 microseconds and only 3% during the first 200 microseconds.

2. The expression {2} points out that the time tick must be locked to the carrier if distortion is to be avoided.

IV. ENVELOPE MEASUREMENTS

IV.-1. *Receivers.*

Reception conditions for transmissions from HBG and WWVB are different. Time pulses from HBG were received at Brussels, a distance of 506 km, under high noise level conditions, whereas time signals from WWVB were usually received at Boulder, a distance of 78.2 km, and at all times under low noise conditions. Two different receivers were constructed having the following characteristics shown in Table II.

TABLE II

		Receiver	
		Brussels [9]	**U.S.A.**
Frequency		75 kHz	60 kHz
Field Strength		650 ±20μV/m	35 mV/m
Antenna	General Characteristics	Ferrite Tube Phillips 56.261.36/3 B	Tuned Loop Primary: 25 turns Secondary: 6 turns
	Resonant Impedance	23.5 kΩ	50 kΩ
	"Q"	50	22
Preamplifier	Gain	56 dB	39 dB
	Voltage Amplification	30	11
Receiver	Output Impedance	2.5 kΩ	0.5 kΩ
	Gain	46 dB	43 dB
	Voltage Amplification	1500	420
	"Q"	Variable between 100 and 300	22

IV-2. *Measuring systems.*

The first problem is to minimize the effects of short term random fluctuations due to propagation, of man-made noise, and of interference from transmitters with carrier or side-band frequencies near the useful signal. The observed signal-to-noise ratio usually lies between 5 and 20. Visual observation of the seconds pulses generally does not give an accuracy better than several hundred microseconds for time comparison.

The accuracy was improved by photographically superimposing many successive time pulses. It is clear that this technique requires the phase between the received signal and the local reference to remain constant during the integrating time. Thus a compromise between the signal-to-noise ratio and the desired accuracy was necessary.

Thus, the higher the receiver "Q" the better the signal-to-noise ratio, but the pulse rise-time increases and lowers the accuracy. This compromise has determined the "Q" of the receivers.

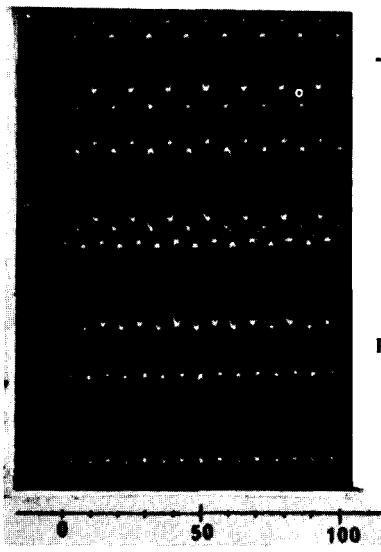

Photo 2 — Brussels, 19 June, 1967, 1605H (U.T.). Sweep: 10 μs/cm; number of pulses: 60.

At Brussels, the envelope of HBG was determined by measuring the amplitudes at selected points on the curve. This accomplished by photographically superimposing several cycles, selected with a variable delay line from a number of consecutive pulses.

For calibration purposes the maximum amplitude is also recorded on the photograph (Photo 2). The measurement precision of the relative value lies between 0.005 and 0.03.

In the United States, with a better signal-to-noise ratio, the entire envelope was recorded on a single photograph. The amplitude was measured to a precision of from 0.002 to 0.008.

Later in the report, Figure 15 shows the timing error versus an amplitude measurement error of 0.01. As might reasonably be expected, the function shows a minimum.

V. EXPERIMENTAL RESULTS

V-1. *Study of transmission characteristics.*

It was desirable to confirm the correspondence between the theoretical model and the radiated signal, for it would be useless to study the model if there was a substantial difference in the radiated signal.

Moreover, this approach allows the transmission characteristics to be considered as initial data.

For HBG, the proximity of other more powerful transmitters has, for now, prevented measurements on the antenna. On the other hand, complete measurements have been made for WWVB.

It was first noted that the emitted signal had a rather complex waveform. For the first 3 milliseconds, the decay was exponential, agreeing with the mathematical model. Then between 3 and 100 milliseconds an overshoot, followed by a damped oscillation, occurred which was probably attributable to the transmission line and antenna matching system. Hereafter the study is limited to the first period.

Measurements on the low-power driving signal show a small amplitude modulation (±2%) and a slight frequency modulation, and they also show that the time required for the signal to reach the reduced level was in the order of 35 microseconds. In addition, a slight overshoot was observed. Despite these defects this signal can be satisfactorily represented by a square wave for mathematical analysis.

The antenna current was then investigated using an untuned loop coupled to the antenna ground lead, the signal from which was observed directly on an oscilloscope. The envelope of the signal agreed with the theoretical one except for a parasitic damped oscillation at 4 kHz with an amplitude of 0.02 and decay time of 310 microseconds.

The radiated signal in the immediate vicinity of the transmitting antenna was studied using the WWVB receiver and a 5 cm whip antenna. The envelope of the signal agreed with theory for a receiver having a "Q" of 22. The damped oscillation was quenched by the receiver filter.

A comparison of the two envelopes showed nonlinearities of the oscilloscope and receiver of less than 1% and 2%, respectively.

The measurements make possible an estimation of the parameters for the theoretical formulas using the least-squares method of fitting curves to the experimental data.[10]

The values obtained are shown below in Table III.

TABLE III

	From Antenna Current	By Receiver with 5 cm Whip Antenna
t_o	27 ± 20 μs	30 ± 35 μs
Q_1	205 ± 5	200 ± 5
A_r	0.90 ± 0.02	0.91 ± 0.02
Q_2	0	22 ± 3
σ_{adapt}	0.0065	0.0065
σ_{exp}	0.003	0.003

The relationship used was formula {3} with n = 2, σ_{adapt} = standard deviation, σ_{exp} = standard deviation, all estimated from measurement conditions.

These measurements emphasize the agreement between observed and predicted envelope shape. They also show whether the observed anomalies are liable to affect the overall accuracy of the measurements.

V-2. *Study of receiving conditions.*

Since the transmission data for HBG were not known accurately, better results were obtained from WWVB as received at Boulder, 78.2 km distance.

Early measurements revealed that the waveshape received in Boulder varied with time. This was in disagreement with the theory, particularly for amplitudes between 1.0 and 0.8. (Deviations are as much as 0.05 with a measurement precision of 0.003.)

These data show that it is necessary to consider the received signal as a composite of several propagation modes. On the other hand, the carrier phase stability is such that, during the day, the same propagation mode prevails.

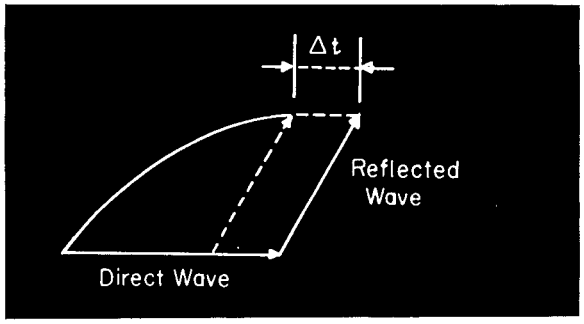

Figure 9. — Vector diagrams for envelope shape.

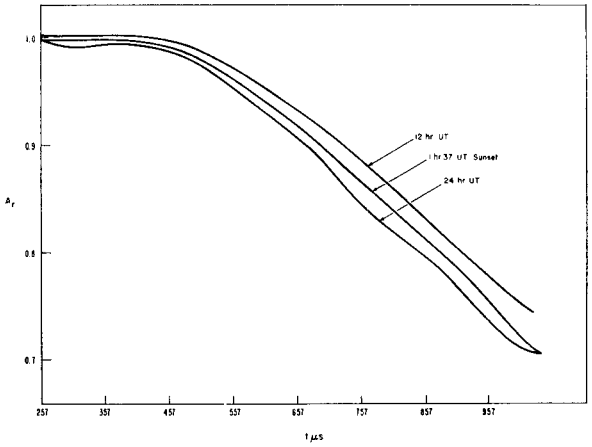

Figure 10. — Variations of envelope shape for a 24-hour period at Boulder.

The hypothesis is then made that propagation occurs with two modes, one of which predominates, the other possibly being present. This hypothesis was then tested to see if it was in agreement with the observations and, if so, to determine the dominant mode and the occurrence of the secondary mode.

In general, one expects for low frequencies that the ground wave is dominant for distances less than 1000 km.

To establish this hypothesis, the envelope of WWVB was measured as a function of distance between the transmitter and receiver for distances from 0 to 800 km. Figure 6 shows the results obtained using the low-level clock pulse as the time of origin. A careful study of these results shows coincident curves for fractional amplitudes less than 0.8, with a standard deviation for the fractional amplitude of 0.003 which corresponds exactly with the measurement error.

Note, however, that Figure 7 shows significant differences when the relative amplitudes lie between 0.8 and 1.0. It is quite evident that the shapes of the envelopes at Boulder and Castle Rock differ markedly from the theoretical single wave shape. These shapes, and also the others, support the presence of a second hop. The pulse beginning can be determined to an accuracy of ±50 microseconds. Figure 8 gives, with the same time scale as the preceding figures, the arrival time of the

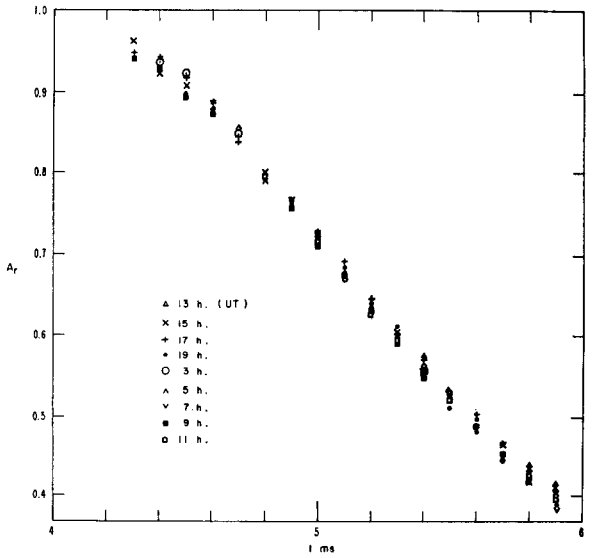

Figure 11. — Variations of envelope shape for a 24-hour period at Brussels.

commencement of the time pulse, from which the propagation time for a direct wave traveling at the speed of light may be deduced. These data demonstrate without doubt that (at least to 500 km) ground wave propagation exists. The propagation velocity is (2.985 ±0.015) 10^8 meters per second.

It is possible to consider that the envelope shape is derived from a dominant ground wave combined with a delayed skywave. It also seems reasonable to assume that the skywave propagates by a single hop. Under these conditions the resultant envelope shape is derived by adding the envelope of two carriers having the previously determined theoretical shape. To perform these calculations three new factors are introduced:

a. Phase difference between the carriers.
b. Skywave time delay (including phase change or reflection).
c. Relative amplitude of skywave.

Using a computer, a set of tables was prepared showing the resultant envelope shapes as a function of these parameters.

Propagation conditions over a 24-hour period were observed both at Boulder and Brussels.

At Boulder, 78.2 km from WWVB, the additional time delay for the skywave is about 260 microseconds assuming the ionospheric reflecting layer is around 70 km high. Results obtained in Boulder are shown in Figure 10. Groundwave propagation accounts for 50% of the observed envelope shapes. Comparing the other envelopes with the calculated tables shows that the skywave varies between 0 and 30% of groundwave amplitude. From this, a phase variation of about 1 microsecond would be expected, which was indeed observed in Boulder. Finally, during the period from 16 hours to 24 hours UT, or from sunrise to several hours before

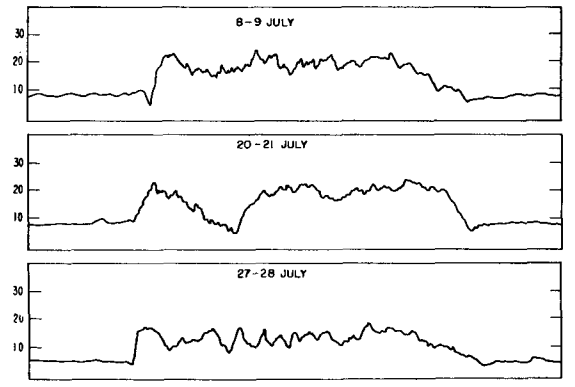

Figure 12. — Recording of field strength of HBG at Brussels.

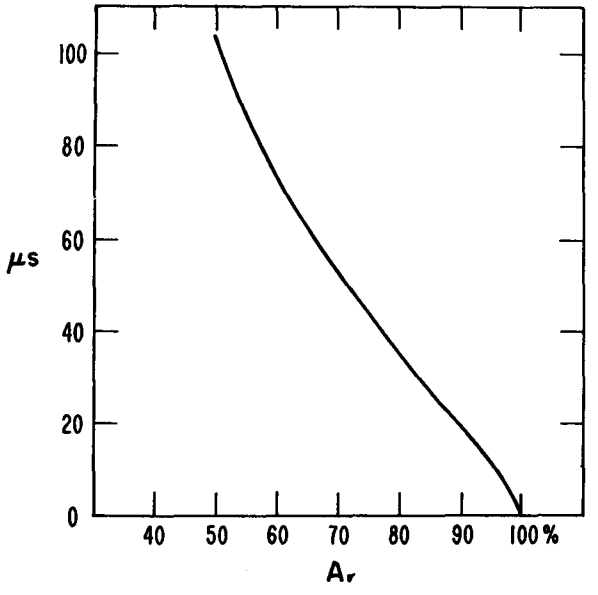

Figure 13. — Timing error due to a 10% variation in "Q" of the transmitting antenna.

sunset, the envelope has the shape predicted for a single mode of propagation.

In Brussels, 506 km from HBG, the additional time delay for the skywave is on the order of 70 microseconds, which fortunately reduces the influence of propagation on the envelope shape. Figure 11 shows the effect of superimposing nine curves taken at regular intervals throughout a 24-hour period. Here also the results are consistent with groundwave propagation during the day and with a nighttime skywave having a relative amplitude of 0 to 30% of its groundwave.

Interesting additional information is seen in the total received amplitude. Figure 12 shows several consecutive graphs. These are not easy to interpret since the amplitude is strongly dependent on the phase difference between the direct and reflected waves. Some points, however, are quite clear:

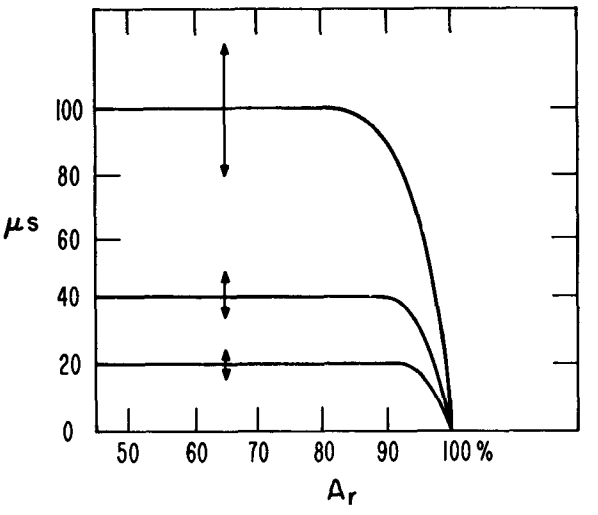

Figure 14. — Timing error due to a change of propagation from 100% ground-wave to 60% ground-wave and 40% sky-wave reflected at an altitude of 70 km.

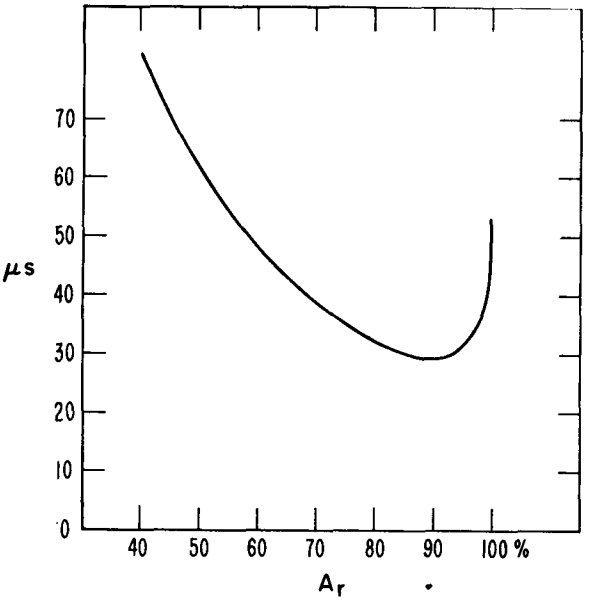

Figure 15. — Timing error due to an amplitude error of 0.01.

a. Daytime propagation is very stable and composed essentially of the groundwave.
b. From shortly before sunset until sunrise skywave also exists.
c. An abrupt change occurs at sunrise.

VI. CONCLUSIONS

The experimental data point out the complexity of the mathematical treatment for the time signal envelope. Unambiguous determination of both the propagation parameters and the transmission parameters is not possible by simultaneous measurements at the receiver.

The first result of this study is to show the desirability of transmitting a pulse with constant, precisely known shape. When this is done, assuming known receiver characteristics, only propagation conditions remain to be determined.

Otherwise, given certain conditions of transmission and reception, the determination of propagation conditions will be facilitated if the "Q"s of the transmitter and receiver are low. This implies powerful transmissions from a low "Q" antenna. The Loran-C transmissions are of this type and permit excellent synchronization.

If one uses time signals as presently transmitted at low frequencies, the time of arrival can be determined from a selected point on the pulse envelope. The timing error in using this method is a function of the amplitude chosen and the following phenomena:

a. Changes in pulse shape due to variations in the transmitting antenna (Figure 13).
b. Variable propagation conditions (Figure 14).
c. Errors in measuring the amplitude of the received pulse envelope (Figure 15).

The overall error (Figure 16) has a minimum depending on the relative magnitudes of the three types of errors. Generally a minimum overall error prevails when the amplitude point is selected between 0.9 and 0.75. Also it seems to be preferable to make the measurements in the mid-afternoon. Figure 17 shows the Brussels' results. Table IV below gives some results for different receiving conditions and supports the conclusions.

The results of similar measurements made at Boulder show a standard deviation of ±20 microseconds. This improved accuracy was principally due to a low noise level.

We then conclude that it is possible, by taking a few simple precautions, to measure the arrival time of a low frequency pulse to a precision of ±40 microseconds or better.

Since synchronization of the transmitters is now only within ±25 microseconds these results are considered very encouraging.

Lastly, the method of envelope analysis should be an effective tool for the study of propagation at low frequencies.

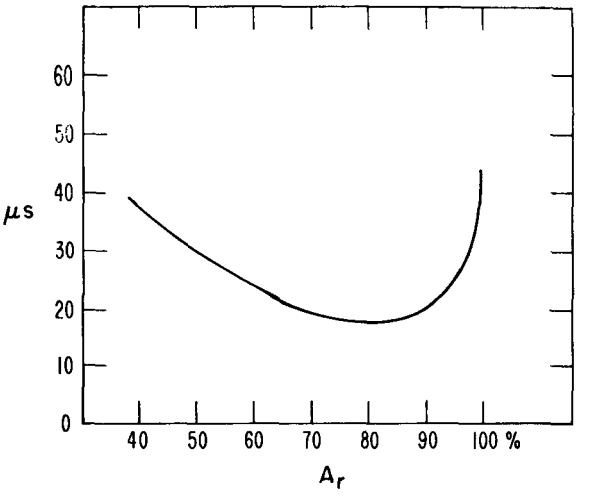

Figure 16. — Total error. $\sigma_Q = 0.05$; σ measured = 0.01; σ sky-wave = 0.40.

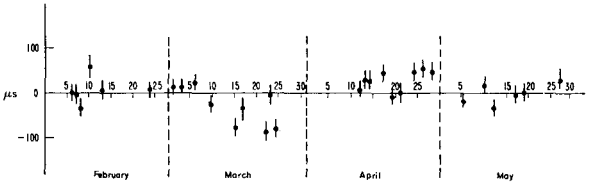

Figure 17. — Deviation of arrival times of HBG time signals as measured in the afternoon. Measurement point $A_r = 0.8$.

TABLE IV

Average Standard Deviations

	Morning (10hUT)	Afternoon (15hUT)
$A_r = 0.5$	120 μs	90 μs
$A_r = 0.8$	70 μs	38 μs

NOTE: The intrinsic precision of a single measurement was between 10 and 30 microseconds.

REFERENCES

[1] Blair, B. E., E. L. Crow and A. H. Morgan, Five years of VLF worldwide comparison of atomic frequency standards, *Radio Science, 2,* 627 (1967).

[2] Pierce, J. S., Intercontinental frequency comparison by very low frequency radio transmission, *Proc. IRE, 45,* 795 (1957).

[3] De Prins, J., J-L. Guisset, J-C. Liévin et J. Tamine, Description du système garde-temps du laboratoire d'étalons de fréquence de l'Université Libre de Bruxelles — *Annales françaises de Chronométrie.* 33e année, tome XIX.

[4] Doherty, R. H., G. Hefley, R. F. Linfield, Timing potentials of Loran-C, *Proc. IRE, 49,* No. 11, 1659 (1961).

[5] U. S. Coast Guard Electronics Engineering Report No. L-33, Calibration of the east coast Loran-C system.

[6] Davis, T. L., R. H. Doherty, Widely separated clocks with microsecond synchronization and independent distribution systems, *IRE Wescon Convention Record, 4, Part V, 3* (1960).

[7] Morgan, A. H., Distribution of standard frequency and time signals, *Proc. IEEE, 55,* 827 (1967).

[8] Chaslain, C., Propagation et réception de signaux horaires en basse fréquence — 1967 — *Memoire* — U.L.B.

[9] Detrie, R., Réception de signaux horaires sur ondes kilométriques (conception du récepteur). *Bulletin de la Classee des Sciences.* 5e série — Tome LII — 1966.

[10] Deleu J. et J. De Prins — Méthodes d'optimisation (To be published in 1968)

[11] Miscellaneous Publication 236, 1967 Edition, U. S. Department of Commerce, NBS standard frequency & time services, Radio Stations WWV, WWVH, WWVB, WWVL, p. 8.

Worldwide Clock Synchronization Using a Synchronous Satellite

LAWRENCE E. GATTERER, MEMBER, IEEE, PAUL W. BOTTONE, AND ALVIN H. MORGAN, MEMBER, IEEE

Abstract—**An experiment performed in late 1967 is reported which investigated the synchronization of widely separated clocks. One-way VHF timing signals were relayed to remote clocks from a reference clock by means of a transponder on a geostationary satellite. The problem of synchronizing clocks using one-way transmission reduces to the problem of predicting the radio propagation delay. The accuracy of predicting the delay was 10 μs or 60 μs depending on the method used. This technique may offer an alternative to transporting atomic standards to geodetic and spacecraft tracking stations around the world in fulfillment of their clock synchronization requirements.**

Manuscript received June 27, 1968. This paper was presented at the 1968 Conference on Precision Electromagnetic Measurements, Boulder, Colo. It is a contribution of the National Bureau of Standards and is not subject to copyright. This work was partially supported by the U. S. Air Force Cambridge Research Laboratories, Cambridge, Mass.

The authors are with the National Bureau of Standards, Boulder, Colo. 80302.

Introduction

CONSIDER a time dissemination system wherein time information derived from a reference clock is broadcast to users who compare the received time with that of their local clocks. The problem of measuring the time difference between a local clock and a remote reference clock reduces to predicting the propagation delay experienced by the radio wave. Station WWV is the transmitter for one such system. The accuracy of predictability of the propagation delay associated with the HF transmissions from WWV is limited to the millisecond region for most users. This limitation arises from the inability to predict the exact route a radio signal follows to the user and from the difficulty of defining the radio refractive index at all points along the path.

The principal advantage of using a geostationary satellite transponder is that the radio path is predominately a free-space line-of-sight path which is more predictable. Those portions of the path for which radio refractive index is a variable constitute only a small percentage of the total path.

Clock synchronization techniques involving two-way transmissions relayed by a satellite transponder between the reference and remote clocks have been described in the literature [1]–[4]. The technique described is of interest because in a one-way system the remote clock station would be relatively simple, cheap, and easy to operate, and the location would not have to be revealed by radio transmissions [5]. Any number of remote clocks could be synchronized simultaneously to the reference clock.

I. Description of Techniques

A. Definitions of Terms Used

Master Clock: the clock that is designated as the time reference point in comparing two or more clocks.

Slave Clock: a clock that is to be synchronized or referenced to the master clock.

Mode I: a satellite clock-synchronization technique involving a one-way communication channel from the master clock to the slave clock, similar in principal to WWV.

Round Robin: a technique for checking Mode II clock synchronization accuracies in a network of three or more stations.

Mode II: a satellite clock-synchronization technique involving a two-way communication channel between the master and slave clocks.

Clock Synchronization: (as used in this paper) the measurement of the time difference between two clocks.

B. Description of the Mode I Clock-Synchronization Technique

In the technique under investigation, Mode I, time signals are sent from the master clock to the slave clock via the satellite. The slave station measures the time difference between the slave clock and the received time signal. Consider the simplest case where the time difference between the master and slave clocks is zero (see Fig. 1). The master station transmits a one-pps signal format, and the slave station oscilloscope displays the received signal format. The sweep speed of the oscilloscope is set to 0.1 cm per second in order to display one sweep per second. Assume that all equipment delays are zero. Since the transmitted pulse train and the slave oscilloscope triggering pulse train are time coincident, the delay from the start of the sweep to the leading edge of the received pulse is equal to the radio propagation delay.

In general, there will be a time difference τ between the master and slave clocks and the equipment delays will be greater than zero. Then the measured delay on the slave oscilloscope will consist of four terms:

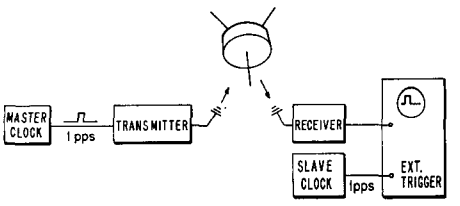

Fig. 1. Block diagram of Mode I clock-synchronization system.

$$R_s = -\tau + P + D_{ms} + D_s,\ \tau < (P + D_{ms} + D_s) \quad (1)$$

where R_s = the reading of the time difference between the slave-clock time tick and the received master-clock time tick, τ = algebraic time difference between master and slave clocks (referred to the master clock), P = radio propagation delay, D_{ms} = sum of the delays of the master transmitting equipment and the slave receiving equipment, and D_s = time delay of the transponder in the satellite.

The problem is to determine the value of τ. The D_{ms} and R_s are measured, D_s must be known, and P is computed. Using these values in (1), τ can be obtained.

With the master transmitting 1 pps the slave can measure τ with an accuracy of perhaps 0.01 second. If the frequency of the transmitted pulse train and the slave oscilloscope triggering train is increased by a factor of 10, the resolution of τ is increased by 10. This process can be continued until limitations are imposed by the system bandwidth. The transmitted 1 pps, 10 pps, 100 pps, etc., are derived from the master clock and they are coherent. Correspondingly, coherent oscilloscope triggering pulse trains are derived from the slave clock.

1) Corrections to Mode I Propagation Delay Calculations to Take Account of Ionospheric Effects: The propagation delay of the radio signals is increased over the free-space value when they pass through the ionospheric layer. An estimate of the increment of delay may be obtained from the relationship

$$\Delta l = \frac{b}{\omega^2}\left[\int_0^s N dh\right]. \quad (2)$$

Here, Δl is the increase in the group path due to the wave traveling through the ionosphere, $b = e^2/(2\ \epsilon_0 M) = 1.6 \times 10^3$ (e is the electronic charge, ϵ_0 is the dielectric constant of free space, M is the mass of the electron), $\omega = 2\pi f$, (f is the signal carrier frequency), and N is the "effective" electron density. The unknown to be determined in the equation is the value of N.

It is possible, in theory at least, to determine N from the measured penetration frequency at vertical incidence. However, such data may not generally be available and therefore another approach was used which seemed suitable for the time accuracies desired here.

Lawrence *et al.* [6] indicate that the value of the integral $[\int_0^s N dh]$ may vary from 10^{16} to 10^{18} electrons for vertical quasi-longitudinal propagation through a square meter column of the layer. These are the midday

values encountered during a sunspot cycle, the maximum value being correlated with the maximum of the sunspot cycle and vice versa. Allowance must be made for the longer path length through the ionosphere for nonvertical propagation. Quasi-longitudinal propagation at VHF implies that the angle between the radio ray path and the earth's magnetic field is less than 89° [7]. This condition holds true for almost all locations other than the subsatellite point.

During the measurements reported here, the sunspot number was about 130 [8], which is the average maximum value for several previous sunspot cycles. Therefore, the value of the integral was chosen as 10^{18}.

Making use of this value of the integral, (2) indicates that the midday increase over the free-space value in one-way group delay of a 135-MHz radio signal traveling vertically through the ionosphere is 7 μs. The nighttime increase may be as small as 1 μs. The uncertainty due to the variability of the sunspot number at corresponding phases of several cycles is estimated to be ± 3 μs for a vertical path.

2) Mode I Timing Error Due to Uncertainty of Receiving Site Location: A determination of the propagation delay requires knowledge of the satellite orbit and the coordinates of both the master and slave stations. The approximate uncertainty in the time synchronization Δt of the slave clock due to the uncertainty in its location, Δd, may be calculated. The geometry is depicted in Fig. 2. It is assumed that the locations of the satellite and the master clock are accurately known so that the time at which the signal leaves the satellite is known. Assuming a spherical earth, it may be shown that

$$\Delta d = r\Delta\theta \cong \frac{c'\Delta t[r^2 + (h+r)^2 - 2r(h+r)\cos\theta]^{1/2}}{(h+r)\sin\theta}, \quad 0 \leq \theta < \frac{\pi}{2} \tag{3}$$

where c' is the effective propagation velocity of the radio signal, r is the earth radius, h is the height of the satellite above the earth, θ is the angle subtended at the earth's center by the satellite and the slave station, and $\Delta\theta$ is the uncertainty in θ due to the uncertainty in the location of the slave station. Equation (3) contains an approximation but is in error by less than 1 percent for values of $\Delta\theta$ less than 8°.

To utilize (3), a parametric curve has been plotted. Fig. 3 illustrates the relationship for $\Delta T = 10$ and 100 μs. At $\theta = 30°$, for example, the slave-clock location must be known to 5 km in order to synchronize it to an accuracy of 10 μs using the Mode I technique.

The effect of a height error can be seen by referring to Fig. 2. At the earth tangent a change in r has no effect on the range to the satellite. At the subsatellite point, however, the range to the satellite changes linearly with the change in distance of the ground station from the center of the earth. At that point there is a timing error of 3 μs per km of height error.

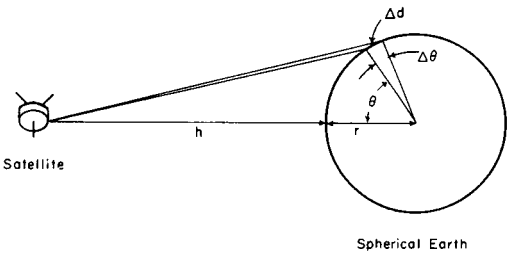

Fig. 2. Geometry of the experiment.

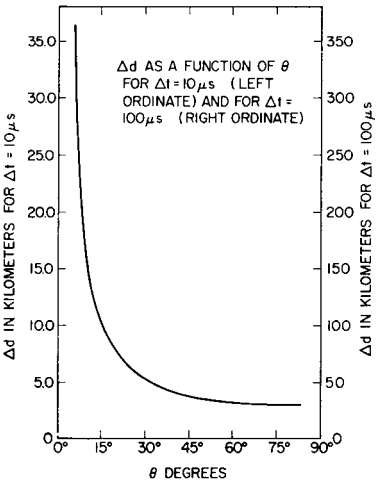

Fig. 3. Time sensitivity of station coordinates.

C. Description of Mode II Clock-Synchronization Technique

This method, which has been used and reported on before [3], was used in support of the Mode I experiment to check the time differences between the station clocks. The locations and ranges of the master and slave clocks need not be known, but both master and slave stations must have transmitters. The slave clock is synchronized as follows: From (1) the master station transmits a 1-pps time signal and the slave observes a time difference R_s:

$$R_s = -\tau + P + D_{ms} + D_s$$

as described in Mode I.

Then the slave station transmits back to the master, which will observe a time difference R_m, where

$$R_m = +\tau + P + D_{sm} + D_s; \tag{4}$$

D_{sm} is the delay associated with the slave transmitting and master receiving equipment, and the other terms are as defined in (1). If radio path reciprocity holds, one can subtract (1) from (4) and solve for τ, thus:

$$\tau = \tfrac{1}{2}[R_s - R_m] + \tfrac{1}{2}[D_{sm} - D_{ms}]. \tag{5}$$

TABLE I

Station	Latitude (°N)	Longitude (°W)	Elevation (meters)	θ (Fig. 2) (approx.)	Magnetic Dip Angle (approx.)	Satellite Range (km)	Satellite Elevation Angle Above Horizon
N	40	105.3	1659	64°	43°	39×10^3	25.26°
V	35.2	116.8	1213	53°	26°	38×10^3	36.24°
A	61.2	149.6	37	63°	43°	39.5×10^3	20.57°

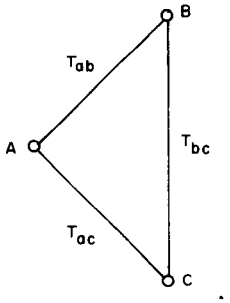

Fig. 4. Round robin check.

Equation (5) describes the case where the clock time difference is less than the sum of the propagation and equipment delays (about a fourth of a second), as in the Mode I discussion.

1) Description of a Mode II Check—Round Robin: A useful check on the accuracy of Mode II synchronizations has been devised for a system of three or more clocks. Fig. 4 shows that

$$T_{ac} = T_{ab} + T_{bc} \tag{6}$$

where T_{ac} is the time difference between the clock at Station *A* and the clock at Station *B* referred to clock *A*, etc.

The time closure *C* is given by

$$C = \left| T_{ac} - (T_{ab} + T_{bc}) \right| \tag{7}$$

and should normally be zero.

The technique is useful in determining whether certain types of operator errors have been made at any station. For example, an oscilloscope trigger slope switch was set incorrectly on several occasions during these measurements. This gave rise to a 50-μs error which was disclosed by applying the round robin technique.

II. Description of the Experiment

A. The Satellite VHF Transponder

The NASA satellite ATS-1 was launched in December, 1966, in near stationary orbit. A part of the ATS satellite system is devoted to supporting experiments at VHF. Signals received at 149.220 MHz with frequency modulation are converted to 135.600 MHz for retransmission to earth. An eight-element phased-array antenna system operating in duplex is used for both receiving and transmitting, while simultaneous signal limiting and bandwidth filtering are employed in the satellite signal chain. Because of this, amplitude modulation is not possible at full satellite power levels and the overall system bandwidth is restricted to 100 kHz. For this experiment frequency modulation was employed. The time delay of the VHF transponder is 7 μs [9].

1) Ground Terminals: Stations were set up for this experiment at the following locations: the National Bureau of Standards Laboratory, Boulder, Colo. (Station *N*); Goldstone Dry Lake Venus facility (Station *V*); Anchorage, Alaska (Station *A*); and the Goldstone Dry Lake Stadan facility. The latter station, which is a command station for ATS-1, was intended to function as the master station and all other stations were to operate as slave stations. However, difficulties with the ATS ground equipment at the Stadan facility prevented its use. In view of these difficulties NASA granted permission to designate the other stations as master stations at various times during the experiment. Data for the stations used are given in Table I.

2) Equipment: All three ground terminals had similar equipment except for transmitter final amplifiers whose outputs were 1 kW, $\frac{1}{2}$ kW, and $\frac{1}{4}$ kW for stations *N*, *V*, and *A*, respectively. The transmitting and receiving antennas at all stations were 10-element yagis with approximately 10-dB gain. Both vertical and horizontal polarization were provided because Faraday rotation occurs at these frequencies. Commercial FM communications transceivers, optimized for 10-kHz tones, were used.

3) Timekeeping Procedures: Commercial cesium beam clocks were maintained at all three stations. These were set using the Mode II technique, and at the end of the experiment the three clocks were brought together for time and frequency comparisons. The time differences between the three clocks were regularly measured during the course of the experiment by means of the Mode II technique, and the clocks at Stations *N* and *V* were compared during the experiment using the JPL Moonbounce technique [10].

The Venus facility, Station *V* of this experiment, is the master terminal for the JPL Moonbounce Radar Time Synchronization System and Station *N* is a slave terminal. This system is similar in principle to the time dissemination technique called Mode I in this paper. The master transmits an *X*-band signal which is reflected by the moon to the slave. The path delay is predicted from knowledge of the lunar ephemeris and is

corrected for Doppler effects introduced by rotation of the earth.

The time difference between clocks during the experiment was recovered to within 1.8 μs, peak to peak.

B. Experimental Results

Experiments were conducted on November 30, 1967, from 1940 to 2140 UT, and on December 1, 1967, from 2000 to 2300 UT. The stations took turns transmitting. All three stations, including the one transmitting, observed the signal transponded by the satellite. Each station measured the time difference between its own clock and the signal received from the satellite. The time duration for a set of three transmissions, including voice acknowledgments, did not exceed eleven minutes. Changes in path length due to satellite perturbations normally do not cause time errors greater than 1 μs during that period of time, although exceptions have been noted [11]. Such exceptions may be related to orbit correction maneuvers in which case they could be anticipated.

1) Mode I Results: Since the time differences between the three station clocks were known, the measurement of the time difference between a received signal and a local clock, corrected for equipment delays, was actually a measurement of propagation delay. The comparison between the measured VHF propagation delay and that computed from the satellite range predictions was the measurement of accuracy of the Mode I technique.

The range predictions were provided by NASA from an existing computer program. Two sets of range values were provided: the first was based on orbital elements of the satellite projected from the past history of the satellite and predicted one week in advance of the experiment; the second set was based on orbital elements which were updated by NASA at the time of these experiments. Results are given in Table II. The Mode I accuracy is given as the average difference between the measured and the computed values of the propagation delay; a positive sign indicates that the latter is larger. The standard deviation follows the accuracy.

2) Mode II Results: By using paired measurements from a given set of measurements, Mode II clock synchronizations were effected. For example, the delay measurements made at Station *V* while Station *N* was transmitting were paired with that made at *N* while *V* transmitted. Results are given in Table III. The accuracy of Mode II is given as the absolute value of the disagreement between the measured (by Mode II) and the known time difference between the clocks. The standard deviation follows the accuracy.

3) Round Robin Closures: The results of the Mode II synchronizations were summed according to (7). The closure for eleven sets of measurements checked by the round robin technique varied from 0.5 μs to 8.4 μs.

4) Moonbounce Results: On November 29, 1967, the Moonbounce radar timing link between Stations *N* and *V* was operated. Ten measurements made between 1925 and 1935 UT were averaged to obtain a clock comparison. This average value differed from the known value by 2.3 μs with a standard deviation of 1.16 μs.

TABLE II

Master Station	Slave Station	Accuracy Using Predicted Values (μs)	Accuracy Using Updated Values (μs)	Number of Observations
November 30, 1967				
N	*V*	−56±1.2	−3.8±2.2	5
N	*A*	−53±5.6	6.6±4.1	5
V	*A*	−33±3.7	16.8±3.7	5
December 1, 1967				
N	*V*	−57±0.1	−8.5±1.6	7
N	*A*	−54±2.1	4.7±3.2	7
V	*A*	−47±4.4	7.4±7.1	7

TABLE III

Master Station	Slave Station	November 30, 1967		December 1, 1967	
		Accuracy (μs)	Number of Observations	Accuracy (μs)	Number of Observations
N	*A*	−5.4±2.9	5	−6.0±3.66	6
N	*V*	−8.8±1.3	5	−7.7±1.98	6
V	*A*	7.9±1.0	5	2.7±2.17	6

C. Error Analysis

1) Mode I Error Analysis: The following sources of error have been considered in connection with the Mode I technique (see Table IV):

a) The ground equipment delay (about 150 μs) was measured frequently during the experiment and was considered to be known to ±2 μs.

b) The satellite transponder delay (7.0 μs) was measured during construction at Hughes Aircraft Company in 1966. The accuracy of measurement was ±1.0 μs [9].

c) The locations of the stations were known to within ±200 meters corresponding to a propagation time uncertainty of ±0.5 μs [from (3)].

Range values provided for Station *V* were inconsistent, apparently because of a programming error. The range values provided for the nearby Stadan terminal were used in computing the propagation delay to Station *V*. It is believed that the range to Station *V* was greater than that to Stadan by 3 km or less. This corresponds to an increase in propagation delay of 9 μs or less.

d) Satellite range values provided by NASA were rounded to the nearest kilometer, corresponding to a propagation delay uncertainty of ±1.5 μs.

e) The up-link frequency is about 150 MHz while the down-link frequency is about 135 MHz. The ionospheric uncertainties discussed earlier in the paper are greater at lower frequencies and so were computed at 135 MHz.

TABLE IV
MODE I ERROR BUDGET

Source	Error (μs)
Equipment	
Uncertainty in measurement of ground equipment delay	± 2
Uncertainty in knowledge of satellite transponder delay	± 1
Geometry	
Uncertainty in propagation delay related to ± 200-meter uncertainty of ground station at $\phi = 65°$ (Stations N and A)	
up link	± 0.7
down link	± 0.7
Uncertainty in propagation delay due to ± 0.5-km uncertainty in satellite range	
up link	± 1.5
down link	± 1.5
Propagation Effects	
Uncertainty in correction to propagation delay due to ionosphere (including difference in up-link and down-link frequencies)	
up link	± 6
down link	± 6
Uncertainty in propagation delay due to troposphere	
up link	0.3
down link	0.3
Rms noise jitter	± 5
Mode I rms error between stations	10.4

For the oblique ionospheric path associated with Stations N, A, and V, the error was estimated to be about ± 6 μs.

f) Noise jitter observed on the slave oscilloscope trace obscured the exact location of the time reference point in the received timing signal. An accuracy of ± 5 μs was assigned to the oscilloscope readings.

g) Other propagation effects associated with VHF ionospheric propagation include Faraday rotation, amplitude and phase scintillation, and ionospheric absorption. These phenomena have negligible effect on the propagation delay [3].

h) The increase in propagation delay (over the free-space value), due to the radio path through the troposphere, was not included in the corrections. The maximum increase under any circumstances would be about 0.3 μs [12].

The Mode I rms error of 10.4 μs is the clock synchronization accuracy to be expected using the equipment of this experiment at stations whose locations are known to 200 meters, using correct satellite range predictions, and computing propagation delays by the methods discussed. The Mode I measurements between Stations N and A, using the updated satellite range values, fall within the predicted error. Using the less accurate projected range values, the discrepancy was about 60 μs.

When the 9-μs allowance is made for the greater uncertainty in the Venus range data, similar results follow from measurements between Stations V and A, and between V and N.

2) Mode II Accuracy: The accuracy associated with the Mode II technique (using the equipment and procedures of this experiment), has been shown to be about 5 μs [3]. The least accurate Mode II synchronizations during this experiment were between Stations N and V (average values were 7.7 and 8.8 μs). It is interesting to note that the clock at Station A, which had not been running prior to arrival at the station, was set using the Mode II technique. At the end of the experiment it was transported to Station N where it was found to be 6 μs from clock N.

3) Moonbounce Accuracy: The accuracy of the Moonbounce Radar Timing System is given as 5 μs [10]. The average accuracy of the measurements made in this experiment was 2.3 μs.

III. Conclusions

A technique for synchronizing widely separated clocks to a reference clock has been investigated. The technique involves the one-way transmission of a radio time signal from the reference clock, relayed by a geostationary satellite VHF transponder to the remote clocks. The problem reduces to predicting the radio propagation delay from the reference clock, by way of the satellite, to the remote clocks. The propagation delay predictability on two days has been studied between three stations. The accuracy of predictability, and hence of clock synchronization, was found to be 60 μs if the propagation delay was computed using a satellite orbit predicted one week in advance of the experiment. The accuracy was 10 μs when the orbit used had been updated to the time of the measurements.

A clock synchronization system using the technique could offer two levels of accuracy. Tables of predictions of propagation delay at future times to specific locations or areas could be distributed or published in advance. Users would observe the radio timing signals when desired, refer to the tables, and compute their time difference from the reference clocks. Those users needing more accurate synchronization would be given after-the-fact propagation delay predictions based on an updated satellite orbit. As a check on the system, key stations could be equipped with transmitters for occasional two-way operations with the reference station or with each other.

If the location of a station were uncertain, the propagation delay could be calibrated by means of a two-way synchronization or a transported clock. Thus, the technique could be applied to navigation problems.

A system based on the technique could provide an alternative to transporting atomic clocks to geodetic and spacecraft tracking stations around the world in satisfying their clock synchronization requirements.

Acknowledgment

U. S. Air Force Cambridge Research Laboratories: Major J. Cook and Capt. D. Abby, for research funding which partially supported the data analysis associated with this experiment.

463-560 O - 72 - 26

U. S. Coast and Geodetic Survey: Lt. (jg) P. F. MacDoran, Environmental Science Services Administration, for suggesting the technique used for eliminating time ambiguity in transmitted time signals, and for his participation in the experiment.

National Bureau of Standards, Time and Frequency Division: L. Fey for participation in the experiment; G. Kamas for circuit designs; D. Hilliard and S. Canova for design and construction of equipment and participation in the experiment; R. Ruppe for assistance with programming and computations; and C. Craig and S. Richmond for assistance in the preparation of this manuscript.

National Aeronautics and Space Administration, Goddard Manned Space Flight Center: R. J. Darcey, J. P. Corrigan, and D. J. Stewart for coordinating ATS operations, providing technical assistance, and computing all range values used in this experiment.

Edgerton, Germeshausen & Grier, Inc.: J. Rennie and R. Smith for operation of the Anchorage station.

Jet Propulsion Laboratories: W. Baumgartner and E. Jackson for their cooperation and assistance in connection with the Moonbounce system and for providing facilities for satellite Station *V*; and R. Fuzie for assistance with timekeeping operations.

Environmental Science Services Administration, Space Disturbances Laboratory: Dr. K. Davies for valuable discussions relating to ionospheric propagation.

References

[1] J. M. Steel, W. Markowitz, and C. A. Lidback, "Telestar time synchronization," *IEEE Trans. Instrumentation and Measurement*, vol. IM-13, pp. 164–170, December 1964.
[2] W. Markowitz, C. A. Lidback, H. Uyeda, and K. Muramatsu, "Clock synchronization via Relay II satellite," *IEEE Trans. Instrumentation and Measurement*, vol. IM-15, pp. 177–184, December 1966.
[3] J. L. Jespersen, G. Kamas, L. E. Gatterer, and P. F. MacDoran, "Satellite VHF transponder time synchronization," *Proc. IEEE*, vol. 56, July 1968.
[4] R. N. Grubb and S. D. Gerrish, "Results of preliminary tests of a time dissemination system using the VHF transponder on the ATS-1 satellite," ESSA Research Lab., Boulder, Colo., Tech. Memo. ERL-TM-SDL-9, March 1968.
[5] L. E. Gatterer, "Clock synchronization experiments at VHF utilizing the ATS-1 transponder," NASA ATS Tech. Summary Rept., February 1968.
[6] R. S. Lawrence, C. G. Little, and H. J. A. Chivers, "A survey of ionospheric effects upon earth-space radio propagation," *Proc. IEEE*, vol. 52, pp. 4–27, January 1964.
[7] K. Davies, ESSA, Boulder, Colo., private communication.
[8] "Solar geophysical data," ESSA, Environmental Data Service.
[9] G. Melton, NASA, private communication.
[10] W. S. Baumgartner and M. F. Easterling, "A world-wide lunar radar time synchronization system," presented at the NATO Advanced Group for Aeronautical Research and Develop., Milan, Italy, September 11, 1967.
[11] L. Fey, NBS, private communication.
[12] J. L. Jespersen, NBS, private communication.

Reprinted from
IEEE Transactions on Instrumentation and Measurement - December 1968

Radio Science, Volume 4, Number 7, pages 579–590, July 1969

TIME AND FREQUENCY

Commission 1

Progress in radio measurement methods and standards

R. W. Beatty, Editor

National Bureau of Standards, Boulder, Colorado 80302

R. C. Baird, J. A. Barnes, R. W. Beatty, G. Birnbaum, M. Birnbaum, H. E. Bussey, E. W. Chapin, G. F. Engen, W. W. Mumford, N. S. Nahman, G. E. Schafer, M. C. Selby, and B. O. Weinschel

(Received March 26, 1969.)

TIME AND FREQUENCY

On Friday, October 13, 1967, the General Conference of Weights and Measures adopted the atomic definition of the unit of time, the second. The development of atomic frequency standards is still most heavily weighted toward cesium beam devices, with considerable work also on hydrogen masers [*Vessot et al.*, 1966; *McCoubrey*, 1967]. Probably because of budget problems, there has been little work on thallium beams. There has been significant interest in optical frequency standards with a notable development of a methane-stabilized laser by John Hall [*Barger and Hall*, 1969]. Current emphasis on atomic frequency standards is toward more nearly optimum performance. Atomic frequency standards have an important use in long baseline interferometry [*Gold*, 1967].

One of the most significant publications on the subject of frequency stability is the special issue of the *Proceedings of the IEEE* volume 54, number 2, (February 1966). Since this publication, there seems to be a fairly general tendency among the more sophisticated time and frequency laboratories to use the variance of frequency fluctuations as defined by *Allan* [1966] as a consistent measure of frequency stability in the time domain. The Allan variance (specifically, $N = 2$) has been referenced several times [e.g., *Vessot et al.*, 1966; *Menoud et al.*, 1967; *Mungall et al.*, 1968; *Vessot et al.*, 1968]. Methods of spectrum estimation [*Bingham et al.*, 1967] and the fast Fourier transform [*Brigham and Morrow*, 1967] are important developments for frequency domain specifications of frequency stability. A subcommittee of the IEEE is preparing standard definitions of frequency stability.

Flicker noise is found to affect the frequency, in long term, of all signal generators [see, for example, *Vessot*, 1968]; to affect the phase, in short term, of oscillators, amplifiers, and frequency multipliers [*Halford et al*, 1968]; and to affect the phase of LF and VLF radio signals [*Allan and Barnes*, 1967; *Guetrot*, 1969]. This area needs much study.

In the area of time and frequency dissemination, satellites have received much attention, with VHF transponder satellites showing capabilities of time synchronization to a few microseconds [*Gatterer et al.*, 1968]. The Omega system is to become operational, and it is expected to allow time synchronization. Other active areas of research include Loran C, portable clocks, HF, LF, and VLF [*Morgan*, 1967].

During the past three years, needs for highly precise time synchronizations have steadily increased. One of the most notable needs that developed is for a 3-sigma tolerance of 0.5 μsec worldwide for the Aircraft Collision Avoidance System (ACAS) [*Holt*, 1968]. It is doubtful that the current UTC system strikes an adequate compromise between needs for Universal Time and Atomic Time. The U. S. Study Group VII supplied recommendations for a new compromise UTC system to the Plenary Session of the International Radio Consultative Committee (CCIR) meeting in Boulder, Colorado, in July 1968. International agreement was not reached, but a Working Party was formed to study the matter. The U. S. Naval Observatory and the National Bureau of Standards (NBS) have coordinated their standard frequency and time signals (beginning October 1968) with time coincidence maintained within ±5 μsec of each other.

Reprinted with corrections and reference addendum, February 1970.

Allan, D. W. (1966), Statistics of atomic frequency standards, *Proc. IEEE, 54*(2), 221–230.

Allan, D. W., and J. A. Barnes (1967), Some statistical properties of LF and VLF propagation, *Proc. 13th EPC/AGARD Symp.*, Ankara, Turkey (to be published).

Barger, R. L., and J. L. Hall (1969), Pressure shift and broadening of methane line at 3.39 micron studied by laser-saturated molecular absorption, *Phys. Rev. Letters, 22*(1), 4–8.

Bingham, C., M. D. Godfrey, and J. W. Tukey (1967), Modern techniques of power spectrum estimation, *IEEE Trans. Audio Electroacoustics, 15*(2), 56–66.

Brigham, E. O., and R. E. Morrow (1967), The fast Fourier transform, *IEEE Spectrum, 4*(12), 63–70.

Gatterer, L. E., P. F. Bottone, and A. H. Morgan (1968), Worldwide clock synchronization using a synchronous satellite, *IEEE Trans. Instr. Meas., 17*(4), 372–378.

Gold, T. (1967), Radio method for the precise measurement of the rotation period of the earth, *Science, 157*(3786), 302–304.

Guetrot, A. G. (1969), Optimum smoothing techniques on VLF time signals, Master of Science thesis, University of Colorado, Boulder.

Halford, D., A. E. Wainwright, and J. A. Barnes (1968), Flicker noise of phase in RF amplifiers and frequency multipliers: Characterization, cause, and cure, *Proc. 22nd Ann. Symp. Freq. Control,* 340–341.

Holt, J. M. (1968), Avoiding air collisions, *Sci. Tech., 78,* 56–63.

McCoubrey, A. O. (1967), The relative merits of atomic frequency standards, *Proc. IEEE, 55*(6), 805–814.

Menoud, C., J. Racine, and P. Kartaschoff (1967), Atomic hydrogen maser work at L.S.R.H., Neuchatel, Switzerland, (Laboratoire Suisse de Recherches Horlogères), *Proc. 21st Ann. Symp. Freq. Control,* 543–567.

Morgan, A. H. (1967), Distribution of standard frequency and time signals, *Proc. IEEE, 55*(6), 827–836.

Mungall, A. G., D. Morris, H. Daams, and R. Baily (1968), Atomic hydrogen maser development at the National Research Council of Canada, *Metrologia, 4*(3), 87–94.

Vessot, R. F. C., H. Peters, J. Vanier, R. Beehler, D. Halford, R. Harrach, D. Allan, D. Glaze, C. Snider, J. Barnes, L. Cutler, and L. Bodily (1966), An intercomparison of hydrogen and cesium frequency standards, *IEEE Trans. Instr. Meas., 15*(4), 165–176.

Vessot, R. F. C. (1968), Atomic hydrogen masers, an introduction and progress report, *Hewlett Packard, J., 20*(2), 15–20.

Vessot, R. F. C., M. W. Levine, L. S. Cutler, M. R. Baker, and L. F. Mueller (1968), Progress in the development in hydrogen masers, *Frequency, 6*(7), 11–17.

Reference addendum to Time and Frequency section.

UNITED STATES DEPARTMENT OF COMMERCE
Maurice H. Stans, Secretary
NATIONAL BUREAU OF STANDARDS • A. V. Astin, Director

TECHNICAL NOTE 379

ISSUED AUGUST 1969
Nat. Bur. Stand. (U. S.), Tech. Note 379, 27 pages (August 1969)
CODEN: NBTNA

STANDARD TIME AND FREQUENCY: ITS GENERATION, CONTROL, AND DISSEMINATION FROM THE NATIONAL BUREAU OF STANDARDS TIME AND FREQUENCY DIVISION

JOHN B. MILTON

Frequency-Time Broadcast Services Section
Time and Frequency Division
Institute for Basic Standards
National Bureau of Standards
Boulder, Colorado 80302

TABLE OF CONTENTS

LIST OF FIGURES

STANDARD TIME AND FREQUENCY: ITS GENERATION, CONTROL, AND DISSEMINATION FROM THE NATIONAL BUREAU OF STANDARDS TIME AND FREQUENCY DIVISION

John B. Milton

The Time and Frequency Division of the National Bureau of Standards produces the NBS time scales, AT(NBS), SAT(NBS), and UTC(NBS). These time scales are developed by utilizing the properties of the NBS frequency standard, NBS-III. The main byproduct of these time scales is the operational clock systems. These operational clock systems are used, among other things, to calibrate the clocks and secondary standards necessary for the operation of the NBS radio stations, WWV, WWVB, WWVL, and WWVH. These stations transmit SAT(NBS), UTC(NBS), and various tones, alerts, and corrections for time-of-day information.

Key Words: clock synchronization; frequency and time dissemination; primary frequency standard; standard frequency broadcasts; time interval; time scales

1. INTRODUCTION

Since its inception in 1901, the National Bureau of Standards has been involved in the design, construction, maintenance, and improvement of standards of frequency and time interval. During the first two decades of the Twentieth Century, the work on these standards was done by quite diverse groups.

The people maintaining the standard of time interval were concerned primarily with problems of navigation, while the standard of frequency was maintained by a group concerned chiefly with radio interference between adjacent channels in the radio spectrum.

The operational time-interval standard has progressed from a pendulum clock with electrical pulse output through crystal clocks to the present-day "atomic clock." During the same period, the operational standard of frequency has evolved from a tuning fork to a quartz crystal oscillator to an atomic beam device. While there may be only a superficial connection between a pendulum clock and a tuning fork, the present-day standards of time interval and frequency are, by their very nature, inseparable.

Along with the maintenance and improvement of these standards came the need to disseminate these standards. In 1923 the National Bureau of Standards radio station WWV was established to disseminate the standard of frequency via experimental broadcasts. Time pulses were added to these broadcasts in 1935. Voice announcements of the time-of-day were added to these broadcasts in 1945.

In 1948, NBS radio station WWVH was placed in operation. In the 1950's, very good commercial standards were controlling both of these high frequency radio stations. At that time, nothing was done at the stations beyond providing good crystal oscillators. Utilizing the ultra-high precision oscillators located at the NBS Boulder Laboratories, the time and frequency of these stations were measured daily. Any deviations from the NBS standard were noted and corrective instructions were relayed to the radio stations.

In 1956, the Boulder Laboratories of the NBS began experimental transmissions on 60 kHz from radio station WWVB. The 60 kHz driving frequency for this station was derived directly from the NBS standard of frequency located at the Boulder Laboratories. There was no control of the transmissions beyond providing this standard driving frequency.

In 1960, utilizing an antenna borrowed from the Central Radio Propagation Laboratory of NBS, radio station WWVL was placed in experimental operation on 20 kHz. This station was located some ten miles west of the Laboratories in a high mountain valley. Direct generation of the transmission frequency by the Boulder Laboratories was not feasible, but a method of phase control using servo systems was employed. Since January 1, 1960, when NBS began using a cesium beam device as its official standard, all broadcast frequencies have been referenced to the cesium resonance frequency.

WWVB and WWVL were moved to Fort Collins, Colorado, and began operation there in July 1963. The original time and frequency control for these stations was accomplished by continuously operating servo systems that compared the phase of these stations as received in Boulder against a phase reference derived from the NBS Frequency Standard. Phase corrective information was then sent to Fort Collins via a radio link.

Primarily in order for NBS to increase the precision and accuracy of the transmissions from station WWV, through more uniform U. S. coverage and the replacement of obsolete transmitting and control equipment, a new facility for that station was installed at Fort Collins, Colorado, in 1966.

Stations WWV, WWVB, and WWVL are, in essence, a composite facility disseminating standards of time and frequency from 19.9 kHz to 25 MHz. At the present time, these stations provide information at both atomic frequency and an internationally agreed upon offset frequency. The offset frequency is used to generate a Universal Time scale, called UTC, which closely approximates the UT2 scale based on the rotation of the Earth.

Even though the time and frequency control of these stations was provided by a highly precise ensemble of clocks and standards, the problem remained of finding a simple, reliable, and inexpensive method of providing a daily calibration of the Fort Collins standards with respect to the NBS reference standards in Boulder.

This paper describes some of the current efforts of the Time and Frequency Division of the NBS. These include the generation of the computed NBS time scales, their translation into real working clocks, and the use of these clocks in coordination efforts with other standards laboratories. The coordination of the Fort Collins site clocks and frequency standards, the measurement and control of LF and VLF radiated phase, and the method of coordination of the Fort Collins master clock with that of NBS/Boulder are also described.

2. STANDARD FREQUENCY AND TIME GENERATION

2.1 Atomic Frequency and Time Standards Section

With the advent of the first working atomic clock system in 1948, developed by Harold Lyons at NBS/Washington, the era of the highly accurate atomic standards was born. The first work at NBS/Boulder was under the project direction of Dr. R. C. Mockler. This early work included, among other things, the refinement of the original NBS cesium-beam device, NBS-I.

In late 1959, the Atomic Frequency Standards Project, including the cesium beam and ammonia maser development work, was combined with the project concerned with theoretical and practical aspects of atomic time scales to form the Atomic Frequency and Time Standards Section.

2.1.1 The NBS Frequency Standard

The operations of the Atomic Frequency and Time Standards Section are presently centered on a device known as NBS-III, which serves as the NBS Frequency Standard. This machine, which is a long-beam cesium resonance standard, is probably the most thoroughly evaluated standard of its kind. The most important requirement for a primary frequency standard is high accuracy, where the term "accuracy" refers to an estimate of how far the output frequency of the standard may deviate from the ideal frequency defined with respect to an isolated cesium atom. In order to determine the limits of accuracy of such a standard, the possible causes, the cures in some cases, and the estimated magnitude of any and all small frequency shifts must be known: hence the continuing study of NBS-III by the Section personnel. NBS-III does not operate continuously; its main function is the frequency measurement of the frequencies of the working ensemble of clocks. These data, as described in the next section, are used in producing the AT(NBS) time scale. The accuracy of NBS-III is $\pm 5 \times 10^{-12}$, based on 3σ estimates of all uncertainties.

2.1.2 Computed or "paper" time scales

The Section maintains six oscillator-clock combinations that are used in producing three computed time scales. One might ask not only what is a "paper" time scale, but also how is it produced, and then how is it used.

The paper time scales, AT(NBS),* SAT(NBS),* and UTC(NBS),* are in fact computer printouts which relate the indicated time of each of the six clocks in the ensemble to the computed scales that are

*See Appendix.

produced by the computer. The computer utilizes the current measured frequency of each oscillator with respect to NBS-III along with the past history of each of the six oscillators to apply a weighting factor to each oscillator based on its performance. The computed scales produced are more uniform than a scale produced by the best unit of the ensemble. The computer output is a set of numbers that are the time differences between each clock output and the computed scales. With this information, one has a mechanism for comparing clocks nationally or internationally and also for comparing the timekeeping performance of individual clocks comprising the time scale system. Figure 1 is a simplified diagram of the system that produces the NBS time scales. More comprehensive versions of all drawings in this document are available from the Frequency-Time Broadcast Services Section of the Time and Frequency Division.

2.1.3 Operational clock systems

The Section maintains three operational clock systems. The outputs of these systems are electrical seconds pulses as well as visual displays of epoch. The time scale based on the primary NBS clock, designated as Clock #7, closely approximates the AT(NBS) time scale. Corrections for Clock #7 relative to the AT(NBS) time scale are computed at regular intervals. Probably the most useful clock in a practical sense is the unit designated Clock #8. This clock's output closely approximates the UTC(NBS) time scale. The daily deviations of Clock #8 from the UTC(NBS) time scale are published monthly in the NBS Time and Frequency Services Bulletin. The deviation of this clock from the UTC(NBS) time scale is constrained to always be less than 1 microsecond and seldom exceeds ± 0.2 microsecond. The third system, operating from an independent quartz crystal oscillator, is a backup atomic rate clock designated Clock #0. A time comparator and 24-hour alarm system

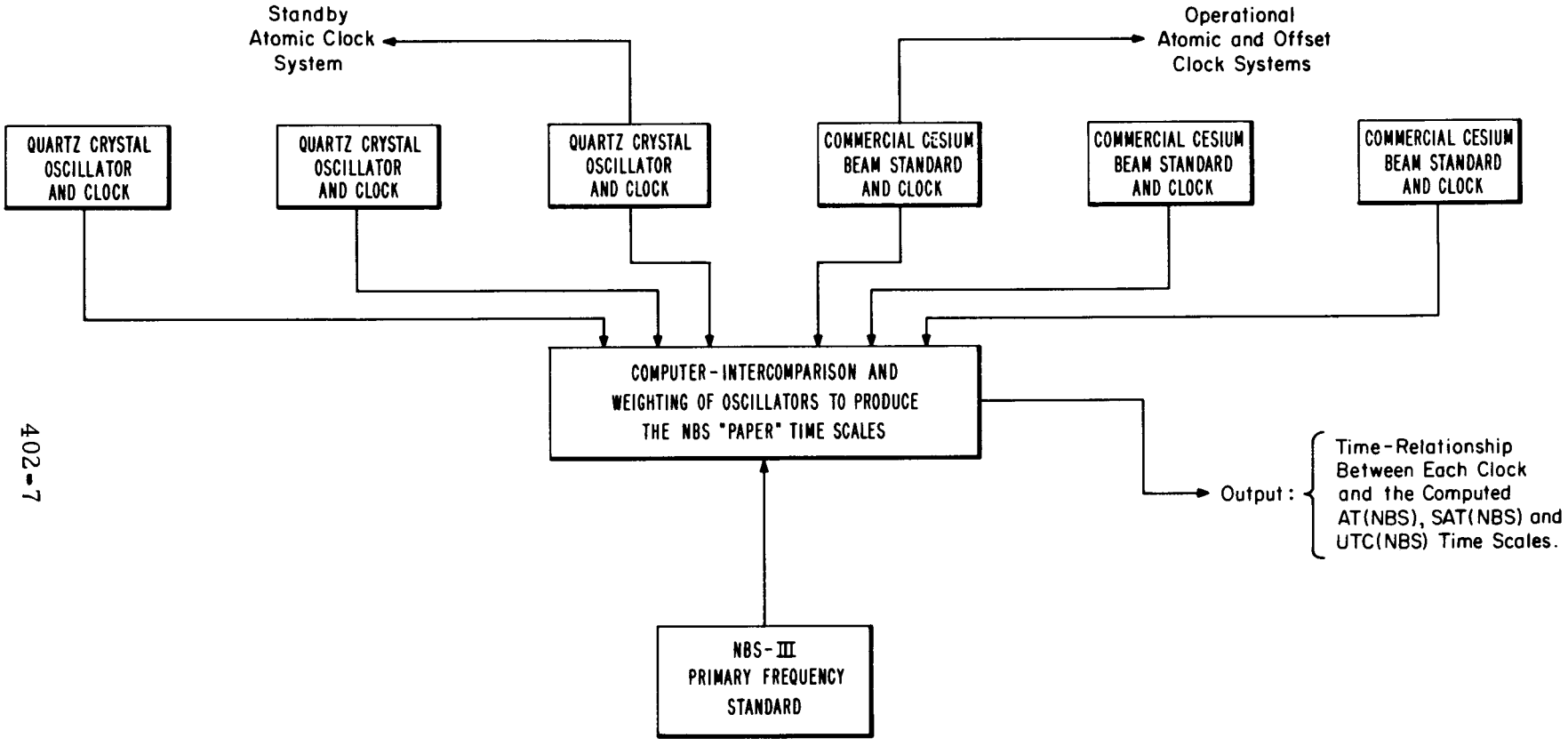

SYSTEM FOR GENERATION OF COMPUTED TIME SCALES
AT(NBS), SAT(NBS), AND UTC(NBS)

Figure 1

are associated with Clock #0 and Clock #7. This alarm is actuated if Clock #7 diverges from Clock #0 by more than 5 microseconds. All of the frequency standards in the operational system operate on the "atomic" frequency. To produce an operational clock whose rate more nearly approximates that of the UTC clock based on the earth's rotation, a fixed frequency offset generator is placed between the atomic standard and the operational clock, such as Clock #8. This offset rate for 1969 is -300×10^{-10}. An adjunct to the operational clock systems is the clock comparison link to Fort Collins that utilizes television synchronizing pulses. Figure 2 is a simplified diagram of these operational clock systems.

2.2 Radio Station WWV, Fort Collins, Colorado

The heart of the time and frequency generation system at WWV is a set of three commercial cesium-beam frequency standards. These standards are the basis for three identical generating units which provide to the transmitters a composite rf signal containing the complete WWV format.

The Cs standards, through a series of dividers and distribution amplifiers, drive the three master clocks or, more specifically, the three WWV time-code generators. These time-code generators provide the standard 600 Hz, 440 Hz, 1 kHz, and all the gates, codes, etc., necessary to produce this rather complex format. Figure 3 shows a simplified drawing of the WWV time and frequency generating system at Fort Collins.

2.3 Radio Station WWVB, Fort Collins, Colorado

The WWVB time and frequency generating system is somewhat similar to that of WWV, although not as elaborate. WWVB uses a highly

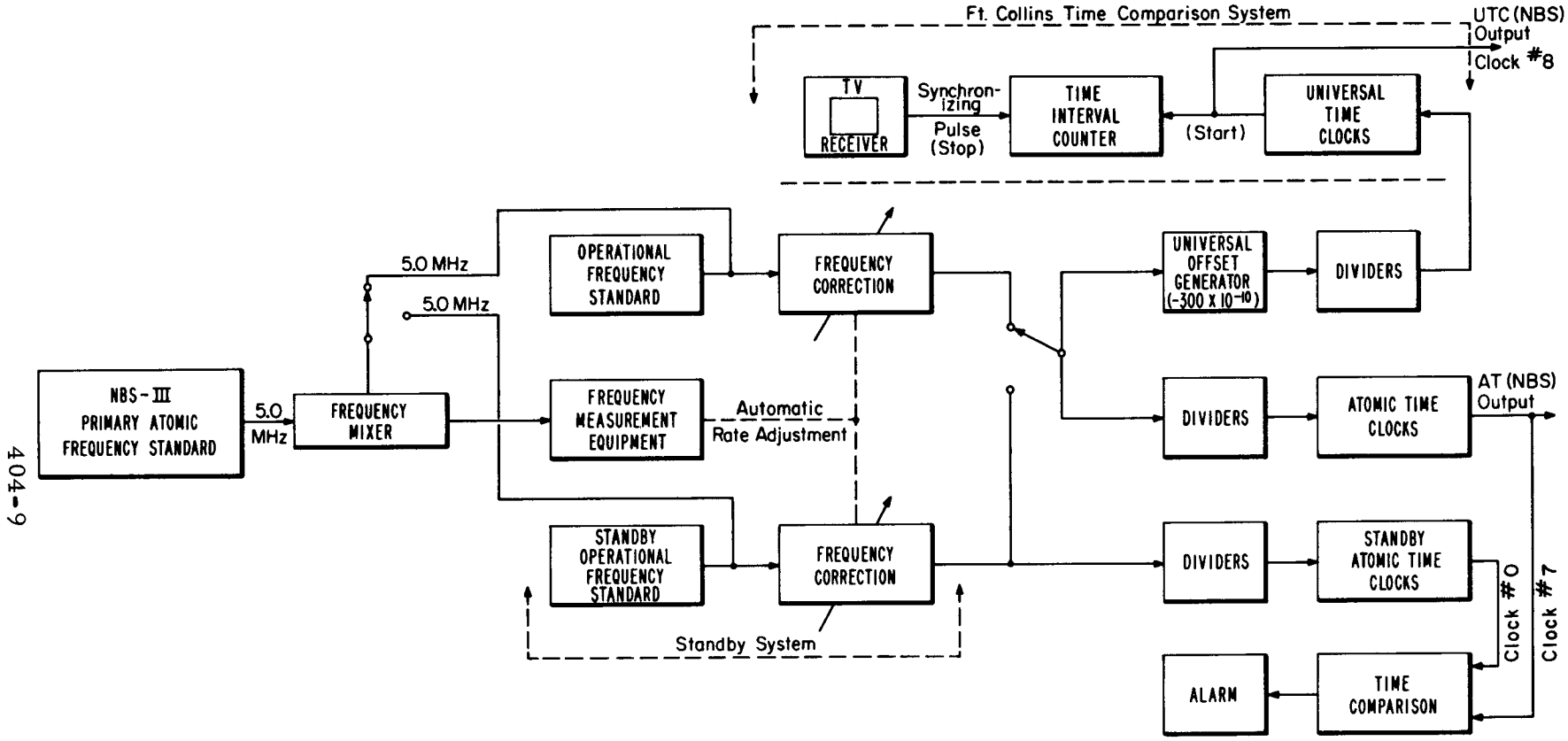

STANDARD FREQUENCY AND TIME INTERVAL GENERATING SYSTEM
TIME AND FREQUENCY DIVISION
SECTION 273.04

Figure 2

463-560 O - 72 - 27

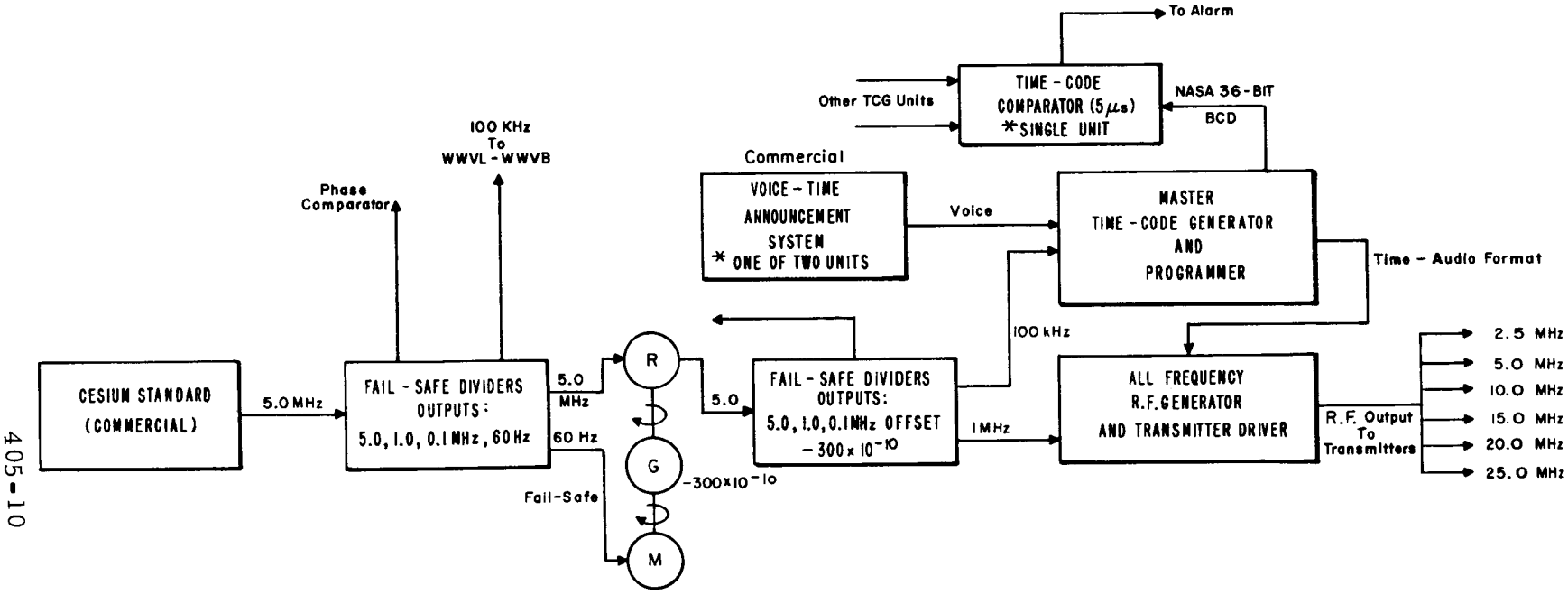

405-10

WWV TIME AND FREQUENCY GENERATION
ONE * OF THREE IDENTICAL SYSTEMS SHOWING INTERCOMPARISONS
FT. COLLINS, COLORADO

Figure 3

stable quartz crystal oscillator as the standard frequency generator. This crystal oscillator is referenced against NBS-III as noted later. Following this quartz crystal oscillator is a device known as a frequency drift corrector, which compensates for both frequency offset and rate change of the quartz crystal oscillator. The format for the time code and the 60 kHz driving frequency are produced by a special time-code generator, while two other generators are driven by a second quartz oscillator. These generators, along with the oscillators and other equipment, provide three semi-independent generating systems. Figure 4 shows the arrangement of this equipment.

2.4 Radio Station WWVL, Fort Collins, Colorado

The frequency generation for WWVL is like that of WWVB in that quartz crystal oscillators and drift correctors are used as the primary frequency generators. Since there is no complex time format in this case, the one or two operating frequencies are programmed to the transmitter by NBS-built equipment. The synthesizers are units from commercial VLF phase-tracking receivers. At present, two frequencies are transmitted alternately every ten seconds. The transmitter is shut off for about 0.1 second out of each ten-second period to allow the frequency changeover. The carrier shutoff is "on time" with respect to the UTC(NBS) time scale. See fig. 5 for a simplified diagram of this system.

A second complete generating and programming system for WWVL is nearing completion. The new system will allow the transmission format to encompass from one to three operating frequencies. The order of frequency transmission and the time length of each can be controlled. The local servo system for the new generation and control equipment is discussed in section 3. Figure 5a shows this new system.

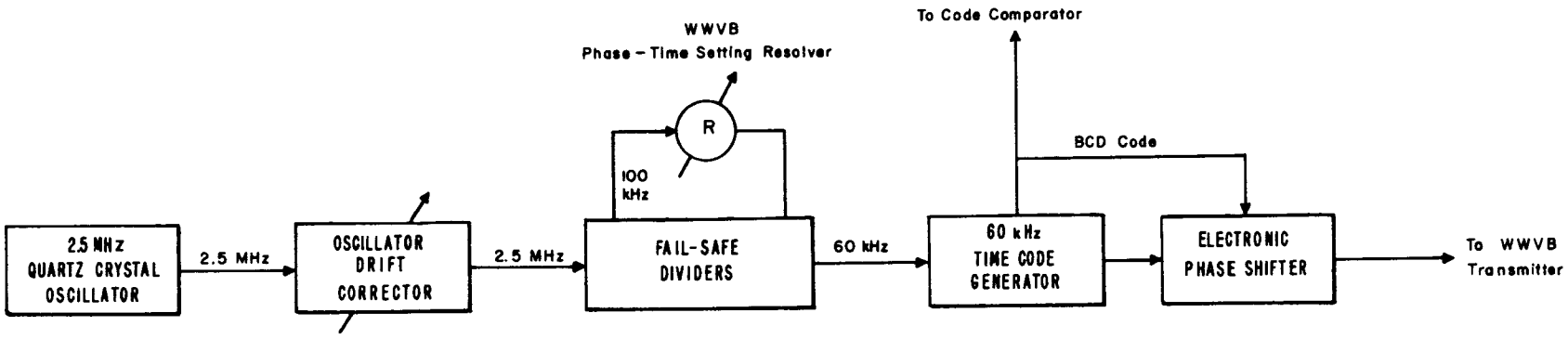

407-12

WWVB TIME AND FREQUENCY GENERATION AND CONTROL - ONE OF THREE SEMI - INDEPENDENT SYSTEMS
FT. COLLINS, COLORADO

Figure 4

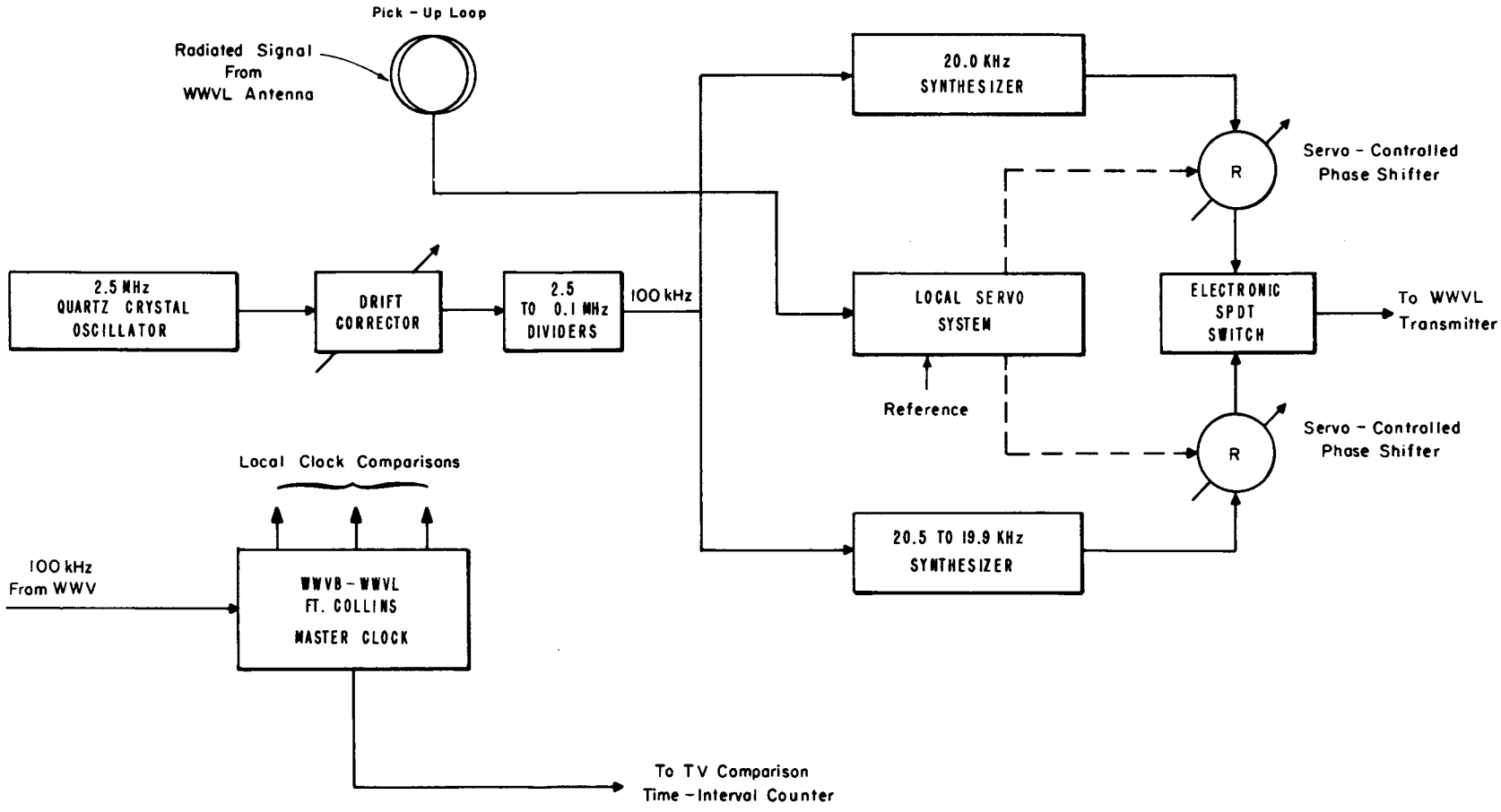

WWVL FREQUENCY CONTROL AND GENERATION SYSTEM 1967 - 1969

Figure 5

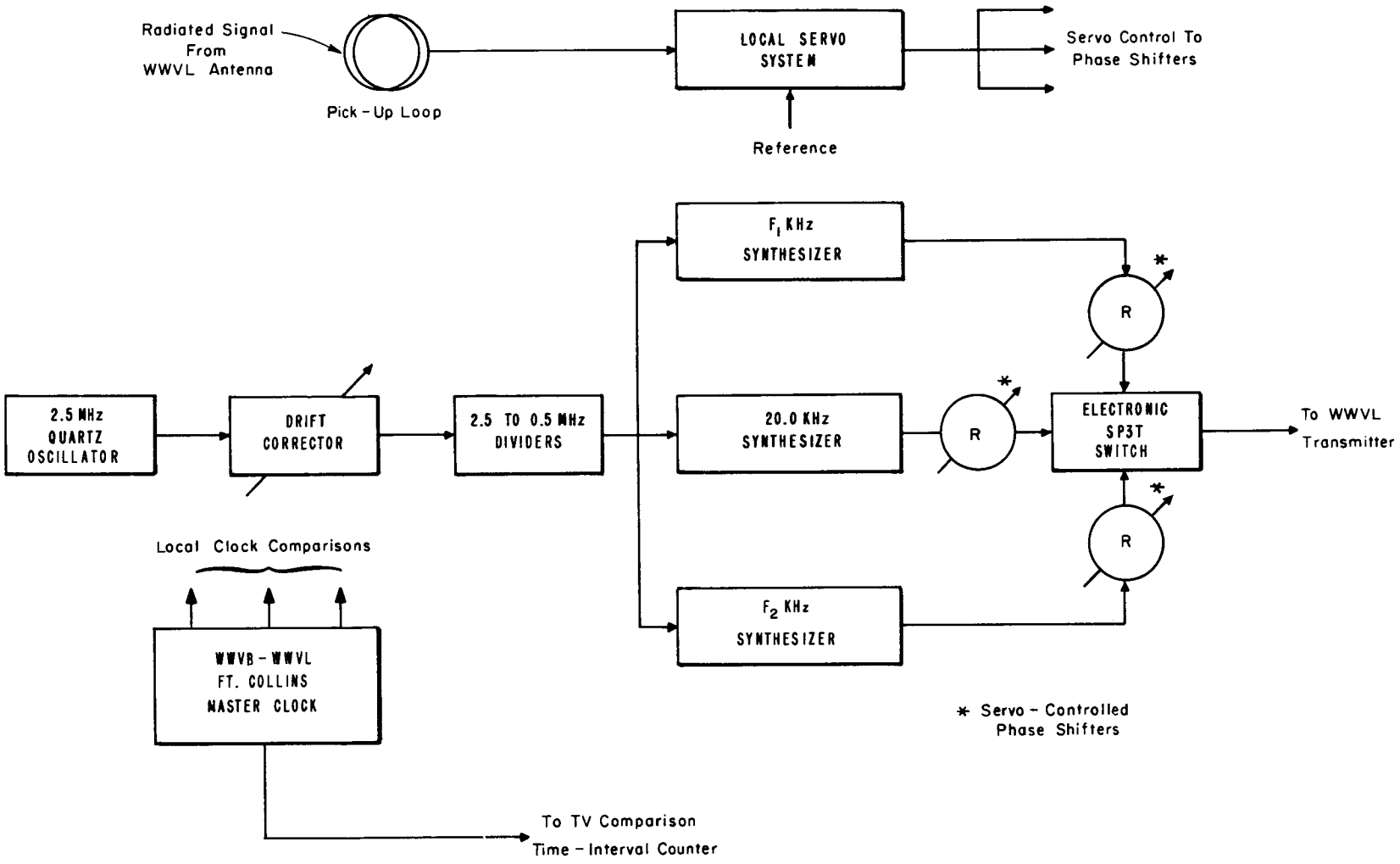

REVISED WWVL FREQUENCY AND TIME GENERATION AND CONTROL SYSTEM

Figure 5a

2.5 Radio Station WWVH, Maui, Hawaii

Station WWVH began operation in 1948 and is now the oldest existing facility operated by the NBS Time and Frequency Division. Because the generation and control systems and equipment have been little modified since 1948, they remain rather primitive. A good quality quartz crystal oscillator provides the driving frequency at 2.5 MHz. This oscillator is referenced indirectly against NBS-III via the NBS VLF broadcasts. The 440 Hz, 600 Hz, and 1200 Hz tones for the format are generated by NBS-constructed equipment. WWVH has one standby clock system.

WWVH is soon going to be completely rebuilt on a new site at Kauai, Hawaii, with operation at the new facility commencing about January 1, 1971. The generation and control equipment for the new WWVH will mirror the system now in operation at WWV. Figure 3 shows the WWV system.

3. TRANSMISSION OF TIME AND FREQUENCY

3.1 Transmission from WWV

The multiple outputs from the rf driver units in the shielded control room are supplied directly to the transmitters. The WWV transmitters are simply high-power linear amplifiers and therefore do not contain audio circuits or modulators. The delay from the time-code generator to the antenna is much less than the transmitted accuracy specified for WWV and is therefore neglected.

The specifications as published in the Time and Frequency Services Bulletin are: frequency within $\pm 5 \times 10^{-12}$ of the NBS Frequency Standard; time within ± 5 microseconds of the UTC(NBS) and UTC(USNO) time scales (these two time scales have been coordinated since October 1968 and are identical to within state-of-the-art comparison techniques).

3.2 Transmission from WWVB

WWVB's transmitter and radiating system have an overall "Q" factor of somewhat less than 100. This "Q" factor is sufficiently low to allow operation without any phase control on the antenna. Future plans call for a "local" servo system to continuously adjust the transmitted phase at the antenna to be in agreement with the local station reference. The local servo system compensates for the phase perturbations due to wind shifting the antenna. These excursions seldom exceed 0.5 microsecond peak-to-peak. To correct for discrete phase shifts that occur whenever the antenna is tuned, a manual phase compensation is made based on a continuously-operating phase monitor.

The relationship between a time pulse or carrier cycle and the epoch of a time scale becomes important when one operates a standard time and frequency station in the LF range. The time at which a particular carrier crossover occurs for WWVB is published on a daily basis in the monthly issues of the Time and Frequency Services Bulletin. This first carrier crossover at the antenna occurs about 6 microseconds after the marker pulse of SAT(NBS).

The following points should be noted: (1) The radiated phase is late relative to the epoch of SAT(NBS) because of the delays through the WWVB transmission system. The master time-code generator at WWVB is maintained in close agreement with SAT(NBS) and any time difference between SAT(NBS) and the WWVB time-code generator is known at all times. (2) When a phase or time error between the epoch of SAT(NBS) and the WWVB time-code generator, and hence the WWVB radiated phase, occurs, the error is corrected by changing the frequency of the WWVB quartz crystal oscillator. The maximum rate of correction is limited to 0.1 microsecond per four-hour period. In other words, during times of phase correction, the frequency of WWVB can be in error with respect to the NBS reference frequency by as much as 6×10^{-12}.

3.3 Transmission from WWVL (Experimental)

The transmitted phase of WWVL is controlled more precisely than that of any other NBS transmission. There are two reasons for this: (1) The realizable stability of the transmission through the medium in the 20 kHz region is quite high, and (2) the susceptibility of the transmission system to phase perturbations is also quite high. The "Q" of the antenna system is of the order of 1000. With a tuning reactance of greater than 500 ohms, a change in this reactance of 0.2% causes a phase shift of 45° or more than six microseconds. Every effort is made to hold the transmitted phase to within ± 0.1 microsecond of its nominal value. This calls for a highly sensitive "local" servo system.

This local servo begins with a pickup loop located in the building containing the antenna loading coil. The voltage from this coil is supplied through a buried coaxial cable to the shielded control room in the transmitter building. This signal, through an AGC amplifier, is compared with the output of the WWVL rf synthesizers. Any phase shifts detected at the loading coil building are quickly compensated for by the local servo-driven phase shifter. There is one of these phase shifters for each transmitted frequency. In addition, the input phase to the transmitter is adjusted so that the zero voltage crossover of the radiated field as measured at the antenna occurs at the epoch of the UTC(NBS) time scale. This is done for all transmitted frequencies.

Mentioned briefly in section 2.4 was the new WWVL generation and control system, which has been tested but is not yet in use. This new system is much improved over the existing control servo. For instance, the "dead-band" of the original system was about 0.2 microsecond. The new system "dead-band" is of the order of 20 nanoseconds. The new system has a single servo motor-amplifier driving the three

phase shifters. Since each phase shifter is continuously driven, any error is "precorrected" by the phase shifter that will be controlling the transmitter in the next transmitting 10-second period. This tends to reduce the phase-noise of the transmission. This noise can be as high as 2 microseconds peak-to-peak in the current system.

Again, as in the case of WWVB, any errors between the radiated phase and the epoch of UTC(NBS) are known at all times, and corrected by the same procedure and at the same maximum rate of $\approx 6 \times 10^{-12}$.

3.4 Transmission from WWVH

Unlike the high-frequency transmitters at WWV, the units at Maui are high-level modulated standard AM transmitters. The 2.5 MHz from the controlling crystal oscillator is fed to each transmitter. Amplification or multiplication of this frequency is carried out by each transmitter as necessary. The various time-ticks, tones, voice announcements, and Morse Code information groups are fed to the modulators of the transmitters. Even though the WWVH master clock is nominally maintained in close agreement with UTC(NBS), the transmitter's modulation circuits degrade this performance somewhat. Station specifications are: frequency within $\pm 5 \times 10^{-11}$ of the NBS Frequency Standard, and time nominally within ± 20 microseconds of UTC(NBS) and UTC(USNO).

4. TIME AND FREQUENCY INTERCOMPARISONS

4.1 Among the Fort Collins Standards

4.1.1 WWV self comparisons

As was mentioned earlier, WWV has three independent time and frequency generating systems. These units are intercompared at three different locations in the systems: First, the phases of the "atomic" 1 MHz outputs from the dividers following the cesium standards are

intercompared. The outputs of the phase detectors used are applied through meter relays to a multi-channel chart recorder with a 1-microsecond full scale. Second, following the motor-driven offset generator, the phases of the 1 MHz outputs from the UTC dividers are intercompared. The phase comparison record is arranged to be on the same multi-channel recorder. The meter relays are so adjusted that a 1-microsecond change in the phase difference between any two standards results in an alarm sounding. The third intercomparison is accomplished at the time-code generators. The 36-bit NASA time code from each generator is monitored by a code comparator. The alarm is sounded if the output from any unit diverges from any other by 5 microseconds, or if a clock jumps phase such that its code is misaligned with respect to that of any other unit. With these three comparison systems any standard, offset generator, divider chain, or time-code generator that fails can be immediately detected. See fig. 3 for a simplified block diagram showing the comparison systems.

4.1.2 WWV to WWVB and WWVL

The standard 100 kHz output from the WWV time and frequency generating system designated "Rack A" is sent by coaxial cable to the WWVB/VL control room. This standard frequency drives a digital clock designated as the "Fort Collins Master Clock." All measurements of the WWVL and WWVB local clocks, which are driven by the quartz crystal oscillators, are in terms of this Master Clock. This Master Clock pulse is also returned by coaxial cable to the WWV control room.

This system of clock intercomparisons effectively prevents undetected clock or time-code generator failures.

In addition to the clock comparisons, the quartz crystal oscillators that form part of the LF and VLF generating systems are continuously compared with the standard 100 kHz signal from WWV (see fig. 6).

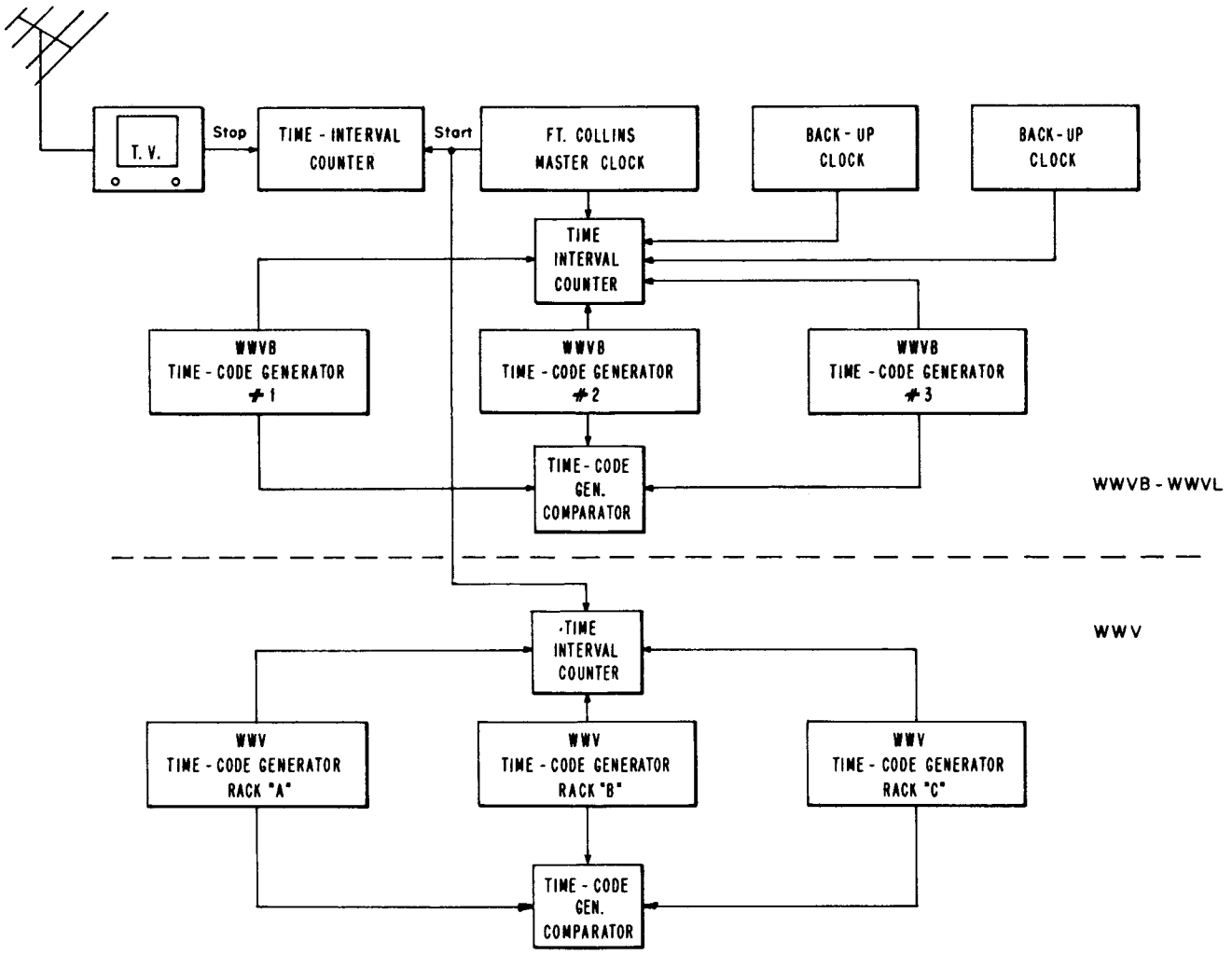

CLOCK INTERCOMPARISON WWV - WWVB - WWVL
FT. COLLINS, COLORADO

Figure 6

4.2 Between the Fort Collins Standards and the WWVH Standard

Station WWVH uses all available information to maintain close ties with the Fort Collins standards. This includes continuous monitoring of stations WWVB and WWVL and frequent comparisons, via portable clock, with a phase stabilized Naval communications station on the island of Oahu. Via portable clocks and other means the relationship between the master clock at this Naval radio station and the clocks at Fort Collins and Boulder is known at all times to within a few microseconds.

4.3 Between the Fort Collins Standards and the NBS Standards

4.3.1 Portable clocks

The most reliable high-precision method of comparing the Fort Collins Master Clock with the NBS/Boulder Clock #8 is to physically carry a cesium-standard-driven clock between the two locations. A highly accurate clock of this sort normally loses or gains less than 0.1 microsecond during the four-hour round trip. To perform this task on a daily basis is expensive and unnecessary. Nevertheless, a portable clock is occasionally carried to Fort Collins when circumstances dictate.

4.3.2 TV synchronizing pulse method

a. Theory

Because the portable clock method for clock synchronization is expensive and time consuming, and the Boulder-Fort Collins continuous phase loop had been eliminated because it added short-term phase errors due to sky-wave interference, a new method had to be found. In 1967, Tolman, et al[1] described a method for comparing remote clocks using television synchronizing pulses for time transfer. Since May 1968,

[1] Tolman, et al, "Microsecond clock comparison by means of TV synchronizing pulses," IEEE Trans. on Instr. and Meas., vol. IM-16, No. 3, September, 1967.

this method has been used to compare the Master UTC Clock at Fort Collins with the NBS Clock #8 at Boulder.

Figure 7 is a space-time diagram of how the method is developed. Assume fig. 7 is a map of the geographical area in question at one instant in time. Located on the map are five TV synchronizing pulses as they might be at this instant.

From the diagram, if the Boulder clock and the Fort Collins clock agree, the delay time over the distance $D_1 - D_2$ is

$$D = \frac{4\lambda}{c} + B - A \text{ microseconds,} \qquad (1)$$

where $\frac{\lambda}{c}$ = one synchronizing pulse period, or 63.55 microseconds. The values B and A are found by using the local clock tick as the start pulse of a time-interval measurement and a synchronizing pulse from a local TV set as the stop pulse. In the case of fig. 7, pulse #1 stops the Boulder time interval measurement at the value "A" and pulse #5 stops the Fort Collins time interval measurement at the value "B". If now the Fort Collins clock is early relative to the Boulder clock, the value B will increase because the interval will be longer. From the diagram, this longer interval B' will be

$$B' = B + \Delta t_e \qquad (2)$$

where Δt_e is the amount early.

Computing the delay time D using great circle distance calculations and substituting eq. (2) into eq. (1),

$$\Delta t_e = \frac{4\lambda}{c} - D + (B' - A) \text{ microseconds.} \qquad (3)$$

b. Results

The TV synchronizing pulse method of clock intercomparisons was put in service in May 1968. The measurements have been made on a daily basis since then. During the actual measurement, some ten to

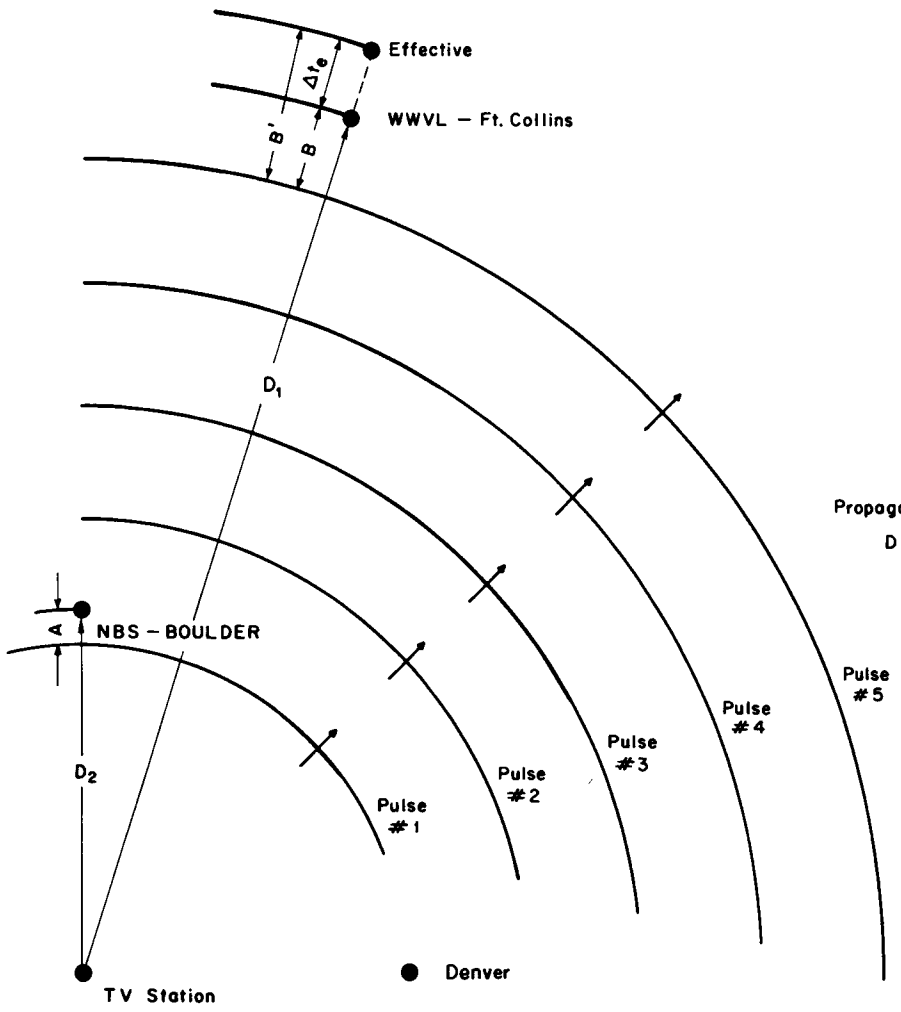

SPACE – TIME DIAGRAM
OF BOULDER TO FT. COLLINS
CLOCK SYNCHRONIZING.
DIAGRAM AT ONE INSTANT OF TIME

Figure 7

twenty readings are taken. The spread over this number of readings has seldom exceeded ± 0.5 microsecond. The average of this group is recorded. When the Fort Collins Master Clock has diverged from NBS Clock #8 by about one-half microsecond, the Fort Collins clocks are all reset to the correct time. These "correct" times will vary from clock to clock. For instance, the master clock at WWVL is maintained at a nominal and arbitrary 18 microseconds early with respect to Clock #8, to allow for easier clock intercomparisons at Fort Collins. The WWV clocks are maintained "on time."

The following table shows the results of the comparisons between the TV synchronizing pulse method and eight portable clock trips from Boulder to Fort Collins, starting in May 1968 and ending in December 1968.

Table 1

Date	Portable Clock Reading Fort Collins Master Clock - #8	TV Reading Fort Collins Master Clock - #8
May 14	17.63 μs	17.92 μs
May 20	17.99 μs	18.64 μs
July 5	17.34 μs	17.74 μs
July 8	17.10 μs	17.20 μs
Oct. 23	17.65 μs	17.57 μs
Nov. 1	17.89 μs	17.79 μs
Nov. 15	18.20 μs	18.24 μs
Dec.	17.33 μs	17.26 μs

It seems probable from the data that as the staff became more familiar with the measurement scheme, the accuracy with respect to the portable clock readings improved.

The method was proved to be satisfactory--the precision and accuracy are of a high order. The drawbacks to the current system are mainly in the measurement technique. The amplified synchronizing pulses themselves are not used; the actual measurement is made with the set's internal oscillator that is phase locked to the incoming pulses. It will be obvious to servo-systems people that this method is fraught with problems (the free-running frequency of the internal oscillator must be preset, for example).

A new system under development at the NBS utilizes the amplified pulses from a more stable color TV system. The new system has promise of improving the accuracy of the measurements by an order of magnitude.

APPENDIX

EXPLANATION OF NBS TIME SCALES

AT(NBS)

AT(NBS) is an Atomic Time Scale, previously called NBS-A, whose rate is determined by the primary frequency standard of the National Bureau of Standards (NBSFS). This standard (NBS-III cesium beam) realizes the second as defined in the International System of Units (SI). The epoch of the scale was in agreement with UTC(NBS) at 0000 UT 1 January 1958.

SAT(NBS)

Stepped Atomic Time is a coordinated time scale; i.e., the International Time Bureau (BIH) determines when steps in epoch of 0.2 second should occur to keep this scale in approximate agreement with UT2. The rate for this scale was the same as for AT(NBS) prior to 1 October 1968. The NBS and the U. S. Naval Observatory (USNO) agreed upon a coordinate rate starting 0000 UT 1 October 1968 for SAT(NBS), and this rate may be written as:

$$f_{coordinate} = (f_{NBSFS})\ (1 + 4 \times 10^{-13}) \text{ from } 10/1/68 \text{ to } 5/1/69$$

$$f_{coordinate} = (f_{NBSFS})\ (1 + 5 \times 10^{-13}) \text{ from } 5/1/69 \text{ to present}$$

In other words, SAT(NBS) presently runs at a rate higher in fractional frequency than AT(NBS) by 5 parts in 10^{13}. SAT(NBS) is the time scale broadcast by Radio Station WWVB. Note: The difference in rate between these scales is relevant only to international and national standards laboratories and observatories such as the BIH and NBS, and this in no way affects all other users of this transmitted signal.

463-560 O - 72 - 28

UTC(NBS)

UTC(NBS) is a coordinated time scale; i.e., the BIH determines when steps in epoch of 0.1 second and changes in rate should occur to keep this Universal Time Scale in approximate agreement with UT2. Near 1 October 1968, the time difference, UTC(USNO) - UTC(NBS), was zero. The NBS and the USNO agreed on a coordinate rate for these two time scales starting 0000 UT 1 October 1968. The coordinate rate was chosen as an average of the two rates, as determined by portable clocks, prior to 1 October 1968. The USNO and NBS intend to maintain synchronization of the UTC scales to within about 5 microseconds by using an appropriate coordinate rate. The present coordinate rate of UTC(NBS) is:

$$f_{UTC(NBS)} = (f_{coordinate}) (1 - 300 \times 10^{-10})$$

or

$$f_{UTC(NBS)} = (f_{NBSFS}) (1 - 299.995 \times 10^{-10}).$$

This last equation is, again, useful only to other standards laboratories.

World-wide Time Synchronization

LaThare N. Bodily, Dexter Hartke, and Ronald C. Hyatt [1]

Continued interest in precise time comparisons provided by the -hp- flying clocks led to a new and more ambitious experiment. This experiment, with higher precision even than before, was performed during the months of May and June. Portable cesium-controlled clocks again were used but with refinements that enabled a potential measurement resolution of 0.02 μs in time comparisons. As a result of the intercomparisons provided by the traveling time standards in the company-funded experiment, many facilities now know with greater precision (about 0.1 μs) how the time of day at their installations compares with those of other time-keeping centers.

The 1966 flying-clock experiment also provided additional data for long-term comparisons between time scales.

Hewlett-Packard Journal, Vol. 17, No. 12, 13–20 (August 1966).

[1] Hewlett-Packard Co., Palo Alto, Calif. 95050, U.S.A.

Progress in the Distribution of Standard Time and Frequency, 1963 through 1965

John M. Richardson [1]

Progress in accurate long distance distribution of standard time and frequency, as reported in the literature from 1963 through 1965, is summarized. Techniques are by VLF, LF, and HF radio propagation, by satellite relay, and by portable clocks. Effects on standard frequency transmissions of variations in VLF propagation with geophysical phenomena are quantitatively understood. VLF and LF transmissions have provided careful, long-term, statistical comparison of remotely located atomic frequency standards. Precision of at least 2 parts in 10^{11} for a 24-hour observation period is possible at 5000 km. The phase of some standard frequency transmitters is routinely steered by VLF at distances up to 5300 km. Global distribution of standard time by VLF to microsecond resolution has been shown feasible. The null beat between two neighboring VLF carriers has been observed to propagate stably enough to mark a particular VLF cycle at 1400 km, and the beat period can be long enough to enable ordinary time signals to mark a particular null beat. Intercontinental time synchronization by microwave pulses has been accomplished via Telstar and Relay II satellites. Accuracy is stated to be several microseconds. Portable cesium clocks have served as global transfer standards with degradation of timing accuracy of only about a microsecond per trip. Results by all the above methods are consistent with each other and with stated accuracies of atomic standards involved.

Progress in Radio Science 1963–1966
Part 1, Proc. XVth General Assembly of URSI, Munich, 40–62
(September 5–15, 1966).

[1] NBS, Boulder, Colo. 80302, U.S.A.

Microsecond Clock Comparison By Means Of TV Synchronizing Pulses

Jirí Tolman, Vladimír Ptáček, Antonín Souček and Rudolf Stecher, IEEE Trans. on Instru. and Meas., Vol. IM-16, No. 3, 247-254 (September 1967).

A new method for precise clocks comparison is described making use of the short rise time of the synchronizing pulse of a current TV picture signal. It is shown that by measuring simultaneously the time interval between one and the same selected TV frame synchropulse and the pulses derived from the respective clocks, these clocks may be compared with microsecond accuracy even if widely separated, provided that appropriate correction for the travel time of the synchropulse is applied.

An experiment concerning international clock comparison between Prague and Potsdam is described, and the numerical results presented. Synchronization of clocks, separated by about 300 km, to about 2 μs was accomplished, and it appears that 0.1 μs is feasible. Further possible applications of this method are discussed.

SIGNAL DESIGN FOR TIME DISSEMINATION: SOME ASPECTS

J. L. Jespersen

The purpose of this paper is to discuss, in a general way, some problems of time signal dissemination in a noisy environment. Most of the paper applies to any timing system, but particular emphasis is given to a CW two-frequency system. This is done for two reasons: first, as will be shown, a two-frequency CW system evolves naturally from fundamental considerations to meet certain user requirements; and second, a two-frequency VLF system is being investigated experimentally at the present time.

Key Words: VHF, HF, VLF, time and frequency dissemination, synchronization, satellite, noise.

NBS Technical Note 357, Issued November 2, 1967

NBS Frequency and Time Broadcast Services

Radio Stations WWV, WWVH, WWVB, WWVL

P. P. Viezbicke, Editor

Special Publication 236, 1970 Edition (Issued 1970). *

Detailed descriptions are given of the technical services provided by the National Bureau of Standards radio stations WWV, WWVH, WWVB, and WWVL. These services are: 1. Standard radio frequencies; 2. Standard audio frequencies; 3. Standard musical pitch; 4. Standard time intervals; 5. Time signals; 6. UT2 corrections; 7. Radio propagation forecasts; and 8. Geophysical alerts. In order to provide users with the best possible services, occasional changes in the broadcasting schedules are required. This publication shows the schedules in effect on February 1, 1970. Annual revisions will be made. Current data relating to standard frequencies and time signals are available monthly in the Time and Frequency Services Bulletin. Advance notices of changes occurring between revisions will be sent to users of NBS broadcast services who request such notice on the basis of need.[2]

* The 1972 Edition is now available.

Key Words: Broadcast of standard frequencies; high frequency; low frequency; standard frequencies; time signals; very low frequency.

[1] NBS, Boulder, Colo. 80302, U.S.A.

[2] Inquiries concerning the Time and Frequency Services Bulletin or the NBS broadcast service policies may be addressed to Frequency-Time Broadcast Services Section, Time and Frequency Division, NBS, Boulder, Colorado 80302.

VLF Propagation Over Distances Between 200 and 1500 km

J. L. Jespersen, G. Kamas, and A. H. Morgan

The measurements discussed in this paper were undertaken as part of an evaluation of the NBS-WWVL (20 kHz) time and frequency station near Fort Collins, Colorado. The main items to be discussed are the: (1) variation in the VLF ground phase pattern as a function of distance from the transmitter; (2) magnitude of the diurnal phase variation as a function of distance from the transmitter; and (3) correlation of the phase fluctuations at 19.9 and 20.0 kHz at a distance of about 1300 km from the transmitter.

Conference on M.F., L.F., and V.L.F. Radio Propagation, (London, England, November 8-10, 1968, W. T. Blackband, Chairman), Inst. Elec. Engrs., (London) Conference Publication No. 36 (Savoy Place, London, England), 74-80, (1967).

STANDARDS AND CALIBRATIONS — WWVL CHANGES BROADCAST FORMAT

For the past several years the broadcasts of NBS Radio Station WWVL (Fort Collins, Colo.) have been used experimentally in a program to study VLF time synchronization capabilities. A time-shared multifrequency concept is being employed to conserve bandwidth and to permit various degrees of receiving equipment sophistication and cost within the same system, as appropriate to timing requirements of the user. WWVL broadcasts on the UTC system so that all frequencies listed here are nominal only and are offset (for 1969 by -300×10^{-10}) from the atomic definition. Future broadcasts will be restricted to use of the following frequencies, which are presently assigned to the National Bureau of Standards: 20.9 kHz, 20.5 kHz, and the band 19.9 to 20.1 kHz.

The previous broadcast schedule of WWVL consisted of alternate ten second transmissions of 20.0 kHz and 20.5 kHz. At 0000 UT on 4 November 1969, the format was changed to the following: Alternate 10 second transmissions of 20.0 kHz, 19.9 kHz, and 20.9 kHz, with the 20.0 kHz transmission alternating between the ten second periods of 19.9 and 20.9 kHz transmissions, that is:

For 10 seconds, 20.0 kHz will be broadcast;
Next 10 seconds, 19.9 kHz will be broadcast;
Next 10 seconds, 20.0 kHz will be broadcast;
Next 10 seconds, 20.9 kHz will be broadcast;
Etc.—

This experimental schedule will continue until further notice. *

*For a description see "NBS FREQUENCY AND TIME BROADCAST SERVICES", Nat. Bur. Stand. (U.S.), Spec. Publ. 236, revised annually, available from the Superintendent of Documents, U.S. Government Printing Office, Washington, D.C. 20402, for 25 cents.

VLF PRECISION TIMEKEEPING POTENTIAL by B. Blair, J. Jespersen and G. Kamas, National Bureau of Standards, Boulder, Colorado, U. S. A.

Timing needs exist today for synchronization of remote clocks to tens of microseconds or better. This paper discusses the potential of dual-frequency VLF transmissions to fulfill those needs. The approach considers corrections for the phase distortions and inter-relationships of the near field measurements at the transmitter, phase relations of the near field to the far field, propagation phase stability, and the resulting time synchronization at a remote VLF reception point. from WWVL at Fort Collins, Colorado, U. S. A. as received at several distant points and compared with local cesium frequency standards. The transmission format of 10 second alternate broadcasts of 19. 9 and 20. 0 kHz signals (100 Hz frequency separation) resulted in less than desirable cycle identification. The 100 Hz separation showed time synchronization possibilities of several hundred microseconds. The format of 20. 0 and 20. 5 kHz time shared signals (500 Hz frequency separation) gave positive cycle identification at several receiving sites. Portable clock comparisons collaborated such time synchronizations to 10 microseconds or less. Theoretical group delay predictions, which include corrections for dispersion effects, have been derived and are presented for the given receiving site locations. For a given distance and direction from a transmitter these theoretical predictions may provide coarse time bases within which framework VLF cycle identification will yield the fine microsecond time synchronization. Because the differential phase variability of the received VLF signals around 20. 0 kHz is essentially identical and the magnification factor, used in determining the group delay, decreases with wider frequency separation of the carriers, the results of this study suggest a frequency separation of perhaps 1000 Hz would offer greater potential for consistent cycle identification.

Reprinted from: International Union of Radio Science (U.R.S.I.) XVIth General Assembly Abstracts (Ottawa, Canada - Aug. 18-28, 1969, Commission I), p.7 (1969). Paper to be published in: Progress in Radio Science 1966-1969, Part I, Proc. XVIth General Assembly of URSI, Ottawa, C. E. White, Editor, (In press).

4. Statistics of Frequency and Time Measurements

Papers

Abstracts

The Power Spectrum and Its Importance in Precise Frequency Measurements*

J. A. BARNES† AND R. C. MOCKLER†

I. Introduction

THE behavior of stable signal sources such as crystal oscillators, frequency multipler chains and masers can be usefully described in terms of their power spectra.

The problem of precise frequency measurement can be understood only by a fairly detailed knowledge of the frequency source and the effect of the measuring system. It is usually sufficient for this "detailed knowledge" to be given in terms of the power spectrum.

In general there are two methods of precise frequency measurement: 1) determining the total elapsed phase in an interval of time with an apparatus like a synchronous clock or a frequency counter, and 2) direct frequency measurement by a resonance method usually involving a molecular or atomic transition.

It can be shown that, in general, a frequency counter will, on the average, measure the frequency of the center of gravity of a power spectrum resulting from frequency modulation of the signal. An atomic or molecular resonance, however, will not, in general, measure the center of gravity of the power spectrum. Thus for a meaningful comparison between an atomic resonance and the output of a frequency multiplier chain, it is essential to know the spectral distribution of the signal from the chain and the spectral distribution of the atomic resonance (including atomic transitions nearby the particular transition of interest).

In practice, of course, one attempts to obtain a monochromatic source of radiation for the measurements. The results of power spectral analysis with the ammonia maser spectrum anayzer[1] are very helpful in this regard. Redesign and modifications can be made until the observed power spectrum has the proper character and purity. The spectrum analyzer system as used at the National Bureau of Standards is shown in Fig. 1.

It is the purpose of this report to discuss certain methods of obtaining the power spectrum and sample results of such experiments. The mean instantaneous frequency and the variance of the instantaneous frequency are related to the power spectrum. These relations are particularly useful in the description of the short-time frequency stability of signal generators particularly in view of the simplicity with which the power spectra can be obtained.

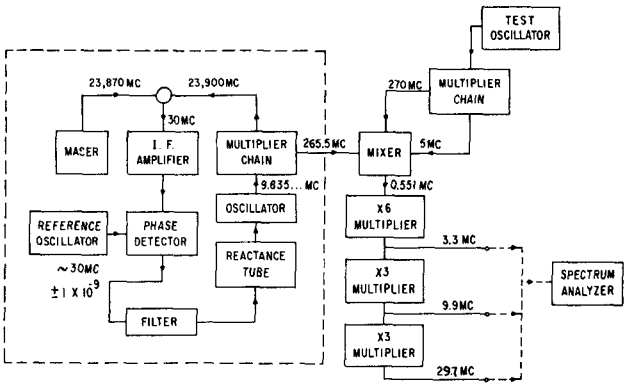

Fig. 1—Ammonia maser—spectrum analyzer system.

II. The Power Spectrum[2]

Suppose that the output voltage of a signal generator is some function of the time, $V(t)$. We can write

$$V(t) = \frac{1}{2\pi}\int_{-\infty}^{\infty} a(\omega)e^{i\omega t}d\omega, \tag{1}$$

provided that $a(\omega)$ vanishes at plus and minus infinity. From the Fourier integral theorem

$$a(\omega) = \int_{-\infty}^{\infty} V(t)e^{-i\omega t}dt. \tag{2}$$

In (2) it is supposed that $V(t)=0$ outside some finite time interval

$$t = -\frac{T}{2} \quad \text{to} \quad t = \frac{T}{2}$$

for the purpose of avoiding convergence difficulties. Then

$$a(\omega) = \int_{-T/2}^{T/2} V(t)e^{-i\omega t}dt. \tag{3}$$

Physically $a(\omega)d\omega$ may be considered the amplitude of the frequency component of $V(t)$ lying in the range ω to $\omega+d\omega$.

* Received by the PGI, July 9, 1960. Presented at the 1960 Conference on Standards and Electronic Measurements as paper 2-5.

† National Bureau of Standards, Boulder, Colo.

[1] J. A. Barnes and L. E. Heim, "A High Resolution Ammonia Maser Spectrum Analyser," to be published.

[2] W. R. Bennett, "Methods of solving noise problems," PROC. IRE, vol. 44, pp. 609–638; May, 1956.

The total energy dissipated in a unit resistor in the time interval

$$-\frac{T}{2} \leqq t \leqq \frac{T}{2}$$

is given by

$$\int_{-T/2}^{T/2} |V(t)|^2 dt = \frac{1}{2\pi}\int_{-T/2}^{T/2} V(t)\int_{-\infty}^{\infty} a^*(\omega)e^{-i\omega t}d\omega dt$$

$$= \frac{1}{2\pi}\int_{-\infty}^{\infty} a^*(\omega)d\omega \int_{-T/2}^{T/2} V(t)e^{-i\omega t}dt$$

$$= \int_{-\infty}^{\infty} \frac{a^*(\omega)a(\omega)}{2\pi}\, d\omega$$

$$\int_{-T/2}^{T/2} |V(t)|^2 dt = \int_{-\infty}^{\infty} \frac{|a(\omega)|^2}{2\pi}\, d\omega. \tag{4}$$

The average power dissipated in this time interval T is given by

$$\bar{P}_T = \frac{1}{T}\int_{-T/2}^{T/2} |V(t)|^2 dt = \int_{-\infty}^{\infty} \frac{|a(\omega)|^2}{2\pi T}\, d\omega, \tag{5}$$

$$\bar{P}_T = \int_{-\infty}^{\infty} P_T(\omega)d\omega \tag{6}$$

where

$$P_T(\omega) = \frac{|a(\omega)|^2}{2\pi T}.$$

$P_T(\omega)$ is the average power dissipated per unit frequency interval at the angular frequency ω and for the particular time interval T. The power spectrum or the power spectral density is sometimes defined as

$$P(\omega) = \operatorname*{Lim}_{T\to\infty} \frac{|a(\omega)|^2}{2\pi T}. \tag{7}$$

This is a proper definition provided that the limit exists. These convergence difficulties can often be avoided by taking the ensemble average. Thus for an ensemble of time functions $V_i(t)$, each member of the ensemble having a time duration T, there corresponds an ensemble $[P_T(\omega)]_i$. The power spectral density can then be defined as

$$P(\omega) = \operatorname*{Lim}_{T\to\infty} \langle [P_T(\omega)]_i \rangle = \operatorname*{Lim}_{T\to\infty} \left\langle \frac{|a_i(\omega)|^2}{2\pi T} \right\rangle \tag{8}$$

where the brackets denote the ensemble average.

III. Some Methods of Power Spectral Analysis

The concern of this report is the experimental determination of the power spectral density of rather narrow banded signal generators. Various methods are possible. The technique that we have found most convenient is described in some detail by Barnes and Heim.[1]

A heterodyne method is used to sweep the power spectrum over a fixed narrow-band filter. In most cases the bandwidth of the filter, $\Delta\omega$, is much narrower than the total width of the power spectrum. The square root of the power spectrum is plotted directly on an x-y plotter in a time short compared to systematic variations but long enough to be consistent with the analyzer's bandwidth.

The power in the frequency bandwidth of the filter—

$$\left(\omega - \frac{\Delta\omega}{2}\right) \quad \text{to} \quad \left(\omega + \frac{\Delta\omega}{2}\right)$$

—at frequency ω is given approximately by

$$P_T(\omega, \Delta\omega) \approx \int_{\omega-(\Delta\omega/2)}^{\omega+(\Delta\omega/2)} P_T(\omega)d\omega \tag{9}$$

where T is the observation time. If T is made indefinitely long, $P_T(\omega,\Delta\omega)$ will tend toward a limit

$$P(\omega, \Delta\omega) = \operatorname*{Lim}_{T\to\infty} P_T(\omega, \Delta\omega). \tag{10}$$

The limit of the ratio $P(\omega,\Delta\omega)/\Delta\omega$ at $\Delta\omega\to 0$ provides a definition of the true power spectral density; *i.e.*,

$$P(\omega) = \operatorname*{Lim}_{\Delta\omega\to 0} \frac{P(\omega, \Delta\omega)}{\Delta\omega}, \tag{11}$$

or

$$P(\omega) = \operatorname*{Lim}_{\substack{\Delta\omega\to 0 \\ T\to\infty}} \frac{P_T(\omega, \Delta\omega)}{\Delta\omega}. \tag{12}$$

This defines the power spectrum in terms more directly related to the experiment than does (8).[3]

The averaging time interval or record length T used in the experiment is not infinitely long, but it is sufficiently long such that any increase in T does not change the character of the plotted spectrum perceptibly (*i.e.*, the reciprocal of the record length, $1/T$, is much less than the bandwidth of the filter). The record length in this type of experiment is the time taken to sweep over a frequency interval equal to the width of the filter bandpass.

In the practical situation, the signal analyzed will have been modified by the transmission characteristics of the detector, filter, amplifier and smoothing circuits. The effects due to the instrumentation must be taken into account and some modification must be made on the previous discussion.

Let us assume that the filter is tuned to some frequency ω_0 and that the transfer function of the filter is given by $G(\omega_0,\omega)$. Also, if the input voltage to the filter, $V(t)$, has its Fourier transform, $a(\omega)$, given by

$$a(\omega) = \int_{-\infty}^{\infty} V(t)e^{-i\omega t}dt, \tag{13}$$

[3] Of course, many traces of the spectrum may be taken for the purpose of obtaining an ensemble average, and this would perhaps provide a more direct relation to the preferred definition based on the ensemble average, (8).

then the output voltage of the filter is given by

$$V_0(\omega_0, t) = \frac{1}{2\pi}\int_{-\infty}^{\infty} G(\omega_0, \omega)a(\omega)e^{i\omega t}d\omega. \qquad (14)$$

The average power delivered to a load by the filter is then proportional to

$$P_0(\omega_0) = \operatorname*{Lim}_{T\to\infty} \frac{1}{T}\int_{-T/2}^{T/2} V_0^2(\omega_0, t)dt. \qquad (15)$$

Comparison of (14) and (15) with (1), (2), and (7) gives

$$P_0(\omega_0) = \int_{-\infty}^{\infty} |\, G(\omega_0, \omega)\,|^2 P(\omega)d\omega, \qquad (16)$$

where $P(\omega)$ is the actual power spectrum of $V(t)$.

$P_0(\omega_0)$ is our estimate of the power density at the angular frequency ω_0. It is an estimate of the local power density, $P(\omega)$, only to the degree to which $|G(\omega_0,\omega)|^2$ approximates a Dirac delta function.

Sample spectra are displayed in Figs. 2, 3, and 4. The discrete line spectrum of Fig. 4 results from the introduction of frequency modulation by two (or more) signals, 60 cps and 120 cps (the oscillator used 60-cps ac filaments). In this particular spectrum the bandwidth of the filter is larger than the total width of any one of the lines of the spectrum.[4] The spectrum was produced by a crystal oscillator in which the crystal was emersed in liquid helium driving a frequency multiplier chain. The power spectrum of Fig. 4 may be written approximately as

$$P(\omega) \approx \sum_{i=1}^{N} q_i\delta(\omega - \omega_i), \qquad (17)$$

in view of the low resolution relative to the width of a single peak. In (17), q_i is a weighting factor for a par-

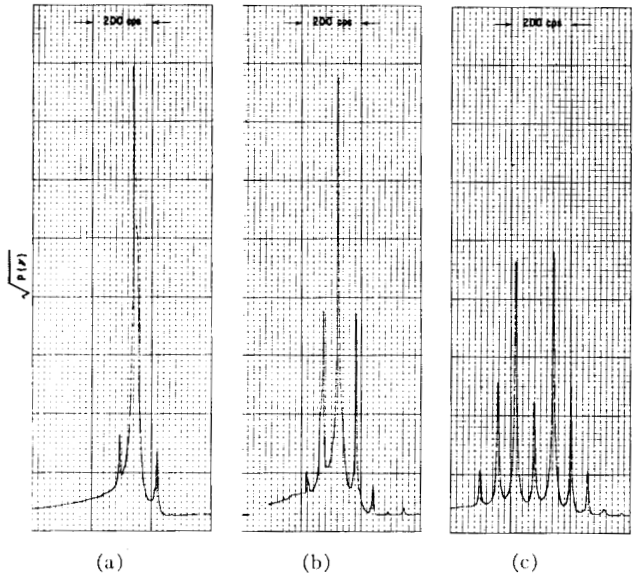

(a) (b) (c)

Fig. 2—(a) shows the square root of the power spectrum for a 3.3 Mc signal; (b) and (c) show the same signal after being multiplied in frequency by factors of 3 and 9, respectively.

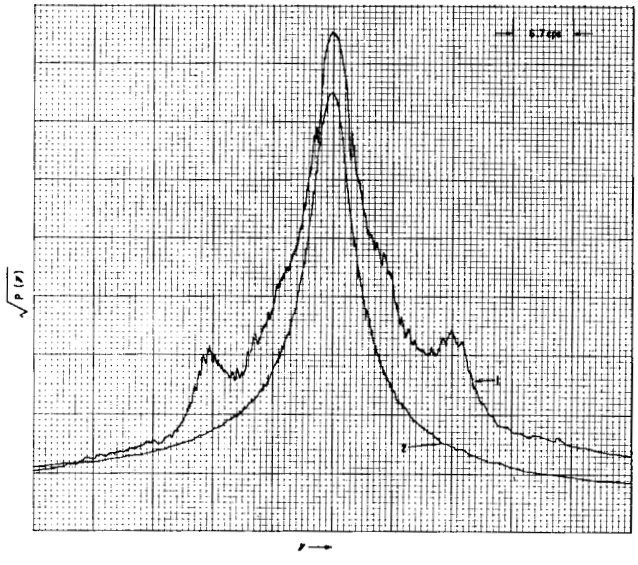

Fig. 3—Trace 1 is a high resolution spectrum of the central peak of a 10-Mc quartz crystal oscillator whose crystal was thermostated in a liquid helium cryostat.[5] The oscillator was equipped with dc filaments but still exhibited 60-cps sidebands about 30 db below the central peak (not shown in this figure). This oscillator operates at about 13.4 cps above 10 Mc and apparently some pickup of the standard is responsible for the sidebands shown in this trace. Trace 2 is the response curve of the spectrum analyzer.

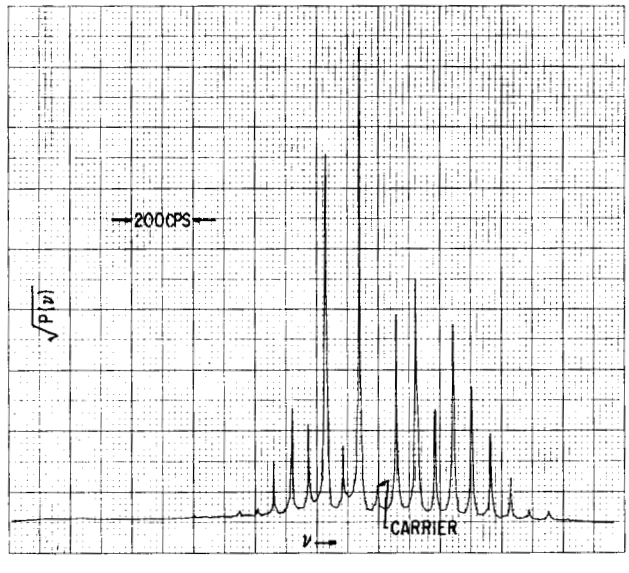

Fig. 4—This spectrum was obtained from the same oscillator as Fig. 3. At the time this trace was made, however, the oscillator was equipped with 60-cps, ac filaments. (Note the different frequency scale.)

[4] In fact the width of these sharp peaks is less than 1 cps. It is not yet certain whether this crystal oscillator is the more stable or the maser is the more stable generator. At the present time it is fashionable to consider the maser the more stable.

[5] This oscillator was designed and constructed by A. H. Morgan and his group at the Natl. Bur. Standards. The quartz crystal was made at the Bell Telephone Labs.

ticular peak at angular frequency ω_i. $\delta(\omega-\omega_i)$ is the Dirac delta function. In order to see the structure of the individual peaks additional frequency multiplication would be required or a substantial decrease in the filter bandwidth.

The power spectrum can also be estimated by a numerical analysis from a recorded plot of $V(t)$. An example of such a plot is shown in Fig. 5. The various methods of analysis of such recordings are to be found in the literature.[6]

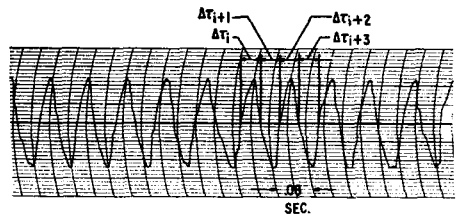

Fig. 5—Recording of direct beat note between free running oscillator and maser. A numerical analysis of these recordings could also be run to determine the power spectrum.

IV. Instantaneous Frequency and Its Relation to the Fourier Frequency Components

In general, there are two methods of precise frequency measurement: 1) determining the total elapsed phase in an interval of time with an apparatus like a synchronous clock or a frequency counter, and 2) direct frequency measurement by a resonance method usually involving a molecular or atomic transition.

The elapsed phase method of frequency measurement has two modifications: 1) a frequency counter which counts the number of cycles in a unit of time, and 2) period measurement which measures the time interval between two positive going crossovers of the signal. Either system gives the "average" frequency in a time interval δT such that

$$\bar{\Omega} = \frac{\delta\phi}{\delta T} = \frac{1}{\delta T}\int_T^{T+\delta T} \dot{\phi} dt \tag{18}$$

where $\delta\phi$ is the elapsed phase in the time interval δT. In the case of the period measuring scheme, $\delta\phi = 2\pi$ and the δT corresponding to this phase change is what is measured.

It is important to realize at this point that these measurements are not simply related to the Fourier components of the signal being measured, at least *a priori*. This is evident since, given a pure sine wave which lasts from T to $T+\delta T$, the Fourier components are spread over a frequency range $\delta\omega \approx 1/\delta T$, and thus a resonance method of frequency measurement would have an uncertainty in the measured frequency of the order of $\delta\omega$. For a period measuring scheme, however, the average instantaneous frequency of the sine wave is possibly measured to an accuracy far exceeding $\delta\omega = 1/\delta T$.

A simple example should serve to illustrate this point: Consider a very stable oscillator which generates a signal of approximately 100 cps. If this signal is used to gate a counter which is arranged to count a very stable and accurate 1-Mc signal, the counter will count for about 1/100 second and the counter will display the period accurate to about ± 1 μsec; that is, to an accuracy of about $\pm 10^{-2}$ cps! Thus with this scheme we have measured the average instantaneous frequency (*not* a Fourier frequency component) in a period of 10^{-2} seconds with a possible error of $\pm 10^{-2}$ cps instead of the ± 50-cps error of measuring the Fourier components. (Similar examples can be worked out for a frequency multiplier-frequency-counter system instead of the period measuring system.)

Returning to (18), let us suppose that the time of measurement, δT, is made small enough that $\phi(t)$ makes no appreciable change in this interval of time. With these conditions satisfied, we see that the measurement gives the instantaneous frequency,

$$\Omega(t) \equiv \dot{\phi}(t) \approx \frac{\delta\phi}{\delta T}.$$

It is possible to obtain some relations between the instantaneous frequency of a signal and its Fourier components for the case of a signal without amplitude modulation. Such a signal is of the form

$$E(t) = \frac{E_0}{2}\left(e^{i\phi(t)} + e^{-i\phi(t)}\right) \tag{19}$$

where E_0 is a constant and $\phi(t)$ is some real function of the time. For the following discussion we will consider only the function

$$f(t) = e^{i\phi(t)}. \tag{20}$$

The second term on the right of (19) only serves to symmetrize the power spectrum [since $E(t)$ is real but $f(t)$ is not]. Thus anything which can be said of the frequency of $f(t)$ can easily be extended to $E(t)$.

The importance of considering only $f(t)$ is that it satisfies the equations

$$\left.\begin{aligned} f^*f &= 1 \\ -if^*\frac{df}{dt} &= \dot{\phi} \end{aligned}\right\}. \tag{21}$$

Thus an instantaneous frequency for $f(t)$ can be defined as

$$\Omega(t) \equiv \dot{\phi}(t) = -if^*\frac{df}{dt}. \tag{22}$$

In order to obtain some connections with the power spectrum of $f(t)$, consider the function $f_T(t)$ defined by

[6] R. B. Blackman and J. W. Tukey, "The Measurement of Power Spectra," Dover Publications, Inc., New York, N. Y.; 1958.

the relations

$$f_T(t) = \begin{cases} f(t) & \text{for } -\frac{T}{2} \leqq t \leqq \frac{T}{2} \\ 0 & \text{otherwise} \end{cases}. \tag{23}$$

Thus $f_T(t)$ can be represented as a Fourier series in the interval

$$-\frac{T}{2} \leqq t \leqq \frac{T}{2}$$

$$f_T(t) = \sum_{n=-\infty}^{\infty} e^{i(2\pi nt/T)} C_n \tag{24}$$

where

$$C_n = \frac{1}{T}\int_{-T/2}^{T/2} e^{-i(2\pi nt/T)} f(t)dt. \tag{25}$$

This is a valid representation for $f_T(t)$ only in the interval

$$-\frac{T}{2} \leqq t \leqq \frac{T}{2},$$

since the Fourier series in (16) is that of a periodic wave of period T beyond this interval. Thus by this rather conventional means[6] we will compute the spectral distribution of $f_T(t)$ and then pass to the limit $T \to \infty$ where

$$f(t) = \operatorname*{Lim}_{T\to\infty} f_T(t).$$

First, define

$$TC_n = a_T\left(\frac{2\pi n}{T}\right)$$

where the paranthesis mean a_T is a function of $(2\pi n/T)$; so (24) and (25) become

$$f_T(t) = \sum_{n=-\infty}^{\infty} a_T\left(\frac{2\pi nt}{T}\right) e^{i(2\pi nt/T)}\left(\frac{1}{T}\right), \tag{24a}$$

$$a_T\left(\frac{2\pi n}{T}\right) = \int_{-T/2}^{T/2} f(t) e^{-i(2\pi nt/T)} dt. \tag{25a}$$

Substitution of (24a) and its complex conjugate into (22) gives

$$\Omega_T(t) = \sum_{m,n=-\infty}^{\infty} \left(\frac{2\pi n}{T}\right) \cdot e^{i(2\pi(n-m)/T)t} a_T\left(\frac{2\pi n}{T}\right)\left(\frac{1}{T}\right)^2 a_T^*\left(\frac{2\pi m}{T}\right). \tag{26}$$

Taking the time average of (26) over the interval

$$-\frac{T}{2} \leqq t \leqq \frac{T}{2},$$

yields

$$\bar{\Omega}_T = \frac{1}{2\pi}\sum_{n=-\infty}^{\infty}\left(\frac{2\pi n}{T}\right)\frac{\left|a_T\left(\frac{2\pi n}{T}\right)\right|^2}{T}\left(\frac{2\pi}{T}\right) \tag{27}$$

since

$$\frac{1}{T}\int_{-T/2}^{T/2} e^{i[2\pi(n-m)t/T]}dt = \begin{cases} 1 & \text{if } n = m \\ 0 & \text{if } n \neq m. \end{cases}$$

If we now pass to the limit as T becomes very large, $2\pi n/T$ approaches a continuous variable, say ω, since each unit change in n changes $2\pi n/T$ by only $2\pi/T$, a very small quantity. Also the first difference of $2\pi n/T$ is $2\pi/T$ which approaches $d\omega$ as T becomes very large. Thus (27) becomes in the limit

$$\bar{\Omega} = \int_{-\infty}^{\infty} P(\omega)\omega d\omega \tag{28}$$

where

$$P(\omega) = \operatorname*{Lim}_{T\to\infty} \frac{|a_T(\omega)|^2}{2\pi T} \tag{7}$$

is the power spectrum of $f(t)$.

The right side of (28) is just the average frequency, $\langle\omega\rangle$, of the Fourier components since from (4)

$$\int_{-\infty}^{\infty} P(\omega)d\omega = 1 \tag{29}$$

for $f(t)$ satisfying (21). Equivalently, the right side of (28) is the center of gravity of $P(\omega)$. Thus (28) shows that the time average of the instantaneous frequency is just the center of gravity of the power spectrum for a frequency modulated signal. Returning to (18) we see that the elapsed phase method of frequency measurement gives the time average of the instantaneous frequency over the interval of measurement and thus if this interval is sufficiently long it will give the frequency of the center of gravity of the power spectrum!

It is also of interest to compute the variance (or mean square deviation from the mean) of the instantaneous frequency; that is, the quantity,

$$\overline{(\Omega(t) - \bar{\Omega})^2} = \overline{\bar{\Omega}^2} - \overline{2\Omega\bar{\Omega}(t)} + \bar{\Omega}^2 = \overline{\Omega^2} - \bar{\Omega}^2. \tag{30}$$

Since $\Omega(t)$ is a real function,

$$\Omega(t) = \Omega^*(t) = if\frac{df^*}{dt};$$

$$\therefore\ \Omega^2(t) = f^*f\frac{df^*}{dt}\frac{df}{dt} = \dot{f}^*\dot{f}. \tag{31}$$

Applying the procedure used above to (31) we obtain

$$\overline{\Omega^2} = \int_{-\infty}^{\infty} P(\omega)\omega^2 d\omega. \tag{32}$$

Combining (28), (30) and (32) we obtain

$$\overline{(\Omega(t) - \bar{\Omega})^2} = \int_{-\infty}^{\infty} P(\omega)\omega^2 d\omega - \left[\int_{-\infty}^{\infty} P(\omega)\omega d\omega\right]^2. \quad (33)$$

But

$$\int_{-\infty}^{\infty} P(\omega)(\omega - \langle\omega\rangle)^2 d\omega = \int_{-\infty}^{\infty} P(\omega)\omega^2 d\omega - \langle\omega\rangle^2 \quad (34)$$

where use has been made of (29) and

$$\langle\omega\rangle \equiv \int_{-\infty}^{\infty} P(\omega)\omega d\omega.$$

Therefore combining (33) and (34) gives

$$\overline{\Omega(t) - \bar{\Omega})^2} = \int_{-\infty}^{\infty} P(\omega)(\omega - \langle\omega\rangle)^2 d\omega. \quad (35)$$

That is, the variance of the instantaneous frequency is just the second moment of the power spectrum.

Returning now to (19), it is easily provable that if the average Fourier frequency, $\langle\omega\rangle$, of $f(t)$ is very large compared to the width of the spectrum, the addition of the term $e^{-i\phi(t)}$ adds a term to the power spectrum of the form $P(-\omega)$, and thus it is possible to treat the so-called "one sided" power spectrum of $E(t)$. Taking into account the multiplicative constant in (19), then (28) and (35) take the form

$$\bar{\Omega} = \frac{2}{E_0^2}\int_0^{\infty} P'(\omega)\omega d\omega \equiv \langle\omega\rangle \quad (28a)$$

$$\overline{(\Omega - \bar{\Omega})^2} = \frac{2}{E_0^2}\int_0^{\infty} P'(\omega)(\omega - \langle\omega\rangle)^2 d\omega \quad (35a)$$

where $P'(\omega)$ is the power spectrum of $E(t)$ and these equations are subject to the condition

$$\bar{\Omega} \gg [\overline{(\Omega(t) - \bar{\Omega})^2}]^{1/2}$$

which is easily satisfied by most oscillators.

As an example of an application of (35a), the second moment of the spectrum of Fig. 4 turns out to be about 30,000 cps^2/sec^2, or the rms frequency deviation is about 174 cps, or more than one part in 10^8. For a one *second* count, however, this oscillator has a spread of only about ± 2 parts in 10^{11} from second to second and a drift of only a few parts in 10^{11} per day. One concludes that this spectrum must be very stable.

V. Conclusion

Power spectra of highly stable signal sources can be observed with the ammonia maser spectrum analyzer in a convenient and rapid way. The short term stability of these sources can be obtained from these observed spectra simply and without the usual laborious analysis of large amounts of data.

The device has use as an instrument for investigating noise properties of signal sources and the multiplication processes in frequency multiplier chains.

Frequency modulation introduced into a crystal oscillator or multiplier chain is enhanced by the frequency multiplication process. In fact the sidebands in the power spectrum are found to be increased in amplitude by the factor of frequency multiplication (see Appendix). This is demonstrated in Fig. 2. It can be demonstrated that the power spectrum of a signal that is frequency modulated by two or more modulating signals of different frequency will in general be unsymmetrical.[7] This is vividly displayed in the power spectrum of Fig. 4.

Spectrum analysis has provided a particularly useful tool in designing crystal oscillators and frequency multipliers such that they yield signals of the highest purity. From a study of the power spectra, one is led to the conclusion that one of the most important things in obtaining a pure signal is to keep the electronics simple, using dc filaments in the oscillator and early stages of multiplication. The signal source that provides the Bureau atomic frequency standards with the purest signals is a system involving a "master and a slave" oscillator. A simple one- or two-tube crystal oscillator that is loosely phase-locked to a more elaborate crystal oscillator (with good long term stability) drives the frequency multiplier chain.

A knowledge of the power spectrum is important not only in describing frequency stability and noise analysis but for other reasons also.

For example, in atomic beam frequency standards, the simple theory of the spectral line shape assumes the atomic transition to be excited by pure sinusoidal or cosinusoidal radiation. In actual fact, of course, the transition is induced by a certain distribution of frequencies. This distribution is determined by the frequency multiplier and crystal oscillator from which the exciting radiation is derived. The radiation in general is composed of the carrier frequency, noise and discrete sidebands resulting from frequency modulation. The discrete sidebands usually result from 60 cps—the power frequency—and multiples thereof. In the atomic clock experiments it is found possible to reduce the noise to a low enough level so that it is not the limiting factor in the precision of the frequency measurements. The discrete sidebands are more difficult to remove. These sidebands are multiplied in intensity by the factor of frequency multiplication. This factor is usually quite large ($\sim$2000) and consequently these sidebands can introduce rather large frequency errors. Errors of this sort are particularly significant if the power spectrum is unsymmetrical. (Shifts of a a few parts in 10^9 have been observed by actual experiments.) Of course, if the power spectrum is known, the proper spectral line shape can be calculated in order to find the proper correction to the measured frequency. It is more desirable

[7] H. S. Black, "Modulation Theory," D. Van Nostrand Co., Inc., New York, N. Y. p. 195; 1953.

—and much simpler—to eliminate these sidebands so that the simple line-shape theory applies. A knowledge of the power spectrum is essential in order to assign a figure of accuracy to the atomic beam frequency standards.

Appendix

As an example of the effect of frequency multiplication on an FM signal, consider just one stage of multiplication. Assume that the current, $I(t)$, in the output tank of the multiplier is related to the input voltage, $V(t)$, by the transfer function, $g(V)$, which is a function of the input voltage; *i.e.*,

$$I(t) = g(V(t))V(t). \tag{36}$$

If the input signal is of the form

$$V(t) = V_0 \cos \phi(t), \tag{37}$$

where $\phi(t)$ is some function of time, then the current becomes

$$I = g(V_0 \cos \phi)V_0 \cos \phi.$$

Since $\cos \phi$ is an even function of ϕ, $g(V_0 \cos \phi)$ is also an even function of ϕ, and therefore I is an even function of ϕ. Therefore I can be expanded as a Fourier cosine series in ϕ; *i.e.*,

$$I = \sum_{n=0}^{\infty} a_n \cos n\phi. \tag{38}$$

To restrict the case to a simple FM wave, let

$$\phi(t) = \omega_0 t + \delta \sin \omega_m t \tag{39}$$

where ω_0 is the carrier frequency, ω_m is the modulating frequency, and δ is the modulation index. Subsitution of (39) into (38) yields,

$$I(t) = a_0 + a_1 \cos (\omega_0 t + \delta \sin \omega_m t) + \cdots + \cdots + a_N \cos (N\omega_0 t + N\delta \sin \omega_m t) + \cdots .$$

If the impedance, $Z(\omega)$, of the output tank is sufficiently peaked about $\omega = N\omega_0$, but broader than $2N\delta\omega_m$, the output voltage, $V'(t)$, is given approximately by

$$V'(t) \simeq a_N Z(N\omega_0) \cos (N\omega_0 t + N\delta \sin \omega_m t). \tag{40}$$

Typically ω_m is very much smaller than ω_0 and the condition that the bandwidth of the output tank is greater than $2N\delta\omega_m$ is easily satisfied. The condition that $Z(\omega)$ is sharp enough to reject $(N-1)\omega_0$ and $(N+1)\omega_0$ usually requires N to be less than 10.

Eq. (40) shows that the modulation index is multiplied by the factor of frequency multiplication and the frequency of modulation is unchanged. Extensive use is made of this fact in FM transmitters.[8]

Fig. 2 (a) shows the square root of the power spectrum ($\sqrt{P(\omega)}$) of a signal while Figs. 2(b) and 2(c) show the same signal after being multiplied in frequency by 3 and 9, respectively.

[8] W. L. Everitt, "Frequency modulation," *Trans. AIEE*, vol. 59, p. 613; November, 1940.

Reprinted from IRE TRANSACTIONS
ON INSTRUMENTATION
Volume I-9, Number 2, September, 1960

A High-Resolution Ammonia-Maser-Spectrum Analyzer*

J. A. BARNES†, MEMBER, IRE, AND L. E. HEIM†

INTRODUCTION

THE problem of precise frequency measurement can be understood only with a fairly complete knowledge of the frequency source and the effect of the measuring system. In particular, the problem becomes more difficult if different methods of frequency measurement are used (*e.g.*, counters and atomic resonances) and if it cannot be assumed that the frequency source is pure.

For almost all systems, the problem of amplitude modulation of the measured signal is of no concern since in practice the signal can be regulated quite well. The problem of frequency modulation, however, is quite another matter. In practice a quartz-crystal oscillator is used and it is assumed to be relatively free of modulation.

It can be shown [3] that in general a frequency counter will, on the average, measure the center of gravity of the frequency-modulation power spectrum. A spectral line in an atomic or molecular transition, however, will not in general measure the center of gravity of the power spectrum. Thus, for a meaningful comparison of frequency counter data and atomic or molecular resonance data, it is essential to know the spectral distribution of the signal being measured.

In practice, of course, one attempts to obtain a monochromatic source of radiation for the measurements. The results of the experiments made with the ammonia-maser-spectrum-analyzer system indicate how relatively pure signals in the microwave region can be obtained.

THEORY

In general, there are two methods of precise frequency measurement: 1) determining the total elapsed phase in an interval of time with an apparatus like a synchronous clock or a "frequency counter;" and 2) direct frequency measurement by a resonance method usually involving a molecular or atomic transition.

If the signal to be measured is composed of several sinusoidal components whose frequencies are near the main component, it is not immediately evident what frequency the two methods will "measure."

Since the frequency counter counts the number of times the signal passes through zero in a positive sense for an interval of time, both the synchronous clock and the frequency counter indicate the total elapsed phase for the period of the measurement. The resonance method, however, must give some sort of an average of all the frequency components present and in general will *not* agree with the elapsed-phase method of measurement. Thus, for a meaningful comparison of these two types of measurement, it is essential that a detailed knowledge of the signal be available.

It is usually sufficient for this "detailed knowledge" to be given in terms of the *power spectrum*. The power spectrum, or spectral density, of a signal can be defined in the following way: If $P(\omega)$ is the power spectrum of a signal, then $P(\omega)d\omega$ is the element of power supplied by those frequency components of the signal in the frequency interval from ω to $\omega+d\omega$. Mathematically it can be shown [1] that if $f(t)$ is the signal, then its power spectrum $P(\omega)$ is given by the time average

$$P(\omega) = \operatorname*{Lim}_{T\to\infty} \frac{1}{2\pi T}\left|\int_{-T/2}^{T/2} f(t)e^{-i\omega t}dt\right|^2.$$

Thus the power spectrum shows the relative energy distribution for the various frequency components and can therefore be used as a measure of the purity of the signal.

For most precise atomic or molecular resonance measurements, a quartz-crystal oscillator at a frequency of a few megacycles is used as the source, either to excite an atomic transition or to compare with an atomic transition. This signal is multiplied in frequency by harmonic multipliers to the atomic or molecular resonance frequency which is usually in the microwave region. This multiplication process has a marked effect on the power spectrum of the signal.

Normally limiters are used throughout the electronic system so that amplitude modulation is not a problem. However, frequency modulation cannot so easily be removed. In fact, it can easily be shown that if a small amount of frequency jitter or modulation is present in the oscillator, it will be *enhanced* by the factor of multiplication.

As an example of the effect of frequency multiplication on an FM signal, consider just one stage of multiplication. Assume that the current $I(t)$ in the output tank of the multiplier is related to the input voltage $V(t)$ by the transfer function $g(V)$, which is a function of the input voltage; *i.e.*,

$$I(t) = g(V(t))V(t). \tag{1}$$

* Received by the PGI, June 13, 1960.

† Radio Standards Div., National Bureau of Standards, Boulder, Colo.

If the input signal is of the form

$$V(t) = V_0 \cos \phi(t), \tag{2}$$

where $\phi(t)$ is some function of time, then the current becomes

$$I = g(V_0 \cos \phi) V_0 \cos \phi.$$

Since $\cos \phi$ is an even function of ϕ, $g(V_0 \cos \phi)$ is also an even function of ϕ, and therefore I is an even function of ϕ. Therefore I can be expanded as a Fourier cosine series in ϕ; *i.e.*,

$$I = \sum_{n=0}^{\infty} a_n \cos n\phi. \tag{3}$$

To restrict the case to a simple FM wave, let

$$\phi(t) = \omega_0 t + \delta \sin \omega_m t, \tag{4}$$

where ω_0 is the carrier frequency, ω_m is the modulating frequency, and δ is the modulation index. Substitution of (4) into (3) yields

$$I(t) = a_0 + a_1 \cos (\omega_0 t + \delta \sin \omega_m t) + \cdots + a_N \cos (N\omega_0 t + N\delta \sin \omega_m t) + \cdots .$$

If the impedance $Z(\omega)$ of the output tank is sufficiently peaked about $\omega = N\omega_0$, but broader than $2N\delta\omega_m$, the output voltage $V'(t)$ is given approximately by

$$V'(t) \simeq a_N Z(N\omega_0) \cos (N\omega_0 t + N\delta \sin \omega_m t). \tag{5}$$

Typically, ω_m is very much smaller than ω_0, and the condition that the bandwidth of the output tank be greater than $2N\delta\omega_m$ is easily satisfied. The condition that $Z(\omega)$ be sharp enough to reject $(N-1)\omega_0$ and $(N+1)\omega_0$ usually requires N to be less than 10.

Eq. (5) shows that the modulation index is multiplied by the factor of frequency multiplication but the frequency of modulation is unchanged. Extensive use is made of this fact in FM transmitters [6].

Fig. 1(a) shows the square root of the power spectrum ($\sqrt{P(\omega)}$) of a signal, while Fig. 1(b) and (c) show the same signal after being multiplied in frequency by 3 and 9, respectively.

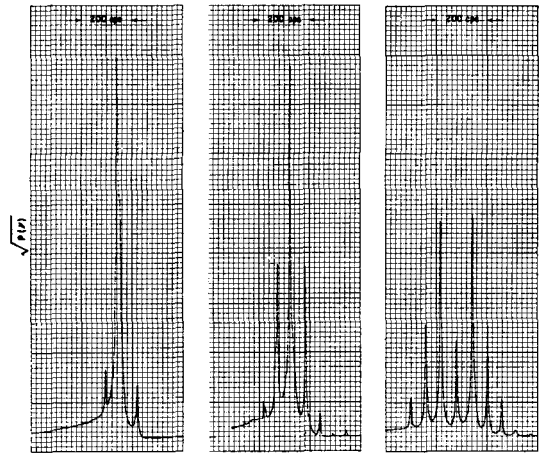

(a) (b) (c)

Fig. 1—Effects of frequency multiplication on a frequency-modulated signal. Fig. 1(a) shows the square root of the power spectrum for a 3.3-Mc signal. Fig. 1(b) and (c) show the same signal after being multiplied in frequency by factors of 3 and 9, respectively.

To return now to the problem of frequency measurement, it can be shown [3] that a frequency counter or synchronous clock measures the center of gravity of the FM power spectrum. An atomic or molecular resonance device such as a cesium beam with Ramsey-type excitation will measure the center of gravity of the power spectrum *only* if the excitation and atomic spectra are both symmetric. (To see that power spectra can, in fact, be quite asymmetric, see Fig. 5.)

It is obvious that a spectrally "pure" signal is the most desirable source for precise frequency measurement. The experiments with the maser-spectrum analyzer indicate some means of obtaining relatively pure signals in the microwave region (see Figs. 2–8, pp. 5–7).

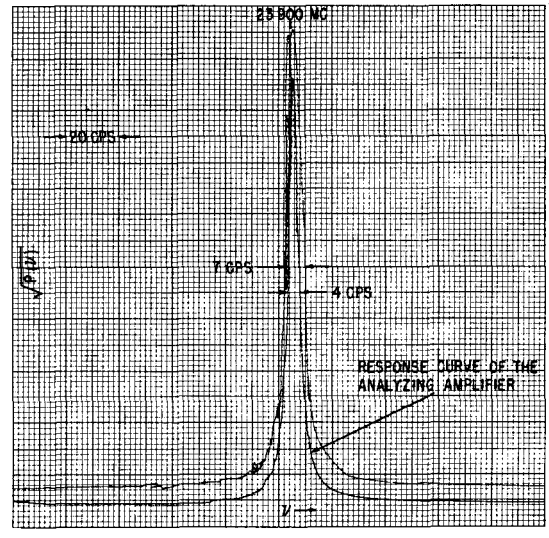

Fig. 2—Spectrum of free-running oscillator used in the spectrum-analyzer system. This spectrum was obtained by analyzing the direct beat note between the *free-running* oscillator-multiplier-chain system and the ammonia maser. It is this oscillator which is phase locked to the maser to give a relatively pure signal to be used in the analyzing of other oscillators. The response curve of the analyzer was obtained by replacing the maser-oscillator beat note by the signal from a high-quality signal generator.

463-560 O - 72 - 29

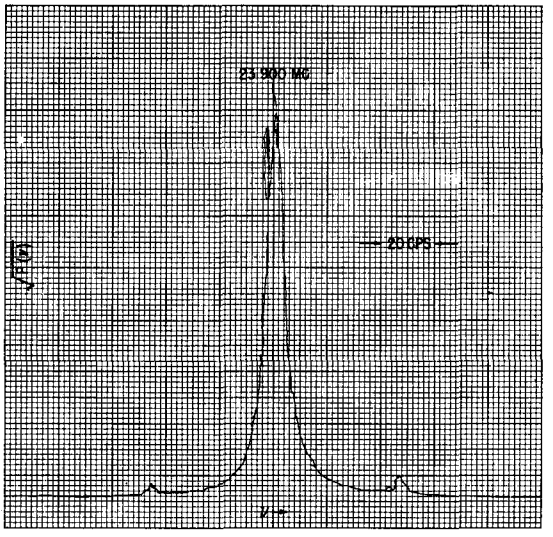

Fig. 3—This spectrum was obtained by intentionally frequency modulating the oscillator of Fig. 2 at a 50-cps rate. The total swing in frequency of the oscillator was about 2 parts in 10^{10} peak to peak. (Note the small sidebands at 50 cps on either side of the central peak.)

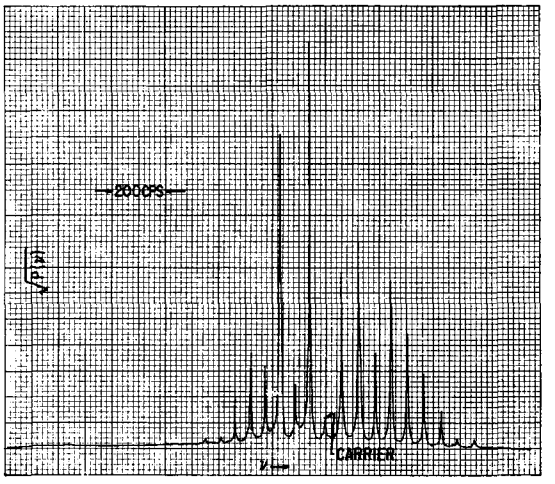

Fig. 5—Asymmetric spectrum of oscillator with ac filaments. This spectrum was obtained from the same oscillator as Fig. 4. At the time this trace was made, however, the oscillator was equipped with 60-cps ac filaments. (Note the different frequency scale.)

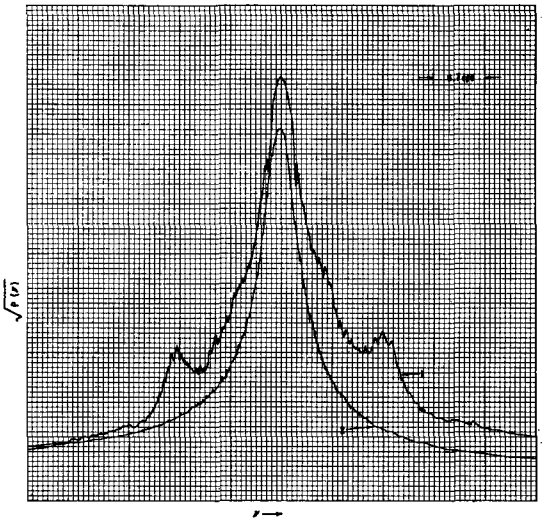

Fig. 4—High-resolution spectrum of liquid helium cooled quartz crystal oscillator. Trace 1 is a high-resolution spectrum of the central peak of a 10-Mc quartz-crystal oscillator whose crystal was thermostated in a liquid helium cryostat [4]. The oscillator was equipped with dc filaments but still exhibited 60-cps sidebands about 30 db below the central peak (not shown in this Figure). This oscillator operates at about 13.4 cps above 10 Mc and apparently some of the pickup of the standard is responsible for the sidebands shown in this trace. Trace 2 is the response curve of the spectrum analyzer.

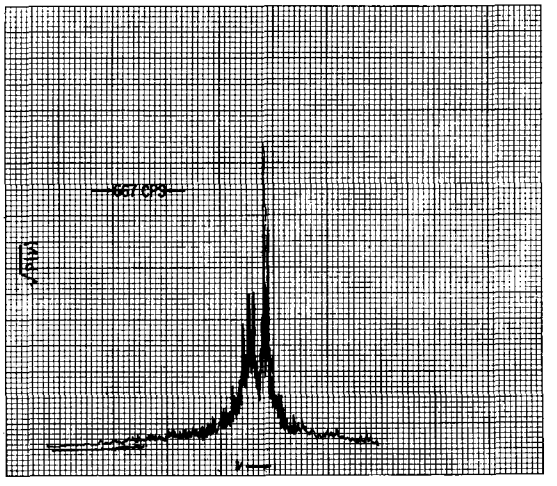

Fig. 6—This spectrum was made from a 100-kc Essen Ring oscillator multiplied in frequency by 145,800. This was the best spectrum ever observed for a 100-kc oscillator multiplied by this factor; however, this spectrum was not consistent, and would have markedly different shape from day to day. (Note the scale.)

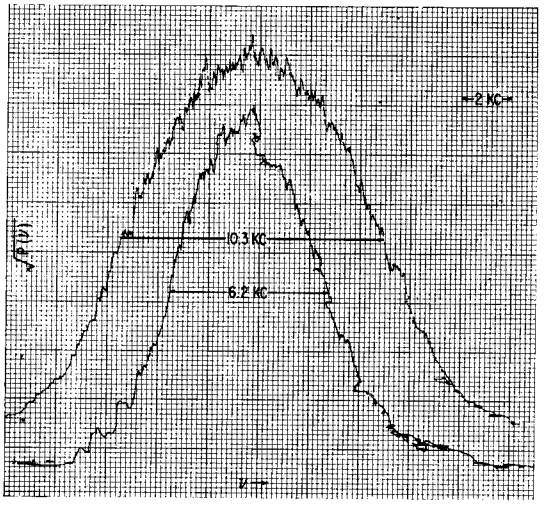

Fig. 7—Effects of warm-up time of multiplier chain on a 100-kc signal. This is a spectrum of a 100-kc oscillator, again multiplied 145,800 in frequency, located two floors above the room containing the maser-spectrum-analyzer system. The signal apparently picked up noise in the long cables connecting the two rooms. The upper trace was taken approximately one hour after the multiplier chain in the spectrum analyzer was first turned on, and the lower trace about 6 hours after the chain was turned on, showing the effect of warm-up time of a multiplier chain on a noisy signal. (Note the scale.)

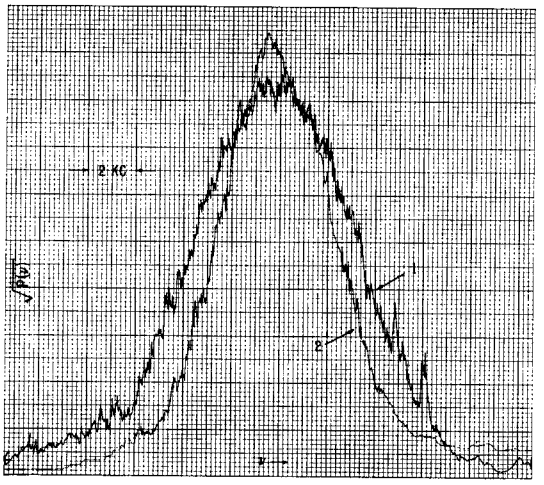

Fig. 8—Effect of buffer amplifier on a noisy 100-kc signal. Again these are the square roots of the power spectra for a 100-kc oscillator multiplied in frequency 145,800 times. Trace 1 employed a buffer amplifier of unit gain between the oscillator and first stage of multiplication, while trace 2 did not use this amplifier.

Experiment

Since it is desired to resolve sidebands of a microwave signal which may be only a few parts in 10^{10} apart, it is essential to use a superheterodyne type of system such as that shown in Fig. 9 (next page). By heterodyning the measured signal with a relatively pure signal, the power spectrum is displaced (ideally without distortion) to lower frequencies (~79 kc) where filters of very narrow bandwidth (~4 cps) can be used.

The first problem is then to obtain a very "pure" signal to heterodyne with the measured signal.

The ammonia beam maser has been recognized as one of the most nearly monochromatic sources of radiation in the microwave region. In fact, the beat note between the two National Bureau of Standards masers demonstrates a bandwidth of somewhat less than about 0.5 cps at 23,870 Mc for a period of several minutes.

Since the maser puts out only about 10^{-9} watts of power and at the rather inconvenient frequency of 23,870 Mc, a crystal-oscillator-multiplier-chain system was phase locked to the maser. As mentioned previously, amplitude modulation can easily be avoided by the use of limiters throughout the multiplier chains. Thus the frequency jitter or modulation of the oscillator is the only problem. By phase locking the crystal oscillator to the maser, nearly the spectral purity of the maser should be imparted to the crystal oscillator.

The oscillator to be tested is multiplied to 270 Mc and 5 Mc and then heterodyned with the 265.551-Mc signal from the maser-stabilized oscillator-multiplier chain. (See Fig. 9.) The frequency multipliers throughout the apparatus are of conventional design operated from dc filament supplies to avoid modulating the signal in the system itself. (The effects of 60-cps filaments in the early stages of multiplication are quite severe.)

The action of this mixer is first to mix the two signals from the test oscillator at 270.0 Mc and 5.0 Mc to obtain the 265.0-Mc beat, and then to mix this signal with the "pure" 265.551-Mc signal from the maser-stabilized oscillator to give a 0.551-Mc beat. This displaces the power spectrum of the 265.0-Mc signal to 0.551 Mc. The fact that heterodyning an FM signal with a pure signal displaces the power spectrum to lower frequencies without distortion is often made use of in FM transmitters and receivers [6].

The 0.551-Mc output of the mixer was then sent to another multiplier with outputs at 3.3, 9.9, 29.7, and 89.3 Mc. The spectra shown in Figs. 4–8 were made by sending the 29.7-Mc signal to the spectrum analyzer shown in Figs. 10 and 11 (next page).

The spectrum analyzer is of rather conventional design. The 29.7-Mc signal to be analyzed is first mixed with a signal from a crystal-controlled frequency synthesizer and then passed through a 79-kc crystal filter whose bandwidth is about 4 cps. Thus by slowly sweep-

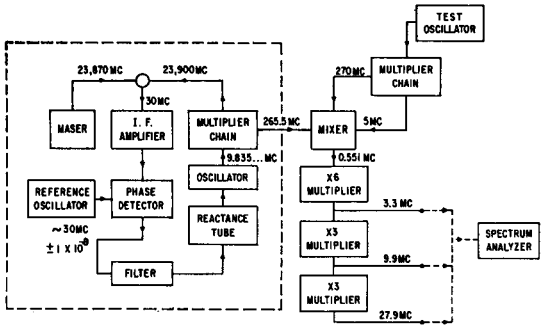

Fig. 9—Block diagram of ammonia-maser-spectrum-analyzer system.

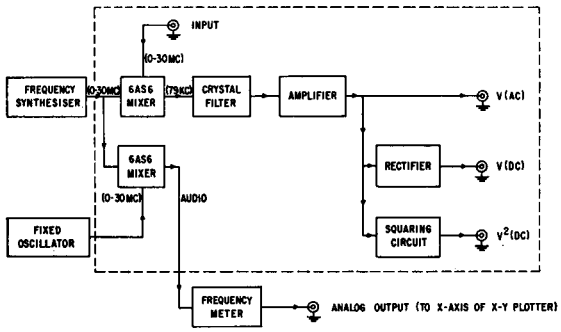

Fig. 10—Block diagram of spectrum analyzer.

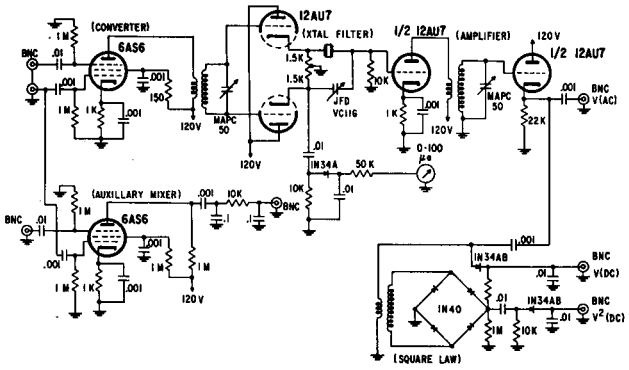

Fig. 11—Circuit diagram of spectrum analyzer.

ing the frequency of the synthesizer, the power spectrum was swept past the analyzing filter.

By separately mixing the signal from the frequency synthesizer with a fixed crystal-controlled oscillator, an analog voltage to the frequency was obtained to drive the x-axis of an x-y plotter. The y-axis was driven by the rectified output of the 79-kc filter. Thus the spectra shown are actually the square root of the power spectra, since the ordinate is nearly linear with voltage instead of power.

Conclusion

From the spectra shown, one is led to the conclusion that the most important things in obtaining a relatively pure signal in the microwave region are to keep the electronics simple, and use dc filaments in the oscillator and early stages of multiplication. Probably the best oscillator would be a system involving a "master and a slave"; that is, a simple one- or two-tube crystal oscillator to drive the chain which is loosely phase locked to a more elaborate crystal oscillator which has good long-term stability. With this system, the amount of electronics affecting the signal directly is kept at a minimum without a sacrifice of stability [5].

The ammonia-maser-spectrum analyzer has proved to be a valuable instrument in the investigation of oscillator and multiplier-chain stability, and noise. In this respect, it is interesting to note an unusual effect which was observed in one of the crystal oscillators at the National Bureau of Standards.

The oscillator was a 5-Mc quartz crystal oscillator with the crystal thermostated in a liquid nitrogen bath. The temperature was maintained constant by regulating the pressure over the liquid nitrogen with a manostat. The oscillator was run on regulated dc filaments and with a well regulated B^+ supply. It was observed that the signal was slightly frequency modulated at about a 10-cps rate. Upon removing the manostat from the liquid nitrogen thermostat so that the temperature of the liquid nitrogen was determined by atmospheric pressure, it was observed that the 10-cps sidebands on the signal slowly reduced in amplitude. After several measurements were made, and the sidebands were observed, first slowly increasing after connecting the manostat and then decaying after disconnecting the manostat, a time constant of about 7 minutes for the build-up of the modulation was determined.

It should be mentioned that the connection of the manostat was virtually instantaneous (compared to 7 minutes). The probable explanation of this is a mechanical vibration of the crystal mount which is excited by the fluctuations in pressure.

In regard to precise frequency measurements, knowledge of the power spectra of the oscillators used to excite the two National Bureau of Standards cesium beam atomic standards has given added reliability to the measurements made with these cesium beams, as well as indicating when a signal is not suited to this form of measurement.

References

[1] See, for example, R. B. Blackman and J. W. Tukey, "The Measurement of Power Spectra," Dover Publications, Inc., New York, N. Y., pp. 84–88; 1958.
[2] For an account of frequency modulation see F. E. Terman, *et al.*, "Electronic and Radio Engineering," McGraw-Hill Book Co., Inc., New York, N. Y., pp. 786–792; 1955.
[3] J. Barnes and R. Mockler, "The power spectrum and its importance in precise frequency measurements," IRE Trans. on Instrumentation, vol. I-9, pp. 149–155; September, 1960.
[4] This oscillator was designed and constructed by A. H. Morgan and his group at the National Bureau of Standards. The quartz crystal was made at the Bell Telephone Laboratories.
[5] This method is presently used quite successfully with the National Bureau of Standards atomic frequency standards.
[6] W. L. Everitt, "Frequency modulation," *Trans. AIEE*, vol. 59, p. 613; November, 1940.

PROCEEDINGS OF THE IEEE

VOL. 51, NO. 2, FEBRUARY, 1963

Spectrum Analysis of Extremely Low Frequency Variations of Quartz Oscillators*

The rather numerous discussions of the spectrum of oscillator frequency fluctuations prompted the application of the Tukey[1] technique of spectrum analysis to five years of daily frequency comparisons between an atomic frequency standard and free-running quartz crystal oscillators at the National Bureau of Standards. Three of the four spectra shown in Fig. 1 were computed from observations made on oscillators 5a and 35 which are 100-kc quartz oscillators utilizing vacuum tubes in amplifiers and automatic level control circuits. The aging rate of these oscillators had stabilized several years before these measurements were begun.

The fourth spectrum of Fig. 1 is an estimate of the contribution to the oscillator spectra due to instrumentation noise. From a series of random numbers this estimate was computed assuming that the daily frequency measurements were in error by as much as ± 1 part in 10^{10} and that the measurement error on any given day was independent of the errors made on neighboring days. Before undertaking the spectrum analyses a detrending procedure described by Norton, *et al.*,[2] was used to remove frequency drifts and variations at frequencies lower than the lowest frequency for which the spectrum was obtained. The spectrum of $\Delta f/f$, the relative or fractional frequency deviations of the oscillator, is shown with normalization such that integration from 0 to ∞ with respect to the Fourier frequency F in cycles per second would formally yield the total

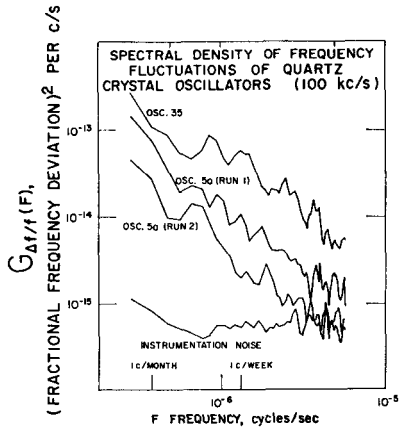

Fig. 1.

relative mean-square fluctuation. Fig. 1 shows spectral densities $G_{\Delta f/f}(F)$ which appear to increase without limit as one considers lower and lower Fourier frequencies. This behavior is similar to that of klystron and LC oscillators at Fourier frequencies about 10^8 times greater than those of Fig. 1.[3,4] A least-squares-type fit to the lowest oscillator curve of Fig. 1 is $G(F)=3.6\times10^{-23}/F^{1.4}$ (fractional frequency deviation)^2 per cycles per second.

Other spectrum measurements were made in a higher fluctuation, or Fourier, frequency range on more recently constructed transistorized 5-Mc quartz oscillators. The equipment consisted of an NH_3 maser, frequency multipliers, a mixer, an electronic frequency meter, and a tunable mean-square indicator. Analysis of these data yielded $G(F)=(5\times10^{-23})/0.9$(fractional frequency deviation)^2 per cycles per second in the range $0.02<F<2$ cps. This result is comparable to that for the lower frequency range. Above $F=2$ cps the spectral density was observed to increase with increasing Fourier frequency F.

For both types of crystal oscillators studied, the spectral behavior observed below $F=2$ cps is similar to that of current fluctuations in current carrying semiconductors. Current noise possessing a spectrum of this type occurs widely in nature and has been referred to as excess noise, flicker noise, or simply $1/F$ noise.[5,6] Excess noise has been observed at frequencies as low as 6×10^{-6} cps.[7] In many theoretical treatments[8-10] of oscillator stability it has been customary to consider only the direct effects of tube shot noise and thermal noise on frequency stability with resulting theoretical spectra which disagree with the actually observed spectra reported here. The effect of flicker noise on oscillator stability has been treated theoretically by Troitsky.[11] His analysis resulted in a spectrum similar to the oscillator spectra of Fig. 1; however, experiments of Driagin[4] failed to verify certain aspects of this theory.

A difficulty associated with the oscillator spectra of the type shown in Fig. 1 is in determining how to extrapolate curves to lower frequencies in a meaningful way. It is desirable to compute for an oscillator such quantities as the power spectrum width, the mean-square frequency variation, and the expected time error of a clock connected to the oscillator. Formal relationships may be easily derived expressing these quantities as integrals over frequency of the frequency fluctuation spectrum times some appropriate filter function which weights the spectrum in accordance with the application under consideration. However, these integrals sometimes diverge at the lower limit if the spectrum is assumed to behave at arbitrarily low frequencies as a straight line extrapolation of Fig. 1 might suggest. The convergence difficulty was discussed by Malakhov[6] with reference to the expressions that lead to the spectral distribution of energy of an oscillator randomly frequency modulated with flicker noise. After disposing of the problem associated with the upper limit, Malakhov proposed proceeding according to the customary formalism that is valid for stationary processes, with the exception that the lower limit $F=0$ was to be replaced by $F=1/T$ where T is characteristic of the duration of an experiment which would determine the width of the power spectrum. This replacement seems reasonable and could be applied in the computation of the fluctuational aspects of various experiments involving oscillators. However, the exact relationship between T and the duration of an observation or experiment is somewhat vague, though this in itself would be of little consequence were it not for the fact that in some cases examined, the pertinent integral was found to be rather dependent on the exact value of the lower limit. Closer analysis of the whole problem might show that the weighting function, rather than the lower limit, could, and should, incorporate the duration of the experiment in such a way as to avoid the difficulty

The authors wish to thank V. E. Heaton, who made and recorded the frequency measurements, A. W. Kirkpatrick, who supplied the program for performing the detrending and spectrum analysis, and J. A. Barnes, who made available the ammonia maser.

W. R. ATKINSON
L. FEY
J. NEWMAN
Radio Standards Lab.
National Bureau of Standards
Boulder, Colo.

* Received August 17, 1962.

[1] R. B. Blackman and J. W. Tukey, "The Measurement of Power Spectra," Dover Publications, Inc., New York, N. Y.; 1959.

[2] K. A. Norton, J. W. Herbstreit, H. B. Janes, K. O. Hornberg, C. F. Peterson, A. F. Barghaussen, W. E. Johnson, P. D. Wells, M. C. Thompson, Jr., M. J. Vetter, and A. W. Kirkpatrick, "An Experimental Study of Phase Variations in Line of Sight Microwave Transmissions," NBS Mono. No. 33; November 1, 1961.

[3] G. A. Espersen, "Noise studies on two-cavity CW klystrons," IRE TRANS. ON MICROWAVE THEORY AND TECHNIQUES, vol. MTT-8, pp. 474-477; September, 1960.

[4] Iu. A. Driagin "Investigating technical frequency drifts in oscillators " 93-97; December, 1958.

[5] D. A. Bell, "Electrical Noise: Fundamentals and Physical Mechanism," D. Van Nostrand Co., Inc., Princeton, N. Y.; 1960.

[6] A. N. Malakhov "Spectra of flicker noise " *Radiotekh. Elektron.*, vol. 4 pp. 54-62, January, 1959.

[7] T. E. Firl and H. Winston, "Noise measurements in semiconductors at very low frequencies " *J. Appl. Phys.* vol. 26 pp. 716-718; June, 1955.

[8] W. A. Edson "Noise in oscillators," PROC. IRE, vol. 48, pp. 1454-1466; August, 1960.

[9] J. A. Mullen, "Background noise in nonlinear oscillators," PROC. IRE, vol. 48, pp. 1467-1473; August, 1960.

[10] M. J. Golay, "Monochromaticity and noise in a regenerative electrical oscillator," PROC. IRE, vol. 48, pp. 1473-1477; August, 1960.

[11] V. S. Troitsky, "Certain problems of the theory of fluctuations in oscillators " *Radiofizika*, vol. 1, pp. 20-23, February, 1958.

Obscurities of Oscillator Noise*

In a recent paper[1] (which will be referred to as paper 1) the origin of crystal oscillator phase noise has been discussed, and an analysis of the measurements reported therein was used to support the hypothesis that crystal oscillator fluctuations arise as a result of thermal noise in the circuitry associated with the oscillator.

Because of the need for knowledge of oscillator noise characteristics and because the results given in paper 1 conflict with those given in a recent paper by the present authors,[2] it was decided that a separate analysis of the data presented in paper 1 should be made in order to ascertain whether any alternative conclusions might be reasonable.

The data analyzed are those presented in Fig. 12 of paper 1, in which good agreement with the calculated curve of Fig. 11, paper 1, has been taken as experimental verification of the hypothesis that the source of oscillator noise is predominantely thermal. Particular importance is to be attached to the higher-frequency portion of the curve to which a single straight line segment was fitted giving a slope of 6-db attenuation per octave with increasing frequency. For the conditions of the experiment described in paper 1, the slope of 6 db/octave would imply noise of a thermal origin.

The present authors feel, however, that this portion of data could better be fitted by two straight line segments rather than by one. In order to test this possibility 78 points were read from Fig. 12 for processing by digital computer. Since the original positions of the plotted points for constructing Fig. 12 were fairly evident, these were the points scaled for analysis.

This spectrum, presented as a phase fluctuation spectrum (in db) in Fig. 12 of paper 1, was converted to a frequency fluctuation spectrum by adding 20 log F in order to facilitate comparison with the data published by the present authors and is plotted in this form in Fig. 1. This presentation appears more suggestive of two regimes of behavior than the original plot, with the dividing point at about 4.6 cps. A horizontal line on this plot would be consistent with noise of a thermal origin.

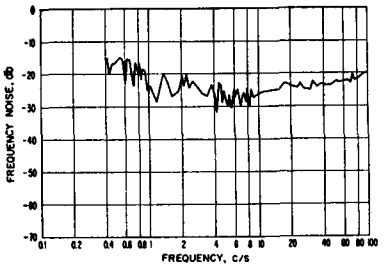

Fig. 1—Crystal-oscillator phase fluctuation noise taken from Fig. 12, paper 1, and replotted as frequency fluctuation noise.

A least squares fit was then made to logarithms of both sides of the equation, $G(F)=AF^{\alpha}$, to determine the value of α which best fit the portion of the data analyzed. This portion excluded the section with frequencies lower than 0.4 cps in order to avoid the region of the curve in the vicinity of f_k, where a departure from a straight line is expected to occur, as is seen in Fig. 11 of paper 1. For the calculation, the program was made to give approximately equal weights to equal frequency intervals. For example, a point at 100 cps was given 10 times the weight of a point at 10 cps. The values of α obtained using this weighting, however, are not greatly different, in the first two cases below, from those obtained using points equally weighted as scaled from Fig. 12. The results were as follows.

* Received August 12, 1963.

[1] L. R. Malling, "Phase-stable oscillators for space communications, including the relationship between the phase noise, the spectrum, the short-term stability, and the Q of the oscillator," PROC. IRE, vol. 50, pp. 1656–1664; July, 1962.

[2] W. R. Atkinson, L. Fey and J. Newman, "Spectrum analysis of extremely low-frequency variations of quartz oscillators," PROC. IEEE, vol. 51, p. 379; February, 1963.

Frequency Range, cps	α
0.4 to 4.6	−0.846
4.6 to 100	+0.442
0.4 to 100	+0.279

Thus, according to this analysis, the frequency fluctuations of the crystal oscillator used in the experiment would, at the lower portion of the frequency interval examined, increase with decreasing frequency as $G_f(F) \sim 1/F^{0.85}$.

This is the behavior noted by the present authors, who found the exponent α to vary from about −0.9 to −1.4 for the oscillators which they studied.[2] Above 4.6 cps the present analysis resulted in a positive α of 0.442, denoting increasing spectral density with increasing frequency, in the range of a few cycles per second to 100 cycles per second, a trend which has also been reported.[2]

Inasmuch as the fitting of two straight lines rather than one to the data gave twice as many parameters that could be optimized for the purpose of improving the goodness of fit, it is not surprising that the average square residual deviation was reduced. No statistical tests were made to see if the observed reduction was significantly larger than the reduction that might be expected to result from the two additional parameters. Rather than to rely on elaborate statistical tests of our own limited data in the 4-cps region and on the data of paper 1, to decide on the universality of the two regimes of spectral behavior, the authors would prefer to examine more data from different laboratories using different instruments for spectral analysis.

In the authors' opinion the origin of frequency fluctuations in oscillators remains sufficiently uncertain to justify the publication of further measurements. The theory of flicker fluctuations in oscillators is particularly obscure and needs clarification.

L. Fey
W. R. Atkinson
J. Newman
National Bureau of Standards
Boulder, Colo.

Author's Reply[3]

It is encouraging to note the interest that has been elicited by the spectral density curve presented in my paper.[1] I think that the additional information provided by Atkinson, Fey and Newman[2] (referred to as paper 2) further clarifies the origin of oscillator phase noise. However, before discussing this, I should like to reiterate the objectives of my paper which are essentially directed at systems behavior rather than at component performance.

The sensitivity and, hence, the range of a deep-space receiver is a function of kTB where T is the thermal-noise temperature and B is the noise bandwidth. It would seem at first that the range in a phase-coherent system could be indefinitely extended by compressing the bandwidth. However, as indicated in my paper,[1] and particularly in Figures 11 and 12, as the bandwidth is compressed the phase-noise of the local oscillator steadily increases. The ultimate range is thus limited by the noise temperature of the system components and the stability of the local oscillator. If the stability of the local oscillator can be expressed in terms of thermal noise, we have then a unified concept of systems performance in relation to range in terms of thermal noise, bearing in mind, of course, differences in spectral responses.

While there has been an industry-wide attack on the reduction of receiver noise-temperatures with numerous and well-documented papers on low noise antennas, masers and parametric amplifiers, for example, very little, if any, data have appeared on oscillator phase-noise, and that which have appeared have not been readily applicable to systems design use. Deep-space components must frequently be held to tolerances of less than 0.1 db to ensure range. This is particularly true of those components located at the input end of the receiver. As the local oscillator is one of the sensitive receiver inputs, its performance specifications must be held quite rigid. Hence one of the major purposes of my paper was to define the problem, establish suitable phase-noise criteria, propose techniques for evaluation and, in addition, provide actual measured systems data to act as guideposts. In addition, if oscillator phase-noise can be related to thermal noise then a language can be readily established for interpreting oscillator stability. Experience with ultra-stable oscillators in coherent systems has shown that phase-noise is primarily a function of crystal-Q and the design of the electronic networks. The difference in stability between two similar oscillators has been shown to be, in almost all cases, due to electronic circuit design.

The foundation of the thermal noise approach is established in Section III of my paper and further expanded in Sections IV and V. The spectral-density curve of Figure 12 was inserted to indicate the nature of phase-noise as measured at the output terminals of a phase-coherent receiver. The close adherence of the curve to a 6-db/octave slope does, however, to a first-order bear out the original premise that the noise originates in the oscillator as white noise having a flat spectrum.

The frequency spectrum covered by Figure 12 is measured for a system bandwidth of $2B_L = 2.5$ cps and is seen to enter the ultra-low-frequency region, a region of particular interest for the authors of paper 2. Generally speaking, a bandwidth of 2.5 cps is lower than could be generally accommodated for space communications due to the correspondingly low information rate achievable. However for the Venus radar experiment commented on in my paper, a $2B_L = 5$ cps was employed. As will be noted in Figure 12 and as commented on by the authors of paper 2, there is an increase in spectral density as the frequency drops below 2 or 3 cps; this had been noted and several explanations suggested. However, it was not possible in the scope of the original paper to expand on this matter. The possibility of the presence of 1/f frequency instability noise from the crystal has been raised in paper 2. 1/f noise is generally recognized to have a slope of 3 db/octave amplitude wise. If we now make the assumption that 1/f crystal phase noise adds directly to the thermal phase noise at the same rate of 3 db/octave, then at frequencies above f_k in Figure 12 the slope would be increased to 9 db/octave and below f_k decreased to 3 db/octave. The problem then arises as to where the 1/f crystal frequency instability noise sets in. The authors of paper 2 favor 2 cps. Hence if we reconstruct Figure 12 with a slope of 6 db/octave above 2 cps, a slope of 9 db/octave from 0.4 cps to 2 cps and a slope of 3 db/octave below 0.4 cps, we arrive at the dotted curve shown in the accompanying figure. This new dotted curve does appear to be a closer match to the measured data. f_k is moved closer to 0.4 cps. As for $2B_L = 2.5$ cps this is a more realistic figure, $f_k \approx B_L/\pi$. I do not think the departure from 6 db/octave at frequencies above 40 cps too significant in this particular case. The spectral components at 60 cps are over 50 db down from the lower frequency components, and instrument noise for this data is becoming a prominent factor at −60 db. I would suggest that the instrumentation accuracy over-all is not better than ±2 db.

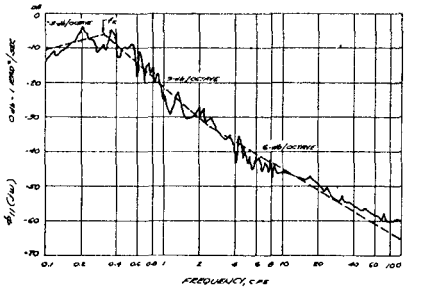

Fig. 2.

Inspection of many records of phase-noise (phase amplitude vs time), as measured at the output terminals of a closed-loop receiver with a meter having dc response, indicates the presence almost invariably of the largest components in the f_k region, and in fact the bandwidth can frequently be estimated from the appearance of the noise. This would appear to indicate then that no significant components are arising below the f_k region that deviate from the proposed laws. Hence extrapolation of 1/f crystal noise at a 3-db/octave rate into the ultra-low-frequency region, *i.e.*, below 1 cps, appears to be justified. As the flicker noise and thermal noise are noncoherent, we might perhaps expect the ±3-db variations in spectral amplitude which appear in Figure 12. I would also mention that similar characteristics have been obtained both for vacuum tube oscillators and solid-state oscillators. Further data in this area from other workers in the field would be, as stated by the authors of paper 2, of extreme interest.

Leonard R. Malling
Jet Propulsion Lab.
California Inst. Tech.
Pasadena, Calif.

[3] Received August 28, 1963.

11. EFFECTS OF LONG-TERM STABILITY ON THE DEFINITION AND MEASUREMENT OF SHORT-TERM STABILITY

J. A. BARNES AND D. W. ALLAN

National Bureau of Standards
Boulder, Colorado

Several authors have reported the measurement of a "flicker noise" spectrum for the frequency fluctuations, below a few cycles per second, of good quartz crystal oscillators. Experimental work carried out at the National Bureau of Standards at Boulder is in good agreement with these results.

The influence of this longer term type of noise turns out to be of considerable importance in the definition and measurement of shorter term noise, since averages of this short-term noise normally cover a total averaging time well into the flicker noise region. A mathematical formalism which satisfactorily avoids convergence difficulties has been developed around a set of physically meaningful quantities. Some theoretically reasonable definitions of short- and long-term stability are given.

It has been established by many people that quartz crystal oscillators are frequency-modulated by a "flicker" or $1/\omega$ type of noise which extends to at least as low a frequency as 1 cycle per year and probably even lower. Because the frequency emitted by any physically realizable device is bounded, this flicker noise behavior must cut off at some low, nonzero frequency ϵ.

It is possible to construct some measure of frequency stability $\langle \chi \rangle$ as the time average of a function $\chi(t)$ of the frequency. This function may or may not depend critically on the cutoff frequency ϵ. Thus, it might be that, if one measures the average value of $\chi(t)$ for some finite time T, this average value $\langle \chi \rangle_T$ will begin to approach $\langle \chi \rangle$ only after T is several times larger than $1/\epsilon$. Such a stability measure is thus said to be "cutoff-dependent" and is an inconvenient measure of frequency stability, since averaging times in excess of several years may be required to obtain a reasonable approximation to $\langle \chi \rangle$.

It is apparent that a necessary condition (not a sufficient condition) on any cutoff independent stability measure $\langle \chi \rangle$ is that $\langle \chi \rangle$ exists in the limit $\epsilon \to 0$. One can show that such quantities as the variance of frequency fluctuations around a uniform drift of frequency are, in fact, cutoff-dependent and hence not a very useful measure of frequency stability.

Some measures of frequency stability which are *not* cutoff-dependent and have direct use in various applications are: (1) variance of frequency fluctuation for finite sampling and averaging times, and (2) the variance of the nth finite difference of the phase for $n \geq 2$.

GENERAL PROBLEM

As stated, it has been established that quartz crystal oscillators are frequency-modulated by a "flicker" or $1/\omega$ type of noise spectrum. It even has been shown that this flicker-noise type of spectrum extends to 1 cycle per year and probably even lower. While this spectral region is not in the realm of "short-term" frequency fluctuations, it does have a very profound influence on their definition and measurement.

This can be seen by considering a crystal oscillator whose frequency fluctuations Ω from a nominal value have a (power) spectral density given by

$$G_\Omega(\omega) = g(\omega) + (h/|\omega|), \qquad (1)$$

where $g(\omega)$ predominates for the higher values of ω and thus gives rise to the "short-term" frequency fluctuations. The second term on the right is the flicker noise term. The total mean square of the instantaneous frequency fluctuation $\langle(\Omega)^2\rangle$ is then given by

$$\langle(\Omega)^2\rangle = 2\int_{\epsilon}^{\infty} G_{\Omega}(\omega)\ d\omega, \qquad \epsilon \geq 0. \tag{2}$$

Since any physical device must emit a finite frequency, Ω *must* be bounded; and thus the integral in Equation 2 must exist. This requires that $\epsilon \neq 0$ in order to insure the existence of

$$\int_{\epsilon}^{\infty} (h/|\ \omega\ |)\ d\omega.$$

From the preceding comments, it is apparent that this "cutoff" frequency ϵ is not known but is certainly less than 1 cycle per year. Thus, any meaningful measure of frequency stability should, in effect, be cutoff-independent; otherwise, averaging times exceeding several years must be employed.

It is possible to consider some function $\chi(t)$ obtained from the frequency (or phase) of the oscillator:

$$\chi(t) = X[f(t)]. \tag{3}$$

The expectation value of $\chi(t)$ is then given by

$$\langle\chi\rangle = \lim_{T\to\infty} T^{-1}\int_{-T/2}^{T/2} \chi(t)\ dt. \tag{4}$$

In principle, it is possible to obtain the Fourier transform of Equation 3 and substitute this in the integral of Equation 4. In this situation, the only quantities $\chi(t)$ which have physical significance (in the sense of being easily measurable) are quantities which do not depend critically on ϵ as $\epsilon \to 0$. In other words, $\lim_{\epsilon\to 0^+}\langle\chi\rangle$ must exist for meaningful quantities. Table 11–1 shows several functions of the frequency which do *not* exist as $\epsilon \to 0^+$. Physically, this can be pictured as follows: One can measure the quantity

$$\langle\chi\rangle_T = T^{-1}\int_{-T/2}^{T/2} \chi(t)\ dt \tag{5}$$

for some given time T, then extend the averaging time to NT and obtain $\langle\chi\rangle_{NT}$. If the sequence $\{\langle\chi\rangle_{NT}\}$ is considered, one might find that

$$\lim_{N\to\infty}\{\langle\chi\rangle_{NT}\} \to \infty.$$

For any finite N and T, the quantity $\langle\chi\rangle_{NT}$ certainly may exist. In the limit, however, the quantity may or may not exist.

TABLE 11–1.—*Cutoff-Dependent Quantities*

Name	Expression
Auto-covariance function of the phase fluctuations	$\lim_{T\to\infty} T^{-1}\int_{-T/2}^{T/2} \phi(t)\phi(t+\tau)\ dt$
Auto-covariance function of the frequency fluctuations	$\lim_{T\to\infty} T^{-1}\int_{-T/2}^{T/2} \bar{\Omega}(t,\tau)\bar{\Omega}(t+\tau',\tau)\ dt,$ where $\bar{\Omega}(t,\tau) = [\phi(t+\frac{1}{2}\tau) - \phi(t-\frac{1}{2}\tau)]/\tau$
Standard deviation of the frequency fluctuations	$\lim_{T\to\infty}\left\{T^{-1}\int_{-T/2}^{T/2}[\bar{\Omega}(t,\tau)]^2\ dt - \left[T^{-1}\int_{-T/2}^{T/2}\bar{\Omega}(t,\tau)\ dt\right]^{-2}\right\}$

MEANINGFUL QUANTITIES

The method of (power) spectral densities is a powerful and often meaningful way of encompassing a broad range of measurements. It certainly has application to the case of flicker noise (Reference 1). Occasionally, however, the quantities of physical interest are not simply related to the spectrum or the spectrum contains more information than is needed. Thus, other measures of frequency stability have been devised. Two additional methods are considered here.

RMS FREQUENCY FLUCTUATIONS

As was stated in Table 11–1, the quantity

$$\sigma_f^2(\tau) = \lim_{T\to\infty}\left\{ T^{-1}\int_{-T/2}^{T/2}\left[\frac{\phi(t+\tau)-\phi(t)}{\tau}\right]^2 dt - \left[T^{-1}\int_{-T/2}^{T/2}\left(\frac{\phi(t+\tau)-\phi(t)}{\tau}\right) dt\right]^2\right\} \quad (6)$$

is cutoff-dependent. However, if one does not pass to the limit $T\to\infty$ but specifies T and τ, the integral most certainly exists even in the limit $\epsilon\to 0$. Thus, one measure of frequency stability is the function

$$\sigma_f^2(\tau, T) = T^{-1}\int_{-T/2}^{T/2}\left[\frac{\phi(t+\tau)-\phi(t)}{\tau}\right]^2 dt - \left[T^{-1}\int_{-T/2}^{T/2}\left(\frac{\phi(t+\tau)-\phi(t)}{\tau}\right) dt\right]^2, \quad (7)$$

which unfortunately depends on *two* parameters τ and T.

THE METHOD OF FINITE DIFFERENCES

It is of value here to digress from short-term stability and consider how quartz crystal oscillators are used in clock systems—a problem in long-term stability. Typically, an oscillator is used as sort of a "fly wheel" in a clock system between regular calibrations with a frequency standard. Thus, one measures an average frequency $\bar{\Omega}$ during some interval $t-\frac{1}{2}\tau$ to $t+\frac{1}{2}\tau$, say. One predicts, then, that (on the average) the total phase accumulated by the oscillator $\Delta\Phi$ in the larger interval $t-\frac{1}{2}T$ to $t+\frac{1}{2}T$ is given by

$$\Delta\Phi \approx T\bar{\Omega} = T\left[\frac{\phi(t-\frac{1}{2}\tau)-\phi(t+\frac{1}{2}\tau)}{\tau}\right] \quad (8)$$

While this may be true "on the average," the frequency fluctuations of the oscillator cause some error $\delta\Phi$, given by

$$\delta\Phi = \Delta\Phi - T\bar{\Omega},$$

$$\delta\Phi = \phi(t+\tfrac{1}{2}T)-\phi(t-\tfrac{1}{2}T) - (T/\tau)[\phi(t+\tfrac{1}{2}\tau)-\phi(t-\tfrac{1}{2}\tau)]. \quad (9)$$

If one now sets $T=3\tau$ and defines the variable ϕ_n defined on the discrete range of the integer n by the relation

$$\phi_n \equiv \phi(t_0+n\tau)$$

and if one writes $t=t_0+\frac{1}{2}T$ in Equation 9, $\delta\Phi$ can be written in the simpler form

$$\delta\Phi = \Delta^3\phi_n, \quad (10)$$

where $\Delta^3\phi_n$ is the third finite difference of the variable ϕ_n (see Table 11–2). Thus the precision of an oscillator used in this system is related to the quantity

$$\langle(\delta\Phi)^2\rangle = \langle(\Delta^3\phi_n)^2\rangle, \quad (11)$$

which certainly must exist if the clock is any good at all.

Indeed, if one considers Equation 10 in the case of flicker noise (Reference 2), not only is $\Delta^3\phi_n$ a stationary function, but the correlation with $\Delta^3\phi_{n+k}$ for $k\geq 3$ is so small that the convergence of the quantity

$$N^{-1}\sum_{n=1}^{N}(\Delta^3\phi_n)^2$$

for large N is essentially that of a random un-

TABLE 11–2.—*Finite Phase Differences*

Variable	Definition	
ϕ_n	ϕ_n	$\phi(t_0+n\tau)$
$\Delta\phi_n$	$\phi_{n+1}-\phi_n$	$\phi_{n+1}-\phi_n$
$\Delta^2\phi_n$	$\Delta\phi_{n+1}-\Delta\phi_n$	$\phi_{n+2}-2\phi_{n+1}+\phi_n$
$\Delta^3\phi_n$	$\Delta^2\phi_{n+1}-\Delta^2\phi_n$	$\phi_{n+3}-3\phi_{n+2}+3\phi_{n+1}-\phi_n$

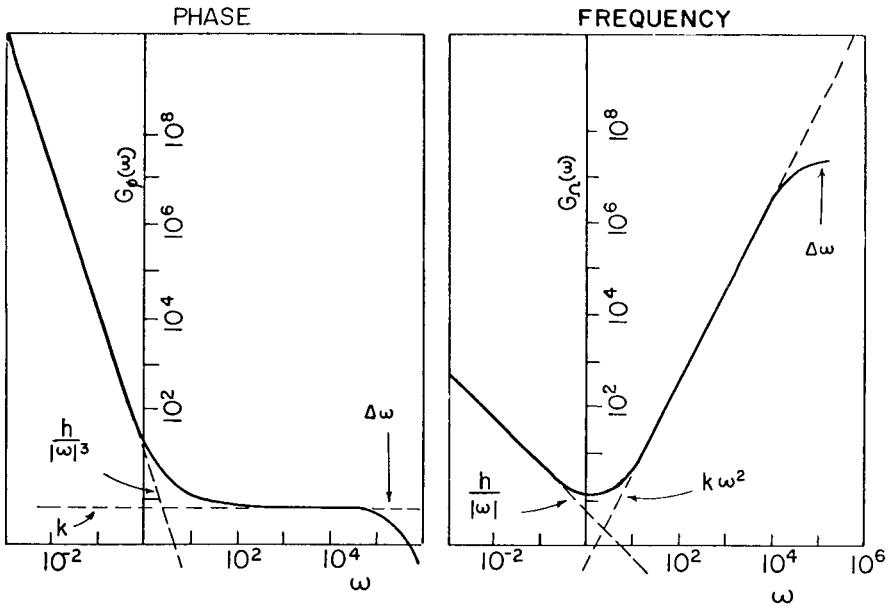

FIGURE 11-1.

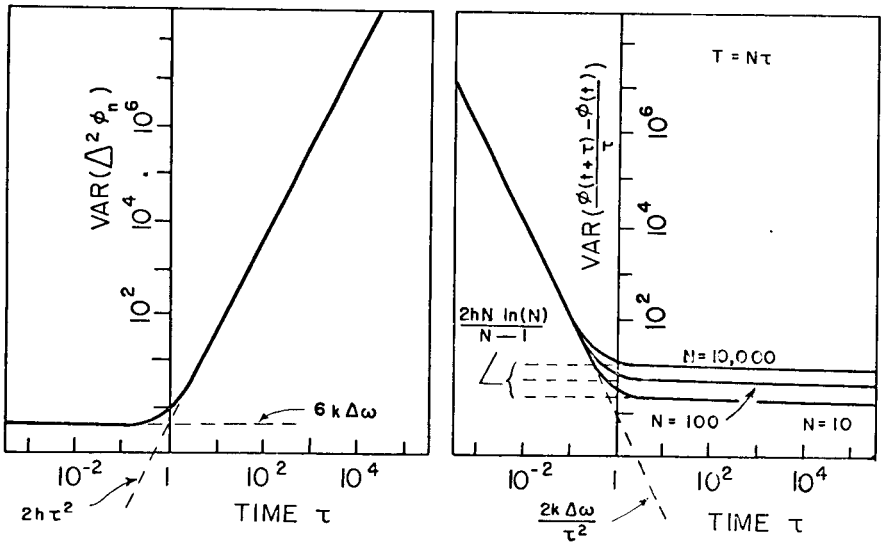

FIGURE 11-2.

correlated variable. Similarly one finds in general that $\Delta^k\phi_n$ is a stationary, cutoff-independent function for $k \geq 2$.

CONCLUSIONS

It is of value now to tie these types of frequency stability together by applying each method to the same theoretical model of an oscillator; in particular, consider an oscillator whose frequency is modulated by a flicker noise. Also, let the system generate an essentially white noise over its bandpass. Since this noise will appear to be half AM and half FM, the spectral densities of frequency and phase will appear as indicated in Figure 11-1. On the basis of this model, the graphs of Figure 11-2 were obtained.

It is interesting to note that the effects of flicker noise on the variance of frequency fluctuations depend on the total averaging time (see Equation 7). Thus, if one were to let $N = T/\tau = 2$ (the smallest possible number for a variance), the oscillator would "appear" better than for any other N. However, one should take the ensemble average of many variances for $N = 2$ to obtain an acceptably precise figure for the variance.

The asymptotes of the curve showing the variance of the second difference differ from the asymptotes of the frequency curve by a function of N and a factor of τ^2. For this specialized case the three numbers k, h, and $\Delta\omega$ serve as a complete measure of frequency stability instead of giving values of a continuous function, such as spectral distribution or variance of the nth finite difference. For the variance of the frequency fluctuations, one has a stability measure which is a function of *two* continuous variables. It also is worth noting that this model, in fact, fits very well a broad class of commercially available oscillators.

One is led to the conclusion that there are some commonly quoted measures of frequency stability which are very impractical. The autocovariance function of phase and frequency and the total rms frequency fluctuations are not useful concepts in the definition of frequency stability, since it is very difficult to obtain them experimentally. While the rms frequency fluctuations for specified sample and averaging times is a meaningful quantity, it is very inconvenient to have a stability measure be a function of two variables. Thus, it is suggested that the more meaningful concepts are (power) spectral densities of phase and frequency fluctuations and the variances of the second and higher finite differences of the phase.

With the difficulty of defining an rms frequency, one sees also the difficulty of measuring the true (power) spectral density of the output voltage of an oscillator. Indeed, as one makes his analyzer narrower in bandwidth and takes longer to sweep the line, the spectrum looks worse and worse.

REFERENCES

1. LIGHTHILL, M., "Introduction to Fourier Analysis and Generalised Functions," Cambridge, 1962.
2. BARNES, J. A., "Atomic Timekeeping and the Statistics of Precession Signal Generators," to be published.

A Statistical Model of Flicker Noise

J. A. BARNES AND D. W. ALLAN

***Abstract*—By the method of fractional order of integration, it is shown that it is possible to generate flicker noise from "white" noise. A formal expression for the relation of flicker noise to white noise is given. An approximate method, amenable to the use of digital computers, is also given for the generation of flicker noise modulated numbers from random, independent numbers.**

INTRODUCTION

FLICKER noise is a noise characterized by a *power* spectral density which varies inversely proportional to frequency. This type of noise has been found in many devices including semiconductors and quartz crystal oscillators. The presence of this type of noise modulating the frequency of high-quality oscillators has been of particular interest to the authors, and it is in this application that the present paper is directed. The principles used, however, are applicable to flicker noise in general but find convenient expression in terms of the phase and frequency of an oscillator.

Manuscript received November 8, 1965.
The authors are with the National Bureau of Standards, Boulder, Colo.

Many books in noise theory [1] establish the relation,

$$S_{\dot{f}}(\omega) = |\omega|^2 S_f(\omega) \tag{1}$$

between the power spectral density $S_f(\omega)$ of a function $f(t)$ and the power spectral density $S_{\dot{f}}(\omega)$ of the derivative of $f(t)$. In the work which follows it will be assumed that if $\dot{f}(t)$ has a power spectral density $S_{\dot{f}}(\omega)$, then $f(t)$ also has a power spectral density $S_f(\omega)$. Equation (1) may be inverted to the form

$$S_f(\omega) = \frac{1}{|\omega|^2} S_{\dot{f}}(\omega). \tag{2}$$

This integration [$\dot{f}(t)$ to $f(t)$] cannot, however, guarantee the stationarity of $f(t)$ and, hence, it is not obvious that the power spectral density of $f(t)$ can be defined in an unambiguous fashion even though $\dot{f}(t)$ may be completely well behaved. Indeed the formal justification for the existence of a flicker noise power spectral density is lacking.

Statistical Model

Consider an ergodic ensemble of functions

$$f_n(t), \qquad n = 1, 2, 3, \cdots$$

such that the ensemble average is given by

$$\operatorname*{Lim}_{N\to\infty} \frac{1}{N} \sum_{n=1}^{N} f_n(t) \equiv \overline{f(t)} = 0, \tag{3}$$

where the bar indicates ensemble average. Since the ensemble is assumed ergodic, the autocovariance function $R_f(\tau)$ is given by

$$R_f(\tau) = \operatorname*{Lim}_{T\to\infty} \frac{1}{2T} \int_{-T}^{T} f_n(t+\tau) f_n(t)\, dt = \overline{f(t+\tau) f(t)},$$

and it will be further assumed that

$$R_f(\tau) = A\delta(\tau), \tag{4}$$

that is, white noise. The power spectral density of $f_n(t)$ is then given by

$$S_f(\omega) = k.$$

If now one assumes that there exists some function $g(t)$ such that

$$\frac{d}{dt} g(t) \equiv \dot{g}(t) = f(t)$$

according to (2) and the assumptions mentioned before,

$$S_g(\omega) = \frac{k}{|\omega|^2}.$$

Similarly, if $\dot{h}(t) = g(t)$, then

$$S_h(\omega) = \frac{k}{|\omega|^4}.$$

That is, each time the function is integrated, a factor of $|\omega|^{-2}$ is applied to the power spectral density. If we define $S_f^{(m)}(\omega)$ to be the power spectral density of the m-fold integral of $f(t)$, we may write

$$S_f^{(m)}(\omega) = \frac{k}{|\omega|^{2m}}.$$

In order to describe flicker noise frequency modulation, we are interested in the case where

$$2m = 1$$

or in other words the $\frac{1}{2}$th order integral of $f(t)$. In this model, $S_f^{(1/2)}(\omega)$ will be taken to represent the power spectral density of the instantaneous frequency. Since the instantaneous frequency of an oscillator is the derivative of the phase $\phi(t)$, one may write

$$S_\phi(\omega) = S_f^{(3/2)}(\omega)$$

for our present model of phase fluctuations.

The concept of fractional order of integration has long been developed and may be found in several references [2]. Thus we may consider an ensemble of oscillators whose phase $\phi_n(t)$ is given by the relation [3]

$$\phi_n(t) = \frac{1}{\Gamma(\lambda)} \int_0^t (t-u)^{\lambda-1} f_n(u)\, du \tag{5}$$

for $\lambda = \frac{3}{2}$, or

$$\phi_n(t) = \frac{1}{\Gamma(\frac{3}{2})} \int_0^t \sqrt{t-u}\, f_n(u)\, du.$$

One may now obtain several relations which are of use later:

$$\overline{\phi(t)} = \frac{2}{\sqrt{\pi}} \int_0^t \sqrt{t-u}\ \overline{f_n(u)}\, du = 0$$

from (3). Similarly

$$\overline{\phi(t)\phi(t+\tau)} = \frac{4A}{\pi} \int_0^t \sqrt{(t-u)^2 + \tau(t-u)}\, du$$

$$= \frac{A}{\pi} \left\{ (2t+\tau)\sqrt{t^2+t\tau} - \frac{\tau^2}{2} \ln \left[\frac{2t+\tau+2\sqrt{t^2+t\tau}}{\tau} \right] \right\} \tag{6}$$

from (4) and the δ-function behavior of $\overline{f(u)f(u')}$. Also

$$\overline{[\phi(t)]^2} = \frac{4A}{\pi} \int_0^t (t-u)\, du$$

$$= \frac{2At^2}{\pi}. \tag{7}$$

It should be noted that both (6) and (7) depend on t [i.e., $\phi_n(t)$ is nonstationary]. In order to further establish the connection of (5) with flicker noise, it is convenient to evaluate the quantity

$$\overline{(\Delta^2\phi)^2} \equiv \overline{[\phi(t+2\tau) - 2\phi(t+\tau) + \phi(t)]^2}.$$

That is the ensemble average of the square of the second difference of the phase [4]. One may write

$$\overline{(\Delta^2\phi)^2} = \overline{[\phi(t+2\tau)]^2} + 4\overline{[\phi(t+\tau)]^2} + \overline{[\phi(t)]^2} - 4\overline{[\phi(t+2\tau)\phi(t+\tau)]} - 4\overline{[\phi(t+\tau)\phi(t)]} + 2\overline{[\phi(t+2\tau)\phi(t)]}. \tag{8}$$

At this point the algebra becomes excessive. It is, however, of value to recognize that flicker noise is normally observed on equipment which has been operating for long periods of time. Thus, it is reasonable to consider the asymptotic behavior of (8) as $t/\tau \to \infty$. If one con-

siders first the terms not involving logarithms, it is possible to expand these terms in τ^2 times a descending series in $\rho \equiv t/\tau$. It is found that the coefficients of ρ^j for $j \geq -1$ vanish identically and thus only the logarithmic terms contribute to the asymptotic value. Thus (8) becomes

$$\overline{(\Delta^2\phi)^2} \approx \frac{2A\tau^2}{\pi} \cdot \ln \left\{ \frac{[2\rho + 1 + 2\sqrt{\rho^2 + \rho}][2\rho + 3 + 2\sqrt{(\rho+1)^2 + \rho + 1}]}{[\rho + 1 + \sqrt{\rho^2 + 2\rho}]^2} \right\} \tag{9}$$

which reduces to

$$\overline{(\Delta^2\phi)^2} \approx \left(\frac{4A}{\pi}\right)\tau^2 \ln 2 \tag{10}$$

for large t/τ. Comparison of this result with another treatment of flicker noise [4] indicates complete agreement for the dependence on τ.

The Generation of "Flicker Noise Numbers"

While it might be possible to have an analog computer evaluate (5), it is of value to generate a series of numbers which behave analogously to (10) for discrete τ. That is if ψ_j [the analog to $\phi(t)$] is a variable defined over the range of the integer j, then

$$\langle(\psi_{j+2N} - 2\psi_{j+N} + \psi_j)^2\rangle = kN^2,$$

where k is a constant and the brackets indicate an average over the entire range of j (N is the discrete analog of τ).

One can show [5] that if a_j is also a discrete variable, the mth-fold finite integral of a_j is given by

$$(\Delta^{-1})^m a_j = \frac{1}{\Gamma(m)} \sum_{i=1}^{j} (j + 1 - i)^{[m-1]} a_i, \tag{11}$$

where the brackets on the exponent are defined to mean

$$\chi^{[l]} \equiv \chi(\chi + 1)(\chi + 2) \cdots (\chi + l - 1). \tag{12}$$

Equation (11) is thus the discrete analog to (5). Unfortunately (12) does not have an obvious generalization to fractional exponents.

This problem was approached in an experimental fashion. A set of numbers ψ_j were generated from a set of random, independent numbers a_i obtained from reference [6]. The ψ_j were related to the a_i according to the equation

$$\psi_j = \sum_{i=1}^{j} \sqrt{j + 1 - i}\, a_i \tag{13}$$

and computed on a digital computer. Using programs described elsewhere [4], [7], an attempt to classify the statistics of the set ψ_j was made. If one assumes that

$$\sqrt{\langle(\psi_{j+2N} - 2\psi_{j+N} + \psi_j)^2\rangle} = \alpha N^{\mu} \tag{14}$$

the values of μ obtained were 0.83 and 0.84. From (10) one sees that for flicker noise, μ should be the integer one.

A modification of (13) to the form

$$\psi_j = \sum_{i=1}^{j} (j + 1 - i)^{2/3} a_i \tag{15}$$

yielded data which conformed to (14) with a μ-value of one as closely as the experimental procedure allowed ($\mu = 1.00 \pm 0.05$). Thus (15) seems to generate flicker noise as precisely as our techniques of analysis can determine.

Conclusions

It has been shown that a half-order integral of white noise displays the properties of flicker noise. The existence of a formal expression relating flicker noise to white noise suggests the possibility of recognizing additional sources and physical mechanisms for the generation of flicker noise. It is possible to generate numbers with a digital computer [using (15)] which present properties similar to flicker noise, which is also of value. Thus it is possible to employ computer simulation of equipment perturbed by flicker noise processes.

Acknowledgment

The authors wish to acknowledge some very valuable discussions with L. Cutler of the Hewlett-Packard Company and Dr. R. Vessot of Varian Associates.

References

[1] W. Davenport and W. Root, *Random Signals and Noise*. New York: McGraw-Hill, 1958, ch. 6.

[2] R. Courant, *Differential and Integral Calculus*, vol. II. New York: Interscience, 1957, ch. IV, sec. 7.

[3] It has been suggested by L. Cutler that this result may also be obtained by multiplication of a white spectral density by $|\omega|^{-2\lambda}$. This corresponds to a filter in frequency domain of transfer function $(j\omega)^{-\lambda}$. The corresponding time function is then the convolution of the white noise time function with the transform of $(j\omega)^{-\lambda}$. This transform is $(t^{\lambda-1})/\Gamma(\lambda)$ for $t > 0$ (Campbell and Foster, *Fourier Integrals*. New York: Van Nostrand, 1948). The convolution is

$$\phi_n(t) = \frac{1}{\Gamma(\lambda)} \int_0^t f_n(u)(t - u)^{\lambda-1} du$$

which agrees with (5).

[4] J. Barnes, "Atomic timekeeping and the statistics of precision signal generators," this issue, page 207.

[5] C. Jordan, *Calculus of Finite Differences*. New York: Chelsea, 1950.

[6] Rand Corp., *A Million Random Digits with 100,000 Normal Deviates*. Glencoe, Illinois: Free Press, 1955.

[7] D. Allan, "Statistics of atomic frequency standards," this issue, page 221.

Atomic Timekeeping and the Statistics of Precision Signal Generators

JAMES A. BARNES

Abstract—Since most systems that generate atomic time employ quartz crystal oscillators to improve reliability, it is essential to determine the effect on the precision of time measurements that these oscillators introduce. A detailed analysis of the calibration procedure shows that the third finite difference of the phase is closely related to the clock errors. It was also found, in agreement with others, that quartz crystal oscillators exhibit a "flicker" or $|\omega|^{-1}$ type of noise modulating the frequency of the oscillator.

The method of finite differences of the phase is shown to be a powerful means of classifying the statistical fluctuations of the phase and frequency for signal generators in general. By employing finite differences it is possible to avoid divergences normally associated with flicker noise spectra. Analysis of several cesium beam frequency standards have shown a complete lack of the $|\omega|^{-1}$ type of noise modulation.

Introduction

AN ORDINARY clock consists of two basic systems: a periodic phenomenon (pendulum), and a counter (gears, clock face, etc.) to count the periodic events. An atomic clock differs from this only in that the frequency of the periodic phenomenon is, in some sense, controlled by an atomic transition (atomic frequency standard). Since microwave spectroscopic techniques allow frequencies to be measured with a relative precision far better than any other quantity, the desirability of extending this precision to the domain of time measurement has long been recognized [1].

From the standpoint of precision, it would be desirable to run the clock (counter) directly from the atomic frequency standard. However, atomic frequency standards in general are sufficiently complex that reliable operation over very extended periods becomes somewhat doubtful (to say nothing of the cost involved). For this reason, a quartz crystal oscillator is often used as the source of the "periodic" events to run a synchronous clock (or its electronic equivalent). The frequency of this oscillator is then regularly checked by the atomic frequency standard and corrections are made.

These corrections can usually take on any of three forms: 1) correction of the oscillator frequency, 2) correction of the indicated time, or 3) an accumulating

Manuscript received September 8, 1965; revised November 6, 1965.

The author is with the National Bureau of Standards, Boulder, Colo.

record of the difference from atomic time of the apparent or indicated time shown by the clock. Both methods 1) and 2) require a calculation of the time difference, and it is sufficient to consider only the last method and the errors inherent in it.

A careful consideration of the calibration procedure leads to the development of certain functionals of the phase which have a very important property—existence of the variance even in the presence of a flicker $(1/|\omega|)$ type of frequency noise. The simplest of these functionals, the second and third finite differences of the phase, turn out to be stationary, random variables whose auto-covariance function is sufficiently peaked to insure rapid convergence of the variance of a finite sample toward the true (infinite sample) variance. These functionals of the phase have the added features of being closely related to the errors of a clock run from the oscillator as well as being a useful measure of oscillator stability.

With the aid of these functionals, it is possible to classify the statistical fluctuations observed in various signal sources. In agreement with work of others [2]–[5], a flicker noise frequency modulation was observed for all quartz crystal oscillators tested. Similar studies on several commercial rubidium gas cells gave uniform indications of flicker noise modulation of levels comparable to those of the better quartz crystal oscillators.

In Section I, the effects on the precision of a time scale due entirely to the calibration procedure of the quartz crystal oscillator and the oscillator's inherent frequency instability are considered.

In Section II, the experimental results of Section I are used as the basis for a theoretical model of oscillator frequency fluctuations, and the results are compared to those of other experimenters.

In Section III, the statistics of an atomic frequency standard of the passive type (e.g., Cs-beam or Rb-gas cell) are considered, and the composite Clock system is treated. Section IV is devoted to a brief discussion of stability measures for signal sources.

I. Quartz Crystal Oscillator Phase Fluctuations

Typical Gross Behavior

Figure 1 shows a typical aging curve for a fairly good quartz crystal oscillator. The oscillator had been operating for a few months prior to the date shown in the graph. On May 1, 1963, the frequency of the oscillator was reset in order to maintain relatively small corrections.

Least square fits of straight lines to the two parts of Fig. 1 yield aging rates of 0.536×10^{-10} per day and 0.515×10^{-10} per day, respectively. This difference in aging rates could be explained by an acceleration of the frequency of about -9×10^{-15} per day per day. This acceleration of the frequency is sufficiently small over periods of a few days when compared to other sources of error that it can be safely ignored. Thus, the frequency of conventional quartz oscillators can be written in the form

$$\Omega(t) = \Omega_0[1 + \alpha t + \epsilon(t)] \tag{1}$$

where α is the aging rate, $\epsilon(t)$ is a variation of the frequency probably caused by noise processes in the oscillator itself, and t can be considered to be some rather gross measure of the time (since α and ϵ are quite small corrections).

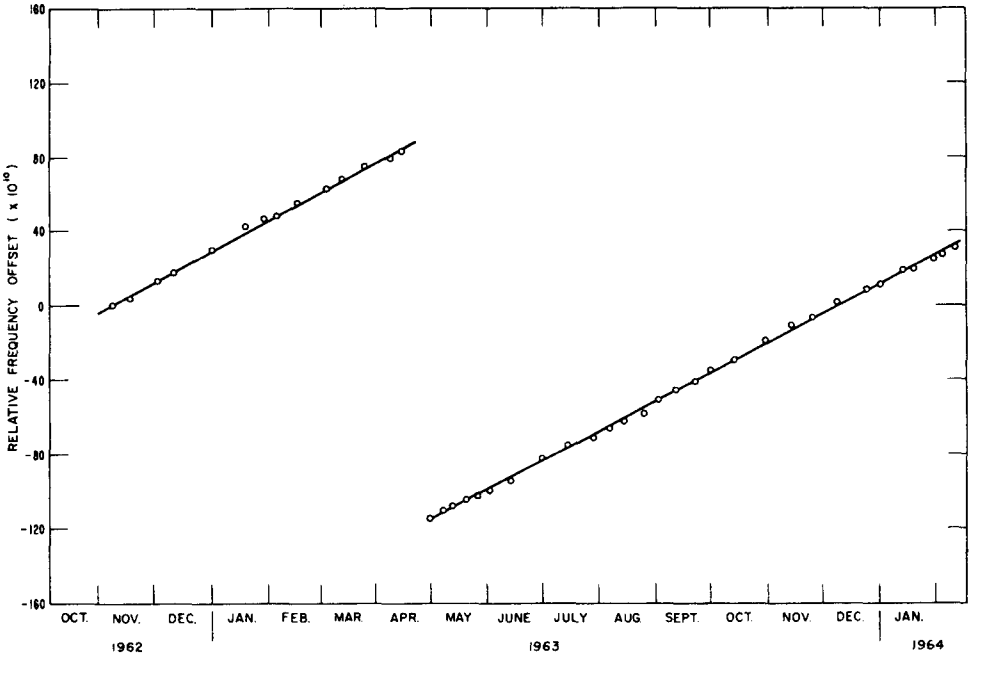

Fig. 1. Frequency aging of a good quartz crystal oscillator.

463-560 O - 72 - 30

Actual Calibration Procedure of a Clock System

The fundamental equation for atomic timekeeping is [6]

$$\Omega = \frac{d\phi}{dt}, \tag{2}$$

where Ω is the instantaneous frequency of the oscillator as measured by an atomic frequency standard, $d\phi$ is the differential phase change, and dt is an increment of time as generated by this clock system. Since *time* is to be generated by this system, and ϕ and Ω are the directly measured quantities, it is of convenience to assume that $\Omega=\Omega(\phi)$ and to write the solution of (2) in the form,

$$\Delta t = \int_{\phi_1}^{\phi_2} \frac{d\phi}{\Omega(\phi)}. \tag{3}$$

If one divides the output phase of the oscillator by Ω_0, and defines the apparent or indicated time t_A to be

$$t_A \equiv \frac{\phi}{\Omega_0}, \tag{4}$$

(1), (3), and (4) can be combined to give

$$\Delta t = \int_{t_{A1}}^{t_{A2}} \frac{dt_A}{1 + \alpha t_A + \dot{\epsilon}(t_A)}. \tag{5}$$

As it is indicated in Fig. 1, it is possible to maintain the magnitude of the relative frequency offset $|\alpha t_A+\dot{\epsilon}|$ within fixed bounds of 10^{-8}. Expanding (5) to first order in this relative frequency offset yields

$$\Delta t \simeq \Delta t_A - \int_{t_A}^{t_{A2}} [\alpha t_A + \dot{\epsilon}(t_A)]\, dt_A. \tag{6}$$

Equation (6) should then be valid to about one part in 10^{16}.

Normally the frequency of the oscillator is measured over some period of time (usually a few minutes) at regular intervals (usually a few days). At this point, it is desirable to restrict the discussion to the case where the calibration is periodic (i.e., period T, determined by t_A) and then generalize to other situations later. One period of the calibration is as follows:

t_A	start of calibration interval
$t_A+\frac{1}{2}(T-\tau)$	start of frequency measurement $(\tau<T)$
$t_A+\frac{1}{2}(T+\tau)$	end of frequency measurement
t_A+T	end of calibration interval,

where τ is the frequency measurement interval. If $\dot{\epsilon}$ were constant in time, the frequency measured during the interval $t_A+\frac{1}{2}(T-\tau)$ to $t_A+\frac{1}{2}(T+\tau)$ would be just the average frequency during the complete measurement interval T since the oscillator would have an exactly linear drift in frequency. Also, if $\dot{\epsilon}$ were constant, (6) could be written as

$$\Delta t = \Delta t_A - T\left\langle \frac{\delta\Omega}{\Omega_0} \right\rangle_\tau, \tag{7}$$

where $\langle\delta\Omega/\Omega_0\rangle_\tau$ is the average relative frequency offset during the interval $t_A+\frac{1}{2}(T-\tau)$ to $t_A+\frac{1}{2}(T+\tau)$.

Even though, in general, $\dot{\epsilon}$ is not constant, ϵ and $\dot{\epsilon}$ are not knowable, and thus one is usually reduced to using (7) anyway. The problem, then, is to determine how much error is introduced by using (7).

The time error δt accumulated over an interval T committed by using (7) can be expressed in the form,

$$\delta t = \int_{t_A}^{t_A+T} [\alpha t_A + \dot{\epsilon}]\, dt_A - T\left\langle \frac{\delta\Omega}{\Omega_0} \right\rangle, \tag{8}$$

where the quantity $\langle\delta\Omega/\Omega_0\rangle_\tau$ is given by

$$\left\langle \frac{\delta\Omega}{\Omega_0} \right\rangle_\tau = \frac{1}{\tau} \int_{t_A+1/2(T-\tau)}^{t_A+1/2(T+\tau)} [\alpha t_A + \dot{\epsilon}]\, dt_A. \tag{9}$$

Equations (8) and (9) can be combined to give

$$\delta t = \epsilon(t_A + T) - \epsilon(t_A) - \frac{T}{\tau}\left[\epsilon\left(t_A + \frac{T+\tau}{2}\right) - \epsilon\left(t_A + \frac{T-\tau}{2}\right)\right]. \tag{10}$$

It is this equation which relates the random phase fluctuations with the corresponding errors in the time determination.

Meaningful Quantities

It is again of value to further restrict the discussion to a particular situation and generalize at a later point. In particular, let $T=3\tau$, then (10) becomes

$$\delta t = \epsilon(t_A + 3\tau) - \epsilon(t_A) - 3[\epsilon(t_A + 2\tau) - \epsilon(t_A + \tau)]. \tag{11}$$

It is now possible to define the discrete variable ϵ_n by the relation

$$\epsilon_n \equiv \epsilon(t_A + n\tau), \qquad n = 0, 1, 2, \cdots$$

and rewrite (11) in the simpler form (see Table I)

$$\delta t \equiv \Delta^3\epsilon_n, \tag{12}$$

where $\Delta^3\epsilon_n$ is the third finite difference of the discrete variable ϵ_n.

TABLE I

FINITE DIFFERENCES

$\epsilon_n \equiv \epsilon(t_A+n\tau)$

Discrete variable		Definition
ϵ_n	ϵ_n	$\epsilon(t_A+n\tau)$
$\Delta\epsilon_n$	$\epsilon_{n+1}-\epsilon_n$	$\epsilon(t_A+\tau)-\epsilon(t_A)$
$\Delta^2\epsilon_n$	$\Delta\epsilon_{n+1}-\Delta\epsilon_n$	$\epsilon(t_A+2\tau)-2\epsilon(t_A+\tau)+\epsilon(t_A)$
$\Delta^3\epsilon_n$	$\Delta^2\epsilon_{n+1}-\Delta^2\epsilon_n$	$\epsilon(t_A+3\tau)-3[\epsilon(t_A+2\tau)-\epsilon(t_A+\tau)]-\epsilon(t_A)$
$\Delta^4\epsilon_n$	$\Delta^3\epsilon_{n+1}-\Delta^3\epsilon_n$	$\epsilon(t_A+4\tau)-4[\epsilon(t_A+3\tau)+\epsilon(t_A+\tau)]$ $+6\epsilon(t_A+2\tau)+\epsilon(t_A)$

Similarly, (2) may be integrated directly using (1) to obtain

$$\phi(t_A) = \Omega_0\left[t_A + \frac{\alpha}{2}t_A^2 + \epsilon(t_A)\right] + \phi(0). \qquad (13)$$

Thus, by defining another discrete variable ϕ_n, the third difference of (13) yields the relation

$$\Delta^3\phi_n = \Omega_0\Delta^3\epsilon_n, \qquad (14)$$

or equivalently,

$$\delta t = \left(\frac{1}{\Omega_0}\right)\Delta^3\phi_n. \qquad (15)$$

It is now possible to set up a table of meaningful quantities for time measurement (see Table II).

If three oscillators are used, it is possible to independently measure the three quantities σ_{12}, σ_{13}, and σ_{23}. Thus there exist three independent equations:

$$\left.\begin{aligned}\sigma_{12}^2 &= \sigma_1^2 + \sigma_2^2\\ \sigma_{13}^2 &= \sigma_1^2 + \sigma_3^2\\ \sigma_{23}^2 &= \sigma_2^2 + \sigma_3^2\end{aligned}\right\}. \qquad (18)$$

While the three equations,

$$\delta t_{ij} = \Delta^3\epsilon_n{}^{(i)} - \Delta^3\epsilon_n{}^{(j)} \qquad \begin{cases} i, j = 1, 2, 3 \\ i < j \end{cases},$$

are not linearly independent, the standard deviations σ_{ij}^2 given by (18), in fact, form linearly independent equations (subject only to certain conditions analogous to the triangle inequalities). Thus, the systems of (18) are solvable for the three quantities $\sigma_i^2 = \langle(\delta t_i)^2\rangle$. It is thus possible to estimate the statistical behavior of each individual oscillator.

TABLE II

MEANINGFUL QUANTITIES

Quantity		Discussion
Phase	$\{\phi_n$	Must exist for all times of interest and be measurable.
First difference of the phase	$\{\Delta\phi_n$	Proportional to the average frequency in the interval τ. Must exist for all time.
Second difference of the phase	$\{\Delta^2\phi_n$	Related to the drift of the oscillator frequency. Must exist for all time.
Variance of the second difference	$\{\langle[\Delta^2\phi_n - \langle\Delta^2\phi_n\rangle]^2\rangle$	(It is possible to construct a time scale even if this does not exist. However, experiment indicates that it is probably finite.)
Third difference of the phase	$\{\Delta^3\phi_n$	Proportional to the clock error in the time interval $T = 3\tau$. Must exist if clock is to be of value.
Mean square third difference	$\{\langle(\Delta^3\phi_n)\rangle^2$	Proportional to the precision of time interval measurements. Must exist if clock is to be of value.

Where all averages are defined by the relation:

$$\langle f(t)\rangle = \lim_{T\to\infty}\frac{1}{T}\int_{-T/2}^{T/2} f(t)dt.$$

Experimental Determination of Phase Fluctuations

If one measures the phase difference between two oscillators, (15) applies to both, and hence the difference phase $\theta_n = \phi_n{}^{(1)} - \phi_n{}^{(2)}$ is related to the difference time $\delta t_{12} = \delta t_1 - \delta t_2$ by the relations

$$\delta t_{12} = \frac{1}{\Omega_0}\Delta^3\theta_n = \Delta^3\epsilon_n{}^{(1)} - \Delta^3\epsilon_n{}^{(2)}. \qquad (16)$$

Provided that the cross-correlation coefficient $\langle(\Delta^3\epsilon_n{}^{(1)})(\Delta^3\epsilon_n{}^{(2)})\rangle$ is zero (i.e., the $\epsilon_n{}^{(i)}$ are noncorrelated), the variance of δt_{12} becomes

$$\sigma_{12}^2 \equiv \langle(\delta t_{12})^2\rangle = \langle(\Delta^3\epsilon_n{}^{(1)})^2\rangle + \langle(\Delta^3\epsilon_n{}^{(2)})^2\rangle, \qquad (17)$$

since it is assumed that $\langle\Delta^3\epsilon_n\rangle = 0$. The assumption that the cross-correlation coefficients vanish is equivalent to postulating an absence of linear coupling between the oscillators either electrically or through their environment. It is of value to develop a scheme which is capable of classifying individual oscillators rather than treating ensembles of assumed identical members. Thus, this development is restricted to time averages of individual oscillators rather than ensemble averages.

Apparatus

A phase meter was used similar to one described in Cutler and Searle [5]. The basic system was aligned with an electrical-to-mechanical angle tolerance of about ± 0.25 percent of one complete cycle, and since the phase meter is operated at 10 Mc/s, this implies the possibility of measuring the time difference to ± 0.25 nanoseconds. The output shaft, in turn, drives a digital encoder with one hundred counts per revolution and a total accumulation (before starting over) of one million. Thus the digital information is accurate to within one ns and accumulates up to one ms. Since measurements are made relatively often, it is easy for a computer to spot when the digital encoder has passed one ms on the data, and this restriction on the data format in no way hampers the total length of the data handled.

Since the oscillator is assumed to have a linear drift in frequency with time, the variance (about the mean)

of the second difference of the phase should depend only on the $\epsilon_n^{(i)}$. For the evaluation of clocks, it is the mean square time error which is important and, thus, the mean square (rather than variance) of the third difference of the phase is the quantity of importance. Calculations of these quantities from the phase θ_n were accomplished on a digital computer. Normally the phase difference is printed every hour for at least 200 hours and the computer program computes the $\Delta^2\theta_n$ and $\Delta^3\theta_n$ for τ equal to 2, 4, 6, 8, etc., hours. Thus it is possible to plot the square root of the variance of the second difference and the root mean square third difference of the phase as a function of the variable τ. A typical plot of these two quantities appears in Fig. 2.

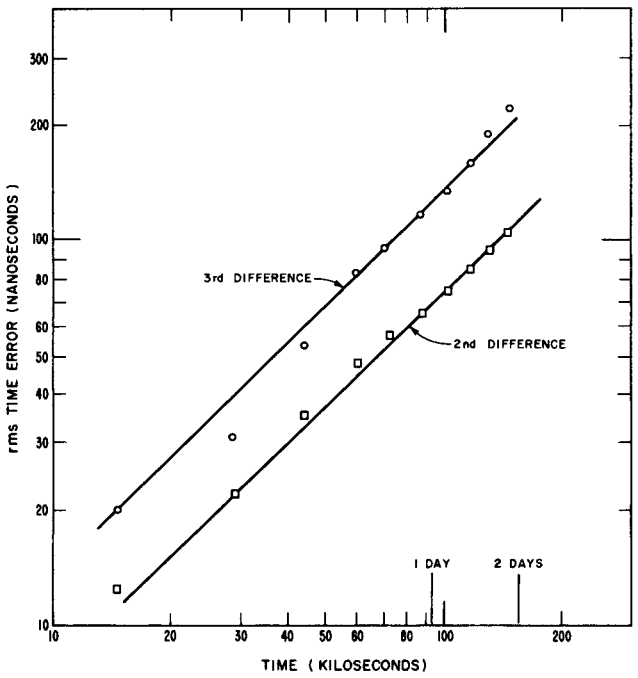

Fig. 2. Variance of second and third difference as a function of τ.

Since many revolutions of the phase meter are normally encountered between data points, the combined effects of nonperfect electrical-to-mechanical phase and rounding errors of the digital encoder can be combined into one stationary, statistical quantity γ, that can be assumed to have delta-function auto-correlation. Let χ represent the rounding errors of the digital encoder defined by the difference between the encoded number and the actual angular position of the shaft. Then these rounding errors form a rectangular distribution from -0.5 ns to $+0.5$ ns, and, thus, contribute an amount

$$\frac{\int_{-1/2}^{1/2} \chi^2\, d\chi}{\int_{-1/2}^{1/2} d\chi} = 0.08 \text{ ns}^2$$

to $\langle\gamma^2\rangle$. The nonperfect electrical-to-mechanical phase conversion is sinusoidal in nature and, thus, contributes an amount equal to

$$\tfrac{1}{2}(0.25)^2 \simeq 0.03 \text{ ns}^2.$$

The final value for $\langle\gamma^2\rangle$ should then be about 0.11 ns^2.

This was checked by taking two very good oscillators operating at a rather large difference frequency ($\sim 5\times10^{-9}$), and printing the phase difference every 10 seconds for several minutes. Since frequency fluctuations of the oscillators are small compared to 1×10^{-10}, the resultant scatter can be attributed to the measuring system. The results of this experiment gave the value 0.19 ns^2 for $\langle\gamma^2\rangle$.

Since γ is assumed to have a delta-function auto-correlation, reference to Table I shows that $\langle(\Delta^3\gamma)^2\rangle = 20\langle\gamma^2\rangle$, and thus (18) may be more precisely written,

$$\left.\begin{aligned} \sigma_{12}^2 &= \sigma_1^2 + \sigma_2^2 + 20\langle\gamma^2\rangle \\ \sigma_{13}^2 &= \sigma_1^2 + \sigma_3^2 + 20\langle\gamma^2\rangle \\ \sigma_{23}^2 &= \sigma_2^2 + \sigma_3^2 + 20\langle\gamma^2\rangle \end{aligned}\right\}. \qquad (18')$$

For the best oscillators tested, σ_{ij}^2 became about $2\langle(\Delta^3\gamma)^2\rangle$ for $\tau = 10^3$ seconds, and, therefore, measurements were limited on the lower end to 20 minutes or 1200 seconds. The longest run made lasted a little over a month or about one thousand hours. Thus the largest value of τ which might have reasonable averaging is about one hundred hours or 3.6×10^5 seconds. This limits the results to about two orders of magnitude variation on τ.

While it is possible to build appropriate frequency multipliers and mixers to improve the resolution of the phase meter and reduce the lower limit on τ, it was considered that the longer time intervals are of greater interest because T $(=3\tau)$ is normally between one day and one week.

II. Theoretical Development

Introductory Remarks

In the development which follows, certain basic assumptions are made. It is assumed that the coefficients Ω_0 and α of (1) may be so chosen that the average value of $\epsilon(t)$ is zero; i.e.,

$$\langle\epsilon(t)\rangle = 0.$$

It is also assumed that a translation in the time axis, $t_A \rightarrow t_A + \zeta$, (stationarity) causes no change in the value of the auto-covariance function,

$$\begin{aligned} R_\epsilon(\tau) &= \langle\epsilon(t)\cdot\epsilon(t+\tau)\rangle \\ &\equiv \langle\epsilon(t+\xi)\cdot\epsilon(t+\xi+\tau)\rangle. \end{aligned} \qquad (19)$$

The only justification of this assumption lies in the fact that the results of the analysis agree well with experiment and the results of others. In the development which follows, one *cannot* assume that

$$R_\epsilon(0) = \langle[\epsilon(t)]^2\rangle$$

exists (i.e., is finite) and, hence, Wiener [7] cannot guarantee that (19) is valid. While it may be that $R_\epsilon(\tau)$ does not exist, quantities such as

$$U(\tau) = 2[R_\epsilon(0) - R_\epsilon(\tau)] \tag{20}$$

may exist and be meaningful if limits are approached properly. It is, thus, assumed that relations such as (20) have meaning and may be handled by conventional means.

Development of Experimental Results

All oscillator pairs tested, which exhibited a stable drift rate as indicated in Fig. 1 and did not have obvious diurnal fluctuations in frequency, showed a definite, very nearly linear dependence on τ for both the standard deviation of the second difference and the root mean square third difference of the phase. It was observed that if an oscillator were disturbed accidentally during a measurement, the plot would have a more nearly $\tau^{3/2}$ dependence. This is probably because the assumption of a negligible quadratic dependence of frequency with time is not valid when the oscillator is disturbed. All oscillators tested, therefore, were shock mounted and all load changes and physical conditions were changed as little as possible.

A least square fit of all reliable data to an equation of the form

$$\sqrt{\langle(\Delta^m\epsilon_n)^2\rangle} = \sqrt{k_m}\tau^\mu \qquad m = 2, 3, 4 \tag{21}$$

gave a value of 1.09 for the average of the μ's. The values of μ ranged from about 0.90 to 1.15 (and even to 1.5 when the oscillators were disturbed during the measurement). It is of interest to postulate that, for an "ideal," undisturbed quartz crystal oscillator, the value of μ is exactly the integer one, and to investigate the consequences of this assumption.

Because certain difficulties arise at the value $\mu = 1$, it is essential to calculate with a general μ and then pass to the limits $\mu \to 1^{(-)}$ for the quantities of interest. This is equivalent to considering a sequence of processes which approach, as a limit, the case of the "ideal" crystal oscillator. Thus (21) may be rewritten for $m = 2$ in the form

$$\langle(\Delta^2\epsilon_n)^2\rangle = k_2 \mid \tau \mid^{2\mu}. \tag{22}$$

Using Table I, (22) may then be rewritten as

$$6\langle[\epsilon(t_A)]^2\rangle - 8\langle\epsilon(t_A)\cdot\epsilon(t_A+\tau)\rangle + 2\langle\epsilon(t_A)\cdot\epsilon(t_A+2\tau)\rangle = k_2 \mid \tau \mid^{2\mu}$$

or, equivalently,

$$6R_\epsilon(0) - 8R_\epsilon(\tau) + 2R_\epsilon(2\tau) = k_2 \mid \tau \mid^{2\mu}. \tag{23}$$

As mentioned above, the function $U(\tau)$ is defined by the relation

$$\begin{aligned} U(\tau) &\equiv \langle[\epsilon(t_A) - \epsilon(t_A + \tau)]^2\rangle \\ &= 2[R_\epsilon(0) - R_\epsilon(\tau)] \end{aligned} \tag{24}$$

and is assumed to exist. Equations (23) and (24) may be combined to give

$$4U(\tau) - U(2\tau) = k_2 \mid \tau \mid^{2\mu}. \tag{25}$$

If a trial solution of the form

$$U(\tau) = A(\beta)\cdot \mid \tau \mid^\beta$$

is used, one obtains

$$A(\beta)\cdot \mid \tau \mid^\beta [4 - 2^\beta] = k_2 \mid \tau \mid^{2\mu}$$

from which one concludes that

$$\beta = 2\mu \leq 2,$$
$$(4 - 2^\beta)A(\beta) = k_2,$$

and

$$U(\tau) = \frac{2}{4 - 2^{2\mu}} \mid \tau \mid^{2\mu}, \tag{26}$$

where $\mu \leq 1$ since $U(\tau)$ and k_2 are non-negative. Equation (21) may, thus, be satisfied if

$$\lim_{\mu \to 1^{(-)}} (4 - 2^{2\mu})A(2\mu) = k_2, \tag{27}$$

which implies that $A(2)$ is infinite. It is for this reason that the limiting process must be employed.

It is not necessary, however, to assume a particular form for $A(2\mu)$ because (27) is sufficient for the purposes of this development.

It is now possible to determine the mean square third difference of ϵ_n; i.e., from Table I,

$$\begin{aligned} \langle(\Delta^3\epsilon_n)^2\rangle &= 20\langle[\epsilon(t_A)]^2\rangle - 30\langle[\epsilon(t_A)\cdot\epsilon(t_A + \tau)]\rangle \\ &\quad + 12\langle[\epsilon(t_A)\cdot\epsilon(t_A + 2\tau)]\rangle - 2\langle[\epsilon(t_A)\cdot\epsilon(t_A + 3\tau)]\rangle, \end{aligned} \tag{28}$$

where use has again been made of (19). Equation (28) may equivalently be written in the form

$$\langle(\Delta^3\epsilon_n)^2\rangle = 15U(\tau) - 6U(2\tau) + U(3\tau), \tag{29}$$

which may be combined with (26) to yield

$$\langle(\Delta^3\epsilon_n)^2\rangle = \frac{k_2 \mid \tau \mid^{2\mu}}{(4 - 2^{2\mu})}[15 + 6(2^{2\mu}) + 3^{2\mu}]. \tag{30}$$

If one now passes to the limit $\mu \to 1^{(-)}$, (30) becomes

$$\langle(\Delta^3\epsilon_n)^2\rangle = \frac{k_2\tau^2(24 \ln 2 - 9 \ln 3)}{4 \ln 2}. \tag{31}$$

Thus, a quadratic dependence of the variance of the second difference of the phase implies a quadratic dependence of the mean square third difference, and the ratio

$$\sqrt{\frac{\langle(\Delta^3\epsilon_n)^2\rangle}{\langle(\Delta^2\epsilon_n)^2\rangle}} = 1.5601 \cdots \tag{32}$$

is independent of τ. The average ratio of the points plotted in Fig. 2 is 1.65. Values ranging from 1.4 to 1.7 were observed for various runs on different oscillator pairs. Average value for all reliable data taken is 1.52.

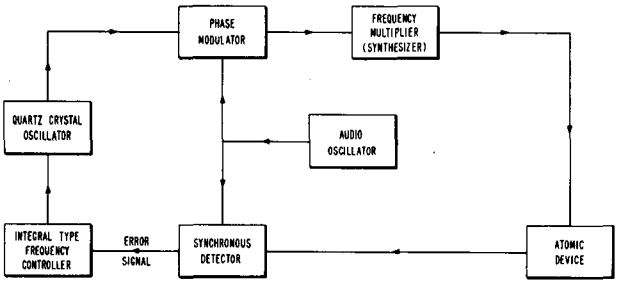

Fig. 3. Typical control loop for an atomically controlled oscillator.

Generalization of the Time Error Problem

The average frequency of an oscillator over an interval of time is just the total elapsed phase in the interval divided by the time interval. Since errors of the frequency standard are not presently being considered, the calibration interval of Section I gives rise to an error time δt which could be expressed as a sum

$$\delta t = \frac{1}{\Omega_0} \sum_{n=0}^{m} a_n \phi(t_A + b_n \tau), \tag{33}$$

where $m+1$ is the total number of terms and the set $\{a_n, b_n\}$ are chosen to fit the particular calibration procedure. Indeed, any calibration procedure must give rise to an error time which is expressible in the form of (33).

There are, however, certain restrictions on the $\{a_n, b_n\}$ which are of importance. First, it is a matter of convenience to require that $b_l > b_n$ for $l > n$. Also, if the oscillator were absolutely perfect, and $\epsilon(t_A)$ were identically zero, one should logically require that the error time δt be identically zero, independent of t_A, the drift rate α, and the basic time interval τ. That is, from (13)

$$\delta t = \sum_{n=0}^{m} a_n \cdot (t_A + b_n \tau) + \frac{\alpha}{2} \sum_{n=0}^{m} a_n \cdot (t_A + b_n \tau)^2 \equiv 0 \tag{34}$$

for all t_A, α, and τ. One is thus led to the three conditions:

$$\sum_{n=0}^{m} a_n = 0, \tag{35}$$

$$\sum_{n=0}^{m} a_n b_n = 0, \tag{36}$$

$$\sum_{n=0}^{m} a_n b_n^2 = 0. \tag{37}$$

It is of interest to form the quantity

$$\left(\sum_{n=0}^{m} a_n b_n^2 \right) \left(\sum_{n=0}^{m} a_l \right) = \sum_{n=0}^{m} a_n^2 b_n^2 + \sum_{n<l}^{m} a_n a_l b_n^2 + \sum_{l<n}^{m} a_n a_l b_n^2, \tag{38}$$

and it is now possible to interchange the subscripts n and l in the last term of (38) and write the equation in the form

$$\sum_{n=0}^{m} a_n^2 b_n^2 + \sum_{n<l}^{m} a_n a_l (b_n^2 + b_l^2) = 0. \tag{39}$$

Subtracting the square of (36),

$$\left(\sum_{n=0}^{m} a_n b_n \right) \left(\sum_{l=0}^{m} a_l b_l \right) = \sum_{n=0}^{m} a_n^2 b_n^2 + 2 \sum_{n<l}^{m} a_n a_l b_n b_l,$$

one obtains

$$\sum_{n<l}^{m} a_n a_l (b_l - b_n)^2 = 0 \tag{40}$$

as another condition on the $\{a_n, b_n\}$. Equation (40) is, of course, not independent of (35)–(37).

For the actual situation where $\epsilon(t_A)$ is not identically zero, one is reduced, as before [see (7)], to using conditions (35)–(37) since $\epsilon(t_A)$ is not knowable. The time error then becomes

$$\delta t = \sum_{n=0}^{m} a_n \cdot \epsilon(t_A + b_n \tau) \tag{41}$$

where use has been made of (13), (33), and the restrictions (35)–(37). Note that (41) is the generalization of (10). The square of (41) can be written in the form

$$(\delta t)^2 = \sum_{n=0}^{m} a_n^2 \epsilon^2(t_A + b_n \tau) + 2 \sum_{n<l}^{m} a_n a_l [\epsilon(t_A + b_n \tau) \cdot \epsilon(t_A + b_l \tau)], \tag{42}$$

which may be averaged over t_A to yield

$$\langle (\delta t)^2 \rangle = \sum_{n=0}^{m} a_n^2 \langle (\epsilon(t_A))^2 \rangle + 2 \sum_{n<l}^{m} a_n a_l \langle [\epsilon(t_A) \cdot \epsilon(t_A + (b_l - b_n)\tau)] \rangle, \tag{43}$$

where use has again been made of (19).

The square of (35) may be written as

$$\sum_{n=0}^{m} a_n^2 + 2 \sum_{n<l}^{m} a_n a_l = 0,$$

and (43) then becomes

$$\langle (\delta t)^2 \rangle = - \sum_{n<l}^{m} a_n a_l \{ \langle \epsilon^2(t_A) \{ 2 \langle \epsilon^2(t_A) \rangle - 2 \langle [\epsilon(t_A) \cdot \epsilon(t_A + (b_l - b_n)\tau)] \rangle \}. \tag{44}$$

Combining (44) with (21) one obtains

$$\langle (\delta t)^2 \rangle = - \sum_{n<l} a_n a_l U((b_l - b_n)\tau). \tag{45}$$

Substitution of (26) in (45) yields

$$\langle(\delta t)^2\rangle = -k_2 |\tau|^{2\mu} \frac{\sum_{n<l}^{m} a_n a_l (b_l - b_n)^{2\mu}}{4 - 2^{2\mu}}, \quad (46)$$

which is indeterminate of the form (0/0) for $\mu = 1$ because of (40). Making use of L'Hospital's rule, the limit of this expression as $\mu \to 1^{(-)}$ is

$$\langle(\delta t)^2\rangle = \frac{k_2 \tau^2}{4 \ln 2} \sum_{n<l}^{m} a_n a_l (b_l - b_n)^2 \ln (b_l - b_n). \quad (47)$$

Equation (47) is thus the generalization of (31). Since many terms appear in the summation in (47), a computer program was written for evaluation with particular sets of $\{a_n, b_n\}$.

Comparison With Others

If one were to assume that (20) could be solved for $R_\epsilon(\tau)$, one would obtain

$$R_\epsilon(\tau) = R_\epsilon(0) - \tfrac{1}{2} U(\tau) \quad (48)$$

which expresses the auto-covariance function in terms of $U(\tau)$. If one assumes still further that the Wiener-Khinchin theorem applies to (48), the power spectral density of $\epsilon(t)$ is then the Fourier transform of $R_\epsilon(\tau)$; i.e.,

$$S^2(\omega) = \text{F.T.}\left[R_\epsilon(0) - \frac{k_2 |\tau|^{2\mu}}{2(4 - 2^{2\mu})}\right].$$

Fortunately, Fourier transforms of functions like $|\tau|^{2\mu}$ have been worked out in Lighthill [8]. The result is

$$S_\epsilon(\omega) = \frac{R_\epsilon(0)}{2\pi} \delta(\omega) - \frac{k_2 \left[\cos \frac{\pi(2\mu + 1)}{2}\right] [(2\mu)!] |\omega|^{-2\mu-1}}{2\pi(4 - 2^{2\mu})}. \quad (49)$$

The factor of $(1/2\pi)$ occurs because $S_\epsilon(\omega)$ is assumed to be a density relative to an angular frequency ω, rather than a cycle frequency ($f = \omega/2\pi$) as is used in [8]. The first term on the right of (49) indicates an infinite density of power at zero frequency, i.e., a nonzero average. The zero frequency components are not measurable experimentally, and hence this term will be dropped as not being significant to these discussions. The second term on the right of (49) is indeterminate for $\mu = 1$. As before, the limit as $\mu \to 1^{(-)}$ may be obtained, yielding

$$S_\epsilon(\omega) = \frac{k_2}{8 \ln 2} |\omega|^{-3} \quad (50)$$

for the final result.

The assumptions needed to arrive at (50) are not wholly satisfying, and it is of value to show that (50) implies that $\langle(\Delta^2 \epsilon_n)^2\rangle$ is indeed given by (21) for $m = 2$. Only one additional assumption is needed, the Wiener-Khinchin theorem. Since $R_\epsilon(\tau)$ and $S_\epsilon(\omega)$ are real quantities, this theorem may be written in the form

$$R_\epsilon(\tau) = 2 \int_0^\infty S_\epsilon(\omega) \cos \omega\tau \, d\omega. \quad (51)$$

From Table I, one may obtain (after squaring and averaging) the expression

$$\langle(\Delta^2 \epsilon_n)^2\rangle = 6R_\epsilon(0) - 8R_\epsilon(\tau) + 2R_\epsilon(2\tau). \quad (52)$$

Substitution of (51) in (52) yields

$$\langle(\Delta^2 \epsilon_n)^2\rangle = 4 \int_0^\infty S_\epsilon(\omega)[3 - 4 \cos(\omega\tau) + \cos(2\omega\tau)] \, d\omega. \quad (53)$$

Using (50) for $S_\epsilon(\omega)$ is a lengthy but straightforward process to evaluate the integral in (53). The result is, in fact,

$$\langle(\Delta^2 \epsilon_n)^2\rangle = k_2 \tau^2,$$

in agreement with (21).

If $g_\epsilon(\omega)$ is the Fourier transform of $\epsilon(t)$, it is shown, for example, in Lighthill ([8] p. 20), that

$$g_{\dot\epsilon}(\omega) = i\omega g_\epsilon(\omega)$$

is the Fourier transform of $\dot\epsilon(t)$. Thus, the power spectral density of $\dot\epsilon(t)$ is related to the power spectral density of $\epsilon(t)$ by the familiar relation

$$S_{\dot\epsilon}(\omega) = \omega^2 S_\epsilon(\omega).$$

Thus, the power spectral density of the *frequency* fluctuations of an "ideal" oscillator may be given as

$$S_{\dot\epsilon}(\omega) = \frac{k_2}{8 \ln 2} |\omega|^{-1},$$

that is, flicker noise frequency modulation. The existence of this type of noise modulating the frequency of good quartz crystal oscillators has been reported by several others [2]–[5], [9].

Comments on the "Ideal" Oscillator

It has thus been shown that the assumptions of stationarity and "ideal" behavior form a basis for a mathematical model of a quartz crystal oscillator which is in quite good agreement with several experiments and experimenters. On the basis of this model, it is now possible to predict the behavior of systems employing "nearly ideal" oscillators with the hope of committing no great errors. There are compelling reasons to believe that $U(\tau)$ actually exists (see Section IV) for real oscillators in spite of (26). Such conditions require that the $|\omega|^{-1}$ behavior for the power spectral density of the frequency fluctuations cut off at some small, nonzero frequency. From some experiments [2] conducted, however, this cutoff frequency is probably much smaller than one cycle per year. Such small differences from

zero frequency are of essentially academic interest to the manufacturer and user of oscillators. Quantities which may be expressed in the form of (41), however, where the coefficients satisfy conditions (35)–(37), have finite averages even in the limit as flicker noise behavior approaches zero modulation frequency. Such quantities are called cutoff *in*dependent in contrast to quantities like $U(\tau)$ which will exist only if the flicker noise cuts off at some nonzero frequency.

III. Atomic Frequency Standards

Passive Devices

There are in use today two general types of atomic frequency standards: 1) the active device such as a maser whose atoms actually generate a coherent signal whose frequency *is* the standard, and 2) the passive type such as a cesium beam or rubidium gas cell. In the passive type, a microwave signal irradiates the atoms and some means is employed to detect any change in the atom's energy state. This paper is restricted to the passive type of frequency standard. Some experiments are in progress, however, to determine the statistical behavior of a maser type oscillator.

It is first of value to discuss in what way a "standard" can have fluctuations or errors. Consider the cesium beam. *Ideally* the standard would be the exact frequency of the photons emitted or absorbed at zero magnetic field in the $(F=4,\ m_f=0)\leftrightarrow(F=3,\ m_f=0)$ transition of cesium^{133} in the ground electronic state for an infinite interaction time. This is, of course, impossible. This means that the standard is at least less than ideal and one is, thus, led to speak, in some sense of the word, about "errors" or even "fluctuations" of the standard.

Figure 3 shows a block diagram of a typical standard of the passive type. An equivalent diagram of this frequency-lock servo is shown in Fig. 4, where $V_1(\omega)$ is the Fourier Transform of the noise generated in the detectors, associated demodulating circuitry, and the frequency multipliers of Fig. 3. $V_2(\omega)$ is an equivalent noise voltage driving the reactance tube in the oscillator to produce the $\epsilon(t_A)$ term in the unlocked oscillator, such that flicker noise FM results. The power spectrum of $V_2(\omega)$, then, is given by

$$C^2S_{V_2} = \frac{h_s}{|\omega|}, \tag{54}$$

where $h_s/|\omega|$ is the power spectral density of the *frequency* fluctuations of the unlocked oscillator.

It is easiest to treat the servo equations by the use of the variable $\dot{\gamma}$, defined to be the difference between the output frequency of the multiplier and the "ideal" frequency of the atomic transition (the output of the "atomic device," as shown in Fig. 4, is then assumed to be the constant zero). In order to preserve the dimensions of voltage for the addition networks, it is convenient to assume that the output of the subtraction network is $-\beta\dot{\gamma}$ where β has the dimensions of volt-seconds. Thus, the equation governing the operation of the servo can be expressed, in the frequency domain, as

$$\left[V_2(\omega) + \frac{V_1(\omega) - \beta\dot{\gamma}(\omega)}{j\omega\tau_1}\right]CN = \dot{\gamma}(\omega). \tag{55}$$

This leads to a power spectral density for $\dot{\gamma}$ given by

$$S_{\dot{\gamma}}(\omega) = \frac{(NC)^2S_{V_1}(\omega) + N^2\tau_1^2h_s|\omega|}{\omega^2\tau_1^2 + (\beta NC)^2} \tag{56}$$

where use has been made of (54).

Normally, $\omega\tau_1$ becomes of the order of (βNC) for ω of the order of 10 s^{-1}. Thus, for small ω, (56) becomes

$$S_{\dot{\gamma}}(\omega) \approx \frac{1}{\beta^2}S_{V1}(\omega) \tag{57}$$

for $|\omega| < 1$ s^{-1}.

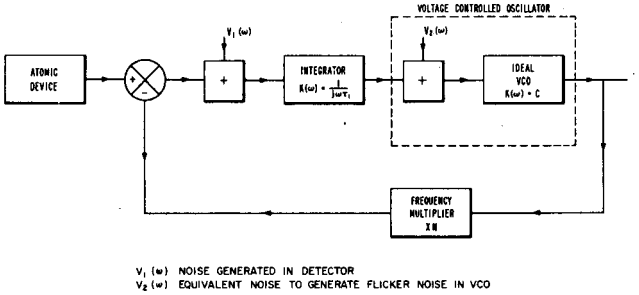

Fig. 4. Equivalent servo diagram of passive type frequency standard.

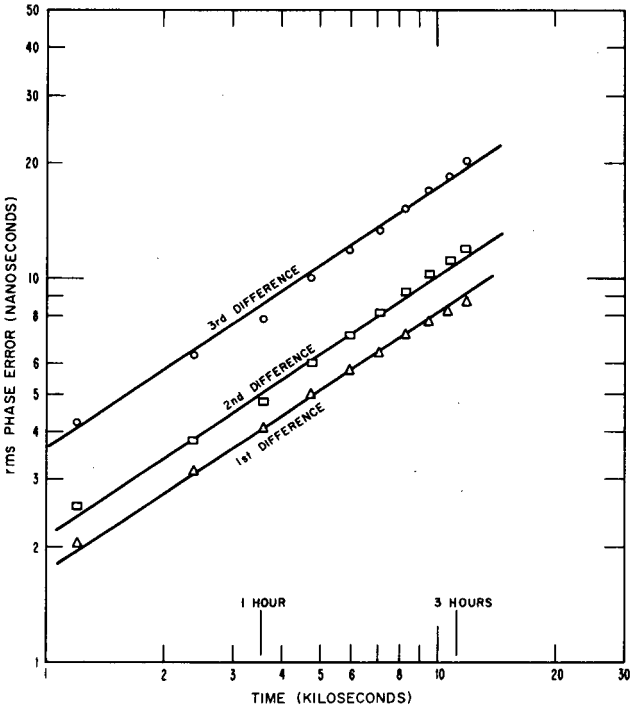

Fig. 5. Variance of differences of the relative phase difference between two atomic standards.

By applying the techniques of Section I to the difference phase of two cesium beams, the curves shown in Fig. 5 were obtained. Through least square fits to the data and comparing the ratios of the variances of differences (see Appendix), the result was obtained that the data fit curves of the form

$$\langle(\Delta^m\gamma_n)^2\rangle = B_m \mid \tau \mid^{\eta}$$

for $\eta = 1.34$, with an uncertainty (standard deviation) of about ± 0.04. Again using [8] as before, this leads to the result that

$$S_{\dot{\gamma}}(\omega) = \frac{g}{\mid \omega \mid^{\mu}}, \qquad g \approx B_1 \frac{\sqrt{3}}{4\pi} \Gamma\left(\frac{7}{3}\right) \tag{58}$$

where $\mu = 0.34 \pm 0.04$. One is, thus, led to the very strange conclusion that the spectral distribution of the detector and multiplier noise varies as $\sim \mid \omega \mid^{-1/3}$. The source of this noise was later traced to a faulty preamplifier. With a proper amplifier used, the spectral distribution appears white as other papers [5], [10], [11] indicate should be the case.

Ideally, for measurements over times large compared to the servo time constant, the error accumulated during one measurement interval should be independent of errors accumulated during nonoverlapping intervals, i.e., mathematically analogous to Brownian Motion [12]. This implies that $S_{\dot{\gamma}}(\omega)$ should be constant for $\mid \omega \mid < 1\ \mathrm{s}^{-1}$.

The Composite Clock System

If an oscillator's frequency is measured by an atomic standard, the error in measurement of the frequency is given by

$$\delta f = \frac{1}{2\pi\tau}\left[\gamma(t_A + \tfrac{1}{2}(T+\tau)) - \gamma(t_A + \tfrac{1}{2}(T-\tau))\right] \tag{59}$$

for a calibration interval as given in Section I. Also, if f_s is the defined output frequency of the frequency standard, the total error time for the entire calibration interval T, due to the Standard, is given by $T\delta f/f_s$, and if the clocks contribute an additional error (uncorrelated to the standard's error), of δt, the total error δT is given by

$$\delta T = \delta t + \frac{T\delta f}{f_s}. \tag{60}$$

It is of value to explore the dependence of $\langle(\delta t)^2\rangle$ on the ratio of T/τ. In particular, let $T = (2n+1)\tau$ for (10). This can be put in the form of (41) with the following assignments:

n	a_n	b_n
0	-1	0
1	$2n+1$	n
2	$-2n-1$	$n+1$
3	1	$2n+1$

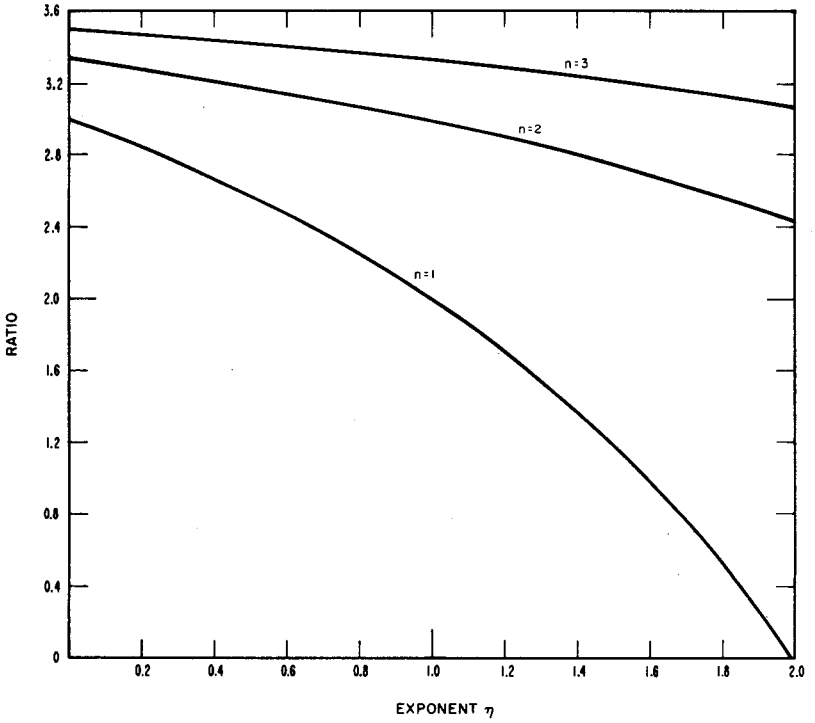

Fig. 6. Ratio of variances, $\langle(\Delta^{n+1}\epsilon m)^2\rangle / \langle(\Delta^n \epsilon m)^2\rangle$, as a function of the exponent η.

It is easy to show that these coefficients satisfy (35)–(37).

Substitution of these coefficients into (47) yields

$$\langle(\delta t)^2\rangle = 2h\tau^2\{-2n^2(2n+1)\ln(n) + 2(n+1)^2(2n+1)\ln(n+1) - (2n+1)^2\ln(2n+1)\}, \quad (61)$$

where $h = k_2/8 \ln 2$.

Since τ is normally small compared to T, it is reasonable to approximate (61) for large n. That is, the relative time error is approximately given by

$$\frac{\sqrt{\langle(\delta t)^2\rangle}}{T} \approx \sqrt{2h \ln(n)}, \quad (62)$$

where the approximations

$$n \gg 1, \ln(n+1) \approx \ln(n) + \frac{1}{n}$$

have been used. It is apparent from (62) that for a given interval T, the errors accumulated by the clock are not *critically* dependent on the measuring time τ, since $\sqrt{\ln(n)}$ is a very slowly changing quantity.

The mean square error associated with the standard, however, can be written in the form

$$T^2\langle(\delta f)^2\rangle = \left(\frac{T}{\tau}\right)^2\langle(\Delta\gamma_n)^2\rangle, \quad (63)$$

since (59) may be written as the first difference of γ_n. From (57) it is apparent that the relative time error is then given by

$$\frac{T^2\langle(\delta f)^2\rangle}{T^2 f_s^2} = \frac{B_1}{(2\pi\tau f_s)^2}\tau^\eta, \quad (64)$$

where $\eta = 1$ ("white" noise). Or, combining (59), (62), and (64),

$$\frac{\sqrt{\langle(\delta T)^2\rangle}}{T} \approx \sqrt{2h \ln(n) + \frac{B_1}{(2\pi f_s)^2\tau}}. \quad (65)$$

As one should expect, for a given T, the errors get less for larger τ but not rapidly. In the limit of $\tau = T$ [not using the approximate (65)], the errors are those of the standard alone, i.e., $\sqrt{B_1\tau/2\pi f_s}$. Also, as $\tau \to 0$, the clock errors are unbounded.

Compounding Time Errors

Equation (65) represents a reasonable approximation to the time errors of a clock system after one calibration interval. The next question is: how do the errors of many calibrations compound to give a total error $\delta(NT)$ after N calibrations? Returning to (59), one may write

$$\delta(NT) = \sum_{n=1}^{N}\delta T_n, \quad (66)$$

where δT_n is the time error associated with the nth calibration interval. There have been papers published [13] that assume that the errors of one calibration interval are not correlated to the errors of any other calibration interval. It is now possible to investigate this assumption more precisely.

In particular, the clock errors (not including the frequency standard errors) δt_n compound to give $\delta(Nt)$, given by

$$\delta(Nt) = \sum_{n=1}^{N}\delta t_n, \quad (67)$$

which can obviously be put in the form of (41). For N equal to any number larger than one, the algebra becomes much too lengthy for actual calculation by hand and it is desirable to make use of a digital computer. Table III shows the results of this calculation for compounding several third-difference-type calibrations. It is interesting to note that, in fact, the total mean square error after N calibrations is very nearly equal to N-times the mean square error after one calibration. This is in quite good agreement with DePrins [13]. Thus, the rms relative eror may be approximated by the relation

$$\sqrt{\frac{\langle(\delta(NT))^2\rangle}{NT}} \approx \sqrt{\frac{2h \ln(n) + B_1\tau}{N}}, \quad (68)$$

where h, n, B_1, f_s, and τ have the same meanings as in (65).

TABLE III
THEORETICAL DETERMINATION OF TIME ERROR PROPAGATION

N	$\frac{\left\langle\left(\sum_{n=1}^{N}\delta t_n\right)^2\right\rangle}{\langle(\delta t_n^2)\rangle}$
2	2.054
3	3.109
4	4.165
5	5.220
6	6.276
7	7.332

The conclusions which can now be drawn are that: 1) the total rms time error of this clock system from an "ideal" atomic clock is unbounded as time increases, and 2) the relative rms error time to total elapsed time (68) approaches zero about as fast as $N^{-1/2}$. It should be mentioned here that systematic errors in the atomic standard have not been considered. While this is a very important problem, it has been treated rather thoroughly elsewhere [10], [11], [14]–[16].

IV. Measures of Frequency Stability

General Restrictions

It is of value to consider the problem of establishing a stability measure in a very general sense. Consider some functional of the phase

$$\chi = \chi(\phi(t)),$$

from which the stability measure Ψ is obtained according to the relation

$$\Psi^2 = \operatorname*{Lim}_{T\to\infty} \frac{1}{T}\int_{-T/2}^{T/2} |\chi|^2\, dt,$$

provided this limit exists.

In practice it is not possible to pass to the limit $T\to\infty$, and, thus, one measures for some fixed time, T; i.e.,

$$\Psi_T^2 = \frac{1}{T}\int_{-T/2}^{T/2} |\chi|^2\, dt.$$

Under favorable conditions, Ψ_T may be a reasonable approximation to Ψ. Unfortunately, this may not always be the case.

The frequency emitted by any physically realizable device must be bounded by some upper bound, say B. The following inequalities must, then, be valid:

$$|\Omega(t)| \leq B, \quad \text{for some } B > 0;$$

$$\operatorname*{Lim}_{T\to\infty} \frac{1}{T}\int_{-T/2}^{T/2} (\Omega(t))^2\, dt \leq B^2.$$

With $S_{\dot\phi}(\omega)$ being the power spectral density of $\Omega(t)$, it follows from the definition of power spectra that

$$\operatorname*{Lim}_{T\to\infty} \frac{1}{T}\int_{-T/2}^{T/2} (\Omega(t))^2\, dt = 2\int_0^\infty S_{\dot\phi}(\omega)\, d\omega$$

for real $\Omega(t)$, and thus

$$2\int_0^\infty S_{\dot\phi}(\omega)\, d\omega \leq B^2. \tag{69}$$

If $S_\phi(\omega)$ has a flicker noise spectrum for small ω, it is apparent that this $1/|\omega|$ type of noise cannot persist to absolute zero frequency or the inequality (69) would be violated. It is, thus, reasonable to postulate the existence of a lower cutoff frequency ω_L for the flicker noise modulation.

It is apparent from the preceding considerations that stability measures may exist for which Ψ_T begins to approach Ψ only after T is several times larger than $1/\omega_L$. From some of the experiments on crystal oscillators [2], this may require T to exceed several years in duration. This is quite inconvenient from a manufacturing or experimental standpoint. The logical conclusion is to consider only those stability measures Ψ which are "cutoff independent," that is, those measures of stability which would be valid even in the limit $\omega_L\to 0^+$.

Finite Differences

It was shown in Section II that an expression of the form

$$\delta t = \frac{1}{\Omega_0}\sum_{n=0}^{m} a_n\phi(t + b_n\tau) \tag{70}$$

will have a finite variance if the $\{a_n, b_n\}$ satisfy conditions (35)–(37). It is easy to show that the first difference of the phase (i.e., frequency) cannot be put in the form of (70) with the coefficients satisfying conditions (35)–(37). Indeed, the limit

$$\operatorname*{Lim}_{\mu\to 1(-)} U(\tau) = \operatorname*{Lim}_{\mu\to 1(-)} \frac{k_2|\tau|^{2\mu}}{4 - 2^{2\mu}}$$

does not exist, and, hence, $U(\tau)$ is not a good measure of stability.

The variances of the second and third finite differences, however, are convergent. It is of interest to note that the first line of Table III may be expressed in the form

$$\frac{\langle|\Delta^3\phi_{n+3} + \Delta^3\phi_n|\rangle}{\langle(\Delta^3\phi_n)^2\rangle} = 2.054,$$

which may be simplified to the form

$$\frac{\langle(\Delta^3\phi_{n+3})(\Delta^3\phi_n)\rangle}{\langle(\Delta^3\phi_n)^2\rangle} = 0.027.$$

This equation expresses the fact that a third difference has a very small correlation (~3 percent) to an adjacent, nonoverlapping third difference. By extending this procedure with the other values given in Table III, it is found that the correlation of one third difference with a nonoverlapping third difference becomes small very rapidly as the interval between these differences becomes large. This is sufficient to insure that the variance of a finite sample of third differences will approach the "true" variance (infinite average) in a well-behaved and reasonable fashion as the sample gets larger.

Variance of Frequency Fluctuations for Finite Averaging Times

Even though the variance of the first difference of the phase does not satisfy the condition of being cutoff independent, it is possible (by specifying both the sample time and the total averaging time) to construct a cutoff independent measure of the frequency fluctuations. Instead of Ψ_T, the variance of N adjacent samples of the frequency will be denoted by $\sigma^2(\tau, N)$ where τ is the sample time for each of the N measurements of frequency. The variance is given by the conventional formula

$$\sigma^2(\tau, N) = \frac{1}{N-1}\sum_{i=1}^{N}\left[\frac{\Delta\phi_i}{\tau} - \frac{\phi_{N+1} - \phi_1}{N\tau}\right]^2.$$

If one neglects the drift rate α, which is essentially equivalent to obtaining the standard deviation around a linear drift, one obtains

$$\langle\sigma^2(\tau, N)\rangle = \frac{1}{(N-1)\tau^2}\left\{N\langle[\epsilon(t+\tau)-\epsilon(t)]^2\rangle - \frac{1}{N}\langle[\epsilon(t+N\tau)-\epsilon(t)]^2\rangle\right\}. \quad (71)$$

For the case of an "ideal" crystal oscillator, (19), (24), and (26) allow (71) to be simplified (after passing to the limit $\mu\rightarrow 1^{(-)}$ to the form

$$\langle\sigma^2(\tau, N)\rangle = \frac{2hN\ln(N)}{N-1}.$$

Thus, as N increases, the expected value of $\sigma^2(\tau, N)$ increases without bound (at least until $N\tau\sim 1/\omega_L$). It is interesting to note that for a given oscillator, $\langle\sigma^2(\tau, N)\rangle$ has a minimum value for $N=2$. Obviously one would have to average several experimental determinations of $\sigma^2(\tau, 2)$ in order to have a reasonable approximation to $\langle\sigma^2(\tau, 2)\rangle$.

While $\sigma(\tau, N)$ is a cutoff independent measure of frequency stability, it has the significant disadvantage of being a function of two variables. Indeed, in order to compare the stability of two oscillators, both the τ's and the N's should have nearly corresponding values.

Delayed Frequency Comparison

In radar work, often the frequency of a signal is compared to the frequency of the same source after it has been delayed in traversing some distance—often a very great distance. One might, thus, be interested in defining a stability measure in an analogous fashion:

$$\Psi^2(\tau, T) = \left\langle\left[\frac{\phi(t+T+\tau)-\phi(t+T)}{\tau} - \frac{\phi(t+\tau)-\phi(t)}{\tau}\right]^2\right\rangle. \quad (72)$$

Again neglecting the drift rate α of the oscillator, (24) and (72) combine to yield

$$\Psi^2(\tau, T) = \frac{1}{\tau^2}[2U(\tau)-U(T-\tau)+2U(T)-U(T+\tau)]. \quad (73)$$

After substitution of (26) into (73) the equation can be rearranged to give (again passing to the limit, $\mu\rightarrow 1^{(-)}$)

$$\Psi^2(\tau, T) = -2h[\rho^2\ln\rho - (1+\rho)^2\ln(1+\rho) - (\rho-1)^2\ln(\rho-1)],$$

where $\rho\equiv T/\tau$. Although this is a rather complicated expression, it may be simplified with the approximation $\rho\equiv T/\tau\gg 1$. The result is

$$\Psi^2(\tau, T) = 4h\left(2+\ln\frac{T}{\tau}\right), \quad \text{for } \frac{T}{\tau}\gg 1 \quad (74)$$

for an "ideal" oscillator. It is interesting to note here that even when considering only $1/|\omega|$ type of noise, one cannot pass to the limit $\tau=0$ for this problem. In the limit as $\tau\rightarrow 0^+$, the expression

$$\lim_{\tau\rightarrow 0^+}\left[\frac{\phi(t+\tau)-\phi(t)}{\tau}\right] \equiv \dot{\phi}(t) \equiv \Omega(t)$$

and thus

$$\lim_{\tau\rightarrow 0^+}\Psi^2(\tau, T) = \langle[\Omega(t+T)-\Omega(t)]^2\rangle \rightarrow \infty$$

from (74), even though $T\ll 1/\omega_L$. The source of this difficulty is the high-frequency divergence of the flicker noise spectrum. If the system is limited at the high frequency by ω_H, then one should pass to the limit $\tau\rightarrow 1/\omega_H$.

Again, $\psi(\tau, T)$ is a function of two variables with all of the associated annoyances. It may, however, be useful in certain applications.

Conclusion

The assumptions of stationarity and "ideal" behavior for a quartz crystal oscillator lead to a statistical model which agrees well with many different experiments. One finds, however, that certain quantities are unbounded as averaging times are extended and it is important to consider only those quantities which have reasonable hope of converging toward a good value in reasonable time. Thus, the concepts of cutoff dependent and cutoff independent measures of frequency stability form a natural classification for all possible frequency stability measures.

On the basis of "ideal" behavior, it has been shown that the errors of a clock, run from a quartz crystal oscillator and periodically referenced to an atomic frequency standard, accumulate error at a probable rate proportional to the square root of the number of calibrations. That is, the errors of one calibration interval are essentially uncorrelated to errors of nonoverlapping intervals in spite of the fact that "ideal" behavior is highly correlated for long periods of time.

It has also been shown that the method of finite differences can be a useful method of determining spectral distributions of noise, as well as being a possible measure of frequency stability. By using higher order finite differences, phase fluctuations with even a higher order pole at zero-modulation frequency can similarly be treated. The need for higher than second or third differences, however, has not yet been demonstrated.

It should be noted that the existence of higher-frequency modulation noise of different origin also has significant affect on stability measures. In general, the factors which limit the system to a finite bandpass are sufficient to insure convergence of the stability measures as $\omega\rightarrow\infty$. If it is primarily the measuring system which limits the system bandpass, however, the results may be significantly altered by the measuring system itself.

Appendix

Ratio of Variances

Let $\epsilon(t)$ be a real generalized function such that $\langle\epsilon(t)\rangle = 0$ and define the discrete variable ϵ_m by the relation

$$\epsilon_m \equiv \epsilon(t + m\tau). \tag{75}$$

Also, let the auto-covariance function of $\epsilon(t)$ be, as before, independent of a simple time transition. One may now write (see Table I)

$$\langle(\Delta\epsilon_m)^2\rangle = 2[\langle(\epsilon_n)^2\rangle - \langle[\epsilon(t+\tau)\epsilon(t)]\rangle] \tag{76}$$

and assume that

$$\langle(\Delta\epsilon_m)^2\rangle = k_1\tau^\eta, \tag{77}$$

where k_1 is a constant for a given η. It is also possible to obtain the variance of the second difference:

$$\langle(\Delta^2\epsilon_m)^2\rangle = 6\langle(\epsilon_m)^2\rangle - 8\langle[\epsilon(t+\tau)\cdot\epsilon(t)]\rangle + \langle[\epsilon(t+2\tau)\epsilon(t)]\rangle. \tag{78}$$

Using (77) and (78), one may obtain

$$\frac{\langle(\Delta^2\epsilon_m)^2\rangle}{\langle(\Delta\epsilon_m)^2\rangle} = \frac{4k_1\tau^\eta - k_1(2\tau)^\eta}{k_1\tau^\eta} = 4 - (2)^\eta. \tag{79}$$

Since (79) must be non-negative (ϵ is real), the exponent is restricted to the range $\eta \leq 2$.

Similarly, one may obtain the variance of the third difference

$$\langle(\Delta^3\epsilon_m)^2\rangle = 15k_1\tau^\eta - 6k_1(2\tau)^\eta + k_1(3\tau)^\eta, \tag{80}$$

and hence the ratio

$$\frac{\langle(\Delta^3\epsilon_m)^2\rangle}{\langle(\Delta^2\epsilon_m)^2\rangle} = \frac{15 - 6\cdot(2)^\eta + 3^\eta}{4 - (2)^\eta}. \tag{81}$$

Similarly,

$$\frac{\langle(\Delta^4\epsilon_m)^2\rangle}{\langle(\Delta^3\epsilon_m)^2\rangle} = \frac{56 - 28\cdot(2)^\eta + 8\cdot(3)^\eta - (4)^\eta}{15 - 6\cdot(2)^\eta + (3)^\eta}. \tag{82}$$

Equations (79), (81), and (82) are plotted in Fig. 6 as a function of the exponent η.

For $\eta = 4/3$, as in Fig. 6, the theoretical ratios,

$$\frac{\langle(\Delta^{n+1}\epsilon_m)^2\rangle}{\langle(\Delta^n\epsilon_m)^2\rangle}$$

for $n = 1$ and 2 are 1.48 and 2.84, respectively. The straight lines drawn in Fig. 5 were made to have these ratios and slope 2/3 (the square root of the variances).

Acknowledgment

The author is sincerely indebted to Drs. P. Wacker and E. Crow of the National Bureau of Standards for some very valuable suggestions and references. The author also wishes to acknowledge the assistance of D. Allan for his aid in data acquisition and analysis, R. E. Beehler for making the cesium beams of the NBS available, and R. L. Fey for some helpful criticism.

References

[1] H. Lyons, "The atomic clock," *Am. Scholar*, vol. 19, pp. 159–168, Spring 1950.

[2] W. R. Arkinson, L. Fey, and J. Newman, "Spectrum analysis of extremely low frequency variations of quartz oscillators," *Proc. IEEE (Correspondence)*, vol. 51, p. 379, February 1963.

[3] L. Fey, W. R. Atkinson, and J. Newman, "Obscurities of oscillator noise," *Proc. IEEE (Correspondence)*, vol. 52, pp. 104–105, January 1964.

[4] V. Troitsky, "Certain problems of the theory of fluctuations in oscillators. The influence of flicker noise," *Izv. Vysshikh Uchebn. Zavedenii, Radiofiz.*, vol. 1, pp. 20–33, 1958.

[5] L. Cutler and C. Searle, "Some aspects of the theory and measurement of frequency fluctuations in frequency standards," this issue, page 136.

[6] J. A. Barnes and R. C. Mockler, "The power spectrum and its importance in precise frequency measurements," *IRE Trans. on Instrumentation*, vol. I-9, pp. 149–155, September 1960.

[7] N. Wiener, *Extrapolation, Interpolation, and Smoothing of Stationary Time Series*. Cambridge, Mass.: Technology Press of Mass. Inst. of Tech., and New York: Wiley, January 1957.

[8] M. Lighthill, *Introduction to Fourier Analysis and Generalized Functions*. New York: Cambridge, 1962.

[9] L. R. Malling, "Phase-stable oscillators for space communications, including the relationship between the phase noise, the spectrum, the short-term stability, and the Q of the oscillator," *Proc. IRE*, vol. 50, pp. 1656–1664, July 1962 (see also [3]).

[10] P. Kartaschoff, "Influence de l'effet de grenaille sur la frequence d'un oscillateur asservi a un etal on a jet atomique," Laboratoire Suisse de Recherches Horlogeres, Neuchatel, Switzerland, No. 08-64-01.

[11] P. Kartaschoff, "Etude d'un etalon de frequence a jet atomique de cesium," Laboratoire Suisse de Recherchess Horlogeres, Neuchatel, Switzerland, November 1963.

[12] S. Basri, "Time standards and statistics," to be published.

[13] J. DePrins, "Applications des masers A $N^{15}H_3$ a la mesure et a la definition du temps," unpublished Doctor of Sciences dissertation, Université Libre de Bruxelles, Belgium, 1961.

[14] R. E. Beehler, W. R. Atkinson, L. E. Heim, and C. S. Snider, "A comparison of direct and servo methods for utilizing cesium beam resonators as frequency standards," *IRE Trans. on Instrumentation*, vol. I-11, pp. 231–238, December 1962.

[15] R. E. Beehler and D. J. Glaze, "The performance and capability of cesium beam frequency standards at the National Bureau of Standards," to be published.

[16] R. E. Beehler and D. J. Glaze, "Evaluation of a thallium atomic beam frequency standard at the National Bureau of Standards," to be published.

Reprinted from the PROCEEDINGS OF THE IEEE
VOL. 54, NO. 2, FEBRUARY, 1966
Pp. 207-220

Statistics of Atomic Frequency Standards

DAVID W. ALLAN

Abstract—A theoretical development is presented which results in a relationship between the expectation value of the standard deviation of the frequency fluctuations for any finite number of data samples and the infinite time average value of the standard deviation, which provides an invariant measure of an important quality factor of a frequency standard. A practical and straightforward method of determining the power spectral density of the frequency fluctuations from the variance of the frequency fluctuations, the sampling time, the number of samples taken, and the dependence on system bandwidth is also developed. Additional insight is also given into some of the problems that arise from the presence of "flicker noise" (spectrum proportional to $|\omega|^{-1}$) modulation of the frequency of an oscillator.

The theory is applied in classifying the types of noise on the signals of frequency standards made available at NBS, Boulder Laboratories, such as: masers (both H and $N^{15}H_3$), the cesium beam frequency standard employed as the U. S. Frequency Standard, and rubidium gas cells.

"Flicker noise" frequency modulation was not observed on the signals of masers for sampling times ranging from 0.1 second to 4 hours. In a comparison between the NBS hydrogen maser and the NBS III cesium beam, uncorrelated random noise was observed on the frequency fluctuations for sampling times extending to 4 hours; the fractional standard deviations of the frequency fluctuations were as low as 5 parts in 10^{14}.

I. Introduction

As ATOMIC TIMEKEEPING has come of age, it has become increasingly important to identify quality in an atomic frequency standard. Some of the most important quality factors are directly related to the inherent noise of a quantum device and its associated electronics. For example, a proper measurement and statistical classification [1] of this inherent noise makes it possible to determine the probable rate of time divergence of two independent atomic time systems, as well as giving insight concerning the precision and accuracy obtainable from an atomic frequency standard.

In the realm of precise frequency measurements, the properties of noise again play an important role. The relative precision obtainable with atomic frequency standards is unsurpassed in any field, and the precision limitations in this field are largely due to inherent noise in the atomic device and the associated electronic equipment. The standard deviation of the frequency fluctuations can be shown to be directly dependent on the type of noise in the system, the number of samples taken, and the dead-time between samples.

A very common and convenient way of making measurements of the noise components on a signal from a frequency standard is to compare two such standards by measuring the period of the beat frequency between the two standards. It is again the intent of the author to show a practical and easy way of classifying the statistics, i.e., of determining the power spectral density of the frequency fluctuations using this type of measuring system.

An analysis has already been made of the noise present in passive atomic frequency standards [1], such as cesium beams, but a classification of the types of noise exhibited by the maser type of quantum-mechanical oscillator has not been made in the long term area, i.e., for low frequency fluctuations. Though this paper is far from exhaustive, the intent is to give additional information on the noise characteristics of masers. Because a maser's output frequency is more critically parameter dependent than a passive atomic device, it has been suggested [2] that the output frequency might appear to be "flicker noise" modulated, where "flicker noise" is defined as a type of power spectral density which is inversely proportional to the spectral frequency $\omega/2\pi$. It has been shown that if "flicker noise" frequency modulation is present on a signal from a standard, some significant problems arise, such as the logarithmic divergence of the standard deviation of the frequency fluctuations as the number of samples taken increases, and also the inability to define precisely the time average frequency. It thus becomes of special interest to determine whether "flicker noise" is or is not present on the signal from a maser so that one might better evaluate its quality as a frequency standard.

Throughout the paper, the paramount mathematical concern is the functional form of the equations with the hope of maintaining simplicity and of providing better understanding of the material to be covered.

II. Methods Employed to Measure Noise

A. Power Spectrum and Variance Relationship

The average angular frequency $\Omega_\tau(t)$ of an oscillator (to distinguish it from spectral frequency ω) over a time interval τ can be written

$$\Omega_\tau(t) = \frac{1}{\tau}\left[\phi(t+\tau) - \phi(t)\right], \tag{1}$$

where ϕ is the phase angle in radians. Now the variance of the frequency deviations is the square of the standard deviation σ. Define the time average of a function as

$$\langle f(t)\rangle = \lim_{T\to\infty} \frac{1}{T}\int_{-T/2}^{T/2} f(t)\,dt. \tag{2}$$

Manuscript received September 17, 1965; revised December 7, 1965.

The author is with the National Bureau of Standards, Boulder, Colo.

One may, therefore, write the square of the standard deviation as follows:

$$\sigma^2 = \langle \Omega_\tau(t)^2 \rangle - \langle \Omega_\tau(t) \rangle^2. \tag{3}$$

One may assume with no loss of generality that the second term in (3) can be set equal to zero by a proper translation, since it is the square of the time average frequency. Therefore, $\Omega_\tau(t)$ is now the frequency deviation from the average value, and $\phi(t)$ the integrally related phase deviation.

Substituting (1) into (3) gives

$$\sigma^2 = \frac{1}{\tau^2}[\langle \phi(t+\tau)^2 \rangle - 2\langle \phi(t+\tau) \cdot \phi(t) \rangle + \langle \phi^2(t) \rangle]. \tag{4}$$

The time average of $\phi(t+\tau) \cdot \phi(t)$ is the autocovariance function of the phase—denoted $R_\phi(\tau)$. One is justified in assuming that a time translation has no effect on the autocovariance function [1], therefore [4],

$$\sigma^2 = \frac{2}{\tau^2}[R_\phi(0) - R_\phi(\tau)]. \tag{5}$$

It is now possible to relate the variance of the squared frequency deviations to the power spectral density by use of the Wiener-Khinchin Theorem, which states that the autocovariance function of the phase is equal to the Fourier transform (F.T.) of the power spectral density of the phase $S_\phi(\omega)$. The power spectral density of the frequency is related to this by the useful equation

$$S_{\dot{\phi}}(\omega) = \omega^2 S_\phi(\omega).$$

Most of the discussion that follows is based on the restriction

$$S_\phi(\omega) = h\,|\,\omega\,|^\alpha. \tag{6}$$

That a singular type of power spectrum predominates over a reasonable range of ω has been verified experimentally. The region of interest for α is $-3 \leq \alpha \leq -1$, and $\alpha = 0$. This covers white noise phase modulation ($S_\phi(\omega) = h$), "flicker noise" frequency modulation ($S_{\dot{\phi}}(\omega) = h\,|\omega\,|^{-1}$), and includes, of course, white noise frequency modulation ($S_{\dot{\phi}}(\omega) = h$). Fortunately, the Fourier transforms of functions of the above form [3] have been tabulated, and the following transforms can be established:

$$\begin{aligned}
&\text{F.T.}\,|\,\omega\,|^\alpha = a'(\alpha) \cdot |\,\tau\,|^{-\alpha-1} \quad \text{for } \alpha \neq 0 \text{ or not an integer} \\
&\text{F.T.}\,|\,\omega\,|^{-0} = \delta(\tau) \\
&\text{F.T.}\,|\,\omega\,|^{-2} = a'(-2) \cdot |\,\tau\,|
\end{aligned} \tag{7}$$

where a' is an α dependent coefficient. A useful substitution is the following [1]:

$$U(\tau) = 2[R_\phi(0) - R_\phi(\tau)]. \tag{8}$$

Because of finite system bandwidths, ω_B, a better representation of $U(\tau)$ is obtained by replacing $R_\phi(0)$ with $R_\phi(1/\omega_B)$ (see Appendix). If the sample time τ is large compared to the reciprocal system bandwidth $1/\omega_B$, then $R_\phi(1/\omega_B)$ is negligible compared to $R_\phi(\tau)$ in the region where $-2 < \mu < 0 (-1 > \alpha > -3)$. $R_\phi(1/\omega_B)$ becomes the larger term, however, in the region of $-1 < \alpha < 0$, and if one assumes $(\omega_B \tau)^{\alpha+1} \gg 1$, then $R_\phi(\tau)$ is neglectable (see Appendix). The following equations for $U(\tau)$ may, therefore, be written:

$$U(\tau) = \begin{cases} |\,a(\alpha)\,|\,|\,\tau\,|^{-\alpha-1}; & -3 < \alpha < -1 \\ a(\alpha)\,|\,\omega_B\,|^{\alpha+1}; & -1 < \alpha \leq 0. \end{cases} \tag{9}$$

The standard deviation squared may, therefore, be written:

$$\sigma^2 = \begin{cases} a(\mu) \cdot |\,\tau\,|^\mu; & -3 < \alpha < -1 \\ a(\alpha)\,|\,\omega_B\,|^{\alpha+1}\,|\,\tau\,|^{-2}; & -1 < \alpha \leq 0 \end{cases} \tag{10}$$

where $\mu = -\alpha - 3$.

$A(\mu)$ has a small dependence on ω_B, implicit within the previous assumptions. Considering the results of (10), the Appendix, and that to be discussed in Section II-D on "flicker noise" modulation ($\alpha = -1$, -3), an informative graph of μ into α may be established as illustrated below.

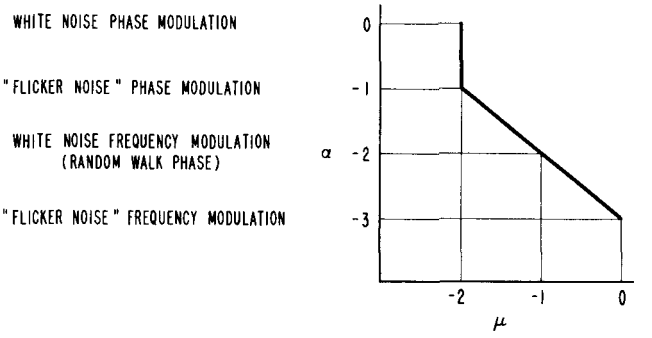

Using (6) and (10) along with the above graph, one may, therefore, deduce the power spectral density from the dependence of the standard deviation of the frequency fluctuations on the sampling time, with restrictions on the experimental parameters as will be shown in the following.

B. Adjacent Sampling of Data

In actual practice, of course, the number of frequency or phase samples must be finite. The case to be considered now is one for which the phase or the frequency is monitored on a continuous basis. Two of the techniques used by the author to accomplish this were as follows: A device, described elsewhere [1], was used to monitor the phase of the beat frequency between two oscillators at prescribed time intervals; the second technique was to measure the period of the beat frequency between two oscillators with two counters so that the dead-time of one counter corresponded to the counting time of the other.

A very powerful and meaningful method of analysis of data taken by a phase monitoring technique has been developed by J. A. Barnes [1] at the National Bureau of Standards, Boulder, Colo. The method employs the use of finite differences and is especialy useful in analyzing

"flicker noise" and long-term frequency fluctuations in general. On the other hand, if one uses the period counting technique for data acquisition, the following form of analysis is useful. It also may be cast in a form where one may use the finite difference technique.

Data are often obtained with one counter measuring the frequency or the period of the beat note between two oscillators with a dead-time between counts.[1] The concern of Section II is with the dead-time being zero, but it is convenient to develop the general case for which the dead-time is nonzero for use in Section III, and specialize this to the continuous sampling case for which the dead-time is zero, which is the case of interest in this section.

Let T be the period of sampling, τ the sample time, and N the number of samples. The standard deviation, $\sigma(N, T, \tau)$, of the frequency fluctuations[2] may, therefore, be written as:

$$\sigma^2(N, T, \tau) = \frac{1}{N-1}\left\{\sum_{n=0}^{N-1}\left[\frac{\phi(nT+\tau)-\phi(nT)}{\tau}\right]^2 - \frac{1}{N}\left[\sum_{n=0}^{N-1}\frac{\phi(nT+\tau)-\phi(nT)}{\tau}\right]^2\right\}. \quad (11)$$

Taking the expectation value of $\sigma^2(N, T, \tau)$ and making the substitution given in (8) yields

$$\langle\sigma^2(N, T, \tau)\rangle = \frac{1}{\tau^2}\left\{U(\tau) + \frac{1}{N(N-1)}\sum_{n=0}^{N-1}(N-n)[2U(nT)-U(nT+\tau)-U(nT-\tau)]\right\}. \quad (12)$$

If the dead-time were zero, then $T=\tau$, and (12) becomes [1]

$$\langle\sigma^2(N, \tau)\rangle = \frac{1}{(N-1)\tau^2}\left[NU(\tau) - \frac{1}{N}U(N\tau)\right]. \quad (13)$$

Remembering that $\mu=-\alpha-3$ and substituting (9) into (13) gives

$$\langle\sigma^2(N, \tau)\rangle = \frac{a(\mu)N|\tau|^\mu}{N-1}[1-N^\mu]; \quad -2<\mu<0 \quad (14)$$

which establishes the interesting result of the dependence of the expectation value of the standard deviation of the frequency fluctuations on the number of samples, the sample time, and the power spectral density. It will be noted that

$$\langle\sigma^2(\infty, \tau)\rangle = a(\mu)|\tau|^\mu; \quad -2<\mu<0 \quad (15)$$

in agreement with (10).

[1] See L. S. Cutler and C. L. Searle, "Some aspects of the theory and measurement of frequency fluctuations in frequency standards," this issue, page 136. This paper shows that the fluctuations $\Delta\tau$ in the period τ are a good approximation to the frequency fluctuations if $\Delta\tau \gg \tau$.

[2] Note that this $\sigma(N, T, \tau)$ is not the same as the σ in (3)–(5), and (10). $\sigma(N, T, \tau)$ is over a finite number of data samples N and, to avoid confusion, the variable N will always be used with σ in the finite sampling case as in (11).

By keeping N constant and assuming μ to be constant over several different values of τ, it may be seen that the value of μ is the slope on a log-log plot of $\langle\sigma^2(N, \tau)\rangle$ vs. τ. This provides a means of determining the power spectral density simply by varying the sample time over the region of interest [4].

It is informative to look at the family of curves obtained from a plot of the dependence of $\langle\sigma^2(N, \tau)\rangle$ as a function of N for various pertinent values of μ to see how it approaches $\langle\sigma^2(\infty, \tau)\rangle$. The family of curves is shown in Fig. 1. One may notice that the convergence is much faster in the region between white noise frequency modulation and white noise phase modulation than between white noise frequency modulation and "flicker noise" frequency modulation.[3] In fact, as $\mu\to 0$, the ratio approaches zero, and one would conjecture that the

$$\lim_{N\to\infty}\langle\sigma^2(N, \tau)\rangle$$

is infinite in the presence of "flicker noise" frequency modulation—a result proven by J. A. Barnes et al. [1].

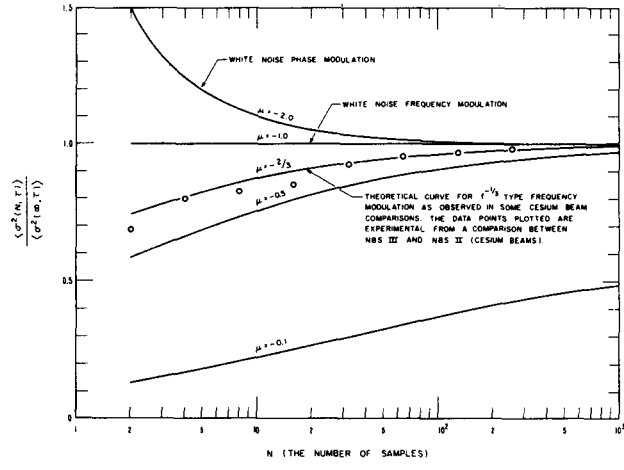

Fig. 1. A plot showing the dependence of the standard deviation of the frequency fluctuation on the number of samples and the type of noise present.

The data points plotted in Fig. 1 were extracted from a cesium beam-cesium beam comparison analyzed elsewhere [1], and exhibit in this new formulation a type of frequency modulation proportional to $|\omega|^{-1/3}$, giving confirmation to this strange type of power spectral density.

It is possible to utilize the dependence of the standard deviation on the number of samples to determine a value of μ by considering a function which takes into account the extreme values of N obtainable from a finite set of data, namely,[4]

[3] To see that $\mu=0$ corresponds to "flicker noise" see Section II-D.

[4] It will be noted that the τ dependence cancels in the expression for χ and hence it is N and μ dependent only. In the table and graphs, the τ dependence is not shown and is, therefore, suppressed since the μ dependence is the thing emphasized.

$$\chi(N, \mu) = \frac{\langle \sigma^2(N, \tau) \rangle}{\langle \sigma^2(2, \tau) \rangle} . \tag{16}$$

Tabulated values of this function are given in Table I, and a plot of $\chi(N, \mu)$ as a function of μ for various values of N is given in Fig. 2. It may be noted that the function is most sensitive in the region between "flicker noise" frequency modulation $\mu = 0$ and white noise frequency modulation $\mu = -1$—one of basic interest. In practice, the table and graph have proven very useful. $\chi(\infty, \mu)$ is plotted for comparison and computational purposes.

Note that $\chi(\infty, 0) = \infty$. In the development thus far, no consideration has been given to the experimental fact that there must exist a lower cutoff frequency that keeps the functions considered from going to infinity, corresponding to certain types of noise, such as "flicker noise." The value of the cutoff frequency is not important other than to say that the functions considered are valid for times up to the order of $1/(\omega \text{ cutoff})$. This time is apparently more than a year for quartz crystal oscillators [5]. If "flicker noise" is present in some atomic frequency standards, the value of $1/(\omega \text{ cutoff})$ is probably less than for quartz crystal oscillators for reasons discussed later, and if "flicker noise" is not present, infinities do not occur in the functions considered for most other types of pertinent noise and hence there is no concern.

TABLE I

THE DEPENDENCE OF $\langle \sigma(N, \tau) \rangle$ ON THE NUMBER OF SAMPLES FOR A FIXED SAMPLE TIME τ, THUS DETERMINING THE VALUE OF μ AND THE STATISTICS. THE VALUES LISTED ARE OF

$$\chi(N, \mu) = \frac{\langle \sigma^2(N, \tau) \rangle}{\langle \sigma^2(2, \tau) \rangle} .$$

μ	N (Number of Samples)					
	4	16	64	256	1024	∞
0.0	1.337	2.133	3.048	4.016	5.004	∞
−0.1	1.288	1.928	2.580	3.190	3.736	7.464
−0.2	1.247	1.753	2.215	2.598	2.899	3.855
−0.3	1.208	1.604	1.928	2.167	2.332	2.660
−0.4	1.171	1.475	1.700	1.847	1.937	2.062
−0.5	1.138	1.365	1.517	1.606	1.655	1.705
−0.6	1.106	1.270	1.369	1.422	1.447	1.467
−0.7	1.077	1.188	1.249	1.278	1.291	1.299
−0.8	1.049	1.116	1.150	1.165	1.171	1.174
−0.9	1.023	1.054	1.068	1.074	1.076	1.076
−1.0	1.000	1.000	1.000	1.000	1.000	1.000
−1.1	0.977	0.952	0.942	0.938	0.937	0.937
−1.2	0.956	0.910	0.893	0.887	0.886	0.886
−1.3	0.937	0.873	0.851	0.844	0.842	0.842
−1.4	0.919	0.841	0.815	0.807	0.805	0.804
−1.5	0.902	0.812	0.784	0.776	0.774	0.773
−1.6	0.886	0.786	0.756	0.748	0.746	0.745
−1.7	0.871	0.763	0.733	0.725	0.723	0.722
−1.8	0.858	0.743	0.712	0.704	0.702	0.701
−1.9	0.845	0.724	0.693	0.685	0.683	0.682
−2.0	0.833	0.708	0.677	0.669	0.667	0.667

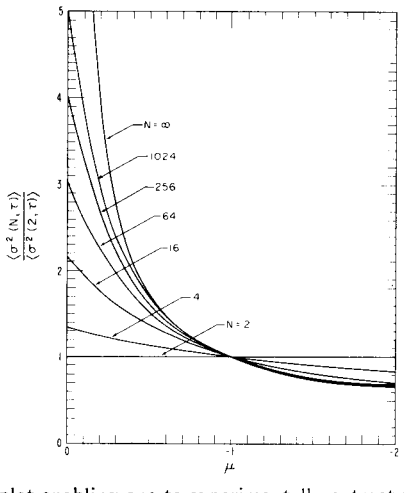

Fig. 2. A plot enabling one to experimentally extract the statistics of an oscillator by knowing the standard deviation for N samples and for two samples using $S_\phi(\omega) = h|\omega|^{-\mu-1}$ except at $\mu = -2$.

C. Non-Adjacent Sampling of Data

The next consideration is to determine the effect of counter dead-time on one's ability to deduce the statistics of an oscillator using the techniques developed in Section II-B. This form of data acquisition is one of the most common, and hence merits attention.

It was shown earlier that (12) is applicable to the present case, and if (9) is substituted into (12), with the assignment that $r = T/\tau$ (the ratio of the period of sampling to the sample time), then

$$\langle \sigma^2(N, T, \tau) \rangle = a(\mu) |\tau|^\mu \left\{ 1 + \sum_{n=1}^{N-1} \frac{(N-n)(nr)^{\mu+2}}{N(N-1)} \left[2 - \left(1 + \frac{1}{nr}\right)^{\mu+2} - \left(1 - \frac{1}{nr}\right)^{\mu+2} \right] \right\}; \qquad -2 < \mu < 0. \tag{17}$$

An important result from (17) is that if N and r are held constant, it is still possible to determine the value of μ by varying τ. Therefore, the relationship between the power spectral density and the standard deviation has the same form as for the continuous sampling case. Additional insight may be obtained by considering some special cases. If $\mu = -1$, $(S_\phi(\omega) = h)$ [6], the series in (17) goes to zero for all possible values of r and hence

$$\langle \sigma^2(N, T, \tau) \rangle = \frac{a(-1)}{|\tau|} \tag{18}$$

for white noise frequency modulation; this is the same result obtained in the continuous data sampling case. One notices that (18) is independent of N as would be espected since the frequency fluctuations are uncorrelated.

If $\mu = -2$, the series in (17) again goes to zero for all values of $r > 1$. The value of α is degenerate except that one may say $-1 < \alpha$. In this domain, the frequency fluctuations appear to be uncorrelated as long as the measurement dead-time is nonzero. Using the proper form of $U(\tau)$ from (9) and substituting into (13) for the case where $r = 1$ (zero dead-time), gives:

$$\langle \sigma^2(N, \tau) \rangle = [a(\alpha) |\omega_B|^{\alpha+1} (N+1)/N\tau^2] .$$

463-560 O - 72 - 31

One, therefore, has the unusual result that

$$\langle \sigma^2(N, T, \tau)\rangle = \frac{N + \delta(r-1)}{N} \cdot \frac{a(\alpha) \mid \omega_B \mid^{\alpha+1}}{\tau^2} \tag{19}$$

where

$$\delta(r-1) = \begin{cases} 1, & r = 1 \\ 0, & r \neq 1, \end{cases} \quad \text{for } -1 < \alpha \text{ and } (\omega_B \tau)^{\alpha+1} \gg 1.$$

A slight N dependence then appears only in the continuous sampling case. Experimentally, one can show that the Kronecker δ-function is replaced by $R_\phi(r-1)/R_\phi(0)$ because of the finite bandwidths involved.

It will be recalled that the curves in Figs. 1 and 2 are for $r=1$ (the dead-time equal zero). The results of (19) show a character change in the curves for $r>1$ and $-2<\mu<-1$, for now the curve for $\mu=-2$ is coincident with the curve for $\mu=-1$ in Fig. 1 and $\chi(N, -2) = \chi(N, -1) = 1.0$ in Fig. 2. No profound character change occurs for $-1<\mu<0$.

It is possible to show that the series in (17) approaches zero as N approaches infinity for all values of $r>1$ and $\mu<0$, hence $\langle \sigma^2(N, T, \tau)\rangle$ has the same asymptotic value as for the continuous sampling technique, independent of the counter dead-time.

If a binomial expansion is made of the second two terms in the series expression of (17), and fourth-order terms and higher in $1/nr$ are neglected, the following simplification occurs:

$$\langle \sigma^2(N, T, \tau\rangle = a(\mu) \mid \tau \mid^{\mu} \left[1 - \frac{(\mu+2)(\mu+1)}{N(N-1)} r^{\mu} \sum_{n=1}^{N} (N-n) n^{\mu} \right]. \tag{20}$$

On the first observation of (20), one may notice that as r becomes large, the standard deviation approaches its asymptotic value. This occurs when one is taking samples much shorter than the capable reset time of the counter. The dependence on N is, therefore, reduced as r^{μ}. In fact, it has been determined by a computer analysis of (17) that the net effect of increasing the dead-time is to collapse the curves in Figs. 1 and 2 towards the unit axis.

D. The "Flicker Noise" Problem

The existence of "flicker noise" frequency modulation on the signal of quartz crystal oxcillators has caused difficulty in handling such quantities as the autocovariance function of the phase and the standard deviation of the frequency fluctuations. As mentioned previously, the development by J. A. Barnes [1] makes it possible to classify "flicker noise" frequency modulation without any divergence difficulties or dependence on the value of the low-frequency cutoff.

Some of the other difficulties associated with the presence of "flicker noise" frequency modulation, as Barnes has shown, are illustrated in the following equations:

$$\langle \sigma^2(N, \tau)\rangle = \frac{2hN \ln N}{N-1}, \tag{21}$$

and

$$\lim_{\tau \to 0} + \left\langle \left[\frac{\phi(t+\tau) - \phi(t)}{\tau} \right] \right\rangle = \langle \Omega(t)\rangle. \tag{22}$$

The fact that the standard deviation diverges with N, as shown in (21), is an annoyance, aside from the fact that it becomes more difficult to write specifications on the frequency fluctuations of an oscillator. The limit expressed in (22) does not exist or is dependent on the low-frequency cutoff; this, of course, affords difficulty in defining a frequency, and would be an unfortunate property to be present in a frequency standard. As has been stated previously for all values of μ considered thus far, $-2<\mu<0$, the limit as N approaches infinity of $\langle \sigma^2(N, \tau)\rangle$ exists; and as the sampling time increases, $\langle \sigma^2(N, \tau)\rangle$ converges toward zero or perfect precision.

Data have been analyzed that indicate the presence of "flicker noise" frequency modulation on the signals from rubidium gas cell frequency standards. It is of concern to determine if this type of noise is present on the signals of other atomic frequency standards, and specifically masers. It is not the intent to determine the source or sources of "flicker noise," as this is a ponderous problem in and of itself, but perhaps only infer where such noise might arise.

Consider, now, ways to establish the presence of "flicker noise." If the data were on a continuous basis, the method of finite differences [1] developed by Barnes would be very useful. One may also notice from (21) that if N is held constant, the value of μ is zero for values of τ in the "flicker noise" frequency modulation region. If data were taken by the common technique of non-adjacent samples, the following considerations are of value.

For "flicker noise" frequency modulation, $U(\tau)$ takes on a different form as a result of the divergence of the autocovariance function of the phase [1],

$$U(\tau) = \lim_{\mu \to 0^-} \frac{k \mid \tau \mid^{\mu+2}}{4 - 2^{\mu+2}}. \tag{23}$$

The constant k is dependent on the quality of the oscillator. If (23) is substituted into (12), letting $\mu \to 0$ ($\mu=0$ corresponds to "flicker noise"), an indeterminate form results for $\langle \sigma^2(N, T, \tau)\rangle$. Applying L'Hospital's Rule, and then passing to the limit, gives the following equation:

$$\langle \sigma^2(N, T, \tau)\rangle = \frac{kr^2}{N(N-1)} \sum_{n=1}^{N-1} (N-n) \left[-2n^2 \ln (nr) + \left(n - \frac{1}{r}\right)^2 \ln (nr+1) + \left(n - \frac{1}{r}\right)^2 \ln (nr-1) \right]. \tag{24}$$

Hence, for a fixed ratio $r = T/\tau$, and a determined number of samples N, the standard deviation is constant,

independent of τ. So for both adjacent and nonadjacent data sampling, the value of μ is zero. One may, therefore, determine if "flicker noise" frequency modulation is present on a signal sampled in a nonadjacent fashion, subject to the above constraints.

A consideration of interest at this point is "flicker noise" phase modulation ($S_\phi(\omega) = h|\omega|^{-1}$). One can show from the work of J. A. Barnes[5] that the value of the function $U(\tau)$ for $\alpha = -1$ is

$$U(\tau) = 4h(2 + \ln \tau\omega_B), \qquad \tau\omega_B \gg 1, \tag{25}$$

where ω_B is the system bandwidth. Substituting (25) into (13) yields the following:

$$\langle\sigma^2(N, \tau)\rangle = \frac{(N+1)4h}{N\tau^2}\left[2 + \ln \tau\omega_B - \frac{\ln N}{N^2 - 1}\right] \qquad \alpha = -1, \quad \tau\omega_B \gg 1. \tag{26}$$

One thus obtains the somewhat unfortunate result that experimentally it would be unlikely that one could distinguish between "flicker noise" phase modulation and any other noise with $-1 < \alpha$ up to and including white noise frequency modulation using the dependence of $\langle\sigma^2(N, T, \tau)\rangle$ on τ, since $\mu \simeq -2$ in this range. However, one might be able to infer from the experimental setup which of the two types of noise was being observed. If this were not possible, one would be forced to determine the type of noise present by some other technique, such as the one employed by Vessot in which he varies ω_B.[6]

If the number of samples N, and the ratio of the period of sampling to the sample time τ, are held constant, the following general equation can be written for both adjacent and nonadjacent sampling of data:

$$\langle\sigma^2(N, T, \tau)\rangle = K(N, \tau)|\tau|^\mu. \tag{27}$$

Using (27) and (6), ($S_\phi(\omega) = h|\omega|^\alpha$), coupled with the results established thus far, one is now able to extract the power spectral density from the dependence of the standard deviation on sample time for values of μ ranging from $-2 < \mu \leq 0$. All of the results have therefore been obtained to make the previous mapping of μ into α for finite data sampling.

III. Atomic Frequency Standards

A. Passive Atomic Standards

Devices such as atomic beam machines and rubidium gas cells have been made to generate impressively stable frequencies [7], [8]. In October, 1964, the appropriately authorized International Committee of Weights and Measures adopted as a provisional definition for the measurement of time, the transition between the $F=4$, $m_F=0$ and $F=3$, $m_F=0$ hyperfine levels of the ground state $^2S_{1/2}$ of the atom of cesium 133, unperturbed by external fields, with the assigned frequency for the transition of 9 192 631 770 Hz. The cesium beam at NBS has also been established as the United States Frequency Standard. The analysis of the theory of operation of these quantum devices has been covered in many publications [7], [8], along with the methods of slave-locking an oscillator to a given transition [8]. An analysis of the noise that should be present in an oscillator servoed to an atomic transition has been made by Kartaschoff [9], Cutler [6], and others. The author desires to reiterate at this point some of the results of these analyses: the frequency should appear white noise modulated; therefore, the phase fluctuations will go as the random walk phenomena, and hence the mean square time error in a clock running from one of these frequency standards would be proportional to the running time. Barnes [1] has also shown that

$$\langle(\Delta^3\phi)^2\rangle \sim \langle(\delta t)^2\rangle, \tag{28}$$

where Δ^3 denotes the 3rd finite difference and δt the clock error time for a running time t, and also that

$$\langle(\Delta^3\phi)^2\rangle \sim |\tau|^{\mu+2} \qquad -2 < \mu \leq 0. \tag{29}$$

The results from combining (28) and (29) are obvious, but still very important, i.e., if either the power spectrum or the dependence of $\langle\sigma^2\rangle$ on the sample time is known, one may then determine the rate of time divergence and conversely [see (7) and 10)],

$$\langle(\delta t)^2\rangle \sim |\tau|^{\mu+2}; \qquad -2 < \mu \leq 0. \tag{30}$$

An example of the above is illustrated by the following: if in fact "flicker noise" frequency modulation is present on the signal of rubidium gas cells, and if one assumes the rms time errors were equal on clocks driven by a rubidium gas cell and a cesium beam of theoretical form at $\frac{1}{3}$ of a day—say, for example, 0.1 microsecond—then the accumulated rms time error after 1 year would be of the order of 100 microseconds for the rubidium cell and 3 microseconds for the cesium beam.

B. Masers

Masers, in contrast to the passive atomic devices discussed in Section III-A, may be used as quantum mechanical oscillators [10]. Since the sources of "flicker noise" frequency modulation could arise from many different mechanisms, the suggestion exists that perhaps the active character of masers could be influenced by one of these mechanisms. Most of the basic experimental research associated with this paper and performed by the author has been to determine if the above suggestion is valid or not, and specifically to determine the type or types of noise present on the signals from masers.

One $N^{15}H_3$ maser has been in operation at NBS for

[5] See Barnes [1], equation (74), page 219.

[6] R. Vessot, L. Mueller, and J. Vanier, "The specification of oscillator characteristics from measurements made in the frequency domain," *this issue*, page 199. (Also see Appendix.)

several years. It is desirable to compare similar atomic devices in looking at noise, so another $N^{15}H_3$ maser was put into operation for direct comparison purposes. Worth considering at this time is the basic operation of a maser so that arguments made later on will be understandable.

Three basic elements of a maser are the source, the energy-state selector, and the resonant cavity. A needle valve and a collimating nozzle are coupled to the source to provide a highly directed beam of $N^{15}H_3$ down the axis of the four-pole focusers. The four-pole focusers are the energy-state selectors and consist of four electrodes with alternate high voltages so that on-axis (in line with the resonant cavity) the electric field is zero, but slightly off-axis the field is large and increases as the distance off axis. Because ammonia has an induced electric dipole moment, an interaction occurs as it enters this electric field region, and as it has been shown [10] the low energy states of the inversion levels of ammonia are defocused while the high energy states are focused on axis and into the resonant cavity. Therefore, if a noise component of the proper frequency is present and the ammonia beam flux is sufficient, a regenerative process will take place in which a high energy-state molecule will decay and radiate a quantum of energy "$h\nu$" causing the field to increase in the cavity and hence inducing other molecules to undergo the transition, etc. The radiation may be coupled off with a waveguide and then, with an appropriate detection scheme, one may observe the maser oscillations at a frequency ν where, neglecting any frequency pulling effects, ν is approximately 22 789 421 700 Hz for $N^{15}H_3$.

There are many parameters that affect the output frequency of an ammonia maser. It is from these parameters that one may expect correlation of frequency fluctuations over long times such as exist for "flicker noise" frequency modulation. To see the mechanism, consider the fundamental pulling equation [10]

$$\nu_0 - \nu \doteq \frac{\Delta\nu_1}{\Delta\nu_c}(\nu_0 - \nu_c) + B, \tag{31}$$

where ν_0 is the unperturbed transition frequency, ν the maser output frequency, $\Delta\nu_1$ the transition line width, $\Delta\nu_c$ the cavity bandwidth, ν_c the cavity's frequency, and B is a term involving the basic parameters such as ammonia beam flux, the voltage on the state selectors, and the magnetic and electric field intensities inside the cavity. Most of the quantities in (31) are dependent on temperature either directly or through the coupling electronics. Some of the quantities in (31) are dependent on the maser's alignment affording another mechanism for correlation of the long-term frequency fluctuations.

As described in detail elsewhere [11], it is possible to construct an electronic servo that will tune the resonant frequency of the cavity to that of the ammonia transition frequency ($\nu_0 = \nu_c$). The tuning is not perfect because of the noise present. The effect this has, as can be seen from (31), is profound, greatly reducing the effect of the basic parameters and almost entirely eliminating cavity dimensional instability. The correlation now existing in the long term frequency fluctuations may well be expected to be masked out by other noise in the system.

Since the servomechanism is of the frequency lock type, and if the noise in the servo is white over some finite bandwidth, then the fluctuations on the output frequency would be white inasmuch as they were caused by the servo. This is the same as for passive atomic devices—a result not altogether unexpected.

IV. Experiments Performed

A. $N^{15}H_3$ Maser Comparison

Two $N^{15}H_3$ masers were compared by the following technique. Each maser has coupled onto its output waveguide a balanced crystal detector and onto each detector a 30 MHz IF amplifier. Since the frequency of the inversion transition in $N^{15}H_3$ is about 22 790 MHz, a local oscillator signal at 22 760 MHz is inserted into each remaining leg of the balanced crystal detectors. The 30 MHz beat frequencies resulting from the output of the IF amplifiers are then compared in a balanced mixer and its audio output is analyzed; the bandwidth of this mixer is about 20 kHz. The frequency of the audio signal can be adjusted to a reasonable value by offset tuning the cavity of one of the masers. The period of this audio signal is determined with a counter; the data are punched on paper tape for computer analysis. The computer determines the average value of the fractional standard deviation σ, along with its confidence limit for pertinent discrete values of the sampling time τ.

In all of the maser data taken it was necessary to subtract out a systematic but well-understood linear drift—due to a change of the ammonia beam flux in the $N^{15}H_3$ maser and due to cavity dimensional drift from changing temperature in the case of the H maser. This was accomplished by the method of least squares [12]. The ability to change the number of samples N was also built into the computer program.

A plot of the computer output for some of the data analyzed in the $N^{15}H_3$ maser comparison is shown in Fig. 4. The output frequencies of the masers were not servo-controlled for these data. The slope is very nearly that of white noise frequency modulation. It will be noted that for a time of one second, the fractional standard deviation of the frequency fluctuations is less than 2×10^{-12}.

B. Cesium Beam, Maser, Quartz Oscillator Intercomparisons

Many comparisons were made between all the different types of atomic devices made available in the Atomic Frequency and Time Standards Section of NBS. Most of the comparisons were made at 5 MHz by measuring the period of the beat frequency with a counter, and the resulting data were processed by a computer.

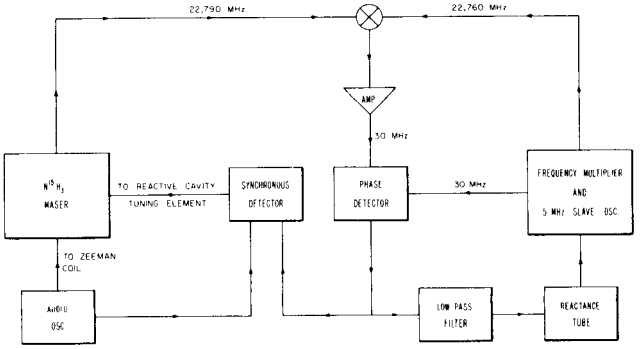

Fig. 3. Block diagram of maser cavity servo system.

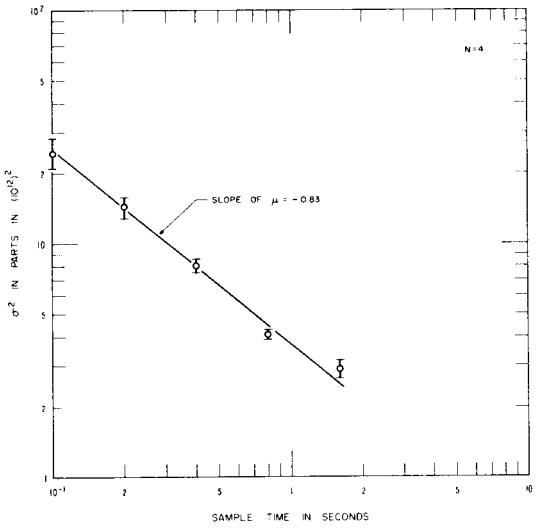

Fig. 4. Comparison of two $N^{15}H_3$ masers; standard deviation of the frequency fluctuations as a function of sampling time.

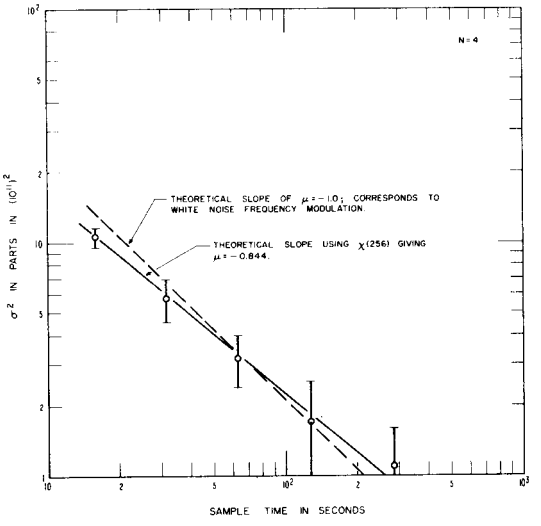

Fig. 5. Cesium beam (NBS III), $N^{15}H_3$ maser (2) comparison; standard deviation of the frequency fluctuations as a function of sampling time.

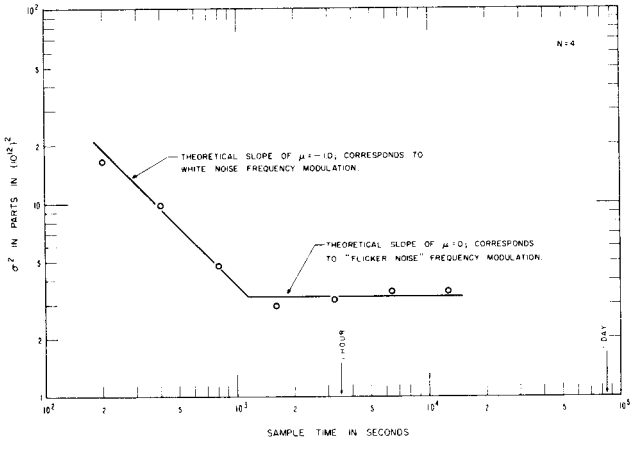

Fig. 6. Cesium beam (NBS III), quartz crystal oscillator comparison; standard deviation of the frequency fluctuations as a function of sampling time.

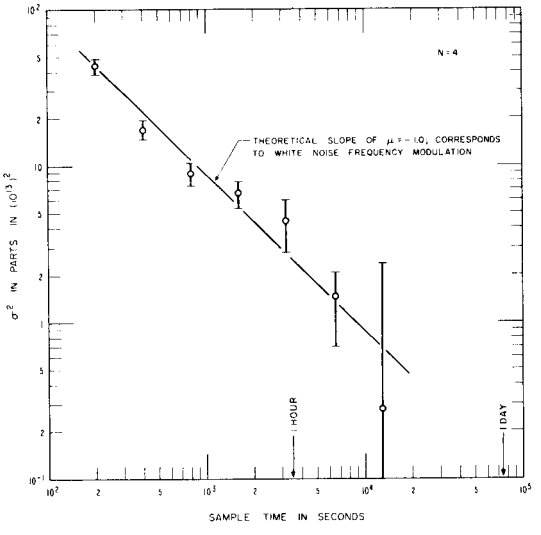

Fig. 7. Cesium beam (NBS III), hydrogen maser comparison; standard deviation of the frequency fluctuations as a function of sampling time.

The bandwidth of the 5 MHz mixer that produces the beat frequency was about 33 Hz.

A comparison was made between the double beam $N^{15}H_3$ maser with the cavity servo in operation as illustrated in Fig. 3, and the NBS III cesium beam. A 5 MHz quartz crystal oscillator of good spectral purity was phase locked by a double heterodyne technique to the output frequency of the maser, and this oscillator was compared with a high quality quartz crystal oscillator that was frequency locked to NBS III. A plot of the data is shown in Fig. 5. The noise is undoubtedly that of the maser cavity servo system, and though it exhibits very nearly its theoretical value of $\mu = -1$ for white noise frequency modulation, the noise level will be seen to be well over an order of magnitude higher than for the free-running maser.

The free-running, single beam, $N^{15}H_3$ maser was compared with NBS III on a longer time basis and indicated the presence of "flicker noise" frequency modulation. There was indicated a fair amount of uncertainty to the data, however.

In Fig. 6 one sees a very interesting plot in the comparison of the NBS III cesium beam with a very high quality quartz crystal oscillator. The comparison was again made at 5 MHz as indicated above. The first part of the curve shows the white noise frequency modulation in the cesium beam servo system, and then the curve changes slope indicating the presence of "flicker noise" frequency modulation as is typically exhibited by quartz crystal oscillators. This shows experimentally the theoretical result discussed previously, that one may have quite a high level of white noise in a system and eventually the system will be better than one with "flicker noise" frequency modulation.

An extended comparison was made (58 hours) between the H maser, NBS III cesium beam, a rubidium gas cell, and a quartz crystal oscillator. Some of the data are still to be analyzed, but some interesting and impressive results have been obtained thus far. Figure 7 shows the analysis of some of the data obtained from the H maser, cesium beam (NBS III) comparison. White noise frequency modulation is exhibited for sampling times extending to 4 hours with the very impressive standard deviation of $\sim 6 \times 10^{-14}$ for $\tau = 4$ hours. "Flicker noise" frequency modulation was observed on both the rubidium gas cell and on the quartz crystal oscillator in this comparison.

V. Conclusions

An invariant quality factor of a frequency standard having definite esthetic value would be the infinite time average, standard deviation of the frequency fluctuations. From the theoretical development a least biased estimate of this factor may be established in terms of the expectation value of the standard deviation for any finite number of samples:

$$\sigma^2 = \frac{(N-1)\langle \sigma^2(N,\tau)\rangle}{N(1-N^{\mu})},$$

$$-2 \le \mu \le 0 \text{ and } |\tau\omega_B|^{|\alpha+1|} \gg 1. \quad (32)$$

σ^2 also has the desirable feature of being dependent on only one variable, τ, except for $\mu = -2$, where it is also necessary to specify ω_B, the system bandwidth. Equation (32) is valid for all types of noise between and including "flicker noise" frequency modulation and white noise phase modulation ($-3 \le \alpha \le 0$). However, if $\alpha = -3$, some other means of specification need be employed, such as Barnes' [1] finite difference technique or $\langle \sigma^2(2,\tau)\rangle$ which, interestingly, is equal to $\langle(\Delta^2\phi)^2\rangle/2\tau^2$ (Δ^2 denotes the second finite difference).

"Flicker noise" frequency modulation was not observed on the frequency fluctuations of the maser type of atomic frequency standard for any of the reliable data obtained—the time coverage here being from about 0.1 second to 4 hours. The presence of "flicker noise" was indicated for free-running masers (both H and $N^{15}H_3$) in the long term range, though the data were somewhat unreliable. This type of noise was eliminated in the case of the $N^{15}H_3$ maser by use of a cavity servo mechanism, and one might infer from the similarities in the masers that the same would hold true for the H maser.

It is acknowledged that if "flicker noise" is present on the frequency fluctuations of a free-running maser for longer times, the lower cutoff frequency might be greater than for quartz crystal oscillators—for indeed the maser operator is himself a part of a cavity servo when he retunes the cavity or perhaps recoats the quartz bulb.

The existence of "flicker noise" frequency modulation on the frequency fluctuations of rubidium gas cells is just another indication that they would not at present make a reliable primary frequency standard. One cannot conclude from the data analyzed that "flicker noise" is not present on masers—even if a cavity servo is employed. It is possible, however, to determine an upper limit for the level of "flicker noise." If $G_\phi(\omega) = h|\omega|^{-3}$, then using (22), the upper limit of h can be determined from the minimum value of $\sigma^2(N,\tau)$. The value of h for $N^{15}H_3$ (determined from Fig. 4) is $\sim 7 \times 10^{-25}$ seconds^{-2}. It is of interest to compare this with the value of h determined for the quartz crystal oscillator shown in Fig. 6—$\backsim 8 \times 10^{-25}$ seconds^{-2}. Though comparable, it should be stated that this oscillator is one of the best that has been analyzed at NBS. The upper limit on h for the H maser, cesium beam (NBS III) comparison shown in Fig. 7 is $\backsim 2 \times 10^{-27}$ seconds^{-2}—being a factor of 350 and 400 times better than the $N^{15}H_3$ maser and quartz crystal oscillator, respectively.

There are many areas where additional data analysis would be informative. It would be very interesting to look at the behavior of the cesium beam, hydrogen

maser comparison, shown in Fig. 7, for extended times. Another analysis of interest would be that of a cavity-servoed H maser. Such a servo system is under development for the NBS H maser. To then compare the cavity-servoed H maser with a cesium beam and its associated servo system would afford great insight into determining which of these competitive atomic standards should be primary.

Appendix

The general expression for the autocovariance function for infinite bandwidth is:

$$R_\varphi(\tau) = a'(\alpha) \mid \tau \mid^{-\alpha-1}, \tag{33}$$

$\alpha \neq 0$, and not an integer, where

$$a'(\alpha) = 2\left[\cos\left(\frac{\pi(\alpha+1)}{2}\right)\right] \cdot \Gamma(\alpha+1).$$

Physically, $R_\varphi(0)$ is kept from diverging in the region $-1 < \alpha$ because of finite system bandwidths, ω_B; i.e., for any $\epsilon < 1/\omega_B$, $R_\varphi(\epsilon) \approx R_\varphi(1/\omega_B)$. A good approximation to $R_\varphi(0)$ in this region is, therefore, $R_\varphi(1/\omega_B)$. One may notice that the variance of the frequency fluctuations diverges [see (5)] with increasing ω_B. The variance of the frequency fluctuations may, therefore, be written:

$$\sigma^2 = \frac{a(\alpha)}{\tau^2}\left[\mid \omega_B \mid^{\alpha+1} - \mid \tau \mid^{-\alpha-1}\right]. \tag{34}$$

In the region $-3 < \alpha < -1$, $R_\varphi(0)$ is approximately zero; and if $\left|\tau\omega_B\right|^{\alpha+1} \gg 1$, then the equations for $U(\tau)$ are as written in (9).

Consider now a finite number of data samples N in the domain where $-1 < \alpha < 0$, and $\left|\tau\omega_B\right|^{\alpha+1} \gg 1$. Using the appropriate form of $U(\tau)$ from (9) and substituting into (13) gives:

$$\langle \sigma^2(N, \tau) \rangle = \frac{N+1}{N} a(\alpha) \mid \tau \mid^{\mu} \mid \tau\omega_B \mid^{\alpha+1}, \tag{35}$$

where

$$\mu = -\alpha - 3.$$

Hence, by keeping N and $\tau\omega_B$ constant, one can determine the value of μ (of α) on a log $\langle \sigma^2(N, \tau) \rangle$ vs. log τ plot, thus eliminating the degeneracy in this region. Equation (35) may also be written:

$$\langle \sigma^2(N, \tau) \rangle = \frac{(N+1) \cdot a(\alpha) \cdot \mid \omega_B \mid^{\alpha+1}}{N\tau^2}. \tag{36}$$

Hence, if N and τ are held constant and ω_B is varied, the slope on a log-log plot of $\langle \sigma^2(N, \tau) \rangle$ vs. ω_B would be $\alpha+1$—affording another technique of determining the spectral density in this domain.

It is of interest to note that the most sensitive parameters to use in arriving at the value of α are: the bandwidth, ω_B, if $-1 < \alpha < 0$; the sample time τ, if $-2 < \alpha < -1$; and the number of samples N, if $-3 < \alpha < -2$.

Acknowledgment

The author wishes to acknowledge the help of many of the personnel in the Atomic Frequency and Time Standards Section of NBS, Boulder, Colo. The author is sincerely indebted to J. A. Barnes for many informative discussions and for much aid in data processing; he has also contributed significantly in making manuscript criticisms for which the author is also very grateful. The help rendered by R. E. Beehler and C. S. Snider in making available the cesium beam frequency standards is greatly appreciated. Appreciation is also expressed to Dr. F. R. Petersen and to Dr. D. Halford for the hydrogen maser availability, and to V. Heaton for his help in data processing.

References

[1] J. A. Barnes, "Atomic timekeeping and the statistics of precision signal generators," this issue, page 207.

[2] J. A. Barnes and R. Vessot, private communication.

[3] M. Lighthill, *Introduction to Fourier Analysis and Generalized Functions*. Cambridge, England: University Press, 1962.

[4] C. L. Searle, R. D. Posner, R. S. Badessa, and V. J. Bates, "Computer-aided calculation of frequency stability," *1964 Proc. Symp. on the Definition and Measurement of Short-Term Frequency Stability*. Washington, D. C.: U. S. Govt. Printing Office, NASA SP-80, pp. 273–277.

[5] W. R. Atkinson, R. L. Fey, and J. Newman, "Spectrum analysis of extremely low frequency variations of quartz oscillators," *Proc. IEEE (Correspondence)*, vol. 51, p. 379, February 1963.

[6] L. S. Cutler, "Some aspects of the theory and measurement of frequency fluctuations in frequency standards," *1964 Proc. Symp. on the Definition and Measurement of Short-Term Frequency Stability*, pp. 89–100.

[7] R. C. Mockler, "Atomic beam frequency standards," *Advan. Electron. and Electron. Physics*, vol. 15, 1961.

[8] R. E. Beehler, W. R. Atkinson, L. E. Heim, and C. S. Snider, "A comparison of direct and servo methods for utilizing cesium beam resonators as frequency standards," *IRE Trans. on Instrumentation*, vol. I-11, pp. 231–238, December 1962.

[9] P. Kartaschoff, "Influence de l'Effect de Grenaille sur la Frequence d'un Oscillateur Asservi A un Etalon a Jet Atomique," Laboratoire Suisse de Recherches Horlogères, Neuchatel, Switzerland, Rapport L.S.R.H. 08-64-01. See also, P. Kartaschoff, "Shot-effect influence on the frequency of an oscillator locked to an atomic beam resonator," *1964 Proc. Symp. on the Definition and Measurement of Short-Term Frequency Stability*, pp. 303–308.

[10] A. A. Vuylsteke, *Elements of Maser Theory*. Princeton, N. J.: Van Nostrand.

[11] J. A. Barnes, D. W. Allan, and A. E. Wainwright, "The ammonia beam maser as a standard of frequency," *IRE Trans. on Instrumentation*, vol. I-11, pp. 26–30, June 1962.

[12] C. R. Wylie, *Advanced Engineering Mathematics*. New York: McGraw-Hill, p. 527, 1951.

ERRATA SHEET

STATISTICS OF ATOMIC FREQUENCY STANDARDS

by

David W. Allan

Equation (12) p.223 should have summation from n = 1 to N - 1 rather than from n = 0

$$\left(\sum_{n=1}^{N-1} (N-n) \left[\quad \right] \right)$$

Equation (22), page 225 should read

$$\lim_{\tau \to 0^+} \left\langle \left[\frac{\varphi(t+\tau) - \varphi(t)}{\tau} \right] \right\rangle = \langle \Omega(t) \rangle \ .$$

Equation (24), page 225 should read

$$\langle \sigma^2(N, T, \tau) \rangle = \frac{k}{N(N-1)} \sum_{n=1}^{N-1} (N-n) \left[-2(nr)^2 \ln(nr) + (nr+1)^2 \ln(nr+1) + (nr-1)^2 \ln(nr-1) \right] .$$

The next to last line in paragraph 1 of the Appendix should read:

"zero; and if $|\tau \omega_B|^{|\alpha+1|} >> 1$, then the equation for $U(\tau)$..." .

FLICKER NOISE OF PHASE IN RF AMPLIFIERS AND FREQUENCY MULTIPLIERS: CHARACTERIZATION, CAUSE, AND CURE

Donald Halford, A. E. Wainwright, and James A. Barnes

Time and Frequency Division
National Bureau of Standards, Boulder, Colorado 80302

(14 December 1967)

Summary

The high phase stability of atomic frequency standards has called for the development of associated electronic equipment of equivalent or superior stability. We have surveyed the performance of existing high quality frequency multipliers and RF amplifiers which operate in the range of 5 MHz to microwave frequencies. We were most interested in the phase noise in the range of Fourier frequencies, f, of about 10^{-2} Hz to 10^{+3} Hz, since most electronic servo systems in existing atomic frequency standards use modulation frequencies which fall within this range. This range also includes the passive linewidths of existing atomic frequency standards.

We found that all state-of-the-art, solid state amplifiers and frequency multipliers in our survey had random phase fluctuations (phase noise) of significant intensity and with a spectral density proportional to 1/f (flicker noise of phase). Surprisingly, the flicker noise of phase was found to be approximately the same in most of the apparatus included in the survey. The typical one-sided spectral density of the phase noise was about $(10^{-11.2}$ radian$^2)/f$ when referred to the input frequency, and the best performance was only 6 dB better. This performance was independent of the input frequency over at least the surveyed range of 5 MHz to 100 MHz, and did not depend upon the multiplication factor. This noise level exceeds by about 20 dB the stability which is needed for full compatibility with existing hydrogen atom masers and with proposed high flux cesium beam designs.

Through our laboratory experimentation, this flicker noise of phase was shown to be due to intrinsic, direct, phase modulation of the RF carrier by the transistors. No large differences in the flicker noise intensity were found among different types of transistors, whether field effect or bipolar (including overlay), silicon or germanium, high f_T or medium f_T, high DC flicker noise or low DC flicker noise, and hermetic can or plastic. With the knowledge that the active elements invariably cause phase noise via intrinsic, direct, phase modulation, we could predict that negative feedback, and only negative feedback, could reduce the phase noise.

By systematically applying local RF negative feedback (emitter degeneration) to each of the transistors in an apparatus, we have realized typically more than 30 dB (up to 40 dB in some cases) reduction of the flicker noise of phase in amplifiers and frequency multipliers. No other circuit

improvements were found which yielded significant additional reduction of the flicker noise of phase. Individual silver mica capacitors (80% of our stock) gave excessive flicker noise of phase, but, by testing and selecting capacitors, this source of noise could always be avoided. Selection of individual transistors had relatively little effect, typically no more than 4 dB.

This improved performance of amplifiers and frequency multipliers comfortably exceeds the requirements for compatibility with contemporary and proposed atomic frequency standard systems. At the Frequency Control Symposium we will discuss

1. our survey of the state-of-the-art,
2. the measurements which proved that the active elements (transistors) were the unavoidable source of the flicker noise of phase,
3. the use of local RF negative feedback as the only practical means of achieving extremely low flicker noise of phase,
4. the measured performance of our new amplifier and frequency multiplier designs, and
5. the outlook for possible similar improvements in oscillators, mixers, and other phase-processing electronic equipment.

Reprinted from:
Proc. of the 22nd Ann. Symp. on Freq. Contr.
(U. S. Army Electronics Command, Ft. Monmouth, New Jersey, Apr. 22-24, 1968)
pp. 340=341 (April 1968).

UNITED STATES DEPARTMENT OF COMMERCE
C. R. Smith, Secretary
NATIONAL BUREAU OF STANDARDS • A. V. Astin, Director

TECHNICAL NOTE 375

ISSUED JANUARY 1969

TABLES OF BIAS FUNCTIONS, B_1 AND B_2, FOR VARIANCES BASED ON FINITE SAMPLES OF PROCESSES WITH POWER LAW SPECTRAL DENSITIES

J. A. BARNES

Time and Frequency Division
Institute for Basic Standards
National Bureau of Standards
Boulder, Colorado 80302

CONTENTS

TABLES OF BIAS FUNCTIONS, B_1 AND B_2, FOR VARIANCES BASED ON FINITE SAMPLES OF PROCESSES WITH POWER LAW SPECTRAL DENSITIES

J. A. Barnes

ABSTRACT

D. W. Allan showed that if y(t) is a sample function of a random noise process with a power law spectral density (i.e., $S_y(f) = h|f|^{\alpha}$), then there is generally bias to the estimated variance of y, defined as

$$\sigma_y^2(N, T, \tau) = \frac{1}{N-1} \sum_{n=1}^{N} (\bar{y}_n - \langle \bar{y} \rangle)^2,$$

where N is the number of samples, $\bar{y}_n$ is the average value of y(t) over the n-th interval of duration τ, T is the time between the beginnings of any two successive sample intervals, and

$$\langle \bar{y} \rangle \equiv \frac{1}{N} \sum_{n=1}^{N} \bar{y}_n .$$

Allan also showed that, under these conditions, the expectation value of the estimated variance is proportional to τ^{μ} where μ is a constant related to α, the exponent in the spectral density; i.e.,

$$E[\sigma_y^2(N, T, \tau)] \propto \tau^{\mu} .$$

Based on this work one may define the two bias functions

$$B_1(N, r, \mu) \equiv \frac{E[\sigma_y^2(N, T, \tau)]}{E[\sigma_y^2(2, T, \tau)]}$$

and

$$B_2(r, \mu) \equiv \frac{E[\sigma_y^2(2, T, \tau)]}{E[\sigma_y^2(2, \tau, \tau)]}$$

where $r \equiv T/\tau$ and the B's are functions of μ through their dependence on y(t).

If one has a sample variance, $\sigma_y^2(N_1, T_1, \tau_1)$, the bias functions allow one to give an unbiased estimate for $\sigma_y^2(N_2, T_2, \tau_2)$ provided the spectral type is known (i.e., μ is known).

The tables give values of $B_1(N, r, \mu)$ and $B_2(r, \mu)$ accurate to four significant figures for the following values of N, r, μ:

μ = -2.0 to 2.0 in steps of 0.2;

N = 4, 8, 16, 32, 64, 128, 256, 512, 1024, ∞ ;

r = 0.001, 0.003, 0.01, 0.03, 0.1, 0.2, 0.4, 0.8, 1, 1.01, 1.1,
2, 4, 8, 16, 32, 64, 128, 256, 512, 1024, 2048, ∞ .

Key Words: statistics, variance, spectral density, unbiased estimate

TABLES OF BIAS FUNCTIONS, B_1 AND B_2, FOR VARIANCES BASED ON FINITE SAMPLES OF PROCESSES WITH POWER LAW SPECTRAL DENSITIES

J. A. Barnes

Consider a random variable y with mean m. The variance of y is defined as the expectation value of $(y - m)^2$, that is

$$\text{Var } y \equiv E[(y - m)^2] .$$

This is defined as an average over the entire ensemble but, for an ergodic process, y(t), it can alternatively be defined as an average over all time, t.

Typically, the variance of y is estimated from a finite set of experimental values according to the relation

$$(\text{Var } y)_{\text{est.}} = \frac{1}{N-1} \sum_{i=1}^{N} (y_i - \langle y \rangle)^2 \qquad (1)$$

where $\langle y \rangle \equiv \frac{1}{N} \sum_{i=1}^{N} y_i$ is the mean of the y_i. The factor $\frac{1}{N-1}$ is used in order that the estimate have no bias for non-correlated y: that is, one typically wants to obtain the true variance which would be obtained as $N \to \infty$. For finite N, the estimated variance has some expected value,

$$E\left[\frac{1}{N-1} \sum_{n=1}^{N} (y_i - \langle y \rangle)^2\right] .$$

If the y_i are independent (actually, non-correlated is sufficient) random variables, then the expected value of this estimated variance for finite

N is exactly equal to the true (infinite N) variance. If the y_i are correlated, however, the estimate based on (1) may indeed be biased. This fact has been recognized and discussed in some detail for the case of power law spectral densities by Allan [1].

The Bias Functions, B_1 and B_2

Following Allan [1], consider a random process y(t) with continuous sample functions. We assume that y(t) has a spectral density, $S_y(f)$, which obeys the law

$$S_y(f) = h|f|^{\alpha}, \quad f_\ell < |f| < f_u \tag{2}$$

where h is a constant, the limit frequencies f_ℓ and f_u satisfy the relations

$$0 \leq f_\ell << f_u < \infty \ ,$$

and any intervals of time, Δt, of any significance satisfy the relations

$$\frac{1}{f_u} << \Delta t << \frac{1}{f_\ell} \ .$$

In short, y(t) has a power law spectral density over the entire range of significance.

Consider a measurement process which determines an average value of y(t) over the interval t to $t + \tau$. That is,

$$\bar{y}(t) = \frac{1}{\tau} \int_t^{t+\tau} y(t')dt' \ . \tag{3}$$

One, now, may determine an estimated variance from a group of N such measurements spaced every T units of time; that is,

$$\sigma_y^2(N, T, \tau) = \frac{1}{N-1} \sum_{n=1}^{N} \left\{ \bar{y}(t+nT) - \frac{1}{N} \sum_{k=1}^{N} \bar{y}(t+kT) \right\}^2, \qquad (4)$$

which is called the "Allan variance" [1].

Allan [1] has shown that under these conditions,

$$E\left[\sigma_y^2(N, T, \tau)\right] \propto \tau^{\mu}, \quad N \text{ and } T/\tau \text{ constant},$$

where μ is related* to α according to the mapping shown in Figure 1 (see references 1 and 2). The relation between μ and α may be given as

$$\mu = \begin{cases} -2 \text{ if } \alpha \geq 1 \\ -\alpha - 1 \text{ if } -3 < \alpha \leq 1 \\ \text{not defined otherwise.} \end{cases}$$

This mapping involves a simple extension of Allan's work [1] to the range $0 < \mu < 2$. This extension was also mentioned in [3].

Allan [1] considered in some detail the case where $T = \tau$. This is the case of exactly adjacent sample averages--no "dead time" between measurements. Allan defined a function, $\chi(N, \mu)$, as follows

$$\chi(N, \mu) \equiv \frac{E\left[\sigma_y^2(N, \tau, \tau)\right]}{E\left[\sigma_y^2(2, \tau, \tau)\right]}, \qquad (5)$$

where it is again assumed that

---

*It should be noted that in reference 1 the exponent, α, corresponds to the spectrum of phase fluctuations while variances are taken over average frequency fluctuations. In the present paper, α is equal to the exponent, α, in [1] plus two. Thus, in this paper, all considerations are confined to one variable, y(t) (analogous to frequency in [1]) and the spectral density of y, $S_y(f)$. This paper does not consider the spectrum of the integral of y(t).

463-560 O - 72 - 32

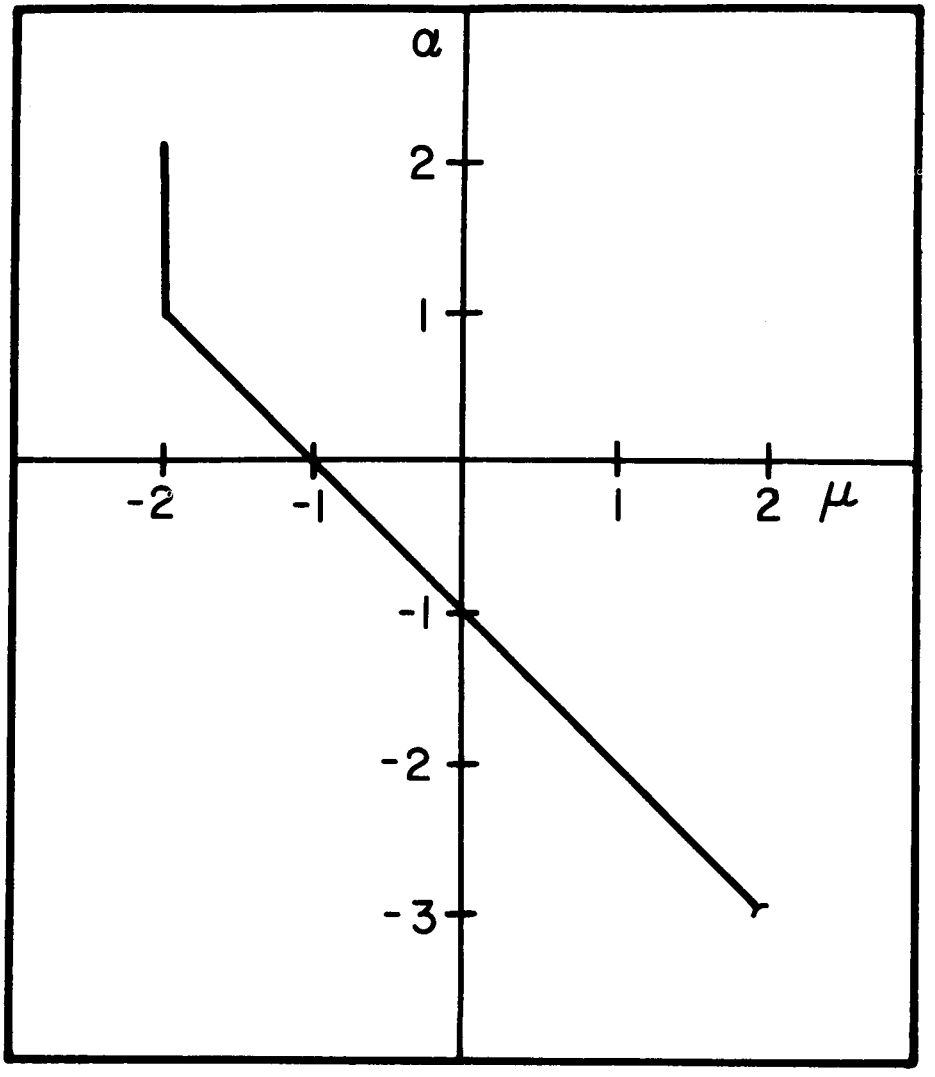

FIG. 1 μ-α MAPPING

$$E\left[\sigma_y^2(N, \tau, \tau)\right] \propto \tau^{\mu}, \quad N \text{ constant} .$$

Allan shows [1] that experimental evaluations of $\chi(N, \mu)$ may be used to infer μ and hence the spectral type by use of the mapping of Figure 1.

Since many experiments actually have dead time present, it is of value to make two different extensions of this function, $\chi(N, \mu)$. First, define $B_1(N, r, \mu)$ by the relations

$$B_1(N, r, \mu) \equiv \frac{E\left[\sigma_y^2(N, T, \tau)\right]}{E\left[\sigma_y^2(2, T, \tau)\right]} \tag{6}$$

where $r \equiv T/\tau$ and

$$E\left[\sigma_y^2(N, T, \tau)\right] \propto \tau^{\mu}, \quad N \text{ and } r \text{ constant} .$$

The second function, $B_2(r, \mu)$, is defined according to the relation

$$B_2(r, \mu) \equiv \frac{E\left[\sigma_y^2(2, T, \tau)\right]}{E\left[\sigma_y^2(2, \tau, \tau)\right]} \tag{7}$$

where $r \equiv T/\tau$. In words, B_1 is the ratio of the expected variance for N samples to the expected variance for 2 samples (everything else fixed); while B_2 is the ratio of the expected variance with dead time to that of no dead time (with N = 2 and τ held constant). The B's, then, reflect bias relative to N = 2 rather than N = ∞. It is apparent that $B_1(N, r=1, \mu) \equiv \chi(N, \mu)$.

For the conditions given above and with reference to Allan [1], one may write expressions for both B_1 and B_2, as follows:

$$B_1(N, r, \mu) = \frac{1 + \sum_{n=1}^{N-1} \frac{N-n}{N(N-1)} \left[2|nr|^{\mu+2} - |nr+1|^{\mu+2} - |nr-1|^{\mu+2} \right]}{1 + \frac{1}{2} \left[2|r|^{\mu+2} - |r+1|^{\mu+2} - |r-1|^{\mu+2} \right]}; \quad (8)$$

in particular for $r = 1$,

$$B_1(N, 1, \mu) = \frac{N(1-N^{\mu})}{2(N-1)(1-2^{\mu})}; \quad (9)$$

and

$$B_2(r, \mu) = \frac{1 + \frac{1}{2} \left[2|r|^{\mu+2} - |r+1|^{\mu+2} - |r-1|^{\mu+2} \right]}{2(1 - 2^{\mu})}, \quad (10)$$

except that by definition, $B_2(1, \mu) \equiv 1$. The magnitude bars are essential on the $r-1$ term when $r < 1$, and, indeed, proper. Since Allan [1] was involved with $r \geq 1$ the magnitude bars were dropped in reference 1.

For $\mu = 0$, equations (8), (9), and (10) are indeterminate of form 0/0 and must be evaluated by L'Hospital's rule. Special attention must also be given when expressions of the form 0^0 arise.

One may obtain the following results:

$B_1(2, r, \mu) \equiv 1$

$B_1(N, r, 2) = \frac{N(N+1)}{6}$

$B_1(N, 1, 1) = \frac{N}{2}$

$B_1(N, r, -1) = 1$ if $r \geq 1$

$B_1(N, r, -2) = 1$ if $r \neq 1$ or 0

$B_2(0, \mu) \equiv 0$

$B_2(1, \mu) \equiv 1.$

$$B_2(r, 2) = r^2$$

$$B_2(r, 1) = \frac{1}{2}(3r - 1) \text{ if } r \geq 1$$

$$B_2(r, -1) = \begin{cases} r \text{ if } 0 \leq r \leq 1 \\ 1 \text{ if } r \geq 1 \end{cases}$$

$$B_2(r, -2) = \begin{cases} 0 \text{ if } r = 0 \\ 1 \text{ if } r = 1 \\ 2/3 \text{ otherwise} \end{cases}$$

Values of the functions $B_1(N, r, \mu)$ and $B_2(r, \mu)$ are tabulated on the following pages for values of N, r, μ as shown below:

μ = -2.0 to 2.0 in steps of 0.2;

N = 4, 8, 16, 32, 64, 128, 256, 512, 1024, ∞ ;

r = 0.001, 0.003, 0.01, 0.03, 0.1, 0.2, 0.4, 0.8,
1, 1.01, 1.1, 2, 4, 8, 16, 32, 64, 128, 256, 512, 1024,
2048, ∞ .

Figure 2 is a graphical representation of $B_2(r, \mu)$ for $0 \leq r \leq 2$ and $-2 \leq \mu \leq 2$.

Examples of the use of the bias functions

The spectral type, that is, the value of μ, may be inferred by varying τ, the sample time [1, 2]. Another useful way, however, of determining the value of μ is by using $B_1(N, r, \mu)$ as follows: calculate an estimate of $E\left[\sigma_y^2(N, T, \tau)\right]$ and of $E\left[\sigma_y^2(2, T, \tau)\right]$ and hence $B_1(N, r, \mu)$; then by use of the tables the value of μ may be inferred.

Suppose one has an experimental value of $\sigma_y^2(N_1, T_1, \tau_1)$ and its spectral type is known--that is, μ is known. Suppose also that one wishes to know the variance at some other set of measurement parameters, N_2, T_2, τ_2. An unbiased estimate of $\sigma_y^2(N_2, T_2, \tau_2)$ may be calculated by the equation:

$$E\left[\sigma_y^2(N_2, T_2, \tau_2)\right] = \left(\frac{\tau_2}{\tau_1}\right)^{\mu} \left[\frac{B_1(N_2, r_2, \mu)B_2(r_2, \mu)}{B_1(N_1, r_1, \mu)B_2(r_1, \mu)}\right] E\left[\sigma_y^2(N_1, T_1, \tau_1)\right]$$

where $r_1 = T_1/\tau_1$ and $r_2 = T_2/\tau_2$.

Obviously one might be interested in $N_2 = \infty$. In this case if $\mu \geq 0$, the expected value of $\sigma_y^2(\infty, T_2, \tau_2)$ is also infinite. This is true because,

$$\lim_{N_2 \to \infty} B_1(N_2, r_2, \mu) = \infty ,$$

for $\mu \geq 0$.

Also, it should be noted that, for $\mu = 2$, $E\left[\sigma_y^2(N, T, \tau)\right]$ is a function of f_ℓ for any $N \geq 2$, T, τ, even though $B_1(N, r, 2)$ and $B_2(r, 2)$ as determined from (8), (9), and (10) are finite and well behaved [3]. In this region, $\mu \sim 2$, the low frequency behavior is critically important.

ACKNOWLEDGEMENT

The author wishes to acknowledge the capable assistance of Mrs. Bernice Bender who wrote the computer programs for evaluating the functions and Messrs. D. W. Allan and D. J. Glaze for many helpful discussions.

REFERENCES

1 D. W. Allan, "Statistics of Atomic Frequency Standards," Proc. IEEE, Vol. 54, No. 2, February 1966, pp. 221-230.

2 R. F. C. Vessot, L. Mueller, and J. Vanier, "The Specification of Oscillator Characteristics from Measurements made in the Time Domain," Proc. IEEE, Vol. 54, No. 2, pp. 199-207, February 1966.

3 J. A. Barnes and D. W. Allan, "An Approach to the Prediction of Coordinated Universal Time," Frequency, Vol. 5, No. 6, November/December 1967, pp. 15-20.

TABLES OF B_1 AND B_2

The tables are photographic reproductions of the computer output. Each entry for the value of the functions, B_1 and B_2 consists of a decimal number followed by an integer which is the exponent of 10. Ten raised to this power should multiply the decimal number. Thus the table entry 2.752 + 003 could be written 2.752×10^{3} or, simply 2752. Similarly, "9.869 - 001" = 9.869×10^{-1} = 0.9869.

B1(N,R,MU) FOR R= 0.001

MU	N = 4	8	16	32	64	128	256	512	1024	∞
2.00	3.333•000	1.200•001	4.533•001	1.760•002	6.933•002	2.752•003	1.097•004	4.378•004	1.749•005	∞
1.80	3.333+000	1.200•001	4.533•001	1.760•002	6.931•002	2.749•003	1.092•004	4.326•004	1.690•005	∞
1.60	3.333+000	1.200•001	4.533•001	1.759•002	6.926•002	2.743•003	1.087•004	4.265•004	1.628•005	∞
1.40	3.333+000	1.200+001	4.532•001	1.758•002	6.916•002	2.734•003	1.078•004	4.187•004	1.560•005	∞
1.20	3.333+000	1.200•001	4.529•001	1.756•002	6.894•002	2.716•003	1.064•004	4.081•004	1.484•005	∞
1.00	3.332•000	1.199•001	4.520•001	1.749•002	6.847•002	2.682•003	1.041•004	3.931•004	1.392•005	∞
0.80	3.328+000	1.195•001	4.497•001	1.733•002	6.743•002	2.617•003	1.001•004	3.708•004	1.276•005	∞
0.60	3.317+000	1.186•001	4.435•001	1.695•002	6.519•002	2.491•003	9.344•003	3.373•004	1.124•005	∞
0.40	3.284+000	1.161•001	4.280•001	1.608•002	6.058•002	2.259•003	8.233•003	2.877•004	9.247•004	∞
0.20	3.200•000	1.101•001	3.943•001	1.435•002	5.220•002	1.875•003	6.563•003	2.200•004	6.786•004	∞
-0.00	3.027•000	9.877•000	3.354•001	1.157•002	3.985•002	1.355•003	4.491•003	1.429•004	4.201•004	∞
-0.20	2.761•000	8.268•000	2.585•001	8.231•001	2.624•002	8.281•002	2.658•003	7.622•003	2.120•004	3.066•005
-0.40	2.450+000	6.549•000	1.837•001	5.269•001	1.520•002	4.365•002	1.235•003	3.399•003	8.860•003	6.507•004
-0.60	2.150+000	5.053•000	1.250•001	3.172•001	8.138•001	2.089•002	5.325•002	1.335•003	3.224•003	1.592•004
-0.80	1.888+000	3.881•000	8.397•000	1.868•001	4.211•001	9.545•001	2.162•002	4.865•002	1.076•003	3.983•003
-1.00	1.667•000	3.000•000	5.667•000	1.100•001	2.167•001	4.300•001	8.567•001	1.710•002	3.417•002	1.000•003
-1.20	1.482•000	2.344•000	3.868•000	6.547•000	1.124•001	1.945•001	3.386•001	5.936•001	1.057•002	2.512•002
-1.40	1.327•000	1.854•000	2.680•000	3.959•000	5.921•000	8.924•000	1.353•001	2.068•001	3.236•001	6.310•001
-1.60	1.198+000	1.487•000	1.890•000	2.442•000	3.185•000	4.179•000	5.511•000	7.317•000	9.946•000	1.585•001
-1.80	1.091+000	1.210•000	1.360•000	1.541•000	1.757•000	2.010•000	2.306•000	2.656•000	3.106•000	3.981•000
-2.00	1.000+000	1.000•000	1.000•000	1.000•000	1.000•000	1.000•000	1.000•000	1.000•000	1.000•000	1.000•000

B1(N,R,MU) FOR R= 0.003

MU	N = 4	8	16	32	64	128	256	512	1024	∞
2.00	3.333+000	1.200+001	4.533+001	1.760+002	6.933+002	2.752+003	1.097+004	4.378+004	1.749+005	∞
1.80	3.333+000	1.200+001	4.532+001	1.759+002	6.917+002	2.732+003	1.072+004	4.112+004	1.514+005	∞
1.60	3.333+000	1.200+001	4.530+001	1.756+002	6.892+002	2.706+003	1.046+004	3.854+004	1.311+005	∞
1.40	3.333+000	1.199+001	4.526+001	1.752+002	6.853+002	2.671+003	1.015+004	3.596+004	1.132+005	∞
1.20	3.332+000	1.198+001	4.516+001	1.744+002	6.788+002	2.620+003	9.774+003	3.330+004	9.717+004	∞
1.00	3.329+000	1.195+001	4.494+001	1.728+002	6.674+002	2.543+003	9.290+003	3.043+004	8.254+004	∞
0.80	3.321+000	1.189+001	4.446+001	1.696+002	6.473+002	2.425+003	8.645+003	2.721+004	6.875+004	∞
0.60	3.302+000	1.173+001	4.342+001	1.634+002	6.124+002	2.242+003	7.765+003	2.346+004	5.536+004	∞
0.40	3.256+000	1.138+001	4.132+001	1.519+002	5.544+002	1.967+003	6.584+003	1.907+004	4.210+004	∞
0.20	3.157+000	1.069+001	3.753+001	1.330+002	4.667+002	1.589+003	5.103+003	1.414+004	2.927+004	∞
-0.00	2.981+000	9.558+000	3.177+001	1.066+002	3.541+002	1.143+003	3.490+003	9.224+003	1.794+004	∞
-0.20	2.729+000	8.054+000	2.474+001	7.694+001	2.377+002	7.169+002	2.061+003	5.175+003	9.470+003	4.488+004
-0.40	2.435+000	6.454+000	1.790+001	5.052+001	1.425+002	3.955+002	1.058+003	2.511+003	4.330+003	1.142+004
-0.60	2.145+000	5.024+000	1.236+001	3.112+001	7.881+001	1.982+002	4.870+002	1.085+003	1.765+003	3.434+003
-0.80	1.887+000	3.876+000	8.372+000	1.857+001	4.167+001	9.363+001	2.085+002	4.326+002	6.638+002	1.066+003
-1.00	1.667+000	3.000+000	5.667+000	1.100+001	2.167+001	4.300+001	8.567+001	1.637+002	2.368+002	3.333+002
-1.20	1.482+000	2.344+000	3.870+000	6.556+000	1.128+001	1.960+001	3.451+001	6.001+001	8.168+001	1.043+002
-1.40	1.328+000	1.854+000	2.681+000	3.964+000	5.941+000	9.001+000	1.386+001	2.159+001	2.756+001	3.264+001
-1.60	1.199+000	1.487+000	1.890+000	2.443+000	3.191+000	4.205+000	5.623+000	7.711+000	9.174+000	1.021+001
-1.80	1.091+000	1.210+000	1.360+000	1.542+000	1.759+000	2.016+000	2.331+000	2.759+000	3.031+000	3.196+000
-2.00	1.000+000	1.000+000	1.000+000	1.000+000	1.000+000	1.000+000	1.000+000	1.000+000	1.000+000	1.000+000

B1(N,P,MU) FOR R= 0.010

MU	N = 4	8	16	32	64	128	256	512	1024	∞
2.00	3.333+000	1.200+001	4.533+001	1.760+002	6.933+002	2.752+003	1.097+004	4.378+004	1.749+005	∞
1.80	3.333+000	1.199+001	4.526+001	1.750+002	6.819+002	2.623+003	9.737+003	3.493+004	1.231+005	∞
1.60	3.332+000	1.198+001	4.514+001	1.738+002	6.688+002	2.493+003	8.637+003	2.793+004	8.697+004	∞
1.40	3.330+000	1.196+001	4.494+001	1.720+002	6.530+002	2.359+003	7.640+003	2.234+004	6.169+004	∞
1.20	3.327+000	1.192+001	4.461+001	1.693+002	6.330+002	2.215+003	6.717+003	1.782+004	4.383+004	∞
1.00	3.319+000	1.185+001	4.403+001	1.653+002	6.066+002	2.055+003	5.842+003	1.412+004	3.109+004	∞
0.80	3.302+000	1.170+001	4.303+001	1.590+002	5.708+002	1.869+003	4.991+003	1.104+004	2.189+004	∞
0.60	3.268+000	1.143+001	4.133+001	1.495+002	5.221+002	1.649+003	4.142+003	8.419+003	1.514+004	∞
0.40	3.203+000	1.095+001	3.857+001	1.354+002	4.572+002	1.390+003	3.287+003	6.172+003	1.014+004	∞
0.20	3.089+000	1.018+001	3.448+001	1.162+002	3.763+002	1.097+003	2.446+003	4.263+003	6.453+003	∞
-0.00	2.912+000	9.076+000	2.909+001	9.282+001	2.857+002	7.951+002	1.672+003	2.719+003	3.826+003	∞
-0.20	2.677+000	7.714+000	2.296+001	6.836+001	1.976+002	5.220+002	1.036+003	1.580+003	2.084+003	5.581+003
-0.40	2.407+000	6.279+000	1.703+001	4.655+001	1.247+002	3.106+002	5.814+002	8.357+002	1.043+003	1.715+003
-0.60	2.134+000	4.959+000	1.205+001	2.977+001	7.296+001	1.697+002	2.995+002	4.076+002	4.851+002	6.423+002
-0.80	1.884+000	3.860+000	8.303+000	1.828+001	4.041+001	8.691+001	1.443+002	1.868+002	2.137+002	2.519+002
-1.00	1.667+000	3.000+000	5.667+000	1.100+001	2.167+001	4.255+001	6.628+001	8.190+001	9.064+001	1.000+002
-1.20	1.482+000	2.346+000	3.880+000	6.598+000	1.145+001	2.026+001	2.947+001	3.486+001	3.754+001	3.980+001
-1.40	1.328+000	1.856+000	2.688+000	3.991+000	6.064+000	9.500+000	1.282+001	1.456+001	1.532+001	1.585+001
-1.60	1.199+000	1.487+000	1.893+000	2.455+000	3.239+000	4.440+000	5.505+000	6.002+000	6.198+000	6.309+000
-1.80	1.091+000	1.210+000	1.360+000	1.545+000	1.772+000	2.089+000	2.349+000	2.456+000	2.494+000	2.512+000
-2.00	1.000+000	1.000+000	1.000+000	1.000+000	1.000+000	1.000+000	1.000+000	1.000+000	1.000+000	1.000+000

B1(N,R,MU) FOR R= 0.030

MU	N = 4	8	16	32	64	128	256	512	1024	∞
2.00	3.333+000	1.200+001	4.533+001	1.760+002	6.933+002	2.752+003	1.097+004	4.378+004	1.749+005	∞
1.80	3.331+000	1.196+001	4.487+001	1.706+002	6.374+002	2.304+003	8.742+003	2.849+004	9.936+004	∞
1.60	3.327+000	1.191+001	4.431+001	1.650+002	5.851+002	1.930+003	6.068+003	1.866+004	5.684+004	∞
1.40	3.320+000	1.184+001	4.360+001	1.588+002	5.352+002	1.615+003	4.535+003	1.228+004	3.276+004	∞
1.20	3.309+000	1.172+001	4.267+001	1.518+002	4.867+002	1.348+003	3.392+003	8.128+003	1.903+004	∞
1.00	3.290+000	1.155+001	4.141+001	1.437+002	4.382+002	1.117+003	2.533+003	5.395+003	1.114+004	∞
0.80	3.257+000	1.128+001	3.966+001	1.339+002	3.887+002	9.152+002	1.879+003	3.580+003	6.554+003	∞
0.60	3.203+000	1.087+001	3.728+001	1.220+002	3.372+002	7.357+002	1.376+003	2.364+003	3.868+003	∞
0.40	3.118+000	1.027+001	3.412+001	1.077+002	2.835+002	5.750+002	9.868+002	1.541+003	2.277+003	∞
0.20	2.992+000	9.460+000	3.013+001	9.127+001	2.296+002	4.324+002	6.856+002	9.834+002	1.328+003	∞
-0.00	2.819+000	8.430+000	2.546+001	7.348+001	1.748+002	3.096+002	4.568+002	6.082+002	7.611+002	∞
-0.20	2.604+000	7.242+000	2.047+001	5.581+001	1.259+002	2.094+002	2.897+002	3.619+002	4.256+002	8.571+002
-0.40	2.362+000	6.005+000	1.566+001	3.993+001	8.524+001	1.335+002	1.744+002	2.066+002	2.314+002	3.099+002
-0.60	2.114+000	4.838+000	1.147+001	2.706+001	5.441+001	8.049+001	9.997+001	1.134+002	1.225+002	1.403+002
-0.80	1.878+000	3.825+000	8.141+000	1.753+001	3.304+001	4.626+001	5.499+001	6.029+001	6.341+001	6.770+001
-1.00	1.667+000	3.000+000	5.667+000	1.100+001	1.928+001	2.560+001	2.929+001	3.127+001	3.229+001	3.333+001
-1.20	1.484+000	2.355+000	3.918+000	6.768+000	1.093+001	1.378+001	1.525+001	1.595+001	1.626+001	1.651+001
-1.40	1.329+000	1.863+000	2.719+000	4.133+000	6.080+000	7.268+000	7.815+000	8.044+000	8.135+000	8.191+000
-1.60	1.199+000	1.491+000	1.910+000	2.532+000	3.341+000	3.782+000	3.963+000	4.030+000	4.053+000	4.064+000
-1.80	1.091+000	1.211+000	1.366+000	1.573+000	1.827+000	1.950+000	1.995+000	2.010+000	2.015+000	2.016+000
-2.00	1.000+000	1.000+000	1.000+000	1.000+000	1.000+000	1.000+000	1.000+000	1.000+000	1.000+000	1.000+000

B1(N,R,MU) FOR R= 0.100

MU	N = 4	8	16	32	64	128	256	512	1024	∞
2.00	3.333•000	1.200•001	4.533•001	1.760•002	6.933•002	2.752•003	1.097•004	4.378•004	1.749•005	∞
1.80	3.315•000	1.174•001	4.252•001	1.517•002	5.330•002	1.858•003	6.467•003	2.250•004	7.830•004	∞
1.60	3.293•000	1.147•001	3.982•001	1.309•002	4.113•002	1.263•003	3.843•003	1.166•004	3.535•004	∞
1.40	3.265•000	1.118•001	3.721•001	1.130•002	3.183•002	8.636•002	2.304•003	6.103•003	1.613•004	∞
1.20	3.230•000	1.084•001	3.463•001	9.728•001	2.470•002	5.943•002	1.394•003	3.232•003	7.453•003	∞
1.00	3.184•000	1.045•001	3.204•001	8.347•001	1.918•002	4.114•002	8.523•002	1.735•003	3.500•003	∞
0.80	3.123•000	9.989•000	2.938•001	7.118•001	1.487•002	2.862•002	5.269•002	9.466•002	1.678•003	∞
0.60	3.043•000	9.445•000	2.663•001	6.014•001	1.149•002	1.999•002	3.295•002	5.265•002	8.254•002	∞
0.40	2.940•000	8.804•000	2.376•001	5.015•001	8.816•001	1.397•002	2.084•002	2.993•002	4.194•002	∞
0.20	2.810•000	8.065•000	2.080•001	4.111•001	6.690•001	9.750•001	1.331•002	1.741•002	2.214•002	∞
-0.00	2.653•000	7.236•000	1.779•001	3.300•001	5.003•001	6.771•001	8.566•001	1.037•002	1.219•002	∞
-0.20	2.472•000	6.344•000	1.481•001	2.585•001	3.673•001	4.664•001	5.542•001	6.314•001	6.989•001	1.156•002
-0.40	2.273•000	5.430•000	1.199•001	1.971•001	2.642•001	3.177•001	3.592•001	3.910•001	4.153•001	8.922•001
-0.60	2.065•000	4.540•000	9.423•000	1.461•001	1.859•001	2.137•001	2.326•001	2.452•001	2.537•001	2.702•001
-0.80	1.860•000	3.720•000	7.204•000	1.055•001	1.281•001	1.419•001	1.502•001	1.550•001	1.577•001	1.616•001
-1.00	1.667•000	3.000•000	5.375•000	7.429•000	8.653•000	9.312•000	9.652•000	9.825•000	9.912•000	1.000•001
-1.20	1.491•000	2.396•000	3.931•000	5.125•000	5.751•000	6.046•000	6.177•000	6.235•000	6.260•000	6.278•000
-1.40	1.337•000	1.907•000	2.832•000	3.477•000	3.772•000	3.892•000	3.938•000	3.954•000	3.960•000	3.962•000
-1.60	1.205•000	1.522•000	2.021•000	2.329•000	2.449•000	2.490•000	2.502•000	2.505•000	2.505•000	2.504•000
-1.80	1.093•000	1.226•000	1.438•000	1.546•000	1.579•000	1.586•000	1.586•000	1.585•000	1.584•000	1.583•000
-2.00	1.000•000	1.000•000	1.000•000	1.000•000	1.000•000	1.000•000	1.000•000	1.000•000	1.000•000	1.000•000

B1(N,R,MU) FOR R= 0.200

MU	N = 4	8	16	32	64	128	256	512	1024	∞
2.00	3.333•000	1.200•001	4.533•001	1.760•002	6.933•002	2.752•003	1.097•004	4.378•004	1.749•005	∞
1.80	3.279•000	1.131•001	3.925•001	1.358•002	4.700•002	1.629•003	5.657•003	1.967•004	6.843•004	∞
1.60	3.222•000	1.065•001	3.404•001	1.053•002	3.209•002	9.729•002	2.946•003	8.923•003	2.703•004	∞
1.40	3.162•000	1.002•001	2.955•001	8.204•001	2.208•002	5.868•002	1.552•003	4.096•003	1.081•004	∞
1.20	3.096•000	9.409•000	2.567•001	6.420•001	1.533•002	3.581•002	8.286•002	1.909•003	4.391•003	∞
1.00	3.024•000	8.811•000	2.229•001	5.044•001	1.074•002	2.215•002	4.501•002	9.072•002	1.821•003	∞
0.80	2.942•000	8.219•000	1.933•001	3.977•001	7.593•001	1.392•002	2.496•002	4.420•002	7.771•002	∞
0.60	2.849•000	7.624•000	1.671•001	3.143•001	5.424•001	8.907•001	1.420•002	2.225•002	3.445•002	∞
0.40	2.743•000	7.023•000	1.438•001	2.488•001	3.912•001	5.811•001	8.330•001	1.166•002	1.607•002	∞
0.20	2.622•000	6.414•000	1.229•001	1.969•001	2.847•001	3.870•001	5.054•001	6.421•001	7.994•001	∞
-0.00	2.487•000	5.796•000	1.042•001	1.555•001	2.088•001	2.631•001	3.180•001	3.733•001	4.288•001	∞
-0.20	2.337•000	5.175•000	8.751•000	1.224•001	1.542•001	1.825•001	2.075•001	2.295•001	2.487•001	3.793•001
-0.40	2.176•000	4.558•000	7.262•000	9.581•000	1.143•001	1.287•001	1.399•001	1.484•001	1.550•001	1.757•001
-0.60	2.008•000	3.958•000	5.949•000	7.450•000	8.497•000	9.211•000	9.692•000	1.001•001	1.023•001	1.066•001
-0.80	1.836•000	3.387•000	4.808•000	5.746•000	6.318•000	6.658•000	6.857•000	6.974•000	7.042•000	7.136•000
-1.00	1.667•000	2.857•000	3.833•000	4.395•000	4.692•000	4.845•000	4.922•000	4.961•000	4.980•000	5.000•000
-1.20	1.505•000	2.379•000	3.016•000	3.333•000	3.476•000	3.539•000	3.565•000	3.575•000	3.579•000	3.582•000
-1.40	1.355•000	1.960•000	2.346•000	2.507•000	2.568•000	2.588•000	2.594•000	2.595•000	2.595•000	2.593•000
-1.60	1.221•000	1.601•000	1.805•000	1.873•000	1.890•000	1.892•000	1.890•000	1.889•000	1.888•000	1.886•000
-1.80	1.102•000	1.300•000	1.378•000	1.390•000	1.387•000	1.382•000	1.378•000	1.376•000	1.375•000	1.374•000
-2.00	1.000•000	1.000•000	1.000•000	1.000•000	1.000•000	1.000•000	1.000•000	1.000•000	1.000•000	1.000•000

B1(N,R,MU) FOR R= 0.000

MU \ N	4	8	16	32	64	128	256	512	1024	∞
2.00	3.333+000	1.200+001	4.533+001	1.760+002	6.933+002	2.752+003	1.097+004	4.378+004	1.749+005	∞
1.80	3.186+000	1.052+001	3.540+001	1.207+002	4.152+002	1.436+003	4.984+003	1.732+004	6.026+004	∞
1.60	3.047+000	9.247+000	2.780+001	8.345+001	2.511+002	7.574+002	2.289+003	6.929+003	2.099+004	∞
1.40	2.915+000	8.151+000	2.197+001	5.825+001	1.536+002	4.046+002	1.066+003	2.810+003	7.412+003	∞
1.20	2.790+000	7.205+000	1.748+001	4.110+001	9.529+001	2.196+002	5.051+002	1.161+003	2.666+003	∞
1.00	2.670+000	6.384+000	1.401+001	2.936+001	6.011+001	1.216+002	2.447+002	4.909+002	9.832+002	∞
0.80	2.555+000	5.670+000	1.131+001	2.126+001	3.868+001	6.908+001	1.221+002	2.144+002	3.752+002	∞
0.60	2.443+000	5.046+000	9.201+000	1.563+001	2.546+001	4.045+001	6.323+001	9.780+001	1.503+002	∞
0.40	2.334+000	4.499+000	7.544+000	1.167+001	1.721+001	2.457+001	3.433+001	4.725+001	6.433+001	∞
0.20	2.227+000	4.017+000	6.232+000	8.870+000	1.196+001	1.556+001	1.973+001	2.454+001	3.009+001	∞
-0.00	2.121+000	3.589+000	5.187+000	6.856+000	8.572+000	1.032+001	1.209+001	1.387+001	1.566+001	∞
-0.20	2.015+000	3.207+000	4.346+000	5.389+000	6.330+000	7.169+000	7.913+000	8.569+000	9.144+000	1.306+001
-0.40	1.909+000	2.864+000	3.664+000	4.305+000	4.811+000	5.208+000	5.516+000	5.753+000	5.936+000	6.518+000
-0.60	1.802+000	2.555+000	3.105+000	3.489+000	3.755+000	3.937+000	4.060+000	4.144+000	4.200+000	4.313+000
-0.80	1.694+000	2.274+000	2.642+000	2.864+000	2.997+000	3.077+000	3.123+000	3.151+000	3.167+000	3.191+000
-1.00	1.583+000	2.018+000	2.254+000	2.376+000	2.438+000	2.469+000	2.484+000	2.492+000	2.496+000	2.500+000
-1.20	1.471+000	1.782+000	1.926+000	1.987+000	2.011+000	2.021+000	2.024+000	2.025+000	2.026+000	2.025+000
-1.40	1.356+000	1.565+000	1.644+000	1.670+000	1.677+000	1.678+000	1.677+000	1.676+000	1.675+000	1.674+000
-1.60	1.240+000	1.363+000	1.401+000	1.408+000	1.408+000	1.406+000	1.404+000	1.403+000	1.402+000	1.402+000
-1.80	1.121+000	1.175+000	1.188+000	1.188+000	1.186+000	1.184+000	1.183+000	1.182+000	1.182+000	1.182+000
-2.00	1.000+000	1.000+000	1.000+000	1.000+000	1.000+000	1.000+000	1.000+000	1.000+000	1.000+000	1.000+000

B1(N,R,MU) FOR Re 0.800

MU	N = 4	8	16	32	64	128	256	512	1024	∞
2.00	3.333+000	1.200+001	4.533+001	1.760+002	6.933+002	2.752+003	1.097+004	4.378+004	1.749+005	∞
1.80	3.032+000	9.694+000	3.213+001	1.089+002	3.739+002	1.292+003	4.483+003	1.558+004	5.421+004	∞
1.60	2.765+000	7.876+000	2.297+001	6.806+001	2.038+002	6.135+002	1.853+003	5.608+003	1.698+004	∞
1.40	2.529+000	6.441+000	1.658+001	4.305+001	1.125+002	2.953+002	7.770+002	2.047+003	5.398+003	∞
1.20	2.319+000	5.306+000	1.210+001	2.762+001	6.317+001	1.447+002	3.319+002	7.617+002	1.749+003	∞
1.00	2.134+000	4.405+000	8.950+000	1.804+001	3.622+001	7.259+001	1.453+002	2.908+002	5.817+002	∞
0.80	1.969+000	3.688+000	6.718+000	1.203+001	2.132+001	3.753+001	6.579+001	1.150+002	2.008+002	∞
0.60	1.823+000	3.117+000	5.128+000	8.225+000	1.296+001	2.018+001	3.116+001	4.782+001	7.310+001	∞
0.40	1.693+000	2.660+000	3.986+000	5.783+000	8.193+000	1.140+001	1.567+001	2.130+001	2.876+001	∞
0.20	1.578+000	2.293+000	3.160+000	4.196+000	5.416+000	6.840+000	8.492+000	1.040+001	1.260+001	∞
-0.00	1.477+000	1.998+000	2.558+000	3.149+000	3.761+000	4.389+000	5.027+000	5.671+000	6.318+000	∞
-0.20	1.387+000	1.760+000	2.115+000	2.446+000	2.749+000	3.023+000	3.267+000	3.483+000	3.673+000	4.968+000
-0.40	1.308+000	1.568+000	1.786+000	1.966+000	2.112+000	2.229+000	2.321+000	2.392+000	2.447+000	2.624+000
-0.60	1.238+000	1.413+000	1.541+000	1.634+000	1.700+000	1.748+000	1.780+000	1.803+000	1.818+000	1.850+000
-0.80	1.177+000	1.287+000	1.357+000	1.400+000	1.427+000	1.444+000	1.454+000	1.461+000	1.464+000	1.470+000
-1.00	1.125+000	1.187+000	1.219+000	1.234+000	1.242+000	1.246+000	1.248+000	1.249+000	1.250+000	1.250+000
-1.20	1.081+000	1.109+000	1.117+000	1.118+000	1.117+000	1.116+000	1.115+000	1.114+000	1.114+000	1.113+000
-1.40	1.045+000	1.050+000	1.045+000	1.039+000	1.035+000	1.032+000	1.030+000	1.029+000	1.028+000	1.028+000
-1.60	1.017+000	1.010+000	1.000+000	9.922-001	9.872-001	9.843-001	9.827-001	9.819-001	9.814-001	9.809-001
-1.80	1.001+000	9.914-001	9.826-001	9.768-001	9.734-001	9.715-001	9.704-001	9.699-001	9.697-001	9.694-001
-2.00	1.000+000	1.000+000	1.000+000	1.000+000	1.000+000	1.000+000	1.000+000	1.000+000	1.000+000	1.000+000

B1(N,R,MU) FOR R= 1.00

	N									
MU	4	8	16	32	64	128	256	512	1024	∞
2.00	3.333•000	1.200•001	4.533•001	1.760•002	6.933•002	2.752•003	1.097•004	4.378•004	1.749•005	∞
1.80	2.988•000	9.490•000	3.138•001	1.063•002	3.646•002	1.260•003	4.372•003	1.519•004	5.286•004	∞
1.60	2.688•000	7.555•000	2.191•001	6.479•001	1.938•002	5.833•002	1.762•003	5.331•003	1.615•004	∞
1.40	2.426•000	6.059•000	1.546•001	3.999•001	1.044•002	2.738•002	7.202•002	1.897•003	5.003•003	∞
1.20	2.199•000	4.900•000	1.104•001	2.504•001	5.717•001	1.308•002	2.999•002	6.881•002	1.580•003	∞
1.00	2.000•000	4.000•000	8.000•000	1.600•001	3.200•001	6.400•001	1.280•002	2.560•002	5.120•002	∞
0.80	1.827•000	3.299•000	5.894•000	1.045•001	1.841•001	3.230•001	5.652•001	9.872•001	1.722•002	∞
0.60	1.677•000	2.750•000	4.424•000	7.004•000	1.096•001	1.698•001	2.614•001	4.005•001	6.114•001	∞
0.40	1.546•000	2.320•000	3.391•000	4.846•000	6.801•000	9.407•000	1.287•001	1.744•001	2.350•001	∞
0.20	1.432•000	1.982•000	2.658•000	3.471•000	4.432•000	5.555•000	6.858•000	8.363•000	1.010•001	∞
0.00	1.333•000	1.714•000	2.133•000	2.581•000	3.048•000	3.528•000	4.016•000	4.509•000	5.005•000	∞
-0.20	1.247•000	1.502•000	1.754•000	1.994•000	2.216•000	2.418•000	2.599•000	2.759•000	2.900•000	3.863•000
-0.40	1.172•000	1.333•000	1.476•000	1.599•000	1.700•000	1.782•000	1.847•000	1.898•000	1.938•000	2.065•000
-0.60	1.107•000	1.197•000	1.271•000	1.327•000	1.370•000	1.401•000	1.422•000	1.438•000	1.448•000	1.470•000
-0.80	1.050•000	1.088•000	1.117•000	1.137•000	1.150•000	1.160•000	1.165•000	1.169•000	1.171•000	1.175•000
-1.00	1.000•000	1.000•000	1.000•000	1.000•000	1.000•000	1.0004000	1.000•000	1.000•000	1.000•000	1.000•000
-1.20	9.569-001	9.284-001	9.105-001	8.997-001	8.933-001	8.897-001	8.877-001	8.866-001	8.860-001	8.854-001
-1.40	9.193-001	8.700-001	8.410-001	8.245-001	8.154-001	8.105-001	8.079-001	8.065-001	8.058-001	8.051-001
-1.60	8.866-001	8.221-001	7.864-001	7.672-001	7.570-001	7.517-001	7.490-001	7.476-001	7.468-001	7.461-001
-1.80	8.581-001	7.827-001	7.431-001	7.226-001	7.122-001	7.068-001	7.042-001	7.028-001	7.021-001	7.014-001
-2.00	8.333-001	7.500-001	7.083-001	6.875-001	6.771-001	6.719-001	6.693-001	6.680-001	6.673-001	6.667-001

463-560 O - 72 - 33

B1(N,R,MU) FOR R= 1.01

MU	N = 4	8	16	32	64	128	256	512	1024	∞
2.00	3.333+000	1.200+001	4.533+001	1.760+002	6.933+002	2.752+003	1.097+004	4.378+004	1.749+005	∞
1.80	2.986+000	9.482+000	3.135+001	1.062+002	3.643+002	1.259+003	4.367+003	1.518+004	5.280+004	∞
1.60	2.685+000	7.542+000	2.187+001	6.466+001	1.934+002	5.822+002	1.758+003	5.321+003	1.611+004	∞
1.40	2.422+000	6.045+000	1.542+001	3.988+001	1.041+002	2.730+002	7.180+002	1.892+003	4.988+003	∞
1.20	2.194+000	4.885+000	1.100+001	2.497+001	5.695+001	1.303+002	2.987+002	6.854+002	1.573+003	∞
1.00	1.995+000	3.985+000	7.966+000	1.593+001	3.185+001	6.369+001	1.274+002	2.547+002	5.095+002	∞
0.80	1.822+000	3.285+000	5.864+000	1.039+001	1.830+001	3.212+001	5.619+001	9.814+001	1.712+002	∞
0.60	1.672+000	2.738+000	4.400+000	6.963+000	1.089+001	1.687+001	2.597+001	3.978+001	6.073+001	∞
0.40	1.541+000	2.309+000	3.371+000	4.814+000	6.754+000	9.340+000	1.277+001	1.731+001	2.332+001	∞
0.20	1.428+000	1.972+000	2.642+000	3.447+000	4.400+000	5.512+000	6.804+000	8.296+000	1.002+001	∞
-0.00	1.329+000	1.706+000	2.120+000	2.563+000	3.025+000	3.500+000	3.984+000	4.472+000	4.963+000	∞
-0.20	1.243+000	1.495+000	1.743+000	1.980+000	2.200+000	2.400+000	2.579+000	2.737+000	2.877+000	3.829+000
-0.40	1.168+000	1.327+000	1.468+000	1.589+000	1.689+000	1.770+000	1.835+000	1.885+000	1.924+000	2.050+000
-0.60	1.104+000	1.193+000	1.265+000	1.321+000	1.362+000	1.393+000	1.414+000	1.429+000	1.440+000	1.461+000
-0.80	1.048+000	1.085+000	1.113+000	1.133+000	1.147+000	1.155+000	1.161+000	1.165+000	1.167+000	1.170+000
-1.00	1.000+000	1.000+000	1.000+000	1.000+000	1.000+000	1.000+000	1.000+000	1.000+000	1.000+000	1.000+000
-1.20	9.599-001	9.331-001	9.160-001	9.056-001	8.995-001	8.960-001	8.940-001	8.929-001	8.924-001	8.917-001
-1.40	9.286-001	8.840-001	8.573-001	8.419-001	8.333-001	8.287-001	8.262-001	8.249-001	8.242-001	8.235-001
-1.60	9.098-001	8.566-001	8.264-001	8.098-001	8.009-001	7.963-001	7.938-001	7.926-001	7.920-001	7.913-001
-1.80	9.156-001	8.682-001	8.425-001	8.288-001	8.217-001	8.181-001	8.162-001	8.153-001	8.148-001	8.143-001
-2.00	1.000+000	1.000+000	1.000+000	1.000+000	1.000+000	1.000+000	1.000+000	1.000+000	1.000+000	1.000+000

B1(N,R,MU) FOR R= 1.10

MU	N = 4	8	16	32	64	128	256	512	1024	∞
2.00	3.333•000	1.200•001	4.533•001	1.760•002	6.933•002	2.752•003	1.097•004	4.378•004	1.749•005	∞
1.80	2.972•000	9.418•000	3.111•001	1.053•002	3.614•002	1.249•003	4.333•003	1.506•004	5.238•004	∞
1.60	2.660•000	7.443•000	2.154•001	6.366•001	1.904•002	5.730•002	1.731•003	5.237•003	1.586•004	∞
1.40	2.391•000	5.929•000	1.508•001	3.897•001	1.016•002	2.666•002	7.011•002	1.847•003	4.870•003	∞
1.20	2.158•000	4.766•000	1.069•001	2.422•001	5.521•001	1.263•002	2.894•002	6.640•002	1.524•003	∞
1.00	1.957•000	3.870•000	7.696•000	1.535•001	3.065•001	6.126•001	1.225•002	2.449•002	4.898•002	∞
0.80	1.783•000	3.177•000	5.637•000	9.954•000	1.750•001	3.068•001	5.365•001	9.366•001	1.634•002	∞
0.60	1.633•000	2.640•000	4.213•000	6.639•000	1.035•001	1.602•001	2.463•001	3.771•001	5.754•001	∞
0.40	1.504•000	2.223•000	3.219•000	4.575•000	6.398•000	8.828•000	1.205•001	1.632•001	2.197•001	∞
0.20	1.393•000	1.898•000	2.521•000	3.272•000	4.160•000	5.199•000	6.404•000	7.797•000	9.402•000	∞
-0.00	1.298•000	1.643•000	2.026•000	2.435•000	2.883•000	3.304•000	3.752•000	4.205•000	4.661•000	∞
-0.20	1.217•000	1.444•000	1.671•000	1.889•000	2.091•000	2.275•000	2.440•000	2.586•000	2.714•000	3.593•000
-0.40	1.147•000	1.288•000	1.416•000	1.524•000	1.617•000	1.692•000	1.751•000	1.797•000	1.832•000	1.948•000
-0.60	1.088•000	1.166•000	1.230•000	1.281•000	1.319•000	1.346•000	1.366•000	1.379•000	1.389•000	1.408•000
-0.80	1.040•000	1.072•000	1.096•000	1.114•000	1.126•000	1.134•000	1.139•000	1.142•000	1.144•000	1.147•000
-1.00	1.000•000	1.000•000	1.000•000	1.000•000	1.000•000	1.000•000	1.000•000	1.000•000	1.000•000	1.000•000
-1.20	9.696-001	9.482-001	9.341-001	9.254-001	9.201-001	9.171-001	9.154-001	9.145-001	9.140-001	9.134-001
-1.40	9.493-001	9.157-001	8.948-001	8.825-001	8.755-001	8.717-001	8.696-001	8.685-001	8.680-001	8.674-001
-1.60	9.415-001	9.048-001	8.831-001	8.709-001	8.642-001	8.607-001	8.588-001	8.578-001	8.574-001	8.569-001
-1.80	9.527-001	9.243-001	9.082-001	8.994-001	8.948-001	8.924-001	8.911-001	8.905-001	8.902-001	8.898-001
-2.00	1.000•000	1.000•000	1.000•000	1.000•000	1.000•000	1.000•000	1.000•000	1.000•000	1.000•000	1.000•000

$B1(N,R,MU)$ FOR R= 2.00

MU	N = 4	8	16	32	64	128	256	512	1024	∞
2.00	3.333+000	1.200+001	4.533+001	1.760+002	6.933+002	2.752+003	1.097+004	4.378+004	1.749+005	∞
1.80	2.908+000	9.132+000	3.006+001	1.017+002	3.487+002	1.205+003	4.179+003	1.453+004	5.053+004	∞
1.60	2.552+000	7.012+000	2.014+001	5.935+001	1.773+002	5.334+002	1.611+003	4.874+003	1.476+004	∞
1.40	2.255+000	5.439+000	1.366+001	3.512+001	9.142+001	2.395+002	6.299+002	1.659+003	4.374+003	∞
1.20	2.007+000	4.271+000	9.409+000	2.114+001	4.800+001	1.096+002	2.510+002	5.756+002	1.321+003	∞
1.00	1.800+000	3.400+000	6.600+000	1.300+001	2.580+001	5.140+001	1.026+002	2.050+002	4.098+002	∞
0.80	1.628+000	2.750+000	4.733+000	8.215+000	1.431+001	2.494+001	4.347+001	7.576+001	1.320+002	∞
0.60	1.486+000	2.264+000	3.485+000	5.371+000	8.262+000	1.267+001	1.937+001	2.955+001	4.498+001	∞
0.40	1.369+000	1.901+000	2.644+000	3.659+000	5.025+000	6.847+000	9.267+000	1.247+001	1.670+001	∞
0.20	1.273+000	1.629+000	2.075+000	2.615+000	3.256+000	4.005+000	4.876+000	5.882+000	7.042+000	∞
-0.00	1.195+000	1.427+000	1.688+000	1.971+000	2.267+000	2.573+000	2.884+000	3.198+000	3.515+000	∞
-0.20	1.133+000	1.277+000	1.425+000	1.568+000	1.702+000	1.824+000	1.934+000	2.031+000	2.117+000	2.704+000
-0.40	1.084+000	1.168+000	1.246+000	1.315+000	1.373+000	1.420+000	1.457+000	1.487+000	1.509+000	1.583+000
-0.60	1.046+000	1.090+000	1.126+000	1.156+000	1.178+000	1.195+000	1.207+000	1.215+000	1.221+000	1.233+000
-0.80	1.019+000	1.035+000	1.048+000	1.058+000	1.064+000	1.069+000	1.072+000	1.074+000	1.075+000	1.077+000
-1.00	1.000+000	1.000+000	1.000+000	1.000+000	1.000+000	1.000+000	1.000+000	1.000+000	1.000+000	1.000+000
-1.20	9.886-001	9.799-001	9.738-001	9.699-001	9.675-001	9.661-001	9.653-001	9.648-001	9.646-001	9.643-001
-1.40	9.837-001	9.719-001	9.641-001	9.593-001	9.565-001	9.550-001	9.541-001	9.537-001	9.534-001	9.532-001
-1.60	9.845-001	9.737-001	9.669-001	9.630-001	9.607-001	9.595-001	9.589-001	9.586-001	9.584-001	9.582-001
-1.80	9.901-001	9.836-001	9.796-001	9.774-001	9.761-001	9.755-001	9.752-001	9.750-001	9.749-001	9.748-001
-2.00	1.000+000	1.000+000	1.000+000	1.000+000	1.000+000	1.000+000	1.000+000	1.000+000	1.000+000	1.000+000

B1(N,R,MU) FOR R= 4.00

MU	N = 4	8	16	32	64	128	256	512	1024	∞
2.00	3.333+000	1.200+001	4.533+001	1.760+002	6.933+002	2.752+003	1.097+004	4.378+004	1.749+005	∞
1.80	2.879+000	9.006+000	2.960+001	1.000+002	3.431+002	1.186+003	4.112+003	1.429+004	4.972+004	∞
1.60	2.504+000	6.819+000	1.952+001	5.745+001	1.715+002	5.160+002	1.558+003	4.714+003	1.428+004	∞
1.40	2.194+000	5.219+000	1.303+001	3.340+001	8.686+001	2.275+002	5.981+002	1.575+003	4.154+003	∞
1.20	1.938+000	4.045+000	8.826+000	1.974+001	4.472+001	1.020+002	2.336+002	5.356+002	1.229+003	∞
1.00	1.727+000	3.182+000	6.091+000	1.191+001	2.355+001	4.682+001	9.336+001	1.865+002	3.726+002	∞
0.80	1.555+000	2.549+000	4.303+000	7.385+000	1.278+001	2.219+001	3.860+001	6.718+001	1.170+002	∞
0.60	1.415+000	2.082+000	3.129+000	4.748+000	7.229+000	1.101+001	1.676+001	2.550+001	3.875+001	∞
0.40	1.303+000	1.742+000	2.356+000	3.196+000	4.326+000	5.834+000	7.837+000	1.049+001	1.399+001	∞
0.20	1.214+000	1.495+000	1.848+000	2.275+000	2.783+000	3.377+000	4.067+000	4.865+000	5.784+000	∞
-0.00	1.144+000	1.318+000	1.514+000	1.726+000	1.949+000	2.179+000	2.414+000	2.651+000	2.890+000	∞
-0.20	1.092+000	1.194+000	1.298+000	1.399+000	1.494+000	1.580+000	1.658+000	1.727+000	1.788+000	2.204+000
-0.40	1.054+000	1.109+000	1.160+000	1.205+000	1.243+000	1.274+000	1.299+000	1.318+000	1.333+000	1.382+000
-0.60	1.027+000	1.053+000	1.075+000	1.093+000	1.107+000	1.117+000	1.124+000	1.129+000	1.132+000	1.140+000
-0.80	1.010+000	1.019+000	1.026+000	1.031+000	1.035+000	1.037+000	1.039+000	1.040+000	1.041+000	1.042+000
-1.00	1.000+000	1.000+000	1.000+000	1.000+000	1.000+000	1.000+000	1.000+000	1.000+000	1.000+000	1.000+000
-1.20	9.953-001	9.916-001	9.890-001	9.873-001	9.862-001	9.856-001	9.853-001	9.851-001	9.850-001	9.849-001
-1.40	9.941-001	9.898-001	9.869-001	9.851-001	9.840-001	9.834-001	9.831-001	9.829-001	9.829-001	9.828-001
-1.60	9.952-001	9.918-001	9.896-001	9.884-001	9.876-001	9.873-001	9.870-001	9.869-001	9.869-001	9.868-001
-1.80	9.974-001	9.957-001	9.946-001	9.940-001	9.936-001	9.935-001	9.934-001	9.933-001	9.933-001	9.933-001
-2.00	1.000+000	1.000+000	1.000+000	1.000+000	1.000+000	1.000+000	1.000+000	1.000+000	1.000+000	1.000+000

B1(N,R,MU) FOR R= 8.00

MU	N = 4	8	16	32	64	128	256	512	1024	∞
2.00	3.333+000	1.200+001	4.533+001	1.760+002	6.933+002	2.752+003	1.097+004	4.378+004	1.749+005	∞
1.80	2.870+000	8.963+000	2.945+001	9.951+001	3.413+002	1.179+003	4.090+003	1.421+004	4.945+004	∞
1.60	2.486+000	6.751+000	1.930+001	5.678+001	1.695+002	5.099+002	1.540+003	4.658+003	1.411+004	∞
1.40	2.170+000	5.135+000	1.279+001	3.276+001	8.515+001	2.230+002	5.862+002	1.544+003	4.071+003	∞
1.20	1.910+000	3.953+000	8.590+000	1.917+001	4.341+001	9.898+001	2.265+002	5.195+002	1.192+003	∞
1.00	1.696+000	3.087+000	5.870+000	1.143+001	2.257+001	4.483+001	8.935+001	1.784+002	3.565+002	∞
0.80	1.521+000	2.453+000	4.101+000	6.996+000	1.206+001	2.090+001	3.630+001	6.315+001	1.099+002	∞
0.60	1.380+000	1.991+000	2.950+000	4.433+000	6.706+000	1.017+001	1.544+001	2.345+001	3.559+001	∞
0.40	1.268+000	1.657+000	2.202+000	2.946+000	3.949+000	5.286+000	7.062+000	9.414+000	1.252+001	∞
0.20	1.181+000	1.420+000	1.720+000	2.083+000	2.514+000	3.019+000	3.606+000	4.284+000	5.066+000	∞
-0.00	1.116+000	1.255+000	1.413+000	1.584+000	1.763+000	1.949+000	2.137+000	2.328+000	2.520+000	∞
-0.20	1.069+000	1.145+000	1.223+000	1.299+000	1.371+000	1.436+000	1.494+000	1.546+000	1.592+000	1.905+000
-0.40	1.037+000	1.075+000	1.110+000	1.142+000	1.168+000	1.189+000	1.207+000	1.220+000	1.231+000	1.264+000
-0.60	1.017+000	1.033+000	1.047+000	1.058+000	1.067+000	1.073+000	1.078+000	1.081+000	1.083+000	1.088+000
-0.80	1.006+000	1.011+000	1.014+000	1.017+000	1.020+000	1.021+000	1.022+000	1.022+000	1.023+000	1.023+000
-1.00	1.000+000	1.000+000	1.000+000	1.000+000	1.000+000	1.000+000	1.000+000	1.000+000	1.000+000	1.000+000
-1.20	9.980-001	9.963-001	9.952-001	9.945-001	9.940-001	9.938-001	9.936-001	9.935-001	9.935-001	9.934-001
-1.40	9.978-001	9.961-001	9.950-001	9.944-001	9.940-001	9.937-001	9.936-001	9.936-001	9.935-001	9.935-001
-1.60	9.984-001	9.973-001	9.966-001	9.962-001	9.960-001	9.958-001	9.958-001	9.957-001	9.957-001	9.957-001
-1.80	9.993-001	9.988-001	9.985-001	9.983-001	9.982-001	9.981-001	9.981-001	9.981-001	9.981-001	9.981-001
-2.00	1.000+000	1.000+000	1.000+000	1.000+000	1.000+000	1.000+000	1.000+000	1.000+000	1.000+000	1.000+000

B1(N,R,MU) FOR R= 16.00

MU	N = 4	8	16	32	64	128	256	512	1024	∞
2.00	3.333•000	1.200•001	4.533•001	1.760•002	6.933•002	2.752•003	1.097•004	4.378•004	1.749•005	∞
1.80	2.866•000	8.949•000	2.940•001	9.934•001	3.406•002	1.177•003	4.083•003	1.419•004	4.936•004	∞
1.60	2.480•000	6.727•000	1.923•001	5.654•001	1.688•002	5.077•002	1.533•003	4.639•003	1.405•004	∞
1.40	2.161•000	5.104•000	1.270•001	3.251•001	8.450•001	2.213•002	5.817•002	1.532•003	4.039•003	∞
1.20	1.898•000	3.914•000	8.491•000	1.894•001	4.285•001	9.769•001	2.236•002	5.127•002	1.177•003	∞
1.00	1.681•000	3.043•000	5.766•000	1.121•001	2.211•001	4.389•001	8.747•001	1.746•002	3.489•002	∞
0.80	1.504•000	2.404•000	3.997•000	6.794•000	1.169•001	2.023•001	3.512•001	6.106•001	1.062•002	∞
0.60	1.360•000	1.939•000	2.848•000	4.254•000	6.409•000	9.696•000	1.469•001	2.228•001	3.379•001	∞
0.40	1.247•000	1.606•000	2.108•000	2.794•000	3.717•000	4.950•000	6.587•000	8.754•000	1.162•001	∞
0.20	1.160•000	1.372•000	1.637•000	1.958•000	2.340•000	2.787•000	3.307•000	3.907•000	4.599•000	∞
.00	1.097•000	1.214•000	1.346•000	1.489•000	1.639•000	1.794•000	1.952•000	2.112•000	2.273•000	∞
-0.20	1.054•000	1.113•000	1.174•000	1.233•000	1.289•000	1.339•000	1.385•000	1.425•000	1.461•000	1.705•000
-0.40	1.026•000	1.053•000	1.078•000	1.101•000	1.119•000	1.135•000	1.147•000	1.157•000	1.164•000	1.188•000
-0.60	1.011•000	1.021•000	1.030•000	1.037•000	1.043•000	1.047•000	1.050•000	1.052•000	1.053•000	1.056•000
-0.80	1.003•000	1.006•000	1.008•000	1.010•000	1.011•000	1.012•000	1.012•000	1.013•000	1.013•000	1.013•000
-1.00	1.000•000	1.000•000	1.000•000	1.000•000	1.000•000	1.000•000	1.000•000	1.000•000	1.000•000	1.000•000
-1.20	9.991-001	9.984-001	9.979-001	9.976-001	9.974-001	9.973-001	9.972-001	9.972-001	9.972-001	9.971-001
-1.40	9.992-001	9.985-001	9.981-001	9.979-001	9.977-001	9.976-001	9.976-001	9.976-001	9.975-001	9.975-001
-1.60	9.995-001	9.991-001	9.989-001	9.987-001	9.987-001	9.986-001	9.986-001	9.986-001	9.986-001	9.986-001
-1.80	9.998-001	9.997-001	9.996-001	9.995-001	9.995-001	9.995-001	9.995-001	9.995-001	9.995-001	9.995-001
-2.00	1.000•000	1.000•000	1.000•000	1.000•000	1.000•000	1.000•000	1.000•000	1.000•000	1.000•000	1.000•000

$B_1(N,R,MU)$ FOR R= 32.00

MU	N = 4	8	16	32	64	128	256	512	1024	∞
2.00	3.333•000	1.200•001	4.533•001	1.760•002	6.933•002	2.752•003	1.097•004	4.378•004	1.749•005	∞
1.80	2.865•000	8.945•000	2.938•001	9.928•001	3.405•002	1.176•003	4.081•003	1.418•004	4.934•004	∞
1.60	2.479•000	6.719•000	1.920•001	5.646•001	1.685•002	5.070•002	1.531•003	4.632•003	1.403•004	∞
1.40	2.158•000	5.091•000	1.266•001	3.242•001	8.425•001	2.206•002	5.799•002	1.527•003	4.027•003	∞
1.20	1.893•000	3.898•000	8.448•000	1.883•001	4.261•001	9.714•001	2.223•002	5.097•002	1.170•003	∞
1.00	1.674•000	3.021•000	5.716•000	1.111•001	2.188•001	4.344•001	8.656•001	1.728•002	3.453•002	∞
0.80	1.494•000	2.378•000	3.940•000	6.685•000	1.149•001	1.986•001	3.447•001	5.992•001	1.042•002	∞
0.60	1.348•000	1.908•000	2.787•000	4.147•000	6.231•000	9.408•000	1.424•001	2.158•001	3.270•001	∞
0.40	1.233•000	1.572•000	2.046•000	2.693•000	3.565•000	4.729•000	6.275•000	8.320•000	1.102•001	∞
0.20	1.146•000	1.338•000	1.579•000	1.871•000	2.218•000	2.625•000	3.097•000	3.643•000	4.272•000	∞
-0.00	1.083•000	1.184•000	1.297•000	1.420•000	1.560•000	1.683•000	1.819•000	1.957•000	2.095•000	∞
-0.20	1.043•000	1.090•000	1.139•000	1.186•000	1.230•000	1.271•000	1.307•000	1.339•000	1.368•000	1.563•000
-0.40	1.019•000	1.039•000	1.057•000	1.073•000	1.087•000	1.098•000	1.107•000	1.114•000	1.119•000	1.136•000
-0.60	1.007•000	1.014•000	1.019•000	1.024•000	1.028•000	1.030•000	1.032•000	1.033•000	1.034•000	1.036•000
-0.80	1.002•000	1.003•000	1.005•000	1.006•000	1.006•000	1.007•000	1.007•000	1.007•000	1.007•000	1.008•000
-1.00	1.000•000	1.000•000	1.000•000	1.000•000	1.000•000	1.000•000	1.000•000	1.000•000	1.000•000	1.000•000
-1.20	9.996-001	9.993-001	9.991-001	9.990-001	9.989-001	9.988-001	9.988-001	9.988-001	9.988-001	9.988-001
-1.40	9.997-001	9.994-001	9.993-001	9.992-001	9.991-001	9.991-001	9.991-001	9.991-001	9.991-001	9.991-001
-1.60	9.998-001	9.997-001	9.996-001	9.996-001	9.996-001	9.995-001	9.995-001	9.995-001	9.995-001	9.995-001
-1.80	9.999-001	9.999-001	9.999-001	9.999-001	9.999-001	9.998-001	9.998-001	9.998-001	9.998-001	9.998-001
-2.00	1.000•000	1.000•000	1.000•000	1.000•000	1.000•000	1.000•000	1.000•000	1.000•000	1.000•000	1.000•000

B1(N,R,MU) FOR RR 64.00

MU	N = 4	8	16	32	64	128	256	512	1024	∞
2.00	3.333•000	1.200•001	4.533•001	1.760•002	6.933•002	2.752•003	1.097•004	4.378•004	1.749•005	∞
1.80	2.865•000	8.943•000	2.938•001	9.927•001	3.404•002	1.176•003	4.080•003	1.418•004	4.933•004	∞
1.60	2.477•000	6.716•000	1.919•001	5.644•001	1.685•002	5.067•002	1.530•003	4.630•003	1.402•004	∞
1.40	2.156•000	5.087•000	1.265•001	3.238•001	8.415•001	2.204•002	5.793•002	1.526•003	4.022•003	∞
1.20	1.890•000	3.891•000	8.429•000	1.879•001	4.251•001	9.690•001	2.218•002	5.085•002	1.167•003	∞
1.00	1.670•000	3.010•000	5.691•000	1.105•001	2.177•001	4.322•001	8.611•001	1.719•002	3.435•002	∞
0.80	1.489•000	2.363•000	3.909•000	6.624•000	1.137•001	1.966•001	3.411•001	5.929•001	1.031•002	∞
0.60	1.341•000	1.889•000	2.749•000	4.080•000	6.119•000	9.229•000	1.396•001	2.114•001	3.203•001	∞
0.40	1.224•000	1.548•000	2.003•000	2.624•000	3.461•000	4.578•000	6.060•000	8.023•000	1.062•001	∞
0.20	1.135•000	1.313•000	1.536•000	1.808•000	2.129•000	2.506•000	2.944•000	3.450•000	4.033•000	∞
-0.00	1.073•000	1.161•000	1.261•000	1.369•000	1.482•000	1.600•000	1.719•000	1.840•000	1.961•000	∞
-0.20	1.035•000	1.073•000	1.112•000	1.151•000	1.187•000	1.220•000	1.249•000	1.275•000	1.298•000	1.456•000
-0.40	1.014•000	1.028•000	1.042•000	1.054•000	1.064•000	1.072•000	1.078•000	1.083•000	1.087•000	1.100•000
-0.60	1.005•000	1.009•000	1.013•000	1.016•000	1.018•000	1.020•000	1.021•000	1.022•000	1.022•000	1.024•000
-0.80	1.001•000	1.002•000	1.003•000	1.003•000	1.004•000	1.004•000	1.004•000	1.004•000	1.004•000	1.004•000
-1.00	1.000•000	1.000•000	1.000•000	1.000•000	1.000•000	1.000•000	1.000•000	1.000•000	1.000•000	1.000•000
-1.20	9.998-001	9.997-001	9.996-001	9.995-001	9.995-001	9.995-001	9.995-001	9.995-001	9.995-001	9.995-001
-1.40	9.999-001	9.998-001	9.997-001	9.997-001	9.997-001	9.997-001	9.997-001	9.996-001	9.996-001	9.996-001
-1.60	9.999-001	9.999-001	9.999-001	9.999-001	9.999-001	9.999-001	9.998-001	9.998-001	9.998-001	9.998-001
-1.80	1.000•000	1.000•000	1.000•000	1.000•000	1.000•000	1.000•000	1.000•000	1.000•000	1.000•000	1.000•000
-2.00	1.000•000	1.000•000	1.000•000	1.000•000	1.000•000	1.000•000	1.000•000	1.000•000	1.000•000	1.000•000

B1(N,R,MU) FOR R= 128.00

MU	N = 4	8	16	32	64	128	256	512	1024	∞
2.00	3.333+000	1.200+001	4.533+001	1.760+002	6.933+002	2.752+003	1.097+004	4.378+004	1.749+005	∞
1.80	2.865+000	8.943+000	2.938+001	9.926+001	3.404+002	1.176+003	4.080+003	1.418+004	4.932+004	∞
1.60	2.477+000	6.715+000	1.919+001	5.643+001	1.684+002	5.067+002	1.530+003	4.629+003	1.402+004	∞
1.40	2.156+000	5.085+000	1.265+001	3.237+001	8.411+001	2.203+002	5.790+002	1.525+003	4.021+003	∞
1.20	1.889+000	3.887+000	8.421+000	1.877+001	4.246+001	9.680+001	2.215+002	5.079+002	1.166+003	∞
1.00	1.668+000	3.005+000	5.679+000	1.103+001	2.172+001	4.311+001	8.589+001	1.714+002	3.426+002	∞
0.80	1.486+000	2.354+000	3.891+000	6.589+000	1.131+001	1.955+001	3.391+001	5.893+001	1.025+002	∞
0.60	1.336+000	1.877+000	2.725+000	4.037+000	6.048+000	9.115+000	1.378+001	2.086+001	3.160+001	∞
0.40	1.217+000	1.532+000	1.973+000	2.576+000	3.388+000	4.471+000	5.909+000	7.813+000	1.033+001	∞
0.20	1.127+000	1.294+000	1.504+000	1.759+000	2.062+000	2.416+000	2.827+000	3.303+000	3.851+000	∞
-0.00	1.065+000	1.144+000	1.232+000	1.329+000	1.430+000	1.534+000	1.640+000	1.748+000	1.856+000	∞
-0.20	1.029+000	1.060+000	1.092+000	1.124+000	1.153+000	1.181+000	1.205+000	1.226+000	1.245+000	1.375+000
-0.40	1.010+000	1.021+000	1.031+000	1.040+000	1.047+000	1.053+000	1.058+000	1.062+000	1.065+000	1.074+000
-0.60	1.003+000	1.006+000	1.008+000	1.010+000	1.012+000	1.013+000	1.014+000	1.014+000	1.015+000	1.015+000
-0.80	1.001+000	1.001+000	1.002+000	1.002+000	1.002+000	1.002+000	1.002+000	1.002+000	1.002+000	1.002+000
-1.00	1.000+000	1.000+000	1.000+000	1.000+000	1.000+000	1.000+000	1.000+000	1.000+000	1.000+000	1.000+000
-1.20	9.999-001	9.999-001	9.998-001	9.998-001	9.998-001	9.998-001	9.998-001	9.998-001	9.998-001	9.998-001
-1.40	1.000+000	9.999-001	9.999-001	9.999-001	9.999-001	9.999-001	9.999-001	9.999-001	9.999-001	9.999-001
-1.60	1.000+000	1.000+000	1.000+000	1.000+000	1.000+000	1.000+000	9.999-001	9.999-001	9.999-001	9.999-001
-1.80	1.000+000	1.000+000	1.000+000	1.000+000	1.000+000	1.000+000	1.000+000	1.000+000	1.000+000	1.000+000
-2.00	1.000+000	1.000+000	1.000+000	1.000+000	1.000+000	1.000+000	1.000+000	1.000+000	1.000+000	1.000+000

B1(N,R,MU) FOR R= 256.00

	N									
MU	4	8	16	32	64	128	256	512	1024	∞
2.00	3.333•000	1.200•001	4.533•001	1.760•002	6.933•002	2.752•003	1.097•004	4.378•004	1.749•005	∞
1.80	2.865•000	8.943•000	2.938•001	9.926•001	3.404•002	1.176•003	4.080•003	1.418•004	4.932•004	∞
1.60	2.477•000	6.715•000	1.919•001	5.642•001	1.684•002	5.066•002	1.530•003	4.629•003	1.402•004	∞
1.40	2.156•000	5.084•000	1.264•001	3.236•001	8.410•001	2.202•002	5.789•002	1.525•003	4.020•003	∞
1.20	1.889•000	3.886•000	8.418•000	1.876•001	4.244•001	9.675•001	2.214•002	5.077•002	1.165•003	∞
1.00	1.668•000	3.003•000	5.673•000	1.101•001	2.169•001	4.305•001	8.578•001	1.712•002	3.421•002	∞
0.80	1.484•000	2.350•000	3.881•000	6.570•000	1.127•001	1.948•001	3.380•001	5.873•001	1.022•002	∞
0.60	1.333•000	1.869•000	2.709•000	4.010•000	6.003•000	9.042•000	1.366•001	2.068•001	3.132•001	∞
0.40	1.212•000	1.520•000	1.952•000	2.541•000	3.335•000	4.394•000	5.800•000	7.662•000	1.012•001	∞
0.20	1.121•000	1.280•000	1.479•000	1.722•000	2.009•000	2.346•000	2.737•000	3.189•000	3.710•000	∞
-0.00	1.059•000	1.130•000	1.210•000	1.296•000	1.388•000	1.482•000	1.577•000	1.674•000	1.772•000	∞
-0.20	1.024•000	1.050•000	1.077•000	1.103•000	1.127•000	1.150•000	1.170•000	1.188•000	1.204•000	1.311•000
-0.40	1.008•000	1.016•000	1.023•000	1.029•000	1.035•000	1.039•000	1.043•000	1.046•000	1.048•000	1.055•000
-0.60	1.002•000	1.004•000	1.005•000	1.007•000	1.008•000	1.008•000	1.009•000	1.009•000	1.010•000	1.010•000
-0.80	1.000•000	1.001•000	1.001•000	1.001•000	1.001•000	1.001•000	1.001•000	1.001•000	1.001•000	1.001•000
-1.00	1.000•000	1.000•000	1.000•000	1.000•000	1.000•000	1.000•000	1.000•000	1.000•000	1.000•000	1.000•000
-1.20	1.000•000	9.999-001	9.999-001	9.999-001	9.999-001	9.999-001	9.999-001	9.999-001	9.999-001	9.999-001
-1.40	1.000•000	1.000•000	1.000•000	1.000•000	1.000•000	1.000•000	1.000•000	9.999-001	9.999-001	9.999-001
-1.60	1.000•000	1.000•000	1.000•000	1.000•000	1.000•000	1.000•000	1.000•000	1.000•000	1.000•000	1.000•000
-1.80	1.000•000	1.000•000	1.000•000	1.000•000	1.000•000	1.000•000	1.000•000	1.000•000	1.000•000	1.000•000
-2.00	1.000•000	1.000•000	1.000•000	1.000•000	1.000•000	1.000•000	1.000•000	1.000•000	1.000•000	1.000•000

B1(N,R,MU) FOR R= 512.00

	N									
MU	4	8	16	32	64	128	256	512	1024	∞
2.00	3.333+000	1.200+001	4.533+001	1.760+002	6.933+002	2.752+003	1.097+004	4.378+004	1.749+005	∞
1.80	2.865+000	8.943+000	2.938+001	9.926+001	3.404+002	1.176+003	4.080+003	1.418+004	4.932+004	∞
1.60	2.477+000	6.714+000	1.919+001	5.642+001	1.684+002	5.066+002	1.530+003	4.628+003	1.402+004	∞
1.40	2.156+000	5.084+000	1.264+001	3.236+001	8.410+001	2.202+002	5.789+002	1.525+003	4.020+003	∞
1.20	1.889+000	3.885+000	8.416+000	1.874+001	4.243+001	9.673+001	2.214+002	5.076+002	1.165+003	∞
1.00	1.667+000	3.001+000	5.670+000	1.101+001	2.168+001	4.303+001	8.572+001	1.711+002	3.419+002	∞
0.80	1.483+000	2.347+000	3.875+000	6.558+000	1.125+001	1.945+001	3.373+001	5.862+001	1.020+002	∞
0.60	1.331+000	1.864+000	2.699+000	3.992+000	5.973+000	8.994+000	1.359+001	2.056+001	3.114+001	∞
0.40	1.209+000	1.512+000	1.936+000	2.516+000	3.296+000	4.338+000	5.721+000	7.553+000	9.973+000	∞
0.20	1.116+000	1.268+000	1.460+000	1.692+000	1.967+000	2.290+000	2.665+000	3.098+000	3.598+000	∞
-0.00	1.054+000	1.118+000	1.191+000	1.270+000	1.353+000	1.438+000	1.526+000	1.614+000	1.703+000	∞
-0.20	1.020+000	1.042+000	1.064+000	1.086+000	1.107+000	1.125+000	1.142+000	1.157+000	1.170+000	1.261+000
-0.40	1.006+000	1.012+000	1.017+000	1.022+000	1.026+000	1.030+000	1.032+000	1.034+000	1.036+000	1.041+000
-0.60	1.001+000	1.003+000	1.004+000	1.004+000	1.005+000	1.006+000	1.006+000	1.006+000	1.006+000	1.007+000
-0.80	1.000+000	1.000+000	1.001+000	1.001+000	1.001+000	1.001+000	1.001+000	1.001+000	1.001+000	1.001+000
-1.00	1.000+000	1.000+000	1.000+000	1.000+000	1.000+000	1.000+000	1.000+000	1.000+000	1.000+000	1.000+000
-1.20	1.000+000	1.000+000	1.000+000	1.000+000	1.000+000	1.000+000	1.000+000	1.000+000	1.000+000	1.000+000
-1.40	1.000+000	1.000+000	1.000+000	1.000+000	1.000+000	1.000+000	1.000+000	1.000+000	1.000+000	1.000+000
-1.60	1.000+000	1.000+000	1.000+000	1.000+000	1.000+000	1.000+000	1.000+000	1.000+000	1.000+000	1.000+000
-1.80	1.000+000	1.000+000	1.000+000	1.000+000	1.000+000	1.000+000	1.000+000	1.000+000	1.000+000	1.000+000
-2.00	1.000+000	1.000+000	1.000+000	1.000+000	1.000+000	1.000+000	1.000+000	1.000+000	1.000+000	1.000+000

B1(N,R,MU) FOR R=1024.00

MU	N = 4	8	16	32	64	128	256	512	1024	∞
2.00	3.333•000	1.200•001	4.533•001	1.760•002	6.933•002	2.752•003	1.097•004	4.378•004	1.749•005	∞
1.80	2.865•000	8.943•000	2.938•001	9.926•001	3.404•002	1.176•003	4.080•003	1.418•004	4.932•004	∞
1.60	2.477•000	6.714•000	1.919•001	5.642•001	1.684•002	5.066•002	1.530•003	4.628•003	1.402•004	∞
1.40	2.156•000	5.084•000	1.264•001	3.236•001	8.409•001	2.202•002	5.789•002	1.525•003	4.020•003	∞
1.20	1.889•000	3.885•000	8.416•000	1.874•001	4.243•001	9.672•001	2.213•002	5.075•002	1.165•003	∞
1.00	1.667•000	3.001•000	5.668•000	1.100•001	2.167•001	4.301•001	8.569•001	1.711•002	3.418•002	∞
0.80	1.482•000	2.345•000	3.872•000	6.552•000	1.124•001	1.942•001	3.369•001	5.855•001	1.018•002	∞
0.60	1.330•000	1.860•000	2.693•000	3.980•000	5.953•000	8.963•000	1.354•001	2.049•001	3.102•001	∞
0.40	1.206•000	1.505•000	1.924•000	2.497•000	3.268•000	4.297•000	5.663•000	7.472•000	9.862•000	∞
0.20	1.112•000	1.259•000	1.444•000	1.668•000	1.934•000	2.245•000	2.607•000	3.025•000	3.507•000	∞
-0.00	1.049•000	1.108•000	1.175•000	1.248•000	1.324•000	1.402•000	1.483•000	1.564•000	1.645•000	∞
-0.20	1.017•000	1.035•000	1.054•000	1.073•000	1.090•000	1.106•000	1.120•000	1.132•000	1.144•000	1.220•000
-0.40	1.004•000	1.009•000	1.013•000	1.017•000	1.020•000	1.022•000	1.024•000	1.026•000	1.027•000	1.031•000
-0.60	1.001•000	1.002•000	1.002•000	1.003•000	1.003•000	1.004•000	1.004•000	1.004•000	1.004•000	1.004•000
-0.80	1.000•000	1.000•000	1.000•000	1.000•000	1.000•000	1.000•000	1.000•000	1.000•000	1.000•000	1.000•000
-1.00	1.000•000	1.000•000	1.000•000	1.000•000	1.000•000	1.000•000	1.000•000	1.000•000	1.000•000	1.000•000
-1.20	1.000•000	1.000•000	1.000•000	1.000•000	1.000•000	1.000•000	1.000•000	1.000•000	1.000•000	1.000•000
-1.40	1.000•000	1.000•000	1.000•000	1.000•000	1.000•000	1.000•000	1.000•000	1.000•000	1.000•000	1.000•000
-1.60	1.000•000	1.000•000	1.000•000	1.000•000	1.000•000	1.000•000	1.000•000	1.000•000	1.000•000	1.000•000
-1.80	1.000•000	1.000•000	1.000•000	1.000•000	1.000•000	1.000•000	1.000•000	1.000•000	1.000•000	1.000•000
-2.00	1.000•000	1.000•000	1.000•000	1.000•000	1.000•000	1.000•000	1.000•000	1.000•000	1.000•000	1.000•000

B1(N,8,MU) FOR P=2048.00

	N									
MU	4	8	16	32	64	128	256	512	1024	∞
2.00	3.333+000	1.200+001	4.533+001	1.760+002	6.933+002	2.752+003	1.097+004	4.378+004	1.749+005	∞
1.80	2.865+000	8.943+000	2.938+001	9.926+001	3.404+002	1.176+003	4.080+003	1.418+004	4.932+004	∞
1.60	2.477+000	6.714+000	1.919+001	5.642+001	1.684+002	5.066+002	1.530+003	4.628+003	1.402+004	∞
1.40	2.156+000	5.084+000	1.264+001	3.236+001	8.409+001	2.202+002	5.789+002	1.525+003	4.020+003	∞
1.20	1.889+000	3.885+000	8.415+000	1.875+001	4.243+001	9.672+001	2.213+002	5.075+002	1.165+003	∞
1.00	1.667+000	3.000+000	5.667+000	1.100+001	2.167+001	4.301+001	8.568+001	1.710+002	3.417+002	∞
0.80	1.482+000	2.345+000	3.870+000	6.548+000	1.123+001	1.941+001	3.367+001	5.851+001	1.018+002	∞
0.60	1.329+000	1.858+000	2.688+000	3.972+000	5.941+000	8.942+000	1.351+001	2.044+001	3.095+001	∞
0.40	1.204+000	1.501+000	1.916+000	2.483+000	3.247+000	4.266+000	5.620+000	7.412+000	9.780+000	∞
0.20	1.108+000	1.251+000	1.431+000	1.648+000	1.906+000	2.209+000	2.560+000	2.966+000	3.434+000	∞
-0.00	1.045+000	1.100+000	1.162+000	1.229+000	1.299+000	1.372+000	1.446+000	1.521+000	1.596+000	∞
-0.20	1.014+000	1.030+000	1.046+000	1.061+000	1.076+000	1.089+000	1.101+000	1.112+000	1.122+000	1.186+000
-0.40	1.003+000	1.007+000	1.010+000	1.012+000	1.015+000	1.017+000	1.018+000	1.019+000	1.020+000	1.023+000
-0.60	1.001+000	1.001+000	1.002+000	1.002+000	1.002+000	1.002+000	1.003+000	1.003+000	1.003+000	1.003+000
-0.80	1.000+000	1.000+000	1.000+000	1.000+000	1.000+000	1.000+000	1.000+000	1.000+000	1.000+000	1.000+000
-1.00	1.000+000	1.000+000	1.000+000	1.000+000	1.000+000	1.000+000	1.000+000	1.000+000	1.000+000	1.000+000
-1.20	1.000+000	1.000+000	1.000+000	1.000+000	1.000+000	1.000+000	1.000+000	1.000+000	1.000+000	1.000+000
-1.40	1.000+000	1.000+000	1.000+000	1.000+000	1.000+000	1.000+000	1.000+000	1.000+000	1.000+000	1.000+000
-1.60	1.000+000	1.000+000	1.000+000	1.000+000	1.000+000	1.000+000	1.000+000	1.000+000	1.000+000	1.000+000
-1.80	1.000+000	1.000+000	1.000+000	1.000+000	1.000+000	1.000+000	1.000+000	1.000+000	1.000+000	1.000+000
-2.00	1.000+000	1.000+000	1.000+000	1.000+000	1.000+000	1.000+000	1.000+000	1.000+000	1.000+000	1.000+000

B1(N,R,MU) FOR R= ∞

MU		N = 8	16	32	64	128	256	512	1024	∞
2.00	3.333•000	1.200•001	4.533•001	1.760•002	6.933•002	2.752•003	1.097•004	4.378•004	1.749•005	∞
1.80	2.865•000	8.943•000	2.938•001	9.924•001	3.404•002	1.176•003	4.080•003	1.418•004	4.932•004	∞
1.60	2.477•000	6.714•000	1.919•001	5.642•001	1.684•002	5.066•002	1.530•003	4.628•003	1.402•004	∞
1.40	2.156•000	5.084•000	1.264•001	3.236•001	8.409•001	2.202•002	5.789•002	1.525•003	4.020•003	∞
1.20	1.889•000	3.885•000	8.415•000	1.875•001	4.243•001	9.672•001	2.213•002	5.075•002	1.165•003	∞
1.00	1.667•000	3.000•000	5.667•000	1.100•001	2.167•001	4.300•001	8.567•001	1.710•002	3.417•002	∞
0.80	1.482•000	2.343•000	3.867•000	6.543•000	1.123•001	1.940•001	3.364•001	5.846•001	1.017•002	∞
0.60	1.327•000	1.854•000	2.680•000	3.958•000	5.916•000	8.903•000	1.344•001	2.034•001	3.080•001	∞
0.40	1.198•000	1.487•000	1.890•000	2.441•000	3.184•000	4.174•000	5.489•000	7.231•000	9.533•000	∞
0.20	1.091•000	1.210•000	1.360•000	1.541•000	1.757•000	2.009•000	2.303•000	2.642•000	3.033•000	∞
-0.00	1.000•000	1.000•000	1.000•000	1.000•000	1.000•000	1.000•000	1.000•000	1.000•000	1.000•000	1.000•000
-0.20	1.000•000	1.000•000	1.000•000	1.000•000	1.000•000	1.000•000	1.000•000	1.000•000	1.000•000	1.000•000
-0.40	1.000•000	1.000•000	1.000•000	1.000•000	1.000•000	1.000•000	1.000•000	1.000•000	1.000•000	1.000•000
-0.60	1.000•000	1.000•000	1.000•000	1.000•000	1.000•000	1.000•000	1.000•000	1.000•000	1.000•000	1.000•000
-0.80	1.000•000	1.000•000	1.000•000	1.000•000	1.000•000	1.000•000	1.000•000	1.000•000	1.000•000	1.000•000
-1.00	1.000•000	1.000•000	1.000•000	1.000•000	1.000•000	1.000•000	1.000•000	1.000•000	1.000•000	1.000•000
-1.20	1.000•000	1.000•000	1.000•000	1.000•000	1.000•000	1.000•000	1.000•000	1.000•000	1.000•000	1.000•000
-1.40	1.000•000	1.000•000	1.000•000	1.000•000	1.000•000	1.000•000	1.000•000	1.000•000	1.000•000	1.000•000
-1.60	1.000•000	1.000•000	1.000•000	1.000•000	1.000•000	1.000•000	1.000•000	1.000•000	1.000•000	1.000•000
-1.80	1.000•000	1.000•000	1.000•000	1.000•000	1.000•000	1.000•000	1.000•000	1.000•000	1.000•000	1.000•000
-2.00	1.000•000	1.000•000	1.000•000	1.000•000	1.000•000	1.000•000	1.000•000	1.000•000	1.000•000	1.000•000

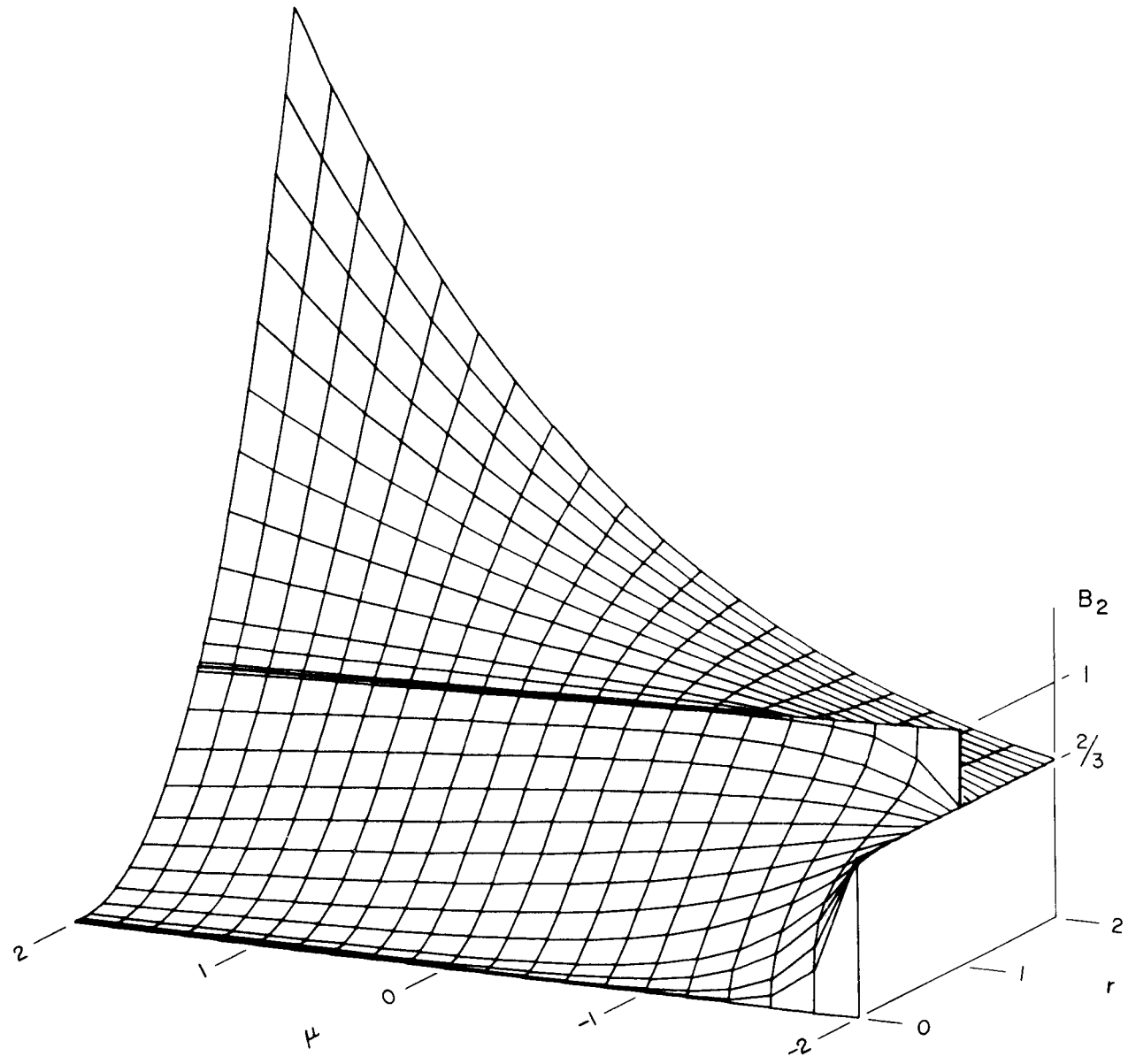

Figure 2 THE BIAS FUNCTION, $B_2(r, \mu)$

B2(R,MU)

MU \ R	0.001	0.003	0.010	0.030	0.100	0.200	0.400	0.800
2.00	1.000-006	9.000-006	1.000-004	9.000-004	1.000-002	4.000-002	1.600-001	6.400-001
1.80	1.072-006	9.645-006	1.072-004	9.642-004	1.070-002	4.263-002	1.686-001	6.525-001
1.60	1.152-006	1.037-005	1.152-004	1.036-003	1.147-002	4.547-002	1.776-001	6.652-001
1.40	1.245-006	1.120-005	1.244-004	1.118-003	1.233-002	4.860-002	1.871-001	6.781-001
1.20	1.356-006	1.221-005	1.355-004	1.216-003	1.333-002	5.207-002	1.972-001	6.910-001
1.00	1.500-006	1.349-005	1.495-004	1.337-003	1.450-002	5.600-002	2.080-001	7.040-001
0.80	1.698-006	1.524-005	1.683-004	1.493-003	1.593-002	6.052-002	2.196-001	7.170-001
0.60	2.001-006	1.788-005	1.955-004	1.708-003	1.773-002	6.583-002	2.321-001	7.299-001
0.40	2.530-006	2.228-005	2.381-004	2.020-003	2.006-002	7.219-002	2.457-001	7.426-001
0.20	3.594-006	3.048-005	3.100-004	2.494-003	2.316-002	7.996-002	2.607-001	7.549-001
-0.00	6.065-006	4.745-005	4.404-004	3.250-003	2.742-002	8.962-002	2.773-001	7.667-001
-0.20	1.260-005	8.606-005	6.921-004	4.507-003	3.340-002	1.018-001	2.959-001	7.775-001
-0.40	3.174-005	1.809-004	1.204-003	6.664-003	4.195-002	1.175-001	3.168-001	7.869-001
-0.60	9.231-005	4.280-004	2.288-003	1.047-002	5.438-002	1.379-001	3.407-001	7.944-001
-0.80	2.949-004	1.101-003	4.662-003	1.735-002	7.271-002	1.646-001	3.682-001	7.992-001
-1.00	1.000-003	3.000-003	1.000-002	3.000-002	1.000-001	2.000-001	4.000-001	8.000-001
-1.20	3.525-003	8.489-003	2.225-002	5.362-002	1.410-001	2.472-001	4.371-001	7.954-001
-1.40	1.276-002	2.467-002	5.081-002	9.828-002	2.032-001	3.104-001	4.808-001	7.832-001
-1.60	4.709-002	7.306-002	1.183-001	1.836-001	2.979-001	3.956-001	5.324-001	7.606-001
-1.80	1.762-001	2.195-001	2.793-001	3.479-001	4.431-001	5.107-001	5.936-001	7.236-001
-2.00	6.667-001	6.667-001	6.667-001	6.667-001	6.667-001	6.667-001	6.667-001	6.667-001

463-560 O - 72 - 34

B2(R,MU)

MU \ R	1.00	1.01	1.10	2.00	4.00	8.00	16.00	32.00
2.00	1.000+000	1.020+000	1.210+000	4.000+000	1.600+001	6.400+001	2.560+002	1.024+003
1.80	1.000+000	1.019+000	1.198+000	3.642+000	1.289+001	4.513+001	1.574+002	5.485+002
1.60	1.000+000	1.018+000	1.186+000	3.316+000	1.039+001	3.188+001	9.706+001	2.947+002
1.40	1.000+000	1.017+000	1.174+000	3.018+000	8.389+000	2.259+001	6.008+001	1.590+002
1.20	1.000+000	1.016+000	1.162+000	2.747+000	6.784+000	1.607+001	3.741+001	8.644+001
1.00	1.000+000	1.015+000	1.150+000	2.500+000	5.500+000	1.150+001	2.350+001	4.750+001
0.80	1.000+000	1.014+000	1.138+000	2.275+000	4.475+000	8.297+000	1.495+001	2.653+001
0.60	1.000+000	1.013+000	1.126+000	2.071+000	3.658+000	6.051+000	9.673+000	1.516+001
0.40	1.000+000	1.012+000	1.114+000	1.886+000	3.007+000	4.473+000	6.404+000	8.951+000
0.20	1.000+000	1.011+000	1.102+000	1.718+000	2.489+000	3.364+000	4.365+000	5.514+000
-0.00	1.000+000	1.010+000	1.089+000	1.566+000	2.078+000	2.581+000	3.082+000	3.582+000
-0.20	1.000+000	1.009+000	1.075+000	1.429+000	1.752+000	2.027+000	2.265+000	2.472+000
-0.40	1.000+000	1.007+000	1.060+000	1.304+000	1.494+000	1.633+000	1.738+000	1.817+000
-0.60	1.000+000	1.006+000	1.043+000	1.192+000	1.290+000	1.351+000	1.392+000	1.418+000
-0.80	1.000+000	1.004+000	1.024+000	1.091+000	1.128+000	1.148+000	1.159+000	1.166+000
-1.00	1.000+000	1.000+000	1.000+000	1.000+000	1.000+000	1.000+000	1.000+000	1.000+000
-1.20	1.000+000	9.929-001	9.693-001	9.181-001	8.990-001	8.912-001	8.879-001	8.865-001
-1.40	1.000+000	9.776-001	9.281-001	8.446-001	8.192-001	8.103-001	8.071-001	8.058-001
-1.60	1.000+000	9.429-001	8.708-001	7.787-001	7.561-001	7.494-001	7.472-001	7.465-001
-1.80	1.000+000	8.614-001	7.883-001	7.196-001	7.062-001	7.028-001	7.018-001	7.015-001
-2.00	1.000+000	6.667-001	6.667-001	6.667-001	6.667-001	6.667-001	6.667-001	6.667-001

B2(R,MU)

MU	R 64.00	128.00	256.00	512.00	1024.00	2048.00	∞
2.00	4.096•003	1.638•004	6.554•004	2.621•005	1.049•006	4.194•006	∞
1.80	1.910•003	6.653•003	2.317•004	8.067•004	2.809•005	9.783•005	∞
1.60	8.937•002	2.710•003	8.215•003	2.490•004	7.550•004	2.288•005	∞
1.40	4.201•002	1.109•003	2.928•003	7.727•003	2.039•004	5.381•004	∞
1.20	1.991•002	4.579•002	1.052•003	2.418•003	5.555•003	1.277•004	∞
1.00	9.550•001	1.915•002	3.835•002	7.675•002	1.536•003	3.071•003	∞
0.80	4.669•001	8.179•001	1.429•002	2.493•002	4.346•002	7.570•002	∞
0.60	2.348•001	3.609•001	5.521•001	8.418•001	1.281•002	1.946•002	∞
0.40	1.231•001	1.674•001	2.260•001	3.031•001	4.050•001	5.395•001	∞
0.20	6.834•000	8.351•000	1.009•001	1.209•001	1.439•001	1.704•001	∞
-0.00	4.082•000	4.582•000	5.082•000	5.582•000	6.082•000	6.582•000	∞
-0.20	2.652•000	2.809•000	2.945•000	3.064•000	3.167•000	3.258•000	3.863•000
-0.40	1.877•000	1.923•000	1.957•000	1.983•000	2.003•000	2.018•000	2.065•000
-0.60	1.436•000	1.447•000	1.455•000	1.460•000	1.463•000	1.465•000	1.470•000
-0.80	1.170•000	1.172•000	1.173•000	1.174•000	1.174•000	1.174•000	1.175•000
.00	1.000•000	1.000•000	1.000•000	1.000•000	1.000•000	1.000•000	1.000•000
1.20	8.859-001	8.856-001	8.855-001	8.854-001	8.854-001	8.854-001	8.854-001
-1.40	8.053-001	8.052-001	8.051-001	8.051-001	8.051-001	8.051-001	8.051-001
-1.60	7.462-001	7.462-001	7.461-001	7.461-001	7.461-001	7.461-001	7.461-001
-1.80	7.015-001	7.014-001	7.014-001	7.014-001	7.014-001	7.014-001	7.014-001
-2.00	6.667-001	6.667-001	6.667-001	6.667-001	6.667-001	6.667-001	6.667-001

AN APPLICATION OF STATISTICAL SMOOTHING TECHNIQUES ON VLF SIGNALS FOR COMPARISON OF TIME BETWEEN USNO AND NBS

Alain Guétrot
Bureau International de l'Heure
Paris, France

Lynne S. Higbie
National Bureau of Standards
Boulder, Colorado 80302

Jean Lavanceau
U. S. Naval Observatory
Washington, D. C. 20390

and

David W. Allan
National Bureau of Standards
Boulder, Colorado 80302

Summary

Recent developments have provided a method for obtaining submicrosecond time comparisons over continental distances. The method was applied to a time comparison between the master clocks at the United States Naval Observatory (USNO) and at the National Bureau of Standards (NBS) in Boulder, Colorado.

There were the following developments. First, if two signals show a reasonable degree of correlation in their fluctuations, then one may derive an optimum linear combination of the two with a mean square error less than for either signal individually. The two signals studied were the transmissions on 21.4 kHz from NSS in Annapolis, Maryland, and on 20.0 kHz from WWVL in Fort Collins, Colorado. It is necessary that receivers be located for both signals at the locations of the controlling clocks. Existence of positive correlation was shown. The positive cross correlation probably was due to the near reciprocal path and the very close transmission frequencies.

Second, the phase fluctuations due to the propagation medium were consistent with a spectral density of the random phase noise proportional to $|f|^{-1}$, commonly called flicker of phase noise. This persisted for Fourier frequencies from one cycle per day down to one cycle per several weeks. The fluctuations on the linear combination of the two signals still behaved as flicker of phase noise but at a lower level.

The phase or time fluctuations of the master clocks however followed a spectral density law proportional to $|f|^{-3}$, flicker of frequency noise, for frequencies lower than one cycle per day.

Third, an optimum linear filter (Wiener filter) giving the minimum mean square error estimate (MMSEE) of the signal has been determined for a random walk of phase signal (spectral density proportional to $|f|^{-2}$) imbedded in white noise (spectral density proportional to $|f|^{0}$). The same filter was shown to be still optimum for spectral densities proportional to $|f|^{-3}$ for the signal and $|f|^{-1}$ for the noise.

Application of the above filter to the appropriate linear combination, defined through correlation properties, of NSS and WWVL signals showed an improvement of 15 dB in the rms day-to-day phase fluctuations. The day-to-day rms time deviations were about 70 ns on the final results. The output estimate of the filter, compared with portable clock measurements, gave a disparity of the order of the final output noise.

The experiment provided an opportunity to determine if there is an effect of mass on frequency and within the uncertainties of the experiment a null result was obtained.

* * *

Reprinted from: Proc. of the 23rd Ann. Symp. on Freq. Contr., (U.S. Army Electronics Command, Ft. Monmouth, N.J., May 6-8, 1969). pp. 248 (May 1969)

519-248

Short-term Frequency Stability: Characterization, Theory, and Measurement

E. J. Baghdady, R. N. Lincoln, and B. D. Nelin [1]

An analysis is first presented of the manner in which oscillator short-term instabilities limit performance in a number of applications. This analysis provides guidelines for theoretical formulations, the definition of "short-term stability" and the development of measurement techniques for characterizing short-term instabilities. The factors that affect short-term stability are then discussed, and basic models for theoretical analysis are formulated. The models are used in investigations of the characteristics of outputs of "stable" sources. Measurement techniques are proposed and compared with techniques employed by other investigators.

Proc. IEEE, 53, No. 7, 704–722 (July 1965).

Manuscript received Dec. 8, 1965; revised March 28, 1965.

[1] Adcom, Inc., Cambridge, Mass. 02139, U.S.A.

Some Aspects of the Theory and Measurement of Frequency Fluctations in Frequency Standards

L. S. Cutler [1] and C. L. Searle [2]

Precision quartz oscillators have three main sources of noise contributing to frequency fluctuations: thermal noise in the oscillator, additive noise contributed by auxiliary circuitry such as AGC, etc., and fluctuations in the quartz frequency itself as well as in the reactive elements associated with the crystal, leading to an f^{-1} type of power spectral density in frequency fluctuations. Masers are influenced by the first two types of noise, and probably also by the third.

The influence of these sources of noise on frequency fluctuation vs. averaging time measurements is discussed. The f^{-1}-spectral density leads to results that depend on the length of time over which the measurements are made. An analysis of the effects of finite observation time is given.

The characteristics of both passive and active atomic standards using a servo-controlled oscillator are discussed. The choice of servo time constant influences the frequency fluctuations observed as a function of averaging time and should be chosen for best performance with a given quartz oscillator and atomic reference.

Proc. IEEE, 54, No. 2, 136–154 (February 1966).

Manuscript received Oct. 11, 1965; revised Dec. 1, 1965.

[1] Physical Research Laboratory, Hewlett-Packard Co., Palo Alto, Calif. 95050, U.S.A.

[2] Dept. of Elec. Eng. and the Res. Lab. of Elect. Mass. Institute of Technology, Cambridge, Mass. 02139, U.S.A.

SOME STATISTICAL PROPERTIES OF LF AND VLF PROPAGATION

D. W. Allan and J. A. Barnes
National Bureau of Standards
Boulder, Colorado

A statistical analysis has been conducted on the daytime phase fluctuations of the standard frequency and time Radio Stations WWVB (60 kHz) and WWVL (20 kHz) as received at Palo Alto, California, and of WWVB as received at NRC, Ottawa, Canada. The analysis technique allows a meaningful determination of the low frequency spectral density, of the variance of the phase and frequency fluctuations, and of some cross-correlations. The analysis techniques used are appropriate for commonly encountered non-stationary as well as stationary noise processes.

The results of the analysis yielded a spectral density of the time fluctuations proportional to the reciprocal spectral frequency ($S_t(\omega) = \frac{h}{|\omega|}$, flicker noise) for the propagation noise on both WWVL and WWVB. The value of h was equal to 7.9×10^{-14} s^2 for WWVL and 2.2×10^{-14} s^2 for WWVB for the Palo Alto path, and h was 4.4×10^{-14} s^2 for WWVB over the Ottawa path. For flicker noise phase modulation, a good model of the standard deviation of the fractional frequency fluctuations is: $\sigma = k|\tau|^{-1}$ where τ is the sample time in days. The values of k were 2.4×10^{-11} days for WWVL and 1.2×10^{-11} days for WWVB over the Palo Alto path and 1.8×10^{-11} days for WWVB over the Ottawa path.

A cross-correlation coefficient of -0.6 was found between WWVL and WWVB for the Palo Alto path. A linear combination of the two transmissions improved the flicker noise level by a factor of 11.5 over WWVL and by a factor of 2.7 over WWVB, allowing a precision of frequency measurement of 1×10^{-12} for a nine day average any time of the year and of 1×10^{-12} for a five day average over the summer months.

Reprinted (with revisions—August 1967) from:
Abstracts of Papers Presented at the XIIIth AGARD-EWP Symp.
Phase and Frequency Instability in Electromagnetic Wave Propagation
(Ankara, Turkey, October 9-12, 1967), p. 16 (1967)

Paper to be published in:
AGARD Conference Proc. No. 33
Phase and Frequency Instability in Electromagnetic Wave Propagation
K. Davies, Editor, Chap. 15 (Technivision Services, Slough, England—in press)

Clock Error Statistics As A Renewal Process

G. E. Hudson and J. A. Barnes

A model ensemble specifying the distribution of clock readings about their average is given which leads to an integral equation of renewal type. Renewal processes are often described by the random times of replacement of mechanical or electrical components. In our case, clocks in the ensemble may repeatedly read correctly and "renew" themselves. Solutions of the equation are discussed and are related to other error statistics.

Proc. 22nd Ann. Symp. on Freq. Contr. (U.S. Army Electronics Command, Ft. Monmouth, New Jersey—April 22-24, 1968), 384-418 (1968).

5. SELECTED FREQUENCY AND TIME REFERENCES

January 1960 —— February 1970

BYRON E. BLAIR

The following selected papers are books, written by both NBS and non-NBS authors, are categorized by various sub-topics within the general area of frequency and time. This is not an exhaustive listing, and many good books and papers have been excluded; on the other hand, we list both elementary and advanced work. Objectives of the listing include: introduction of frequency and time aspects to readers unfamiliar to the field; availability of the publications to the general public; documentation of some important studies, showing both scope and worldwide extent of frequency and time work over the past decade; and lastly, a call of attention to advanced research being actively pursued or considered today.

This compilation supplements the papers given in the previous four sections, and we would encourage the reader also to consult the many excellent references listed there. In many cases we have selected review papers, summaries of relevant work, and recent publications; these, in turn, usually reference earlier work in the field. Papers showing a CFSTI notation are available from the Clearinghouse for Federal Scientific and Technical information as follows:

National Technical Information Service
U. S. Department of Commerce
Springfield, Virginia 22151

A USGPO notation indicates availability from:

Superintendent of Documents
U. S. Government Printing Office
Washington, D. C. 20402

Reprints of research articles usually are available from authors and/or sponsoring groups or journals.

To aid in the location of the source material, there has been a vigorous attempt to list complete references in consistent form, using accepted journal title abbreviations as given in the "1961 Chemical Abstracts —— Lists of Publications" or the "1966 Revised and Enlarged Word Abbreviation List for USASI Z39.5-1963"-"American Standard for Periodical Title Abbreviations". We trust the selected publications prove useful and welcome any suggestions for references which are felt to be contributory to the intent of this listing. The valuable assistance of Mrs. Carol Wright in typing these selected references is gratefully acknowledged.

CONTENTS

5.1. Frequency and Time Standards

[1] BASOV, N. G., and LETOKHOV, V. S., "Optical frequency standards," (translated from USPEKHI FIZICHESKIKH NAUK., vol. 96, December 1969), SOVIET PHYSICS--USPEKHI, vol. 11, no. 6, pp. 855-880 (American Inst. of Phys., New York, N.Y., 10017, May-June 1969).

[2] ERMAKOV, V. I., PUSHKIN, S. B., and SACHKOV, V. I., "State standard of time and frequency," (translated from IZMERITEL'NAYA TEKHNIKA, no. 11, November 1967), MEAS. TECH. (USSR), pp. 1344-1354 (Consultants Bureau, New York, N.Y., 10011, November 1967).

[3] HELLWIG, H., "The hydrogen storage beam tube--a proposal for a new frequency standard," METROLOGIA, vol. 6, no. 2, (April 1970) (in press).

[4] _____, "Areas of promise for development of future primary frequency standards," PROC. 24th ANN. SYMP. ON FREQUENCY CONTROL (U.S. Army Electronics Command, Ft. Monmouth, N.J., 07703, April 27-29, 1970)(in press).

[5] HEWLETT-PACKARD STAFF, Frequency and Time Standards, APPL. NOTE 52, 91 pages (H-P, Palo Alto, California, 94304, November 1965).

[6] NICHOLSON, W., and SADLER, D., "Atomic standards of frequency and the second of ephemeris time," NATURE, vol. 210L, no. 5032, p. 187 (April 9, 1966).

[7] REDER, F. H., "Atomic frequency control--achievements and problems," FREQUENCY, vol. 1, no. 5, pp. 32-45 (July-August 1963).

[8] RICHARDSON, J. M., and BROCKMAN, J. F., "Atomic standards of frequency and time," THE PHYS. TEACHER, vol. 4, no. 6, pp. 247-256 (September 1966).

[9] RILEY, W. J., "Characteristics of precision frequency sources," GEN. RADIO FREQ./TIME NOTEBOOK, no. 1, 7 pages (August 1967).

a. Atomic oscillators, clocks

[10] BANGHAM, M., "Hydrogen maser work at the National Physical Laboratory," PROC. COLLOQUE INTERNATIONAL DE CHRONOMETRIE (International Horological Symp., Paris, France, Sept. 16-20, 1969), Paper A7, 12 pages (Nouvelle Faculte des Sciences, 11, Quai St., Paris, (5°), France, 1969).

[11] BARNES, J. A., "Frequency measurement errors of passive resonators caused by frequency modulated exciting signals," IEEE TRANS. on INSTRUM. AND MEAS., vol. IM-19, no. 3 (August 1970) (in press).

[12] CHI, A. R., MAJOR, F. G., and LAVERY, J. E., "Frequency comparison of five commercial cesium standards with a NASA experimental hydrogen maser," PROC. IEEE (LTR), vol. 58, no. 1, pp. 142-143 (January 1970).

[13] ELKINA, L. P., ELKIN, G. A., and STRAKHOVSKII, G. M., "Measurement of the frequency drift of a hydrogen standard owing to atomic impacts on the flask wall," (translated from IZMERITEL'NAYA TEKHNIKA, no. 6, June 1968), MEAS. TECH. (USSR), pp. 841-842 (Consultants Bureau, New York, N.Y., 10011, June 1968).

[14] ESSEN, L., and SUTCLIFFE, D. S., "Improvement to the National Physical Laboratory atomic clock," NATURE, vol. 223, no. 5206, pp. 602-603 (August 9, 1969).

[15] HELLWIG, H., "Untersuchung der frequenzgenauigkeit des ammoniakmasers auf der 3-2-linie," (Investigation of the frequency stability of the ammonia maser on the 3-2 line), Z. ANGEW. PHYS., vol. 21, no. 3, pp. 250-255 (1966).

[16] _____, and PANNACI, E., "Maser oscillations with external gain," J. of APPL. PHYS., vol. 39, no. 12, pp. 5496-5498 (November 1968).

[17] HELLWIG, H., "Hydrogen spin exchange frequency shifts," NAT. BUR. STAND. (U.S.) TECH. NOTE 387, 13 pages, (USGPO, in press).

[18] _____, VESSOT, R. F. C., LEVINE, M., ZITZEWITZ, P. W., PETERS, H. E., ALLAN, D. W., and GLAZE, D. J., "Measurement of the unperturbed hydrogen hyperfine transition frequency," CPEM DIGEST (1970 Conf. on Precision Electromagnetic Meas., Boulder, Colo., 80302, June 2-5, 1970), 2 pages (in press).

[19] HIBBARD, L. U., "The hydrogen maser as an Australian frequency standard," PROC. I.R.E.E. (Australia) vol. 28, no. 12, pp. 453-461 (December 1967).

[20] LACEY, R. F., "Thallium beam frequency standards," METROLOGIA, vol. 3., no. 3., pp. 70-78 (July 1967).

[21] MENOUD, CH., and RACINE, J., "Resultats nouveaux obtenus avec les masers a hydrogene H2 et H3 du LSRH," (New results obtained with the LSRH hydrogen masers, H2 and H3), PROC. COLLOQUE INTERNATIONAL DE CHRONOMETRIE (International Horological Symp., Paris, France, Sept. 16-20, 1969), Paper A8, 13 pages (Nouvelle Faculte des Sciences, 11, Quai St., Paris, (5°), France, 1969).

[22] MUNGALL, A. G., BAILEY, R., DAAMS, H., and MORRIS, D., "A re-evaluation of the N.R.C. long cesium beam frequency standard," METROLOGIA, vol. 4., no. 4, pp. 165-168 (October 1968).

[23] PETERS, H. E., JOHNSON, E. H., and McGUNIGAL, T. E., "NASA's atomic hydrogen standards," PROC. COLLOQUE INTERNATIONAL DE CHRONOMETRIE (International Horological Symp., Paris, France, Sept. 16-20, 1969), Paper A6, 29 pages (Nouvelle Faculte des Sciences, 11, Quai St., Paris, (5°), France, 1969).

[24] RAMSEY, N. F., "The atomic hydrogen maser," AMER. SCI., vol. 46, no. 4, pp. 420-438 (Winter 1968).

[25] RISLEY, A. S., et al., "Long term frequency stability of a NASA prototype hydrogen maser," CPEM DIGEST (1970 Conf. on Precision Electromagnetic Meas., Boulder, Colo., 80302, June 2-5, 1970), 2 pages (in press).

[26] STEINER, C., "Atomic clocks," Parts I, II, and III, FREQUENCY, vol. 6, no. 3, pp. 29-38; vol. 6, no. 4, pp. 20-24; vol. 6, no. 5, pp. 25-33 (March, April, May 1968).

[27] THRONE, D. H., "A report on the performance characteristics of a new rubidium vapor frequency standard," FREQUENCY TECHNOL., vol. 8, no. 1, pp. 16-19 (January 1970).

[28] VESSOT, R.F.C., LEVINE, M. W., CUTLER, L. S., BAKER, M. R., and MUELLER, L. F., "Progress in the development of hydrogen masers," FREQUENCY, vol. 6, no. 7, pp. 11-17 (July 1968).

b. Crystal oscillators

[29] ADAMS, C., KUSTERS, J., and BENJAMINSON, A., "Measurement techniques for quartz crystals," FREQUENCY, vol. 6, no. 8, pp. 22-25 (August 1968).

[30] GERBER, E. A., and SYKES, R. A., "Quartz frequency standards," PROC. IEEE, vol. 55, no. 6, pp. 783-791 (June 1967).

[31] HORTON, W. H., and BOOR, S. B., "Comparison of crystal measurement equipment," PROC. 19th ANN. SYMP. ON FREQUENCY CONTROL (U.S. Army Electronics Command, Ft. Monmouth, N.J. 07703, April 20-22, 1965), (AD-471 229), pp. 436-467 (CFSTI, 1965).

[32] SIMON, E., "Long-term frequency stability of crystal oscillators," U.S. ARMY ELECTRON. COMMAND REP. NO. ECOM-2787, 29 pages (Ft. Monmouth, N.J., 07703, December 1966).

c. Frequency stability

[33] CHI, A. R. (Chairman), Proc. IEEE-NASA Symp. on Short-Term Frequency Stability, (Goddard Space Flight Center, Greenbelt, Md., 20771, Nov. 23-24, 1964), NASA REP. NO. SP-80, 317 pages (USGPO, 1965).

[34] _____ (Editor), Special Issue on Frequency Stability, PROC. IEEE, vol. 54, no. 2, pp. 101-280 (February 1966).

[35] _____, et al., "Long-term frequency stability measurement of rubidium gas cell frequency standards," PROC. 22nd ANN. SYMP. ON FREQUENCY CONTROL (U.S. Army Electronics Command, Ft. Monmouth, N.J., 07703, April 22-24, 1968), (AD-844 911), pp. 592-604 (CFSTI, 1968).

[36] CUTLER, L.S., "Present status in short term frequency stability," FREQUENCY, vol. 5, no. 5, pp. 13-15 (September-October 1967).

[37] LACEY, R. F., HELGESSON, A. L., and HOLLOWAY, J. H., "Short-term stability of passive atomic frequency standards," PROC. IEEE, vol. 54, no. 2, pp. 170-176 (February 1966).

[38] STRATEMEYER, H. P., "The stability of standard-frequency oscillators," GEN. RADIO EXP., vol. 38, no. 6, 16 pages (June 1964).

[39] VAN DUZER, V., "Short-term stability measurements," Proc. IEEE-NASA Symp. on Short-Term Frequency Stability, (Goddard Space Flight Center, Greenbelt, Md., 20771, Nov. 23-24, 1964), NASA REP. NO. SP-80, pp. 269-272 (USGPO, 1965).

d. Portable frequency standards, clocks

[40] BODILY, L. N., "Performance characteristics of a portable cesium beam standard," PROC. 20th ANN. SYMP. ON FREQUENCY CONTROL (U.S. Army Electronics Command, Ft. Monmouth, N.J., 07703, April 19-21, 1966),(AD-800 523), pp. 448-463 (CFSTI, 1966).

e. Time scales, time

[41] ALLAN, D. W., GRAY, J. E., and MACHLAN, H. E., "The NBS atomic time scale system: AT(NBS), SAT(NBS), and UTC(NBS)," PROC. 24th ANN. SYMP. ON FREQUENCY CONTROL (U.S. Army Electronics Command, Ft., Monmouth, N.J., 07703, April 27-29, 1970)(in press).

[42] BIPM (International Bureau of Weights and Measures), "Changement de la définition de la seconde," (Change of the definition of the second), Comptes Rendus des Séances de la Trièzieme Conférence Générale Des Poids et Mesures, (Proc. Meet. of 13th General Conf. of Weights and Measures, October 10-16, 1967; October 15, 1968, Paris, France), pp.58-60; Unit of time (second) resolution, p. 103 (Gauthier-Villars & Cie, Paris, France, 1969).

[43] CIPM (International Committee of Weights and Measures), Comité Consultatif pour La Définition de la Seconde (Consultative Committee for the Definition of the Second), 3e Session-1963, 72 pages; 4e Session-1967, 29 pages (Gauthier-Villars & Cie, Paris, France, 1964; 1968).

[44] ESSEN, L., "A revolution in time-keeping," Proc. of Conf. on Freq. Generation and Control for Radio Syst. (C. E. Tate, Chairman, London, England, May 22-24, 1967) INST. ELEC. ENG. (London) CONF. PUBL. NO. 31, pp. 11-15 (Savoy Place, London, England, 1967).

[45] KARTASCHOFF, P., and BRANDENBERGER, H., "A digital servo for frequency and time scale conversion," PROC. 20th ANN. SYMP. ON FREQUENCY CONTROL (U.S. Army Electronics Command, Ft. Monmouth, N.J., 07703, April 19-21, 1966),(AD-800 523), pp. 577-586 (CFSTI, 1966).

[46] KHALFIN, L. A., "A fundamental method for measuring time," SOVIET PHYS. JETP, vol. 12, no. 2, pp. 353-354 (February 1961).

[47] SIMKIN, G. S., "Establishment of a single time and length standard," (translated from IZMERITEL'NAYA TEKHNIKA, no. 11, October 1968), MEAS. TECH. (USSR), pp. 1308-1314 (Consultants Bureau, New York, N.Y., 10011, October 1968).

f. Other

[48] GOULD, G., "Laser frequency standards," FREQUENCY, vol. 1, no. 6, pp. 14-16 (September-October 1963).

5.2. Dissemination of Frequency and Time

[49] BEGLEY, W. W., and SHAPIRO, A. H., "Aspects of precision timing systems," Aerospace Corp. (El Segundo, Calif.),(AD-695 458), 115 pages (CFSTI, October 1969).

[50] GARDNER, R. K., "Time and coordinate system studies," Mitre Corp. (Bedford, Mass.), REP. NO. TM-04059,(AD-615 034), 110 pages (CFSTI, March 1965).

[51] JESPERSEN, J. L., "A survey of time and frequency dissemination techniques, PROC. 24th ANN. SYMP. ON FREQUENCY CONTROL (U.S. Army Electronics Command, Ft. Monmouth, N.J., 07703, April 27-29, 1970),(in press).

[52] RADIO SCIENCE, Cumulative Tables of Contents (1959-1967) and Contents, vol. 3 (New Series), January through December, 1968, RADIO SCI., vol. 3 (New Series), no. 12, pp. 1184-1200; I-IX (USGPO, December 1968).

[53] RADIO SCIENCE, Contents of 1969 Volume, RADIO SCI., vol. 4, no. 12, pp. 1389-1397 (Amer. Geophys. Union (AGU), Washington, D.C., 20037, December 1969). NOTE: RADIO SCI. contains many excellent papers relating to frequency and time dissemination by radio signals.

[54] SPERRY GYRO. CO. STAFF, "Study of methods for synchronization of remotely located clocks," REP. NO. HP 9224-0234, NASA CR-738,(N67-19896), 206 pages (USGPO, March 1967).

[55] WINKLER, G.M.R., "World-wide time review," DOT/FAA Meet. on Utilization of Time/Frequency in Collision Avoidance Systems (CAS), (FAA, Washington, D.C., 20590, August 27-28, 1968),(AD-681 881), pp. 111-124 (CFSTI, 1968).

[56] WITT, S. N., JR., "Design guidelines for frequency standard and distribution systems," FREQUENCY, vol. 2, no. 1, pp. 32-33 (January-February 1964).

a. Radio broadcasting

[57] BEERS, Y., "WWV moves to Colorado," Parts I and II, QST, vol. LI, no. 1, pp. 11-14 (January 1967); vol. LI, no. 2, pp. 30-36 (February 1967).

[58] BONANOMI, J., CHASLAIN, Cl., and RENTSCH, E., "Le service horaire HBG, experiences et resultats apres 3 annees d'exploitation," (The Hourly Service HBG, Experiences and Results after 3 Years of Operation), PROC. COLLOQUE INTERNATIONAL DE CHRONOMETRIE (International Horological Symp., Paris, France (September 16-20, 1969), Paper A23, 6 pages (Nouvelle Faculte des Sciences, 11, Quai St., Paris, (5°), France, 1969).

[59] C.C.I.R., Documents of the XIth Plenary Assembly, (Oslo, Norway, 1966), vol. 3 (standard frequencies and time signals), pp. 281-324 (Int. Telecommun. Union, Geneva, Switzerland, 1967).

[60] CREIGHTON, J. L., and WASE, A.E.N., "The new very-low-frequency transmitter at Rugby radio station," POST OFFICE ELEC. ENG. J. (London), vol. 61, part 4, pp. 232-237 (January 1969).

[61] GOULD, R. N., and CARTER, W. R., "Very low frequency electromagnetic waves," WIRELESS WORLD, vol. 68, no. 4, pp. 186-190 (April 1962).

[62] PALIY, G. N., "Transmission of standard frequency using a broadcasting station," (translated from IZMERITEL'NAYA TEKHNIKA, no. 11, November 1967), MEAS. TECH. (USSR), pp. 428-431 (Consultants Bureau, New York, N.Y., 10011, November 1967).

[63] STEELE, J. McA., "Standard frequency transmissions," WIRELESS WORLD, vol. 73, no. 9, pp. 443-448 (September 1967).

[64] STONE, R., JR., "Frequency control of Navy VLF stations," REP. of NRL PROGR. (U.S. Naval Res. Lab., Washington, D.C., 20390), pp. 8-16 (CFSTI, February 1967).

[65] SÜSS, R., "The generation of time measurement markers," NTZ COMMUN. J. (PROC. NACHRICHTENTECHNISCHE GESELLSCHAFT -VDE), vol. 5, no.6, pp. 249-256 (1966).

[66] WINKLER, G.M.R., "USNO time service announcements," (U.S. Navy transmission changes, phase values, schedules of standard time and frequency broadcasts),(U.S. Naval Observatory, Washington, D.C., 20390).

(1) Systems (including navigation)

[67] BROGDEN, J. W., "The OMEGA navigation system," NAVIGATION, vol. 15, no. 2, pp. 115-118 (Summer 1968).

[68] CROMBIE, D. D., "The effect of waveguide dispersion on VLF timing systems," IEEE TRANS.on ANTENNAS AND PROPAGATION, vol. AP-15, no. 2, pp. 322-323 (March 1967).

[69] HARTLEY, H. F., "Analysis of some techniques used in modern LF-VLF radiation systems," IEEE TRANS. on COMMUN. TECHNOL., vol. COM-16, no. 5, pp. 690-700 (October 1968).

[70] LACY, E. A., "OMEGA - a VLF radionavigation system," ELECTRON. WORLD, vol. 82, no. 6, pp. 47-49, 69 (December 1969).

[71] PHIPPS, C. R., JR., "OMEGA-system synchronization in the absolute mode of operation," NAVAL ELECTRON. LAB. CENTER RES. REP. 1544, 32 pages (NELC, Command Control and Commun., San Diego, Calif., 92152, March 1968).

[72] PIERCE, J. A., "OMEGA," IEEE TRANS. on AEROSP. and ELECTRON. SYST., vol. AES-1, no. 3, pp.206-215 (December 1965).

[73] SHAPIRO, L. D., "LORAN-C timing," FREQUENCY, vol. 3, no. 2, pp. 32-37 (March-April 1965).

[74] STRINGER, F. S., "Hyperbolic radio navigation systems," WIRELESS WORLD, vol. 75, no. 1406, pp. 353-357 (August 1969).

[75] TATE, C. E., (Chairman), Proc. of Conf. on Freq. Generation and Control for Radio Syst. (London, England, May 22-24, 1967), INST. ELEC. ENG. (London) CONF. PUBL. NO. 31, 191 pages (Savoy Place, London, 1967).

[76] THOMAS, G., "Étude et réalisation d'un oscillateur asservi a la phase d'une onde étalon périodiquement interrompue," (Design and construction of an oscillator phase controlled by by a standard transmission periodically interrupted), L'ONDE ELECTRIQUE, vol. 46, no. 474, pp. 986-988 (September 1966).

[77] WATT, A. D., VLF Radio Engineering, 701 pages (Pergamon Press, Inc., Long Island City, N.Y., 11101, 1967).

(2) Propagation factors

[78] BELROSE, J. S., "The lower ionosphere - a review," Proc. Conf. on M.F., L.F. and V.L.F. Radio Propagation (W. T. Blackband, Chairman, London, England, November 8-10, 1967), INST. ELEC. ENG. (London), CONF. PUBL. NO. 36, pp. 331-338 (Savoy Place, London, England, 1967).

[79] BLACKBAND, W. T. (Editor), Propagation of Radio Waves at Frequencies Below 300 Kc/s, (Proc. 7th Meet. of the AGARD Ionos. Res. Comm., Munich, Germany, 1962), 478 pages (Pergamon Press, Ltd. Oxford, England, 1964).

[80] _____ (Chairman), Proc. Conf. on M.F., L.F. and V.L.F. Radio Propagation (London, England, November 8-10, 1967), INST. ELEC. ENG. (London), CONF. PUBL. NO. 36, 354 pages (Savoy Place, London, England, 1967).

[81] BOVA, N. T., LAIKHTMAN, I. B., and MOLEBNYI, V. V., "Methods of measuring group velocity and group delay time," (translated from IZVESTIYA VUZ. RADIOTEKHNIKA, vol. 8, no. 4), SOVIET RADIO ENG. (USSR), pp. 276-284 (July/August 1965).

[82] BRILLOUIN, L., Wave Propagation and Group Velocity, 154 pages (Academic Press, New York, N.Y., 10003, 1960).

[83] BUDDEN, K. G., Radio Waves in the Ionosphere, 542 pages (Cambridge University Press, London, England, 1961).

[84] CHILTON, C. J., CROMBIE, D. D., and JEAN, A. G., "Phase variations in V.L.F. propagation," (Chap. 19, Propagation of Radio Waves at Frequencies Below 300 Kc/s, W. T. Blackband, ed.), pp. 257-290 (Pergamon Press, Ltd., Oxford, England, 1964).

[85] CROMBIE, D. D., "The waveguide mode propagation of VLF radio waves to great distances," (A survey) Proc. Conf. on M.F., L.F. and V.L.F. Radio Propagation (W. T. Blackband, Chairman, London, England, November 8-10, 1967), INST. ELEC. ENG. (London), CONF. PUBL. NO. 36, pp. 138-158 (Savoy Place, London, England, 1967).

[86] DAVIES, K., Ionospheric Radio Propagation, NAT. BUR. STAND. (U.S.) MONOGR. 80, 470 pages (USGPO, corrected reprinting November 1965).
NOTE: Essentially devoted to propagation of HF radio; two chapters included on lower frequency bands (LF and VLF) and upper frequency band (VHF).

[87] _____, Ionospheric Radio Waves, 460 pages (Blaisdell Publishing Co., Waltham, Mass.,02154, 1969).

[88] _____ (Editor), Phase and Frequency Instability in Electromagnetic Wave Propagation, (AGARD-EWP XIII Symp., Ankara, Turkey, October 9-12, 1967), AGARD CONF. PROC. NO. 33, K.Davies, Ed. (Technivision Services, Slough, England,in press).

[89] JOHLER, J. R., "Propagation of an electromagnetic pulse from a nuclear blast," IEEE TRANS. on ANTENNAS AND PROPAGATION, vol. AP-15, no. 2, pp. 256-263 (March 1967).

[90] LAWRENCE, R. S., LITTLE, C. G., and CHIVERS, H.J.A., "A survey of ionospheric effects upon earth-space radio propagation," PROC. IEEE, vol. 52, no. 1, pp. 4-27 (January 1964).

[91] WAIT, J. R., Electromagnetic Waves in Stratified Media, 372 pages (Pergamon Press, Inc., Long Island City, N.Y., 11101, 1962).

(a) HF propagation

[92] BOWHILL, S. A., "Diversity effects in long distance high frequency radio pulse propagation," J. RES. NBS, vol. 65D (Radio Propagation), no. 3, pp. 213-223 (May-June 1961).

[93] DAVIES, K., and BAKER, D. M., "On frequency variations of ionospherically propagated HF radio signals," RADIO SCI.,vol. 1 (New Series), no. 5, pp. 545-556 (May 1966).

[94] FENWICK, R. B., and VILLARD, O. G., JR., "A test of the importance of ionosphere-ionosphere reflections in long distance and around-the-world high-frequency propagation," J. GEOPHYS. RES., vol. 68, no. 20, pp. 5659-5666 (October 1963).

[95] JULL, G. W.,"Short-term and averaged characteristics of nonreciprocal HF ionospheric paths," IEEE TRANS. on ANTENNAS AND PROPAGATION, vol. AP-15, no. 2, pp. 268-277 (March 1967).

[96] LOMAX, J. B., "High-frequency propagation dispersion," Phase and Frequency Instability in Electromagnetic Wave Propagation, (AGARD-EWP XIII Symp., Ankara, Turkey, October 9-12,1967), AGARD CONF. PROC. NO. 33, K. Davies, Ed.(Technivision Services, Slough, England, in press).

[97] TOMAN, K., "Ionospheric phase- and group-path," J. of ATMOS. and TERR. PHYS., vol. 29, no. 8, pp. 1019-1023 (August 1967).

[98] _____, "Frequency variations of an oblique 5 MHz ionospheric transmission," Phase and Frequency Instability in Electromagnetic Wave Propagation, (AGARD-EWP XIII Symp., Ankara, Turkey, October 9-12, 1967), AGARD CONF. PROC. NO. 33, K.Davies, Ed. (Technivision Services, Slough, England, in press).

[99] TREHARNE, R. F., et al., "Some characteristics of the propagation of skywaves over short ionospheric paths," PROC. I.R.E.E. (Australia), vol. 26, no. 8, pp. 245-254 (August 1965).

(b) LF propagation

[100] BERRY, L. A., "Wave hop theory of long distance propagation of low-frequency radio waves," RADIO SCI., J. RES. NBS/USNC-URSI, vol. 68D, no. 12, pp. 1275-1284 (December 1964).

[101] JOHLER, J. R., "Propagation of the low-frequency radio signal," PROC. IRE, vol. 50, no. 4, pp. 404-427 (April 1962).

(c) VLF propagation

[102] ALPERT, YA. L., and FLIGEL, D. S., Propagation of ELF and VLF Waves near the Earth, 172 pages (Plenum Publishing Corp., New York, N.Y., 10011, 1970).

[103] BURGESS, B., "Navigation errors using Omega at ranges close to a transmitter," PROC. INST. ELEC. ENG. (London), vol. 117, no. 1, pp. 51-55 (January 1970).

[104] BURTT, G. J., "Observations on phase stability of signals from NBA (18 kc/s) Panama as received in New Zealand," PROC. INST. ELEC. ENG. (London), vol. 110, no. 11, pp. 1928-1932 (November 1963).

[105] CHILTON, C. J., MURPHY, A. C., STEELE, F. K., and RADICELLA, S. M., "The normal phase variations of the 18 Kc/s signals from NBA observed at Tucuman, Argentina," INST. ENVIRON. RES. TECH. REP. IER 3-ITSA 3-6, (PB-173 828), 30 pages (CFSTI, July 1966).

[106] CROMBIE, D. D., "Phase and time variations in VLF propagation over long distances," RADIO SCI. J. RES. NBS/USNC-URSI, vol. 68D, no. 11, pp. 1223-1224 (November 1964).

[107] CROMBIE, D. D., "Further observations of sunrise and sunset fading of very-low-frequency signals," RADIO SCI., vol. 1 (New Series), no. 1, pp. 47-51 (January 1966).

[108] HAMPTON, D. E., "Group-velocity variations of V.L.F. signals," PROC. INST. ELEC. ENG. (London), vol. 114, no. 6, pp. 689-695 (June 1967).

[109] KAISER, A. B., "VLF propagation over long paths," J. ATMOS. and TERR. PHYS., vol. 29, pp. 73-85 (January 1967).

[110] _____, "An explanation of VLF diurnal phase change observations," RADIO SCI., vol.4, no. 1, pp. 17-21 (January 1969).

[111] REDER, F. H., ÅBOM, C. J., and WINKLER, G.M.R., "Precise phase and amplitude measurements on VLF signals propagated through the artic zone," RADIO SCI., J. RES. NBS/USNC-URSI, vol. 68D, no. 3, pp. 275-281 (March 1968).

[112] _____, "VLF propagation phenomena observed during low and high solar activity," Progress in Radio Science 1966-1969, Part 1, C. E. White, Ed., (Proc. XVI General Assembly of URSI, Ottawa, Canada, 1969)(in press).

[113] STEELE, F. K., and CHILTON, C. J., "Measurement of the phase velocity of VLF propagation in the earth-ionosphere waveguide," RADIO SCI., J. RES. NBS/USNC-URSI, vol. 68D, no. 12, pp. 1269-1273 (December 1964).

[114] SWANSON, E. R., "Time dissemination effects caused by instabilities of the medium," Phase and Frequency Instability in Electromagnetic Wave Propagation, (AGARD-EWP XIII Symp., Ankara, Turkey, October 9-12, 1967) AGARD CONF. PROC. NO. 33, K. Davies, Ed. (Technivision Services, Slough, England, in press).

[115] _____, and HEPPERLEY, E., "Composite OMEGA: OMEGA navigation using a combination of information from radiations at 10.2 and 13.6 kHz," NAVAL ELECTRON. LAB. REP. NO. NELC-1657, (AD-863 791), 66 pages (CFSTI, October 1969).

[116] THOMPSON, A. M., ARCHER, R. W., and HARVEY, I.K., "Some observations on VLF standard frequency transmissions as received at Sydney, N.S.W.," PROC. IEEE, vol. 51, no. 11, pp.1487-1493 (November 1963).

[117] WAIT, J. R., "Introduction to the theory of VLF propagation," PROC. IRE, vol. 50, no. 7, pp. 1624-1647 (July 1962).

[118] _____, and SPIES, K. P., "Characteristics of the earth-ionosphere waveguide for VLF radio waves," NAT. BUR. STAND. (U.S.) TECH. NOTE 300, 94 pages (USGPO, 1964); 1st suppl., 24 pages (February 1965); 2nd suppl., 14 pages (March 1965).

[119] _____, "Recent theoretical advances in the terrestrial propagation of VLF electromagnetic waves," Advan. Electron. and Electron. Phys., L. Marton, Ed., vol. 25, pp. 145-209 (Academic Press, Inc., New York, N.Y., 10003, 1968).

[120] WESTFALL, W. D., "Diurnal changes of phase and group velocity of VLF radio waves," RADIO SCI. vol. 2 (New Series), no. 1, pp. 119-125 (January 1967).

b. Other means of dissemination

(1) Portable clocks

[121] BENTICK, J. P., "A transfer standard of time for use over great distances," ROYAL AIRCRAFT ESTAB. (England), TECH. REP. NO. RAE-TR-67296, (AD-833 068), (CFSTI, November 1967).

[122] BODILY, L. N., and HYATT, L. C., "'Flying clock' comparisons extended to East Europe, Africa, and Australia," HEWLETT-PACKARD J., vol. 19, no. 4, pp. 12-20 (H-P, Palo Alto, Calif., 94304, (December 1967).

[123] KUGEL, C. P., "OMEGA system synchronization - NELC propagation prediction capability evaluated by U.S. Naval Observ. flying clock meas.," NAVAL ELEC. LAB. CENTER RES. REP. 1529, 24 pages (NELC, Command Control and Commun., San Diego, Calif., 92152, Januarv 1968).

[124] REDER, F. H., WINKLER, G.M.R., and BICKART, C., "Results of a long-range clock synchronization experiment," PROC. IRE, vol. 49, no. 6, pp. 1028-1032 (June 1961).

(2) Satellites

[125] KERSHNER, R. B., and NEWTON, R. R., "The transit system," J. INST. NAVIG. (England), vol. 15, no. 2, pp. 129-144 (April 1962).

[126] LAIOS, S. C., "STADAN clock synchronization via GEOS-II satellite," GODDARD SPACE FLIGHT CENTER NASA REP. NO. X-570-69-159, 33 pages (NASA-GSFC, Greenbelt, Md., 20771, March 1969).

[127] MARKOWITZ, W., LIDBACK, C. A., UYEDA, H., and MURAMATSU, K., "Clock synchronization via relay II satellite," IEEE TRANS. on INSTRUM. AND MEAS., vol. IM-15, no. 4, pp. 177-184 (December 1966).

[128] MAZUR, W. E., and LAIOS, S. C., "A compendium of satellite time-synchronization techniques," GODDARD SPACE FLIGHT CENTER NASA REP. NO. X-573-69-394, 13 pages (NASA-GSFC, Greenbelt, Md., 20771, August 1969).

[129] STEELE, J. McA., MARKOWITZ, W., and LIDBACK, C. A., "Telstar time synchronization," IEEE TRANS. on INSTRUM. AND MEAS., vol. IM-13, no. 4, pp. 164-170 (December 1964).

(3) Telephone lines/cables

[130] GRIMSLEY, S. W., and MILLER, M. J., "Phase comparison of frequency standards," PROC. I.R.E.E. (Australia), vol. 29, no. 1, pp. 14-17 (January 1968).

[131] HASTINGS, H. F., "Transmission to Naval Observatory of reference frequency derived from hydrogen masers at NRL," REP. NRL PROG. (U.S. Naval Res. Lab., Washington, D.C., 20390), pp. 46-47 (CFSTI, March 1965).

5.3. Radio Reception Techniques-Local Synchronization/Comparison/Navigation

[132] ABLOWICH, D., JR., "Frequency and time synchronization," MEAS. AND DATA, vol. 1, no. 1, pp. 30-47 (January-February 1967).

[133] ALPERT, A., and MURPHY, D. J., "Establishing, synchronizing and maintaining a standard clock for the USAF calibration program," FREQUENCY, vol. 6, no. 5, pp. 17-21 (May 1968).

[134] NBS, "Standard frequencies wired into NBS labs," FREQUENCY, vol. 6, no. 8, pp. 6,8 (August 1968).

[135] SOSIN, B. M., and HAYWOOD, H., "A frequency distribution scheme," FREQUENCY, vol. 5, no. 4, pp. 35-36 (July/August 1967).

a. HF reception/measurement

[136] HILL, G. E., and HERMAN, J. R., "WWV reception in the Arctic during ionospheric disturbances," J. RES. NBS, vol. 67D (Radio Propagation), no. 2, pp. 179-182 (March-April 1963).

[137] MERRELL, R., "Keeping accurate time with WWV," BROADCAST ENG., vol. 10, no. 9, pp. 14-17 (September 1968).

b. LF reception/measurement

[138] PAKOS, P. E., "Use of the Loran-C system for time and frequency dissemination," FREQUENCY TECHNOL., vol. 7, no. 7, pp. 13-18 (July 1969).

[139] SHAPIRO, L. D., "Loran-C skywave delay measurements," IEEE TRANS. on INSTRUM. AND MEAS., vol. IM-17, no. 4, pp. 366-372 (December 1968).

c. VLF reception/measurement

[140] BRADY, A. H., "On the long term phase stability of the 19.8 kc/s signal transmitted from Hawaii and received at Boulder, Colorado," RADIO SCI. J. RES. NBS/USNC-URSI, vol. 68D, no. 3, pp. 283-289 (March 1964).

[141] BURGESS, B., "Experimental observations on the phase variability of 200 Hz difference frequencies derived from VLF transmissions obtained over large distances," ROYAL AIRCRAFT ESTAB. (England) TECH. REP. NO. 68150, (AD-840 697), 7 pages (CFSTI, 1968).

[142] CHI, A. R., and WITT, S. N., "Time synchronization of remote clocks using dual VLF transmissions," PROC. 20th ANN. SYMP. ON FREQUENCY CONTROL (U.S. Army Electronics Command, Ft. Monmouth, N.J., 07703, April 19-21, 1966), (AD-800 523), pp. 588-611 (CFSTI, 1966).

[143] COUZENS, R., "The 'beat 2 receiver' - a twin channel OMEGA receiver," ROYAL AIRCRAFT ESTAB. (England) TECH. REP. NO. 68225, (AD-686 454), 7 pages (CFSTI, August 1968).

[144] ECHOLS, J. D., "Calibrating frequency standards with VLF transmissions," ELECTRONICS, vol. 35, no. 17, pp. 60-63 (April 1962).

[145] EGIDI, C., "Narrow band time signals," ALTA FREQUENZA, vol. 37, no. 5, pp. 129E-139E (1968).

[146] HARTKE, D., "Simplified local comparisons with USFS," FREQUENCY, vol. 2, no. 2, pp. 32-33 (March-April 1964).

[147] IIJIMA, S., TORAO, M., and FUJIWARA, K., "Phase variations of VLF waves, GBR and GBZ, as received," ANNALS OF TOKYO ASTRON. OBSERV., 2nd Series, vol. XI, no. 1, pp. 1-28 (1968).

[148] LAPANNE, L., "Using wave analyzers to maintain frequency standards," FREQUENCY, vol. 2, no. 5, pp. 20-22 (September-October 1964).

[149] MOOSER, L., "Frequency and phase control of local oscillators by transmitters of standard frequency," PROC. 14th ANN. SYMP. ON FREQUENCY CONTROL (U.S. Army Res. and Dev. Lab., Ft. Monmouth, N.J., 07703, May 31-June 2,1960), (PP-153 716), pp. 421-428 (Libr. of Congr., Washington, D.C., 20006, 1960).

[150] PIERCE, J. A., "The use of composite signals at very low radio frequencies," HARVARD UNIV. TECH. REP. NO. 552, 31 pages (Div. Eng. and Appl. Phys., Harvard Univ., Cambridge, Mass., 02138, February 1968).

[151] RAWLES, A. T., and BURGESS, B., "Results of two-frequency VLF transmission experiments from Criggion GBZ," RADIO SCI., vol. 2 (New Series), no. 11, pp. 1295-1301 (November 1967).

[152] ROEDER, J. H., and SHAWE, M. E., "Dual VLF timing capability observed at some intermediate ranges," GODDARD SPACE FLIGHT CENTER REP. NO. X-521-69-346, 28 pages (NASA-GSFC, Greenbelt, Md., 20771, June 1969).

[153] STANBROUGH, J. H., JR., "A VLF radio relative navigation system," J. INST. OF NAVIG., vol. 11, no. 4, pp. 417-428 (January 1965).

[154] STONE, R. R., JR., "Synchronization of local frequency standards with VLF transmissions," PROC. 16th ANN. SYMP. ON FREQUENCY CONTROL (U.S. Army Res. and Dev. Lab., Ft. Monmouth, N.J., 07703, April 25-27, 1962), (PP-162 343), pp. 227-240 (CFSTI, 1962).

[155] BEATTY, R. W., and WEINSCHEL, B. O. (Editors), Special Issue on Radio Measurement Methods and Standards, PROC. IEEE, vol. 55, no. 6, pp.737-1063 (June 1967).

[156] GOLDING, J. F., "Counter methods of frequency measurements," BRITISH COMMUN. AND ELECTRON., vol. 8, no. 11, pp. 848-853 (November 1961).

[157] GRIMSLEY, S. W., and MILLER, M. J., "Phase comparison of frequency standards," PROC. I.R.E.E. (Australia), vol. 29, no. 1, pp. 14-17 (January 1968).

[158] KOIDE, F. K., "Frequency and time distribution," MEAS. AND DATA, vol. 1, no. 3, pp. 98-108 (May-June 1967).

[159] MARKOWITZ, W., "Time and frequency measurement, atomic and astronomical," FREQUENCY TECHNOL., vol. 7, no. 1, pp. 13-18 (January 1969).

[160] NOORDANUS, J., "Frequency synthesizers-a survey of techniques," IEEE TRANS. on COMMUN. TECHNOL., vol. COM-17, no. 2, pp. 257-271 (April 1969).

[161] PARSEN, B., "Comparators for evaluation of frequency standards," FREQUENCY, vol. 1, no. 5, pp. 53-55 (July-August 1963).

[162] WINKLER, G.M.R., "Convention used for reporting clock differences: the algebraic method," FREQUENCY, vol. 6, no. 11, pp. 5-6 (November 1968).

[163] WITT, S. N., "Frequency standards and calibration techniques," ELECTRON. INSTRUM. DIGEST, vol. 5, no. 3, pp. 10-18 (March 1969).

a. Computer program analysis

[164] CRARY, J. H., "Extension of programs for calculations of great circle paths and sunrise-sunset times," NAT. BUR. STANDS. (U.S.) TECH. NOTE 303, 19 pages (USGPO, February 1965).

[165] DAVID, F., et al., "Correlation measurements on an HF transmission link," IEEE TRANS. on COMMUN. TECHNOL., vol. COM-17, no. 2, pp.245-256 (April 1969).

[166] JOHLER, J. R., and MELLECKER, C., "Theoretical LF, VLF field calculations with spherical wave functions of integer order," ESSA TECH. REP., 82 pages; Supplement-Computer Program, 99 pages (USGPO, in press).

[167] SEARLE, C. L., POSNER, R. D., BADESSA, R. S., and BATES, V. J., "Computer-aided calculation of frequency stability," PROC. IEEE-NASA SYMP. on the DEFINITION and MEAS. of SHORT-TERM FREQ. STABIL. (Goddard Space Flight Center, Greenbelt, Md., 20771, November 23-24, 1964), NASA REP. NO. SP-80, pp. 273-277 (USGPO 1965).

b. Standards of measurement

[168] ASTIN, ALLEN V., "Standards of measurements," SCI. AMER., vol. 218, no. 6, pp. 50-62 (June 1968).

[169] HUNTOON, R. D., "Status of the national standards for physical measurement," SCIENCE, vol. 150, no. 3693, pp. 169-178 (October 1965).

[170] JEAN, A. G., TAGGART, H. E., and WAIT, J. R., "Calibration of loop antennas at VLF," J. RES. (NBS) Sec. C-ENG. and INSTRUM., vol. 65, no. 3, pp. 189-193 (July-September 1961).

[171] LEWIS, E. D., and SODERMAN, R. A., "Radio-frequency standardization activities," PROC. IEEE, vol. 55, no. 6, pp. 759-773 (June 1967).

[172] McNISH, A. G., "Fundamentals of measurement," ELECTRO-TECHNOL., vol. 71, no. 5, pp. 113-128 (May 1963).

[173] RICHARDSON, J. M., and BROCKMAN, J. F., "The U.S. basis of electromagnetic measurements," IEEE SPECTRUM, vol. 1, no. 1, pp. 129-138 (January 1964).

c. Statistical analysis/measurement techniques

[174] BINGHAM, C., GODFREY, M. D., and TUKEY, J. W., "Modern techniques of power spectrum estimation," IEEE TRANS. on AUDIO ELECTROACOUSTICS, vol. AU-15, no. 2, pp. 56-66 (June 1967).

[175] BLACKMAN, R. B., Linear Data-Smoothing and Prediction in Theory and Practice, 182 pages (Addison-Wesley Publ. Co., Inc., Reading, Mass. 01867, 1965).

[176] BRIGHAM, E. O., and MORROW, R. E., "The fast Fourier transform," IEEE SPECTRUM, vol. 4, no. 12, pp. 63-70 (December 1967).

[177] CROW, E. L., "The statistical construction of a single standard from several available standards," IEEE TRANS. on INSTRUM. AND MEAS., vol. IM-13, no. 4, pp. 180-185 (December 1964).

[178] EDSON, W. A., "Noise in oscillators," PROC. IRE, vol. 48, no. 8, pp. 1454-1466 (August 1960).

[179] LIGHTHILL, C. M., Introduction to Fourier Analysis and Generalized Functions, 79 pages (Cambridge University Press, London, England, 1962).

[180] MULLEN, J. A., "Background noise in nonlinear oscillators," PROC. IRE, vol. 48, no. 8, pp. 1467-1473 (August 1960).

[181] SILVER, S. L., "Electronic measurements using statistical techniques," ELECTRON. WORLD, vol. 79, no. 6, pp. 49-53 (June 1968).

5.5. Advanced Frequency and Time Research

a. Aircraft collision avoidance system (ACAS)

[182] FRYE, E. O., and KILLHAM, D. E., "Aircraft collision avoidance systems," IEEE SPECTRUM, vol. 3, no. 1, pp. 72-80 (January 1966).

[183] HOLT, J. M.,"Avoiding air collisions," SCI. AND TECHNOL., no. 78, pp. 56-63 (June 1968).

[184] McINTIRE, O. E., et al., DOT/FAA Meet. on Utilization of Time/Frequency in Collision Avoidance Systems (CAS), (FAA, Washington, D.C., 20590, August 27-28, 1968), (AD-681 881) 125 pages (CFSTI, 1968).

[185] THORNBURG, C. O., "Master timing of CAS ground stations," IEEE TRANS. on AEROSP. AND ELECTRON. SYST., vol. AES-4, no. 2, pp. 265-272 (March 1968).

[186] WHITE, F. C. (Editor), Special Section on Aircraft Collision Avoidance, IEEE TRANS. on AEROSP. AND ELECTRON. SYST., vol. AES-4, no. 2, pp. 234-314 (March 1968).

b. Aircraft flyover

[187] BESSON, J., and CUMER, J., "Synchronisation precise de bases par simple survol," (Precise in-flight synchronization of ground stations), PROC. COLLOQUE INTERNATIONAL DE CHRONOMETRIE (International Horological Symp., Paris, France, September 16-20, 1969), Paper A-27, 24 pages (Nouvelle Faculte des Sciences, 11, Quai St., Paris, (5°), France, 1969).

[188] LAY, M. D., and DAVIS,D. T., "A simple airborne system for calibration of remote precision clocks," FREQUENCY TECHNOL., vol. 7, no. 12, pp. 13-22 (December 1969).

c. Communications/deep space tracking

[189] BALTAS, M. M., "Frequency and timing control in future military communications," FREQUENCY, vol. 2, no. 4, pp. 16-17 (July-August 1964).

[190] FILIPOWSKY, R. F., and MUEHLDORF, E. I., Space Communications Systems, 575 pages (Prentice-Hall, Inc., Englewood Cliffs, N.J., 07632, 1965).

[191] SYDNOR, R., CALDWELL, J. J., and ROSE, B. E., "Frequency stability requirements for space communications and tracking systems," PROC. IEEE, vol. 54, no. 2, pp. 231-236 (February 1966).

[192] TRASK, D. W., and MULLER, P. M., "Timing: DSIF two-way Doppler inherent accuracy limitations," JPL PROGRAMS SUMMARY 37-39, vol. III, pp. 7-16 (JPL, Calif. Inst. of Technol., Pasadena, Calif., 91103, May 1966).

[193] VIARS, T. C., "Application of precise time-frequency technology in multi-function systems," PROC. 23rd ANN. SYMP. ON FREQUENCY CONTROL (U.S. Army Electronics Command, Ft. Monmouth, N.J., 07703, May 6-8, 1969) pp. 8-13 (Electron. Ind. Ass., Washington, D.C., 20006, 1969).

d. Long-base interferometry

[194] BURKE, B. F., "Long-base interferometry," PHYS. TODAY, vol. 22, no. 7, pp. 54-63 (July 1969).

[195] ROGERS, A.E.E.,and MORAN, J. M., "Very long baseline interferometry as a means of world-wide time synchronization," LINCOLN LAB. TECH. REP. 478, 16 pages, (Lincoln Lab., M.I.T., Boston, Mass., 02173, February 1970).

[196] SHAPIRO, I. I., "Possible experiments with long-baseline interferometers," NEREM RECORD, vol. 10, pp. 70-71 (AD-685 687), (CFSTI, 1968).

e. Meteor trail

[197] LATORRE, V. R., "Messages by meteor," ELECTRONICS, vol. 38, no. 21, pp. 102-106 (October 1965).

[198] MARCH, D. N., TASHIRO, S., and SANDERS, W. R., "Meteor trail forward scatter time synchronization," FREQUENCY, vol. 6, no. 2, pp. 12-17 (February 1968).

[199] SANDERS, W. R., ALBRIGHT, D. L., TASHIRO, S., and MARCH, D. N., "A meteor burst clock synchronization experiment," IEEE TRANS. on INSTRUM. AND MEAS., vol. IM-15, no. 4, pp.184-189 (December 1966).

[200] SUGAR, G. R., "Radio propagation by reflection from meteor trails," PROC. IEEE, vol. 52, no. 2, pp. 116-136 (February 1964).

f. Moonbounce

[201] BAUMGARTNER, W. S., and EASTERLING, M. F., "A world-wide lunar radar time synchronization system," Advanced Navigational Tech., (papers of 14th AGARD/AVIONICS Panel Meet., Milan, Italy, September 12-15, 1967), AGARD CONF. PROC. NO. 28, pp. 143-162, W. T. Blackband, Ed. (Technivision Services, Slough, England, February 1970).

[202] COFFIN, R. C., EMERSON, R. F., and SMITH, J. R., "Time-synchronization system," JPL PROGRAMS SUMMARY 37-45, vol. III, pp. 72-75 (JPL,Calif. Inst. of Technol., Pasadena, Calif., 91103, May 1967).

g. Pulsars

[203] BOYNTON, P. E., PARTRIDGE, R. B., and WILKENSON, D. T., "Precision time measurements of optical pulsars," PROC. 23rd ANN. SYMP. ON FREQUENCY CONTROL (U.S. Army Electronics Command, Ft. Monmouth, N.J., 07703, May 6-8, 1968), p. 313 (Electron. Ind. Ass., Washington, D.C., 20006, 1969).

[204] REICHLEY, P. E., DOWNS, G. S., and MORRIS, G. A., "Time-of-arrival observations of eleven pulsars," ASTRON. J., vol. 159 (LET.), pp. L35-L40 (January 1970).

[205] TILSON, S., "Pulsars may be neutron stars," IEEE SPECTRUM, vol. 7, no. 2, pp. 42-55 (February 1970).

h. Satellite/clocks

[206] BASOV, N. G., et al., "Operational test of a molecular generator on an artificial earth satellite," (Edited translation of KOSMICHESKIE ISSLEDOVANIYA (USSR), vol. 5, no. 4, pp. 608-616, by F. Dion), (AD-678 441), 14 pages (CFSTI, December 1967).

[207] EASTON, R. L., et al., "Crystal oscillator satellite experiment," PROC. 22nd ANN. SYMP. ON FREQUENCY CONTROL (U.S. Army Electronics Command, Ft. Monmouth, N.J., 07703, April 22-24, 1968), (AD-844 911), pp. 342-353 (CFSTI, 1968).

[208] GATLAND, K. W. (Editor), Telecommunication Satellites, 441 pages (Prentice-Hall, Inc., Englewood Cliffs, N.J.07632, 1964).

[209] OSBORNE, E. F., "Global timing systems of nanosecond accuracy using satellite references," JOHN HOPKINS UNIV. APL TECH. MEMO NO. TG-1086, 182 pages (CFSTI, October 1969).

[210] SEKIMOTO, T., and PUENTE, J. G., "A satellite time-division multiple-access experiment," IEEE TRANS. on COMMUN. TECHNOL., vol. COM-16, no. 4, pp. 581-588 (August 1968).

[211] THOMAS, P., "Crowding in the synchronous orbit," SPACE AND AERONAUT., vol. 49, no. 4, pp. 66-74 (April 1968).

[212] WEIFFENBACH, G. C., "Time dissemination by satellite," DOT/FAA Meet. on Utilization of Time/frequency in Collision Avoidance Systems (CAS) (FAA, Washington, D.C., 20590, August 27-28, 1968), (AD-681 881), pp. 85-88 (CFSTI, 1968).

i. Television (Commercial), TV

[213] DAVIS, D. D., JESPERSEN, J. L., and KAMAS, G., "The use of television signals for time and frequency dissemination," PROC. IEEE (LTR.), vol. 58, no. 6 (in press).

[214] PARCELLIER, P., "Développement des synchronisations de temps par télévision," (Development of television time synchronization), PROC. COLLOQUE INTERNATIONAL DE CHRONOMETRIE (International Horological Symp., Paris, France, September 16-20, 1969), Paper A26, 6 pages (Nouvelle Faculte des Sciences, 11, Quai St., Paris, (5°), France, 1969).

j. Other

[215] KLEPPNER, D., "Frequency comparison system for spacecraft relativity experiment," PROC. 21st ANN. SYMP. ON FREQUENCY CONTROL (U.S. Army Electronics Command, Ft. Monmouth, N.J.,07703, April 24-26, 1967), (AD-659 792), pp. 509-511 (CFSTI, 1967).

[216] MUNGALL, A. G., DAAMS, H., BAILEY, R., and MORRIS, D., "Mass-frequency effect on VLF and portable clock comparisons of atomic frequency standards," METROLOGIA, vol. 5, no. 1, pp. 31-32 (January 1969).

[217] SHERIDAN, K. V., "Use of atomic frequency standards for phase calibration of large aerial arrays," ELECTRON. LETT., vol. 5, no. 16, pp. 363-365 (August 1969).

[218] VESSOT, R.F.C., KLEPPNER, D., and RAMSEY, N.F., "Application of the hydrogen maser to experimental relativity," IEEE J. QUANTUM ELECTRON., vol. QE-4, no. 5, pp. 376-377 (May 1968).

[219] WOODWARD, R. H., "Distance measurement with ultra-stable oscillators," FREQUENCY, vol. 2, no. 1, pp. 16-20 (January-February 1964).

5.6. National-International Coordination of Frequency and Time

[220] BECKER, G., FISCHER, B., and KRAMER, G., "Methoden und ergebnisse im internationalen zeitvergleich mit längstwellen," (Methods and results in international time comparison with very long waves), PROC. COLLOQUE INTERNATIONAL DE CHRONOMETRIE (International Horological Symp., Paris, France, September 16-20, 1969), Paper A22, 24 pages (Nouvelle Faculte des Sciences, 11, Quai St., Paris, (5°), France, 1969).

[221] ESSEN, L, and STEELE, J. McA., "The international comparison of atomic standards of time and frequency," PROC. INST. ELEC. ENG. (London), vol. 109, part B, no. 43, pp. 41-47 (January 1962).

[222] GUINOT, B., "Formation de l'échelle de temps coordonné par le Bureau International de l'Heure," (Formation of the coordinate time scale by the BIH), PROC. COLLOQUE INTERNATIONAL DE CHRONOMETRIE, (International Horological Symp., Paris, France, September 16-20, 1969), Paper A20, 8 pages (Nouvelle Faculte des Sciences, 11, Quai St., Paris, (5°), France, 1969).

[223] MITCHELL, A.M.J., "Frequency comparison of atomic standards by radio links," NATURE, vol. 198, no. 4886, pp. 1155-1158 (June 23, 1963).

[224] RICHARDSON, J. M., "The functions of Commission I of the International Scientific Radio Union," PROC. IEEE, vol. 55, no. 6, pp. 743-745 (June 1967).

[225] SILVER, S., "URSI, the International Scientific Radio Union," RADIO SCI., vol. 4, no. 1, pp. 3-6 (January 1969).

[226] SMITH, H., "International co-ordination of radio time signal emissions," PROC. 23rd ANN. SYMP. ON FREQUENCY CONTROL (U.S. Army Electronics Command, Ft. Monmouth, N.J.,07703, May 6-8, 1968), pp. 18-20 (Electron. Ind. Ass., Washington, D.C., 20006, 1969).

[227] WHITE, C. E., "World-wide control of industrial radio-electronic measurement accuracy," PROC. IEEE, vol. 55, no. 6, pp. 748-758 (June 1967).

5.7. General References

HOADLEY, G. B. (Editor), CPEM Special Issues (International Conference on Precision Electromagnetic Measurements, held at Boulder, Colorado, 80302, every two years), IEEE TRANS. on INSTRUM. AND MEAS. (fall, winter issue, even years).

NOTE: These Special Issues contain many useful and state-of-the-art papers in the frequency and time area.

The proceedings of the Symposium on Frequency Control, sponsored annually by the U. S. Army Electronics Command, Ft. Monmouth, N.J.,07703, contain a wide variety of frequency/time papers, including general interest subjects, progress reports, and well-documented, state-of-the-art accounts. The proceedings for the last ten years are listed below, with identifying information, to aid any interested reader:

Symp. No.	Date	Proceedings Accession No.	Pages	Availability
14	May 31 - June 2, 1960	PP-153 716	443	Library of Congress Washington, D.C., 20006
15	May 31 - June 2, 1961	AD-265 455	335	CFSTI
16	April 25-27, 1962	PP-162 343	455	CFSTI
17	May 27-29, 1963	AD-423 381	618	CFSTI
18	May 4-6, 1964	AD-450 341	597	CFSTI
19	April 20-22, 1965	AD-471 229	673	CFSTI
20	April 19-21, 1966	AD-800 523	679	CFSTI
21	April 24-26, 1967	AD-659 792	579	CFSTI
22	April 22-24, 1968	AD-844 911	620	CFSTI
23	May 6-8, 1969	----------	313	Electronics Industries Ass. 2001 Eye St., NW Washington, D. C. 20006

Author Index

A

B

C

D

E

F

G

J

K

L

M

N

T

Volume and Page

V

W

Volume and Page

Subject Index[1]

[1] [Reference is to volume number, boldface, followed by page number of this volume.]

A

B

E

F

G

H

I

L

463-560 O - 72 - 35

O

P

Q

R

S

T

U

V

W

Y

Z

Official SI Unit Names and Symbols

[For a complete statement of NBS practice, see NBS Tech. News Bull. Vol. 55, No. 1, Jan. 1971.]

Name	Symbol	Name	Symbol
meter	m	newton	N
kilogram	kg	joule	J
second	s	watt	W
ampere	A	coulomb	C
kelvin [1]	K	volt	V
candela	cd	ohm	Ω
radian	rad	farad	F
steradian	sr	weber	Wb
hertz	Hz	henry	H
lumen	lm	tesla	T
lux	lx		

Additional Names and Symbols approved for NBS use

curie [2]	Ci	mole	mol
degree Celsius [3]	°C	siemens [4]	S
gram	g		

[1] The same name and symbol are used for thermodynamic temperature and temperature interval. (Adopted by the 13th General Conference on Weights & Measures, 1967.
[2] Accepted by the General Conference on Weights & Measures for use with the SI.
[3] For expressing "Celsius temperature"; may also be used for a temperature interval.
[4] Adopted by IEC and ISO.

Table for Converting U.S. Customary Units to Those of the International System (SI) [5]

To relate various units customarily used in the United States to those of the International System, the National Bureau of Standards uses the conversion factors listed in the "ASTM Metric Practic Guide", designation: E 380–70. These are based on international agreements effective July 1, 1959, between the national standards laboratories of Australia, Canada, New Zealand, South Africa, the United Kingdom, and the United States.

To convert from:

(1) inches to meters, multiply by 0.0254 exactly.
(2) feet to meters, multiply by 0.3048 exactly.
(3) feet (U.S. survey) to meters, multiply by 1200/3937 exactly.
(4) yards to meters, multiply by 0.9144 exactly.
(5) miles (U.S. statute) to meters, multiply by 1609.344 exactly.
(6) miles (international nautical) to meters, multiply by 1852 exactly.
(7) grains (1/7000 lbm avoirdupois) to grams, multiply by 0.064 798 91 exactly.
(8) troy or apothecary ounces mass to grams, multiply by 31.103 48 . . .
(9) pounds-force (lbf avoirdupois) to newtons, multiply by 4.448 222 . . .
(10) pounds-mass (lbm avoirdupois) to kilograms, multiply by 0.453 592 . . .
(11) fluid ounces (U.S.) to cubic centimeters, multiply by 29.57 . . .
(12) gallons (U.S. liquid) to cubic meters, multiply by 0.003 785 . . .
(13) torr (mm Hg at O °C) to newtons per square meter, multiply by 133.322 exactly.
(14) millibars to newtons per square meter, multiply by 100 exactly.
(15) psi to newtons per square meter, multiply by 6894.757 . . .
(16) poise to newton-seconds per square meter, multiply by 0.1 exactly.
(17) stokes to square meters per second, multiply by 0.0001 exactly.
(18) degrees Fahrenheit to kelvins, use the relation $T_{°s} = (t_F + 459.67)/1.8$.
(19) degrees Fahrenheit to degrees Celsius, use the relation $t_{°s} = (t_F - 32)/1.8$.
(20) curies to disintegrations per second, multiply by 3.7×10^{10} exactly.
(21) roentgens to coulombs per kilogram, multiply by $2.579\ 760 \times 10^{-4}$ exactly.

[5] Système International d'Unités (designated SI in all languages).